

THIRD EARTH RESOURCES TECHNOLOGY SATELLITE-1 SYMPOSIUM

Volume I: Technical Presentations Section A

*The proceedings of a symposium held by
Goddard Space Flight Center
at Washington, D.C.
on December 10-14, 1973*

Compiled and Edited by

*Stanley C. Freden
Enrico P. Mercanti
Missions Utilization Office*

and

*Margaret A. Becker
Technical Information Division
Goddard Space Flight Center*

Prepared at Goddard Space Flight Center



Scientific and Technical Information Office
NATIONAL AERONAUTICS AND SPACE ADMINISTRATION
1974
Washington, D.C.

This document is "made available under NASA sponsorship in the interest of early and wide dissemination of Earth Resources Survey information and without liability for any use made thereof." (NPD 8000.2A March 16, 1973)

PREFACE

The Third Symposium on Significant Results Obtained from the first Earth Resources Technology Satellite (ERTS-1) was held from December 10-14, 1973 at the Statler Hilton Hotel in Washington, D. C. The Symposium was sponsored by the National Aeronautics and Space Administration, Goddard Space Flight Center. The structure of this Symposium was similar to the one held from March 5-9, 1973. The Opening Plenary Session on Monday morning contained two papers of general interest to the entire audience, one on the status of the ERTS-1 system and a report on the Canadian ERTS program. The next two and one-half days were devoted to contributed papers in the various disciplines presented during three parallel sessions. These papers are contained in Volume I of the Proceedings.

The Thursday Summary Session, as before, was designed to highlight and summarize the significant results from the first three days and also to present some typical examples of the applications of ERTS data for solving resources management problems at the national, state and local levels. This Session was highlighted by an introductory address by Dr. James C. Fletcher, NASA Administrator, and by a keynote address by Dr. John C. Whitaker, Under Secretary of the Interior, U.S. Department of the Interior. The presentations from this session are contained in Volume II of the Proceedings.

Volume III contains the Discipline Summary Reports. These are based on a report produced from a two-week long series of intensive interviews with the individual ERTS-1 Principal Investigators and then updated and extended from the material presented at the Third ERTS Symposium. The interviews were organized and directed by Dr. O. Glenn Smith of the Earth Resources Program Office at the Johnson Space Center and were held at the Goddard Space Flight Center from October 22 to November 2, 1973. The Discipline Summary Reports were written by Working Groups in each of the disciplines which were convened on Friday, December 14. These Working Groups were chaired by the respective discipline session chairmen and were composed of selected specialists in the various disciplines. Opinions and recommendations expressed in these reports are those of the panel members and do not necessarily reflect an official position of NASA.

Stanley C. Freden
Symposium Chairman

TABLE OF CONTENTS

<u>Paper No.</u>		<u>Page</u>
	ERTS-1 SYSTEM PERFORMANCE OVERVIEW, John H. Boeckel,	1 ✓
	CANADIAN ERTS PROGRAM PROGRESS REPORT, L. W. Morley and A. K. McQuillan	13 ✓
	AGRICULTURE/FORESTRY/RANGE RESOURCES	
A 1	ESTIMATE OF WINTER WHEAT YIELD FROM ERTS-1, Stanley A. Morain and Donald L. Williams	21 ✓
A 2	USER ORIENTED ERTS-1 IMAGES, Seymour Shlien and David Goodenough . . .	29 ✓
A 3	AN EVALUATION OF MACHINE PROCESSING TECHNIQUES OF ERTS-1 DATA FOR USER APPLICATIONS, David Landgrebe and Staff . . .	41 ✓
A 4	THE UTILITY OF ERTS-1 DATA FOR APPLICATIONS IN AGRICULTURE AND FORESTRY, R. Bryan Erb	75 ✓
A 5	CROP IDENTIFICATION AND ACREAGE MEASUREMENT UTILIZING ERTS IMAGERY, William H. Wigton and Donald H. Von Steen	87 ✓
A 6	VEGETATION DENSITY AS DEDUCED FROM ERTS-1 MSS RESPONSE, C. L. Wiegand, H. W. Gausman, J. A. Cuellar, A. H. Gerbermann, and A. J. Richardson	93 ✓
A 7	REGIONAL AGRICULTURE SURVEYS USING ERTS-1 DATA, William C. Draeger, James D. Nichols, Andrew S. Benson, David G. Larrabee, William M. Senkus, and Claire M. Hay	117 ✓
A 8	FOREST AND LAND INVENTORY USING ERTS IMAGERY AND AERIAL PHOTOGRAPHY IN THE BOREAL FOREST REGION OF ALBERTA, CANADA, C. L. Kirby	127 ✓
A 9	SO ₂ DAMAGE TO FORESTS RECORDED BY ERTS-1, Peter A. Murtha	137 ✓
A 10	A TIMER INVENTORY BASED UPON MANUAL AND AUTOMATED ANALYSIS OF ERTS-1 AND SUPPORTING AIRCRAFT DATA USING MULTISTAGE PROBABILITY SAMPLING, James D. Nichols, Mike Gialdini, and Sipi Jaakkola	145 ✓
A 11	APPLICATION OF ERTS-1 IMAGERY TO LAND USE, FOREST DENSITY AND SOIL INVESTIGATIONS IN GREECE, N. J. Yassoglou, E. Skordalakis, and A. Koutalos	159 ✓

PRECEDING PAGE BLANK NOT FILMED

TABLE OF CONTENTS (Continued)

<u>Paper No.</u>		<u>Page</u>
A 12	ERTS-1 MSS IMAGERY: ITS USE IN DELINEATING SOIL ASSOCIATIONS AND AS A BASE MAP FOR PUBLISHING SOILS INFORMATION, Frederick C. Westin	183 ✓
A 13	MAPPING SOILS, CROPS, AND RANGELANDS BY MACHINE ANALYSIS OF MULTI-TEMPORAL ERTS-1 DATA, Marion F. Baumgardner, James A. Henderson, Jr., and LARS Staff	205 ✓
A 14	APPLICATION OF ERTS-1 IMAGERY IN MAPPING AND MANAGING SOIL AND RANGE RESOURCES IN THE SAND HILLS REGION OF NEBRASKA, Paul M. Seevers, David T. Lewis, and James V. Drew	225 ✓
A 15	ERTS SURVEYS A 500 KM ² LOCUST BREEDING SITE IN SAUDI ARABIA, D. E. Pedgley	233 ✓
A 16	REMOTE SENSING EXPERIMENT IN WEST AFRICA, N. H. MacLeod	247 ✓
A 17	NATURAL RESOURCE INVENTORIES AND MANAGEMENT APPLICATIONS IN THE GREAT BASIN, Paul T. Tueller, Garwin Lorain, and Ronald M. Halvorson	267 ✓
A 18	USEFULNESS OF ERTS-1 SATELLITE IMAGERY AS A DATA-GATHERING TOOL BY RESOURCE MANAGERS IN THE BUREAU OF LAND MANAGEMENT, R. Gordon Bentley	291 ✓
A 19	VEGETATION MAPPING FROM ERTS IMAGERY OF THE OKAVANGO DELTA, Douglas T. Williamson	301 ✓
A 20	MONITORING VEGETATION SYSTEMS IN THE GREAT PLAINS WITH ERTS, J. W. Rouse, Jr., R. H. Haas, J. A. Schell, and D. W. Deering	309 ✓
A 21	ERTS-1 DATA UTILIZATION IN THE FIELD OF AGRICULTURE IN THAILAND, Pradisth Cheosakul	319 ✓
LAND USE & MAPPING		
L 1	COMPUTER-IMPLEMENTED LAND USE CLASSIFICATION WITH PATTERN RECOGNITION SOFTWARE AND ERTS DIGITAL DATA, Armond T. Joyce and Thomas W. Pendleton	331 ✓
L 2	REMOTE SENSING OF LAND USE CHANGES IN U.S. METROPOLITAN REGIONS: TECHNIQUES OF ANALYSIS AND OPPORTUNITIES FOR APPLICATION, James R. Wray	339 ✓

TABLE OF CONTENTS (Continued)

<u>Paper No.</u>		<u>Page</u>
L 3	ERTS-1 ROLE IN LAND MANAGEMENT AND PLANNING IN MINNESOTA, Joseph E. Sizer and Dwight Brown	341 ✓
L 4	INTERACTIVE ANALYSIS AND EVALUATION OF ERTS DATA FOR REGIONAL PLANNING AND URBAN DEVELOPMENT: A LOS ANGELES BASIN CASE STUDY, Surendra Raje, Richard Economy, Gerald Willoughby, and Jene McKnight	351 ✓
L 5	EVALUATION OF ERTS-1 DATA FOR ACQUIRING LAND USE DATA OF NORTHERN MEGALOPOLIS, Robert B. Simpson, David T. Lindgren, and William D. Goldstein	371 ✓
L 6	THE VALUE OF ERTS-1 IMAGERY IN RESOURCE INVENTORIZATION ON A NATIONAL SCALE IN SOUTH AFRICA, O. G. Malan, C. N. MacVicar, D. Edwards, B. N. Temperley, and L. Claassen and collaborators	383 ✓
L 7	CHANGE IN LAND USE IN THE PHOENIX (1:250,000) QUADRANGLE, ARIZONA BETWEEN 1970 AND 1973: ERTS AS AN AID IN A NATIONWIDE PROGRAM FOR MAPPING AND GENERAL LAND USE, John L. Place	393 ✓
L 8	THE APPLICATION OF ERTS-1 DATA TO THE LAND USE PLANNING PROCESS, James L. Clapp, Ralph W. Kiefer, Edward L. Kuhlmeier, and Bernard J. Niemann, Jr.	425 ✓
L 9	THE UTILITY OF ERTS-1 DATA FOR APPLICATIONS IN LAND USE CLASSIFICATION, John E. Dornbach and Gerald E. McKain	439 ✓
L 10	APPLICATION OF ERTS-1 SATELLITE IMAGERY FOR LAND USE MAPPING AND RESOURCE INVENTORIES IN THE CENTRAL COASTAL REGION OF CALIFORNIA, John E. Estes, Randolph R. Thaman, and Leslie W. Senger	457 ✓
L 11	EVALUATION OF ERTS-1 IMAGERY FOR LAND USE/RESOURCE INVENTORY INFORMATION, Ernest E. Hardy, James E. Skaley and Elmer S. Phillips	491 ✓
L 12	IMPACT OF ERTS-1 IMAGES ON MANAGEMENT OF NEW JERSEY'S COASTAL ZONE, Edward B. Feinberg, Roland S. Yunghans, JoAnn Stitt, and Robert L. Mairs	497 ✓
L 13	CARETS—AN EXPERIMENTAL REGIONAL INFORMATION SYSTEM USING ERTS DATA, Robert H. Alexander	505 ✓
L 14	CONCEPTS OF INTEGRATED SATELLITE SURVEYS, J. A. Howard.	523 ✓

TABLE OF CONTENTS (Continued)

<u>Paper No.</u>		<u>Page</u>
L 15	TOWARDS AN OPERATIONAL ERTS - REQUIREMENTS FOR IMPLEMENTING CARTOGRAPHIC APPLICATIONS OF AN OPERATIONAL ERTS TYPE SATELLITE, Alden P. Colvocoresses	539 ✓
L 16	EARTH RESOURCES TECHNOLOGY SATELLITE DATA COLLECTION PROJECT, ERTS - BOLIVIA, Dr. Carlos Brockmann	559 ✓
L 17	AN OPERATIONAL APPLICATION OF ERTS-1 IMAGERY TO THE ENVIRONMENTAL INVENTORY PROCESS, James D. O'Neal and James R. Bwins	579 ✓
L 18	PHOTOINTERPRETATION OF ERTS-A MULTISPECTRAL IMAGES ANALYSIS OF VEGETATION AND LAND USE FOR THE VALENCIA LAKE BASIN REGION, F. Salas, M. Pineda, and A. Arismendi	585 ✓
 MINERAL RESOURCES, GEOLOGICAL STRUCTURE AND LANDFORM SURVEYS 		
G 1	APPLICATION OF THE ERTS SYSTEM TO THE STUDY OF WYOMING RESOURCES WITH EMPHASIS ON THE USE OF BASIC DATA PRODUCTS, Robert S. Houston, Ronald W. Marrs, Roy M. Breckenridge, and D. L. Blackstone, Jr.	595 ✓
G 2	SUMMARY OF AN INTEGRATED ERTS-1 PROJECT AND ITS RESULTS AT THE MISSOURI GEOLOGICAL SURVEY, James A. Martin, William H. Allen, David L. Rath, and Ardel Rueff	621 ✓
G 3	ANALYSIS OF STATE OF VEHICULAR SCARS ON ARCTIC TUNDRA, ALASKA, Ernest H. Lathram	633 ✓
G 4	THE INFLUENCE OF SEASONAL FACTORS ON THE RECOGNITION OF SURFACE LITHOLOGIES FROM ERTS-IMAGERY OF THE WESTERN TRANSVAAL, Jan Grootenboer	643 ✓
G 5	STRATIGRAPHIC SUBDIVISION OF THE TRANSVAAL DOLOMITE FROM ERTS IMAGERY, Jan Grootenboer, Ken Eriksson, and John Truswell	657 ✓
G 6	AN INVESTIGATION OF MAJOR SAND SEAS IN DESERT AREAS THROUGHOUT THE WORLD, Edwin D. McKee and Carol S. Breed	665 ✓
G 7	A NEW METHOD FOR MONITORING GLOBAL VOLCANIC ACTIVITY, Peter L. Ward, Elliot T. Endo, David H. Harlow, Rex Allen, and Jerry P. Eaton	681 ✓
G 8	EVALUATION OF ERTS IMAGERY FOR SPECTRAL GEOLOGICAL MAPPING IN DIVERSE TERRANES OF NEW YORK STATE, Y. W. Isachsen, R. H. Fakundiny, and S. W. Forster	691 ✓

TABLE OF CONTENTS (Continued)

Paper No.		Page
G 9	GEOLOGIC APPLICATIONS OF ERTS IMAGES ON THE COLORADO PLATEAU, ARIZONA, Alexander F. H. Goetz, Fred C. Billingsley, Donald P. Elston Ivo Lucchitta, and Eugene M. Shoemaker	719 ✓
G 10	ERTS-1, EARTHQUAKES, AND TECTONIC EVOLUTION IN ALASKA, Larry Gedney and James VanWormer	745 ✓
G 11	STRUCTURAL INVESTIGATIONS IN THE MASSIF-CENTRAL — FRANCE, J-Y. Scanvic	757 ✓
G 12	STRUCTURAL GEOLOGY OF THE AFRICAN RIFT SYSTEM: SUMMARY OF NEW DATA FROM ERTS-1 IMAGERY, P. A. Mohr	767 ✓
G 13	TECTONIC ANALYSIS OF EAST AND SOUTH EAST IRAN USING ERTS-1 IMAGERY, Khosro Ebtehadj, Ali Ghazi, Farrokh Barzegar, Reza Boghrati, and Bahman Jazayeri	783 ✓
G 14	MINERAL EXPLORATION WITH ERTS IMAGERY, Stephen M. Nicolais	785 ✓
G 15	ERTS-1 IMAGERY AS AN AID TO THE UNDERSTANDING OF THE REGIONAL SETTING OF BASE METAL DEPOSITS IN THE NORTH WEST CAPE PROVINCE, SOUTH AFRICA, Dr. Richard P. Viljoen	797 ✓
G 16	MAPPING OF HYDROTHERMAL ALTERNATION ZONES AND REGIONAL ROCK TYPES USING COMPUTER ENHANCED ERTS MSS IMAGES, Lawrence C. Rowan, Pamela H. Wetlaufer, F. C. Billingsley, and Alexander F. H. Goetz	807 ✓
G 17	AN EVALUATION OF THE SUITABILITY OF ERTS DATA FOR THE PURPOSES OF PETROLEUM EXPLORATION, Robert J. Collins, F. P. McCown, L. P. Stonis, Gerald Petzel, and John R. Everett	809 ✓
G 18	PRELIMINARY ROAD ALINEMENT THROUGH THE GREAT KAVIR IN IRAN BY REPETITIVE ERTS-1 COVERAGE, Daniel B. Krinsley	823 ✓
G 19	RELATIONSHIP OF ROOF FALLS IN UNDERGROUND COAL MINES TO FRACTURES MAPPED ON ERTS-1 IMAGERY, Charles E. Wier, Frank J. Wobber, Orville R. Russell, Roger V. Amato, and Thomas V. Leshendok	825 ✓
G 20	A STUDY OF THE TEMPORAL CHANGES RECORDED BY ERTS AND THEIR GEOLOGICAL SIGNIFICANCE, Harold D. Moore and Alan F. Gregory	845 ✓
G 21	GEOLOGIC EVALUATION AND APPLICATIONS OF ERTS-1 IMAGERY OVER GEORGIA, S. M. Pickering and R. C. Jones	857 ✓

TABLE OF CONTENTS (Continued)

<u>Paper No.</u>		<u>Page</u>
G 22	ALTITUDE DETERMINATION AND DESCRIPTIVE ANALYSIS OF CLOUDS ON ERTS-1 MULTISPECTRAL PHOTOGRAPHY, Carlos Albrizzio and Adelina Andressen	869 ✓
G 23	GEOLOGICAL PHOTOINTERPRETATION OF THE PARAGUANA PENINSULA USING ERTS-A MULTISPECTRAL PHOTOGRAPHY, Carlos Albrizzio	883 ✓
G 24	SIGNIFICANCE OF SELECTED LINEAMENTS IN ALABAMA, James A. Drahovzal, Thornton L. Neathery, and Charles C. Wielchowsky	897 ✓
G 25	GEOLOGIC INTERPRETATION OF ERTS-1 SATELLITE IMAGES FOR WEST ASWAN AREA, EGYPT, E. M. El Shazly, M. A. Abdel-Hady, M. A. El Ghawaby and I. A. El Kassas	919 ✓
G 26	ERTS-A MULTISPECTRAL IMAGE ANALYSIS CONTRIBUTION FOR THE GEOMORPHOLOGICAL EVALUATION OF SOUTHERN MARACAIBO LAKE BASIN, F. Salas, O. Cabello, F. Alarcón and C. Ferrer	943 ✓
G 27	GEOLOGIC HYPOTHESES ON LAKE TANGANYIKA REGION, ZAIRE, DRAWN FROM ERTS IMAGERY, Ulyera Wolyce and Sendwe Ilunga	955 ✓
G 28	PRELIMINARY RESULTS OF ERTS-INVESTIGATIONS BY W-GERMAN INVESTIGATORS, Richard Mühlfeld	969 ✓

WATER RESOURCES

W 1	MAPPING SNOW EXTENT IN THE SALT-VERDE WATERSHED AND THE SOUTHERN SIERRA NEVADA USING ERTS IMAGERY, James C. Barnes, Clinton J. Bowley, and David A. Simmes	977
W 2	SNOW-EXTENT MAPPING AND LAKE ICE STUDIES USING ERTS-1 MSS TOGETHER WITH NOAA-2 VHRR, D. R. Wiesnet and D. F. McGinnis, Jr.	995
W 3	NEW SPACE TECHNOLOGY ADVANCES KNOWLEDGE OF THE REMOTE POLAR REGIONS, William R. MacDonald.	1011
W 4	ERTS-1 DATA IN SUPPORT OF THE NATIONAL PROGRAM OF INSPECTION OF DAMS, G. E. Graybeal, F. G. Hall, B. H. Moore, and E. H. Schlosser	1023
W 5	DYNAMICS OF PLAYA LAKES IN THE TEXAS HIGH PLAINS, C. C. Reeves, Jr.	1041
W 6	WATER-MANAGEMENT MODELS IN FLORIDA FROM ERTS-1 DATA, Aaron L. Higer, Alfred E. Coker, and Edwin H. Cordes	1071

TABLE OF CONTENTS (Continued)

<u>Paper No.</u>		<u>Page</u>
W 7	MEASURING WATERSHED RUNOFF CAPABILITY WITH ERTS DATA, Bruce J. Blanchard	1089
W 8	AN EVALUATION OF THE ERTS DATA COLLECTION SYSTEM AS A POTENTIAL OPERATIONAL TOOL, Richard W. Paulson	1099
W 9	RETRANSMISSION OF WATER RESOURCES DATA USING THE ERTS-1 DATA COLLECTION SYSTEM, R. A. Halliday, I. A. Reid, and E. F. Chapman	1113
W 10	ERTS-1 FLOOD HAZARD STUDIES IN THE MISSISSIPPI RIVER BASIN, Albert Rango and Arthur T. Anderson	1127
W 11	OPTICAL DATA PROCESSING AND PROJECTED APPLICATIONS OF THE ERTS-1 IMAGERY COVERING THE 1973 MISSISSIPPI RIVER VALLEY FLOODS, Morris Deutsch and F. H. Ruggles	1167
W 12	APPLICATION OF ERTS IMAGERY TO ENVIRONMENTAL STUDIES OF LAKE CHAMPLAIN, A. O. Lind	1189
W 13	A REAL TIME DATA ACQUISITION SYSTEM BY SATELLITE RELAY, Saul Cooper	1197
W 14	HYDROLOGIC APPLICATIONS OF ERTS-1 DATA COLLECTION SYSTEM IN CENTRAL ARIZONA, Herbert H. Schumann	1213
W 15	APPLICATIONS OF ERTS DATA TO COASTAL WETLAND ECOLOGY WITH SPECIAL REFERENCE TO PLANT COMMUNITY MAPPING AND TYPING AND IMPACT OF MAN, Richard R. Anderson, Virginia Carter, and John McGinness	1225
W 16	INVENTORIES OF DELAWARE'S COASTAL VEGETATION AND LAND-USE UTILIZING DIGITAL PROCESSING OF ERTS-1 IMAGERY, V. Klemas, D. Bartlett, R. Rogers, and L. Reed	1243
W 17	EVALUATION OF REMOTE SENSING AND AUTOMATIC DATA TECHNIQUES FOR CHARACTERIZATION OF WETLANDS, Robert H. Cartmill	1257
MARINE RESOURCES		
M 1	RELATIONSHIPS BETWEEN ERTS RADIANCES AND GRADIENTS ACROSS OCEANIC FRONTS, George A. Maul and Howard R. Gordon	1279
M 2	OCEAN INTERNAL WAVES OFF THE NORTH AMERICAN AND AFRICAN COASTS FROM ERTS-1, John R. Apel and Robert L. Charnell	1309

TABLE OF CONTENTS (Continued)

<u>Paper No.</u>		<u>Page</u>
M 3	A REVIEW OF INITIAL INVESTIGATIONS TO UTILIZE ERTS-1 DATA IN DETERMINING THE AVAILABILITY AND DISTRIBUTION OF LIVING MARINE RESOURCES, William H. Stevenson, Andrew J. Kemmerer, Buddy H. Atwell, and Paul M. Maughan	1317
M 4	UPDATING COASTAL AND NAVIGATIONAL CHARTS USING ERTS-1 DATA, Fabian C. Polcyn and David R. Lyzenga	1333
M 5	SEDIMENT CONCENTRATION MAPPING IN TIDAL ESTUARIES, A. N. Williamson and W. E. Grabau	1347
M 6	MONITORING COASTAL WATER PROPERTIES AND CURRENT CIRCULATION WITH ERTS-1, V. Klemas, M. Otley, C. Wethe, and R. Rogers	1387
M 7	CALIFORNIA COASTAL PROCESSES STUDY, Douglas M. Pirie and and David D. Steller	1413
M 8	THE UTILIZATION OF ERTS-1 DATA FOR THE STUDY OF THE FRENCH ATLANTIC LITTORAL, Pierre G. Demathieu and Fernand H. Verger	1447
M 9	ERTS IMAGERY APPLIED TO ALASKAN COASTAL PROBLEMS, F. F. Wright, G. D. Sharma, D. C. Burbank, and J. J. Burns	1451
M 10	MONITORING ARCTIC SEA ICE USING ERTS IMAGERY, James C. Barnes and Clinton J. Bowley	1453
M 11	APPLICABILITY OF ERTS TO ANTARCTIC ICEBERG RESOURCES, John L. Hult and Neill C. Ostrander	1467
 ENVIRONMENT SURVEYS 		
E 1	THE USE OF ERTS-1 IMAGERY IN AIR POLLUTION AND MESO- METEOROLOGICAL STUDIES AROUND THE GREAT LAKES, Walter A. Lyons, and Richard A. Northouse	1491
E 2	A METHOD TO MEASURE THE ATMOSPHERIC AEROSOL CONTENT USING ERTS-1 DATA, Michael Griggs	1505
E 3	AUTOMATED STRIP-MINE AND RECLAMATION MAPPING FROM ERTS, Robert H. Rogers, Larry E. Reed, and Wayne A. Pettyjohn	1519
E 4	SIGNIFICANT APPLICATIONS OF ERTS-1 DATA TO RESOURCE MANAGEMENT ACTIVITIES AT THE STATE LEVEL IN OHIO, D. C. Sweet, F. G. Pincura, C. J. Meier, G. B. Garrett, L. Herd, G. E. Wukelic, J. G. Stephan, and H. E. Smail	1533

TABLE OF CONTENTS (Continued)

<u>Paper No.</u>		<u>Page</u>
E 5	ERTS IMAGERY AS A SOURCE OF ENVIRONMENTAL INFORMATION FOR SOUTHERN AFRICA, Douglas T. Williamson and Brian Gilbertson	1559
E 6	APPLICATION OF ERTS IMAGERY IN ESTIMATING THE ENVIRONMENTAL IMPACT OF A FREEWAY THROUGH THE KNYSNA AREA OF SOUTH AFRICA, Douglas T. Williamson and Brian Gilbertson	1569
E 7	APPLICATIONS OF ERTS-1 IMAGERY TO TERRESTRIAL AND MARINE ENVIRONMENTAL ANALYSES IN ALASKA, D. M. Anderson, H. L. McKim, W. K. Crowder, R. K. Haugen, L. W. Gatto, and T. L. Marlar	1575
E 8	AN INTERDISCIPLINARY STUDY OF THE ESTUARINE AND COASTAL OCEANOGRAPHY OF BLOCK ISLAND SOUND AND ADJACENT NEW YORK COASTAL WATERS, Edward Yost, R. Hollman, J. Alexander, and R. Nuzzi	1607
E 9	AIRCRAFT AND SATELLITE MONITORING OF WATER QUALITY IN LAKE SUPERIOR NEAR DULUTH, James P. Scherz, Michael Sydor, and John F. Van Domelen	1619
E 10	QUANTITATIVE WATER QUALITY WITH ERTS-1, Harold L. Yarger, James R. McCauley, Gerald W. James, Larry M. Magnuson, and G. Richard Marzolf	1637
E 11	AN EVALUATION OF THE USE OF ERTS-1 SATELLITE IMAGERY FOR GRIZZLY BEAR HABITAT ANALYSIS, Joel R. Varney, John J. Craighead, and Jay S. Sumner	1653
E 12	UTILITY OF ERTS FOR MONITORING THE BREEDING HABITAT OF MIGRATORY WATERFOWL, Edgar A. Work, Jr., David S. Gilmer, and A. T. Klett	1671

INTERPRETATION TECHNIQUES

I 1	TECHNIQUES FOR COMPUTER-AIDED ANALYSIS OF ERTS-1 DATA, USEFUL IN GEOLOGIC, FOREST AND WATER RESOURCE SURVEYS, Roger M. Hoffer and Staff	1687
I 2	MULTISPECTRAL COMBINATION AND DISPLAY OF ERTS-1 DATA, Vidal Raphael Algazi	1709
I 3	AFFINE TRANSFORMATIONS FROM AERIAL PHOTOS TO COMPUTER COMPATIBLE TAPES, F. G. Peet, A. R. Mack, and L. S. Crosson	1719
I 4	ESIAC: A DATA PRODUCTS SYSTEM FOR ERTS IMAGERY (Time-lapse Viewing and Measuring), William E. Evans and Sidney M. Serebreny	1725

TABLE OF CONTENTS (Continued)

<u>Paper No.</u>		<u>Page</u>
I 5	ADVANCED PROCESSING AND INFORMATION EXTRACTION TECHNIQUES APPLIED TO ERTS-1 MSS DATA, William A. Malila and Richard F. Nalepka	1743
I 6	INTERPRETATION OF ERTS-1 IMAGERY AIDED BY PHOTOGRAPHIC ENHANCEMENT, U. Nielsen	1773
I 7	A TECHNIQUE FOR CORRECTING ERTS DATA FOR SOLAR AND ATMOSPHERIC EFFECTS, Robert H. Rogers, Keith Peacock, and Navinchandra J. Shah	1787
I 8	THE PENN STATE ORSER SYSTEM FOR PROCESSING AND ANALYZING ERTS DATA, G. J. McMurtry, F. Y. Borden, H. A. Weeden and G. W. Petersen.	1805
I 9	ERTS IMAGE DATA COMPRESSION TECHNIQUE EVALUATION, Curtis L. May	1823
I 10	EVALUATION OF DIGITALLY CORRECTED ERTS IMAGES, John E. Taber	1837
I 11	AUTOMATED THEMATIC MAPPING AND CHANGE DETECTION OF ERTS-1 IMAGES, Nicholas Gramenopoulos.	1845
I 12	PRINCIPAL COMPONENTS COLOUR DISPLAY OF ERTS IMAGERY, M. M. Taylor	1877
I 13	APPLICATIONS OF ERTS DATA TO RESOURCE SURVEYS OF ALASKA, Albert E. Belon and John M. Miller	1899
I 14	SCENE CORRECTION (PRECISION PROCESSING) OF ERTS SENSOR DATA USING DIGITAL IMAGE PROCESSING TECHNIQUES, Ralph Bernstein	1909
I 15	SPECTRAL AND TEXTURAL PROCESSING OF ERTS IMAGERY, R. M. Haralick and R. Bosley	1929
I 16	DIGITAL IMAGE ENHANCEMENT TECHNIQUES USED IN SOME ERTS APPLICATION PROBLEMS, Alexander F. H. Goetz and Fred C. Billingsley	1971
	AUTHOR'S INDEX	1993

TABLE OF CONTENTS

VOLUME II

SUMMARY SESSION

INTRODUCTION TO SUMMARY SESSION

Dr. James C. Fletcher, Administrator
National Aeronautics and Space Administration

KEYNOTE ADDRESS

Hon. John C. Whitaker
Under Secretary of the Interior
U.S. Department of the Interior

SELECTED SIGNIFICANT ACCOMPLISHMENTS

REPORT ON THE CANADIAN ERTS PROGRAM, Lawrence W. Morley

ENVIRONMENTAL SURVEYS IN ALASKA BASED UPON ERTS DATA, John M. Miller

GEOLOGIC AND RELATED APPLICATIONS OF ERTS IMAGERY IN GEORGIA, Samuel M. Pickering

AN EVALUATION OF THE SUITABILITY OF ERTS DATA FOR THE PURPOSES OF PETROLEUM
EXPLORATION, John R. Everett and Gerald Petzel

APPLICATIONS AND KEY FINDINGS

ERTS PROGRAM OF THE U.S. ARMY CORPS OF ENGINEERS, John W. Jarman

A REVIEW OF INITIAL INVESTIGATIONS TO UTILIZE ERTS-1 DATA IN DETERMINING THE
AVAILABILITY AND DISTRIBUTION OF LIVING MARINE RESOURCES, William H. Stevenson,
Andrew J. Kemmerer, Buddy H. Atwell and Paul M. Maughan

AUTOMATED STRIP-MINE AND RECLAMATION MAPPING, Wayne A. Pettyjohn, Robert H. Rogers
and Larry E. Reed

UTILITY OF ERTS FOR MONITORING THE BREEDING HABITAT OF MIGRATORY WATERFOWL,
Edgar A. Work, Jr., David S. Gilmer and A. T. Klett

SUMMARIES IN SELECTED DISCIPLINES

AGRICULTURE, FORESTRY, RANGE RESOURCES, Robert M. MacDonald

WATER RESOURCES, Vincent V. Salomonson

LAND USE AND MAPPING, Armond T. Joyce

MINERAL RESOURCES, GEOLOGICAL STRUCTURE AND LANDFORM SURVEYS, Nicholas M. Short

TABLE OF CONTENTS
VOLUME III
DISCIPLINE SUMMARY REPORTS

AGRICULTURE, FORESTRY, RANGE RESOURCES, William J. Crea

LAND USE AND MAPPING, Armond T. Joyce

MINERAL RESOURCES, GEOLOGICAL STRUCTURE AND LANDFORM SURVEYS, Nicholas M. Short

WATER RESOURCES, Vincent V. Salomonson

MARINE RESOURCES, E. Lee Tilton

ENVIRONMENT SURVEYS, Lawrence R. Greenwood

INTERPRETATION TECHNIQUES, James L. Dragg

N74 30706

ERTS-1 SYSTEM PERFORMANCE OVERVIEW

John H. Boeckel, NASA, Goddard Space Flight Center

ABSTRACT

The ERTS-1 Spacecraft had a life of one year as a design goal. At the end of one year, the spacecraft was still providing about 130 scenes per day in multispectral images having resolution and radiometric accuracy better than prelaunch predictions.

INTRODUCTION

The mission of the ERTS-1 spacecraft and its supporting systems was to demonstrate the feasibility of multispectral remote sensing from space for use in practical earth resources management applications. Most of the papers presented during the symposium deal with the utility of the data for use in various scientific disciplines and practical applications. This paper provides the background of spacecraft and system performance which results in the data which the investigators have used.

THE ERTS SPACECRAFT

The ERTS spacecraft weighs about 950 Kg and is earth oriented, aligned to the local vertical within 0.7 degrees. The solar arrays provide about 500 watts when illuminated for the operation of the spacecraft subsystems and the payload which consists of the Multispectral Scanner (MSS), the Return Beam Vidicon Camera (RBV), two Wide-Band Video Tape Recorders (WBVTR), and a Data Collection System (DCS). The imaging instruments (RBV and MSS) provide multispectral images of the earth approximately 185 Km by 185 Km whenever turned on.

The orbit of ERTS-1 is sun synchronous with an inclination of 99.1 degrees crossing the equator in a North-South direction at about 0942 local time. Successive orbits are separated by about 2870 Km at the equator. On the following earth-day, the orbit will have moved approximately 159 Km to the west. This orbit results in repeating the same ground track every 18 days. In order to maintain the ground track within ± 18 Km, the spacecraft includes an orbit-adjust propulsion system.

SPACECRAFT PERFORMANCE

The primary objective of the ERTS-1 observatory was "the acquisition of synoptic, multispectral repetitive images from a satellite for a period of three months from which useful data can be obtained for investigations in such disciplines as: agriculture, geology, geography, hydrology, ecology, and oceanography." The design life for the spacecraft was one year (minimum).

00503 47V

Since its launching, the spacecraft has experienced two unexpected malfunctions and one anticipated degradation. During orbit 148 (August 3, 1972), a noise transient was experienced when WBVTR No. 2 was turned on. Analysis indicates that the problem was caused by internal shorting of the tape recorder power supply. Since that time, only WBVTR No. 1 has been used. During orbit 196 (August 6, 1972), a power transient was experienced when the RBV was turned on. In this case, analysis indicates a failure of a relay in the Power Switching Module of the spacecraft leaving the relay in a permanently "on" state. RBV turn-off (and "on") can still be accomplished by using a set of relays which control individual RBV functions. However, because of the difficult command sequence and the excellent performance of the MSS, the RBV has not been reactivated. Some 1,400 RBV scenes are available for analysis of the instrument's performance. A degradation in the performance of WBVTR No. 1 occurred during orbit 3462 (March 29, 1973) after the recorder design-life had already been exceeded. This has resulted in reducing the capacity of the recorder from its original thirty (30) minutes to approximately twelve (12) minutes. This capacity is still sufficient to record approximately one hundred scenes per day when out of contact with the receiving sites at Greenbelt, Maryland; Goldstone, California; and Fairbanks, Alaska.

Despite the anomalies experienced, the spacecraft and its payload are judged to have far exceeded their success criteria and design goals. After sixteen months in orbit, world-wide coverage was still being obtained at the rate of 130 scenes per day.

THE MULTISPECTRAL SCANNER

Because the vast majority of the data on which subsequent papers will be based are the result of observations by the MSS, a more detailed description of this instrument will be given.

The Multispectral Scanner Subsystem (MSS), gathers data by imaging the surface of the earth in four spectral bands simultaneously through the same optical system.

For ERTS-1, the four spectral bands are:*

- Band 4 0.5 to 0.6 micrometers
- Band 5 0.6 to 0.7 micrometers
- Band 6 0.7 to 0.8 micrometers
- Band 7 0.8 to 1.1 micrometers

Bands 4 through 6 use photomultiplier tubes as detectors; Band 7 uses silicon photodiodes.

The MSS scans cross-track swaths of 185 kilometers (100 nm) width, imaging six scan lines across in each of the spectral bands simultaneously. The object plane is scanned by means of an oscillating flat mirror between the scene and the telescope. The 11.56 degree cross-track field of view is scanned as the mirror oscillates ± 2.89 degrees about its nominal position. The MSS system is illustrated schematically in Figures 1 and 2.

*The number sequence for MSS bands corresponds to the image annotation convention used by the data processing facility.

The along-track scan is produced by the orbital motion of the spacecraft. The nominal orbital velocity causes an along-track motion of the subsatellite point of 6.47 km/sec neglecting spacecraft perturbation and earth rotation effects.

The line scanned by the first detector in one cycle of the active mirror scan lies adjacent to the line scanned by the sixth detector of the previous mirror scan.

The instantaneous field of view of each detector subtends an earth-area square of 79 meters on a side from the nominal orbital altitude. Field stops are formed for each line imaged during a scan, and for each spectral band, by the square input end of an optical fiber. Six of these fibers in each of four bands are arranged in a 4 by 6 matrix in the focused area of the telescope.

Light impinging on each glass fiber is conducted to an individual detector through an optical filter. An image of a line across the swath is swept across the fiber each time the mirror scans, causing a video signal to be produced at the scanner electronics output for each of 24 channels. These signals are then sampled, digitized and formatted into a serial digital data stream by a multiplexer. The sampling interval is 9.95 sec, corresponding to a cross track motion of the instantaneous field of view of 56 meters.

Due to the fiber optics physical separation and the detector time sampling, the spacing between fibers is set for different spectral bands to permit the radiometric levels to be compared without interpolating data. For a given selected spacing, this time interval between commutator samples in adjacent bands is made to coincide with the time interval between instantaneous fields of view. The commutator will then sample exactly the same point on the ground in each band.

During the retrace when the scan mirror makes the transit from east to west, a shutter wheel closes off the optical fiber view to the earth and a light source is projected onto the fibers through a variable neutral density filter on the shutter wheel. This process introduces a calibration wedge into the video data stream during this retrace interval. The calibration lamp makes it possible to obtain a check of the relative radiometric levels and also to equalize gain changes which may occur in the six detectors of a spectral band.

To produce "map like" images from data as obtained by the MSS, corrections must be made for the following factors:

- Non-linearity of mirror velocity
- Earth Rotation
- Attitude Rates
- Altitude Variation

These corrections (and others) are made in the NASA Data Processing Facility (NDPF) by merging spacecraft telemetry, ephemeris data, MSS calibration data, and the MSS video signal.

SYSTEM PERFORMANCE

The ERTS "product" which is employed by the majority of users is a photographic image. In addition to imagery, Computer Compatible Tapes (CCT's) are also available. The properties of images and CCT's which result from the serial action of the ERTS system (MSS, spacecraft, data acquisition, image generation, and photographic processing) are discussed below.

An attempt has been made through orbit adjustment (cross-track) and accurate timing (along-track) to hold the center of each image of the same ground region within as small an area as possible. Prelaunch predictions indicated a circle of 64 Km diameter could be achieved. Three orbit adjustments have been made to date. Figure 3 gives the cross-track drift which has been experienced since launch on July 23, 1972. Overall image framing in the March to October 1973 time period has held the center point within a 22 Km diameter circle two-thirds of the time.

The annotation of each ERTS image includes latitude and longitude tick marks. The position of these marks is computed from ephemeris data which gives the spacecraft position and spacecraft telemetry which gives the pointing direction. Prelaunch predictions estimated the annotation accuracy at about 800 meters. After some initial difficulties as reported at the last symposium, annotation accuracy was within 1000 meters during early 1973. After that time, the error became greater but is now becoming smaller again as shown in Figure 4. This variation may be a seasonal effect caused by the manner in which the spacecraft attitude measurement data are interpreted in computing spacecraft pointing direction.

Band to band spectral registration for the MSS has been measured as being better than 50 meters RMS. This is three times better than prelaunch predictions.

Temporal registration, i.e., from a scene taken at one time in a given band to a scene taken at another time in the same band, has also been significantly better than predicted. After fitting two images by translation and rotation, the RMS error is about 150 meters versus a prelaunch prediction of about 275 meters.

The usefulness of the ERTS images as a map depends not only on the quality of the images but also on the map projection to which they are being compared. It is not possible to make an indefinitely large mosaic of ERTS images because it is not possible to make a flat map of the curved surface of the earth while preserving the scale in two orthogonal directions. Within a given MSS image, the use of a single scale factor results in errors of less than 200 meters RMS in measuring the location of one feature relative to another.

The ability to see small features in an image is limited by the instantaneous field of view (IFOV) among other factors. As discussed above, the IFOV is 79 meters square. This numerical value is in fact the measured resolution for relatively good contrast linear targets such as piers in a harbor. For long, high-contrast targets, such as concrete bridges over water, structures as narrow as 40 meters can be observed. Investigators report routine observation of ponds 7 acres and larger in size. Such a pond would be about 180 meters in diameter.

Radiometric accuracy of the system depends on optical performance of the instrument, stability of the calibration lamp, lack of noise in the electrical transformations and transmissions, proper computer processing, and correct utilization of the radiometric transfer characteristics of the film recording medium. The radiometric stability of the MSS instrument and spacecraft system is evidenced by the fact that radiance measured over Death Valley on the same calendar date at a one year interval has varied less than two (2) percent. The radiance over this site during the year follows a cosine curve in phase with the sun angle as would be expected, Figure 5.

Many investigators have observed "banding" or "striping" in images. This is caused in part by the fact that a single image in a given spectral band is made by six individually calibrated detectors and also because the eye of the observer is more sensitive to changes in radiance than is the on-board calibration system. A change in the manner in which the calibration data is applied and

a correction of an error have reduced banding after December 1972. On recently produced CCT's, radiometric noise while viewing a uniform scene is less than 5% of measured radiance.

The utility of film for radiometric measurements depends in part on the accuracy of the gray-scale calibration steps. Data for 264 images processed in October 1973 are presented in Figure 6. Here, nominal transmission of the gray-scale steps is shown together with the variation allowed by the original specification. Actual performance is shown as one-sigma bars for the thirty-one samples measured. It is well within specification.

EARTH COVERAGE

A history of the coverage obtained by ERTS-1 from the receiving sites during each 18 day coverage cycle is given in Figure 7; 20 cycles are accomplished in one year. As can be seen, there was a dip in the scenes acquired during the tape recorder difficulties in March 1973, and a somewhat lower overall level thereafter. However, recent experience shows that while the sun angle is low in the Northern Hemisphere, 50 scenes per day are currently being collected at U.S. receiving sites via real-time transmissions and 85 scenes per day via tape recorder.

The secondary objectives of the ERTS-1 mission were: (1) the acquisition of complete United States' coverage, largely cloud free, with either the Multispectral Scanner or the Return Beam Vidicon camera systems, or both; (2) the acquisition of coverage over the major land masses of the earth with either the Multispectral Scanner or the Return Beam Vidicon camera system, or both; and (3) demonstration of the relay of data from remote ground based platforms via the ERTS-1 satellite.

All of the United States has been covered at least once with less than 30% cloud cover. Some areas have been covered more than twenty times. World-wide coverage with less than 30% cloud cover during the first year of operation is illustrated in Figure 8. Recently, as the requirements of investigators have been reduced, the spacecraft has been operated to begin filling in the blank areas. It should be noted that this "map" is a projection in which ERTS orbits are vertical and latitudes are measured in terms of ERTS frames. Therefore, the land masses are distorted.

Over one hundred data collection platforms have been in use for the past eight months. The original requirement was that at least one data transmission be collected from each platform every twelve hours. Actual performance has provided an average of eight transmissions in every twelve hour period.

COOPERATIVE DATA ACQUISITION

In addition to the data acquired by U.S. Receiving stations, ERTS data are acquired by Canada at Prince Albert and by Brazil at Cuiaba. Total statistics for scenes acquired through November 1973 are approximately as follows:

United States	76,140
Canada	12,403
Brazil	<u>4,527</u>
Total Scenes	93,070

These data are available to any purchaser who may wish to use them for the better utilization of the earth's resources.

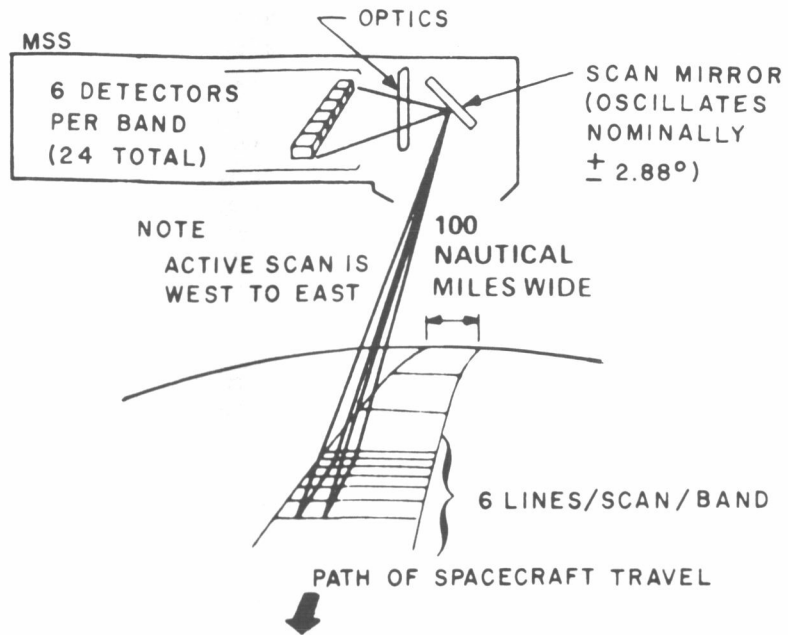


Figure 1.

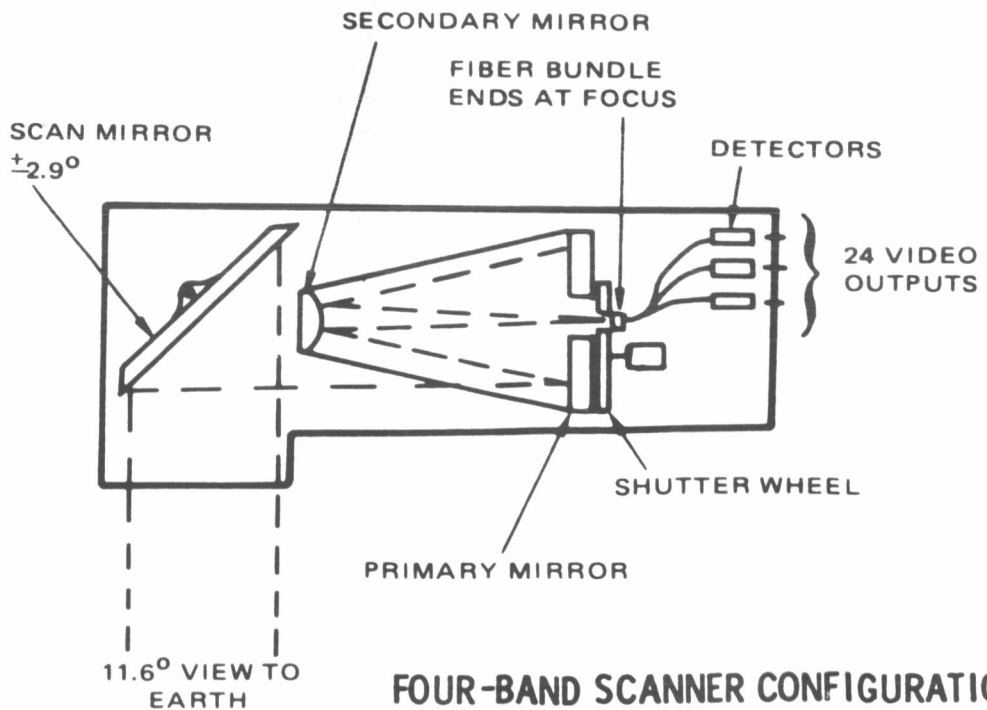
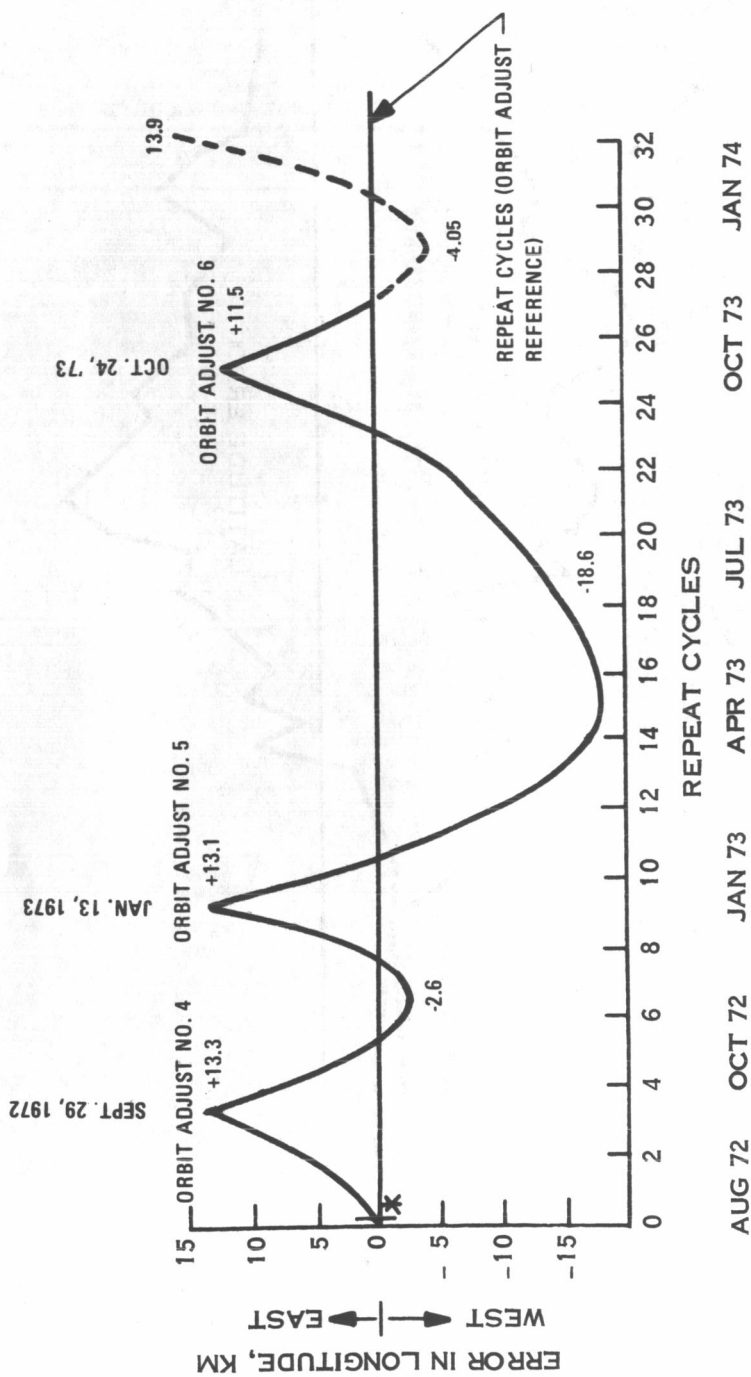


Figure 2.

CROSS TRACK DRIFT



*ORBIT ADJUST NO'S 1,2,3, TO
ACHIEVE NOMINAL PARAMETERS

Figure 3.

TICK MARK PLACEMENT ERROR

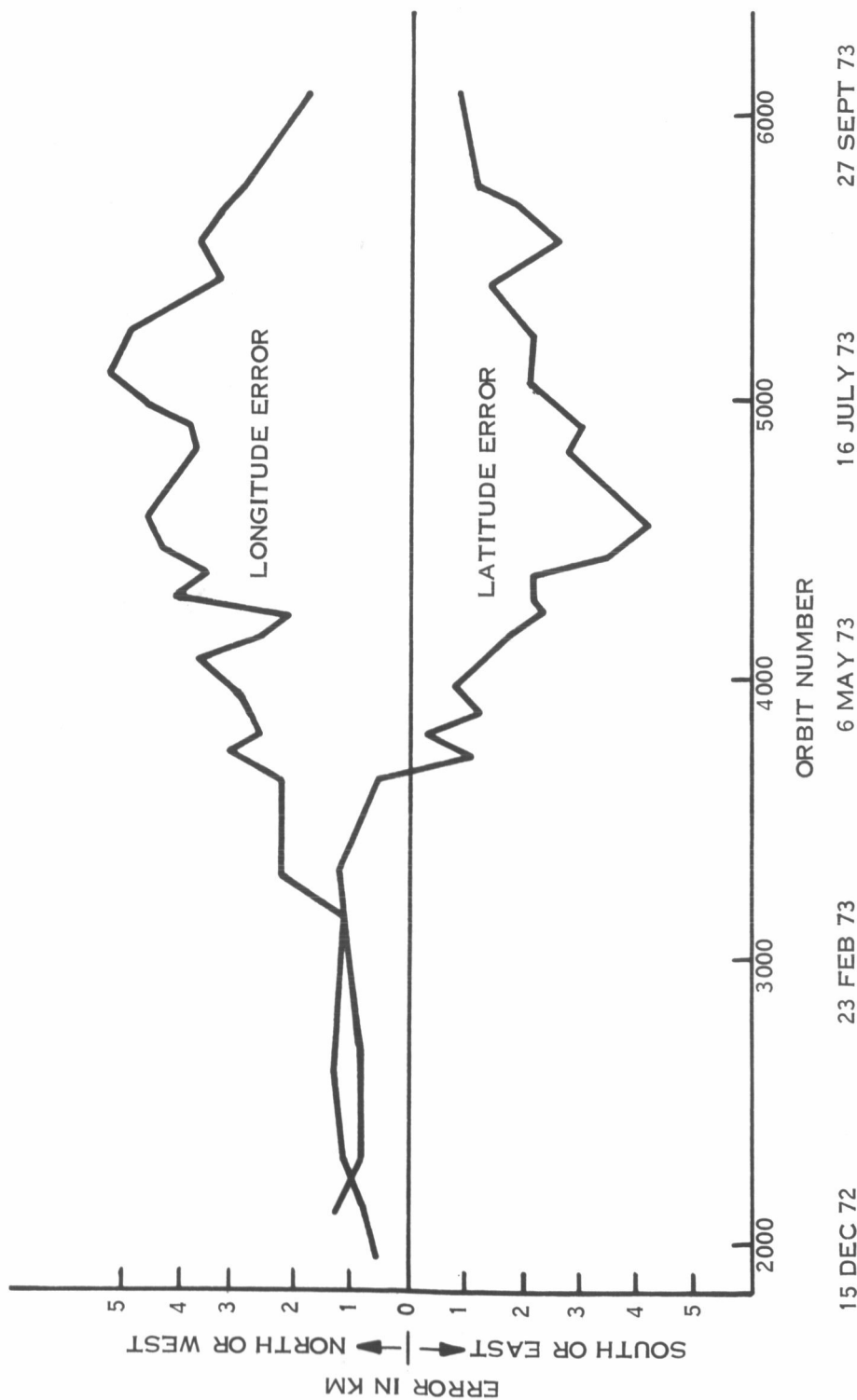


Figure 4.

AVERAGE RADIANCE MEASURED AT 11 DATES OVER 1 YEAR

RADIANCE EXTRAPOLATION

DATA		K COS Z		MSS BAND 7	
9/9/73	38%	9/9/73	36%	15 MEASUREMENTS PER IMAGE 9.5 IN. 3RD GENERATION POSITIVE DEATH VALLEY TEST SITE	
9/14/72	37%	9/14/72	35%		
Δ	1%	Δ	1%		

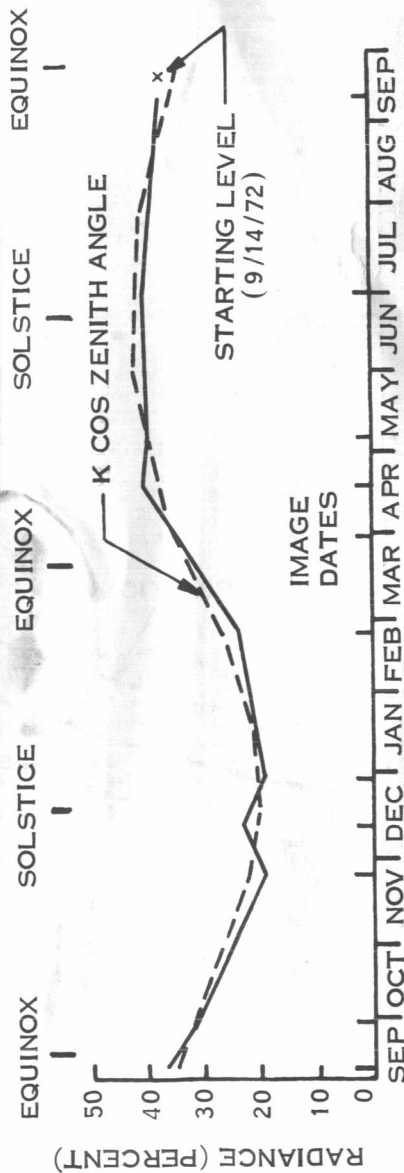


Figure 5.

3rd GENERATION 70 mm FILM DENSITY VS GRAY SCALE

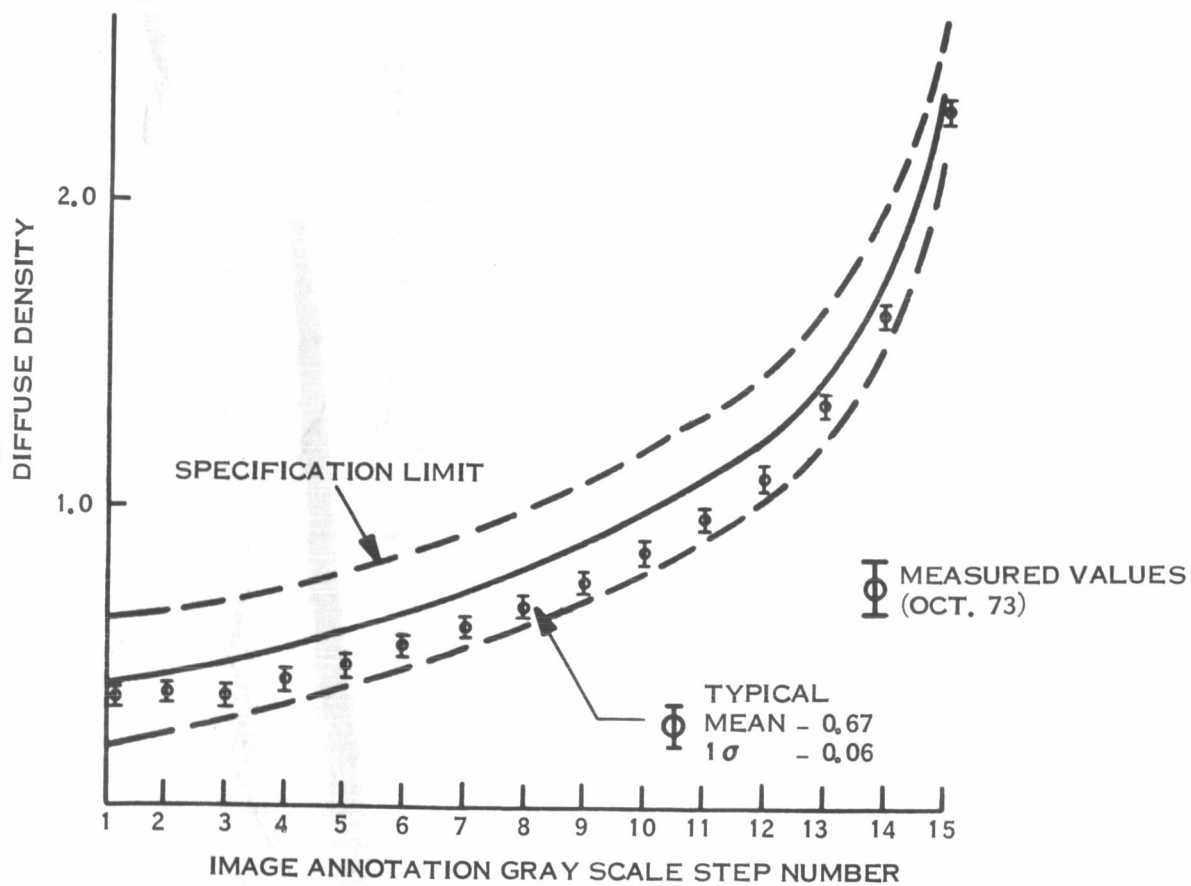


Figure 6.

ERTS SCENE ACQUISITION HISTORY BY CYCLE

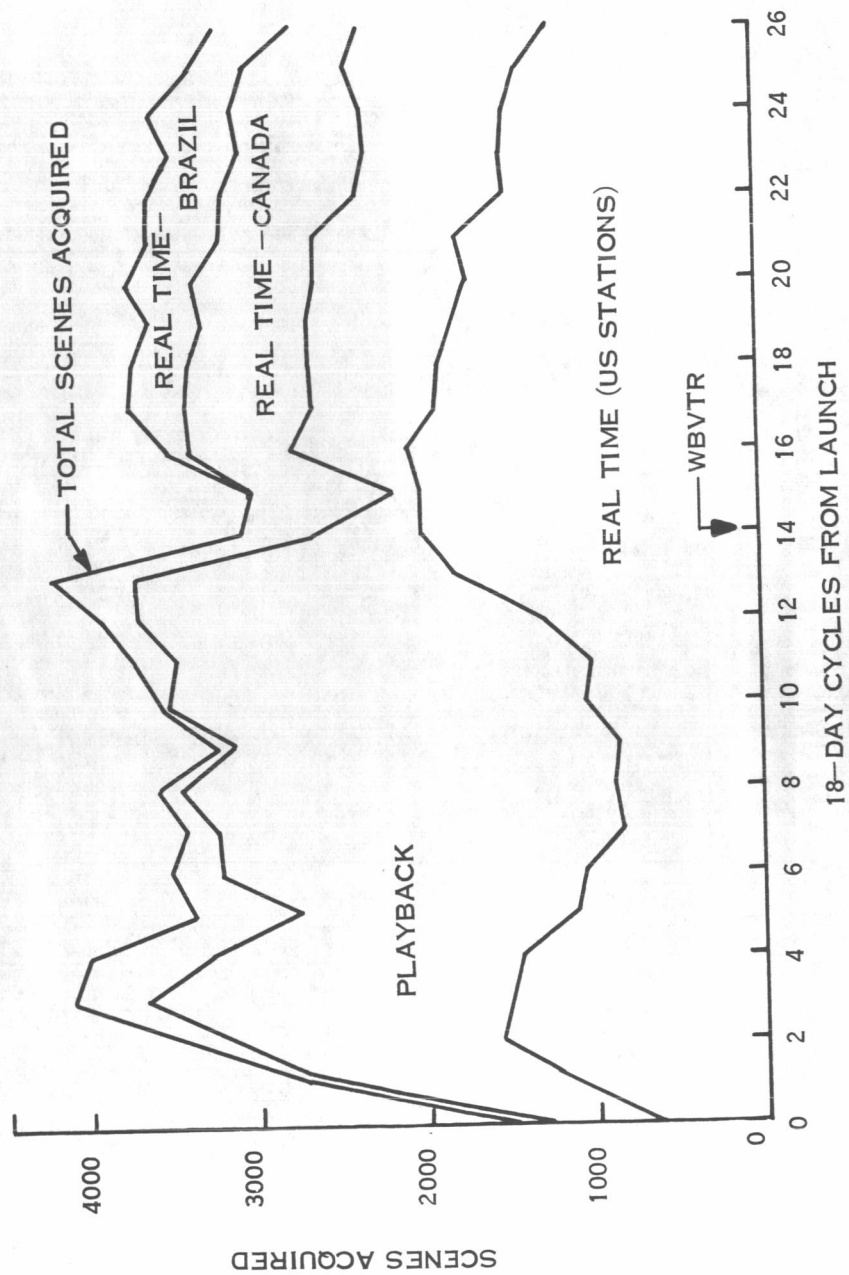


Figure 7.

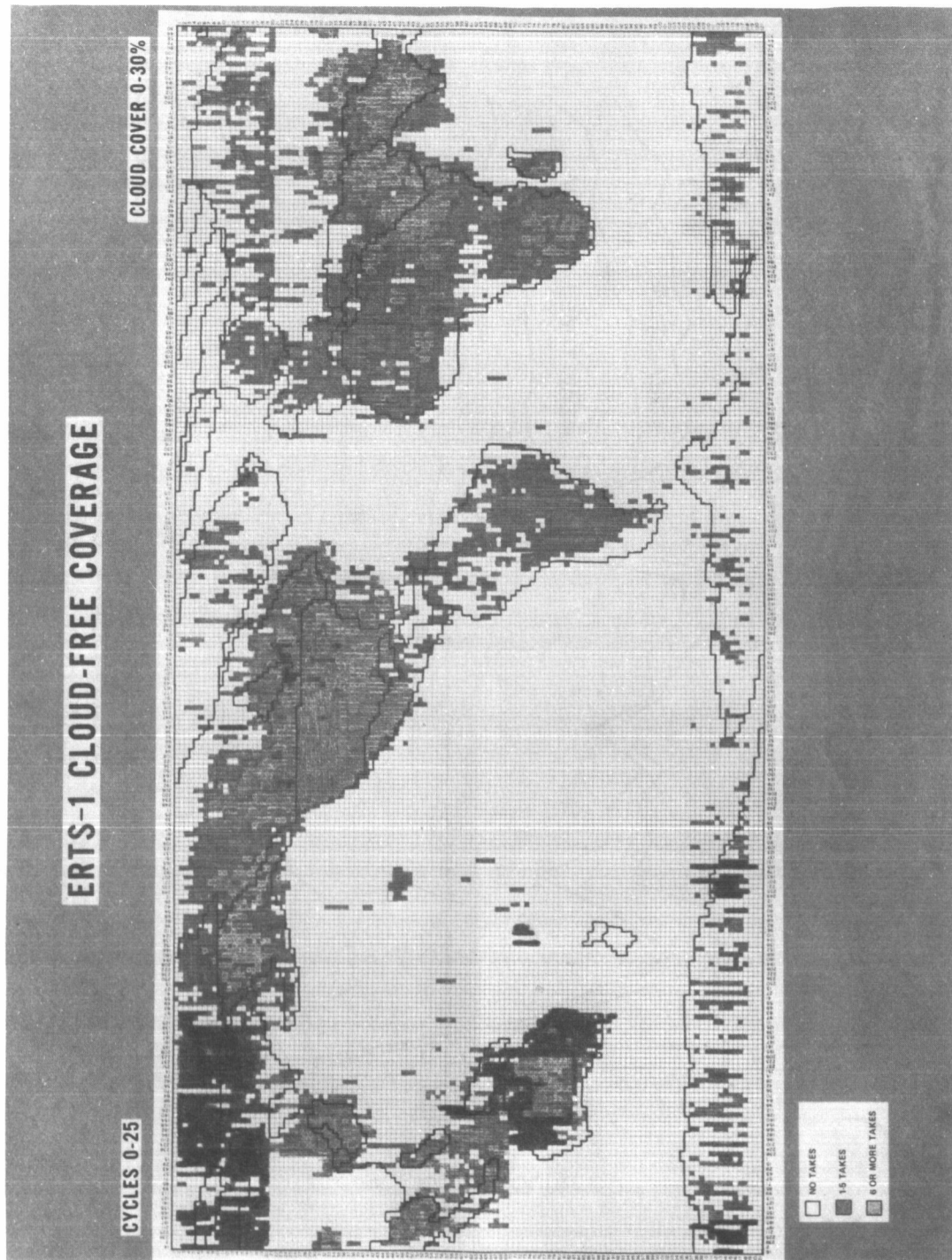


Figure 8.

CANADIAN ERTS PROGRAM PROGRESS REPORT

L. W. Morley and A. K. McQuillan, *Canada Centre for Remote Sensing, Department of Energy, Mines and Resources, Ottawa, Canada*

ABSTRACT

This paper reports on the progress of the Canadian ERTS program providing statistics on the production and role of ERTS images both from the CCRS in Ottawa and from the Prince Albert Saskatchewan satellite station. The types of products, difficulties of production and some of the main applications in Canada are discussed.

Under a 4-yr. collaborative agreement between the United States and Canada, the Canada Centre for Remote Sensing reads out and distributes the ERTS data of Canada.

The Canadian receiving station is at Prince Albert, Saskatchewan (Fig. I) shows the range circle of this station. The MSS data of Canada are recorded on high density magnetic tape and then immediately played back through the Quick Look Cathode Ray tube recorder where all the uncorrected images are photographed onto 70 mm. black and white film. 9 x 9 enlargements are made from this film and are sold at a dollar a print by Don Fisher and Associates, a private contractor who was awarded this franchise. He does the photographic processing at the station in Prince Albert and mails the copies directly to his customers from there within two days of the satellite pass.

Immediately after the Quick Look information is extracted, the tapes are air expressed to Ottawa where they are played through the ground data handling system onto electron beam recorders providing all 4 bands and false colour images for distribution by the National Air Photo Library. The National Air Photo Library, Reproduction Centre, located in the same building as the CCRS Ground Data Handling Centre, is fully equipped with automatic film processing equipment for black and white and colour reproduction in quantity.

Investigators in Canada are not centrally funded by the Canada Centre for Remote Sensing. They must seek their funding from the appropriate mission-oriented agency whether such agency is in the federal government, any of the provincial governments, the universities or private industry. CCRS does carry out research in the methodology of interpretation both of the analogue and digital analysis kind.

1 N 74 30707

Fig. II shows the organization of the CCRS and its committee structure. We communicate with users directly and also through the working groups which are organized both by geographic region and by discipline. The working groups meet independently about 3 times a year to initiate remote sensing projects and to make recommendations. The heads of the working groups meet once a year and make recommendations to the CCRS.

A large Canadian symposium on remote sensing is held once every two years. The next one will be held at the University of Guelph April 30 - May 2, 1974.

Ground Data Handling Centre Production

Since the ERTS-1 launch on July 23, 1972, about 25,000 scenes of Canada have been recorded. Of these, 10,428 scenes have been translated into images in all 4 bands and have been placed in inventory. 976 false colour scenes and 111 computer compatible tapes have been produced. The reason for the large backlog has been the unreliability of the electron beam recorders. These are going to be re-furbished and later replaced by a colour laser-beam image reproducer.

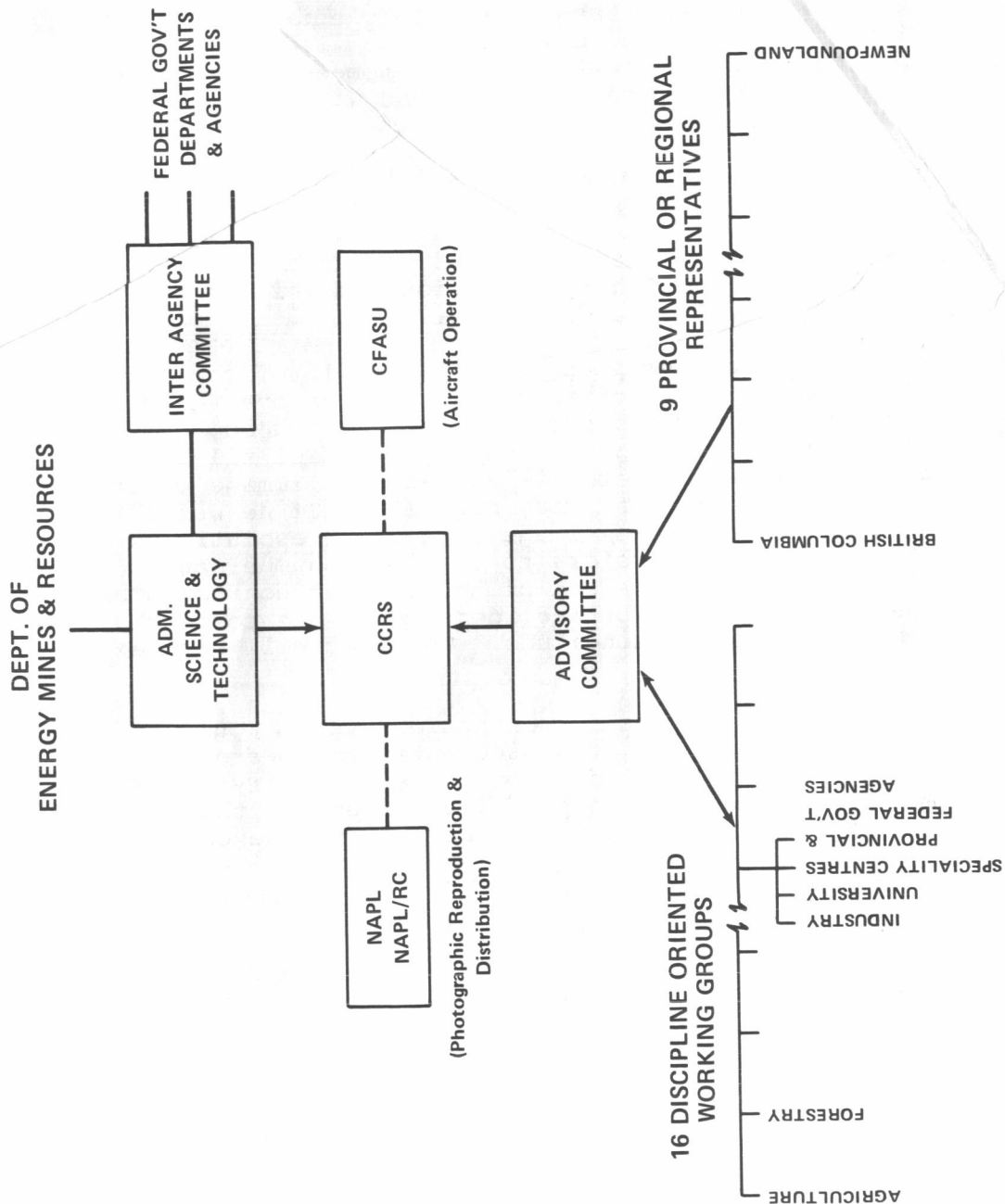
Total number of ERTS images produced by the National Air Photo Library	272,800
This was in response to 1159 orders for data.	

Total production of black and white Quick Look images by Donald Fisher & Associates at Prince Albert is about 9 x 9 black and white images.	50,000
---	--------

Map Corrected Imagery

The Ground Data Handling System in Ottawa was designed with the capability of producing map-corrected images. Because of the instability of the electron beams in the recorders, it has not been possible to produce accurately corrected images. This program will be resumed after delivery of the laser beam image reproducer in September 1974.

E. A. Fleming of the Surveys and Mapping Branch did a study of the planimetric accuracy of an ERTS image corrected for earth rotation only. She found that this image compared favourably in accuracy to the standard 1:1,000,000 topographical map published by the Surveys and Mapping Branch. The standard deviation was less than a millimeter on a number of points over the whole image. The practical result of this is that it is possible to mosaic ERTS images that have this correction made while uncorrected images produce unsatisfactory mosaics.



ELEMENTS OF "THE NATIONAL PROGRAM ON REMOTE SENSING"

Quick Look Images

The Quick Look images produced at Prince Albert utilize the full 2,400 lines of the MSS but they only have about half the resolution of the images produced by the electron beam recorders in the Ground Data Handling system at Ottawa.

The big advantage of the Quick Look is that there is no backlog, all orbits are processed immediately and the only limitation is the speed of the mail delivery. Facsimile service is available at Prince Albert with some considerable loss of resolution. It is used in a limited way by the ice reconnaissance people.

Plans for the future of Prince Albert call for upgrading of the resolution of the Quick Look system, the installation of automatic photo processing equipment, the setting up of a microfiche service on all ERTS imagery of Canada and earth rotation correction. New higher resolution facsimile equipment may be installed if there is a demand for it.

Donald Fisher and Associates plan: to produce microfiche cards containing Quick Look images of each day's orbits over Canada. Subscribers will get 365 cards per year and all images, clouds or not, will be shown in one band. The images will all be annotated with the orbit number (1 - 75) and the image centre number (1 - 31) as well as the date, Fig. III. If he wants to order either a 9 x 9 Quick Look image or a high resolution image from Ottawa he simply refers to the image number and date. This should eliminate a lot of the present confusion about trying to specify % cloud cover and identifying the corners of the area by latitude and longitude. The user will know exactly what he is getting.

It strikes me that such a data dissemination system would be useful in meeting the demands of sensed nations who are insisting on getting copies of data over their country and who want it before third parties see it. The system has the advantage of being quick, cheap and methodically indexed by date and area.

Ground Data Collection Platforms

To date 14 DCP units have been installed and tested at various locations across Canada. Fig. IV. Reliable data retrieval from all units was demonstrated. The Water Resources Branch of the Department of the Environment has 9 units measuring river velocity, water level, precipitation, ice thickness and ice movement. The Mackenzie River data is used by the river boat traffic and the Columbia river data to forecast runoff for dam control.

The Canada Centre for Inland Waters uses its platforms to monitor water quality in Lake Ontario. The Atmospheric Environment Service monitors precipitation, humidity, air and water temperature at

its installations. Applications for 6 new units will be made soon.

Data are recorded at CCRS on magnetic tape from the Goddard telephone line in parallel with a hard copy print out. Each morning the data are put into the PDP-10 computer at CCRS where it is sorted, converted into engineering units and stored on a user disc files. The user may then retrieve his data in hard copy through Telex from any location in Canada.

The data retransmission system through CCRS has been operating since January 1973 to the complete satisfaction of all users to date. Users are looking forward to expanding the number of units.

Some Demonstrated and Potential Economic Benefits

1. The Arctic

- (a) Seismic survey ships operating in the Arctic require information on ice conditions of the type provided by ERTS, that is a broad enough coverage to show the general ice conditions in the area but of high enough resolution to ensure the ships can run straight survey lines. This summer, because of ERTS imagery, one survey company operating in Norwegian Bay was able to survey an area it would not have otherwise. Quick-look ERTS imagery obtained 2 days after passage of the satellite showed the presence of open water beyond a large ice floe and was useful to the captain in navigating within the floe. The information which could not be obtained from helicopter support on board the ship because of the extent of the floe, permitted survey of an additional 75 miles which represented over \$100,000 additional revenue to the company. They also know in hindsight from ERTS imagery of at least 250 other miles representing close to \$400,000, they could have surveyed with the one ship stationed in the area had they been able to receive coverage in a more timely manner. They are therefore examining possibilities of relaying ERTS images directly to their ships from Prince Albert.

This company expects that ERTS will also be valuable to them in their winter seismic studies. They have been studying ice floes moving down and consolidating so they will have information on ice type and surface roughness. This will aid the company in deciding where to take contracts for winter surveys and what type of equipment to use.

- (b) Ice Forecasting Central of the Department of the Environment has recommended that April aircraft flights used to determine ice conditions in the Arctic be replaced by ERTS quick-look imagery. The flights utilize about 50

hours at a cost of about \$50,000 compared to a cost of ERTS imagery of \$1,500. The imagery will permit an initial analysis of ice conditions for the seasonal outlook and permit the May aircraft flights to concentrate on key areas so defined. Ice Forecasting Central recommends that ERTS imagery be obtained from April through September to give increased information about ice conditions and permit a better deployment of reconnaissance aircraft.

- (c) In 1972 a geophysical survey company spent 6 weeks in difficulty in ice-congested waters in and near Barrow Strait. Bellot Strait, an alternate route was open for 4 days and navigable for some time beyond that with ice breaker support. In this region ERTS has 5 - 6 consecutive days of overlap out of 18. The probability of obtaining a useful ERTS photo showing the ice free conditions of Bellot Strait (taking into account cloud cover) was then about 10%. Barrow Strait which was closed in would be covered by a different series of orbits so that the probability of obtaining information which would have helped the ship was at least twice that or 20%. The company believe they could have saved 1.5 million dollars with better information on ice conditions in the area. ERTS gave a 20% probability of providing this information.
2. ERTS imagery is being used in Saskatchewan in mapping forest fire burns. 42 burns across the northern part of the province are being mapped. Helicopters have been used in the past in the mapping of such burns. Using approximate values for helicopter time of one hour per burn for mapping and transit time the cost at \$253 per hour would be over \$10,000 for the helicopter. ERTS imagery costs less than \$100 and the manual time involved in using satellite imagery is less. The accuracy of the mapping is greatly improved using ERTS imagery.
3. A profitable application of ERTS imagery is in the mapping of large reservoirs in hydro power development projects. An accurate knowledge of reservoir storage is necessary to determine how much firm power can be generated. In one northern Canada project, the reservoir was flown with aircraft three times when the reservoir was filling up at a cost of the order of 1/4 million dollars. The reservoir could be covered by 2 ERTS images. During the course of one survey the water level changed 1 foot because of the time factor in covering the entire reservoir. Satellite data taken at one point in time would give a much less expensive and better volume estimate. This would result in a better estimate of firm power capability and would affect the contracts for power generation entered into by the company. In the project mentioned above there are now indications that the reservoir storage is several percent greater than expected. They believe this could be translated into about 1% extra power generation (worth 1 million dollars). They will try to use ERTS to assess the extra storage capacity. Although they have entered into

a long term contract, they could still make it known to the customer that they had the capability of generating this extra amount of power.

ERTS imagery is being considered in the mapping of Reindeer Lake in Saskatchewan which will be used as a storage reservoir for a power development on the Churchill River. Reindeer Lake has been surveyed by aircraft at a cost of \$46,000. A mosaic from which an area measurement could be made would cost \$35,000. The reservoir can be covered by 2 ERTS frames and several ERTS images taken at various lake water levels should give a better extrapolation to the final reservoir storage when the new dam is built. E. A. Fleming, of the Department of Energy, Mines and Resources, investigating ERTS for topographic mapping purposes, has concluded from a study of the reservoir formed by Kettle Rapids Dam in Manitoba that the reservoir outline from ERTS for 1:250,000 mapping would be more accurate than could be obtained from 85 pictures at 2,000 foot/inch.

4. High Benefit Applications of ERTS imagery are in land use mapping and in the selection of routes for pipelines, transmission lines and highways. ERTS imagery is being used together with larger scale imagery in studies to select a route for the Polar Gas pipeline. Preliminary estimates of updating of present land use mapping in Western Canada indicate cost savings of about 4 to 1 for high altitude photography over conventional aerial survey photography and approximately 20 to 1 if satellite imagery is used. The satellite imagery would have to be used in digital form to give the required resolution.

Conclusions:

The greatest difficulty we experience is with potential users who are reluctant to change their way of doing things because they don't realize the obvious advantages to using the satellite data. It will take time.

References:

Remote Sensing in Canada - Newsletters Nos. 1 - 5
The Canadian Advisory Committee on Remote Sensing 1972 Report
Resource Satellites and Remote Airborne Sensing for Canada:
Proceedings of the First Canadian Symposium on Remote
Sensing, February, 1972.

The above reports are all available through the Canada Centre for Remote Sensing, Department of Energy, Mines and Resources, Ottawa, Canada KIA OE\$, Tel. (613) 993-3350.

AGRICULTURE/FORESTRY/RANGE RESOURCES

ESTIMATE OF WINTER WHEAT YIELD FROM ERTS-1

Stanley A. Morain and Donald L. Williams, *Department of Geography and Space Technology Center, University of Kansas, Lawrence*

ABSTRACT

A model for estimating wheat yield per acre has been applied to acreage estimates derived from ERTS-1 imagery to project the 1973 wheat yields for a ten county area in southwest Kansas. The results (41.04 million bushels) are within 3 per cent of the preharvest estimates for the same area prepared by the USDA Statistical Reporting Service (39.91 million bushels). The projection from ERTS data is based on a visual enumeration of all detectable wheat fields in the study area and was completed while the harvest was in progress. Visual identification of winter wheat is readily achieved by using a temporal sequence of images (band 5 for Sept.-Oct.; band 5 for Dec.-Jan.; and band 5 & 7 for March-April). Identification can be improved by stratifying the project area into subregions having more or less homogeneous agricultural practices and crop mixes. By doing this, small changes in the spectral appearance of wheat related to soil type, irrigation, etc. can be accounted for. The interpretation rules developed by visual analysis can be automated for rapid computer surveys.

INTRODUCTION

Recent events in international politics have had great impact on the economy of U. S. agriculture. The "new" agricultural economics has focused attention on the need for rapid and timely estimates of crop acreage, yield, and general crop condition. Increasing world demand for U. S. agricultural products, coupled with increasing domestic demand, requires the development of means for assessing the status of major crops over large geographic areas at several points in the growing season. Even though present crop reporting methods are reliable for U. S. agriculture, a major shortcoming for efficient planning is the time lag between collection and dissemination of statistics. Techniques that can reduce the time lag in normal crop reporting procedures will undoubtedly have an impact on American agriculture. Similarly, any technique that will improve timeliness and accuracy of information on foreign agricultural production will benefit American agricultural policy makers. In this paper we describe our methods and results for estimating the winter wheat acreage and yield for a ten county area in southwest Kansas.

1 N 74 30708

METHODOLOGY

Acreage, and yield per acre, represent the two measures required for a "crude" crop projection for any geographic area. We describe this as a crude projection because it does not consider differences in crop variety, protein content, crop lost during harvesting or other refinements on the amount of grain actually delivered to storage bins. Nevertheless, by using ERTS as the data base, projections can be announced several months in advance of current, equally crude, projections announced by the crop reporting service.

Wheat Acreage Estimates

A report on our technique for estimating winter wheat acreage in southwest Kansas was published in the Goddard Symposium on Significant Results using ERTS Imagery (Williams, et. al., 1973). In this document, a procedure for visually detecting and enumerating wheat fields on ERTS imagery is described.

Basically the technique requires the interpreter to:

- 1) delineate county boundaries on the imagery;
- 2) recognize and delineate agricultural subregions within each county on the basis of differences observed in the imagery (the boundaries of many of these subregions will cut across county boundaries;
- 3) compare the results of step 2 with soil and landform maps (for those counties where they exist) in order to better estimate the importance of the crop in each land-use region;
- 4) learn to distinguish the image tones of wheat in fields 80 acres (approx. 32 ha) or larger from those of other important crops in the subregion and convert these into interpretation rules applicable to that subregion, and;
- 5) visually locate and estimate the acreage of wheat fields in each subregion using the interpretation rules developed in step 4. From the subregion totals a composite acreage is obtained for the entire project area.

Accuracy and Advantages of ERTS Visual Analysis--By using the above procedure we have found through comparisons with ground truth and aircraft underflight data that 99 per cent of all the wheat fields and 99 per cent of the total acreage can be accurately estimated. Although the interpretation rules are created from grey tones of fields larger than 80 acres, the rules can be applied to all field sizes as small as 10 acres providing there is high tone contrast with their surroundings. An obvious advantage in the Winter Wheat Belt is that, once identified as wheat, the acreage of each field can be accurately estimated because field sizes, by the township and range system of survey, are characteristically 10, 40, 80, 120, 160 or 320 acres (4, 16, 32, 48, 64 or 128 ha respectively).

There are at least three other advantages of visual interpretation from ERTS. First, with experienced interpreters who are familiar with the cultivation of winter wheat, the time involved for a complete enumeration of each county is on the order of one hour per 250 square kilometers. While this is considerably longer than would be

required using a computer (assuming it could be trained to identify wheat) it is also much cheaper. Secondly, by visual analysis, we obtain a nearly complete enumeration of the crop and learn how its spectral properties vary geographically and temporally. Thirdly, because we identify and locate each field early in the crop cycle, the need for ground truth and aircraft data diminishes through time and allows us to concentrate those activities in areas where spectral anomalies (disease, stress) begin to appear.

The Need for Sequential ERTS Data--Estimates of winter wheat acreage would not be possible without sequential ERTS data. The crop calendar for wheat is unique among those crops commonly grown in the Great Plains. It is planted in September or October depending upon weather conditions. By late November it is the only green crop in the agricultural scene and can be readily detected and enumerated on MSS band 5 (the chlorophyll absorption band). It is significant that these circumstances coincide with the most cloud-free season of the year over this region. With a high probability for at least one cloud and snow-free image, a complete enumeration of wheat planted is virtually a fait accompli. In addition, by virtue of slight tonal variations at this time of year, we feel that it will be possible, given more detailed observation, to categorize differences in planting time and general wheat condition.

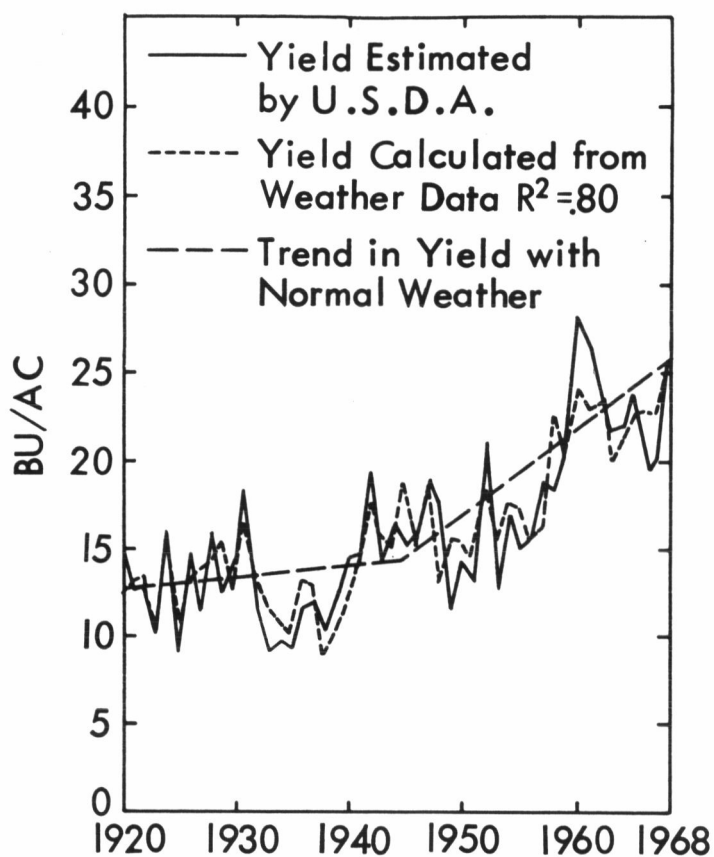
A second look at wheat is required during March or April in southwest Kansas. We used imagery from this time period to adjust the initial acreage estimate and to assess general wheat condition. This was necessary because a popular practice in western Kansas is to plant wheat as a winter forage and soil protection measure with no intention of later harvesting the crop. In spring the field is turned under to provide green manure and replanted to another crop. Such acreage must be subtracted from the initial estimate. A combination of the red and infrared bands is desired for these early spring observations.

A final ERTS observation is recommended during the harvest season. This is perhaps not as important at present as it could be in the future, after we learn to interpret and adjust estimates for crop loss due to disease, hail damage, etc. Individual fields can be turned under as late as June and still produce a cash crop. An estimate of wheat acreage actually harvested therefore is desirable. It is, of course, true that other crops, in addition to wheat, can be surveyed using the same set of above images. Alfalfa, for example, can be visually distinguished from wheat in May and early June on band 7. At this time of year alfalfa is growing vigorously (bright on band 7) while wheat is drying for harvest (medium tone on bands 5 and 7).

Yield Per Acre Estimate

The model we have used for estimating average yield per acre was proposed by Thompson (1969). It is based on departure from average weather conditions. According to his results, highest yields in Kansas are associated with above normal precipitation from August through March (normally a total of 325 mm.). Each additional 25 mm. at this time of year results in a gain of approximately 0.63 bushels per acre. High yields are also associated with above normal rainfall in April, normal rainfall in May and below normal rainfall in June. As a rule these months receive 88, 120 and 103 mm. of moisture respectively. Finally, for optimal yields in Kansas, below normal temperatures during April, May and June are best. With these data, it is possible to calculate an expected yield per acre. A comparison of actual and calculated yields is given in Figure 1.

ACTUAL AND CALCULATED YIELDS AND TREND OF WHEAT YIELD IN KANSAS (FROM THOMPSON, 1969)



Weather data suitable for use in the model are published by the U. S. Weather Bureau in its monthly climatological survey of each state. These data are published for each station and the stations are grouped into districts. The southwestern Kansas district includes the ten counties surveyed in this report and mean weather conditions in that district were used in solving the equation developed by Thompson.

Semi-Automatic Interpretation

The interpretation rules developed for visual interpretation can be specified in a computer compatible form for rapid wheat acreage surveys. At present the technique is termed semi-automatic because both the pre- and post-processing time involve human activities. In broad outline the procedure requires the interpreter to:

- 1) specify the coordinates of subareas on the image which match county boundaries or other geographic localities. Care must be taken to specify the location of towns or other non-cropland sites in order to exclude these from later tabulations.
- 2) create a frequency histogram for the 128 "tones" on the data tape for each area specified in step 1.
- 3) divide the histogram into 15 levels (roughly equivalent to the 15 gray level steps found on each MSS image).
- 4) determine the total number of resolution cells contained within those gray levels that have been determined by visual analysis to closely correspond to wheat. Since each resolution cell is approximately equal in size to one acre (.4 ha), the number of cells is considered to be roughly equal to the wheat acreage.

An estimate from this procedure for an 840 sq. mile (2,184 sq. km) area in Finney and Gray Counties totaled 165,000 acres. The same area, by visual tabulation, contained 162,000 acres. Although the time required for the semi-automatic approach was about half (10 hrs. vs. 5 hrs.), the cost was almost four times (\$120 vs. \$30). At present we do not consider these differences to be meaningful because of the research environment under which they all were derived. Our two strongest views at this stage of development are that:

- 1) we see no way of ever eliminating the pre-processing human time required for crop surveys, simply because there are too many decisions and "bookkeeping" operations involved in a reliable inventory, and;
- 2) we may require a visual analysis in any case so that we can locate and monitor individual fields.

RESULTS

Table 1 gives our estimate of wheat acreage for the ten county survey area (approximately 8,071 sq. miles or 21,000 km) and compares it with estimates prepared by the Statistical Reporting Service (SRS) of USDA. The ERTS estimate was prepared in March whereas the data available from SRS represent their May and August estimates of "harvestable" acreage. Final figures from SRS will not be available until February 1974, but, assuming that their August estimate is more accurate than their May estimate, the final tally should not differ significantly from the original ERTS total. The March ERTS estimate is within 0.5 per cent of the SRS August estimate.

Table 1
Comparative Estimates of 1973 Wheat Acreage (and yield in bu/ac)
for Ten Counties in SW Kansas
as Compiled by USDA, SRS and by Analysis of ERTS Imagery

County	SRS Acreage Est.		Ave. Yield	ERTS Acreage Est.	
	May 1973	Aug. 1973		March 1973	
Finney	205,000	198,000	(37)	239,000	
Grant	81,000	87,000	(34)	74,000	
Gray	157,000	162,000	(36)	174,000	
Haskell	104,000	109,000	(43)	110,000	
Kearney	117,000	119,000	(31)	115,000	
Meade	141,000	132,000	(36)	151,000	
Morton	91,000	97,000	(24)	72,000	
Seward	83,000	80,000	(36)	78,000	
Stanton	135,000	132,000	(24)	108,000	
Stevens	85,000	87,000	(31)	86,000	
	1,199,000	1,202,000	(33.2 ave.)	1,207,000	(34)

Also shown in Table 1, in parentheses, are the SRS projected average yields per acre, for August, for each of the ten counties. Our estimate for the entire area, as calculated by the Thompson model, is given in parentheses in the row of totals. These values have been combined into a matrix as shown in Table 2. The upper left cell represents the total crude yield that would be obtained using the traditional, time-tested techniques and an average of 33.2 bushels/ac. The lower right cell gives the expected wheat yield using ERTS imagery and the methodology reported in this paper. The ERTS estimate of total wheat bushels is 2.8 per cent higher than the SRS estimate. It predates the SRS estimate by about two months.

Table 2
Matrix of Total Estimated Yield
Comparing SRS and ERTS Data

		Average Yield/Acre	
		SRS (33.2 bu/ac) as of 8/73	ERTS (34 bu/ac) as of 6/73
Harvestable Acreage	SRS (1.202×10^6) as of 8/73	$39.906 \times 10^6 \text{ bu}$	$40.848 \times 10^6 \text{ bu}$
	ERTS (1.207×10^6) as of 3/73	$41.193 \times 10^6 \text{ bu}$	$41.038 \times 10^6 \text{ bu}$

DISCUSSION OF THE RESULTS

The above results include several points that need amplification. One could argue, first, that if the ERTS acreage estimate is based on a total enumeration of fields instead of a sample, as normally employed by SRS, and that, further, if SRS has a more sophisticated technique for calculating average yield per acre than that proposed by Thompson, the combination of these two values might give an even better estimated yield. This value is presented in the lower left cell of Table 2 and is approximately 3.1 per cent higher than the SRS tally. Final figures, when presented, may support this argument.

A second argument concerns the complex economics of irrigated wheat and wheat planted as winter forage. Irrigation by center pivot methods is increasing rapidly on the lighter textured soils of the southwest (Williams and Barker, 1972). In past years many irrigated fields have been planted to wheat as a winter cover crop and replanted in spring to feed grains. However, the recent high price of wheat, combined with the prospect for continued international wheat trading and low domestic reserves has stimulated growers to harvest wheat that would otherwise have been turned under. Yields on irrigated wheat fields in 1973 are estimated on the basis of past performance at 53 bushels/acre. We estimate from ERTS imagery that in 1973 174,000 acres of harvestable wheat were irrigated in the project area. Using these inputs we can revise the original yield estimate, as shown in Table 3, to a total of 44.344 million bushels, or 17 per cent higher than the August SRS estimate. Again, only the final figures, when released by SRS, will reveal whether this refinement is reasonable. No distinction is made between irrigated and dryland wheat in the SRS estimate presented but such distinction is made in the final February data. We believe that our ERTS derived estimate for harvestable irrigated wheat in 1973 is reasonable since SRS reported 202,000 acres of planted irrigated wheat in 1972 (personal communication).

Table 3
Revised Yield Estimate
from ERTS to Include Irrigated Acreage

Type	Acres ($\times 10^3$)	Ave. Yield (Bu/Ac)	Total Yield ($\times 10^6$ Bu)
Irrigated	174	53	9.222
Dryland	1033	34	35.122
Totals	1207	-	44.344

REFERENCES

ERTS-1 Imagery:

<u>DATE</u>	<u>FRAME NUMBER</u>	<u>QUALITY</u>
8-16-72	1024-16511-5	Excellent
9-21-72	1060-16505-5	Good, partial cloud cover
9-21-72	1060-16512-5	Good, partial cloud cover
9-22-72	1061-16564-5	Good
9-22-72	1061-16570-5	Good
12-21-72	1151-16575-5	Good, partial snow cover
3-20-73	1240-16523-5	Good, partial snow cover
5-31-73	1312-16520-5	Excellent
7-24-73	1366-16512-5	Excellent

Thompson, Louis M. (1969), "Weather and Technology in the Production of Wheat in the United States," Journ. of Soil and Water Conservation 24:6 (Nov.-Dec.), pp. 219-224.

Williams, D. L. and Barker, B. (1972), "Center Pivot Irrigation in Finney County, Kansas: An ERTS-1 Interpretation Procedure." Lawrence, Ks: Center for Research, Inc. NASA-CR-131208, 14 p.

Williams, D. L., Morain, S. A., Barker, B. and Coiner, J. C. (1973), "Identification of Winter Wheat from ERTS-1 Imagery," in Symposium on Significant Results Obtained From the Earth Resources Technology Satellite-1, Vol. 1, edited by S. C. Freden, E. P. Mercanti, and M. A. Becker. Washington D. C: National Aeronautics and Space Administration, pp. 11-18.

USER ORIENTED ERTS-1 IMAGES

Seymour Shlien and David Goodenough, (*Canada Centre for Remote Sensing*), Ottawa, Canada

ABSTRACT

Photographic reproductions of ERTS-1 images are capable of displaying only a portion of the total information available from the Multispectral Scanner. For these reasons, methods are being developed by the Applications Division of the Canada Centre for Remote Sensing, to generate ERTS-1 images oriented towards special users such as agriculturists, foresters, and hydrologists by applying image enhancement techniques and interactive statistical classification schemes.

Spatial boundaries and linear features can be emphasized and delineated using simple filters. Linear and nonlinear transformations can be applied to the spectral data to emphasize certain ground information.

An automatic classification scheme was developed to identify particular ground cover classes such as fallow, grain, rape seed or various vegetation covers. The scheme applies the maximum likelihood decision rule to the spectral information and classifies the ERTS-1 image on a pixel by pixel basis. The user must first furnish the classifier a set of training areas for the classes of interest so that the statistical information can be extracted. The classifier then gives the user an estimate of how well it can distinguish the classes on the basis of these data and attempts to classify a designated area. Preliminary results indicate that the classifier has limited success in distinguishing crops, but is well adapted for identifying different types of vegetation.

Illustrative examples are presented for areas in the ERTS-1 frame, 1007 - 16531, which covers the area around Winnipeg, Manitoba.

1 N74 30709

INTRODUCTION

Owing to the fact that photographs are only able to display a fraction of the total information available from ERTS imagery, digital methods that directly process the original data were investigated. The goal of this study was to develop techniques that automatically interpret the images or enhance different characteristics of the images. The investigation was carried out with the use of a Bendix "Multispectral Analyzer Display" which was interfaced to a time-sharing DEC PDP-10 computer system. All the methods described were applied to the ERTS-1 frame 1007 - 16531 which was imaged on July 30, 1972 and covered the area centered on Winnipeg, Manitoba (Figure 1).

The three methods described are presently at different stages of development. Most of the emphasis in this report will be given to supervised digital classification which was studied extensively. The two other image processing techniques applied by us are summarized briefly.

BOUNDARY ENHANCEMENT AND DETECTION

Linear features such as boundaries between agricultural fields, topographical features, and roads are important in the production of maps. If the spatial boundaries of different ground cover classes were known in advance then the data pixels enclosed by the boundaries could be classified more rapidly and accurately. A simple scheme involving minimum computation to enhance these features is a form of differentiation. The image is displaced one or two pixel units and a new image is determined from the absolute difference of the original and displaced image. High spatial frequency content such as texture and boundaries is amplified at the expense of the DC components. Thresholding techniques and logical manipulations as described by Holdemann and Kazmierczak (1971) are necessary to extract and follow the linear features. The method was very successful for very sharp boundaries such as water land interfaces seen in band 7 but only moderately successful for agricultural fields.

CANONICAL TRANSFORMATION OF SPECTRAL INTENSITIES

The chromaticity transformation conceived by Taylor (1973) and described in a separate paper at this conference was applied to agricultural and forested areas of the ERTS frame. The technique works basically as follows. By use of a canonical transformation (Kendall and Stuart, 1968) the spectral intensities are transformed to a set of uncorrelated variables, thus eliminating the redundant information. The new variables are then transformed to a set of chromaticity coordinates. In this

presentation the intensity of the red and green guns of the "Multispectral Analyzer Display" were controlled by the eigenvector with highest eigenvalues, the ratio of red to green was controlled by the second highest eigenvector, and the blue gun was controlled by the third eigenvector. This transformation of eigenvectors to colour is far from optimum, but is one of several easy transformations tried.

Very impressive colour images were generated in this way. Small shades in intensities show up dramatically as different hues.

To get the optimum transformation, the statistical characteristics of the portion of the original image should be used.

AUTOMATED CLASSIFICATION OF GROUND COVER TYPES

Rapid and timely evaluation of Canada's agriculture, forest, and water resources has important economic benefits. For this reason a study to determine the feasibility of automatic classification using the maximum likelihood decision rule was made. The emphasis in this study was the determination of classes which are easily separable using ERTS data and the estimation of the misclassification error.

The maximum likelihood decision rule basically partitions the observation space, consisting here of the four spectral bands, into 4-dimensional regions associated with these classes. The underlying assumption to this statistical classification scheme is that the probability distributions associated with each of the ground cover classes are known exactly. Provided that this is true then it has been shown (Van Trees, 1968) that the scheme is optimum in sense of minimum misclassification error. Though this assumption is not strictly true for ERTS imagery, the maximum likelihood decision rule was still favoured since it is one of the most established statistical schemes and includes the minimum distance rule (Sebestyen, 1960) in special cases.

The maximum likelihood decision rule was applied as follows. Given the spectral intensities of a particular pixel the likelihoods of observing these intensities are computed for each of the possible classes in consideration. The class with the maximum likelihood is chosen. If the maximum likelihood is below a certain threshold then no decision is made. To reduce the problems inherent in the determination of the likelihoods it was assumed that the four MSS bands can be adequately approximated by a multivariate normal distribution. Crane, Malila and Richardson (1972) found that there is not serious loss in accuracy due to this assumption. Letting

$\bar{m}_i^T = (m_4, m_5, m_6, m_7)$ and C_i be the mean vector and covariance matrix

associated with class i , then the logarithm of the likelihood of observing sample $\bar{x} = (x_4, x_5, x_6, x_7)$ is given by equation (1).

$$l(x|i) = -2 \ln (2\pi |C_i|) - (\bar{x} - \bar{m}_i)^T C_i^{-1} (\bar{x} - \bar{m}_i) \quad (1)$$

Where $| \cdot |$ denotes determinant, the superscript "T" denotes transpose and C_i^{-1} denotes the inverse matrix of C_i .

Two contrasting areas were studied in the determinations of the performance of the classification scheme. The first area located 40 miles SE of Winnipeg contained various types of vegetation. The second area in the Red River Basin was entirely agricultural. Ground truth was obtained from Thie (1973) and Woo (1973) for the two respective areas. Using this ground truth we determined the statistical parameters of a set of classes. They are listed in Tables 1 and 2.

Several independent methods were used to estimate the class separability and the misclassification error. In the first method the divergence measure (Kullback, 1959) was calculated for each pair of classes i and j using equation (2):

$$J(i,j) = \frac{1}{2} \text{tr} (C_i - C_j) (C_j^{-1} - C_i^{-1}) \\ + \frac{1}{2} \text{tr} (C_i^{-1} + C_j^{-1}) (\bar{m}_i - \bar{m}_j) (\bar{m}_i - \bar{m}_j)^T$$

Where $C_i, C_j, \bar{m}_i, \bar{m}_j$ are the covariance matrices and mean vectors of the two classes i and j and "tr" denotes the sum of the diagonal elements of the following matrix the divergence measure is always positive, and is zero only when the two classes have identical distributions (Kullback, 1959; Wacker and Landgrebe, 1971; Fu and Min, 1968). There is no exact relation between the divergence and the misclassification error. However, some lower and upper bounds have been established by Maill and Green (1963) and Kadota and Shepp (1967). For 95% classifications accuracy the divergence measure should be above 50. The divergence matrices are listed in Tables 3A and 4A.

In the second method, the original "training" data were run through the classifier and the maximum likelihood classifications obtained was compared with the true classification. The results of this analysis are listed in the confusion matrices in Tables 3B and 4B. In the third approach synthetic data having the class means and covariances were generated by Monte Carlo methods and run through the classifier. The results of this last approach are listed in Tables 3C and 4C.

The three different approaches give similar results. Except for Jack Pines, Black Spruce and Tamarack the different vegetation types were distinguishable with less than 3 per cent error. Black Spruce and Tamarack were most difficult to distinguish. A projection of the decision ellipses in observation space is given in Figure 2.

The agricultural aclasses were considerably more difficult to discriminate. Fallow and rape seed were the only classes that could be discriminated with certainty. The statistical distributions of the grain stubble, grain fields, corn, and sunflower had much overlap resulting in a high misclassification. Wheat was correctly identified more than 95% of the time but this result is probably optimistic since the ground truth was obtained from only two fields.

CONCLUSIONS

The main conclusions of this study are listed below.

1. The visual appeal of colour ERTS-1 images can be remarkably improved by transforming the spectral data from the 4 bands to a set of uncorrelated coordinates and displaying the transformed data in chromaticity coordinates to which the eye is most sensitive. Small changes in intensities stand up better in the new colour images.
2. The maximum likelihood decision rule can discriminate the vegetation classes Jack Pines, Black Spruce, Sedges, Trembling Aspen, Community Pasture, and Tamarack with more than 85 per cent accuracy. Errors were largely due to confusing Jack Pines, Black Spruce and Tamarack. The classifications of the different agricultural crops was found to be more difficult. The only agricultural classes that could be identified with certainty were fallow, rape seed, and possibly wheat.

ACKNOWLEDGEMENTS

We would like to thank Dr. M. Taylor of the Defence and Civil Institute of Environmental Medicine for his very valuable discussions.

Dr. J. Thie and Dr. F. Peet of the C.C.R.S. have provided us with considerable assistance in obtaining the data used in this study.

Also, thanks go to Dr. S. Vishnubhatla and Dr. I. Crain of the C.C.R.S. for providing us with computer routines to do matrix manipulations.

REFERENCES

- Crane, R.B., W.A. Malila, and W. Richardson (1972). Suitability of the normal density assumption for processing multispectral scanner data. IEEE Trans. Geoscience Electronics GE-10 158-165.
- Fu, K.S., and P.J. Min (1968). On Feature Selection in Multiclass Pattern Recognition. Tr. EE68-17. Purdue University.
- Holderman, F., and H. Kazmierczak (1972). Preprocessing, of gray-scale pictures. Computer Graphics and Image Processing 1 66-80.
- Kendall, M.G., and A. Stuart (1968). The Advanced Theory of Statistics Vol. 3 Charles Griffin & Company (London).
- Kullback, S. (1959). Information Theory and Statistics. Dover Publications.
- Marill, T., and D.M. Green (1963). On the Effectiveness of Receptors in Recognition Systems. IEEE Trans. Information Theory IT-9 11-17.
- Sebestyen, G. (1960). Classification Decisions in Pattern Recognition TR 381. Research Laboratory of Electronics, Massachusetts Institute of Technology.
- Taylor, M. (1973). Principal Components colour display of ERTS imagery. ERTS-1 Symposium December 10-13, 1973.
- Thie, J. (1973). Personal communication.
- Van Trees, H.L. (1968). Detection, Estimation and Modulation Theory Part 1. John Wiley & Sons.
- Wacker, A.G., and D.A. Landgrebe (1971). The Minimum Distance Approach to Classification. LARS Information Note 100771.
- Woo, V. (1973). Red River Crop Type Study. Technical Report, Manitoba Remote Sensing Office.

TABLE 1

VEGETATION COVER ERTS FRAME 1007-16531

<u>Mean Intensities</u>					
<u>Class</u>	<u>Band</u>	<u>4</u>	<u>5</u>	<u>6</u>	<u>7</u>
Water		21.5	17.4	10.0	1.4
Jack Pines		14.5	12.6	22.3	13.1
Black Spruce		14.9	11.7	24.7	15.0
Sedges		17.3	17.8	25.5	16.8
Trembling Aspen		14.6	11.3	35.1	29.6
Community Pasture		21.9	21.6	39.0	30.2
Tamaracks		15.4	12.3	26.9	18.2

<u>Covariance Matrix</u>											
<u>Class</u>	<u>Bands</u>	<u>4,4</u>	<u>5,4</u>	<u>5,5</u>	<u>6,4</u>	<u>6,5</u>	<u>6,6</u>	<u>7,4</u>	<u>7,5</u>	<u>7,6</u>	<u>7,7</u>
Water		0.5	0.1	0.7	0.0	0.1	0.9	0.0	0.0	0.1	0.3
Jack Pines		1.0	1.0	2.4	0.9	1.3	2.1	0.7	1.2	1.1	1.3
Black Spruce		0.5	0.0	0.7	0.3	0.3	1.8	0.3	0.4	1.3	1.8
Sedges		0.5	0.0	0.8	0.1	0.2	1.2	-0.1	0.0	0.2	0.4
Trembling Aspen		0.5	0.1	0.9	0.0	-0.2	2.3	-0.2	-0.4	1.2	2.0
Community Pasture		1.0	0.7	1.9	1.0	0.6	5.1	0.9	0.3	4.3	5.4
Tamarack		0.4	0.0	0.6	0.1	0.2	1.8	0.1	0.1	0.9	1.2

TABLE 2

AGRICULTURAL COVER ERTS FRAME 1007-16531

Class	<u>Mean Intensities</u>				
	<u>Band</u>	<u>4</u>	<u>5</u>	<u>6</u>	<u>7</u>
Fallow		18.0	17.4	18.4	7.6
Wheat		17.9	16.4	27.7	18.0
Grain Stubble		19.5	18.7	31.7	21.8
Corn		17.9	15.2	33.8	26.1
Rape		22.2	20.4	43.2	36.5
Sunflower		18.1	15.8	31.8	23.6
Grain Field		19.0	17.9	32.7	24.0

		<u>Covariance Matrix</u>										
		<u>Bands</u>	<u>4,4</u>	<u>5,4</u>	<u>5,5</u>	<u>6,4</u>	<u>6,5</u>	<u>6,6</u>	<u>7,4</u>	<u>7,5</u>	<u>7,6</u>	<u>7,7</u>
<u>Class</u>												
Fallow		0.8	0.6	1.7	0.7	1.4	2.2	0.4	0.7	0.9	0.9	
Wheat		0.7	0.5	1.6	0.2	0.4	1.3	0.2	0.4	0.4	0.9	
Grain Stubble		3.2	4.9	8.8	0.5	1.2	4.3	-1.3	-2.1	3.0	4.8	
Corn		0.9	0.6	2.1	0.5	0.0	8.9	0.3	-0.9	10.6	14.9	
Rape		0.9	0.6	2.0	-0.2	0.9	2.8	-0.3	0.9	3.4	6.5	
Sunflower		0.6	0.7	3.0	0.0	-0.7	2.7	-0.2	-1.3	2.0	3.3	
Grain Field		2.2	3.2	7.3	0.4	-0.2	8.5	-0.6	-1.9	8.1	11.1	

VEGETATION COVER ERTS FRAME 1007-16531

DIVERGENCE MATRIX

TABLE 3A

<u>Class</u>	1	2	3	4	5	6	7
<u>Class</u>							
1	0.						
2	559.	0.					
3	645.	9.	0.				
4	761.	54.	75.	0.			
5	1702.	307.	141.	284.	0.		
6	1673.	186.	181.	291.	149.	0.	
7	836.	35.	7.	69.	98.	208.	0.

CONFUSION MATRIX ± TRAINING AREAS

TABLE 3B

<u>True Class</u>	1	2	3	4	5	6	7
<u>Chosen Class</u>							
0	0	0	0	0	4	2	3
1	550	231	0	0	0	0	0
2	0	21	16	1	0	0	0
3	0	8	192	0	0	0	41
4	0	0	0	613	0	0	0
5	0	0	0	0	275	0	0
6	0	0	0	0	0	472	0
7	0	0	28	0	1	0	554

CONFUSION MATRIX - MONTE CARLO

TABLE 3C

<u>True Class</u>	1	2	3	4	5	6	7
<u>Chosen Class</u>							
0	0	0	0	0	0	0	0
1	100	0	0	0	0	0	0
2	0	91	10	1	0	0	0
3	0	8	77	0	0	0	10
4	0	0	0	99	0	0	0
5	0	0	0	0	100	0	0
6	0	0	0	0	0	100	0
7	0	1	13	0	0	0	90

Legend: (0) Neither (1) Water (2) Jack Pines (3) Black Spruce
 (4) Sedges (5) Trembling Aspen (6) Community Pasture
 (7) Tamarack

AGRICULTURAL COVER ERTS FRAME 1007-16531

DIVERGE MATRIX

TABLE 4A

<u>Class</u>	1	2	3	4	5	6	7
<u>Class</u>							
1	0.						
2	203.	0.					
3	213.	20.	0.				
4	383.	62.	8.	0.			
5	865.	309.	74.	49.	0.		
6	313.	31.	6.	4.	98.	0.	
7	270.	36.	2.	4.	50.	4.1	0.

CONFUSION MATRIX - TRAINING AREAS

TABLE 4B

<u>True Class</u>	1	2	3	4	5	6	7
<u>Chosen Class</u>							
0	0	0	2	0	0	0	1
1	171	0	0	0	0	0	0
2	0	169	1	3	0	1	4
3	0	1	34	3	0	3	22
4	0	0	0	53	0	10	17
5	0	0	0	0	49	0	1
6	0	0	39	22	0	43	44
7	0	1	4	8	0	0	54

CONFUSION MATRIX - MONTE CARLO

TABLE 4C

<u>True Class</u>	1	2	3	4	5	6	7
<u>Chosen Class</u>							
0	0	0	0	2	0	0	3
1	100	0	0	0	0	0	0
2	0	96	8	2	0	3	5
3	0	1	55	0	0	8	21
4	0	2	6	61	0	10	11
5	0	0	0	0	100	0	0
6	0	0	23	31	0	72	26
7	0	1	8	4	0	7	34

Legend: (0) Neither (1) Fallow (2) Wheat (3) Grain Stubble (4) Corn
 (5) Rapeseed (6) Sunflower (7) Grain Field

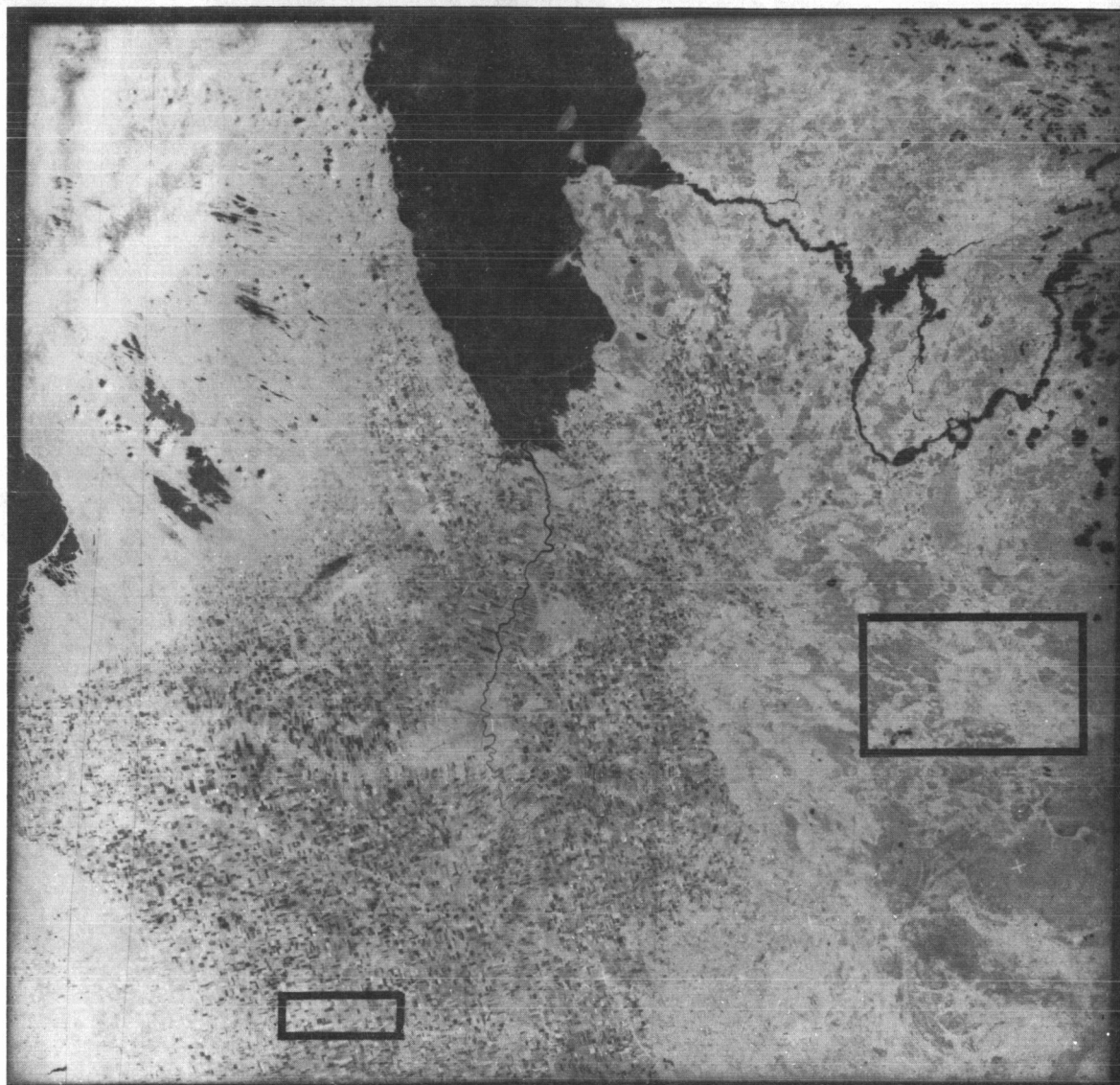


Fig 1: ERTS-1 frame 1007-16531 band 7 imaged July 30 1972. The agricultural area is indicated at the lower left. The vegetation area is indicated on the right and extends about 30 kilometers beyond the southern boundary.

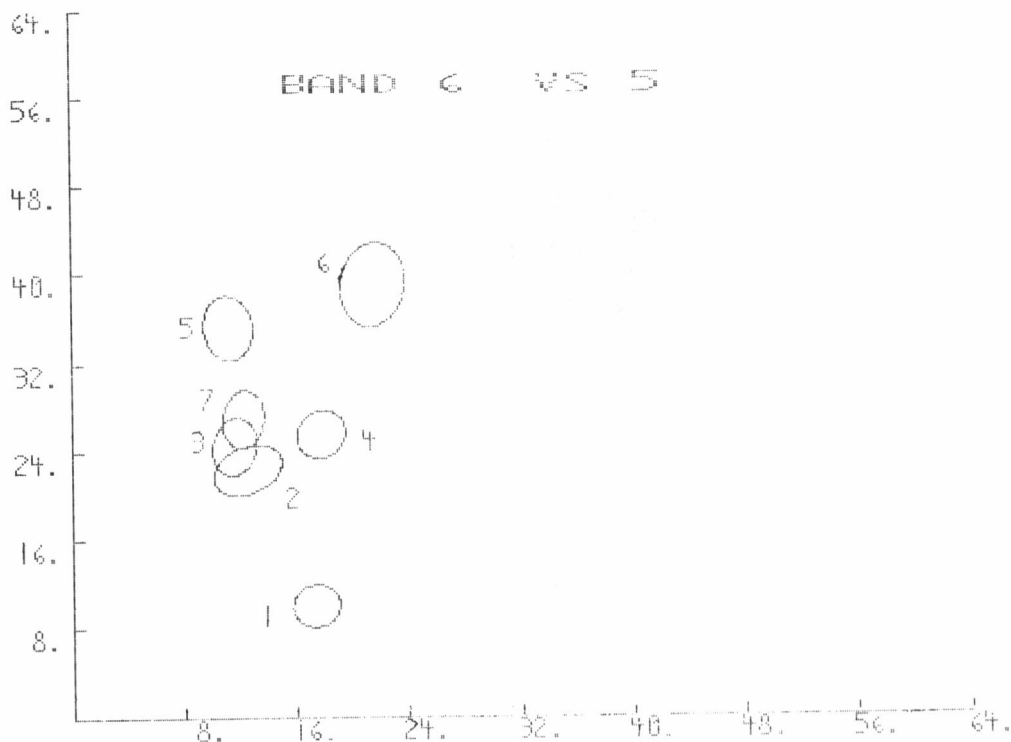


Figure 2: Projection of the vegetation decision regions in observation space. (1) Water (2) Jack Pines (3) Black Spruce (4) Sedges (5) Trembling Aspen (6) Community Pasture (7) Tamarack.

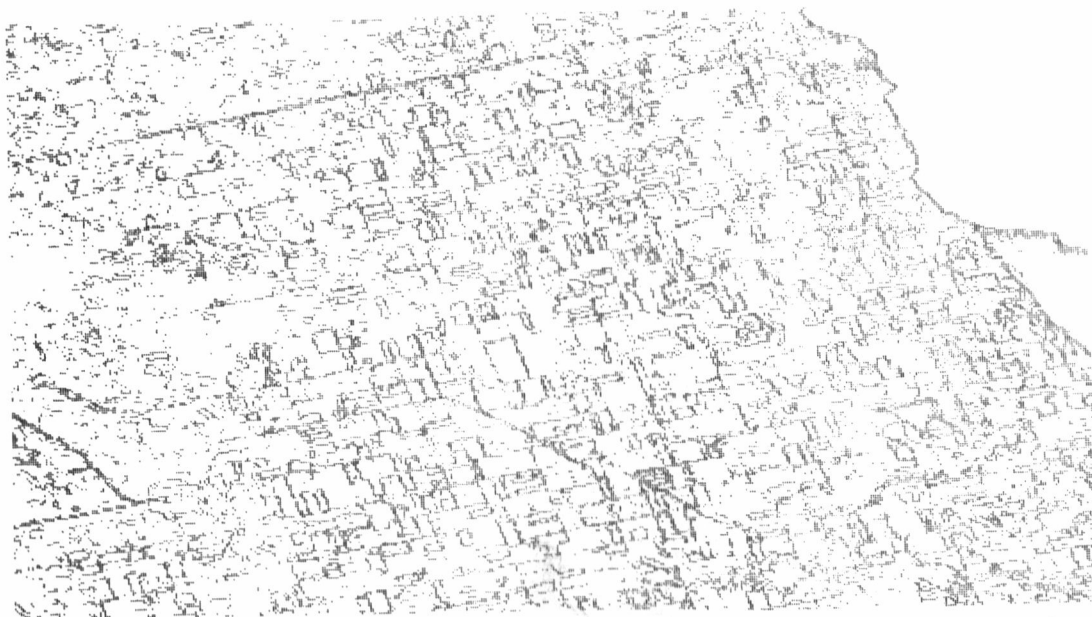


Figure 3: Boundary detection applied to agricultural area East of the Southern end of Lake Winnipeg.

AN EVALUATION OF MACHINE PROCESSING TECHNIQUES OF ERTS-1 DATA FOR USER APPLICATIONS

David Landgrebe and Staff

INTRODUCTION: A Context for the Work

For some years research has been underway to learn how to use computing machines for the processing and analysis of remotely sensed data. The motivation of this work is not to produce an automatic analysis system, but to utilize computing machinery for the repetitive and routine aspects of the total analysis and processing problem in order to minimize the costs and increase the throughput rate.

By the time of the launch of ERTS-1 this research had identified a number of machine processing algorithms useful for both preprocessing and analysis of the data. Some of these processing algorithms have been embodied into a software system known as LARSYS¹, and this system has been widely used and thoroughly tested on several different problems utilizing aircraft scanner data. Thus, an important task with the launch of ERTS-1 was to test this processing method relative to the high volume, high quality data which ERTS-1 was expected to produce.

The vantage point adopted in devising this test is based on attempting to visualize the complete spectrum of information which might be obtainable from remotely sensed data. An earth resources information tree (see Figure 1) is one way to visualize this spectrum of information. In the information tree concept, the totality of surface features is first broken down into relatively simple classes such as:

- Vegetation
- Soils and Geologic Features
- Urban Features
- Hydrological Features
- Atmospheric Features

Each of these in turn may be broken down into more detail. For example, vegetation might be subdivided into natural and cultural vegetation; under cultured vegetation there would be croplands and this could be further broken down to species, variety, yield, etc. In this way one can visualize the information derivable through remote sensing of surface features as being

1 N 74 30710

essentially a continuum of data classification possibilities. Although it is not precisely true in every case, generally the deeper one goes down the information tree the more difficult the classification task.

From this vantage point then and realizing the importance of being able to ultimately satisfy an actual user's needs, a suitable test of a new processing approach might be devised by selecting a set of study projects which (a) are associated with specific user problems of importance and (b) which suitably sample this spectrum of information possibilities from left to right and from top to bottom. Following this approach for our study, five specific application investigations were selected.* These were:

1. General Earth Feature Identification
2. Crop Species Identification
3. Soil Association Mapping
4. Urban Land Use Analysis
5. Water Resource Identification

State and regional information users were also identified for each of these tasks and their cooperation secured so that each of these application investigations could be directed at a specific user need.

Along with these application investigations four supporting technology tasks were also proposed. These tasks were needed in order to bring the existing technology of processing and analysis into compatibility with the new data source. The four supporting technology tasks were:

- .Analysis Technique Development
- .Reformatting and Temporal Registration
- .Atmospheric Modeling
- .System and Scene Corrected Data Comparison

The purpose of this presentation is to present some new results on several of these study projects. Before doing so however, it will add to the overall perspective to briefly note results presented on these study projects in earlier ERTS-1 Symposia. At the first ERTS-1 meeting in September, 1972 a report² was presented which treated classes of earth surface features similar to those of application investigation number 1, above; however the real purpose of this study was to test rapid turn-around analysis possibilities and to gain an initial indication of the quality of the data which the satellite was producing. The analysis of the so-called Texoma ERTS frame, the first frame produced in computer compatible tape form by the ground station, was carried out within 48 hours after receipt of the data and within 72 hours after the data was gathered. Successful machine classifications were obtained for such

*In addition to the ERTS-Wabash Valley Study (UN 127, D. Landgrebe, Principal Investigator) two other were conceived as a part of the overall test. They are UN 103, R. Hoffer, Principal Investigator for problems involving especially terrain relief and UN 630, M. Baumgardner, Principal Investigator for other types of agricultural and range situations, e.g. dry land and irrigation farming. These are reported on elsewhere in this symposium.

classes as: forest, several categories of rangeland, cropland, and several categories of water. A quantitative evaluation of classification accuracy was not conducted.

At the March, 1973 ERTS-1 Symposium a report³ was provided on preliminary urban land use inventory studies using these methods. Preliminary analysis of data over Milwaukee, Wisconsin; Chicago, Illinois; and Indianapolis, Indiana were reported. Urban land use categories such as older housing, newer housing, industry, commerce, wooded areas, water and grassy areas were utilized. The results were evaluated on a qualitative basis. Later in this report we shall give the results of a replication of this study together with a quantitative analysis of the accuracy.

Also in the March 1973 ERTS Symposium, the results of a relatively extensive agricultural crop classification study were reported.⁴ Utilizing test areas involving 500 agricultural fields scattered over a three county area, a demonstrated accuracy in excess of 80 percent was reported; in addition, the results of extrapolating training from one county to another were reported as successful and preliminary results on the use of temporally registered data for improving classification accuracy was given. Additional work of this type has been undertaken with data from other parts of the country where cropping patterns are significantly different. Some of this work is being done in cooperation with the Statistical Reporting Service, USDA (Mr. Don VonSteen and Mr. Bill Wigton). This work is reported elsewhere in this meeting.

In the remainder of this report, we will provide results from additional studies and urban land use analysis, soil association mapping, and in reformatting and temporal registration, thus further filling in the profile of possible performance and future utility of satellite data coupled with machine processing.

URBAN LAND USE ANALYSIS

Figure 2 shows an ERTS image centered over the southern tip of Lake Michigan. This data was gathered on October 1, 1972. In order to determine the repeatability of urban land use mapping possibilities which ERTS provides a replication of an earlier urban land use mapping test was conducted using the Gary-Hammond, Indiana area.

In conducting such an experiment the first task is to display the data in a suitable fashion to the analyst. Figure 3 shows the same data displayed electronically from computer compatible tape data rather than by conventional photographic means. This image, formed on a digital image display device,

utilized three channels of ERTS data in a fashion similar to standard color products available from the ERTS ground station. However, in this case rather than balancing the display of the three spectral bands in the conventional fashion the contrast of each band has been maximized in this presentation based on the actual range in this data. In theory, this results in a large quantity of information being displayed. However, of course, training in interpreting this new media would be required to realize it.

One of the advantages of electronically displaying data is in the additional flexibility it provides over conventional means. For example, in this case our interest is to be focused on the southern-most tip of Lake Michigan. The next four figures show displays of this same region at successively increasing levels of detail (Figure 4, 5, 6, and 7).

The analysis proceeds by selecting small areas typical of each land use class to be used. This is done with the aid of a clustering algorithm. The set of training samples resulting is used to classify the entire study area, using the Gaussian maximum likelihood classifier of LARSYS.

The resulting classification is shown in conjunction with the raw data (Figure 8), and as Figure 9. Important features and land use classes are located with letters or numbers in Figure 9 and are also listed in Table 1. Gray levels used for the display of the spectral classes are as follows:

Industrial/Commercial	Medium Gray
Older Housing	Black
Newer Housing	White
Trees	Light Gray
Grassy (open, agricultural)	Dark Gray
Water	Black
Smoke	White

Older housing and water have been assigned the same gray level (black), but consideration of their areal distributions prevents confusion between the two. Water is largely restricted to Lake Michigan and to several other water bodies, such as Wolf Lake. Older housing is located between coastal industrial establishments and newer housing. Smoke and newer housing also have the same gray levels (white). Smoke, however, is found only over Lake Michigan, while newer housing is located to the south.

Agricultural areas (shown as dark gray) were identified in the southern part of the study area. This class included cropland, pasture, and idle land in rural areas, as well as parks, golf courses, and open land in urban areas. Wooded areas (shown as light gray) are commonly associated with the drainage pattern of the study area. Three principal stands of trees appeared, in conjunction with the Little Calumet River, Deep River, and the Dunes Park area along Lake Michigan. Water,

displayed as black, is located in Lake Michigan and other, smaller water bodies such as Wolf Lake.

Newer housing developments, shown as white, are located on the fringes of the urbanized area, in the municipalities of Munster, Highland, Griffith, and Merriville. The majority of the structures were built since World War II. Lawns (grass) and streets are the two primary constituents of this spectral class. Therefore, four-lane highways were also classified as newer housing.

Older residential, displayed as black, consists of areas developed prior to World War II. They are found in Hammond, Whiting, East Chicago, and Gary. Closely spaced rooftops, along with mature vegetation (large trees) are the reasons for the spectral separability of this class.

Industrial/commercial areas (shown as medium gray) are usually void of vegetation. They are characterized by the occurrence of rooftops, parking lots, streets, and bare ground. Examples include Inland Steel, U.S. Steel, Standard Oil, Bethlehem Steel, the Gary Central Business District, and Broadway Plaza Shopping Center (Figure 9).

The land use classes identified in this study correspond well with the classes proposed by Anderson, Hardy, and Roach in the U.S. Geological Survey Circular 671⁵ and also with those developed in previous ERTS urban analyses (2, 7, 11, 13). Further investigations were made, however, into industrial areas in this analysis because of their large areal extent in the Gary-Hammond area.

Five spectral classes of commercial/industrial land use were developed. Two of the classes are associated with closely spaced rooftops; the other three are associated with gravel or sandy areas in industrial areas, adjacent to the rooftop classes. The northern part of the classification image is shown in Figure 10. Gray levels used for the classification image are as follows:

Rooftops (dark reflectance)	Black
Rooftops (bright reflectance)	Dark Gray
Gravel/Sandy areas (3 classes)	Medium Gray
Smoke	White
All Other Classes	Light Gray

The reader will note that the same classification is shown in both Figure 9 and Figure 10; the only idfference is the assignment of gray levels to the spectral classes.

The class shown as black in Figure 10 is associated primarily with dark roofing material, but also with large coal piles. Large areas of this spectral class are associated with

the three large steel firms in the study area -- Inland, U.S., and Bethlehem. The other rooftop class, displayed as dark gray, is associated with brighter reflecting rooftops. Reasons for the three spectral categories of gravel/sandy areas (all displayed as medium gray) are not entirely clear at this time but they probably relate to both the color of the material and the presence/lack of sparse vegetative cover. Two large areas of gravel/sandy material are located in the northwest part of the study area, one between the large building complexes of Inland and U.S. Steel companies and the second in the large oil refining district in the Whiting-East Chicago area. In the northeastern part of the study area, another large area of gravel/sand is located west of the buildings of Bethlehem Steel. This area was dominated by one of the three classes of gravel/sand, and had a particularly high spectral reflectance in both the visible and infrared portions of the spectrum. The ground cover in this area is the dune sand typical of this locale.

The final class used in this classification scheme, the white areas in Lake Michigan, is speculated to be smoke coming from coastal industrial establishments. Spectrally, the class is similar to water, having a very dark reflectance in the infrared (Figure 8-B). Several facts, however, when considered as a whole, lead one to conclude it is smoke. The linear, parallel arrangements of the data points, extending some 30 miles into Lake Michigan, are contrary to the circulation patterns in the lake. Moreover, the meteorological records report that the wind was out of the southwest on the morning of the ERTS pass.

While smoke was probably identified in the western part of the study area, the smoke data points along the coast in the east were probably water. Moreover, the large area classified as smoke northwest of Bethlehem Steel was probably a thin cloud. Despite the spectral confusion in these areas, the partial separability does warrant further investigation of the phenomena of smoke located over water bodies.

CLASSIFICATION ACCURACY

An attempt was made to determine the classification accuracy by a sampling method. A number of rectangular test areas were determined for each land use, and the class accuracy determined (Table 2). Water, wooded areas, older housing, and newer housing were all identified with over 90 percent accuracy. Trouble was encountered in industrial/commercial areas, most of the misclassification being attributed to older housing. The poorest classification accuracy was in grassy and agricultural areas, where less than 70 percent of the data points were accurately classified. Misclassification of these areas was of two major types. One, areas in agricultural regions associated with darker colored soils proved difficult to separate from older housing. One such area was located south of Little Calumet River, in Munster and Highland. The other type of misclassifi-

cation was in undeveloped marshland adjacent to industrial areas. Large areas south of U.S. Steel and along U.S. Highway 12 were misclassified as older housing.

Important tabular data can be generated from the machine processing of ERTS data. Table 3 contains an estimate of the proportion of the study area (excluding Lake Michigan) allocated to the various land uses, obtained by a simple tallying of the numbers of data points in each land use. Adjustments were made for agricultural/grassy areas, commercial/industrial, and older housing, relative to the misclassification between these three land uses. Acreages were obtained by multiplying the number of data points by 1.1, the approximate resolution of ERTS. The data in Table 3 could have been reported by smaller areal units, such as municipalities, townships, or census tracts, by storing the desired boundaries in the computer.

SOIL ASSOCIATION MAPPING

Computerized analysis of ERTS MSS data has yielded images which will prove useful in such programs as the ongoing Cooperative Soil Survey program, involving the Soil Conservation Service of USDA and other state and local agencies. In the present mode of operation, a soil survey for a county may take up to 5 years to be completed. Results reported here indicate that a great deal of soils information can be extracted from ERTS data by computer analysis. This information is expected to be very valuable in the premapping conference phase of a soil survey for a county, resulting in more efficient field operations during the actual mapping. It is expected to result in greater accuracy of mapping and decrease the time required to produce the soil survey.

Several states are presently accelerating their soil survey programs in light of the increased pressure on our soil resources for production of food and fiber. Since soils are a primary consideration in land use planning, these inventories of soils resources are desperately needed at the present time.

The task being pursued in our ERTS-1 study is concerned primarily with comparison of generalized county soil maps with multispectral maps produced by computer analysis of ERTS MSS data. A typical soil association map is given in Figure 11. Initial investigation of discriminability of individual soil types for more detailed mapping are also being conducted.

The procedure being followed in determining the utility of ERTS data involves direct comparisons of ERTS images of various types to existing soil association maps. Techniques were developed during the course of the project to facilitate making such comparisons independent of the spectral characteristics of the soils. Essentially, this is accomplished by the digital geometric correction of ERTS MSS data where necessary

(in the computer analysis phases) and direct overlay of conventional soil maps onto the ERTS images.

Four types of techniques are being tested:

- 1) B/W photographic image-single band
- 2) B/W electronic image-single band
- 3) Color electronic image-three bands
- 4) Computer classification image-four bands

In each case an attempt was made to draw boundaries between generalized soil associations onto the image. This was followed by comparison with a soil association map in transparent overlay form. The overlay was photographically manipulated to the same scale as the ERTS image containing the interpreted boundaries.

An inspection and test of data from various dates has verified the original assumption that data gathered at a time of maximum soil exposure provides the best results. This occurs in late Spring in the Wabash Valley. For example on June 9, 1973 it was found that 55% of Tippecanoe County, Indiana was nonvegetated.

The generation of the black and white images is straightforward with the exception that the electronically generated one has its contrast optimized relative to the scene data range. The electronically generated color image is generated in the same fashion as Figures 3 through 7.

The fourth type, the computer classification is a non-supervised classification of the four band data. An example is shown in Figure 12 which includes the soil map overlay. It was found in this case that the data could be partitioned into 10 multispectral classes such that none were spectrally similar to one another.

In this figure the very dark colors represent vegetated areas while intermediate and light colors show nonvegetated soils. A close inspection of the image relative to the map boundaries reveals that some generalized soil boundaries are mislocated on the conventional map. An example is seen in the upper left part of the image, where a light colored area extends from soil association 81 (Miami-Russell-Fincastle) across the area mapped as soil association 73 (Raub-Ragsdale) and into soil association 89 (Sidell-Parr). The Raub-Ragsdale soil association would not typically contain such large delineations of these well-drained soils.

Several soil associations can be delineated very well in Figure 12. Soil association 16 (Elston-Wea) is very distinctive in the left center of the image. Soil association 66 (Fincastle-

Ragsdale-Brookston) has a distinctive appearance in the upper right portion of the image as well as in other areas. Soil associations 73 and 89 are easily delineated from soil associations 66 and 81 in several areas.

Table 4 shows results of comparing false color electronic images and computer classification images with the soil association map. The computer classification most closely agreed with the soil map, and the discrepancies noted are associated with errors in the conventional map.

Table 5 gives results of the investigation of spectral separability of individual soil types. The overall accuracy of 89% indicates that ERTS data can be used to assist in identification and mapping of individual soil types.

Although these studies have not been completed, it seems that several positive conclusions will be forthcoming. Geometric correction of ERTS MSS data and direct overlay of existing conventional soil maps facilitated specific and precise comparisons. Used together, these two sources provide increased information on soil characteristics which should be extremely useful in the National Cooperative Soil Survey. Computer classification images contained more soils information than any other images investigated. This advantage of computer analysis, coupled with the advantages of being compatible with other data storage and retrieval systems for soils and land use data make the computer analysis approach highly desirable. Since soils are a major consideration in land use and land use planning, this type of analysis will likely become of even greater utility in the next few years.

GEOMETRIC CORRECTION AND TEMPORAL REGISTRATION OF ERTS DATA

Earlier it had been indicated that supporting technology tasks in the ERTS Wabash Valley Study involved reformatting and temporal registration, and scene corrected data comparisons. In the case of the latter it had been assumed prior to the launch of ERTS that the geometric accuracy present in scene corrected data would prove very helpful in locating specific ground points, both in the classifier training process and in the evaluation and utilization of results. This has certainly proved to be the case. A geometric correction software system which used the ERTS orbital and sensor system parameters as inputs is utilized to deskew, rotate and rescale computer compatible tape data. For example, in one test, data from Tippecanoe County was geometrically adjusted to achieve a 1:24,000 scale computer line printer printout of the area. To test the geometry the printout was then overlaid on

a standard 1:24,000 quadrangle map and significant landmarks traced onto the printout. In this manner it was determined that a maximum error of 1.3 picture elements was obtained.

If greater accuracy is required ground control points can be introduced to reduce the geometric error still further. If it is desired to precisely align data from one ERTS pass onto that of another, the same system can be used, but achieving still smaller relative error between the two data sets by allowing final adjustment of the geometry to be under the control of a two dimensional correlation algorithm. Table 6 shows accuracies which appear to be typical of using these techniques to adjust the geometric qualities of ERTS-1 data. In essence, this system amounts to a digital implimentation of the scene correction capability of the ERTS ground station, but with the addition of an inter-image correlator. It has proven immensely valuable in reducing the time required for an analyst to train a classifier and to evaluate its performance by greatly simplifying the problem of locating specific ground location. It also provides a basis for developing multitemporal data sets from subsequent passes of ERTS-1 so that the value of multitemporal, multispectral classification can be tested.

CONCLUSIONS

In this presentation a broad study has been described, the purpose of which is to evaluate a set of machine analysis and processing techniques applied to ERTS-1 data. The analysis phase of this study still has several months to completion. However, based on the analysis results in urban land use analysis and soil association mapping together with previously reported results in general earth surface feature identification and crop species classification, a profile of general applicability of this procedure is beginning to emerge. Put in the hands of a user who knows well the information he needs from the data and also is familiar with the region to be analyzed it appears that significantly useful information can be generated by these methods. When supported by pre-processing techniques such as the geometric correction and temporal registration capabilities, final products readily useable by user agencies appear possible. In parallel with application, through further research, there is much potential for further development of these techniques both with regard to providing higher performance and in new situations not yet studied.

ACKNOWLEDGEMENTS

This work was supported by NASA Grant NAS5-21773 and NGL15-005-112. A number of LARS staff members contributed significantly to this work. Mr. William J. Todd conducted the urban land use analysis. Dr. Friedrich Quiel, of the University of Munich, a visiting scientist at LARS, assisted in collecting ground observations for the urban land use study. Dr. Jan Cipra leads the Soil Association Mapping team. Mr. Paul Anuta leads the geometric correction and temporal registration task area.

REFERENCES

1. LARSYS Software Documentation, Copyright 1973, Purdue Research Foundation, West Lafayette, Indiana.
2. Landgrebe, D. A., Hoffer, R. M., Goodrick, F. E., and Staff, LARS. An Early Analysis of ERTS-1 Data. Proceedings of the Earth Resources Technology Satellite-1 Symposium, Goddard Spaceflight Center, Greenbelt, Maryland, September 29, 1972.
3. Todd, William J., Paul W. Mausel, and Kenneth A. Wenner. Preparation of urban land use inventories by machine-processing of ERTS MSS data. Proceedings of Symposium on Significant Results Obtained from the Earth Resources Technology Satellite-1. Goddard Spaceflight Center, Greenbelt, Maryland, March 5-7, 1973. Volume I, Section B, page 1031-1039.
4. Bauer, Marvin E., and Jan E. Cipra, Identification of Agricultural Crops by Computer Processing of ERTS MSS Data. Proceedings of the Symposium on Significant Results Obtained from the Earth Resources Technology Satellite-1, NASA/Goddard Spaceflight Center, Greenbelt, Maryland, March 5-7, 1973. Volume I, Section A, page 205-212.
5. Anderson, James R., Ernest E. Hardy, and John T. Roach. 1972. A land use classification system for use with remote sensor data, U.S. Geological Survey Circular 671. U.S. Geological Survey, Washington, D. C. 16 p.
6. Anuta, Paul E. 1970. Spatial registration of multispectral and multitemporal digital imagery using fast fourier transform techniques. IEEE Transactions on Geoscience Electronics. GE-8(4):353-368.
7. Ellefsen, R., P.H. Swain, and J. R. Wray. 1973. Urban land use mapping by machine processing of ERTS-1 multispectral data: A San Francisco Bay area example. Proceedings of Conference on Machine Processing of Remotely Sensed Data. Laboratory for Applications of Remote Sensing, Purdue University, West Lafayette, Indiana, October 16-18, 1973. P. 2A-7 - 2A-22.
8. Landgrebe, David A. 1971. Systems approach to the use of remote sensing, LARS Information Note 041571. Laboratory for Applications of Remote Sensing, Purdue University, West Lafayette, Indiana. 19p.

9. LeBlanc, P. N., C. J. Johannsen, and J. E. Yanner. 1972. Land use classification utilizing remote multispectral scanner data and computer analysis techniques, LARS Information Note 111672. Laboratory for Applications of Remote Sensing, Purdue University, West Lafayette, Indiana. 98p.
10. Phillips, T. (ed). 1973. LARSYS User's Manual. Laboratory for Applications of Remote Sensing, Purdue University, West Lafayette, Indiana 613p.
11. Simpson, R. B. 1972. Urban-field land use Southern New England: A first look. Conference Proceedings, Earth Resources Technology Satellite-1. Goddard Spaceflight Center, Greenbelt, Maryland, September 29, 1972. P. 100-107.
12. Swain, Philip H. 1972. Pattern recognition: A basis for remote sensing data analysis, LARS Information Note 111572. Laboratory for Applications of Remote Sensing, Purdue University, West Lafayette, Indiana. 40p.
13. Todd, William J., and M. F. Baumgardner. 1973. Land use classification of Marion County, Indiana by spectral analysis of digitized satellite data. Proceedings of Conference on Machine Processing of Remotely Sensed Data. Laboratory for Applications of Remote Sensing, Purdue University, West Lafayette, Indiana, October 16-18, 1973. P. 2A-23 to 2A-32.
14. Todd, William J., Paul W. Mausel, and M. F. Baumgardner. 1973. Urban land use monitoring from computer-implemented processing of airborne multispectral data. LARS Information Note 061873. Laboratory for Applications of Remote Sensing, Purdue University, West Lafayette, Indiana. 17p.

Table 1. Features of interest, land uses, and major highways indicated in Figure 9.

¹ L	² Feature, land use, or highway	³ Spectral class
A	Smoke plume	smoke
B	Inland Steel	commercial/industrial
C	United States Steel	commercial/industrial
D	Bethlehem Steel	commercial/industrial
E	Oil Refineries	commercial/industrial
F	Wolf Lake	water
G	Lake Michigan	water
H	Gary-Central Business District	commercial/industrial
J	Highland-subdivision	newer housing
K	Indiana Harbor	commercial/industrial
L	Port of Indiana	commercial/industrial
M	Gary Municipal Airport	newer housing
N	Indiana Dunes State Park	wooded
O	Agricultural area	grassy/agricultural
P	Indiana-Illinois state line	-----
Q	Wicker Memorial Park	grassy/agricultural
R	Trees along Deep River	wooded
S	Hammond-residential area	older housing
T	East Chicago-residential area	older housing
U	Munster-subdivision	newer housing
V	Gary-residential area	older housing
2	Interstate Highway 80-94	newer housing
3	Interstate Highway 80-90	newer housing
4	U.S. Highway 12	newer housing
5	Interstate Highway 94	newer housing
6	Illinois Highway 394	newer housing
7	U.S. Highway 41	newer housing
8	Interstate Highway 65	newer housing
9	U.S. Highway 30	

¹White letter or number indicated in Figure 9.

²Features of interest of land uses are indicated by letters; highways are indicated by numbers.

³Five spectral categories of commercial/industrial land use were used in the classification scheme.

Table 2. Classification accuracy for test samples

Land Use	Percentage of Data Points Classified As:					
	C/I ¹	OHg ²	NHg ³	Wod ⁴	A/G ⁵	Wat ⁶
Cmrc/Inds. ¹	<u>89.8</u>	7.3	0.3	-	0.2	2.5
Old Hsng. ²	0.9	<u>97.9</u>	0.9	0.3	-	-
New Hsng ³	0.6	4.0	<u>94.0</u>	-	1.4	-
Wooded	-	2.0	-	<u>94.4</u>	3.5	-
Agrc/Grsy ⁵	0.8	27.4	3.2	3.1	<u>65.5</u>	-
Water	0.8	-	-	-	-	<u>99.2</u>

\bar{X} Classification accuracy by class = 90.3%.

- ¹ Commerce/Industry
- ² Older Housing
- ³ Newer Housing
- ⁴ Wooded
- ⁵ Agricultural/Grassy
- ⁶ Water

Table 3. Land use area claculations for study area (excluding Lake Michigan).

Land Use	Number of Data Pts.	Number of Acres	Number of Hectares	% of Study Area
Cmrce/Indstry ¹	25766	28343	11479	8.2
Older Housing ¹	56528	62181	25183	.18.0
Newer Housing	28540	31394	12714	9.1
Wooded	52346	57581	23320	16.6
Agric/Grassy ¹	150982	166080	67262	48.0
Water	499	549	222	0.2
TOTAL	314661	346127	140181	100.0

¹ Adjustments made in accordance with test classification accuracy (see Table 2.)

Table 4. ERTS-Wabash Valley Study

SOIL ASSOCIATION MAPPING COMPARISON

Soil Association	Percent Difference Within Association		
	Color Image	Electronic Image	Computer Classi- fication Image
73 Raub-Ragsdale	35.0		8.5
89 Sidell-Parr	11.0		27.0
16 Elston-Wea	0		0
81 Miami-Russell-Fincastle	20.0		3.8
66 Fincastle-Ragsdale-Brookston	<u>3.0</u>		<u>3.1</u>
AVERAGE (Weighted)	15.0		7.3

Table 5. ERTS-Wabash Valley Study

SOIL TYPE SEPARABILITY TEST

SOIL TYPE	PERCENT CORRECT (TRAINING SAMPLES)	
Ragsdale	90.6	
Fincastle	81.8	
Genesee	100.0	
Wea	98.6	
Sidell	84.0	
Miami	77.3	
Ockley	<u>76.9</u>	
OVERALL	89.0	246 DATA POINTS

Table 6. GEOMETRIC CORRECTION & TEMPORAL

REGISTRATION ACCURACY FOR

ERTS-1 MSS CCT DATA	
<u>Task</u>	<u>Typical Error</u>
Geometric correction (estimated parameters)	1-2% accumulative
Geometric correction (ground control)	Maximum 1.33 pixels RMS .65 pixels
Temporal registration (correlation control)	Maximum 1.4 pixels RMS .5 pixels

FIGURE CAPTIONS

- Figure 1. An Earth Resources Information Tree
- Figure 2. An ERTS-1 image of the southern Lake Michigan region October 1, 1972
- Figure 3. Electronically displayed ERTS-1 data from Computer Compatible Tape
- Figure 4. Electronically displayed data showing increasing detail
- Figure 5. Electronically displayed data showing increasing detail
- Figure 6. Electronically displayed data showing increasing detail
- Figure 7. Electronically displayed data showing increasing detail
- Figure 8. Photos from digital display, showing relationship between gray scale imagery and land use classification. Image in A is from the visible portion of the spectrum (Band 4, 0.5-0.6 μ m); B is from the reflective infrared (Band 6, 0.7-0.8 μ m); C is a computer-implemented classification of the study area (see text for explanation of gray levels). Images in A, B, and C show the entire study area; enlargements of the northwestern portions of those three images are shown in D, E, and F, respectively. Horizontal length of A, B, and C is 54 kilometers (34 miles); vertical length is 46 kilometers (29 miles). Horizontal length of D, E, and F is 27 kilometers (17 miles); vertical length is 23 kilometers (14.5 miles). The true north-south line is rotated about 18 degrees counterclockwise to vertical. Horizontal scale is approximately three-fourths that of the vertical scale.
- Figure 9. Photo from digital display of computer-implemented land use classification of Gary-Hammond area (see text for explanation of gray levels). Letters/numbers refer to features of interest, a listing of which is found in Table 1.
- Figure 10. Photo from digital display of computer-implemented land use classification of Gary-Hammond area (northern part of study area) using gray levels which emphasize the industrial land uses. Class shown as black is dark roofing material; dark gray is lighter colored roofing material; medium gray is gravel/sandy areas; smoke is white. All other spectral classes are shown as light gray.

Figure 11. A typical conventional soil association map.

Figure 12. A nonsupervised computer classification of ERTS-1 data showing 10 spectral classes.

Surface Features



- ① Soil Conservation Service
- ② Department of Natural Resources - Indiana
- ③ Agricultural Stabilization and Conservation Service
- ④ Marion County Plan Commission
- ⑤ Statistical Reporting Service
- ⑥ Wabash Valley Interstate Commission

Figure 1



Figure 2. An ERTS-1 image of the southern Lake Michigan region October 1, 1972.

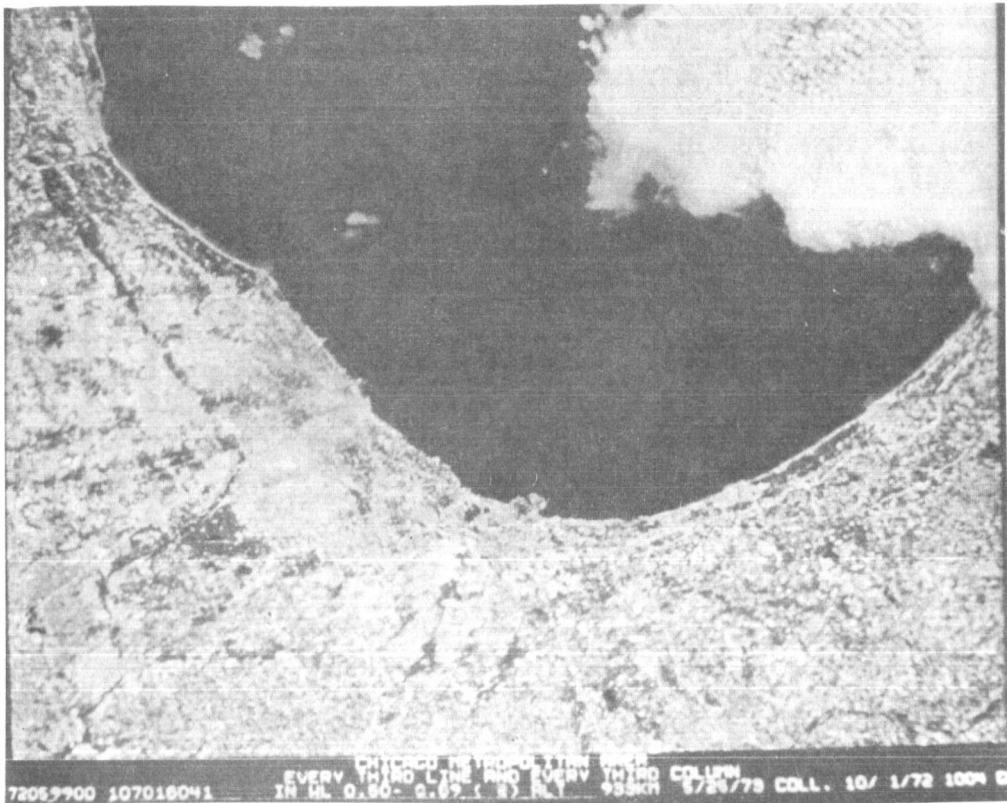


Figure 4. Electronically displayed data showing increasing detail.

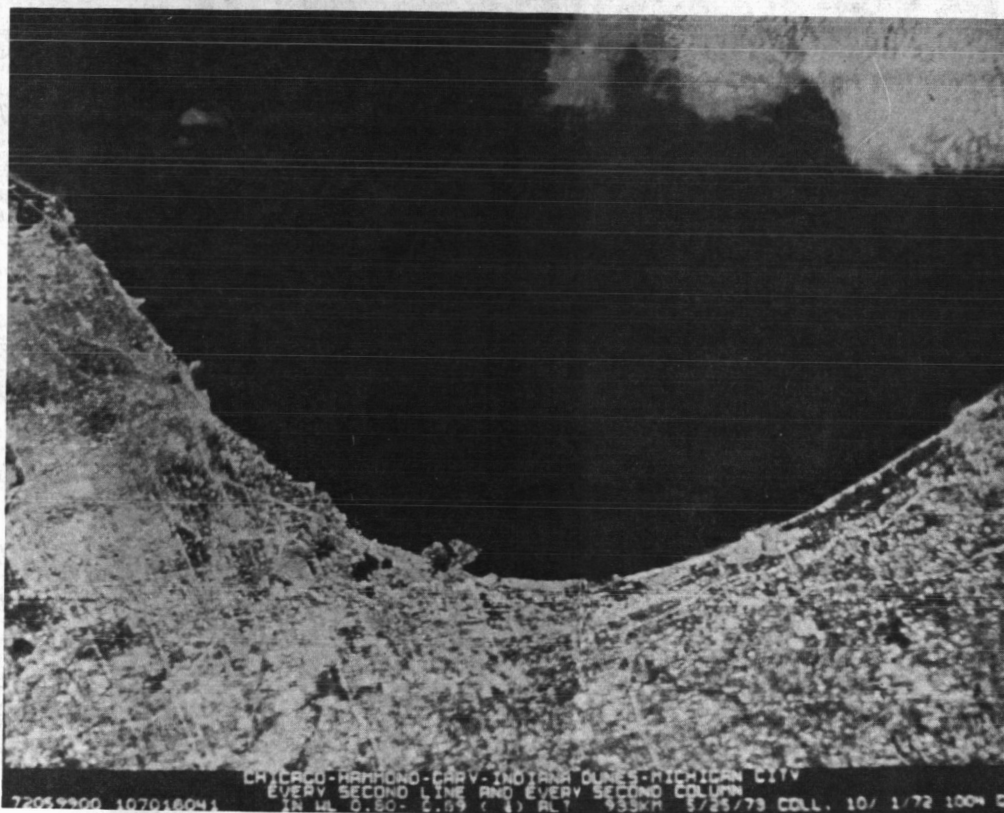


Figure 5. Electronically displayed data showing increasing detail.



Figure 6. Electronically displayed data showing increasing detail.



Figure 7. Electronically displayed data showing increasing detail.

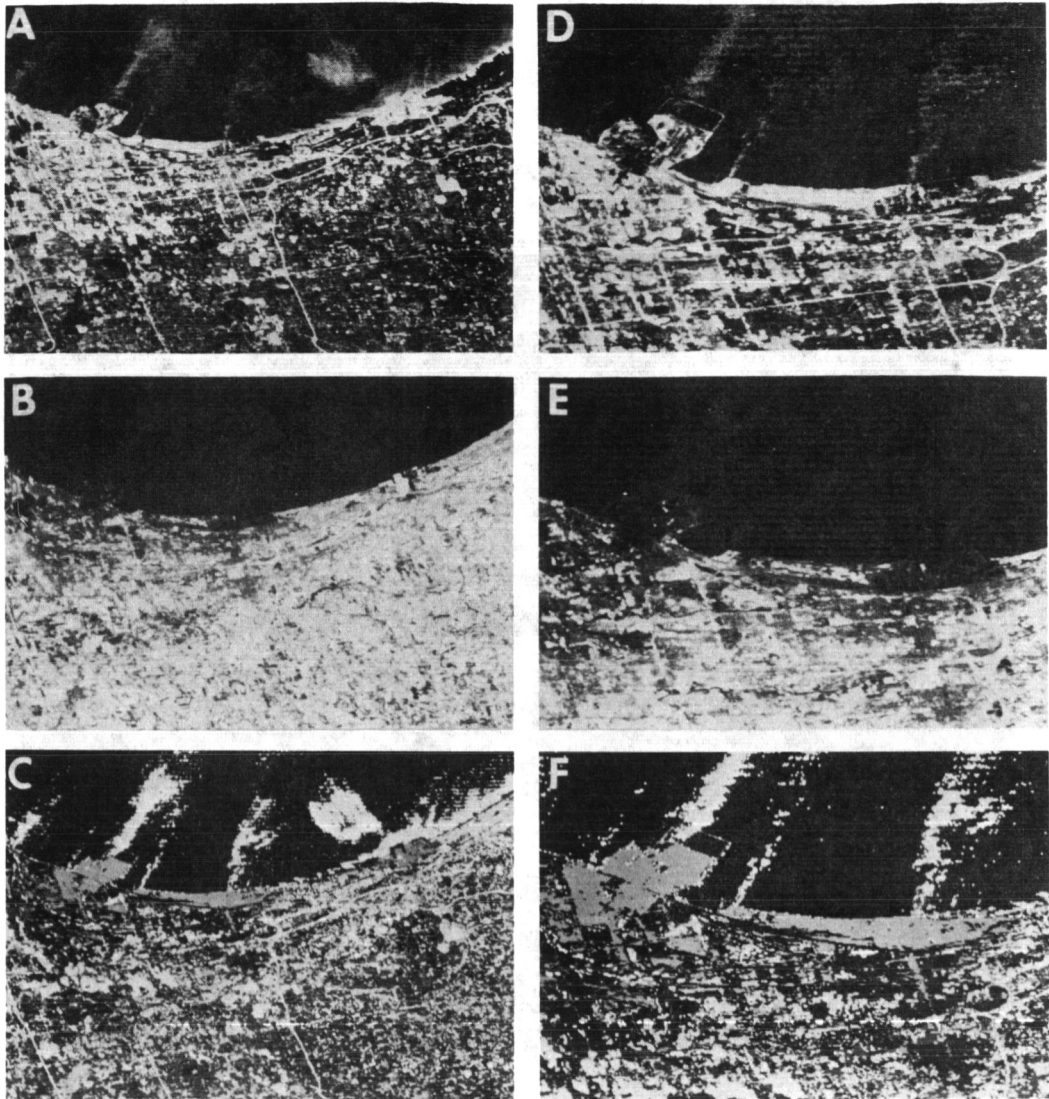


Figure 8. Photos from digital display, showing relationship between gray scale imagery and land use classification. Image in A is from the visible portion of the spectrum (Band 4, 0.5-0.6 μ m); B is from the reflective infrared (Band 6, 0.7-0.8 μ m); C is a computer-implemented classification of the study area (see test for explanation of gray levels). Images in A, B, and C show the entire study area; enlargements of the northwestern portions of those three images are shown in D, E, and F, respectively. Horizontal length of A, B, and C is 54 kilometers (34 miles); vertical length is 46 kilometers (29 miles). Horizontal length of D, E, and F is 27 kilometers (17 miles); vertical length is 23 kilometers (14.5 miles). The true north-south line is rotated about 18 degrees counterclockwise to vertical. Horizontal scale is approximately three-fourths that of the vertical scale.

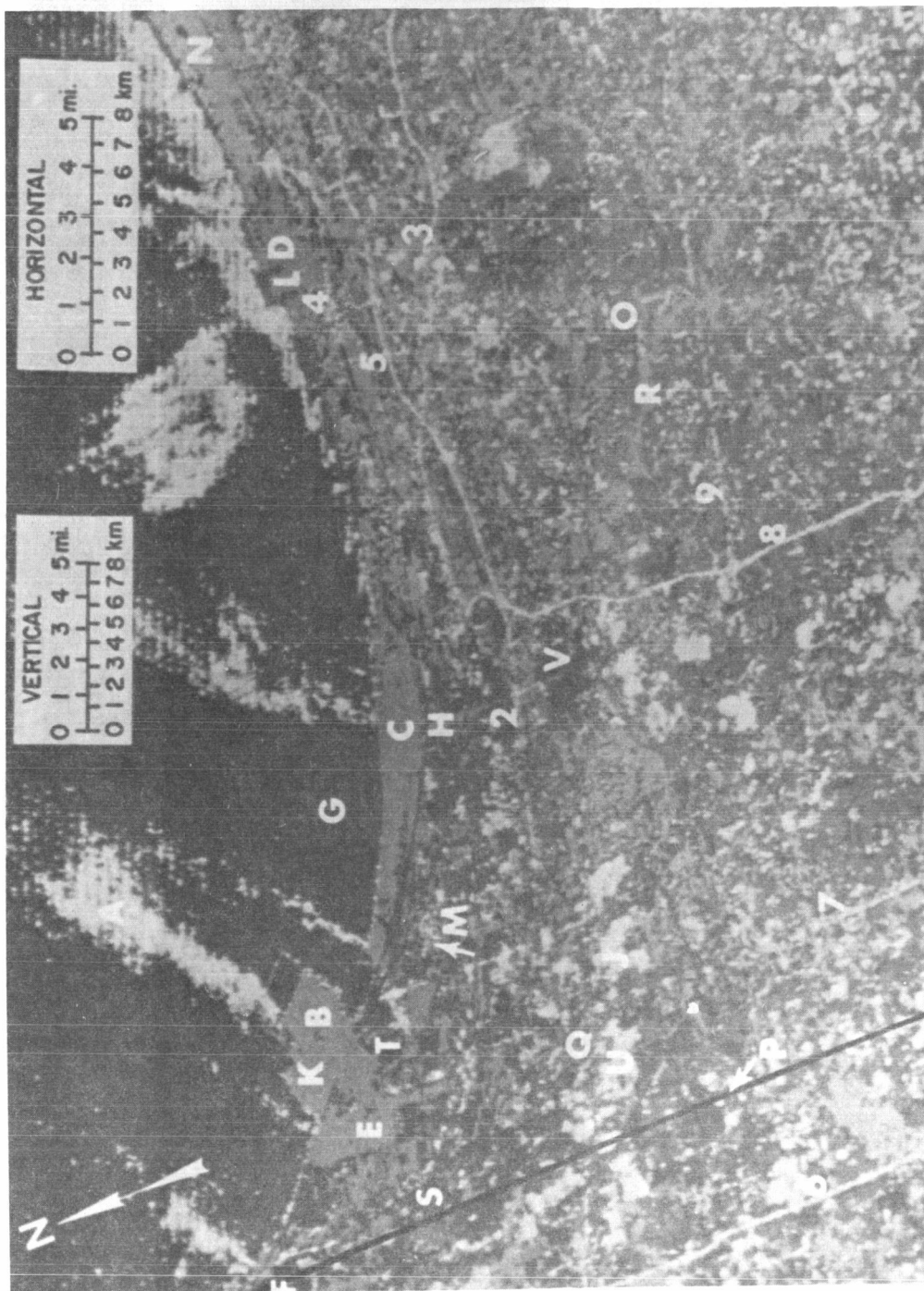


Figure 9. Photo from digital display of computer-implemented land use classification of Gary-Hammond area (see text for explanation of gray levels). Letters/numbers refer to features of interest, a listing of which is found in Table 1.

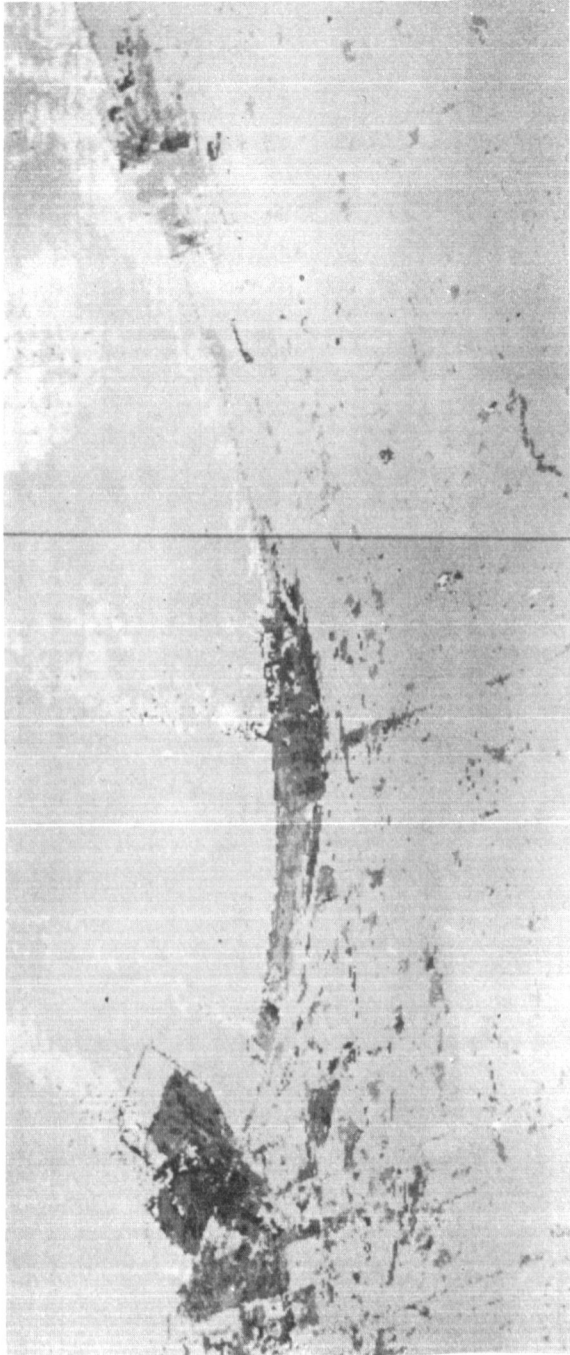


Figure 10. Photo from digital display of computer-implemented land use classification of Gary-Hammond area (northern part of study area) using gray levels which emphasize the industrial land uses. Class shown as black is dark roofing material; dark gray is lighter colored roofing material; medium gray is gravel/sandy areas; smoke is white. All other spectral classes are shown as light gray.

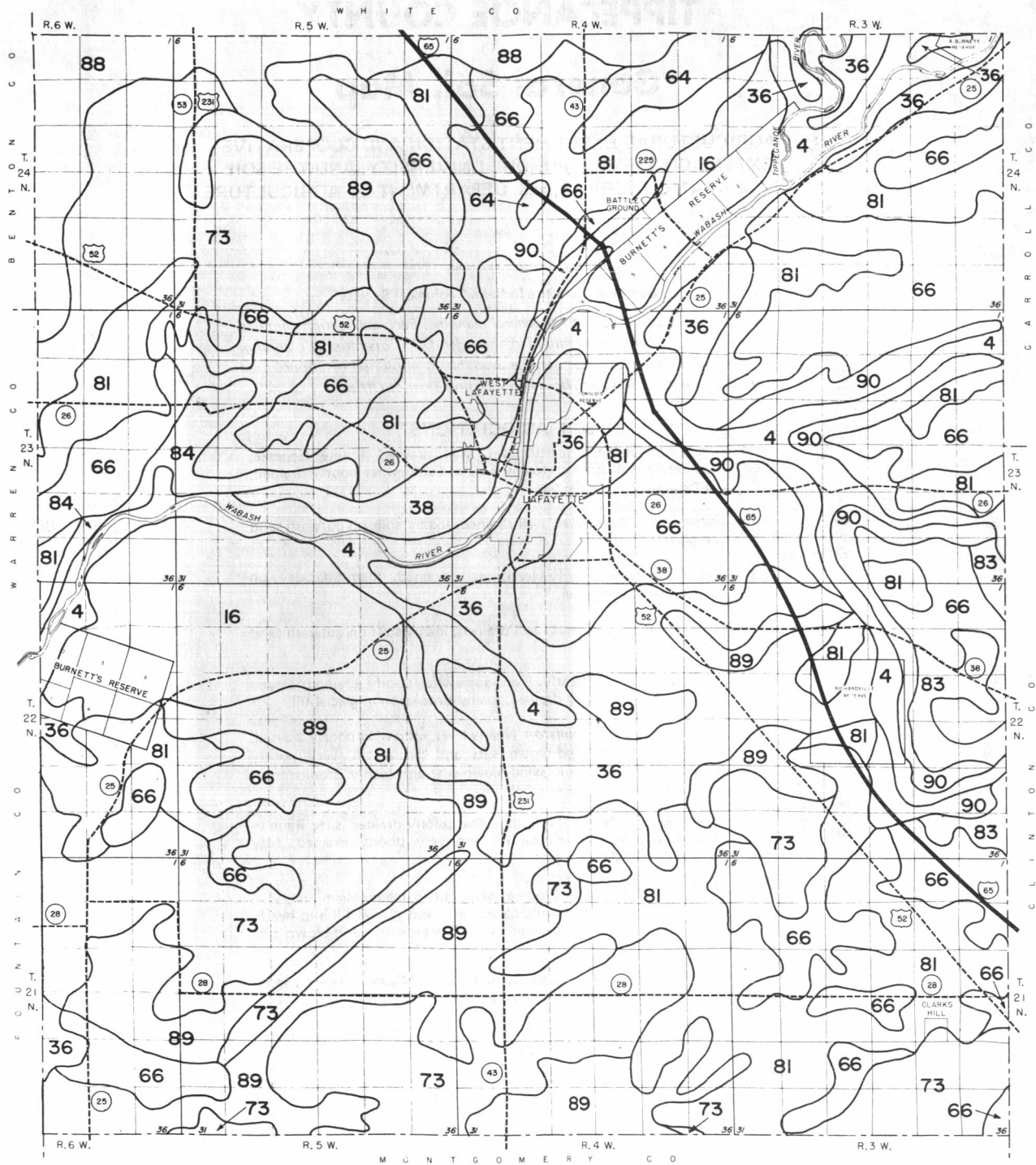
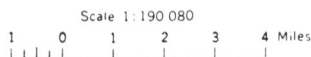


Figure 11. A typical conventional soil association map.

TIPPECANOE COUNTY

General Soil Map

AGRICULTURAL EXPERIMENT STATION AND COOPERATIVE
EXTENSION SERVICE, PURDUE UNIVERSITY; AND THE SOIL
CONSERVATION SERVICE, U.S. DEPARTMENT OF AGRICULTURE



Base map from the Indiana Geological Society

Note: This map is intended for general planning. Each delineation contains soils different from those shown in the legend. For operational planning, use detailed soil maps that may be available in published or unpublished form at the local Soil and Water Conservation District Office.

SOIL ASSOCIATIONS

4. *Genesee-Shoals-Eel*: Nearly level, well drained, loamy Genesee, moderately well drained, loamy Eel, and somewhat poorly drained, loamy Shoals in alluvial deposits.
16. *Elston-Wea*: Nearly level, well drained, loamy soils on outwash sand and gravel.
36. *Ockley-Westland*: Nearly level, well drained, loamy Ockley on outwash sand and gravel.
38. *Ockley-Fox*: Nearly level, well drained, loamy soils on outwash sand and gravel.
64. *Crosby-Brookston*: Nearly level, somewhat poorly drained, clayey Crosby and very poorly drained, loamy Brookston in glacial till.
66. *Fincastle-Ragsdale-Brookston*: Nearly level, somewhat poorly drained, silty Fincastle in wind-blown silts and glacial till, very poorly drained, silty Ragsdale in wind-blown silts and loamy Brookston in glacial till.
73. *Raub-Ragsdale*: Nearly level, somewhat poorly drained, silty Raub in wind-blown silts and glacial till and very poorly drained, silty Ragsdale in wind-blown silts.
81. *Miami-Russell-Fincastle*: Sloping, well drained, loamy Miami in glacial till and silty Russell in wind-blown silts and glacial till and nearly level somewhat poorly drained, silty Fincastle in wind-blown silts and glacial till.
83. *Miami-Crosby*: Sloping, well drained, loamy Miami and nearly level, somewhat poorly drained, clayey Crosby in glacial till.
84. *Miami-Hennepin*: Sloping, well drained, loamy Miami and steep, well drained, shallow, loamy Hennepin in glacial till.
88. *Odell-Chalmers*: Nearly level, somewhat poorly drained, loamy Odell and very poorly drained, loamy Chalmers in glacial till.
89. *Sidell-Parr*: Sloping, well drained, silty Sidell in wind-blown silts and glacial till and loamy Parr in glacial till.
90. *Hennepin-Rodman*: Steep, well drained, shallow, loamy Hennepin in glacial till and excessively drained, shallow, sandy Rodman on sand and gravel.



November, 1971

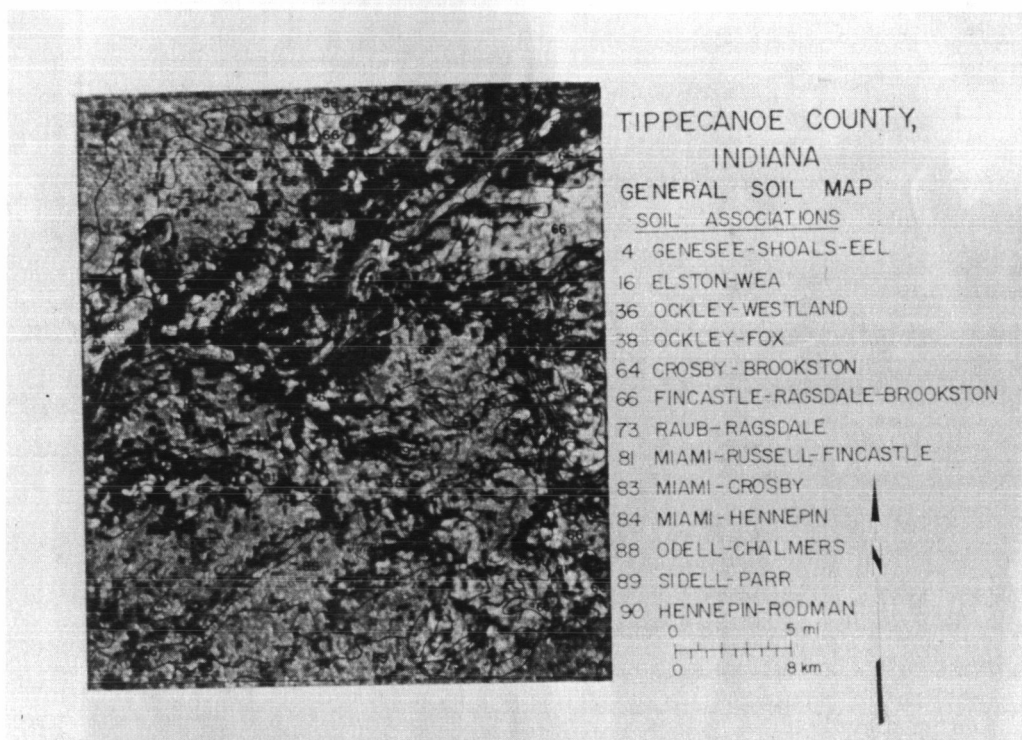


Figure 12. A nonsupervised computer classification of ERTS-1 data showing 10 spectral classes.

THE UTILITY OF ERTS-1 DATA FOR APPLICATIONS IN AGRICULTURE AND FORESTRY

R. Bryan Erb, NASA, Johnson Space Center, Houston, Texas

ABSTRACT

A comprehensive study has been undertaken at the NASA Johnson Space Center to determine the extent to which ERTS-1 data could be used to detect, identify (classify), locate and measure features of applications interest in the disciplines of Agriculture and Forestry. The study areas included: six counties in five states in which were located examples of the most important crops and practices of American agriculture; and a portion of the Sam Houston National Forest, a typical Gulf coastal plain pine forest.

The investigation utilized conventional image interpretation and computer-aided (spectral pattern recognition) analysis using both image products and computer compatible tapes. The emphasis was generally upon the computer-aided techniques.

It was concluded that ERTS-1 data can be used to detect, identify, locate and measure a wide array of features of interest in agriculture and forestry.

INTRODUCTION

This study was part of a comprehensive investigation carried out at the Johnson Space Center (JSC) to support the goals of the Center in exploring applications of space remote sensing. In general, this effort attempted to determine the role of ERTS, aircraft and ground data in the definition and development of the technology for an Earth Resources Survey program.

More specifically, the objectives of the portion of the investigation reported in this paper were:

- (1) To assess the utility of ERTS data to detect, identify, locate and measure features of applications interest in agricultural and forest areas.
- (2) To conduct a cooperative program with the U.S. Department of Agriculture (USDA) - Agricultural Stabilization and Conservation Service (ASCS) to evaluate the utility of ERTS-1 data for their crop inventory needs.

PRECEDING PAGE BLANK NOT FILMED

1 N 74 30711

This investigation was supported by both NASA and the USDA. The involvement of ASCS field personnel was essential to obtaining ground truth and ASCS also supported the analyses with staff located at Houston. The U.S. Forest Service (USFS) also has staff members located at Houston, and they supported the investigation in both analysis and field work.

TEST SITES

The agricultural test sites, one each in Montana, Nebraska, Iowa and Georgia and two in California, were chosen by ASCS to cover examples of the most important crops and practices in American agriculture. The six sites chosen comprise a subset of 18 sites in which ASCS is conducting, at the county level, an image interpretation investigation of ERTS data. The ASCS County executive personnel acquired complete descriptions of all crops in a 3 by 10 km (2 x 6 miles) test area once each year and then provided updates of the descriptions for 50 fields in each area synchronous with each ERTS pass. No aircraft flights were made over these test sites, however, ASCS photography was available.

The forest test area was the Raven District of the Sam Houston National Forest (SHNF). This is a typical pine forest of the Gulf coastal plain, located about 90 miles north of the city of Houston. The USFS Team at JSC has been carrying out remote sensing investigations in the SHNF for over two years and had acquired detailed ground data and several aircraft flights which were utilized by the ERTS investigation team.

APPROACH

The investigation utilized a number of analytical techniques and made some attempt at comparisons among them in terms of the ability to extract information from the ERTS data. The investigation teams were organized to include specialists in the appropriate scientific disciplines, persons skilled in image interpretation and others skilled in digital techniques. This mix of skills worked well and provided excellent cross-training of all personnel.

Image interpretation was carried out on several types of materials as follows:

- a. GSFC Material: Enlarged 70 mm B&W
 9 1/2 inch B&W
 Color Composites

- b. JSC first generation images created from digital tapes.

Some efforts were expended on image enhancement and additive color projection techniques. Equipment used included:

- a. I²S Model 2000 multichannel film viewer
- b. I²S Mini Addcol

c. Itek Additive Color Viewer/Printer

The main thrust of the investigation was focused on computer-aided processing of the digital data by spectral pattern recognition techniques. Both nonsupervised and supervised techniques were employed.

For each area of investigation an attempt was made to quantify how well applications features could be:

- a. detected - i.e., established that something unique was there
- b. identified - i.e., assigned to some classification
- c. located - i.e., position established with respect to a geographic grid or readily identified control points
- d. measured - i.e., the areal extent determined.

The term "applications features" means regions on the ground which can be precisely located and described and which are directly related to some resource which is manageable and to which remote sensing could be applied. For example, a stand of pine timber or a field of corn would be an applications feature.

It was found that a classification hierarchy was almost indispensable in conducting an investigation such as this. The classification scheme served as a guide to increasingly refined discriminations and as a meterstick against which to compare performance of various information extraction techniques. The classification hierarchy used for the most general descriptions is close to that given in USDI Circular 671, but modified at the Level II to accommodate computer-aided spectral analysis rather than human interpretation of the spatial cues contained in the data. The classifications at the more detailed levels were generated by the investigators for the purposes of the present effort and are shown in Figures 1 and 2.

RESULTS

The results reported herein represent only the highlights of the investigation. Much more detailed accounts will be given in documents to be published by JSC.

Detection

Agricultural vs. nonagricultural and cropland vs. noncropland could be distinguished quite well by image interpretation using essentially spatial cues. The same discrimination using nonsupervised computer-aided techniques was only fair. Image interpretation techniques were used to detect individual fields. In areas of strip/fallow farming for green winter wheat, fields aligned north-south could be detected as small as

45-60 meters in width. Fields aligned east-west, however, could not be detected unless 90-135 meters wide. Rectangular fields with good contrast could be detected in parcels down to 4-16 hectares in size. The boundary between fields of like appearance could be detected when the gap was 12 meters and of high contrast to the fields. Pine timber stands could be detected by image interpretation down to plots 4 hectares in size. Water bodies were detectable under the best conditions down to 1 or 2 hectares in size. Rural settlements, being more complex features, could not be detected with confidence unless 40 hectares in size. Forest right-of-ways, such as for roads, power or pipelines, could be detected when as narrow as 28 meters.

A test of detectability limits for various image media was carried out on 30 forest features which included: timber stands of 2-75 hectares, right-of-ways and streams 14+M width and lakes of 2 or more hectares in areal extent. Using six different image media various numbers of the features could be detected as follows:

° JSC color composites from CCT	21 of 30 features
° Band 5, 9 1/2" transparency	20
° Band 6	16
° GSFC color composite	15
° Band 7	11
° Band 4	4

Identification

A major portion of the investigation effort was focused on the identification or classification of specific features on the ground. The test areas were classified by the various techniques discussed above and the results were displayed in the form of classification maps. The classifications resulting from image interpretation were depicted by conventional cartographic techniques. The results of image enhancement efforts were recorded photographically. Results of digital classifications were recorded on film using the same tape-to-film screening and recording device (data analysis station) with which first generation color composites were made from ERTS digital data. Typical examples of the classification results from the digital analysis are shown in Figures 3 through 5 for Hill County, Montana, Holt County, Nebraska and the SHNF in Texas.

The details of the classification performance for these and other sites is given in Figures 6 and 7 for agriculture and forest features respectively.

The results shown in Figure 6 pertain to data acquired during the 1972 growing season. In the case of Hill County, Montana, data was obtained late in the year (August) and much of the wheat had been harvested. Recent work for a series of three data sets spanning the 1973 growing season shows improved performance in classification of wheat if registered

data sets from two or three ERTS passes are used. Wheat classification accuracies in the range of 90-95% were obtained with 5-10% of the confusion crops (barley) identified as wheat when such temporal data sets were analyzed.

Location

Some effort was devoted to assessing the accuracy with which specific features could be located on the earth's surface. One technique used involved the construction of a custom Universal Transverse Mercator (UTM) grid from control points taken off 1:24,000 topographic maps. Distinct features in the ERTS data such as field corners in Hill County, Montana, could then be located to an accuracy of approximately 200 meters. A similar approach was used to superimpose a UTM grid on a portion of an ERTS scene by correcting the location of each pixel digitally again using control from maps. An example of this is described in a companion paper.* It should be noted that the 200 meter figure is considered to hold only close to the region for which control was established.

Measurement

The areal extent of the various features was determined by several techniques both manual and semi-automatic. The results of typical determinations are given in Figure 8.

SCIENTIFIC AND TECHNICAL FINDINGS

The main scientific and technical findings were:

- ° Agricultural and cropland can be separated from other classes of land use and this is best done by conventional image interpretation using spatial cues.
- ° Crop types can be classified best by spectral pattern recognition techniques. Accuracies in the range of 70-90% can be achieved with single data sets. It should be noted that this is as good performance as has been historically achieved with aircraft data.
- ° Use of a registered data set (two or more passes) can improve classification performance to the 95% range.
- ° A phenomena of the MSS data known as blooming is apparent at boundaries of fields of high contrast, thus obscuring the true boundary and making accurate area measurement difficult.
- ° Surface features can be located to within about 200 meters of their true position on the earth (over small geographic areas).

* "The Utility of ERTS-1 Data for Applications in Land Use Classification," J. E. Dornbach and G. E. McKain, Third ERTS Symposium, Washington, D.C., December 10-12, 1973.

- ° Area measurements of selected fields can be made from ERTS data to accuracies on the order of 90%.

- ° Classification hierarchy is useful for focusing an investigation and ERTS data can be used to discriminate between some classes to Level IV, (e.g., alfalfa vs. cotton) and in one case to a Level V (corn vs. popcorn).

- ° Training field data derived in Imperial County was used to classify in Butte County (700 Km distance) with some success. For some features no recognition was obtained but for alfalfa and bare soil test field results were 70 and 80% respectively.

- ° ERTS data can be used to detect, classify and measure some Level III and IV features typical of Texas forests.

- ° Accuracy of classification is in the range of 75 to 90%.

- ° Classification accuracy at Levels III and IV is better by ADP techniques than by image interpretation.

- ° Area measurement of large timber stands from ERTS data agrees with data from aircraft imagery to a typical accuracy of 89%.

- ° Effects of a light ground fire (set to clear brush) over a 40 hectare stand were clearly visible on ERTS data.

- ° A two hectare portion of a pine stand which was infested by pine-bark beetle was detected indirectly in exploring the cause for misclassification in a supervised ADP analysis.

APPLICATIONS

Two applications activities with user agencies are underway utilizing in part the understanding and techniques derived in this investigation.

One application is a crop acreage inventory activity with the USDA. A plan is currently being developed for a large area survey of wheat.

The other is a project with the Southern and Pacific Northwest Regions of the U.S. Forest Service. This activity is a continuation of a project to explore the application of aircraft data which started in 1971 with the SHNF test site. Two Forest Service employees resident at JSC are undertaking analysis of ERTS data over the Sabine National Forest to compare ERTS results with those derived from aircraft and from the Skylab Earth Resources Experiment Package (EREP).

CONCLUSIONS

The general conclusions which can be stated at this time are the following:

- ° ERTS-1 data can be used to detect, identify, locate and measure a wide array of features of interest in agriculture and forestry.
- ° The utility of the information extracted from ERTS-1 data is likely to be greatest for large area applications.
- ° The computer-aided analysis techniques perform as well or better than conventional image interpretation, especially for the more detailed classifications, but both techniques will be useful for most Earth Resource Surveys.
- ° Classification performance with ERTS data is as good as has been historically achieved with aircraft data.
- ° The feasibility of large area crop and forest resource classification has been demonstrated and elements of appropriate agencies are working with NASA to pursue specific applications.

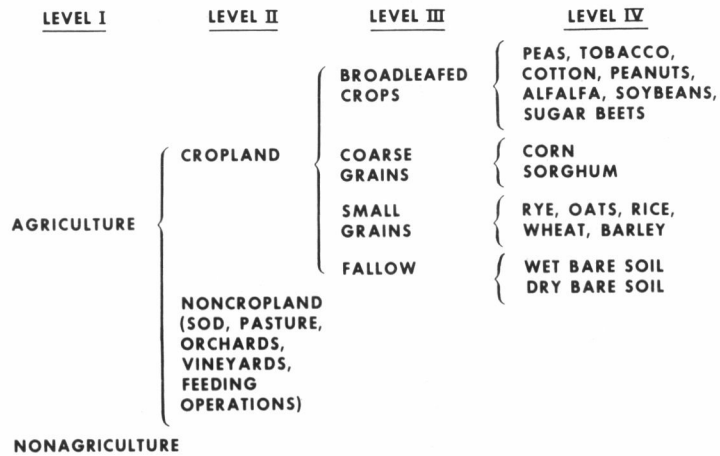
AGRICULTURE CLASSIFICATION HIERARCHY

Figure 1

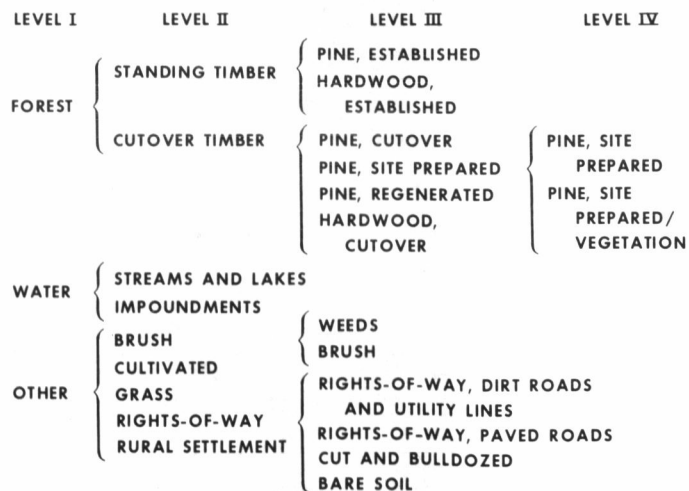
FOREST CLASSIFICATION HIERARCHY

Figure 2

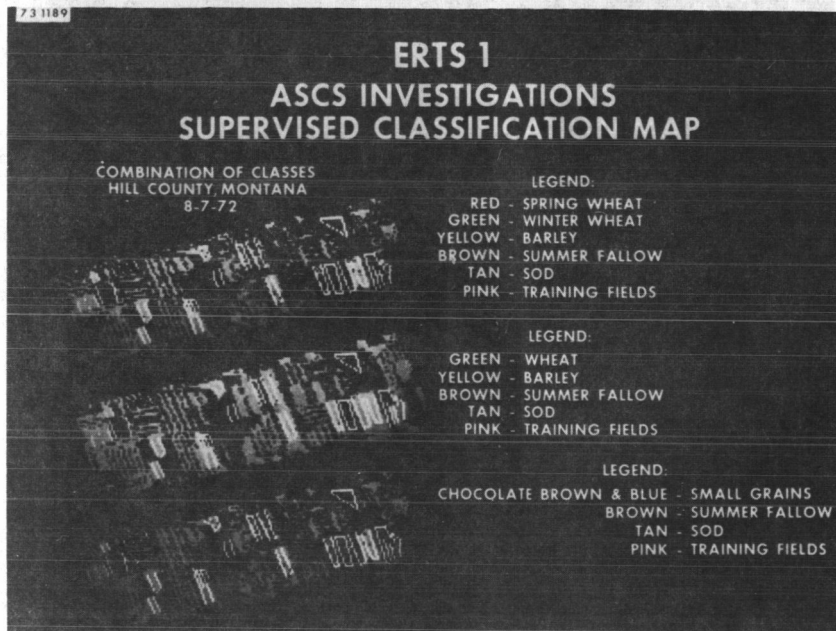


Figure 3

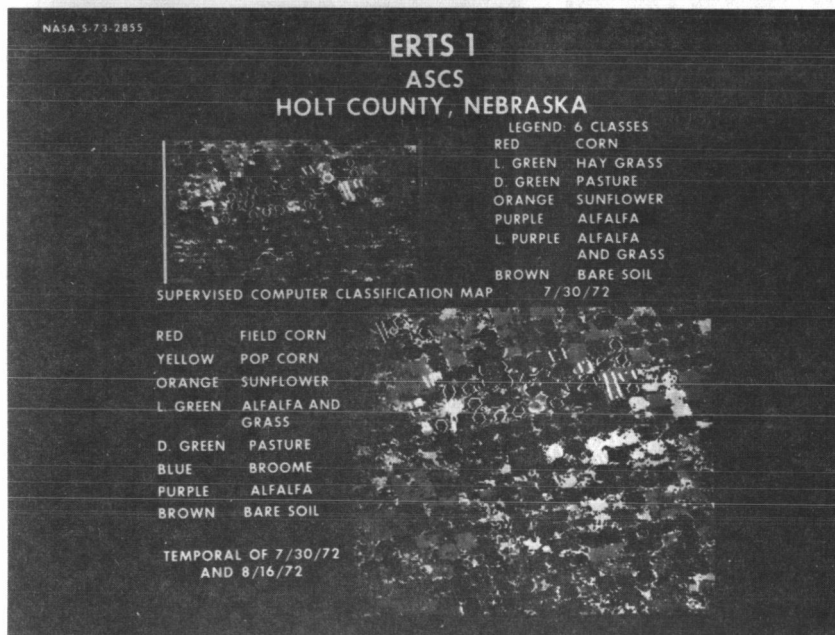


Figure 4

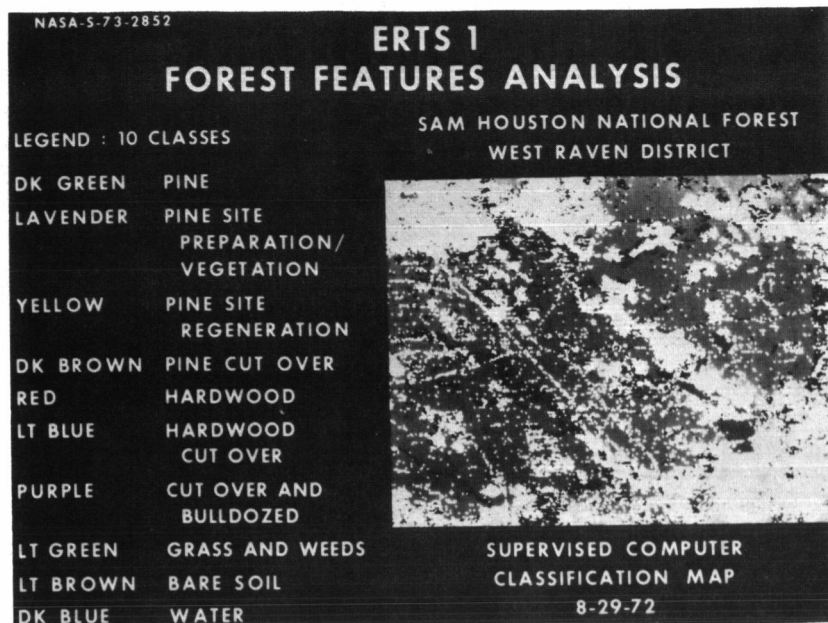


Figure 5

NASA-5-73-3274

AGRICULTURE-RESULTS IDENTIFICATION (CLASSIFICATION)

FEATURE	METHOD	PERFORMANCE %
● SMALL GRAINS, GRAIN STUBBLE	IMAGE INTERPRETATION (SINGLE DATA SET)	33-59
● SOD		91
● SUMMER FALLOW		88
● SMALL GRAINS	SUPERVISED ADP (SINGLE DATA SET)	96
● SOD		90
● SUMMER FALLOW		87
● WHEAT, BARLEY		65-88
● TRUCK FARMING CROPS		78
● CORN FIELDS	SUPERVISED ADP (SINGLE DATA SET)	73 OF 76 FIELDS
● CORN, POPCORN, SUNFLOWERS	SUPERVISED ADP (REGISTERED SET OF TWO PASSES)	95-99

Figure 6

FOREST - RESULTS

IDENTIFICATION (CLASSIFICATION)

<u>FEATURE</u>	<u>METHOD</u>	<u>PERFORMANCE</u>
● TIMBER CLASSES AT LEVEL III PINE, SITE PREPARED, REGENERATED	SUPERVISED ADP	85 - 100%, TEST BY PIXEL
● TIMBER CLASSES AT LEVEL IV SITE PREPARED VS SITE PREPARED/VEGETATED		88 - 100%, TEST BY PIXEL
● 14 FOREST CLASSES ACCURACY OF CLASSIFICATION COMPARED TO GROUND TRUTH MAPS	IMAGE INTERPRETATION SINGLE BAND MULTIPLE BANDS JSC COMPOSITE I ² S ENHANCEMENT UNSUPERVISED ADP SUPERVISED ADP	7 CLASSES 56% 10 66 10 69 7 59 14 87 12 78

Figure 7

AGRICULTURE AND FOREST - RESULTS

MEASUREMENT

<u>FEATURE</u>	<u>METHOD</u>	<u>PERFORMANCE</u> (% ERROR) REFERENCE TO GROUND TRUTH
● ESTABLISHED PINE 3000+ HECTARES	SUPERVISED ADP PLANIMETERING OF RECTIFIED CLASSIFI- CATION MAP UNSUPERVISED ADP PIXEL COUNT	- 11% ± 3 TO 15%
● LONG NARROW FIELDS 12 - 70 HECTARES	HILL CO., MONTANA PLANIMETERING OF SCALED COLOR ENHANCEMENTS	± 2 - 17%
● SQUARE TO RECTANGU- LAR FIELDS, 30 OR LARGER HECTARES	IMPERIAL CO., CALIF.	± 1 - 3%
● RICE, 65 HECTARES	SAN JOAQUIN, CALIF. COUNT OF ADP PIXELS	± 5 - 10%

Figure 8

CROP IDENTIFICATION AND ACREAGE MEASUREMENT UTILIZING ERTS IMAGERY

William H. Wigton and Donald H. Von Steen, *Statistical Reporting Service, U. S. Department of Agriculture*

ABSTRACT

The Statistical Reporting Service of the U.S. Department of Agriculture as a principle investigator for NASA, is evaluating ERTS-1 imagery as a potential tool for estimating crop acreage. The Statistical Reporting Service makes crop and livestock forecasts and estimates throughout the year, across the U.S. A main data source for the estimates is obtained by enumerating small land parcels that have been randomly selected from the total U.S. land area. These small parcels are being used as ground observations in this investigation. The test sites are located in Missouri, Kansas, Idaho, and South Dakota. The major crops of interest are wheat, cotton, corn, soybeans, sugar beets, potatoes, oats, alfalfa, and grain sorghum. Some of the crops are unique to a given site while others are common in two or three States. This provides an opportunity to observe crops grown under different conditions. Results for the Missouri test site are presented in this report. Results of temporal overlays, unequal prior probabilities, and sample classifiers are discussed. The amount of improvement that each technique contributes is shown in terms of overall performance. The results show that useful information for making crop acreage estimates can be obtained from ERTS-1 data.

INTRODUCTION

SRS of the U.S. Department of Agriculture is the main fact-gathering agency of the USDA. The name of the agency has changed several times, but the objective of collecting and disseminating primary data on agriculture has remained the same for more than 100 years. Crop acreage and production as well as livestock, prices, labor, and farm expenditures are estimated.

Many of these estimates are generated from a general purpose land area sample survey conducted in June and based on 17,000 segments selected at random from the total U.S. land area. This is a sample stratified by States and within states by land use. Segments for a State are defined within each category of land use or stratum and a sample of these segments is selected. Stratification by land use has made it possible to sample more efficiently for all items because sample segments are allocated to each stratum individually. At the time of field enumeration, the interviewer must be able to identify the boundaries of the sample segment and collect information which applies to the land inside these boundaries. ERTS imagery may also be helpful in stratification and in the segment selection process; we have not used ERTS for these purposes yet, but plan to try this soon.

1 N 74 30712

Keep in mind that we use these segments to generate livestock and price estimates as well as crop acreages, and for this reason, ERTS will not replace our present system for major items. Secondly, our estimates have sampling errors between 2 percent and 5 percent at the U.S. level, and between 5 and 10 percent at the state level for major commodities. We do not go much below the state level for our probability survey since the sample was not designed to provide estimates below the state level.

PROCEDURES

Twenty-nine segments of approximately one square mile size were located in two ERTS frames covering most of Crop Reporting District No. 9 in Southeast Missouri. The segments are located over a 10,000 square mile area. Information on the crop and acreage of each field was obtained by SRS enumerators during the summer of 1972; this data has been used for training the classifier and testing its performance. ERTS data from three dates was included in the analysis. Data collected September 14 and October 2, 1972 was registered (overlaid) to data collected August 26, 1973. The temporal overlay alleviated the necessity of locating fields in three different data sets, as well as permitted a test of the utility of temporal data in the classification.

The ERTS data was also geometrically corrected to facilitate locating the coordinates of segments and fields. In the geometric correction process the MSS data is rotated, deskewed, and scaled to 1/24,000 scale. The geometrically corrected data was overlaid on 1/24,000 scale topographic maps on which the segments had been outlined. The individual segments were then classified (clustered) using the non-supervised classifier in LARSYS. Field coordinates were located on the map output from this classification. Final classifications were carried out using the supervised classifier in LARSYS.1/

RESULTS

The results are presented in the form of a classification matrix. Table 1 shows the classification results obtained when using quadratic discriminant functions with equal prior probabilities. That is, it is assumed that the probability of occurrence of corn is the same as the probability for cotton, and so forth. Because of the small size of the data set the whole data set was used in training the classifier. This is a nine channel classification with data from three ERTS passes. The four major classes, cotton, corn, soybeans, and grass were classified 74, 59, 40, and 57 percent correctly, respectively. Overall performance was 59 percent.

1/

We gratefully acknowledge the assistance of Dr. Marvin Bauer, Purdue, LARS, for technical assistance and in reviewing this paper. Also, LARS for giving support in providing the temporal overlays for this analysis. However, the authors accept responsibility for the suitability of the methods employed and interpretation of the results.

The assumption of equal prior probabilities is many times not valid, but is frequently used because of lack of information. The prior probabilities used in this study came from an earlier survey, the June 1972 Enumerative Survey. Other sources of prior probability information are historic data, for example, last year's farm census. Classification results using unequal prior probabilities are shown in Table 2. Comparing the results in Table 1 to those in Table 2 it is seen that the overall performance has been increased from 59 to 71 percent; and secondly, that the total number of points classified into each class is much closer to the actual number of points present. For example from Table 2, the total number of points classified as cotton is 906 which is considerably closer to 927, the actual number present. The total number of corn points, 43 is rather close to the actual 58 present. For soybeans, the total of 866, is very close to the actual 852 present. Two hundred seventy-seven (277) points were classified as grass compared to 240 actual points of this crop. Further, the statistical properties of estimates made on this basis are better since, if the assumption of normality for the data set is correct, and the prior probabilities are correct, we obtain unbiased estimates.

Most classifications reported by other researchers have not used prior probabilities. While the overall error rate reported here is higher than reported by some researchers, this study was based on a statistical sampling of the entire land area in the study areas rather than on purposely selected test sites.

Table 3 shows results of using a sample classifier rather than a point classifier used in the above work. In a point classifier system each point in a field can be assigned to any of the groups. With the sample classifier all points in the field are assigned to the same class or crop. One drawback to this procedure is that there were a large number of fields that were not classified because the technique requires $p+1$ data points in order to form the statistics necessary to assign it to a crop (where p is the length of the vector of measurements). However, if enough points are present, classification performance has generally been found to be better than for the point classifier.

In the work we have done in Missouri using the sample classifier, about 40 percent of the fields were not classified because the required number of points for the classifier (10 in this particular case) exceeded the number of points present within the defined fields. Of the total number of fields 33 percent were correctly identified. Considering only those fields which were classified, 54 percent were classified correctly.

In Missouri 71 percent of the fields were less than 20 acres, but account for 32 percent of the total area. In our Kansas site, 20 percent of the fields were less than 20 acres, but account for only 1.5 percent of the total land areas. In South

Dakota, 40 percent of the fields were less than 20 acres, and account for 15 percent of the area. In Idaho, 74 percent of the fields were less than 20 acres, and account for 25 percent of the area. If 20 acres is a critical field size for the classifier, we would expect to do well in making acreage estimates, in Kansas, but in Missouri only a little more than 50 percent of the acreage would be accounted for.

Next, the information gained from the temporal overlay is evaluated. In Table 4 classification results for single dates are compared to the multitemporal classifications already presented. The overall classification performance was improved about 10 percent by the addition of temporal data with even greater improvement for several of the individual classes.

DISCUSSION

The results presented do not show the classification accuracy to be as high as that found by other investigators. The lower performance level is primarily attributed to the greater variation in crops, soils, and weather over a 10,000 square mile area than is found over smaller areas. And, secondly to the kind of crops which were being discriminated. Still, the classifications contain enough information to be useful in estimating crop acreages over large areas, particularly if regression or some other technique is used to improve the estimate.

A regression estimator can be used to reduce the variance of the estimate. For example, if a large area is classified and there is an r^2 of .50 between the discriminant function classification and what the ground acreage data shows. We can adjust our area sample estimates by the complete classified data and obtain a reduced variance of $\Sigma y^2 (1-r^2) / n(n-2)$ where r^2 is the correlation coefficient squared. The estimate of the variance of the comparable statistic without using ERTS data is $\Sigma y^2 / n(n-1)$ which would be nearly twice as large when $r^2 = .50$.

If we were to classify a sample of points we would have a double sample and the variance would be:

$$\frac{\Sigma y^2 (1-r^2)}{n(n-2)} + \frac{\Sigma y^2 (r^2)}{n m}$$

where n = the sample size from JES and m = the sample size from ERTS.

Table 1. Classification matrix of quadratic discriminant functions with equal prior probabilities using data from three overflights,¹ Missouri Study Area.

	No. of sample points	Percent Correct	Number of samples classified into				
			Cotton	Corn	Soybean	Grass	Misc.
Cotton	927	74.3	689	21	83	36	98
Corn	58	58.6	4	34	3	10	7
Soybeans	852	39.7	101	49	338	137	227
Grass	240	57.1	34	22	22	137	25
Misc.	140	75.0	14	5	7	9	105
Totals	2217		842	131	453	329	462

Overall performance 58.8 percent

- ¹ August 26, 1972, MSS bands 4, 5, 7.
September 14, 1972, MSS bands 5, 7.
October 2, 1972, MSS bands 4, 5, 6, 7.

Table 2. Classification matrix of quadratic discriminant functions with unequal prior probabilities using data from three overflights,¹ Missouri Study Area.

	No. of sample points	Percent Correct	Number of samples classified into				
			Cotton	Corn	Soybean	Grass	Misc.
Cotton	927	79.7	739	2	137	26	23
Corn	58	44.8	9	26	7	14	1
Soybeans	852	71.8	99	12	612	96	23
Grass	240	53.3	42	1	66	128	2
Misc.	140	89.3	17	2	44	13	64
Totals	2217		906	43	866	277	125

Overall performance 70.8 percent

- ¹ August 26, 1972, MSS bands 4, 5, 7.
September 14, 1972, MSS bands 5, 7.
October 2, 1972, MSS bands 4, 5, 6, 7.

Table 3. Sample classification matrix based on data from 3 overflights. Missouri Study Area.

Group	No. of fields	Per-cent fields correct	No. of points	Per-cent points correct	Cotton	Corn	Soy beans	Grass	Misc.	Not classified
Cotton	38	63.2	927	85.0	24	0	2	0	1	11
Corn	7	14.3	58	20.7	0	1	0	1	1	4
Soybeans	58	25.9	852	44.2	9	3	15	3	8	20
Grass	31	9.7	240	29.6	3	1	1	3	2	21
Misc.	9	44.4	140	65.7	1	0	1	1	4	2
Totals	143	32.9	2217	60.4	37	5	19	8	16	58

Table 4. Comparison of multitemporal classification performance to classifications of single dates.^{1,2} Missouri Study Area.

Group	Multitemporal	Aug. 26	Sept. 14	Oct. 2
Cotton	79.7	60.6	69.7	73.2
Corn	44.8	10.3	0.0	12.1
Soybeans	71.8	86.0	67.6	62.4
Grass	53.3	8.3	42.1	27.9
Misc.	89.3	31.4	22.8	17.9
Overall	70.8	61.6	61.1	59.2

¹Unequal prior probabilities were used for all classifications.

²August 26, 1972, MSS bands 4, 5, 7.
 September 14, 1972, MSS bands 5, 7.
 October 2, 1972, MSS bands 4, 5, 6, 7.

VEGETATION DENSITY AS DEDUCED FROM ERTS-1 MSS RESPONSE

C. L. Wiegand, H. W. Gausman, J. A. Cuellar, A. H. Gerbermann, and A. J. Richardson,
USDA, Agricultural Research Service, Weslaco, Texas

ABSTRACT

Reflectance from vegetation increases with increasing vegetation density in the 0.75- to 1.35- μ m wavelength interval. Therefore, ERTS-1 bands 6 (0.7 to 0.8 μ m) and 7 (0.8 to 1.1 μ m) contain information that should relate to the probable yield of crops and the animal carrying capacity of rangeland. On the other hand, reflectance from vegetation is typically less from vegetation than from bare soil and is essentially constant in the visible wavelengths as vegetation density increases; consequently, the decreased response observed in ERTS bands 4 (0.5 to 0.6 μ m) and 5 (0.6 to 0.7 μ m) as vegetation increases is mainly caused by vegetation obscuring soil reflectance. The ratio of band 5 to band 7 (5/7) or band 7 minus band 5 (7-5) are, in addition to bands 6 and 7, practical indicators of vegetative cover and density for users of ERTS-1 data.

The results of an experiment designed specifically to test the relations among leaf area index (LAI), plant population, plant cover and plant height, and the ERTS-1 MSS responses for 3 corn, 10 sorghum, and 10 cotton fields are also given. Because of clouds, only one ERTS-1 pass (May 27, scene 1308-16323) yielded MSS data and that for only bands 4, 5, and 6. The coefficient for the linear correlation between LAI and band 6 digital counts was 0.823** for the 10 cotton fields and 0.841** for the combined sorghum and corn fields. The correlation coefficient between LAI and band 6 minus band 5 digital counts was 0.888** for cotton fields and 0.768** for the corn and sorghum fields. The four plant parameters explained 87 to 93% of the variability in the band 6 digital counts and from 59 to 90% of the variation in bands 4 and 5. Plant population was as useful as LAI for characterizing the sorghum and corn fields, and plant height was as good as LAI for characterizing cotton fields. These findings generally support the utility of ERTS-1 data for explaining variability in green biomass, harvestable forage and other indicators of productivity.

N74 30713

INTRODUCTION

The earth's vegetation is one of its most valuable resources. Plants are the traceable source of most of the food and fiber needed by humans and other animals, and past generations of plants provide the energy reserves of coal and petroleum that concern us today. Plants are also intimately involved in the hydrologic and energy balances of the earth.

Net assimilation, or dry matter production, by vegetation is related to the number and photosynthetic area of leaves. Fortunately, the spectral response observed when viewing vegetation from space is dominated by the leaves. Thus the spectral response of vegetation in the ERTS-1 data is worth examining in terms of vegetation cover, vegetation density, and other productivity indicators of range, forest, and crop land.

Agriculturalists, foresters, and range scientists use various parameters to indicate the vegetation density or potential productivity of vegetation. Foresters use tree girth, crown diameter, tree height, leaf area index, and timber volume. Range scientists use harvestable forage and animal carrying capacity (acres or hectares required to maintain an animal year round). Ecologists use estimates of biomass. Agriculturalists use leaf area index (LAI), percent ground cover, plant height, plant population per unit ground area, and other measures of vegetation conditions.

The purposes of this paper are (a) to point out the information available to ERTS users about vegetative cover and density in the ERTS-1 multispectral scanner (MSS) data and (b) to report data relating the MSS response to leaf area index (LAI), plant population, ground cover, and plant height.

LITERATURE REVIEW

ERTS-1 bands 4, 5, and 7 color composites yield images with color tones similar to those of color infrared photographic film. Thomas et al. (1966, 1967) and Stanhill et al. (1973), respectively, have shown that light reflectance from cotton and wheat fields is strongly affected by the amount of plant material or percent ground covered by the vegetation. In their studies, light transmission of color infrared film accounted for 75 and 49% of the variation in cotton lint and wheat grain yields, respectively.

Von Steen, Leamer, and Gerbermann (1969) found statistically significant correlations among preharvest yield indicators (open bolls, number of plants, percent ground cover, plant height, weight plant material per plot) and optical density of aerial infrared film for cotton, grain sorghum, carrots, cabbage, and onions.

Stoner, Baumgardner, and Cipra (1972) related the LAI of corn to the ratio of visible and reflective infrared channels of aircraft optical mechanical scanner data on two flight dates in July. The combined MSS data for the two flight dates yielded a coefficient of determination, R^2 , of 0.968 between LAI, that ranged from 0 to 4, and the ratio of two MSS channels ($1.0 - 1.4 \mu\text{m} / 0.61 - 0.70 \mu\text{m}$).

Pearson and Miller (1972) developed and tested both a two-channel ratioing technique and a multispectral pattern recognition technique to compare spectral biomass estimates of grassland with biomass values taken from clipped plots. Biomass estimates were made with an accuracy greater than 95% with a two-channel spectral ratio method using a small hand-held radiometer. Eighty to 90% of the variation in biomass values taken from clipped plots along a flight line could be explained by the airborne MSS data over the same area. Kanemasu (In Press) found that the ratio of reflectances at 0.545 and 0.655 closely followed crop growth and development and concluded that it was a good indicator of soil exposure and crop maturity.

A number of practical applications of the ERTS-1 data to determining vegetation types and amounts, or seasonal effects were previously reported (Freden, Mercanti, and Becker, 1973). For example, Carneggie and DeGloria (1973) obtained information from the ERTS-1 scenes of California on the distribution, yield, condition and availability of forage. Seevers and Drew (1973) identified gross differences in forage density and range condition within given range sites in the sand hills of Nebraska. Heath and Parker (1973) used computer-aided interpretations to classify timber stands and range plants in the Houston area. Dethier (1973) reported that the brown wave (fall vegetation senescence) could be readily detected in the Appalachian and Mississippi Valley corridors and suggested that specific phenological events such as crop maturity and leaf fall could be mapped for specific sites and possibly entire regions from the ERTS-1 data.

PRINCIPLES

The wavelengths of light that are effective for photosynthesis cover the interval from 0.4 to 0.7 μm . Bands 4, 5, 6 and 7 of the ERTS-1 MSS correspond to the spectral intervals 0.5 to 0.6, 0.6 to 0.7, 0.7 to 0.8, and 0.8 to 1.1 μm , respectively. Laboratory data on the spectral reflectance of leaves in terms of the number of leaf layers is given in Fig. 1, taken from Allen and Richardson (1968), except that the ERTS-1 MSS bands have been superimposed. Notice that in the 0.75- to 1.35- μm interval, the reflectance of vegetation is very high and that the signal strength increases as the number of leaf layers, or the vegetation density, increases. This finding indicates that ERTS-1 band 7 responses, and to a lesser extent band 6 responses, should clearly indicate differences in vegetation density.

There is a one-to-one correspondence between yield and vegetation density of crops grown for hay or forage. For plants grown for their seed, fruit, roots, or fiber, there is usually a close correlation between potential production and plant vigor. Axiomatically, healthy non-stressed plants develop larger and more dense canopies and yield better than those growing under suboptimal conditions.

The ERTS-1 responses can be related to the stage of crop development. Spectral crop calendars useful in temporal analyses are possible (Steiner, 1970; Lauer, 1971). The ERTS-1 responses can also be directly related to percent ground cover, plant height or other crop parameters that are correlated with reflectance.

Figure 1 also shows that in the interval 0.5 to 0.75 μm , the reflectance from vegetation is virtually the same regardless of the number of layers of leaves in the plant canopy. The implication here is that the photosynthetic potential of green plants can not be deduced directly from the photosynthetically active wavelengths. Physiological disturbances in plants that decrease chlorophyll content may be detectable, compared with healthy plants, because chlorophyll is a strong absorber of visible light. Thus, the ERTS-1 bands 4, 5, and 6 are valuable to help identify deviations from healthy plants. Plants with physiological disturbances are less vigorous than healthy plants as manifested by fewer leaves or foliar discoloration (Wiegand, Gausman, and Allen, 1972). The information about plant density inferred from the reflective infrared bands 6 and 7 and the information about plant pigmentation obtained from bands 4 and 5 complement each other.

In ERTS-1 bands 6 and 7, the observed reflectance of the soil background is usually less than that of vegetation whereas in bands 4 and 5 it is typically greater than that of vegetation. Therefore, in ERTS-1 band 4 and 5 wavelengths, the soil background dominates the signal up to a fairly high vegetative cover.

Because the ERTS-1 MSS signals recorded for variable ground cover conditions (vegetation density conditions) are a mixed signal for soil and vegetation, the ratio of band 5 to band 7 (5/7) or band 7 minus band 5 (7-5) are practical indicators of vegetative cover and density for users of ERTS-1 data. The decreased radiance observed in ERTS-1 bands 4 (0.5 to 0.6 μm) and 5 (0.6 to 0.7 μm) as vegetation density increases is mainly caused by the increasing amount of soil obscured by the vegetation.

Vegetation density is also dependent on stage of the growing season, or time of the year. Deciduous trees shed their leaves in fall but conifers retain theirs. Thus the two are best contrasted when the deciduous trees are dormant. The progress of the vernal advance (green wave) and fall senescence (brown wave) can be assessed for natural stands of plants and cultivated perennials. Development of annual crops can also be monitored and be interpreted in relation to major weather events such as freezes, drought, and rainfall distribution.

Figure 2 presents the observed radiometric response of the MSS bands 4, 5, and 6 for one corn and two sorghum fields in ERTS-1 scene 1308-16323 that had ground cover of 55, 90, and 90% and LAI of 2.46, 4.08, and 6.92. Also shown is the spectrum for bare soil (Mercedes clay). The radiances (Potter, 1972; conversion factors from digital counts to radiances are .19528, .15748, .13858, and .24286 for bands 4, 5, 6, and 7, respectively) decrease in bands 4 and 5 with increasing vegetation density, expressed as LAI, or with the increasing amount of soil obscured by the plants. The radiances in band 6 are in the order of LAI. The missing band 7 radiances should be about the same or slightly higher than those for band 6, but unlike band 6 they should be pure reflective infrared responses and not a mixture of visible and reflective infrared signals. The band 6 radiances do yield spectra similar in shape to the data for stacked leaves measured with a laboratory spectrophotometer given in Fig. 1. The radiance values for bare soil were obtained from a bare field close to the grain sorghum fields in the ERTS-1 scene. Compared with other ERTS-1 scenes, the radiance in band 6 is high for the particular bare field represented in Fig. 2.

THEORY

Allen and Richardson (1968) applied the Kubelka-Munk theory to reflectance of light by plant canopies and produced the equation

$$LAI = \frac{1}{2 \ln b} \ln \frac{(a-R)(1-aR_g)}{(a-R_g)(1-aR)} \quad [1]$$

for predicting leaf area index (LAI) of plant canopies from their reflectance measured remotely. The equation applies over the reflective infrared plateau wavelength interval, 0.75 to 1.35 μm . In eq. [1], R is the canopy reflectance, R_g is the reflectance of the soil background, and a and b are optical constants that have been determined for many plants (Gausman and Allen, 1973; Allen, Gausman, Richardson, and Wiegand, 1970; Gausman et al., 1973).

A completely different total reflectance model in terms of fractional plant cover can be expressed by

$$R_T = f R_c + (1-f) R_g \quad [2]$$

wherein R_T is total reflectance, R_c is vegetation canopy reflectance, R_g is soil background reflectance, and f is an indicator of plant density, such as, percent ground cover, LAI, or plant height.

Upon rearranging eq [2],

$$R_T = R_g + (R_c - R_g)f. \quad [3]$$

Comparing eq. [3] with the standard linear regression model

$$R_T = a_0 + a_1 f \quad [4]$$

it is seen that

$$R_g = a_0, \text{ the reflectance intercept when } f = 0, \text{ and} \\ (R_c - R_g) = a_1 \text{ so that } R_c = a_0 + a_1.$$

R_c is the reflectance characteristic of the crop or plant community the data are from. If f is expressed in LAI, then it is the reflectance of the canopy with a leaf area index of unity. If in percent ground cover, it is the reflectance of the canopy when ground cover is 1%. In the ERTS-1 MSS signals, R_T is a mixed signal for the vegetation and soil background. The simplified model presented enables one to estimate R_g , and the regression coefficient $(R_c - R_g)$ identifies the rate of change of reflectance per unit change in f .

As shown in Fig. 1 and discussed by Wiegand et al. (1971), the reflectance of vegetation in the visible region (ERTS-1 bands 4 and 5) is virtually the same for leaves one layer deep or stacked in enough layers to insure infinite reflectance, R_∞ (Allen and Richardson, 1968), and usually lower than that of soil. Thus R_T should be virtually constant for vegetation once the soil is obscured, and $(R_c - R_g)$ in eq. [3] should be small and negative. In the reflective infrared, however, R_T should increase as the vegetation density increases up to a LAI corresponding to R_∞ , requiring that $(R_c - R_g)$ be positive.

R_T and R_c are expressed in the ERTS-1 MSS signal by the digital counts of the system-corrected digital tapes, by the data expressed as radiance (Potter, 1972), or as a normalized response relative to the digital count maximum (127 for bands 4, 5, and 6 and 63 for band 7) for each band. Calibration of the MSS data directly in terms of reflectance needed for eq. [1] is not available to the authors.

In practice ERTS-1 data users will want to express the MSS responses in terms of quantities that are highly correlated with reflectance--dry matter production, biomass, LAI, percent ground cover, e.g. Once the relation is calibrated for a particular crop, plant community, or ecosystem of interest, the ERTS-1 data should be expressible directly in the productivity estimator of interest to the user. Atmospheric conditions that vary from one ERTS-1 pass to another should shift the data along the axes for any one band, but should not greatly affect the relative position of the data points to each other. If differences between two bands

are used, such as band 7 minus band 5, atmospheric interference effects are reduced possibly permitting pooling of data from multiple ERTS-1 passes for analysis. A ratio of responses in bands both in the visible, as 4/5, or both mainly in the infrared, as 6/7, should minimize atmospheric interference effects in the absence of random noise since both numerator and denominator would be similarly affected by atmospheric attenuation.

METHODS

Data being presented in this paper arise from two different sources. One source is the ground truth that has been taken to support the ERTS-1 analysis effort for one whole county. It was taken to (a) have well-documented fields to judge the accuracy of ERTS-1 classification results against, (b) provide statistical estimates of the acreages devoted to various crops to compare with ERTS-1 estimates, and (c) help establish what ground truths are meaningful in terms of the ERTS-1 spectral data. The data consist of observations of the soil surface condition, species, plant height, percent ground cover by the crop and by weeds, stage of plant maturity, and observations on the general condition of the crop, and stresses in four interpenetrating samples located throughout the county. Almost 1500 fields are involved.

The other source of data is an experiment conducted in the spring of 1973 specifically to determine the leaf area index (LAI) of 3 corn, 10 grain sorghum, and 10 cotton fields selected from the 1500 fields to have a range in planting dates, hence crop maturity, over several ERTS passes. The overall purpose was to test eq. [1] using the ERTS-1 data. Ten average-sized plants were cut off at ground level at each of eight sites in each field, the leaves were removed, and the area of each leaf was determined using a photoelectric planimeter. The area of the leaves was cumulated for each plant and sampling site and expressed as the ratio of area of the leaves to the ground area occupied by the plants. This ratio is by definition, LAI.

The number of plants per 10 m segments of row was determined on four adjacent rows at each of eight locations in each field to establish the plant population and hence the LAI characteristic of each field. The LAI determination was to be repeated each 2 weeks in each field between April and June to insure data near ERTS-1 overpasses. However, the large manpower requirement for LAI determinations and heavy rainfall prevented maintenance of the schedule.

The procedure used to determine the percent of ground covered by the plant canopies differed depending upon whether the crop plants produced a solid canopy (bare soil exposed only in the inter-row area) or an open canopy (bare soil visible through the canopy as well as in the inter-row area). For the solid canopy crops, such as cotton and thick stands of corn and sorghum, the bare soil width (BW) and row spacing (RS) were measured. By definition, BW is the width of the bare soil showing between the leaf canopies of adjacent crop rows, and RS is the average spacing between crop rows. For the solid canopy the percent crop cover is calculated from these measurements using

$$\left(\frac{RS - BW}{RS} \right) 100 = \text{percent cover}$$

where RS and BW are measured in cm.

For the open canopy crops--such as onions, immature cantaloupe, and corn and sorghum planted to low plant populations--the "open" canopies were considered solid, and the above formula was used to determine the percent cover. Then a subjective estimate was made of the percent open spaces in the leaf canopy by looking downward on them and this percentage was subtracted from the estimate calculated by the formula to obtain an estimate of actual cover

The computer compatible digital tapes (CCT) from the National Data Products Facility (NDPF) were displayed on a cathode ray tube (CRT), and a coordinate system was overlain to aid in locating the fields of interest in the CCT. The digital data corresponding to the approximate coordinates of the fields and sample segments of interest were transferred to a secondary tape. These data were displayed as gray maps using a line printer and were intensively studied to establish field locations and field boundaries. The digital counts for the pixels, or instantaneous ground resolution elements, within the test fields were averaged for each MSS band.

The space data were used as (a) digital counts, (b) radiance ($\text{mw}/\text{cm}^2\text{-sr-}\mu\text{m}$) using the conversion factors provided by Potter (1972), or (c) pseudo-reflectance by ratioing the CCT digital counts by the maximum possible count (127 for bands 4, 5, and 6 and 63 for band 7).

RESULTS

Due to excessive clouds, data are available for only three ERTS-1 passes, Dec. 16, 1972, Jan. 21, 1973, and May 27, 1973, corresponding to scene I.D. 1146-16323, 1182-16322, and 1308-16323, respectively. The May 27 scene is the only one for which LAI data are available; ERTS band 7 data for this scene delivered to date have a "venetian blind" effect in them and are not useable. The NDPF is redigitizing this scene.

Figures 3a and 3b present the relation between LAI and band 6 digital counts, the band 6 minus band 5 digital count difference, and the ratio of digital counts in bands 5 and 6 ($5/6$) separately for the combined grain sorghum and corn fields and for the cotton fields. LAI of sorghum and corn account for 67.7% of the variation in band 6 digital count, 59% of the variation in the 6-5 difference, and 45.2% of the variation in the band $5/6$ ratio. Thus band 6 alone is superior to the difference, and to the ratio of visible-to-infrared response.

For the cotton fields, a quadratic equation was used to fit the band 6, and the band 6 minus band 5 optical count difference but a linear equation was fitted to the $5/6$ ratio data. LAI explains 83%, 90%, and 78% of the variation in digital counts using band 6, 6-5, and $5/6$, respectively. For cotton, then, the band 6 minus band 5 digital counts were the best indicator of vegetation density.

The sorghum and corn plants averaged 94 cm high and were approaching full canopy development, whereas the cotton plants averaged only 37 cm in height and were at or very near first bloom stage of development. The plants also differ considerably in growth habit or architecture. Corn and grain sorghum display their long curved leaves in umbrella fashion, whereas cotton plants are conical and their leaves are heliotropic. Such characteristic differences help to discriminate among crops and plant communities spectrally and must contribute useful information for texture analyses. They also suggest that crops or plant communities typical of a given locale or region might be spectrally "calibrated" against the ERTS-1 data one or more times during the year; identifications in subsequent years would be based on the calibration so that extensive ground truth would be unnecessary.

Most investigators use the ERTS-1 MSS digital counts as provided by the NDPF system-corrected CCT. Table 1 presents the linear and quadratic equations for the regression of CCT digital counts (DC) on LAI. For cotton, the quadratic equation explained a statistically significant amount of variance over the linear equation, but it did not for sorghum. The equations for band 6 are repeated from Figs. 3a and 3b but the equations for bands 4 and 5 are presented anew.

The sorghum and corn plants obscured the soil so the correlation in the visible, where responses are due mainly to soil, are poor. For the cotton, both the exposed soil and the vegetation yielded an appreciable signal so that correlation coefficients in both the visible and infrared are significant at 0.01 probability level. The improvement in fit for cotton using a quadratic expression is appreciable, and suggests that a more complicated physical model is required when plant cover is incomplete. Three considerations are sun angle as it affects the length of shadows cast by the plants, row direction, and row spacing.

LAI is only one measure that agriculturalists use to indicate vegetation density. The simple correlations between LAI and plant population (POP; plants per 40 meters of row), percent ground cover (PC), and plant height (PH) are given in table 2 as well as the multiple regression equations expressing LAI as a function of the other plant parameters. LAI of cotton is most highly correlated with PH (0.783) and least correlated with plant population (0.382), whereas LAI of sorghum and corn is most highly correlated with plant population (0.829) and least correlated with PH (0.165). These data seem to indicate that different plant parameters are needed to characterize different crops.

Any useful plant and soil parameters for characterizing crop, range, and forest scenes must necessarily account for most of the variation in the MSS data. Table 3 summarizes regression equations produced relating the CCT digital counts to the vegetation ground truths: LAI, plant population (POP), plant cover (PC), and plant height (PH).

As expected, the plant parameters explain more of the variation in digital counts in the reflective infrared than in the visible. The regression coefficient for the population term was zero for sorghum and corn in bands 4 and 5, causing this variable to be dropped from the estimating equation. Evidently the high correlation ($r = 0.829$) between LAI and POP shown in table 2 caused plant population to contribute nothing to the estimation of the digital counts that was not explained by LAI. This finding has practical consequences. Plant population is easy to determine by counting stalks at a number of locations in fields, or it can be estimated from the amount of seed planted per hectare. Determination of LAI, on the other hand, is laborious and the plants are destroyed in the process. Thus if plant population suffices to characterize corn and sorghum fields in terms of LAI and ERTS-1 radiances, verifying ground truth is easy to obtain. Of course, the plant population remains constant once a crop stand is established. The plants would grow and the radiances measured by satellite would change from one satellite pass to another as the plants develop. However, the radiances for a given set of fields would remain in the same relative position to each other as the plant populations do. Thus one population count should be good for a whole growing season (several ERTS passes).

If there is a good relation between plant population or ERTS radiances and yields, a procedure is suggested for determining the optimum population on a regional basis. Then one can work to get the optimum population widely adopted by growers.

As shown in table 2, PH for cotton was highly correlated with LAI. Coefficients for the linear correlation of LAI and PH with DC calculated in arriving at the equations of table 3 were:

			Band 4	Band 5	Band 6
			- - - - - r - - - - -		
DC	vs	LAI	-.726**	-.855**	+.823**
DC	vs	PH	-.769**	-.825**	+.925**

The similarity among correlation coefficients for the correlation of LAI and PH with DC in all bands and the very high coefficient for the correlation of DC with PH in band 6, suggest the possibility that PH can substitute for LAI at least during the prebloom and early fruit set periods of development of this crop.

The 93.4% and 87.3% ($R^2 \times 100$) of the variation in digital counts explained in band 6 for cotton and the combined sorghum and corn, respectively, by the plant parameters used to characterize the crops indicate that (a) characteristics of the vegetation are mainly responsible for the recorded ERTS-1 signals, and (b) useful plant parameters are available for the crops studied.

As stated earlier, one objective of this study was to test eq. [1] for predicting LAI from the ERTS MSS data. Table 4 gives the optical constants a and b, defined by Gausman and Allen (1973), needed to solve eq. [1]. They are calculated from absolute reflectance and transmittance spectra obtained spectrophotometrically on leaves typical of the crops. The values given for "sorghum and corn" are an average of values for each of the two crops.

Inspection of eq. [1] shows that it is limited to conditions when the canopy reflectance R is larger than the soil background reflectance. Additionally, the last term becomes negative if 'a' gets very large.

LAI was calculated for band 6, using the digital count observed in the MSS data divided by 127 to obtain a pseudo-reflectance of the crop, R, and the intercept of the pseudo-reflectance at LAI = 0 was used as the reflectance of the soil background.

The coefficients for the linear correlation of calculated LAI with manually measured LAI were high at 0.815** for cotton and 0.872** for sorghum and corn, respectively. However, the calculated LAI never exceeded 2.0. Thus the predictions of LAI from eq [1] are not satisfactory.

The possible reasons for poor results include (a) the constants 'a' and 'b' are in inappropriate units for this application, (b) the pseudo-reflectance used is inappropriately normalized, (c) band 7 MSS data should be used, (d) the reflectance for soil estimated from the intercept at $f = 0$ is too high, (e) the theoretical requirements of the equation (diffuse isotropic incident radiation) are not met, and (f) the row pattern of crops distributes the leaves nonuniformly against the background. Optical constants derived from laboratory data have been successfully applied to other field studies.

Efforts to use eq. [1] will continue because of the potential it has as a practical tool for deducing biomass or yield from ERTS-1 and other remotely measured near-infrared reflectance.

The second model proposed, typified by eq. [3], was also applied. It should describe the physical events better in the visible (bands 4 and 5) than in the infrared; in the infrared it is too simple to describe the multiply-reflected light from successive leaf layers. In applying eq. [3] the digital counts from the ERTS-1 data, R_T , are plotted against any plant parameter of interest such as fractional cover, LAI, or even plant height. R_g is the intercept on the R_T axis when fractional ground cover, LAI, or height of the plants of interest is zero, that is, the soil is bare.

Table 5 gives the values of R_g , $(R_c - R_g)$ and R_T calculated from eq. [3] for each MSS band for the three ERTS-1 scenes we have data from. For the May 27 pass, the calculated R_T value is given as a function of LAI, but for the other two dates as a function of percent ground cover. The calculated R_T values increase from the R_c value in the infrared bands as vegetation density increases from LAI = 1, but decrease in the visible with increasing LAI above 1. Even though LAI for the cotton plots ranged up to 3.0, the ground cover was only 18 to 40%; consequently considerable soil reflectance should be recorded in the ERTS signals. The measured LAI ranged up to 8.5 in the sorghum and corn fields, but the ground cover recorded ranged from 35 to 90%. Consequently some soil (or shadow) signals were included even for fields with high LAI.

The January 21, 1973, data represent 28 vegetable fields as follows: broccoli, 2; carrot, 6; cabbage, 6; onion, 8; tomato, 3; lettuce, 1; beet, 1; and spinach, 1. Ground cover ranged from 2 to 90%. The December 16, 1972, data represent 106 vegetable fields consisting of crop and number of fields, respectively, as follows: lettuce, 14; pepper, 5; tomato, 11; onion, 26; cabbage, 19; carrot, 25; broccoli, 5; and beet, 1. Percent ground cover of these fields ranged from 1 to 100%. The regression coefficient ($R_c - R_g$) is negative on all dates for the visible bands and positive for the reflective infrared bands.

The digital count values for the May 27 ERTS-1 scene are higher than for the other two scenes. The predominant soil type for the December 16 and January 21 data is Harlingen clay and other heavy-textured alluvial flood plain soils. The May 27 data were obtained from upland soils further from the Rio Grande, which are as light-textured as fine sandy loam. Local soils are generally more reflective the coarser the texture. This, combined with the higher incident solar radiation in May than in December or January would account for the higher digital count values in the scene in May than in the winter months. The higher (Rc-Rg) values in May than the winter months for vegetation also agree with the larger digital counts being due to more incident solar radiation available for reflectance in May than in winter. For all scenes, the ERTS-1 MSS operated on low gain, hence MSS gain is not a factor.

In summary, we have shown that the ERTS-1 MSS data do relate to vegetation density and potential productivity and that vegetation parameters explain most of the variation in band 6 and 7 responses. We also presented and discussed two different equations for relating vegetation reflectance to the ERTS-1 MSS responses. We trust that operational methods for assessing the condition and animal carrying capacity of rangeland and the yield of crops using space data will incorporate procedures based on the principles presented.

LITERATURE CITED

- Allen, W. A. and Richardson, A. J. 1968. Interaction of light with a plant canopy. *J. Opt. Soc. Amer.* 58:1023-1028.
- Allen, W. A., H. W. Gausman, A. J. Richardson, and C. L. Wiegand. 1970. Mean effective optical constants of thirteen kinds of plant leaves. *Appl. Opt.* 9:2573-2577.
- Carnegie, D. M. and S. D. DeGloria. 1973. Monitoring California's forage resource using ERTS-1 and supporting aircraft data. p. 91-95. In *Proc. Symp. on Significant Results Obtained from ERTS-1. Vol. I*, NASA SP-327. U.S. Govt. Printing Ofc., Washington, DC.
- Dethier, B. E., M. O. Ashley, B. Blair, and R. Hopp. 1973. Phenology satellite experiment. p. 157-165. In *Proc. Symp. on Significant Results Obtained from ERTS-1. Vol. I*, NASA SP-327. U.S. Govt. Printing Ofc., Washington, DC.
- Freden, S. C., E. P. Mercanti, and M. A. Becker (eds.). 1973. *Proc. Symp. on Significant Results Obtained from ERTS-1*, New Carrollton, MD., Mar. 5-9, 1973. 2 Vol., 1730 p., NASA SP-327. U.S. Govt. Printing Ofc., Washington, DC.
- Gausman, H. W. and W. A. Allen. 1973. Optical parameters of leaves of 30 plant species. *Plant Physiol.* 52:57-62.
- Gausman, H. W., W. A. Allen, C. L. Wiegand, D. E. Escobar, R. R. Rodriguez, and A. J. Richardson. 1973. The leaf mesophylls of twenty crops, their light spectra, and optical and geometrical parameters. *Tech. Bul.* 1465. U.S. Dept. Agric. 60 p. U.S. Govt. Printing Ofc., Washington, DC.
- Heath, G. R. and H. D. Parker. 1973. Forest and range mapping in the Houston Area with ERTS-1. p. 167-172. In *Proc. Symp. on Significant Results Obtained from ERTS-1. Vol. I*, NASA SP-327. U.S. Govt. Printing Ofc., Washington, DC.
- Kanemasu, E. T. In Press. Seasonal canopy reflectance patterns of wheat, sorghum and soybean. *Remote Sensing of Environment*.
- Lauer, D. T. 1971. Testing multiband and multirate photography for crop identification. *Proc. Int'l. Workshop on Earth Resource Survey Systems*. II:33-46. U.S. Govt. Printing Ofc., Washington, DC.
- National Aeronautics and Space Administration (NASA). 1972. *Data Users Handbook*. Doc. No. 71SD4249. p. A-11. Goddard Space Flight Center, Greenbelt, MD.
- Pearson, R. L. and L. D. Miller. 1972. Remote mapping of standing crop biomass for estimation of the productivity of the shortgrass prairie, Pawnee National Grasslands, Colorado. II:1355-1379. *Proc. Eighth Intern'l. Symp. on Remote Sens. of Environ.*, Univ. of Mich., Ann Arbor.

- Potter, J. F. 1972. Response of the ERTS multispectral scanner. Tech. Memo. 642-044. 7 p. Lockheed Electronics Co., Inc., Houston, TX.
- Seevers, P. M. and J. V. Drew. 1973. Evaluation of ERTS-1 imagery in mapping and managing soil and range resources in the sand hills region of Nebraska. p. 87-89. In Proc. Symp. on Significant Results Obtained from ERTS-1. Vol. I, NASA SP-327. U.S. Govt. Printing Ofc., Washington, DC.
- Stanhill, G., V. Kafkafi, M. Fuchs, and Y. Kagan. 1973. The effect of fertilizer application on solar reflectance from a wheat crop. Israel J. Agric. Res. 22:109-118.
- Steiner, D. 1970. Time dimension for crop survey from space. Photogram. Engin. 36:187-193.
- Stoner, E. R., M. F. Baumgardner, and J. E. Cipra. 1972. Determining density of maize canopy: II. Airborne multispectral scanner data. Laboratory of Applications of Remote Sensing, Purdue Univ., West Lafayette, Ind. LARS Print 111272. 16 p.
- Thomas, J. R., V. I. Myers, M. D. Heilman, and C. L. Wiegand. 1966. Factors affecting the light reflectance of cotton. p. 305-312. Proc. Fourth Symp. on Remote Sens. of Environ., Univ. of Mich., Ann Arbor.
- Thomas, J. R., C. L. Wiegand, and V. I. Myers. 1967. Reflectance of cotton leaves and its relation to yield. Agron. J. 69:551-554.
- Von Steen, D. H., R. W. Leamer, and A. H. Gerbermann. 1969. Relationship of optical density to yield indicators. p. 1115-1122. Proc. Sixth Int'l. Symp. on Remote Sens. of Environ., Univ. of Mich., Ann Arbor.
- Wiegand, C. L., H. W. Gausman, and W. A. Allen. 1972. Physiological factors and optical parameters as bases of vegetation discrimination and stress analysis. p. 82-102. Proc. Operational Remote Sensing, Am. Soc. of Photogrammetry, Falls Church, VA.
- Wiegand, C. L., R. W. Leamer, D. A. Weber, and A. H. Gerbermann. 1971. Multibase and multiemulsion space photos for crops and soils. Photogram. Engin. 37:147-156.

Table 1. Linear and quadratic equation regressions of ERTS-1 MSS digital counts (DC) on leaf area index (LAI) for bands 4, 5, and 6, scene ID 1308-16323.

Crop(s)	Band	Regression equation	Correlation coefficient
Cotton	4	DC = 43.8-3.5(LAI)	r = -0.746*
		DC = 47.5-11.0(LAI)+2.5(LAI) ²	R = 0.867**
	5	DC = 40.0-5.0(LAI)	r = -0.856**
		DC = 42.6-10.3(LAI)+1.8(LAI) ²	R = 0.888**
	6	DC = 50.2+5.1(LAI)	r = 0.823**
		DC = 45.5+14.4(LAI)-3.1(LAI) ²	R = 0.911**
Sorghum & Corn	4	DC = 42.9-0.9(LAI)	r = -0.441
	5	DC = 38.8-1.5(LAI)	r = -0.464
	6	DC = 44.4+2.8(LAI)	r = 0.841**

**Statistically significant at the 0.01 level.

*Statistically significant at the 0.05 level.

Table 2. Simple correlation coefficients among LAI and plant population (POP), percent cover (PC), and plant height (PH) for cotton and for grain sorghum and corn, and LAI expressed as a function of the other plant parameters.

CROP			
	POP (Plants/40m of row)	PC %	PH (cm)
- - - - - r - - - - -			
Cotton	LAI vs: 0.382	0.589	0.783**
LAI = -2.392-0.00003(POP)+0.0211(PC)+0.0829(PH)			
$R^2 = 0.628$			
Sorghum & corn	LAI vs: 0.829**	0.555**	0.165
LAI = 0.234+0.0023(POP)+0.038(PC)-0.0046(PH)			
$R^2 = 0.753$			

**Significant at the 0.01 level.

Table 3. Digital counts (DC) in ERTS-1 bands 4, 5, and 6 as estimated from four plant parameters, LAI, plant population (POP), percent ground cover (PC), and plant height (PH).

Crop	Band	Regression Equation	R ²
Cotton	4	DC = 47.51-2.215(LAI)-.006(POP)+.369(PC)-.367(PH)	.899**
	5	DC = 48.40-3.270(LAI)-.009(POP)+.006(PC)-.175(PH)	.853**
	6	DC = 31.09+1.243(LAI)+.005(POP)+.236(PC)+.391(PH)	.934**
Sorghum & corn	4	DC = 53.38-.600(LAI)-.034(PC)-.098(PH)	.590**
	5	DC = 56.11-1.049(LAI)-.023(PC)-.192(PH)	.653**
	6	DC = 45.93+3.09(LAI)-.00001(POP)-.111(PC)+.060(PH)	.873**

**Significant at the 0.01 level.

Table 4. Optical constants a and b for cotton, sorghum, and corn needed to solve eq. [1] over the ERTS-1 MSS wavelengths. Eq. [1] applies best to the reflective infrared wavelength interval 0.75 to 1.35 μm .

Wavelength μm	Cotton		Sorghum and Corn	
	a	b	a	b
.50	10.1149	12.4133	7.2990	28.2740
.55	8.3252	7.5888	5.9500	11.1809
.60	12.4855	14.4815	7.9804	34.5618
.65	13.0149	24.0333	9.8553	235.3162
.70	3.1282	2.9818	3.5587	3.9962
.75	1.4551	1.4357	1.4636	1.4417
.80	1.3295	1.3161	1.3193	1.2968
.85	1.3178	1.3024	1.2939	1.2706
.90	1.3446	1.3251	1.2914	1.2659
.95	1.4000	1.3736	1.3422	1.3082
1.00	1.3546	1.3318	1.3013	1.2704
1.05	1.3015	1.2825	1.2483	1.2224
1.10	1.3462	1.3226	1.2702	1.2408
1.15	1.5294	1.4858	1.4426	1.3885
1.20	1.5337	1.4875	1.4426	1.3862
1.25	1.5097	1.4640	1.4038	1.3504
1.30	1.6882	1.6114	1.5390	1.4596
1.35	2.0774	1.9230	1.8046	1.6679
1.40	4.2764	3.5637	3.3571	2.9117

Table 5. Digital count values of R_g , R_c , and R_T calculated using eq.[3]
for ERTS-1 MSS bands 4, 5, 6 and 7 from three ERTS-1 scenes.

ERTS Scene and Date	Crop	Band	R _g (R _c -R _g)		R _T				
					LAI				
					1	2	4	6	8
			Digital Counts						
1308-16323 5/27/73	Cotton	4	43.8	-3.5	40.3	36.8	29.8	--	--
		5	40.0	-5.0	35.0	30.0	20.0	--	--
		6	50.2	+5.1	55.3	60.4	70.6	--	--
	Sorghum and Corn	4	42.9	-0.9	42.0	41.1	39.3	37.5	35.7
		5	38.8	-1.5	37.3	35.8	32.8	29.8	26.8
		6	44.4	+2.8	47.2	50.0	55.6	61.2	66.8
			DC	% ⁻¹			PC (%)		
					10	20	40	60	80
	1182-16322 1/21/73	Vegetables	4	27.82	-.024	27.6	27.3	26.9	26.4
(8 crops; 28 fields)		5	25.63	-.058	25.0	24.5	23.3	22.2	21.0
		6	20.69	+.180	22.5	24.3	27.9	31.5	35.1
		7	26.59	+.187	28.5	30.3	34.1	37.8	41.5
1146-16323 12/16/72	Vegetables	4	31.35	-.037	31.0	30.6	29.9	29.1	28.4
	(8 crops; 106 fields)	5	28.60	-.065	27.9	27.3	26.0	24.7	23.4
		6	29.91	+.063	30.5	31.2	32.4	33.7	35.0
		7	28.65	+.108	29.7	30.8	33.0	35.1	37.3

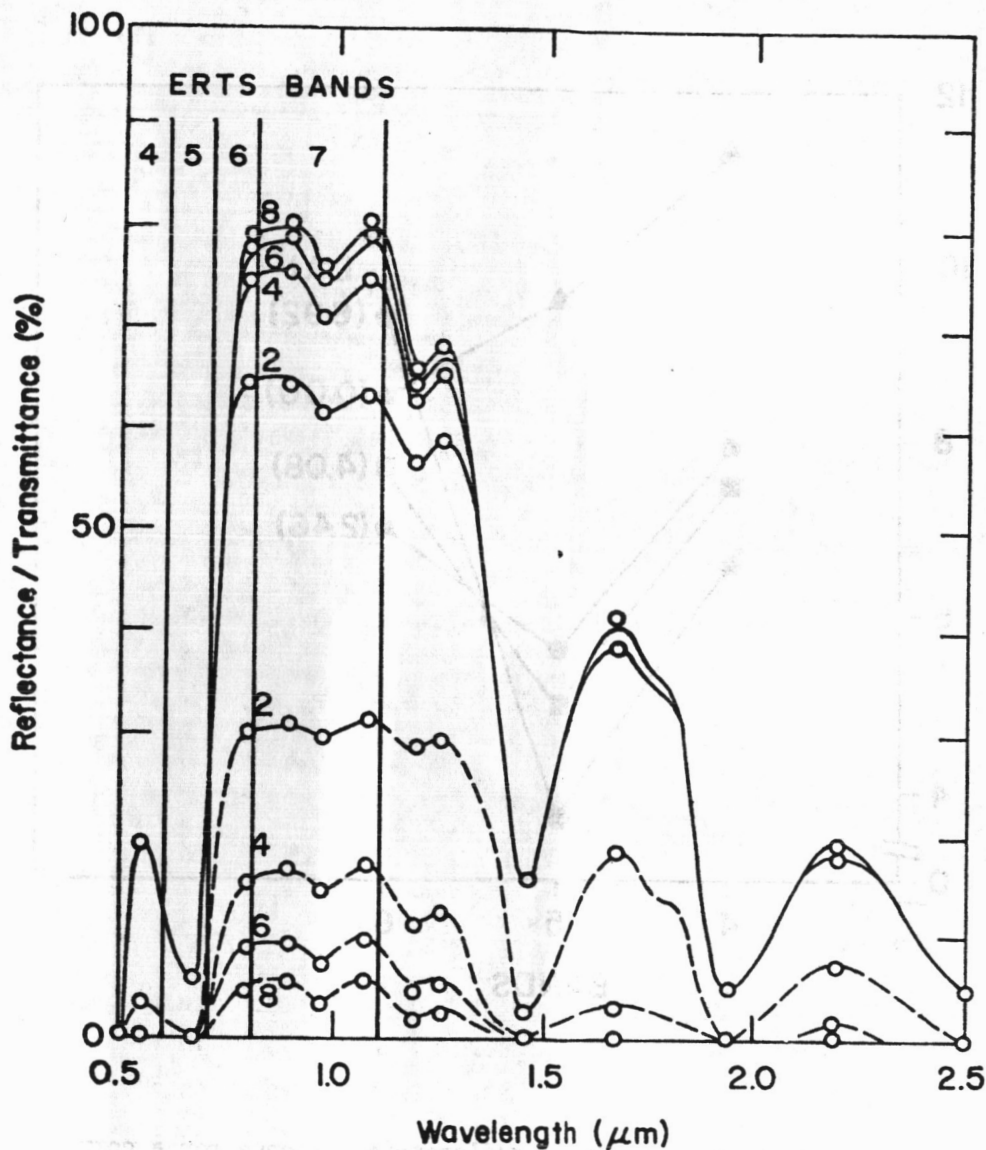


Fig. 1. Reflectance (solid lines) and transmittance (dashed lines) of 2, 4, 6, 8, stacked mature cotton leaves. The lines are theoretical; the circles are experimental. (Allen and Richardson, 1968.) Reflectance from vegetation is dependent on leaf area index in ERTS bands 6 and 7 but not in bands 4 and 5.

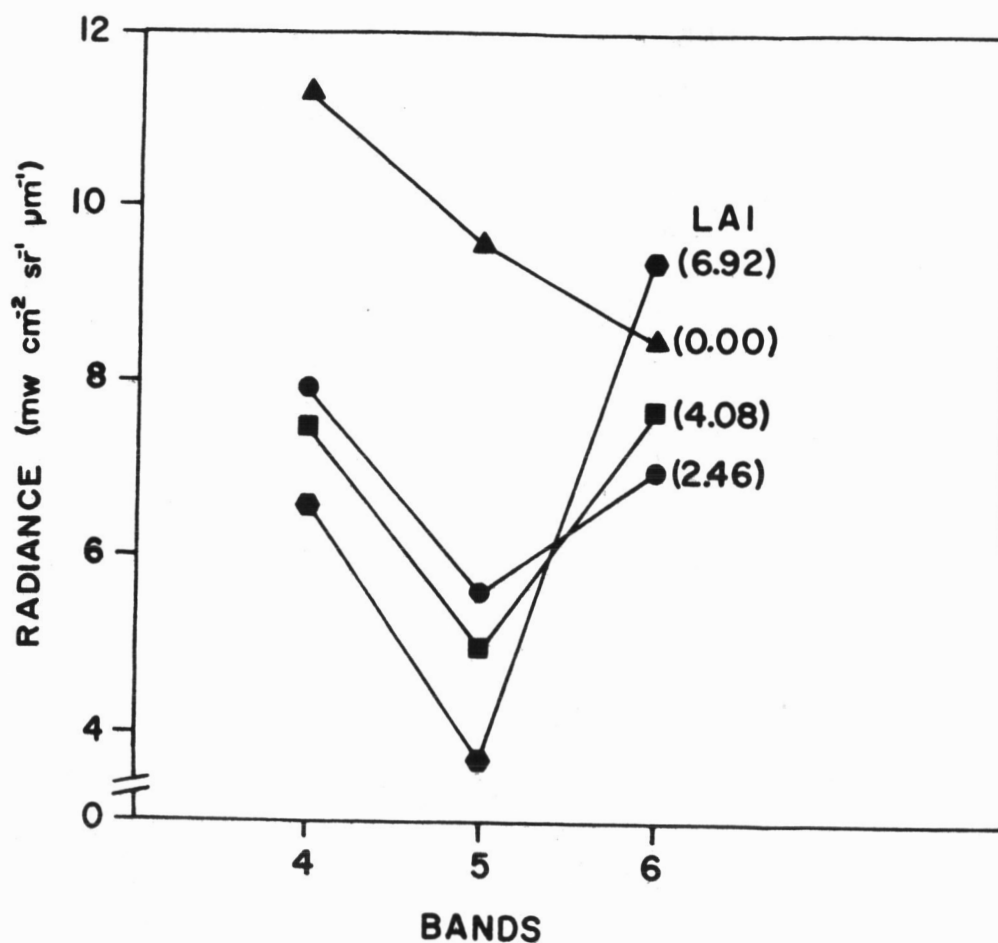


Fig. 2. ERTS MSS bands 4, 5, and 6 radiometric response for a corn, two sorghum, and a bare soil field with leaf area to ground area (leaf area index, LAI) of 2.46, 4.08, 6.92, and 0.0, respectively. ERTS response in bands 4 and 5 is mainly due to the soil obscured by vegetation, whereas in the reflective infrared vegetation dominates the ERTS signals. Note: Radiance of bare soil is that observed in ERTS data for lone bare field located near sorghum fields; its radiance is believed to be atypically high by approximately $2 \text{ mw cm}^{-2}\text{-sr}^{-1}\text{-}\mu\text{m}^{-1}$.

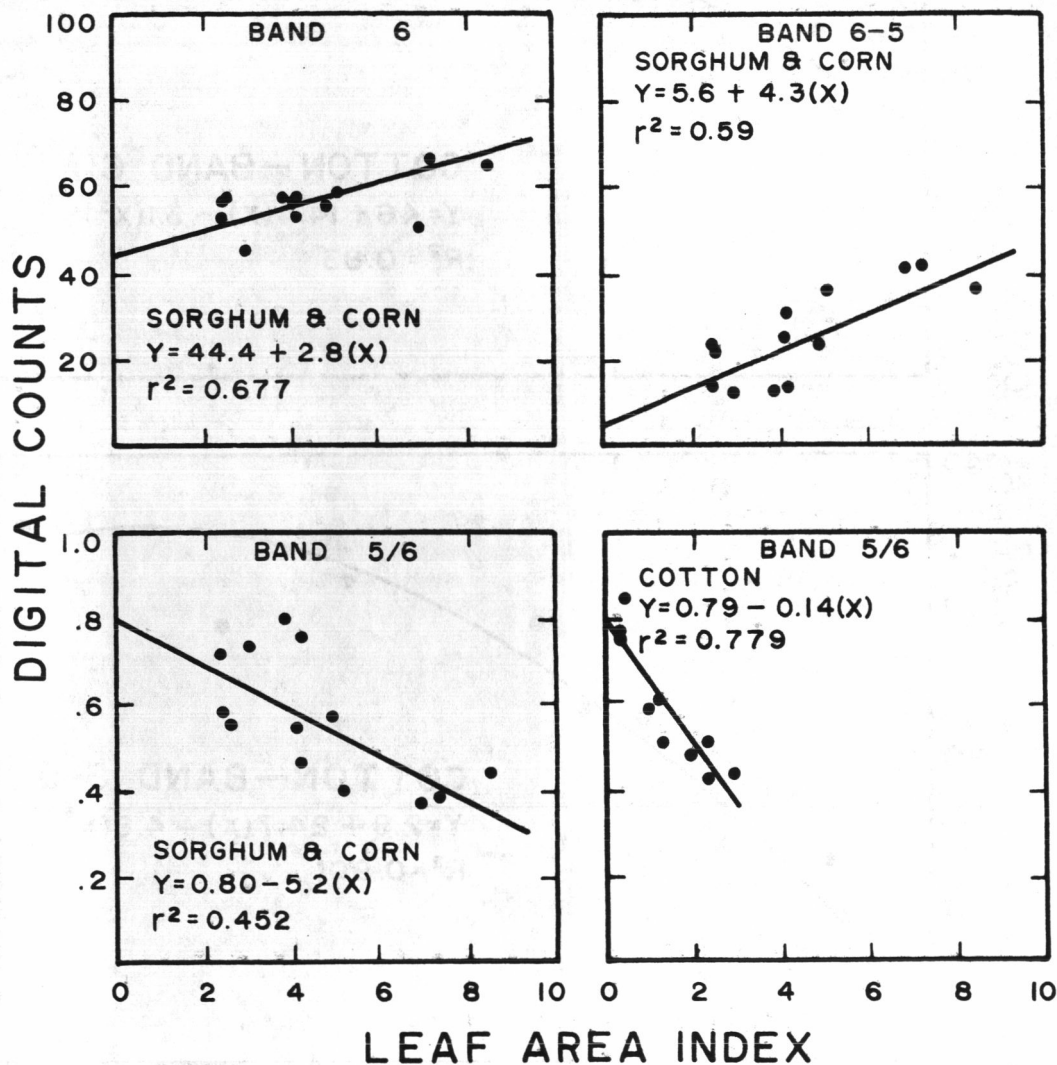


Fig. 3a. Combinations of CCT digital counts (band 6), digital count differences (band 6 minus band 5), and digital count ratios (band 5/band 6) for sorghum and corn combined into one crop type and for cotton versus LAI.

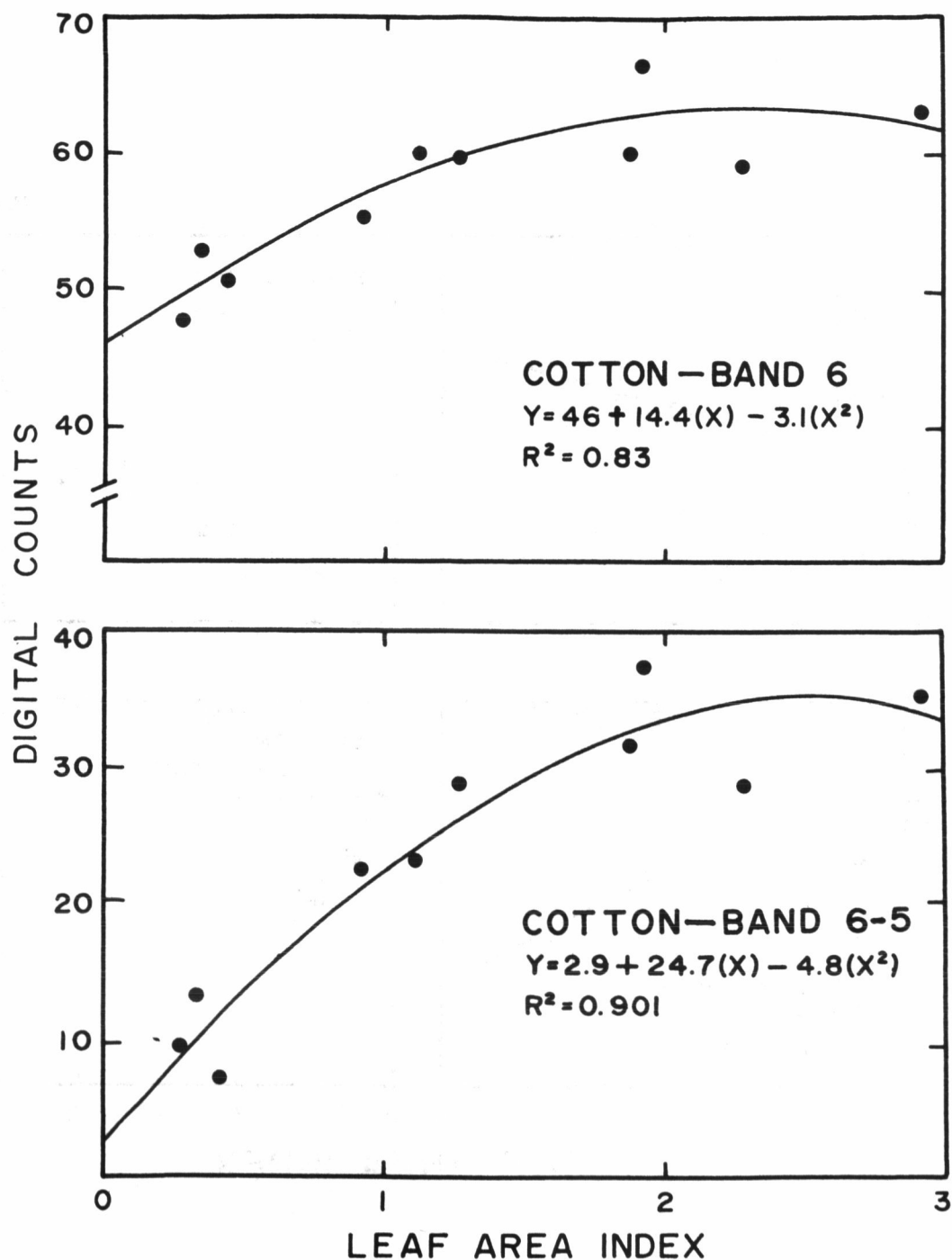


Fig. 3b. LAI of 10 cotton fields versus band 6 digital counts and band 6 minus band 5 count differences. In the regression equations Y symbolizes digital counts and X symbolizes LAI. $R^2 \times 100$ is the percent of variation attributable to the relation between LAI and digital counts.

REGIONAL AGRICULTURE SURVEYS USING ERTS-1 DATA

William C. Draeger, James D. Nichols, Andrew S. Benson, David G. Larrabee, William M. Senkus and Claire M. Hay,
Center for Remote Sensing Research, University of California, Berkeley, California 94720

ABSTRACT

During the past year, the Center for Remote Sensing Research (CRSR) at the University of California has conducted studies designed to evaluate the potential application of ERTS data in performing agricultural inventories, and to develop efficient methods of data handling and analysis useful in the operational context for performing large area surveys.

This work has resulted in the development of an integrated system utilizing both human and computer analysis of ground, aerial, and space imagery, which has been shown to be very efficient for regional crop acreage inventories. The technique involves (1) the delineation of ERTS images into relatively homogeneous strata by human interpreters, (2) the point-by-point classification of the area within each strata on the basis of crop type using a human/machine interactive digital image processing system, and (3) a multistage sampling procedure for the collection of supporting aerial and ground data used in the adjustment and verification of the classification results.

INTRODUCTION

In the United States, the Department of Agriculture presently conducts an enumerative program in which virtually all agricultural land is inventoried annually. In addition, numerous other federal, state and local agencies conduct extensive crop inventories, land use surveys, and soils mapping projects of varying magnitude. On a worldwide basis it would seem that the principal obstacles to providing enough food for all persons are not merely ones of production but also problems of allocation and distribution. What is needed is knowledge as to where and how much food is now being produced, and how crop production is changing with time. Considering the present needs for regional, national, and worldwide inventory and evaluation data, coupled with the particular capabilities of the ERTS system, agricultural

1 N 74 30714

applications appear to be especially promising as an area in which important benefits might be realized from the use of such technology.

Up to the present time agricultural inventories have required a tremendous effort on the part of on-the-ground enumerators, and have presented a formidable data compilation task. However, a satellite sensing system, with which large areas of land can be surveyed in their entirety on one image, and which can provide uniform worldwide coverage with a relatively small number of images, offers great promise as a data collection tool for alleviating these problems. Furthermore, the dynamic nature of agriculture requires not a single evaluation in most cases, but rather a continual updating of conditions. In fact, it has been shown that desired information about agricultural crops can often be obtained only by capitalizing on a knowledge of the patterns of change exhibited by particular crop types under various growing conditions. Again, this suggests that a satellite sensing system such as ERTS, which makes possible regular, frequent observations of each spot on the earth's surface, can provide a service which is both highly desirable and totally infeasible using conventional techniques.

Based on these facts, plus the encouraging results achieved using both high altitude aircraft and spacecraft imagery for crop inventory experiments over the past several years, the Center for Remote Sensing Research (CRSR) at the University of California undertook the experiment described in this paper. The experiment was designed to evaluate the feasibility of using satellite data regionally to provide needed agricultural information on an operational basis. The experiment was performed in Maricopa County, Arizona and San Joaquin County, California in cooperation with a number of state and federal agencies.

In an effort to accurately determine the amount of detail which can be extracted from ERTS-1 data, and the optimum use of "subsampling" in the form of aerial photography and ground truth data for various agricultural-related tasks, the investigation was carried out in a stepwise fashion beginning with agricultural land use stratification, and progressing to very detailed surveys. These investigations entailed the use of both human image analysts and automatic classification and data handling techniques, and an evaluation of the optimum mix of human and machine techniques for each analysis problem. In each case, an attempt was made to ensure that the types of information compiled (e.g., maps, tabular data, crop acreages, etc.) conformed to actual requirements or desires as expressed by those persons currently involved in resource evaluations and planning in the test site.

In the area of agricultural land stratification, particular attention was paid to quantitative analyses of the stratifications to ascertain the extent to which they did provide meaningful crop type and condition information. In so doing, use was made of ground cell information,

point sampling along transects (using observers flying in light aircraft), and comparisons with existing land classifications using the CRSR MAPIT techniques. In addition, a study was made of the variation in delineations made at different times during the growing season.

Crop classification and inventory studies progressed concurrently with the stratification investigations, as it seemed likely that any operational inventory procedures would be heavily dependent on an initial stratification of agriculture on ERTS or other small-scale imagery. Very significant progress was made on the development of automatic data processing techniques for the detailed classification of agricultural lands. In particular, emphasis was placed on the optimum interface between human interpreters and the computer. Thus, initial stratifications of agricultural land were performed manually, and the resultant information used in the classification process. In addition, a sampling procedure was designed which would optimize processing of remote sensing and ground data by reducing the amount of ground information required. Incorporated in the design is provision for the weighting of classification errors based on the relative importance of errors regarding various crops. Finally, studies were conducted to estimate the relative costs of performing crop inventories using various combinations of human and computer data processing inputs.

A PRACTICAL INVENTORY SYSTEM

The principal result of the ERTS-1 investigation was the development of an integrated data handling and analysis system which utilizes both human and computer analysis of ground, aerial and space imagery and which has been shown to be very efficient for regional crop acreage inventories.

The initial step in the inventory process consists of the delineation of ERTS images into relatively homogeneous strata by human interpreters. The total image is first divided into agricultural and non-agricultural areas, after which the agricultural areas are subdivided on the basis of predominant crop types using only gross image characteristics and a general knowledge of cropping practices.

In an attempt to evaluate the use of satellite imagery for this purpose, all land within San Joaquin County was delineated by image analysts into broad land use and crop category classes based on their appearance on the ERTS-1 July 26 (summer season) color composite image. The stratification of the agricultural land use categories proved to be a relatively simple task, taking each of three interpreters approximately 30 minutes to complete. The three interpretations were quite similar, requiring only minor revisions to produce a "consensus" stratification. A total of thirteen different agricultural strata were recognized, differing both in general field size and relative proportions of crop types and field conditions. Upon comparing these interpretations we concluded that nearly all boundaries were truly

representative of differing cropping practices. In a number of cases, the stratifications agreed almost exactly with major soil type boundaries as drawn by earlier soils surveys.

Certainly a much more detailed and up-to-date stratification was produced from the ERTS image than is currently used by the Statistical Reporting Service, USDA. The obvious questions arise, however, as to whether: (1) the strata as drawn on the image are meaningful in terms of actual land use conditions, (2) the strata delineations would change throughout the year, and (3) such a detailed delineation could enable the Statistical Reporting Service to more efficiently and accurately estimate the parameters of interest on a statewide basis.

In addition to their possible use by agencies such as the Statistical Reporting Service, the stratifications performed by the human interpreters proved to be of great value as the preliminary step prior to detailed classification of crop types on a field by field basis, since it was found that by far the most practical and cost-effective method for producing "automated crop inventories" involves the use of manual interpretation at several stages in the process. In particular, it has been found that automatic classification done stratum by stratum, using training data specific to each stratum, results in much greater classification accuracy than would be possible otherwise. Furthermore, it is much more efficient to allow a human to do the preliminary stratification than to attempt this with automated techniques. Thus an interactive man-machine system, in which each is used to perform only those tasks for which it is best suited, results in the greatest overall efficiency in terms of time and money expended for a given level of classification accuracy.

At this point in the inventory process, political and administrative boundaries may also be superimposed on the imagery to define the geographic area of interest. Next, to train the discriminant analysis program, fields identified by ground data or photo interpretation representing the various resource or vegetation types of interest in each stratum are located on small-scale photos for extraction from the digital tapes. The number of training fields required for each crop class depends on the variability of the spectral signature of the various crops present. This variability is caused by such factors as different cropping practices, local soil differences, and genetic variations within a particular crop type. For a crop such as alfalfa where there may be several stages of maturity present at the time of image acquisition, five or more fields per stratum may be required. In the case of less complex crop classes such as corn, one training example may be adequate. These training fields must also be large enough to be identifiable on the imagery acquired by the remote sensing system used in the first stage. On ERTS-1 imagery the minimum area is around 20 acres with a minimum dimension on one side of 800 feet. These fields are identified on and extracted from the spacecraft imagery and

supplied as training to the discriminant analysis system. The multispectral data are then run through the discriminant analysis to obtain a point-by-point classification of the entire area by strata (as defined by the human interpreter). This provides an initial estimate of the acreage of the vegetation classes by strata.

The discriminant analysis results must then be sampled in some manner to determine the relationship between the discriminant analysis estimate and the true value or ground estimate of the resource. Sampling units are defined by breaking the entire area into rectangular areas which in the case of the ERTS study were based on the coordinate grid generated by the MSS system. The size and shape of each rectangular area are determined by the information requirements of the manager, the change in variability of the estimates for the SUs as their size is changed, the cost of making further estimates on the SUs, and the difficulty of recognizing the sampling units on conventional larger-scale imagery.

To evaluate the relative utility of the discriminant analysis of ERTS-1 multispectral-multidate imagery in estimating the area of agricultural crops the information obtained from the discriminant analysis, ground data and high flight imagery of the intensive test site in San Joaquin County were used to determine the optimum size of the sampling unit and the number of samples required to obtain acceptable estimates of crop area for the entire county. The optimum size of the primary (first stage) sampling unit was found to be 25 x 35 picture elements (equivalent to 386 hectares on the ground). This was determined from the estimates of the coefficient of variation, and the plot of expected error in transferring the ERTS sampling units to the corresponding photography for precise area measurement.

At this point there are two basic models that can be applied to estimate the number of sampling units to comprise the second stage sample. If an estimate of the quantity of a resource present is needed, and if it is found that the variance of the estimate is proportional to the value of the resource, then probability sampling will generally be the most efficient model. If, however, in-place mapping is desired, a sampling scheme using regression estimation to establish the relationship between the discriminant analysis estimate and the ground estimate for the resource is used. Therefore, the sampling units for the second stage are selected using information derived in the first stage initial classification, thus reducing the amount of aerial and ground data needed.

The second stage of the model is based on aerial photography of the selected sampling units on which precise field size measurements can be made. In cases where only surface area cover estimates are needed, the second stage imagery and associated ground data are all that are needed. In other cases where estimates of yield per unit area are

required, three or more stages may be required to obtain adequate information. When the "correct" area and classification for each field in the sampling units has been determined, this information is used to adjust the estimates obtained in the initial classification.

CONCLUSIONS

The techniques and results discussed in this paper have their real significance in that they indicate the very real possibility of eventually performing operational agricultural surveys on a regular basis using satellite data as a basic input. The particular procedure which has been explained is presented, not as an answer to the entire problem of agricultural surveys using spacecraft data, but rather as an example of how the problem can be approached and as an indication of some of the possible techniques that might be used.

Obviously there are a number of questions that must be answered before the design and feasibility of an operational system can be defined. Among the unanswered questions are those relating to the area effectiveness of training and calibration data (i.e., over how large an area is a given set of training data useful), to the applicability of such techniques to all crops in all parts of the world (and what kinds of adaptations of the techniques might prove necessary), and to the accuracy with which crop yields as well as acreages might be estimated. Furthermore, a limited study of the sort described here working with data from an experimental satellite such as ERTS-1 can only indicate the potential usefulness of such a system. Certainly a commitment by agencies actually involved in the collection of agricultural information, and an operational data processing system providing for the rapid availability of data which is so crucial in the agricultural situation are necessary before the final questions can be answered.

Town or City	1969 Urbanized Area (Acres)	1972 Urbanized Area (Acres)	Amount of Agricultural Land (Acres) Lost
Chandler	1,920	2,880	960
Glendale	4,000	6,240	2,240
Mesa	8,320	13,440	5,120
Phoenix*	56,680	64,680	8,000
Scottsdale*	6,400	9,600	3,200
Tempe	7,200	15,840	8,640

*1972 urbanized area totals do not include sparse residential developments in wildland areas.

Figure 1. Measurements of urban areas in Maricopa County, Arizona made using stratifications of Apollo 9 photos taken in 1969 and ERTS-1 imagery obtained in 1972 indicate the extent to which prime agricultural areas are being converted to urban use.

FIELD BY FIELD RESULTS OF CLASSIFICATION
OF TEST AREAS FROM ERTS-1 TAPE DATA
STRATUM 16 SAN JOAQUIN COUNTY, CALIFORNIA

		GROUND DATA										TOTAL	COMMISSION ERROR
		ASPA	CORN	HARV	BARE SOIL	POTA	SAFF	SUG BEET	FL IRR	ALFA	TOMA		
CLASSIFICATION	ASPA	126			4	3						133	5
	CORN	7	59									66	11
	HARV			19								19	0
	BARE SOIL	5			5							10	50
	POTA	2				4						6	35
	SAFF	1	1				6					8	25
	SUG BEET		1			2		5				8	37
	FL IRR								3			3	0
	ALFA											0	-
	TOMA		3				1					4	100
TOTAL		141	64	19	9	9	7	5	3	0	0	257	
% CORRECT		89	92	100	56	44	86	100	100	-	-	227	88.3

TOTAL PERCENT CORRECT - 88.3

Figure 2. Preliminary classification tests on sample areas within a field-crop stratum in San Joaquin County resulted in an overall percent correct identification based on number of fields of 88 percent.

	GROUND										DATA										TOTAL
	1	2	3	4	5	6	7	8	9	10	11	12	13	14	15	16	17	18	19	20	
ASPARAGUS	132	1		4	1																145
SAFFLOWER	1	12				1															14
SUGAR BEETS				2	4	1															45
ALFALFA	1	2	2	6	2		1														40
TOMATO	18	4	1	3	33	3	2														66
WALNUT						11	2														16
CORN	7					63															70
HARVESTED					1	23		2													27
BARE SOIL	5					5															10
FLOWED	2			2		1	18	2		3											24
PASTURE	2			3	2																35
BURNED								1													1
ROAD				3																	3
WATER										10											10
GRAPES							2														15
TREES										1											34
LIMA BEANS				1	1																7
RICE																					14
PEPPER																					12
SORGHUM																					9
SQUASH				1																	17
POTATO	2																				1
OTHER				1	1																2
TOTAL	168	17	33	67	43	13	70	28	9	19	33	1	0	11	11	6	20	20	4	2	9
% CORRECT	71	63	11	76	77	85	90	82	55	15	82	100	-	11	73	100	50	60	25	25	50
																					44
																					612
																					1

TOTAL % CORRECT = 77.9

CROP TYPE	STUDY AREA					TEST EXTRACTIONS				
	CLASSIFIED POINTS	RECLASSIFIED POINTS	W/WEIGHTS	ACRES	% OF TOTAL	CLASSIFIED POINTS	ACRES	% OF TOTAL		
ASPARAGUS	56,371	56,833	57,857	62,070	28.23	17,446	19,190	33.2*		
HARVESTED	36,103	31,282	30,416	35,377	16.09	5,159	5,675	9.83		
CORN	26,662	31,320	31,280	29,135	13.36	8,720	9,592	16.60		
SUGARBET	15,646	14,689	15,046	17,238	7.84	4,309	4,740	8.20		
SAFFLOWER	11,089	9,127	9,513	12,225	5.56	2,945	3,240	5.51		
WATER	10,189	12,188	10,189	11,235	5.11	2,404	2,644	4.58		
POTATO	5,749	3,022	3,137	6,332	2.88	1,866	2,053	3.55		
BARE SOIL	1,450	973	1,450	1,583	.72	647	712	1.23		
TOMATO	30,409	29,384	30,059	33,457	15.23	7,019	7,721	13.37		
ALFALFA	9,532	10,382	10,643	10,950	4.98	1,994	2,193	3.80		
TOTALS	199,600	199,600	199,600	219,872	100.00	52,509	57,760	99.98		

Figure 3. The table on the left illustrates the results of preliminary classification of over 600 test fields in the field-crop strata in San Joaquin County. On the right are the results of a classification of all of one field crop strata comprising an area of over 200,000 acres (80,000 ha). This essentially comprises a description of the entire stratum in terms of the area classified as each of the various crop types.

	STRAT- IFIED NO CALSCAN	MULTI DATE CALSCAN			CALSCAN NO STRAT- IFICATION
		ONE DATE	TWO DATES	THREE DATES	
STRATIFICATION	120	120	120	120	0
TRAINING EXTRACTION	0	660	660	660	1370
CALSCAN ANALYSIS	0	210	570	1176	8260
SAMPLING GROUND ENUMERATION and CALCULATION	n=82 8835	n=22 2430	n=11 1275	n=9 1060	8835
TOTAL COST	8955	3420	2625	3021	18,465
RELATIVE COST	1.0	.38	.29	.34	2.06

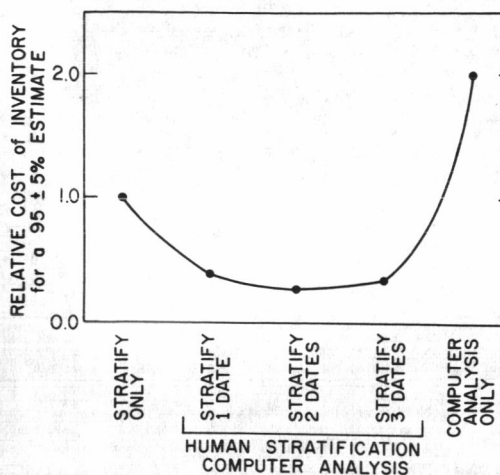


Figure 4. The table and accompanying plot illustrate the estimated relative costs in dollars of performing a crop inventory in San Joaquin County. The estimates assume an accuracy of classification of ± 5 percent at the 95 percent confidence level. Note that it would appear that the least expensive survey would involve both initial stratification by human interpreters and computer classification of crops within strata.

FOREST AND LAND INVENTORY USING ERTS IMAGERY AND AERIAL PHOTOGRAPHY IN THE BOREAL FOREST REGION OF ALBERTA, CANADA

C. L. Kirby*

Satellite imagery and small-scale (1:120,000) infrared ektachrome aerial photography for the development of improved forest and land inventory techniques in the boreal forest region are presented to demonstrate spectral signatures and their application. The centre point of the study area is at 57°N and 118°W (Figure 1).

The forest is predominately mixed, stands of white spruce and poplar, with some pure stands of black spruce, pine and large areas of poorly drained land with peat and sedge type muskegs. This work is part of coordinated program to evaluate ERTS imagery by the Canadian Forestry Service.

Figure 2 is a satellite scene obtained by the multispectral scanner of ERTS on September 2, 1972. The scene has been geometrically and radiometrically corrected. Mapping precision of this satellite frame is similar to that obtainable on a national topographic map at a scale of 1:250,000 (50 meters), and serves as a useful base map—because of the detail—for transferring information from the small-scale aerial photography. The green, red and first infrared bands have been combined with an electron beam image recorder by the Canada Center for Remote Sensing in Ottawa to produce a false color picture somewhat similar to that obtained with small-scale (1:120,000) aerial photography.

Geological and hydrological features that the satellite picture brings out are: areas of sand dunes (a dead ice moraine) (1), beach lines and glacial spillways (2) (3), and lakes filled with algae and sedges (4). An inventory of all ponds giving not only location but also water quality is possible. Interpretation such as this, over time, will clearly indicate the direction of many hydrologic processes. Water with algal growth and tall sedges because of the high I. R. reflectance, appears light pink. Water with high amounts of sedimentation, such as the Peace River, shows as blue. The sand bars in the Peace River have a high reflectance and appear nearly white.

*Canadian Forestry Service, Northern Forest Research Centre, Environment Canada, 5320 122nd Street, Edmonton, Alberta. T6H 3S5

N74 30715

Line detail includes: roads (5), railroads (6), oil pipelines with a width of only 30 meters (100 feet) (7), clearcut strips (8), and patches (9), and oil well sites as small as 200 meters square (10).

Forest covertypes in evidence are: coniferous (11) and hardwood (12) stands, muskeg (13), and burned-over areas (14). Coniferous forests appear dark red, hardwood forests appear red, and muskegs and burned-over areas show as light blue, yellow or white.

In the upper right-hand corner of the ERTS frame, a brown-to-purplish tone (15) is evident; this apparently is the result of many small patches of coniferous forest surrounded by water. The patches are less than the size of an ERTS resolution element and we get an averaging of water and coniferous forest.

These are only a few obvious spectral signatures and their interpretation. As one would expect, spectral signatures of all targets are subject to many changes depending on the season, phase of vegetation, and atmospheric pass.

A comparison of small-scale (1:120,000) aerial photograph with a portion of the previously discussed ERTS scene is shown in Figure 3.

ERTS imagery obtained on January 7, 1973 brings out surface relief of stream beds more clearly than the previous summer scene. The interpretation of vegetation types was not possible at this date because of the low sun angle and confused reflectance patterns, except to positively identify muskegs with low vegetation because they are covered with snow.

The following ERTS images are just to the south of the picture in Figure 2. These images cover an area upon which we had a detailed forest inventory done from small-scale false-color aerial photography. On this aerial photography it was possible to accurately identify all covertypes and to classify forests into twenty-foot height classes.

On May 14 before the poplar trees had leafed out but the grasses and herbs had greened up, Band 5 portrayed the bones of the test area. The high reflectance of the vegetation along the streams showed the drainage patterns. In addition because the aspen were without leaf areas where a dense spruce understory was present were indicated.

On September 17, 1973, Band 5 appears to be considerably different from Band 5 on May 14, 1973. This is attributed to the first frosts in fall and to the changing reflectance patterns of the poplar leaves. Considerable caution in the interpretation of vegetation using photography or satellite imagery must be

exercised in the fall. Imagery at this date may indicate when killing frosts occur. In addition to rapid phenological changes in the aspen, there are phenological changes in the muskeg. Muskegs and softwood forests both have low reflectance on Band 5 in September.

Band 7 on September 17, 1973, was different from any previous Band 7 received. On this band, roads and line detail previously found only on Bands 4 and 5 now appear.

Color composites were made using a color additive viewer, Bands 4, 5 and 6 were combined with blue, green and red filters respectively. A forest burned-over in 1971 appears in the September composite, but not in the May composite. Therefore it is suggested that mapping of burned-over forest may be best done with fall imagery after the first killing frosts.

The May image indicated the location of the coniferous forest on Band 5, while Bands 4, 5, 6 of the September imagery showed the location of the hardwood forest. Therefore we combined the spring and fall imagery as follows:

<u>Date</u>	<u>Band</u>	<u>Filter</u>
September 17, 1973	4	Blue
" " "	5	Red
" " "	6	Green
May 14, 1973	5	Red

This combination of spectral bands and seasons gave good separation between water, conifers, muskegs and hardwood stands. In addition the location of forest cutting and road construction is enhanced. An updating of the forest cover map is possible with this type of information.

These trials illustrate that by combining phenological knowledge with the knowledge of spectral reflectance patterns the interpretation of vegetation types from ERTS imagery is improved.

A multistaged forest inventory system using satellite imagery, and aerial photography of small-scale (1:120,000) I.R. ektachrome (Kodak film 2445) and large-scale (1:1000) with aero color negative film (Kodak film 2445) is being developed.

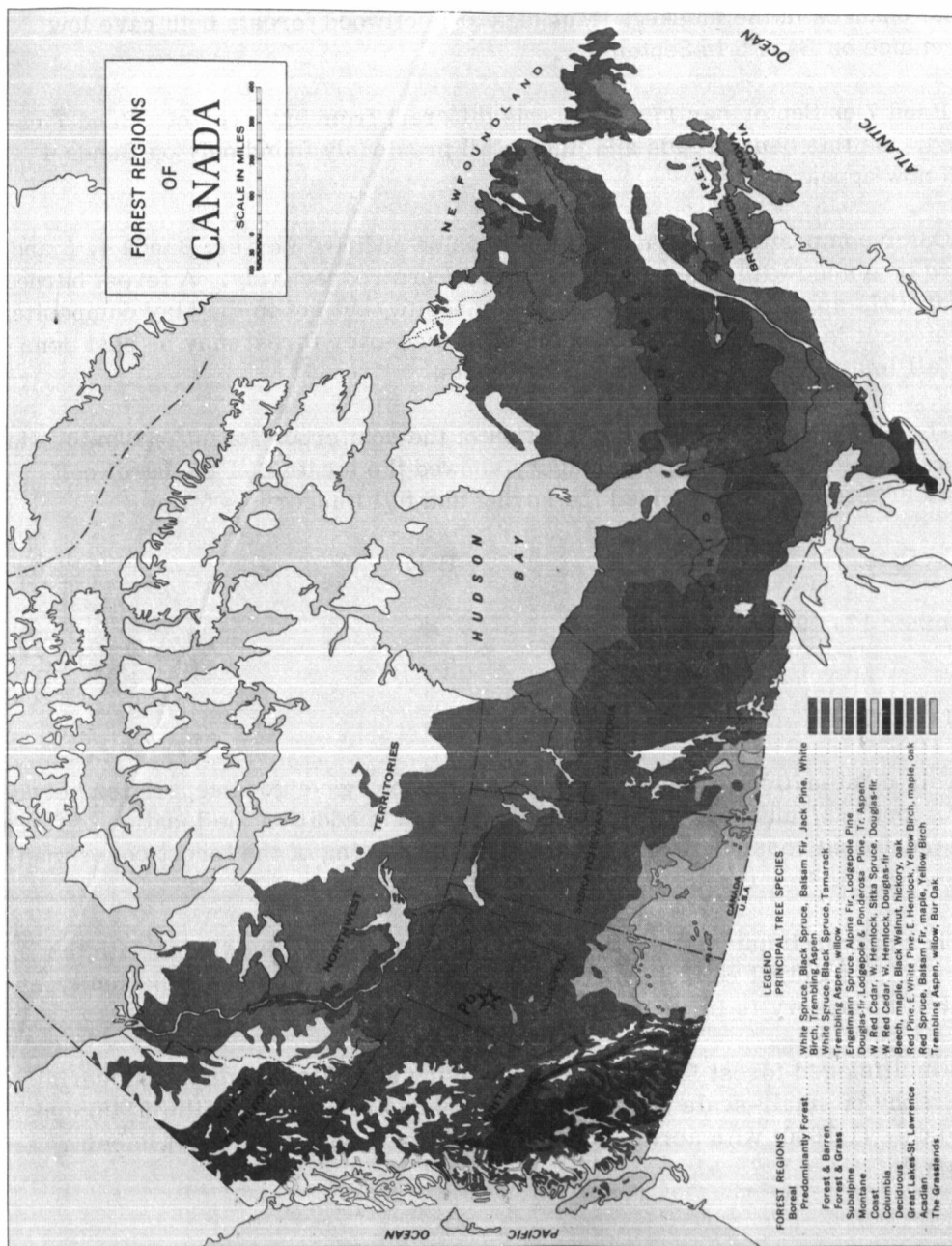


Figure 1. Location of P-6 Test Site in the Boreal Forest Region

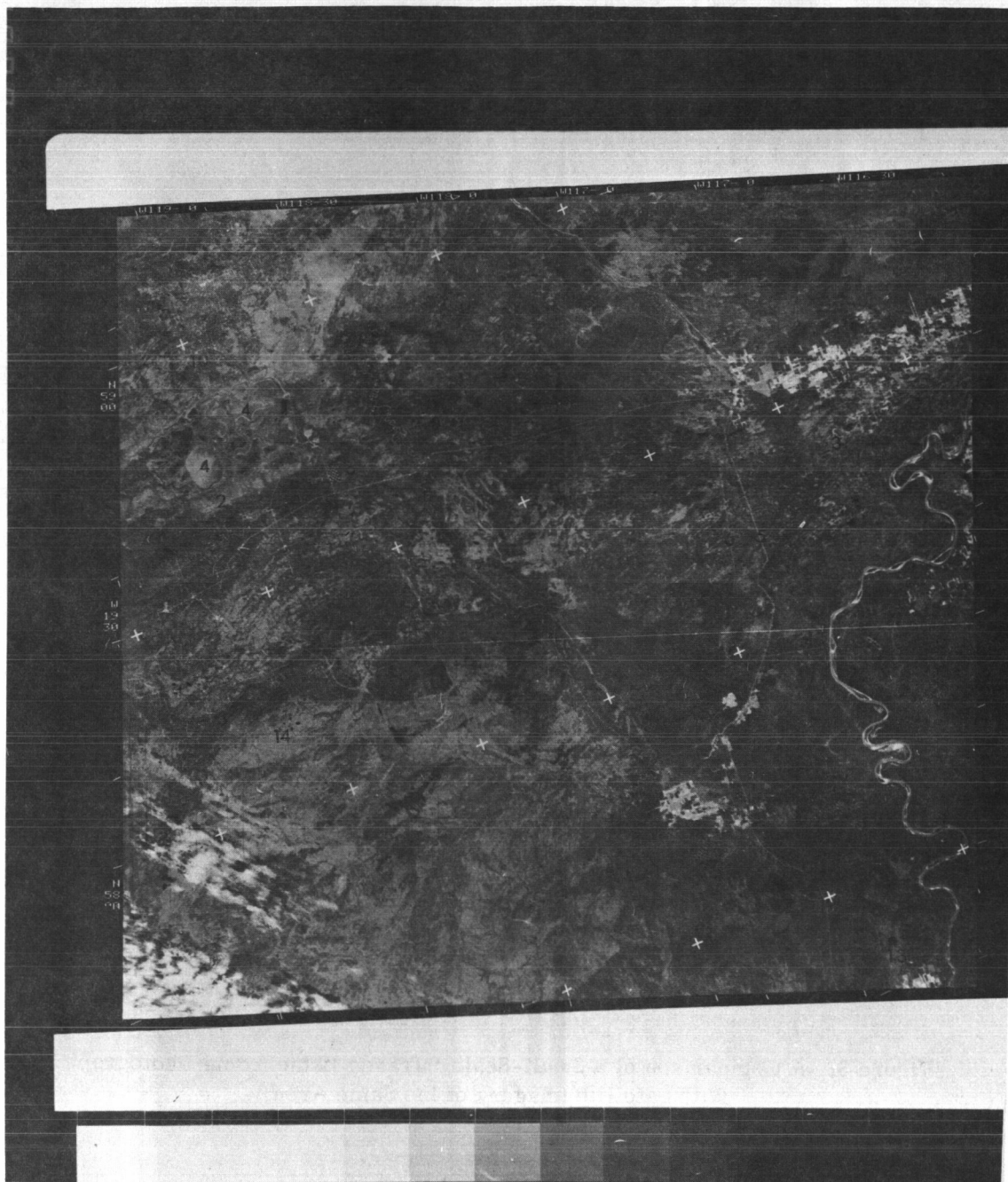


Figure 2. ERTS Image of Northwestern Alberta Obtained September 2, 1972

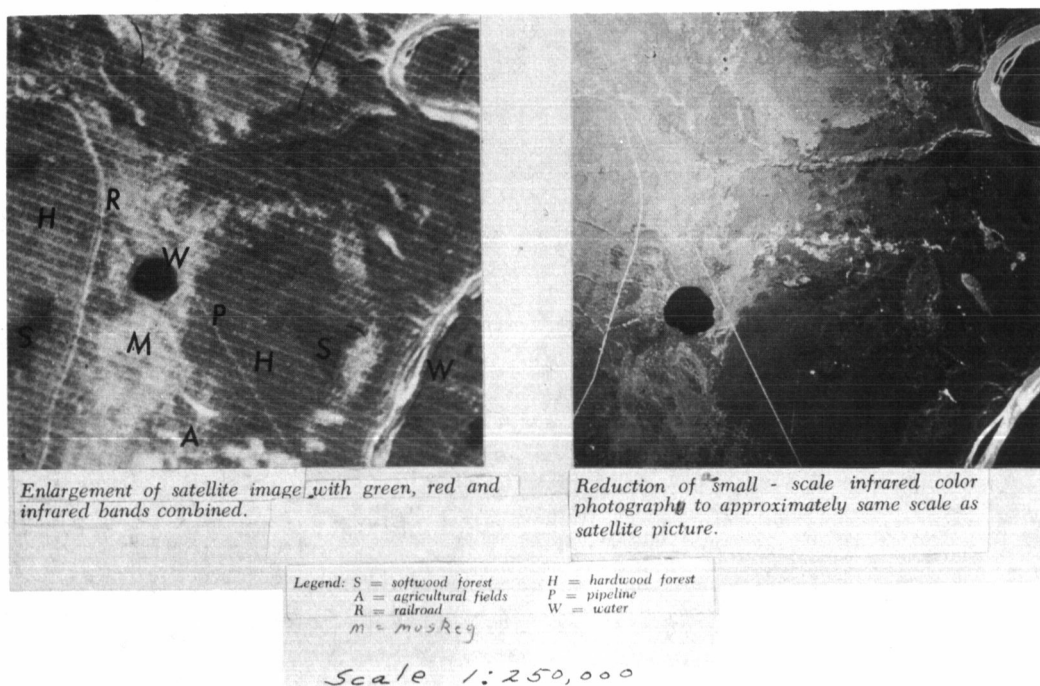


Figure 3. A Comparison of a Small-Scale Infrared Ektachrome Photograph With Satellite Imagery of the Same Area



Figure 4. Forest Covertypes as an Overlay on a Small-Scale Photograph

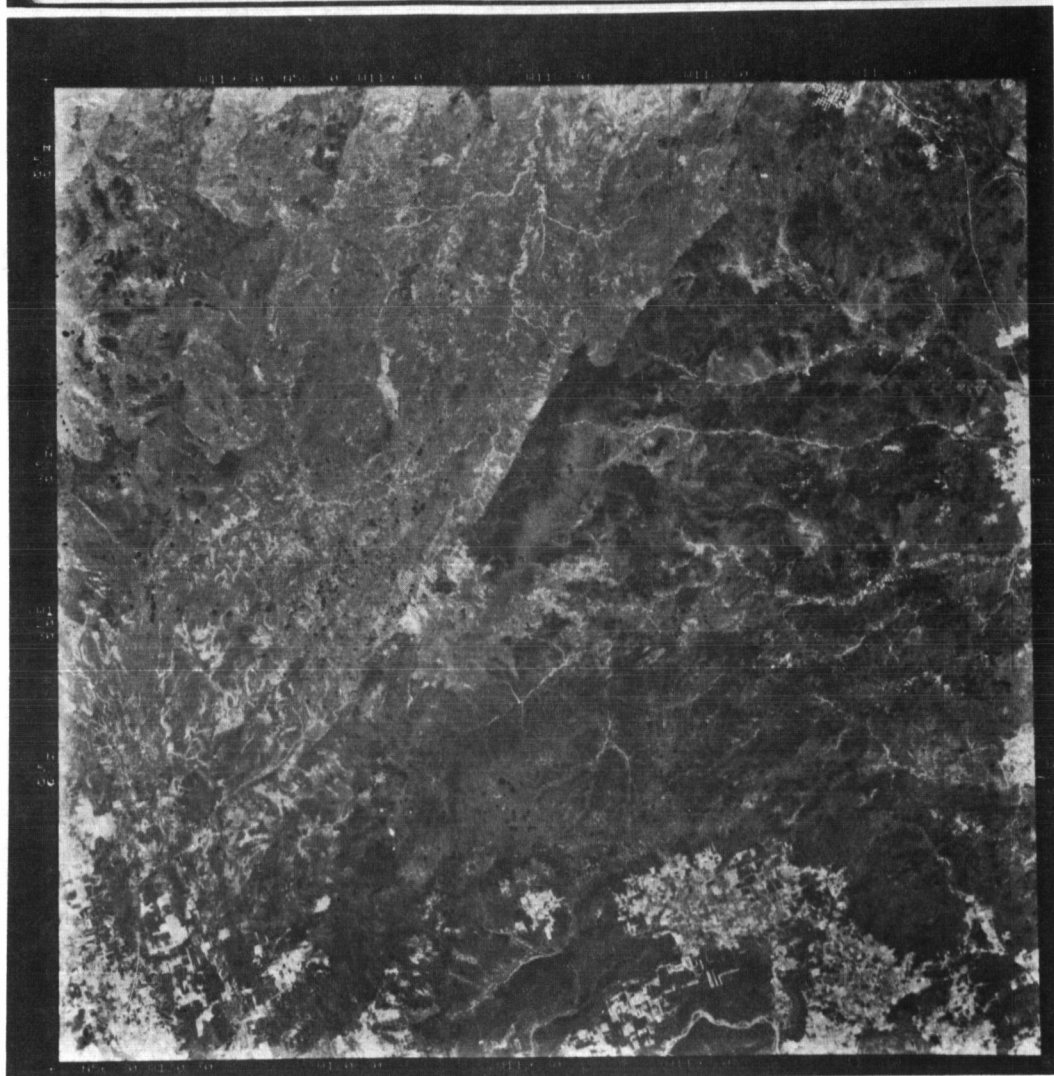
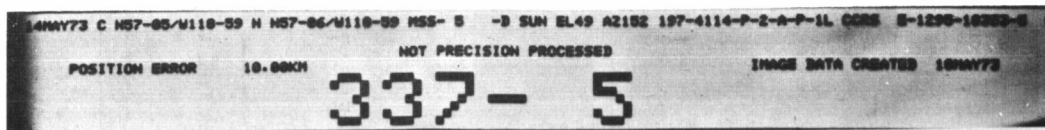


Figure 5. ERTS image Band 5, May 14, 1973.
Drainage patterns and coniferous forests are indicated.

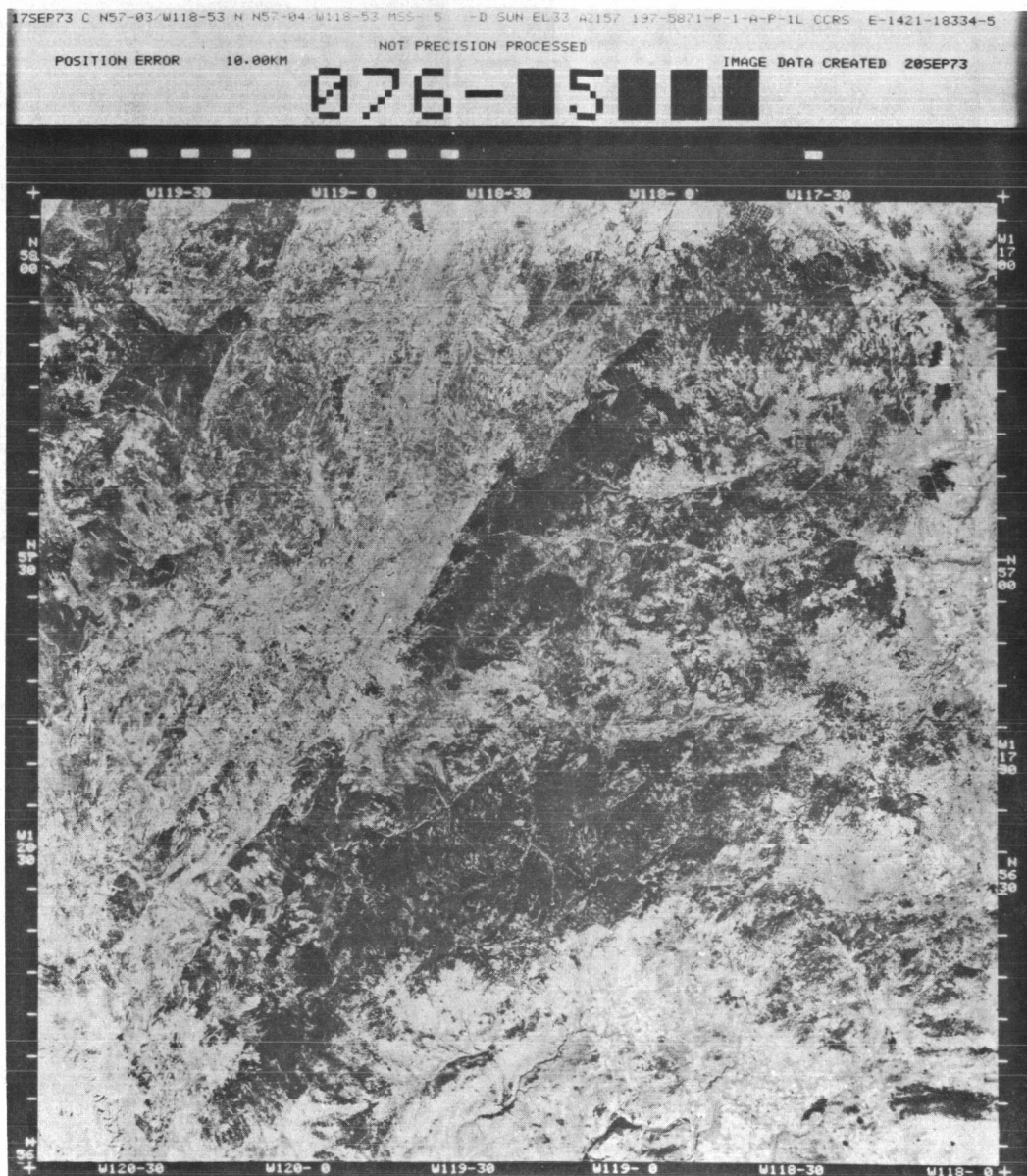


Figure 6. ERTS Image Band 5, September 17, 1973

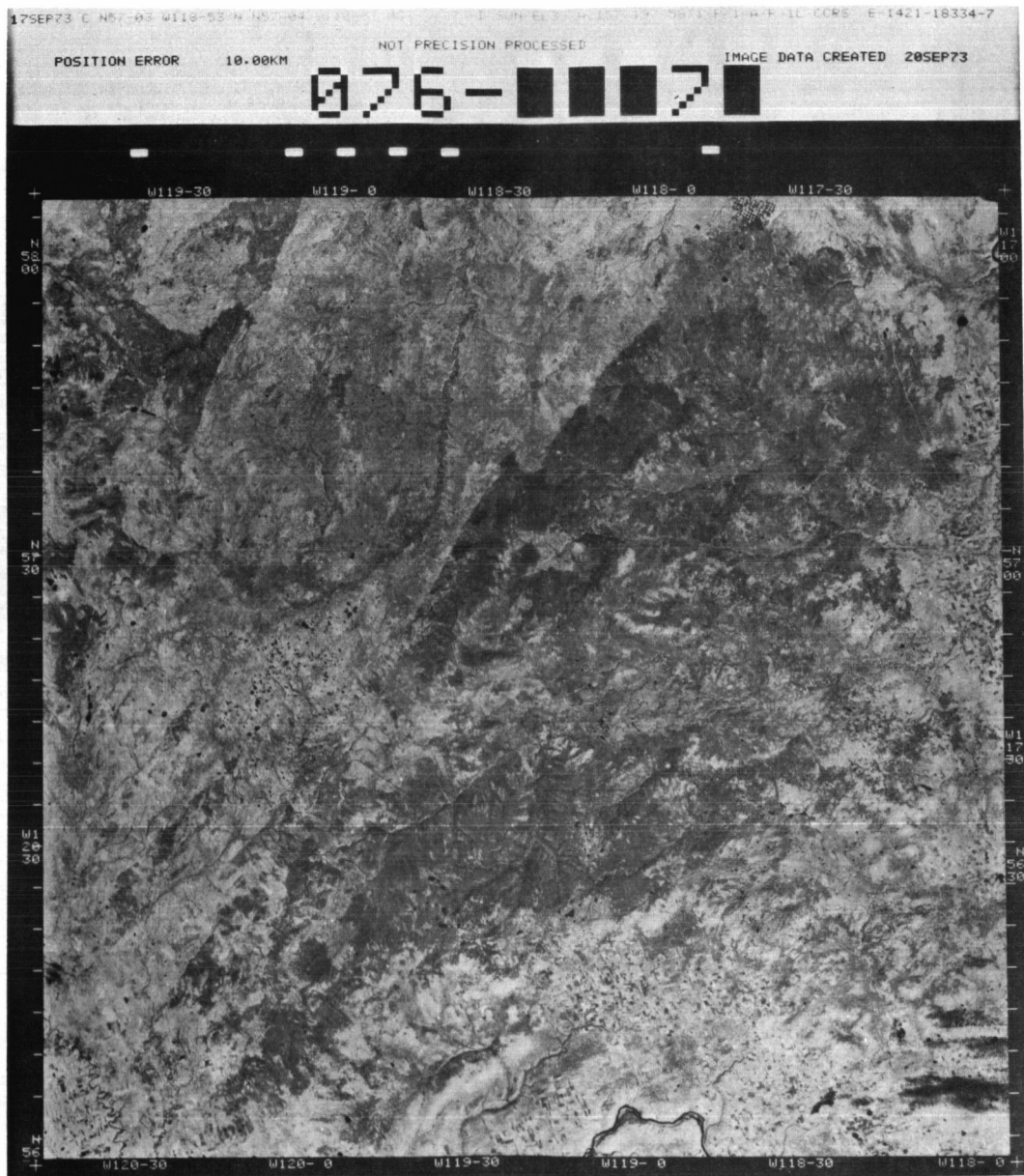


Figure 7. ERTS Image Band 7, September 17, 1973

SO₂ DAMAGE TO FORESTS RECORDED BY ERTS-1

Peter A. Murtha, *Research Scientist, Forest Management Institute, Canadian Forestry Service,
Department of the Environment, Ottawa, Canada*

ABSTRACT

SO₂ fumes have been affecting the forests around Wawa, Ontario, which have been under surveillance for a number of years and were recently covered by ultra-small-scale (1:160,000) air photography for damage-assessment purposes. The area was selected as a Canadian Forestry Service ERTS test site and was imaged on four successive ERTS-1 passes during the summer of 1973.

Image interpretation supported by electronic colour enhancement was used to delineate on ERTS imagery three damage zones (total-kill, heavy-kill and medium-damage zones). The zones delineated on ERTS imagery are similar to the results of aerial sketch-mapping and air photo interpretation. Band 5 provided the greatest detail for assessing the damage to the forests, followed in successive order by bands 4, 6 and 7. Comparison with ERTS images obtained in the winter showed that even though the total-kill could be separated from heavy-kill damage zones, total-kill could not be consistently separated from clear-cut logging, burned areas, frozen lakes and bogs.

INTRODUCTION

Between May 4 and September 8, 1973, a CFS test site near Wawa, Ontario (Sayn-Wittgenstein and Moore, 1972) was imaged six times (twice in the spring and four times in the summer); each time virtually cloud-free conditions existed. The best images were obtained on August 3, and September 8; this paper deals with these images.

SUMMARY OF RESULTS

Band 5 was the best band to delineate the extent of vegetation damage on both dates. The boundaries of damage on the August 3, band-5 image (Figure 1) coincided most closely with the results of the photo interpretation and aerial sketch-mapping. Figure 2 depicts the image for band 4: Figures 3 and 4 are the corresponding imagery for September 8. Figure 5 and 6 are photos of the total-kill and medium-damage zones.

¹This paper is the synthesis of 2 previous publications (Murtha 1972 and 1973).

1 N74 30716

The SO₂ fume damage to the vegetation was the most obvious on the band 5, August 3 image for the following reasons:

- (i) exposed rock, sand, tree bark, and dry, dead foliage have their highest spectral reflectance in the red spectral region (Steiner and Gutermann, 1966);
- (ii) chlorophyll of green vegetation absorbs in the red spectral region, thus vegetated areas would be "dark" on band 5.

Analysis of the damage zones showed that:

- (i) the total-kill zone (Figure 5) where almost no vegetation exists, is "brightest" on the image;
- (ii) the heavy-kill zone, where only patches of less vegetation are found, has a darker tone than does the total-kill zone;
- (iii) the medium-damage zone (Figure 6) where some of the trees have been killed, is darker in tone than either of the others, but is still not as dark as the forested areas outside the damage zones;
- (iv) it was impossible to delineate the area of light injury on the ERTS-1 image;
- (v) at ERTS-1 scale (1:1,000,000) the small variations in the boundaries of the damage zones are not evident;
- (vi) as the growing season ended and autumnal coloration occurred, it was increasingly difficult to delineate the perimeters of the damage zones.

Discrimination between the SO₂ fume damage zones and other forest "disturbances", such as fire and logging, was facilitated because of the particular characteristics of the SO₂ pollutant damage, and was influenced to a great extent by the prevailing wind. Thus,

- (i) there is a strong point-source (e.g. factory location at Wawa. See arrows Figures 1 to 4);
- (ii) the damage billows (expands) in a direction coincident with the prevailing winds; and
- (iii) the damage decreases in intensity as the distance from the point-source increases.

Logging activities and forest fires have sharply defined boundaries associated with them whereas the areas of SO₂ damage did not.

If the total-kill and heavy-kill damage zones had not been present, it would have been virtually impossible to delineate the medium-damage zone, let alone designate the cause of damage as an air pollutant. It was only because of *a priori* knowledge that the Wawa damage was attributed to SO₂. The only interpretation possible from the ERTS-1 image was to indicate that the damage was wind-associated.

The sequence of the dates and bands indicates that there is an optimum date during the growing season at which to delineate the damage. Obviously any

date prior to the growing season is unsuitable because of the large component of leafless, perfectly healthy trees and "exposed terrain". In the latter part of the growing season, autumnal coloration "colours" the interpretation of results. The best results would then come during the early part of August.

In conclusion, it seems that ERTS-1 imagery should provide a simple means of mapping and monitoring large forest areas affected by severe SO₂ fume damage, provided sufficient time has elapsed for the damaged forest region to take on the characteristics of the air pollutant (SO₂) damage. It is impossible to map areas of "light injury" from the satellite imagery.

REFERENCES

- MURTHA, P.A. 1972. SO₂ forest damage delineation on high-altitude photographs. Proc. 1st Can. Symp. on Remote Sensing, vol. 1, p. 71-82.
- MURTHA, P.A. 1973. ERTS records SO₂ fume damage to forests, Wawa, Ontario. For. Chron. 49(6); *In Press*.
- SAYN-WITTGENSTEIN, L., and W.C. MOORE. 1972. The ERTS experiments of the Canadian Forestry Service. Proc. 1st Can. Symp. on Remote Sensing, vol. 2, p. 705-712.
- STEINER, D. and T. GUTERMANN. 1966. Russian data on spectral reflectance of vegetation, soil and rock type. Dep. Geog., Univ. Zurich, Zurich, Switz. 232 p.

POSITION ERROR

10.00KM

NOT PRECISION PROCESSED

IMAGE DATA CREATED 6AUG73

360-5

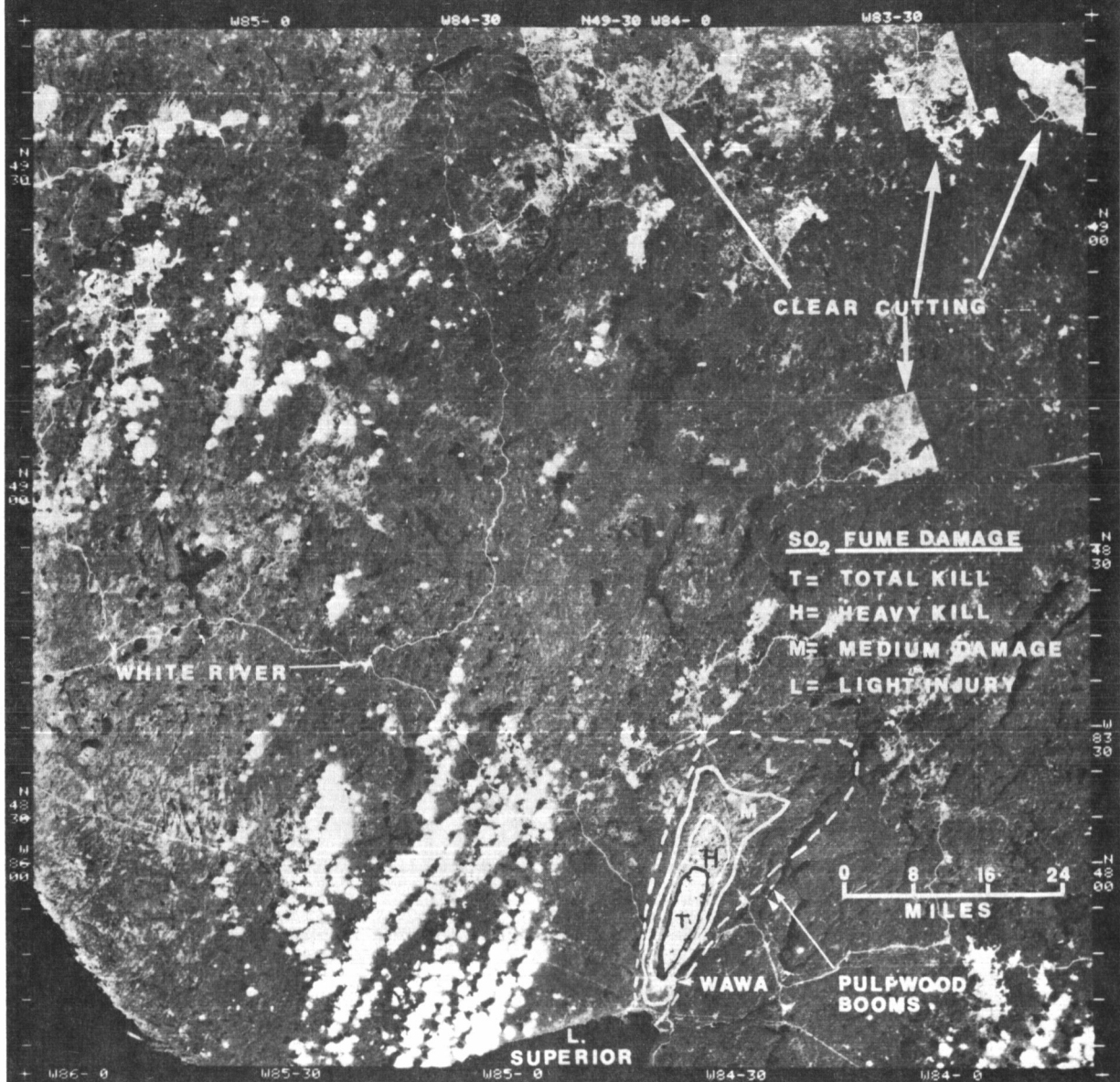


Figure 1. ERTS-1 frame no. 1376-16020; band 5; 3 August, 1973. Three SO₂ fume-damage zones are delineated covering about 390 square kilometers. (Refer to Murtha (1972) for definitions of the damage zones.) Total-kill = T; Heavy-kill = H; Medium-damage = M; and light-injury = L. The light-injury zone was not interpreted from the ERTS-1 image but was transferred from air photos. The T, H, and M zones are consistent with the photo-interpretation results.



Figure 2. ERTS-1 frame no. 1376-16020; band 4; 3 August 1973. Note the decreased detail and size of damage area when compared with Figure 1.

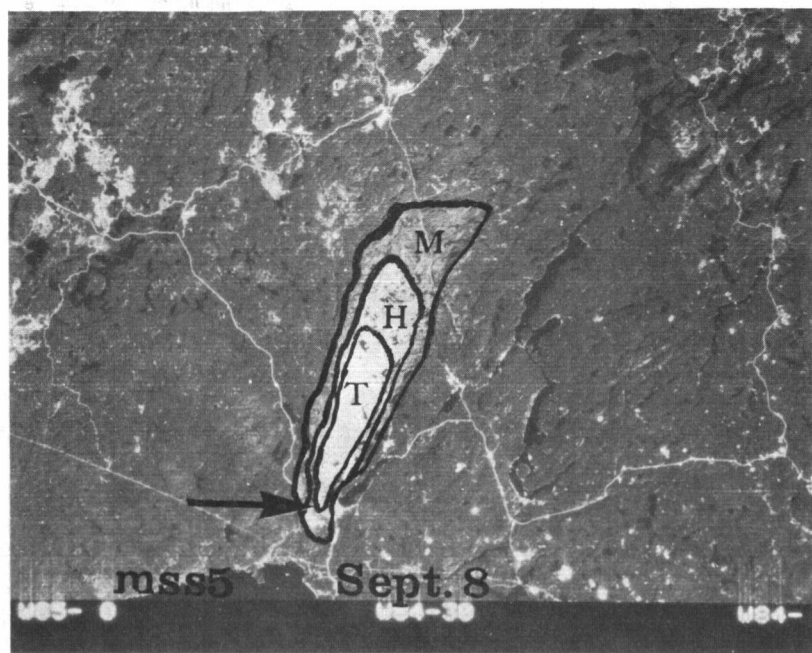


Figure 3. ERTS-1 frame no. 1412-16013; band 5; 8 September 1973. Although the damage zones may be delineated, the size of the medium-damage zone is not as large as the zone delineated in Figure 1. The other two zones are virtually the same as that shown in Figure 1.

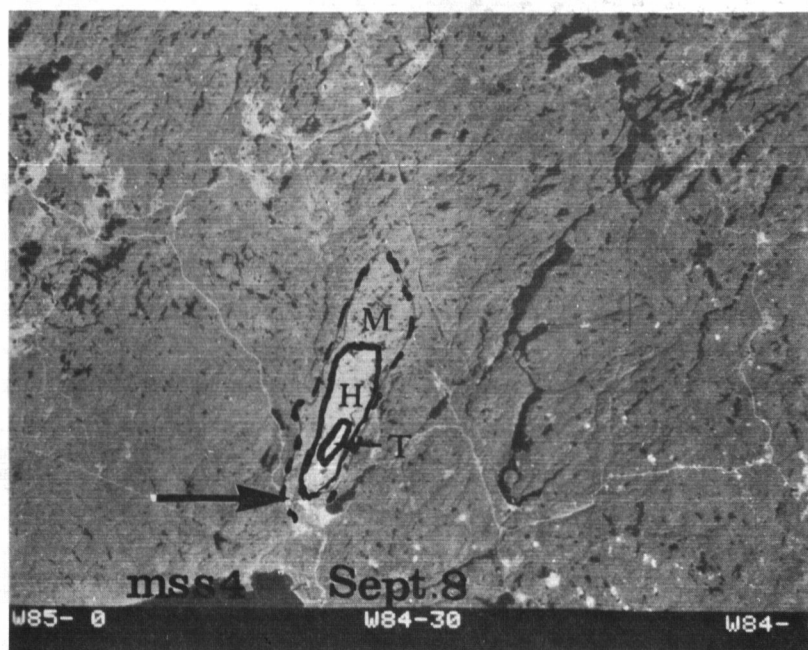


Figure 4. ERTS-1 frame no. 1412-16013; band 4; 8 September 1973. Note the decreased size of the damage zones.



Figure 5. The centre of the total-kill zone is characterized by the complete absence of vegetation. The exposed rock, which has a high red spectral reflectance, causes the very light tone of the total-kill zone on satellite image. (Photo by FMI).



Figure 6. The medium-damage zone is characterized by high white birch (*Betula papyrifera* Marsh) mortality, with no significant mortality of other hardwoods and conifers. (Photo by FMI).

A TIMER INVENTORY BASED UPON MANUAL AND AUTOMATED ANALYSIS OF ERTS-1 AND SUPPORTING AIRCRAFT DATA USING MULTISTAGE PROBABILITY SAMPLING

James D. Nichols, Mike Gialdini and Sipi Jaakkola, *Center for Remote Sensing Research, 260 Space Sciences Laboratory, University of California, Berkeley, California*

ABSTRACT

A quasi-operational study demonstrating that a timber inventory based on manual and automated analysis of ERTS-1, supporting aircraft data and ground data was made using multistage sampling techniques.

The inventory proved to be a timely, cost-effective alternative to conventional timber inventory techniques. The timber volume on the Quincy Ranger District of the Plumas National Forest was estimated to be 2.44 billion board feet with a sampling error of 8.2 percent. Costs per acre for the inventory procedure at 1.1 cent/acre compared favorably with the costs of a conventional inventory at 25 cents/acre. A point-by-point comparison of CALSCAN-classified ERTS data with human-interpreted low altitude photo plots indicated no significant differences in the overall classification accuracies.

SECTION I: INTRODUCTION AND PROCEDURES

In order to test the usefulness of ERTS imagery for wildland resource inventories, a timber inventory was performed in which the ERTS imagery acted as the first stage of a multistage sampling design. The objective of the inventory was to estimate the standing volume of merchantable timber within the Quincy Ranger District (215,000 acres) of the Plumas National Forest in California. Secondary objectives of the inventory were: (1) to test the operational efficiency of the sampling procedures of the multistage sampling design; (2) to test the effectiveness of the CALSCAN classifier on the ERTS data; (3) to determine the value of ERTS data and the aircraft data in reducing the sample error; and (4) to compare the costs of this timber inventory with other inventories that utilize conventional procedures.

A three stage sampling design was tested in which "timber volume" was the variable estimated. At each stage timber volume estimates were made from sampling units whose probability of selection in the sample was proportional to the predicted volume. Timber volume estimates were made from three stages: (1) the first stage involved automatic classification of the timberland on the ERTS data tapes into four timber volume classes. Within the classified area subsamples were selected (called primary sampling units; PSU) from which a more refined estimate

IN 74 30717

of timber volume could be made in the second stage; (2) the second stage involved the acquisition of low altitude photograph of selected primary sampling units to choose photo plots based on a second timber estimate made by comparison with photo-volume tables; (3) the third stage involved selecting individual trees within selected sample photo plots by photo measurement of all merchantable trees. The selected trees were then precisely measured for volume on the ground and these volume measurements in turn were expanded through the various stages of the sample design to estimate total timber volume over the national forest land within the Quincy Ranger District.

The statistical procedures for expanding the timber volume estimates through the various stages of the timber inventory are discussed in Section II of this study. The procedures for selecting sampling sites and estimating timber volumes from ERTS and aircraft imagery at each of the stages of the sample design are described in subsequent sections in order to demonstrate how the ERTS and supporting aircraft data were necessary components in performing the timber inventory.

Stage I. CALSCAN Classification of ERTS Data and Primary Sample Unit Selection

ERTS-1 data tapes of the Quincy Ranger District, Plumas National Forest, were classified on the CRSR interactive human-computer system using a CALSCAN point-by-point classification routine. The coordinates of the Ranger District boundary and those of non-national forest land within the District were identified on the tapes so that only those picture elements associated with national forest land were classified and incorporated into the inventory. This procedure considerably reduces the costs of classification.

The classification was based on four timber volume classes, namely (1) non forest; (2) forest sites containing less than 10,000 Bd. ft./ac.; (3) forest sites containing 10,000-20,000 Bd. ft./ac.; and (4) forest sites containing more than 20,000 Bd. ft./ac. The classifier was trained to recognize each of the four timber volume classes based upon photo-interpretation selection of 33 training cells whose range of timber volumes was based on crown closure and average crown diameter. The training cells were selected from interpretation of high altitude color-infrared photography (scale 1/120,000). Each of the training cells was located on the ERTS imagery and digitized. Point-by-point classification of all ERTS data points within the Quincy Ranger District proceeded by matching each data point (picture element) with the training cells. The results were grouped into the four timber volume classes. The accuracy achieved by automatic classification of ERTS tapes (Tables 1 and 2) demonstrates the efficiency which can be attained in the timber inventory through analysis of ERTS data tapes in the initial stages of the sample design.

The classified ERTS data (CALSCAN classification) of the Quincy Ranger District was divided into rectangular sampling units (called primary sampling units). Each unit measured 1325 ft. wide by one and a half miles long. The size of these sampling units was based upon a practical area which could be photographed in a single flight line by a light aircraft using a 35 mm camera system, the ability of the ground crew to complete the ground work for a flight line in one day, and the variation between sampling units. For each primary sampling unit, the following information was computed.

- (1) The number of points in each volume class (within the unit).
- (2) The weighted total volume for each volume class.*
- (3) The sum of the weighted totals for all classes.
- (4) A cumulative sum of the weighted totals.
- (5) The mean volume for all sampling units.
- (6) The variance of the sampling units.

Based upon the information either estimated or computed for each primary sampling unit (PSU), four units were selected for further sampling in the timber inventory. The four units were selected with probability of selection proportional to their estimated volumes. The location of the four selected PSU's was transferred from the ERTS classified images to the color-infrared high altitude aerial photography (scale 1/120,000) to facilitate locating them accurately from the air when they are photographed from a lower altitude as part of the second stage of the timber inventory.

Stage II. Volume Estimation on Low Altitude Photography

Two 35 mm cameras were used to obtain low altitude photography of the selected primary sampling units at two different scales. A 24 mm focal length wide-angle lens was used to acquire complete coverage of each sampling unit at an approximate scale of 1/7500, and a 200 mm focal length lens obtained large scale stereo triplicates, scale approximately 1/1000, from which to make precise photo estimates of timber volume. The camera with the telephoto lens was equipped with a motorized film drive which enabled each stereo triplicate to be taken within one second at five second intervals, while the camera with the wide-angle lens was operated manually to obtain single frames at five second intervals. The photo coverage for each PSU consisted of 10 stereo triplicates and 10 wide-angle photographs.

The wide-angle photos of each primary sampling unit were formed into a mosaic to show its full area. The center of the middle photo for each stereo triplicate was used as a plot center and was located and marked on the mosaic. Each plot center was also located on a topographic map and its elevation was determined.

*The weighted total volume was determined by multiplying the number of points in each volume by the assigned weight for that class:
non-timber = 0; less than 10,000 Bd. ft./ac. = 1; 10,000-20,000 Bd. ft./ac. = 2; 20,000 Bd. ft./ac. and above = 3.

Discriminant Analysis		NF	T1	T2	T3
Photo Interpretation on 1:1000 color photography	NF	90.0	5	0	5
	T1	0	93	7	0
	T2	7	19	67	7
	T3	0	0	25	75
% change in class		+5%	+20	-7%	-8

NF = Non forest

T1 = Less than 10,000
board feet per acre

T2 = 10,000 to 20,000
board feet per acre

T3 = Greater than 20,000
board feet per acre

Table 1

The accuracy obtained in a comparison of classified ERTS data with photo interpreter classification from a photo scale of 1/1000. The diagonal of the matrix shows the percentage correct classification when comparing the discriminate analysis of ERTS data with the large scale photographs. The values not along the diagonal represent the percentage of points which were classified into adjacent timber volume classes. The values at the bottom of each column indicate the percentage of points classified by discriminate analysis of ERTS data which were greater than (+) or less than (-) the points classified by interpreters on large scale aerial photographs.

Discriminant Analysis of ERTS-1 data

	Coni	Soil/R	BR	H.W.	Wat.	Conv.	Grass
Coni	95.7	.9	0	3.8	0	0	.9
Soil/R	0	71.8	0	14.1	0	7.0	7.0
BR	14.3	0	48	13.0	0	1.3	23.4
H.W.	13.2	.9	1.9	74.5	0	3.8	5.7
Wat.	0	0	0	0	100	0	0
Conv.	12.5	12.5	0	43.8	0	31.25	0
Grass	15.6	9.4	3.1	6.35	0	6.3	59.4
% change in class	+5.6	-16.9	-48.1	+13.2	0	+6.25	+59.4

Photo Interpretation on 1:120,000
CIR and ground dataCONI = Commercial conifer consisting of
pure fir and mixed conifer stands.

SOIL/R = Soil and Rock.

BR = Brush lands made up several species
in mixed and pure stands.

HW = Hardwoods included Oak and riparian.

WAT = Water.

CONV = Brush lands converted to conifer
plantations.GRASS = Grass lands included dry and
wet meadows.

TABLE 2. The results obtained in comparing classified ERTS data with photo-interpretation-classification of land vegetation categories on small scale aerial photographs (1/120,000). The diagonal of the matrix shows the percentage correct classifications when comparing the discriminant analysis of ERTS data with the training cell classes delineated on the small scale photograph. The values not along the diagonal represent the percentage of points which were classified into adjacent categories. The values at the bottom of the columns indicates the percentage of points classified by discriminant analysis which are greater than (+) or less than (-) the points associated with the training cells.

The scale of each photo plot was determined, and a .4 acre circular plot was drawn about the photo plot center. Timber volume in each .4 acre photo plot was estimated by referring to photo-volume tables based upon interpretation of % crown closure and measurement of average stand height using a parallax bar (Chapman, 1965). Within each primary sampling unit, two out of the ten possible photo plots were chosen with probability of selection proportional to the estimated volume.

Stage III. Selection of Trees for Precise Ground Measurement of Timber Volume

In the third stage, all trees of merchantable size within each selected photo plot were pin-pricked and numbered. For each of these trees, the average crown diameter was determined based on the longest and shortest dimension of their crowns. After adjustments for scale, the average crown diameter value was cubed (raised to the third power) to be used as a relative measure of individual tree volume for the third stage volume estimation. Four trees were selected from the population of merchantable trees found within each photo plot to be measured by a dendrometer on the ground. (Selection again was based upon probability proportional to the estimated volume of each tree.)

A two-man crew went into the Quincy Ranger District with a Barr and Stroud optical dendrometer to measure the selected trees. The large scale (low altitude) photographs were used to locate the photo plot centers as well as the trees within the plots to be measured. In addition to the dendrometer measurements, an easily recognizable feature on the ground near the plot center was measured in order to get a more accurate estimation of the photo scale of the plot. The dendrometer measurements were brought back from the Quincy Ranger District and entered into a computer program that calculated volumes for the individual trees. The tree volumes were then expanded through each stage of the sample design to estimate total volume on the District, consistent with the statistical methods for variable probability sampling (see Section II).

SECTION II. STATISTICAL METHODS FOR TIMBER VOLUME ESTIMATION

Timber volume predictions were made from three stages of the timber inventory of the Quincy Ranger District for the purpose of selecting sample plots whose probability of selection was proportional to the volume predictions. Thus, variable probability sampling methods were used to estimate the total volume in this timber inventory. Three variables proportional to timber volume were used in generating the selection probabilities: (1) "Volume" estimate of the ERTS picture element based on the spectral signatures on four bands and subsequent training and classification; (2) volume estimate of a plot on a 1:1000 scale color print based on the photo-volume tables (Chapman, 1965); and (3) volume estimate on a large scale photo based on a rough volume estimate - crown diameter cubed.

Using a scheme where probability of selection is proportional to the estimated volume, the effort is focused on the areas of higher timber volume and adds to the overall cost-efficiency. The ability to list the populations at each stage prompted the selection of list sampling as the variable probability sampling scheme.

Method of Estimation

The method of estimation was based on "unequal expansion" as implied by the probability scheme discussed above. At each of the three stages, the probability proportional to estimated size (p_i) was obtained by listing the volume estimates of the sampling units (x_i), and dividing them by the total of volume estimates $\left(\sum_{i=1}^n x_i \right)$:

$$p_i = \frac{x_i}{\sum_{i=1}^n x_i}$$

A sample of a chosen size was then drawn by applying random integers from 1 to $\sum_{i=1}^n x_i$ and observing the probability interval and the corresponding sampling unit which contains the randomly selected integers.

In the first and second stages the timber volumes of the selected sampling units were estimated by subsequent sampling, whereas in the third stage the volume was carefully measured by a precision dendrometer. The entire three stage estimation procedure was as follows:

Stage I: A sample of n_h out of the N_h PSU's was drawn from stratum h with probability proportional to estimated size (ppes). The estimate of the total volume then becomes:

$$\hat{V} = \sum_{h=1}^L \frac{1}{n_h} \sum_{i=1}^{n_h} \frac{y_{hi}}{p_{hi}}$$

where: L = total number of strata

p_{hi} = selection of probability of the i th PSU in the h th stratum

\hat{y}_{hi} = total volume of the i th PSU in the h th stratum (remains to be estimated by subsequent stages).

Stage II: To estimate the total volume (y_{hi}) of the i th PSU, a sample of n_{hi} out of the N_{hi} secondary sampling units (.4 acre plots) is drawn with probability proportional to estimated volume. This would give:

$$y_{hi} = \frac{1}{n_{hi}} \sum_{j=1}^{n_{hi}} \frac{y_{hij}}{p_{hij}}$$

However, in order to include area expansion from circular sample plots to the full PSU, plus stratify the second stage plots into four volume strata, the estimator becomes:

$$\hat{y}_{hir} = \sum_{r=1}^R \frac{1}{p_{hir}} \frac{A_{hir}}{a_{hir}} \frac{1}{n_{hir}} \sum_{j=1}^{n_{hir}} \frac{\hat{y}_{hirj}}{p_{hirj}}$$

where: $r = 1, 2, \dots, R$ refers to the CALSCAN volume strata

p_{hir} = selection probability of the r th volume stratum of the i th PSU in the h th stratum

A = area (indices as above)

a = sample area (indices as above)

n = sample size (indices as above)

p_{hirj} = selection probability of the j th plot of the r th volume stratum, of the i th PSU in the h th stratum

\hat{y}_{hirj} = plot volume (to be estimated by Stage III)

Stage III: To estimate the total volume of the j th plot, a sample of n_{hirj} out of the N_{hirj} tertiary sampling units (trees) is drawn with pps. Then ...

$$\hat{y}_{hirj} = \frac{1}{n_{hirj}} \sum_{k=1}^{n_{hirj}} \frac{y_{hirjk}}{p_{hirjk}}$$

where: p_{hirjk} = the selection probability of the k th sample tree of the j th plot of the r th volume stratum of the i th PSU of the h th stratum.

y_{hirjk} = the dendrometer measured volume of the k th sample tree of the j th plot of the r th volume stratum of the i th PSU of the h th stratum.

Combining the various stages above, the entire estimator becomes:

$$v = \sum_{h=1}^L \frac{1}{n_h} \sum_{i=1}^{n_h} \sum_{r=1}^R \frac{1}{p_{hir}} \frac{A_{hir}}{a_{hir}} \frac{1}{n_{hir}} \sum_{j=1}^{n_{hir}} \frac{1}{p_{hirj}} \frac{1}{n_{hirj}} \sum_{k=1}^{n_{hirj}} \frac{y_{hirjk}}{p_{hirjk}}$$

Variance of the Estimator

In multistage sampling, when the number of first stage units is large, most of the variability in the population is due to the first stage. Therefore, it suffices to consider only the first stage values (here \hat{y}_{hi}) to estimate the population variance and, consequently, the variance of the estimator (Durbin, 1953, p. 262; Kendall and Stuart, 1967, vol. 3, p. 200; Langley, 1971, p. 131).

Thus for the first stage our stratified sampling estimator becomes (Cochran, 1963, p. 260):

$$\hat{v} = \sum_{h=1}^L \frac{1}{n_h} \sum_{i=1}^{n_h} \frac{y_{hi}}{p_{hi}}$$

Its variance is:

$$\text{Var}(\hat{v}) = \sum_{h=1}^L \frac{1}{n_h} \sum_{i=1}^{N_h} p_{hi} \left(\frac{y_{hi}}{p_{hi}} - v_h \right)^2$$

which has an unbiased estimator

$$\text{Var } (\hat{V}) = \sum_{h=1}^L \frac{1}{n_h (n_h - 1)} \sum_{i=1}^{n_h} \left(\frac{y_{hi}}{p_{hi}} - \hat{V}_h \right)^2$$

For proportional allocation, $n_h = n (N_h/N)$ and

$$\text{Var } (\hat{V}) = \sum_{h=1}^L \frac{N}{n N_h} \sum_{i=1}^{N_h} p_{hi} \left(\frac{y_{hi}}{p_{hi}} - V \right)^2$$

$$\text{Var } (\hat{V}) = \sum_{h=1}^L \frac{N^2}{n N_h (n N_h - 1)} \sum_{i=1}^{n_h} \left(\frac{y_{hi}}{p_{hi}} - \hat{V}_h \right)^2$$

The last equation is an unbiased estimator of $\text{Var } (\hat{V})$ and can be used for the estimation of the sampling error of the inventory.

SECTION III. RESULTS AND CONCLUSIONS

The total volume of timber in the Quincy Ranger District of the Plumas National Forest was estimated to be 407 million cubic feet (approximately 2.44 billion board feet) based on eight selected photo plots located within four primary sampling units. The sampling error associated with this estimate was 8.2% which falls below the expected sampling error of 20% for the Quincy Ranger District. This indicates that the true volume of merchantable trees in the Quincy Ranger District will fall into the interval 2.11 - 2.77 billion board feet with 80% probability.

There were only 31 trees total measured by an optical dendrometer on the ground at the eight plots (32 trees should have been measured but one plot out of the eight contained only three merchantable trees which could be measured). The field work required one week's time from a two-man crew, and the total area of the ground plots measured was 3.2 acres, representing a sampling fraction of approximately 1/67,000.

Table 1 lists the costs of the timber inventory on 215,000 acres using the multistage sampling design as an operational system. The expected costs of an inventory using the above procedures, on the entire Plumas National Forest (1,161,554 acres) would be approximately \$15,000 and would take 5 months to complete. In comparison, the U. S. Forest Service in 1970 completed an inventory of the Plumas National Forest using the 10 point system, a conventional procedure, at a cost

of \$300,000 and took two years to complete. Some deficiencies of that inventory were: (1) that it did not provide in-place mapping of timber volumes and (2) it used interpolation to arrive at the volumes for each ranger district which tends to reduce the accuracy of the volume estimates for each district, as compared to the estimate for the entire forest. The CRSR system would inventory each ranger district as a separate unit, thereby achieving more precise estimates and could also provide in-place mapping of volume.

The Forest Service inventoried the entire El Dorado National Forest (858,496 acres) using WRIS (Wildland Resource Inventory System) at a cost of approximately \$31,300. While WRIS closely resembles the CRSR system in design, the results again lacked in-place mapping of volume as well as not treating each ranger district as a stratum. In terms of inventory costs per acre for each system, the CRSR system appears to be best (10-point system = 25¢/acre, WRIS = 3.6¢/acre, and CRSR = 1.1¢/acre) while still providing more information with little or no loss in precision. It should also be noted that the multistage design used here becomes more efficient as the total area considered increases. For example, if the entire State of California were inventoried, the per acre costs would be .175¢.

TABLE 3
COST ESTIMATE-TIMBER INVENTORY
BASED ON 215,000 ACRES - QUINCY RANGER DISTRICT

Computer Processing

CALSCAN Training and Photo Interpretation	\$ 120	
CALSCAN Classification	210	
Statistical Break-up	40	
CALSCAN Statistics	<u>12</u>	
		\$ 382

Aerial Photography

Aircraft and Crew	\$ 210	
Film and Processing	<u>90</u>	
		\$ 300

Supplies and Expenses

Travel	\$ 350	
Miscellaneous	<u>50</u>	
		\$ 400

Personnel

1 Project Scientist		
2 mos. F.T.E. @ \$1100/mo.	\$2,200	
1 Software Consultant		
.5 mo. F.T.E. @ \$1300/mo.	550	
1 Statistician		
.5 mo. F.T.E. @ \$1100/mo.	550	
2 Lab Assistants		
1 mo. F.T.E. Each @ \$620/mo.	<u>1,240</u>	
Salary Subtotal	\$4,640	

Associated Overhead \$968

\$5,568

TOTAL \$6,640

SUMMARY

The preliminary results of the timber inventory of the Quincy Ranger District indicate that the procedures employed in the multi-stage sampling design are valid and substantially reduce both the costs and the amount of time required to perform a timber inventory for a large area. This study demonstrates the value of ERTS data for accurately correlating picture elements with timber volume estimates as a fundamental first step in selecting primary sampling units in the first stage of the inventory. The inventory procedures utilized here will be applied to two additional districts of the Plumas National Forest in an effort to estimate the total timber volume on the forest to a desired sampling error of 10%.

Future activities will include the investigation of the ability of the CALSCAN classifier to correlate timber condition classes with picture elements to provide information for use in forest simulators. This would enable forest managers to project long-range results of management practices to determine their effectiveness. Also, similar inventory procedures will be developed for application to other vegetation types to provide timely, cost-effective, and useful information for resource management planning, such as fuel mapping for fire control and management and rangeland-condition mapping for carrying-capacity determinations.

APPLICATION OF ERTS-1 IMAGERY TO LAND USE, FOREST DENSITY AND SOIL INVESTIGATIONS IN GREECE

N. J. Yassoglou, *Athens Faculty of Agriculture*; E. Skordalakis, *NRC/Democritos*; and A. Koutalos, *Department of Agriculture*

ABSTRACT

The information, which is available at present, on land use, site quality and soil conditions in Greece, is not adequate.

Photographic and digital imagery received from ERTS-1 was analyzed and evaluated as to its usefulness for the assessment of agricultural and forest land resources.

Black and white, and color composit imagery provided spectral and spatial data, which, when they were matched with temporal land information, provided the basis for a semidetailed land use and forest site evaluation chartography.

Color composit photographs have provided some information on the status of irrigation of agricultural lands.

Computer processed digital imagery was successfully used for detailed crop classification and semidetailed soil evaluation.

The results and techniques of this investigation are applicable to ecological and geological conditions similar to those prevailing in the Eastern Mediterranean.

INTRODUCTION

During the Mycenaean and Classical Eras, the inhabitants of Greece had a remarkable knowledge of the properties and of the potentialities of their land resources. There is ample evidence that the utilization of land, during those times, was based on quite sophisticated systems securing its conservation. From the time of the Roman Conquest of the country up to the present time, little attention was given to land resources. Thus the lack of data is a serious hindrance to the elaboration of modern land development projects.

The objective of this investigation was to determine whether remote sensing data obtained from ERTS-1 could be used in recognizing, evaluating and mapping land features and resources. Emphasis was placed on the study of signatures related to agriculture and forestry such as: present land use, ecological sites, forest density, soil properties and soil chartography.

PRECEDING PAGE BLANK NOT FILMED

1 N74 30718

METHODS AND MATERIALS

ERTS-1 was successfully launched on July 29, 1973 and provided photographic and digital imagery of selected areas of Greece.

Two frames covering the Athens-Delphi and Eastern Peloponnese provinces in the south eastern part of the country were studied in this investigation. The studied remote sensing information was recorded on the 2nd of August, 1973. The local time was about 10.30 a.m.

Ground truth information was collected prior to the launching of ERTS-1. Data affected by temporal variations were collected on the date that the satellite obtained information over Greece.

Black and white photographic imagery was studied first and gray scale classes were related to land use features and to forest density.

False color composit photographs were used next, to further separate land use features, evaluate agricultural and forest sites and classify soils into broad categories.

Digital imagery was processed at LARS (Fu and Langrebe 1969) using the LARSYSAA computer program to determine detailed land use classes, map crop distributions and to recognize salinity and drainage condition of the soil in selected small areas.

Land feature maps, prepared from photographic and digital imagery, were checked in the field and their accuracy was tested. Thus improved relationships between ground truth and spectral information were achieved.

RESULTS AND DISCUSSION

A n a l y s i s o f P h o t o g r a p h i c I m a g e r y

Multispectral scanner and RBV photographic imagery was analyzed and the following land features were recognized.

Land Use Patterns.

The recognition of the land use patterns was based on the study of the gray scale classes and of the spatial characteristics of the RBV and MSS black and white and of the false color composit images.

Vegetation was best separated from bare land on the RBV channel 2 and MSS channel 5 imagery.

The photographs were studied with the use of a magnifying viewer and a stereoscope. Eight gray scale classes were visually recognized on the RBV channel 2 black and white transparencies. Detailed ground truth data were used for

the assignment of land features to each gray scale class.

On the basis of spectral and spatial information derived from the ERTS-1 photographic imagery, a land classification scheme was developed as shown in table 1.

Table 1 shows that each gray scale class corresponds to more than one land use features, which in some cases are quite different. From the practical point of view it is necessary that these groups of land use features be separated. This separation was achieved by making use of existing geographical and geomorphological information and by the use of the false color composite pictures as follows:

Water corresponds to the darkest gray scale class on the black and white photographic imagery.

The next darkest, class 1 covers well irrigated annual and perennial agricultural crops as well as dense fir and austrian pine forest stands.

The agricultural crops can be separated from the forest by their geographical distribution. Well irrigated crops are grown on flat bottom land, while fir and austrian pine are grown on ragged mountainous terrain, at high elevations. These two land forms can be easily recognized and separated on the 1:1,000,000 photographic imagery by their characteristic texture as it is described in the discussion of the soils.

On the false color composites the irrigated agricultural crops are bright red, while the fir-austrian pine forests are dark red. Thus they can easily be separated from each other.

In gray scale class 2, dense halepo pine and hardwood forests could not be separated on the black and white picture from marginally irrigated orchards and other crops. It is known, however, that Halepo pine grows mainly along the coastal areas of Southern Greece, at an elevation not exceeding the 800 meters. In contrast, hardwood species form forest stands in the central part of the country and at elevations usually exceeding the 500 meters. Thus in most cases, with few exceptions, halepo pine can be separated from the deciduous forests. In false color composites the deciduous forest shows a brighter red color than the pine forest. This subject will be elaborated on in the study of ecological sites.

Orchards are found in Greece mainly on recent alluvial or quaternary deposits, which are easily delineated on the 1:1,000,000 scale space photograph. Small localized areas covered with orchards are also found on some mountain slopes along with pine and deciduous forest. These can not be separated from each other on the 1:1,000,000 photograph.

In gray scale class 3 the separation of thin pine forests from thin deciduous forests and shrubs presents similar problems, which can be also solved by considering the geographical distribution of the species.

Table 1. Classification of land features based on ERTS-1 photographic imagery

Gray scale class	Appearance in color composit photograph	Geographic and spatial characteristics	Land use class
0	Dark blue	Sea, lake, river	Water
1	Bright red	Flat land, geometrical shapes	Well irrigated agriculture
	Dark red	High mountains ragged terrain	Fir-Austrian pine forest
2	Reddish brown-pink	Coastal slopes	Dense Halepo pine forest
	Bright red	Inland mountains	Dense hd-wood forest
	Red to pink	Flat land, fragmented fields	Marginally irrigated agriculture
3	Mottled (red,brown, yellow, purple)	Coastal slopes	Thin Halepo pine, shrubs
		Inland mountains	Thin hardwoods, shrubs
4	Mottled, mostly red-dish brown and yellowish	Ragged terrain	Shrubs, pines, olive trees, bare soil and rocks intermixed
5	Yellowish white to orange	Flat or gently sloping land	Non irrigated olive groves, vineyards with some pines and shrubs
6	White,yellowish white, bluish white.	Flat or gently sloping land	Non irrigated winter crops, bare soil
		Ragged terrain	Thin shrubs and rocks
7	White to blue	Ragged mountain slopes	Bare wasteland
		Residential patterns	Cities and towns

This class, due to the irregular mixing of thin forest stands with shrubs, bare soil and some dense stands, has a characteristic texture consisting of small areas of different brightness.

Gray scale class 4 corresponds to degraded sloping land, which due to severe grazing and lumbering, has lost a great part of its vegetational cover. Consequently intensive erosion has exposed the bedrock on a large portion of surface of the land. Due to the high reflectivity of the bare soil and exposed bedrock, the pattern of this class is brighter than that of the previous class. The texture, however, is the same in both classes.

Olive groves and vineyards in Greece are in most cases non irrigated crops. Bare soil represents about 50% of the total area and it contributes significantly to the reflectivity of the land surface. Due to the dry climate and the lack of irrigation, the plants suffer during the summer months from moisture stress and thus they absorb less visible light. Consequently this class is only slightly darker than the bare soil. Geomorphologically, these crops grow mostly in Southern Greece on quaternary deposits and on the slopes of tertiary formations.

The separation of this class from the following class of winter crops on the black and white photographs is difficult.

On the false color composit, class 5 shows a yellowish orange tinge, thus it can be separated from the yellowish white colored class 6. The separation of class 5 from class 4 is relatively easy because of the difference in the brightness of the surface.

Due to the fragmentation of the cultivated areas and the brightening effect of the large portion of the bare soil, the separation of vineyards from the olive groves is not feasible on the 1:1,000,000 space photographs.

Gray scale class 6 is brighter than the previous classes, because during the period of August, when the data were obtained by ERTS-1, the respective land surfaces consisted either of bare soil or of harvested winter crops, principally wheat and barley.

Class 6 is not easily recognized from class 7 in the gray scale. Class 7, however, is mainly found on mountainous terrain while class 6 is located on the quaternary and tertiary deposits of lower lands.

In the false color composit photograph class 6 is predominantly white to yellowish white, with some bluish spots corresponding to cultivated bare soils.

Class 7 corresponds mainly to bare soil and rock outcrops located on the eroded mountainous land and to residential areas, which, in Greece, usually have sparse vegetation.

The vegetation of the lands of class 7 consists of sparse small shrubs of predominantly xerophytic species. Thus the reflection pattern is determined by the soil and bedrock surface.

Class 7 is the brightest of all the recognized by naked eye gray scale classes. Its separation, however, from class 6 is difficult on the black and white photograph. On the false color composit photograph, however, it has a distinct bluish white color peculiar to this class.

Figures 1 and 2 show land use maps of Southeastern Greece made on the basis of ERTS-1 photographic imagery.

Ecological Site Evaluation

The subhumid and the semi-arid climatic zones cover the greatest part of Greece's productive lands. Therefore the water supplying power of the soil during the dry months is a critical and in many cases the limiting factor for the growth of the plants.

The conditions which affect the water supplying power of the soil in the agricultural lands are the natural soil drainage and the applied irrigation water.

In the forest and range lands these conditions are the local climate, the geology, the soil depth and texture, the slope of the land and its geographical orientation (aspect).

The tension of the soil moisture affects the structural characteristics and the leaf area of the plants. These parameters determine the reflectivity of the vegetational cover of the soil (Mayers 1970). Consequently the reflectivity of the vegetation can be used as a measure of the effectiveness of irrigation in the agricultural lands and of the site quality of the forest and range lands.

The false color composit space photographs show a range of red colors corresponding to vegetation. A close inspection of the areas of various degrees of brightness of the red color on the photograph indicated the possibility of assigning them to respective site classes. (Orme et al. 1971, Krumpke et al 1971 and Colwell 1972).

Ground truth data collected through extensive field observations confirmed the above hypothesis.

It was found on high elevations, where the climate is humid to subhumid, that the dominant factor which influences the water supplying power of the soil is its depth. In these areas the bright color corresponds to vegetation grown on deep soil, while less bright red color is found on sites with shallower soils.

The deep residual soils are normally found in Greece on mica schist and on

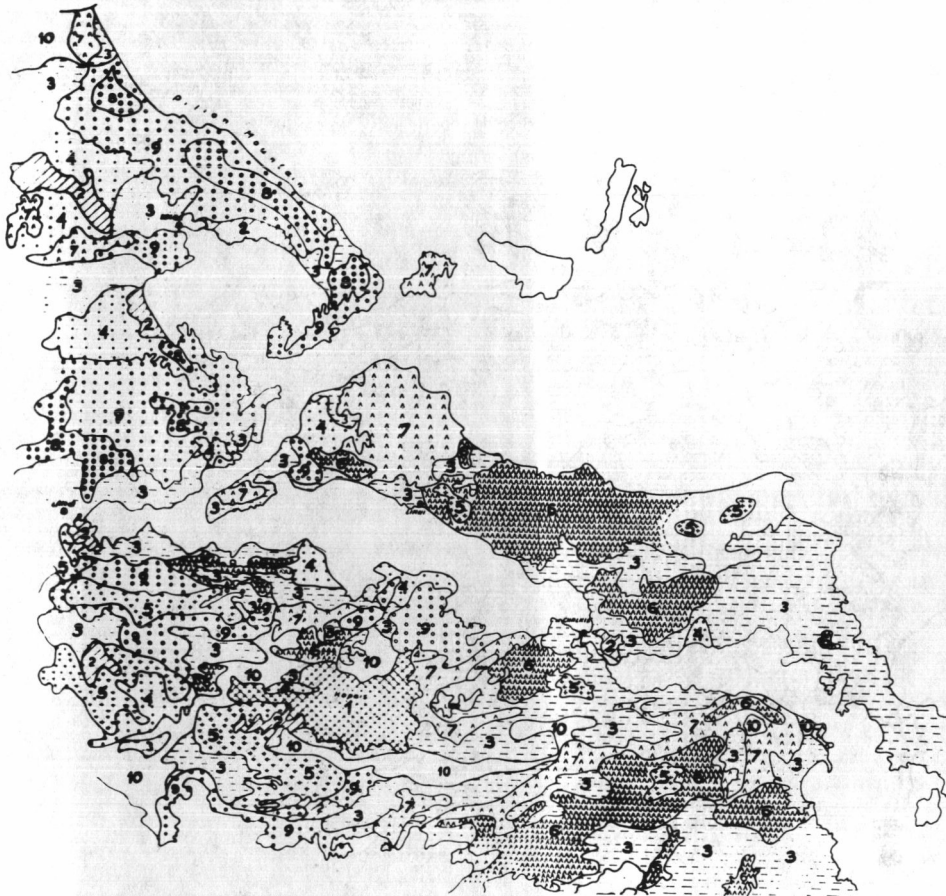


Fig. 1. Land use map of Central Greece

1. Well irrigated agricultural crops. 2. Marginally irrigated crops, vineyards, olive trees, orchards. 3. Non irrigated agricultural crops, olive groves, vineyards, annual crops. 4. Non irrigated winter crops and bare soil. 5. Fir and austrian pine. 6. Dense halepo pine. 7. Thin halepo pine. 8. Dense deciduous forest. 9. Thin deciduous forest, shrubs, scattered olive trees. 10. Shrubs, sparsely covered wild land and urban areas.

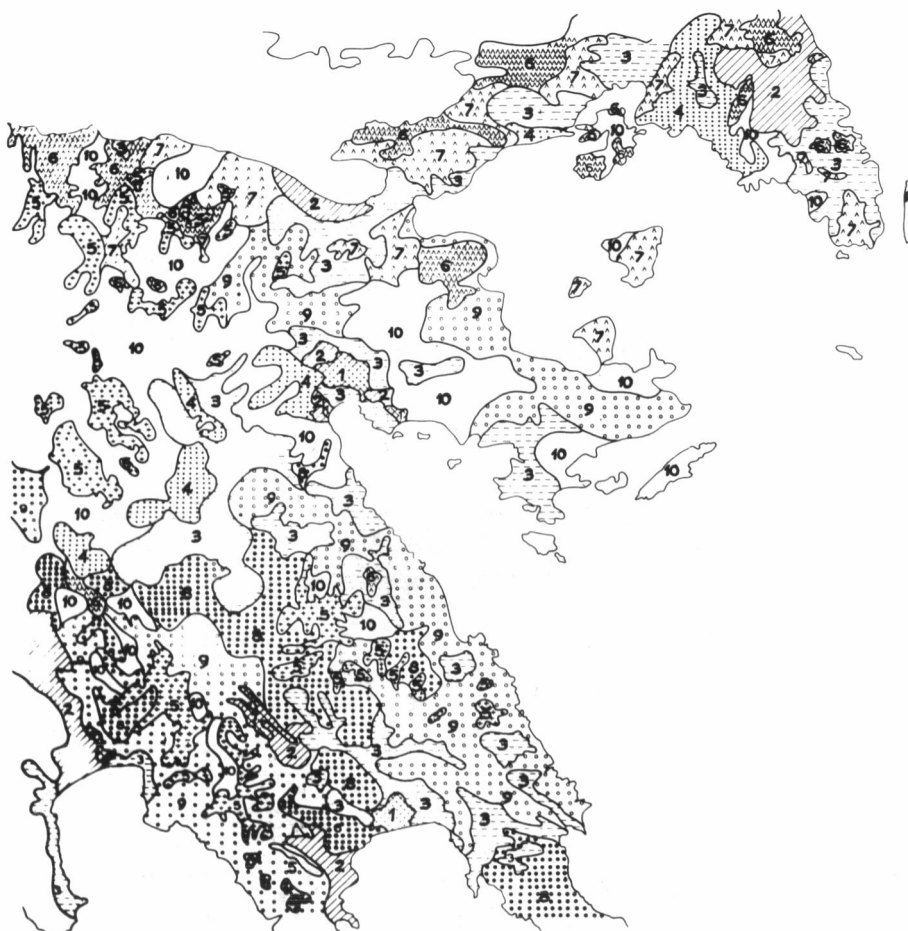


Fig. 2. Land use map of Eastern Peloponnese, Greece.

1. Well irrigated agricultural crops. 2. Marginally irrigated crops, vineyards, olive trees, orchards. 3. Non irrigated agricultural crops, olive groves, vineyards, annual crops. 4. Non irrigated winter crops and bare soil. 5. Fir and austrian pine. 6. Dense halepo pine. 7. Thin halepo pine. 8. Dense deciduous forest. 9. Thin deciduous forest, shrubs, scattered olive trees. 10. Shrubs, sparsely covered wild land and urban areas.

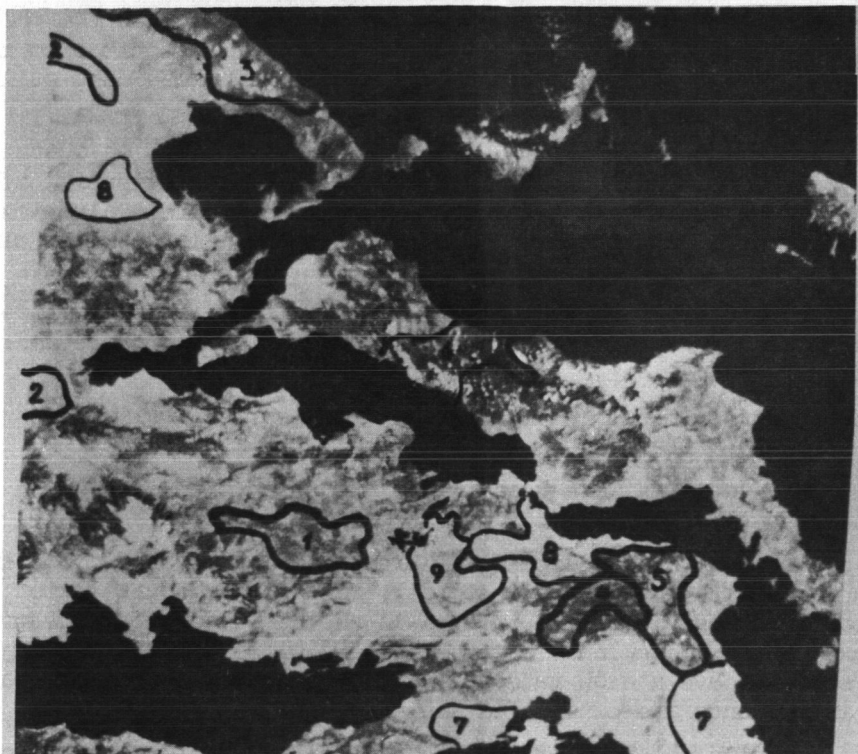


Fig. 3. Site evaluation map of Central Greece.

interbedded sandstone, siltstone and shale. Thus, the colors on the photograph can be correlated with the geological substratum. Exceptions to this observation are few, confined to areas of small slope, where deep soils form also on other parent materials.

On the lower lands and hills, where deep soils are developed on quaternary and tertiary deposits, the dominant site factor is the distribution of the rainfall throughout the year and not the soil depth. A site evaluation map was made on the basis of the above observations. The following site classes have been recognized and mapped in Central Greece shown in figure 3.

Site 1 corresponds to well irrigated agricultural lands. The bright red colors in the plain of Kopais and in the alluvial fan of Lamia are characteristic of the well irrigated summer crops, in this site.

Site 2 includes agricultural lands, where irrigation is localized and water is applied in limited quantities.

The forest and range lands were classified into three site classes on the basis of the visually estimated brightness of the red color.

Site class 3, shown in the map of Central Greece, has bright red color and it includes lands with relatively deep soil, which has adequate water storage capacity. These lands are located in the humid zones of the mountains. A typical example of these lands are the eastern slopes of Pilion Mountain. The forest species have a high rate of growth, the reforestation is easy and returns of investments are considered satisfactory.

Site class 4 shows on the photograph a less bright red color than class 3. The lands of this class are located: a) on humid mountainous regions with soils of moderate depths and b) on subhumid lowlands and hills with soils of adequate depth. In both cases the water supply power of the soil during the summer is relatively low. Thus, the productivity of the lands of site 4 is moderate.

Site class 5 shows a reddish brown color on the photograph. The lands of this class are characterized by a summer drought and/or shallow soil. The growth rate of the forest species is low, reforestation success is limited and pastures are dry during the summer and fall months. Investments for the development of these lands will produce limited or doubtful returns.

Site class 6 is exceptionally dark on the color composite photograph. Ground truth data show that the area consists of broken halepo pine stands, which have suffered severe resin extraction treatments. The cleared areas are used for dry farming and for grazing.

The foliage of the pine trees is yellowish due to the large scars that have been made on their trunks. Thus, the dark color in the photograph may be

attributed to the stress of the trees.

The areas 7,8 and 9 in figure 3 correspond to olive groves and vineyards, nonirrigated winter crops and bare soil and rock outcrops respectively, as it was described in the land use analysis.

The site classification map, which was made on the basis of false color composit 1:1,000,000 scale space photograph, can be used for the planning of the forest and range development of Greece on a more solid and scientific basis than it has been done so far. The results of this investigation could possibly be extended to other countries with similar climatic conditions.

Soil Features.

The following classes of soil groups have been recognized on the black and white and on the color composit space photographs:

Severely eroded mountain soils.

Mountainous lands have lost most of their soil and the bedrock is exposed on the largest part of the surface. Due to the absence of soil, deep enough to support vegetation, these lands are bright on the black and white photograph and bluish white on the false color composite. Since their soil is considered practically unproductive, the knowledge of its extent and distribution in the country is necessary for the planning of resource development. The space photographs provide a quick, inexpensive and relatively accurate estimate of these soils. Class 10 in the land use map of figures 1 and 2 represents this group of soils.

Saline soils.

Most of the saline soils of Greece are associated with the imperfectly and poorly drained soils of the coastal plains. Due to salt limitations, the vegetation is poor and in the summer months is either dry or under stress. The color of the soil is dark, except in small spots, where due to the precipitation of fine salt crystallites, is almost white.

Since the saline soils are localized in relatively small areas, where they are mixed with non saline soils, the 1:1,000,000 scale space photograph is not very convenient for their identification in the coastal plains of Greece.

Black and white photographs produced by the computer at LARS from digital

MSS data at x 16 magnification were used for the identification of the coastal saline soils of Greece, as it is shown in figure 4.

The separation was made by comparing the computer produced photographs of the green channel with those of the infrared channel.

A test area was selected in the Skala coastal plain south of Sparta in Peloponnese, where detailed ground truth information was collected.

In August, irrigated crops, wet land and saline soils are shown dark on the green channel photographs. Thus, they cannot be separated. On the photograph of the infrared channels, however, irrigated crops and vegetation on wet land are highly reflective and cover light areas in the photograph. In contrast the saline soils are dark both in the green and in the infrared band. Due to moisture stress, the reflectivity of the vegetation is also low and contributes to the darkness of salt affected areas (Mayers 1970, Gausman 1971).

Saline soils can be separated from the non saline bare soils of the area by comparing the above photographs. Bare non saline soils are less reflective than the saline soils in the infrared band. Thus, they are shown as light spots in the green channel and dark in infrared channel, while as it was indicated above the saline soils appear dark in both channels.

Wet soils.

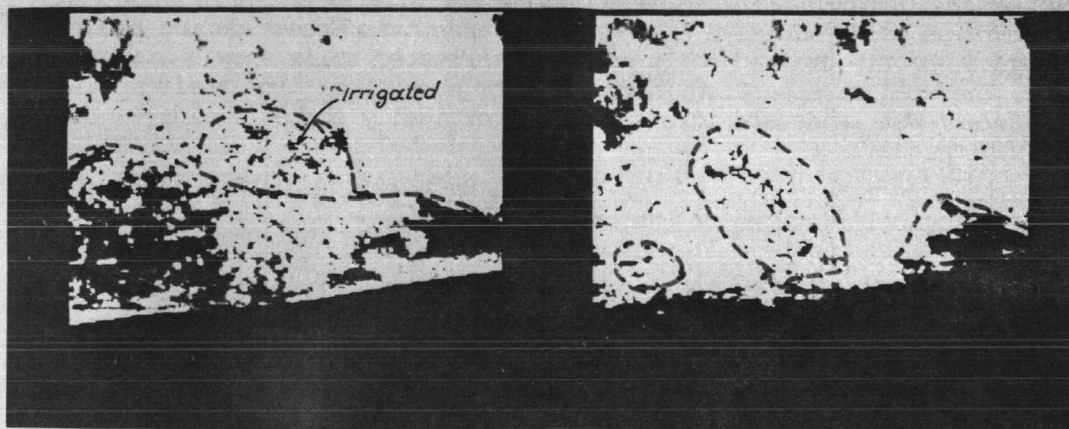
Poorly drained soils are generally darker than well drained soils. Their differences in the reflectivity were not great enough to allow a direct soil drainage classification in the 1:1,000,000 scale photographs. Temporal differences may be a useful tool, but at present such data are lacking.

The recognition of poorly drained soils and wet lands in a semiarid and subhumic country, such as Greece, can be based on the reflectance of the vegetation.

As it was discussed in the land use and the site evaluation sections of this report, a high water supply capability of the soil causes a sharp decrease in the reflectivity of the vegetation in the visible bands and an increase in the infrared bands.

The reflectivity of the plant leaves is known to decrease in all bands with increasing water content (Mayer 1970). The increase in the brightness of the red color in the false color composite photographs which was observed on sites with adequate supply of soil water can be explained by the denser vegetational cover in these areas.

In areas where soil water is a limiting factor for plant growth, an increase



a

b

Fig. 4. Computer processed digital MSS imagery of Scala Plain, Sparta, Greece.

- a. Green band showing wet and saline soils.
- b. Infrared band showing the saline soils and bare surfaces.

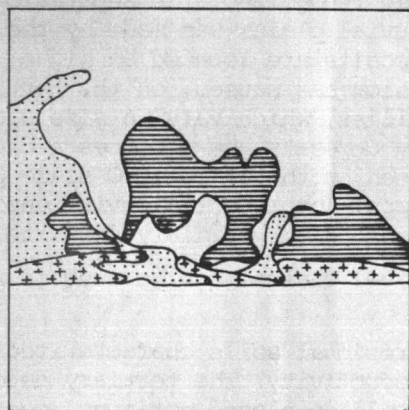


Fig. 4. Soil map of Scala Plain, Sparta, Greece.

- Saline soils.
- Poorly drained soils.
- Sand dunes

in soil moisture increases the number and the size of the plants and consequently the ratio of vegetation to bare soil becomes greater. Thus, an enhancement of the reflectivity in the near infrared band is observed in wet soils during the dry months of the year.

In the false color additive photographs, taken over Greece during the month of August, poorly drained soils and well irrigated soils show a bright red color. They can be separated, however, from each other from their spatial signatures. Wet lands are idle and no geometrically shaped fields can be observed on them.

Geomorphological features of the soil.

Important soil characteristics such as parent material, relief, erosion, drainage, stage of development and productivity are related to geomorphology.

The black and white and false color composit photographs can be used for the classification of the geomorphological features. The best imagery for this purpose was the infrared black and white and the false color composit.

The following three classes, which bear importance to soils, were recognized in the 1:1000,000 scale imagery:

- (1) Mountain slopes.
- (2) Gently sloping tertiary deposits.
- (3) Flat recent alluvial plains.

The above classes were recognized from their characteristic textures in the photographs. The mountainous regions characterized by deep and large valleys, gullies and faults were easily recognized. The separation of the tertiary deposits from the recent alluvial plains was made by the use of microscopic stereoscope. The tertiary deposits are located on higher elevations than the recent alluvial deposits. Erosion has caused, on the tertiary deposits, the formation of a network of gullies, which vary in size and orientation. This network dissects the tertiary deposits and produces a characteristic texture, which in many cases can be seen on the 1:1000,000 scale photograph by the use of a magnifying stereoscope. The recent alluvial deposits are flat and thus lack the erosional patterns of the tertiary deposits.

The above three geomorphological classes can be used in reconnaissance soil classification and mapping.

On the mountain slopes form residual soils characterized by erosion hazards, depth limitations and low productivity. The tertiary deposits are the parent material of deep soils with well developed horizons, moderately eroded and in many cases calcareous. These soils are used for dry farming. Their agricultural value is moderate to low.

The recent alluvial soils are young in age, calcareous and they lack in well developed horizons. They are the best suited soils for intensive agriculture.

The ERTS-1 photographic imagery was used for the correction of the boundaries of soils developed on tertiary and recent alluvial deposits in the 1:1,000,000 scale soil map of Greece.

A n a l y s i s o f D i g i t a l I m a g e r y

Digital data of the frames: ERTS-1010-08375 (Eastern Peloponnese) and ERTS-1010-08373 (Central Greece) were reformatted and processed by the IBM system/360 Model 67 Computer at LARS of Purdue University. The LARSPLAY and the LARSYSAA programs (6) were used for the processing of the data.

Feature vectors were analyzed and classified into 15 spectral classes by the LARSYSAA program. The computer was instructed to print maps of the above two provinces of Greece by assigning alphanumeric symbols to each of the classes.

A more detailed study of the fifteen classes was conducted in the Kopais plain, where sufficient ground truth data were collected during the month of August of 1972.

The Kopais plain is located about 70 miles north west of Athens. It consists of a drained lake bed, which is primarily used for irrigated agriculture. The plain is surrounded by hills consisting of limestone rock outcrops with sparse vegetation and of tertiary and quaternary deposits, which have areas covered by shrubs and trees, intermixed with fields used for nonirrigated winter crops.

The spectral classes of the Kopais plain were correlated with ground truth data. Their spectral signatures were also studied and visible/infrared ratios of reflected energy were calculated. On the basis of spectral properties, land features were assigned as following:

Spectral Classes.

The characteristics of the spectral classes of the Kopais plain are given in table 2. The modality of the histograms for each class and channel is shown in table 3. The classes can be characterized as unimodal except for the classes 4 and 14, which could be separated into two subclasses.

Table 2. Relative reflectivity of the spectral classes of the Kopais Plain

Spectral class	Total Energy λ (μ)	%	%	Ratio
		Energy at	Energy at	$\frac{\% 0,50 - 0,70}{\% 0,70 - 1,10}$
		λ (μ) 0,50 - 0,70	λ (μ) 0,70 - 1,10	
1/15	201.31	54.85	45.15	1.215
2/15	167.47	32.96	67.03	0.492
3/15	155.26	37.35	62.64	0.596
4/15	163.51	46.58	53.41	0.872
5/15	145.45	44.11	55.88	0.787
6/15	168.78	54.23	45.77	1.185
7/15	152.31	53.56	46.44	1.153
8/15	138.09	53.97	46.02	1.173
9/15	147.57	50.10	49.89	1.000
10/15	136.86	39.24	60.75	0.645
11/15	134.36	49.39	50.60	0.976
12/15	126.07	42.42	57.57	0.737
13/15	123.82	51.35	48.64	1.056
14/15	109.14	52.54	47.45	1.107
15/15	63.29	75.25	24.74	3.041

Table 3. Modality of the histograms of spectral classes.

Spectral class	Channels			
	1	2	3	4
1/15	unimodal	bimodal	unimodal	unimodal
2/15	uni -	uni -	bi -	uni -
3/15	uni -	uni -	bi -	uni -
4/15	uni -	bi -	uni -	bi -
5/15	uni -	uni -	uni -	uni -
6/15	uni -	uni -	uni -	uni -
7/15	uni -	uni -	uni -	uni -
8/15	uni -	uni -	uni -	uni -
9/15	uni -	uni -	uni -	uni -
10/15	uni -	uni -	uni -	uni -
11/15	uni -	bi -	uni -	uni -
12/15	uni -	uni -	uni -	uni -
13/15	uni -	bi -	uni -	uni -
14/15	uni -	bi -	bi -	bi -
15/15	uni -	uni -	uni -	uni -

Land Use Classes.

On the basis of ground truth data and their spatial and spectral characteristics the fifteen classes were assigned to eight land use classes as it is shown in table 4.

Table 4. Correspondence of spectral classes to land use classes.

Land Use Classes	1	2	3	4	5	6	7	8	9	10	11	12	13	14	15
1. Corn										+		+			
2. Wheat							+								
3. Alfalfa			+												
4. Trees-shrubs									+		+		+	+	
5. Cotton				+											
6. Unknown					+	+			+						
7. Soil							+		+						
8. Eroded Soil		+													
9. Water															+

Table 4 shows that in many cases more than one spectral classes had to be grouped into one land use class. This was necessary because land use subclasses were not spatially separable and it was to some extent, justified by the proximity of the spectral ratios of the grouped spectral classes shown in table 2.

The modality of the land use classes was tested from the histograms, which were calculated by the statistics processor of the LARSYSAA program. The results of these calculations are shown in figure 5.

The most reflective spectral class 1 was assigned to soils with light colored surface. The parent material of the drained lacustrine soil is a whitish marl. Upon oxidation of the thin organic surface layer and deep

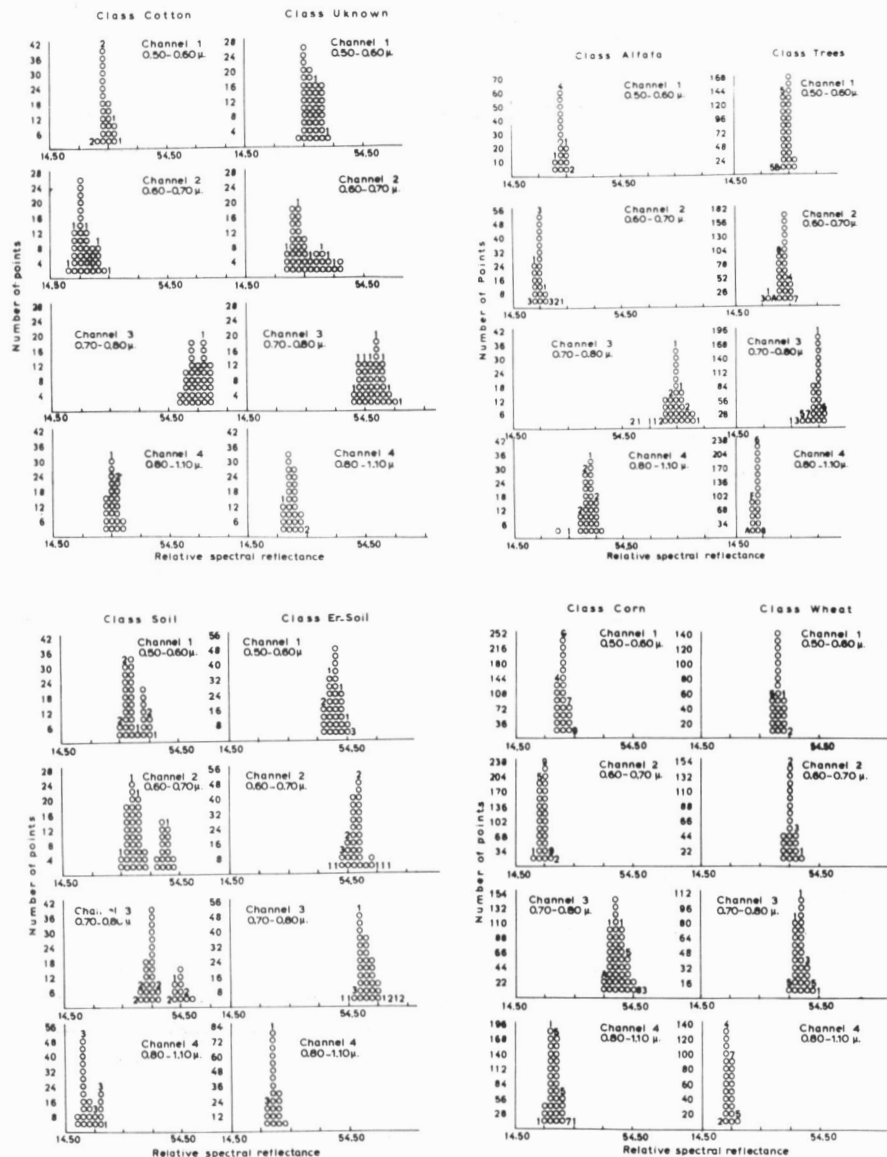


Fig. 5. Spectral histograms of land use classes.

ploughing, the marl was brought to the surface of the soil in many locations. This soil surface has the highest total reflectivity of all the other surfaces in the studied area. The reflected energy in the visible part of the spectrum is greater than in the infrared due to the lack of vegetational cover. Eroded alfisols having their red colored Bt horizon exposed on the surface belong also to the spectral class 1.

This land use class named "eroded soils", is found both on the marly bottom land and on the eroded slopes of the tertiary deposits.

The spectral classes 6 and 8 were assigned to the bare soil surface. From these two classes the first has higher total reflectivity than the second one. Their spectral ratios, however, are about the same. The histograms in figure 5 also indicate that two bare soil surfaces can be recognized.

Indeed, ground truth data have shown that the brighter spectral class 6 should be assigned to flat bare soil surfaces of the bottomland in areas where the marly parent material has not been exposed. Class 8 should be assigned to the rocky surfaces of the surrounding the bottomland hills. These hills have the limestone bedrock exposed on the greater part of their sloping surfaces. The vegetation is sparse and it was mostly dry during the recording of the spectral data by ERTS-1.

The roughness of the surface and the presence of dry vegetation could possibly explain the lower reflectivity of spectral class 8 as compared to spectral class 6.

The recognition, separation and mapping of the above three classes of soil can be regarded as a significant achievement toward the assessment of the productivity of the studied area. Thus, spectral class 6 corresponds to highly productive soil and spectral class 1 corresponds to unproductive soil.

Spectral class 7 was assigned to wheat fields. In August, at the time that the data were recorded by ERTS-1, the wheat fields had been harvested and only, short dry straw remained on the ground. Thus bare soil constituted a large portion of the reflecting surface. Accordingly the spectral data (table 2) of class 7 do not deviate significantly from those of the classes 6 and 8, which were assigned to bare soil. Due to the uniform distribution and the minuteness of the soil and straw surfaces, the whole reflecting surface appears uniform. For this reason the respective histograms are narrow.

Spectral classes 2 and 3 were assigned to alfalfa and cotton respectively. Both classes are characterized by low spectral ratios. Both crops were irrigated and thus were highly reflective in the infrared wave lengths. However, during the month of August alfalfa fields present a denser and a greener surface than cotton fields. Consequently alfalfa has a smaller spectral ratio than cotton.

The unknown land use class consists of greatly fragmented fields of various irrigated crops intermixed with wheat fields, bare soil, trees, and shrubs. Due to the small size of the fields, the resolution was poor and the separation was not feasible. The variability in the spectral signatures of this land use class is also reflected in the histograms, which are distinctly bimodal. The spectral classes 4, 5 and 9 were assigned to this land use class.

Corn fields covered a large area in the irrigated bottomland. Two spectral classes were associated with the cornfields: class 10 and class 12. As it can be seen in tables 2 and 4, the two classes have similar characteristics and the histograms of the land use class are unimodal.

At the time of the spectral recording by ERTS-1, corn was approaching maturity and irrigation was not as intensive as in alfalfa and cotton. Thus, the relative reflectance of corn fields in the infrared region was somewhat lower than that of the other two crops.

Spectral class 10 has lower ratio than class 12. The difference may be attributed to variations in irrigation and in the maturity stage of the crop.

The land use class trees and shrubs covers the surrounding hills of the Kopais plain. This land use class is characterized by broken forest and shrub vegetation, growing on soils developed on tertiary and quaternary deposits as well as on soils developed on limestone. The depth of the soil is adequate for the growth of vegetation. Its moisture regime, however, is not favorable. In small scattered areas, the native vegetation has been cleared out and the land is used for dry farming olive groves and vineyards. A number of these farms have been abandoned.

The spectral classes, which were associated with this land use class, were the 11, 13 and 14. These three classes differ in their total reflectivities but the reflected energy is about equally distributed between the visible and the infrared range in all of them. Thus, the spectral ratios approach unity, a value which lies between that of the bare soil and the green vegetation.

Water is characterized by low reflectivity, especially in the infrared range. Spectral class 15 was therefore the appropriate one to be assigned to water, which was in complete agreement with ground data.

Training and test fields were selected in the computer print of the spectral classes. The fields were selected on the basis of ground truth information. The training class performance is shown in table 5.

Table 5. Training class performance for the Kopais Plain

Class	No. of samples	Percent correct classification	Corn	Wheat	Alfalfa	Trees	Cotton	Unknown	Soil	Er. Soil	Threshold
1. Corn	468	96.8	453	0	0	0	1	14	0	0	0
2. Wheat	248	91.1	0	226	0	0	0	1	20	0	1
3. Alfalfa	98	94.9	0	0	93	0	2	3	0	0	0
4. Trees-shrubs	345	98.0	0	0	0	338	0	0	0	0	7
5. Cotton	75	97.3	0	0	0	0	73	0	0	0	0
6. Unknown	84	98.8	0	0	0	0	1	83	0	0	0
7. Soil	110	95.5	0	0	0	4	0	0	105	1	0
8. Eroded Soil	136	97.1	0	0	0	0	0	0	0	132	4
Total	1564		453	226	93	342	77	101	125	133	12

Over all Performance (1503/1564) = 96.1%

Average Performance by class (769.4/8) = 96.2%

Table 6. Approximate accuracy of the land use map

Land use class	% Classified correctly	Incorrect classifications
1. Corn	90	shrubs as corn
2. Wheat	95	Dry weeds as wheat
3. Alfalfa	90	Cotton as alfalfa
4. Trees and shrubs	90	Vine, alfalfa as shrubs
5. Unknown	100	-
6. Soil and rocks	100	-
7. Eroded soil	100	-

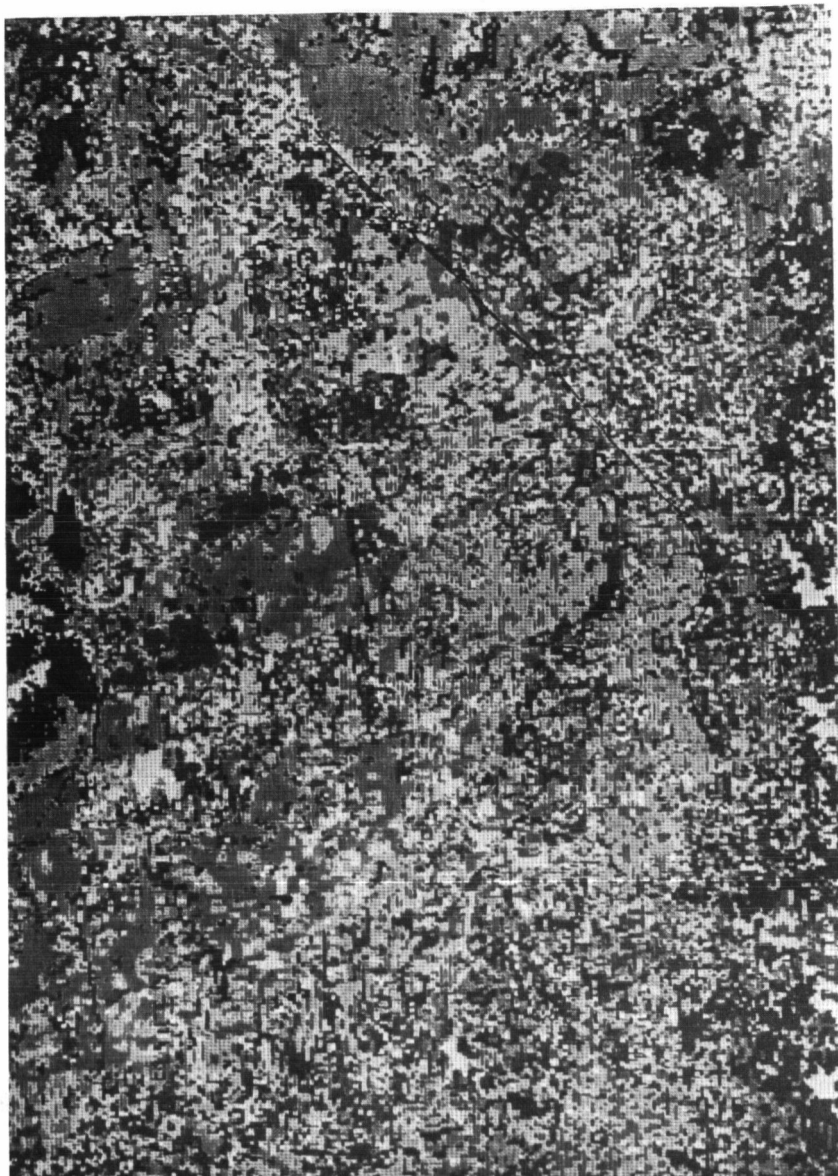


Fig. 6. Computer print of land use map of Kopais Plain.

olive green = corn, red = wheat, blue = cotton, green = bare soil,
orange = eroded soil, dark green ■ trees and shrubs, white = un-
known, mustard = alfalfa.

Land Use Mapping

The computer was instructed to print a land use map, shown in figure 6, in which the nine classes were represented by alphanumeric symbols. The scale of the map was about 1:22,000. A threshold of 0,5%, which corresponded mainly to residential areas, was used in the process of grouping spectral features into land use classes. The map was then checked against detailed ground truth information. Its approximate accuracy is shown in table 6.

The data in table 6 suggest that the accuracy of the land use classification and mapping was satisfactory.

The high accuracy of the classes unknown, soil-rocks and eroded soils can be explained by the broadness of feature characteristics that they include.

CONCLUSIONS AND SUMMARY

Photographic and digital imagery of Central Greece and Eastern Peloponnese were analyzed.

On the basis of information extracted from black and white, false color composite photographic imagery and spatial information the following land use classes were recognized and mapped.

- a. Forests: dense and thin stands of fir, austrian pine and halepo pine.
- b. Shrubs and idle land: dense shrubs, thin shrubs and rocky idle lands.
- c. Agricultural lands: well irrigated and marginally irrigated crops, winter farmland, olive groves and vineyards.

The accuracy of the above maps was satisfactory.

Photographic imagery and photographs printed from the digital display were used to recognize and map recent alluvial soils, tertiary soils, eroded residual soils, wet soils and saline soils,

False color composites made through additive process from RBV and MSS 1:1,000,000 scale photographic images were used to identify and map agricultural forest and range site evaluation classes, based on the water supplying capability of the soil.

Digital data from the Kopais plain were analyzed at LARS by the use of LARSYSSA computer program. Fifteen spectral classes were assigned to respective detailed crop and semidetailed soil classes. Alphanumeric computer maps of about 1:22,000 scale were printed, showing the distribution of these nine classes. These maps provide information on the degree of proper utilization of land resources in the studied area.

The feature recognition patterns, which were developed in this investigation, are strongly influenced by the local ecological, spatial and land parameters. Thus the results found and the techniques proposed in this report may have applications to areas of ecological, land and agricultural conditions similar to those of Southeastern Greece.

ACKNOWLEDGEMENTS

Acknowledgements are gratefully made to NASA for providing the ERTS-1 data and to IARS of Purdue University for its technical assistance. Special thanks are given to Drs. M. Baumgardner, S. Kristof and J. Cipra for their help in handling the digital data.

REFERENCES

- 1) Colwell, R.N., 1972, ERTS-1 Applications to California Resource Inventory. NASA Proc. Sym. Earth Resources Technology Satellite-1, p.7
- 2) Fu, K.S., Langrebe, D.A. and Phillips, T.L., 1969, Information Processing of Remotely Sensed Agricultural Data, Proceedings of the IEE, Vol.57, No 4, p.639.
- 3) Gausman, H.W., 1971, Photographic Remote Sensing of "Sick" Citrus Trees, Int. Workshop on Earth Resources Survey Systems, Vol.II, p.15, U.S. Government.
- 4) Kristof, S.J. and Zachary, A.L., 1971, Mapping Soil Types from Multispectral Scanner Data, Proc. VII Int. Sym. Remote Sensing of Environment, Vol. III, p.2095.
- 5) Krumpke, P.E., De Selm, H.R. and Amundsen, C.C., 1971, An Ecological Analysis of Forest Landscape Parameters, VII Int. Sym. Remote Sensing of Environment, Vol.1, p.715.
- 6) IARS, 1970, Remote Multispectral Sensing in Agriculture, Research Bulletin 873.
- 7) Mayers, V.I., 1970, Soil, Water and Plant Relations, In Remote Sensing, National Academy of Sciences Washington.
- 8) Orme, A.R., Bowden, L.W. and Minnigh, R.A., 1971, Remote Sensing of Disturbed Insular Vegetation from Color Infrared Imagery, Proc.VII Int. Symp. Remote Sensing of Environment Vol. II, p.1235.

ERTS-1 MSS IMAGERY: ITS USE IN DELINEATING SOIL ASSOCIATIONS AND AS A BASE MAP FOR PUBLISHING SOILS INFORMATION.¹

Frederick C. Westin, *Plant Science Department and Remote Sensing Institute, South Dakota State University, Brookings, South Dakota*

ABSTRACT

ERTS 1 imagery is a useful tool in the identification and refinement of Soil Association areas and an excellent base map upon which soil association information can be published. Prints of bands 5 and 7 were found to be most useful to help delineate major soil and vegetation areas. For example band 7 was found to give superior definition to steeply sloping soils while band 5 gave the best contrast between trees and grass. After delineating major soil areas, over 4800 land sale prices covering a period of 1967-72 were located in the soil areas and averaged. A legend explaining land use, dominant slope and soil parent materials of each delineated area was developed. The soil associations then were described as Soil Association Value Areas and published on a 1:1,000,000 scale ERTS mosaic of South Dakota constructed using negative prints of band 7. The resulting map describes the kind of agriculture and soils and allows readers to see how soils actually are being used on a near orthographic current map. Furthermore, it gives information about what buyers think the soils are worth. The map is intended for use by state and county revenue officers to equalize land values in South Dakota, by individual buyers and sellers of land and lending institutions as a reference source, as a reference map by those planning road routes and cable lines and pipelines, by conservationists in helping to keep current conservation needs inventories, by agronomists needing current information on distribution and patterns of crop growth and by crop yield forecasters to guide sampling strategy.

^{1/} SDSU-RSI-J-73-11 Supported in part by contract No. NAS-5-21774

1
N74
30719

INTRODUCTION

Soil maps are an integral part of an effective agricultural research and advisory program. Soil maps are used for farm and ranch planning, for crop and grass yield estimates, for evaluating land, for land use planning, for irrigation planning, for drainage planning, for assessing potentialities for special crops, for rural zoning, and for forest management.

Soil maps are of different scales ranging usually from 1:15,840 to 1:7,000,000. The large scale maps necessary for detailed land planning show the extent of individual soils, and are made by boring holes and walking over the land so that delineations are observed over their entire extent. These soil survey maps are expensive to make and publish.

Small scale soil maps, called soil association maps, are geographic associations of one or several soils and usually are at scales of 1:500,000 to 1:1,000,000. Simonson (1971) states that each soil association consists of a set of geographic bodies that are segments of the soil mantle covering the land surface.

Soil Associations are soil landscapes that occur in repeating patterns. They may contain like or unlike soils but the association itself is homogeneous and different from other soil associations when viewed on the imagery.

Field checking of soil association maps is done at infrequent intervals depending upon the scale and use of the map. Although soil association maps of small scale are not as precise for interpretations as detailed soil maps of large scale, they cost much less to make and they do have use for broad planning purposes and for education.

It should be emphasized that the soils shown on soil maps are not defined in terms of profiles alone. According to the soil survey staff of the USDA (1951), each soil unit is a particular kind of landscape and it is these landscapes of soils that are classified and shown on soil association maps. Although soil profiles cannot be seen on air or satellite imagery, soil landscapes are visible. In this regard it should be stated that soil survey experience is necessary if maximum use is to be made of ERTS-1 MSS imagery for identifying soil associations.

Soil landscapes exhibit a characteristic surface geometry such as relative frequency of streams, and a characteristic surface composition such as the percentage of bare soil areas. Other features used in differentiating soil landscapes include vegetation and hydrology.

Five factors control the formation and distribution of soils and soil associations. These are: climate, organisms (dominantly native vegetation), soil parent material, topography and time. With the exception of time these factors define the environment of soil formation. Time gives the total potential for change, and is not considered in this study as a separate factor resulting in recognizable boundaries. Climate and native vegetation are closely related and usually are considered together since both are dynamic factors acting upon soil parent materials on different topographic sites.

Aerial photographs have been widely used to differentiate soil association landscapes for 40 years. The bulk of these photographs have been black and white panchromatic prints although color infrared materials have had some use. The aircraft has been the primary platform for obtaining these images. Now, since the summer of 1972, ERTS-1 MSS satellite imagery available in 4 spectral bands and at 18-day intervals brings a new tool to the study of soil association landscapes.

The objective of this study was the recognition of Soil Association boundaries on ERTS-1 images and mosaics and the publication of a soil association map on an ERTS-1 mosaic of South Dakota.

PROCEDURE

The ERTS-1 multispectral scanner records the electromagnetic energy that comes from features on the earth's surface. The radiation is in four bands as follows: band 4 - 0.5-0.6 μm ; band 5 - 0.6-0.7 μm ; band 6 - 0.7-0.8 μm ; and band 7 - 0.8-1.1 μm . The spectral energy coming from a soil or crop or other feature depends on its molecular composition. Consequently the various earth's features exhibit unique tonal signatures on the different bands. Tonal signatures can result from multiband viewing or from monochromatic prints derived from one spectral band and shown in gray tones.

The ERTS-1 imagery used for this study consisted of 9-inch transparencies at a scale of 1:1,000,000. From these transparencies two kinds of images were prepared for study: 1) color transparency composites at 1:1,000,000 scale made from bands 4, 5, and 7. These were viewed over a light table under magnification; 2) negative prints of scale 1:500,000, 1:250,000, 1:100,000 and 1:60,000.

In this study an effort was made to study ERTS-1 imagery using equipment usually available to a soil survey office. This consists mainly of access to a darkroom with a good enlarger having a non-diffuse light source. A diffuse light enlarger tends to blend and smooth out boundaries on the images which is not desired.

CHARACTER OF SOIL BOUNDARIES DUE TO CLIMATE AND VEGETATION AND THEIR RECOGNITION

Soil profiles cannot be seen on either air or satellite imagery and for a large part of the growing season each year even the surface soil of South Dakota is covered with vegetation. Thus, recognition of soil association boundaries must be inferred in part from the patterns made by the present vegetation since this is the principal way that climate and native vegetation are expressed.

Soil Association boundaries separate kinds of agriculture. For example, corn and soybeans are grown in South Dakota in the eastern and southeastern part where the soils have developed under a warm-moist climate and tall grass vegetation. Moving northwest, spring wheat takes over as the main crop. Spring wheat is at its peak of green growth in June at which time corn is just beginning to mantle the soil. Thus, band 7 of May ERTS passes will show high reflectance where spring wheat is the dominant crop. On August imagery the corn and soybean-growing soil associations will reflect strongly while the soil associations used for spring wheat will have low reflectance. Thus, both the temporal and multispectral characteristics of ERTS imagery are utilized in recognizing boundaries of soil associations. Other characteristics used include field size (larger in wheat area) and percentage of the soils in pasture or range grass (larger in wheat area).

Some role in soil formation is played by both precipitation and temperature. Precipitation affects the amount of water that enters the soil and hence the chemical and physical weathering processes, eluviation and ion movement. Moisture relationships also affect the amount of residues that are returned to the soil and the speed of their decomposition.

Temperature controls the heat available for the physical, chemical and biological processes of soil formation. Weathering generally increases with an increase in temperature if moisture is not limiting. Also, higher temperatures generally increase the rate of organic matter decay.

The general characteristics of soils can be related to climate. Although there are many interrelationships, the most significant ones generally relate to a single soil property such as organic matter content and a single climatic component like precipitation. The climate in South Dakota is subhumid in the eastern part and semiarid in the central and western parts. Tall grass prairie was the principal vegetation in the subhumid east while mid and short grasses were the native vegetation types in the semiarid central and western parts.

The principal biotic factor in soil formation is vegetation since it is the major source of organic matter. The effect

of vegetation on soil properties differs with the kind of vegetation. Grasses contribute large amounts of organic matter that darken the upper layers of soil. The intensity of the development of these upper horizons correlates well with the climate resulting in darker and thicker dark colored horizons in eastern South Dakota and gradually thinning and becoming lighter colored in moving to the northwest corner. Since climate is a continuum the soil thickness and darkness also are a continuum. As long as soil parent material and topography are constant factors the soil boundaries related to climate and native vegetation are gradual. Thus, the problem of delineating soil boundaries which are due to climate has been difficult by conventional means since no one aerial photograph or county mosaic covered sufficient area to see evidence of soil differences that could be attributed to climate and vegetation.

ERTS scenes cover larger areas, however, and this synoptic view provides an opportunity to observe soil associations and their use over an area of climatic change. As mentioned, however, climatic change is gradual and as long as soil parent material and topography remain constant, the soil association boundaries that result from climatic change are gradual. Fortunately, however, there often is a topographic or soil parent material change which provides a distinct boundary and the climatic continuum can be partitioned in this manner. Figures 1 and 2 illustrate this point. Figure 1 is of western Minnesota along latitude 44°15'. The climate gradually is becoming drier from east to west. This is seen in the gradual darkening of the tone of the MSS-7 negative print. This tone darkening is due to an increased percentage of spring grain which is near its peak of green growth on 17 June. The more humid eastern area is planted to corn and soybeans neither one of which has produced much vegetation by this date. Three soil parent material boundaries occur on the scene at roughly right angles to the climatic change. These soil parent material boundaries then serve also to partition the climatic continuum. Figure two is from east-central South Dakota. Here, also, the climate gradually is becoming drier from east to west and this is seen on the MSS-7 negative print as a gradual darkening of the tone of the image due to a change in crops grown from more corn to less corn. This ERTS scene is of 16 May when corn is in the process of being planted and thus the corn land reflects very light gray on the negative print of MSS-7 while the wheat, which is present in larger proportion on the west, has a dark tone. The light tones signifying corn land are present in larger proportion on the east part of the figure. Crossing at nearly right angles to this climatic change is a soil parent material change which then also serves as a boundary for a climate change.

RECOGNITION OF SOIL ASSOCIATION BOUNDARIES CAUSED BY SOIL PARENT MATERIALS

Soil parent materials may be classified into one of three groups: residual, transported and organic. Since organic materials are not present in soil associations in South Dakota they are not discussed further here.

Residual soil parent materials include hard igneous and metamorphic rocks, as well as hard and soft sedimentary rocks. The hard rocks weather very slowly to produce thin soils. In South Dakota these occur in the Black Hills and are further distinguished by rugged mountainous relief. These areas of different rocks have sharp boundaries visible on MSS-5 and 7 of ERTS (see figure 3). They have greatest reflectance differences with surrounding areas on band 5 than the other bands. Softer sedimentary rocks include sandstones, limestones and shales. These along with alluvium and loess characterize the west half of South Dakota.

Soil Association boundaries caused by a change in the soft sedimentary rocks are sharp in South Dakota, and visible on ERTS images in any season and on bands 5, 6, and 7 or on color composites. Several kinds of soft sedimentary rock soil parent material are shown of figures 4 and 5. The Sand Hills consist of unconsolidated deep coarse sands on undulating or hummocky relief used for range grasses. The Pine Ridge is from a partially cemented calcareous sandstone and the soils here are generally shallow sandy loams on steep, north-facing slopes. This environment is suited for range grasses and Ponderosa Pine. The pine grows generally on the steepest valley sides and its reflectance is much lower on band 5 than is the grass. Thus on this band there is a unique veining pattern following the location of the Ponderosa Pine.

The siltstone in this area is high in calcium carbonate and light tan to white in color. The soils that develop from them are thin, especially on the slope breaks and knobs and the whitish parent material gives a high reflectance on band 5 of ERTS. The siltstone area erodes to barren badlands where a slope differential or wall occurs but otherwise is used mainly for growing range grasses and occasionally a field of winter wheat. The appearance of the siltstone area on ERTS imagery then is one of uneven tone caused by the association of moderately deep and shallow soils and the boundaries separating the area from the adjacent soil associations is sharp.

The shale in this area is a rather dense, very fine-textured marine deposit and the relief on which it occurs is rolling. The fine textures and strong relief result in high runoff so the production of grass (which is the main use) is low. Thus the IR reflectance generally of these areas is low. The high

runoff from these clay materials is carried from the uplands mainly by a fine network of closely spaced streams. This stream network and the low IR reflectance are two features identifying the shale soil parent materials. The boundary separating shale from associated soil parent materials in this area usually is sharp and is visible on the ERTS images, especially on band 7. Figure 5 shows the delineation of soil association boundaries between a dense shale and a sandstone.

Transported soil parent materials usually are named to show the principal agency responsible for transportation and deposition. A common feature of transported soil parent materials is that they occur in an unconsolidated state, thus they give rise to deeper soils generally than do residual materials.

The transported soil parent materials can be subdivided into deposits from running water, glacial deposits, and wind-laid sediments. Running water deposits include alluvium and terrace materials. For major rivers, boundaries of both deposits can be distinguished on ERTS images. Alluvial deposits are identified by stream proximity, linear shape and usually by having a network of drains. In addition, the valley floor and bluff usually have a sharp boundary caused by reflective differences of the valley floor vegetation and the sparser vegetation of the steep valley sides. Figure 6 shows the delineation of the Big Sioux River bottomland and a terrace near Brookings.

Terrace soil parent materials also occur near streams, but back from the alluvial plain. They also usually have linear shapes but lack a network of drains since they are above the level of flooding. Since they occur on flat topography and the materials are friable, the soils usually are among the most productive for their area of occurrence and are under cultivation. Thus a field pattern of cropland with few, if any, areas of grass or trees further characterizes terraces in South Dakota. Since these soils are the most productive in their area, the total biomass produced is larger than surrounding areas and terraces have higher reflectance on band 7 than adjacent areas.

Glacial soil parent materials in South Dakota include till and outwash. Till is generally medium textured and is deposited in undulating ground moraines and steep end moraines. Glacial outwash, which is coarse textured, is carried by water beyond the ice front onto a plain. Glacial till soil parent materials on undulating or nearly level slopes and outwash plains generally are under cultivation and so have a pattern of field boundaries. Steeply sloping or hilly glacial soil parent materials generally are in grass or trees, thus land use is useful in the separation of these two kinds of glacial till

soil parent material. Figure 7 illustrates the distinct boundaries on MSS-7 imagery that separate a dead ice moraine, an end moraine, and ground moraine in north central South Dakota. Each of these is a Soil Association area.

In general, boundaries separating glacial soil parent materials can be distinguished from residual soil parent materials on ERTS. The residual soil parent materials are on an erosional landscape consisting of broad ridge tops, valley sides and well defined stream courses. The glacial landscape is one where the land forms have been constructed by glaciers. It consists of broad plains interrupted by hilly ridges. The stream drainage pattern is less well defined and often the glacial plain is dotted with morainic depressions, marshes and lakes. See figure 8.

Boundaries separating mature glacial plains can further be distinguished from immature glacial plains in that the former has a well developed network of streams and the latter is characterized by poorly drained areas and no stream surface drainage network. See figure 7. Band 7 is superior for boundary detection in glacial areas since all water bodies are clearly shown.

The wind-deposited soil parent materials in South Dakota include loess which is silt size, and eolian sand. Loess deposits are superior soil parent materials since they are friable and permeable. Thus they are cultivated for the most part even in semiarid climates. Figure 9 is an ERTS image from southeast South Dakota. Here a thick loess occurs on a rolling upland which dictates use of a high percentage of close-growing crops like small grain to help control water erosion. On June imagery these crops are near their peak of green growth and thus reflect strongly on MSS-7. The flat areas are used for corn and soybeans primarily and these crops have not grown sufficiently by mid June to give much reflectance on MSS-7. Therefore, these areas have light tones on the negative prints of figure 9.

Field patterns often indicate loess soil parent materials in western South Dakota. See figure 4. The boundaries separating loess from eolian sand and residual sandstone are sharp as is shown in the figure. Eolian sand soil parent materials also have sharp boundaries with loess and sandstone. The identification keys for eolian sand soil parent materials are that the areas are in grass (because of the severe wind erosion hazard), they lack any surface streams and their general configuration is one of hummocks and ridges interspersed with small flats, dips and depressions. The boundaries delineating eolian sand soil parent material are distinct on ERTS images.

RECOGNITION OF SOIL ASSOCIATION BOUNDARIES CAUSED BY TOPOGRAPHY

Topography affects soil formation mostly by modifying the climate. Precipitation effectiveness is influenced by runoff which is controlled by topography. Likewise the slope aspect and degree of slope affect the amount of solar radiation received which in turn affects soil temperature and evaporation. Thus the climatic environment induced by topography affects the vegetation and the boundaries delineating this climatic effect can be observed on ERTS images. This is shown on figure 10 where the steep slope of the Prairie Coteau appears as a wide, dark area on MSS-7 while it is not apparent on MSS-5. The evidence of steep slopes along valley sides can also be inferred from the close spacing of drains into a river valley as is shown in figure 11. Here the evidence is apparent on both bands 5 and 7.

Differences in soil moisture regimes influenced by topography are significant. In the sandhills the low lying basins receive runoff and have poorly drained soils high in organic matter. Although small basins usually are not individually separated on soil association maps, their presence or absence is a characteristic of the soil association, and hence being able to see their boundaries on ERTS is significant.

Upland and lowland is a broad topographic classification of soil associations. Lowlands include alluvium and terrace soils which usually have well defined boundaries visible on ERTS.

Upland soils on undulating topography generally are described as mature since they reflect the normal expression of the climate of the area. On steep slopes thin profiles generally erodes as fast as new soil develops. These thin soils produce less vegetation than the associated normal soils for two reasons -- they are thinner and less well supplied with nutrients and they receive less effective moisture for plant growth. Thus the MSS-7 is the most useful to distinguish the boundaries of these thin, steeply sloping soils. This is shown on figures 10 and 11.

THE RELATIONSHIPS AMONG THE SOIL FORMING FACTORS

Variation in any of the factors of soil formation can change the soil association. Often the factors interact and the effect is additive or one may nullify another.

In figures 1 and 2 a climatic change is apparent from east to west as corn acreage decreases and spring wheat acreage increases. The climatic boundary is gradual but distinct topographic or soil parent material boundaries occur. Thus a topographic or a soil parent material boundary also serves to divide the climatic continuum. Soil parent material and

topography usually change abruptly and these changes produce boundaries visible on ERTS. Because of the reflective contrasts produced on MSS-7 by vegetative differences, the seasonal greening of vegetation coupled with crop calendar information provides a good tool to distinguish Soil Association boundaries. This temporal advantage coupled with the multispectral advantages make ERTS a valuable tool in distinguishing Soil Associations.

USE OF AN ERTS-1 MOSAIC OF SOUTH DAKOTA AS A BASE FOR PUBLISHING A SOIL ASSOCIATION VALUE MAP

Soil Association maps for large areas at scales of 1:1,000,000 and 1:500,000 usually are published as line maps or in color. The cost of publishing these maps on conventional aerial photographs would be excessive. 1/ A mosaic constructed from ERTS costs relatively little, however, since only 20 ERTS scenes are needed to cover the entire state of South Dakota. Moreover, the image approximates an orthographic view resulting in little distortion. Another advantage of ERTS is that a near real-time view of the scene is afforded and so the current use of the soil associations can be observed and studied. The map also can be updated each year with current ERTS imagery.

A Soil Association Value Map of South Dakota on an ERTS-1 mosaic has been published as SDSU-RSI-73-17 and is available from the Remote Sensing Institute, South Dakota State University, Brookings 57006. This map was constructed as follows. After delineating the major Soil Associations with the aid of ERTS imagery, over 4800 land sale prices covering a period of 1967-72 were located in the soil areas and averaged. A legend explaining land use, dominant slope and soil parent materials of each delineated area was developed. The soil associations then were described as Soil Association Value Areas on a 1:1,000,000 scale ERTS mosaic of South Dakota constructed using negative prints of band 7. 2/ Negative prints were used because they are a generation closer to the ERTS imagery than positive prints. MSS-7 was used because of its usefulness in detecting growing vegetation, its good contrast, its ability to delineate water and its ability to penetrate haze. The resulting map describes the kind of agriculture and soils and allows readers to see how soils actually are being used on a current map having very little distortion. Furthermore, it gives information about what buyers think the soils are worth. The map is intended for use by state and county

1/ It is estimated that it would take about 30,000 conventional aerial photographs to cover South Dakota.

2/ Appreciation is expressed to Jack Smith, Photographic Technician, RSI, SDSU, Brookings, for preparing the ERTS mosaic of South Dakota.

revenue officers to equalize land values in South Dakota, by individual buyers and sellers of land and lending institutions as a reference source, as a reference map by those planning road routes and cable lines and pipelines, by conservationists in helping to keep current conservation needs inventories, by agronomists needing current information on distribution and patterns of crop growth and by crop yield forecasters to guide sampling strategy.

REFERENCES

Soil Survey Staff. 1951. Soil Survey Manual ARS, USDA, Wash. D. C. p. 131.

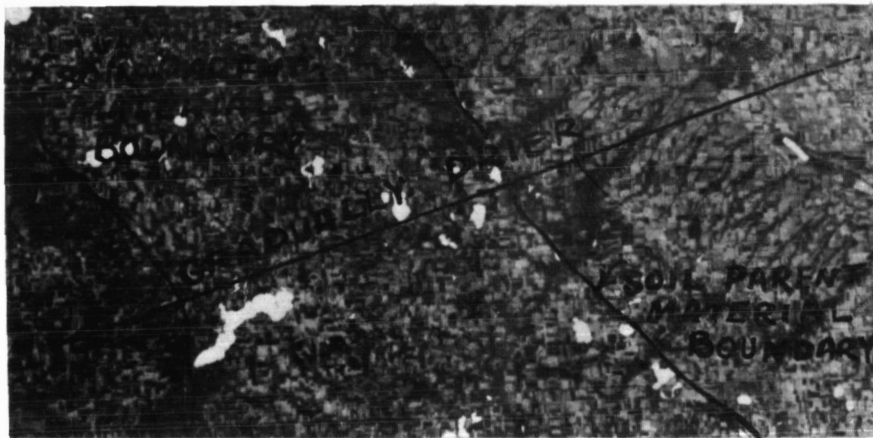
Simonson, R. W. 1971. Soil Association Maps and Proposed Nomenclature. Soil Sci. Soc. Amer. Proc. 35: pp. 959-963.

Figure 1

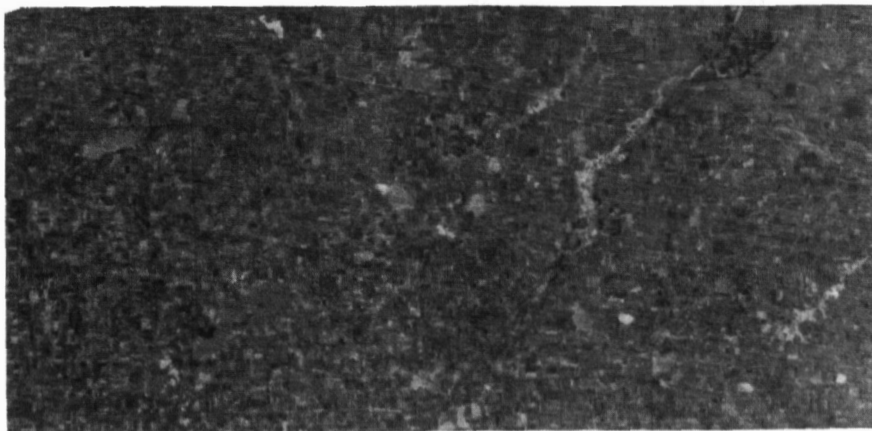
Use of ERTS-1 to detect Soil Association boundaries due to climatic differences

Negative prints, Scale 1:500,000, Western Minnesota 17 June '73

Along 44° latitude precipitation decreases in western Minnesota as the South Dakota state line is approached, and this fact is recognized by farmers who increase the proportion of small grain (a crop requiring less moisture) relative to corn and soybeans. On MSS-7 of this negative print from 17 June imagery, the lighter tones are on the more humid east, where most of the land has been planted to corn or soybeans about a month earlier. These crops have not yet mantled the soil so a large part of the reflectance on MSS-7 is of the soil. Moving west the number of fields in small grain (which is at its peak of green growth on 17 June and thus reflects strongly on MSS-7) increase, gradually increasing the proportion of dark tones on MSS-7. MSS-5 does not show these tonal differences.



MSS-7



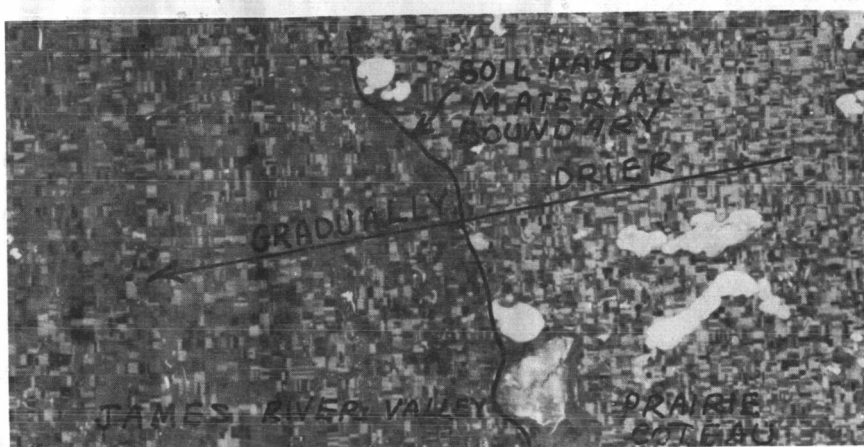
MSS-5

Figure 2

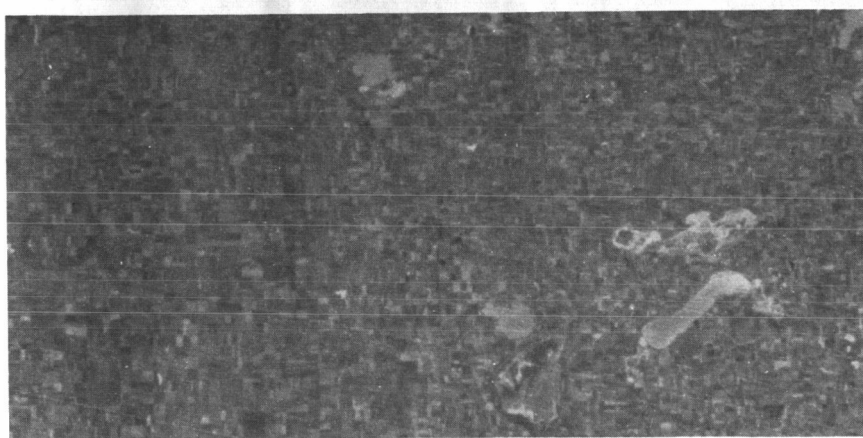
Use of ERTS 1 to detect Soil Association boundaries due to climatic differences

Dry subhumid and moist subhumid climates, glacial soils

In this May 16, 1973 ERTS scene, the moist subhumid Prairie Coteau (Udic soil subgroups) on the east has a higher proportion of corn and soybeans than the dry subhumid James Valley (Typic soil subgroups) which is primarily in spring grain and grass. Since the spring grain and grass are near their peak of green growth on this date, they have higher reflectance on band 7 than the Prairie Coteau which has a smaller mass of vegetation and hence has a comparatively low reflectance. This climatic boundary is apparent on MSS 7 but not MSS 5. Scenes taken in August also will show this but the reflectances on band 7 will be reversed from that shown on the May scene.



MSS-7



MSS-5

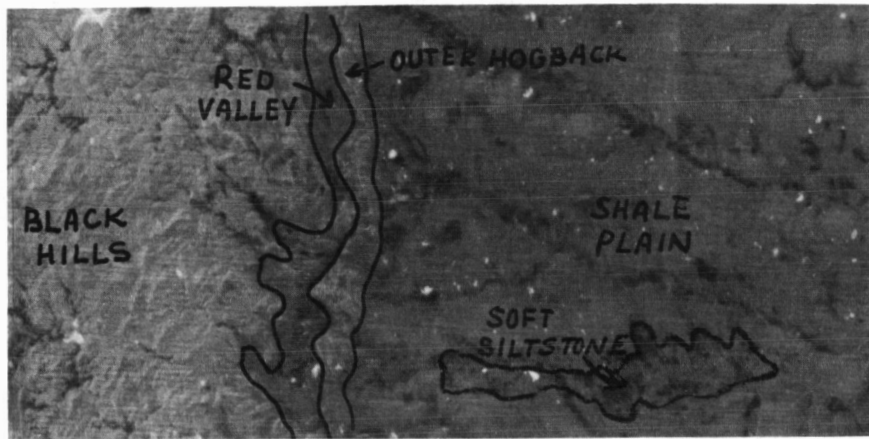
Figure 3

Use of ERTS 1 to detect Soil Association boundaries due to
soil parent material differences

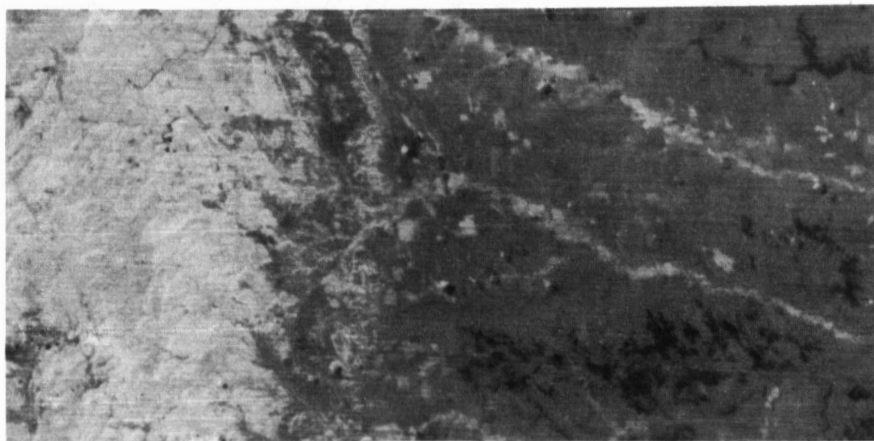
Limestone, Sandstone, Shale, Siltstone

Negative Prints, Scale 1:500,000, Western South Dakota

On this May 16, 1973 scene, the Black Hills area shown is developed from a hard limestone and is mantled with coniferous vegetation; the Red Valley is from a soft shale and is in grass; the Outer Hogback is from a hard sandstone and is partly in grass, partly in trees; the soft shale plain is in grass; and the light-colored soft siltstone area is barren badlands. The boundaries of each of these soil parent materials are apparent on both MSS 5 and 7 of ERTS but the contrast among these materials is more pronounced on MSS 5 than on 7.



MSS-7



MSS-5

Figure 4

Use of ERTS 1 to detect Soil Association boundaries due to soil parent material differences

Sandhills, Loess, Sandstone (Semiarid climate)

Negative Prints, Scale 1:500,000, Southwestern S. D.

On this May 1973 scene, the boundaries separating sandhills, loess and sandstone are readily apparent on both MSS 5 and 7, however, the gray tones denoting reflective differences are most apparent on MSS 5. Both the Sandhills, and the Pine Ridge are in grass but the latter has a well developed network of streams denoting low soil infiltration rates due to steep topography or slowly permeable soils or both. The nearly white fringe area along the drains is due to the low reflectance of the Pine trees and is seen best in MSS-5. The Sandhills has no drainage network indicating a high infiltration rate as would be expected on a sandy soil. The loess area is characterized by a field pattern of fallow (light gray on MSS 7) winter wheat (dark gray on MSS 7) and milo (also light gray on MSS 7). In the semiarid climate characterizing this area, only the most favorable soils are cropped. Conversely, since the income from wheat and milo is higher than from grass, few favorable soils are not cropped; thus, in this area land use correlates with soil quality.



MSS-7



MSS-5

Figure 5

Use of ERTS 1 to detect Soil Association boundaries due to
soil parent material differences

Dense Shale and Sandstone, Semiarid Climate

Negative Prints, Scale 1:500,000, Western South Dakota

On this May 15, 1973 scene, the dense shale soil area is nearly barren of vegetation while the sandstone area has a modest cover of cool season grasses and an occasional field. On band 7 the dense shale-derived Winler soil area has very low reflectance appearing nearly white on the print. Tonal differences between these two soil parent materials is not as pronounced on band 5.



MSS-7



MSS-5

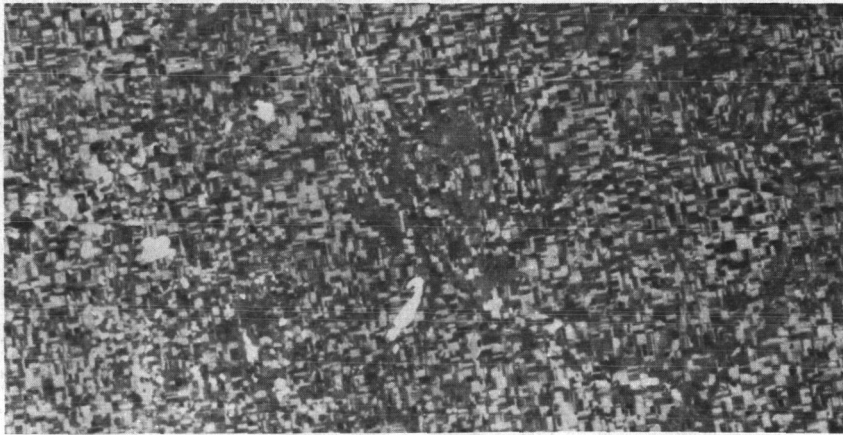
Figure 6

Use of ERTS 1 to detect Soil Association boundaries due to soil parent materials and land form differences

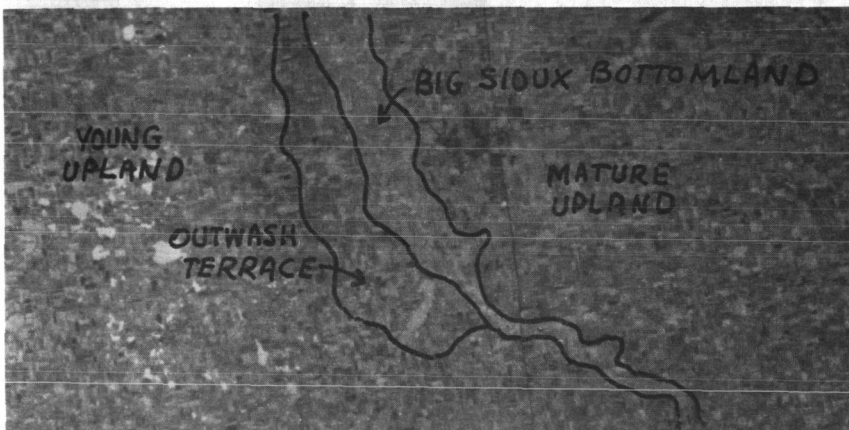
Bottomland, Terrace and Upland

Negative Prints, Scale 1:500,000, Eastern South Dakota

On this 17 June 1973 scene the boundaries of a bottomland, an outwash terrace, and two glacial uplands are apparent on MSS-5. The distinguishing features include reflective differences shown in gray tones, regularity of field patterns, presence or absence of streams, presence or absence of lakes and marshes. The last named feature is also seen on MSS-7. The reflective differences apparent between the poorly drained bottomland and the well drained terrace are due to the high incidence of grass vegetation on the bottomland which is near the peak of growth on 17 June. The higher lying terrace has well drained soils and is used exclusively as cropland. The west-lying glacial upland is dotted with marshes and lakes while the east-lying glacial upland has no lakes but instead has a stream drainage network.



MSS-7



MSS-5

Figure 7

Use of ERTS 1 to identify Soil Association boundaries due to soil parent material differences

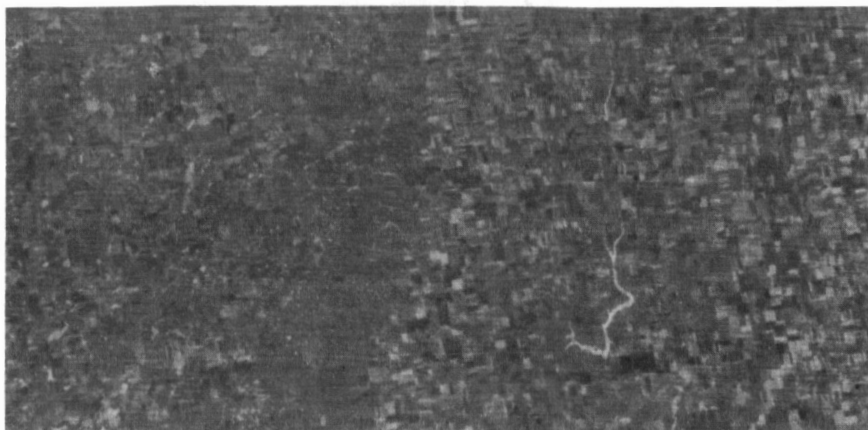
Dead-Ice Glacial Moraine, End Moraine, Ground Moraine

Negative Prints, Scale 1:500,000, Northcentral S. D.

On this 1 June 1973 scene the boundaries separating three kinds of soil parent materials are distinct on both MSS 7 and 5. The slight haze present however, was not penetrated as well by the MSS-5 as by the MSS-7 wavelengths resulting in a sharper image for the latter. The distinctness of the boundaries separating these soil parent materials is due to 1) unique land and water patterns of the strongly undulating Dead-Ice area seen especially well on MSS-7; 2) the uniform gray band of the steep, stony end moraine; and 3) the regular field pattern almost uninterrupted by lakes or grassed areas of the ground moraine.



MSS-7



MSS-5

Figure 8

Use of ERTS 1 to distinguish Soil Association boundaries due to
soil parent materials

Residual and Glacial Soil Association-Landscapes

Negative Prints, 15 May '73 Scale 1:500,000, Central South Dakota

The Oahe reservoir in central South Dakota occupies the trench of the Missouri River. East of this trench are friable medium textured glacial soil parent materials on a gently undulating surface having morainic depressions, marshes and lakes. West of the trench are firm clayey soil parent materials on a rolling surface characterized by broad ridges, steep valley sides and stream courses. The clayey residual soils on strong slopes are used primarily for rangeland, while the friable medium textured soils on gently undulating surfaces are mostly cropped to winter and spring wheat and corn.



MSS-7



MSS-5

Figure 9

Use of ERTS 1 to identify Soil Association boundaries due to soil parent material differences

Loess and Alluvium

Negative prints, Scale 1:500,000, Southeast South Dakota

On this 17 June 1973 scene boundaries between two loess areas are apparent on both MSS 5 and 7. In addition, the alluvial area boundaries are distinct on MSS-7 from the thick loess area having rolling relief. The thin loess area having flat relief and the alluvial plain have similar reflectances. The agricultural land use in southeast South Dakota consist of raising corn and soybeans and some alfalfa and small grains on flat or nearly level soils while close-growing crops like small grains dominate steeper slopes. On 17 June the small grains are near their peak at vegetative growth thus reflecting strongly on MSS-7 while the flats having more corn and soybeans have soil exposed over much of the area (as these crops were planted only about a month earlier) and have low reflectance. An August scene would show reverse reflectances as the areas having more corn and soybeans would give higher reflectance than the associations with more small grain.



MSS-7



MSS-5

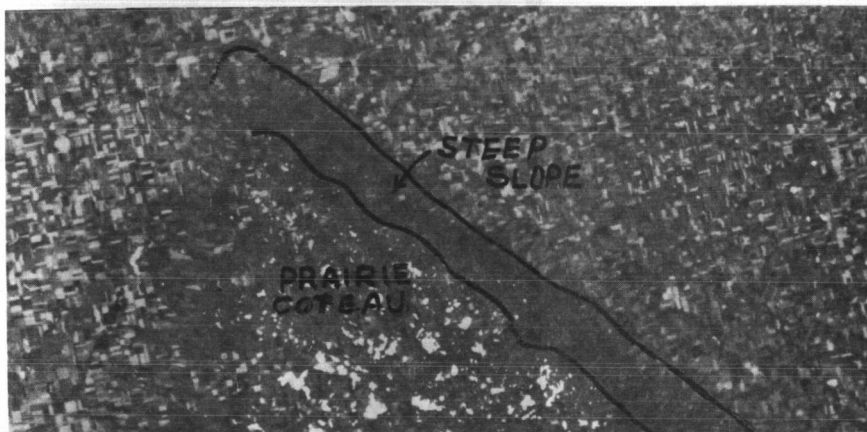
Figure 10

Use of ERTS 1 to distinguish Soil Association boundaries due to topography

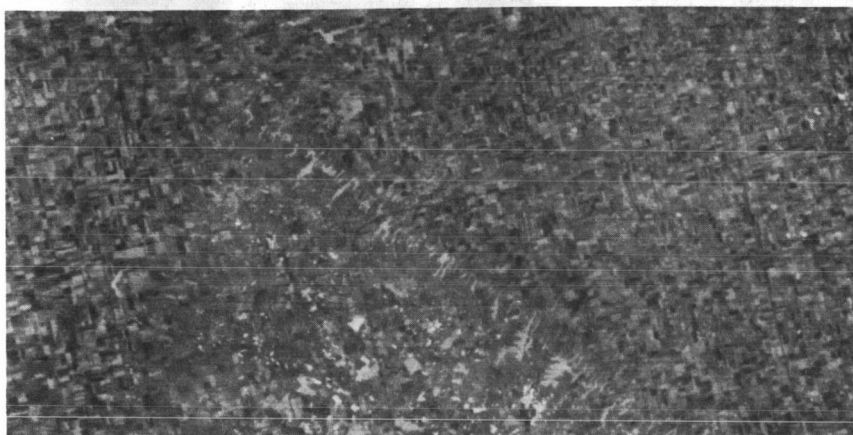
Glacial Area, Eastern South Dakota

Negative Prints, Scale 1:500,000,

On these July '72 prints the steep, escarpment of the Prairie Coteau stands out on MSS-7 as a broad dark band with distinct boundaries. This area is in grass because of its rugged topography and stoniness. On 29 July this grass is growing vigorously and hence reflects highly on MSS-7. On the Coteau lighter tones are prominent accentuated by many lakes on the crest of the Coteau. The lower-lying areas east and west of the Prairie Coteau have a field pattern indicating intensive cultivation. The light-toned fields shown on MSS-7 in this area have recently been planted to corn which has not grown enough at this time to have much reflectance on MSS-7. The steep slope is marked on MSS-5 by closely spaced parallel drains.



MSS-7



MSS-5

Figure 11

Use of ERTS 1 to distinguish Soil Association boundaries due to topography

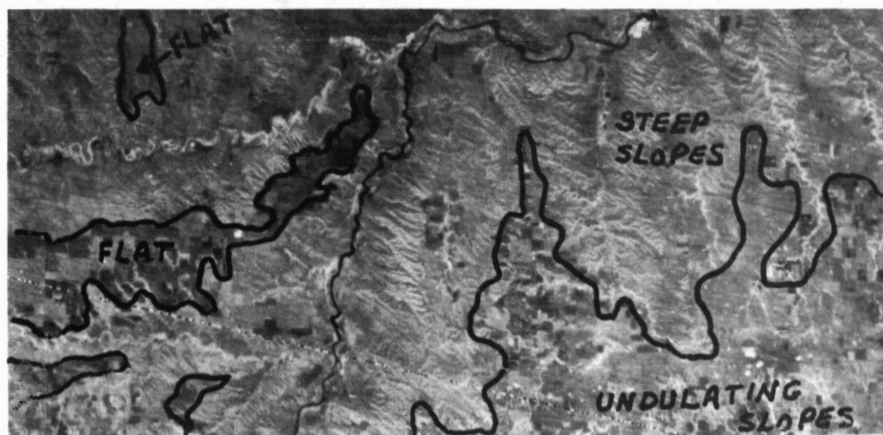
Residual Area, Western South Dakota

Negative prints, Scale 1:500,000

On these 9 July 1973 prints the steep valley sides of the Cheyenne and Belle Fourche rivers stand out with distinct boundaries on both MSS-5 and 7 from the adjacent less sloping areas. These steep areas, exclusively in grass, have thin clay soils derived from shale and produce less vegetation than the deeper, more friable soils occurring on less steep topography. Thus they have a reflective difference apparent on MSS-7 and this reflective difference correlates with the topographic boundary. On MSS-5 the reflective difference between the steep and less steep areas is less pronounced but the closely spaced stream network of the valley sides is more sharply etched, thus both MSS-5 and 7 aid in distinguishing the steep valley side boundaries.



MSS-7



MSS-5

MAPPING SOILS, CROPS, AND RANGELANDS BY MACHINE ANALYSIS OF MULTI-TEMPORAL ERTS-1 DATA

Marion F. Baumgardner, James A. Henderson, Jr., and LARS Staff, *Laboratory for Applications of Remote Sensing, Purdue University, West Lafayette, Indiana*

ABSTRACT

ERTS-1 data, obtained during the period 25 August 1972 to 5 September 1973 over a range of test sites in the Central United States, have been used for identifying and mapping differences in soil patterns, species and conditions of cultivated crops, and conditions of rangelands. Multispectral scanner data from multiple ERTS passes over certain test sites have provided the opportunity to study temporal changes in the scene.

Geometric correction was performed on the digital data for several dates and for several test sites. This made much easier the task of locating specific data points and of comparing the analytical results with other maps and data sources.

Multispectral classifications delineating soils boundaries in different test sites compared well with existing soil association maps prepared by conventional means.

Spectral analysis of ERTS data was used to identify, map, and make areal measurements of wheat in western Kansas.

Multispectral analysis of ERTS-1 data provided patterns in rangelands which can be related to soils differences, range management practices, and the extent of infestation of grasslands by mesquite (Prosopis fuliflora) and juniper (Juniperus spp.)

INTRODUCTION

Results of the analysis and interpretation of ERTS-1 multispectral data obtained over several Great Plains test sites on multiple dates are presented in this paper. These test sites were selected because they present a variety of problems associated with the development and management of land resources in the Great Plains.

The purpose of the studies reported here is to examine the utility of ERTS-1 data and machine processing techniques in (1) identifying winter wheat and measuring its areal extent, (2) delineating soil association boundaries, (3) characterizing and mapping rangeland conditions, and (4) inventorying land use in a semiarid region.

Identification and Areal Measurement of Winter Wheat

Hard red winter wheat (*Triticum vulgare*) is the principal crop in Greeley County, Kansas. This area in western Kansas is typical of much of the winter wheat belt of the United States. ERTS-1 digital data obtained on 19 June 1973 were analyzed to separate wheat from other cover types and to measure the area in wheat.

On 14 May 1973 color and color infrared photography was obtained by a NASA aircraft at an altitude of 9500 m along a north-south flightline centered over Greeley County. By photo-interpretation of the color infrared photography three cover types were identified: wheat, fallow (bare soil) and permanent pasture. Training sets representing each of these three cover types were selected.

Using a clustering algorithm the ERTS-1 data for the area along the aircraft flightline were separated into eight spectrally separable classes in order to enhance the field boundaries. It was then possible to locate in the ERTS data the training fields selected from the aerial photography. A supervised algorithm was then used to classify the entire county into three categories: wheat, fallow, and pasture (Figure 1). A set of test fields was selected from the aerial photography and used to evaluate the classification results. Later the computer classification results of several fields were verified by the cooperative agricultural extension agent in Greeley County.

The classification accuracy is recorded in Table 1.

Table 1. Results of Computer Classification of ERTS-1 MSS Data, Greeley County, Kansas, 19 June 1973.

Class	% Correct Recognition of Tested Fields*
Pasture	96.1
Wheat	97.0
Fallow	97.9

*From underflight photography and limited ground observations.

From the classification results the area of wheat in Greeley County was then calculated, and the results were compared with estimates made by the Statistical Reporting Service (U.S. Department of Agriculture). These comparisons are presented in Table 2.

Table 2. 1973 Wheat Area Estimates for Greeley County, Kansas.

<u>Source of Estimate</u>	<u>Hectares</u>
SRS (USDA)	73,000 + 5%
ERTS	77,000

Delineation of Soil Associations

One of the important uses of ERTS imagery is in the delineation of soil associations or groups which may have different physical and chemical properties. The Soil Conservation Service (U.S. Department of Agriculture) is vitally concerned with the classification and mapping of soils, with the use and management of soils, and with the monitoring of changing land uses. Digital data from ERTS-1 have been studied to determine their application in each of these concerns of SCS.

The soil association map (Figure 2) of Crosby County, Texas, shows the northern one-third of the county to consist of deep clays and silty clay loams. The soils in the central part of the county west of Blanco Canyon are mixed lands--silt loams and silty clay loams. To the south of this area the soils grade into the lighter sandy loams. The soil association map shows in the southwest part of the county on the High Plains an area of deep sandy soils. The Caprock Escarpment separates the soils of the High Plains from the soils of the Rolling Plains. Just below the rim of the Escarpment is a band of steep shallow soils. As the slopes flatten out below the Escarpment sandy loams predominate. However, there are two areas of deep sands in the southeast part of the county.

An examination of an image (Figure 3) of Crosby County produced from bands 4, 5, and 7 of the 9 October 1972 ERTS pass reveals rather well the gross soil patterns, including the clearly defined Caprock Escarpment. Using all four bands of the 9 October 1972 ERTS MSS data a nonsupervised or clustering algorithm was used to produce a classification with fourteen spectral classes (Figure 4). Examination of the patterns reveals subtle changes which correspond to the changes in soils from the heavy clay soils in the north to the sandy loams and sands in the south and southeast.

Fourteen spectral classes produced with MSS data from the 2 December 1972 ERTS pass reveal similar soil changes from north to south (Figure 5). In the 12 spectral classes produced from the 18 June 1973 ERTS MSS data the soils patterns seem to be less distinct (Figure 6). However, the Caprock Escarpment and the deep sands are easily delineated.

A closer view of the 9 October and 2 December spectral classifications of the Blanco Canyon area east of Crosbyton reveals

the sharp break between the High and Rolling Plains (Figures 7 and 8). There are also subtle spectral differences which relate to the steep shallow soils and the less steep, rolling sandy soils between the Caprock Escarpment. In the immediate future data from these three dates will be geometrically corrected so that temporal overlay analysis can be done. At that time a soil association map will be produced with the use of ERTS imagery as a base.

Characterizing and Mapping Rangeland Conditions

To a very large degree man is dependent upon the rangelands in the arid and semiarid regions of the world for producing animal protein. The task of monitoring and managing these rangelands is great. Millions of hectares of rangeland in the Western United States are subject to overgrazing and mismanagement. Temporal data from ERTS can provide very useful information and monitoring services for private organizations and public agencies whose responsibility it is to manage rangelands.

A spectral classification of an area around the T Bar Ranch in Lynn County, Texas was produced from ERTS MSS data obtained on 9 October 1972 (Figure 9). The purpose of the classification was to delineate spectrally different conditions of rangelands. Although it is difficult to quantify the results, an examination of low altitude aerial photography indicates that a good separation has been obtained between three conditions: (1) range grasses, (2) a mixture of grasses and mesquite (Prosopis fuliflora) and (3) heavy mesquite infestation (Figure 10).

An area of rangeland in the southeastern part of Crosby County around the White River Reservoir was also examined. Images produced from ERTS MSS bands 4, 5, and 7 and classifications using all 4 MSS bands were generated from the 18 June 1973 ERTS MSS data. The image (Figure 11) indicates where the more dense green vegetation is located and delineates the rangeland from the cultivated fields. The classification (Figure 12) suggests where the heavy vegetation and more uniform areas are. It also illustrates the mottled area west of the White River Reservoir which seems to be related to differences in topography, soil productivity, soil depth, and vegetative cover.

Land Use Inventory in Semiarid Region

In the coming decade the United States may be challenged as never before in the tasks of land management and agricultural production. Permanent vegetation on millions of hectares of marginal land is now being sacrificed to the plow. Lands which are highly susceptible to wind and water erosion are being brought under cultivation to take advantage of the record high prices for agricultural products. Changing land use patterns call for faster and more accurate methods of monitoring land use change.

MSS data from two ERTS passes over Lubbock County, Texas have been studied. The dates are 2 December 1972 and 18 June 1973.

Images produced from ERTS MSS bands 4, 5, and 7 for these two dates reveal some striking differences (Figures 13 and 14). In December the urban and rural scenes are easily separated. However, the scarcity of green vegetation subdues the spectral differences between different features in both urban and rural areas. In the June image differences in green vegetation present more contrast and enhance the separability between parks, residential areas, and commercial-industrial zones in the city of Lubbock.

A computer-generated classification of the June data for Lubbock County (Figure 15) illustrates spectral classes related to rural lands, urban residential, commercial-industrial, and water.

A closer look at the city of Lubbock reveals more clearly the differences between the two dates (Figures 16 and 17). In the image for June the residential areas are easily delineated from the commercial-industrial areas and the major transportation arteries. The classification (Figure 18) is a map of the city illustrating five spectral classes--residential, commercial-industrial, water, dense green areas (parks, grass), and rural (non-green fields).

Many features identified on aerial photography can be identified in the classification of the ERTS data. Two examples are the Lubbock Airport (Figure 19) and the large complex of cotton warehouses southeast of Lubbock (Figure 20).

The most recent updating of the Lubbock City map was in 1971. A careful comparison of the classification of ERTS data and the city map reveals many areas of land use change on the outskirts of the city since 1971.

Conclusions

Results reported in this paper strongly support the need for an operational satellite for observing, mapping, and monitoring earth resources. In the opinions of the authors of this paper the feasibility has been established for using satellite-acquired multispectral scanner data and computer-implemented pattern recognition techniques to identify and measure area of crops, to assist in mapping soils, to characterize and monitor rangeland conditions, and to prepare and update land use inventories.

ATTACHMENT A

ERTS Data Analyzed

<u>Test Site</u>	<u>ERTS-1 Scene I.D.</u>	<u>Date of Pass</u>
Greeley County, Kansas	1331-16571	19 June 1973
Crosby County, Texas	1078-16524	9 Oct 1972
Crosby County, Texas	1132-16532	2 Dec 1972
Crosby County, Texas	1330-16531	18 June 1973
Lubbock County, Texas	1132-16532	2 Dec 1972
Lubbock County, Texas	1330-16531	18 June 1973
Lynn County, Texas	1330-16531	18 June 1973

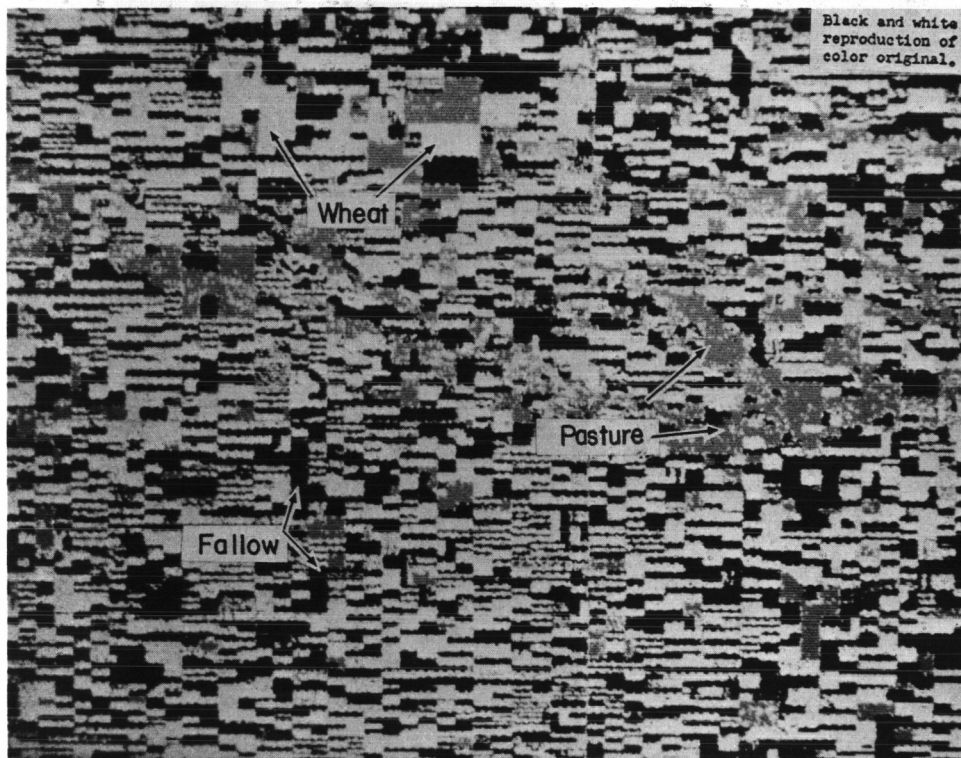


Figure 1. Identification of wheat, fallow (bare soil), and permanent pasture in Greeley County, Kansas by computer analysis of multispectral scanner data from the 19 June 1973 ERTS pass.

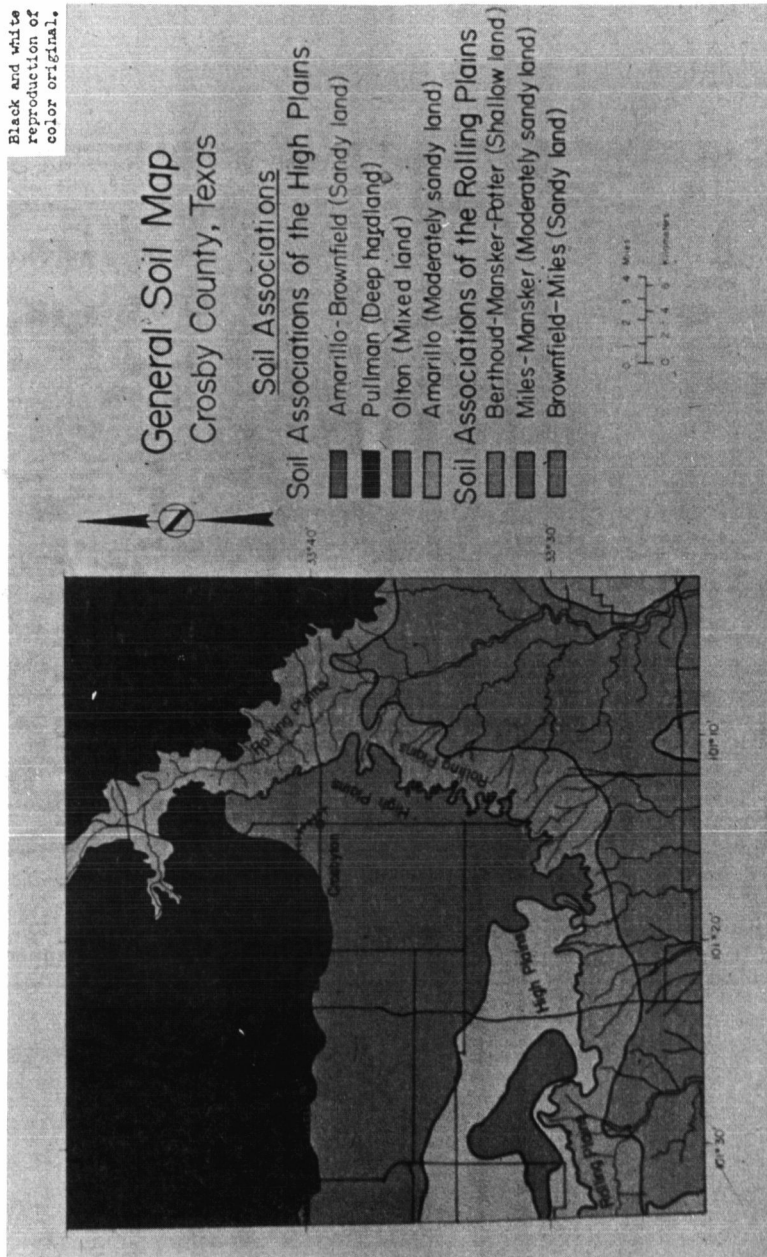


Figure 2. Soil association map of Crosby County, Texas.

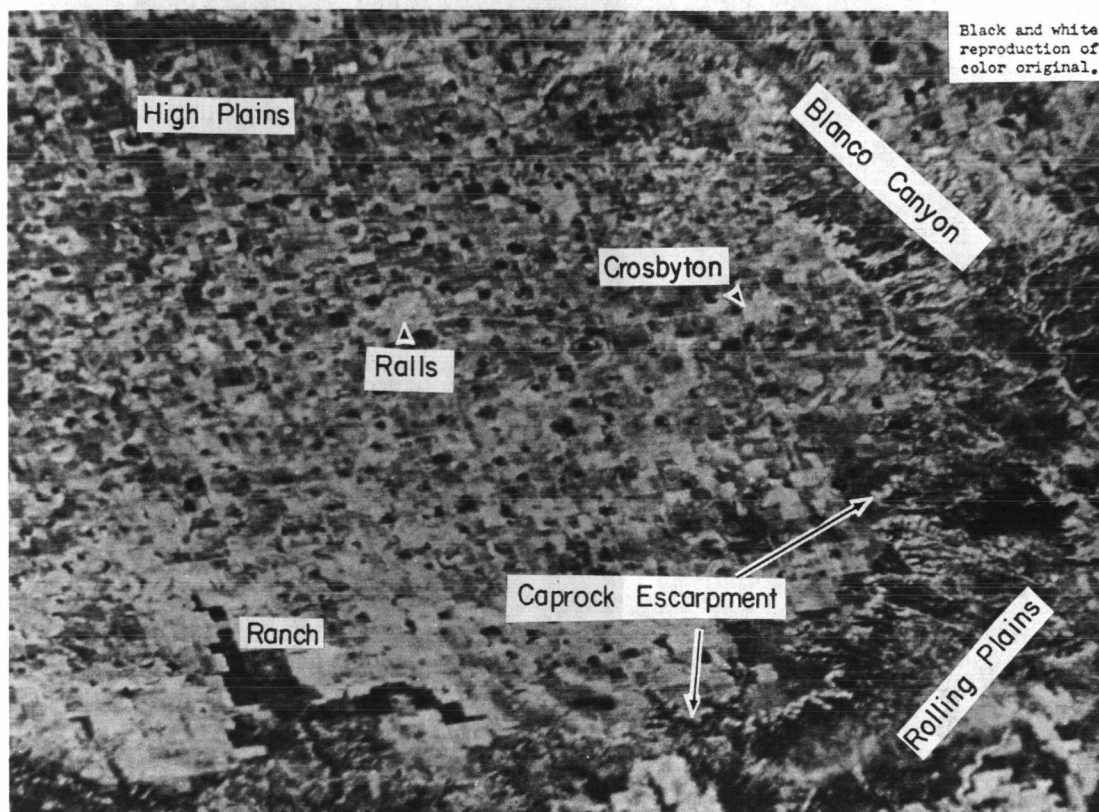


Figure 3. Image of Crosby County, Texas produced by computer analysis of MSS data from 9 October 1972 ERTS pass.

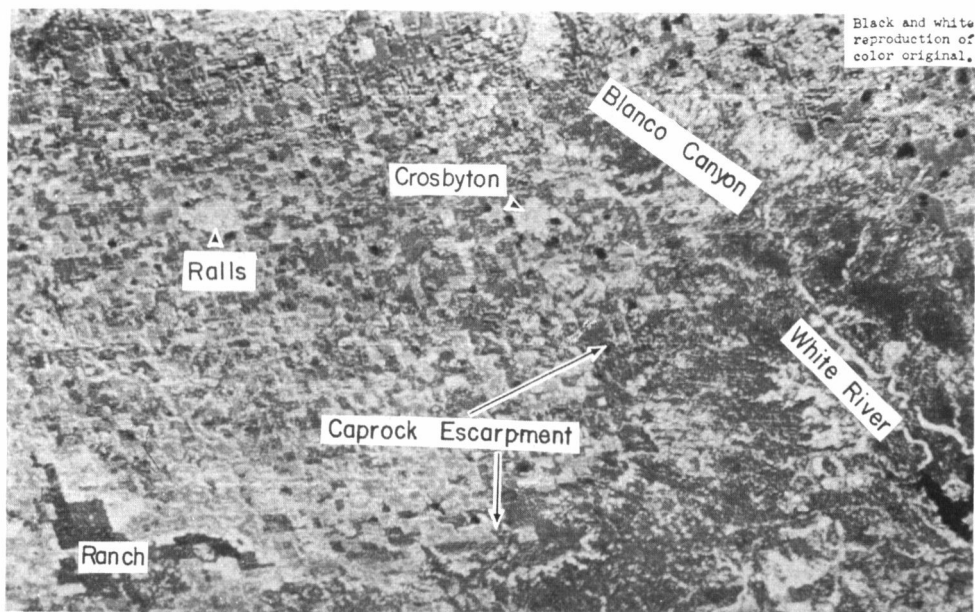


Figure 4. Fourteen spectral classes (representing different ground cover types or conditions in Crosby County, Texas) produced by computer analysis of MSS data from the 9 October 1972 ERTS pass.

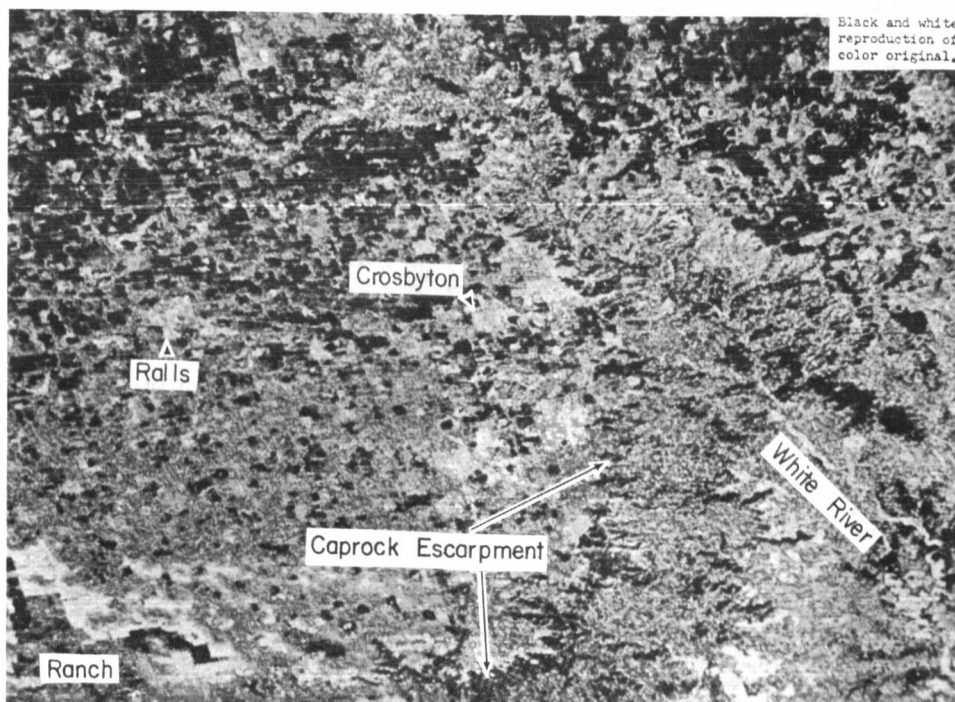


Figure 5. Fourteen spectral classes produced by computer analysis of MSS data from the 2 December 1972 ERTS pass over Crosby County, Texas.

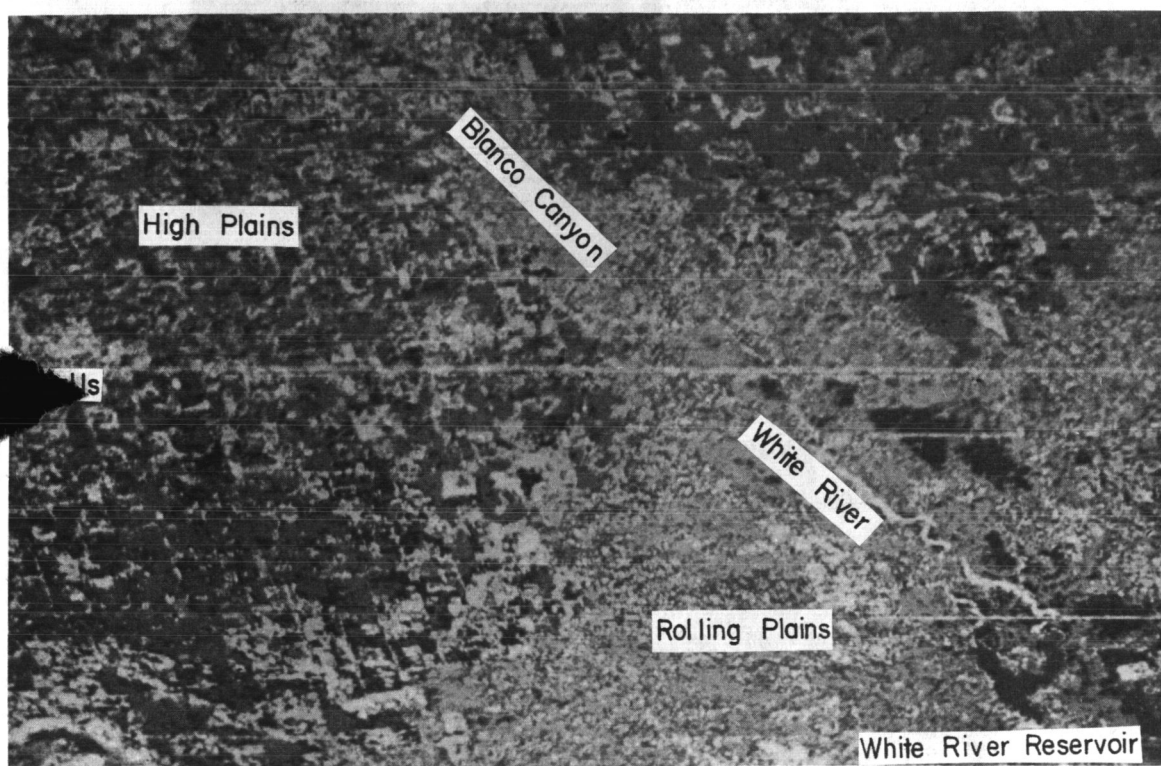


Figure 6. Twelve spectral classes produced by computer analysis of MSS data from the 18 June 1973 ERTS pass over Crosby County, Texas.

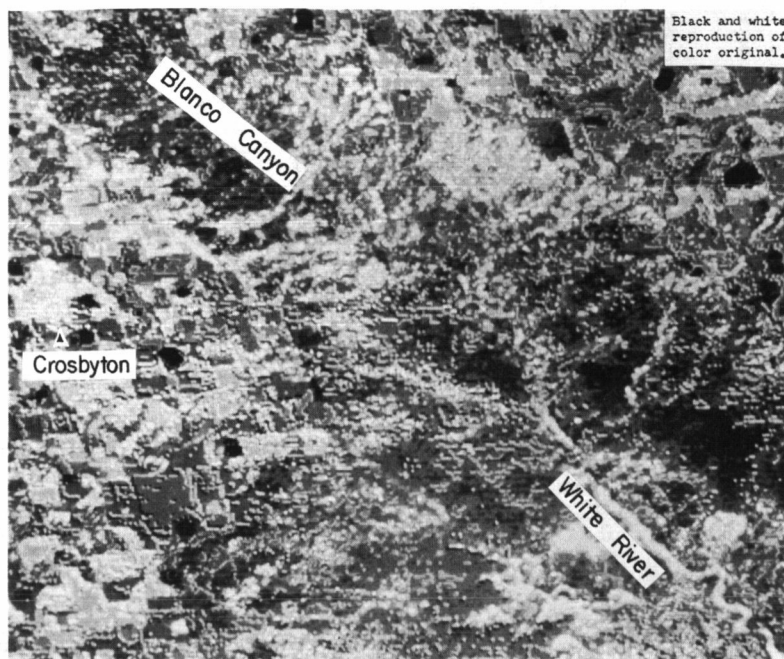


Figure 7. Fourteen spectral classes of Blanco Canyon area east of Crosbyton, Texas; produced from 9 October 1972 ERTS data.

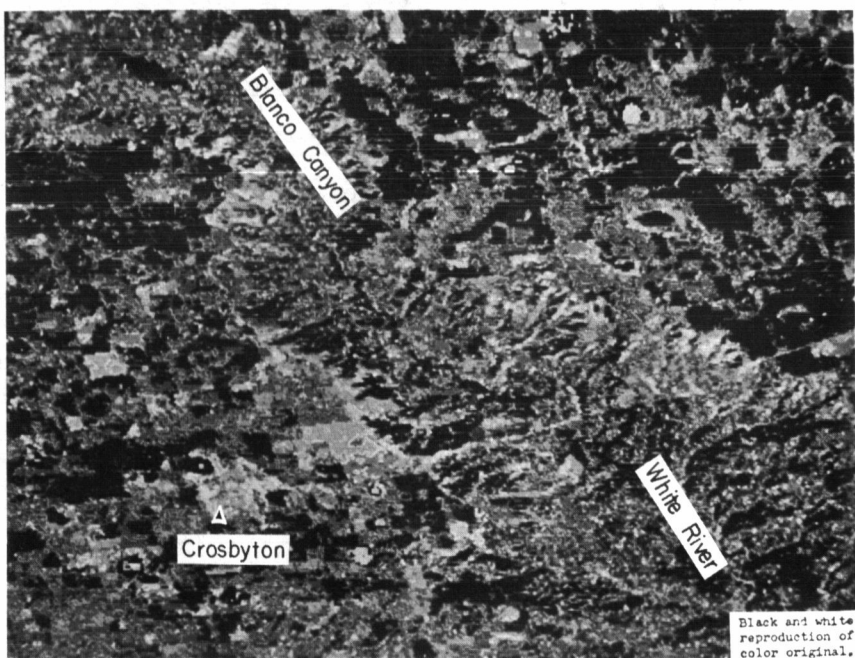


Figure 8. Fourteen spectral classes of Blanco Canyon area east of Crosbyton, Texas; produced from 2 December 1972 ERTS data.

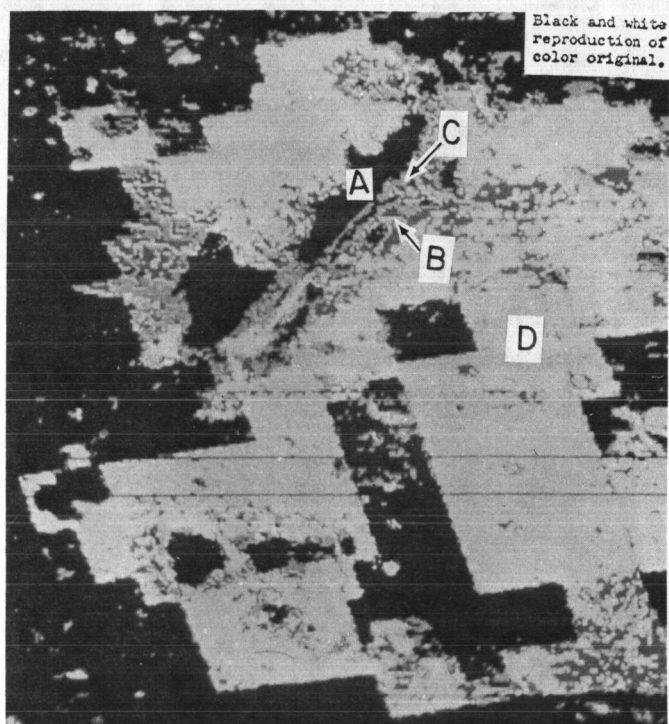


Figure 9. Four spectral clases of T Bar Ranch area in Lynn County, Texas, produced from 18 June 1973 ERTS data; A = Double Lakes; B = heavy mesquite infestation; C = moderate mesquite infestation; D= little or mesquite infestation.

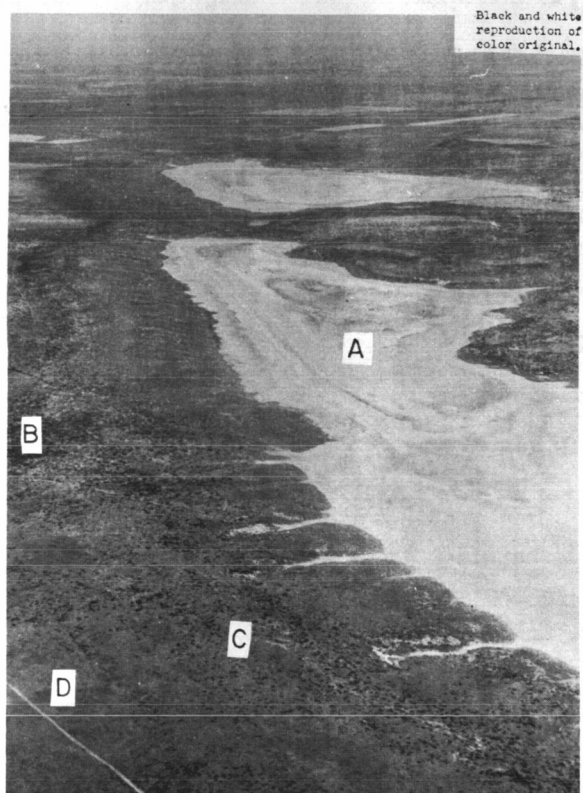


Figure 10. Aerial photograph taken over T Bar Ranch on 5 July 1973; A = Double Lakes; B = heavy mesquite infestation; C = moderate mesquite infestation; D = little or no mesquite infestation.

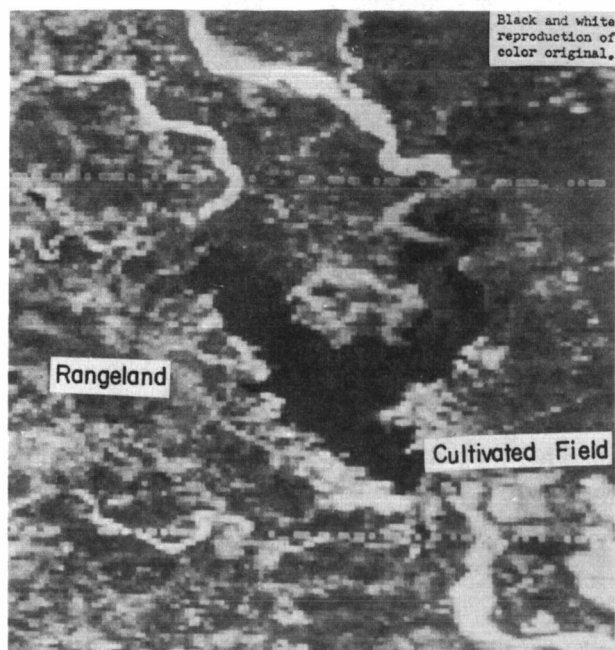


Figure 11. Image of White River Reservoir area produced by computer analysis of MSS data obtained from 18 June 1973 ERTS pass.

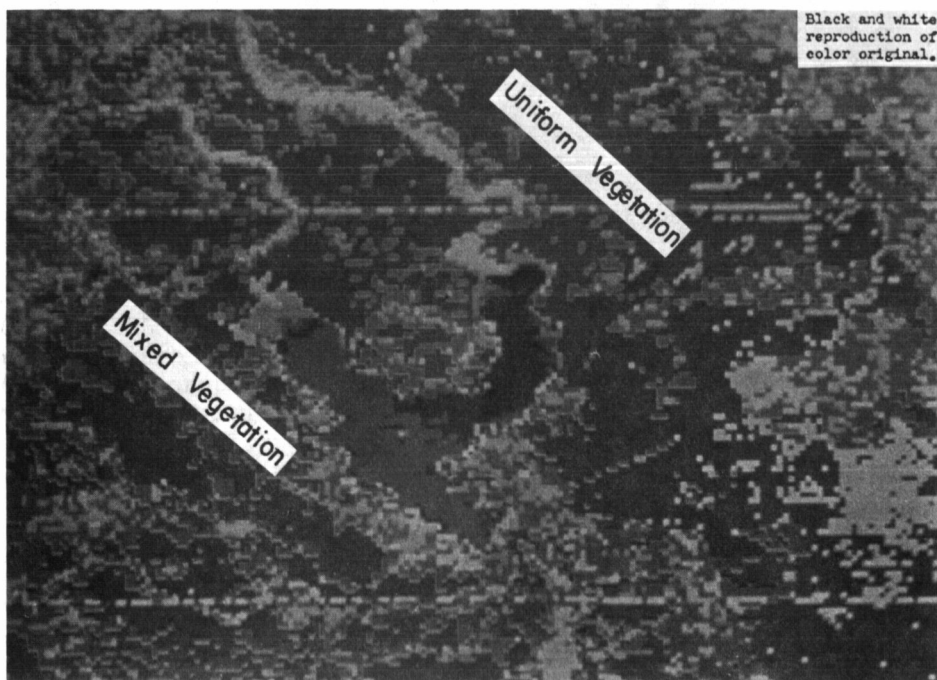


Figure 12. Nine spectral classes of White River Reservoir area in Crosby County, Texas; produced from 18 June 1973 ERTS data.

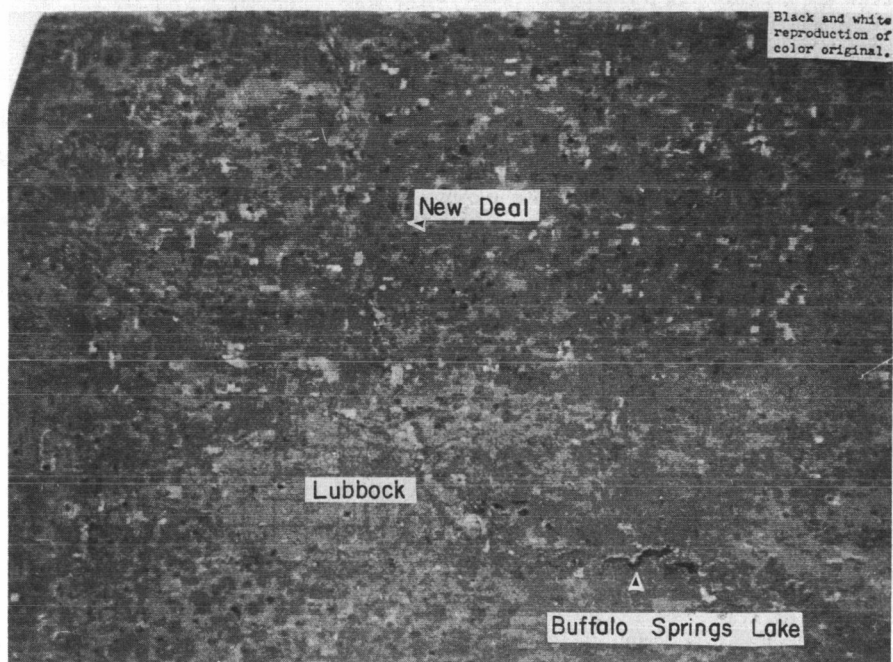


Figure 13. Image of Lubbock County, Texas produced by computer Analysis of MSS data obtained from 2 December 1972 ERTS pass

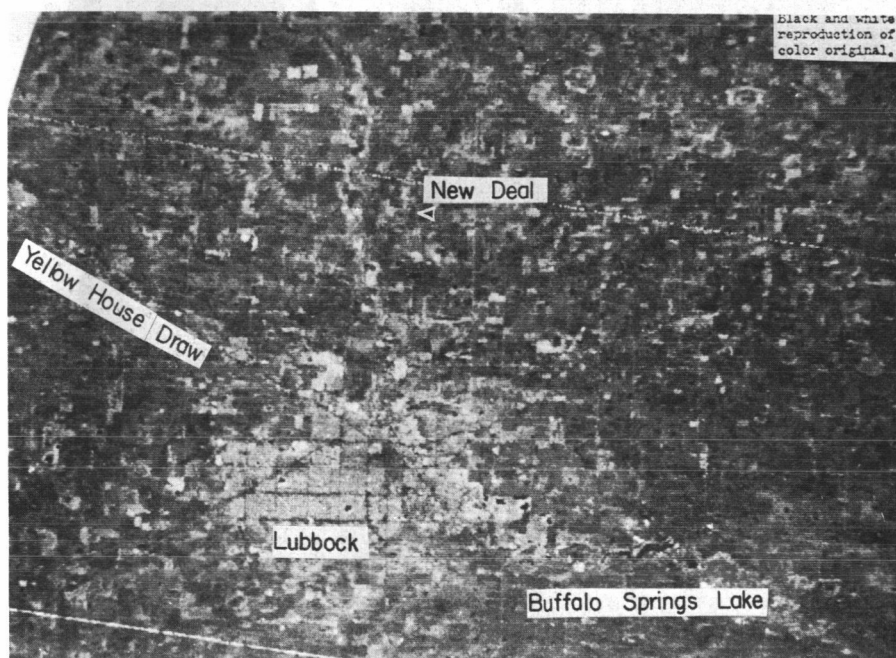


Figure 14. Image of Lubbock County, Texas produced by computer analysis of MSS data obtained from 18 June 1973 ERTS pass.

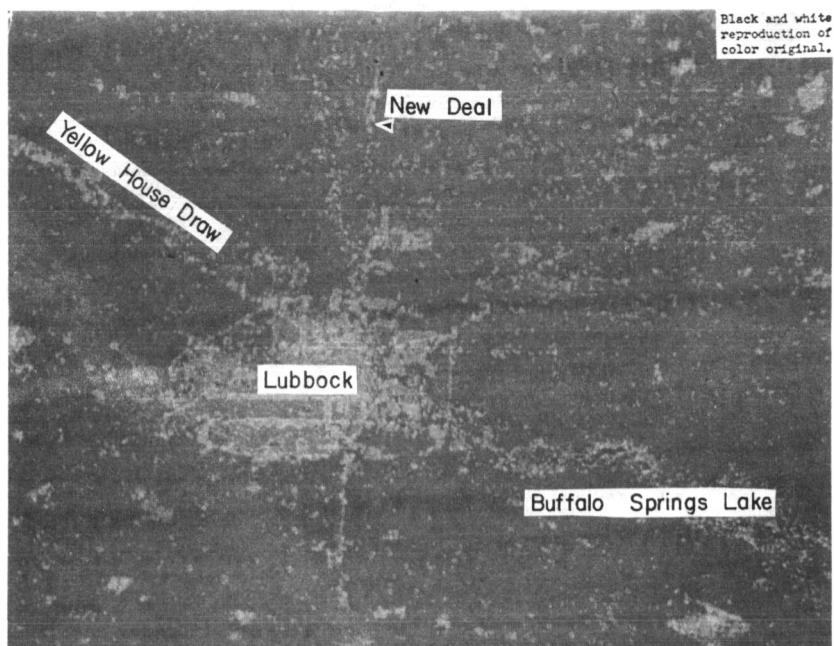


Figure 15. Four spectral classes of Lubbock County, Texas; produced from 18 June 1973 ERTS data.

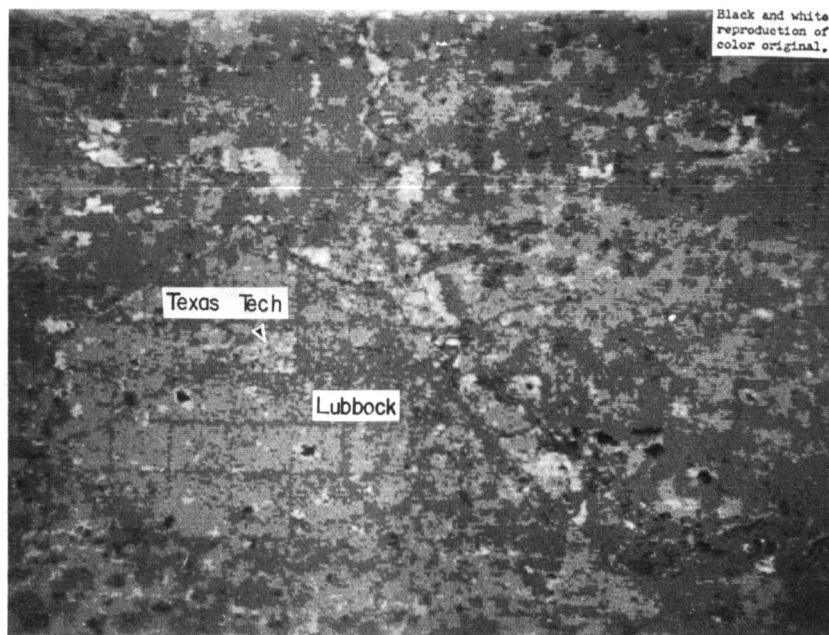


Figure 16. Image of Lubbock, Texas produced by computer analysis of MSS data obtained from 2 December ERTS pass.

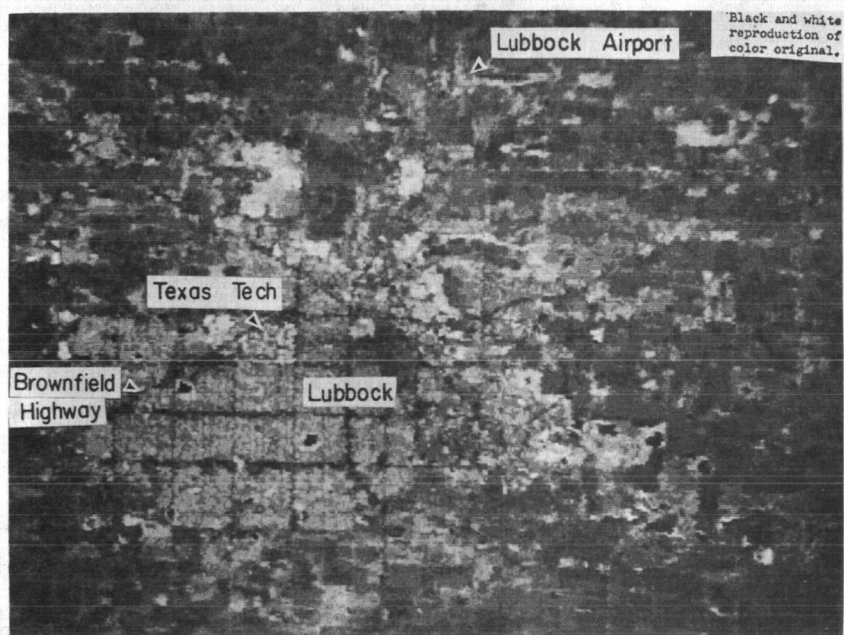


Figure 17. Image of Lubbock, Texas produced by computer analysis of MSS data obtained from 18 June 1973 ERTS pass.

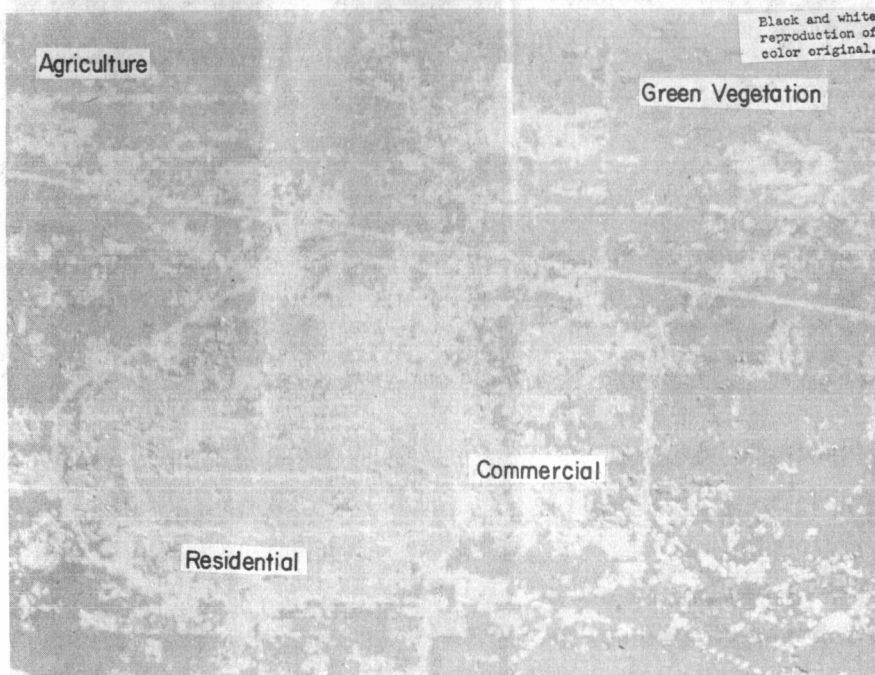


Figure 18. Four spectral classes of Lubbock, Texas area; produced from 18 June 1973 ERTS data.

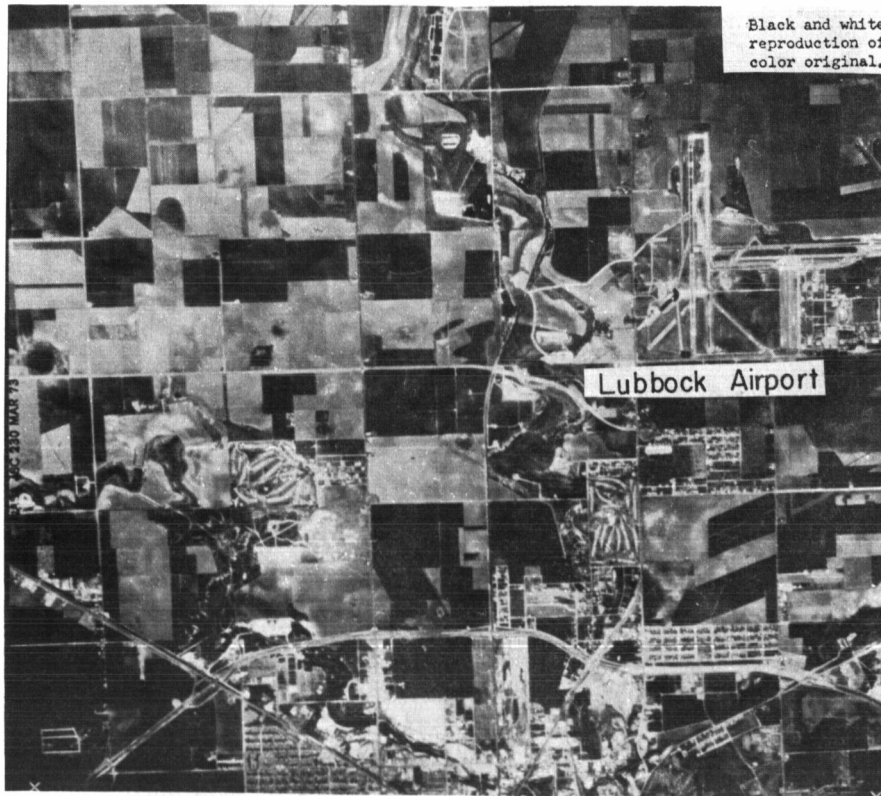


Figure 19. Aerial photograph taken on 20 March 1973 north of Lubbock, Texas.



Figure 20. Oblique aerial photograph taken on 5 July 1973, over southeast Lubbock, Texas.

APPLICATION OF ERTS-1 IMAGERY IN MAPPING AND MANAGING SOIL AND RANGE RESOURCES IN THE SAND HILLS REGION OF NEBRASKA

Paul M. Seevers, David T. Lewis and James V. Drew, *Department of Agronomy, University of Nebraska-Lincoln, Lincoln, Nebraska 68503*

ABSTRACT

Maximum sustained beef production within the 32,000 square kilometers of the Sand Hills region of Nebraska is directly related to range management decisions based on range sites and interpretations of range condition classes. Interpretations of imagery from the Earth Resources Technology Satellite (ERTS-1) indicate that soil associations and attendant range sites can be identified on the basis of vegetation and topography using multi-temporal imagery. Optical density measurements of imagery from the visible red band of the multispectral scanner (MSS band 5) obtained during the growing season were related to field measurements of vegetative biomass, a factor that closely parallels range condition class on specific range sites. ERTS-1 imagery also permitted inventory and assessment of center-pivot irrigation systems in the Sand Hills region in relation to soil and topographic conditions and energy requirements. The following resource maps of the Upper Loup Natural Resource District located entirely within the Sand Hills region were prepared from ERTS-1 imagery: (1) Location of subirrigated range sites and lakes, (2) Frequency of blowouts and areas affected by severe wind erosion, (3) Areas with less than 10% vegetative cover and severe wind erosion hazard, (4) Distribution of center-pivot irrigation systems identified according to production of perennial forage crops or annual crops.

INTRODUCTION

The objective of this investigation is to evaluate the use of MSS imagery acquired by ERTS-1 as a tool in mapping and managing soil and range resources in the Sand Hills region of Nebraska. This region occupies the north-central one-third of Nebraska, is composed of approximately 32,000 square kilometers of eolian sand dunes interspersed with nearly level valleys, and is stabilized by grass and grass-like plants. The dominant economic enterprise within the region is the production of beef cattle and centers on cow-calf operations involving the utilization of rangeland forage. In 1972 there were 518,300 beef cows and 606,700 calves and yearlings within the Sand Hills region, representing an aggregate value of \$263,820,000.

PRECEDING PAGE BLANK NOT FILMED

1 N 74 30721

Beef animals raised within the Sand Hills region obtain virtually all of their feed units from forage. Consequently, domestic and foreign demands for beef translate into demands for efficient use of existing forage as well as for more forage. Maximum sustained beef production within the Sand Hills region is directly related to the optimum use of rangeland according to management practices determined on the basis of range sites and range condition classes. In addition, the development of center-pivot irrigation systems has considerable potential for increasing and stabilizing forage yields under the erratic climatic conditions of the Great Plains.

The model tested in this study is that shadow patterns from the dune topography of the sandhills and the spectral reflectance of the rangeland vegetation will permit interpretations of soil associations and attendant range sites, range condition and degree of forage utilization from reflectance measured by sensors aboard ERTS-1. A major goal in developing this model was to determine the optimum level of generalization suitable for consistent and accurate interpretations using the scale and resolution of ERTS-1 imagery.

SOIL ASSOCIATIONS AND RANGE SITES

Multi-temporal ERTS-1 imagery of McPherson, Hooker and Thomas Counties within the Sand Hills region of Nebraska permitted human image interpretation of soil

Table 1. Relationships of Topographic Features, Soil Associations and Range Sites Within the Sand Hills Region of Nebraska

<u>TOPOGRAPHIC FEATURES</u>	<u>SOIL ASSOCIATIONS</u>	<u>RANGE SITES</u>
1. Rolling and steeply sloping (choppy) uplands with dry valleys	Valentine-Dunday	Sands, Choppy Sands and Sandy
2. Rolling uplands with dry valleys	Valentine-Anselmo	Sands and Sandy
3. Steeply sloping (choppy) uplands	Valentine, hilly	Choppy Sands
4. Rolling uplands with subirrigated valleys	Valentine-Elsmere-Gannett	Sands and Subirrigated
5. Rolling uplands, dry valleys and subirrigated valleys	Valentine-Dunday-Loup	Sands, Sandy, Subirrigated
6. Rolling uplands	Valentine, rolling	Sands
7. Rolling uplands with dry valleys of sand hills - loess border	Anselmo-Valentine-Dunday	Sands, Sandy

associations comparable with recently published soil association maps for these counties. Specific soil associations and range sites defined in terms of soil and topographic features are shown in Table 1.

Color composites generated from spring imagery (MSS bands 4, 5 and 6 of image 1295-16564) obtained on May 14, 1973 prior to summer haying operations were used to identify the Valentine-Elsmere-Gennett soil association consisting of dunes and subirrigated valleys. Within this association, Elsmere and Gannett soils (Subirrigated range sites) exhibited relatively dense and physiologically active vegetation and provided strong reflectance in MSS band 6 in comparison with Valentine soil (Sands range site) that is not subirrigated. Moreover, standard management practices involving mowing or grazing of the Subirrigated sites prevent the annual accumulation of dead vegetation and permit near-infrared reflectance from vegetative growth produced during the spring. In contrast, the relatively low density of vegetation on the choppy, steeply sloping uplands permitted tentative identification of the Valentine, hilly, soil association.

The Valentine, hilly association (Choppy Sands range site) as well as the other soil associations differing in topographic expression were readily identified from winter imagery (MSS band 6 of image 1170-17020) obtained on January 9, 1973 showing topographic features enhanced by continuous snow cover and low sun angle. Shadow patterns allowed the delineation of the Valentine-Dunday soil association (Sands, Choppy Sands and Sandy range sites) consisting of large dunes separated by rolling valleys, the Valentine-Anselmo soil association (Sands and Sandy range sites) consisting of rolling dunes and swales, the Valentine, rolling soil association (Sands range site) consisting of rolling uplands, and the Valentine, hilly soil association (Choppy Sands range site) consisting of choppy sandhills with no major intervening valleys.

Color composites generated from summer imagery in MSS bands 5, 6 and 7 permitted the identification of patterns of cultivated cropland and the delineation of the Anselmo-Valentine-Dunday soil association (Sands and Sandy range sites) in the sandhills-loess border.

Relationships established through comparisons of ERTS-1 imagery with published soil association maps of McPherson, Hooker and Thomas Counties permitted construction of a soil association map for Cherry County, Nebraska, an adjacent sandhills county for which no comparable soil association map was available. Comparisons of the soil association map constructed for Cherry County with data obtained from field observations and from high altitude color-infrared aerial photography indicate a high degree of accuracy for the soil association map interpreted directly from ERTS-1 imagery (MSS bands 4, 5 and 6 of image 1295-16562 and MSS band 6 of image 1170-17013). Because of unique combinations of vegetation and land surface configuration within the Sand Hills region, ERTS-1 imagery is suitable for interpreting soil units and range sites at a level of generalization intermediate between county soil association maps and standard soil surveys made by observations of soil profiles and landscapes on the ground.

RELATIONSHIPS OF VEGETATIVE BIOMASS AND OPTICAL DENSITY

Identification of soil associations and attendant range sites within the Sand Hills region provides a basis for the measurement and interpretation of total vegetative biomass from ERTS-1 imagery. Because of the total spectral response of the sandy soils, differences in image density in relation to vegetative biomass are more distinct in the Sand Hills region than in other rangeland areas of Nebraska.

Field studies in Cherry County, Nebraska, completed within one day of the ERTS-1 overpass on July 26, 1973 indicate relationships between total vegetative biomass and the optical density of imagery from MSS band 5 (image 1386-17011) measured at specific study sites (Table 2). The optical density measurements reported fall within the upper one-half of the gray scale, the optimum range for image evaluation.

Numerous field observations within the Sand Hills region suggest that range condition classes based on field estimates of climax vegetation for a given range site are also closely related to vegetative biomass. Nevertheless, comparison of values for optical density and range condition between different range sites (e.g., Sandy v.s. Subirrigated) is not feasible because variations in range condition on similar range sites result in overlapping values for optical density.

Table 2. Relationships of total vegetative biomass to optical density of ERTS-1 image, MSS band 5, for selected range sites within the Sand Hills region of Nebraska.

<u>RANGE SITE</u>	<u>RANGE CONDITION</u>	<u>VEGETATIVE BIOMASS</u> ¹ kg/ha dry wt.	<u>OPTICAL</u> ² <u>DENSITY</u>
Sandy	Poor	367	0.49
Choppy Sands	Fair	598	0.58
Subirrigated	Fair	1428	0.64
Sandy	Good	1418	0.67
Sands	Good	1288	0.64

¹Field data obtained July 25, 1973

²ERTS-1 overpass July 26, 1973

When the soil association and attendant range site are known, however, range condition class can be estimated from optical density measurements of imagery from MSS band 5 obtained during the growing season. Range condition class is a major factor in determining animal stocking rates for Sand Hills rangeland.

APPLICATIONS

The Sand Hills region includes all or part of several Natural Resources Districts within Nebraska. Each district is governed by a local board of directors and is authorized to develop a variety of resource programs including range management. In addition, the Soil Conservation Service, USDA, is responsible for soil surveys and range site interpretations and for developing conservation ranch plans within the Sand Hills region. ERTS-1 imagery has substantial potential for use by these organizations in planning and monitoring operational programs in range management.

The Upper Loup Natural Resources District is located centrally within the Sand Hills region. Four resource maps have been prepared from ERTS-1 imagery for this District as follows:

Subirrigated Range Sites and Lakes

Forage production from Subirrigated range sites and the location of sandhills lakes are significant factors in planning range management within the Upper Loup Natural Resources District. Consequently, a map showing the distribution of these features (Fig. 1) was prepared from imagery obtained from MSS bands 5 and 7 on May 14 and 15, 1973 (images 1295-16564 and 1296-17023).

Wind Erosion Hazard

Overgrazing in the Sand Hills region is particularly critical in view of the fragile nature of the sandy rangeland and its potential for destruction by wind erosion. Continued overgrazing results in a sharp decrease in range condition class and increases wind erosion hazard.

ERTS-1 images from MSS band 5 obtained on August 17 and 18, 1972 (images 1025-16554 and 1026-17012) and May 14 and 15, 1973 (images 1295-16564 and 1296-17023) were used to map areas with less than 10% vegetative cover on these dates within the Upper Loup Natural Resources District (Figure 2). Areas that did not recover to more than 10% vegetative cover by mid-May, 1973 are potentially hazardous in terms of wind erosion.

Blowout Land

Within the Sand Hills region, areas from 2 to 50 hectares or more in size that have been stripped of vegetative cover by wind erosion and that are actively eroding are readily interpreted from ERTS-1 imagery obtained during the growing season. A map showing the number of blowouts per township within the Upper Loup Natural Resources District (Fig. 3) was prepared from ERTS-1 imagery from MSS band 5 obtained on May 14 and 15, 1973 (images 1295-16564 and 1296-17023). This map identifies areas where blowouts have severely reduced forage production and where erosion control is needed.

Center-Pivot Irrigation

The production of forage irrigated by center-pivot systems to supplement forage produced by native rangeland is a recently established procedure for increasing the production of beef cattle within the Sand Hills region. One

hectare of properly irrigated forage in the Sand Hills region provides an animal carrying capacity approximately equal to 20 hectares of dryland range. Imagery obtained from MSS band 5 on May 14 and 15, 1973 (images 1295-16564 and 1296-17023) was used to locate all center-pivot irrigation systems within the Upper Loup Natural Resources District and to identify these systems according to perennial forage crops or annual crops (Fig. 4).

ERTS-1 imagery permits an assessment of center-pivot irrigation systems in relation to soil and topographic conditions within the Sand Hills region. Primary problems in establishing irrigated crops on the sandy soils involve wind erosion following severe land leveling, and the accumulation of surface water in subirrigated locations. Image interpretation has potential for delineating areas unsuited for the installation of center-pivot irrigation. In addition, an accurate inventory of center-pivot systems permits an analysis of energy requirements necessary to maintain irrigated production.

SUMMARY

The synoptic view provided by imagery from ERTS-1 is of substantial value for inventorying and measuring rangeland resources across the 32,000 square kilometers of the Sand Hills region. Interpretations of multi-temporal imagery within the region identified associations of soils and attendant Sandy, Sands, Choppy Sands and Subirrigated range sites at a level of generalization intermediate between county soil association maps and standard soil surveys made by detailed observations on the ground. Recognition of seven established soil associations permitted the delineation of these units in a portion of the region where modern soil association maps do not exist.

Optical density measurements of imagery from MSS band 5 obtained during the growing season were related to field measurements of vegetative biomass, a factor that closely parallels range condition class on defined range sites within the Sand Hills region. Consequently, range condition classes defined according to determinations of climax vegetation in the field may be estimated from the optical density of ERTS-1 imagery when range sites are known. Refinement of these relationships will permit operational interpretations of range condition in the Sand Hills region for use in timing livestock grazing and in selecting stocking rates. Overgrazing in the Sand Hills is particularly critical in view of the fragile nature of the sandy rangeland and its potential for destruction by wind

The following resource maps for use in planning range management programs in the Upper Loup Natural Resources District within the Sand Hills region have been prepared from ERTS-1 imagery: (1) Location of Subirrigated range sites and lakes, (2) Areas of erosion hazard with less than 10% vegetative cover in August, 1972 and May, 1973, (3) Frequency of blowout land and areas affected by severe wind erosion, and (4) Distribution of center-pivot irrigation systems identified according to the production of perennial forage crops or annual crops

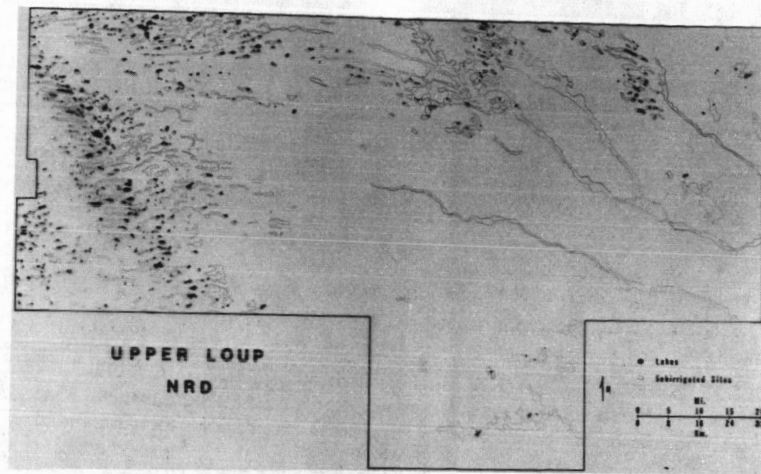


Figure 1. Distribution of Subirrigated range sites and lakes within the Upper Loup Natural Resources District, Nebraska.

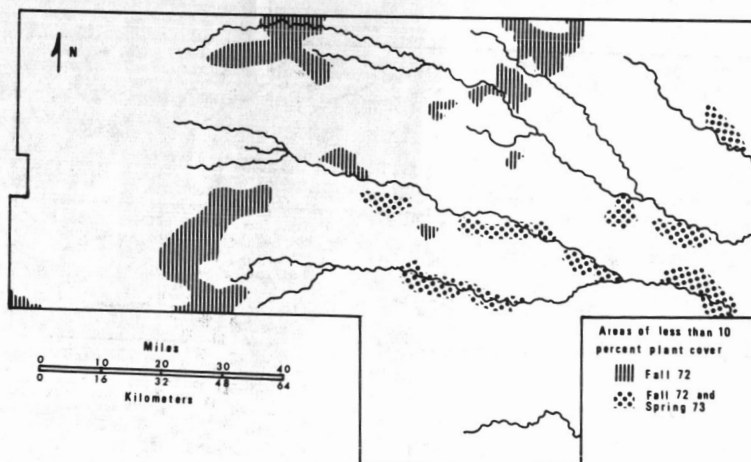


Figure 2. Distribution of areas with less than 10% vegetative cover on August 17 and 18, 1972 and May 14 and 15, 1973 within the Upper Loup Natural Resources District, Nebraska. Areas in which vegetative cover has not increased above 10% by mid-May, 1973 are susceptible to wind erosion.

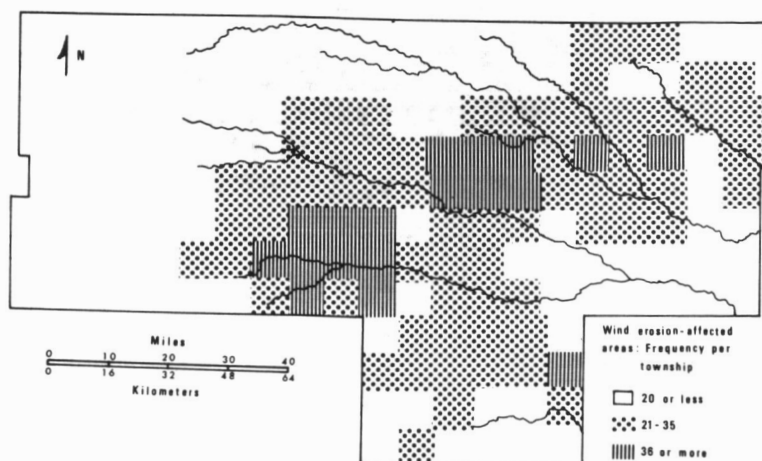


Figure 3. Frequency of blowouts 2 to 50 hectares in size within townships in the Upper Loup Natural Resources District on May 14 and 15, 1973.

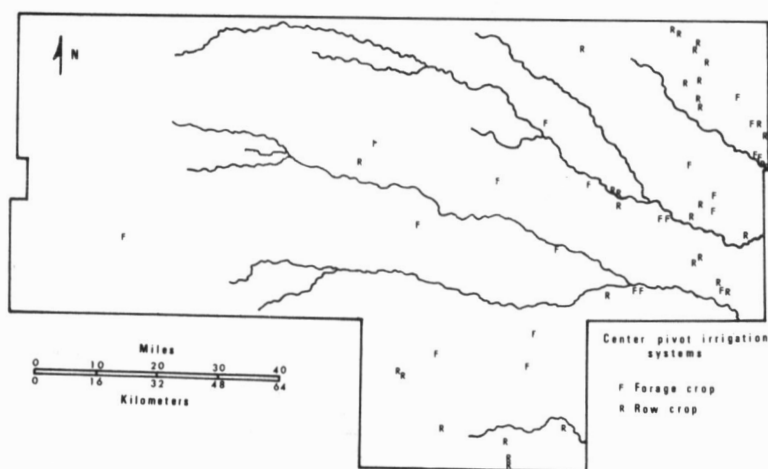


Figure 4. Distribution of center-pivot irrigation systems identified according to the production of perennial forage crops or annual crops within the Upper Loup Natural Resources District on May 14 and 15, 1973.

ERTS SURVEYS A 500 KM² LOCUST BREEDING SITE IN SAUDI ARABIA

D. E. Pedgley, Centre for Overseas Pest Research, London W8 5SJ, England

ABSTRACT

From September 1972 to January 1973, ERTS-1 precisely located a 500 km² area on the Red Sea coastal plain of Saudi Arabia within which the Desert Locust (*Schistocerca gregaria*, Forsk.) bred successfully and produced many small swarms. Growth of vegetation shown by satellite imagery was confirmed from ground surveys and raingauge data. The experiment demonstrates the feasibility of detecting potential locust breeding sites by satellite, and shows that an operational satellite would be a powerful tool for routine survey of the 3×10^7 km² invasion area of the Desert Locust in Africa and Asia, as well as of other locust species in the arid and semi-arid tropics.

INTRODUCTION

ERTS-1 has been used to test the feasibility of locating potential locust breeding sites by satellite. Sites favourable to breeding by the Desert Locust (*Schistocerca gregaria*, Forsk.) are places in the arid and semi-arid regions of northern and eastern Africa, and south-western Asia, that have been wetted recently by rain or runoff, and where vegetation has started to grow. Moist ground is needed for successful incubation of eggs laid in it; vegetation is needed to provide food and shelter for both parents and the subsequent flightless, nymphal stages. Preferred sites are those with a soil comprised of silty sand, not drying to a hard surface that would impede oviposition yet retaining moisture at depth of 5-10 cm. The rain needed to produce such a habitat is that which will wet a minimum of, say, 15 cm of soil to its field capacity. The necessary amount of rain depends on such factors as soil texture, slope and drainage, but in general falls greater than 20 mm are usually considered to be sufficient. Runoff along wadis from distant sources can provide locally favourable habitats. Incubation takes 10 days or more, increasing with lower temperatures, and the five nymphal stages each take five days or more, again increasing with lower temperatures. Hence, from laying to fledging as a flying insect can take as little as six weeks, even allowing a further five days for wings to become fully usable. Since rain in the regions concerned is largely seasonal, several successive falls may produce a breeding habitat suitable for up to several months, during which more than one generation may be produced.

At the end of 1972, the Desert Locust rapidly increased in numbers on the Red Sea coastal plain of Saudi Arabia. By early 1973, over 40 reports of swarms had been received from the area, and it was clear that a potentially dangerous situation had developed, sufficient to threaten the start of a

N 74 30722

new plague if the swarms had been able to escape and breed successfully for the next generation or two. In fact, timely applications of insecticide greatly reduced the threat.

During the build-up period, ERTS-1 was monitoring the area. This note discusses the interpretation of satellite imagery, using vegetation surveys and rainfall records.

ACTIVITIES

The area chosen for field tests was the Red Sea coastal plain of Saudi Arabia from Gizan (17°N) to Yenbo (24°N) - see Fig. 1. Within this area, a smaller, routine sampling area was chosen, in which a series of 51 sampling points was set up at approximately 5 km intervals along the road northward from Jiddah towards Medina, as far as Badr (Fig. 2). At each of these points samples of soil moisture and assessments of greenness of the vegetation were taken at 18-day intervals from 22 November 1972 to 28 March 1973 (i.e. 8 sets of observations), coinciding with overpasses of ERTS-1. These points were chosen because it was hoped they would be able to help locate the edges of areas wetted by rain, and because they could be visited easily in one day using a good, hard-surface road. Routine sampling to the south of Jiddah, although an area more likely to receive rain, would have involved difficult logistic problems. In that area there are only rough tracks and five days would have been needed for each survey; resources of men and vehicles were not sufficient for the necessary 18-days repetition.

Unfortunately, negligible rains fell over the routine sampling area, so there were no changes in soil moisture or vegetation greenness that could be detected by ERTS-1. Moreover, the scanty rains that did fall were followed by a drying of the topmost 5 mm of soil within a day. Even with much heavier rain a similar rapid surface drying would have been likely, so that detection of surface moisture by satellite using changes in albedo is unlikely to be useful in such sandy and silty areas, except perhaps where there is persistent standing water, which would usually require runoff.

Despite this set-back, it was possible to take advantage of substantial rains that fell between October 1972 and January 1973 over the field test area south of Jiddah, particularly between Lith and Qunfidah (Fig. 1). Here the coastal plain is a gently undulating region 10-30 km broad, consisting essentially of alluvial deposits. Silty soils of the deltas associated with the major wadies contrast with the intervening sandy or gravelly plains (Fig. 6). Wind-blown deposits often encroach on the foothills to the east, beyond which the country is very broken as far as the south-west facing scarp that continuously reaches an altitude of about 2 km. The alluvial plains effectively end near $18^{\circ} 30'\text{N}$, where extensive lava sheets reach the sea, but there are some small areas of lava to the north. Salt flats fringe much of the coast.

COMPARISON OF SATELLITE IMAGERY WITH GROUND OBSERVATIONS

Comparisons could be made on only two days.

8 December 1972 (image 1138-07122). Fig. 3(a) shows the approximate boundaries of magenta colouration (possible vegetation), found by visual inspection; they are subjective and to some extent unreal because the edges of areas of natural vegetation resulting from particular falls of rain are vague, in contrast with the edges of cultivated areas. Fig. 3(b) shows approximate edges found on a ground survey between 26 November and 8 December. The only region of overlap is between Wadi Qamunah and Wadi Yiba (for place names see Fig. 6), where agreement is not close although both maps show areas free of green vegetation on the seaward side. This vegetation mostly consisted of the perennial tussock grass Panicum, and communities of annuals, especially Dipterygium and Heliotropium, both of which are preferred food plants of the Desert Locust. (In the southern Sahara, these plants are replaced by Schouwia and Tribulus, but in all parts of the locust's invasion area various grasses are also eaten extensively.)

13 January 1973 (images 1174-07113 and 1174-07115). Fig. 4 compares field reports with areas of possible vegetation observed by satellite. Agreement is good. Widespread vegetation was present on the coastal plain south of Wadi Lith, whilst the satellite image (1174-07113) suggested Wadi Iyar as the northern limit. This small discrepancy may have been partly caused by difficulties in locating the boundaries. An aircraft survey on 19 February gave the northern edge between Wadi Iyar and Wadi Shaqah ash Shamiyah, indicating a drying out of the northernmost vegetation. Two particular points are worth noting.

- (a) A small area of dry vegetation south-east of the delta of the Wadi Shaqah al Yamaniyah lay in a barren region on the satellite image. The existence of this area was confirmed by an aircraft survey on 19 February, and a further ground survey on 3 March.
- (b) The region of sparse vegetation between the deltas of Wadis Yiba and Hali is well known on image 1174-07115.

These two examples indicate that although sparse vegetation can be detected by the satellite such vegetation can also be missed.

SPREAD OF NATURAL VEGETATION, SEPTEMBER 1972 TO JANUARY 1973

The reasonable agreement between observed vegetation distribution and the areas of possible vegetation on satellite images allows an analysis of other images. This is attempted for five separate occasions when false-colour imagery was available, from which the spread of vegetation over the four-month period September 1972 to January 1973 could be deduced. The results will be applied in the following two sections to known occurrences of rain and locusts.

For 26-27 September, false colour imagery covered the whole area from Wadi Lith to Wadi Yiba (images 1065-07055, 1066-07110, 1066-07113), parts of which were used to construct Fig. 5(a). Variations in contrast between images made some comparisons difficult. The inferred vegetation may be divided into three types.

- (i) Irrigated cultivations such as gardens, date palmeries and grain fields, mostly located
 - (a) in valleys near the foot of the scarp, and
 - (b) where major wadis cross the plains, especially in their deltas.Their magenta colouration persisted from one image to another although there were changes in area, presumably corresponding to extensions in areas planted or harvested.
- (ii) Natural perennial vegetation, e.g. coastal mangrove and areas of *Salvadora* in some wadis. Areas of salt bush (*Sueda*) in deltas and near the coast showed as dark patches and were only vaguely magenta; they occupied the same areas on each image.
- (iii) Natural ephemeral vegetation, presumably renewed as a result of recent rains, and characterised by large changes in both area and colour intensity. Some areas occurred along the scarp, increasing in size southwards, as is to be expected from the occurrence of monsoon rains (see next section), but there was no such vegetation on the coastal plains. Boundaries were not clear-cut, perhaps because runoff was rapid. Parts of these areas may be relict woodland, which is known to be preserved on certain isolated mountain massifs and parts of the higher scarp.

By 19 November, not only had wadi cultivations increased in extent but also there were patches of vegetation on the plains between Wadis Qanunah, Yiba and Hali (for place names see Fig. 6). Although the patches are likely to be mostly natural vegetation, there are known to have been some cereal plantings such as *Pennisetum*, another preferred food plant of the Desert Locust. By 8 December, Fig. 3(a), there had been a further increase in the extent of vegetation patches on the plains.

On 26 December, most of the area was again covered by images 1156-07114 and 1156-07121, parts of which have been used to construct Fig. 5(b). Comparing with Fig. 5(a), there were two significant changes.

- (i) Wadi cultivations. There were notable increases in area in the four deltas of Wadis Hali, Yiba, Qanunah and Shaqah ash Shamiyah, and increases in length along the lower courses of many wadis. There was also some tendency for a decrease in the amount of cultivation in the upper courses of the wadis.

- (ii) Natural vegetation. There had been a large increase in area - to almost the whole coastal plain south of Wadi Duqah, together with patches near the two Wadis Shaqah, but some large areas were still devoid of green vegetation. In many places there was an increase in intensity of the magenta colouration (shown in Fig. 5(b) as denser shading), presumably reflecting increases in both density and height of vegetation. Areas of salt bush remained dark.

By 13 January (Fig. 4) there had been a further increase in the area covered by natural vegetation - almost the whole coastal plain south of Wadi Iyar.

OCCURRENCE OF RAIN AND ITS RELATION TO THE SPREAD OF VEGETATION

The usual distribution of rains over the coastal plains and adjacent scarp between Lith and Qunfidah (based on about six years' records from eight gauges in the network of the Hydrology Division of the Saudi Ministry of Agriculture and Water Resources - Fig. 6) is as follows.

- (i) July-September (summer, or monsoon rains):
scattered showers along the scarp, increasing in frequency and intensity from north to south; a few light showers on the plains, but amounts are likely to be less than 10 mm.
- (ii) October-February (winter rains):
some showery days on both scarp and plains; on the plains this is the only 'rainy season', with totals averaging 50-150 mm, increasing southwards.
- (iii) March-June (spring rains):
scattered showers on some days along the scarp but almost none on the plains.

The observed distribution from these eight gauges was as follows. After a dry July, there were a few showers in the last week of August; amounts were mostly less than 10 mm, and they are unlikely to have provoked much vegetation. This is consistent with the absence of vegetation shown in Fig. 5(a), four weeks later. In September, the only rain was a few millimetres at Wadi Hali on the 24th. During the last week of October there were scattered showers giving 15-20 mm from Wadi Qarma southwards. These rains were no doubt the origin of the diffuse patches of vegetation seen on 19 November (image 1119-07064), i.e. three weeks later, and more extensively on 8 December (Fig. 3(a)). In November, there were only isolated light showers on the last few days, but December brought two good spells of rain:

5th-11th, when falls exceeded 10 mm at all gauges, and were about 50 mm over central parts of the area;

27th-31st, when 25-75 mm fell, mostly in the north of the area.

Rains continued during the first week of January 1973, with falls generally 50-100 mm. The last rain was reported from Wadi Hali at the end of the second week. No rain fell in February or March, so the seasonal total, October to January, was about 150 mm at most places - near average in the south but above average in the north.

The increase in area and density of vegetation shown in Fig. 5(b) must represent growth initiated by the rains of late October and further stimulated by the rains of early December, i.e. about three weeks before picture time. The northern limit of dense inferred vegetation at Wadi Duqah is consistent with the observed northern limit of October rains, whereas the sparse growth further north was probably initiated by the early December rains. The further increases in area and density seen on 13 January (Fig. 4) presumably indicate continued growth stimulated by the late December and early January rains, i.e. one to two weeks before picture time. The inferred vegetation boundary at Wadi Iyar on 13 January suggests that effective December and January rains were at most only isolated further north. Moreover, the ground survey between 20 January and 7 February, and the aircraft survey on 19 February both support this suggestion.

OCCURRENCE OF LOCUSTS AND THEIR RELATION TO THE SPREAD OF VEGETATION

First reports of Desert Locusts on the coastal plain since December 1971 were of scattered adults and hoppers (the nymphal stages) in late July and early August 1972 among cultivations in Wadis Qarma and Nawan. Since a ground survey across the whole area on 3-7 March had found no locusts, it is possible that the observed population had come in the meantime from the highlands to the north-east, where scattered adults had been seen at several places in May, June and July. Alternatively an inconspicuous or unreported low density population may have persisted among cultivations, or even on the nearby plains following showers in mid-June (there having been no significant rain in May), but these rains were almost certainly insufficient for breeding outside irrigated cultivations. Low density populations of adults and hoppers continued to be reported from cultivations between Wadi Shaqah ash Shamiyah and Wadi Qarma in September and October.

In early November, a swarm of unknown size was seen near Habil on the Wadi Yiba (Fig. 6). The origin of this swarm is still in doubt. It is unlikely to have been produced from the small populations already mentioned, but it could have come from unreported breeding further south, or even east among the foothills, or alternatively it could have come from much further east in the Arabian peninsula, particularly since strong east winds had swept the area in late October when a tropical cyclone had taken a most unusual track westwards along the Gulf of Aden.

Following the swarm report, survey and control teams came on to the coastal plain. Scattered and grouping adults were found widely from the second half of November onwards between Wadi Shaqah ash Shamiyah and Wadi Yiba, with a maximum density of 4000 per hectare over 20 km² near the swarm sighting.

Most of these locusts probably invaded the area from outside. They bred widely, so that some bands of hoppers were seen marching across country by early December. This successful breeding had clearly occurred because the soil had been wetted sufficiently for egg-laying following the first significant rains late in October. The resulting growth of vegetation between the wadis (Fig. 3) had provided widespread and ample food and shelter outside cultivated areas. The increase in population and its northward spread continued so that during January there were 47 reports of swarms between Wadi Lith and Wadi Hali - all small, the maximum size being 3 km². Although there were only three more swarm reports in February, widespread scattered adults and hoppers continued to be reported into March, with groups of adults and bands of hoppers. A second generation was being produced, but by April the main population was found in Wadi Lith and Wadi Shaqah ash Shamiyah, and there were no reports in May. This rapid decline in April can safely be attributed to the application of insecticides, including the use of two spray aircraft in February and March. In addition, the absence of rain in February and March led to a drying of the vegetation, already detectable in places by early March, and widely so by April.

Thus, locusts arrived (probably in late October or early November), in time to take advantage first of all of the late October rains and subsequently of the heavier and more widespread rains in December and January, and multiplied in two generations to give a serious situation that was brought under control by the timely application of insecticide.

CONCLUSIONS

Although there were only a few ground observations to check satellite imagery, they enabled analysis to be made of false colour images on a sequence of five occasions which, together with rainfall data, give a consistent pattern of the growth and spread of vegetation on the Red Sea coastal plain of Saudi Arabia from about Lith to Qunfidah following three spells of rain between October 1972 and January 1973. None of these rains fell less than two days before the dates of available images. Two gauges had falls of about 10 mm 2-3 days before the image for 8 December but there was no evidence of the presence of surface soil moisture as might be expected by a darkening of the ground. This is consistent with 2-3 days being sufficient for drying out of the topmost 1 cm or more of soil.

On the other hand, the arrival and subsequent breeding by numerous locusts (sufficient to produce many small swarms) in a region where the spread of vegetation was clearly shown by satellite imagery, demonstrates the powerful potentialities of an earth resources satellite in routine surveying for potential breeding sites. The breeding area involved in this study was small, some 500 km²; moreover, it was relatively easily accessible to survey and control teams. However, the two vegetation surveys used here needed approximately 100 man-days and about 3000 km driving along rough tracks or across country. If this is contrasted with:

- (i) the 3×10^7 km² within which breeding can occur during plague periods, depending upon the incidence of suitable rains, and
- (ii) the vastly greater expenditure on money, manpower and machines needed to provide surveys as detailed as those made here (for the size of area, probably as detailed as any undertaken before and in any country subject to invasion by the Desert Locust), than that usually available for survey,

it is clear that the only way of obtaining routine data of comparable standard over the whole region open to infestation is by use of a satellite. The same satellite could be used to gather similar data for other locust species, e.g. in South America, South Africa and Australia.

It has been demonstrated that ERTS-1 located a potential locust breeding site. Whether breeding actually takes place must be found by conventional surveys. If an operational satellite were to be used to locate potential breeding sites, it would be necessary for images to be in the hands of potential users within four weeks, and preferably two weeks. Within such periods, locusts can reach an advanced nymphal stage, or even fledge prior to migration. Little time would then be left to send control teams into areas likely to be infested. Thus an automatic picture transmission (APT) system would be desirable, preferably with a simple receiver, bearing in mind the probable costs to the 60 or so countries involved. Moreover, the combination of images from several spectral bands for simple visual interpretation of false colour products may prove too complex for routine operation. Perhaps APT channel 5 images would be sufficient - a time series would show the development of vegetated areas, particularly if picture quality was comparable on all orbits. With an APT system, images at intervals of about two weeks would be adequate for tactical planning by national or international control organizations.

ACKNOWLEDGEMENTS

Grateful thanks are due to Salem Hadramy, Director, Locust Research Station, Jiddah for willingly providing staff, vehicles and equipment for surveys made during the course of this project. Members of his staff directly involved were Yagoub Ashour, Ahmed Ibrahim and Ahmed Assad. Staff members from the Centre for Overseas Pest Research who provided data and assistance were G.B. Popov, J. Tunstall, M.J.K. Paskin, A.R. Wooler, D.E. Padgham and A.W. Harvey. Thanks are also due to Dr. J.C. Davies, head of the CQPR team in Jiddah.

This note is produced with the permission of the Director, Centre for Overseas Pest Research, London.

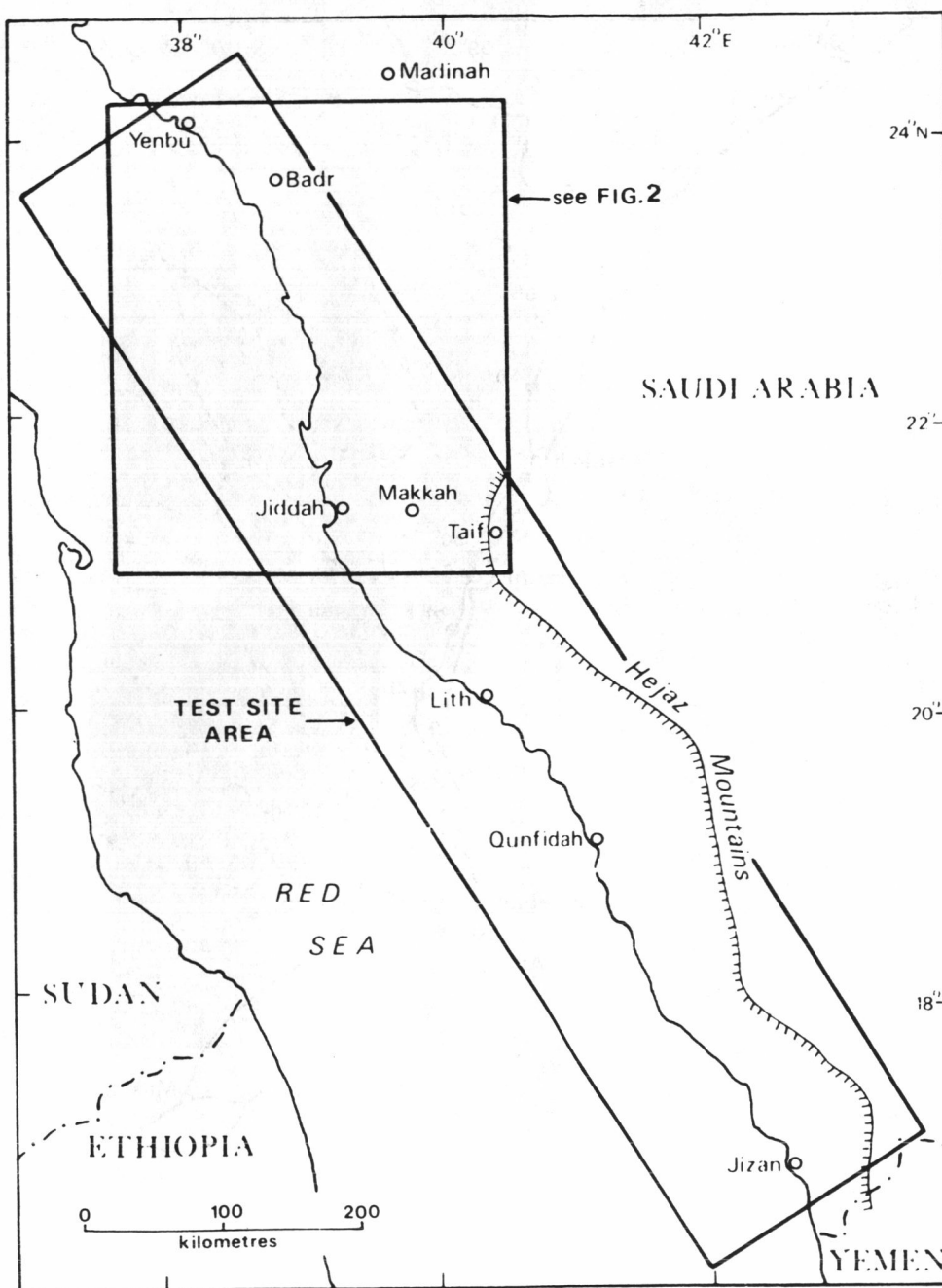


Fig. 1. Location map showing ERTS-1 test site area on the Red Sea coastal plain of Saudi Arabia.

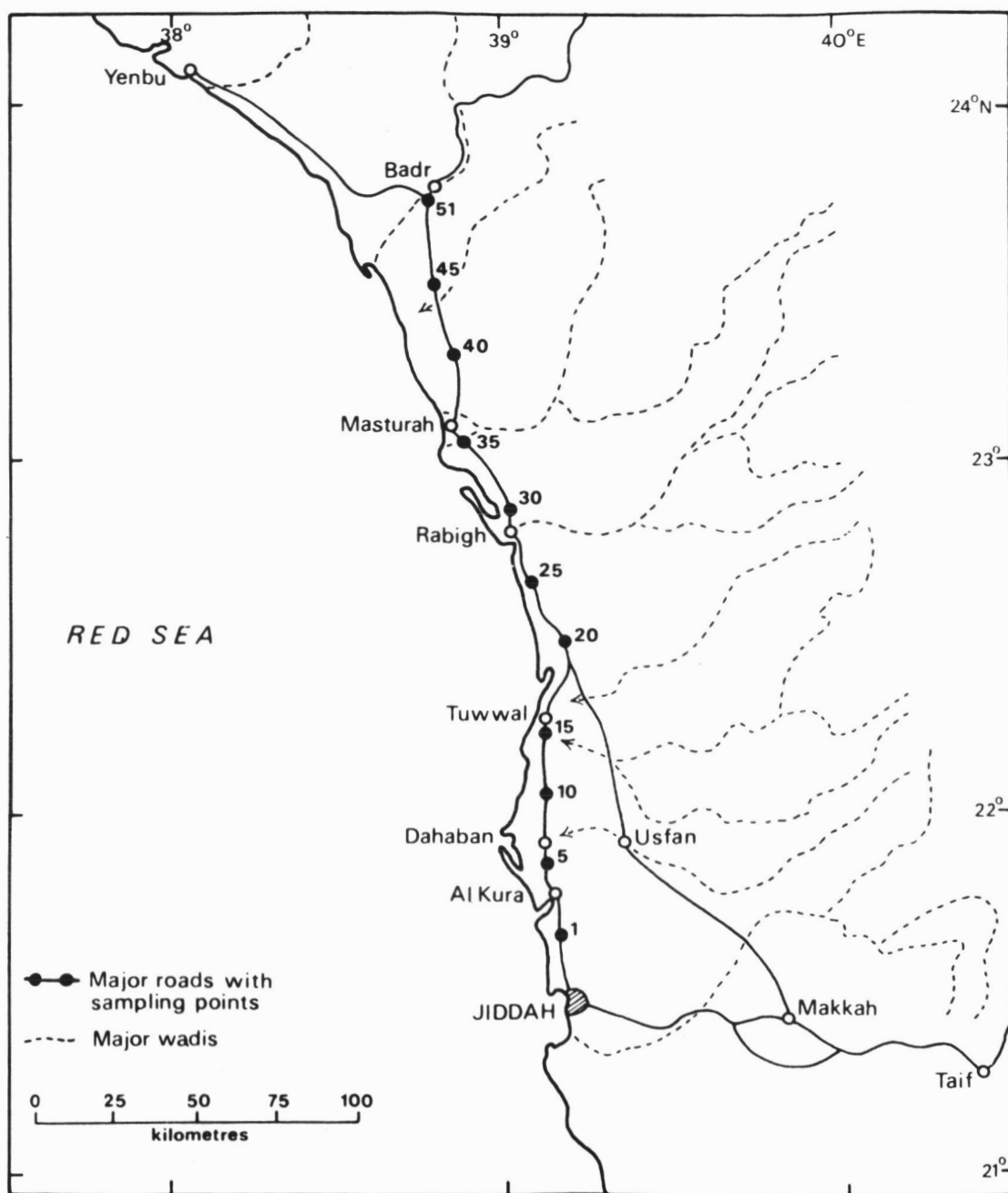


Fig. 2. Location map showing positions of 51 sampling points along the road between Jiddah and Badr.

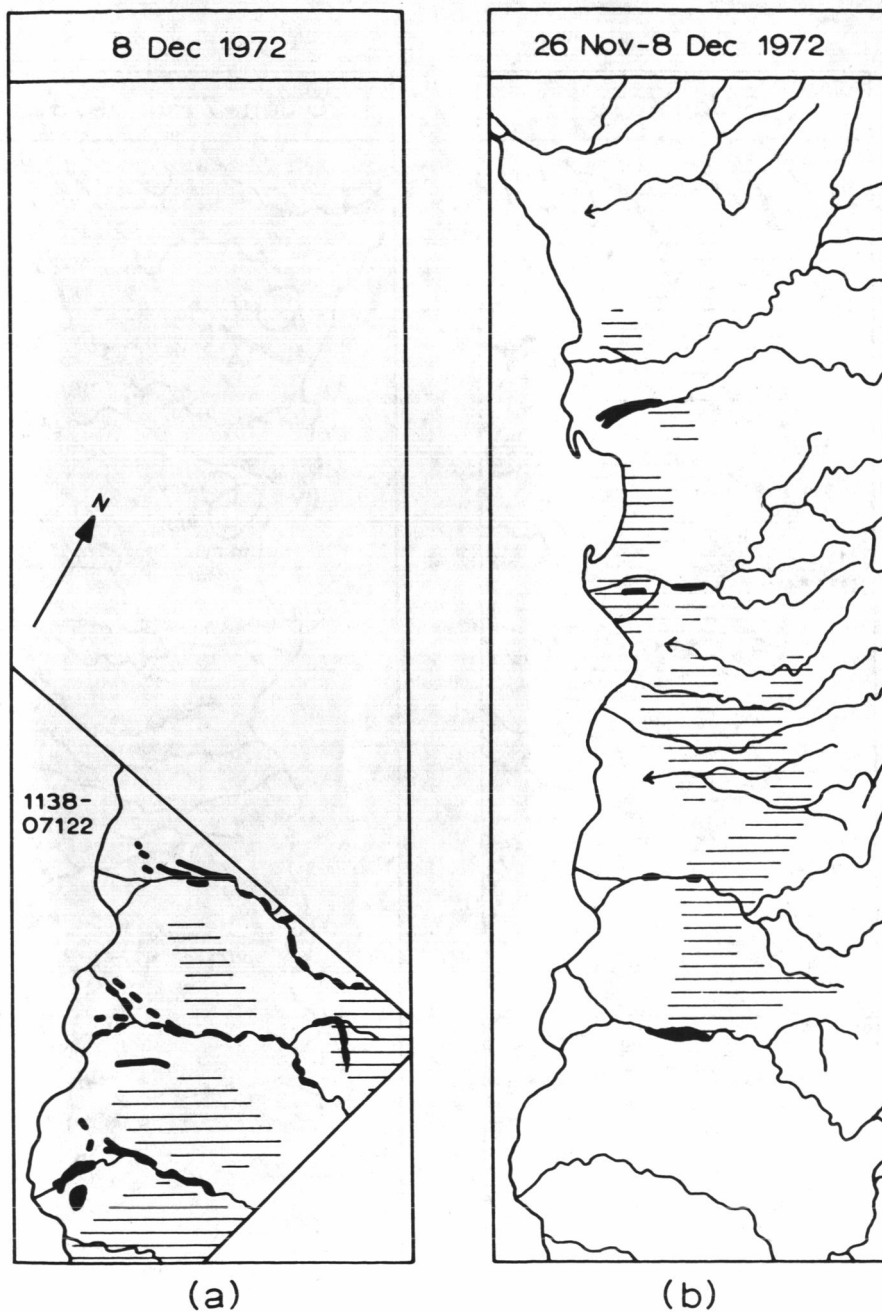


Fig. 3. (a) Approximate distribution of areas of possible vegetation (magenta colouration) on ERTS-1 image 1138-07122 for 8 December 1972.

(b) Approximate distribution of areas of vegetation seen on a ground survey from 26 November to 8 December 1972.

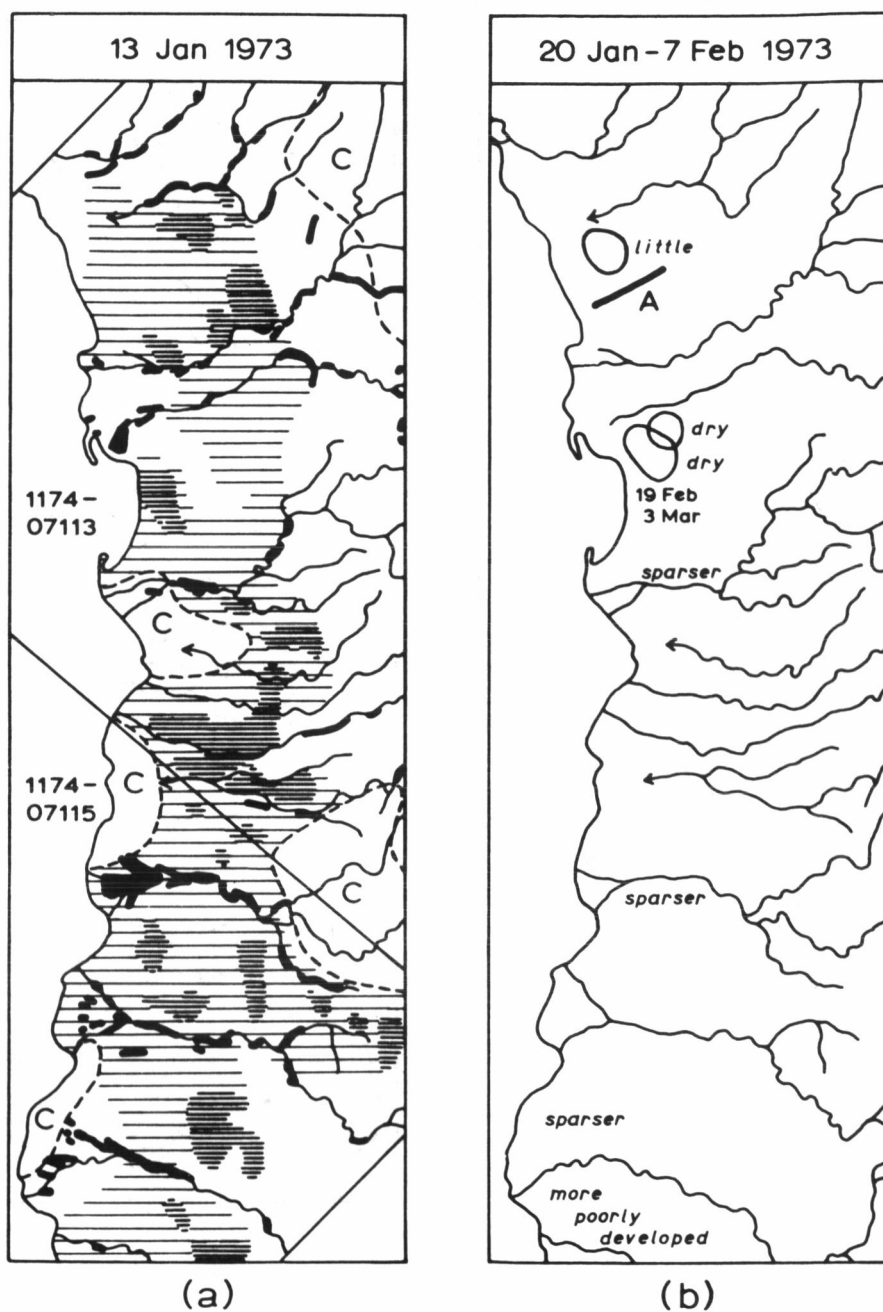


Fig. 4. Similar to Fig. 3, but for 13 January 1973 (images 1174-07113 and 1174-07115) and 20 January to 7 February 1973. Denser shading shows areas of stronger magenta colouration.

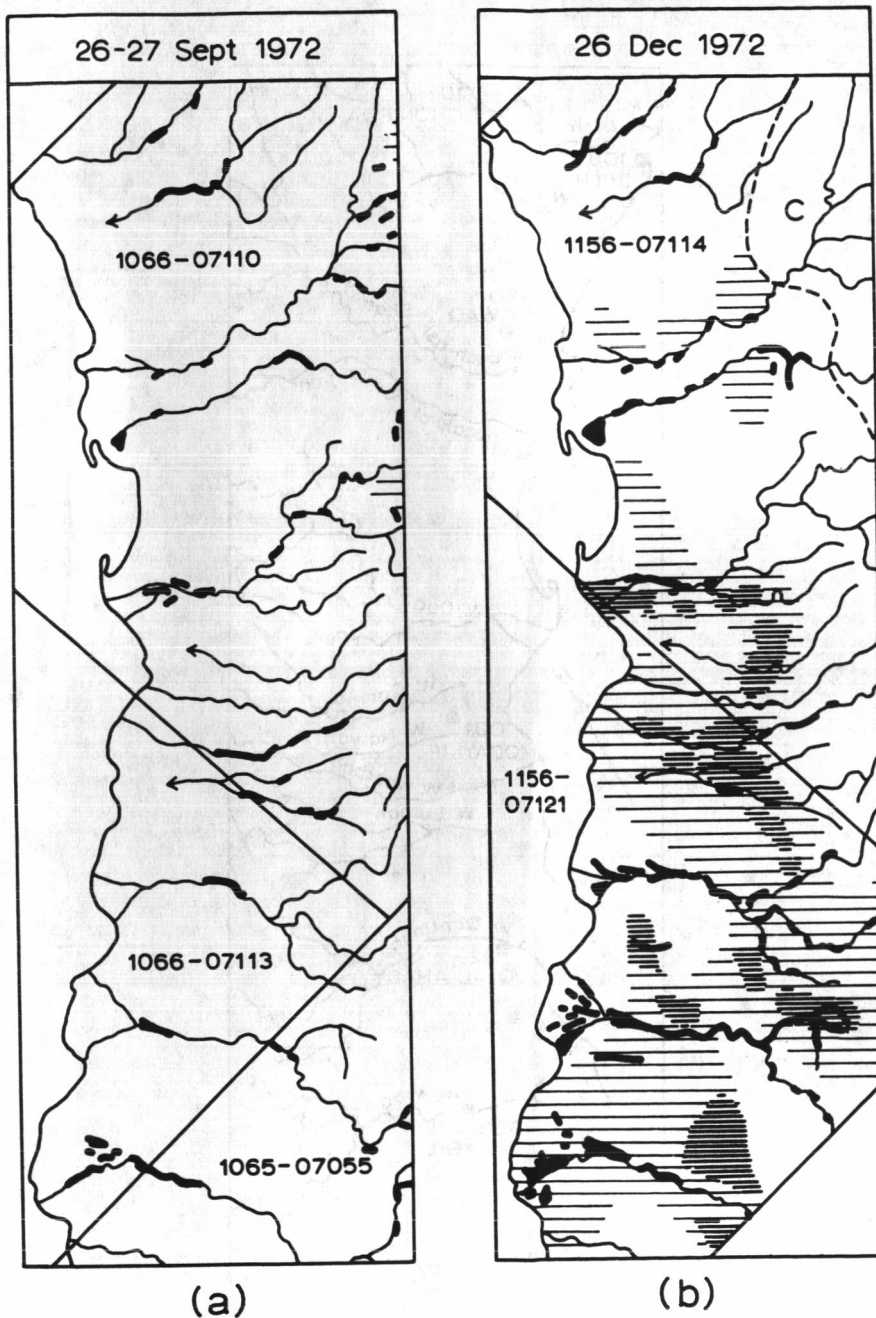


Fig. 5. (a) Inferred distribution of vegetation, based on parts of images 1065-07055 (26 September 1972) and 1066-07110 and 1066-07113 (27 September).

(b) Similar to (a), but based on parts of images 1156-07114 and 1156-07121 (26 December 1972).

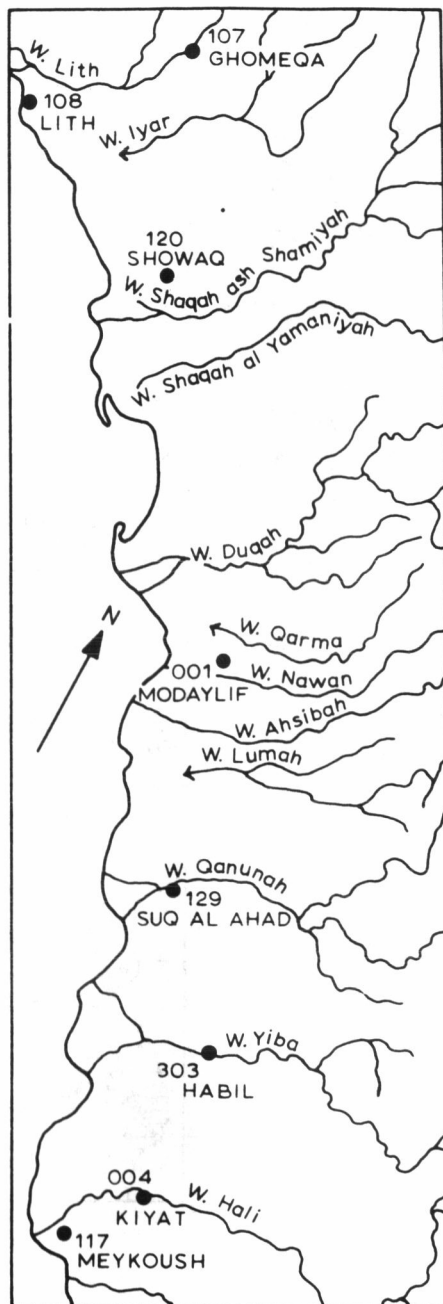


Fig. 6. Locations of places named in the text. Also positions of raingauges.

REMOTE SENSING EXPERIMENT IN WEST AFRICA

N. H. MacLeod, *Department of Biology, The American University, Washington, D.C.*

There are substantial needs of the Sahelian Zone to detail the state of regional agricultural resources in the face of a sixth year of serious drought conditions. While most of our work has been done in the Republic of Niger, the principles which have emerged from our analysis seem to be applicable to much of the Sahel. The discussion relates to quite specific rehabilitation and development initiations under consideration in Niger which are based in part upon direct analysis of ERTS imagery of the country, in part on field surveys and on discussions with Nigerian officials and technicians. Again, because the entire Sahelian Zone (including Niger) has large zones of similiar ecologic characteristics, modifications of the approaches suggested for Niger are applicable to the solution of rehabilitation of the desert, the savannah and the woodlands of West Africa in general.

Figure 1 defines the zonation of aridity in Africa under normal conditions, that is, those conditions found during the past fifty years or so. The three desertic regions are subcontinental in size and would normally be considered as classic cases of meteorologically defined deserts — that is, deserts formed as a result of the descent of cold dry air from the upper atmosphere, a part of the phenomena of global atmospheric circulation (Fig. 2). We have some reason to doubt that the Sahara is formed in such a manner, our doubts being based on archeological and ecological considerations. This is not just a passing comment. If the Sahara and the Sahel are so dry entirely because of meteorological phenomena, then the rehabilitation of the Sahel will be very difficult indeed.

On the other hand if there are cultural factors which have changed many microclimates through such means as the destruction of vegetation and if those cultural factors continue to play their role in climatic modification, then there is hope that these factors may be identified and changed to reverse the process of desert formation. The analysis of ERTS imagery of the Sahel and especially of Niger gives considerable hope that the process of desert formation can be reversed (Fig. 3). To reverse desert formation and to rehabilitate the desert and the Sahel, we are using the indications from satellite imagery to derive a set of operating principles upon which we are basing our recommendations to the Niger Government and our discussions of national development programs.

In field surveys in the Republic of Niger, we were able to substantiate the observations made in the Laboratory in Washington, D. C. In addition we had

the opportunity to discuss the country's development goals with government officials and to develop a better understanding of social and economic impediments to presently envisioned development initiatives.

By February of this year there had developed a realization that short-falls in grain production in West Africa, the basic source of food for most West Africans, was due to a persistent drought. The accumulated effects of the drought since 1969 had evolved into an emergency situation. In March, six Sahelian countries declared themselves a disaster area and appealed to the United Nations for assistance in meeting the food requirements of their peoples. As part of the response to that appeal NASA began to acquire as much ERTS imagery as possible over the Sahel. To process and deliver useful information to the afflicted area, a Drought Analysis Laboratory was established at Goddard Space Flight Center, a cooperative effort of Goddard, The American University and Catholic University. It is from analysis of this imagery in conjunction with field studies and literature surveys that we have derived a concept of the regional dynamics of the Sahel.

In the 12-frame ERTS mosaic, including Niger, Upper Volta, and Mali, several of the major surface features of the Sahelian Zone are quite visible. Not only the Niger River itself, but the remnants of major Saharan drainage systems of Tertiary or Quaternary age are prominent features throughout the Central Sahel area (Fig. 4). From the large size of these ancient channels one can surmise that the intensity of rainfall during the earlier pluvial periods of formation was formidable, even in the Central Sahara. Since that early time the desert has formed; the Sahara and the Sahel both retain the marks of more humid times. The transition process to the present aridity is called desertification, a process which is going on today at an apparently faster and faster pace.

Our view is that the desertification process is linear, largely culturally induced and reversible. To a great extent the viewpoint is derived from analysis of ERTS imagery (Fig. 5). The banding of sand encroachment, and amount of vegetative cover are progressive north and south, as seen in this (Fig. 6) and other ERTS mosaics of the Sahel. A cyclic climatic variation should leave outliers or more mesic plant communities in favorably situated sites. Such outliers are not found in the Sahel. However, culturally induced equivalents are found, wherever cultural pressures on ecological systems are reduced or controlled in the Sahel. A rapid and positive change in plant cover is observed. A particularly interesting example is the Ekrafane Ranch, seen in the North-east corner of Figure 3 and in Figure 7.

The ranch is visible because of vegetative and soil changes occurring in the past five years, or the period since 1968 when this 110,000 hectare ranch was

fenced and controlled access and grazing were introduced (Fig. 8). Aerial photography taken previous to 1968 shows no difference in general appearance between the present inside and outside of the ranch area. The ranch has five powered wells to supply man and cattle with water — but not for irrigation.

Outside the ranch in the Azouauk Valley, there are three powered wells installed at about the same time, with no control of access. Figure 9 shows the result of uncontrolled access to wells — hundreds of square kilometers of barren ground. This is in strong contrast to the effects of managed range in Ekrafane Ranch in an adjacent, actually less favored ecosystem. Figure 10 shows the border of the Ranch from the Air, and Figure 11 at the ground near the border fence.

The fencing and controlled grazing have resulted in greater seeding, seedling survival, and plant vigor and also in reduction of sand movement. These changes add up to a favorable change in both microclimate and carrying capacity. Indeed the changes represent a reversal of desert encroachment, a demonstration of the feasibility of rehabilitation of the Sahel. The Ekrafane Ranch is not unique: it is large, only five years in production; the five years being the worst years of drought in this century. The ranch is productive, not simply reserved land taken out of production and there are other such areas — in Niger, in Upper Volta, in Mali and Senegal. These areas are also visible in the ERTS MSS images because of the rehabilitative effect of reducing or removing unmanaged cultural pressures on quite fragile ecosystems.

In this ERTS scene we see not only the Ekrafane Ranch, but also that there is opportunity for more ranching establishments in the same region — regions identified by seasonal assessment of the ERTS sequential images as more heavily vegetated grassland, and more favorably watered. On mosaicing of most of the interior zone of the Sahel west of Lake Chad, we find that similar opportunities are located across the Sahel. Ground observations in a significant portion of the Nigerien Sahel have substantiated the space observations (Fig. 12). These observations have been brought to the attention of the Niger government and are currently being formed into a set of recommendations for that government. Similar observations have been discussed with planners in the governments of Upper Volta and Mali as well.

In addition to the ranch observations just discussed, one can also see in Figure 7 the remnant drainage channels mentioned earlier. Particularly striking are the meanders in these channels, formed during the last stages of stream channel sedimentation. The soils in these meanders are heavy — mostly clays and silts — and unvegetated. The lack of vegetation may be due to the low rainfall in this particular area — less than 300 mm — and the higher water

holding capacity of the soil. It is likely that these soils do not receive enough precipitation to hold water in excess of the wilting point. Where these soils are irrigated they are quite productive, with excellent crops of grains, produce and forage.

It was our impression, developed during image analysis, field survey and discussion with technical specialists, that the channels themselves are phreatic aquifers — that is, annually recharged near-surface water bearing systems (Fig. 13). In other papers we have discussed this phenomenon and proposed that the conditions exist for rainfall to penetrate the sand cover of the watersheds, and then to run-off underlying impermeable laterites into the old stream channels. We have started mapping these heavy soils, using the ERTS Analysis System developed by J. S. Schubert at the Goddard Space Flight Center for computer MSS analysis with maximum geographic resolution. We are doing so to prepare ourselves and others for the possibility of recommending seriously that these soil and water resources be used for irrigated crop production to be conducted on a year-round basis. Because of a serious short-fall in grain production the Sahel this year, a short-fall greater by a factor of three than last year in Niger alone, these soil and water resources may have to be brought into production on an emergency basis. As they do not appear on conventional soil maps in general, the identification and location of these resources is being done as expeditiously as possible.

The ERTS mosaic is again of use in understanding the process of desertification as it occurs in zones of traditional sedentary cultivators where grains and other crops are grown (Fig. 14). The recognition of the problem comes through examination of the portion of the arable land that is actually in cultivation, that which is in fallow, and that which is covered by perennial vegetation. In areas which can be used for cultivation — are free of disease, and have sufficient average rainfall to support rainfed agriculture — the proportion of land in cultivation is alarmingly high. In previous decades, the normal rotation was twenty or more years, providing sufficient time for some recovery of soil fertility. We have observed in the ERTS images and on the ground that two ominous trends have developed. One is the reduction of the rotational periods to three years or less — sometimes to zero; the other is the expansion of rainfed grain production into regions where rainfall is normally insufficient to make a crop. The expansion is accompanied by destruction of vegetative cover prior to cropping — a prime cause of ecological instability in the Sahel. In addition some of the areas of traditional cropping are now given over to cash cropping — cotton and peanut production on a commercial basis. While the decision to carry on cash cropping is an economic one, and probably necessary to obtain scarce foreign exchange funds, the decision nonetheless effectively reduces the land area available for stable production of basic food stuffs necessary to the support of the growing populations.

This particularly difficult problem of over-use of soil resources has led to the establishment of a vicious circle, i. e. , over-use leads to losses in soil fertility and yield, which in turn requires less productive soils to be used to obtain an adequate harvest. How to break the cycle?

Among suggestions are the following:

1. creating multicrop rotation to replace the present monoculture
2. bringing livestock production into sedentary agriculture
3. to irrigate those alluvial soils located through ERTS image analysis (Fig. 15).

All these suggestions involve social changes which are largely unexamined. Such social changes can impose serious obstacles to development programs.

In closing, a few comments about the relationship of development in the Sahel to resource management in the United States. The Sahelian countries and the United States are in ecological and economic trouble. The Sahel, with its fewer people, less urbanization and technological infrastructure, is comprehensible. One can study the whole system. In the United States, however, we are confronted with segments of natural systems and an incomprehensible matrix of overlapping interests of land-use authorities, including private property, city planning, federal reserves, and commercial vs. environmental groups. As we begin to comprehend the Sahel through analysis of remote sensing imagery, we also learn to comprehend our problems here at home.

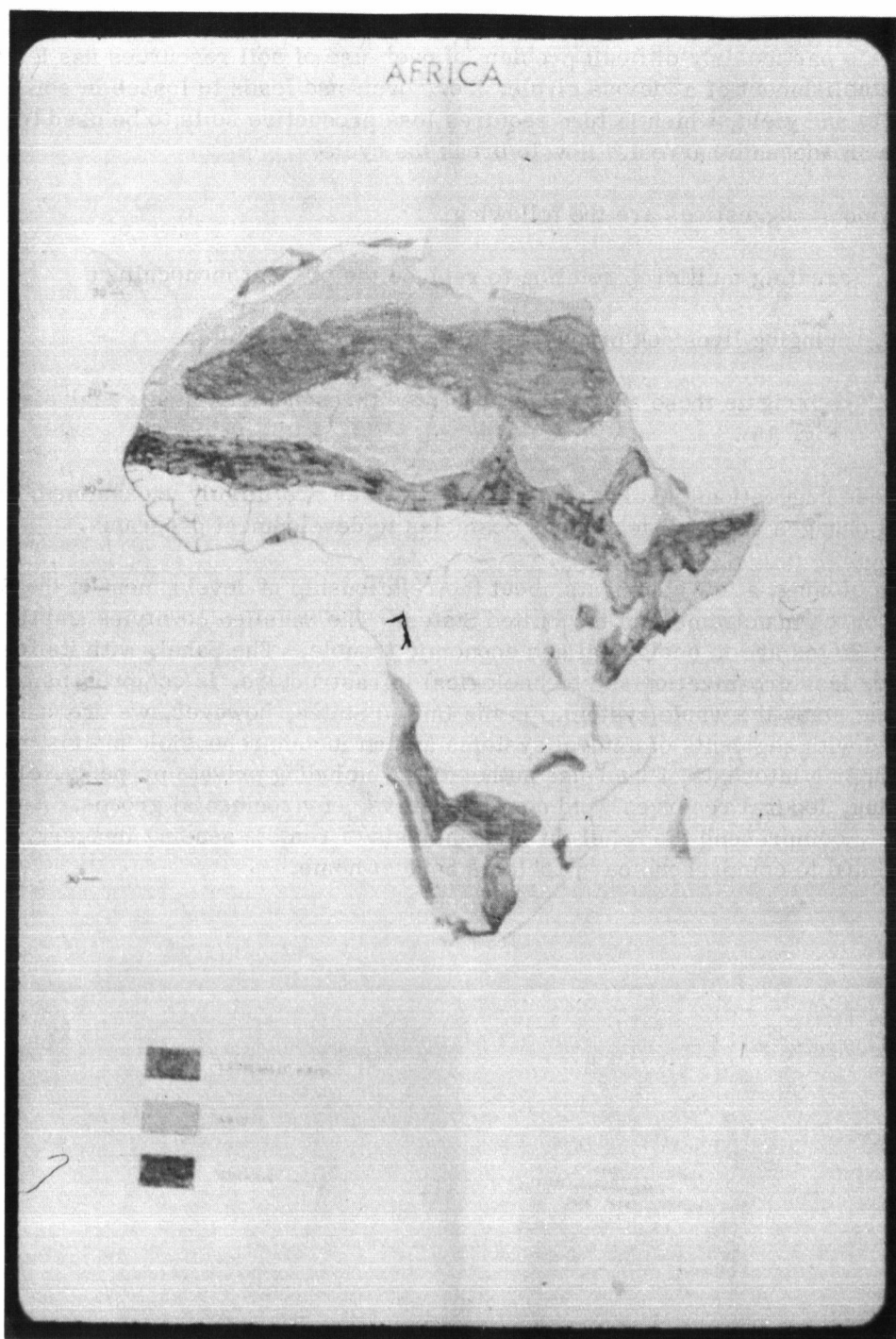


Figure 1.

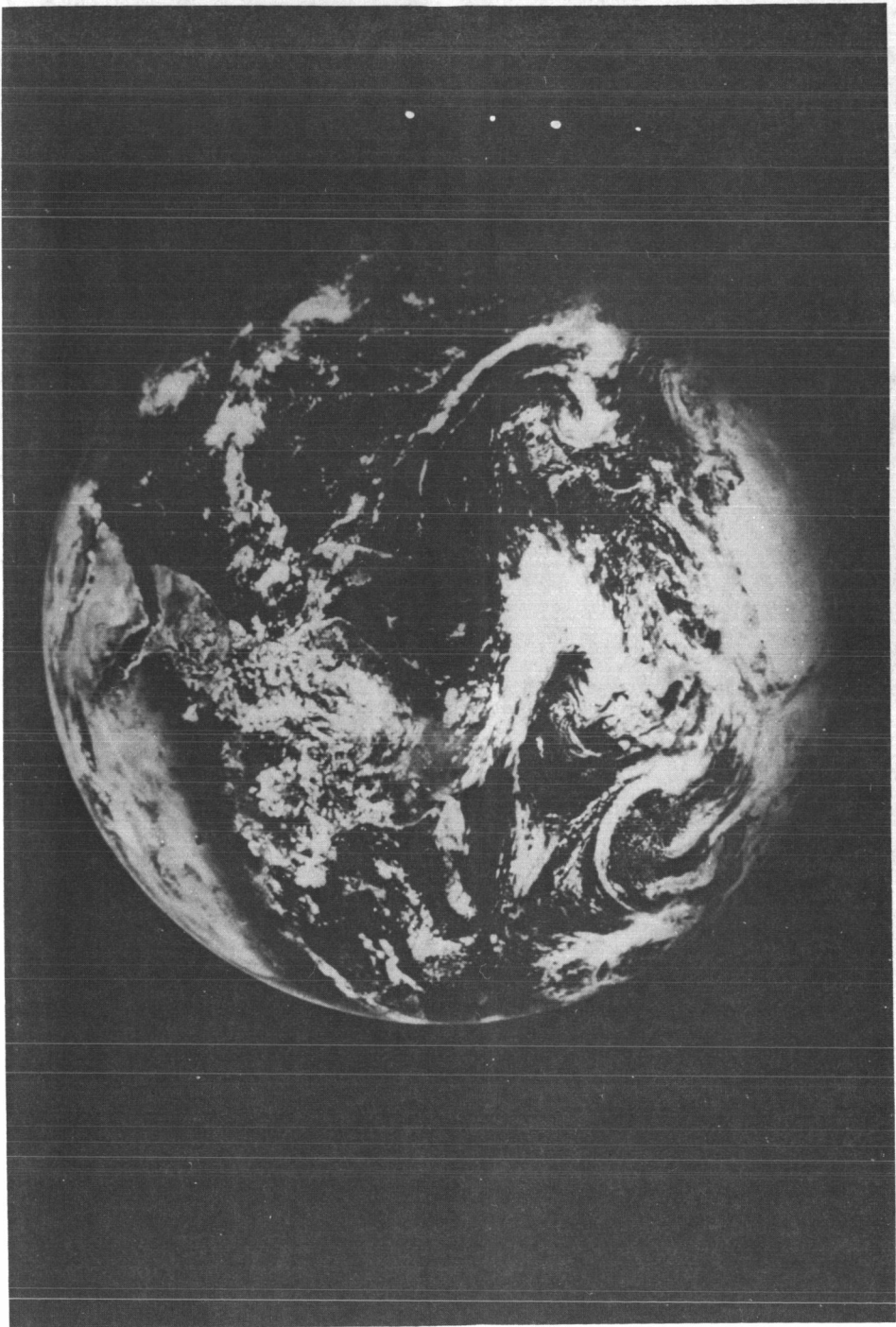


Figure 2.



Figure 3.

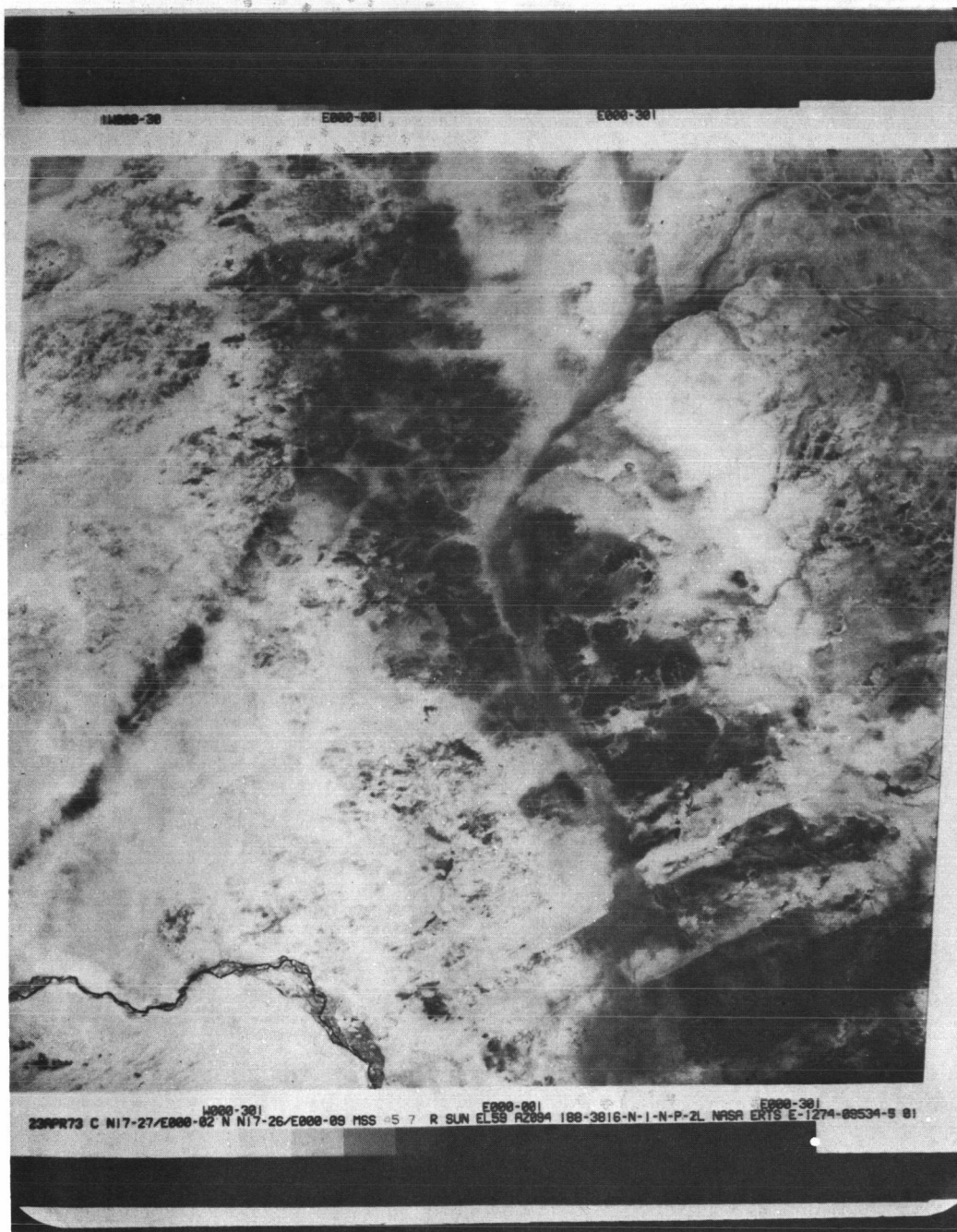


Figure 4.



Figure 5.

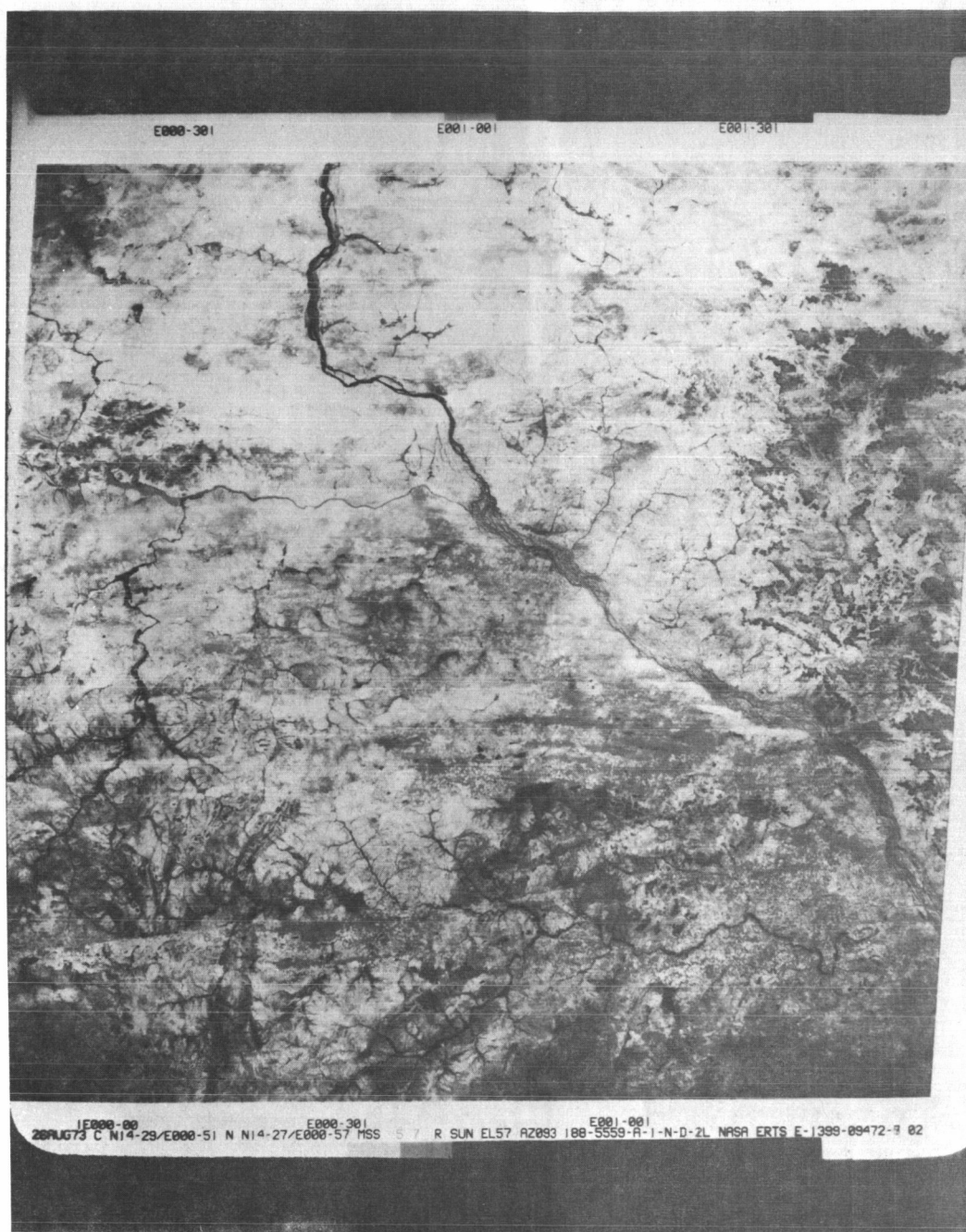


Figure 6.

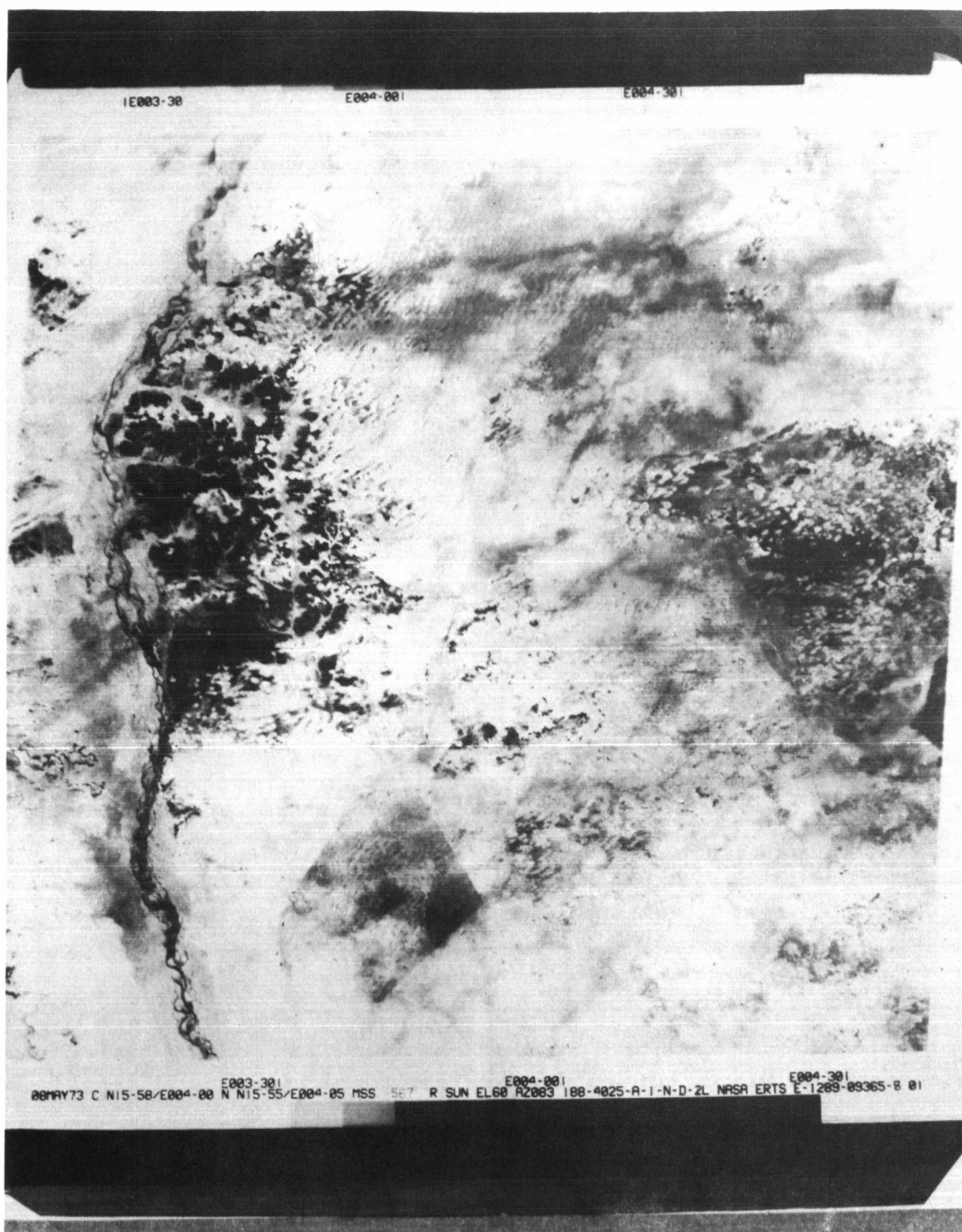


Figure 7.

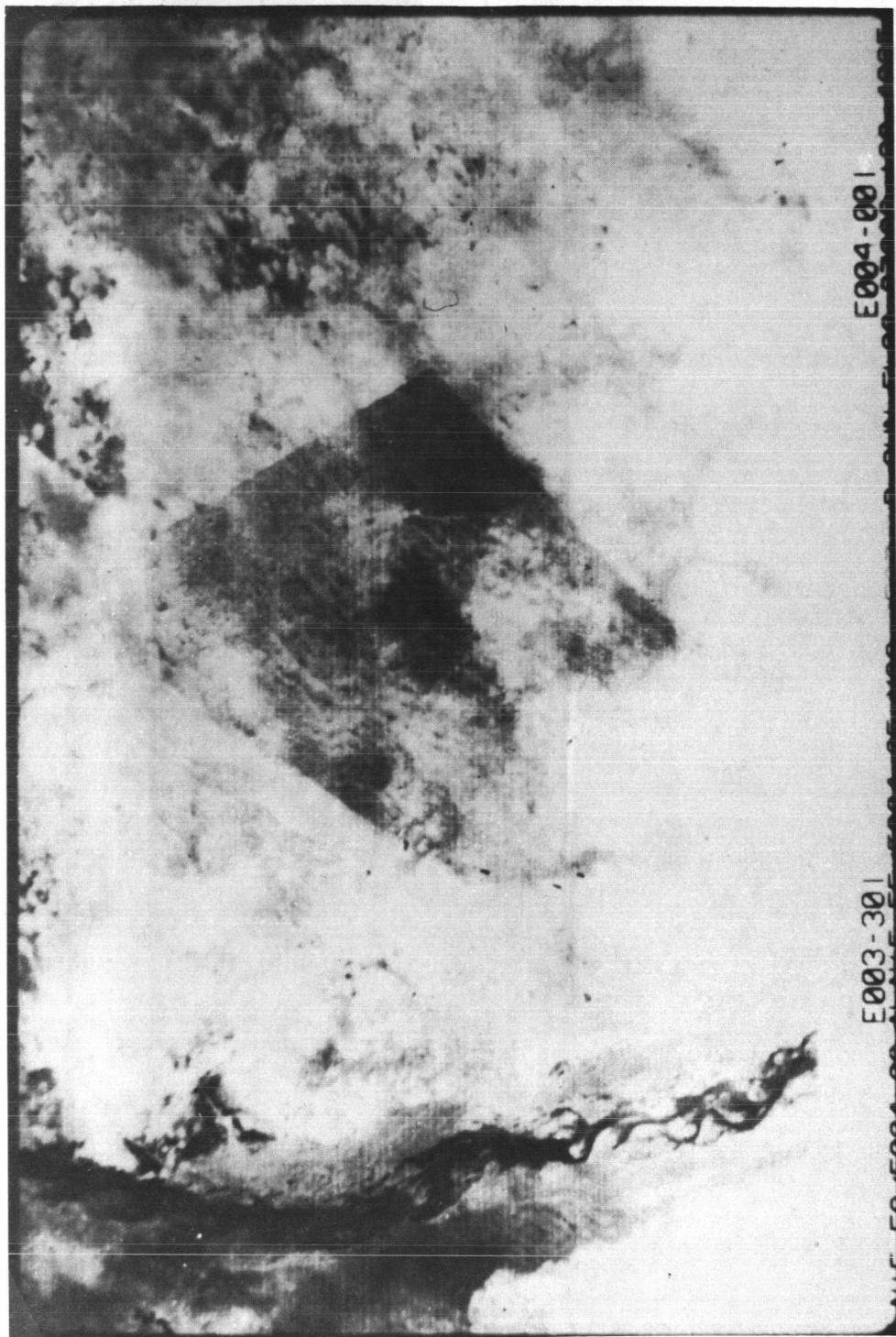


Figure 8.

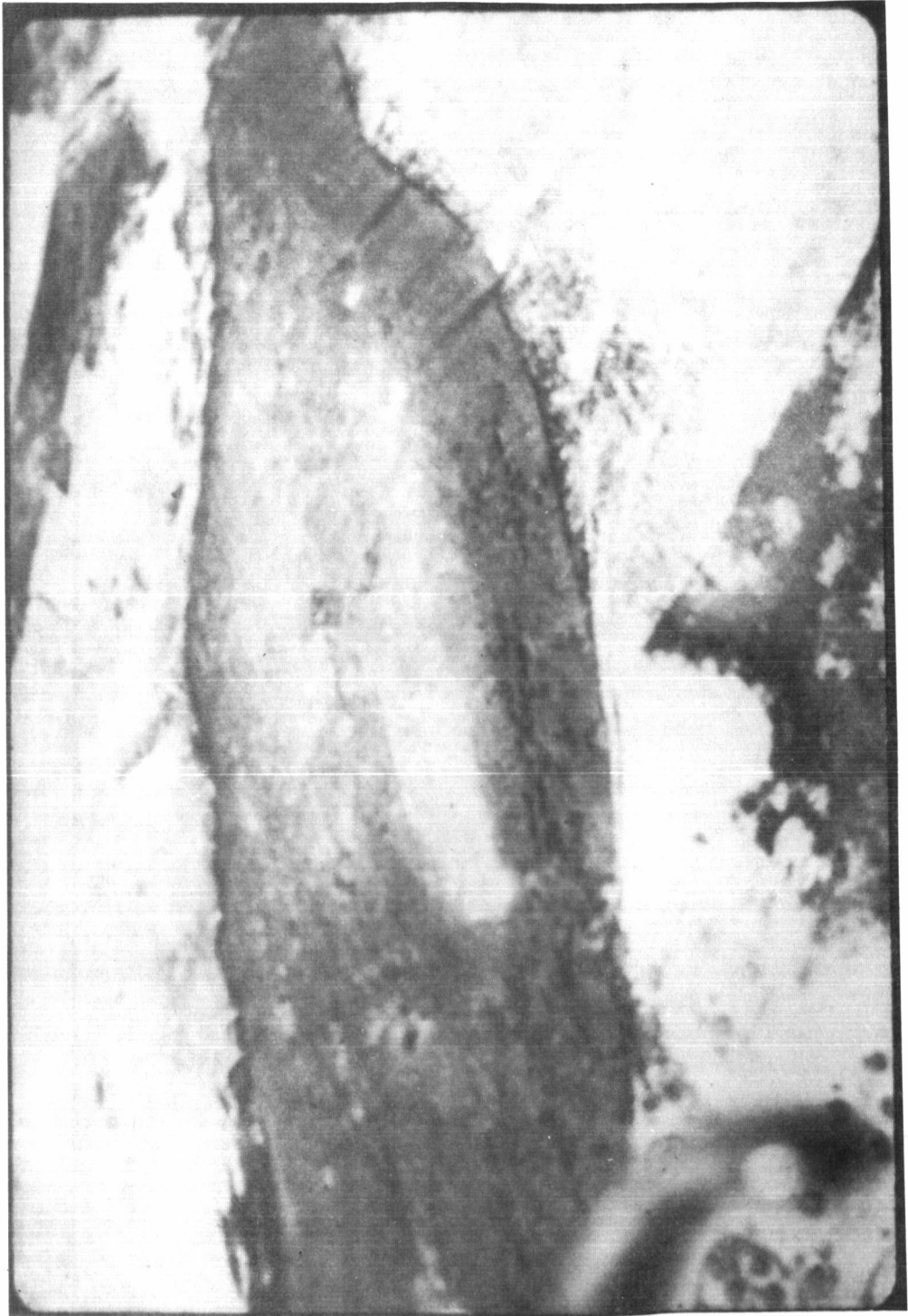


Figure 9.

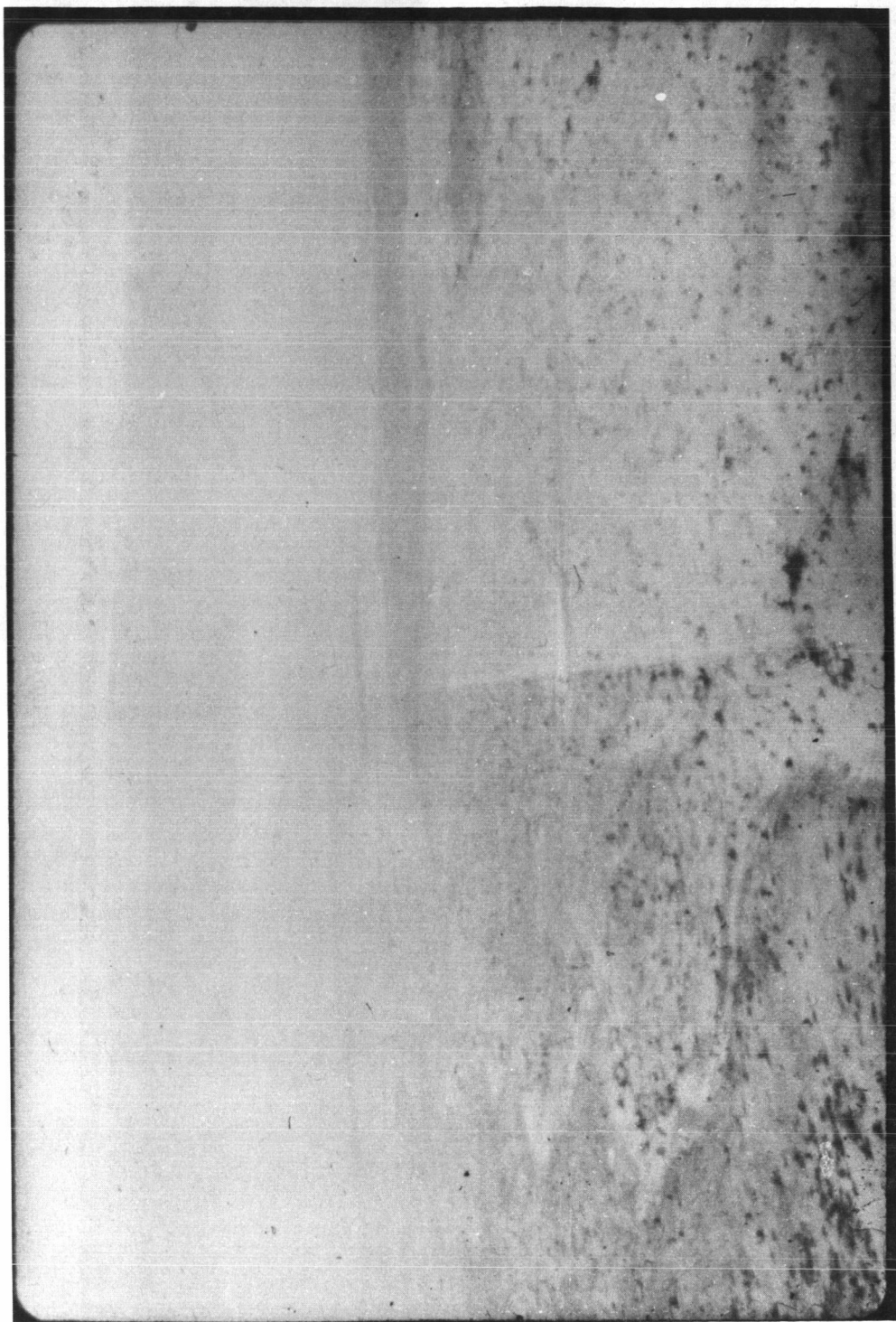


Figure 10.

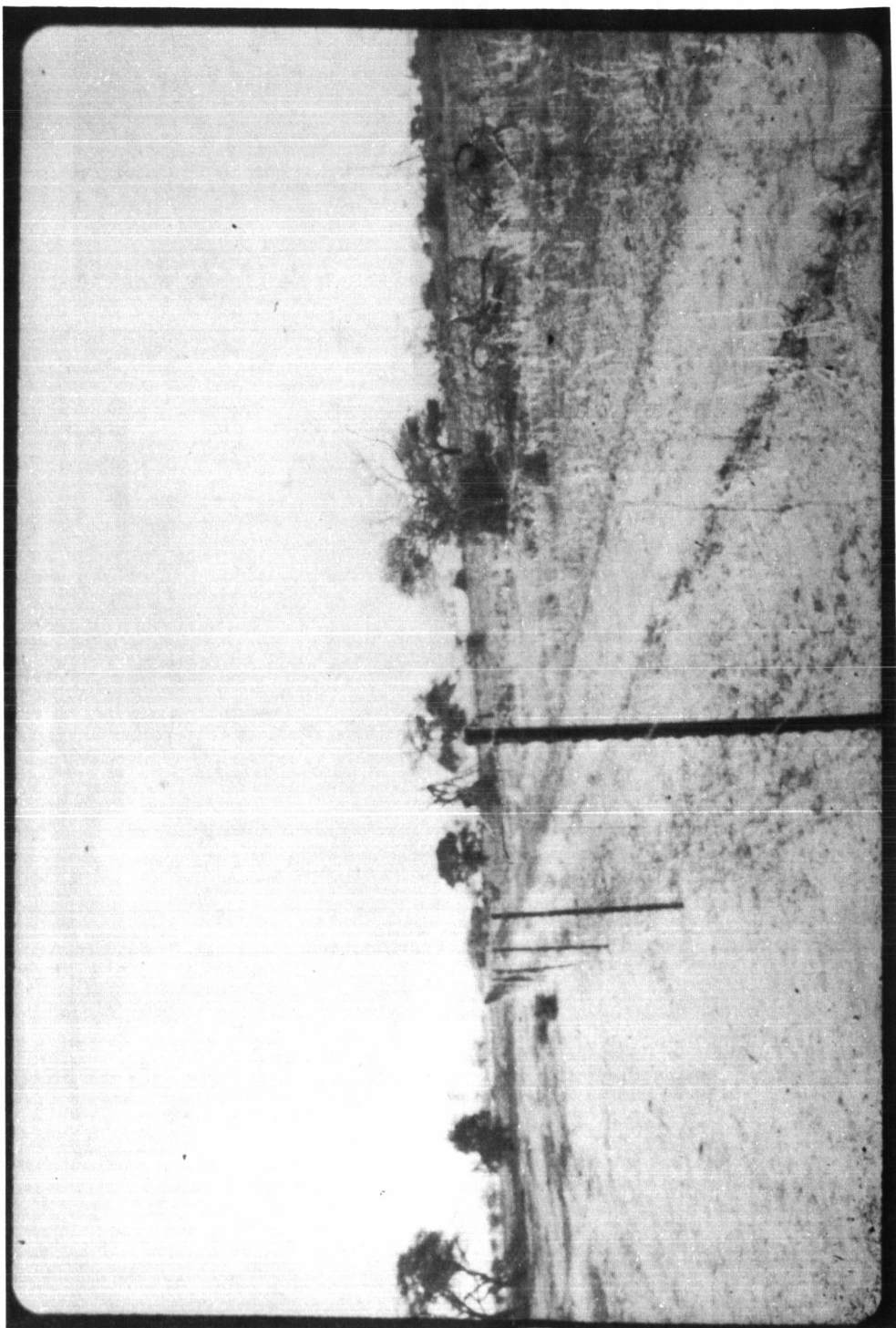


Figure 11.

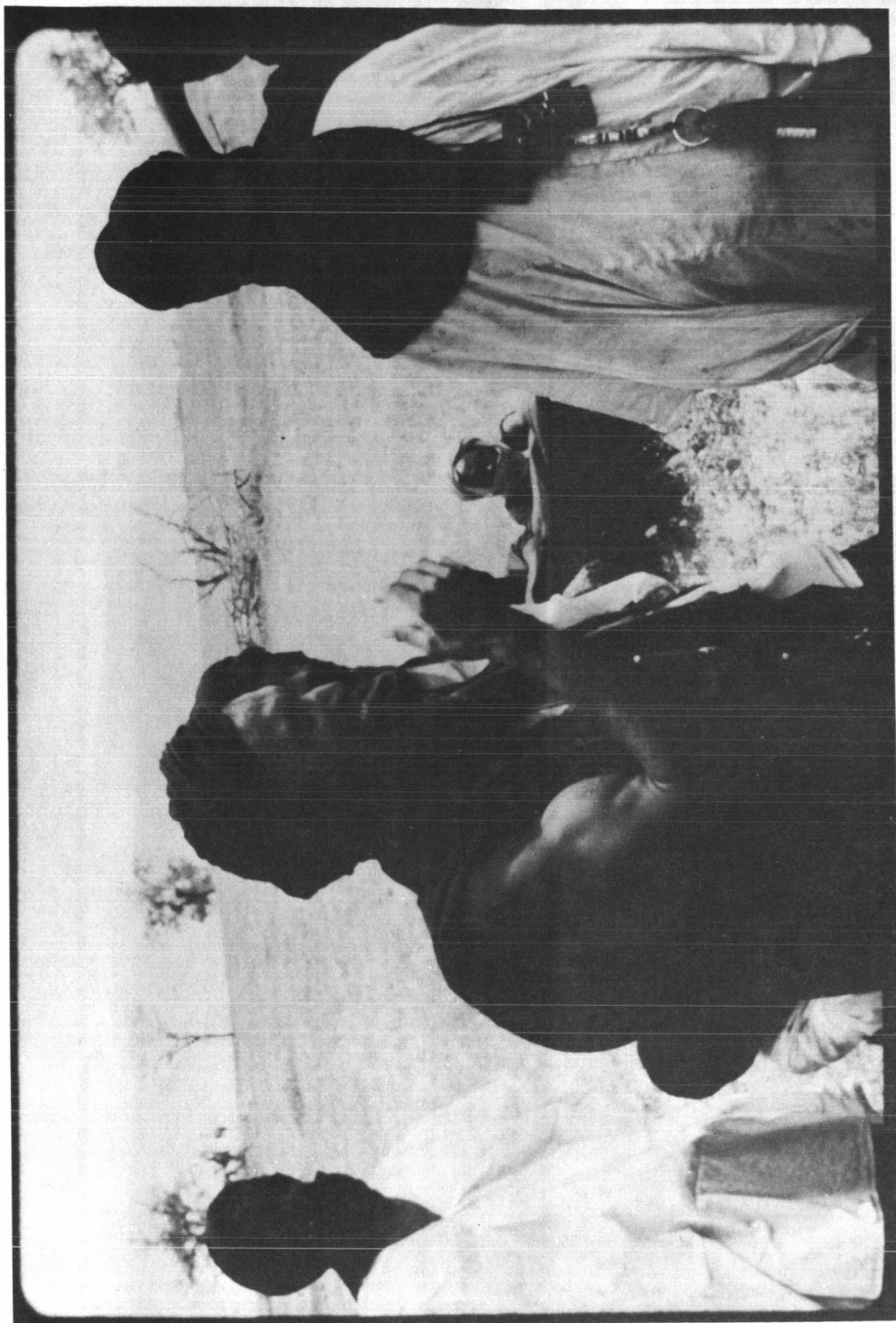


Figure 12.

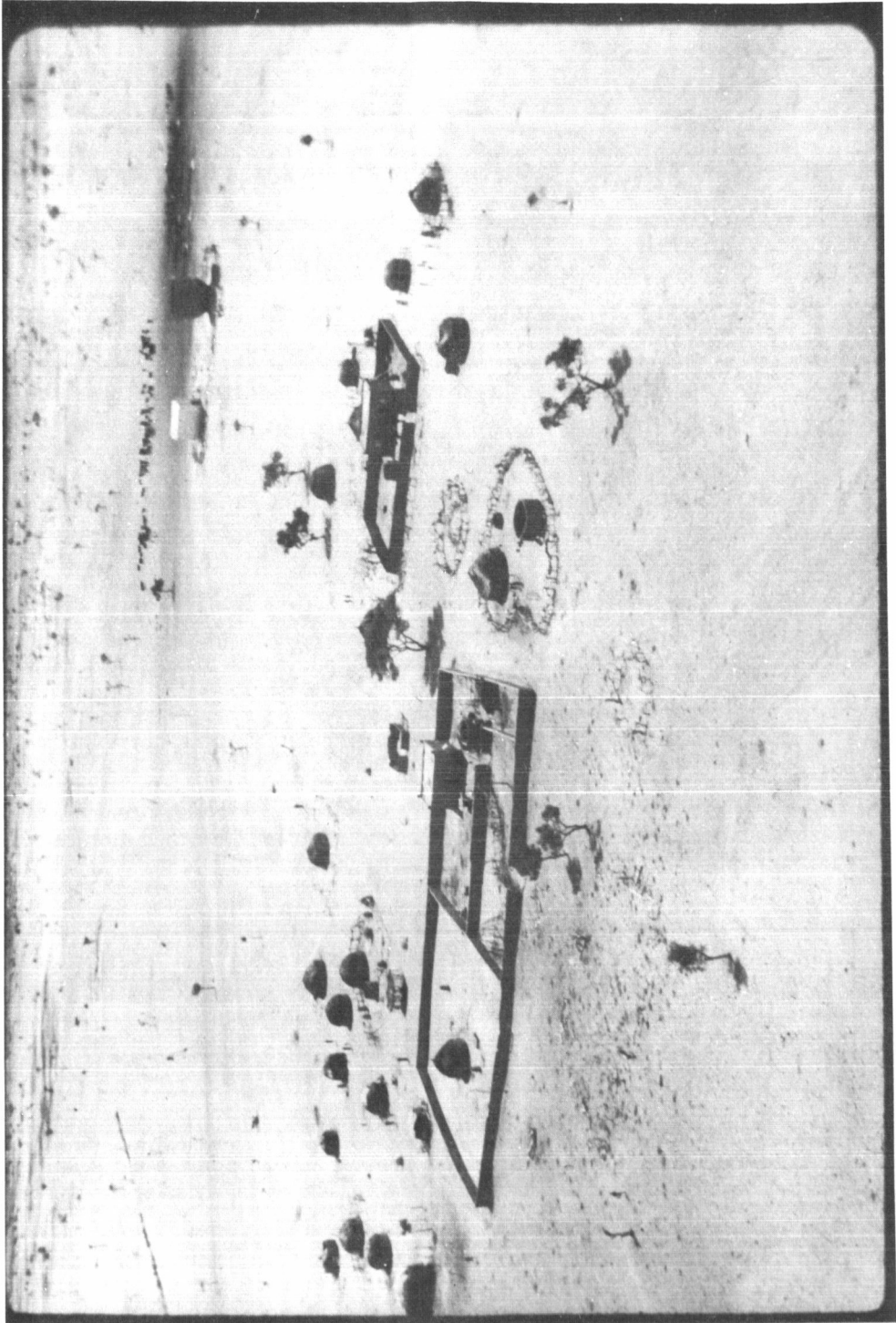


Figure 13.

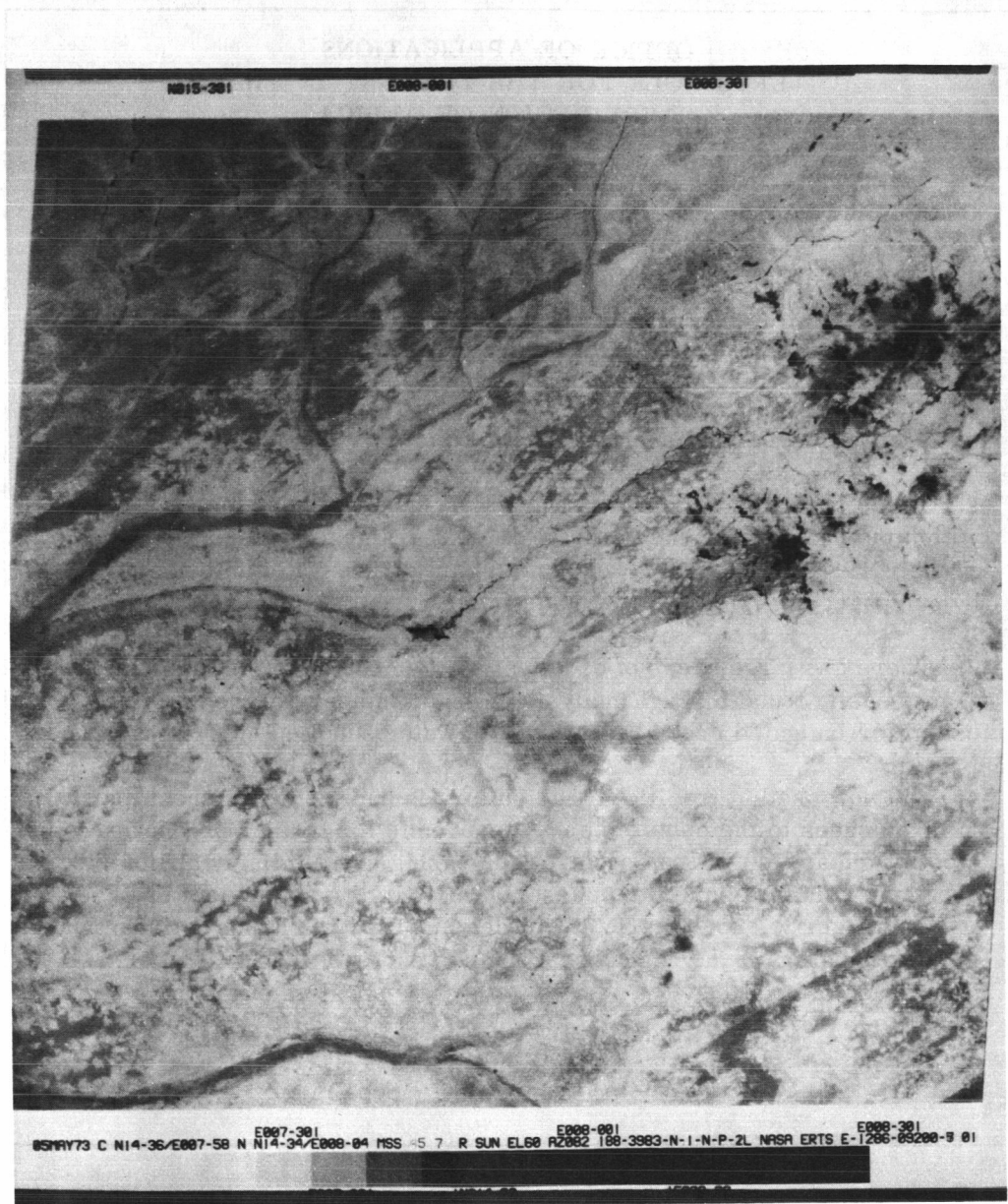


Figure 14.

OFFICE OF APPLICATIONS
ERTS ROLE FOR THE DROUGHT IN THE
SAHEL REGION OF AFRICA

CONCLUSIONS:

1. The Ekrafane Ranch demonstrates the feasibility and usefulness of controlled grazing management in the Sahelian Zone. Benefits from improved practices are far more profound in terms of reversal of desertification than simply rationalized livestock production in the Zone. Improvement of water, soil and vegetation resources is quite apparent even after only five years of enclosure (cloture).
2. Large reserves of near-surface water, annually replenished, exist within the channels of the extensive ancient drainage systems identified in the ERTS-1 imagery. A very small part of this water is being used, by pumpage, for livestock and human water supplies—none for irrigation.
3. There are large areas of excellent soils in the channels, whose location is easily found through analysis of space imagery. The soils are useful for irrigated crop production with water supplied by pumpage.
4. Soil now used in traditional agriculture is badly eroded (sheet erosion), in many cases to the point of being uneconomic for further production. Most of the areas used in uncontrolled grazing are similarly afflicted by erosion — wind erosion in this case. While traditional agriculture has enabled Niger to export agricultural commodities in the past, its unmodified continuation in the region we examined can only lead to further deterioration of productivity and also to the deterioration of the agricultural resource base.

September 1973

NATURAL RESOURCE INVENTORIES AND MANAGEMENT APPLICATIONS IN THE GREAT BASIN

Paul T. Tueller, Garwin Lorain and Ronald M. Halvorson, *Remote Sensing Laboratory, University of Nevada/Reno, Reno, Nevada*

ABSTRACT

ERTS-1 resolution capabilities and repetitive coverage have allowed the acquisition of several statewide inventories of natural resource features not previously completed or that could not be completed in any other way. Familiarity with landform, tone, pattern and other converging factors, along with multitemporal imagery, has been required. Nevada's vegetation has been mapped from ERTS-1 by the following categories: southern desert shrub, salt desert shrub, northern desert shrub, pinyon/juniper woodland, mountain brush, aspen, meadows and marshlands, wheatgrass seedings, phreatophytes and cropland.

Dynamic characteristics of the landscape have been studied. Sequential ERTS-1 imagery has proved its usefulness for mapping vegetation, following vegetation phenology changes, monitoring changes in lakes and reservoirs (including water quality), determining changes in surface mining use, making fire fuel estimates and determining potential hazard, mapping the distribution of rain and snow events, making range readiness determinations, monitoring marshland management practices and other uses. Land use capability classification work is in progress. A wide variety of other uses has been proposed and users identified. Feasibility has been determined, but details of incorporating the data in management systems awaits further research and development. The need is to accurately define the steps necessary to extract required or usable information from ERTS imagery and fit it into on-going management programs.

INTRODUCTION

The synoptic view of the Great Basin afforded by ERTS-1 and especially the repetitive cloud free coverage has proved to be very valuable for the inventory of natural resource features in the Great Basin of the United States. Resource managers can derive considerable useful information from ERTS-1, although the specific procedures for incorporation of the data into management programs is lacking. This investigation has developed a catalog of information derivable from ERTS-1 space imagery as well as an appraisal of new uses and user groups. Problems associated with the use of the imagery have been identified.

N74 307224

MS 430254

The principal objective of our study has been to investigate the usefulness of MSS imagery from ERTS-1 as a supplementary tool for the management of renewable natural resources within the Great Basin. Subsidiary objectives can be listed as follows:

1. To develop a key to broad vegetation units and assess their relation to soil order and landform.
2. To evaluate MSS spectral signatures for vegetation phenology for a complete growing season.
3. To map the natural vegetation of Nevada.
4. To determine the usefulness of specific bands for evaluating a variety of wildland management functions.

METHODS

Initially, our ERTS analysis consisted of identifying different classes of roads, cities, towns, small water bodies, stream channels, fields, landforms, gross vegetation types, and other features that we were familiar with. Our initial finding was that we were able to identify many more features than we first thought possible. This was a matter of gaining experience and familiarity with the imagery.

Secondly, we began to measure the area of water bodies, vegetation types and both natural and man-made vegetation units. Several grids were constructed with different size squares and calibrated to ERTS scale. The grids were generally 0.1 mm square, 1 mm square, and 4 mm square. Very large areas were measured with dot grids having 990 or 3960 dots per square decimeter (64 or 256 dots per square inch). More recently we have used our Zoom Transfer Scope to blow up features for more accurate measurement.

We have used human interpretation techniques almost exclusively. Tone, texture, shape, pattern and size were the main photo interpretation factors utilized. When interpreting certain features, we relied heavily on physiographic location, soil appearance and field experience with these features. Color composites added infinitely to interpretations, especially for vegetation types having greater than 50% cover. Diazochrome transparencies proved useful when of good quality. Even slightly dark transparencies produced poor diazochrome color composites.

A mosaic of the state was constructed using 21 black and white prints at a scale of 1:1 million (8.5 by 12.7 decimeter sheet; 24 by 36 inch sheet) and 1:2

million (4.25 by 6.37 decimeters; 12 by 18 inch sheet). The red band (MSS 5) was used to construct the mosaic because landform features appeared more striking. This mosaic is being used as a base to map resource features and compare changes on other imagery types and dates.

To determine accuracy of ERTS-based vegetation maps, test points were established along highways which traversed the state. These test points were systematically located at 16 kilometer (10 mile) intervals. The vegetation next to the highway was recorded as to type (salt desert shrub, pinyon/juniper, etc.) and physical location. These points were located on a 1:1 million scale topographic map using a Lietz opsometer and USGS topographic maps at a scale of 1:250,000. Accurate point location on the 1:1 million scale map was thus made.

Once the point locations were established, the vegetation map overlays (scale 1:1 million) were superimposed on the base map. At each point the vegetation was recorded as observed in the field and as identified on ERTS. This data was treated as an interpretation test. Known field points became identification cells and the maps became an interpretation of these cells. Two types of error were possible: commission and omission. A commission error occurred when the map identified a cell as being of a certain type when it was not. An omission error occurred when it was not identified correctly, i. e., it was omitted. An interpretation test table was generated from this data.

To correlate satellite imagery with ground events, accurate and often detailed notes were taken at several study sites. Three main factors determined optimum time to record "ground truth". The first factor was the eighteen day overflights. Ground truth must be recorded every eighteen days coinciding with the ERTS overflights.

The second factor was plant maturity. Since much of our ground data was concerned with plant phenology, the period of active plant growth and development was critical. Ground data was obtained for northern Nevada sites between April and October, the active growing season. During the remainder, most vegetation is dormant. Data was obtained for southern Nevada sites year-long due to diverse climatological conditions caused by elevational differences of 3.2 kilometers in 48-64 linear kilometers (2 miles in 30 or 40 linear miles). The greatest growth period for the low elevation southern sites was between February and November.

The third factor was accessibility. Winter storms caused many northern sites to be inaccessible due to road conditions. This was a determining factor in making ground data collection trips.

The dominant species were listed, along with their phenological stage. Soil moisture, snow pack, etc., were also observed. In general, our observations shifted from detailed, small area observations to general, large area observations. It was felt that these generalized observations were more compatible with our project goals and research capabilities. The ability to ascertain ground measurements that correlate with image features was a difficult one due to the great heterogeneity of features that appeared homogeneous on an ERTS-1 image.

A densitometer was used to correlate vegetation reflectance on ERTS with ground phenology data. Only Reno and Las Vegas study areas could be used, however, due to extensive cloud cover over the rest of the state during critical overpasses.

The initial study sites were found to be too small for use with our densitometer. The area which could be "read" with the densitometer was a 1 mm diameter circle on the image, or about 80 hectares (200 acres) on the ground. With this in mind, larger sites were selected such as a large native meadow, a large alfalfa field, an extensive area of mountain brush, and other similarly large areas.

MSS 5 and 7 bands were used, as these are most indicative of vegetation change. Large water bodies were measured to create a standard to compensate for exposure. It was hoped that the MSS 7 image of these water bodies could be transformed to a constant value. Once this constant value was found, the vegetation data was transformed accordingly. This transformed data was then ratioed ($MSS\ 5 \div MSS\ 7$) or the differences were found ($MSS\ 5 - MSS\ 7$). The ratios or differences were used to detect vegetation phenology change.

ACCOMPLISHMENTS

Resource Inventories

We have completed ERTS-1 derived maps for the principle Great Basin vegetation types statewide: southern desert shrub, salt desert shrub, northern desert shrub, pinyon/juniper woodland, mountain brush, aspen, meadowland, agricultural and phreatophytic vegetation and wheatgrass seedings. Most other vegetation types, e.g., stands of bristlecone pine, white fir or other specific plant associations, were not mappable with the color composite data available, or the resolution limits of ERTS-1.

Native vegetation has frequently been plowed and planted to introduced grasses in Nevada to increase grazing capacity. Nearly a million acres were found in the state (Figure 1). MSS band 7 was the most useful for identifications. Seedings were delineated by ownership or administration: public, private,

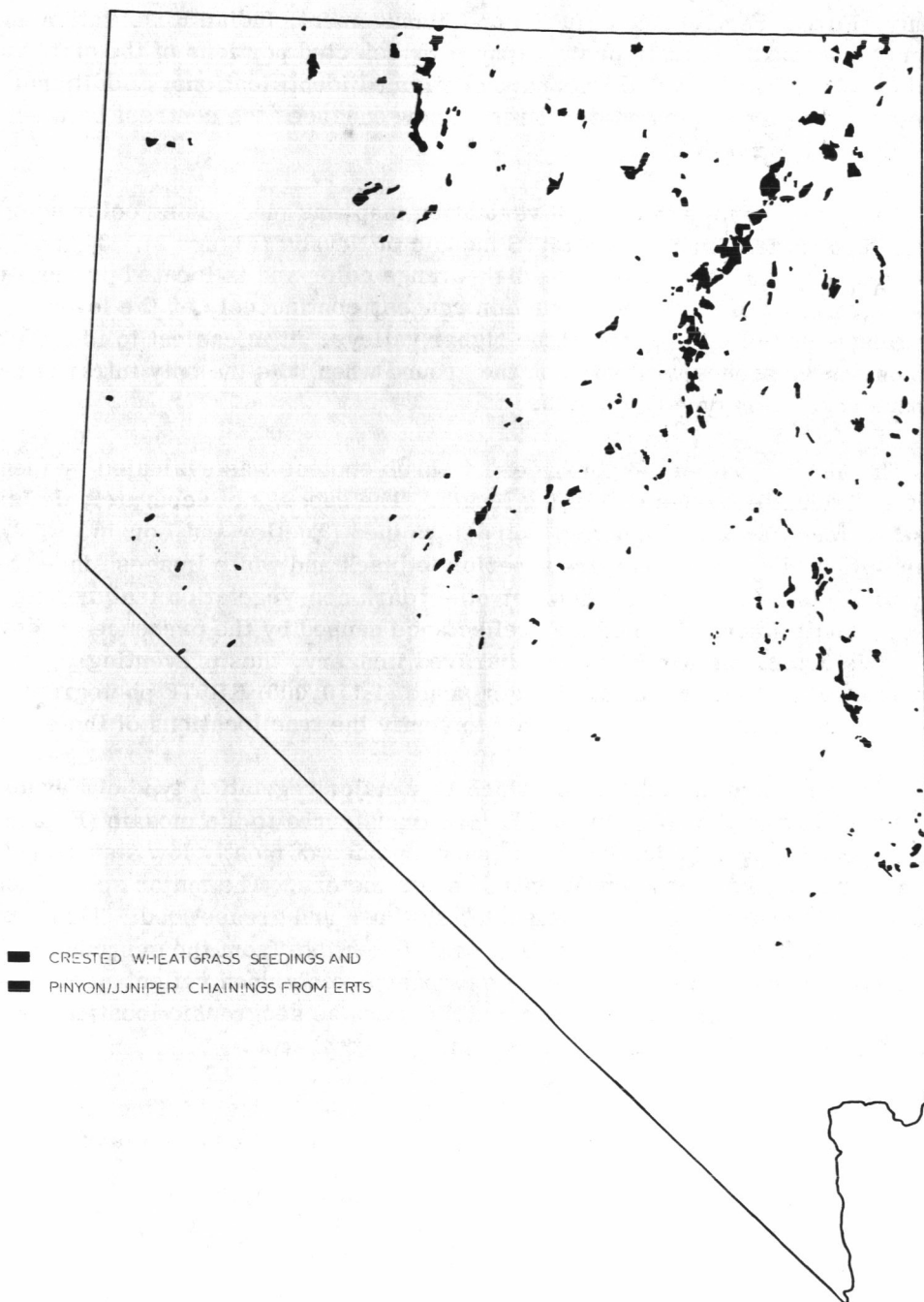


Figure 1. Perennial wheatgrass seedings in Nevada. Their distribution is closely related to the distribution of valleys adjacent to the higher mountain ranges.

county, Forest Service, Bureau of Land Management, Indian Reservation and other. Intermediate scale photography over selected portions of the state and field checking by aircraft flights have confirmed identifications. Additional seedlings were located on winter dates. Snow enhanced the contrast between seedlings and native brush.

The pinyon/juniper woodland vegetation map was made using color composites, then transferring to the ERTS mosaic of Nevada (Figure 2). This vegetation type is characterized by a reddish-orange color and is located primarily in belts on most of the higher mountain ranges, continuously on the lower mountain ranges and often in some of the higher valleys. It is easiest to identify and map on winter scenes with snow on the ground when it is the only infrared reflective vegetation type (Figure 3).

The pinyon/juniper-northern desert shrub ecotone was evaluated by identifying individual ecotones of varying length. The success of accurately defining these ecotones on ERTS imagery was determined (Tueller and Lorain, 1973). Color infrared composites were superior to black and white images since it was easy to mistake landform shadows or other dark non-vegetation features for ecotones. Small amounts of infrared reflectance caused by the presence of pinyon/juniper is detectable with the color infrared imagery, thus preventing possible confusion with other features. Larger scale (1:110,000) RB57F photography and aerial reconnaissance have been used to verify the true locations of the ecotones.

Salt desert shrub vegetation, which is a major vegetation type of Nevada, was mapped from the color infrared, then transferred to the mosaic (Figure 4). This vegetation type is dominated by brush species of mostly low stature ($1/4$ to $1/2$ meter tall), but occasionally reaches 1-2 meters. The major species in this type are halophytes including shadscale, saltbush and greasewood. This vegetation was difficult, if not impossible, to differentiate from the surrounding northern and southern desert shrub types based solely upon reflectance. Therefore, it was necessary to use other criteria such as geographic location, soil reflectance, and elevation in identifying this vegetal type.

Interpreter experience is very important in identifying this vegetation type as the following criteria all have to be taken into account before a decision is made:

1. It is generally below 1500 meters (5,000 feet), except for some higher, internal drainage basins.
2. It is usually associated with light colored, highly reflective alkali soils where water frequently stands or moves and evaporation is high.

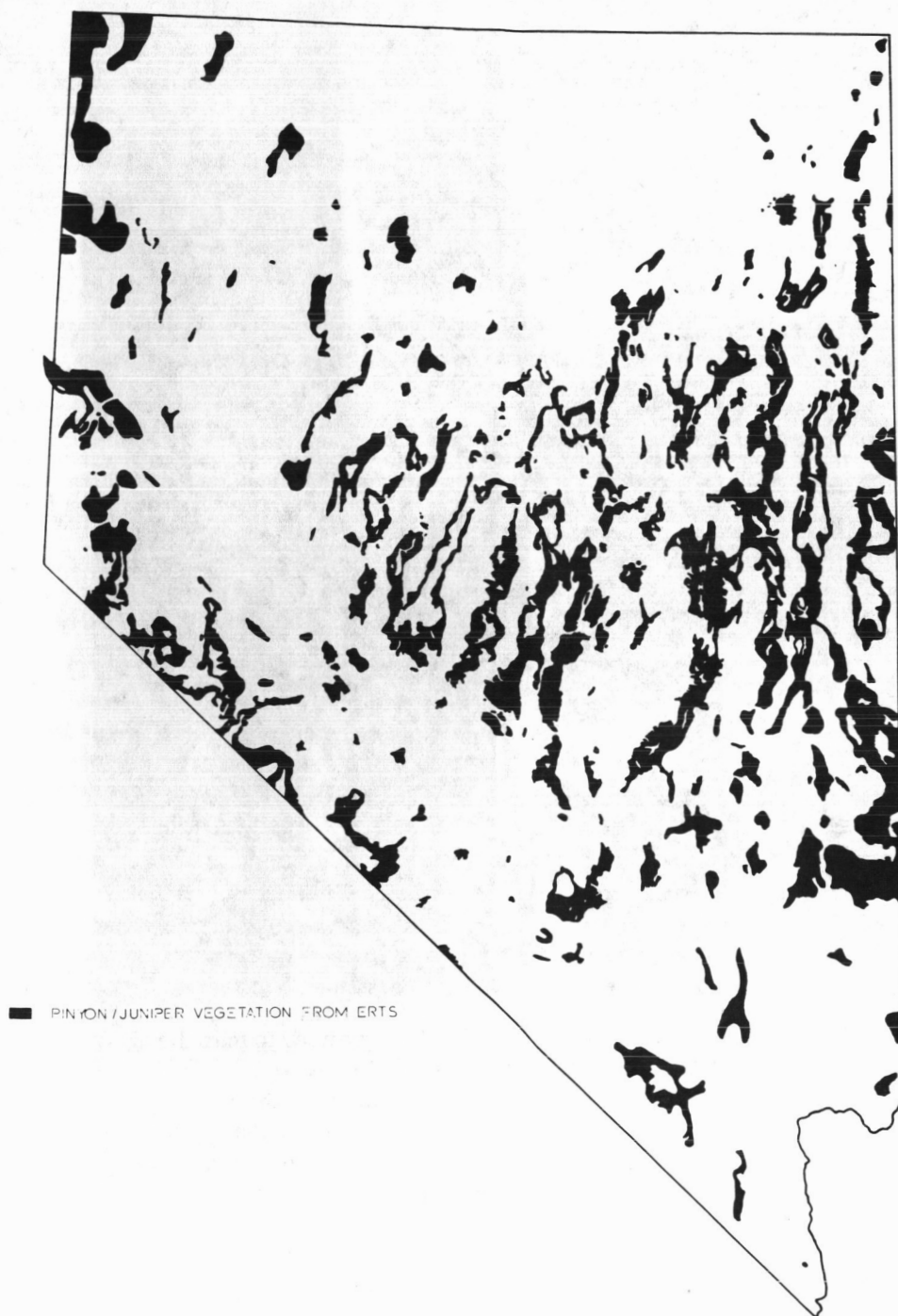


Figure 2. Pinyon/Juniper Woodland in Nevada.

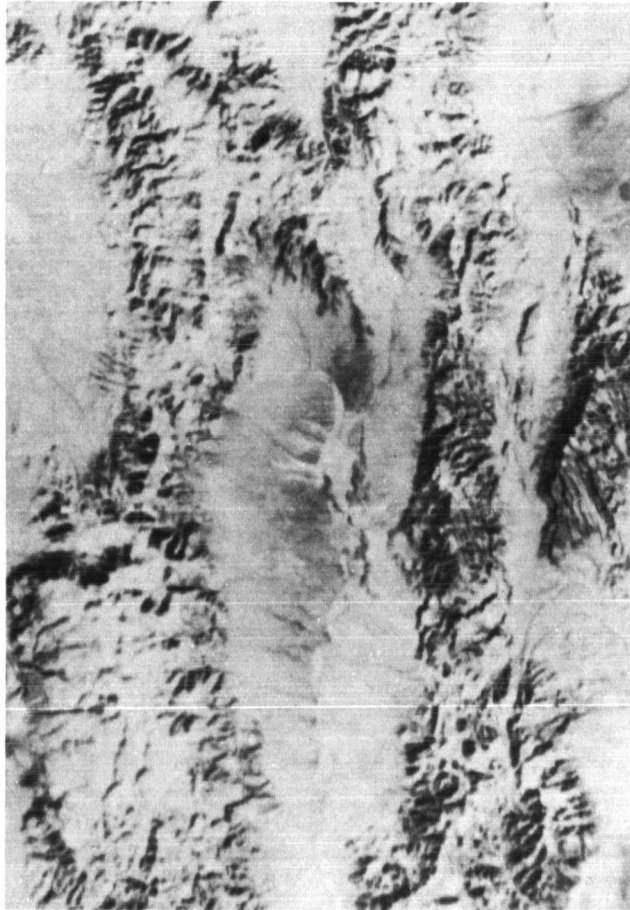


Figure 3. Winter ERTS-1 scene used to map the Pinyon/juniper woodland. Note how the pinyon/juniper woodland is found in belts on the higher mountain ranges (Monitor Range on left) and goes to the top on lower portions of the Hot Creek Range on the right. (Image 1144-18003-4, 5, and 7)

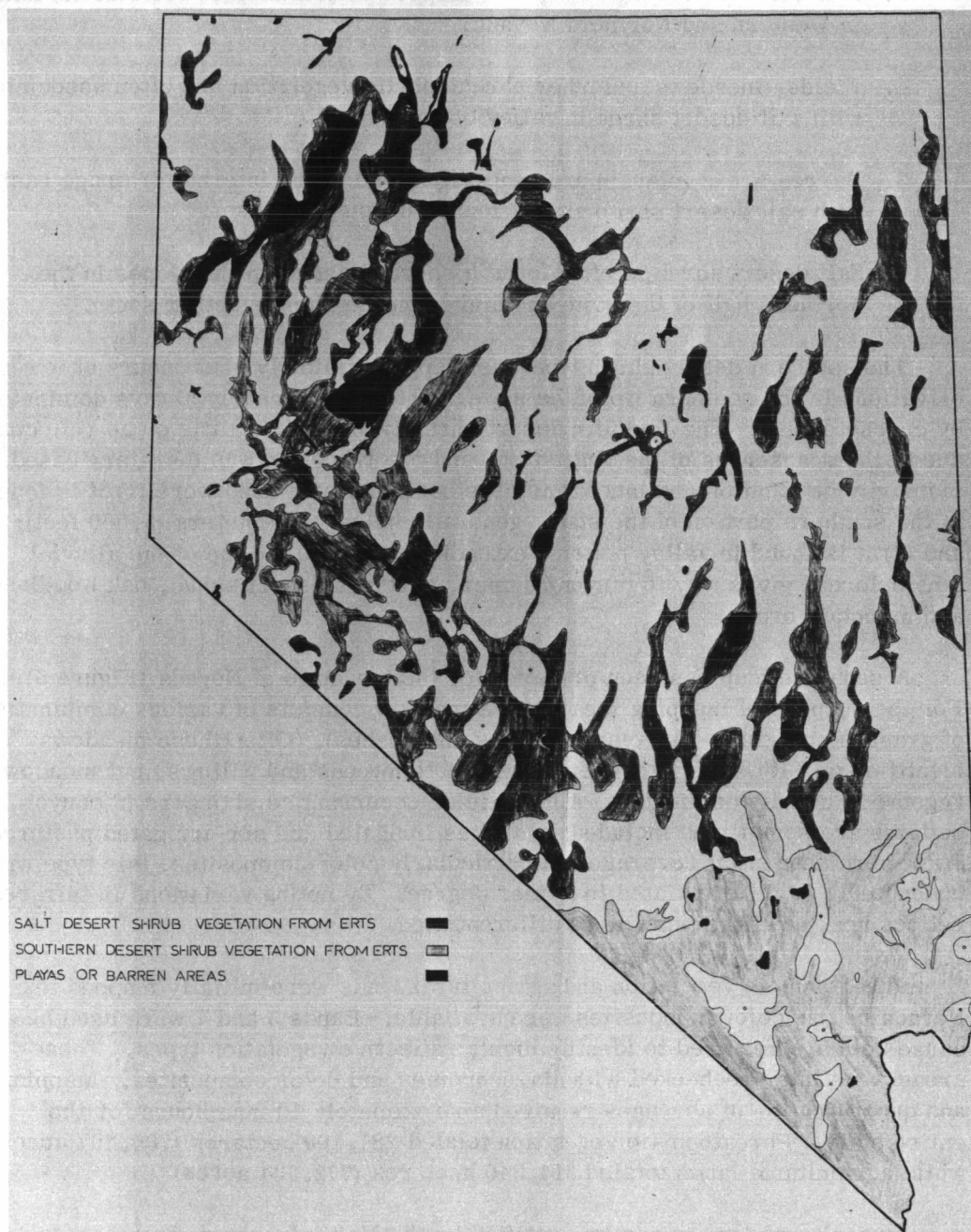


Figure 4. Southern Desert Shrub (Primarily Mojave Desert) and Salt Desert Shrub Vegetation in Nevada.

3. It is closely correlated with the mapped distribution of Pleistocene lakes in Western and Northern Nevada.
4. Fields, meadows and other phreatophytic vegetation are often associated with salt desert shrub in valley bottoms.
5. Barren areas (playas) are generally found in the internal drainage basins with salt desert shrub always found surrounding them.
6. Salt desert shrub is often found a short distance up the slopes in the northern half of the state and higher on the slopes further south.

The southern desert shrub type was mapped similarly, but occurs at lower elevations in the southern tip of the state. This type is nearly always dominated by creosote bush. The southern desert shrub type exhibits little or no reflectance due to the sparseness of the vegetation, and identification was therefore based primarily on location and landform. The basic criteria used were (1) it is found in the southern portion of the state, generally below 1500 meters (5,000 feet); and (2) it is found in valley bottoms extending nearly to the top of the alluvial fans before it gives way to pinyon/juniper, northern desert shrub, oak woodland and mountain brush.

A separate map has been prepared for the meadows of Nevada (Figure 5). For the purpose of mapping meadows, a meadow consists of various combinations of grasses and grass-like plants (sedges and rushes). Often these meadows identified on ERTS are interspersed with cottonwoods and willows, but meadow vegetation usually dominates. Alfalfa fields occurring as stringers in canyon bottoms are sometimes included as well as irrigated and sub-irrigated pastures. With more sequential coverage and particularly color composites, this type will undoubtedly be differentiated to a finer degree. By noting variations in infrared reflectance, alfalfa fields can be differentiated.

Phreatophytic vegetation and agricultural lands were initially mapped in Nevada before color composites were available. Bands 5 and 7 were used because both are required to identify highly reflective vegetation types. These areas were later rechecked with diazochromes and color composites. Mapping and quantification of acreages required approximately 10 man hours for the entire state. Phreatophytic vegetation totaled 287,100 hectares (705,407 acres), while agricultural lands totaled 314,340 hectares (772,334 acres).

Agricultural land is easily identified by the high infrared reflectance during the growing season and the orderly, usually square or rectangular shape of the individual fields. Fallow fields are easily identified by their light tone on all bands including color infrared composites. Phreatophytes were identified by

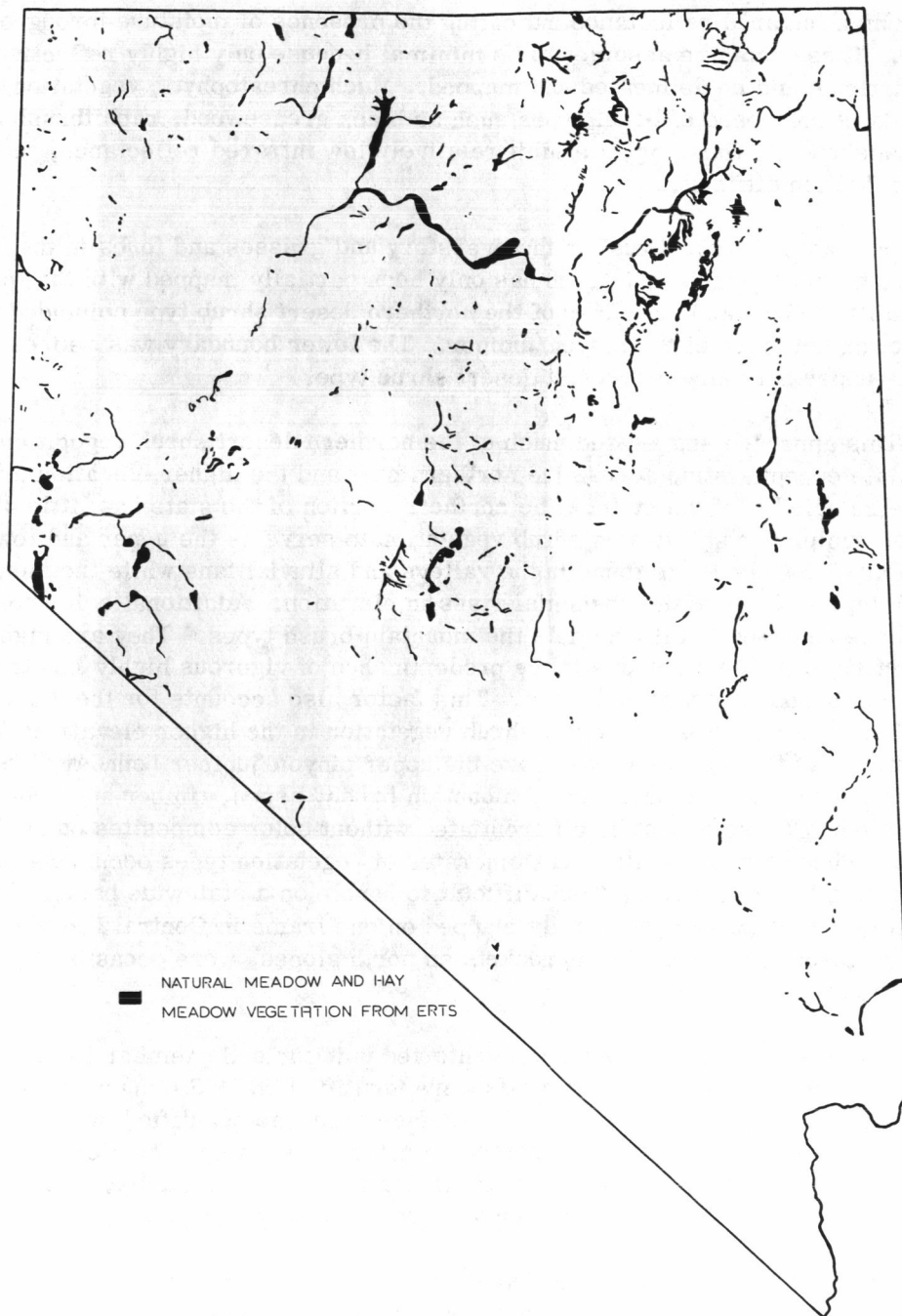


Figure 5. The Distribution of Native and Hay Meadow Vegetation in Nevada as derived from ERTS-1 Color Composites.

their high infrared reflectance indicating the presence of moisture throughout the year. These data are assumed to be minimal because only highly reflective vegetation could be delineated and mapped. Much phreatophytic vegetation in Nevada is composed of brush types such as black greasewood, rabbitbrush and big sagebrush. These types exhibit relatively low infrared reflectance, making quantification difficult.

Dominated by sagebrush in the overstory and grasses and forbs in the understory, the northern desert shrub has only been partially mapped with the imagery available. The upper boundary of the northern desert shrub type coincided with the lower boundary of the pinyon/juniper. The lower boundary was delineated by the upper boundary of the salt desert shrub type.

This approach segregated much of the northern desert shrub vegetation in the state except a strip across the northern part and the higher elevation areas in the remainder of the state. The northern portion of the state has little or no pinyon/juniper or salt desert shrub vegetation to serve as the upper and lower boundary. Sagebrush is found in the valleys and alluvial fans while the mountain brush type is found with substantial rises in elevation. Additional color composites are required to differentiate the mountain brush types. They are highly reflective in the summer due to the predominance of vigorous highly infrared reflective shrubs, grasses and forbs. This factor also accounts for the difficulty of differentiating northern desert shrub vegetation in the higher elevations in the remainder of the state. Areas above the upper pinyon/juniper boundary are a mixture of northern desert shrub, mountain brush, aspen, timber and sub-alpine vegetation. These cannot be differentiated without color composites on additional dates. These types are also conglomerates of vegetation types occurring in fairly small areas, making them difficult to handle on a statewide basis. The aspen type was fairly successfully mapped on one frame in Central Nevada. Timber types, usually occurring in pockets on north slopes, were occasionally identified.

Standing water surfaces were inventoried using mid-September imagery as a base. Reservoirs, lakes and ponds were identified on MSS images and named from existing topographic maps. The surface area was quantified by acreage using a system similar to that described earlier for seedings (Tueller and Lorain, 1973). This water inventory can be updated seasonally or annually. A number of other inventories are underway or have recently been completed.

Soil-vegetation relationships have been considered. Some general relationships specifically oriented to landform-vegetation-soil correlations are readily apparent. For example, there is a close relationship between salt desert shrub vegetation and old beaches, between the mountain brush, pinyon/juniper,

mountain mahogany complex and mollisols, and the northern desert shrub vegetation and the distribution of andisols.

Vegetation mapping accuracy results show an overall correct figure of 74% (Table 1). Much of the incorrect results is due to the inability at times to distinguish northern desert shrub from salt desert shrub, and the poor identification of low density pinyon/juniper. Very sparse pinyon/juniper cannot be detected on ERTS imagery and there was a high percentage of omission errors associated with this type. It may have been appropriate to eliminate many pinyon/juniper identification cells because of their proximity to a mapped ecotone, but this was not done. Hence, the results may not correctly describe the accuracy of this vegetation map, but they do give an indication of the types of errors that can be expected in identifying this vegetation type. There was also error associated with the discrimination between small playas and salt desert shrub. Perhaps the salt desert shrub and playa identification cells should be combined due to the fact that not all playas were indicated on the vegetation map.

Analysis of Repetitive ERTS-1 Imagery

Sequential imagery has proved its usefulness for a wide variety of purposes: vegetation mapping, following vegetation phenology changes, monitoring changes in standing water in lakes and reservoirs, evaluating changes in surface mining use, determining freezing and thawing dates for ponds, lakes and reservoirs, determining wet and dry periods on playas in relation to storm events, making fire fuel estimates and hazard estimates, mapping storm and snow distribution patterns in relation to large downstream erosion or flood events, making range readiness determinations, and other uses.

Unique winter scenes provided by ERTS were highly beneficial for identifying and mapping certain features. Color infrared composites from December 14, 1972 (Figure 3) greatly aided the mapping of pinyon/juniper vegetation in Nevada. These frames provided a unique situation in which pinyon/juniper (tree) was the only infrared reflective vegetation type at this time. All other vegetation types were either dormant or were covered with snow at this time. Unfortunately, only two frames in Nevada were available of this unique scene. The lower boundary of pinyon/juniper is easily recognized on summer color composites, but the upper boundary diffuses into other highly infrared reflective types. Pinyon/juniper was very accurately mapped where these winter scenes existed, but was still more accurately mapped where they did not exist than any map available.

Another example of interpretation aided by snow cover is shown at Coils Creek. Coils Creek has been one of our intensive soils/vegetation study sites for the past 6 or 7 years (Blackburn, et al., 1969). Later, the vegetation/soils

Table 1
Results of an ERTS-1 Interpretation Test for
Vegetation Type Identification in Nevada.

Vegetation	northern desert shrub	southern desert shrub	salt desert shrub	playas ¹	pinyon/juniper	coniferous	agriculture	seedings	points not used ²	TOTALS (excluding points not used)	TOTALS (including points not used)
No. Test Cells	31	20	70	3	22	1	9	3	9	159	168
No. Correct	29	17	48	0	10	1	9	3	-	117	-
No. Commission	32	0	7	1	2	0	0	0	-	42	-
No. Indicated	61	17	55	1	12	1	9	3	9	159	168
No. Omitted	2	3	22	3	12	0	0	0	-	42	-
% Omitted	6	15	31	100	55	0	0	0	-	26	-
% Committed ³	103	0	10	33	9	0	0	0	-	26	-
% Committed ⁴	52	0	13	100	17	0	0	0	-	26	-
% Correct	94	85	69	0	45	100	100	100	-	74	-

¹All playas were not indicated on the map

²These points were not used due to problems with ecotones

³Based upon no. of type present

⁴Based upon no. of type indicated

map compiled in 1969, plus field trips were used to see if these same vegetation communities could be recognized on color, color infrared, and multispectral photography. Color infrared is available of this entire watershed at a scale of 1:24,000. Multispectral imagery is available at a scale of 1:62,500, from which color composites and enhancements were made to study the vegetation. NASA's RB57F flew the area in the fall with 9 sensors including color, color infrared, and black and white multispectral. These were all intensely studied. One vegetation ecotone, a very sharp boundary between big sagebrush and low sagebrush plant communities, could never be identified, even on the 1:24,000 color infrared. This boundary can now be clearly identified on December 14, 1972 color composites. Optimum snow cover is felt to be the reason for this identification. This could only be accomplished by sequential coverage over the same areas by the ERTS satellite. There is no question that sequential coverage adds invaluable information for vegetation mapping. Obtaining coverage in different winters where snowpack varies will also provide additional information.

As another example, we have evaluated a big sagebrush chemical control project occurring on the northern alluvial fan of Antelope Peak in the Monitor Range. The area is about 2 miles long by 1 mile wide with the chemical control accomplished in strips where sections between strips were left uncontrolled. This area is fairly easy to identify on 1:108,000 color infrared imagery obtained in the fall. This area is not visible on ERTS diazochrome composites in September, but is readily visible on December 14, 1972, ERTS black and white or color composites. The plant succession of this area can be monitored by ERTS from year to year as the area eventually returns to big sagebrush vegetation.

Changes in lakes, ponds and reservoirs are measurable. Determinations can be made of changes in surface standing water and correlated with water availability for irrigation, waterfowl habitat, and similar uses (Figure 6).

Numerous other examples can be cited. Many wildfires occurred in Western Nevada in the summer of 1973. Several of these fire scars were measured in a matter of minutes and compared favorably to Bureau of Land Management records. These fire scars were identified with the greatest ease on MSS 7 (Figure 7). Analysis of imagery before and after a significant storm event in Central Nevada has shown the potential of evaluating erosion features such as the widening or cutting of major washes. The Ruby Marshes are being monitored for waterfowl and fisheries management purposes. Water level controls are correlated with vegetation changes resulting in tone changes on ERTS color composites.

Phenology change has been successfully detected by using a densitometer and ratioing the transformed values for MSS bands 5 and 7. Figure 8 shows the typical phenologic change of a native meadow. The plants are initially green in

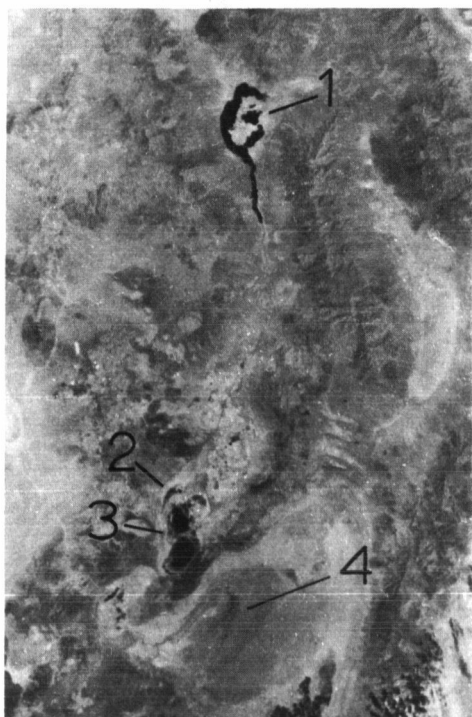


Figure 6. Left - ERTS-1 MSS 7 on August 11, 1972. Note the standing water in Rye Patch Reservoir (1), Toulon Lake (2), Humboldt Lake (3), and the Carson Sink (4). (Image 1019-18050-7)

Right - The same frame September 16, 1972. Note the significant reduction in total standing water. (Image 1055-18050-7)

C-4

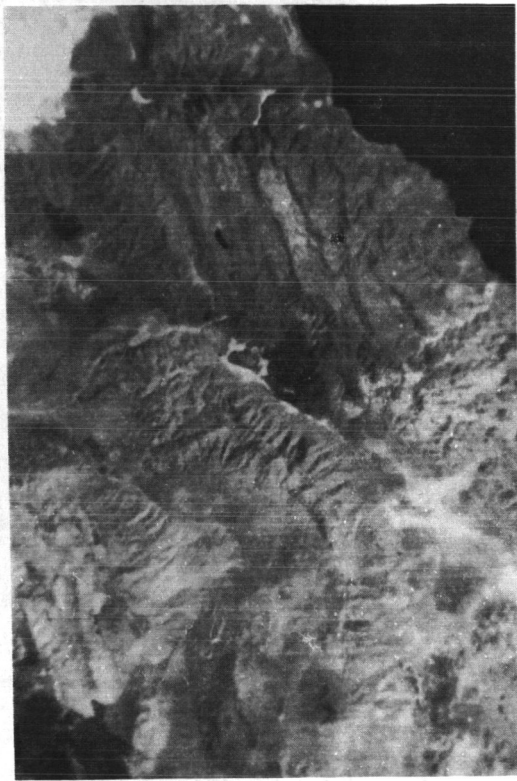


Figure 7. Fire scars, such as these between Pyramid Lake and Reno, can easily be delineated and quantified on ERTS imagery. (Image 1380-18104-7)

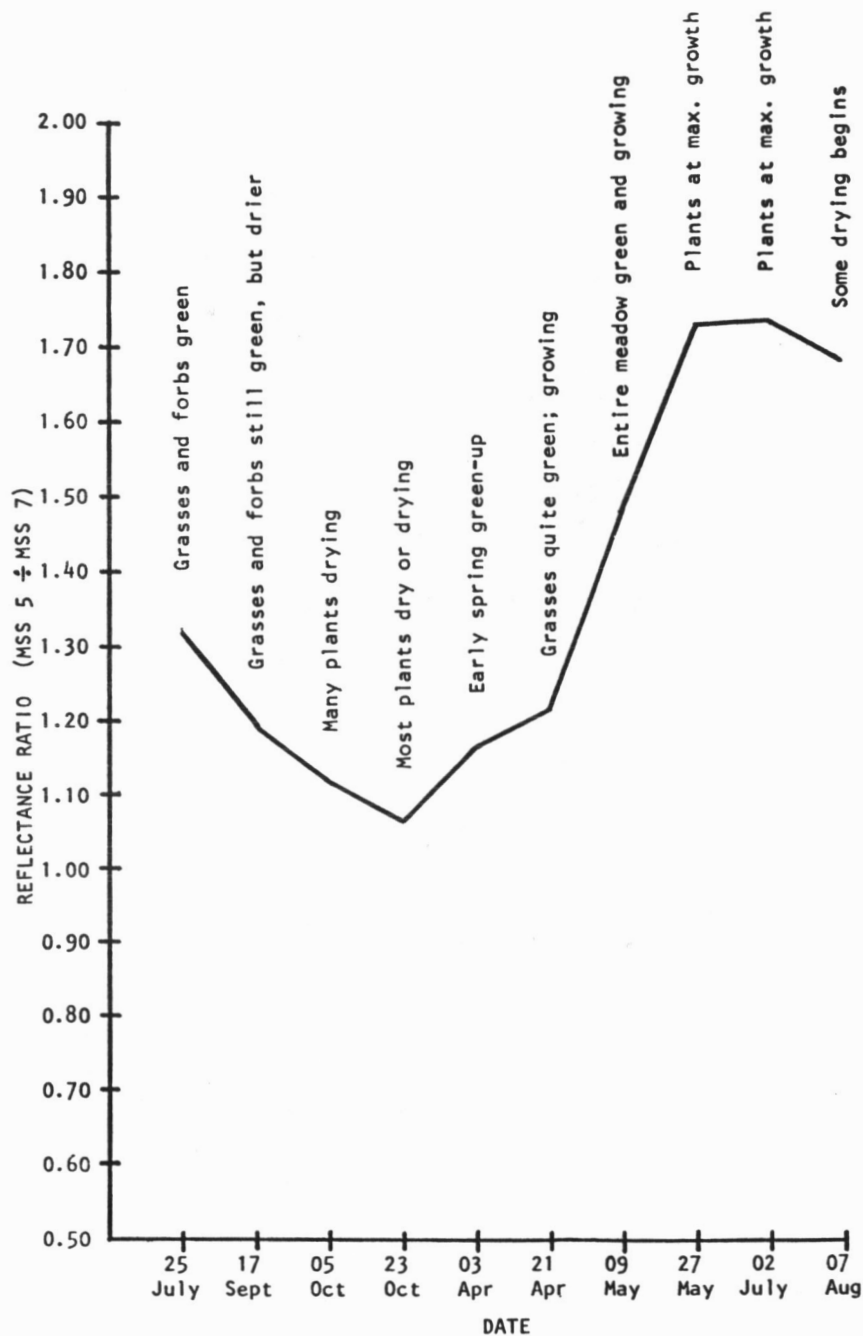


Figure 8. Phenologic Change of a Native Meadow in Washoe County as Detected on ERTS Imagery

the summer and exhibit fairly high infrared reflectance. The MSS 5 band records this as a dark tone, while the MSS 7 band shows it much lighter. Hence, the ratio between these bands is greater than 1. As the year progresses and the plants mature, this reflectance and the ratio decrease. With the onset of spring, the plants green up and the ratio increases. The phenology change is dependent on many factors, especially climate, and will vary from year to year.

Figure 9 shows the phenology change of a mountain brush community. The plants are initially green, but as fall approaches the deciduous species lose their leaves. This lowers the ratio but it still remains above 1. Snowfall covers the remaining leaves and the reflectance ratio drops below 1. Snowmelt, together with the emergence of new leaves, is detected as the ratio again rises above 1.

Similar results were observed for an irrigated field, an alfalfa field, and a marsh area. Annual vegetation such as cheatgrass exhibits the same reflectance properties, although the reflectance is not as easily measured except in the spring. Tests run on sparse vegetation types in the Las Vegas area showed that the phenology cannot be monitored for this type. The soil, not the vegetation, is the main contributing factor to the tone signature or infrared reflectance exhibited on ERTS imagery.

DISCUSSION AND CONCLUSIONS

The data we have extracted from ERTS-1 imagery is proving to be very useful to state and federal agencies and private firms. Many groups that we have worked with in Nevada have already shown an interest in and used these data. Our project has provided inventory information in the kind of detail never before available in Nevada on a statewide basis. The ERTS-1 imagery as a monitoring system is invaluable and only a few of the potential uses have been evaluated. The ERTS imagery has created considerable interest for monitoring water availability in reservoirs, snowpack determinations, fire fuel estimates, and measuring urban sprawl. Various other inventory and monitoring systems have been proposed. However, one important problem is the need for more timely delivery of products.

A tremendous amount of information is available from ERTS-1 imagery that has not been exploited in Nevada due to the sheer bulk of the data and the need for more research, including ground data. New uses are constantly being brought to light by exposing the imagery to different people (e.g., the Nevada Fish and Game Department has suggested and is using ERTS-1 imagery for the following: eagle and hawk inventory planning, aspen mapping in relation to beaver inventories). Our Desert Research Institute is using the imagery to survey sites in the Great Basin that have potential for the placement of solar energy

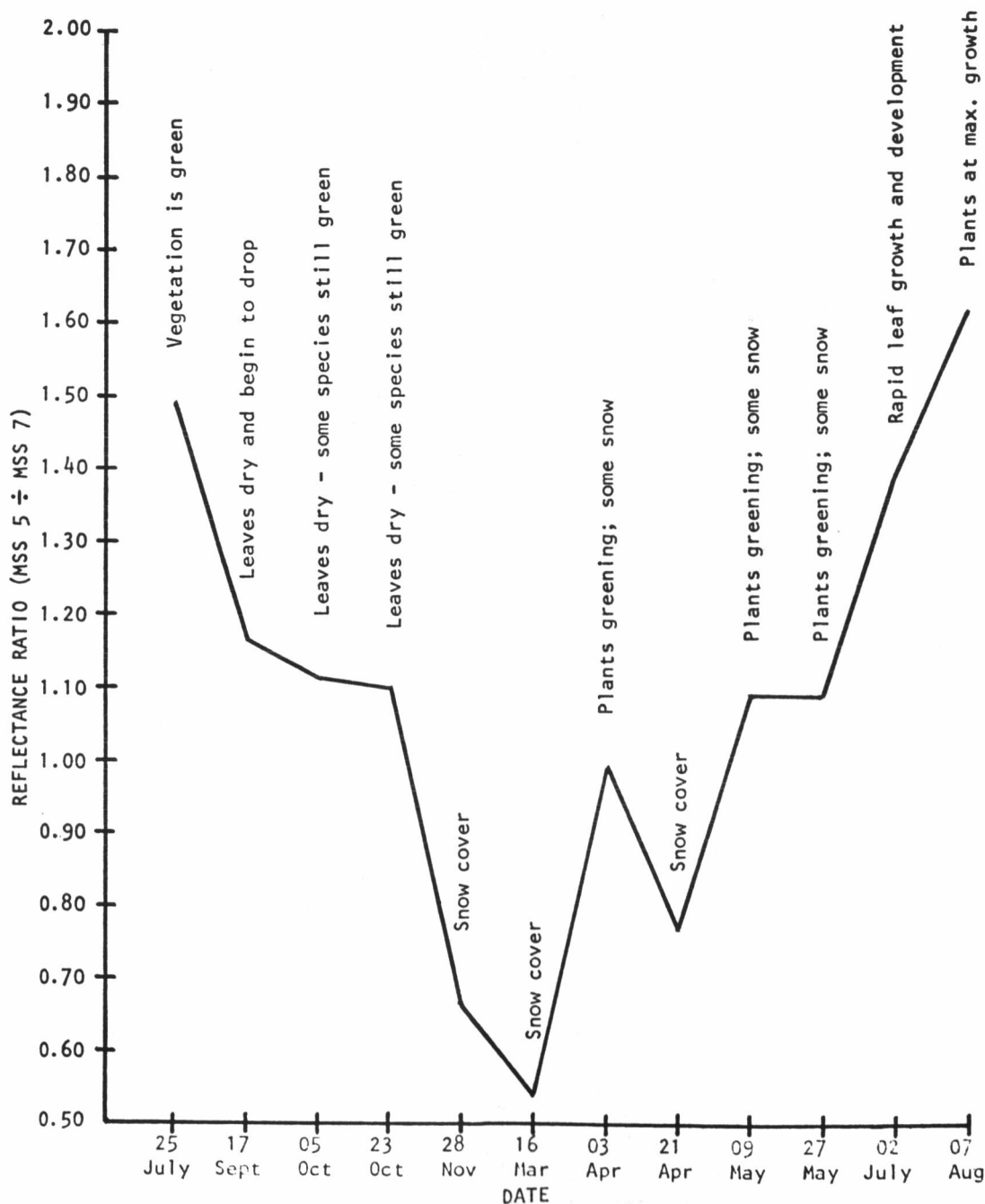


Figure 9. Phenologic Change of a Mountain Brush Community in the Sierras as Detected on ERTS Imagery

panels; The Nevada Division of Water Resources is utilizing updated surface water inventories and surveying the state for potential locations for new atomic energy plants and for inventorying the location and extent of surface mining activities.

The full potential of sequential imagery cannot be fully realized at this time due to factors such as cloud cover and exposure or processing problems. More coverage will undoubtedly show additional uses. The comparison of year to year dates (we are just beginning to evaluate this) will also yield more information on the correlations between precipitation, vegetation production and reflectance on ERTS imagery. Many unique signatures on ERTS have appeared which were not evaluated because we were not aware of their existence at the time field notes were gathered. As these ideas are plugged into our future field work, we can check these unique signatures as ERTS passes over and exploit their values for future uses. Finally, many critical dates for mapping vegetation types were missed due to cloud cover problems. The addition of dates in subsequent years and their related unique conditions will aid further mapping in the state (e.g., pinyon/juniper winter mapping scenes) and for updating maps.

ERTS will have considerable input to Nevada's new land use planning legislation (land use capability classification). County managers will also find it useful for land use planning. For example, we have had a request for a mosaic of Washoe County to be used by the Washoe County Sheriff's Department in their law enforcement planning efforts.

The Bureau of Land Management and Forest Service are finding our vegetation inventories to be useful for management purposes. Measurement of phenological changes in the vegetation has important management implications, e.g., for monitoring grazing management systems, fire hazard estimates and range readiness. Feasibility has been determined, but details of incorporating the data into management systems awaits further research and development.

More information is needed to document vegetation phenology and the means for accurately measuring the appropriate signatures. Additional detailed field notes on specific vegetation types (e.g., meadow and aspen) would be helpful along with larger scale underflights to document signatures as they appear on ERTS. Many variations in reflectance are apparent in seedings. These need further investigation to determine why they occur, and if they can be correlated with grazing management requirements.

The unique ability to infer snow depths and to determine snow distribution by storm event offers great potential for more accurately mapping vegetation types and to map other vegetation units that are not identifiable to date on ERTS-1 data.

There is also further need to describe these uses to state and local agencies, individuals and firms in the Great Basin. Information from our study has not yet been widely disseminated.

ERTS lends itself well to countywide or statewide inventorying and monitoring systems. The resolution was adequate for identifying most major vegetation types or zones in the Great Basin. Higher resolution would definitely be an advantage where more vegetational detail is required. Small stock ponds, critical to the livestock industry, could be monitored with a higher resolution system. The 18-day interval would be adequate for our study if there were no cloud cover, except for the critical growing season. The growing season requires more frequent coverage for optimum information. Cloud cover on only one overpass tends to leave large gaps in the data. For example, two of our study areas had no coverage between January and mid-June, a critical portion of the growing season. For the statewide inventories already described, ERTS-1 has proved its usefulness.

MSS 4 was evaluated routinely, but it was soon determined that this band was of little use to our investigations. MSS 5 and 7 bands were found to be the most useful for our investigation. MSS 5 provided the best resolution while MSS 7 has important uses for evaluating standing water surfaces and certain highly reflective vegetation types. For most of our analyses, MSS 6 offered no additional advantages.

NASA high flight data has been invaluable to us for purposes of supplementing ground data. Additional flights in other areas would also be of benefit in support of ERTS data.

Use of ground data is required in certain instances, but many times one cannot get the perspective from the ground required to accurately interpret ERTS data. We have found difficulty in sampling ERTS-1 signatures on the ground because of the variation found on the ground on seemingly homogeneous sites as viewed on ERTS-1 imagery. This is where NASA high flight imagery and our own 70 mm color and color infrared imagery is useful because it provides the overview and the resolution to see necessary detail and to make comparison.

REFERENCES

- Blackburn, W.H., Paul T. Tueller and Richard E. Eckert. 1969. Vegetation and soils of the Coils Creek Watershed. Nevada Agricultural Expt. Sta. Tech. Bull. Report R48. 80p.
- Tueller, Paul T. and Garwin Lorain. 1973. ERTS-1 evaluations of natural resource management applications in the Great Basin. First ERTS-1 Symposium on Significant Results. New Carrollton, Maryland. March.

USEFULNESS OF ERTS-1 SATELLITE IMAGERY AS A DATA-GATHERING TOOL BY RESOURCE MANAGERS IN THE BUREAU OF LAND MANAGEMENT

R. Gordon Bentley, *Bureau of Land Management, Denver, Colorado*

ABSTRACT

ERTS-1 satellite imagery can be an effective data-gathering tool for resource managers. Techniques are developed which allow managers to visually analyze simulated color infrared composite images to map perennial and ephemeral (annual) plant communities. Tentative results indicate that ephemeral plant growth and development and potential to produce forage can be monitored.

INTRODUCTION

The United States Department of the Interior, Bureau of Land Management (BLM) administers the natural resources of approximately 470 million acres of public domain lands in the 11 western states and Alaska. Funds and manpower have become more and more limited as costs rise and additional tasks are required by a public demanding increased services and a higher quality environment. A tool is needed which will allow resource managers to quickly collect initial information and effectively update that information on a regular schedule. Approximately 160 million acres of public lands in the western United States are grazed by livestock. A knowledge of the soils and vegetation of this land is basic to good resource management.

Studies were conducted during 1973 on public lands in Arizona, California, Oregon and Alaska. Results show that color composite satellite imagery can be used to map soils and vegetation to varying intensities depending upon the area being studied and the scale to which satellite imagery has been reproduced. For example, the density and height of vegetation affect how well soil boundaries can be mapped. In the California desert, where only three to five percent of the ground is covered by perennial vegetation, soils can be mapped accurately to the series level. In southeastern Oregon, where 30 to 50 percent of the ground is covered by perennial vegetation, soils are not as easily delineated. In the desert region of southern Arizona, production of ephemeral forage can be mapped fairly easy on sites which have a very open cover of Larrea tridentata - creosotebush, but this is a more difficult task on sites with a dense cover of mixed desert trees and shrubs. On all sites, photo enlargements yielded more information than the 1:1,000,000 contact prints.

Results from all sites lead to the conclusion that satellite imagery can be a useful tool. However, only detailed results for the south central Arizona study site are reported in this paper, see Figure 1. Of equal importance to

N74 30725

results is a knowledge of the techniques employed in deriving this information from satellite imagery. The techniques described below can be applied on any grazing lands administered by BLM. For a detailed discussion of results the reader is referred to the authors' Type III Final Report due January, 1974.

USE OF IMAGERY

General Procedure

Color composite simulated color infrared images at 1:1,000,000 scale were used for gathering resource information. Color composites were made by the Principal Investigator from NASA 9x9 inch multiband positive transparencies using a camera triple-exposure technique described in the authors' final report. The following is a discussion of the specific techniques used to obtain vegetation data from satellite imagery.

At the time of the satellite overpass ground truth data is collected. The resource manager (interpreter) gathers data concerning plant species composition, percent of ground covered by perennial plants and pounds per acre of ephemeral forage plants. This data is gathered on representative sample sites. It is important that data be gathered on at least one site representing each of the several different homogeneous areas identified on satellite imagery. If imagery of a previous flight is not available to help guide the location of sample ground truth sites, the resource manager should be careful to locate sites in vegetative types with obvious differences as seen on the ground. If sites are improperly located, corrections can be made when measurements are taken to record changes in vegetation later in the growing season. After the initial selection of sample sites, collection of ground truth data takes about one and one half days per satellite frame. The manager traverses five to ten percent of the 13,225 square miles as best he can depending upon the available road network.

When a current color composite satellite image is received it is first analyzed visually in the office by an interpreter. Homogeneous areas on the image are delineated on the basis of color, tone and texture, Krumpal (1973). Boundaries around distinct areas are recorded directly on overlay material. This process requires two to three hours. The interpreter then makes a reconnaissance flight from low flying aircraft (up to 10,000 ft. AGL) over the area covered by the ERTS-1 frame, using the satellite image and overlay for reference. During the flight he checks the content of homogeneous areas and boundaries between them with what he can see on the ground. Necessary corrections are made directly on the overlay. This process takes two to three hours.

Finally, information gained from analysis of satellite imagery is correlated with ground truth data taken on the representative sites. A specific color tone and textural pattern (signature) which separates one homogeneous area from another on the image is matched with the combination of topography and vegetative community which produced that particular signature. All areas scattered over the image with the same signature are then assigned the same

vegetative characteristics as identified by ground measurements collected on a representative site. Subsequent field checks made as the growing season progresses provide an opportunity to check the accuracy of this extrapolation process. The end product is an up-to-date map of vegetative conditions.

Detailed Analysis

Using ERTS-1 color composite frame 1085-17330, 16 Oct. 72, three distinct areas important to livestock management in the desert were clearly apparent. Dark blue areas with a rough texture identified desert mountain rock outcrops; sites with a shallow rocky soil which produce a light cover of ephemeral forage and impede access by livestock. Light blue or bluish-purple areas with a striated texture identified a complex mixture of desert trees and shrubs (Table 1) located on foothills and upper bajada slopes at the base of mountains. White areas with a striated to smooth texture identified nearly pure stands of creosotebush (Table 1) located on lower bajadas and valley floors.

Analysis of ERTS-1 color composite frame 1211-17334, 19 Feb. 73, revealed three broad classes of ephemeral forage production for both the tree-shrub and creosotebush sites. The color-texture key shown in Table 2 was used to separate areas producing various amounts of forage. Because the creosotebush sites produce very little perennial vegetation and have a potential to produce a large quantity of ephemeral forage they were designated as Ephemeral sites (Tables 2 & 3). The tree-shrub sites producing a large amount of perennial vegetation and a good variety of ephemeral species but a smaller quantity of ephemeral forage were designated as Perennial-Ephemeral sites (Tables 2 & 3). Forage classes for each of these two vegetative types showing pounds of ephemeral forage per acre are shown in Table 3.

PRODUCTS OBTAINED FROM ANALYSIS OF SATELLITE IMAGERY

Forage production of ephemeral plants was mapped for central Arizona from ERTS-1 color composite frame 1211-17334, 19 Feb. 73, 1:1,000,000 scale, see Figure 2. Growth and development of ephemeral plants can be monitored on periodic images taken during the growing season. Even slight differences can be seen when comparing images 1085-17330, 16 Oct. 72 and 1103-17332, 03 Nov. 72. Potential of areas to produce ephemeral forage can be determined, see Figure 3. This was done by comparing current forage production from Figure 2 with precipitation data from several stations scattered over the general study area and elevation of each specific site. The potential map is tentative since it is based on only one years data.

BENEFITS TO RESOURCE MANAGERS

Satellite imagery can theoretically be useful to resource managers as a data gathering tool. In a discussion of the usefulness of satellite imagery the assumption is made that imagery in a usable form can be placed

in the hands of the resource manager within one week of the date of the satellite overpass. At present, the most useful form of imagery is a second generation color composite at a scale of 1:250,000. This is because sophisticated analysis equipment is not readily available. Also, most BLM field personnel are trained in visual analysis techniques and additional training needed to use satellite imagery would be minimal. The 1:250,000 scale corresponds to the scale of U.S.G.S. Quadrangle maps now being used in many field offices.

When the ERTS system is fully operational, data such as shown in Figure 2, will be useful as a guide to the numbers of livestock which can properly harvest ephemeral livestock forage in the southwest. Ephemeral forage conditions are subject to extreme changes within a very short time (weeks). Periodic satellite imagery can be used as a tool to monitor these changes, providing up-to-date information over very large areas. This kind of information would be difficult to collect on the ground because of long distances and very short time periods involved.

REFERENCES

Krumpe, P.F. 1973. A regional approach to wildland resource distributional analysis utilizing high altitude and earth orbital imagery. Proc. American Soc. of Photogrammetry, 39th Annual Meeting, Washington, D.C. March 11-16, 1973. 336-371 p.

Figure 1 - Map showing location of the central Arizona test site.

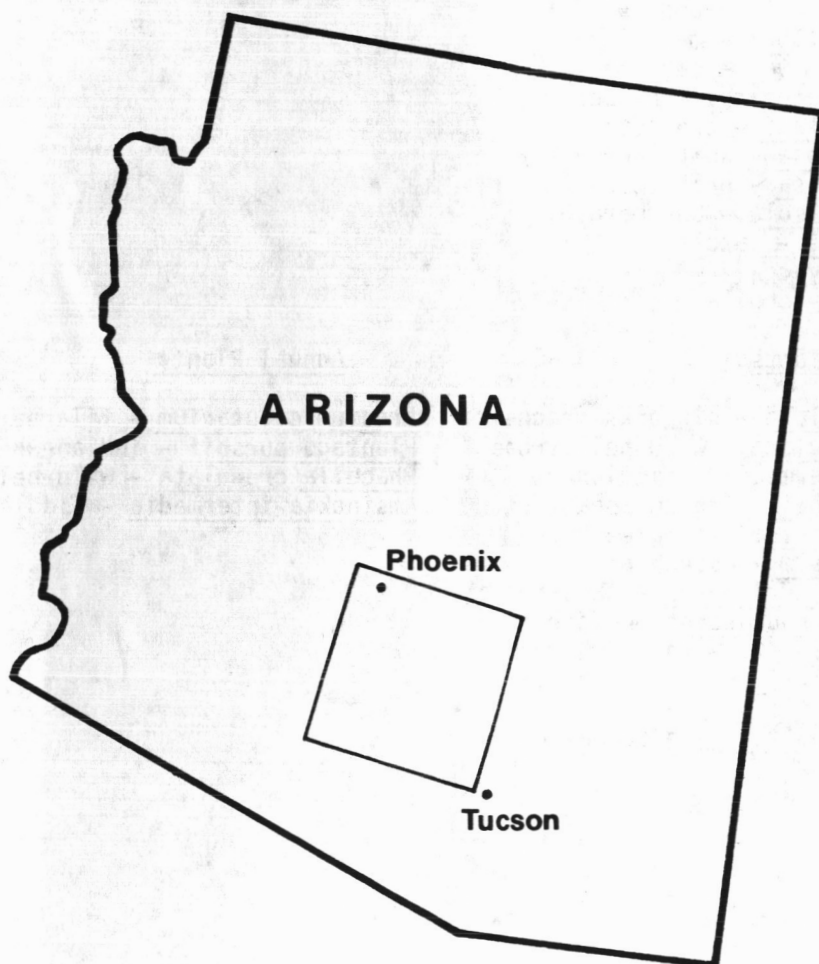


TABLE 1. List of perennial and ephemeral plants found on tree-shrub and creosotebush sites in central Arizona.

<u>Tree-Shrub Sites</u>	<u>Creosotebush Sites</u>
<u>Perennial Plants</u>	<u>Perennial Plants</u>
<u>Cercidium floridum</u> - paloverde <u>Olneya tesota</u> - ironwood <u>Prosopis juliflora</u> - mesquite <u>Carnegiea gigantea</u> - saguaro <u>Berberis haematocarpa</u> - barberry <u>Larrea tridentata</u> - creosotebush <u>Franseria dumosa</u> - white bursage <u>Encelia farinosa</u> - brittlebush <u>Hymenoclea salsola</u> - burrobrush <u>Acacia greggii</u> - catclaw <u>Yucca</u> spp. - yucca <u>Opuntia</u> spp. - cholla	<u>Larrea tridentata</u> - creosotebush
<u>Annual Plants</u>	<u>Annual Plants</u>
<u>Festuca octoflora</u> - sixweeks fescue <u>Phacelia crenulata</u> - wild-heliotrope <u>Amsinckia intermedia</u> - fiddleneck <u>Plantago purshii</u> - indian-wheat <u>Erodium cicutarium</u> - filaree <u>Eriogonum densum</u> - buckwheat <u>Nemacladus glanduliferus</u> - threadplant <u>Orthocarpus purpurascens</u> - escobita <u>Descurainia pinnata</u> - tansy-mustard <u>Astragalus nuttalianus</u> - milkvetch <u>Lupinus sparsiflorus</u> - lupine <u>Sphaeralcea coulteri</u> - globemallow	<u>Erodium cicutarium</u> - filaree <u>Plantago purshii</u> - indian-wheat <u>Phacelia crenulata</u> - wild-heliotrope <u>Amsinckia intermedia</u> - fiddleneck

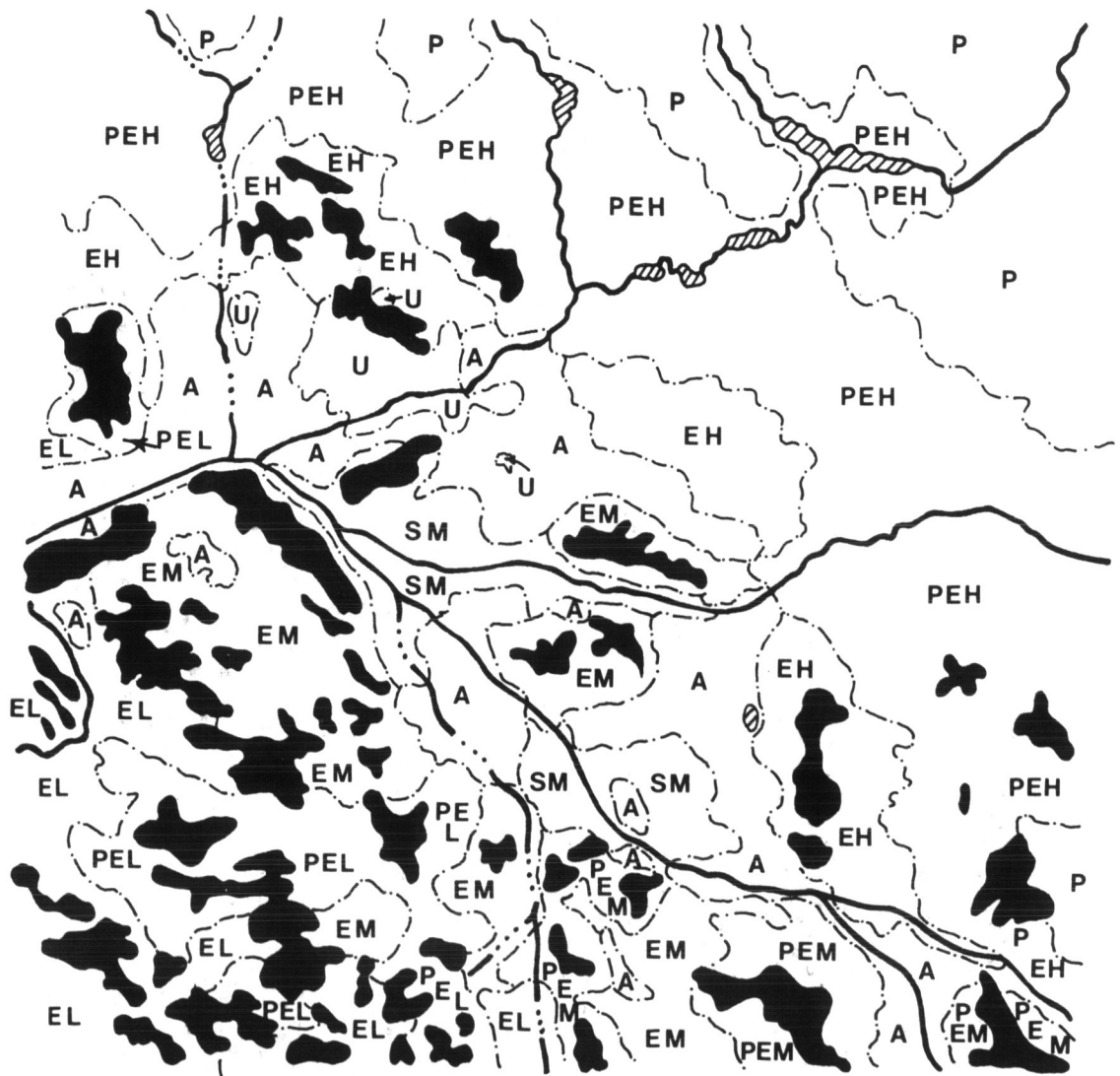
Table 2 - Color-texture key used to separate ephemeral forage production classes.

<u>Color</u>	<u>Texture</u>	<u>Vegetation Type</u>	<u>Ephemeral Forage Production Class</u>
Blue with red spots & streaks intermixed	Striated	Perennial-Ephemeral	Heavy
Bluish gray with pink blotches	Striated to smooth	Perennial-Ephemeral	Moderate
Blue	Striated to smooth	Perennial-Ephemeral	Light
Bright red	Mottled to smooth	Ephemeral	Heavy
Pink	Smooth	Ephemeral	Moderate
Light pink to white	Smooth	Ephemeral	Light
White, dark purple to red	Streaked	Drainage channel	Moderate
Blue to gray	Rough	Desert Mtn. outcrops	Light
Red to brownish red	Rough	Perennial	None

Table 3 - Ephemeral forage production for Winter Season 1972-73, as of April 18-19, 1973

<u>Vegetation Type</u>	<u>Production Class</u>	<u>Forage Production lbs./acre</u>
Urban	----	----
Agricultural Land	----	----
Perennial	----	----
Perennial - Ephemeral	Heavy	1000-1500
Perennial - Ephemeral	Moderate	500-1000
Perennial - Ephemeral	Light	up to 500
Saltbush (drainage channels)	Moderate	500-1000
Ephemeral	Heavy	3000-5000
Ephemeral	Moderate	2000-3000
Ephemeral	Light	up to 2000
Perennial - Ephemeral (Desert mtns-rock outcrops)	Light	up to 1000

Figure 2 - Ephemeral forage plant production as determined from ERTS satellite frame 1211-17334, 19 Feb. 73.

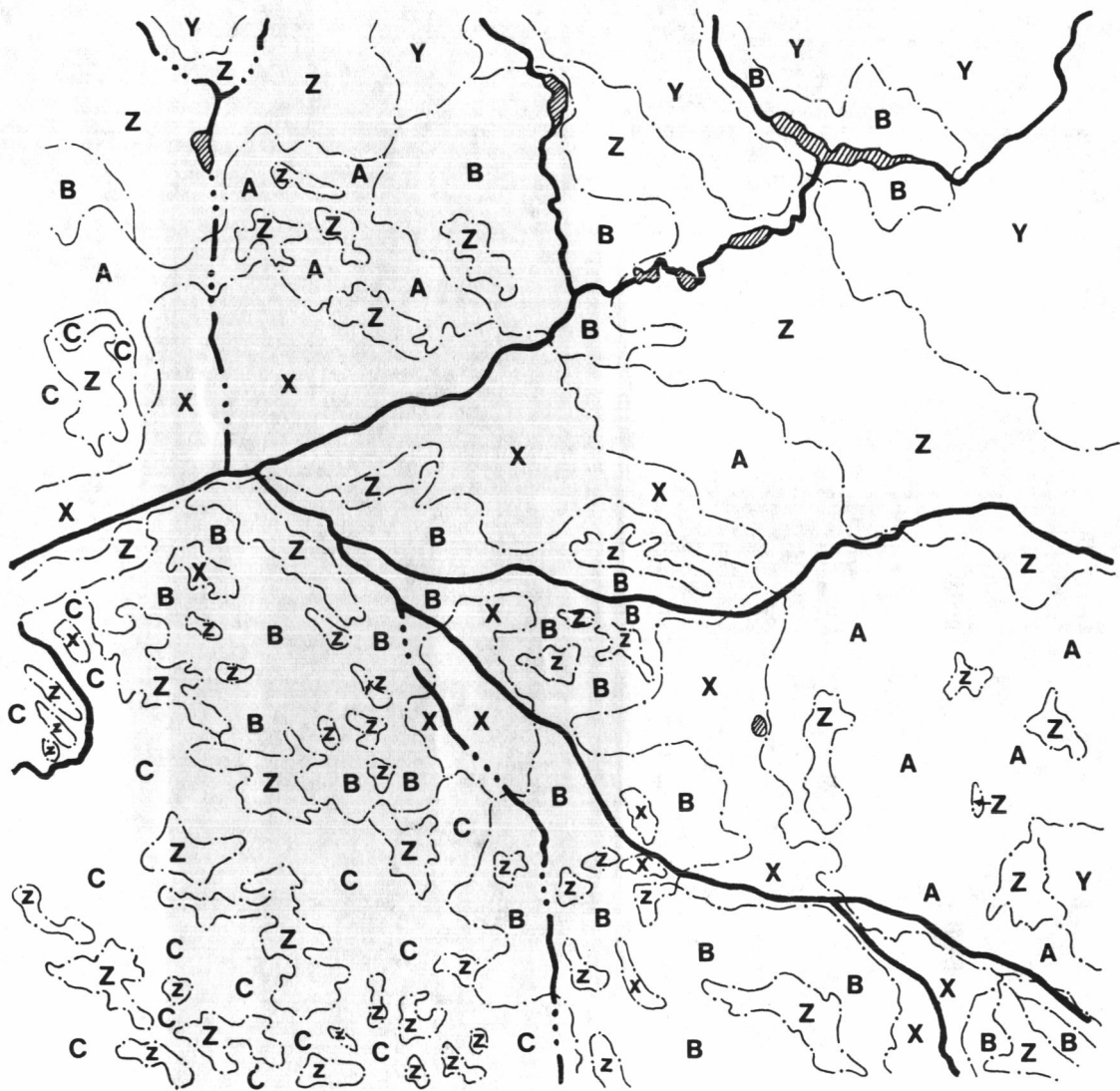


LEGEND

U - Urban Area
 A - Agricultural Land
 P - Perennial Plants
 PE - Perennial - Ephemeral
 E - Ephemeral
 S - Saltbush

H - Heavy Production
 M - Moderate Production
 L - Light Production
 ● - Rock Outcrop
 (light production)
 ▨ - Lake

Figure 3 - Potential of areas to produce ephemeral forage plants.



LEGEND

X - No Ephemeral Potential
(urban & agriculture)
Y - No Ephemeral Potential
(perennial plants)
Z - Low Useable Ephemeral
(steep topography)

A - High Ephemeral Potential
B - Moderate Ephemeral Potential
C - Low Ephemeral Potential

VEGETATION MAPPING FROM ERTS IMAGERY OF THE OKAVANGO DELTA

Douglas T. Williamson, *Spectral Africa (Pty) Limited, P.O. Box 2, Randfontein, Rep. of South Africa*

ABSTRACT

The Okavango is Botswana's major water resource. As yet it is essentially undeveloped and supports large wild life populations both within the system itself and in the adjacent semi-arid areas. Development of the delta for its water resources and recreational potential is inevitable and imminent. Much basic resources data is urgently required to facilitate sound planning.

Other workers have studied ERTS imagery of the delta from a geological and hydrological perspective. The present study has been specifically directed at mapping vegetation types within the delta and generally concerned with finding what information of value to plant and animal ecologists could be extracted from the imagery. To date it has been found that

- (i) It is possible to map broad vegetation types from the imagery. This has enabled preparation of a vegetation map of the delta which considerably refines existing maps.
- (ii) Imagery of the delta records the state of the system in a manner which will facilitate long-term studies of plant succession.
- (iii) Phenological events can be detected. This may allow inferences to be drawn about seasonal movements of animal populations.
- (iv) The imagery can be used to detect and map wild fires. This will be useful in determining the role of fire in the ecology of the region.

Using the imagery it is thus possible to map existing vegetation and monitor both short and long-term changes.

These results have been obtained after a few months of work using only colour composites of the delta and without sophisticated, automated techniques of data extraction and analysis. They demonstrate that ERTS type imagery can be

N 74
30726

a valuable tool to those responsible for planning and managing the exploitation of natural resources in the developing world.

INTRODUCTION

Botswana is a developing country in Southern Africa. It has an area of 570 000 km², much of which is sandy, featureless tree and shrub savanna. It is sparsely populated and its people are predominantly rural. The economy of the country has recently been stimulated by mineral discoveries but it is still almost entirely pastoral and agricultural with a significant fraction of the population living at a subsistence level. Several factors account for this low level of development, aridity being amongst the most important of these.

The Okavango delta is a major water resource but, although it obviously has a pivotal role in the future of Botswana, it remains essentially undeveloped. Its rich fauna and flora are largely intact and until recently were utilized primarily to meet individual subsistence requirements. The survival of the delta in a relatively pristine condition is probably attributable to its remoteness and the presence of the tsetse fly (Glossina morsitans) host to the trypanosome organisms which cause fatal diseases in man and his domestic stock. However, this state of affairs is rapidly changing. With improved communications, tourism and hunting are increasing. The projected eradication of the tsetse fly will result in penetration of the delta for pastoral and possibly agricultural exploitation. The recent mineral discoveries in Botswana mean that development of the Delta's water resources for industrial purposes is inevitable and imminent.

At this point the ecology of the Delta is poorly understood and much environmental data is urgently required if the impending developments are to be implemented on a sound basis.

The entire Okavango Delta has been covered by ERTS imagery. The imagery has thus far been studied from the perspectives of geology (Akehurst, 1973) and hydrology (Wilson, 1973). The main aim of the present study is to map broad vegetation types in the Delta region. This objective was selected because, as pointed out by Anderson et al (1973), knowledge of the distribution and importance of vegetation types can be applied in a wide range of fields such as plant ecology, hydrology, soil science, meteorology, wild life biology and management and land use planning.

VEGETATION MAPPING

Only photographic ERTS-1 products have been available for the vegetation mapping program. A variety of products, detailed in the Table, are being used.

TABLE : PHOTOGRAPHIC PRODUCTS USED IN OKAVANGO STUDY

PRODUCT	SCALE	APPLICATION
1. Black and White paper prints, MSS Bands 4, 5 & 7.	1:1 000 000	Annotation in the field
2. Black and White paper prints, individual MSS bands	1:1 000 000	Delineating features accentuated in individual bands
3. Color composite transparencies MSS bands 4, 5 & 7.	1:1 000 000	Differentiating color tones by transmission densitometry.
4. Color composite paper prints, MSS bands 4, 5 & 7.	1:1 000 000	Interpretation and mapping at this scale
5. Color composite paper prints, MSS bands 4, 5 & 7.	1:500 000	Mosaic for field work aid to interpretation.
6. Color composite paper prints, MSS bands 4, 5 & 7.	1:250 000	Interpretation and mapping at this scale.

for identifying and delineating vegetation types the color composites have proved markedly superior to the black and white prints, the latter being used for field annotation simply because they are less expensive to produce.

Three images have so far been studied in detail for vegetation mapping. These are NASA ERTS-E-1054-07565 and 1054-07571 of September 15, 1972 and ERTS-E-1055-08023 of September 16, 1972. Image ERTS-E-1054-07565 which portrays a large portion of the delta, is reproduced as figure 1.

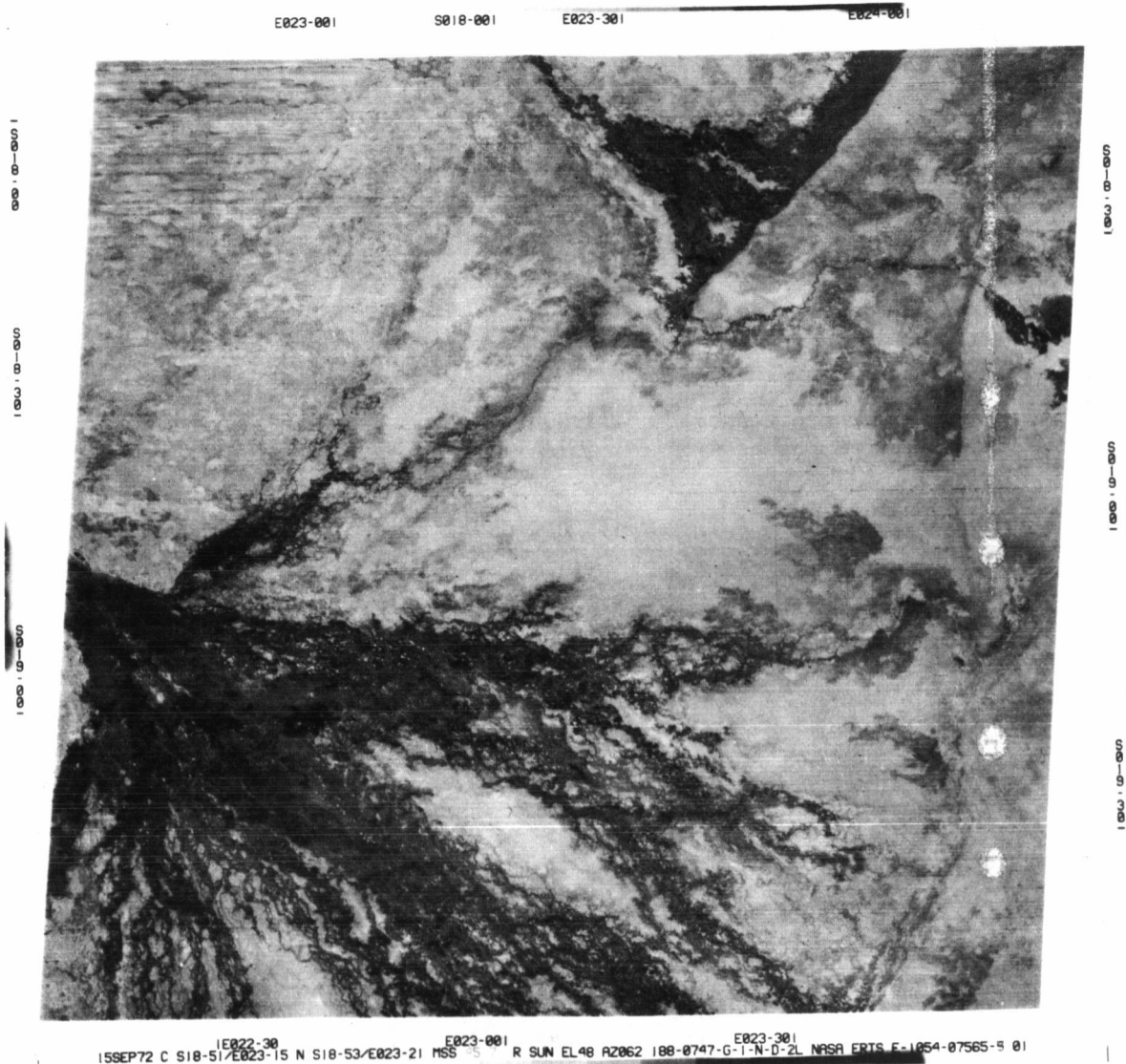


FIG. 1 : ERTS-image of the Okavango Delta.

Initial interpretation of vegetation patterns was based on ground truth gathered by photographing vegetation on the ground at some 86 points in the delta and the adjacent semi-arid areas.

On the basis of this data a provisional vegetation map has been prepared from ERTS imagery in which six habitat types are identified, namely (i) inundated swamp (ii) dried-up swamp (iii) closed woodland (woodland/savanna woodland), (iv) open woodland (tree and shrub/scrub savanna), (v) mosaic of trees, shrub/scrub and grass, (vi) grassland. The interpretation and mapping has been checked by aircraft overflight and found to be substantially correct.

Comparison of figures 2 and 3 shows that the map prepared from ERTS imagery constitutes a considerable refinement of existing vegetation maps of the region. On the ERTS based map vegetation types are delineated with significantly more detail and precision than on existing maps.

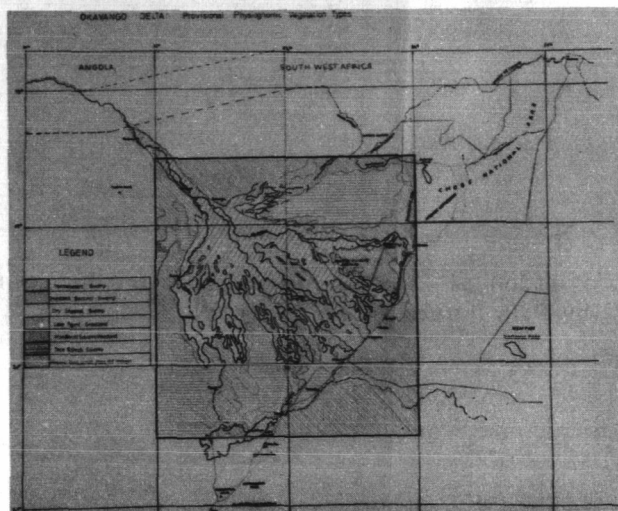
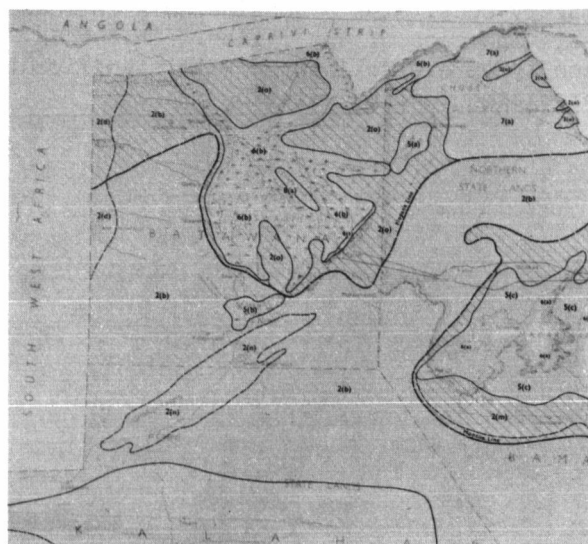


FIG. 2 : Vegetation map prepared from ERTS imagery of the Okavango Delta.



**FIG. 3 : Portion of Provisional Vegetation Map of Botswana
by P.R. Weare and A. Yalala.**

It is hoped that it will be possible to further refine the map by a comparative study of sequential imagery, to which I have not yet had access. This hope is based on the likelihood that the sequential imagery will enable two important distinctions to be made. Firstly it should be possible to separate areas that are seasonally flooded from areas of permanent swamp. Secondly it should be possible to distinguish areas dominated by individual species, such as mopane (Colophospermum mopane), on the basis of phenological characteristics.

FUTURE AREAS OF STUDY

The application of ERTS imagery in other ways seems feasible and needs to be investigated in further studies. For example, of considerable importance is the fact that the imagery records the vegetation of the delta in a way that will facilitate long-term studies of plant succession. The imagery was gathered before any major development or exploitation of the delta and it records important features, for instance the wetland-upland boundary, very clearly. It is almost certain that impending developments will induce successional changes. Comparison with imagery of a later date will rapidly reveal any degradation or adverse changes which may result from such developments.

The imagery also records phenological events. By observing seasonal changes in vegetation and the distribution of surface water it should be possible to draw inferences about the seasonal movements of animal populations.

Finally, Wightman (1973) has shown that ERTS imagery can be used to detect and map wildfires. This will for the first time enable the compilation of a comprehensive record of burning and provide a definitive insight into the role of fire in the ecology of the region.

SUMMARY AND CONCLUSION

The present study has been in progress for five months. It has used no sophisticated techniques of data extraction and analysis. Using ERTS color composites existing vegetation maps of the Okavango delta have been improved and study of sequential imagery is expected to allow further refinement of vegetation mapping. It will very likely be feasible to monitor both short- and long-term changes in the vegetation of the delta with ERTS type coverage. The ERTS system thus enables the inventory and surveillance of a key environmental component.

This capability will clearly enhance Botswana's ability to manage its natural resources. ERTS imagery can thus be a valuable tool to those responsible for planning and managing the exploitation of natural resources in the developing nations.

REFERENCES

Akehurst, S.M.

1973 ERTS-1 Type I and Type II Reports for period September 1972 to May, 1973.

S.R. No. 9643. Catalogue No. 1019.

Anderson, James H., Lewis Shapiro and Albert E. Belon

1973. Vegetative and Geologic Mapping of the Western

Seward Peninsula, Alaska, Based on ERTS-1 imagery.

Proc. Symp. Significant Results from ERTS-1 March, 1973,

Vol. 1 pg. 67-74.

Wightman, J.M.

1973. Detection, Mapping and Estimation of Rate of Spread of Grass Fires from Southern African ERTS-1 imagery.

Proc. Symp. Significant Results from ERTS-1, March, 1973.

Vol. 1. pg. 593-601.

Wilson, B.H.

1973. ERTS-1 Type I Report for the period September to December, 1972.

SR. No. 9643. Catalogue No. 1019.

MONITORING VEGETATION SYSTEMS IN THE GREAT PLAINS WITH ERTS

J. W. Rouse, Jr., R. H. Haas, J. A. Schell and D. W. Deering, *Remote Sensing Center, Texas A&M University, College Station, Texas*

ABSTRACT

The Great Plains Corridor rangeland project being conducted at Texas A&M University utilizes natural vegetation systems as phenological indicators of seasonal development and climatic effects upon regional growth conditions. A method has been developed for quantitative measurement of vegetation conditions over broad regions using ERTS-1 MSS data. Radiance values recorded in ERTS-1 spectral bands 5 and 7, corrected for sun angle, are used to compute a band ratio parameter which is shown to be correlated with aboveground green biomass on rangelands.

INTRODUCTION

The Great Plains of the central United States produces over forty percent of the nation's beef and much of the country's grain. The beef industry in this region is a \$23 billion operation, which is extremely vulnerable to adverse seasonal or climatic conditions. The stability of the beef and agricultural products industry in the Great Plains is contingent upon decisions made by the 400,000 farm and ranch owners in this region. These private operators need timely information on regional range forage conditions and crop production levels upon which to base their management decisions. This paper reports on an ERTS-1 study of rangelands in the Great Plains that has established the potential for using ERTS-type data to provide quantitative regional vegetative condition information required in support of these agricultural operations.

The Great Plains Corridor rangeland project utilizes natural vegetation systems as phenological indicators of seasonal development and climatic effects upon regional growth conditions. The basic task is that of monitoring the vernal advancement and retrogradation of vegetation (green wave effect) throughout the uniform Mixed Prairie Grassland Association extending from south Texas into Canada. The objective of the work is to determine the feasibility of using ERTS-type data to map regional vegetation conditions throughout the growing season for the Great Plains.

1 N74 30727

The study employs a network of ten test sites in six states extending from south Texas into North Dakota. Ground observations recorded every eighteen days at each site include green biomass, moisture content of vegetation, weather information, etc. ERTS-1 MSS data have been acquired for all sites for four full seasons.

The ERTS-1 MSS data were computer processed for selected areas of each site. Spectral reflectance data were analyzed for each available date for each site. The measurements were corrected for seasonal sun angle differences to permit temporal comparisons. Radiance values recorded in ERTS-1 spectral bands 5 and 7 were used to compute a Band Ratio Parameter which is shown to be correlated with aboveground green biomass and vegetation moisture content.

This research has established a method for obtaining a quantitative measurement of vegetation conditions over broad regions using ERTS-1 MSS data. It is anticipated that this capability will be further developed to provide regional rangeland vegetation condition and growing condition information needed in rangeland management and agribusiness activities in the Great Plains.

OBJECTIVES

The objectives of the Great Plains Corridor Project were established to examine three basic hypotheses:

Hypothesis 1: The vernal advancement and retrogradation of vegetation (green wave effect) can be discriminated on a regional basis using repetitive multispectral data.

Hypothesis 2: Natural vegetation parameters provide a new information source for regional agri-business use.

Hypothesis 3: Temporal effects are important in discriminating broad landforms, soil associations, vegetation types, and other natural resource features.

The specific objectives are:

1. Establish a test site network for collection of ERTS-1 correlated ground data in the Great Plains Corridor.
2. Use ERTS-1 data for charting the "Green Wave Effect" in the Great Plains Corridor.
3. Correlate changes in reflectance characteristics of vegetation measured by ERTS-1 with environmental and growth conditions.

4. Evaluate the use of ERTS-1 data for measuring the kind, amount, and condition of rangeland vegetation.
5. Evaluate the feasibility of an operational satellite system for monitoring the status of natural vegetation in the Great Plains Corridor.

GREAT PLAINS CORRIDOR

An effective rangeland test site network was established within the Great Plains Corridor region during the initial phases of the ERTS-1 investigation. This test site network consists of ten study sites (Fig. 1), nine of which lie within the Mixed Prairie grassland association. The headquarters study site at College Station, Texas occurs within the closely allied but somewhat more humid True Prairie grassland association.

With the exception of the College Station and Weslaco study sites, which are at elevations of 314 and 225 ft., respectively, the Great Plains Corridor test site elevations span only 1800 ft., from Texas through North Dakota. Their elevations range between 1100 and 2900 ft.

Loamy soils predominate on most of the study areas within the Corridor. However, one southern site (Woodward) and one northern site (Sand Hills) are dominated by sandy soils. Two southern sites (Sonora and Throckmorton) and one northern site (Cottonwood) are dominated by clayey soils.

Important community dominants within the Corridor include warm-season grasses (bluegrams, buffalograss, sideoats grams, and big and little bluestems) and cool-season grasses (western wheatgrass, needle-and-thread, and Texas wintergrass). Stipa and Bouteloua genera are considered to be characteristic of the Mixed Prairie and are present throughout the association. The relative homogeneity of the Great Plains Corridor and of the included study sites, in terms of climate and soils as evidenced through vegetation expression, is demonstrated in Figure 2.

Each of the ten sites is an established research area of a state agricultural experiment station or the USDA. All sites are monitored by the experienced personnel normally associated with the several stations. The ground observations recorded coincident with the ERTS-1 passes include green biomass, standing biomass, moisture content of vegetation, and phenology of dominant species. Ground photography and grass clippings are obtained during each sampling. Weather information is also recorded for all sites.

DATA PROCESSING

The objectives of this study require the acquisition of ERTS-1 measurements showing temporal changes at each of ten locations throughout the Great Plains Corridor. The problem of obtaining radiance data from identical locations on multiple orbits has been handled in two stages. In the first stage, a 7km x 7km area centered on the test site is located, using a computer greymap, and the integrated radiance is computed for each of the MSS bands. The data presented in this paper were obtained from this type processing. The second stage involves "masking" the 7km x 7km sections to remove non-grassland areas. For many sites, this procedure removes only a small percentage of the scene, e.g. Throckmorton.

The radiance measured in each MSS band is computed from the ERTS CCT counts and corrected for seasonal sun angle differences by dividing the CCT value by the sine of the inclination angle of the sun. The correction procedure has been tested using measurements of temporally independent targets.

The data processing procedure has been formalized and implemented on a digital computer to generate the Site Processing Report shown in Figure 3 for each frame of usable data.

SPECTRAL ANALYSIS

The processing of ERTS MSS data provides four parameters which can be analyzed relative to the ground observations. However, previous studies have shown that combinations of these four parameters can provide more useful parameters for specific comparisons. For the purposes of this project, the parameter obtained by taking the difference between the radiance values in bands 5 and 7 has been found to be of particular significance. Although other combinations have been found which correlate with vegetation condition, this project has established that bands 5 and 7 do provide a single quantity indicative of the aboveground green biomass, and consequently the present analysis activity has been restricted to this parameter.

The specific parameter employed is the Band Ratio Parameter (BRP) defined as the difference in the ERTS radiance value measured in bands 5 and 7, divided by their sum. The normalization procedure is used to eliminate seasonal sun angle differences and to minimize the effect of atmospheric attenuation. To avoid working with negative BRP values and the possibility that the variance of the ratio would be proportional to the mean values, a square-root transformation is also computed. This parameter, termed the

Transformed Vegetation Index (TVI), is equal to the square-root of the BRP plus an arbitrary constant. The constant selected was 0.5.

A step-down regression analysis of twenty-nine data sets from the five southern test sites indicated that dry biomass, percent green estimate, moisture content, and their interactions accounted for 60% of the variation in TVI values computed from the heterogeneous 7km x 7km areas. However, data from the uniform grassland site near Throckmorton, Texas show that TVI is highly correlated to vegetation condition. At Throckmorton, the vegetation moisture content and percent green estimate, along with their interaction, accounts for 99% of the variation of TVI for eight sampling dates. The green biomass parameter alone accounts for 89% of the variation in TVI. Addition of the vegetation moisture content and green biomass interaction to the regression of green biomass with TVI increases the accountable variation to 93%. Figure 4 shows the relationship of TVI and green biomass measured for eight dates at the Throckmorton test site.

Analysis of these data suggest that a threshold exists such that the TVI is insensitive to biomass and/or vegetation moisture content below the threshold values. The implication is that sparsely vegetated areas are not amenable to TVI characterization. However, further analysis is necessary to confirm this preliminary indication.

The TVI parameters appear to be most adequate for monitoring the vernal progression and retrogradation of vegetation within the Great Plains Corridor and has good potential for measuring green biomass in increments to useful for regional agricultural applications.

CONCLUSION

This paper provides a brief summary of selected aspects of the Great Plains Corridor Project being conducted at Texas A&M University. The emphasis here is on the quantification of ERTS-1 MSS data to provide measurements of vegetation conditions on a regional basis. The project includes other analysis activities using ERTS-1 data, including image analysis, using color composites and black and white images, and interactive computer analysis. The net result of these activities is confirmation that the basic hypotheses of the study are true.

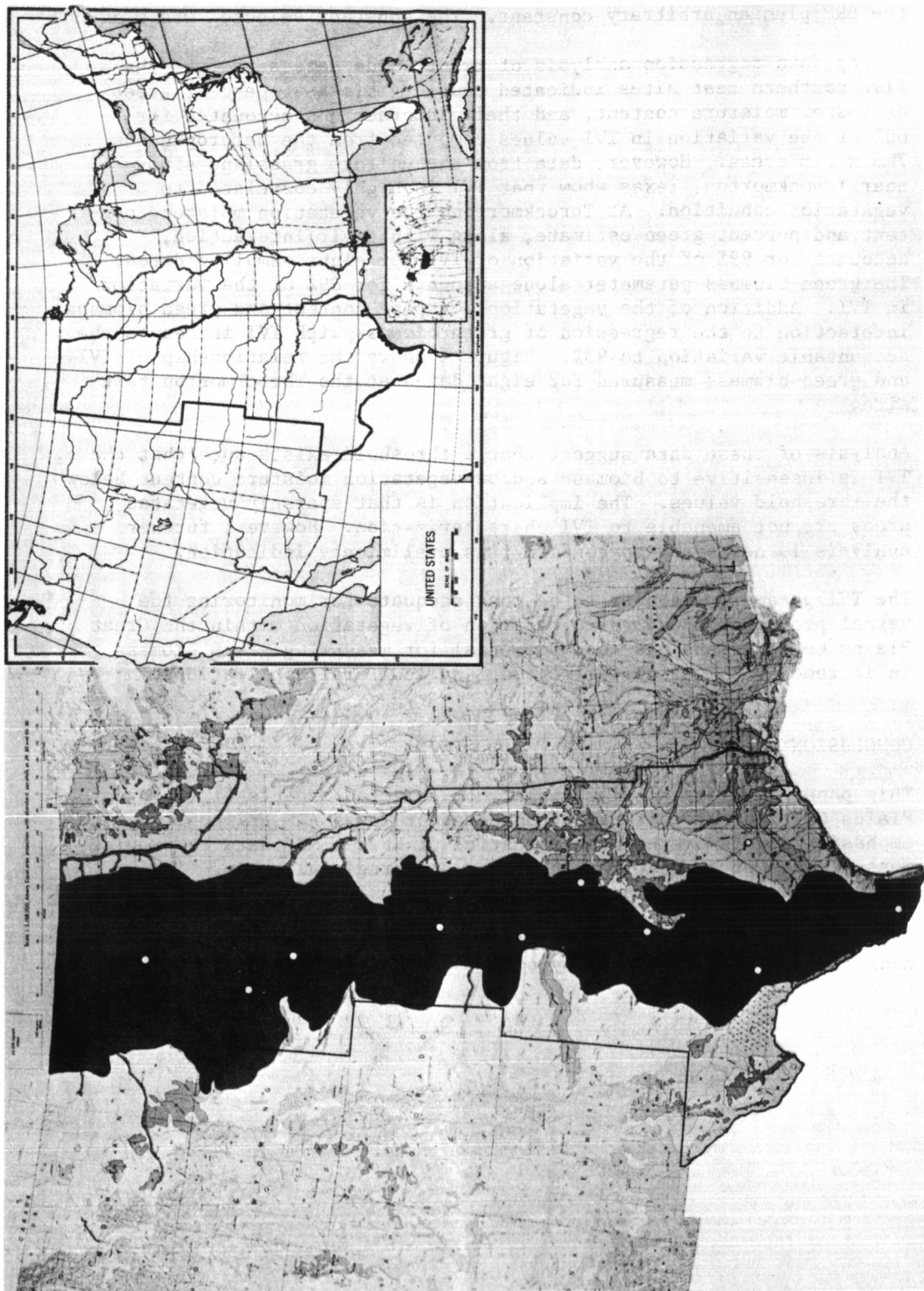


Figure 1. Great Plains Corridor and test site network.

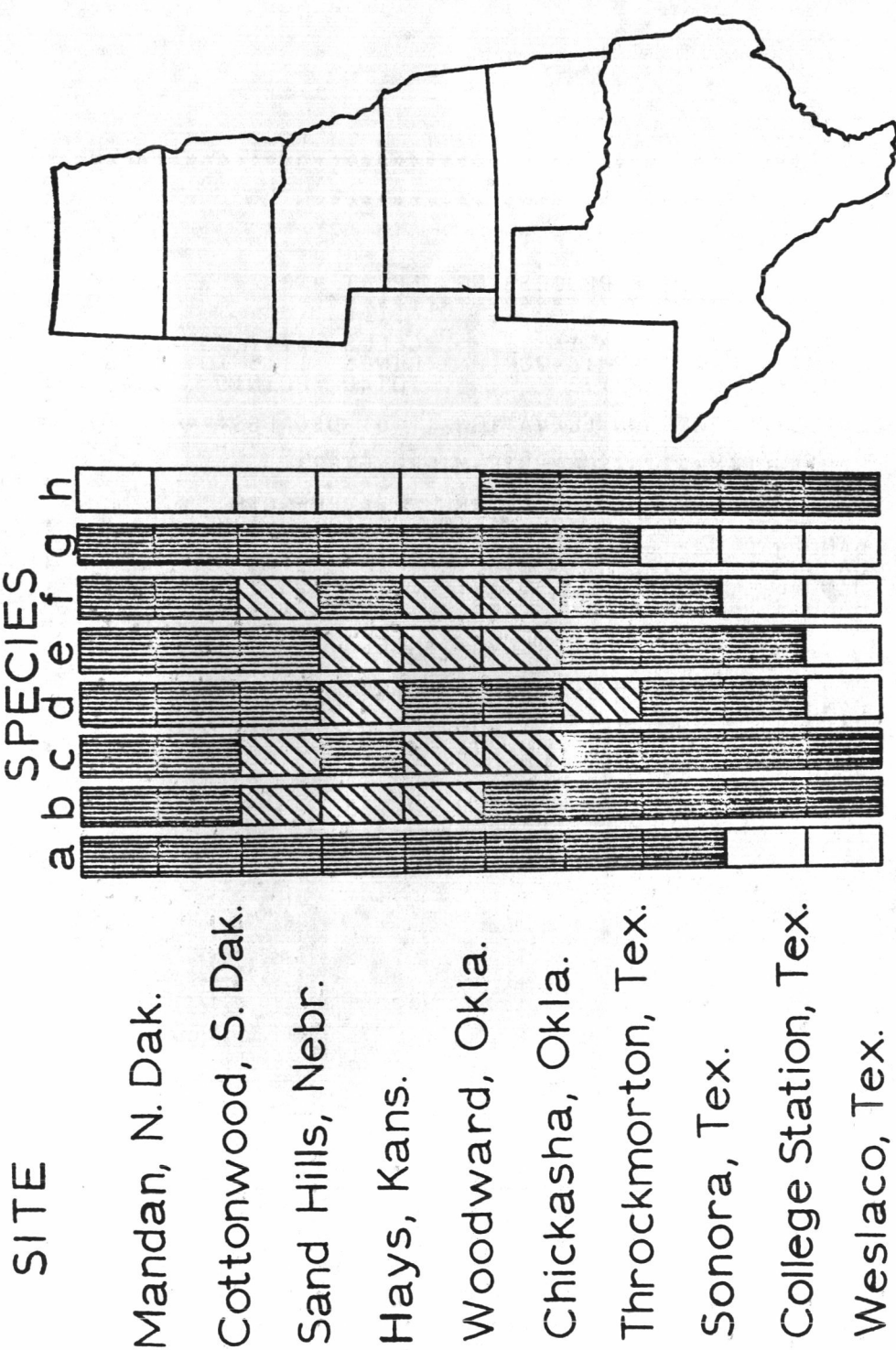


Figure 2. Occurrence of eight dominant grasses on the Great Plains Corridor test sites (vertical stripes), or within the region indicated (diagonal stripes). Dominant grasses are: a) blue grama, b) sideoats grama, c) buffalograss, d) little bluestem, e) big bluestem, f) western wheatgrass, g) needle-and-thread, h) Texas wintergrass.

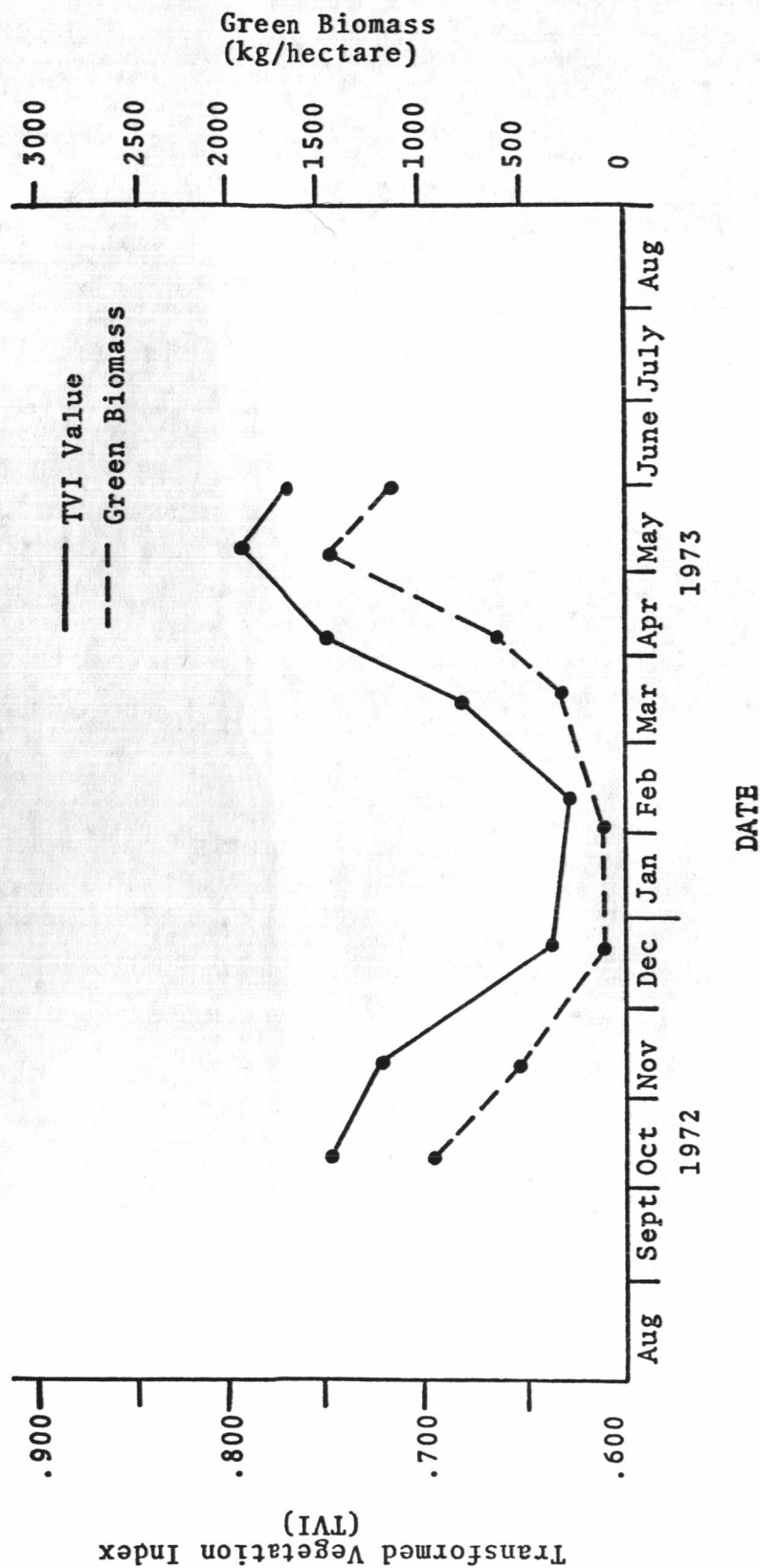
GREAT PLAINS CORRIDOR PROJECT

```
*****  
*                                     *  
*               ERTS-1              *  
*    SITE PROCESSING REPORT    *  
*****  
  
SITE DESIGNATOR: GP 3# 1          CELLS   1147 TO   1266  
IMAGE IDENTIFIER: 1292-16420      LINES   1115 TO   1196  
DATE ACQUIRED:     11MAY73        TOTAL POINTS 9840  
  
***CORRECTED FOR SUN ELEVATION    61 DEGREES***  
  
RADIANCE(MWATTS/SQCM-STR-MICROMETER)  
  
            MEAN           STANDARD       WAVELENGTH  
            DEVIATION      (MICROMETERS)  
BAND 4      8.01             1.59         .5 - .6  
BAND 5      5.22             0.80         .6 - .7  
BAND 6      7.56             0.57         .7 - .8  
BAND 7      6.76             0.58         .8 -1.1  
  
NORMALIZED COVARIANCES  
  
BAND 4      BAND 5      BAND 6      BAND 7  
BAND 4      1.000       0.301       0.084      -0.025  
BAND 5      0.301       1.000       0.278      -0.059  
BAND 6      0.084       0.278       1.000       0.803  
BAND 7     -0.025      -0.059       0.803       1.000  
  
BAND RATIO PARAMETER 0.128  
TRANSFORMED PARAMETER 0.793  
  
+-----+  
| 16.0 | +  
|      | |  
|      | |  
|      | |  
|      | |  
| 8.0  | +  
|      | |  
|      | |  
|      | |  
|      | |  
|      | |  
| 0.0  | +-----+  
|      | | 0.5  | 0.6  | 0.7  | 0.8  | 0.9  | 1.0 |  
|      | | RADIANC VS WAVELNGTH  
+-----+  
  
PREPARED BY:TEXAS A&M UNIVERSITY, REMOTE SENSING CENTER  
DATA ANALYSIS LABORATORY 11SEP73
```

Figure 3. Site Processing Report.

GREAT PLAINS CORRIDOR PROJECT
THROCKMORTON TEST SITE

Figure 4. ERTS-1 Transformed Vegetation Index Values Vs. Green Biomass Data



AGRICULTURAL UTILIZATION OF ERTS-1 DATA IN THAILAND

Pradisth Cheosakul, Boon Indrambarya, Joseph O. Morgan and Suvit Vibulsresth, *Thailand National Programme* of the Earth Resources Technology Satellite*

I shall take this opportunity to report briefly on recent advances made in three disciplinary areas that are of major importance to Thailand. They are Agriculture, Forestry, and Land Use Classification.

ERTS investigations are currently underway in some six or seven government departments. As has already been reported, a six week intensive training course in remote sensing was given in Bangkok last year, under the auspices of the U.S. Operation Mission to Thailand and the U.S. Geological Survey. Thai scientists and technicians who attended that course have since been working on a variety of ERTS projects in several disciplinary areas.

Preliminary investigations of the ERTS-1 Data have been so successful that the Thai Government has decided to develop a remote sensing data handling and research center, and USOM has agreed to provide additional training and support for a period of two years.

We have in hand more than 379 scenes from the ERTS multispectral scanner. Since the entire country has been covered, in some places as many as nine times, we have a considerable amount of data to work with and can envisage to do much constructive work.

Now I will present some of the current project work by means of 15 figures.

AGRICULTURE

The task of delineating agricultural regions directly from ERTS images is carried out in the Ministry of Agriculture and Cooperatives. A small task force of trained technicians is presently carrying out this work and is evaluating several types of processed data.

Figure 1 shows a partially annotated color enlargement, obtained from the General Electric Company (scale about 1:350,000), which has been checked rather extensively by means of field trips and aircraft flights. It shows the large rice growing region to the north of Bangkok (Bangkok is at lower right) and areas of other crops that can be differentiated by experienced interpreters.

Figure 2 is a computer printout furnished by Purdue LARS. Although it was made by use of an unsupervised clustering processing routine, and by scientists at LARS who are quite unfamiliar with Thailand, it is an accurate and informative representation. This hand colored printout shows inundated rice paddies in blue (October scene), vegetated areas in orange and red, and bare soil and clouds in white. It has been determined that the areas colored orange represent orchard crops quite accurately. The rectangular area, is seen better in the next figure.

*National Research Council, 196 Phahonyothin Road, Bangkok 9 Thailand

IN 74 30728

Figure 3 is a large Buddhist compound edged by a moat or canal. The center area of the compound is vegetated, and the small area at center right is slightly raised, bare ground with a single large monastery, as shown in Figure 4.

Figure 5 is an Ektachrome view of a part of the compound and the surrounding moat.

Figure 6 is an Ektachrome infrared view from another angle; the area containing the building is at center right. Our investigating teams use these two films routinely, in 35 mm format, in low altitude aerial reconnaissance surveys.

Figure 7 The color print of the Bangkok region is shown again, to point out a very large alluvial fan that had not been identified as such until this ERTS image became available.

Figure 8 shows this alluvial fan as portrayed on the analogue display unit at the University of Kansas in January 1973.

Figure 9 shows a color scene made from two MSS band 7 frames imaged during different months, once (red color) in October 1972, when the Mun river was over its banks, and again (blue color) in January 1973, when the flood water had subsided. This technique of change detection has proven to be an accurate and rapid means of investigating flood patterns and is being used by the Agriculture and Irrigation Departments.

FORESTRY

The Royal Forestry Department is using 1:500,000 scale band 5 and band 7 prints, diazochrome color composites, and existing air photos of 1:50,000 scale to map changes in forest area. This is an important project for Thailand, because it is not possible, with available resources, to patrol all of the remote forest areas - hence they are not effectively protected against illegal destruction of nomadic tribes, farmers needing new land, and unlicensed timber cutters.

Our foresters have measured the decrease in forest area in six of the 72 provinces of the country, since the most recent previous survey. In Chonburi province, where no survey has been made since 1961, evaluation of ERTS images shows a decrease in forest area of more than 23%. The Department will complete a new survey of the entire country in the current fiscal year, a task which requires ten years and many millions of baht if made from new aerial photography.

Figure 10 shows the new forestry map of one region which has been drastically cut back in recent years. It was made in 1973 from 7-8 frames of ERTS images taken in 1972 and 1973.

Figure 11 is a band 5 image of part of this area, and

Figure 12 is a color infrared aerial photo of a partially destroyed forest. The green areas have been slashed down and burned over. Some older burned areas, in pink, have been planted in tapioca and other crops. Some of these areas will soon be more carefully documented, using our four lens aerial camera and four channel multispectral viewer.

Land Use Classification

It is found that existing land use maps of Thailand can be improved and updated with the aid of ERTS images. The Land Development Department is currently using 1:500,000 scale black and white prints, drawing the boundaries directly on the print as illustrated in the following three figures.

Figure 13 showing the Central plain of Thailand.

Figure 14 showing the Northern part of the Central plain.

Figure 15 showing the Mekhong River

Aerial photos and ground data are used to verify vegetation and soil types. The information is then transferred to a base map.

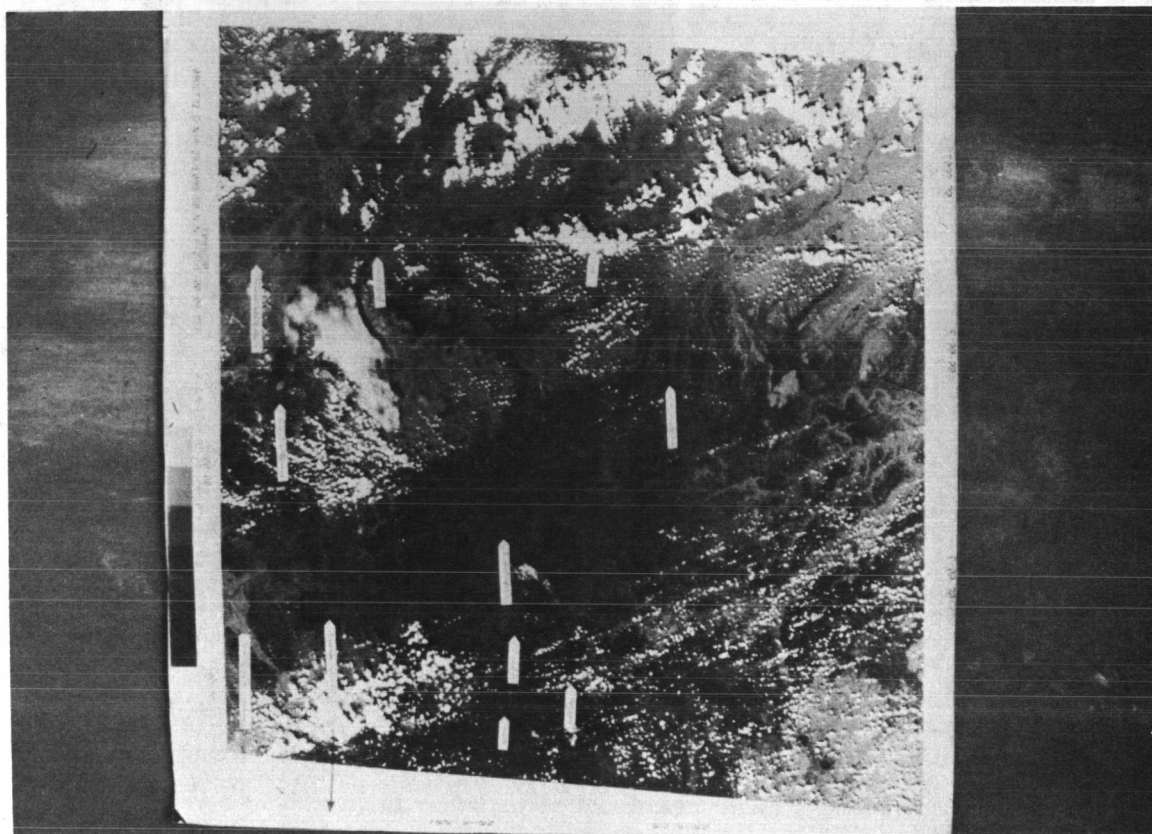


Figure 1

SERIAL NUMBER----- 50534601
ROW NUMBER----- 126601
FLIGHT LINE--- 10780320 1881
DATA STORAGE TAPE/FILE-- 1771
REFORMATTING DATE- JUNE 5, 1973

CLASSIFIED- MAY 15, 1973
DATE----- OCT 9, 1972
TIME----- 1012 HOURS
ALTITUDE----- 3062000 FEET
GROUND HEADLINE----- 108

CHANNELS USED

CHANNEL 1	SPECTRAL BAND	0.5 TO 0.60 MICROMETERS	CALIBRATION CODE = 1	CO = 0.0
CHANNEL 2	SPECTRAL BAND	0.60 TO 0.70 MICROMETERS	CALIBRATION CODE = 1	CO = 0.0
CHANNEL 3	SPECTRAL BAND	0.70 TO 0.80 MICROMETERS	CALIBRATION CODE = 1	CO = 0.0
CHANNEL 4	SPECTRAL BAND	0.80 TO 1.10 MICROMETERS	CALIBRATION CODE = 1	CO = 0.0

CLASSICS

SYMBOL	CLASS	GROUP
	NS- 1/10	CLOUDS
	NS- 2/10	CLOUDS
	NS- 3/10	CLOUDS
	NS- 4/10	VEG 1
	NS- 5/10	VEG 2




SYMBOL	CLASS	GROUP
+	NS- 6/10	VEG 3
.	NS- 7/10	SOILURBN
	NS- 8/10	VEG 4
	NS- 9/10	WATER
	NS-10/10	SHADSH20



Figure 2

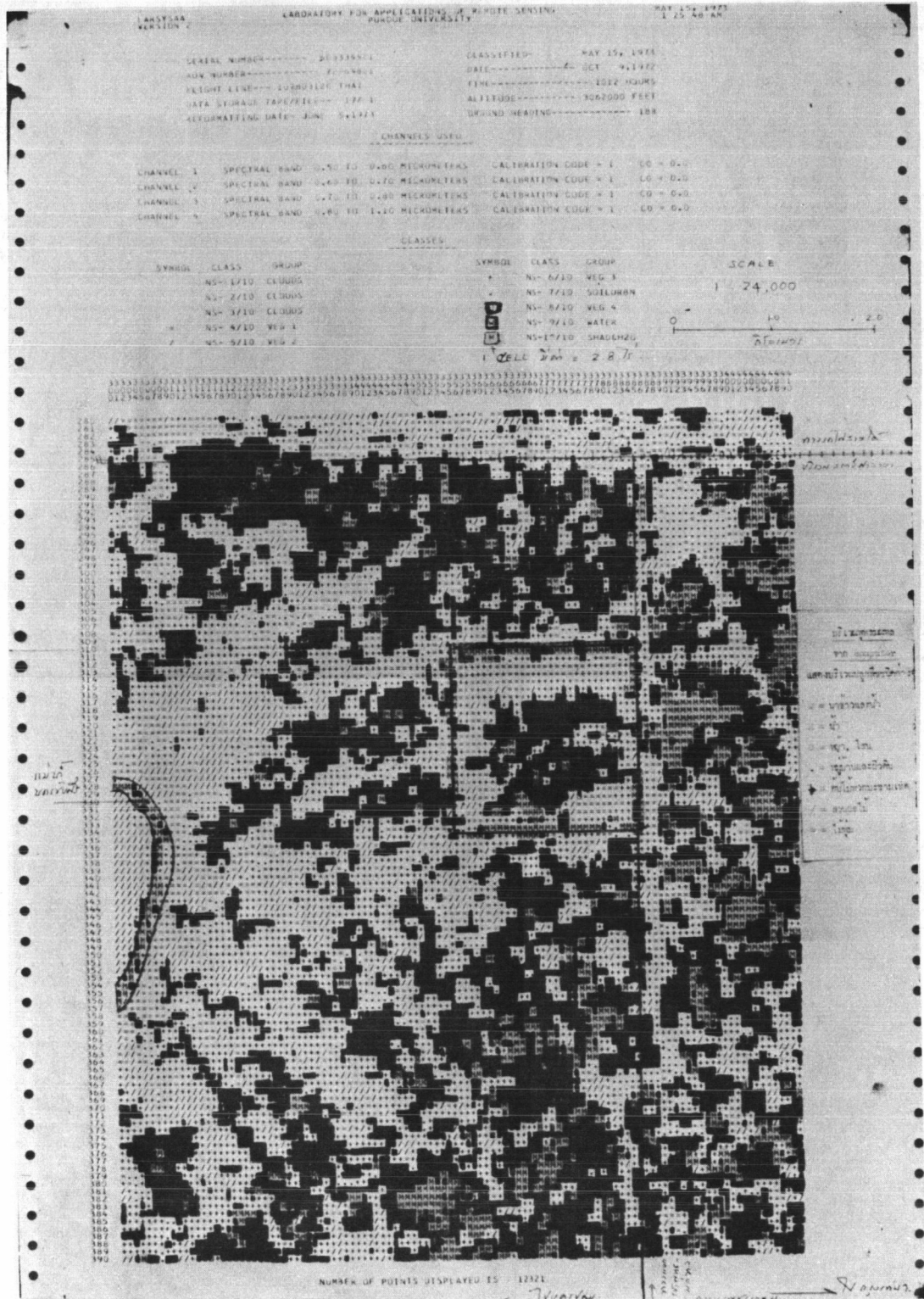


Figure 3



Figure 4

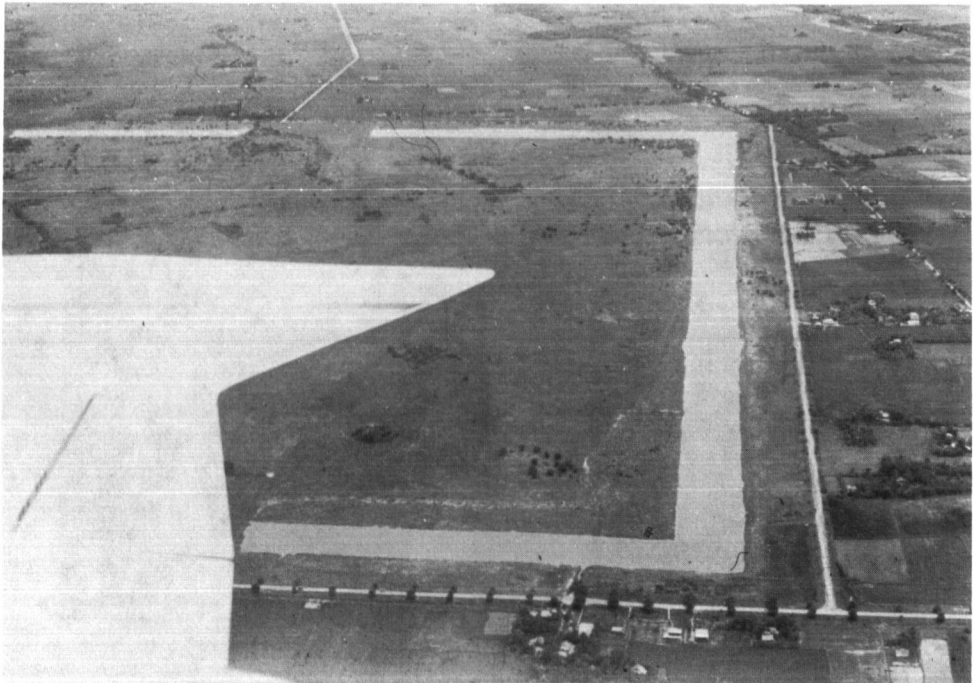


Figure 5



Figure 6

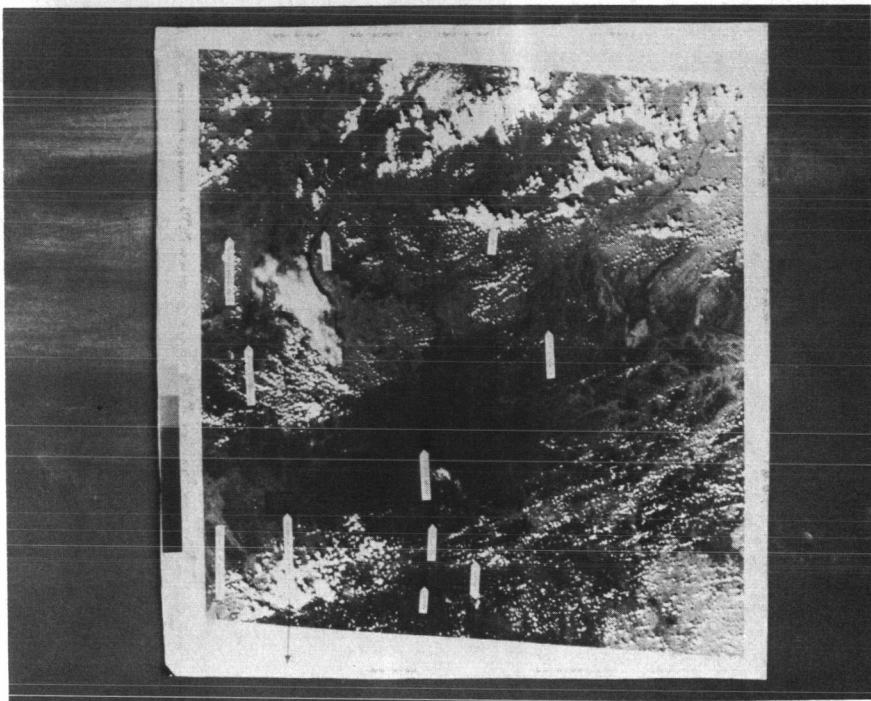


Figure 7

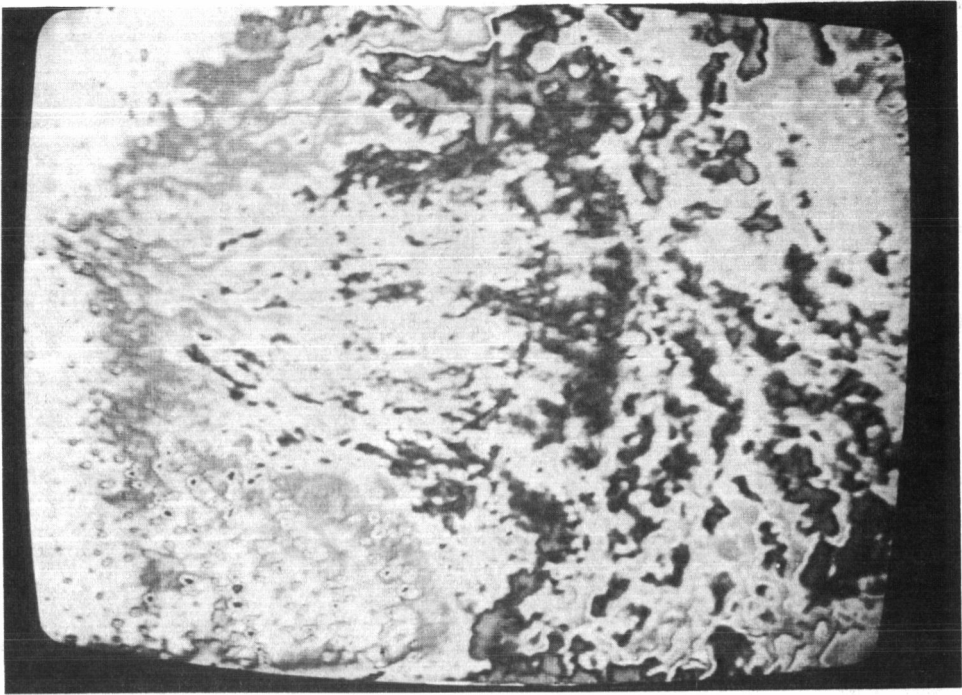


Figure 8

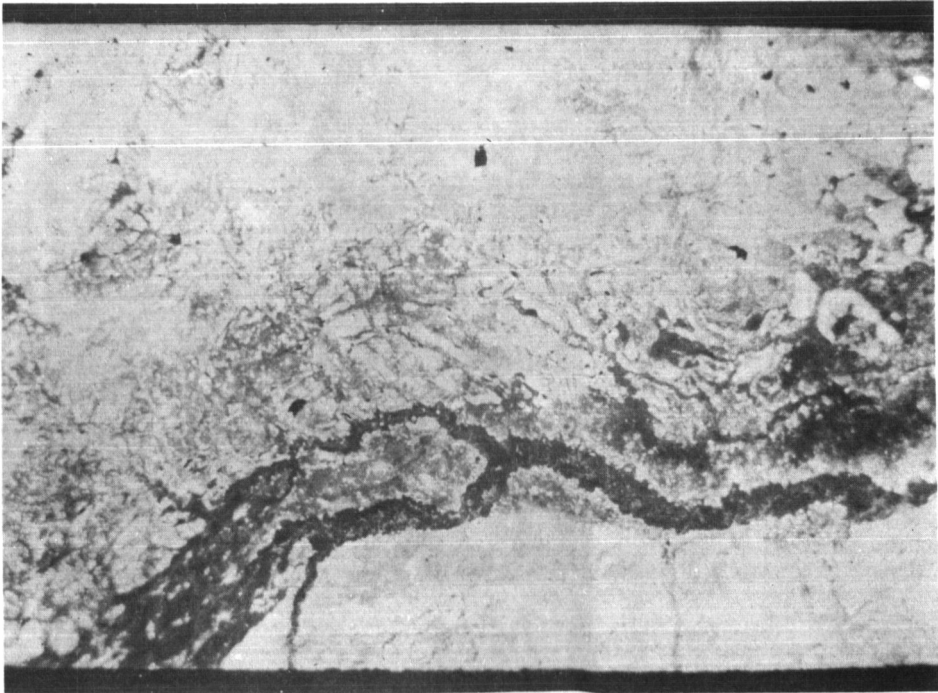


Figure 9

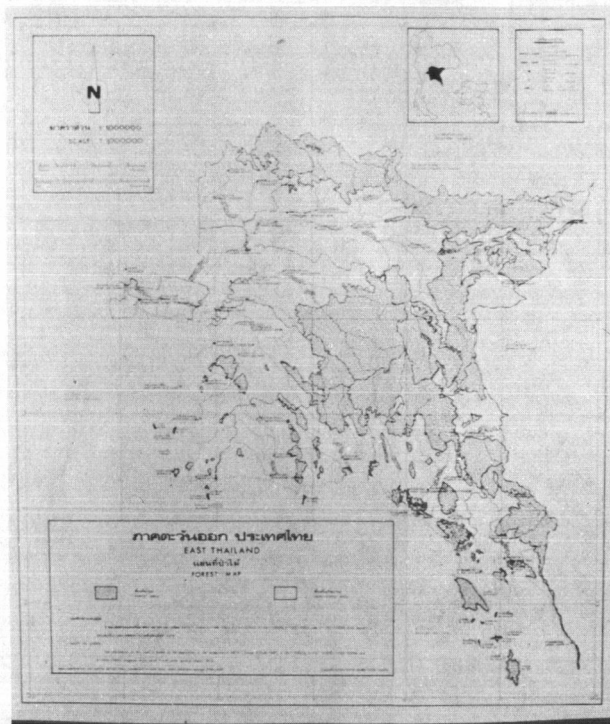


Figure 10

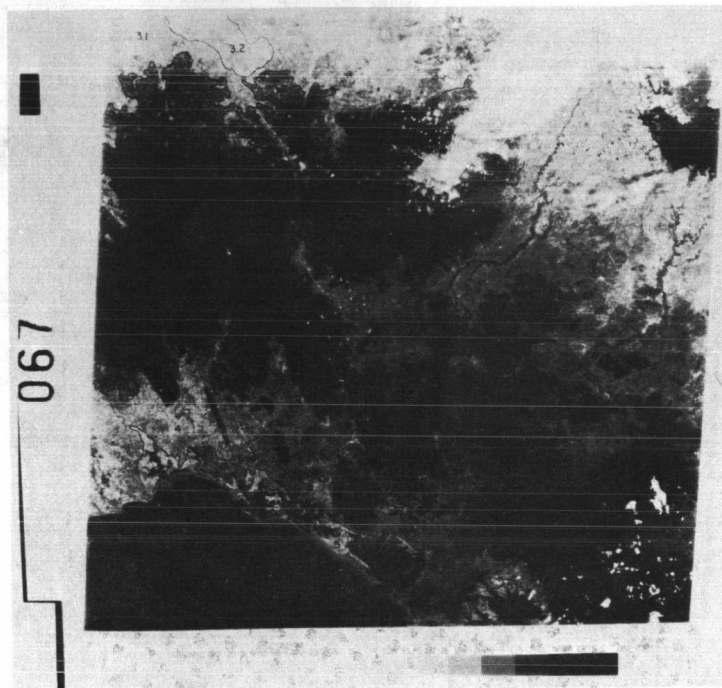


Figure 11

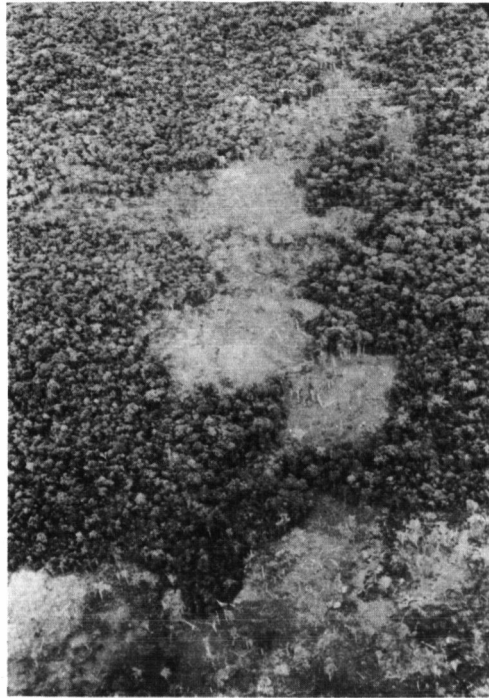


Figure 12

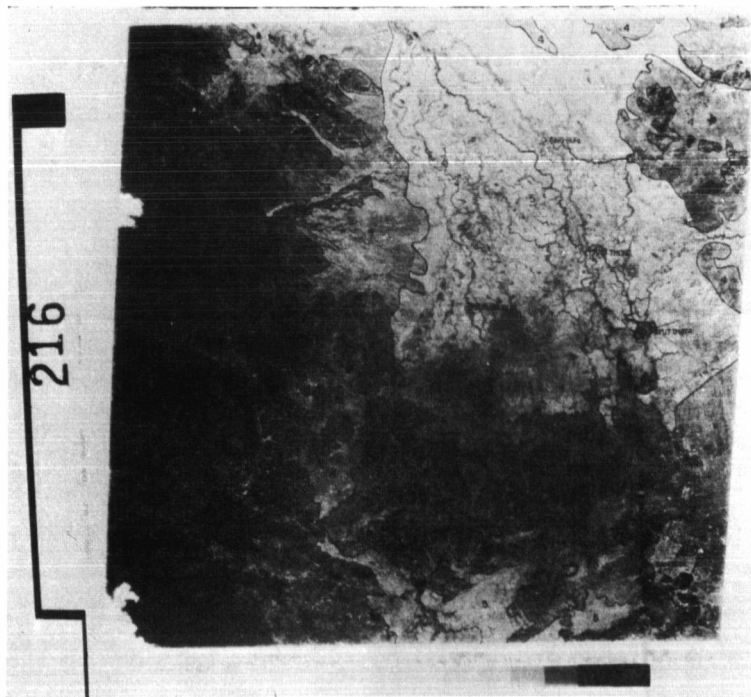


Figure 13

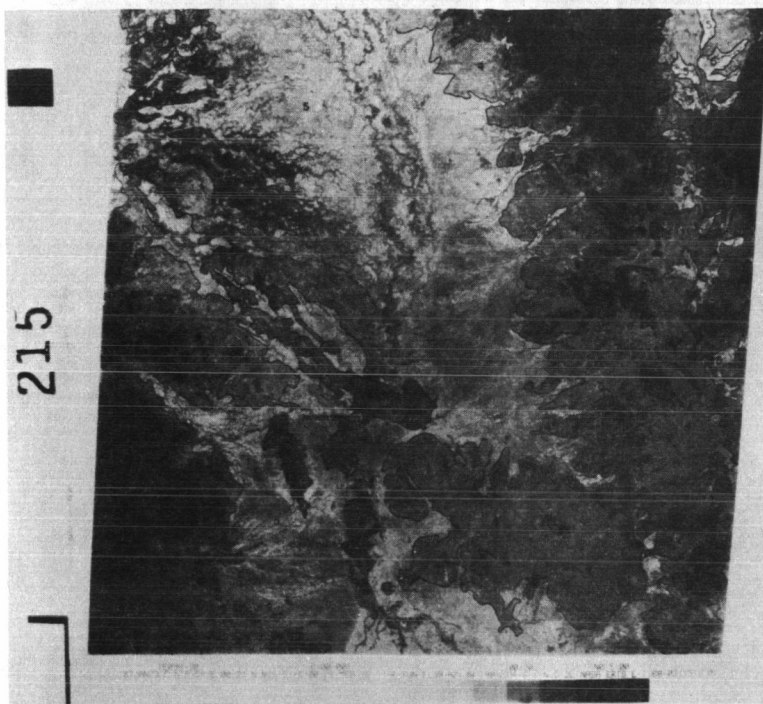


Figure 14

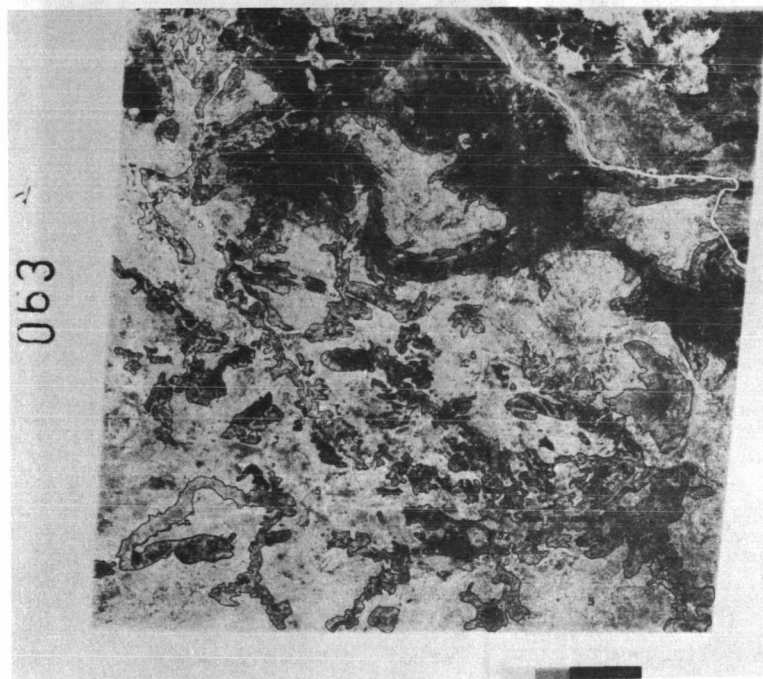


Figure 15

LAND USE & MAPPING

COMPUTER-IMPLEMENTED LAND USE CLASSIFICATION WITH PATTERN RECOGNITION SOFTWARE AND ERTS DIGITAL DATA

Armond T. Joyce, *NASA Earth Resources Laboratory, Mississippi Test Facility, Bay St. Louis,
MS 39520* and Thomas W. Pendleton, *Ibid*

ABSTRACT

Significant progress has been made in the classification of surface conditions (land uses) with computer-implemented techniques based on the use of ERTS digital data and pattern recognition software. The supervised technique presently used at the NASA Earth Resources Laboratory is based on maximum likelihood ratioing with a digital table look-up approach to classification. After classification, colors are assigned to the various surface conditions (land uses) classified, and the color-coded classification is film recorded on either positive or negative 9 1/2" film at the scale desired. Prints of the film strips are then mosaicked and photographed to produce a land use map in the format desired. Computer extraction of statistical information is performed to show the extent of each surface condition (land use) within any given land unit (e.g. township, county, drainage, etc.) that can be identified in the image. Evaluations of the product indicate that classification accuracy is well within the limits for use by land resource managers and administrators. Classifications performed with digital data acquired during different seasons indicate that the combination of two or more classifications offer even better accuracy. Future emphasis will include adaptation of software to general purpose computers, development of low-cost hardware for image display, and establishment of ground truth logistics for widespread implementation over large areas, e.g. statewide.

INTRODUCTION

ERTS-1 data offers the land use analyst several new dimensions. A single ERTS pass results in the collection of data over a swath approximately 100 nautical miles wide, whereas imagery acquired with mapping cameras flown in aircraft commonly cover swaths from two to fifteen nautical miles. ERTS repetitive coverage on an eighteen day cycle provides possibilities for a rapid detection of cultural changes on the earth's surface as well as seasonal differences in vegetation and land use practices. In addition, the digital form of the data is conducive to automated data processing based on computerized systems.

The objective of the study reported in this paper was to perform computer-implemented land use classifications utilizing ERTS digital data and pattern recognition software for two sets of data, each pertaining to a different season of the year, and to compare the two classifications as to their portrayal of seasonal differences in vegetation and agricultural practices. ERTS digital data acquired over the Mississippi coastal plains on August 5, 1972, and again on January 16, 1973 were selected for the study.

*Nasa Earth Resources Laboratory, Mississippi Test Facility, Bay St. Louis, MS 39520

**Ibid.

1 N 74 30729

DATA PROCESSING

Land use classification at the Earth Resources Laboratory is performed using a Data Analysis Station (DAS) and UNIVAC 1108 software. The DAS consists of a Varian 620f computer with 16,000 16 bit words, two nine track digital tape decks, a color television display device (CRT) with light pen capability, a Singer color film recorder, a card reader and a line printer. The UNIVAC 1108 software consists of several modules which constitute a supervised maximum likelihood classification scheme based on Gaussian statistics. The modules are a statistical module, a training sample separation module, and a classification module.

The initial stage of data processing consists of reformatting on the DAS the nine track ERTS computer compatible bulk data tapes received from the Goddard Space Flight Center. The reformatting operation produces a data tape in a format suitable for the 1108 software and a display tape which can be used to drive the DAS CRT or the DAS film recorder. Using the display tapes and the light pen capability of the DAS CRT, the coordinates of surface areas with known land use, called training samples, are determined. These scan line and scan line element coordinates allow the training sample areas to be located in the data in a supervised classification system. Using the training sample coordinates and the reformatted bulk data tapes, the training sample data is extracted and stored on a training sample edit tape which can be used with the UNIVAC 1108 software.

The statistical module on the UNIVAC 1108 is used to compute means and covariance matrices and to plot histograms for each training sample. The information output by the statistical module is used to edit the training sample data and is used for input to the separation module. The separation module computes a measure, "divergence," of the similarity of pairs of training samples. The measure, while quantitative, is difficult to relate to physical processes. However, it is known that the larger the measure the greater the difference between the training samples. ERL uses the measure to determine which training samples can be grouped to form a training class and which training samples cannot be grouped but must be treated as subclasses. In particular, for the classification of the two subject ERTS frames, the divergences between all training samples which potentially belonged to a single class were computed. Those training samples which had a divergence of less than approximately 15 were grouped into a single subclass.

As an example of training sample grouping we could consider the class "forest" from the 7 August 1972 data set as shown in Figure 1. The training information for the "forest" class consisted of fifteen training samples identified as pine and twelve samples identified as hardwood. The divergence criteria grouped these training samples into three subclasses of pine and four subclasses of hardwood. Hence, the forest classification was derived from seven forest subclasses. In general, the six class classification was derived from twenty-three subclasses which were three soybean subclasses, one corn subclass, two exposed soil subclasses, two grass subclasses, one pasture subclass, three marsh subclasses, three water subclasses, one urban industrial subclass and the previously mentioned seven forest subclasses.

COMPUTER DERIVED LAND USE CLASSIFICATION OF ERTS-1 DATA
ACQUIRED AUGUST 7, 1972 - MISSISSIPPI GULF COAST



Fig. 1 Computer Generated Color-Coded Land Use Map

URBAN/INDUSTRY

WATER

FOREST

MARSH

GRASS

CULTIVATED

OTHER



prepared by

NASA/JSC Earth Resources Laboratory
Mississippi Test Facility
Bay St. Louis, Mississippi

Based on the groupings indicated in the previous paragraph, the statistical module was used to generate information used by the classification module to classify the reformatted ERTS bulk data tapes. The classification algorithm is based on pre-storing in the computer a representation of each data element and the class to which it is to be assigned. This technique eliminates the need to compute for re-occurring data elements the probability that the data element belongs to each subclass, and the comparison of all such probabilities. The classification algorithm can process one ERTS computer compatible tape in eight minutes. However, the algorithm is limited to twelve classes. Since we used twenty-three classes, two passes were required per data tape. Therefore, four tapes or one ERTS frame requires about one hour to process. The resulting classification is stored on tape as a color-coded classification symbol for each data element.

The classification tape is displayed in false color on the DAS CRT and is displayed on the DAS film recorder. When the classification is displayed on the film recorder, rectification allows overlaying the classification data with a map of desired scale. The rectification technique considers scan angle, scan rate, sample rate, V/H ratio of the platform, rotation rate of the earth, and the characteristics of the film recorder. A quantitative evaluation of the rectification has not yet been made, but rectified data has been overlayed with a 1:250,000 scale map on a Traverse Mercator Projection. The match between the rectified data and the map appears to be very good in a region 25 x 100 nautical miles which corresponds to 1/4 of an ERTS frame and it is expected that the entire ERTS frame will match equally as well.

DATA ANALYSIS

The classifications for both sets of data were performed using the same geographic locations for training sample areas. There were eighty-two training sample areas which together encompassed 4376 resolution cells. The results of the classifications within training sample areas are shown in Table 1.

Overall, the classification within training sample areas indicates that the August 1972 data yielded a more accurate classification than the January 1973 data (94.8% versus 89.0%), but both classifications are well within the limits for use by land resource managers, administrators, or planners. The ground evaluation is still in progress, but preliminary findings show that classification accuracy within the entire test area (six counties) is not substantially different from the results of the classification within training sample areas. However, in viewing the statistics in Table 1, it is evident that certain surface conditions were classified more accurately with one set of data than with the other.

The forested areas of the Mississippi coastal plains are mainly pine forests, but there are also large areas covered by swamp hardwood forest in the bottom-lands adjacent to the major rivers. Pine tree foliage is green during January at which time most other vegetation is either dead or leafless. Most hardwood trees are leafless during January, and, although there are some evergreen brush species in the understory, the hardwood forests should be spectrally distinct from other vegetation that may exist. Therefore, it was hypothesized that the total forest area could be most accurately classified utilizing ERTS data acquired in January, and that pine forests could be better distinguished from

Table 1. Classifications within training sample areas expressed as percentage of total cells representing a given surface condition classified as pertaining to that surface condition.

<u>Surface Condition</u> <u>(Land Use)</u>	<u>Aug. 1972</u> <u>data</u>	<u>Jan. 1973</u> <u>data</u>
Total forested area	92.4	97.8
Pine forest	81.4	91.5
Hardwood forest	72.7	88.5
Total cropland area	84.6	84.2
Soybeans	80.0	-
Corn	96.0	-
Exposed soil	92.0	-
Winter ryegrass	-	89.1
Stubble	-	69.8
Grass (improved and unimproved pasture)	89.0	80.4
Marsh (non-forested wetlands)	94.9	67.4
Water	97.6	98.9
Inert materials (asphalt, concrete, metal, etc.)	94.9	65.9
Overall	94.8	89.0

hardwood forests with the same data. The validity of this hypothesis is indicated by the classification results shown in Table 1 which show that the classification within forest training sample areas was 92.4% for August data and 97.8% for January data. Furthermore, the scorecard classification within pine forest training samples was 81.4% for August data versus 91.5% for January data.

During August 1972, on the Mississippi coastal plains, the main agricultural crop was soybeans, although there was some corn and some exposed soil in cultivated areas. Soybeans and corn are spectrally similar, and both crops are spectrally similar to grass vegetation. However, exposed soil is spectrally distinct from all green vegetation during August. During January, some of the cultivated area contains winter ryegrass in a green growing condition; and the remainder of the cultivated area contains stubble (dead soybean or corn stalks) or dead vegetation that is spectrally distinct from ryegrass but spectrally similar to dead grass and dead marsh vegetation. Therefore, it was hypothesized that there was not

likely to be a significant difference in land use classification accuracy between January data and August data for the total cultivated area, but that the ryegrass classification attained with the January data was likely to be more accurate than the soybean classification attained with the August data. The validity of this hypothesis is also indicated by the scorecards. The classification within all training samples for cultivated areas was 84.6% for August data and 84.2% for January data, but the soybean classification with August data was 80.0% and the ryegrass classification with January data was 89.1%.

Marsh vegetation is in a vigorously growing state during August; whereas, except for a few evergreen brush species in some areas, marsh vegetation is dead during January, and should be spectrally similar to dead grass, stubble and leafless hardwood. Therefore it was hypothesized that the most accurate classification of marsh vegetation could be attained with August data. The scorecard results show 94.4% for August data and 67.4% for January data. The low accuracy for the marsh classification with January data is attributed to a similarity between a marsh spectral signature and a spectral signature for a flooded condition under leafless hardwood swamp forest. In the January classification, 21.7% of "marsh" training sample cells were classified as "hardwood."

A computer-derived classification, as used in this study, is based on separating surface conditions that have different spectral characteristics caused by differences in reflected energy as measured from above. Urban, commercial, industrial, and residential land uses can be separated from the other land uses only in-as-much as their surface conditions with inert materials (asphalt, concrete, metal, wood, etc.) are spectrally different from vegetation or other material (sand, water, etc.). Residential or urban areas that have foliated trees overtopping the buildings as well as lawns and shrubs occupying surface areas as seen from above are likely to be classified as vegetation. However, the color assigned to inert materials (asphalt, concrete, etc.) and the colors assigned to other surface conditions (grass, trees, etc.) that may be in the urban environment will form color patterns on a color presentation that can be interpreted so as to enable delineations of urban areas, especially to separate urban commercial and industrial centers with large concentrations of inert surface materials, residential areas with associated vegetation, and other land uses. In this context, the classification results within training sample areas is meaningless to the accuracy of the classification of the total urban commercial, industrial, or residential area. However, in-as-much-as the hardwood trees that overtop one-story or two-story buildings are leafless and lawn grasses are dead during January, a larger portion of the urban areas outside of training sample areas was classified as having inert material (asphalt, concrete, etc.) on the surface when utilizing ERTS data acquired in January than when utilizing data acquired in August when all vegetation is green.

CONCLUSIONS

In summary, it was shown that August data yielded the best classification to determine the extent of the area occupied by marsh vegetation, soybeans, and exposed soil; whereas, the January data yielded the best classification of the forested areas (as well as separating pine forest from hardwood forest), winter ryegrass and urban areas. It was also shown that there were no significant differences.

between the August and January classifications of the total agricultural area, or water bodies. These findings suggest that even better classifications may be attained for certain surface conditions utilizing data acquired during other seasons (e.g. for the total cultivated area during May when most fields are in some phase of soil preparation and have no significant amounts of green or dead vegetation). If this hypothesis is valid, it may be possible to attain the most accurate classification of surface conditions by integrating land use classifications made with ERTS data acquired during each season of the year.

Work is proceeding to produce a land use classification with ERTS data acquired during the spring when nearly all cropland is in some state of soil preparation, and during the fall when deciduous species have changed leaf color but have not shed their leaves. A comparison of four classifications of data acquired during the four seasons will determine the extent to which land use classification can be improved by combining two or more classifications for different seasons.

Future work will also include adaptation of software to general purpose computers, and establishment of ground truth logistics for the implementation of computer implemented land use classifications over areas larger than the 100 nautical mile by 100 nautical mile area encompassed by this study.

REMOTE SENSING OF LAND USE CHANGES IN U.S. METROPOLITAN REGIONS:
TECHNIQUES OF ANALYSIS AND OPPORTUNITIES FOR APPLICATION

James R. Wray, *U.S. Geological Survey, Geographic Applications Program, Washington, D.C.*

ABSTRACT OF ILLUSTRATED REPORT OF FINDINGS

With twin slide projectors and screens this ERTS investigator describes graphically the "Census Cities" ERTS experiment in urban change detection using remote sensors. Sample pages from a prototype looseleaf Atlas of Urban and Regional Change record land use at selected U.S. urban test sites at the time of the 1970 census, and the changes occurring 1970 to 1972. The relationship or model between land use data from sensors and socio-demographic data from the census is partly demonstrated. The example suggests how knowledge of land use changes acquired by sensors can be used to make estimates of population, and other attributes. The feasibility of nationwide mapping of land use, and land use changes, by direct computer classification of ERTS-1 multispectral digital data is also demonstrated. An integrated system of time series coverages and sensor platforms, and the packaging of results in a user-interactive format, offers new opportunities for resource management. Potential applications in state and regional planning are many, and some are named. But the longer-range gains are likely to be improved understanding by legislators, managers and voters as to what it is that makes our country tick. One of the specific tasks could be the allocation of revenues to be shared. Because of ERTS our land and our world will never be the same to us again. In telling us the finiteness of both it challenges us to be better stewards of the remarkable--and only--home we have.

1 N 74 30730

Publication authorized by Director, U.S. Geological Survey.
Prepared for oral/visual presentation at NASA ERTS-1 Symposium,
Washington, D.C., December 10-13, 1973.

PRECEDING PAGE BLANK NOT FILMED

03708 4271

ERTS-1 ROLE IN LAND MANAGEMENT AND PLANNING IN MINNESOTA

Joseph E. Sizer, *State Planning Agency*; Dwight Brown, *University of Minnesota*

ABSTRACT

Research on applications of ERTS-1 imagery to land use has focused on evaluating the ability of ERTS-1 imagery to update and refine the detail of land use information in the Minnesota Land Management Information System. Work has been directed toward defining the capabilities of the ERTS-1 system to provide information about surface cover by identifying forest, water, and wetland resources; urban and agricultural development; and testing and evaluating data input and output procedures. As capabilities were developed, meetings were held with administrators and resource information users from various agencies of government to identify their information needs.

A full scale systems test for several selected pilot areas in the state is nearly complete. Users have been identified for each test area and they have been instrumental in identifying data requirements and analysis needs for administrative purposes. Users have both rural and urban orientations and provide a basis for evaluation of the results.

INTRODUCTION

The Minnesota State Planning Agency and University of Minnesota are engaged in a cooperative effort to develop and evaluate the utility of the ERTS-1 imagery to update and refine the detail of land use information in the Minnesota Land Management Information System (MLMIS). There are three basic objectives for this work effort.

1. To define the capabilities of ERTS-1 imagery to provide information about surface cover by identifying water and wetland resources, urban development, agriculture, and forestry; and testing data input and output procedures.
2. To utilize ERTS-1 imagery in ongoing research and planning operations of land management agencies in the state.

PRECEDING PAGE BLANK NOT FILMED

1 N 74 30731

3. To transfer the developed capabilities for using remote sensing data to state and regional agencies charged with planning, policy development, and management of land-based resources in Minnesota.

This paper focuses on what has been done and what is being done to achieve these objectives.

SURFACE COVER INFORMATION CAPABILITIES

The ability to extract surface cover information from ERTS-1 imagery of Minnesota is highly variable among the range of surface cover types found in Minnesota. Each broad class of land cover has its own optimal season(s) for interpretation. For an individual class this season may vary as a function of location or local site conditions.

Based on analysis of 12 months of coverage, the ability to add detail to the surface cover classes also varies from place to place. Table 1 shows the kind and detail of information that can be extracted reliably throughout the state and those details that can be added on occasion in some areas.

Many of the second and third land cover classes are limited by the unit size necessary for discrimination and the necessity of coverage in an extremely narrow time period in order to discriminate some features from their surroundings. For example, a small seasonal wetland with open water will probably be detectable for only a few days to a few weeks at most; and seasonal wetlands with uniform emergent vegetation are not reliably detected below 75 acres in size in certain parts of the state. These problems would probably be greatly reduced with thermal infrared band images, more frequent coverage, or reductions in cloud cover.

DEMONSTRATION PROJECTS

Three demonstration projects have been selected to encompass the range of surface cover conditions found in Minnesota. Potential users have been identified and are to provide the basis for evaluation of results. Itasca County was selected because of the importance of forests, iron ore resources, and substantial local interest in information sources for use at the county level. The Twin Cities Metropolitan Area was selected because of the urban uses, rapid change, and user interest. Monitoring of plowing in west central Minnesota was selected as a demonstration solely on the basis of intense user interest.

Table 1

Classes of Land Surface Cover for Minnesota Obtained from ERTS-1 Imagery

<u>Level I</u>	<u>Level II</u>	<u>Level III</u>
Extractive	Iron Mining	Tailings pond Tailings basin Tailings & stripping piles Pits
	Gravel Rock Sanitary Landfill*	
Urban	Residential	Mixed single/multiple units Single unit, high density* Single unit moderate density*
	Commercial/Industrial/ Institutional	Commercial core outlying centers and strips
Water	Lakes	Natural basin Excavated basin (mine, pits, etc.)
	Rivers	
Wetlands	Northern Bogs Southern Perennial* Southern Seasonal*	Several vegetation types
Forests	Conifer* Hardwoods* Mixed*	
Cultivated	Season of Tillage	
Open and Other	(non-cultivated farmland, pasture, & open non-farmlands)	

* Indicates classes of cover that can be added locally depending on proper seasons of coverage and local environmental conditions.

Surface cover for the southern one-third of Itasca county was mapped. Foresters in the county are now evaluating the results under the direction of Dr. Merle Meyer of the University of Minnesota. Two townships, having a wide range of cover types, were selected to test cathode-ray tube entry procedures for ERTS-1 updating of MLMIS. A sample output of the stored information is shown in Figure 1. The system is capable of producing this output for all townships in the state and land cover information can be compared with a variety of environmental information stored for the same area. Data can be manipulated to map change, non-conforming use, use by type of ownership, etc.

860408

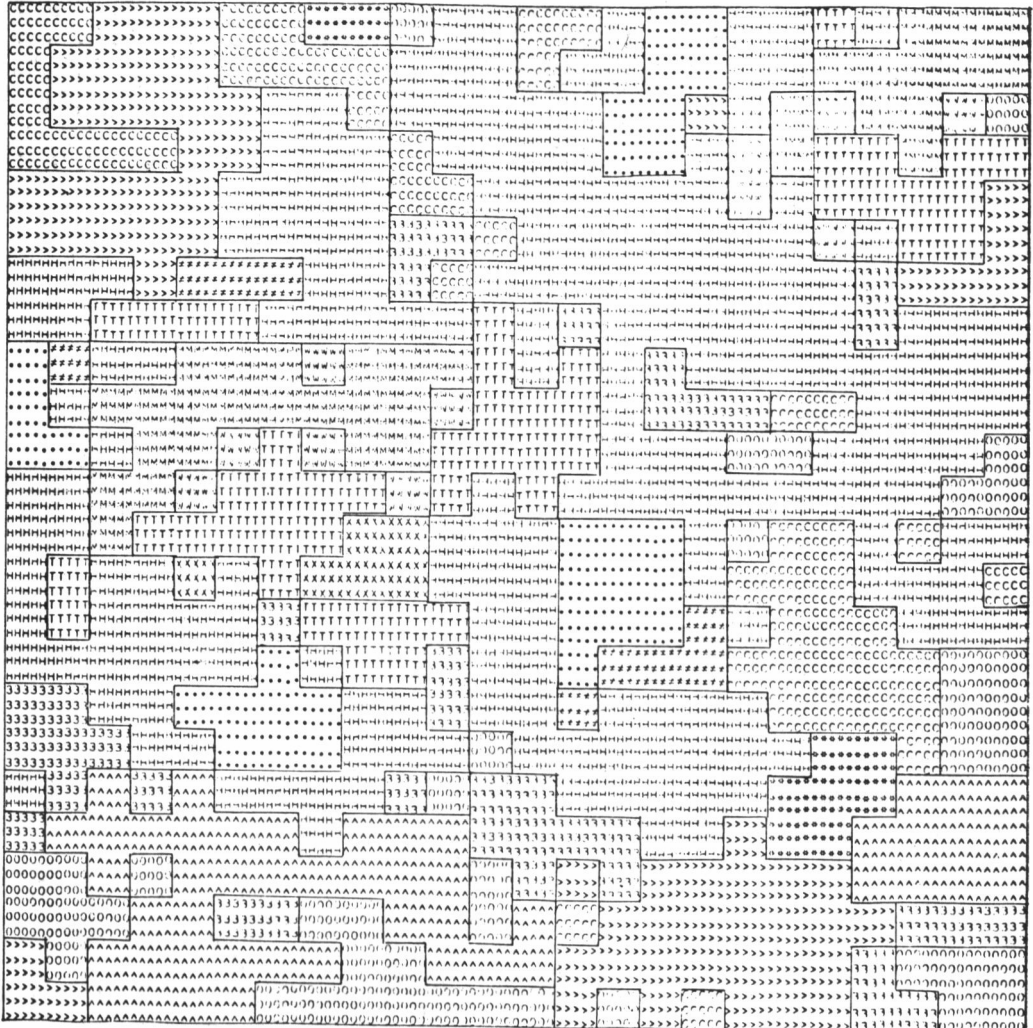


Figure 1

ERTS I
METROPOLITAN LAND USE CLASSES
Twin Cities, Minnesota

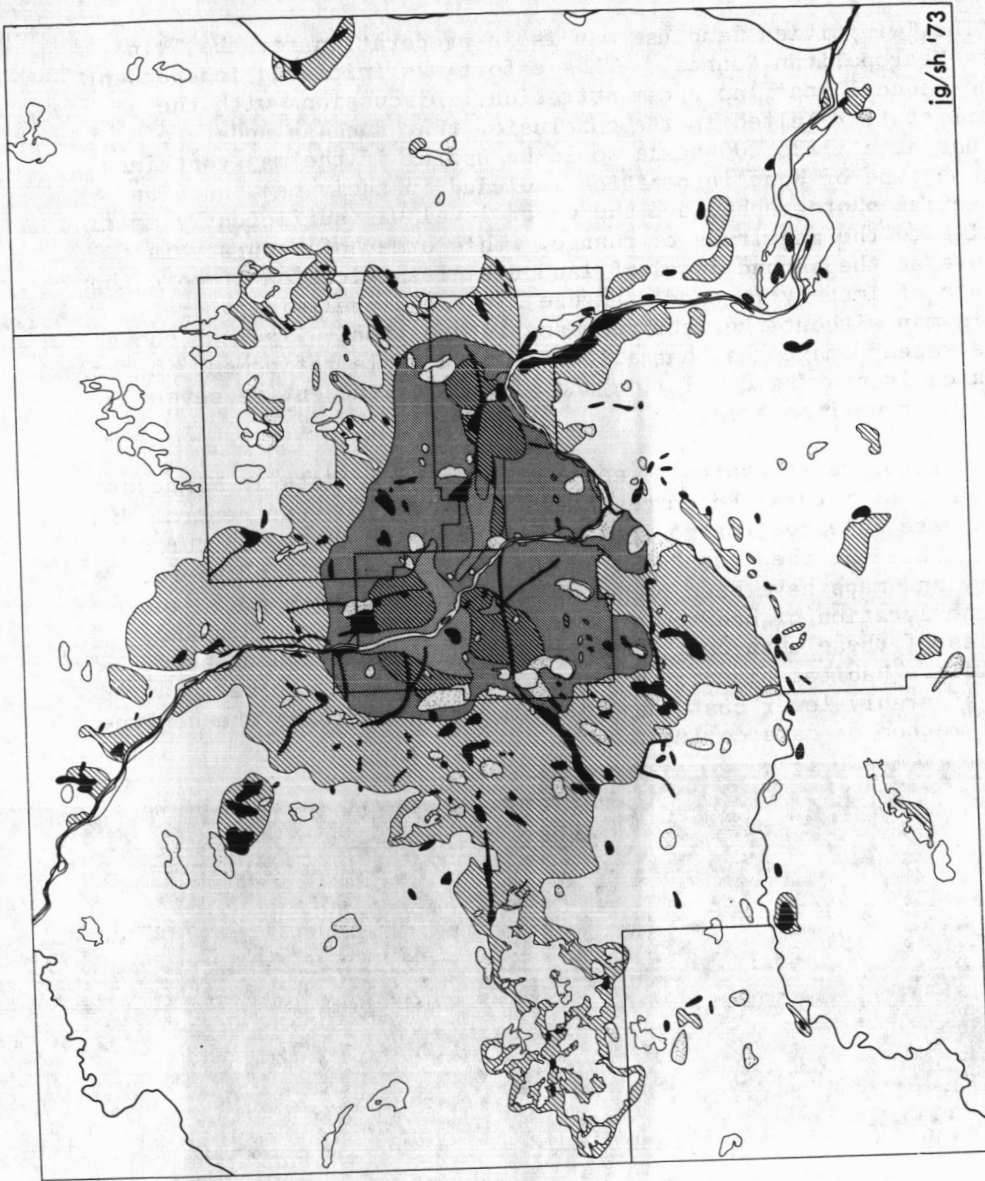
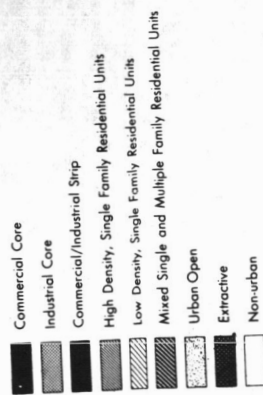


Figure 2

The Twin Cities land use map is in preparation for the Twin Cities Metropolitan Council. This effort was initiated independent of the Council staff as a demonstration. Discussions with the Council staff resulted in the conclusion that such an update of land use at a 1:125,000 scale would be useful if the map contained the same type of base information included in their map based on 1966 aerial photography, and the error level was sufficiently small relative to the magnitude of change. This order of accuracy is possible at the second level of land use classification if more than one date of imagery is used. Figure 2 shows a preliminary draft of this map without the required base information. Figure 3 shows a more recent image that has allowed considerable refinement in the map which is nearing completion and will cover the entire seven county metropolitan area.

In response to expressed needs of game biologists in Minnesota Department of Natural Resources seven townships in west central Minnesota were selected for monitoring the seasonal change in surface cover. Thus far the area has been covered by ten sets of useful imagery and maps have been prepared for each. Figures 4, 5, and 6 show the location of one township in west central Minnesota and examples of these changes. These maps are currently being used in wildlife habitat planning projects, and the data can be acquired at considerably lower cost than field mapping, which is the conventional method of data collection.

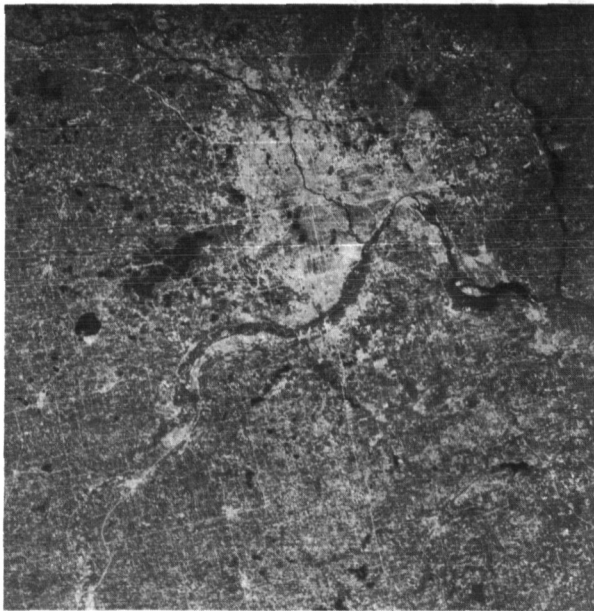
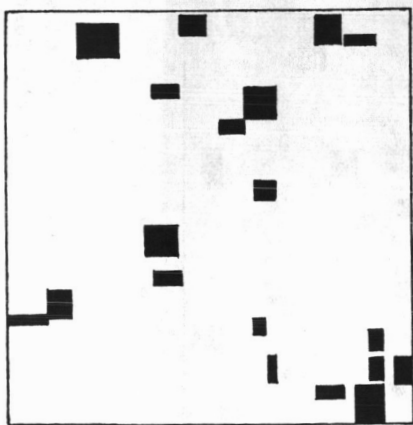


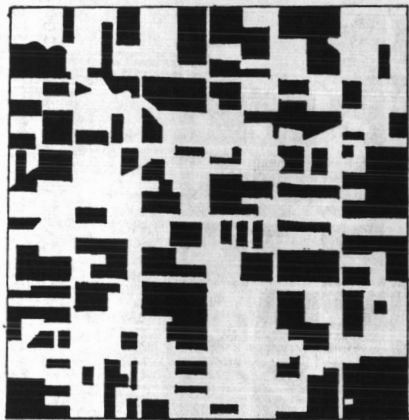
Figure 3. Twin Cities Minnesota color combined bands 5 and 7, July 3, 1973.



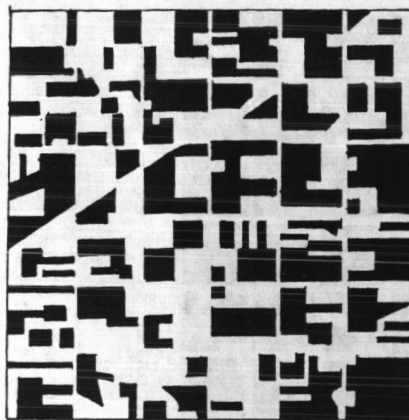
Figure 4. West Central Minnesota location of Croke township, Traverse County. September 21, 1972 color combined ERTS-1 image.



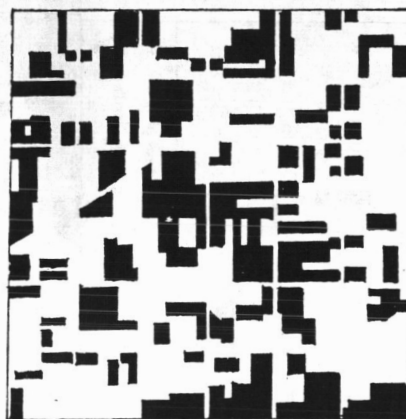
16 August 1972



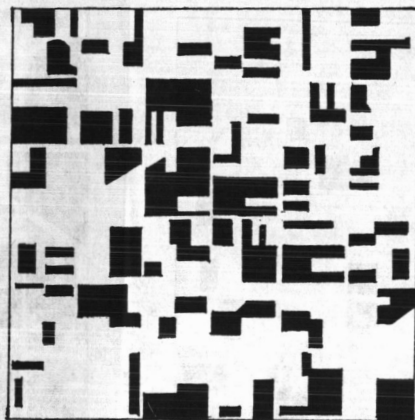
21 September 1972



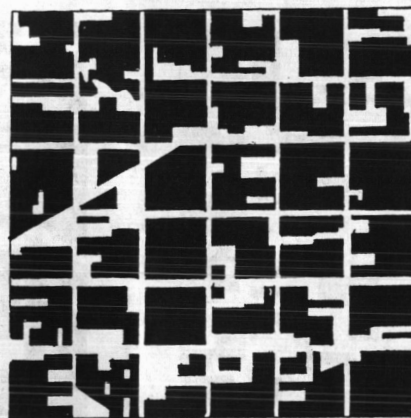
8,9 October 1972



30,31 May 1973

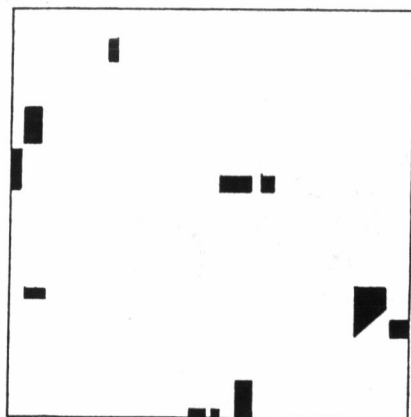


17 June 1973

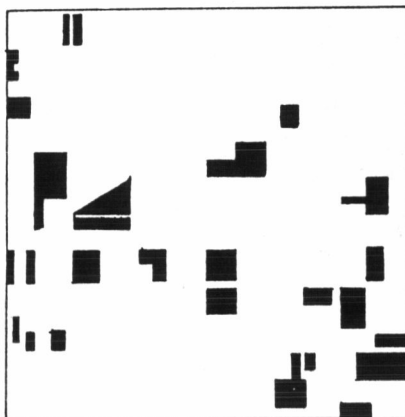


Composite

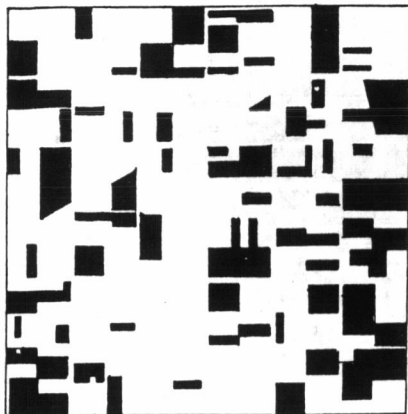
Figure 5. Bare, plowed fields for five dates and composite map for Croke Township, Traverse County, Minnesota. August, 1972 - June, 1973.



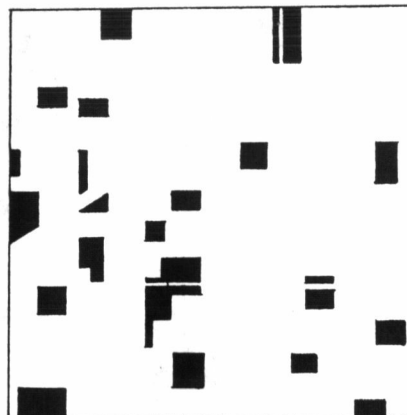
5, 6 July 1973



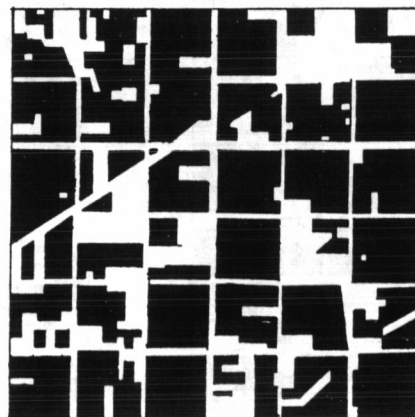
10 August 1973



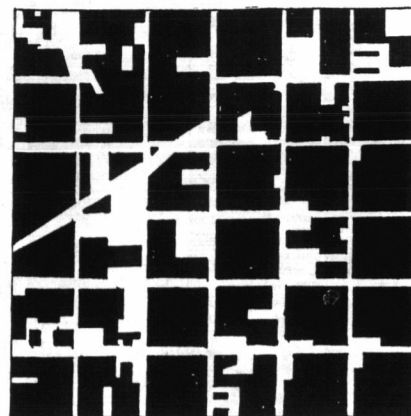
28, 29 August 1973



4 October 1973



22 October 1973



Composite

Figure 6. Bare, plowed fields for five dates and composite map for Croke Township, Traverse County, Minnesota. July through October, 1973.

TRANSFER OF CAPABILITIES

In order to transfer ERTS-1 information capabilities to governmental agency users we have worked through local units of government and the new regional development commissions which encompass the entire state. The required development commissions have as a major function the coordination of planning within their geographical boundaries. Two of these regional units offer unique opportunities to explore, demonstrate, and transfer the ability to use ERTS-1 imagery in their development, planning, and resource management programs.

The regional unit covering the Twin Cities Metropolitan area is particularly concerned with the rate and location of developmental activities in the Twin Cities Metropolitan area.

Because of the capability of seasonal monitoring, the ERTS-1 imagery provides the opportunity for the Metropolitan Council to identify open space and wetlands that require some level of protection. Monitoring urban growth further allows the identification of major service corridors in an effort to guide development and to adjust plans for areas in the initial stages of development. The first effort of cooperation has been the development of an updated land use map as a demonstration project.

The Commission covering northeastern Minnesota, which includes the second largest metropolitan area, the largest forested area, and the entire Mesabi Iron Range, is concerned with extractive operations and the management of forest resources. The apparent capabilities of ERTS-1 imagery to identify forest and extractive resources and to monitor their changes led to the early selection of a demonstration project in this area.

In addition to the two regional unit studies, we have been working closely with Department of Natural Resources and State Highway Department personnel to develop user capabilities for managers in a variety of fields. Thus far, limited funds have allowed one demonstration project in this area dealing with seasonal change in surface cover.

Efforts to transfer capabilities to the user community are in the formative stages. We have been working with personnel in the State Planning Agency, State Highway Department, and Department of Natural Resources to identify the information needs and to specify user personnel in each agency. Key personnel in these agencies are assisting in this effort and are being trained to serve as continuing faculty for state and local unit training programs.

The lists of specific personnel and resource management application areas have been identified for several working units in the above agencies. These problem areas will serve as the focus for the first in a series of workshops for resource management staff, to begin in early February.

The Minnesota State Legislature has shown interest in the materials produced by the ERTS-1 program. They have held a special hearing for a presentation on ERTS-1 applications to Minnesota resource management problems. As a follow-up, the House Appropriations Committee toured the EROS data center and met with their staff personnel to identify the kind of product support that EROS could provide to Minnesota users. The Legislature has also provided an initial \$25,000 to one agency to begin development of a broad based remote sensing program.

State-wide programs now under way in land use planning and water resource planning are beginning to employ imagery where adequate coverage exists. It is anticipated that the imagery will be used in the coastal zone planning program scheduled to begin in Spring, 1974.

IMAGE IDENTIFICATION

<u>Figure</u>	<u>Image Type</u>	<u>Date</u>	<u>I. D.</u>	<u>Band</u>
1	Color Combined	7 Oct. 72	1076-16370	4,5,6
2	Color Combined	6 Oct. 72	1075-16321	5,7
3	Color Combined	3 July 73	1345-16322	5,7
4	Color Combined	21 Sept. 72	1060-16485	5,7
5	70mm Bulk (+)	16 Aug. 72	1024-16484	7
5	70mm Bulk (+)	21 Sept. 72	1060-16485	7
5	70mm Bulk (+)	8 Oct. 72	1077-16431	7
5	70mm Bulk (+)	9 Oct. 72	1078-16490	7
5	70mm Bulk (+)	30 May 73	1311-16435	7
5	70mm Bulk (+)	31 May 73	1312-16493	7
5	70mm Bulk (+)	17 June 73	1329-16434	7
6	70mm Bulk (+)	5 July 73	1347-16432	7
6	70mm Bulk (+)	6 July 73	1348-16491	7
6	70mm Bulk (+)	10 Aug. 73	1383-16430	7
6	70mm Bulk (+)	28 Aug. 73	1401-16424	7
6	70mm Bulk (+)	29 Aug. 73	1402-16482	7
6	70mm Bulk (+)	4 Oct. 73	1438-16473	7
6	70mm Bulk (+)	22 Oct. 73	1456-16470	7

INTERACTIVE ANALYSIS AND EVALUATION OF ERTS DATA FOR REGIONAL PLANNING AND URBAN DEVELOPMENT: A LOS ANGELES BASIN CASE STUDY

Surendra Raje and Richard Economy, *General Electric Co., Space Division, Valley Forge, Pa.*
Gerald Willoughby, *OVAACS International Inc., Columbia, Maryland* and Jene McKnight, *County of Los Angeles - Regional Planning Commission, Los Angeles, California*

ABSTRACT

N74 30732

The progression endemic to the ERTS Data Use Experiment SR 124 in data quality, analysis sophistication and applications responsiveness is reviewed.

The roles of the variety of ERTS products, including the supporting underflight aircraft imagery at various scales, are discussed in the context of this investigation.

The versatility of interpretation techniques and outputs developed and implemented via the General Electric Multispectral Information Extraction Systems (in both the prototype laboratory - GEMS - version and the production field - IMAGE 100 - model) is described and exemplified by both system-expository and applications-explanatory products.

The wide-ranging and in-depth applications studied in the course of this experiment can be characterized as community-oriented and agency-directed. In the former, generic category, which is primarily data-contentual, problems analyzed dealt with agricultural systems, surface water bodies, snow cover, brush fire burns, forestry, grass growth, parks - golf courses - cemeteries, dust storms, grading sites, geological features and coastal water structure. The ERTS MSS band selectivity and measurements thresholds were of primary interest here.

The agency-directed application areas have been user-evaluational in nature. Beginning with overall urbanized regional analysis of land cover density-development intensity, residential areas were analyzed for ascertaining if housing types could be aggregated with any degree of reliability. It does appear that with the A-3 configurational U2 imagery for both input preparation and output evaluation, the ERTS CCT data analyzed interactively on the IMAGE 100 yields so-called Level III results of interest in certain on-going user-agency programs that would enable the users to monitor environmental factors using ERTS-IMAGE 100 outputs.

Presented at
THIRD ERTS SYMPOSIUM
Washington, December 1973

PART 1
Presented by Gerald Willoughby

The results described in this presentation are drawn from ERTS-1 experiment SR 124; the Principal Investigator: Surendra Raje, the General Electric Company; the Co-Investigators: Dr. Richard Economy, GE; Jene McKnight, the County of Los Angeles Regional Planning Commission; and Gerald Willoughby, OVAAC8 International Inc. (Fig. 1).

28508 474
The presentation will be given in two parts; the second half will be given by Mr. Raje. The first part is a synopsis of a substudy we began in October 1973 and which is not yet concluded. The information extraction techniques employed in the study are those provided by GE's IMAGE 100, the production model of the R&D GEMS System. Since IMAGE 100 only recently came on line, the entire SR 124 experiment has benefitted from just a few hours on the system. . . also the first opportunity for us to work with digital data instead of imagery. The data sources for the results that you will see are CCT's of March 1972.

The objective of the study was to test the compatibility of ERTS data in relation to an urban land use classification system of a user agency. . . that of our partner on the team. . . the Los Angeles County Regional Planning Commission. The objective entails a number of substudies, one for each land class. In the short time available to us we have looked at and have results for only residential.

Before I begin to describe the method we use, I would like to comment upon the objective and in particular the concept of compatibility. We are land planners. . . we make a very significant distinction between earth surface conditions, the physical properties of objects, and land use, the institutionalization of a social abstraction. For purposes of regional and urban planning the distinction is extremely important. I would illustrate by drawing your attention to the similarities and differences among a public park, a private golf course and a cemetery; or a shopping center and light industry.

Los Angeles Housing

We chose housing to begin because of Los Angeles priorities. At the present time the County's planning process is wholly directed towards complying with State requirements which dictate the need for a General Plan. The Plan must include policy with respect to nine social, economic and natural environmental systems, called elements in the LA General Plan (Table 1). The Commission believes its present data base is adequate; one outstanding exception is housing. In order, then, that any results might be immediately applicable, operationally, housing was chosen.

METHODOLOGY OVERVIEW

In the distinction between Class Analysis (supervised learning) and Cluster Analysis (unsupervised learning) the results (in Part 1) have been generated wholly from the former. Class Analysis utilizes the technique of training on a test site which is known to contain the class of interest. Using IMAGE 100 we trained on residential test sites selected from aerial photography* (Fig. 2). The test sites were homogeneous with respect to their distinguishing housing types and community structure. Following the training procedure and electronic analysis, color enhanced "themes" supposedly representative of the residential class are provided across the entire field of view on a TV monitor. We took slides of these themes and compared them to land uses given on Los Angeles base maps.

METHODOLOGY IN DETAIL

The primary residential classifier we used is Dwelling Units Per Acre; this will have to be expanded, we know, to include Floor Area Ratios, Building Coverage and Net Green Space values (green space contrasted with open space). Secondary classifiers consist of two subsets. The first describes community structure: for example, the street system. . . single or double loading and the existence of rear yard servicing. The second set describes predominant features of the individual lot: for example, roof tones (a consistent and recognizable pattern in most Los Angeles developments), the frequency of swimming pools, and laneway characteristics. . . single/double, asphalt/concrete, to front yard garage or to rear yard garage.

*See page 7

We selected test sites using U2 1:32,000 aerial photography and recorded them by ink drawings on tracing paper. We had anticipated photoreducing these to register with the digital data display on the TV monitor but found this step unnecessary* due to the very high quality of the digital data; all test sites were easily located (Figs. 3 and 4).

IMAGE 100 has the capacity to enlarge any given field of view. The scale factor chosen, 3 in our work, is largely a tradeoff between the quality of detail required to train by, and the overall size of the field of view required for results (Fig. 5).

Themes are areas which appear on the TV monitor color enhanced (Fig. 6). Hopefully they represent classes having similar spectral properties. . .but such a conclusion is the result of the evaluation stage. After a site is selected for analysis, it is so identified by means of an electronic cursor, a theme is produced following the completion of two routines:

1. One dimensional histograms are constructed for each channel; these give the upper and lower limits in the reflectance scale and the distribution of pixels within the range bounded at the limits. The limits are first set by choosing a threshold for pixel counts but may be adjusted later if a more selective or less selective reflectance range is desired (Fig. 7).
2. The second routine provides four dimensional histograms. Color space is cellularly divided according to criteria prescribed by the analyst for the number of divisions in each of the four reflectance scales derived during routine one. The cells which contribute to the final spectral signature upon which a color enhanced theme is generated are chosen according to the number of pixels they contain, per cell, in relation to a lower limit, or threshold (Fig. 8).

When the two routines are complete a spectral signature is in theory established. All pixels, having similar spectral properties, over the entire field of view are color enhanced providing the theme.

Three parameters influence the generation of themes:

1. The upper and lower limits in the 1-D histograms
2. The number of divisions per channel in the 4-D histograms
3. The threshold for pixel counts in the 4-D histograms

Experimentation during analysis, an advantage of IMAGE 100, is required in the choices to be made for each parameter. Through an iterative process of changing choices and checking monitor results at selected locations for which ground truth information does exist (the selected test sites for example) many themes can be generated: with varying results. A 16-level, 4-D histogram may tend to be too inclusive: yet a 64-level, 4-D histogram too selective. The objective, of course, is to produce as discrete a spectral signature as possible, representative of the class.

For illustrative purposes the slides † show four themes corresponding to different criteria used in their generation. The test site is in Beverly Hills and is residential, single family detached with a density of 1.3 units/acre.

- | | |
|----------|---|
| Theme 1: | 1-D limits were established, a 4-D threshold of 2 prescribed and a 64-level, 4-D histogram run |
| Theme 2: | 1-D limits were narrowed, the 4-D threshold kept at 2, and a 32-level, 4-D histogram run |
| Theme 3: | 1-D limits were held, the 4-D threshold changed to 38 and the 32-level, 4-D histogram repeated |
| Theme 4: | 1-D limits were broadened, the 4-D threshold changed to 2, and the 32-level, 4-D histogram repeated |

EVALUATION

The themes displayed on the monitor were recorded on slides and later projected onto Los Angeles land use maps and the two registered. A Dot planimeter was used to record observations.

†Not all slides presented at the meeting are included in this paper.

For illustrative purposes typical analysis results are shown for a test site in San Fernando Valley. Each column of the chart, headed by a color, represents a theme; for this test site we generated six themes Table 3 gives the raw data.

In Table 4, summarizing the analysis, the first column gives the land uses. In each theme column the figures given under "a" give the area of the land use class which is color enhanced as a percentage of the total color enhanced area or theme. In each theme column the figures under "b" give the area of the land use class which is color enhanced as a percentage of the total land area for the class. Essentially this method looks at classification accuracy two ways, although as planners we are more interested in those figures under "b".

The results show for this test site, which is not a typical, that we can identify, using the best value attained, 82.1% of the residential land use class upon which we trained, and this class in turn represented 76.6% of the total land area. Percentage wise, we are picking up high values for other land uses, although these do represent very little acreage.

Again, I would repeat, we have had very little machine time and our sample size is therefore small. For evaluation purposes we feel we could achieve more reliable results using U-2 photography although the choice would tend to weaken our purpose of working with a user agency and their land classification system, Table 5. We have now decided to use both sources, maps and aerial photos, and compare results which should be interesting.

The Los Angeles land classification was consciously used as the vehicle to test. . . the objective of the study: you can see some of the difficulties we encounter where classes are loosely defined. . . the last five, for example:

RECREATION

PUBLIC

SERVICES

OPEN SPACE

VACANT

From our viewpoint, as planners, a concept of much more interest than land use, proposed by us at a previous NASA symposium and as well at an Los Angeles ERTS symposium, is the concept of "development intensity." Land is classified according to its ground cover, either natural or man made, and ranked according to the proportions of each. Used by imaginative planners this information can enormously impact upon policy and standards for the use of land. Using the identical analysis methods I have described, information much more tractable and appropriate can be extracted from ERTS data and, based on previous work we have done using imagery, we are very confident in getting good results. . . particularly now that we have a digital analysis capability. We expect to continue both the land use experimentation and experimentation in the development intensity concept.

Question by Dr. L. W. Morley, Director, Canada Center for Remote Sensing: Could you elaborate upon your use of the U2 imagery ?

Answer by Mr. Willoughby: In this substudy, the U2 imagery was used to prepare the training-sites definition for IMAGE 100 runs which themselves used ERTS CCT inputs. As I mentioned, we are also using the U2 imagery to evaluate the IMAGE 100 outputs.

Comment by Mr. Raje: The use of U2 imagery mentioned by Mr. Willoughby was "light-box" use, visual photo-interpretive and in quasi-ground-truth sense. We are also machine-analysing, i. e., signature-acquiring, the multispectral underflight aircraft data for evaluating the corresponding ERTS-products analyzed results. This work will be reported later.

PART 2
Presented by Surendra Raje

Mr. Willoughby reported on the application of the more common approach, the Training-Testing Method, of machine analysis of multispectral data. I am reporting briefly on the application we have made extensively of the Slicing-Clustering Approach. The terminology here refers to spectral or color space: slicing the available spectral region into predetermined sequence or interactively defined volumes; clustering the actual distribution of cells in color space that yield the dominant themes in the entire field of view.

This method is more appropriately applied to large areas, such as the Urban Regions. We have thus analysed some eight regions in the metropolitan Los Angeles Basin. I shall briefly discuss the Central Los Angeles -- Regional Core -- area. Most of this work was done on the GEMS facility at GE's Valley Forge Center and analysed by the County of Los Angeles co-investigators. Some of it has been reported previously. I am describing the IMAGE 100 'Re-Runs' of this sub-study, with CCT input since GEMS only accepted film input .

It will be instructive, in passing, to compare the same area as seen first on the GEMS, then on IMAGE 100 in film input and on it in CCT input.

It will be further informative to compare this standard, linear input Fig. 9 with the Hadamard TransforMed View of the Same Scene Fig. 10. It should be pointed out that while this Rotation of Axes in Color Space yields dramatic patterns of interest to an Urban Planner, as Mr. Willoughby and Mr. McKnight have often reported before, so far this is only what Dr. Economy describes as Preprocessing.

Proceeding with actual signature acquisition, which yields to Theme Generation, per se, let us begin at one end of spectral space in this field of view: we obtain the Theme of Water. (The number given to a theme, here No. 3, is only pertinent to the selection of the color, here it is blue!).

Next in spectral sequence is the Theme: Heavy Industrial followed by Heavy Commercial Fig. 11. The so-called windowing feature on the IMAGE 100 enables a closer visual inspection of any area of special interest. Here, e.g., the LA CBD was enlarged X3 times the scale in the main field of view which incidently is loaded at 1 ERTS pixel to 1 TV pixel. Next in the theme, Low Density Residential, we pick up the higher quality housing, e.g., in west and south Los Angeles. Finally, the greener ground areas emerge in this theme of Parks, Golf Courses, Cemeteries.

What is the significance of this sequence of themes? First of all, each theme in itself reveals what Mr. Willoughby previously characterized as Land Cover Density - Development Intensity as obtained in the ground scene covered. What is of particular interest to urban planners in this application of the Slicing-Clustering Method is the interrelationship of these various themes within a given area: thus they find this 8-Theme Composite picture (Fig. 13) of tremendous interest. This should be compared with LA Land Use Map. What it brings out, our planner-co-investigators excitedly say, is an entire new insight into Urban Structure never before offered to them. Let me emphasize here that we are looking at internal delineation. . . intraurban as contrasted with interurban relationships here.

Mr. Jene McKnight and his associates in Los Angeles have found this and similar sets of urban regional analyses of the Los Angeles Basin giving new insights into the problems of the LA Regional Core. They plan to pursue using this output in Urban Design Studies they had proposed before CoLAGE - ERTS activity began.

This brings us to address briefly to the Cost-Benefit Analyses questions generally and specifically those raised in the EarthSat-Booze-Allen-Hamilton Study for the Department of the Interior. As the County of Los Angeles co-investigators pointed out to the Interviewers in Los Angeles and we did in the Sioux Falls Interview and Questionnaire, the Dollar Value of this effort exceeds the total investment committed to the project by NASA, GE and the County. The Underflights Aircraft Imagery CoLA-RPC has received alone exceeds in benefits the total cost as the County and the Community at large in Los Angeles assess it.

As for the ERTS Data proper, as analysed photo-interpretationally as well as electronically, let us briefly look at the Applications Overview (Table 6) of the type of problems tackled in this project. We barely had time to review only the Agency-Directed Items. While we are attempting to estimate the Dollar Value of the results both to CoLA-RPC and the Community at Large there and elsewhere, all of us on the Colage Team feel very strongly that the fact that ERTS provides entirely new type of data and IMAGE 100 analyses it in very novel and flexible fashion, we should be and are addressing to the problems of newer and more appropriate uses of these new products rather than to jam these results into older practices-procedures. At a recent National Land Use Institute held in Washington, I found very keen interest expressed by Urban and Regional Planners from around the Country to these newer products and tools and approach.

Referring back to the Los Angeles County Comprehensive General Plan elements, Mr. McKnight intends to use results shown above in the Seismic Safety Element work getting underway at the County early in 1974. Mr. Charness, his associate in charge of the Environmental Assessment Group, has already been using results from this project in the Conservation Element work. He also has entered the item in the Comprehensive General Plan issued by the County last August. As pointed out in a previous report, the County created a Position of Remote Sensing Planner in the early phase of this joint project.

The use of the products from this project by the Secondary Users in the Los Angeles Region has been rather extensive, especially since early May when we had organized a Regional Meeting to Review Results of this and other ERTS Projects in the Southern California.

In conclusion, I should like to indicate that the major objectives set forth for this investigation have been met already. In view of the Program Procession, we hope to report some of the more exciting items underway, such as Temporal Compositing Analyses in the final report due in the first quarter of 1974. Finally, both the Los Angeles Planning Community, through the County and vicinity, and ourselves are looking forward to operationalize all the items researched and developed during this project. . . prior to ERTS-B launch, I might add".

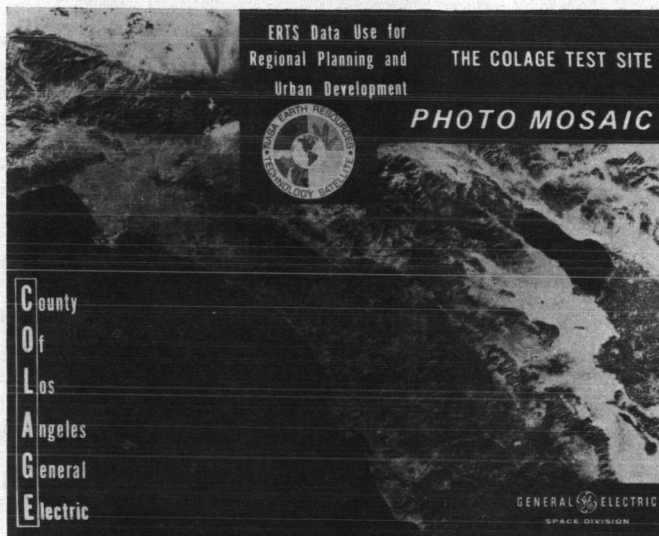


Figure 1. CoLAGE Test Site Overview

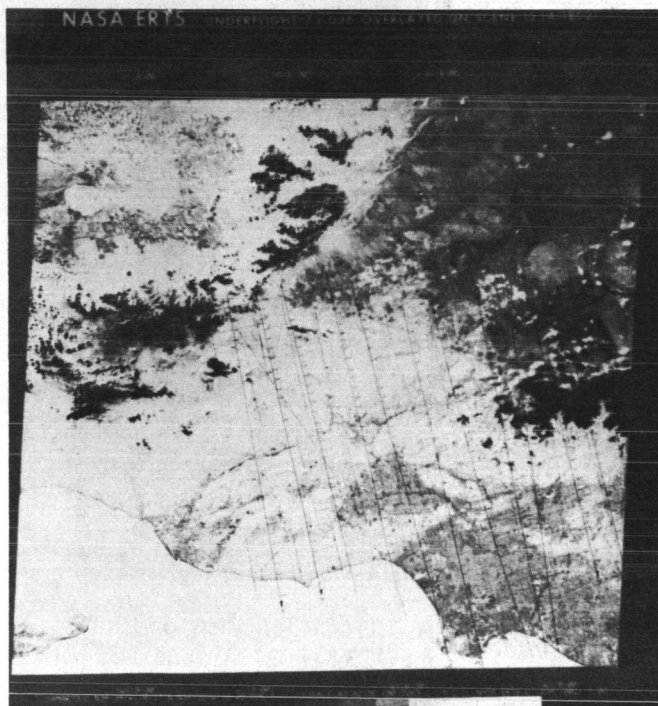


Figure 2. Flightlines of U2 with A-3 Configuration Flown 3/14/73 during which ERTS Overflow



Figure 3. Portion of Frame 178. Flt 73-036 Showing Residential Areas Around Los Alamitos Naval Air Station



Figure 4. IMAGE 100 CRT View of ERTS Scene 1234-18021 Around Los Alamitos Naval Air Station, CCT Input @ 3 by 4 Enlargement in X to Y. Note Area 4

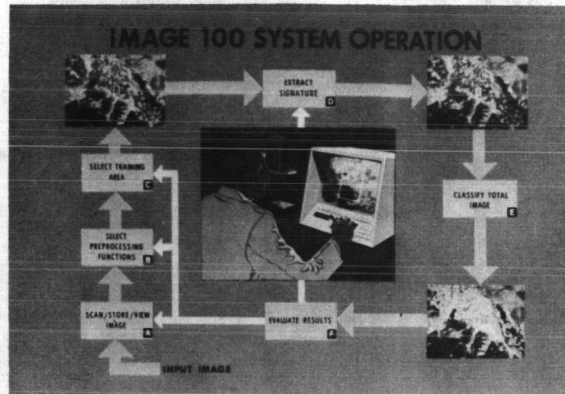


Figure 5. Functional Flow Around IMAGE 100



Figure 6. Theme Alarm Corresponding to Training Site 4 of Fig. 4

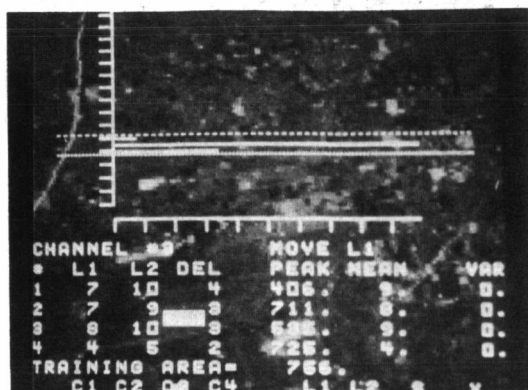


Figure 7. 1D Histogram Display, Channel 3 for Signature of Site 4 of Fig. 4



Figure 8. 2D Cluster Display, Ch 2 vs Ch 4, Projected for 4D Histogram

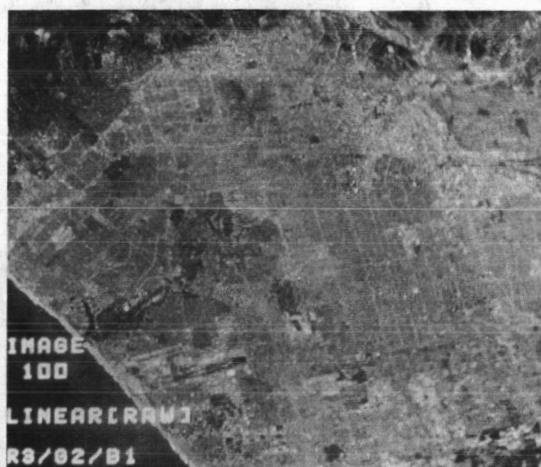


Figure 9. West Central Los Angeles - CCT -
Loaded in Standard, Linear Mode for Display



Figure 10. Hadamard Transformed
Representation of Scene from Fig. 9



Figure 11. Predominately Heavy Commercial Areas Enhanced by Slicing in Color Space
LA CBD Enlarged 3X



Figure 12. Green Spaces in the Field of View Enhanced. Enlargement of Wilshire CC 3X



Figure 13. An 8-Theme Composite Superposing the Above Themes Generated Sequentially

TABLE 1
ELEMENT PRIORITIES
(OCTOBER 15, 1973)

MANDATED BY STATE LAW: MUST BE COMPLETED BY SEPTEMBER 1974	1ST PRIORITY	1. SEISMIC SAFETY 2. PUBLIC SAFETY 3. SCENIC HIGHWAYS 4. TRANSPORTATION NOISE 5. CIRCULATION 6. WATER AND WASTE MANAGEMENT	THESE ARE DONE BUT WILL BE RE- EVALUATED FOLLOWING COMPLETION OF 1-6 ABOVE
	2ND PRIORITY	7. HOUSING 8. LAND USE 9. OPEN SPACE 10. CONSERVATION 11. PUBLIC SERVICES AND FACILITIES	
COMPLETED BY SEPTEMBER 1975 RPC CRITERIA	3RD PRIORITY	12. RECREATION 13. HUMAN RESOURCES 14. ENVIRONMENTAL QUALITY	

GENERAL PLAN TO BE COMPLETED BY SEPTEMBER 1975 THEN PERIODIC REVIEW

TABLE 2
COLA REGIONAL PLANNING
COMMISSION ORGANIZATION

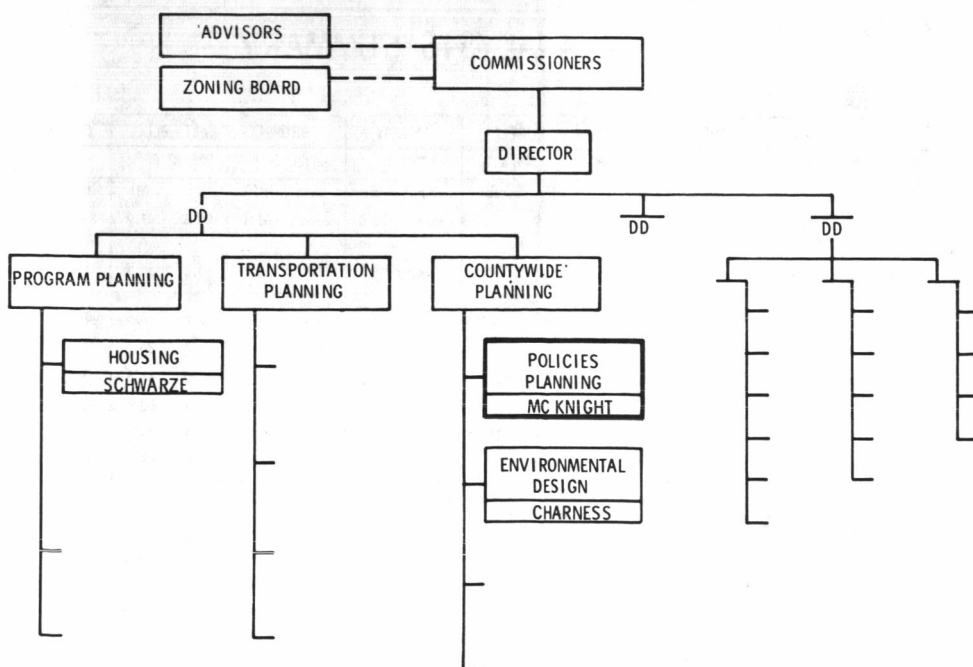


TABLE 3
COLAGE IMAGE 100 HOUSING STUDY
TEST SITE NO. 1
SAN FERNANDO VALLEY
RAW DATA OBSERVATIONS

Land Use		Theme					
Classification		Purple	Yellow	Brown	Lt.Blue	Dk.Blue	Black
Single-family residential	(L)	918	827	683	528	417	189
Multiple-family residential	(M)	3	2	1	1	2	0
Commercial	(C)	33	11	8	4	4	1
Recreational	(R)	11	4	6	8	7	1
Public	(P)	24	27	21	11	15	5
Services	(S)	89	29	21	30	27	23
Open Space	(O-1)	109	66	56	35	29	10
Vacant	(Z-1)	4	3	2	1	1	1
Area Alarmed		1,081	969	798	618	502	230
Total Area		1,360	1,435	1,394	1,470	1,394	1,344

TABLE 4
HOUSING TEST SITE NO. 1
SAN FERNANDO
ANALYSIS SUMMARY

THEME			PURPLE		YELLOW		BROWN		LT. BLUE		DK. BLUE		BLACK	
AREA ALARMED %			79.5		67.5		57.2		42.0		36.0		17.1	
	(ACRES)	(%)	(A)	(B)	(A)	(B)	(A)	(B)	(A)	(B)	(A)	(B)	(A)	(B)
SINGLE-FAMILY RESIDENTIAL	1,020.2	76.6	84.9	82.1	85.3	74.0	85.6	61.1	85.4	47.2	83.1	37.3	82.2	16.9
MULTIPLE-FAMILY RESIDENTIAL	5.5	0.4	0.3	50.0	0.2	33.3	0.1	16.7	0.2	16.7	0.4	33.3	0.0	0.0
COMMERCIAL	42.9	3.2	1.1	70.2	1.1	23.4	1.0	17.0	0.6	8.5	0.8	8.5	0.4	2.1
RECREATION	25.6	1.9	1.0	39.3	0.4	14.3	0.8	21.4	1.4	28.6	1.4	25.0	0.4	3.6
PUBLIC	31.9	2.4	2.2	68.6	2.8	77.1	2.6	60.0	3.0	31.4	3.0	42.9	2.2	14.3
SERVICES	88.5	6.6	2.0	91.8	3.0	29.9	2.6	21.6	5.4	30.9	5.4	27.8	10.0	23.7
OPEN SPACE	125.0	9.4	8.1	81.3	6.8	49.3	7.0	41.8	5.8	26.1	5.8	21.6	4.3	7.5
VACANT	4.6	0.3	0.4	80.0	0.3	60.0	0.3	40.0	0.2	20.0	0.2	20.0	0.4	20.0
	1,332.3	100.0	100.0		100.0		100.0		100.0		100.0		100.0	

(A) AREA ALARMED AS A % OF THE THEME,
e.g., AREA IDENTIFIED IN PURPLE (79.5% OF SCENE)

(B) AREA ALARMED AS A % OF THE CLASS,
e.g., LAND USE

TABLE 5

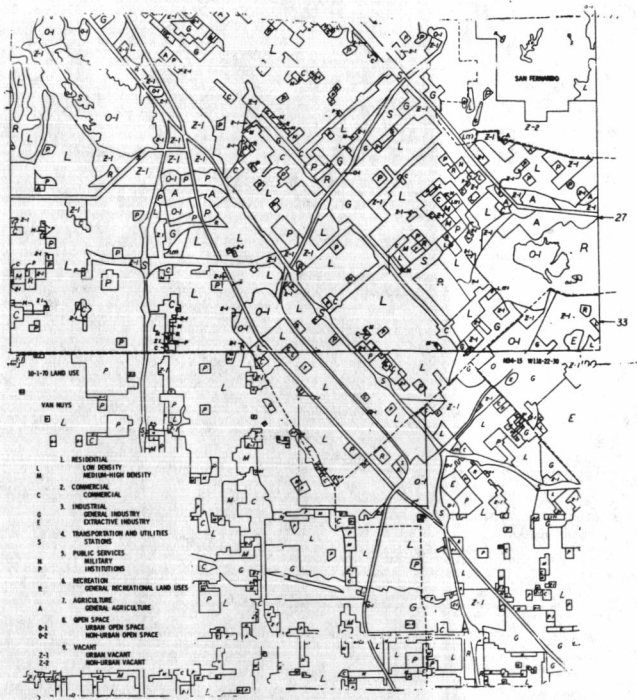


TABLE 6
APPLICATIONS OVERVIEW

COMMUNITY-ORIENTED

- DATA-CONTENTUAL
 - AGRICULTURAL SYSTEMS
 - SURFACE WATER BODIES
 - SNOW COVER
 - BRUSH FIRE BURNS
 - FORESTRY
 - GRASS GROWTH
 - PARKS, GOLF COURSES
 - DUST STORMS
 - GRADING SITES
 - GEOLOGICAL FEATURES
 - COASTAL WATER STRUCTURE

AGENCY-DIRECTED

- USER-EVALUATIONAL
 - URBANIZED REGIONS
 - RESIDENTIAL AREAS
 - HOUSING TYPES

EVALUATION OF ERTS-1 DATA FOR ACQUIRING LAND USE DATA OF NORTHERN MEGALOPOLIS

Robert B. Simpson, David T. Lindgren and William D. Goldstein, *Dartmouth College Project in Remote Sensing, Hanover, N.H.*

ABSTRACT

State planners are increasingly becoming interested in ERTS as a possible method for acquiring land use data. An important consideration to them is whether ERTS can provide such data at a savings in both time and money over alternative systems. The following is a preliminary evaluation of ERTS as a planning tool.

INTRODUCTION

Among the investigations funded by NASA under the ERTS-1 Program was one for the investigation of the land use of northern Megalopolis by the Dartmouth College Project in Remote Sensing. Specifically the objectives of this investigation were (1) to map and digitize the land use of the northern third of Megalopolis, and (2) to evaluate ERTS as a planning tool. At present we have completed the mapping and digitizing phase of the project; the evaluation of ERTS as a planning tool is in progress.

For aid in orientation, a map showing the Boston-Washington Megalopolis among the urban concentrations of the United States has been included (Fig. 1), as well as a map displaying the location and boundaries of the test area (Fig. 2).

Mapping the Land Use of Northern Megalopolis

The Color-Coded Version. Good weather over New England in mid-October 1972 provided the first fully useful imagery of our test area. Nine-by-nine transparencies of the four necessary scenes became available from the NDPFC on 18 December 1972, and the General Electric Photo Laboratory in Beltsville, Maryland, provided the essential unenhanced 1:250,000 CIR transparencies of those scenes on 3 January 1973. Working from the CIR transparencies a single photointerpreter completed the three-state land use map in draft form within three months (1 April 1973). However, it took another two months (1 June 1973) to complete the final color-coded map (Fig. 3). Thus, it took five months to complete the map by conventional photointerpretation techniques. Furthermore, because of a variety of constraints we did not use multi-seasonal coverage, we relied exclusively on MSS bulk-processed products, and we made infrequent use of the individual bands.

PRECEDING PAGE BLANK NOT FILMED

1 N74 30733

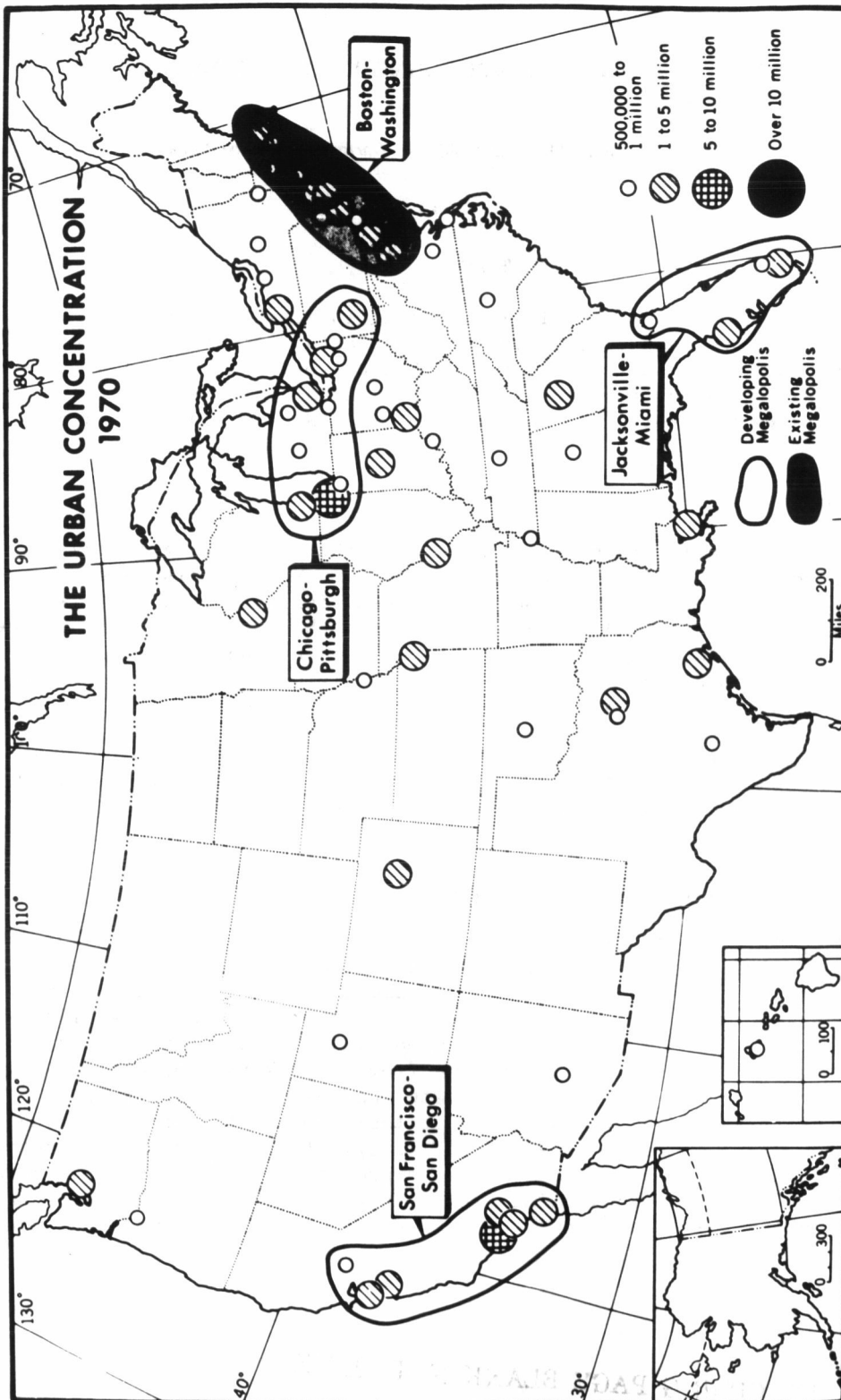


Figure 1. The Boston-Washington Megalopolis.

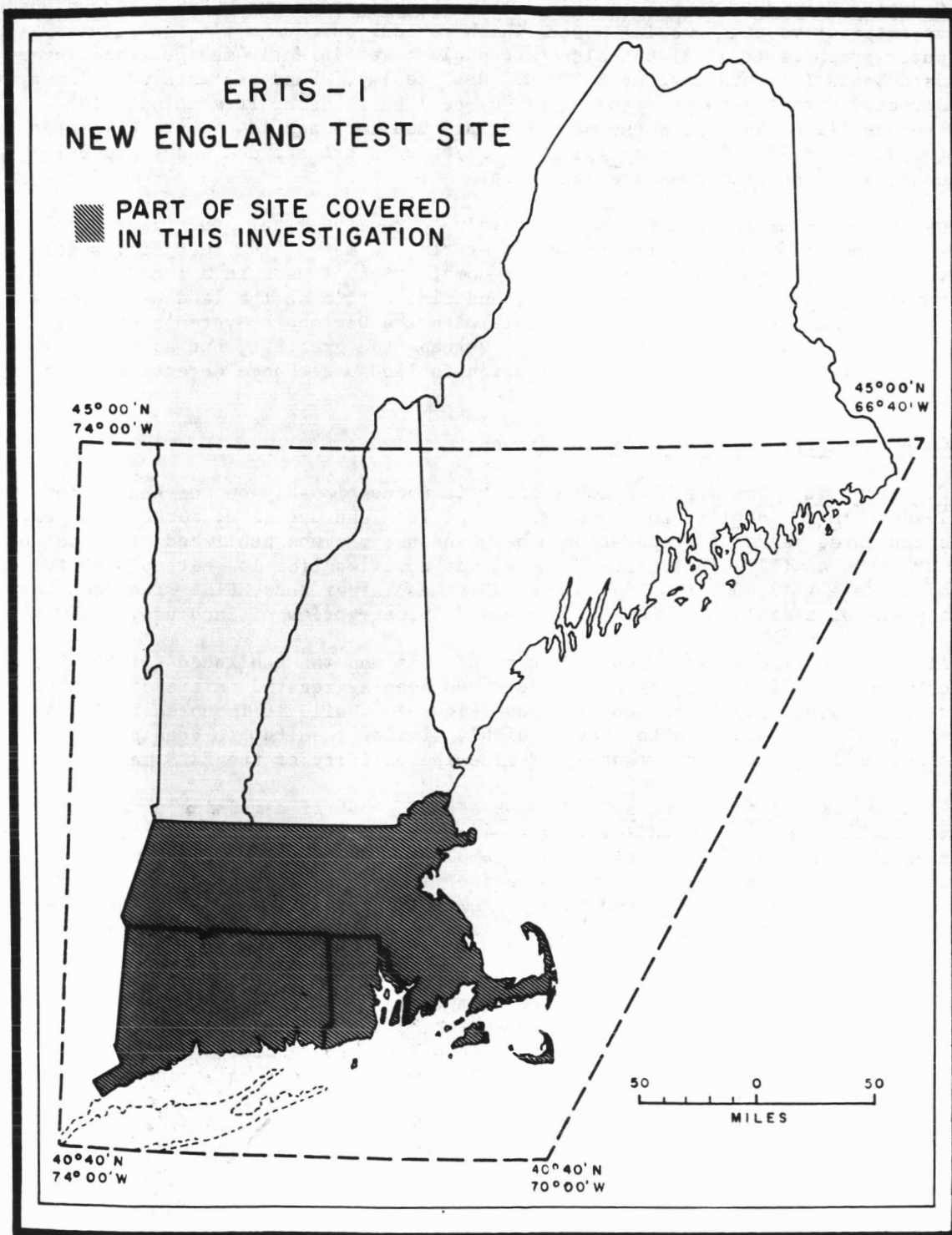


Figure 2. The Test Area.

Computer Version. In the course of this investigation the DCPRS has developed an interactive time-sharing system which not only produces fine quality computer graphics (Fig. 4) but also is capable of efficiently manipulating large data bases (in this case over 600,000 data cells). Land use data were input directly into the computer on a cell-by-cell basis using free-format disc-storage files, by typing the majority land use for each 1/4 square kilometer (62 acres) cell. Subsequently, these files were transformed under program control to the true-to-scale data base.

On the basis of these data it is possible to receive within thirty minutes real time and but a few minutes computer time, a map of the test site which visually highlights any single use or combination of uses in a form less visually complex than the multi-colored maps, and also a file on the land use summary tabulations formatted to be compatible with the Dartmouth System's correlation, regression, and clustering routines. Perhaps the greatest, but as yet untapped, asset of this system is its application to land use change detection investigations.

Comparability, Cost and Time Effectiveness.

Comparability. The state of Connecticut is unquestionably one of the national leaders in the quality and completeness of its land use data. Just this year after three years of preparation a new land use map was published at a cost of more than a million dollars. This map was compiled from low-altitude photos of a scale 1:12,000, that is, almost 90 times larger than ERTS. The resultant map was of a scale 1:24,000 and contained 55 categories of land use.

At the same time a small-scale version of this map was published (1:250,000) on which the 55 categories of land use had been aggregated into eleven, thus corresponding closely to the ERTS map (Fig. 5). While it is unrealistic to expect the two products to provide highly similar results, it does provide an opportunity to at least visually examine the validity of the ERTS map.

Cost and Time Effectiveness. We have assumed that if a meaningful land use map could be made from ERTS-1 imagery it would be at a savings in time and money over other means of production. The completion of the three-state ERTS map makes it possible to test this assumption. In the evaluation which follows, the cost of land-use mapping from ERTS is compared to that from high-altitude aircraft (RB-57 and U-2, scale 1:100,000) and from medium-altitude aircraft (scale 1:20,000).

The ERTS-1 figures have been derived from the present investigation, which has involved mapping approximately 15,000 square miles of southern New England at a scale of 1:250,000 from a single set of CIR transparencies prepared by photo laboratory processes only. The high altitude figures were also derived from the experience of the Dartmouth College Project in Remote Sensing in the investigative mapping of land use in the Boston and New Haven areas (Approximate 1,500 square miles) using NASA RB-57 photography under USGS/GAP contract in 1970-71.



Fig. 3 Land Use Map of Northern Megalopolis

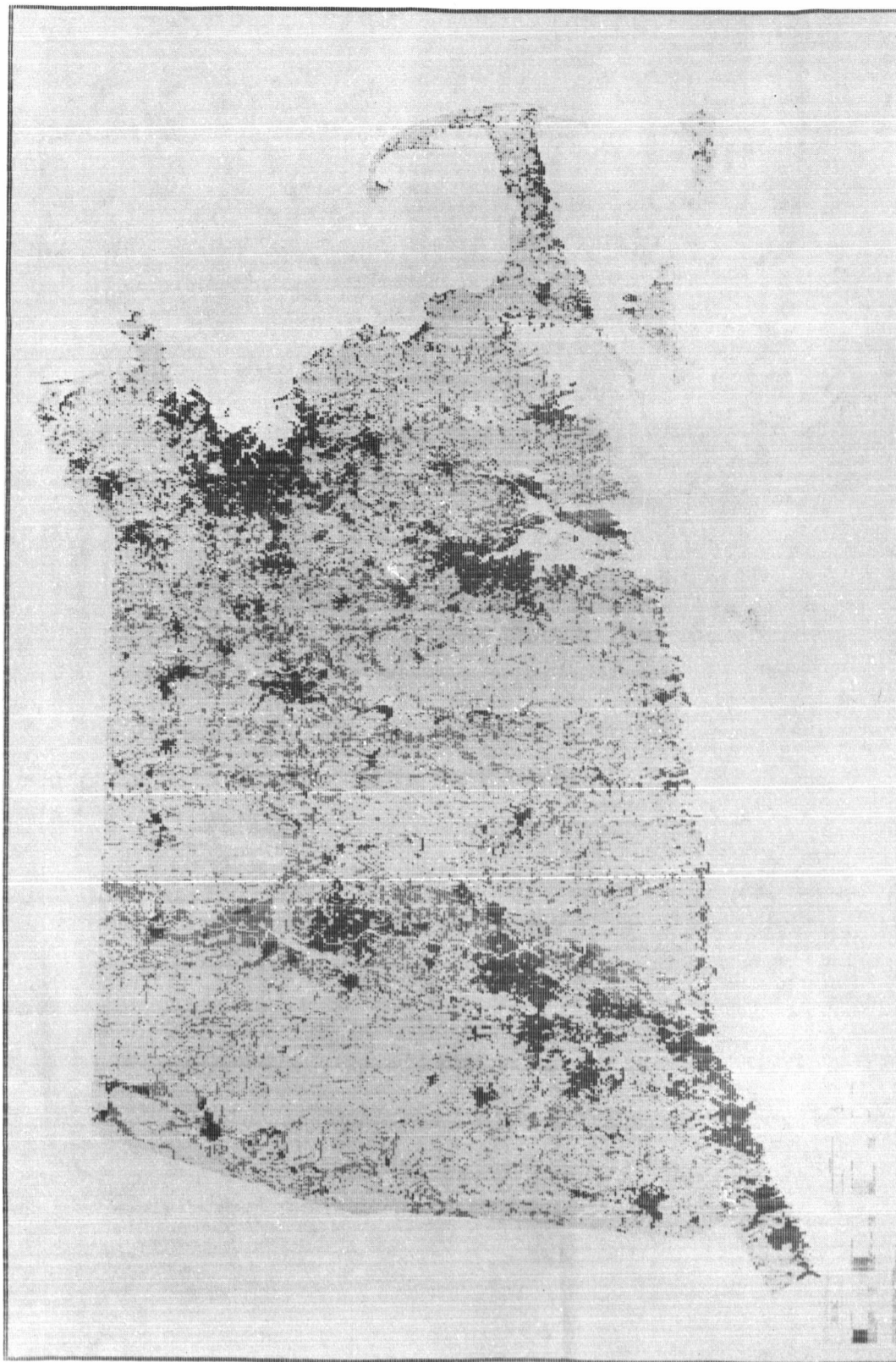


Fig. 4 Computer Map Illustrating Built-Up Land Uses Within Test Site

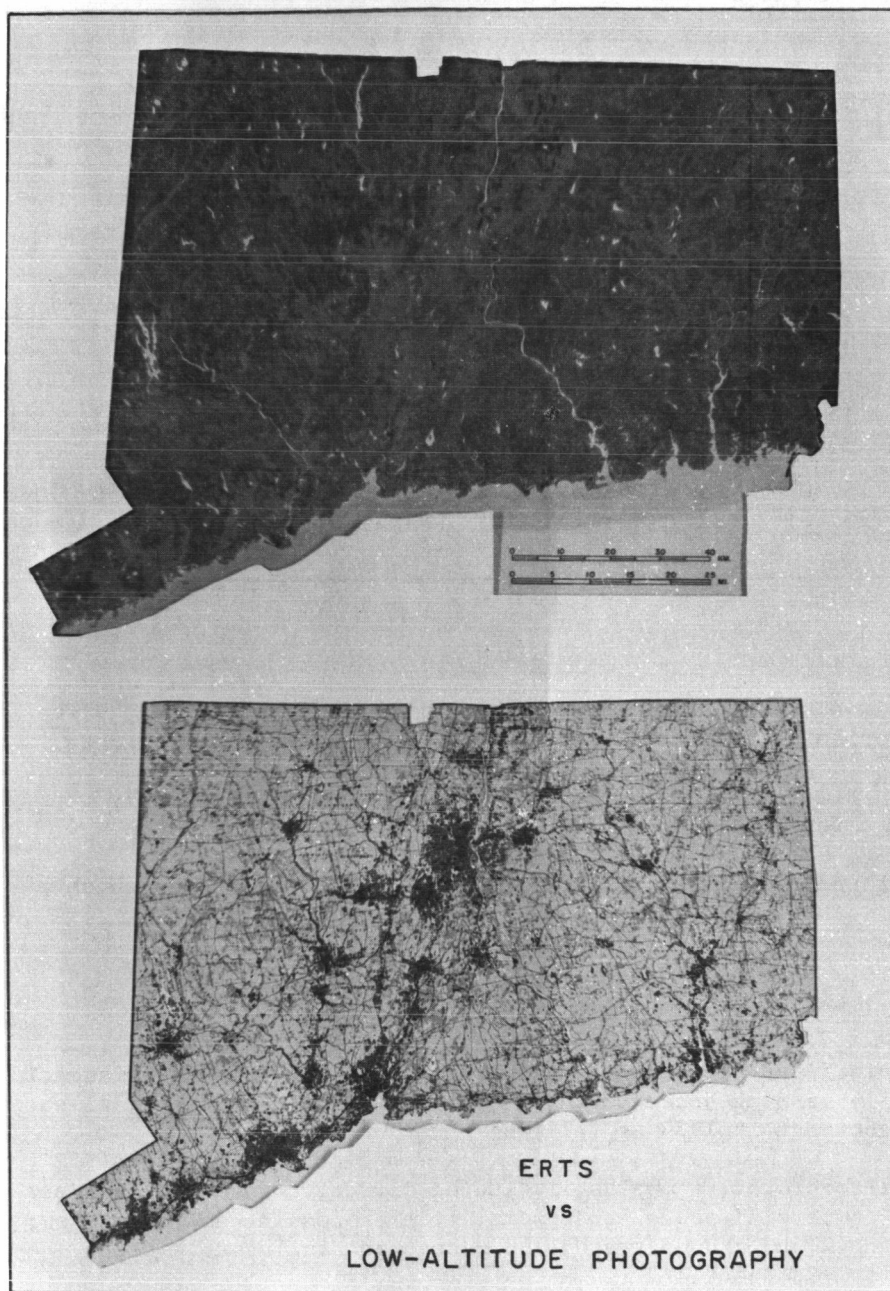


Fig. 5 Comparison of Connecticut Land Use Map with ERTS

Fig. 6

Estimates of ComparativeCost- and Time-Efficiency in Land UseMapping

	(a) <u>Cost</u>		(b) <u>Time</u>		(c) <u>Scale of</u> <u>Imagery</u>		(d) <u>Status</u>
	(\$/sq.mi.)(ratio)		(interp.hrs/ 1000 sq.mi.)(ratio)			(ratio)	
ERTS-1	\$ 1.06 ¹	1:	45 ⁵	1:	1:1,000,000	1:	Experimental
<u>High-altitude</u> <u>aircraft</u>	10.46 ²	10:	328 ⁶	7:	1:100,000	10:	Experimental
<u>Medium-altitude</u> <u>aircraft</u>	15.50 ³ (23.80) ⁴	15: (22:)	1,380 ⁷	31:	1:20,000	50:	Operational

Assumptions:

- * Product is a numerically coded b/w, or rough color-coded, map with 11 categories of land use
- * Costs and time shown are for imagery interpretation phase only (no charge for imagery)
- * Bases for individual derivations are shown in the footnotes which follow

Footnotes:

¹ Basis: This figure represents an approximation of DCPRS experience in experimentally mapping three southern states of New England (14,371 sq. mi.) under NASA contract in 1973 as follows:

Photo interpreter, 4 months, including direct, fringe and indirect costs; commercial photo lab special film processing and enlarging; field check and ground truth; and management including direct, fringe and indirect)

Total \$ 15,300

Average cost of \$ 1.06/sq. mi.

² Basis: based on DCPRS experience in experimentally mapping the Boston area (1,100 sq. mi.) under USGS contract in 1970.

Photo interpreter time reduced from 12 to 9 weeks due to reduction of categories mapped from 24 to 11, and elimination of extensive hand coloring.

Total \$ 11,506

Average cost of \$10.46 sq. mi.

³ Basis: cost estimates received from three commercial mapping agencies, for mapping an area similar to state of Connecticut (5,000 sq. mi.)

Average of the 3 was \$15.50 per sq. mi. (for interpretation and map making only)

⁴ Basis: this figure represents \$15.50 plus \$8.30/sq. mi. for photography the average of prices submitted by the 3 companies.

⁵ Basis: same as for footnote (1)

14,371 sq. mi. in 4 months (640 hrs.) of interpretation time

Average of 45 hrs. interpretation per 1,000 sq. mi.

⁶ Basis: same as for footnote (2)

1,100 sq. mi. in 9 weeks (360 hrs.) of interpretation time

Average of 328 hours interpretation per 1,000 sq. mi.

⁷ Basis: Average of the time estimates received from the three contractors referred to in footnote (3) above

1,000 sq. mi. in 1,380 hrs. interpretation time

Average of 1,380 hrs. interpretation per 1,000 sq. mi.

The lower (medium-altitude) aircraft figures represent the numerical averages of estimates provided by three commercial air-photo mapping organizations with extensive experience in Northeastern United States.

In each case purely human - visual image interpretation is assumed using conventional photo laboratory products. Field checking would be limited, but readily available published ground truth would be used extensively.

Column (a) shows that the image interpretation phase of land use mapping can be done from ERTS for about \$1/sq. mi. in comparison with approximately \$10/sq. mi. from high-altitude aircraft and \$15/sq. mi. from medium-altitude aircraft. The latter estimate maybe more conservative than the other two since it is based upon competitive commercial experience rather than on investigative research programs.

Column (b) reveals a greater spread in time-in-work estimates than in dollar-cost estimates. As much area can be mapped in one day of ERTS land use interpretation as in 7 days of U-2 or RB-57 interpretation or in 31 days of conventional photo mapping.

In summary, these figures have been compiled from experience probably as extensive as is yet available in the ERTS program, but it is regional experience and the figures should be revised as national experience accrues.

Conclusions and Recommendations.

On the basis of our research we have concluded that it is completely practical to compile an 11-category land use map for a state or group of states utilizing unenhanced ERTS-1 imagery and conventional manual photointerpretation techniques. Furthermore, the savings in both dollars and time using ERTS as opposed to aircraft are an order of magnitude more.

We have also concluded that the manual read-in by grid cell provides planning offices with a rapid and inexpensive method of converting a manually - compiled land use map to a much more broadly useful and flexible data base. We have likewise found continued user interest in the traditional color-coded land use map.

Our preliminary evaluation of ERTS' utility to planners suggests almost open-ended capabilities for the future. Initial conferences with planners in several of the New England states have revealed a near unanimity in interest in ERTS as a source of land use data. However, their degree of enthusiasm appears inversely proportional to the quality and detail of the land use information which they already have at their disposal. For example, those states which have very detailed maps and statistics perceive ERTS-1 in its present form as a tool of limited value although they see great possibilities in the earth resources satellite concept - in a platform with the performance capabilities proposed for EOS, for example. On the other hand, those states possessing little current land use information can visualize an immediate utility for ERTS-1 data.

It should certainly be pointed out, however, that both types of states are reserving any final judgement on ERTS until further statistical evaluation has been completed. To that end we expect to make an evaluation of the accuracy of our ERTS-1 land use data using land use data acquired by the Connecticut Office of State Planning as a base. Since much of the ERTS research, particularly in land use, has been conducted in the semi-arid West where landscapes are more homogeneous and parcel sizes larger, we feel that the humid Northeast with its smaller parcel sizes, its complex physiographic and cultural landscapes, and its heavier population densities, provides a better test of ERTS' land use capabilities. The smaller size of eastern states, especially in New England, also gives us an opportunity to work with a variety of land use philosophies and planning organizations.

In the remaining months of our ERTS-1 research we of the Dartmouth College Project in Remote Sensing hope to more effectively evaluate ERTS in terms of planners needs. In ERTS-1 we have gathered land use data and prepared maps which we are taking to planners for their evaluation. Under ERTS-B it is proposed that the planners, in this case from the New Hampshire Office of Comprehensive Planning, work with us from the very start, and that the evaluation take place continuously as we compile from ERTS a single comprehensive state land use map for New Hampshire utilizing the latest and most efficient techniques. This map will be compiled with New Hampshire on a cost-sharing basis and when completed should enable us to provide the most penetrating evaluation of ERTS from a land use planning viewpoint yet undertaken.

Finally, we are eagerly looking for progress towards a true second generation earth resources satellite. The 10-meter resolution proposal for EOS should provide us with a truly effective land use mapping tool.

THE VALUE OF ERTS-1 IMAGERY IN RESOURCE INVENTORIZATION ON A NATIONAL SCALE IN SOUTH AFRICA

O. G. Malan, *National Physical Research Laboratory, CSIR, Pretoria*; C. N. MacVicar, *Soil and Irrigation Research Institute, Pretoria*; D. Edwards, *Botanical Research Institute, Pretoria*; B. N. Temperley, *Geological Survey, Pretoria*; and L. Claassen and collaborators, *Department of Planning and the Environment, Pretoria*

ABSTRACT

It has been shown that ERTS imagery, particularly in the form of 1:500 000 scale false colour photolithographic prints, can contribute very significantly towards facilitating and accelerating (dramatically, in some cases) resource surveys and geologic mapping. Fire mapping on a national scale becomes a feasibility; numerous new geologic features, particularly lineaments, have been discovered, land-use can be mapped efficiently on a regional scale and degraded areas identified.

The first detailed tectonic and geomorphological maps of the Republic of South Africa will be published in the near future mainly owing to the availability of ERTS images.

INTRODUCTION

This paper reports some of the results of ERTS participation proposal SR-9616 'To Assess the Value of Satellite Imagery in Resource InventORIZATION on a National Scale', Principal Investigator, O.G. Malan.

This project was managed by an ERTS Investigator's Committee, under the chairmanship of the Principal Investigator, which included representatives of the cooperating agencies; the Soil and Irrigation Research Institute and Botanical Research Institute, both of the Department of Agricultural Technical Services, the Geological Survey of the Department of Mines and the Department of Planning and the Environment as well as from organizations rendering support services.

The general approach in this study was an attempt to integrate ERTS results on a broad scale into current resource survey programmes, rather than to create an intensive new research project.

- 1) National Physical Research Laboratory, CSIR, Pretoria
- 2) Soil and Irrigation Research Institute, Pretoria
- 3) Botanical Research Institute, Pretoria
- 4) Geological Survey, Pretoria
- 5) Department of Planning and the Environment, Pretoria

1 N 74 30734

The advantage of this approach was that it was possible to draw on the experience of a larger number individuals from a variety of agencies representing mainly 'end users' confronted with practical resource survey and management problems rather than purely academic issues. Also use could thus be made of existing organisational structures, facilities and field personnel.

A disadvantage was that, because of other priorities in current programmes of the agencies involved, progress sometimes was slower than expected and all objectives could not be achieved before the deadlines imposed by NASA. Furthermore, because the priorities of different agencies did not coincide geographically, a truly multidisciplinary investigation has not been achieved. Such an approach would most probably have yielded considerably more information than the sum of the separate investigations.

Besides the cooperating agencies, useful contributions were also received from individual scientists attached to universities and other research organizations.

COVERAGE

All 77 scene positions covering the Republic of South Africa were imaged, of which only 7 were not imaged at least once with less than 5 % cloud cover. Of these, 30 % cloud cover was the worst. The remaining scene positions were imaged cloud free up to seven times. With the exception of six RBV frames, all imagery was MSS.

Unfortunately these images were not evenly distributed temporally: No images were acquired over the Republic during the autumn-winter months April to July. This is to be regretted for three reasons:

- 1) No mid-winter images, with the lowest sun angles accentuating topographic features, were available.
- 2) The possibility of detecting urban air pollution, which is worst during winter mornings in the interior, could not be tested.
- 3) Experience with high level false colour aerial photography indicated that maximal discrimination between some vegetation types could be expected during autumn.

DATA HANDLING

Initially an organization was set up to produce and distribute 1:1000 000 scale black and white photographic prints produced from 70 mm positives. Although these were usually adequate for the identification of geologic structural features, it soon became apparent that for vegetation and land use purposes, this product was unsatisfactory.

Experiments were therefore undertaken to produce economically a large scale false colour product. The optimum product in terms of ease of production and handling, cost and information content was found to be 1:500 000 scale false colour photolithographic prints. Since the NDPF 70 mm positive transparencies were often unsharp, these were produced from 9 inch positive transparencies in the following manner:

In order to obtain a final scale as closely as possible to 1:500 000, a cartographic analysis was undertaken. This indicated that a cross track registration mark separation of on the average 397 mm (compared to 395 mm nominal) was required.

In one step the NDPF 9 inch positive was enlarged to a negative screen of this scale with 175 screen points per inch (giving 6.5 million screen points per colour compared with 7.5 million theoretical data points per band). Simultaneously the contrast was also increased by processing step 5 and step 14 of the grey scale, respectively, to 0 % and 100 % transmission (in the negative screen). Densitometry on a few selected scenes have indicated that very little information is lost by sacrificing the extreme ends of the grey scale in favour of increased contrast.

MSS bands, 4, 5 and 7 were then offset printed in a set of trichromatic colours, respectively yellow, magenta and cyan.

It is gratifying to note, as indicated by the example of the street pattern of Paulpietersburg situated at approximately 30° 50' E, 27° 25' S in scene 1047-07191 (Fig. 1), that the 'resolution' has apparently improved through the three additional generations (screen, plate, print) after the NDPF product.

This product has received very favourable comment from all investigators both with respect to ease of interpretation and annotation. It can be highly recommended since it can be produced by a process which is commonly commercially available at a reasonable cost (locally approximately US \$200 per scene per first 100 copies, rising US \$7 per additional 100 copies).

It proved to be so popular with scientists from universities, exploration companies, governmental agencies etc., that total coverage of the Republic is currently being produced on a subscription basis.

An I²S Mini-Addcol Additive Colour Viewer was also employed in some investigations and Computer Compatible Tapes were received, but too late to include any results in this paper.

RESULTS

Only some major results of the investigation will be highlighted. The complete Type III report, which will be released by NASA in due course, should be consulted for more details.

Soil Mapping--Identification of soil types was only possible where a close correlation exists between soil type, vegetation, terrain morphology, geology, climate or land use. Nevertheless ERTS imagery draws attention to differences within specific areas and in special cases allowed personnel to determine some of the known boundaries more accurately and faster.

Geomorphological Mapping--The possibilities of application of ERTS images in geomorphological mapping are very promising - particularly in arid regions. This data base, being ideally commensurate with the small scale mapping, eliminates the cost and drudgery associated with conventional sources of information. Geomorphological features such as mountains, ridges, river valleys and alluvium, footslopes, plateaux, canyons, alluvial, colluvial and aeolean deposits, etc. could be identified consistently.

The first detailed 1:1500 000 scale geomorphological map of the Republic of South Africa will be taken from its present second approximation to the final publication edition solely as a result of ERTS imagery. In Figure 2 a portion of this map is shown.

Agricultural Land Use and Planning--It is possible to distinguish cultivated land, natural grazing land and irrigation schemes. In special cases further subdivision is possible.

Areas where mismanagement has led to over exploitation of natural vegetation or the invasion of degraded vegetation types can be identified.

On the basis of ERTS images it is also possible to delineate homogeneous agricultural areas for the purpose of planning for optimal land utilization as shown in Figure 3 for the Springbok Flats and adjacent region.

Urban and Regional Land Use--Except when applied to very broad and large scale components of a metropolitan area, the scale of ERTS images is too small to yield significant results in urban land use.

For land use on a regional scale as shown, for example, by a comparison of Figures 4 and 5, ERTS images yield information which differs negligibly from that provided by conventional aerial photography. The time required for the analysis of a 1:500 000 false colour ERTS print of this area was minimal in comparison.

This means that ERTS images enables a rapid inventory of land use on a regional scale for the entire Republic - a task which, by conventional means, would have been well-nigh impossible.

Roads and railways can be located depending on the contrast with the surroundings. Roads are particularly visible during or soon after construction or when surfaced with light coloured materials such as calcrete. Railways can be located over long distances in some areas, probably owing to deliberate burning of grass along the tracks to prevent coal burning steam engines from igniting grazeland.

Water reservoirs and larger ponds can be identified as well as political boundaries such as those between the Republic and South West Africa, Lesotho and Swaziland.

Vegetation Mapping--Major vegetation types can be mapped, often with a high degree of accuracy, as established by ground control or by comparison with aerial photography, in spite of the fact that in most cases images were acquired during a season when differentiation was less than optimum. Maximal differentiation can be obtained for dense wooded forest and scrub as well as for sparse vegetation types.

These surveys, for example those illustrated in Figure 6 and 7, could be completed within a matter of weeks as opposed to periods of years by conventional means.

Failure to resolve some vegetation types such as open savanna from grassland or natural forest from exotic tree plantations and shrub might be due to the unfavourable time of imagery.

Fire Mapping--An unexpected result of great importance for management purposes has been the ease with which burnt area can be mapped. This applies to both grassland in the interior and shrub vegetation such as 'fynbos' (macchia) in the Western Cape (Figure 7).

In the case of grassland, which may be burnt annually, a preliminary survey in Natal has shown that the position, extent as well as time of burning to within less than 18 days can be determined with ease. In the case of 'fynbos', which is burnt every few years, the age of the vegetation in burnt areas could be estimated up to 5 years and more.

Thus by use of ERTS imagery the monitoring of veld fires on a national scale becomes a practicability for the first time.

Geology--The most significant contribution of ERTS imagery in South African geology to date has been the discovery of numerous previously unknown lineaments, such as indicated in Figure 8.

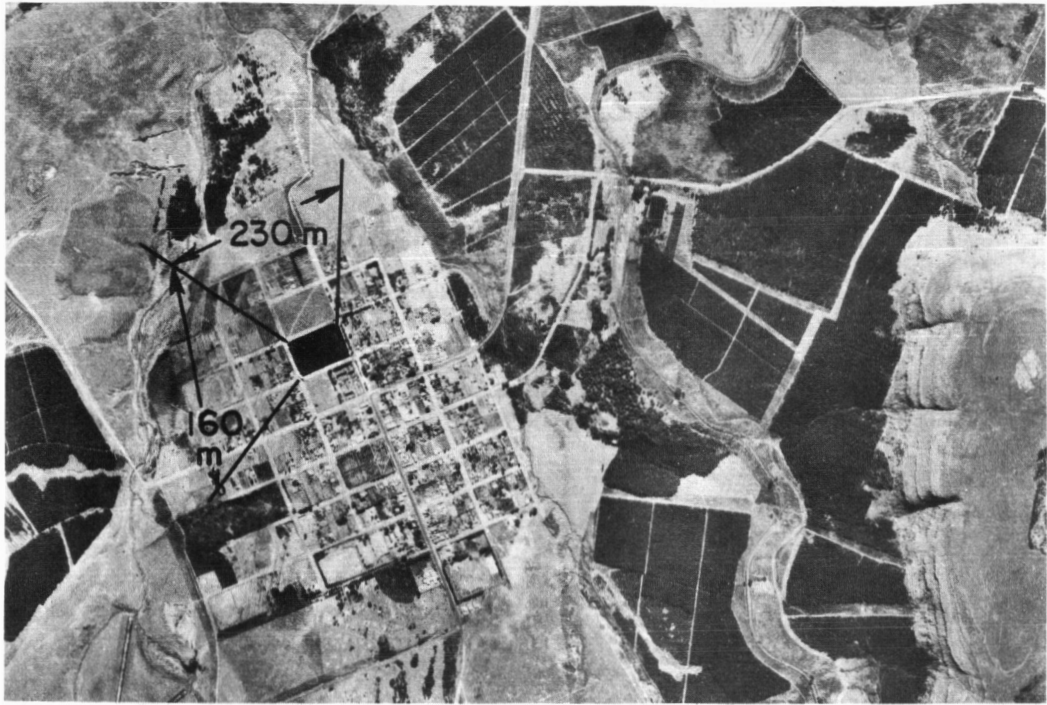
ERTS imagery has been so informative that it is already being used routinely in all current survey and small scale mapping and map revision programmes.

The compilation of the first detailed tectonic map of the Republic of South Africa has been initiated as a result of the availability of ERTS images.

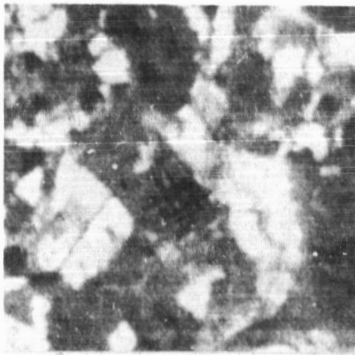
The potential benefit of ERTS to economic geology may be judged from the very lively interest of local mining and exploration companies in the 1:500 000 false colour prints.

CONCLUSION

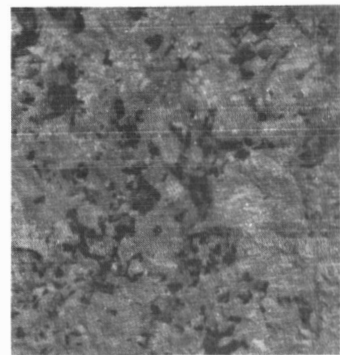
1. An ERTS image product, 1:500 000 scale false colour photolitho prints can easily be mass produced in consistent quality at a reasonable cost.
2. This product is easy to interpret with limited training and can be phased into current resource survey programmes without specialized equipment or major problems.
3. Being ideally commensurate with mapping scales at regional or national level, ERTS images can reduce the cost of and time required for national resource inventorization very significantly and make previously impossible types of survey a practicability.
4. Those government agencies most familiar with ERTS imagery in the Republic of South Africa, already routinely use them in their current survey programmes.



a) Aerial Photograph, 1:27 000



b) Negative print
Band 5
ca 1:150 000



c) False colour
Bands 4, 5 & 7
1:500 000

FIG. 1 Aerial and ERTS photography
of Paulpietersburg

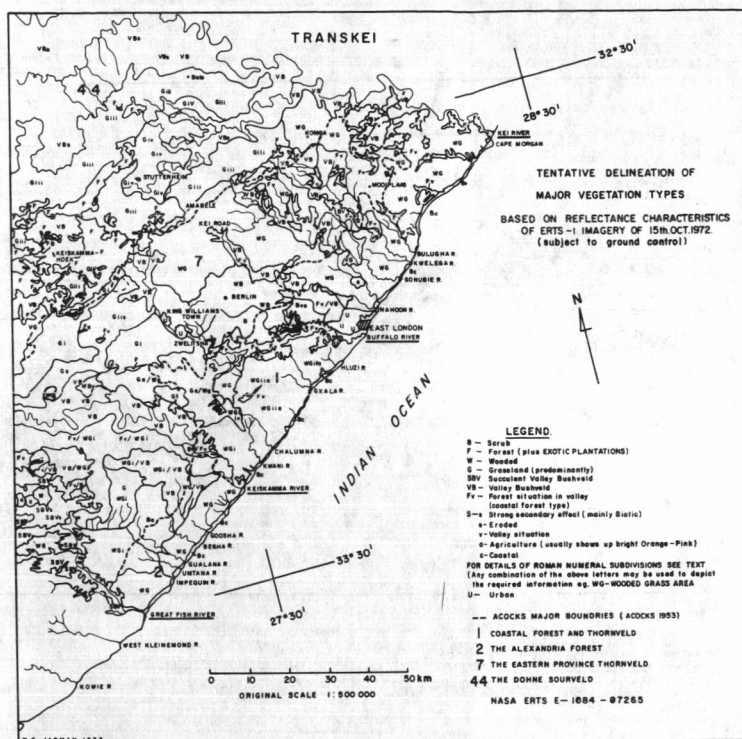


FIG. 6 Vegetation map of Eastern Cape based on E 1084-07265 1:500 000 false colour lithoprint

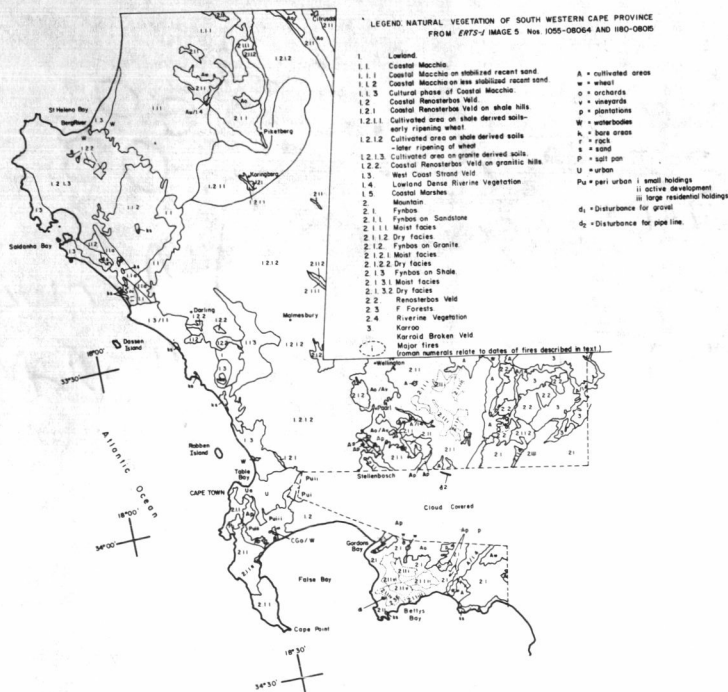


FIG. 7 Vegetation map of Southwestern Cape based on E 1055-08064 and E1180-08015 1:500 000 false colour lithoprints

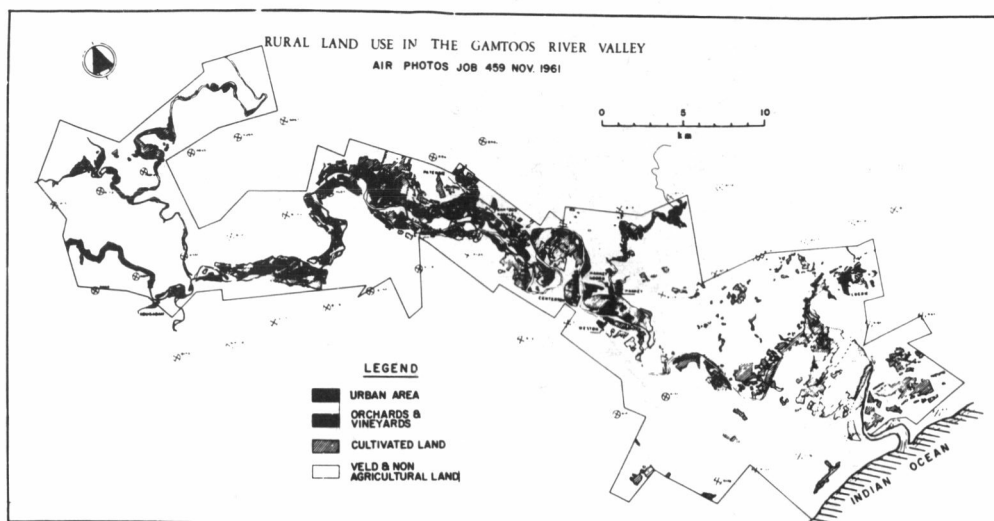


FIG. 4 Rural land use in Gamtoos River Valley from aerial photography

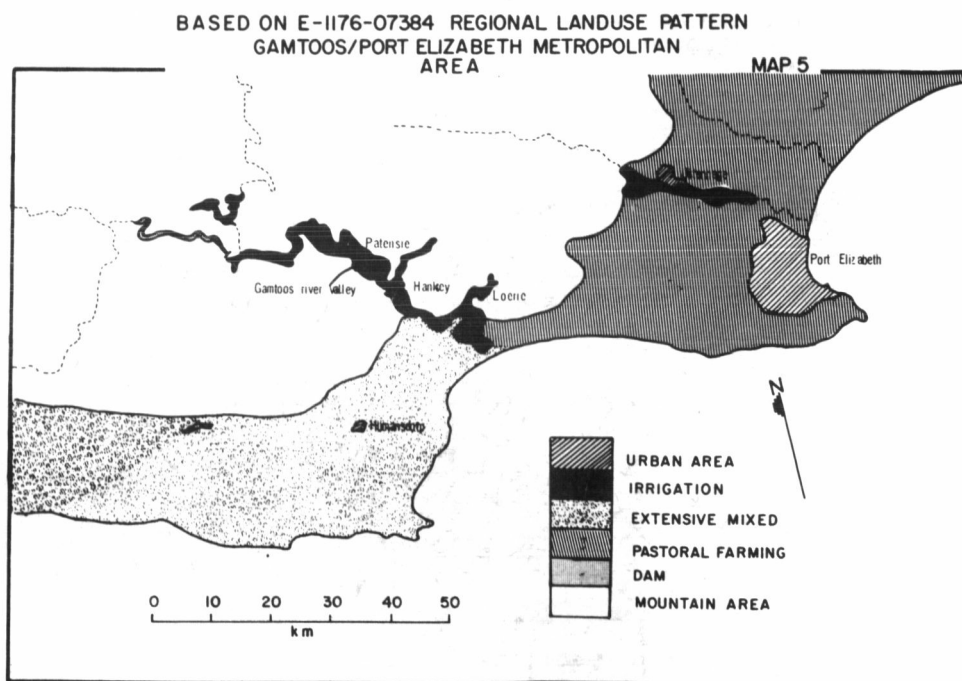


FIG. 5 Regional land use in Gamtoos River Valley based on E-1176-07384 1:500 000 false colour lithoprint

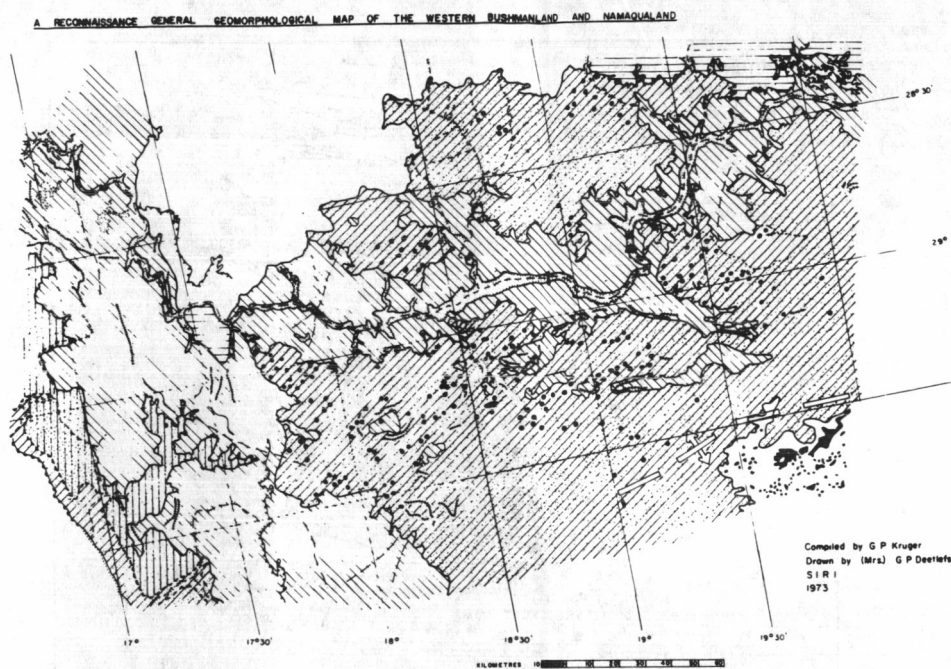


FIG. 2 Reconnaissance general geomorphological map of western Bushmanland and Namaqualand

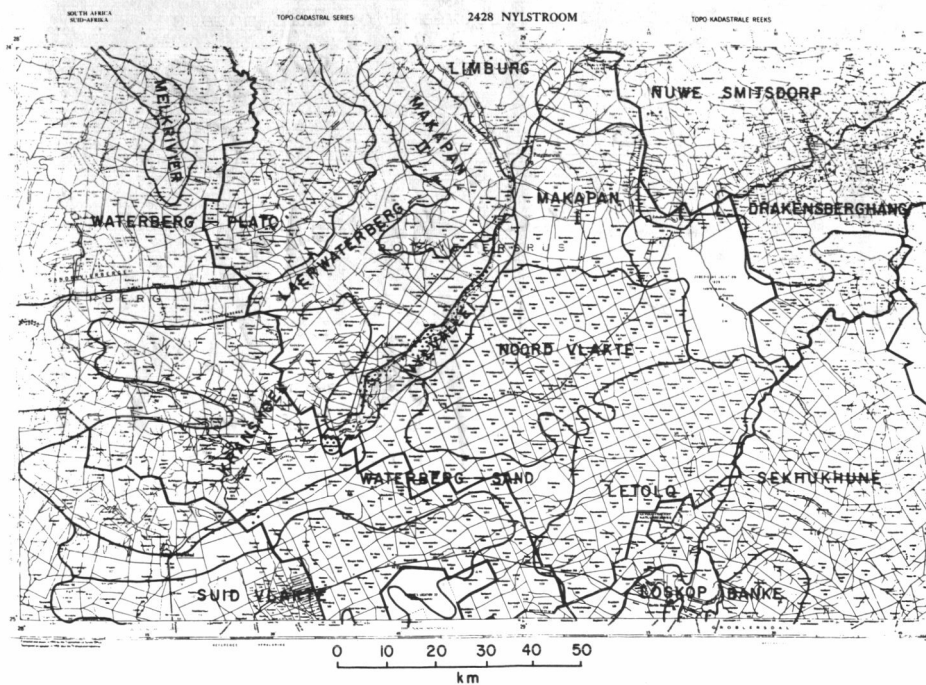


FIG. 3 Broad agricultural regions based on E 1049-07295 superimposed on topocadastral map

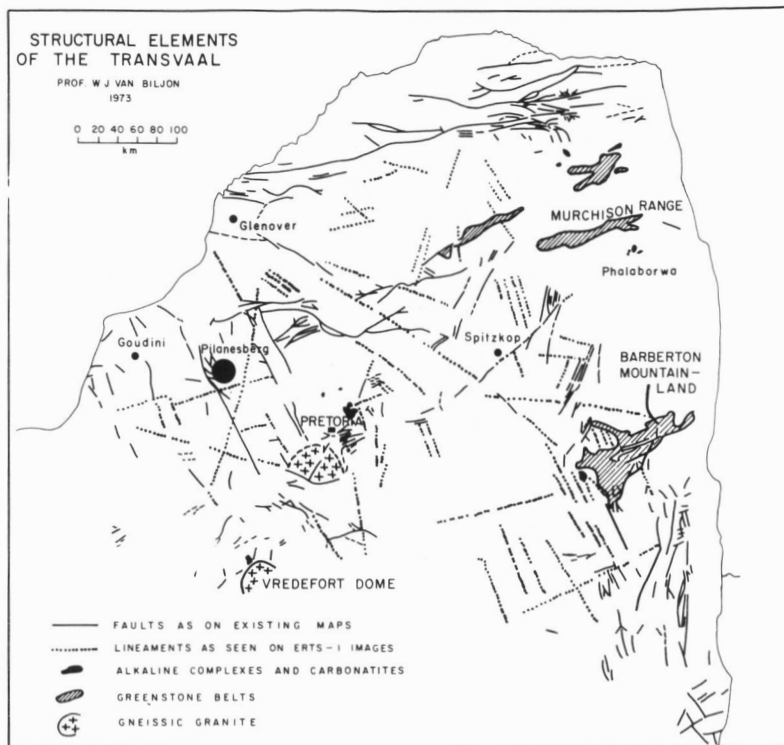


FIG. 8 Structural elements of the Transvaal, known and new features discovered on ERTS mosaic

**CHANGE IN LAND USE IN THE PHOENIX (1:250,000) QUADRANGLE, ARIZONA
BETWEEN 1970 AND 1973: ERTS AS AN AID IN A NATIONWIDE PROGRAM FOR
MAPPING GENERAL LAND USE**

John L. Place, *U.S. Geological Survey, Geographic Applications Program, Washington, D.C.*

ABSTRACT

Changes in land use between 1970 and 1973 in the Phoenix (1:250,000 scale) Quadrangle in Arizona have been mapped using only the images from ERTS-1, tending to verify the utility of a standard land use classification system proposed for use with ERTS images. ERTS 9 x 9 transparencies, interpreted by several techniques, were used to update a land use map previously compiled with 1970 air photos. Types of changes detected have been (1) new residential development of former cropland and rangeland; (2) new cropland from the desert; and (3) new reservoir fill-up. The seasonal changing of vegetation patterns in ERTS has complemented air photos in delimiting the boundaries of some land use types. Inasmuch as air photos normally are a year or more out of date, ERTS provided currency.

ERTS images, in combination with other sources of information, can assist in mapping the generalized land use of the fifty states by the standard 1:250,000 quadrangles. Several states are already working cooperatively in this type of mapping. This monitoring of land use change can be of value to planners and resource managers at Federal, state, and regional levels, both for resource development and environmental protection in broad areas of the United States. The ERTS images focus attention on those areas requiring more intensive study.

Approved for publication by Director, U.S. Geological Survey, paper to be given at the NASA/ERTS-1 Symposium, Washington, D.C. December 10-13, 1973.

1 N 74 30735

The objectives of ERTS investigation number SR 186 have been (1) to test the interpretability of ERTS-1 images for use in the mapping of generalized land use, and (2) to test the applicability of ERTS-1 images in detecting changes and updating maps.

After using the ERTS images, it is apparent that they will be of help, in combination with other sources of information, in mapping the generalized land use of the fifty states by 1:250,000 quadrangles. A cooperative program has already been established to do this with several states and multi-state regional commissions. The ERTS coverage could be of particular value in selecting which quadrangles are in greatest need of update in the first cycle of revision.

Figure 1 is the most recent map showing land use for most or all of the United States. It presents information that was collected by conventional means over a period of several years, and it was in part out of date at the time that it was published by the USGS in the National Atlas of the United States. With the advent of earth satellite sensors, supplemented by air photos, it became possible to monitor land use changes on a nearly real-time basis. It was believed that to reduce costs, the mapping and updating should be computerized and should be built around the standard 1:250,000-scale topographic quadrangles, the largest scale of maps for which we have complete coverage of the fifty states.

The Phoenix quadrangle in Arizona (see Figure 2) was selected as the pilot project, and it would also serve as a test of land use mapping in arid lands. Figure 2 shows a 2 x 2 matrix of four quadrangles in southern Arizona. The Phoenix quadrangle is the one to the northwest. The other three were investigated under sponsorship of the EROS Program as a complementary effort.

The first step in producing a computerized map of land use is to compile by hand, as shown in Figure 3, while interpreting high-altitude air photos, supplemented by satellite imagery. This particular hand-compiled map of land use in the Phoenix Quadrangle was drawn from U-2 photos taken in November 1970.

The data from the land use maps were read into a computerized data bank along with data on land ownership, soils, drainage, and census codes for state, county and tracts as listed in Figure 4.

Figure 5 illustrates the first example of an automated plot of land use from the computer data bank. The general land uses are shown in color. The black plate from the standard topographic quadrangle has been overlain to provide place names, linear patterns and much of the marginal information.

Figure 6 shows a blow-up of the eastern edge of that last map, showing most of the Phoenix metropolitan area. The colors represent the first level of our land use classification system, and different symbols are used to show the second level of detail.

Figure 7 presents the land use classification system which was used in the Arizona study. It has been published in USGS Circular 671. The first level was designed for interpreting satellite imagery; the second level for high-altitude aircraft photography. It is open ended for users to add other levels as desired.

An example of one color plate of the land use map is presented in Figure 8. Our Calcomp 763 plotter plotted this cropland plate. The dense symbols are tree crops, in this case citrus, and the lighter patterns are other crops. Changes in the land use record can be made very simply by card input to update specific cells.

Change detection has been an important part of our work, with special emphasis on our ERTS experiment. Of the many techniques that we have used to interpret ERTS images, the one that worked best was the seasonal comparison of ERTS color composites.

Figure 9 is a color composite of the Phoenix area in August 1972, right after the launch of ERTS-1. Our processing got better later, but desert vegetation looks drab, colorless during the summer. The irrigated fields near Phoenix show red. Here the MSS 4, 5, and 6 bands are combined.

An October view of the same area is shown in Figure 10. Improved color results from the substitution of the 7 band in place of the 6 band in the composite. However, the natural vegetation still looks dry and colorless before the beginning of the primary rainy season.

Figure 11 is a February ERTS scene during a very rainy winter. The natural grasses in the desert show bright red, and desert brush appears redder and lusher. These are bands 4, 5, and 7.

Figure 12 is the May ERTS scene of the same area. The natural grasses are beginning to brown out. The pattern of Phoenix urban land use is particularly clear in this ERTS composite. The upper end of the new Painted Rock Reservoir is visible near the southwest corner. Study of reservoir fluctuation may be one use of ERTS.

Figure 13 is a September ERTS scene from the pass west of the one shown in the previous three figures. In September, the Painted Rock Reservoir downstream from Gila Bend has not yet started to fill. The fall vegetation is too drab to silhouette man-made features well; however, the mine tailings and pits at Ajo show up clearly.

An I²S Color Additive Viewer was used to create experimental color composites. This viewer handles 70 mm film chips. As illustrated in Figure 14, to get greater magnification, 70 mm chips were cut out of 9 x 9 transparencies, and these were mounted in the film viewer.

Figure 15 illustrated what the chip looks like when blown up onto the display screen of the I²S viewer. At a scale of 1:380,000 on the scope, it resembled the 1:250,000 scale of the 1970 hand-drawn map that we were trying to update.

When that MSS 5 band was combined with bands 4 and 6 in the viewer, the color composite shown in Figure 16 was created. This is a photograph of the display scope, one way to keep a record of experimental settings.

When ERTS images from different time periods were overlain using different color filters, it was expected that differences of changes would be enhanced. They were as shown in Figure 17, but primarily it enhanced differences in stage of vegetation growth, not differences in general land use. This technique was a little disappointing. Quick-flip technique also showed too much clutter.

We also tried density slicing of an ERTS 5 band image using a Data Color Viewer as shown in Figure 18. This gave us experience in planning for the use of computer compatible tapes which are now being investigated. We learned to focus in on areas of relatively homogenous use, that is, urban or rural, but not both. In Figure 18, by focussing-in on downtown Phoenix, business streets and commercial-industrial districts are enhanced, but it is still cluttered.

From all these image interpretation techniques, particularly the color composites of the ERTS images, we compiled maps

of change detected using ERTS. Early efforts had many inaccuracies, but as seasonal changes in vegetation were monitored by ERTS, a much more accurate delineation was possible. The muted colors shown in Figure 19 are the original 1970 land use map. The brighter colors are the changes detected using only ERTS images. The red is new urban, the green is new cropland, and the dark blue is new water surfaces, as shown in the legend in Figure 20.

As a check of accuracy, we did the same change detection shown in Figure 21, using U-2 air photographs taken November 1972. This map of change is more detailed than the ERTS change map, but the ERTS map is more up-to-date reflecting changes of the past few months. The total areas of change are similar in the two maps, and the distribution pattern is also similar. ERTS and air photos complement each other. ERTS certainly focusses attention on rapidly-changing areas.

In Figure 22, the total change in the Phoenix quadrangle has been summarized from data bank in this matrix of change "from" and "to".

The utility of having other factors combined in the data bank is illustrated in Figure 23 where that last change matrix is divided up in four matrices by land ownership classes, private, state, public lands, and Indian lands.

As examples of queries that we have made to the Phoenix data bank, we asked, how much land has been lost from agriculture to urban use in Maricopa County between February and November 1970? The answer: 6 square kilometers. Of the best agricultural soil, how many square kilometers are still in rangeland? The answer: 1760 square kilometers. Used for urban? 349 square kilometers. And these areas could be plotted as maps.

In the past few weeks, more effort has been given toward plotting the original digitized polygons in map form, thus gaining greater accuracy over the cellular maps. In Figure 24, the land use patterns on the east side of Phoenix are outlined as polygons by a Calcomp 763 plotter.

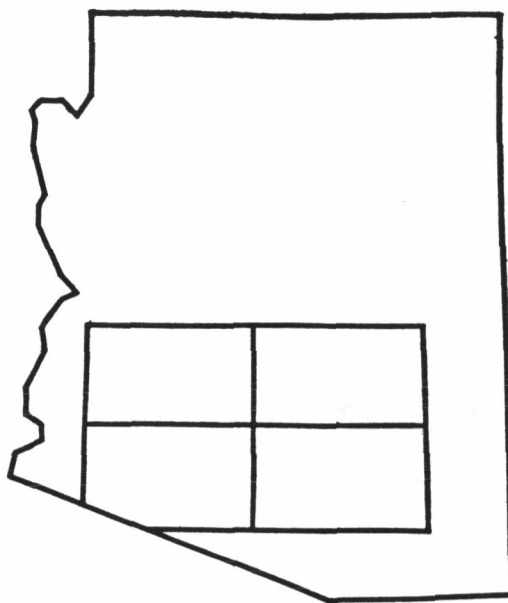
In Figure 25, land use polygons are filled-in automatically with colored symbols. In this case, the area is around Gila Bend, Arizona.

We have the capability to convert the polygons automatically to cells in order to exploit our existing soft-ware for statistical analysis.

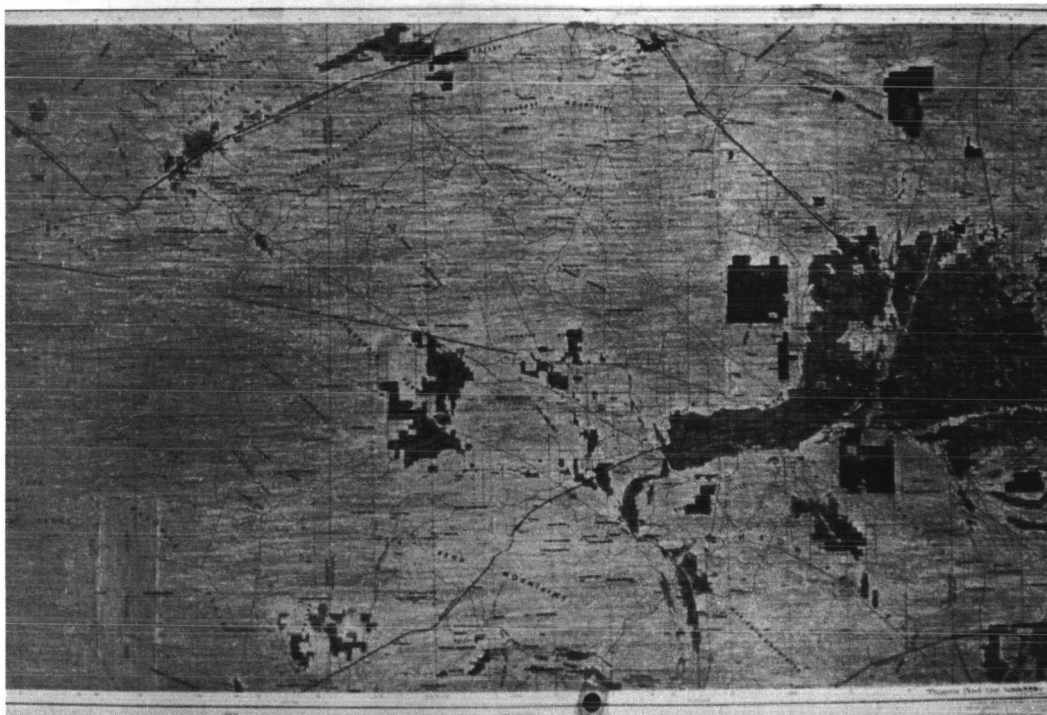
Primarily we have been creating an array of procedures to be applied to various tasks. The USGS has been attempting to work with individual states, mostly through multi-state regional organizations and have established cooperative working arrangements with the Ozark Regional Commission and the Appalachian Regional Commission to map parts of their regions, using the procedures that I have just described, developed originally for the Phoenix Quadrangle, utilizing all available sources of information, including ERTS images. The ERTS images provide currency and improved interpretation of land use where seasonally-changing patterns help to indicate use.



1. The land use map from the National Atlas of the United States. This is the most recent map of land use covering all or most of the country, but it took several years to compile and is many years out of date.



2. An orientation map of the four 1:250,000 scale quadrangles currently being worked on in Arizona. The Phoenix quadrangles is the one on the northwest.



3. Hand-drawn land use map of the entire Phoenix Quadrangle (scale 1:250,000), compiled from aerial and satellite photography. The ERTS images were compared to this type of map in order to detect changes. This map is merely an interim working step in digitizing the computerized model and map.

FACTORS IN DATA BANKS

LAND USE

DRAINAGE

OWNERSHIP

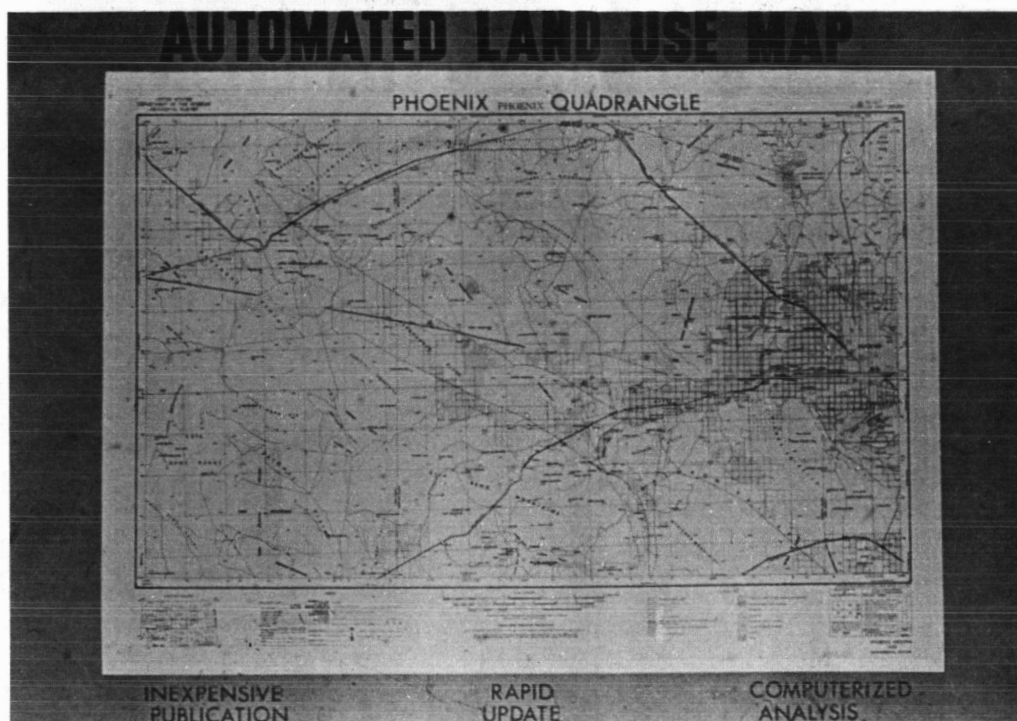
STATE CODE

SOILS

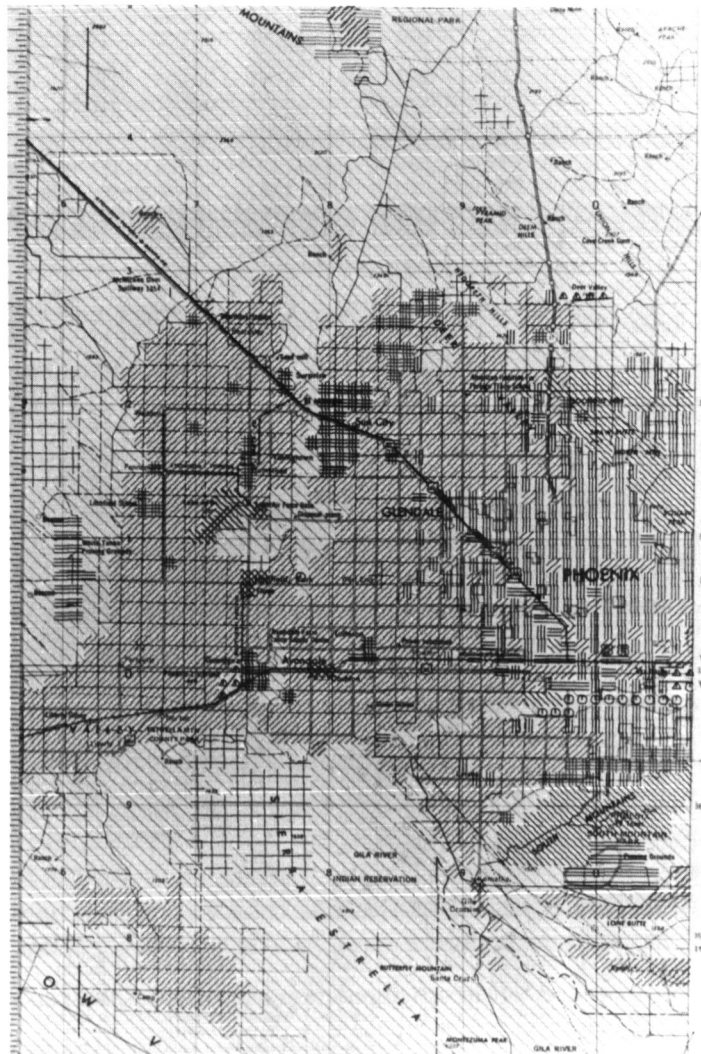
COUNTY

TRACT

4. A list of the factors recorded in the computer data bank for the Phoenix Quadrangle. The date of the land use information is also recorded.



5. Land use map of the entire Phoenix (1:250,000) Quadrangle plotted automatically from the computerized data bank and overlain with the black plate from the standard topographic sheet. This data bank and map represents land use in 1970; it will be updated through use of ERTS images.



6. Land use map plotted automatically from a computer data bank of the Phoenix Quadrangle. This shows the City of Phoenix on the eastern edge of the map. The changes detected in the ERTS images will be used to update this data bank.

LAND USE CLASSIFICATION SYSTEM FOR USE WITH REMOTE SENSOR DATA

LEVEL I CATEGORIES

LEVEL II CATEGORIES

01 URBAN AND BUILT-UP

- 01 RESIDENTIAL
- 02 COMMERCIAL & SERVICES
- 03 INDUSTRIAL
- 04 EXTRACTIVE
- 05 MAJOR TRANSPORT ROUTES & AREAS
- 06 INSTITUTIONAL
- 07 STRIP & CLUSTERED SETTLEMENT
- 08 MIXED
- 09 OPEN & OTHER

02 AGRICULTURAL

- 01 CROPLAND & PASTURE
- 02 ORCHARDS, GROVES, BUSH FRUITS, VINEYARDS & HORTICULTURAL AREAS
- 03 FEEDING OPERATIONS
- 04 OTHER

03 RANGELAND

- 01 GRASS
- 02 SAVANNAS (PALMETTO PRAIRIES)
- 03 CHAPARRAL
- 04 DESERT SHRUB

04 FORESTLAND

- 01 DECIDUOUS
- 02 EVERGREEN (CONIFEROUS & OTHER)
- 03 MIXED

LEVEL I CATEGORIES

LEVEL II CATEGORIES

05 WATER

- 01 STREAMS & WATERWAYS
- 02 LAKES
- 03 RESERVOIRS
- 04 BAYS & ESTUARIES
- 05 OTHER

06 NON-FORESTED WETLAND

- 01 VEGETATED
- 02 BARE

07 BARREN LAND

- 01 SALT FLATS
- 02 SAND (OTHER THAN BEACHES)
- 03 BARE EXPOSED ROCK
- 04 BEACHES
- 05 OTHER

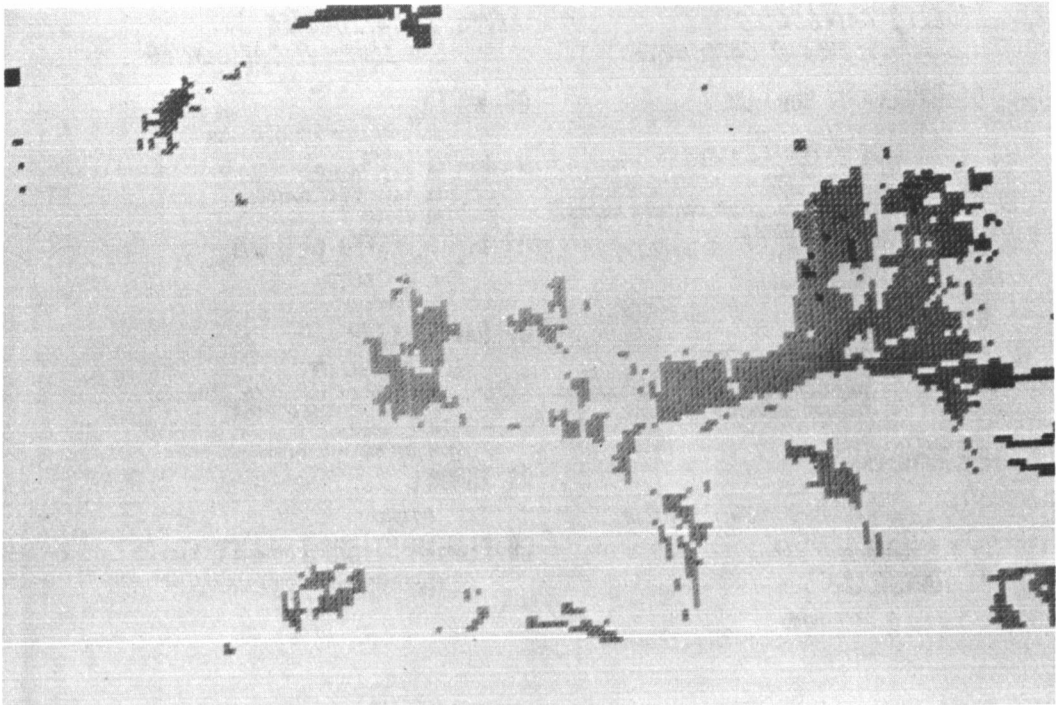
08 TUNDRA

- 01 TUNDRA

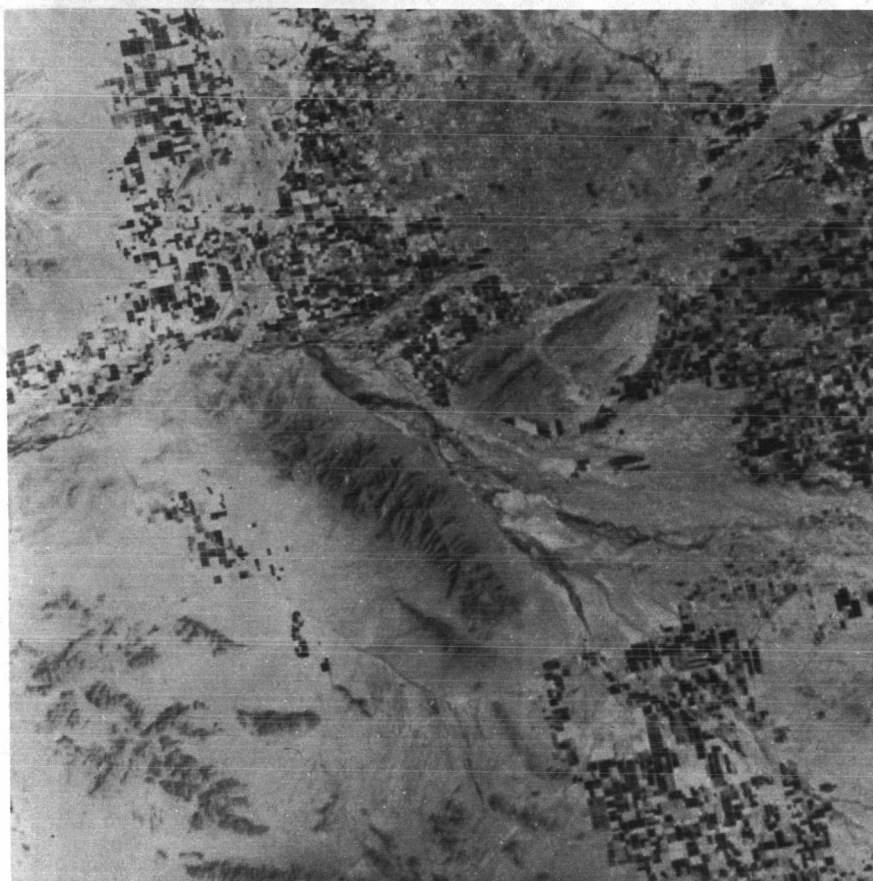
09 PERMANENT SNOW AND ICE FIELDS

- 01 PERMANENT SNOW & ICE FIELDS

7. The land use classification system designed for use with ERTS images (Level I) and with high altitude NASA aerial photographs (Level II). It was found that some of the Level II categories could be distinguished from ERTS images most of the time. The classification system is being used with the Phoenix Quadrangle project.



8. Example of an automated plot in the form of the color plate for cropland. Tree crops are indicated by denser symbols. Combining of such color plates produces the colored map shown in figures 5 and 6.



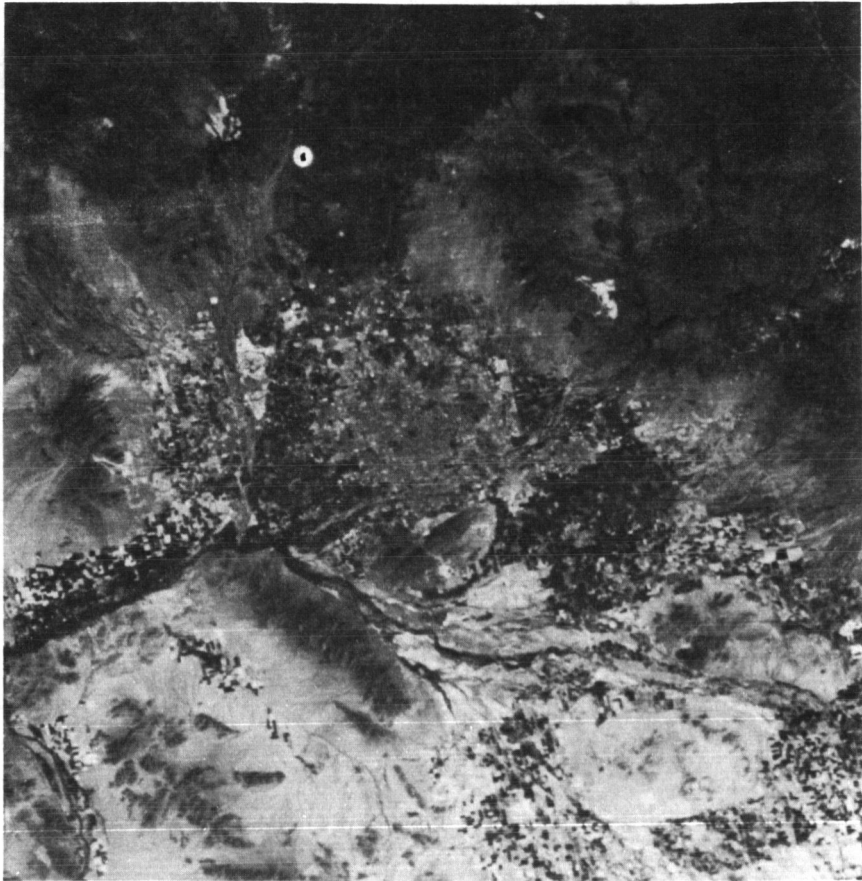
9. Print of ERTS color composite with an approximate scale of 1:1,000,000. This shows Phoenix and vicinity on August 23, 1972. This was one of the first ERTS frames and the processing was not as good as it became later. Nevertheless, the dryness, i.e., absence of red tones, can be seen as the desert vegetation has withered during the summer dry season. Mines appear as blue scars. Color composite was made with bands 4, 5, and 6.



10. Print of an ERTS color composite with an approximate scale of 1:1,000,000. This shows Phoenix and vicinity on October 16, 1972. The desert shrubs are dry and colorless at the end of the dry season. Many fields are fallow along the edge of the desert. Only by comparing crop patterns for all seasons can we accurately delineate the land use boundaries. Color composite was made with bands 4, 5, and 7.



11. Print of an ERTS color composite with an approximate scale of 1:1,000,000. This shows Phoenix and vicinity on February 19, 1973. This shows lush desert grasses present during a particularly wet rainy season. Note that the irrigated crops are not redder than in the images from other seasons. Color composite was made with bands 4, 5, and 7.



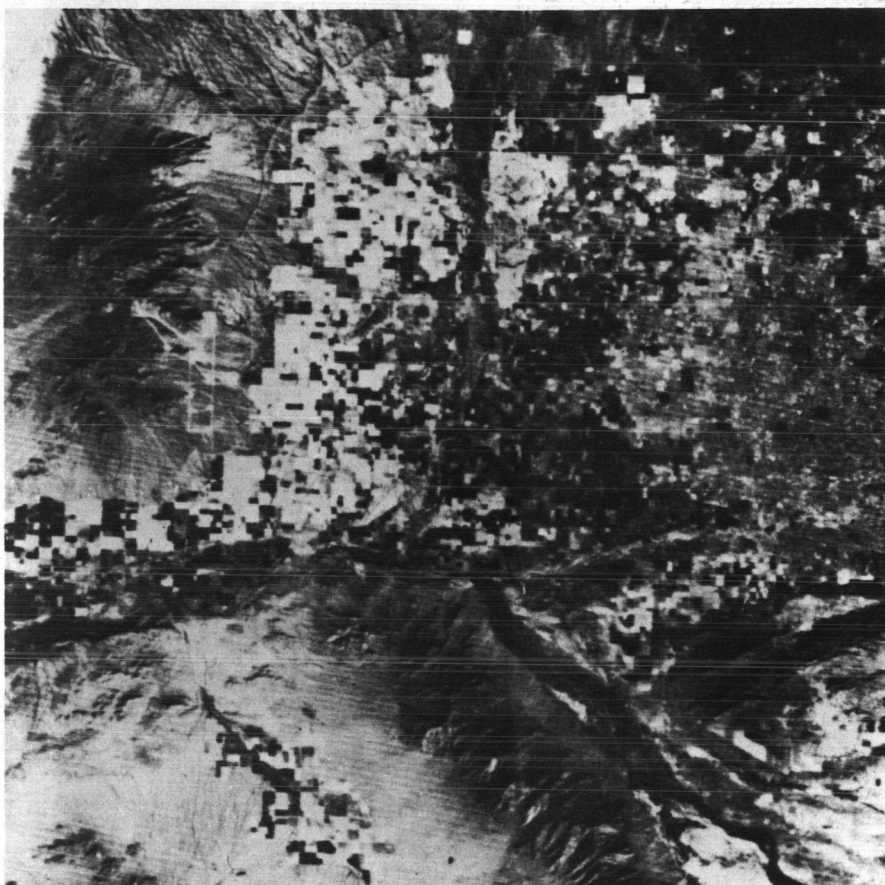
12. Print of an ERTS color composite with approximate scale of 1:1,000,000. This shows Phoenix and vicinity on May 2, 1973. The urban patterns within Phoenix show up as blue line commercial streets. With ten times magnification, the textures of industrial districts and the central business district are discernable. The residential areas are purplish pink. The Painted Rock Reservoir is full of water for the first time. Its upper end is visible on the west edge of the image. Salt River also has surface water, revealing channel locations, a rare sight. Color composite was made with bands 4, 5, and 7.



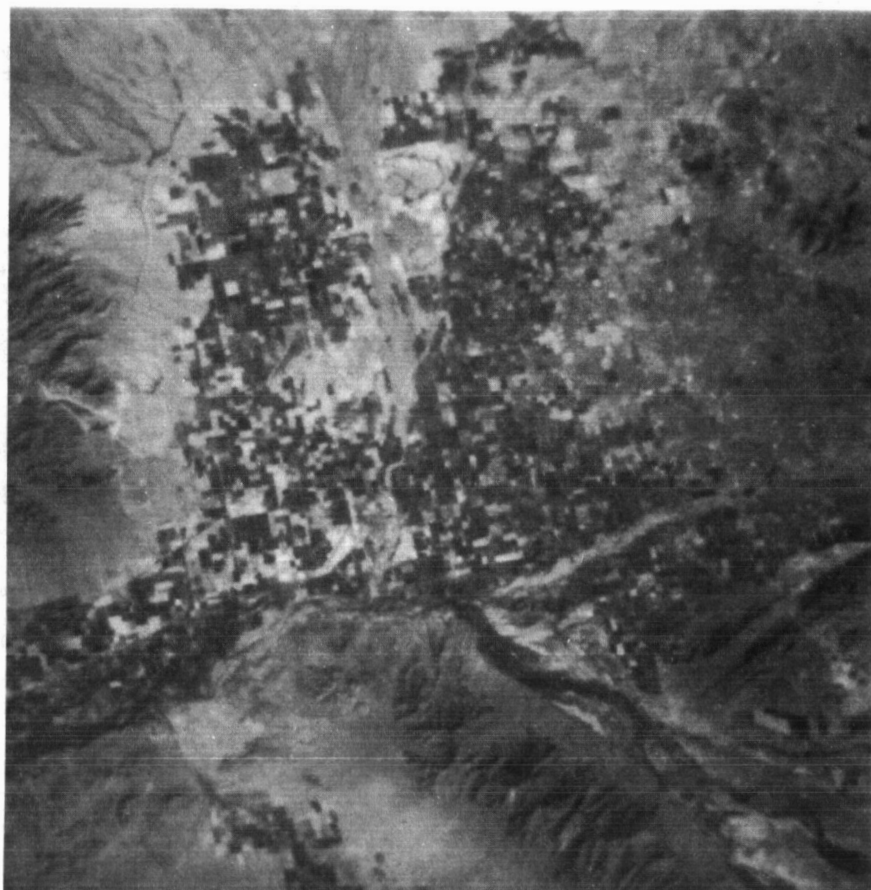
13. Print of an ERTS color composite with approximate scale of 1:1,000,000. This shows much of the Phoenix Quadrangle southwest, of Phoenix on November 4, 1972. Notably it showed the Painted Rock Reservoir before it was allowed to fill. The May 1973 image shows the upper end of that reservoir full of water. Note the open pit copper mines showing clearly at Ajo in the lower right of the image. Color composite was made with bands 4, 5, and 7.



14. Example of how a 70 mm chip is cut out of a 9 x 9 transparency showing south-central Arizona. The 70 mm chip is to be used in an I²S Color Additive Viewer where it will be magnified from 1:1,000,000 to a scale of about 1:380,000 on the display scope of the viewer. This scale approximates the base mapping scale of 1:250,000 used in the Phoenix Quadrangle Project.



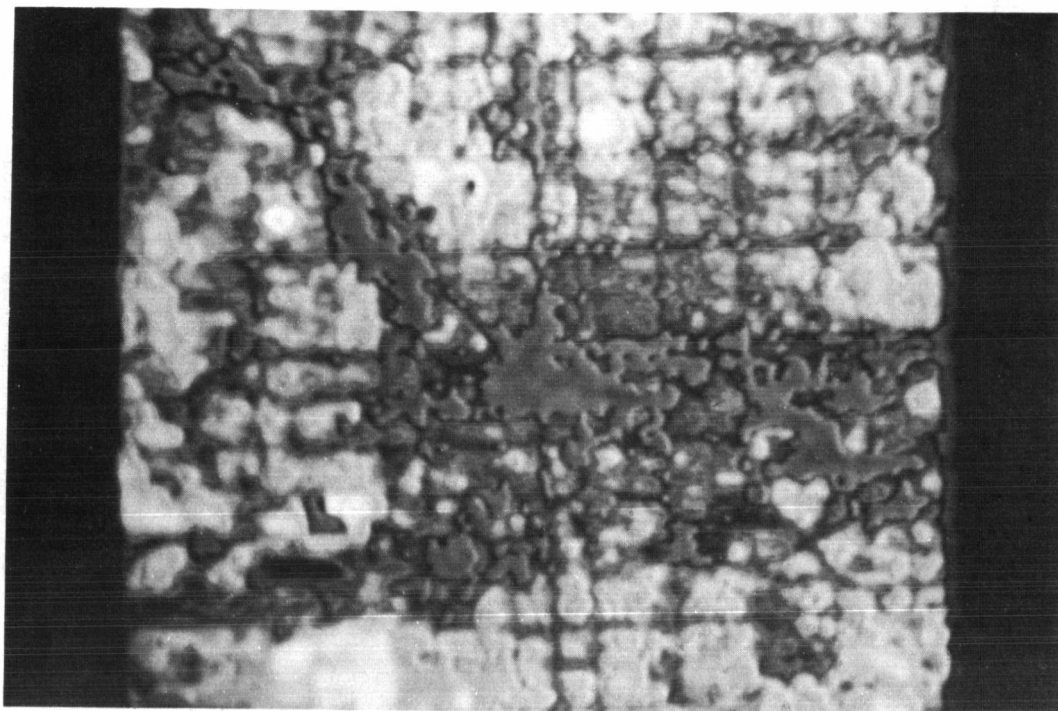
15. Examples of a three-times magnification of the 70 mm chip shown in the previous illustration. This approximates its scale on the display screen of the I²S viewer, however, in the viewer it would be combined into a color composite with identical chips from other bands. This is a band 5 image of the Phoenix area.



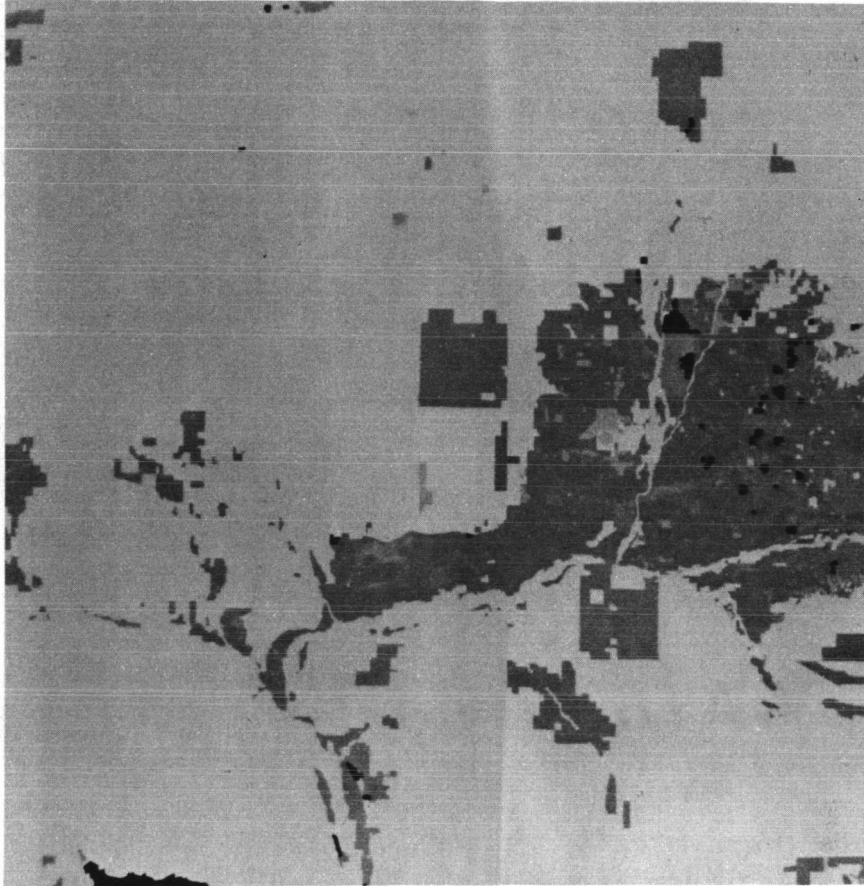
16. Example of a color photograph taken of the display screen of the I²S Color Additive Viewer. This one is the ERTS color composite (bands 4, 5, and 6) of the west side of Phoenix taken in November 1972. Scale approximately 1:300,000.



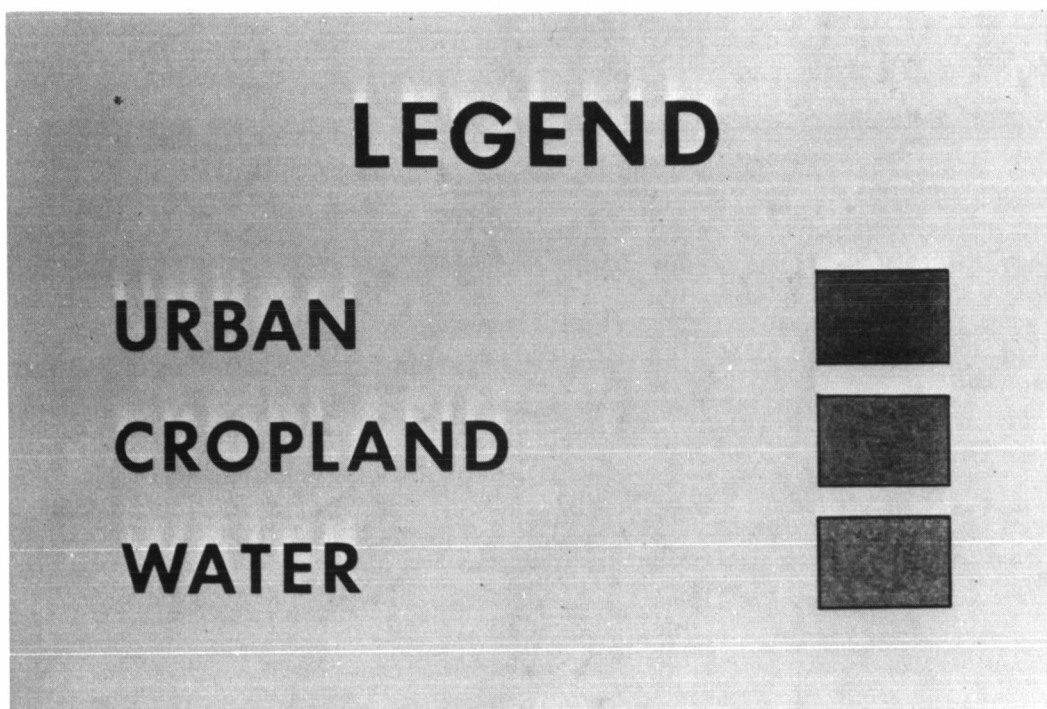
17. An attempt at change detection by using ERTS images two month's apart with different color filters. Different satellite positions causes some blurring and clutter. In general, unchanged areas cancel out as brown. Yellow or blue colored areas indicate possible change, but most is due to different stages of the agricultural cycles, not change in land use. These were band 5 images taken west of Phoenix in August and October 1972. A one year change will be tested.



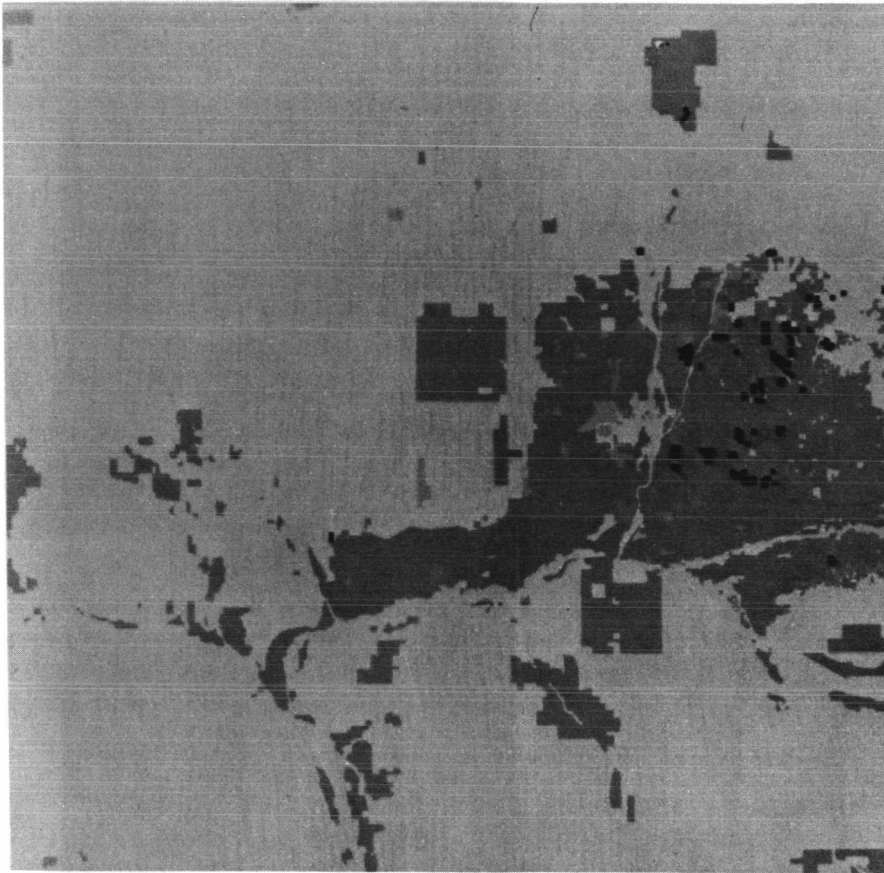
18. Using the Data Color Viewer to focus in on central Phoenix and to slice gray-scale densities, non-vegetated commercial and industrial districts appear dark blue, business streets red, and residential areas pale blue and green. An ERTS band 6 was used.



19. Change in land use detected using only ERTS images obtained throughout the period August 1972 and May 1973. The area shown is the eastern half of the Phoenix Quadrangle. It is important that total areas of urban growth detected by aerial photography or by satellite sensing are similar and the location of the primary clusters are essentially the same. New areas of change since the date of the aerial photos show how the two collection systems complement each other.



20. Legend for the maps of land use change, figures 19 and 21.



21. Change in land use detected using ERTS-underflight aerial photography taken in November 1972 in the vicinity of Phoenix. The southernmost 10% of the Phoenix Quadrangle was never covered by the aerial photography. The red change is new residential, the green is cropland, and the blue is surface water.

CHANGE OF LAND USE IN THE PHOENIX
QUADRANGLE AS DETECTED FROM ERTS

NOVEMBER 1970 TO MAY 1973

(SQUARE KILOMETER CELLS)

	TO			
	RESIDENTIAL	CROPLAND	DESERT SHRUB	RESERVOIR
FROM RESIDENTIAL	-	0	0	0
CROPLAND	3 0	-	0	1 9
DESERT SHRUB	3	2 3	-	5 5
RESERVOIR	0	0	0	-

U.S. GEOLOGICAL SURVEY

GEOGRAPHIC APPLICATIONS PROGRAM

22. Matrix of change found in the Phoenix Quadrangle between 1970 and 1973. Areas are in square kilometers.

CHANGE OF LAND USE BY LAND OWNERSHIP TYPE IN
THE PHOENIX QUADRANGLE AS DETECTED FROM ERTS

NOVEMBER 1970 TO MAY 1973

(SQUARE KILOMETER CELLS)

PRIVATE

T O

RESIDENTIAL CROPLAND DESERT RESERVOIR

SHRUB

RESIDENTIAL	-	0	0	0
CROPLAND	30	-	0	17
DESERT SHRUB	1	3	-	39
RESERVOIR	0	0	0	-

FEDERAL PUBLIC LAND

T O

RESIDENTIAL CROPLAND DESERT RESERVOIR

SHRUB

RESIDENTIAL	-	0	0	0
CROPLAND	0	-	0	0
DESERT SHRUB	2	15	-	9
RESERVOIR	0	0	0	-

STATE

T O

RESIDENTIAL CROPLAND DESERT RESERVOIR

SHRUB

RESIDENTIAL	-	0	0	0
CROPLAND	0	-	0	1
DESERT SHRUB	0	5	-	3
RESERVOIR	0	0	0	-

INDIAN LAND

T O

RESIDENTIAL CROPLAND DESERT RESERVOIR

SHRUB

RESIDENTIAL	-	0	0	0
CROPLAND	0	-	0	1
DESERT SHRUB	0	0	-	2
RESERVOIR	0	0	0	-

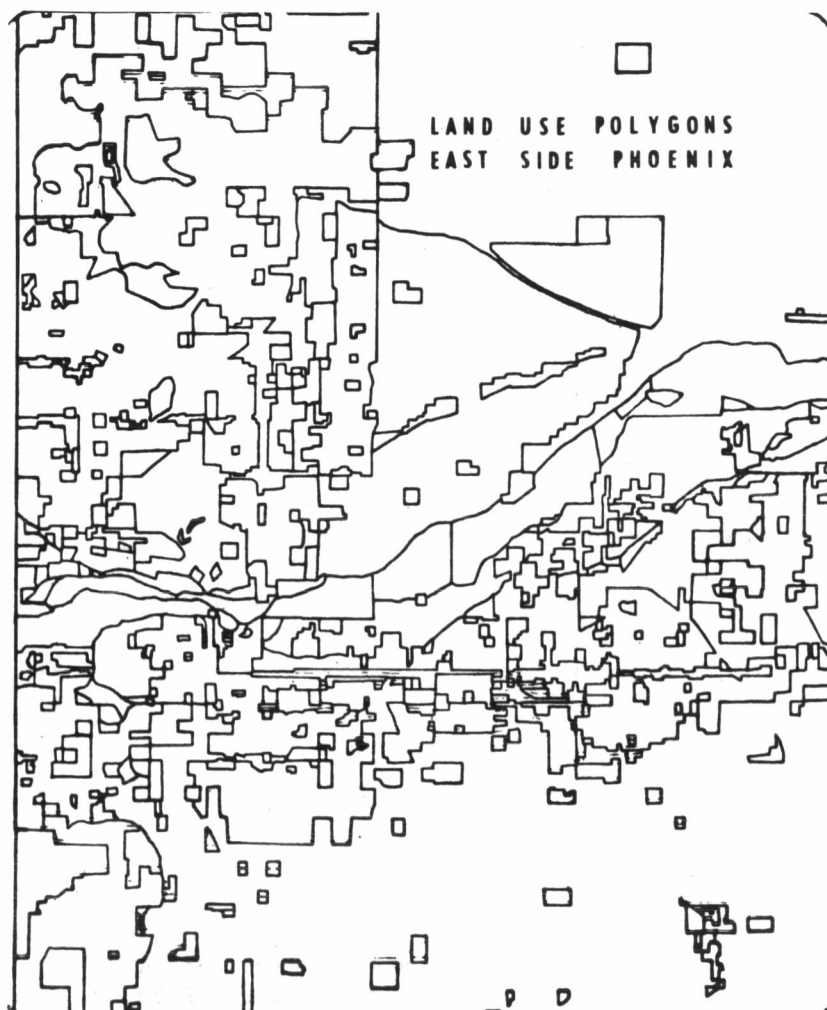
U.S. GEOLOGICAL SURVEY

GEOGRAPHIC APPLICATIONS PROGRAM

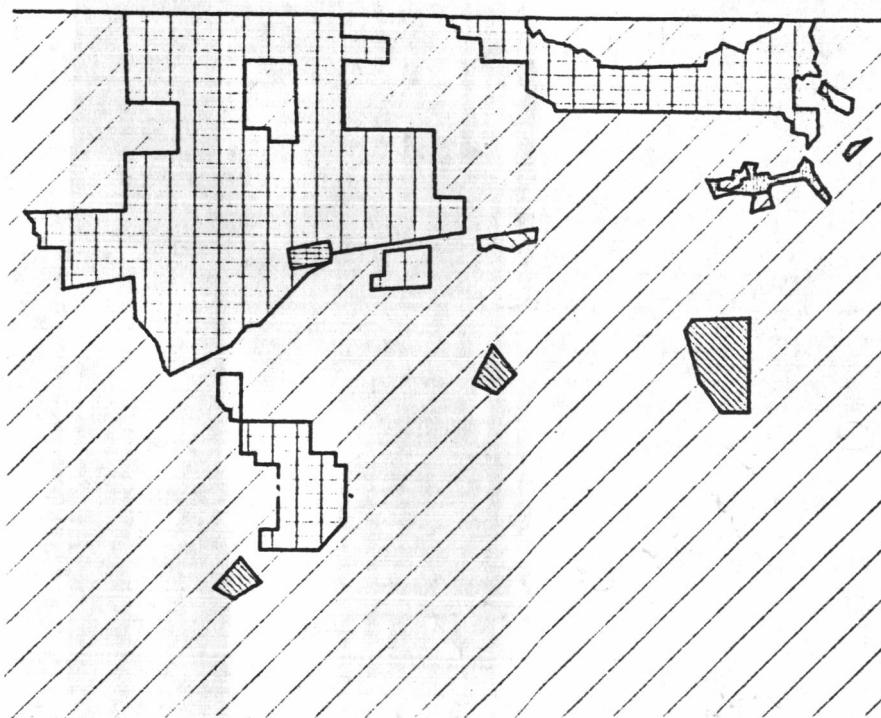
U.S. GEOLOGICAL SURVEY

GEOGRAPHIC APPLICATIONS PROGRAM

23. Changes, presented in Figure 22, broken down by land ownership class.



24. Example of an automated plot (1:120,000) of the land use map of the east half of Phoenix. The computer data bank contains the digitized record of polygon boundaries and the type of land use represented. A capability exists to fill in symbols or cells within the polygons. This is merely a test check on polygon boundary lines. Although this was made from photos, ERTS images could be used to update such a map record.



25. New technique for automated plotting of land use polygons from the computer data bank. Color symbols or cross-hatching are used to indicate land use types. This shows Gila Bend, Arizona.

THE APPLICATION OF ERTS-1 DATA TO THE LAND USE PLANNING PROCESS

James L. Clapp, Ralph W. Kiefer, Edward L. Kuhlmeier and Bernard J. Niemann, Jr., *Environmental Monitoring and Data Acquisition Group, University of Wisconsin, Madison, Wisconsin*

ABSTRACT

The need for the development and implementation of methods for the detection, inventory and monitoring of land resource variables is reflected in present and pending federal and state legislation. ERTS can provide an operational data source for many of the significant land use variables at the policy level.

Land resource data has been extracted on a percent of cell basis from ERTS imagery, RB-57 color infrared imagery and best available conventional sources for a 10,000 square kilometer test area in eastern Wisconsin.

First, the data from the three sources is compared on a spatial basis for a 300 square kilometer portion of the test area. For those land resource variables associated with cover, ERTS derived resource data compared favorably with both the RB-57 and conventional data. In the case of those variables which change with respect to time and are not regularly monitored by conventional means, the ERTS derived data is superior to conventional data.

Second, the effect of the data source on land use decisions is examined. Three interstate highway corridors are located through the same region based upon data extracted from each of the three sources. A policy of preserving natural environmental systems was used as a basis for the corridors selection in each case. The resulting three corridors compare favorably.

INTRODUCTION

The urban population growth, the demands of population centers for recreational resources, the growing need and concern for environmental resource planning, all dictate the need for better data in the land use planning process. This need for a relevant and environmentally responsive regional planning and management data base is crucial to the economic future for an assuring quality of life. At present, the regional decision maker typically lacks reliable basic information on

1 N 74 30736

the use, the composition, character, and the temporal change of the region. The most basic forms of these data, such as the extent of vegetation cover, wetlands distribution, urban growth and the ecological well-being of the landscape are examples of data that have been traditionally unavailable in formats directly useable in the regional planning process. The results of this study, while clearly demonstrating that ERTS-generated information will not be a panacea for all regional planning data needs, does offer a technique by which the data acquisition process can be significantly improved.

METHOD OF INVESTIGATION

The investigation was conducted in three basic phases. The first phase consisted of the determination of which land use variables could be extracted from ERTS and RB-57 images. The second phase consisted of the quantitative and spatial comparison of land resource variables extracted from ERTS, RB-57 and available conventional data sources. The third phase, which is still under investigation, compares the spatial effects of the data sources on land use planning decisions.

Test Site

The principal test site employed in the investigation, called REMAP-I, consists of a 10,000 square kilometer area between Milwaukee and Green Bay, Wisconsin, shown in Figure 1. A smaller portion of the area, the 10 x 30 kilometer Sheboygan Test Site, was employed in some of the analyses. A computer-based data bank had been developed for REMAP-I area by the Environmental Awareness Center of the University of Wisconsin from conventional data sources to assist the Wisconsin Department of Transportation in the location of a corridor for Interstate 57. Thirty-eight land resource variables, made up of 132 data items, are stored for each 1 km cell in REMAP-I on a percent-of-cell basis. The cells are spatially organized on a UTM base. Any combination of variables, which can be individually weighted, can be developed as a spatial density printout for comparisons with ERTS and RB-57 derived information. Figure 2 shows a sample printout for the variable "Existing Agricultural Land Use." Figure 3 illustrates the use of the REMAP-I data base to generate a spatial density printout of the study area employing a particular policy. The policy illustrated in Figure 3 is environmental impact. All variables which relate to environmental considerations are weighted high. The resulting lighter areas should be protected under this policy. The policy can be modified by changing the weights assigned to the variables.

In the construction of the REMAP-I data bank significant difficulties were encountered. These centered on the non-availability of compatible data sources. The "best available" sources of appropriate data varied in format, scale, accuracy, vintage, controlling agency and spatial reference. The cost of data

extraction from these varied sources was estimated at \$10 per cell or \$100,000 for the entire 10,000 cell REMAP-I area.

Interpretation Technique

Conventional air photo interpretation techniques were employed to extract data from the ERTS and RB-57 images. Nine-inch transparencies were used for both ERTS and RB-57 sources as the basic image format. Data extraction on a percent-of-cell basis was made using a zoom stereoscope. A 1 km cell grid was superimposed on the imagery by navigation with respect to identifiable features on the imagery. Extracted data were keypunched and input to the computer data bank. This procedure was followed for each variable identifiable. An ERTS-1 Interpretation Matrix was prepared which lists the REMAP-I variables, data and coverage interpreted, the band employed, a classification of identification by difficulty, and the image format and date most appropriate for each variable identification. This matrix is viewed as incomplete at this time due to inadequate spring and fall ERTS coverage caused by poor weather conditions.

SPATIAL COMPARISONS OF VARIABLES

Figures 4, 5 and 6 illustrate the spatial comparison of three of the land resource variables for the Sheboygan Test Site, a 10 x 30 kilometer portion of the REMAP-I data bank. The figures are computer-generated spatial-referenced quantitative information as derived from (1) ERTS-1 multispectral imagery, (2) RB-57 high altitude color-infrared photography, and (3) the REMAP data bank constructed from conventional sources. Each cell is one square kilometer in size, spatially referenced to the UTM system. The density of the symbol printed in each cell indicates the percentage of that cell occupied by the resource in question. Beneath the spatially represented areas are given the total area occupied by each resource as determined from each data source. Numbers of occurrence and areas for each of the three data sources are presented for each level of occurrence.

Figure 4, the printout for the variable "Agriculture," shows the spatial/statistical comparison for the amount of land in the Sheboygan Test Site devoted to agricultural land use (land used directly or indirectly for the growth of food products, including crop, animal and poultry farming; includes both crop land and grazing land). There is excellent agreement among all three data sources and ERTS imagery is useful for the determination of lands devoted to agricultural use. Because of the continuing change in the use of agricultural lands, there is a real need for monitoring this variable on a regular basis.

Figure 5, the variable "Forest," shows spatial/statistical comparisons for the land covered with forests (those land areas with at least 50% tree canopy cover). "Upland Forest and Lowland

Forest" were treated as separate variables in the original REMAP-I and RB-57 data extractions, but are combined into the one category "Forest" in the case of ERTS. There is reasonable agreement among all three data sources, but it should be emphasized that the ERTS interpretation contains less discrete information than RB-57 and REMAP-I. It is possible that the ERTS derived data could be refined by (1) coverage over an entire season, and (2) more sophisticated methods of data extraction.

Figure 6, the variable "Open Water and Wetlands," shows the spatial/statistical comparisons for land covered with open water and wetlands. Four resource variables, "rivers," "lakes," "lakes smaller than 50 acres," and "open wetlands," were individually analyzed for ERTS, RB-57 and REMAP. For the purposes of this comparison they were combined to yield that component of the land covered by open water (rivers and lakes) and wetlands (principally areas occupied by such biotic communities as those dominated by grasses, sedges, emergent aquatics, dogwoods, shrubwillows, and alders). There is reasonable agreement between ERTS and RB-57 in identifying the major open water and wetland areas in the test site. However, in many cases where only a small percentage of each cell is occupied by open water and/or wetland, detection was not made on the ERTS imagery, as shown by the number of occurrences.

It can be seen that there is not a good agreement between the REMAP areas and the RB-57 and ERTS areas for open water and wetlands. In order to investigate the possible reasons for this discrepancy, a field check was undertaken. It showed that many areas classified as "open wetlands" in the REMAP data bank are now covered by "lowland forest" tree species. Such areas are, therefore, shown as "forest" on the ERTS and RB-57 printouts and as "open wetlands" on the REMAP printout. When printouts for "lowland forest" and "open wetlands" were compared for RB-57 and REMAP, it indicated that the total areas of "lowland forest" plus "open wetlands" are quite close for these two data sources.

WETLANDS VERIFICATION

Variable	Total Km ² as derived from		
	ERTS	RB-57	REMAP
Open Wetlands	10.8	9.2	20.8
Lowland Forest		<u>31.9</u>	<u>18.9</u>
TOTAL		41.1	39.7

This example points clearly illustrates that (1) land cover changes with time and 40-year-old data are probably inadequate, (2) field checks are an essential part of remote sensing data extraction studies, and (3) resource definitions must be carefully drawn.

EFFECT OF DATA SOURCE ON LAND USE DECISIONS

A spatial comparison of data derived from the three sources, although valuable, does not approach the more fundamental question of how the source of the data affects the decisions based upon the data.

In order to approach this question, Policy Models were established for the Sheboygan Test Site for each of the three data sources. This was accomplished by resource disciplines assigning weights to each variable according to its significance with respect to that policy. Figure 7 shows the printout for the Policy Minimum Environmental Impact for each of the data sources. The more dense cells represent those areas which have a high sensitivity to impact and should be avoided under this Policy. Note that if there are differing opinions or changes in perception over variable weights to be assigned to a policy, the spatial effect of a change of weights or policy can be quickly examined.

The ERTS model is based upon five variables, the RB-57 model upon eight variables, and the REMAP-I model upon all 38 variables. This reflects the varying degree of discreteness of the respective data sources and the greater dependence upon varying sources required for REMAP I.

In order to examine the effect of the three data sources on land use decisions, a computer optimization program was developed which selects an interstate highway corridor through the test site based upon minimum environmental impact as established by the policy. These corridors are shown in Figure 7 as the dark lines.

Although this portion of the investigation is only preliminary, an examination of Figure 7 reveals some interesting features. First, all three sources produce corridors which are quite similar. Second, as the data become more discrete, the corridors become less direct. A significant amount of investigation remains to be done on this question, particularly on the optimization of the data base using each source for those variables for which that source is most appropriate.

STATE LAND INFORMATION SYSTEM

In order to meet the data needs of the land use planning process it is necessary that four key elements be represented. These are shown diagrammatically in Figure 8. First, there must be a hierarchy of data sources, including earth resources satellites. Second, the data needs and definitions must be established by the user groups. Third, the legislative support must be provided. Fourth, an information system must be designed to be responsive to all these elements. These components must be dynamic and responsive to social and technological change.

PRELIMINARY CONCLUSIONS

1. Land resource data/information, regardless of source, must be spatially referenced to be of maximum value for planning.
2. It is essential to establish precise definitions of critical land resources and the parameters which determine them in terms of measurement techniques economically available.
3. It is essential to establish precise criteria and data required for the establishment and measuring of the relative quality of critical resources.
4. ERTS derived data/information is potentially superior to conventional land use data for those items (1) which change rapidly with time, and (2) for which conventional data is not available.
5. For broad land cover assessments, data derived from ERTS by non-sophisticated methods is sufficient for initial resource assessments at the state or regional policy level.
6. More specific land resource information is available from ERTS if machine-based analysis techniques are employed.
7. Machine-based data extraction systems should be interactive, employing the man to identify and the machine to analyze and measure.
8. A state or regional data/information system must encompass a hierarchy of data sources including satellites, high-altitude aircraft, low-altitude aircraft, and ground-based surveys.
9. ERTS has provided a focus from which the regional land use planning data/information problem can be approached.
10. Any effort directed toward the implementation of a data/information system for regional land use planning must be multidisciplinary.
11. It is essential to integrate development funds from multiple sources in order to develop and implement a comprehensive data/information system for state and regional planning.
12. The effective implementation of a state or regional data/information system requires the assignment of responsibility, authority and funds to a single agency.
13. The successful implementation of a state or regional data/information system requires interagency cooperation and may require interagency reorganization.

4	4	UTM
1	1	
0	9	
0	0	
0	0	
0	0	

SHEBOYGAN TEST SITE
VARIABLE 63 AGRICULTURE

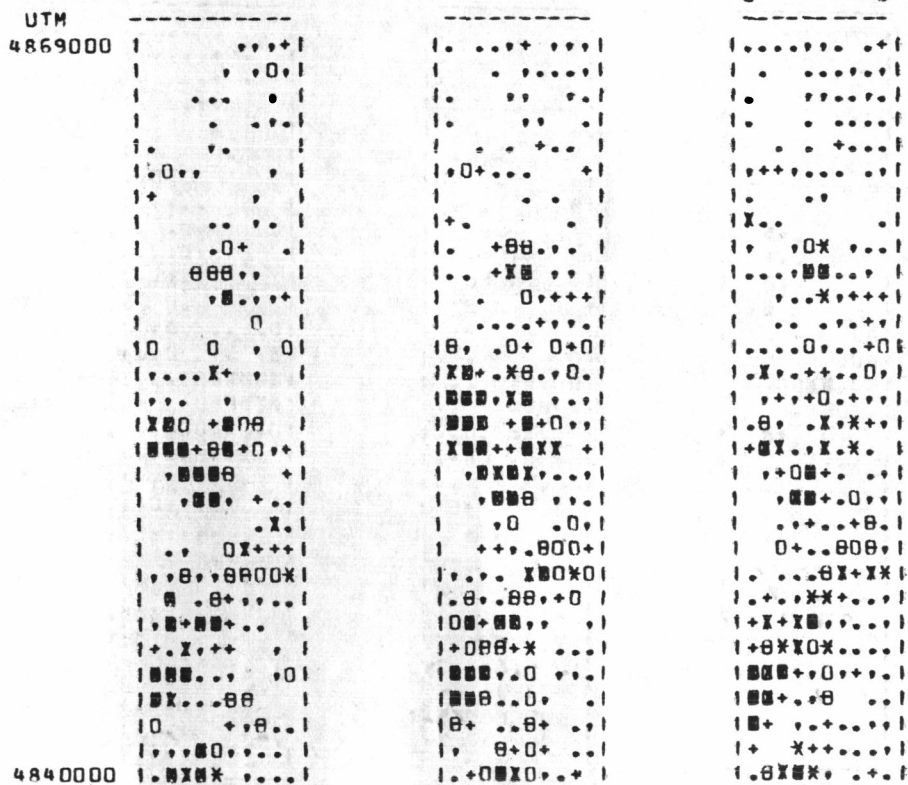
[illegible]

		A ERTS 183.630			B RBS7 181.600			C REMAP I 198.110			
TOT. SQ.KM	LEVELS	1	2	3	4	5	6	7	8	9	10
		+++++	00000	00000	XXXXX	XXXXX	00000	00000	00000
SYMBOLS		+++++	00000	00000	XXXXX	XXXXX	00000	00000	00000
		+++++	00000	00000	XXXXX	XXXXX	00000	00000	00000
RANGE (%)		1-9	10-19	20-29	30-39	40-49	50-59	60-69	70-79	80-89	90-99
	A	10	16	17	13	15	9	18	39	49	88
OCCUR	B	12	15	13	24	15	19	35	33	51	63
	C	11	7	7	12	17	15	34	42	66	71
	A	.47	1.97	3.70	4.05	6.12	4.70	11.35	28.60	40.33	82.34
SQ.KM	B	.68	2.20	3.12	8.34	6.43	10.44	22.55	24.81	43.46	59.57
	C	.63	1.08	1.65	3.99	7.50	8.24	21.74	31.28	55.97	66.03
ERTS BAND		5	14. SEPTEMBER, 1972				1053-16093-5				

434

ERTS-1 INVESTIGATION: CONTRACT # NAS 5-21754
 ENVIRON. MONITORING AND ACQUISITION GROUP
 INSTITUTE FOR ENVIRONMENTAL STUDIES
 UNIVERSITY OF WISCONSIN - MADISON

SHEBOYGAN TEST SITE
 VARIABLE 24+25 FOREST



	A ERTS 48.830			B RB57 59.470			C REMAP I 51.990			
TOT. SQ.KM	1	2	3	4	5	6	7	8	9	10
LEVELS	++++	00000	88888	XXXXX	XXXXX	88888	88888	88888
SYMBOLS	++++	00000	88888	XXXXX	XXXXX	88888	88888	88888
RANGE (%)	1-9	10-19	20-29	30-39	40-49	50-59	60-69	70-79	80-89	90-99
OCCUR	A	43	48	21	16	13	2	7	9	7
	R	62	48	32	21	15	3	10	8	10
	C	100	52	37	11	8	11	11	3	9
SQ.KM	A	2.36	6.38	4.73	5.30	5.42	1.10	4.48	5.13	7.43
	B	2.84	5.96	7.39	6.79	6.35	1.58	6.27	6.40	6.55
	C	4.33	7.10	8.92	3.62	3.39	5.85	7.09	2.16	7.62
ERTS BAND	5	14. SEPTEMBER, 1972				1053-16093-5				

FIGURE 5. FOREST LAND COVER
 ERTS and RB-57 INTERPRETATIONS
 vs REMAP-I DATA BANK

ERTS-1 INVESTIGATION: CONTRACT # NAS 5-21754
 ENVIRON. MONITORING AND ACQUISITION GROUP
 INSTITUTE FOR ENVIRONMENTAL STUDIES
 UNIVERSITY OF WISCONSIN - MADISON

SHEBOYGAN TEST SITE

VARIABLE 20+21+26+147 OPEN WATER AND WETLANDS

4 4 UTM
 1 1
 0 9
 0 0
 0 0
 0 0

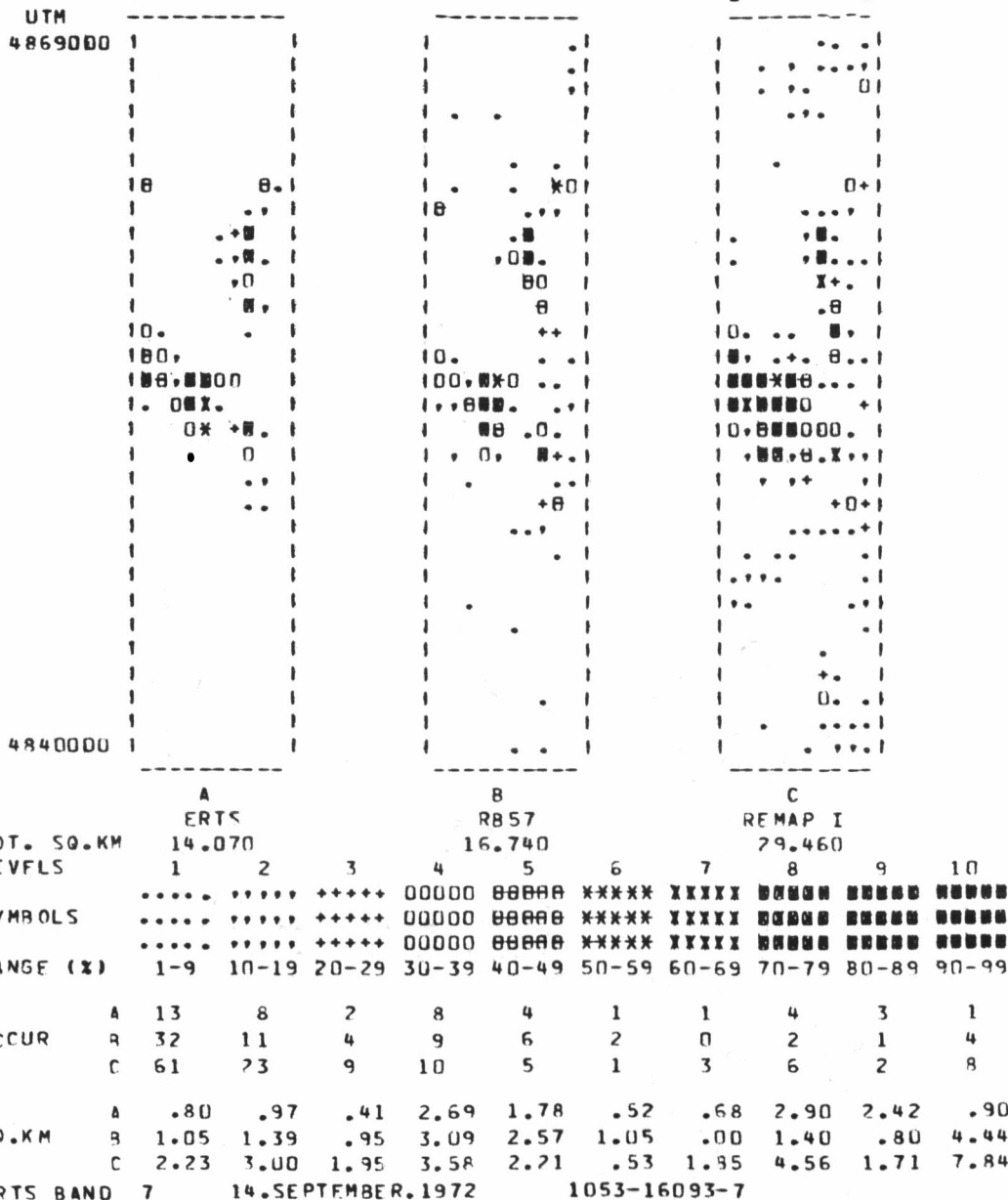


FIGURE 6. OPEN WATER AND WETLANDS
 ERTS and RB-57 INTERPRETATIONS
 vs REMAP-I DATA BANK

ERTS-1 INVESTIGATION: CONTRACT # NAS 5-21754
 ENVIRON. MONITORING AND ACQUISITION GROUP
 INSTITUTE FOR ENVIRONMENTAL STUDIES
 UNIVERSITY OF WISCONSIN - MADISON

SHEBOYGAN TEST SITE
 VARIABLE ECOLOGICAL SYSTEM

4 4 UTM
 1 1
 0 9
 0 0
 0 0
 0 0

UTM
 4869000

4840000

	A ERTS			B RB57			C REMAP I			
TOT. SQ.KM	13.250			26.250			22.780			
LEVELS	1	2	3	4	5	6	7	8	9	10
SYMBOLS	+++++	00000	00000	XXXXX	XXXXX	00000	00000	00000
RANGE (%)	1-9	10-19	20-29	30-39	40-49	50-59	60-69	70-79	80-89	90-99
OCCUR	A 108	52	5	1	0	0	0	0	0	0
	B 115	63	11	14	7	2	1	0	0	0
	C 142	60	20	7	2	0	0	0	0	0
SQ.KM	A 3.93	7.73	1.21	.38	.00	.00	.00	.00	.00	.00
	B 4.74	9.08	2.64	4.95	3.14	1.03	.68	.00	.00	.00
	C 6.36	8.23	5.04	2.34	.81	.00	.00	.00	.00	.00

FIGURE 7. LAND USE DECISION MODEL
 "LINE FINDER". HIGHWAY ALIGNMENT.
 WEIGHTED TOWARDS ENVIRONMENTAL
 CONSIDERATIONS

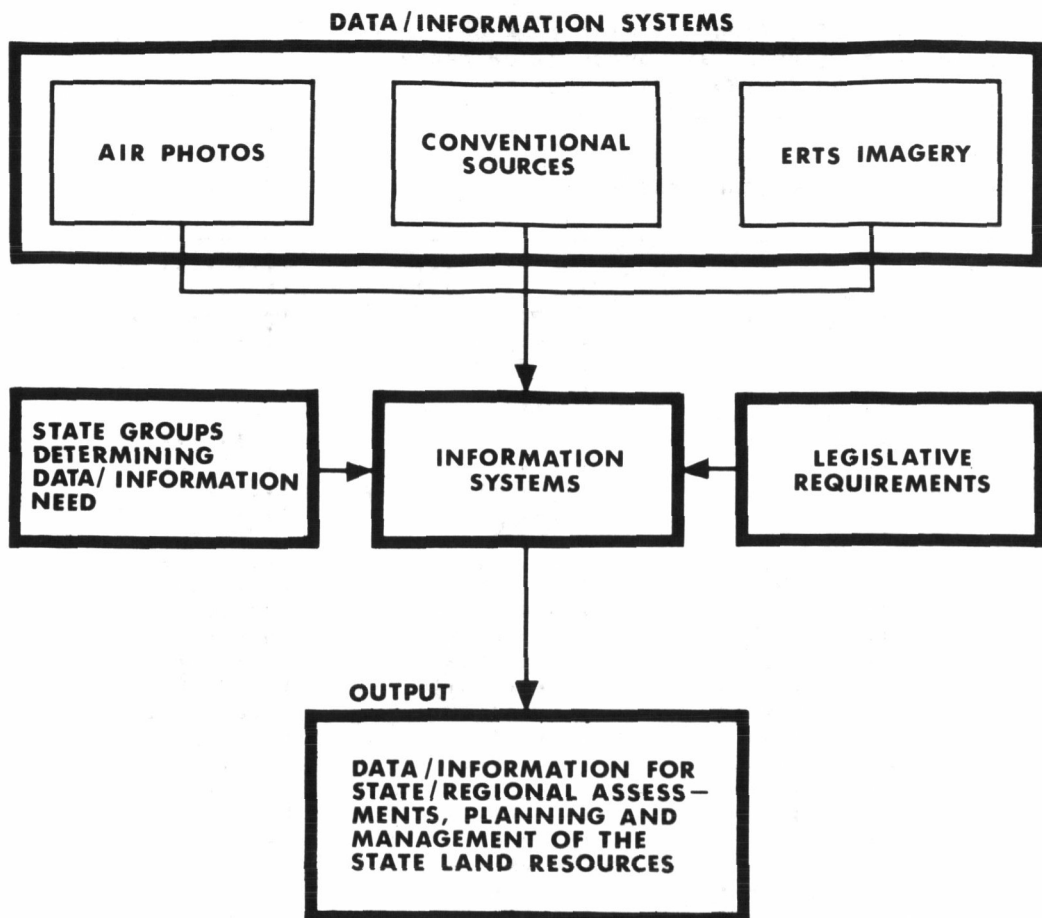


FIGURE 8. DATA/INFORMATION AND LEGISLATIVE REQUIREMENTS FOR STATE INFORMATION SYSTEMS

THE UTILITY OF ERTS-1 DATA FOR APPLICATIONS IN LAND USE CLASSIFICATION

John E. Dornbach and Gerald E. McKain, *NASA, Johnson Space Center, Houston, Texas*

ABSTRACT

A comprehensive study has been undertaken at the Johnson Space Center to determine the extent to which conventional image interpretation and computer-aided (spectral pattern recognition) analysis techniques using ERTS-1 data could be used to detect, identify (classify), locate, and measure current land use over large geographic areas.

It can be concluded that most of the Level I and II categories in the USGS Circular #671 can be detected in the Houston-Gulf Coast area using a combination of both techniques for analysis. These capabilities could be exercised over larger geographic areas, however, certain factors such as different vegetative cover, topography, etc. may have to be considered in other geographic regions.

The best results in identification (classification), location, and measurement of Level I and II type categories appear to be obtainable through automatic data processing of Multispectral Scanner computer compatible tapes. To achieve these results, however, a slight modification of the Circular #671 categories and definitions would be required.

INTRODUCTION

The purpose of this paper is to report on one part of the ERTS-1 investigation at the Johnson Space Center (JSC). In particular, this report will focus on the use of the ERTS-1 Multispectral Scanner System (MSS) data as a source of information for compiling land-use inventories, such as those which might be required as part of recent coastal zone and pending national land-use legislation. The work of the Earth Observations Division Investigation Teams and the Land-Use/Urban Analysis Teams in particular are acknowledged.

The objectives of the ERTS-1 land-use investigation were as follows:

- ° General - Within the Houston Area Test Site (HATS), determine the role of ERTS-1, aircraft, and ground data in the definition and development of the technology for land-use classification over a large geographic (multi-county) region.

N74 30737

° Specific

1. Using MSS imagery, establish the land-use categories which can be detected, identified, located and measured by conventional image interpretation techniques.
2. Using MSS computer compatible tapes (CCT's), determine the degree to which automatic data processing (ADP) techniques can be applied to detect, identify, locate, and measure the various categories of a land-use classification system.
3. Using existing or by developing new manual and automatic techniques, produce land-use classification maps of a portion of the test site.
4. Using aircraft and ground data, relate results from the above to land use present at the time of the ERTS-1 overflight.

The investigation teams used imagery generated not only at the National Data Processing Facility (NDPF) at the Goddard Space Flight Center (GSFC) but also color-composite imagery generated directly from the MSS CCT's at JSC.

The 18-county Houston Area Test Site (HATS) covers an area about 41,600 square kilometers (16,000 square miles) around the City of Houston. It is an extremely diverse land-use study area possessing a large Central Business District, a rapidly expanding urban fringe, a large petrochemical industrial complex, many square kilometers of extractive industries, extensive agricultural and range lands, coastal zone features, and the Sam Houston National Forest. Figure 1 illustrates the general area covered by the ERTS-1 scenes which were studied. The area covered by the one-fourth scene CCT which was used in automatic data analysis, is the area which is outlined and that which received the most intensive analysis. Therefore, in the remainder of this paper, this area will be referred to as the Prime Study Area.

CLASSIFICATION SCHEME

The classification scheme used in this investigation is that described in the U.S. Department of the Interior Geological Survey, Circular #671 (Reference 1). This scheme (or a planned revision thereto) is being considered for possible application on a national basis, in the event legislation such as contained in the Senate Bill 268, "Land Use Policy and Planning Assistance Act" is enacted. Although not specifically an objective of this task, the results of this investigation illustrate the applicability of the Circular #671 scheme to the Central Gulf Coast Region and what, if any, modifications might be recommended to produce a more meaningful classification, if ERTS MSS data is to be one of the major data sources. These modifications are especially significant if ADP techniques are to be the main source of data analysis, since Circular #671 on Page 6 recognizes that, "As further advances in technology

are made, it may be necessary to modify the classification system for use with automatic data analysis."

DATA USED

ERTS-1 MSS data from two passes over HATS were utilized in the investigations on Land-Use Classification. These passes, on August 28 and 29, and October 3 and 4, 1972, occurred in generally clear conditions with only a small percentage of cloud cover. The major analysis activities used the August and October data. During the August pass, high altitude underflights were flown over a portion of the test site.

Both system-corrected imagery and digital data were acquired from the NDPF. The black and white 70 mm and 240 mm (9 inch) imagery from the NDPF were utilized primarily in the form of black and white prints of each band enlarged from the 70 mm transparencies to a scale of approximately 1:250,000. For this land-use study, the color composites from the NDPF were not analyzed, due to the availability of higher resolution color composites directly from the digital tapes. The digital tapes were used in two ways; they were used for computer-aided classification by spectral pattern recognition using supervised and nonsupervised techniques, and were also used to produce two or three band color composites using the film recorder on the JSC multispectral Data Analysis Station, giving essentially a first generation, positive transparency film product at a scale of approximately 1:250,000.

CONVENTIONAL IMAGE INTERPRETATION

° Level I and II Classification of GSFC Black and White Imagery

Conventional image interpretation for a Level I classification was conducted using black and white transparencies and enlarged prints from Bands 5 and 7 over the prime study area. The following Level I categories of Circular #671 were detected and identified:

Urban and Built-Up Land	Forest Land
Agricultural Land	Water
Rangeland	Non-Forested Wetland

There were no Barrenlands identified in the area covered by this data. Also, the categories of Tundra and Permanent Snow and Icefields are not found in Texas.

As individual categories, Agricultural Land and Rangeland were usually easily identifiable from everything else. However, the least reliable of the Level I determinations was delineating the boundary between these two categories, even when field sizes and shapes were used. It was necessary to define all identifiable pastureland as Rangeland, in order to alleviate this problem. The authors are aware that this is probably a problem unique to this part of the United States. In the remainder of this report, Agricultural Land and Rangeland will be

treated as a single Level I category.

There was also a definitional problem regarding the Level I classification of oil and gas Extractive areas versus the Rangeland and Non-Forested Wetland categories, since in Texas many oil and gas fields are grazed. Generally on ERTS-1 imagery, clues to the existence of oil or gas fields are far below the resolution of the system. However, close in to the urbanized area, this use probably would be defined as Open and Other; hence, would fall into the urbanized category. As distance from the urban fringe increases, it becomes more difficult to make the Extractive versus Rangeland decision. Near the Gulf of Mexico, much of the Non-Forested Wetland is also grazed and therefore, the decision becomes even more difficult.

Highly reflective areas in the two bands were also often difficult to classify, especially at the urban fringe, since the interpreter did not have enough clues to determine whether it were urban (new subdivision or industry), agriculture (bare soil), or cleared forest (to be reforested). It is significant to note that the definitions in Circular #671 did not adequately cover the commercial timber cutting which occurs each year in different parts of the Sam Houston National Forest or the extensive cutting and clearing which is occurring north of the City of Houston, where new fresh water reservoirs for municipal surface-water supplies are being constructed.

From a standpoint of the minimum size of Level I features which were detected by this procedure, the following results were achieved:

<u>Feature</u>	<u>Performance</u>
Agricultural Fields	4 Hectares
Forest Stands	4 Hectares
Rights-of-Ways in Forest	28 Meters (width)
Water Bodies	1 to 2 Hectares
Rural Settlements	40 Hectares

The performance accuracy in Level I classification using this technique ranged between 80 to 98 percent. A more detailed comparison of the performance of the three techniques used for each category is given in the results section of this paper. Also, as will be seen later, the color composite generated at JSC provided a better data source for attempts at conventional image interpretation for Level II and hence Level II classification was not attempted using black and white imagery.

° Level I and II Classification of JSC Generated Color Composite

One computer compatible tape was used to produce a first generation, positive color transparency on the digital tape to film recorder which is part of the Data Analysis Station equipment at JSC. The composite was produced with Channel 1 (Band 4) portrayed as blue, Channel 2 (Band 5) as green, and Channel 4 (Band 7) as red. The result was a 1:250,000

scale (approximate), false-color infrared ektachrome transparency which was of considerably higher resolution than the color prints received from the NDPF. This is understandable since the NDPF goes through several image reproduction and scanning steps prior to production of a 1:1,000,000 scale system-corrected, color composite paper print.

Conventional image interpretation for Levels I and II was conducted using this transparency (Figure 2). Each category was annotated on a stable base mylar overlay and keyed to the color composite film strip. The following Level I and II categories of Circular #671 were detected and identified:

Level I

Urban and Build-Up Land

Forest Land

Agricultural Land/Rangeland

Water

Non-Forested Wetland

Level II

Residential and Open

Commercial and Industrial

Transportation, Communications
and Utilities

Strip and Clustered Settlements

Extractive

As previously explained in the Section on the conventional interpretation of NDPF black and white imagery; Barren Lands, Tundra, and Permanent Snow and Icefields were not present. Furthermore, other category classifications at the Level II were not attempted by the Land-Use Study Team for the following reasons:

Agricultural Land - All land in this category could only fall into either the Cropland and Pasture or the Other category. It was impossible to determine unused cropland or brushland from vacant or unused land in the Urban category of Mixed or Open and Other, especially in the multi-county, urban fringe area.

Rangeland - According to the Circular #671 definitions, only the Grass category of Level II was present in the Prime Study Area.

Forest Land - Since only single date imagery was used, decisions on Level II were not possible. However, other study teams using growing and dormant season imagery could make this type determination.

Water - Almost all water features in the Prime Study Area would have had to be classified as Reservoirs. Due to the scale involved, the image interpreters did not attempt to identify (classify) water areas smaller than 16 hectares (40 acres) which would have been the Water - Other Category at Level II. No streams were wider than 200 meters

(1/8 mile) as defined in Circular #671 except in one instance, where a classification decision could not be made due to the tidal nature of the mouth of the stream.

Non-Forested Wetland - Only a very small percentage of this category was found in the Study area, and that which existed was vegetated. It is uncertain how well this technique could differentiate the vegetated from the bare in the Non-Forested Wetland category.

As will be seen in the results section, the performance accuracy in Level I and II classification was slightly better than when using the black and white enlargements. The ability to detect minimum size objects was also about the same.

During the first and second phases of this study, i.e., those which used conventional image interpretation techniques, special enhancements were produced using black and white transparencies of two or three bands in various optical and electro-optical additive color viewers and printers available at JSC. It was found that these did not appear to provide better or faster results than use of the black and white enlargements or JSC color composites. In fact, the enhancing process appeared to degrade the ability to measure the acreage of certain types of land use.

° Level I and II Classification Using Computer-Aided Techniques

The two methods of computer-aided processing used to analyze the digital tape data were supervised maximum likelihood classification (LARSYS II, Purdue LARS) and unsupervised classification using clustering techniques (ISOCLS - Iterative Self-Organizing Clustering Program, JSC). The first method of processing requires information from training fields that are defined by the analyst and then all other data is classified into the various defined classes (i.e., into the classes that had been input into the computer). A threshold is usually specified, so that data points that are far from the mean of each class are left unclassified. The second method of processing organizes all of the data into spectrally homogeneous groups (clusters) and produces classification-type clustering maps, in which the clusters require identification and interpretation in a postprocessing analysis. It is also possible to use the ISOCLS clustering algorithm to generate statistics for LARSYS II classification in lieu of training field statistics.

The digital data used for this analysis was a 9 track, computer compatible tape from the August 29, 1972, ERTS-1 overpass of the Houston area.

Using the computer-aided techniques, the following Level I and II categories of Circular #671 were detected and identified:

Level I

Urban and Built-Up

Level II

Residential

Level I

Agricultural Land/Rangeland
Forest Land
Water
Non-Forested Wetlands

Level II

Commercial, Industrial and
Transportation
(Open and Other)

When attempts were made to classify Level I categories for the entire Prime Study Area, it was found that there was a marked spectral similarity between highly vegetated Urban categories such as Open and Other and the Cropland and Pasture categories under Agricultural Land (Figure 3). The following performance percentages were determined by computing the area of a predetermined test location which had been correctly classified:

All Level I categories, except Urban	91 - 97%
Level I, Urban	44%

When an effort was made to limit the area to be classified to what might be termed the area inside the urban fringe, the following range of Level II results were obtained:

Residential	67 - 83%
Commercial, Industrial & Transportation	60- 94%
Open and Other	72%

Figure 4 is an example of a supervised classification limited to the highly urbanized area around Houston. Please note that the category Vegetated was used as a class to include urban and non-urban land use which was spectrally similar. It was found that to produce this classification, it was necessary to select more training fields than would be normally required in classifying more homogeneous data sets such as forest or water. Even when many types of residential areas were selected as training fields which could conceivably be considered representative of a class called general residential land use, it appeared that picture elements for all urban categories other than Commercial/Industrial/Transportation were being classified as either Residential or Open and Other (Vegetated). Due to the difficulty in selecting training fields representative of a class, no attempt was made to generate performance statistics on the supervised analysis.

Figure 5 is an example of the use of ISOCLS as a preprocessor to organize certain clusters into meaningful categories of urban land use. In the process, clusters consisting of a few pixels or those with large distances from the mean of the chosen clusters were eliminated. The organizing process used aircraft underflight imagery to correlate the urban land use with each specific cluster. Using this technique, it was shown that not only could some Level I and II categories be mapped,

but the Residential category could further subdivided into what might be termed Level III.

A sampling technique was developed for this classification based on the random selection of grid squares superimposed on a base map, which contained land use as interpreted from the 1:120,000 scale high altitude aircraft imagery. By comparison on a picture element by picture element basis within the selected grid squares, it was possible to determine how well the clusters agreed with existing land use. The following table illustrates how well the classifications derived from the clusters agreed with the image interpretations on the base map.

Agreement With Base (%)		Commercial/Industrial/ Transportation	Residential	Mixed Urban	Vegetation (Woody)	Vegetation (Non-Woody)	Water
Commercial/Industrial/ Transportation	94.2	5.5					0.3
Residential	2.6	66.8	23.0	4.5	3.2		
Mixed Urban	1.0	20.8	51.1	3.8	23.5		
Vegetation (Woody)		0.7	0.2	95.1	4.0		
Vegetation (Non-Woody)	1.1	12.1	25.7	4.8	56.2		
Water	3.9	3.0	1.9	2.2	1.5	87.7	

As was the case with the supervised classification, the Commercial/Industrial/Transportation, the Woody Vegetation (Forest and Brush), and Water categories were well differentiated. The major problem to be encountered in the use of the Circular #671 categories would be in differentiating picture elements with similar spectral response in all four channels in the urban and non-urban areas, as illustrated by the Mixed Urban and Vegetation (Non-Woody) categories.

This study indicated also that if those clusters combined as Residential were analyzed, it was possible to identify each cluster as a separate category which could be classified as Residential, Residential (New) and Residential Mixed. These categories could be considered to be a Level III classification. They appeared to agree generally well with interpretations made from aerial photographs, but a system was not developed which could provide repeatable results with these categories included with the other Level I and II categories.

A limited experiment was conducted to determine how well the areal extent of certain urban land use categories could be measured. The following table illustrates these results:

Accuracy of Areal Extent of Land Use Categories Delineated by Computerized

Classification Technique (ISOCLS)

<u>Residential Study Area</u>	<u>Ratio of Area Acreage $\frac{C^*}{B}$</u>
Cloverleaf (Area L)	1.12
Garden Villas (Area N)	1.16
Center City (Area P)	0.91

- * B = Acreage of Area as delineated on an aerial photograph.
- C = Acreage of Area as delineated on computer classification map (manual picture element count)

Insofar as location of features is concerned, a capability has been developed at JSC to reformat the ERTS-1 CCT as received from the NDPF to correct for:

1. Differential in line and sample spacing
2. Earth Rotation
3. Scale and aspect ratio of the JSC film recorder

The reformatted (registered) tape can then be used to generate a color composite image or after classification by LARSYS II, a color-coded classification map upon which a 10 square kilometer Universal Transverse Mercator (UTM) grid is superimposed (Figure 6). A cursory analysis has indicated that within a local area, this grid is located with respect to the position of features on the earth's surface to much better than 500 meters. Larger areas, as for example an entire CCT, suffer some degradation in the position of all features, due mainly to the instability inherent in the film recorder.

Another paper at this Symposium from JSC will address the locating of ERTS-1 picture elements classified as water to an accuracy of at least 300 meters (1,000 feet) at a 1:24,000 scale. This was made possible by assigning scan line and sample numbers to control points selected from the USGS 1:24,000 scale topographic map series. On the basis of this work and in recognition the UTM overlay previously referred to, it has been demonstrated that it is possible to locate picture elements which have been classified as some specific category of land use, to an accuracy of at least 300 meters or better. Due to the "mixed" or "unresolved object" picture element problem between the different categories of land use, it is not believed that the boundary could be located more accurately. It should not, however, be more than 300 meters or less than two millimeters on a 1:250,000 scale land use map. Depending upon the manner in which the land use maps were to be used, this may be

acceptable to those agencies interested in regional or national land use mapping of Level I and II categories.

RESULTS

1. The results of this land use investigation and those of the other ERTS-I Teams at JSC indicate that using ERTS MSS data as the only information source, a Level I and II Land Use Map of the Texas-Louisiana Gulf Coast Region could be produced. This would require a slight modification in the categories and definitions contained in Circular #671. Assuming that growing and dormant season data is available and that both conventional image interpretation and computer-aided processing are utilized, the following categories could be classified for areas in excess of 4 hectares (10 acres):

<u>Level I</u>	<u>Level II</u>
Urban and Built-Up Land	Residential Commercial and Industrial Extractive Transportation, Communications, Utilities Strip and Clustered Settlements Open and Other
Agricultural Land	Cropland Other
Rangeland	Open Wooded
Forest Land	Deciduous Evergreen (Coniferous and Other) Mixed
Water	Streams and Waterways Lakes Reservoirs Bays and Estuaries Other
Non-Forested Wetland	Swamp Marsh Non-Vegetated
Barren Land	Beaches Sand Other Than Beaches Other

2. All three techniques examined for producing Level I land use maps produced acceptable results insofar as classification accuracy was concerned. As indicated in the paper, when much of the open and heavily vegetated areas inside the urban fringe were treated separately from non-urban areas, the classification accuracy was in the order of 67 to 83%. A comparison of the accuracies achieved by comparing the three classification products with a standard base derived from image interpretation of aerial photography is as follows:

GSFC B&W Images JSC Color Composite Computer-Aided

Land Use Category

Forest Land	98.4%	99.9%	97.4%
Agriculture Land/ Rangeland	89.9	92.3	92.9
Water	79.6	76.0	91.1
Urban and Built-Up Land	93.7	96.5	44.1 (67-83)*

* Accuracy achieved when Urbanized area classified separately from non-urban.

3. When classifying at Level II or higher order categories, computer-aided techniques appear to have a decided advantage over conventional image interpretation. As evidence of this, the following is the only quantitative comparison of classification accuracy which was conducted in this study at the Level II:

Classification Product

Land Use Category	JSC Color Composite (%)	Computer-Aided (%)
Residential	64.7	83.0
Commercial, Industrial, and Transportation	43.8	60.2
Open and Other	-	72.0

The above was conducted only within the urbanized area and was achieved by comparing the classification product with a standard base derived from image interpretation.

4. Investigations at JSC have indicated that computer-aided classification appears to offer greater potential for Level II and higher order category classification than conventional image interpretation. This advantage is assumed to be related to scale and resolution and is probably directly attributable to the capability of the computer-aided classification technique to work near the spatial resolution limits of the sensor system. That is, the human eye-brain combination can readily organize general categories over large areas, as for example Level I at a 1:250,000 scale, but this ability becomes taxed as the number of categories increase and the average area of the units to be classified, decreases. In contrast, the computer-aided classification technique can theoretically detect and potentially identify (classify) each 0.5 Hectare (1.2 acre) picture element as some land surface feature, independent of scale. However, the "mixture" or "unresolved object" picture element problem must be better understood before this becomes practical. Experience at JSC in using computer-aided techniques in classifying surface water from everything else, using Bands 4 and 7, has shown that when three contiguous picture elements have been classified as surface water, there is a high probability that surface water of 4 Hectares (10

acres) or greater in areal extent is present.

Three conclusions may be derived from this:

a. If it can be concluded that computer-aided land use classification works best when used for Level III or IV classification with aggregation back through Level II to Level I, a sampling strategy would have to be developed and used, due to the magnitude of the data processing problem when dealing with the mapping of large areas. The sampling strategy would also have to take into consideration the "mixed" picture element problem and would require a modification to the existing Circular #671 categories.

b. Improvements may be needed in boundary location accuracy due to the degradation caused by "mixed" picture elements which will be found on the perimeter of each classified category.

c. Improvements are needed in the accuracy of area measurement due to the "mixed" picture element problem, especially for classified features less than 100 Hectares (250 acres) in size, since the proportion of the perimeter picture elements increases as the area of the feature decreases.* Classification errors of commission as well as omission must be considered as part of this area measurement problem.

5. When efforts were concentrated on mapping coastal zone features and allowing many of the Level I and II categories to be considered "Other", the following features were classified using the ISOCLS non-supervised clustering procedure:

Clearest Water	Mixed Hardwood and Pine Forest
Less Clear Water	Pine Forest
Most Turbid Water	Wet Bare Soil
Shell Beach and Concrete	Fresh & Brackish Marsh & Wet Rice Fields
Swamp	Other (Urban, Grassland, Dry Cropland)

6. Temporal data sets of Band 7 from two overpasses, registered to each other, were used to automatically determine changes (decrease or increase) in surface water and changes in the tidal limits.

SUMMARY

This study and those of other investigators in the ERTS-1 Program have demonstrated the feasibility of using ERTS-type satellite scanner data for conducting regional and national land use surveys. They have also indicated that monitoring of land use change can be accomplished at

* Work by Nalepka and Hyde (Reference 2) in assuming a hypothetical 100 x 100 meter spatial resolution found that the "mixed" picture element problem could lead to a 25% error in the determination of area of a 44 Hectare (110 acre) square field and a 51% error in the area of a 68 Hectare (170 acre) rectangular field.

intervals commensurate with the requirements of States and other agencies. Although the feasibility has been demonstrated, there has not been as yet a systematic application of land use classification, location, and area measurement procedures, using either conventional image interpretation or computer-aided techniques. This systematic application will require evaluating the performance and accuracies necessary to meet the specific needs of land resource management agencies, prior to development of an operational capability.

References

1. "A Land-Use Classification System for Use with Remote-Sensor Data," Anderson, James R. et al, Geological Survey Circular #671, Washington, D.C., 1972.
2. "Estimating Crop Acreage from Space-Simulated Multispectral Scanner Data," Nalepka, R. F. and Hyde, P. D., Environmental Research Institute of Michigan Report ERIM 31650-148-T, Ann Arbor, Mich., August 1973, pp. 7 and 8.

NASA-S-73-1542

ERTS-1

LAND USE FEATURES ANALYSIS

MANUAL CLASSIFICATION OF LEVELS I AND II
LAND USE IN PRIME STUDY AREA

URBAN AND BUILT-UP	YELLOW
RESIDENTIAL AND OPEN	PINK
COMMERCIAL AND INDUSTRIAL	GREEN
TRANSPORTATION,	BROWN
COMMUNICATION,	BLUE
AND UTILITIES	LIGHT BLUE
STRIP AND CLUSTERED	
SETTLEMENTS	
EXTRACTIVE	ORANGE
FOREST LAND	PINK
AGRICULTURE AND RANGELAND	GREEN
WATER	BROWN
NON-FORESTED WETLAND	BLUE

SOURCE: 1:250,000 SCALE JSC COLOR COMPOSITE
FROM MSS SYSTEM-CORRECTED
CCT - BANDS 4, 5, AND 7
ACQUIRED ON AUGUST 29, 1972



Figure 1 -
The 18 County Houston Area Test Site.
Outlined Area Indicates The Prime Study
Area Covered By One ERTS-1 Computer
Compatible Tape. Houston Is At The
Lower Left of This Study Area.

Figure 2 - Land Use Classification of Prime Study Area
Using Conventional Image Interpretation of
Color-Composite Generated at JSC From Digi-
tal Tape.

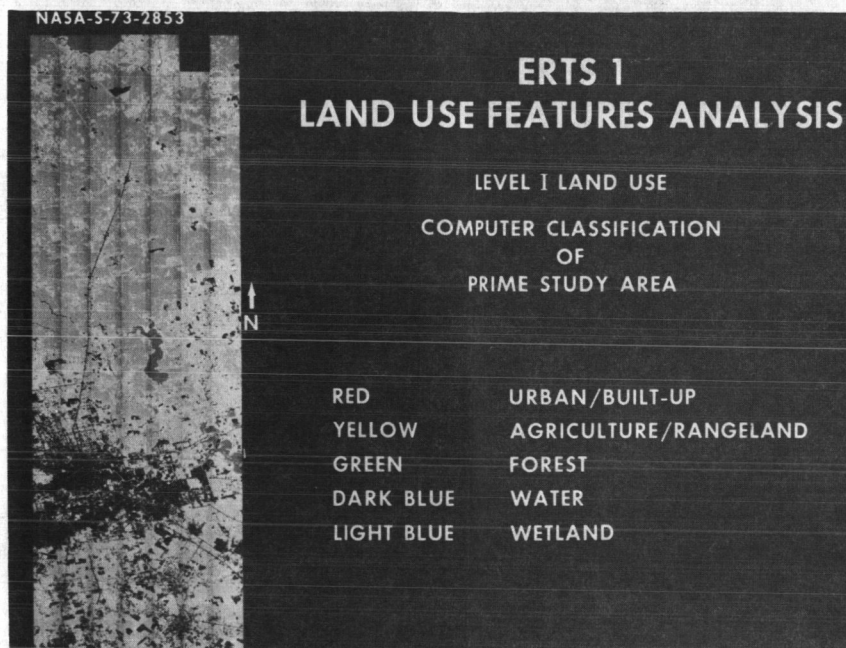


Figure 3 - Level I Computer-Aided Classification of Entire Prime Study Area.

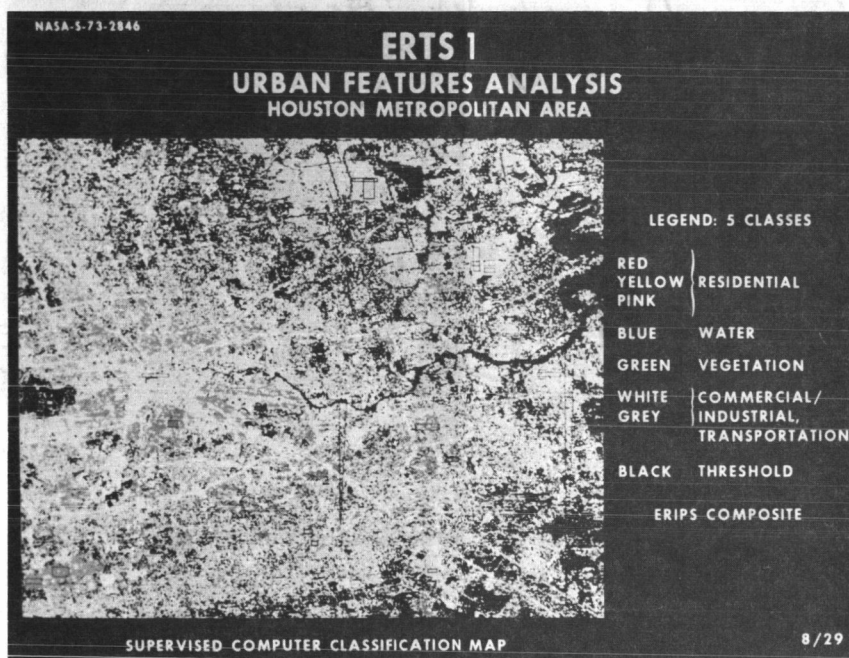
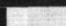








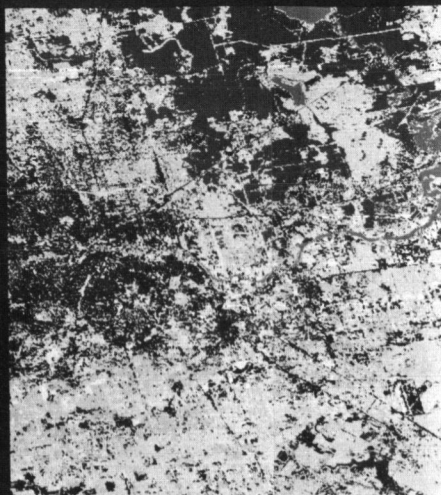
Figure 4 - Supervised Computer-Aided Classification of The Houston Metropolitan Area Portion of The Prime Study Area.

ERTS 1 UNSUPERVISED CLASSIFICATION MAP

ISOCLS
LEVEL III
8-29-72

LEGEND: 7 CLASSES

-  COMMERCIAL / INDUSTRIAL / TRANSPORTATION
-  RESIDENTIAL
-  RESIDENTIAL (NEW)
-  RESIDENTIAL MIXED
-  VEGETATION (FOREST)
-  VEGETATION (OTHER)
-  WATER



HOUSTON METROPOLITAN AREA

Figure 5 - Nonsupervised Computer-Aided Classification of The Houston Metropolitan Area Portion of The Prime Study Area.

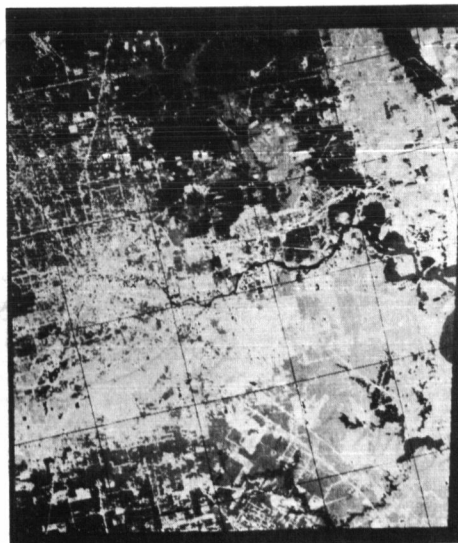


Figure 6 - 1:250,000 Scale Black and White Photograph of The Color Composite Generated At JSC From Part Of A Digital Tape. A Ten Square Kilometer UTM Grid Is Automatically Registered On The Film Recorder Output.

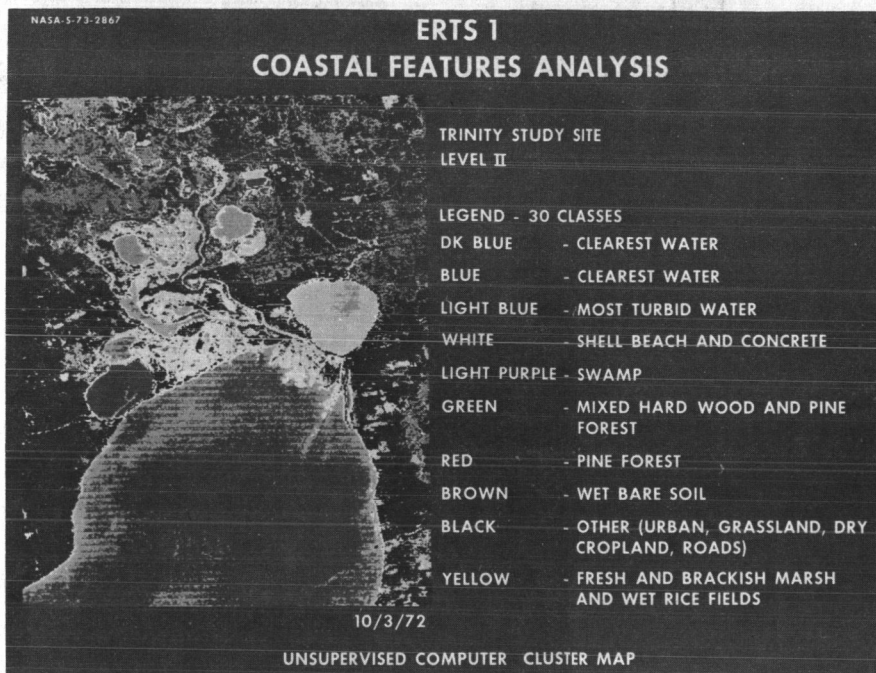


Figure 7.

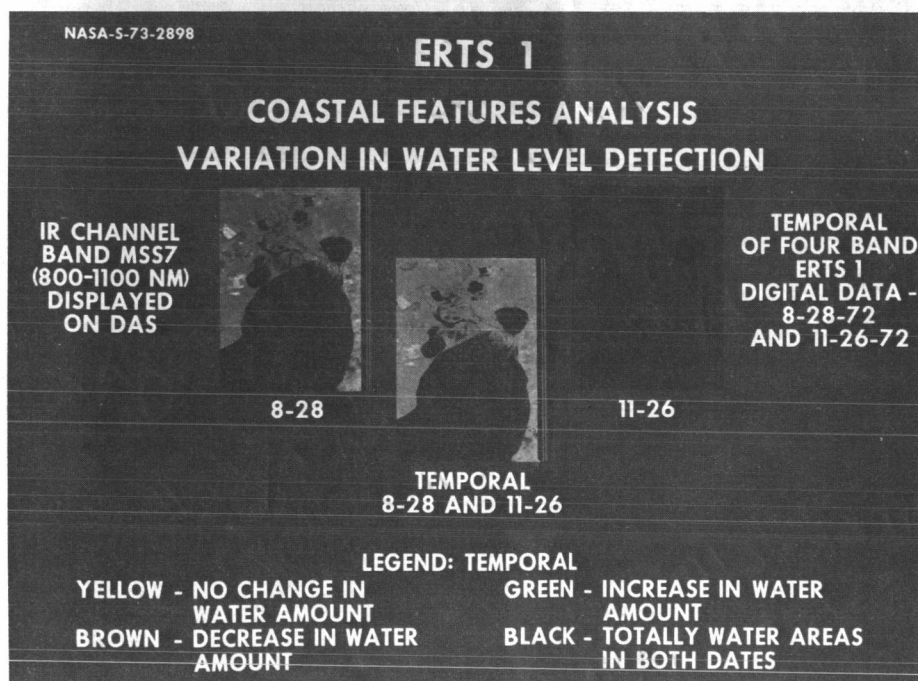


Figure 8.

APPLICATION OF ERTS-1 SATELLITE IMAGERY FOR LAND USE MAPPING AND RESOURCE INVENTORIES IN THE CENTRAL COASTAL REGION OF CALIFORNIA

John E. Estes, Randolph R. Thaman and Leslie W. Senger, *Geography Remote Sensing Unit [GRSU], University of California, Santa Barbara*

ABSTRACT

ERTS-1 Satellite imagery has proved a valuable data source for land use as well as natural and cultural resource studies on a regional basis. ERTS-1 data also provide an excellent base for mapping resource related features and phenomena. The investigations reported on here are focused on a number of potential applications which are already showing promise of having operational utility.

INTRODUCTION

The purpose of this paper is to describe the significant findings resulting from an evaluation of ERTS-1 imagery as a data source for land use studies and the inventory and monitoring of selected environmental parameters. The paper will be divided into three sections: 1] a description of research carried out by the Geography Remote Sensing Unit [GRSU], University of California, Santa Barbara, California, from July 1972 to July 1973; 2] a discussion of the significance of the results; and, 3] a brief discussion of envisioned follow-on studies and the uses of ERTS-1 data that, at present, seem to have the most promise on an operational basis.

DESCRIPTION OF RESEARCH

The objectives of the research, performed by the GRSU, were to: 1] determine the feasibility of using ERTS as a data source for the detection, identification and mapping of various land use types; 2] identify specific land use parameters within the diverse environmental and cultural settings constituting these test areas; and, 3] to compile data base maps for land use and other important resources in the Central California test site. Specific features under examination included: natural vegetation, geomorphology, hydrology, and cultural features such as urbanized areas, transportation routes and networks. The areal focus of these studies was on the Central Regional Test Site, California, covers approximately 52,213 square kilometers [see Figure 1]. Included within the site are several million people and all, or portions of, ten California counties.

In order to successfully evaluate ERTS-1 data for generating resource data for this area it was first necessary to: 1] develop flexible classification schemes for both urban and rural terrain features and, 2] to develop a data base for the test site, against which the value of ERTS-1 imagery as a data source could be evaluated.

PRECEDING PAGE BLANK NOT FILMED

N 74 30738



Figure 1: Central Regional Test Site, California covering approximately 52,213 square kilometers.

Classification Systems

The classification systems were designed so that they could be either collapsed or expanded to accommodate different levels of generalization, e.g., classifications developed would be applicable to either conventional aerial photography or ERTS satellite imagery. Four major classification schemes were devised: 1] land use; 2] land forms; 3] hydrology; and, 4] natural vegetation [see Appendix A]. The land use classification scheme included general categories such as agriculture, extractive industries, public facilities, recreational facilities, industrial areas, transportation networks, commercial areas, residential areas and non-developed land. Each of these categories are, in turn, subdivided for more specific identification of terrain features, e.g., recreation was broken down into campgrounds, golf courses, parks, stadiums, marinas, etc., or as in the case of residential areas, into single family and multi-family dwellings.

The land form [geomorphology] classification scheme included general categories related to fluvial, glacial, eolian, marine, volcanic and other complex geomorphological features. Again these categories were further broken down into more specific land forms.

Hydrologic features were broken down into streams [which were classified according to their "stream orders"], lakes, springs, estuaries, marshes, swamps and man-made hydrologic features such as reservoirs, canals, wells, sumps, etc.

Finally, the natural vegetation classification included both terrestrial and aquatic vegetation. Again, these categories were subdivided into sub-categories such as marine aquatic, freshwater aquatic, strand grassland, woodland-savanna, scrub, forest and riparian. These sub-categories were, in turn, further broken down into more specific vegetation associations such as: salt marsh, valley grassland, coastal chaparral, cut-over forest, desert scrub, hardwood forests, coniferous forests, etc. Again, in all cases the classification systems derived were amenable to application to both conventional high altitude NASA photography and the more generalized ERTS-1 images.

Data Base

In preparation for the analysis of ERTS-1 data, baseline information on the Central Regional Test Site was acquired prior to the acquisition of the first ERTS-1 images. These data were compiled utilizing 1:60,000 and 1:120,000 high altitude photography; 1:600,000 NASA U-2, ERTS-1 support photography; and selective ground reconnaissance. Based on interpretational analysis of these data, GRSU personnel were able to prepare land use, land-form, hydrology and natural vegetation maps for almost the entire Central California test site. In all cases, the above mentioned classification schemes were used as guidelines for data acquisition and mapping. The data

and maps compiled provided an excellent basis for evaluating the potential of ERTS-1 type imagery for supplying similar or incremental data on either a more timely or, less costly basis than is presently possible.

ERTS-1 Analysis

After the classification systems had been prepared and the data base for the test site completed, the analysis of the ERTS-1 imagery began. The analysis of the ERTS-1 imagery was accomplished in six phases: 1] an initial phase during which the image interpreters familiarized themselves with the unique scale, resolution, contrast and tonal and textural characteristics of ERTS-1 imagery; 2] preliminary interpretation of the imagery for representative test sites to determine the interpretability and classification related information content of the ERTS imagery; 3] evaluation and modification of classification schemes based on the preliminary studies; 4] completion of data base maps for the entire Central California test site; 5] the application of ERTS data to ancillary problems with particular focus on interfacing with and trying to encourage resource management agencies and other user groups to attempt to utilize ERTS-type data on an operational basis; and, 6] a final analysis and summary of the value of ERTS-1 imagery based on the studies performed by the GRSU.

Phase 1: The familiarization phase entailed intensive study of ERTS images of known areas to determine which features and/or environmental parameters could be consistently identified. An examination was also made of the interpretation techniques which would be most suitable for ERTS analysis.

As part of this phase, interpretation and analysis were performed on both the original 9 1/2 x 9 1/2 inch black-and-white transparencies as well as on ten times [10x] enlargements of selected portions of ERTS images. In most cases the analysis performed entailed the study of both conventional high altitude aerial photography and ERTS images of the same area, in concert, to familiarize the interpreter with the relative appearance of the landscapes and to gain a general idea of which features could be detected, identified, mapped, measured, and/or monitored.

Phase 2: The preliminary interpretation of ERTS-1 imagery for selected test sites was again, a phase of the study designed to familiarize interpreters with the problems associated with an overall interpretation of ERTS imagery for specific test areas so that they would be better prepared to complete the data base for the entire 52,213 square kilometer Central Region test site. Furthermore, at this juncture in the study, multitemporal imagery taken during both summer and winter seasons was unavailable, so a decision was made to delay the production of the final test area maps until additional data from subsequent ERTS over-flights became available, in order to achieve highest mapping accuracy for the finished product.

Preliminary maps were completed for land use, land forms and natural vegetation and formed the basis for modification of the original classification systems to render them more applicable to the information content of ERTS imagery. Figure 2 is an example of one of the preliminary vegetation maps of the area around Morro Bay, California, utilizing ten times enlargements of July 25, 1972 ERTS-1 imagery. Similarly, a preliminary

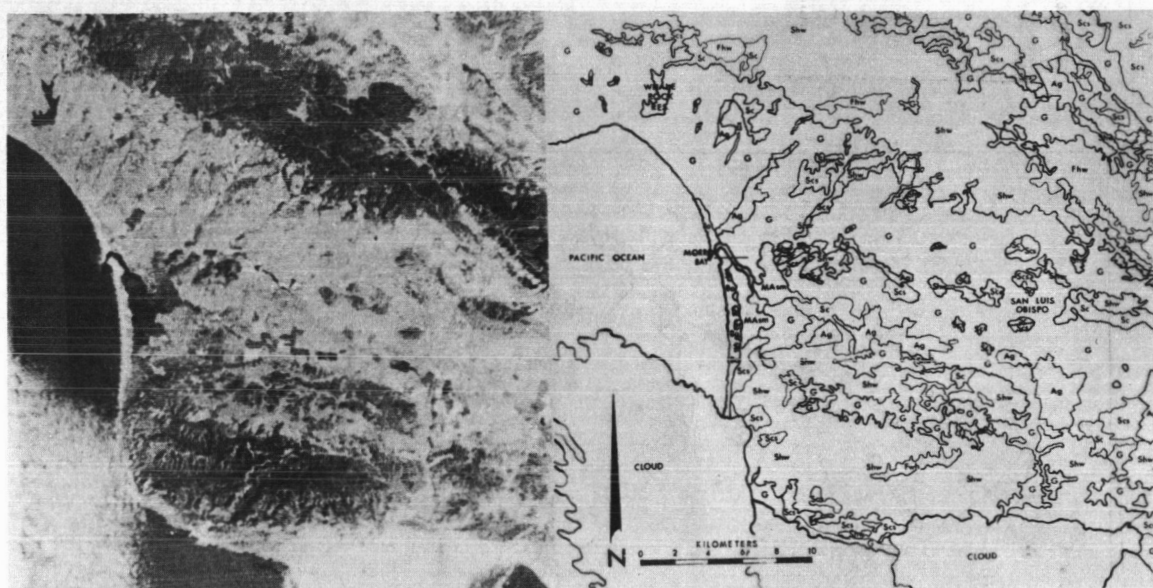


Figure 2. Preliminary natural vegetation maps prepared from ten times [10x] enlargements of July 25, 1972 ERTS-1 satellite imagery of the area surrounding Morro Bay, California.

map of land use is shown in Figure 3 while another preliminary vegetation map is shown in Figure 4. In all cases, the experience gained in preparing these maps was invaluable for the ensuing mapping of the entire test site as well as providing valuable insight for an accurate estimation of the value of ERTS data for such studies.

Phase 3: Based on these preliminary studies, a number of modifications were made in the classification systems to provide for a more generalized type of information [see Appendix B]. For example, urban areas under 4,000 persons in population were very difficult to detect. Consequently, classifications such as single or multiple family dwellings became insignificant as important categories [at least in the California environment]; likewise, certain vegetation categories such as hard chaparral and soft woodland were generally difficult and were modified for the final operational classification. Accordingly, the original detailed classification schemes shown in Appendix A were modified and more generalized categories, such as those shown in Appendix B, became the operational categories utilized for the production of the final data base maps.

Actual completion of the data base maps for the Central Regional Test Site required the use of portions of seven different ERTS-1 images such as those shown below in Figures 5 and 6. For each section of the test site at least two ERTS bands [generally band 5 and either band 6 or 7,

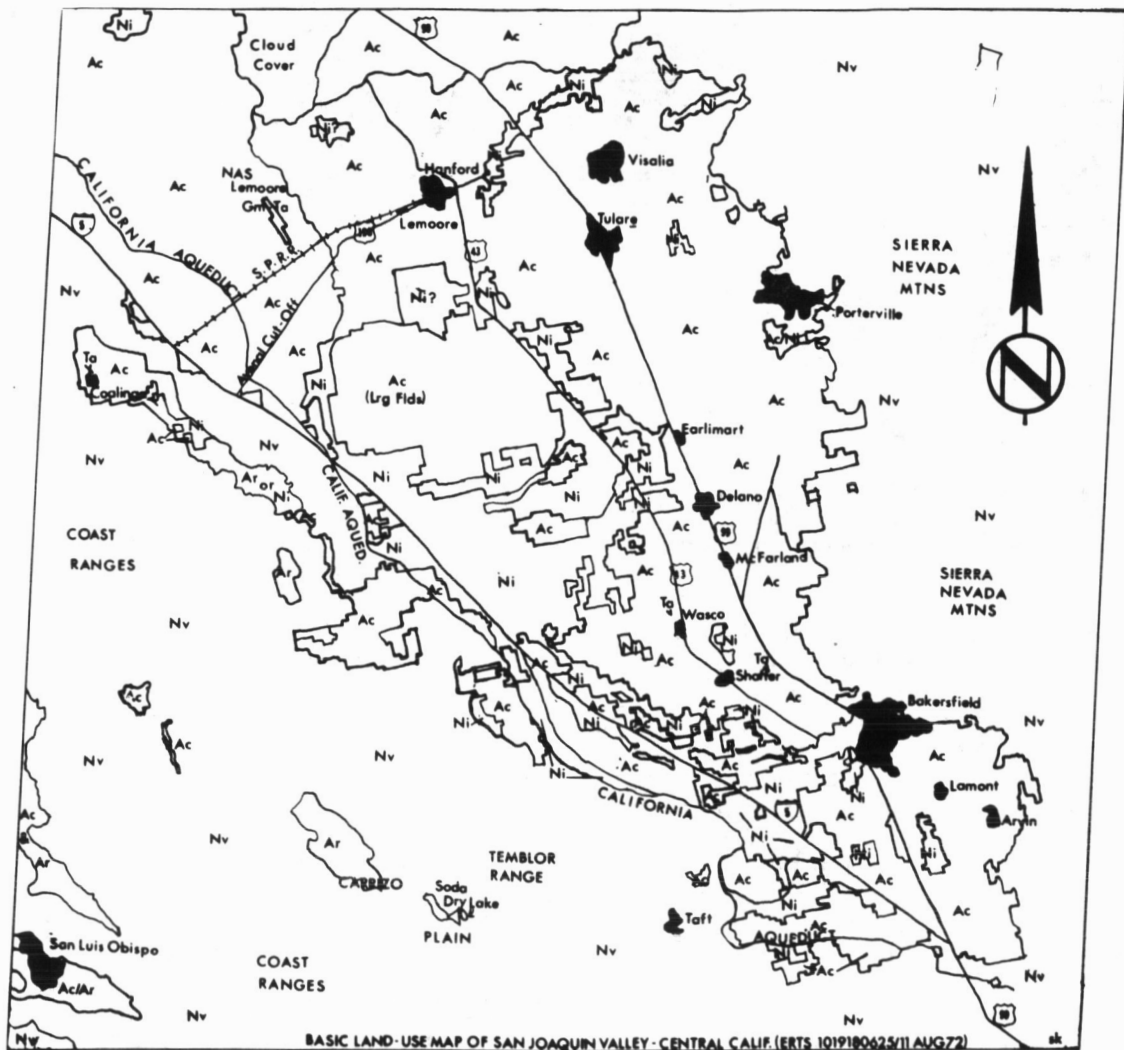
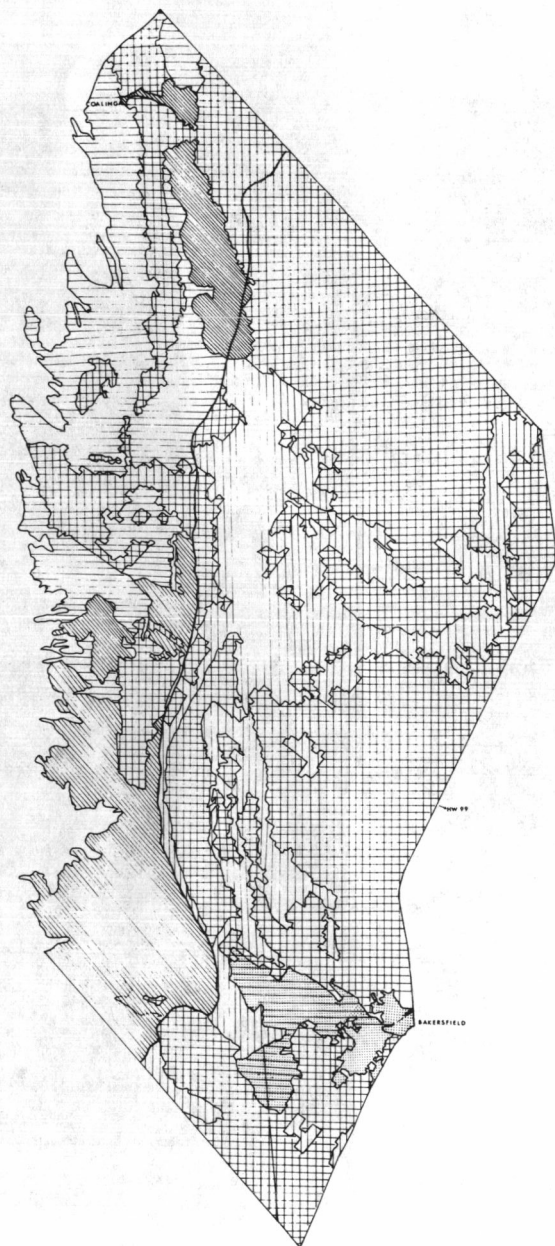


Figure 3. Preliminary land use map constructed using August 11, 1972 ERTS-1 imagery of the southern end of the San Joaquin Valley, California.



WEST SIDE VEGETATION - 1972



SOURCE: ERTS-1, MSS BAND 5

Figure 4. Preliminary vegetation map of the southern end of the San Joaquin Valley, California constructed using an August 11, 1973 ERTS-1 image.

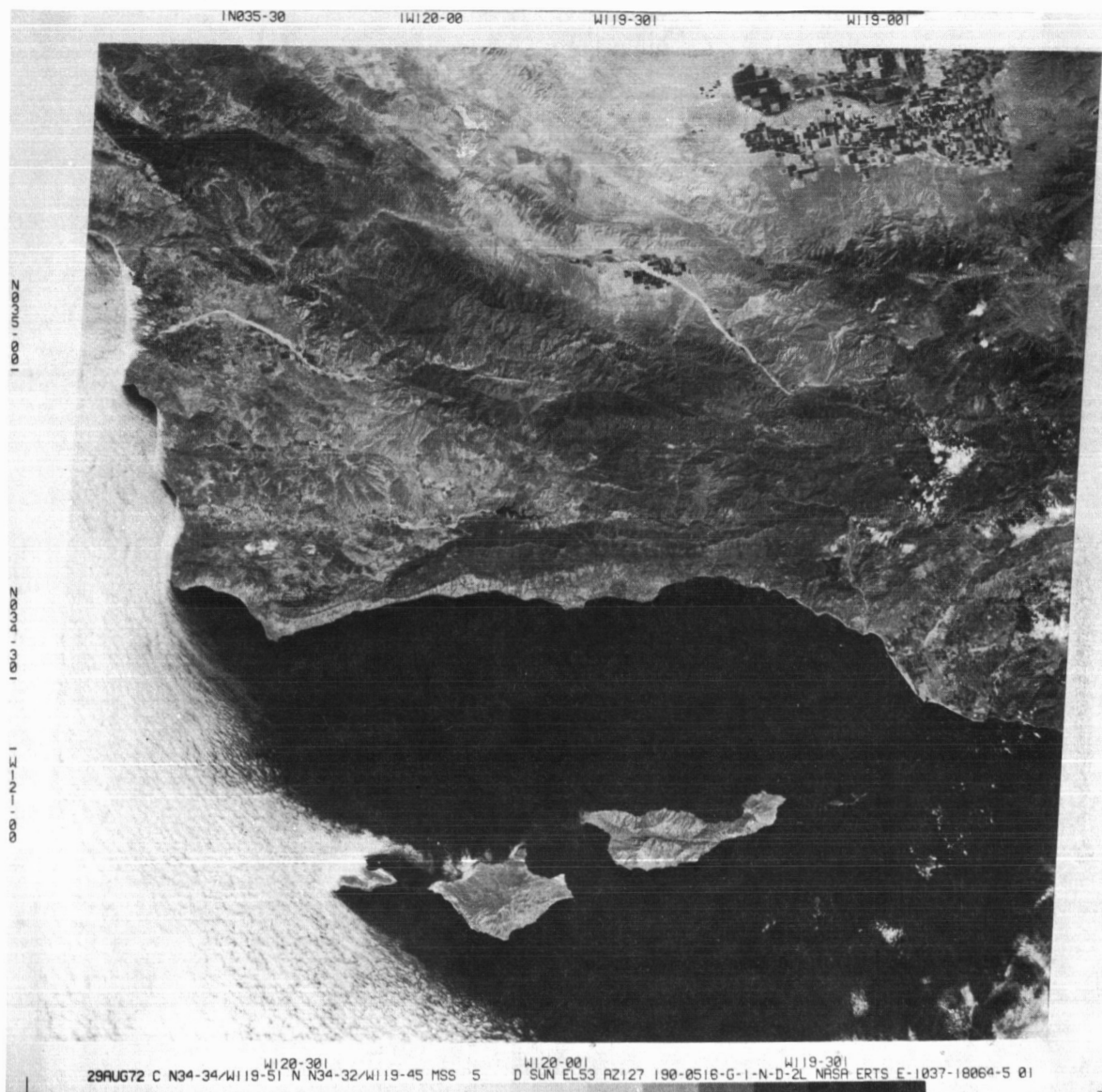


Figure 5. An example of a 9 1/2 x 9 1/2 inch (1:1,000,000) ERTS-1 band 5 image used for the completion of regional data base maps of the Central Regional Test Site. This image is centered on the town of Santa Barbara, California.

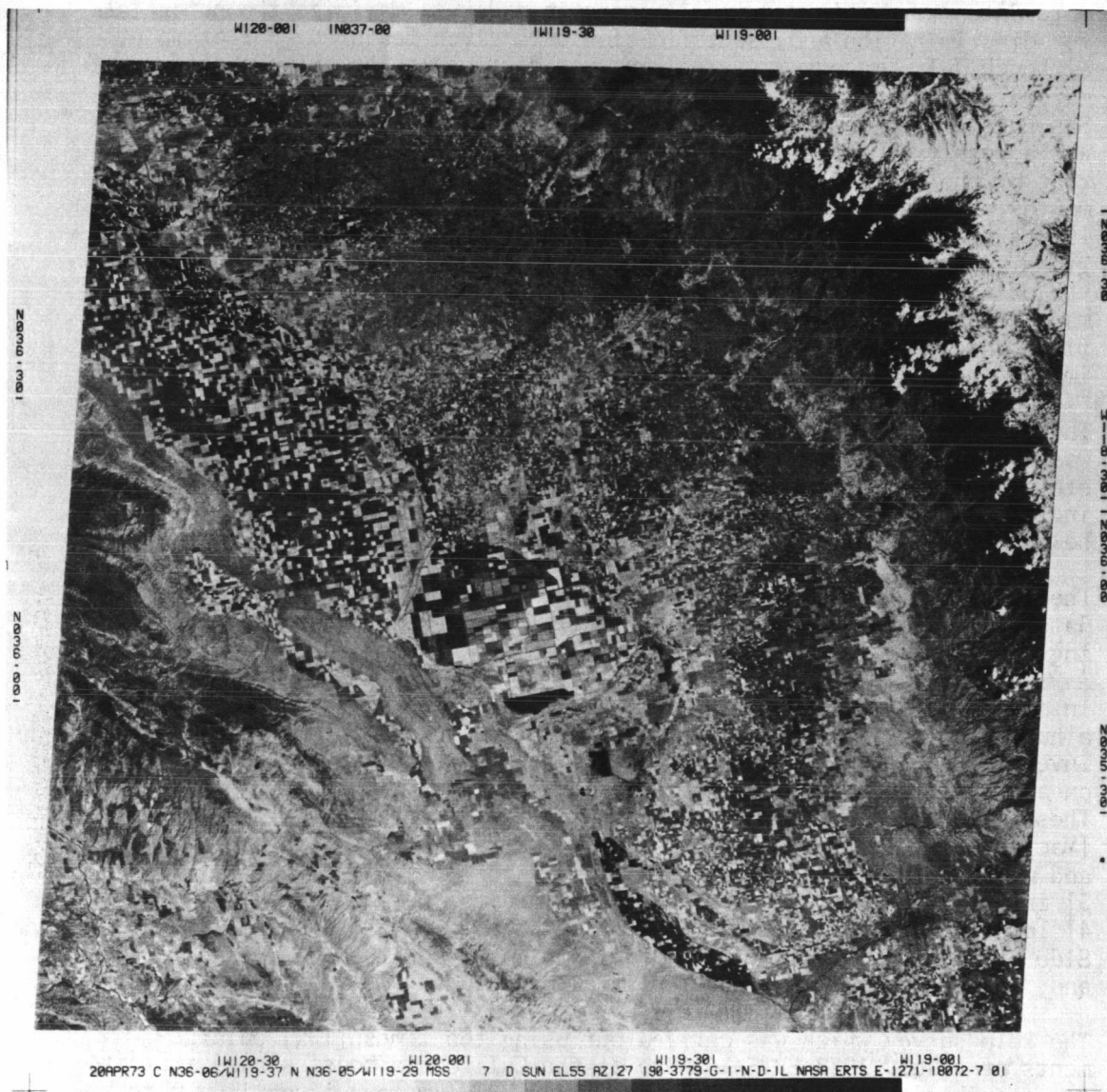


Figure 6. An example of a 9 1/2 x 9 1/2 inch (1:1,000,000) ERTS-1 image used for the completion of regional data base maps of the Central Regional Test Site. This image is centered on the Tulare Lake area of the San Joaquin Valley, California.

although in a few instances band 4 was used] were employed to utilize the multiband capabilities of ERTS-1 imagery. Similarly, data from two or more dates were utilized in all cases in order to maximize the potential for discrimination and identification of a given feature. For example, although July imagery was excellent for distinguishing between different major vegetation types, it was almost impossible to locate the city of San Luis Obispo [population of approximately 30,000] at this date. This was a result of the similarity of the light toned urban signature with that of the surrounding annual grassland, which is dry during the summer months. In March, however, when the annual grassland had turned green, the limits of San Luis Obispo showed up clearly against the background annual grassland. In all cases the actual interpretation was carried out using the original 9 1/2 x 9 1/2 inch, 1:1,000,000 scale ERTS images with the maps being constructed on mylar overlays. Interpreters used hand magnifiers and Zeiss stereoscopes [when reinforcement and/or combination of images was desired, or when limited stereoscopic viewing was feasible].

The minimum mapping unit, i.e., the smallest area that was classified, was 2.641 square kilometers. At a scale of 1:1,000,000, 2.641 kilometers equals approximately 0.026 square centimeters on the image. Accordingly, it was felt that units smaller than 2.641 square kilometers would be comparatively insignificant, and unmappable, at a scale of 1:1,000,000.

The resultant final land use, land form, hydrology and vegetation data base maps for the Central Region Test Site can be seen on the following pages.

In addition to the completion of the data base maps discussed above, a number of additional studies were performed in an attempt to develop inventory techniques which would have a high probability of being adopted on an operational basis by various user agencies with area responsibilities. These studies have included: 1] mapping the distribution of kelp [*Macrocystis*] concentrations along the Central California coast; 2] mapping and monitoring fire damage and recovery rates of a major forest fire; 3] inventory of irrigated agricultural land for Kern County, California; 4] location and delineation of areas of perched water tables in the West Side of the San Joaquin Valley, California; 5] monitoring of land use change; and, 6] identification of agricultural crops.

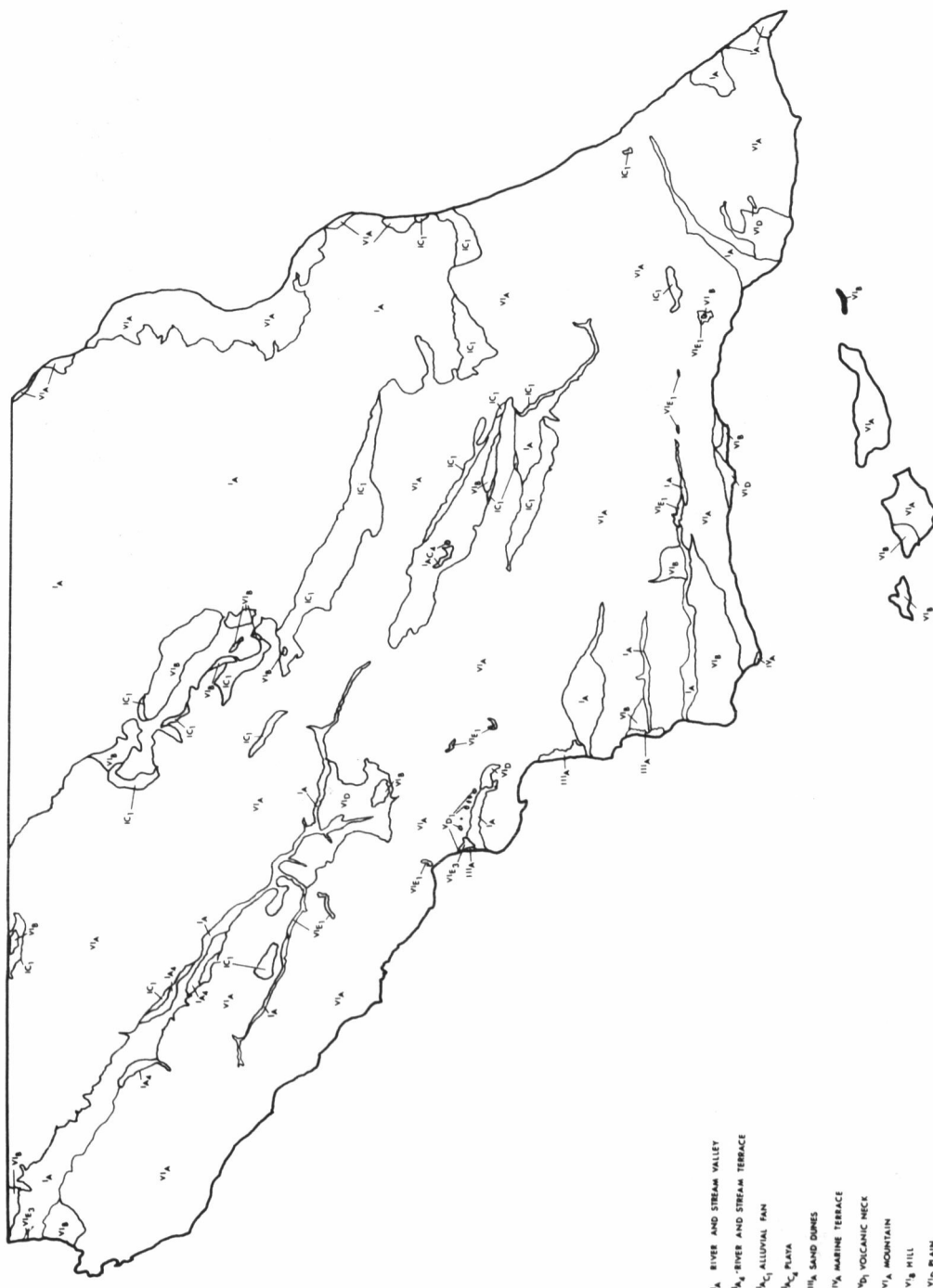
The kelp survey which was carried out using ten times [10x] enlargements of a July 1972 ERTS-1 image of the California coast showed that it was possible to accurately map kelp using ERTS imagery if optimum meteorological, tidal, water temperature, current conditions, etc. occur at the time of overflight. The map showing the areal extent and location of the kelp concentrations and an estimate of their surface area can be seen on the following pages [Figure 7 and Table 1].

The investigation of the usefulness of ERTS-1 data for delimiting fire damage areas was based on the U.S. Forest Service's common practice of delimiting the area of each major fire area using conventional aerial photog-

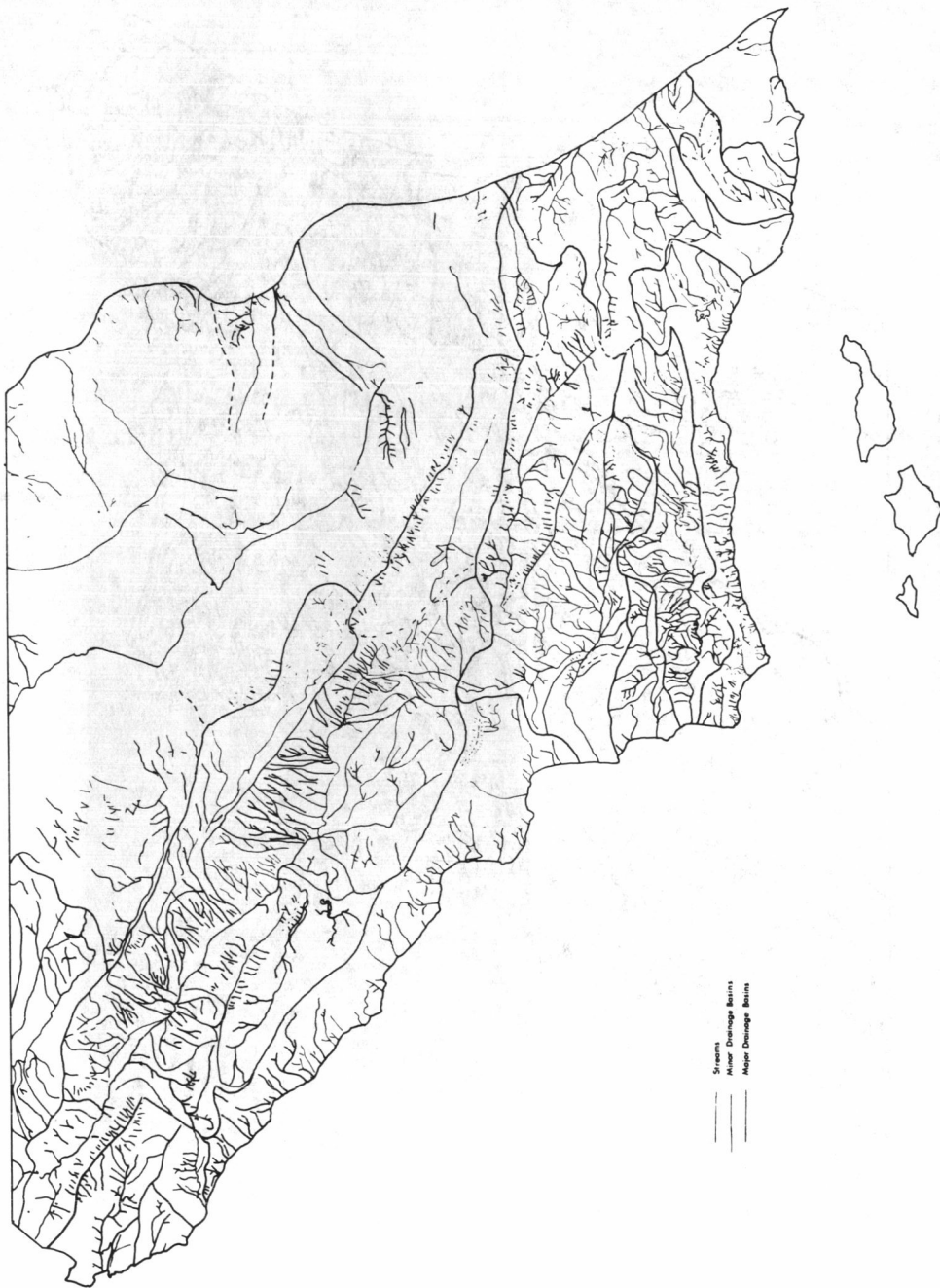
LEGEND

Ac	Cropland
Ar	Rangeland
Em	Mining
Gm	Military Facility
Ni	Idle Land
Nv	Natural Vegetation
Te	Airfield
D	Highways
S	Interstate
O	State
B	Urban

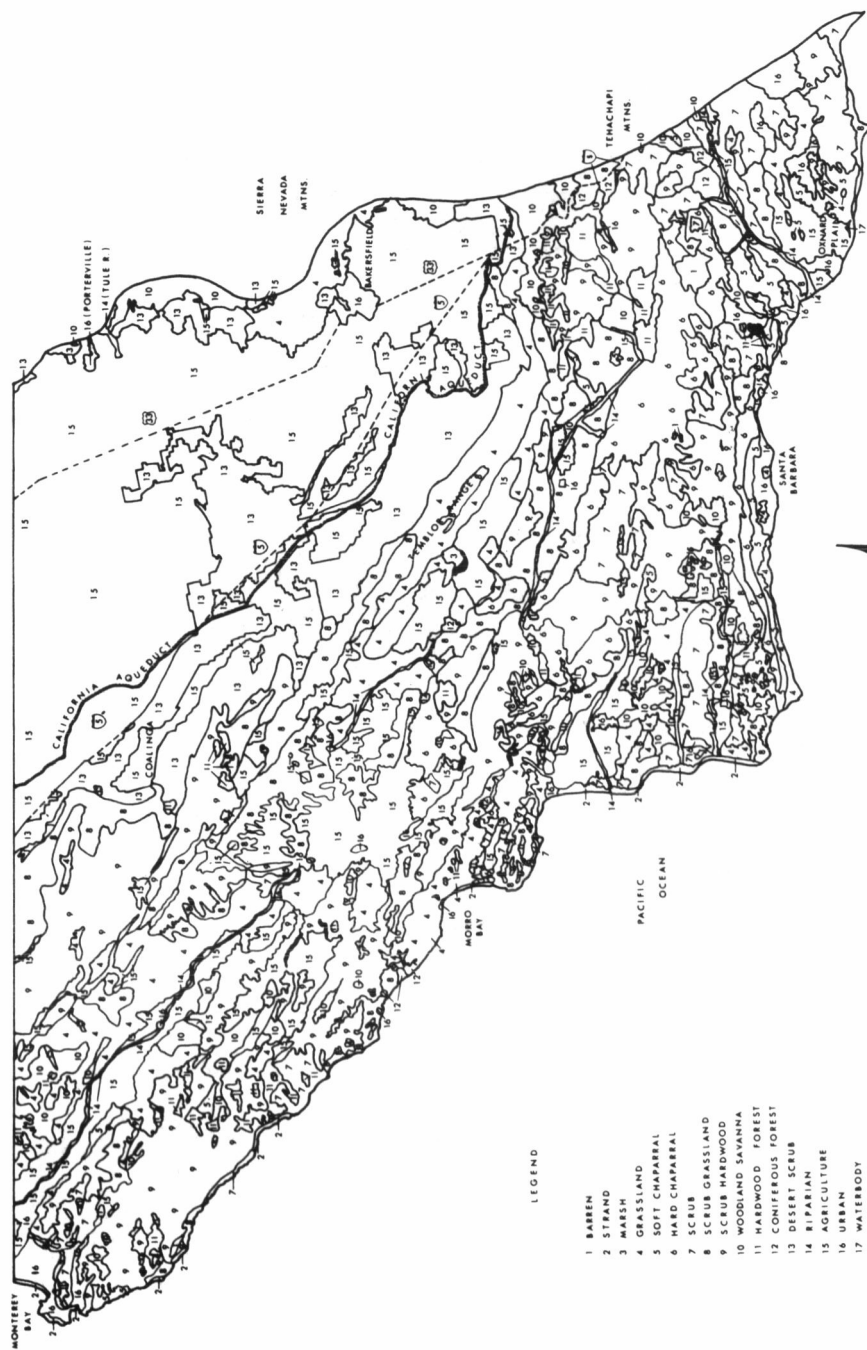
CENTRAL REGION LANDFORM DATA BASE



Central Region Drainage Data Base



CENTRAL REGION VEGETATION DATA BASE



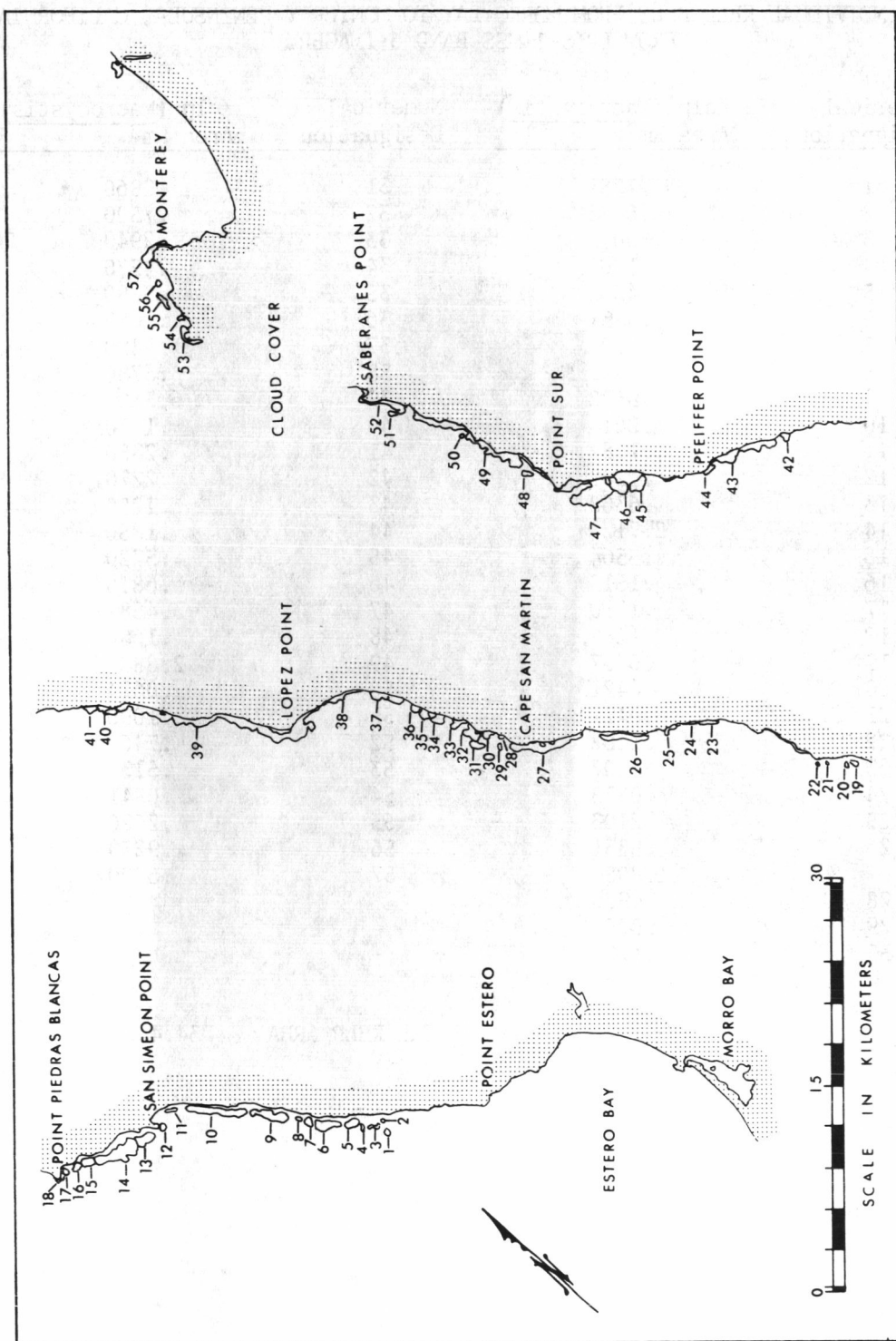


Figure 7. Map showing the areal extent and location of kelp beds (*Macrocystis*) along the California coast from Morro Bay north to the Monterey Peninsula. Land area is shown by the stippled pattern while individual kelp concentrations are indicated by numbers (1-57).

TABLE 2. QUANTITATIVE ESTIMATES OF SURFACE AREA
OF INDIVIDUAL KELP BEDS FROM MORRO BAY TO MONTEREY PENINSULA, CALIFORNIA
FROM ERTS-1 MSS BAND 6 IMAGERY

Numerical Designation	Kelp (<u>Macrocystis</u>) Area Km ²	Numerical Designation	Kelp (<u>Macrocystis</u>) Area Km ²
1	.1282	31	.2860
2	.0673	32	.7500
3	.0013	33	.2940
4	.1002	34	.4370
5	.4205	35	.3280
6	.8831	36	.1680
7	.2520	37	.8490
8	.0841	38	.3780
9	.9672	39	6.510
10	1.261	40	.1770
11	.1282	41	.2350
12	.1282	42	.2270
13	.6308	43	.1250
14	2.712	44	.1850
15	.3364	45	.5720
16	.1513	46	.6810
17	.1010	47	3.458
18	.1282	48	.1680
19	.0757	49	2.882
20	.0421	50	.0674
21	.0421	5k	.1090
22	.1682	52	.7460
23	.2607	53	.5130
24	.0873	54	.0841
25	.2103	55	.2020
26	.8831	56	.9250
27	1.808	57	.6900
28	.0925		
29	.0757		
30	.1700		

TOTAL KELP AREA 34.4432

graphy. The study was focused on an area west of Santa Barbara burned by the "Bear Fire" in August 1972 which burned approximately 17,260 acres of scrubland and forest vegetation. Upon receipt of the October 1973 ERTS-1 imagery, it was found possible, on band 7, to accurately map the areal extent of the fire as well as unburned islands of vegetation within the fire area at a considerable time savings over the use of conventional areal photography. Furthermore, with the receipt of ERTS data on an 18-day basis it was possible to monitor the vegetation recovery rate of the burned area.

The inventory of irrigated agricultural land using ERTS-1 data has also shown considerable promise. This project entailed the inventory of all irrigated agricultural land in Kern County, California. Data were generated on the acreage of irrigated land in the county and sent to the Kern County Water Agency [KCWA] for verification. The area was first mapped using NASA high altitude photography and later using ERTS-1 imagery. The results of these inventories is shown below in Table 2 along with K.C.W.A. figures for the same area:

Table 2
Comparison of Data on Irrigated Agricultural Land, Kern County, California

<u>SOURCE</u>	<u>AGRICULTURAL ACREAGE ESTIMATE</u>
1. NASA High Flight [70mm] - 1971	753,369
2. K.C.W.A. - 1971	795,280 [including fallow]
3. 1969 Crop Survey [Kern County]	746,104 [excluding fallow]
4. ERTS-1	748,050

An indication of the accuracy of these figures [less than 1% error when fallow ground is excluded] is the fact that the K.C.W.A is now using ERTS-1 data on irrigated agricultural land supplied to them by the GRSU as data input to their water supply/demand models. The following maps are examples of March and July 1973 inventories of irrigated agricultural land based on ERTS-1 data which are being supplied to the K.C.W.A. on a regular basis.

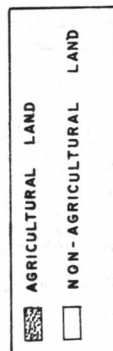
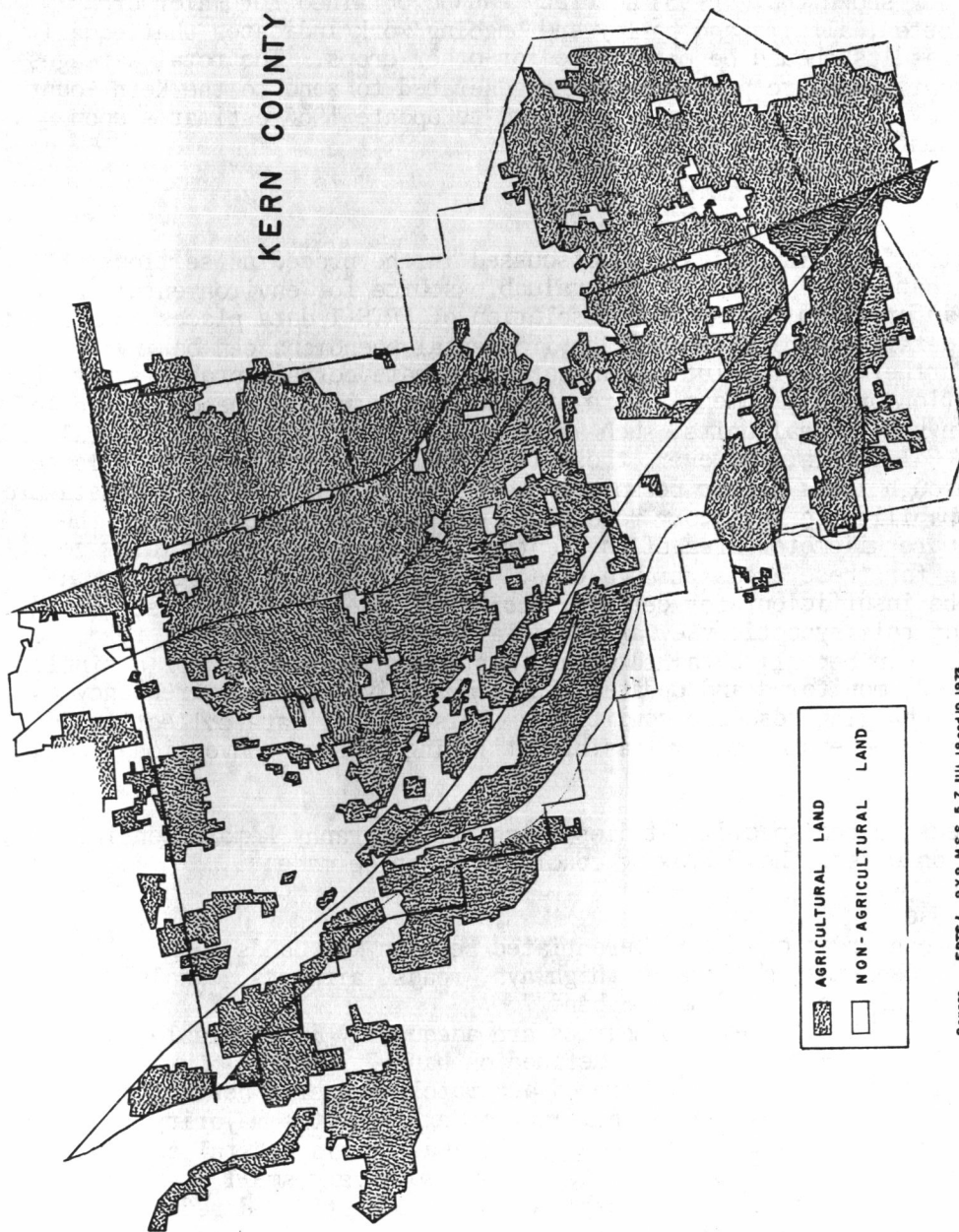
Other work in progress with K.C.W.A. and the Department of Water Resources of the State of California indicated that areas of perched water tables and excessive soil salinity, both pressing problems in the irrigated lands of the West Side of the San Joaquin Valley, can be monitored effectively using multirate ERTS type imagery.

Land use change studies are also of critical importance to planning agencies because land use changes rapidly, especially in rapidly developing agricultural areas such as the West Side of the San Joaquin Valley, California, and it is important to monitor this phenomena. Accordingly, studies were also conducted to see if ERTS-1 imagery might be suitable for detecting and monitoring land use change. The following map and table show 1971 and 1972 data on land use change in an area of the West Side of the San Joaquin Valley constructed from 1971 high altitude photography and ERTS-1 imagery,

KERN COUNTY



KERN COUNTY



Source ERTS 1 9X9 MSS 5, 7 JUL 18 and 19, 1973

respectively. In this case, the ERTS-1 imagery provided for adequate monitoring of land use change.

Finally, the use of ERTS-1 imagery, should provide accurate data on the relative acreages of different agricultural crops. Preliminary studies have already shown that 90-95% accuracy can be obtained for major crops such as cotton, alfalfa and barley and ongoing work indicates that equally accurate results should be obtainable for other crops. The total acreages of different crops are presently being generated to send to the Kern County Water Agency so that they can be utilized to update 1960 estimates upon which present water allocations are based.

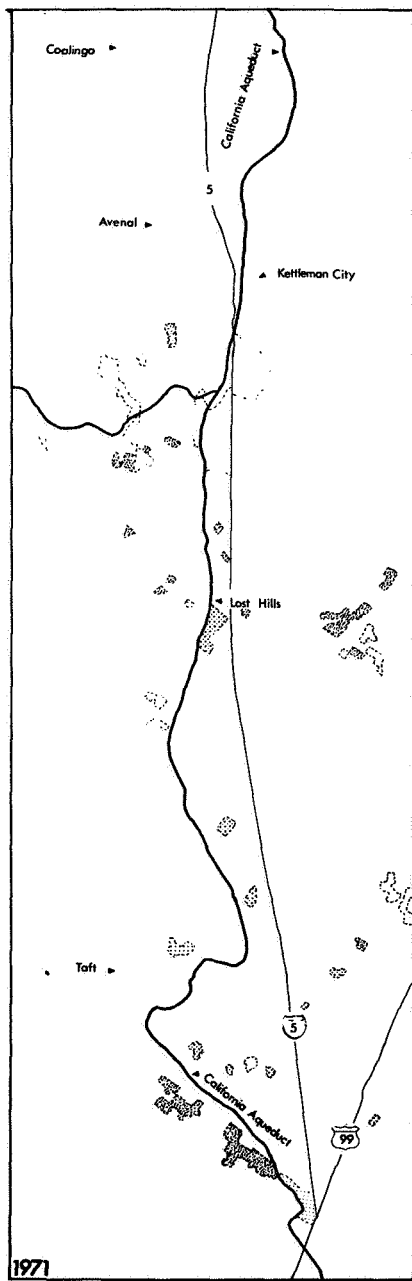
CONCLUSIONS

The results of the investigations discussed in the preceding sections indicate that ERTS-1 data can be a valuable source for environmental resource information needs. The resolution of ERTS-1 data places constraints upon the detail to which specific environmental phenomena can be investigated. Furthermore, resolution limitations create certain problems for the investigation of environments where diverse environmental phenomena are localized in small areal units, such as the coastal portion of the Central Region of California. However, these limitations are mitigated to a large degree through the synoptic perspective afforded by ERTS-1. ERTS-1 data provide a capability to inventory resources over extensive areas [e.g., the 52,213 square kilometer area of the Central Region], and sequentially generate data for these areas through time. Although the detail of information may be insufficient for certain specialized user requirements, the advantages of this synoptic view are that large scale environmental resource information can be: 1] obtained within a standardized format for a single date; and, 2] monitored and updated with comparative ease and frequency to reflect changing resource conditions. This type of data collection does not appear to be economically feasible utilizing present conventional data collection methods.

With respect to the specific studies which the Geography Remote Sensing Unit has conducted, the following conclusions can be made:

Land Use

1. Urban areas can be differentiated best on MSS bands 4 and 5.
2. Transportation linkages [highways, roads, airports, canals] are most readily defined from MSS band 7.
3. Agricultural field boundaries are adequately identifiable on MSS bands 4 - 7, and most clearly defined on band 7.
4. Cultivated land can be mapped accurately [under 5 percent error] from MSS band 5. Fallow land identification explains the majority of error.
5. Land use is difficult to map in the California coastal environment because many individual use categories occupy very small areal units; land use mapping is easier and capable of more sophisticated refinements in the arid California Central Valley.



LAND USE CHANGE

WEST SIDE

1971-1972



KEY:

Cropland	
Grazing	
Oil Extraction	
Nonproductive Land	

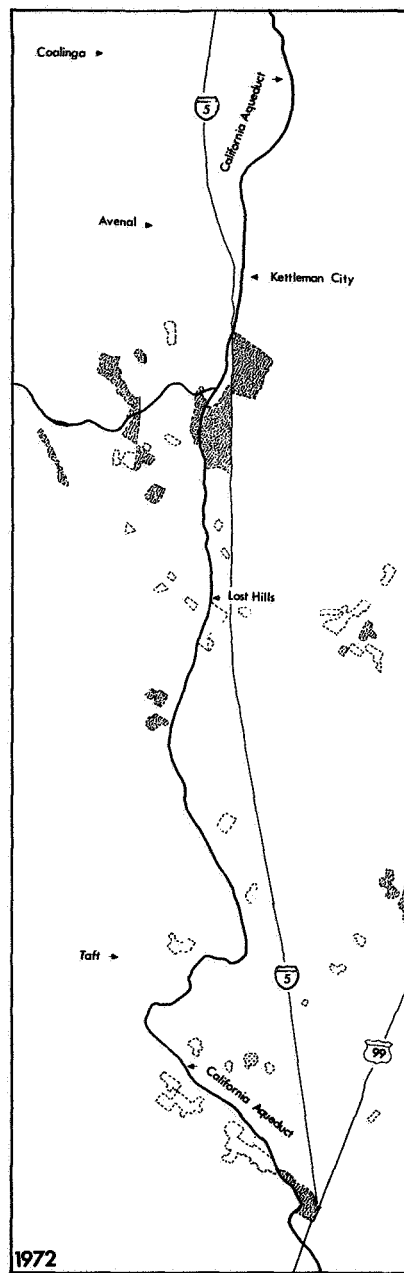
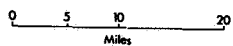


TABLE 3. LAND USE CHANGES 1971 - 1972

1971	1972 LAND USE CHANGES (IN ACRES)				TOTAL
	CROPLAND	GRAZING	OIL EXTRACTION	NON-PRODUCTIVE	
CROPLAND		49,152		896	50,048
GRAZING	22,258				22,258
OIL EXTRACTION	2,074				2,074
NON-PRODUCTIVE	7,163				7,163
TOTAL CHANGE IN LAND USE ACREAGE	31,495	49,152		896	81,543

NET CHANGE IN LAND USE CATEGORIES (ACRES)				
CROPLAND	GRAZING	OIL EXTRACTION	NON-PRODUCTIVE	
Loss: 50,048	Loss: 22,258	Loss: 2,074	Loss: 7,163	
Gain: 31,494	Gain: 49,152	Gain: N/A	Gain: 896	
Change: -18,553	Change: +26,894	Change: -2,074	Change: -6,267	

6. Macro-level land use change can be identified, mapped, and measured with a high degree of reliability.

Crop Identification

1. Non-vegetated [bare soil] field conditions are identifiable with almost 100 percent accuracy [negligible errors of omission or commission].
2. It is difficult to identify specific crops on a single date because of signature overlap.
3. Identification accuracies can be improved and approach an accuracy of 90% or higher if multirate analytical approach is used, since crop growth cycles are reflected in progressively changing tonal signatures on ERTS-1 imagery over time.

Drainage and Landform Mapping

1. Drainage networks and basins can be mapped with sufficient accuracy to permit updating of U.S.G.S. 1:250,000 topographic maps.
2. Macro-scale landform mapping is feasible.

Kelp [Macrocystis]

1. Kelp concentrations can be identified and located accurately.
2. Boundaries of kelp concentrations can be delimited accurately and good areal estimations made.
3. Internal variations within kelp concentrations are detectable [probably related to density] and may, in conjunction with estimates of areal extent, provide an indication of biomass.

Forest Fire Damage

1. The perimeter of forest fire damage can be accurately delimited.
2. "Islands," or pockets of unburned vegetation, can be identified and mapped.
3. Burn area of previous forest fires [at least one year in the past] can be identified and mapped.

Vegetation Mapping

1. Barren land, Coastal Strand, Coastal Salt Marsh, Grassland, Scrub Hardwood, and Agricultural vegetation exhibit good differentiation.
2. Coastal Sagebrush, Chaparral, Woodland-Savannah, Forest Hardwood, and Riparian vegetation exhibit limited differentiation.
3. Coniferous forest is difficult to differentiate.
4. Individuals, with comparatively minor training in photo interpretation and vegetation identification, can perform vegetation mapping at reasonable levels of accuracy; more specifically, at the association rather than the community level. This indicates that ERTS-1 type technology should be transferable into operational usage for this type of resource inventory.
5. Some problems in the interpretation of specific vegetation associations may be mitigated through selective use of ground or light aircraft reconnaissance.

Successes resulting from these specific investigations are primarily attributable to: 1] the multiband [opportunity to view phenomena that are highlighted in different bands]; and, 2] multirate [certain phenomena are more observable during particular seasons of the year] approach which is characteristic of ERTS-1 data. Perhaps most significantly, it is estimated that each of the Central Region data base maps [encompassing an area of approximately 52,213 square kilometers] could be constructed for a different time period in approximately one man-week. These considerations indicate that ERTS-1 type data should provide significant input to resource management and planning at regional, or larger scales. Indeed the GRSU is presently actively pursuing the potential planning applications of these data with several local and regional agencies including: the Central California Coastal Commission, State of California Department of Water Resources, Fresno Office, Kern County Water Agency and the Santa Barbara County Planning Department, among others.

In short, the ERTS-1 satellite data provides an excellent mapping base for regional resource inventories utilizing generalized classification systems. In order to achieve high interpretation accuracy, the mapping should be performed by interpreters who are well acquainted with the landscape features and their geographic distribution. The major opportunities for the operational use of ERTS-1 type imagery seem to be in generating more specific, timely and accurate data such as the total acreage of irrigated agricultural land, rates and magnitude of land use change, the monitoring of kelp resources, the inventory of acreages of important agricultural crops or studies of similar critical environmental parameters which provide input for important resource management decisions.

Appendix A. Original Classification Schemes for Land Use, Land Forms, Hydrology and Natural Vegetation

Key:

General Category ex. A [Agriculture]
Type within Category ex t [tree crops]
Specific Type ex c [citrus]
Total Code: Atc

Note that the more specific notation depends upon ability to identify
and additional types and specific types can be added to the system as
they are encountered.

	CODE
Agriculture	A
Crops	Ac
Grain Crops	Acg [type]
Horticulture	Ach [type]
Row Crops	Acr [type]
Tree Crops	Act [type]
Livestock	Al
Stock farming [beef]	Alsb
Stock farming [sheep]	Alss
Stock Farming [dairy]	Alsd
Rangeland	Ar
Pasture [improved]	Arpi
Pasture [unimproved]	Arpu
Extractive	E
Seawater mineral recovery	Es [type]
Petroleum production fields	Ep [type]
Mining Operations	Em [type]
Public Facilities	G
Governmental, administrative	Ga [type]
Governmental, military	Gm [type]
Cemeteries	Gc
Protection, Police and Fire	Gf [type]
Hospitals	Gh
Prisons	Gp
Waste disposal [solid & liquid]	Gd [type]
Education	Ge [type]
Parks & Recreation	P
Campground	Pc
Golf Course	Pg
Park	Pp
Stadium	Ps
Marinas	Pm
Resort	Pr

Appendix A cont'd.

	CODE
Industrial	I
Primary Conversion	Ip
Steel mill	Ips
Ship building	Ipb
Saw mills [or pulp]	Ipw
Assembly	Ia
Auto	Iaa
Electronic	Iae
Food Processing	If
Canneries, fish	Ifc
Canneries, fruit	Iff
Storage	Is
Port warehousing	Isp
Rail warehousing	Isr
Transportation	T
Airports	Ta [type]
Highways	Th [type]
Railroads & Yards	Tr [type]
Canals	Tc [type]
Docks	Td
Commercial	C
Clustered	Cc [type]
Strip	Cs [type]
Residential	R
Single family	Rs
Multi-family	Rm [type]
Non-developed	N
Natural Vegetation	Nv [type]
Idle Land	Ni [type]
Barren Land	Nb [type]
Water Bodies	Nw [type]

LANDFORM CLASSIFICATION

- I. Fluvial
 - A. River and stream valley
 - 1. meander
 - 2. oxbow lake
 - 3. meander scar
 - 4. terrance
 - 5. channel bar
 - 6. point bar
 - 7. delta bar
 - 8. channel filling
 - 9. natural levee
 - 10. crevasses
 - 11. distributaries, passes, or mouths
 - B. Deltas
 - 1. esturine
 - 2. arcuate
 - 3. digitate [birdsfoot]
 - C. Other
 - 1. alluvial fan
 - 2. alluvial cone
 - 3. bajada
 - 4. playa
 - 5. alkali flat
 - 6. salinas
 - 7. washes [wadis]
- II. Glacial
 - A. Alpine
 - 1. cirque
 - 2. tarn
 - 3. trough valley
 - 4. hanging valley
 - 5. steps
 - 6. pater noster lakes
 - 7. aretes
 - 8. moraine
 - 9. esker
 - 10. kame
 - 11. kame terrace
 - 12. fjords
 - 13. fiards
 - 14. ice
 - B. Continent
 - 1. mamillated
 - 2. till plain
 - 3. drumlin
 - 4. kettle
 - 5. kame

LANDFORM CLASSIFICATION [page 2]

- 6. kame terraces
 - 7. esker
 - 8. moraine
 - 9. ice
- III. Eolian
 - A. Dunes
 - 1. sand shadows
 - 2. barchan or crescent
 - 3. longitudinal or seif
 - B. Sand sheets
 - C. Whole backs
 - D. Deflation basins
 - E. caves or arches
- IV. Waves and Currents
 - A. Terraces
 - B. Tidal zone
 - 1. beach
 - 2. bays
 - 3. inlet
 - 4. sea arch
 - 5. stack
 - 6. bar
 - 7. spit
 - 8. forwland
 - C. Offshore zone
 - 1. tombolo
 - 2. stack
 - 3. bar
 - 4. spit
 - 5. foreland
 - 6. island
- V. Volcanic
 - A. Cones
 - 1. strata or composite
 - 2. shield
 - 3. cinder
 - 4. spatter
 - B. Depressions
 - 1. craters
 - 2. calderas
 - C. Lava fields or plains
 - 1. tumuli
 - 2. squeeze-ups
 - 3. pressure ridges
 - 4. lava blisters
 - D. Skeletons
 - 1. neck
 - 2. plug
 - 3. dike
 - 4. sill

LANDFORM CLASSIFICATION [page 3]

VI. Complex and Compound

- A. Mountain
- B. Hill
 - 1. monadnock
 - 2. inselberg
 - 3. other
- C. Ridge
 - 1. cuesta
 - 2. hogback
 - 3. homoclinal
 - 4. other
- D. Plain
 - 1. lacustrine
 - 2. outwash
 - 3. other
- E. Water body
 - 1. lake
 - 2. lagoon
 - 3. estuary
 - 4. tidal marsh
 - 5. tidal flat
 - 6. other

VII. Other

- A. Karst
 - 1. sinkhole
 - 2. uvala
 - 3. karst plain
 - 4. bland valley
 - 5. karst valley
 - 6. rise pits
 - 7. hums
- B. Atolla and reefs
- C. Meteorite craters
- D. Carolina bays
- E. Man made forms
- F. Other

C-6

HYDROLOGIC CLASSIFICATION

- I. Streams
 - A. 1st Order
 - B. 2nd Order
 - C. 3rd Order
 - D. 4th Order
 - E. 5th Order
 - F. 6th Order
- II. Lakes
 - A. Permanent
 - 1. Freshwater
 - 2. Saline
 - B. Ephemeral
 - 1. Freshwater
 - 2. Saline
- III. Springs
- IV. Estuaries
- V. Marshes
- VI. Swamps
- VII. Man Induced Changes in Hydrology
 - A. Reservoirs
 - B. Canals
 - C. Wells
 - D. Other

NOTE: Drainage basins would be delimited on the same map, but would not be classified.

NATURAL VEGETATION CLASSIFICATION SCHEME

<u>Plant Community</u>	<u>Code</u>
I. Aquatic	
A. Marine (Aquatic)	M
1. Nearshore (Kelp and seaweed)	Mn
2. Intertidal	Mi
B. Freshwater (Aquatic)	Fw
C. Marsh	Ma
1. Salt Marsh	Ma (sm)
2. Freshwater Marsh	Ma (fm)
II. Terrestrial	
A. Barren	Ba
B. Strand	Sr
C. Grassland	G
1. Coastal Prairie	Gcp
2. Valley Grassland	Gvg
3. Meadows	Gme
D. Woodland-Savanna	Ws
E. Scrub	S
1. North Coast Shrub	Snc
2. Coastal Sagebrush (soft chaparral)	Scs
3. Cut-over Forest	Scf
4. Chaparral (hard chaparral)	Sc
5. Scrub-Hardwood	Shw
6. Desert Scrub	Sd
a. Mesquite	
b. Sagebrush	
c. Saltbush	
F. Forest	F
1. Hardwood	Fhw
2. Mixed Evergreen	Fme
3. Coniferous	Co
a. Redwood	Co (rw)
b. North Coast	Co (nc)
c. Douglas Fir	Co (df)
d. Pine	Co (pc)
G. Riparian	R
H. Agriculture	A

Appendix B. Revised operational land use and vegetation classification schemes which were used for the preparation of regional data base maps from ERTS-1 imagery.

KEY:

General Category, ex A (Agriculture)
 Type within Category, ex. c (crops)
 Specific Type, ex. g (grain)
 Total Code: Acg

<u>General Category</u>	<u>Code</u>	<u>Comments</u>
AGRICULTURE	A	
Field Crops	Ac (type)	may include row type (r); grain type (g); and tree/orchard (t). Additional sub-types could be added.
Range Areas	Ar (type)	grassland differentiated from surrounding vegetation and often showing signs of fencing (square borders). May include improved (i) or unimproved (u).
EXTRACTIVE	E	
Mining Operations	Em (type)	may include open pit (o), etc. and additional sub-types.
Petroleum Production Fields	Ep	usually identified by maze of crossing access roads
PUBLIC FACILITIES	G	
Governmental, military	Gm (type)	may include air bases (ta), army installations (indicated by Fort ____), etc.
PARKS AND RECREATION	P	
Golf Course	Pg	readily identifiable on MSS band 7 if of eighteen hole variety
Marinas	Pm	identifiable due to geometrical signature along coastlines
INDUSTRIAL	I	
Port Facilities	Ip	As Pm but larger
TRANSPORTATION	T	
Airports	Ta	signature depends on locational content to other features and runway material.
Highways (roads, etc.)	Th*	*roads are normally mapped using their federal, state or county number (i.e., 101 rather than the code).
Railroads	Tr*	*railroads are usually mapped using the abbreviations for their operating company (i.e., S.P.R.R.-Southern Pacific Railroad Company).

Appendix B cont.

<u>General Category</u>	<u>Code</u>	<u>Comments</u>
Canals	Tc*	*canals are normally identified by name (i.e., California Aqueduct).
URBAN	U*	*urban areas, undifferentiated between commercial. Residential are normally identified by the city name (i.e., OJAI) in bold type and their extent shaded in.
NON-DEVELOPED	N	
Barren Land	Nb	includes extensive sand or bare rock areas
Idle Land	Ni	land within or bordering agricultural or urban areas which has been cleared but not used for commercial purposes.
Natural Vegetation	Nv	see natural vegetation data key and map for specific vegetation associations.
Water Bodies	Nw* (type)	*normally indicated by lake (l), river (r), or ocean (o) name on map.

VEGETATION CLASSIFICATION USED FOR
VEGETATION DATA BASE MAPPING OF THE CENTRAL REGION TEST SITE

1. Barren
2. Strand
3. Marsh
4. Grassland
5. Soft Chaparral
6. Hard Chaparral
7. Scrub
8. Scrub Grassland
9. Scrub Hardwood
10. Woodland Savanna
11. Hardwood Forest
12. Coniferous
13. Desert Scrub
14. Riparian
15. Agriculture
16. Urban
17. Waterbodies

EVALUATION OF ERTS-1 IMAGERY FOR LAND USE/RESOURCE INVENTORY INFORMATION

Ernest E. Hardy, *Senior Research Associate*; James E. Skaley, *Project Coordinator* and Elmer S. Phillips, *Photography Consultant*, (New York State College of Agriculture and Life Sciences, Cornell University, Ithaca, New York)

ABSTRACT

The objective of this investigation was to develop a low cost, manual technique for enhancing ERTS-1 imagery and preparing it in suitable format for use by users with wide and varied interests related to land use and natural resources information. The goals of the project were: to develop enhancement techniques based on concepts and practices extant in photographic sciences, to provide a means of allowing productive interpretation of the imagery by manual means, to produce a product at low cost, to provide a product that would have wide applications, and one compatible with existing information systems.

Through the use of photography techniques, standardization of the 70mm film chip received from NASA is achieved. A subtractive color process is employed to produce step enlargements of the 1:3,300,000 images to scales up to 1:66,000. Diazo transparencies are then produced in magenta, cyan, and yellow for each of the four MSS bands.

Data retrieval can be achieved from any of many thousands of diazo color combinations. Each color diazo combination can provide a unique kind of information. Direct map transfer is readily accomplished at the scale of 1:250,000 and larger. Enlargement to much larger scales (1:50,000 to as large as 1:10,000) is feasible with quality overhead projectors.

Cost of preparation of the photographically enhanced, enlarged negatives and positives and the diazo materials is about 1¢ per square mile. Cost of creating and mapping a land use classification of twelve use types at a scale of 1:250,000 is only \$1 per square mile. The product is understood by users, is economical, and is compatible with existing information systems. Hard copy mylar maps for reproduction are produced, from which information for computer manipulation is prepared. Many user applications of this system are already in use.

1 N 74 30739

This is a report on the progress and some of the results of research carried out in relation to NASA Investigation No. 358, Evaluation of ERTS-A Imagery for Land Use/Resource Inventory Information. The research has been conducted by the New York State College of Agriculture and Life Sciences, by the Department of Natural Resources at Cornell University. A full-time professional research staff of five people assisted by consultants in photography and computer sciences has been responsible for the research work of this project.

Among the goals of the project were the development of photographically enhanced imagery at a low cost, suitable for use in manual interpretation of ERTS-A imagery. If produced in a format compatible with existing land use classification and computer graphic systems, this would provide an opportunity to develop a very wide range of applications.

In our approach to meeting the goals of the project, it was understood that photo enhancement was not satisfied by simply enlarging the imagery from the basic material as received from NASA. It was recognized early in the research program that photographic techniques, when carefully applied to both the positive and negative 70mm film chips, offered an opportunity to enhance the imagery to a very high degree. Enhancement at this stage of the work then lead to the development of processes that:

1. allow for extreme enlargement of scale while still maintaining suitable quality
2. provides an opportunity to produce a great array of color combinations
3. provides for color isolation of any particular form of resource information or land use

By obtaining large-scale images from the photographically enhanced images, at low cost, suitable means of manual interpretation of the data have been developed.

Experience has shown that the more sophisticated the method of processing resource information, the smaller is the number of potential users of that information. Most local officials who make the majority of the resource management decisions do not feel at ease with, or trust, information prepared in a manner they themselves cannot accomplish or duplicate. Therefore, the use of low cost, manual interpretation techniques, based on "hard copy" imagery, is proving to be the key to our widening range of applications.

In all stages of the research on this project, care has been taken to insure compatibility with present land use classification, referencing, and retrieval systems currently in use, especially the New York State Land Use and Natural Resource Inventory (LUNR).

Our approach was to use the LUNR information for our basic ground truth. Additional field checking was done to verify the degree of accuracy of LUNR data in specific areas and to record the rate of land use change in selected study areas. Staff members had previous experience as LUNR research technicians and this phase of the work was rapidly completed.

We then developed the photo enhancement techniques that have been the major factor in developing satisfactory techniques for the application of ERTS-A imagery to resource and land use classification and inventory.

New classification systems were developed, based on the capability of the photographically enhanced ERTS-A imagery. Suitable conversions of the LUNR classification were made, to enable comparisons between the two systems of data acquisition. Data from both sources were related to standardized map bases, and evaluation of accuracy levels were undertaken.

High correlations were obtained for classification systems developed for 8 to 12 land use categories. Many of our tests indicated over 90% correlation, but we consider 85% a more typical figure.

The high correlation figures encouraged us to consider other applications for use of ERTS-A imagery. Many have been tried successfully.

Within the photographic process, a number of steps and procedures should be mentioned. From the photographer's viewpoint, the imagery, as received from NASA, is out of balance. For accurate color reproduction, the density ranges should approximate one another. We realized that if we could use photographic processes to approximate false color reproduction, it would be feasible through the use of subtractive color theory to assign combinations of colors and bands, negative or positive, for clear demarcation in any desired color of any specific object.

Through experimentation, proper films, filters, and process techniques have been determined to provide images of more nearly balanced density. Through step enlargement procedures, the images may be enlarged from the 1:3,300,000 70mm chip up to 1:1,000,000 and then up to ratios of 1:150,000 or larger.

Carefully prepared, and by following prescribed calculations, positive transparencies from the negatives can be produced. These are then run through the diazo process, where any of the desired wavelengths may be produced in cyan, magenta, or yellow. To continue the original test to produce false color, band 4 was printed yellow, band 5 magenta, and band 7 cyan. When superimposed, they produced a high quality false color image.

As a further test of this process, the false color images were enlarged to scales as large as 1:66,000 and there was still suitable information for land use classification.

The photographic steps have shown that by using subtractive color theories to produce the desired false color, an extremely wide range of color combinations is possible. Although work needs to be continued on development of a prediction model of the possible combinations of color, and what they relate to, we have been able to identify any desired land

use information by isolating it in a color of unique contrast with its surrounding areas.

The number of possible color combinations from any one frame of imagery is greater than 20,000. When imagery from two time periods is used, the number of possible combinations increases exponentially.

The diazo process enables us to use manual manipulation of spectral bands and hues to elevate the contrast level of any spectral category of interest. Then, by color coding desired density levels to approximate a desired classification unit, interpretation and geographic referencing of like spectral zones is a satisfactory way of applying the satellite imagery to a resource classification system.

We have not yet found major difficulties in geographic referencing. The imagery, as prepared, has high resolution capability, and boundaries between contrasting colors and hues are sharp. There is ample opportunity to use this imagery for direct transfer of data at ratios of 1:250,000 or 1:150,000 or even larger. Projection techniques and inexpensive equipment are readily available to provide excellent results at scales of 1:24,000 and larger.

Data takeoff techniques have proven satisfactory when relatively straightforward Guidelines are followed. They are:

1. Prepare a base map at the desired scale with a few geographic references such as lakes or streams.
2. Trace regions of like hue identified as a homogeneous spectral category onto the overlay.
3. Construct a spectral map from different composites to fill in the desired information for the mapped area.
4. Relate areas to UTM coordinates and record on appropriate forms for computer storage and retrieval.

The results of this approach can be, and have been, verified by comparison with low-altitude photographs, existing geographically referenced land or resource surveys (LUNR), or by field checking. Results to date have shown a high degree of correlation, usually close to or over 90%.

The final hard copy map output from this process may be at practically any desired scale. Direct transfer may be made at ratios of 1:250,000 and 1:125,000 with map units of about 25 hectares and 10 hectares, respectively. When projected imagery is used, it is quite routine to go to scales of 1:12,000 with minimum map units of two hectares or less.

There is a major opportunity to make satellite imagery available and useful to large numbers of people through this processing approach. We have found it very productive as a source of data for such uses as:

1. updating previous inventories
2. analysis of seasonal change
3. compilation of new maps, such as forestry, drainage, agriculture
4. isolation of one specific land type or land use
5. generation of new kinds of data, such as sequential snow cover maps

Many other applications have been requested and are currently being tested. The apparent advantages of this process are found in:

1. low costs - as low as \$1 per square mile for up to 12 classification units
2. that it does not require sophisticated or expensive hardware at any step of the process
3. that it limits subjective interpretation so it can be readily taught to non-technical users
4. the extremely wide range of color selections allowing adaptation for great numbers of applications
5. high accuracy levels achieved
6. letting the user select the scale of his choice for any application
7. the material being readily understood
8. the whole process able to be carried out anywhere in the world with equipment costs of \$10,000 or less
9. that it is, or can be, compatible with existing resource information systems

Current applications include use by planning agencies, a number of state agencies, and by university faculty and students for research projects.

The potential for the future appears very great, with the inherent capabilities of the satellite system offering information that was previously unavailable. With the development of a suitable color prediction model, we can predict continuous rewards. Our current efforts at broadening the applications of ERTS-acquired imagery have been directed toward introducing the process to the local administrators of the state. To this end, the assistance of the Cooperative Extension Service has been obtained, and the development of a service organization, capable of introducing the use of ERTS imagery to anyone desiring to use it, is now underway.

.

.

IMPACT OF ERTS-1 IMAGES ON MANAGEMENT OF NEW JERSEY'S COASTAL ZONE

Edward B. Feinberg, Roland S. Yunghans, JoAnn Stitt (*New Jersey Department of Environmental Protection, Trenton, N.J.*) and Robert L. Mairs (*Earth Satellite Corporation, Washington, D.C.*)

ABSTRACT

The thrust of New Jersey's ERTS investigation is development of procedures for operational use of ERTS-1 data by the Department of Environmental Protection (DEP) in the management of the State's coastal zone. Four major areas of concern were investigated: detection of land use changes in the coastal zone; monitoring of offshore waste disposal; siting of ocean outfalls; and allocation of funds for shore protection.

ERTS imagery was not useful for shore protection purposes; it was of limited practical value in the evaluation of offshore waste disposal and ocean outfall siting. However, ERTS imagery shows great promise for operational detection of land use changes in the coastal zone. Some constraints for practical change detection have been identified.

INTRODUCTION

The New Jersey Department of Environmental Protection (DEP) is a regulatory agency charged by law with protecting and enhancing the State's total environment. The Department is oriented toward implementing and enforcing environmental statutes. While DEP is not a research organization, we do pursue mission oriented research when that research offers good prospects for successful application to practical problems. Remote sensing research has played and will continue to play an important role in DEP programs. Our wetlands and coastal zone statutes could not have been implemented without remote sensing tools.

New Jersey's ERTS-1 investigation, which is being conducted in conjunction with Earth Satellite Corporation, is aimed at developing procedures for operational use of ERTS data by DEP

PRECEDING PAGE BLANK NOT FILMED

1 N 74 30740

in managing the State's coastal zone. Four significant problem areas have been identified as potentially benefiting from information derived from ERTS data:

1. Monitoring of offshore waste disposal;
2. Siting of ocean outfalls for regional sewage treatment plants;
3. Allocation of funds for shore protection;
4. Detection of land use changes in the coastal zone.

OFFSHORE WASTE DISPOSAL

The offshore waste disposal problem is important because of proximity to New Jersey's coastline of two major Federally regulated marine waste disposal sites--one off Sandy Hook near the New York Bight and the other off Cape May near Delaware Bay. DEP is concerned with the effects this waste disposal will have on future recreational use of waters and beaches, fish resources, and public health.

The Federal Environmental Protection Agency has designated five dumping areas within the New York Bight site for the disposal of the following waste materials: industrial acid, sewage sludge, dredge spoil, construction debris and wrecks. ERTS imagery primarily records acid and dredge spoil. We are monitoring the dumping with each ERTS overpass to determine geographical extent and generalized dispersion characteristics. These analyses are helping the Department to better understand the extent of the problem; they will also help to support a case with EPA for possible alternate disposal sites, if the data demonstrate this need. However, the long delay in receiving ERTS imagery has caused it to be useless in helping to monitor impacts of individual dumpings, even for the limited use of guiding water quality sampling by DEP inspectors.

OCEAN OUTFALLS

The Department presently is engaged in a long term program of converting New Jersey sewage waste disposal from hundreds of local, often improperly operated, primary and secondary treatment plants to a small number of regional secondary treatment plants with long ocean outfalls. While ocean discharge of sewage effluent is not the ideal solution to the problem, it poses much less hazard to the environment than

the alternatives available to New Jersey, e.g., discharging into ground water and estuarine areas, which have been traditional recipients of these wastes.

A review of the outfall design criteria found in engineering reports indicates that little or no systematic use has been made of nearshore circulation of surface dispersion information derived from remote sensing techniques. Furthermore, effectiveness of ocean outfall systems rarely has been confirmed after construction. Using ERTS data, repetitive black and white aircraft photography dating back to 1940, and other historical data, we have developed tidal and wind driven surface current information for direct input into the design of New Jersey's sixteen proposed ocean outfalls. These data have been received enthusiastically by the sewage authorities and their environmental consultants, but it is still too early to tell if, of themselves, the data will be definitive.

The Department must determine if outfall design specifications are being met and must insure that effluents have a minimal impact on nearshore waters and beaches. Federally imposed standards also must be attained. These determinations can best be made with aircraft photography and collateral ground truth data. We are planning to verify the models from which most outfalls presently are designed by injecting dye at the treatment plant, photographing the outfall site, contouring areas of equal density on the photography and relating in situ measurements of dye concentration to film density. In this way, we hope to confirm the initial dilution ratio of the outfall from the sea bottom to the ocean surface.

ERTS still may be of benefit in these analyses. The capacities of the proposed outfalls are much greater than all but one outfall now in operation, and this outfall presently is operating far below design capacity. We intend to conduct a dye study at this outfall (when it begins operating at capacity) in conjunction with an ERTS overpass. To date ERTS imagery of dye studies has not provided useful information, however, the larger outfalls may be detectable with ERTS. If this proves to be the case, repetitive coverage will be of great value in demonstrating the effectiveness (or lack of effectiveness) of the outfall design.

SHORE PROTECTION

New Jersey (through DEP) annually spends several million dollars of State funds for construction and maintenance of shore protection structures. These expenditures are in the

form of matching grants to local municipalities (on a seventy five percent State--twenty five percent local basis) and represent only ten percent of the total requests for aid.

New Jersey is probably one of the best (or worst) examples of beach preservation structures in the United States. The Atlantic shoreline consists of groin upon groin all the way down the coast. Over the years, the State has been building and repairing these structures and/or replenishing the sand-eroded areas without a clear understanding of the effectiveness of these measures. Only recently, the United States Park Service decided to abandon completely shore protection measures on their lands and let the beaches return to a natural condition.

ERTS proved to have insufficient resolution to address this problem, both directly in measuring beach erosion rates and indirectly in measuring nearshore currents. Perhaps, with an increase in resolution to tens of feet or even feet, repetitive ERTS coverage will be valuable in monitoring impacts and effectiveness of shore protection structures, but the imagery from ERTS-1 is not useful for this purpose.

COASTAL ZONE LAND USE

The New Jersey Wetlands Act, which took effect in November, 1970, requires that the Department map the wetlands and regulate their use. Approximately 938 maps are being prepared, over 500 of which have already been completed, at a scale of 1:2400. These maps show the upper wetlands boundary and an inventory of wetlands vegetation down to five acre units, for approximately 450 square miles of wetlands. In preparing these maps, stereo aerial photography was taken, in both natural color and color infrared, for over 1300 square miles of New Jersey's coastal area. This photography is at a scale of 1:12000.

The New Jersey Coastal Area Facility Review Act took effect in September, 1973. This Act regulates use of lands adjacent to the wetlands and extends DEP responsibility to approximately 1750 square miles. The Coastal Area Act defined the boundaries of the area in terms of roads and railroads and listed the facilities to be regulated. The Act also required that the DEP prepare an environmental inventory for the coastal area. Since the Act contained a grandfather clause for facilities already under construction on the effective date, the Department obtained stereo color infrared aerial photography on that date throughout the coastal area for legal documentation. This photography, at a scale of 1:35000, also will be used to help prepare the environmental inventory.

DEP, by virtue of these two statutes, has the authority to control major development within the coastal area of New Jersey. This area constitutes approximately twenty-five percent of the State. Enforcement of these laws must deal with two basic situations:

1. Monitoring authorized development projects to ensure compliance with permit conditions.
2. Detecting clandestine or unauthorized major land use modifications.

In the past, the Department has approached the enforcement problem by using ground inspectors, supplemented by occasional observations from light aircraft and helicopters. Hand held photography was obtained frequently for legal evidence, both on the ground and in the air. This approach was satisfactory when the areas over which DEP had enforcement powers were more limited; however, it is far too costly and slow a method to adequately cover twenty-five percent of the State.

The wetlands and coastal area photography, referred to previously, have demonstrated clearly the value of systematic aerial photography in monitoring the coastal area. These photographs are scanned to detect land use changes and to direct a limited number of inspectors to the precise locations of changes. This leads to far more effective

utilization of the inspectors' time. Simultaneously, the photographs provide a legal record of changes. Periodic aerial photographic coverage (three to four times a year) would provide cost effective surveillance, but there would be several months interval between observations. With modern construction equipment, extreme destruction of land can occur rapidly. More frequent observations are needed, but the cost for frequent aerial coverage of the entire coastal area would be prohibitive. For this reason, the Department has turned to ERTS as a potential surveillance tool for detecting land use changes.

Comparisons of ERTS images for the period 10 October 72 through 7 July 73 have detected two hundred seventy-six changes. These changes are plotted on 1:24000 scale photomaps, which are used to guide field inspectors. We have successfully detected changes as small as two to three acres. At present we are refining our interpretation techniques to distinguish developmental changes from agricultural and seasonal changes.

DISCUSSION

For the first three problem areas -- offshore waste disposal, ocean outfalls and shore protection -- we have concluded that repetitive high-altitude aerial photography provides for more useful information than does ERTS. The resolution of ERTS-1 is insufficient for addressing these problems. An increase in resolution to tens of feet or feet may provide the needed information.

We believe that repetitive ERTS coverage has great potential value to the State for the fourth problem area -- operational detection of land use changes in the coastal area. A responsive change detection system initially would be used to enforce our coastal zone and wetlands statutes. Specifically, it would guide on-ground inspections, help us plan intelligently for local aircraft surveillance, and establish legal records for court use. All of these promote efficiency in management of our coastal zone and are cost effective in terms of time and personnel.

To realize this potential in change detection, certain limitations of the present ERTS system must be overcome:

1. Change detection must be automated (digital tapes should be used for analysis in conjunction with imagery);
2. Approximately one acre resolution must be achieved;

3. The repetitive coverage interval of 18 days should be reduced (this is highly desirable but not limiting);
4. Thirty to sixty day imagery delivery times from NASA for standing orders are shortened substantially (to four to seven days);
5. Requests for additional data are met in a timely fashion (rather than six months or longer as at present).

The Department is prepared to initiate an operational test of change detection utilizing ERTS-1 imagery. This test requires rapid delivery of imagery by NASA. We will analyze the imagery rapidly and immediately provide the information to DEP inspectors. Timeliness of the information is most important in motivating our inspectors to use it. With timely information, our inspectors can halt unauthorized land use changes before great environmental damage has occurred. Stale information is of historical interest only, and will have no meaningful impact on operational management of our coastal zone. To conduct this test, we have requested that imagery be made available within five working days after each ERTS overpass, for five consecutive overpasses. The number of overpasses requested will allow for possible cloud cover. This test, using visual interpretive techniques, will provide detailed data on the effectiveness of ERTS in operational change detection.

DEP also will propose to NASA an extension of our ERTS investigation to improve the timeliness and accuracy of our change detection capability by shifting to automatic data processing of ERTS digital tapes. We hope that NASA will act favorably on this proposal. It represents a major step toward a fully operational change detection system.

RECOMMENDATIONS

In dealing with the real world problems of a regulatory agency, our work indicates that ERTS data coupled with repetitive aircraft coverage will be most productive and cost effective. We recommend that NASA take into account these kinds of needs and fund either in whole or in part worthwhile aircraft and ERTS supporting programs that are aimed at specific operational problems of state and local governmental agencies. The success of our ERTS investigation in addressing these real world problems has convinced the State of New Jersey to include in its next budget fifty thousand dollars to participate in the kinds of activities mentioned above.

We appreciate the opportunity to participate in the ERTS program with NASA.

CARETS—AN EXPERIMENTAL REGIONAL INFORMATION SYSTEM USING ERTS DATA

Robert H. Alexander, *U.S. Geological Survey, Geographic Applications Program, Reston, Virginia 22092*

ABSTRACT

The U. S. Geological Survey CARETS (Central Atlantic Regional Ecological Test Site)/ERTS investigation is testing the applicability of ERTS data as input to an environmental information system for a multi-state mid-Atlantic region surrounding the Chesapeake and Delaware Bays. The "information system" framework encompasses a flow of information through several stages from sensor to user, and involving evaluation and feedback from several potential users. Basic assumptions of the CARETS project model are that there is a measurable environmental impact associated with land use and land use change as determined with remote sensor data, and that the ERTS-derived land use data sets, when properly calibrated, may thus provide regional planners and administrators with a shortcut to an understanding of the environmental changes that are going on in their regions. Mid-way through the investigation, data sets on land use from both aircraft and ERTS sources have been compiled for the 73,000 km² area of the test region. These data sets are being prepared for user evaluation in both graphic and digital form, and a variety of area measurement and accuracy computations are being performed to assist in evaluating the ERTS and aircraft data as aids in the planning process.

N74 30741

INTRODUCTION

This paper is a brief description and progress report of the Central Atlantic Regional Ecological Test Site (CARETS) demonstration project, an interdisciplinary, interagency cooperative investigation in which data from the Earth Resources Technology Satellite (ERTS-1) are being tested as input to an experimental regional environmental information system.

The project arose through a process of negotiation, beginning in 1970, among several scientists and administrators in both the National Aeronautics and Space Administration (NASA) and the U. S. Geological Survey, who had felt that something was lacking in the pattern of widely-scattered, single discipline experiments which existed at that time in NASA's program of research on remote sensing for earth resources applications.

Publication authorized by the Director, U. S. Geological Survey

It was felt that the detailed experimentation with the matching of sensor records and known ground conditions at single, well-documented test sites, while necessary for establishing the feasibility of applying the space observations to earth resources problems, was not sufficient. What was needed in addition, it was determined, was the regional integration of the results of a number of experiments, with emphasis on reaching the user with data meaningful to him in terms of solving his problems. To address the need for interdisciplinary and regionally-integrated research packages, NASA developed the concept of "ecological test sites", and established a number of them throughout the U. S. In addition to economizing on the use of aircraft test flights by concentrating on fewer regions, the ecological test site concept was supposed to take advantage of the actual interaction of the various environmental phenomena which could be observed by the remote sensors. There was even some talk that ecological models might be developed which would take advantage of the availability of remotely-sensed observations of the earth's surface in unprecedented amounts, and hasten the solution of environmental problems that are characterized by complex interconnections among the phenomena involved. Thus the CARETS project was established as one of the NASA-sponsored ecological test sites.

Project Design and Structure

CARETS is a project of some complexity, addressing environmental problems in a heavily-urbanized mid-Atlantic area of some 73,000 km² (28,000 mi²). Since there are a number of interdisciplinary environmental problem-solving projects or programs throughout the country at the present time, some of them statewide in scope and operated by agencies of state government, some attention will be given to an explanation of the CARETS project design and structure, so that the reader can compare it with other efforts with which he may be familiar.

The size of the test region would place it in rank between the 40th (South Carolina) and the 41st (West Virginia) of the 50 states arranged in order of total area. Only two states, however, (California and New York) have larger numbers of people than the 13,404,558 living within the confines of the CARETS area in 1970. The demonstration project is thus expected to be comparable in level of effort to that required for a similar land use information system in a typical heavily-urbanized and populous state.

The project was designed with the aim of bringing space technology and information systems technology together to assist in solving environmental problems. Its situation in the Geological Survey allows application of that agency's long-standing expertise in earth sciences and mapping, and in addition permits taking advantage of a recent USGS thrust aimed at integrating the contributions of many discipline specialists to bring the earth sciences specialties more quickly to bear on the solution of pressing environmental problems centering on the land use issue.

The basic project design takes advantage of the two-way linkage between land use and the processes and responses of the biophysical environment. According to this linkage, land use (incorporating land cover in the USGS land use classification for use with remote sensors--Anderson et al., 1972) evolves under constraints set by processes of the physical environment, with socio-economic processes determining the particulars of how a given land use pattern develops within the environmental limits; certain environmental factors, on the other hand, are functions of land use and land use change, as for example runoff, sediment yield, micro-and meso-climates, water quality, atmospheric dust, etc. Reliable and timely data on regional hydrology, geology, micro-climatology, water quality, etc., are expensive and often slow to obtain over large regions in forms suitable for analysis of environmental impact. The surface expression or resultant of all the environmental and socio-economic processes, however, can be readily observed and monitored with the aid of remote sensors carried in satellites or aircraft; that surface expression is what is here called "land use."

If the land use that is monitored and mapped can be properly "calibrated" in terms of its probable environmental impact, then a land use data base can be a powerful tool of inference concerning, for example, environmental quality--not replacing direct measurement of critical environmental parameters, but rather providing a basis for extrapolating those measurements region-wide for more rapid determination of environmental impact of new development--hopefully in time to assist in the critical decisions as to how and where that development should occur.

Further detail on project structure and integration of the various elements of the CARETS project can be gained by reference to the flow chart depicted in Figure 1. The top portion of the diagram illustrates the flow of activities involved in the preparation and checking of the land use data base, and the comparison and evaluation of ERTS and aircraft data sets on land use. The lower portion of the diagram illustrates the flow of environmental and socio-economic data largely from non-remote sensing sources. The shaded portion of each box in Figure 1 indicates the portion completed at the time of the mid-project review in October 1973.

The color infrared photography obtained by the NASA high-altitude aircraft flights over the test region in 1970 was used to provide the mapping base, a controlled photomosaic at a scale of 1:100,000 for the entire test region, except for a few border areas that were missed and were added with data from 1972 flights. The aircraft land use data base has been completed in map form for the entire region. ERTS data have been used to compile a land use data set at a scale of 1:250,000, using the aircraft-derived data only as a training set to aid in identifying land use classes by a manual (visual) photo-interpretation technique.

Land use change over a two to three year period is determined by comparison of the 1970 data base with more recent photography obtained from NASA aircraft flights. A similar procedure will be performed with ERTS data for 1973-1974. An important component of the project is the determination of accuracy figures for the land use data, first by establishing accuracy levels for the aircraft-derived data, using field checks where necessary, and then applying the measures to the ERTS-derived data sets using spatial sampling techniques.

The CARETS investigation is also making available other data sets to aid in regional environmental analysis. An entirely new geologic map is being compiled for the region, at a scale of 1:100,000, emphasizing surficial materials, slope, and engineering characteristics of the terrain; it will be used in conjunction with the land use data to aid users in estimating geological suitability of the yet-undeveloped areas. Selected hydrological data on runoff and sediment yield are being compared with land use in small drainage basins to illustrate the calibration of land use data in terms of hydrological impact. Air quality and micro-climatological impact of land use patterns are also being investigated for portions of the test region. Overlay maps of census tracts have been prepared to the same format as the land use data base, so that land use-population relationships can be determined.

The various types of data will be overlaid and merged as indicated by the arrows in the diagram, and a demonstration will be made of how these processes can aid in regional analysis and planning assessment of the test region or portions thereof. Finally, the whole package, including the remote sensing data, the processed maps and graphics, the statistical summaries, and the analytical reports, will be presented to users in the test region, to solicit their evaluation in terms of their data needs and particularly in support of decisions they have to make about future land use in their regions. The dashed line in Figure 1, illustrating "feedback to data sources" is used to indicate a process that it is hoped will continue after the CARETS investigation is completed; that is, once the results of this and other possible approaches to improving environmental decisions are evaluated, it is hoped that the data producers indicated at the left side of the diagram will respond with whatever programs may be necessary to fulfill the federal responsibilities in assistance to states and localities in the solution of environmental problems associated with land use change.

The objectives, then, of the CARETS project may be summarized as follows:

Overall objective: to test the applicability of data from ERTS as input to a regional environmental information system for the CARETS region. The "information system" referred to encompasses a flow of data from sensor to user, incorporating a specific process of land use analysis in intermediate stages of this information flow.

Sub-objectives:

- a. Land use analysis: to provide uniform quantitative data sets (maps and statistical summaries) on land use and land use change, from ERTS and aircraft data, summed by counties and other planning jurisdictional areas for the entire region; make quantitative comparisons of ERTS and aircraft data sets.
- b. Environmental impact assessment: to perform sample interpretations and analyses of remote-sensor-derived land use data sets in terms of the environmental impact of land use patterns and land use changes.
- c. User services: to provide for experimental use, evaluation, and critique of land use information products derived from this investigation; the use, evaluation, and critique to be obtained from representative user institutions with responsibilities for planning and managing future land uses.

Elements of the CARETS Geographic Information System

The CARETS project structure is one of a class that is beginning to be called "geographic information systems" (Tomlinson, 1972), that is, information systems in which a location identifier is carried along with each data element. Such information systems are useful where large amounts of environmental data are required, and where quantitative assessments and manipulations must be performed on the kinds of information customarily stored in map form.

In the CARETS information system maps themselves constitute one of the intermediate steps in the information flow process. Conceptually the "intermediate map" stage might be bypassed, since what is desired is a flow or communication of information about places on the earth's surface to users who are coming more and more to have requirements for environmental information in numerical form. Technological developments such as the ERTS multispectral scanner with its output potentially available in digital form with each data element identified with a spot on the earth's surface are possibly forerunners of information systems which can bypass the map in communication of vital information from the earth through the remote sensor to the user/decision maker. The CARETS information system anticipates such automated developments in the future. For the present, the CARETS data are transformed into map form for intermediate processing, using a combination of manual and machine methods which are within the capability of available technology, and which simulate the processing capabilities of future information systems that will be more fully automated.

The elements of the CARETS geographic information system may be better understood by referring to an abbreviated list of steps, as follows. Note that the list begins and ends with the users, whose needs are the reasons for existence of any information system.

a. User needs assessment. Prior to the official beginning of the CARETS project an assessment was made of the region's users of environmental information of the type available from the remote sensors. While a wide variety of users or potential users were identified, the user needs assessment concentrated on those who were in a position to make or influence decisions on land use, in accordance with the basic CARETS model. These were the various planning and management agencies of federal, state, and local governmental units. Approximately 200 individuals representing these and other regional user institutions were brought together in Washington in June 1971 for an initial users conference. Attendees were exposed to brief presentations on CARETS and on the capabilities of the sensors, and were then asked for indications of ways that the proposed systems could be of use. In addition to the initial users' conference, a study was made of Virginia State agencies and how the data of the kind to be produced in the CARETS project could be of use in their activities (Adams, Goodell, et al., 1971). The results of these efforts were the identification of a community of users with similar kinds of needs for land use data, which characteristically were required in quantitative form, retrievable for a given geographic area of the users' jurisdiction, and in such a format that the land use data could be used in conjunction with other environmental or socio-economic data sets as required for zoning, forecasting, determination of environmental impact, or other application of land use data.

b. Preparation of maps for digitizing. This step encompasses the extraction, in map form, of data sets from the remote sensing data, both aircraft and satellite, and preparing the maps so that they could be transformed into digital format. The test region has been mapped on 48 separate map sheets for the aircraft data base; locations of these sheets are indicated in Figure 2. Controlled photomosaics, land use maps, and land use change maps are available on open file at the U. S. Geological Survey, along with hydrology, census, and location maps to aid in use and interpretation of the land use data. ERTS maps, being at a smaller scale, have been compiled on sheets covering larger areas, as indicated on Figure 3. Examples of an ERTS image and corresponding land use map derived therefrom are shown in Figures 4 and 5. Key to categories of land use identified on ERTS imagery (with numerical codes that identify the land uses depicted in Figure 5) is contained in Table 1.

c. Digitizing map data. Transforming the information on the line maps to digital format followed a decision to create a data base with as much of the detail in the original maps as possible, so that even after the completion of the ERTS experiment, a valuable digital file of the region's land use would remain. This decision meant that a "polygon" system would be used, i.e. one which creates a file of all the areas or polygons bounded by a discrete line on the map. Digitizing of CARETS maps to date was done using two methods: manual line following, using a USGS coordinate digitizer; and automatic optical scanning, using the drum scanner belonging to the Canadian government, Department of the Environment, Canadian Geographic Information System, Ottawa.

d. Processing data for conversion to polygon file. This step involves computer programming and data processing which enables the raw tape or card files of the digitized boundary line data to be converted into a tape which identifies each polygon according to its location and land use type (or other appropriate label).

e. Plotting, editing and correcting errors. Errors, whether operator caused or in the data themselves, are removed by a sometimes laborious process of plotting, editing, and performing certain computer tests.

f. Preparation of area summaries. This task involves computation of areas occupied by the various land use types, a task readily performed in the computer once an error-free tape of the land use boundaries is available.

g. Merging of land use and land use change files to produce update. Once a land use data base is established for a given time (1970 for the CARETS aircraft data and 1972 for the ERTS data), its updating is perhaps most efficiently accomplished by examining later remote sensing data for indications of land use change, mapping the areas where change has taken place, and merging the two maps to produce the updated or revised map. So far the merge has been done manually, although it is hoped that the capability will soon be available for accomplishing the merge in the machine, i.e., using digital records of the original and change maps.

h. Overlaying land use maps with census, hydrology and geology maps. To achieve the desired flexibility in retrieval of the land use information, the system should have the capability of retrieving quantitative data sets geographically ordered according to the area of the user's jurisdiction, or other geographic area that may be of interest for environmental analysis, for example, within a certain distance of the coastline or an urban area, or within a certain drainage basin, or according to characteristics of surficial geology when desired for land use suitability analysis. Commonly, for data of the type dealt with in this project, "output" will be required county-by-county, since administration, planning, and other data-gathering activities are often organized by counties or groups of counties. The geographic areas represented by counties (and Virginia independent cities) are illustrated in Figure 6.

The CARETS geographic information system is developing the capability of performing the map overlay operation within the digital computer, i.e., interrogating the digital files of the land use data along with those of any other map with boundaries of areas for which land use summaries are required. This capability greatly expands the utility of the digitized land use file, making possible not only quantitative comparisons of ERTS and aircraft data for any portion of the region, but also the partitioning of the basic data set into rectangular grid cells of any specified dimensions. The overlay capability already exists in the Canada Geographic Information System, and successful system tests of a portion of the CARETS data have already been performed through a cooperative arrangement with the Canadian government. In this test land use data for the Norfolk-Portsmouth Standard Metropolitan Statistical Area were overlayed and retrieved and summed by census tracts, allowing computations of relationships among population and land use for that area. At this writing, steps are being taken to achieve an overlay capability on USGS hardware.

i. Statistical analysis of digitized data. As a final stage in the USGS processing of the CARETS data sets, a variety of analytical techniques will be utilized, for example, area summaries, comparisons of one map with another, multiple regression analyses of land use data versus other environmental or socio-economic data sets, formatting of land use data for experimental input to simulation or forecasting models, and analysis of land use time series. Examples of machine-derived data summaries for a portion of CARETS (the Norfolk-Portsmouth Standard Metropolitan Statistical Area) are shown in Table 2.

j. User evaluation and feedback. Cooperating user institutions are involved in the entire process of developing the experimental CARETS information system. A systematic evaluation of the entire range of data sets being produced by CARETS is being performed by these users, and their responses are to be fed back for inclusion in the final report. A series of questionnaires has been prepared to systematize user response to CARETS products. The first in the series, "CARETS User Indication of Interest" is reproduced as Figure 7. Potential users who respond by submitting such a form will be contacted by a CARETS staff member to provide the data requested, if possible, and to follow up with more detailed inquiry about the uses to which the products would be put. It is hoped that continuing arrangements with those users can survive the NASA-funded part of the demonstration project and provide the basis for an operational user-interactive system to follow.

ACKNOWLEDGMENTS

Most of the staff members of the Office of the Chief Geographer have contributed to the CARETS project, and their contributions have been essential to the evolution of the project and the development of its products. In particular, special acknowledgment and thanks are due to the "core" staff members in the final phase of CARETS, Peter Buzzanell, Katherine Fitzpatrick, Harry F. Lins, Jr., and Herbert K. McGinty. The project has also benefitted from the advice and assistance of the International Geographical Union Commission on Geographical Data Sensing and Processing, and the Canada Geographic Information System, Department of the Environment, Ottawa.

REFERENCES

- Adams, D., H. G. Goodell, et al., 1971. The potential of remote sensing as a data base for state agencies: the Virginia model, University of Virginia technical report.
- Anderson, James R., Ernest E. Hardy, and John T. Roach, 1972. A land-use classification system for use with remote-sensor data, Geological Survey Circular 671.
- Tomlinson, R.F., (ed), 1972. Geographical data handling, Symposium edition, I.G.U. Commission on Geographical Data Sensing and Processing, UNISCO/IGU Second Symposium on Geographical Information Systems, Ottawa, Aug 1972.

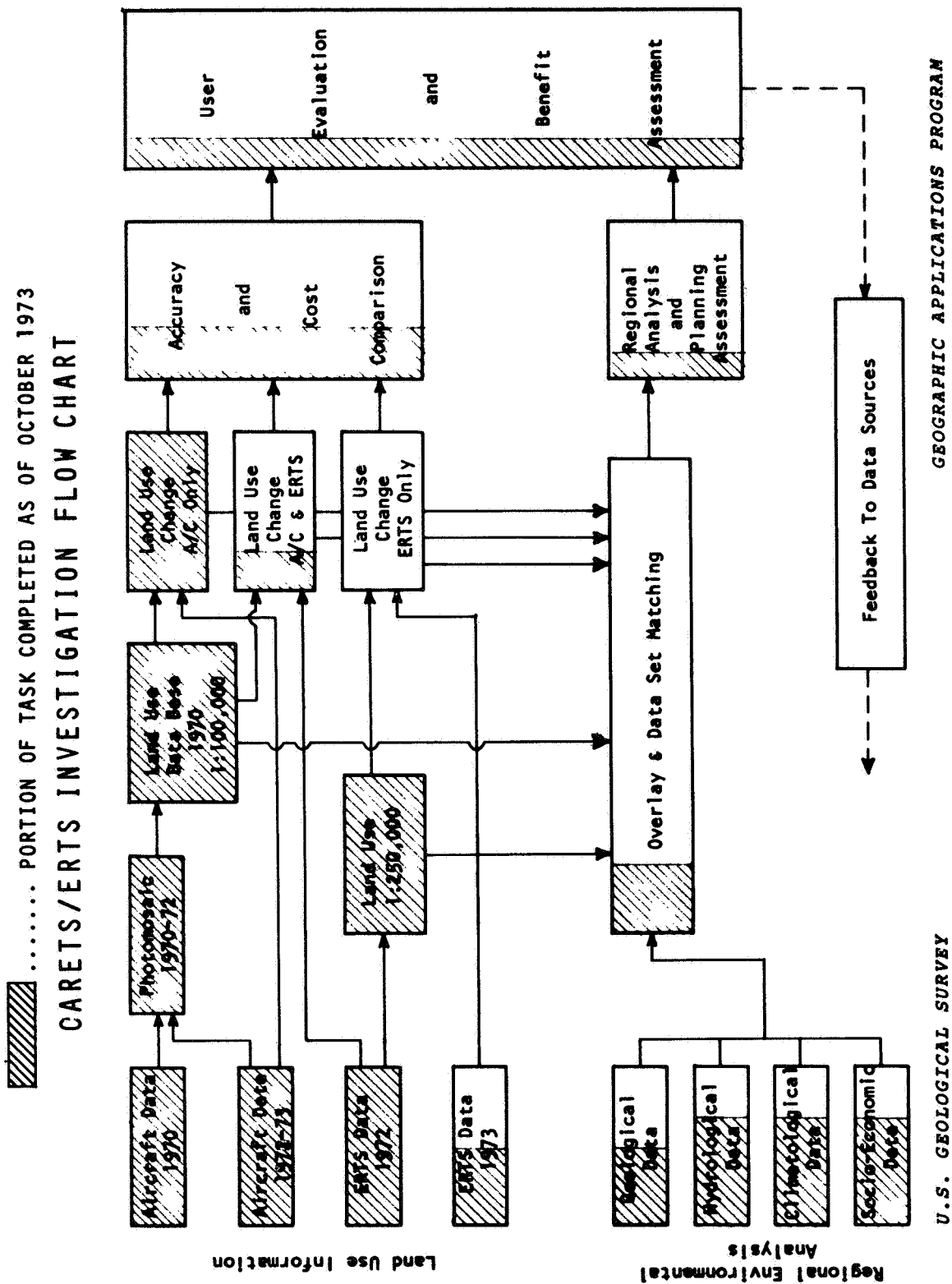
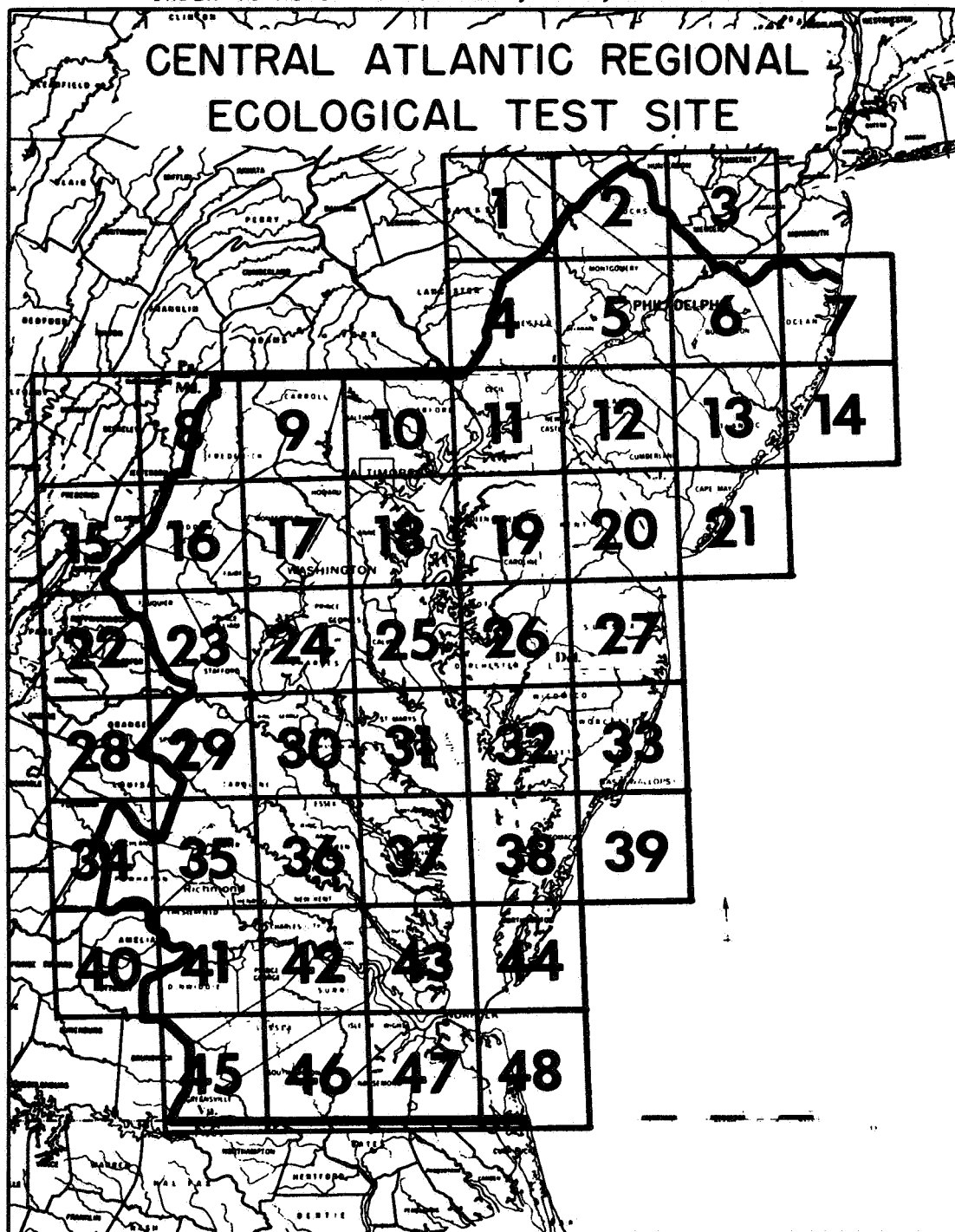


Figure 1

INDEX TO AIRCRAFT COMPILED, 1970, LAND USE MAPS



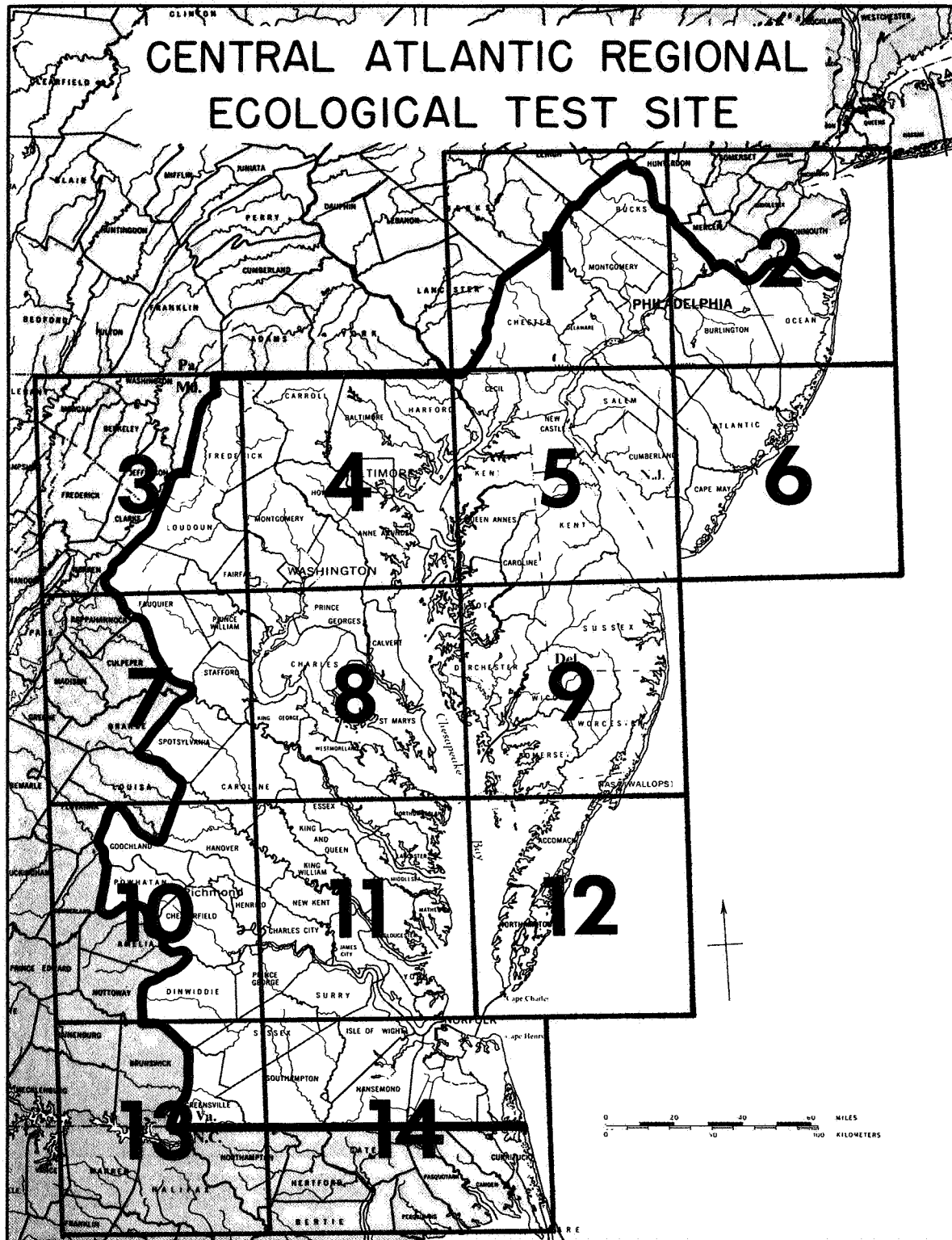
U.S. Geological Survey

Geographic Applications Program

INT: 760-72

Figure 2

INDEX TO ERTS COMPILED, 1972, LAND USE MAPS



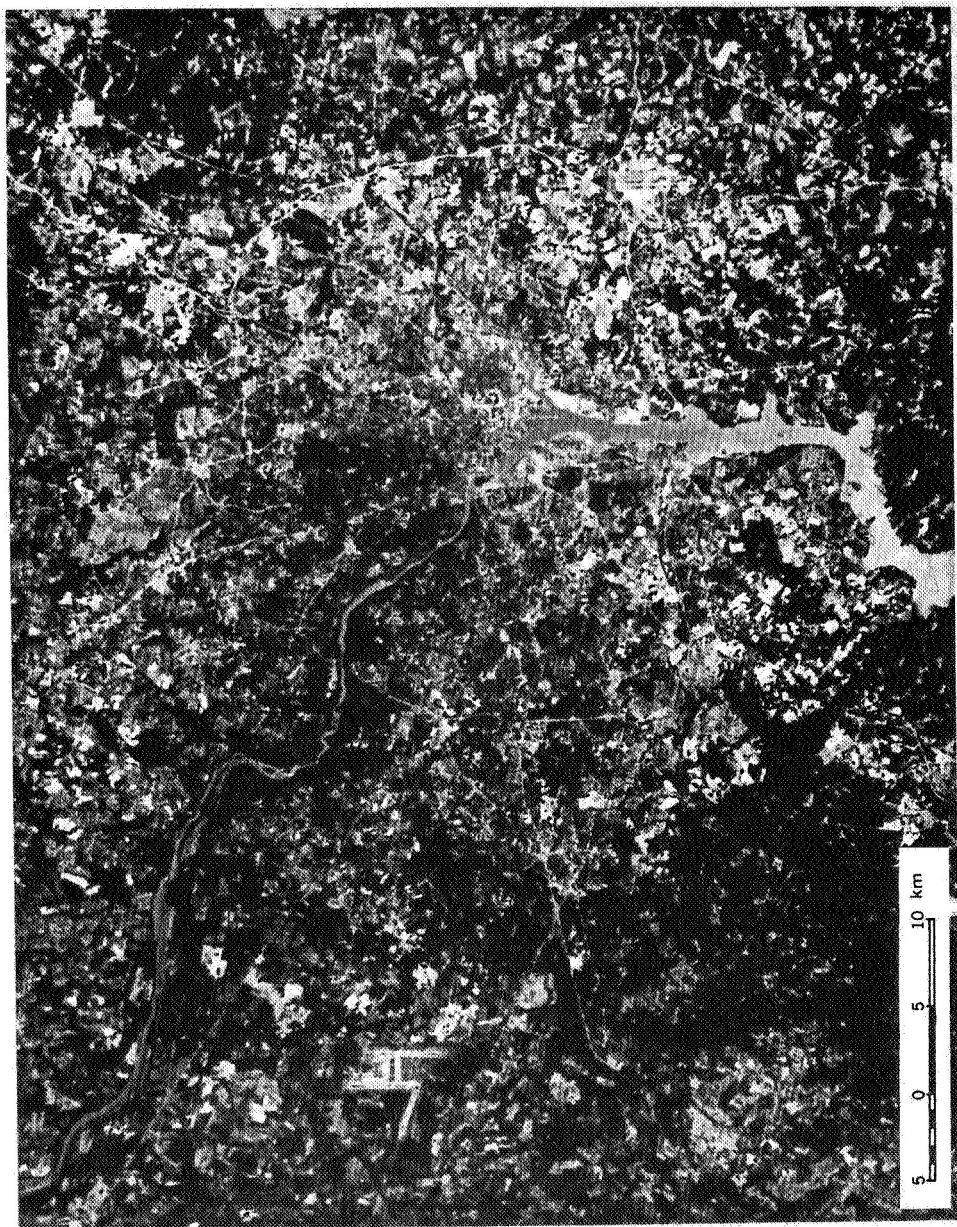
U.S. Geological Survey

Geographic Applications Program

Figure 3

INT: 760-72

ERTS Color Composite Image of the Washington, DC Area
(Frame 1080-15192/Bands 4,5,7/11 Oct 72)



U.S. Geological Survey

Geographic Applications Program

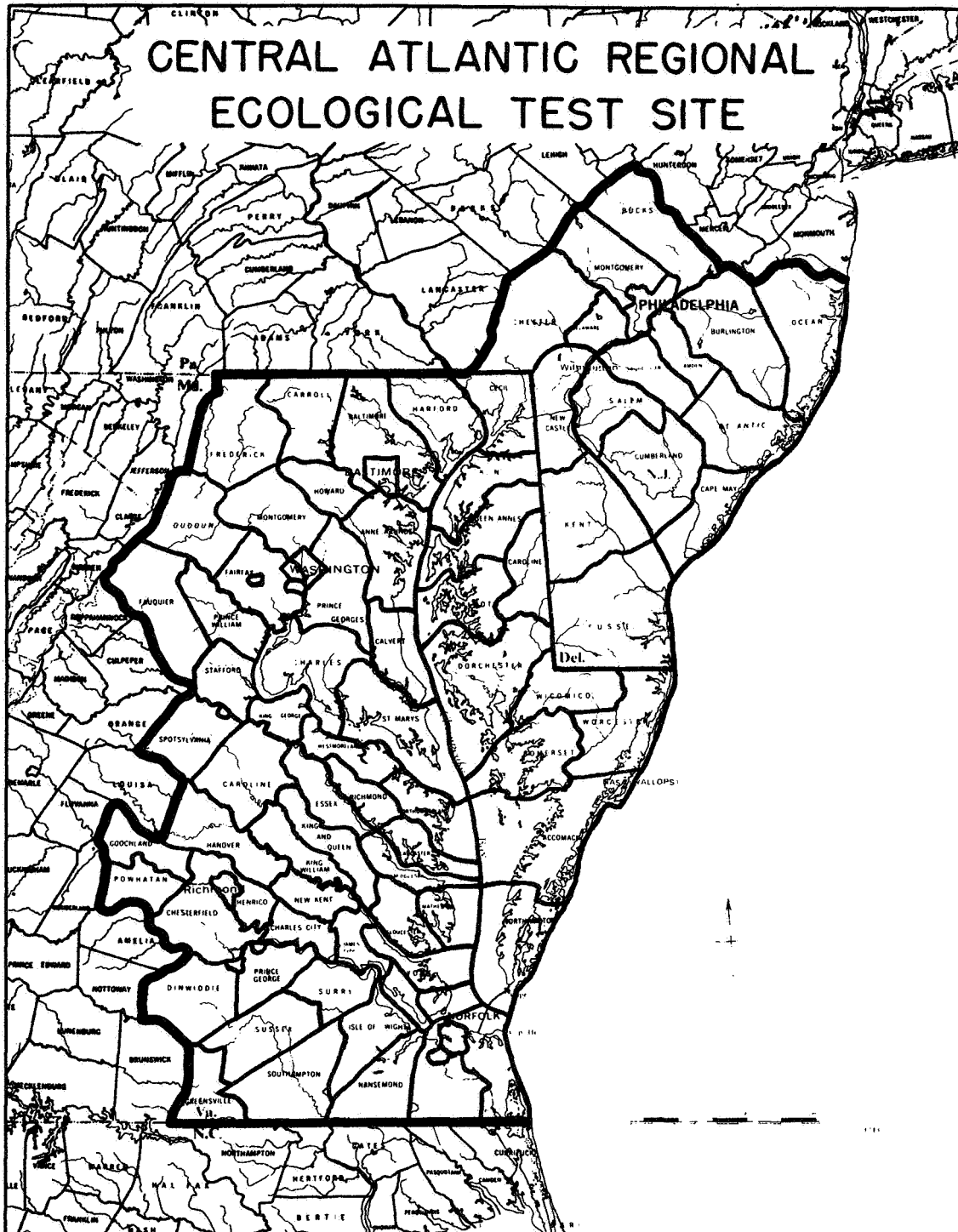
Figure 4

The map displays the Kura River and its tributaries, including the Kura, Kura, and Kura. The terrain is characterized by numerous contour lines and elevation markers, indicating a complex topography. The map also shows the locations of various settlements and infrastructure, such as the Kura, Kura, and Kura. A scale bar in the bottom right corner indicates distances of 0, 5, and 10 km.

Geographic Applications Program

518

COUNTY AND INCORPORATED CITY BOUNDARIES



U.S. Geological Survey

Geographic Applications Program

INT 760-72

Figure 6

CARETS USER INDICATION OF INTEREST

MEMORANDUM

Date: _____

To: Robert H. Alexander Mail Stop 115
U.S. Geological Survey
Reston, Virginia 22092

From: Name: _____
Agency or Organization: _____
Mailing Address: _____
Phone: _____

I am interested in problems of land use and related environmental impact in the Central Atlantic Region. Pursuant to those interests, I wish to inquire about the suitability of land use data and related information being made available through the NASA-USGS Central Atlantic Regional Ecological Test Site (CARETS). In exchange for any information I receive, I agree to supply information on its utility for my purposes.

Types of CARETS products of interest to me:

- ☐ "raw" remote sensing data products (e.g. ERTS imagery, aerial photos)
- ☐ processed graphics (e.g. orthophotomaps, land use maps)
- ☐ data listings and statistical summaries (e.g. amount of land in certain uses)
- ☐ interpretive reports (e.g. analysis of regional land use trends and their environmental implications)

Geographical area(s) of my principal interest:

- ☐ Virginia ☐ Maryland ☐ District of Columbia
- ☐ Delaware ☐ Pennsylvania ☐ New Jersey
- ☐ Other (specify) _____

I would intend to use the information for:

- ☐ recommendation to land use decision-making authority
- ☐ general background information on my region of interest
- ☐ education/public relations purposes
- ☐ research
- ☐ delivery to another person or agency (specify) _____
- ☐ Other (specify) _____

Signature

Figure 7

CARETS LAND USE CATEGORIES IDENTIFIED ON ERTS IMAGERY

<u>LEVEL I</u>	<u>LEVEL II</u>	<u>LEVEL III (PROPOSED)</u>
1 URBAN AND BUILT-UP	11 RESIDENTIAL	111 SINGLE FAMILY RESIDENTIAL UNITS
	12 COMMERCIAL AND SERVICES	121 RETAIL TRADE AREAS
	14 EXTRACTIVE	142 SAND AND GRAVEL PITS
	15 TRANSPORTATION, COMMUNICATION AND UTILITIES	151 HIGHWAYS
		152 RAILROADS AND FACILITIES
		153 AIRPORTS
		154 MARINE CRAFT FACILITIES
	16 INSTITUTIONAL	
	17 STRIP AND CLUSTERED SETTLEMENT	
	18 MIXED	
	19 OPEN AND OTHER	
2 AGRICULTURAL	21 CROPLAND AND PASTURE	
4 FOREST	41 DECIDUOUS FOREST	
	42 EVERGREEN FOREST	
5 WATER	51 STREAMS AND WATERWAYS	
	52 LAKES	
	53 RESERVOIRS	
	54 BAYS AND ESTUARIES	
6 NON-FORESTED WETLAND	61 VEGETATED	
	62 BARE	
7 BARREN LAND	74 BEACHES	

GEOGRAPHIC APPLICATIONS PROGRAM

U.S. GEOLOGICAL SURVEY

Table 1

COMPARISON OF AIRCRAFT AND ERTS
LAND USE MEASUREMENTS
NORFOLK-PORTSMOUTH SMSA

	1972 AIRCRAFT DATA (HECTARES)	1972 ERTS DATA (HECTARES)
URBAN	41,207	47,148
AGRICULTURAL	49,293	47,381
FORESTED	76,124	73,848
NON-FORESTED WETLANDS	7,793	4,583
BARREN LANDS	1,446	1,749
TOTAL	175,863	174,709

Table 2

CONCEPTS OF INTEGRATED SATELLITE SURVEYS

J. A. Howard, *Senior Officer (Remote Sensing), Food and Agriculture Organization of the United Nations, Rome, Italy*

ABSTRACT

FAO initially contracted with NASA to carry out investigations in three countries; but now as the result of rapidly increasing interest, ERTS imagery has been/is being used in 7 additional projects related to agriculture, forestry, land-use, soils, land forms and hydrology. Initially the ERTS frames were simply used to provide a synoptic view of a large area of a developing country as a basis to regional surveys. From this, interest has extended to using re-constituted false colour imagery and latterly, in co-operation with Purdue University, the use of computer generated false colour mosaics and computer generated large scale maps. As many developing countries are inadequately mapped and frequently rely on outdated maps, the ERTS imagery is considered to provide a very wide spectrum of valuable data. Thematic maps can be readily prepared at a scale of 1:250,000 using standard NASA imagery. These provide coverage of areas not previously mapped and provide supplementary information and enable existing maps to be up-dated. There is also increasing evidence that ERTS imagery is useful for temporal studies and for providing a new dimension in integrated surveys.

Looking towards the future, ERTS imagery or equivalent imagery is seen as providing developing countries with relatively inexpensive information as a basis to regional surveys, management surveys and local and regional planning activities.

As we are well aware, there has been a technological revolution in recent years in the methods of aerial survey. This revolution has been accompanied by publications on integrated surveys of land-use and natural resources using aerial photographs (e.g. Christian, 1958; Becket & Webster, 1962; Brink et al., 1966; Hardy, 1970; Howard, 1970, 1971); but these do not take into account the role of and the impact of satellite imagery on integrated surveys. In fact, the potential contribution of satellite imagery to integrated surveys in developing countries is only beginning to be appreciated. In the past, national inventories of rural resources have seldom been undertaken using complete coverage by aerial imagery, although national inventories of land-use and natural resources are in general recognized as a prime requisite to effective national rural planning and rural management. As indicative of the expanding role of satellite

1 N 74 30742

imagery, the Food and Agriculture Organization of the United Nations (FAO) initially contracted with NASA to carry out three investigations using Earth Resources Technological Satellite (ERTS) imagery (Sudan, Colombia, Philippines); but the Organization is now extending the use of its satellite imagery to seven additional countries.

SOME BASIC CONSIDERATIONS

When attempting to interpret ERTS imagery for integrated surveys, we should bear in mind the following pertinent facts:

1. ERTS-1 imagery is confined to four contiguous bands (bands 4-7) of reflected solar energy in the visible and near infra-red spectra.
2. Although band 4 (0.5/0.6 microns) covers the peak of spectral reflectivity of vegetation in the visible spectrum (i.e. c. 0.54 microns), its value may be lost by the somewhat similar reflective characteristics of the other surfaces (cf. spectral curves 1 & 2 with 3 - Figure 1). An exception, lies in its penetrative quality of ocean surfaces by solar energy of this waveband. High density phytoplankton, associated with high density fish populations, may contrast well against the surrounding ocean in band 4, due to the higher reflectivity of phyto-plankton. Similarly band 4 may reveal near in-shore features not to be observed in the other bands.
3. Band 5 (0.6/0.7 microns) covers the spectral range of maximum chlorophyll absorptivity by plants at about 0.655 microns (cf. curves 1, 2 - Figure 1). As most other natural surfaces, water excepted, have a much lower spectral absorptivity, and hence higher spectral reflectivity, this band provides good contrast between vegetal surfaces and exposed dry soil and sand. When there exists a high correlation between vegetal cover and soil type or sub-soil water, then this band is of value to soil surveyors and hydrologists.
4. Bands 6 (0.7/0.8 microns) extends from the far-red of the visible spectrum into the near infra-red and includes the spectral range in which the shoulder of the plant spectral reflectivity curve is sensitive to disease, severe drought and mineral changes. Investigators have variously put the commencement of the near infra-red band, as between 0.70 microns and 0.78 microns (cf. Howard 1970); but most commonly it is accepted as beginning between 0.72 to 0.75 microns. The writer accepts a value of 0.75 microns, since this is beyond the shoulder of the curve for healthy plant foliage. As water surfaces and moist surfaces are highly absorptive in the infra-red, these are usually readily distinguishable in this band (cf. Figure 1), provided their characteristic reflectivity is not masked by vegetation.

5. Band 7 (0.81/1.1 microns) is entirely in the near infra-red, but includes two hydroroxyl absorbing bands (0.95, 1.1 microns). Improved penetration of alto-stratus clouds can be observed on some imagery in band 7.

6. Due to the altitude of the satellite (i.e. 920 km, 560 miles), ERTS imagery provides a perspective of the Earth approaching a plan view, which can often be used directly for small-scale planimetric mapping with relatively few ground control points.

7. As a single ERTS frame covers a ground area of about 26,000 km², it offers advantages associated with a synoptic view and favours deductive reasoning rather than inductive reasoning. Recognition of the latter is important, since much of our present-day approach to research depends on well tried methods developed for working from the particular to the general (i.e. by inductive reasoning).

8. As the electromagnetic data recorded in a single signal by the tape of the ERTS optical mechanical scanner covers an area of approximately 65 m x 70 m, this is often considered to be the minimal resolving power of the imagery. However, objects with a size smaller than this may be identified sometimes by interpreting the mixed signal of the data cell. For several reasons, a resolution of about 70 m will usually not be obtained when working from 1:1,000,000 ERTS black-and-white prints or transparencies. Using this type of imagery, it is frequently difficult to identify features related to landform, soils, vegetation and crops with a ground area less than about 0.5 sq. km.

9. As ERTS-1 has an 18-day cycle, it enables time-dependent information (e.g. seasonal flooding) to be studied. However, clouds may be a limiting factor to frequent time dependent studies. As shown by Table A, which summarizes ERTS data (<30% cloud cover) for one-year for Africa, South America and Southern Asia, cloud can be an important limiting factor to studies, particularly in South America.

Table A

ERTS-1 Imagery - % of Frames with <30% Cloud: 1972/73

Continental Area	Frames % Satisfactory for Spatial Studies	Frames % Satisfactory for time-dependent Studies
South America	50	38
Africa	85	63
Southern Asia	93	88

TYPE OF ERTS IMAGERY

As follows, FAO's investigations are indicative of the increasing range of ERTS imagery formats, etc. from which to choose for integrated surveys. These are:

- a. 70 mm black-and-white transparencies in the four spectral bands at a scale of 1:3,369,000.
- b. 18 cm x 18 cm, net image area, black-and-white transparencies in the four spectral bands at scales of 1:1,000,000. This format is also referred to as 9" 9-1/2".
- c. as b. but black-and-white prints in the four spectral bands at scale of 1:1,000,000 and 1:500,000.
- d. multi-spectral imagery (reconstituted colour) at 1:1,000,000, 1:290,000 and 1:70,000/1:100,000 using additive viewing techniques.
- e. multi-spectral colour mosaics formed from an assembly of computer-compatible video-tape displays at 1:158,000 or from multi-spectral imagery.
- f. computer print-outs at 1:25,000.

18 cm transparencies and black-and-white prints have been found suitable for a range of field activities, where the final mapping scale does not exceed about 1:200,000. There is increasing evidence that with adequate ground checking, a range of discipline oriented thematic maps can be prepared at 1:250,000. These will be useful to national planning and to regional and reconnaissance surveys. However, the information to be obtained from the imagery is seldom useful in local surveys and local management planning. For these latter purposes, maps usually require to be at scale of about 1:50,000 or larger. In the past, conventional aerial photography has often been taken at scales between 1:30,000 and 1:60,000 without recognizing the fact that smaller scales would be as satisfactory, since the final map scale will be 1:250,000. Under these circumstances, ERTS black-and-white imagery in 2 bands may suffice, particularly if the imagery is enlarged 2-4 times for field use. It may require emphasizing that, as many developing countries are remote from experienced aerial survey companies, aerial photography is expensive and often exceeds a \$100,000 per mission.

Seventy millimeter chips, unless used in conjunction with a slide projector or with an additive viewer in a multi-spectral study, has the limitation of working at a much reduced scale (i.e. 1:3,369,000). Chips are therefore only used in additive colour viewing or occasionally by copying them on to a 35 mm format

for slide studies in black-and-white using a standard 35 mm projector and a viewing screen. There is little doubt that multi-spectral colour imagery at about 1:1,000,000 is quicker and less tedious to interpret than black-and-white imagery at the same scale. Although, what is obvious from multi-spectral colour imagery can also be observed often by back-checking to 35 mm slides, data has been observed from multi-spectral imagery, which even with back-checking was not adequately detected from black-and-white material.

A colour mosaic assembled from video-tape displays by Purdue University is now being used in a desk-study in Rome. It seems to be intermediate in value between the ERTS prints and computer compatible tape print-outs; but also requires a critical appraisal with multi-spectral colour imagery at 1:70,000 to 1:100,000. Print-outs at 1:25,000 provides information, which is not observable from imagery at 1:1,000,000 or enlargements thereof.

ANALYSIS OF SELECTED ILLUSTRATIONS

For integrated surveys related to land-use and natural resources, small-scale ERTS imagery (i.e. 1:1,000,000) is useful for (a) preparing small-scale thematic maps (e.g. 1:250,000) of areas as yet not covered by planimetric maps (b) planning reconnaissance and pre-investment surveys in areas not adequately covered by existing maps (c) planning conventional aerial photography (including contract preparation) of selected areas of development, so as to ensure that the area will be fully covered at the most suitable scale and in the best film-filter combination (d) amending existing small-scale maps to eliminate planimetric errors (e) amending existing maps, so as to include details previously omitted (f) up-dating land-use information contained on existing maps (e.g. new forest boundaries in areas of recent settlement and agricultural development) (g) two to four times enlargements of black-and-white imagery to serve as photo-mosaics. In addition, using an additive viewer, a colour inter-negative is obtained and from this a two to four times colour enlargement is prepared, which may then be used as substitute for a colour photo-mosaic from aerial photographs.

Three examples from Africa, indicative of the type of information obtained from the ERTS imagery are as follows. A comparison of ERTS imagery and existing maps of Morocco have shown that it is practicable to prepare quite detailed thematic geological maps from the imagery as many structural features are clearly defined (e.g. major and minor faults to north-east of Agadir). Also, the existing maps may be amended to correct planimetric errors in water-course alignments and additional information enables the length of water-courses to be extended. The synoptic view of the arid coast of Morocco provided information on the former coast lines in this region.

A reconstituted multi-spectral additive colour image of Awash Valley, Ethiopia, and prepared by Huntings Aerial Surveys Ltd. (London), has been found useful in providing a better understanding of the hydrology of the area. The colour imagery also assisted in the geomorphic and groundwater (thematic) mapping of the region (Currey, 1973). Several unknown sources of freshwater were discovered. If the imagery had been available prior to the aerial photography at 1:40,000 of the commercially irrigated cotton growing areas, the flight-plan would have been amended to advantage of the follow-up survey. In the vicinity of the irrigated cotton crops, induced and natural vegetation was identified and delineated on the imagery and Papyrus swamp was clearly recognizable along the edge of the major lake.

Imagery of the Sudan (El Obeid, El Fula) has been examined from black-and-dispositives and prints (Mitchell, 1973). Selected areas are in the process of being examined using computer generated data (Baumgardner, 1973) and some checking of ground-truth against print-outs has been completed (Ramsay, 1973). The author has made a comparison of these two sources of information. Prints at 1:1,000,000 can be magnified to about 1:200,000 before film graininess becomes conspicuous, but multi-spectral additive colour viewing is possible at about 1:70,000 using 1:1,000,000 black-and-white chips. On the multi-spectral colour mosaic and on the multi-spectral additive colour imagery, an aureole of weathered material surrounding the inselbergs could be identified. Several vegetal types, two dune formations and soil-types are readily observed. Areas of induced vegetation may be delineated. Drainage patterns are conspicuous and often characterize the types of bedrock. It is also practicable to divide the areas into land-systems. A temporal desk-study of imagery in the vicinity of El Fula indicates major changes in the surface features due to the rapid evaporation of surfaces water during the dry season.

DISCUSSION AND CONCLUSIONS

As a basis to integrated land-use and resource surveys, a number of authors have described and discussed the significance of land-units as observed on conventional aerial photographs (see Howard 1971). These papers provide adequate evidence of the role of aerial photo-interpretation in integrated surveys. Now, on the basis of the separate information derived to date from the FAO studies of the ERTS imagery, the imagery seems satisfactory for use in integrated surveys. The approach recommended by the author is to apply a hierarchical subdivisive system in which the largest land-units are identified and delineated on the imagery on the basis of a paramount discipline, (vide Table B). These land-units are then further sub-divided into smaller and smaller land-units on the basis of other paramount disciplines. Eventually small land-units are obtained, which are homogeneous in a number of environmental factors useful to future rural planning and development, and including the preparation of thematic maps.

Checking in the field will be necessary; but this can be minimized by attempting to identify beforehand the land-units of varying magnitude.

Table B provides a brief description of the hierarchical land-units to be observed on satellite imagery (cf. Howard 1971, 1970a, b). Land-unit is used here as a general term. The paramount disciplines, used to subdivide the ground area portrayed on the imagery into smaller and more homogenous units, is also given in column 2. The final column summarizes the attributes considered most useful to integrated surveys. It will be observed that land units at the level of the land-system and land-catenas are uniform in macro-climate, lithology and landforms; and land-facets, if identified, are uniform not only in these factors but also in terms of natural vegetation soil type and certain environmental characteristics which may be imbedded in the vegetation (e.g. aspect, macro-climate, water table).

Table B
Land-Units Observable on ERTS Imagery

Land-unit	Paramount Discipline	Comments and Description
Land-division ↓	Regional geography	The synoptic view provided by the satellite imagery is valuable for the identification of these extensive land-units having a gross landform expressive of a continental structure and in which its regional climate is evidenced by the uniform fit of the vegetation (panformation) to its landform.
Land-province ↓	Physical geography	The synoptic view provided by the satellite imagery is valuable for the identification of these extensive land-units, which are recognizable as a distinctive assemblage of surface forms expressive of a second order structure.
Land-region ↓	Geology	A land-unit, usually of considerable magnitude, which is identifiable mainly through the image characteristics of its land-system(s). The land-region has surface properties of a lithological unit with a small range of surface forms.

Table B (Continued)

Land-unit	Paramount Discipline	Comments and Description
Land-system ↓	Geomorphology	A recurrent landform pattern of geographically and geomorphologically related smaller land-units. Its drainage pattern is distinctive and provides boundaries coinciding with geomorphic features.
Land-catena ↓	Geomorphology	These land-units are often difficult or impossible to identify from small-scale imagery (e.g. 1:1,000,000); but large-scale computer based and additive viewing techniques are providing encouraging results. A land-catena constitutes a major recurrent (geomorphic) unit of the land-system (vide Howard, 1971). Each land-catena contains a distinctive grouping of geographically and geomorphologically related land-facets.
Land-facet ↓	Phyto-geomorphology (Botany/ Geomorphology)	Not normally recognizable from small scale imagery; but large-scale techniques indicates that some land-facets are identifiable provided they are extensive in ground area. A land-facet comprises a distinct unit of topography with which is associated an equally distinctive vegetal structure at the level of the plant subformation. Usually, climatic uniformity can be inferred from the vegetal structure; and the soil-type should be found to be uniform.
Land-element ↓	Botany	Not observed on ERTS imagery.

REFERENCES

- Baumgardner, M. F. (1973), Personal communication LARS, Purdue University, USA.
- Becket, P. H. & Webster, R. (1962), The storage and collation of information on terrain. Military Engineering Experimental Establishment, U.K.

- Brink, A.B., Mabbutt, J.A., Webster, R. & Beckett, P.H. (1966), Report of the working group on land classification and data storage. M.E.X.E. No. 940, Christchurch.
- Christian, C.S. (1958), The concept of land units and land systems. Proc. 9th Pacific Science Congress 20: 74-81.
- Colvocoresses, A.P. (1972), Image resolution for ERTS, Skylab and Gemini/Apollo. Photogramm. Engng: 38(1): 33-5.
- Currey, D.T. (1973), Personal communication, c/-AGS Division, FAO, Rome.
- Hardy, E.E. (1970), Inventorying New York's land-use and natural resources. New York's Food and Life Sciences 3 (4):
- Howard, J.A. (1970), Aerial Photo-Ecology, Faber & Faber, London, 325 pp.
- Howard, J.A. (1970), Stereoscopic profiling of land-units from aerial photographs. Austr. Geogr. 11: 259-68.
- Howard, J.A. (1971), Multi-band concepts of forested land-units. Proc. 3rd Intern. Symposium on Photo-Interpretation. International Society of Photogrammetry, Dresden, G.D.R.
- Mitchell, C. (1973), Personal communication, Reading University, United Kingdom.
- Ramsay, D. (1973), Personal communication, c/-AGS Division, FAO, Rome.

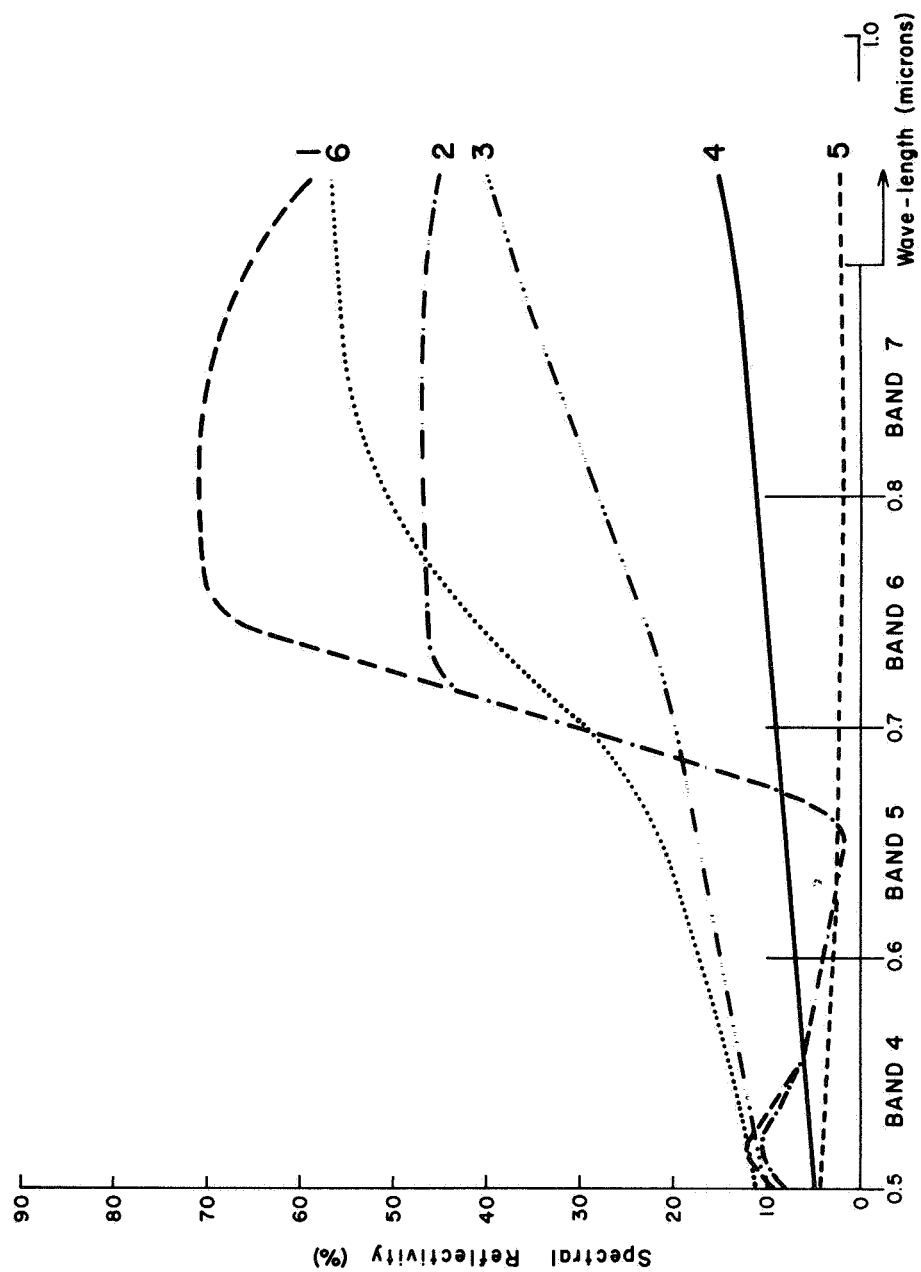
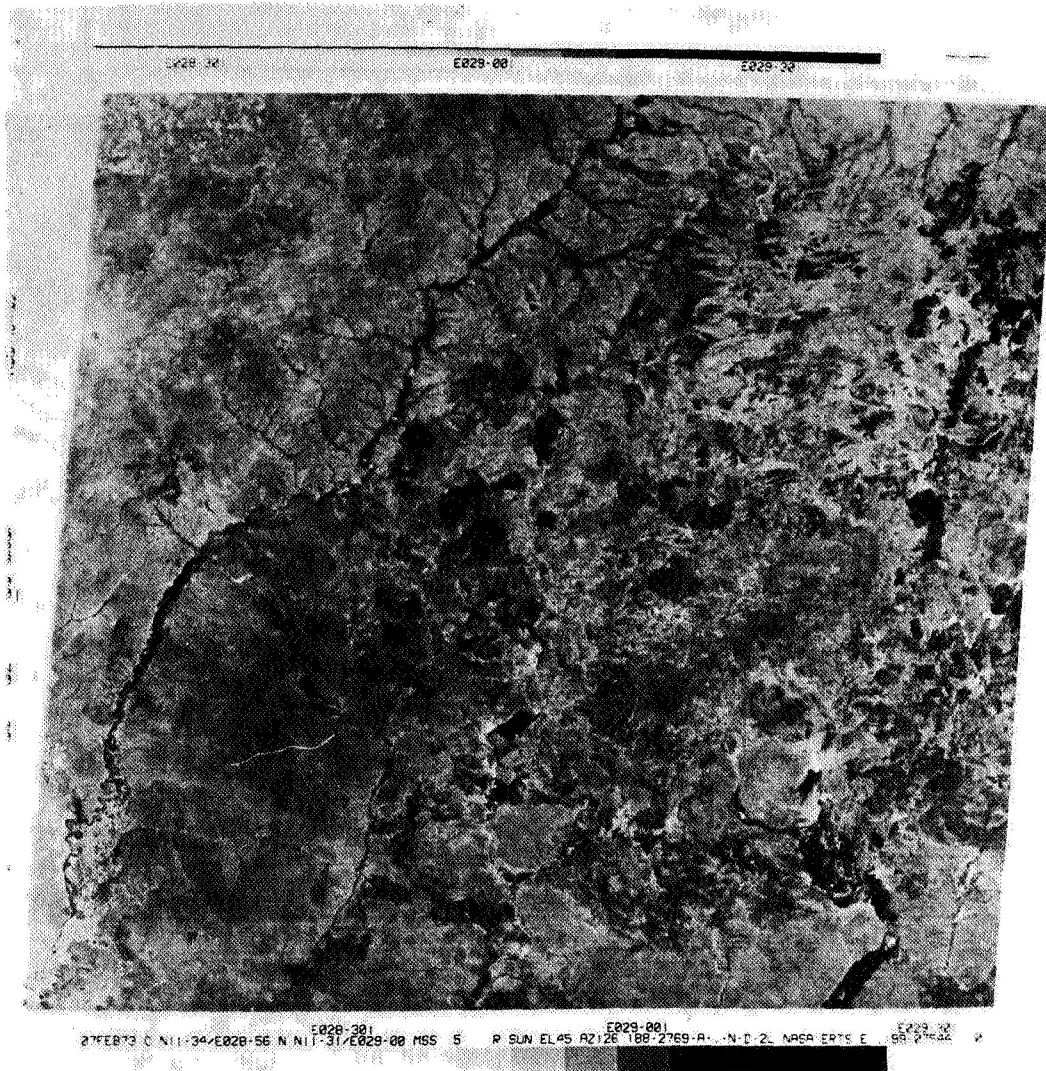
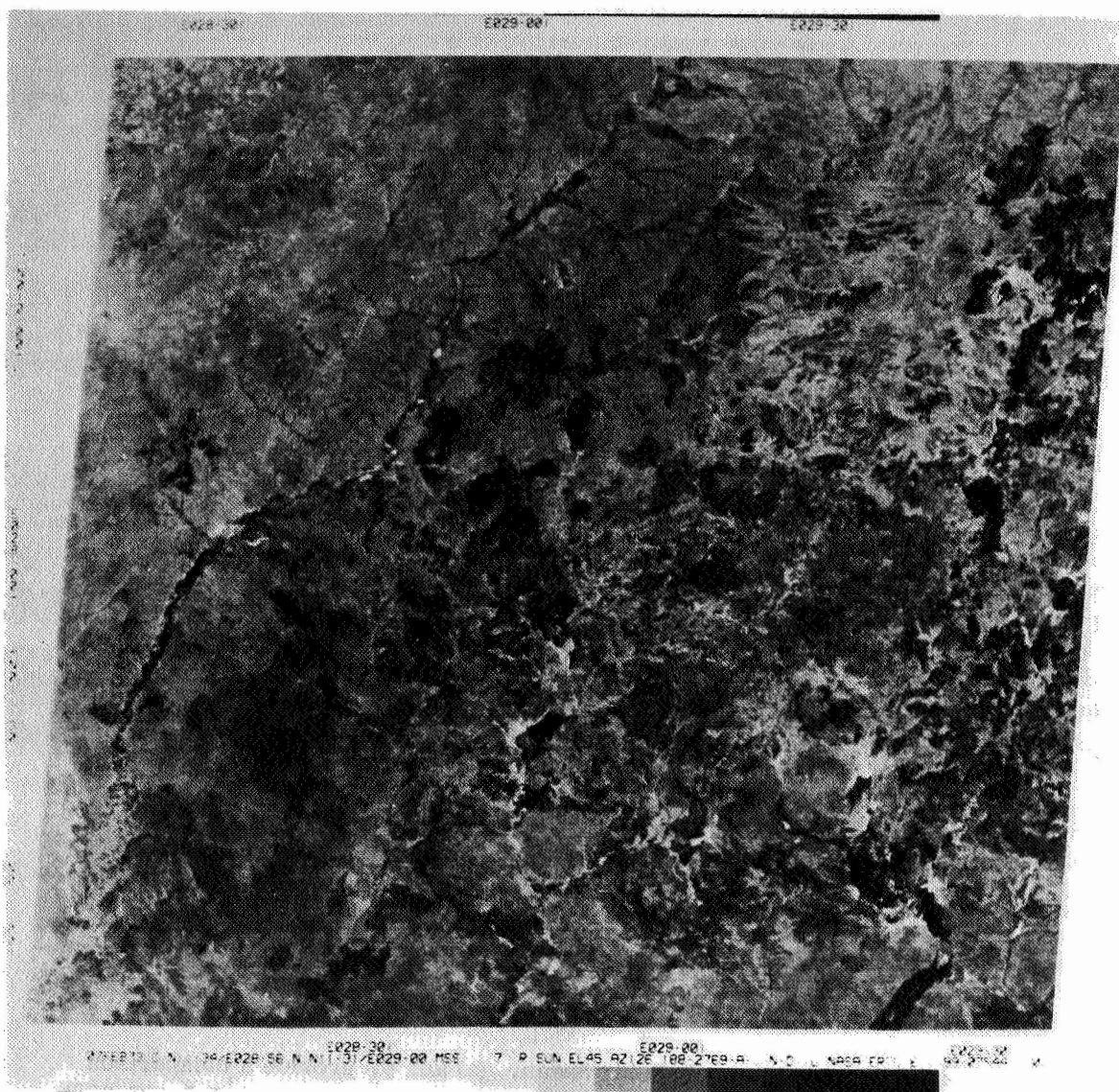


Figure 1. Characteristic spectral reflectivity curves of several natural surfaces: (1) healthy green vegetation (leaf area index: 4); (2) healthy green vegetation (leaf area index: 1); (3) dry loam; (4) wet loam; (5) water surface; (6) dry grasses.



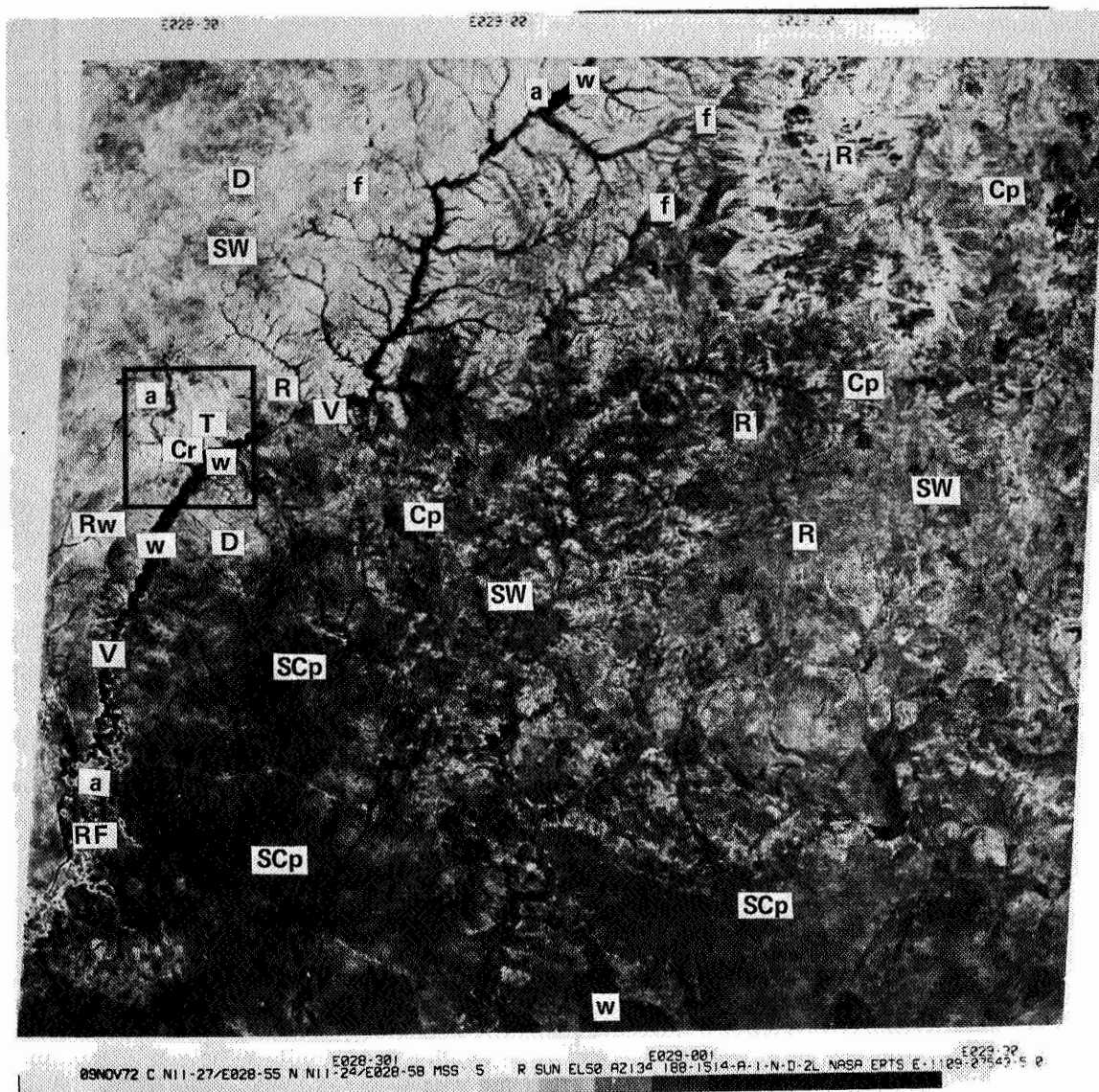
(a)

Figure 2. ERTS imagery, El Fula, Sudan. (a) and (b) provide a comparison of spectral bands 5 and 7 taken on 27 February 1973 (dry season) (1:1,000,000). Note the better definition of the drainage system in band 5, but band 7 (infrared) enables water surfaces (moist areas) to be easily identified. (c) band 5 taken 29 November 1972 at end of wet season. A comparison with (b) (i.e. time-dependent study) shows changes related to vegetation and water moisture. (d) Part of a multi-spectral colour mosaic (1:158,000) obtained from the magnetic tape replays (29 November). Note the easier recognition of features than in black-and-white, including soil boundaries and water surfaces/moist areas.



(b)

Figure 2 (Continued)



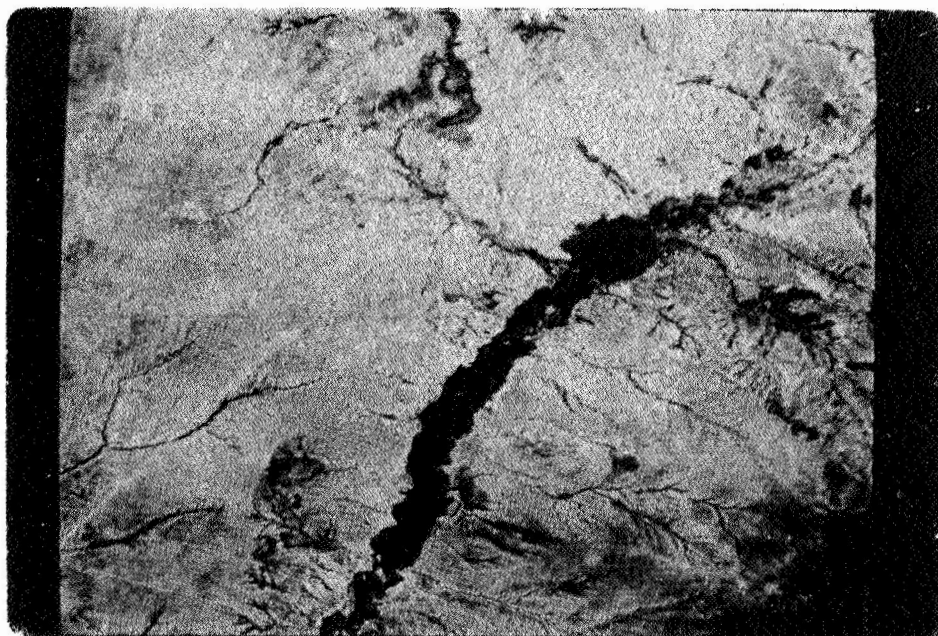
(c)

Figure 2 (Continued)

Key

f: fault
 D: dunes
 a: alluvium
 w: water surfaces
 Cp: clay plain
 SCp: smooth clay plain
 R: rock outcrop
 V: main valley

RF: riparian forest
 SW: sayanna woodland
 Cr: cultivation (crops)
 T: town
 Rw: railway
 d: dense
 s: sparse
 h: hydromorphic



(d)

Figure 2 (Continued)

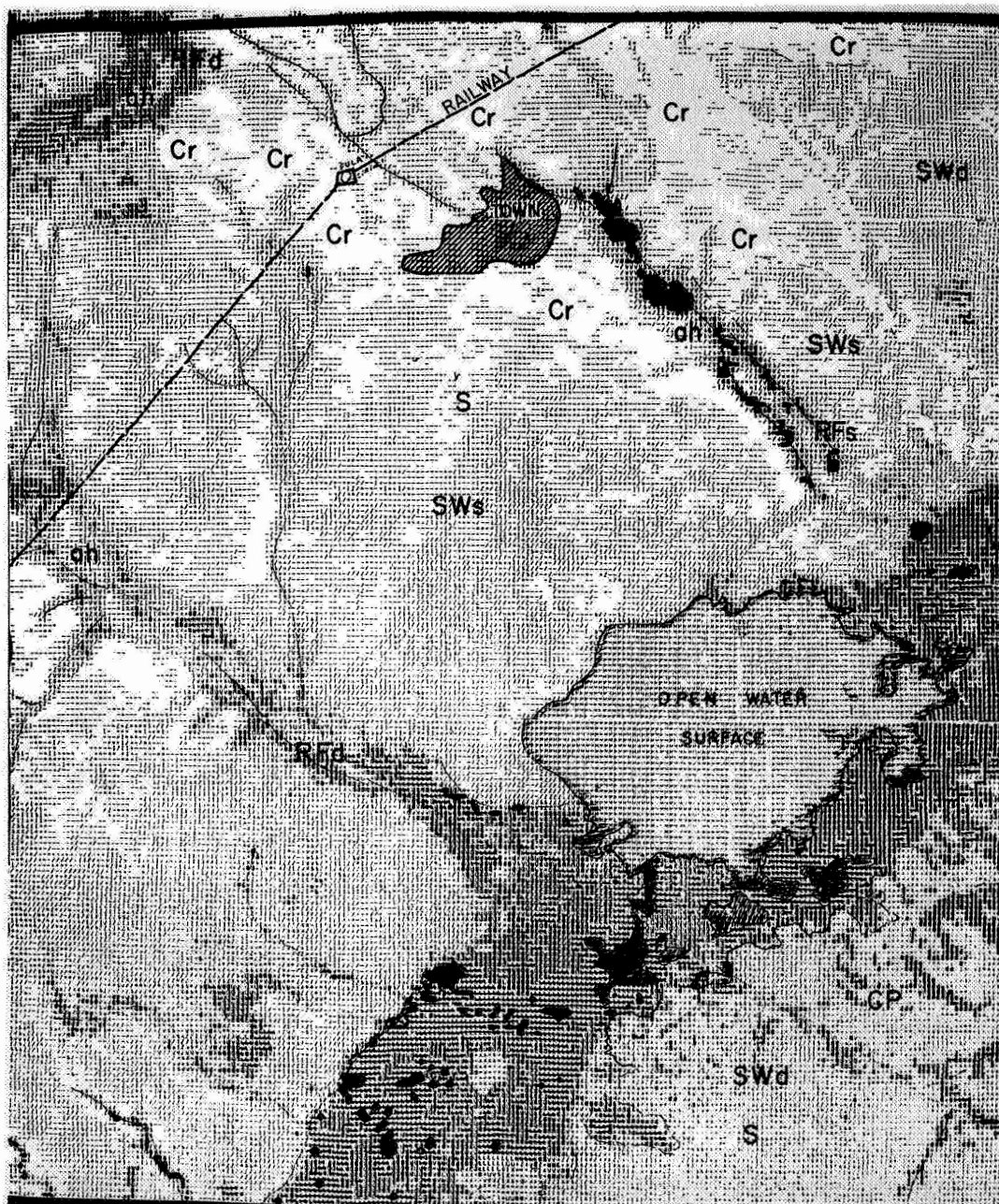


Figure 3. Computer print-out at 1:25,000 from tapes of 29 November of area within small square (2c). Note the further increase in ground information as compared with Figure 2. Black areas and water surfaces/areas of very high moisture content.

TOWARDS AN OPERATIONAL ERTS - REQUIREMENTS FOR IMPLEMENTING CARTOGRAPHIC APPLICATIONS OF AN OPERATIONAL ERTS TYPE SATELLITE

Alden P. Colvocoresses, *U.S. Geological Survey, Reston, Virginia*

Background

After nearly 18 months of successful operation of the first Earth Resources Technology Satellite (ERTS-1), a careful look at the future is obviously in order. Judging from the results of ERTS-1 experiments, public sales of ERTS-1 products and overall worldwide response it is believed that ERTS-1 has demonstrated an Earth sensing mode that should become operational. It is recognized that several studies leading to the definition of an operational ERTS have been made. However cartographic requirements are generally more basic and demanding than those of the Earth science disciplines and are therefore treated separately in this paper. One assumption made is that the configuration of ERTS, particularly with respect to the Multispectral Scanner (MSS) and data transmission rates cannot be materially altered.

General

Although the ERTS-1 experiment was not designed for mapping applications, cartographers (foreign as well as domestic) have examined and evaluated ERTS-1 imagery. The consensus of these investigators is that an operational ERTS-type satellite can have many valuable applications, particularly where the image itself serves as the cartographic base for medium- and small-scale maps. The requirements for implementing these applications are based on capabilities as demonstrated by ERTS-1 or as defined for a future ERTS-type satellite as follows:

- Continuous operation which, subject to visibility, covers the earth from 82° N to 82° S every 18 days.
- Near-real-time reception of data.
- Near orthogonal imagery (ERTS-1 has a maximum angle off axis of only 5.76°).
- Geometric fidelity, which permits accurate positioning at scales as large as 1:250,000.

PRECEDING PAGE BLANK NOT FILMED

1 N 74 30743

- Spatial frequency (resolution) commensurate with an instantaneous field of view in the 40- to 80-meter range.
- Radiometric fidelity in several simultaneously acquired wavebands including the near infrared.

Spatial Frequency

Requirement - Image quality suitable for detection and identification of image control points and major planimetric features, such as roads, railroads, canals, field boundaries, urban boundaries, and water-land interfaces.

Rationale - Need to produce imagery suitable for reproduction at scales as large as 1:250,000 - a standard medium scale accepted throughout the world. Much useful information for many disciplines can be derived from these products and be referenced to the figure of the earth.

Present Performance - Instantaneous field of view (IFOV) of MSS is a 79-m square and the recorded net pixel is 79 by 59 m. The Return Beam Vidicon (RBV) line width is equivalent to 45 m and theoretically should produce the higher resolution, although empirical tests to date have not borne this out; the RBV is rated equivalent to the MSS with an effective pixel size of about 80 m.

Changes - To obtain the image quality required for more useful cartographic products, one relatively broad band of imagery (0.5 - 0.7 μm) should have an effective pixel size of about half the side dimension of that of the present sensors.

Suggested Solution - Increase (perhaps double) the focal length of the RBV(s), limit its response to one spectral band, and maintain the same width of coverage as the MSS. Considerable spatial frequency increase can be obtained before image motion compensation (IMC), which is a complex modification, would be needed. Current criteria for acceptable image motion is that the degradation along track should not exceed 50% of the cross track resolution. The existing 79 m IFOV would be suitable for the MSS bands.

Spectral Frequency

Requirement - Record a minimum of two bands in the visible and two in the near IR.

Rationale - These spectral bands are needed to differentiate fixed and temporal phenomena, such as cultural features, open water, areas of vegetation cover, snow and ice, topographic features, local atmospheric anomalies, and the various meaningful variations and combinations of these phenomena insofar as unique recordable spectral responses exist.

Present Performance - Two visible and two near IR bands are now recorded by the MSS. The three RBV bands provide redundancy to the four MSS bands.

Changes - None - except reduction of RBV bands from 3 to 1.

Temporal Frequency

Requirement - Near global coverage every 18 days.

Rationale - The frequency of repetitive coverage of ERTS-1, which promises to produce complete cloud-free coverage of the U.S. on an annual basis and coverage of selective representative areas on a seasonal or even monthly basis, is considered adequate except for monitoring short-lived phenomena. Increasing the number of satellites would increase frequency, but the cost of data acquisition and handling would probably negate this advantage. If short-lived phenomena are in fact to be monitored from space, a geosynchronous system capable of selective area coverage is believed to be the most feasible solution.

Present Performance - 18-day global coverage except for latitude higher than 82°.

Changes - None

Reception and Processing Time

Requirements - The conversion of selected sensor response into cartographic products in a matter of days - maximum of one week.

Rationale - Although ERTS is not considered suitable for the monitoring of short-lived phenomena, it does record certain items that should be rapidly disseminated in cartographic form. Examples involve the delineation of water boundaries which includes surface water distribution, flood conditions and the water-ice interface in polar regions. The seasonal delineation of infrared reflective vegetation is another.

Present Performance - Except for coverage of the eastern U.S. data tapes must be flown to Goddard for processing. Precision processing or otherwise relating imagery to ground control and preparing products for distribution now involves manual procedures which may take a month or so to accomplish. However, a single gridded ERTS product at 1:1,000,000 scale (Lake Tahoe) was brought to the reproduction stage in a matter of 15 days after acquisition.

Changes - Provide direct real time reception to the processing centers insofar as possible. For the U.S. a reception station in South Dakota and another in Alaska is suggested. Processing centers should be equipped to produce selected imagery in cartographic form (precisely referenced to the

figure of the Earth) within a matter of 2 or 3 days after reception. By use of digital or optical density slicing certain of these signatures should be reduced to thematic binary form and thus simplify the processing.

Geometric Properties of Imagery

Requirements - Independent spatial positioning of imagery compatible with requirements for 1:1,000,000 scale and, with the benefit of ground control, for 1:250,000 scale at National Map Accuracy Standards (NMAS).

Rationale - An operational remote sensing system must not only record identifiable data but also have a means of spatial reference. An accepted system of reference is one that relates to the figure of the earth as described in spherical coordinates (lat/long) or plane coordinates (X Y). For remote areas, 1:1,000,000 scale is adequate for delineation and changes of gross features, but 1:250,000 scale is needed to portray changes to developed areas and indicate where more precise mapping is required. A 1:250,000-scale map that just meets NMAS contains root mean square (rms) errors of about 80 m. Thus accuracy and MSS pixel size would be of the same approximate size, which is a logical relationship.

Present Performance - Positioning of ERTS data with control only by orbital and sensor parameters (independent mapping) now involves errors in the order of 2,000 m (rms). This is compatible with maps of 1:6,000,000 scale. With the aid of ground control, a system-corrected (bulk) image when fitted to a conventional map projection involves errors of 200-450 m, which is marginal for 1:1,000,000-scale mapping. Fitting a geodetic grid to an MSS image reduces these errors to the 50 to 100 m range, which is compatible with 1:250,000-scale mapping. However this involves the use of the existing projection of the MSS image which is semiperspective and lacks the conformality of geodetic projections. Scene-corrected (precision processed) MSS imagery has errors in the 100- to 200-m range but because of degraded image quality is considered suitable for reproduction at no larger than 1:500,000 or possibly 1:1,000,000 scale. On a portion (1/16) of an MSS bulk image on which at least two control points can be identified, points which are part of a defined pattern (shore line, field lines, highways, etc.) can be located to within 20 to 30 m (like all other accuracy figures stated herein these are rms figures).

Changes - Increase the independent positioning capability from 1:6,000,000 (2,000 m) to 1:1,000,000 scale (300 m) if possible. Define the imaging system so that either bulk or precision images can be produced with less than 80 m error in areas where suitable control exists. All such imagery to retain the spatial frequency (quality) of the original data.

Suggested Solution - Slightly improve positional and attitude determination devices. Modify the system corrected (bulk) printing of MSS to a conformal (Space Oblique Mercator)* projection. For those who may not accept the

*A description of this projection is contained in a memorandum (EC-18-ERTS) which is attached and made a part of this paper.

Space Oblique Mercator projection provisions for precision processing without loss of image quality and on a conventional projection such as the UTM should be provided. It is believed that demands for this product will be relatively small since the Space Oblique Mercator projection accommodates the conventional geodetic grids without measurable distortion and the precise relationship between the projections can be mathematically defined. In polar regions such precision processing would normally be on a polar stereographic projection. Incorporate one RBV band with maximum spatial frequency and an engineered reseau of approximately 30 points, most of which are near the image border.

Image Repeatability

Requirement - Hold successive images of the same scene to a maximum of ± 13 km from the nominal scene center.

Rationale - An ERTS satellite system has the potential of repeating image positions to the indicated requirements. If accomplished, this would provide a worldwide system of formats based on the nominal scene with very high assurance that the formats will be completely covered by subsequent corresponding scenes. Such maps could be published in perhaps 1/10 the time and effort now required for conventional formats, which normally involves mosaicking images from several orbital passes. Use of the image format would permit publication and distribution of ERTS imagery in a timely and relatively inexpensive form.

Present ERTS Performance - The ERTS orbit is permitted to drift (cross-track direction) about ± 15 km before corrections are made. Attitude variations produce up to ± 11 km offsets. Thus the cross track maximum variation may be ± 26 km whereas the minimum side lap at the equator is only 26 km or ± 13 km. Along-track image boundaries are generally within ± 5 km.

Changes - Hold orbital drift, attitude variation, and along-track image boundaries of the MSS so that the resultant scene has a maximum cross track deviation of ± 13 km, and no more than ± 5 km deviation in the along-track direction to a prescribed scene center point.

Suggested Solution - Improve orbital and attitude correction parameters and maintain standards for defining along-track image boundaries of the MSS.

Sensor Alignment

Requirement - Obtain a square MSS image format at the midlatitudes.

Rationale - Scanners and frame images should cover the same area. A square format is the more efficient to process and also is more esthetically pleasing.

Present Performance - MSS has a 3° nominal image skew at the midlatitudes--
 4° at the equator and 0° at maximum inclination (81°).

Changes - Define a nominally square image for the MSS at the midlatitudes.

Suggested Solution - Turn the spacecraft or sensors 3° to the right of the spacecraft velocity vector. This will create 1° skew at the equator, near 0° at the midlatitudes on the descending node, and 3° at the maximum inclination (82°) where it is of lessor concern.

Summary

The attached table summarizes the cartographic requirements for an operational ERTS type satellite.

CARTOGRAPHIC REQUIREMENTS FOR AN OPERATIONAL ERTS TYPE SATELLITE

Requirements	Rationale	Present Performance	Changes and Suggested Solution
<u>Spatial Frequency</u> 1 band 40 m pixel 4 bands 80 m IFOV	Identification of key cultural features Reproduction at 1:250,000 and smaller scales	80 m effective pixel size (RBV) 80 m IFOV (MSS)	Increase focal length of RBV and reduce to one band
<u>Spectral Frequency</u> 2 bands in visible 2 band in near IR 1 redundant RBV band (in visible)	Differentiation of fixed and temporal phenomena	2 bands in visible (MSS) 2 bands in near IR (MSS) 3 RBV bands redundant to MSS	Reduce RBV to 1 broader band
<u>Temporal Frequency</u> Near global coverage every 18 days	Optimum for this type of satellite system. ERTS orbit unsuited for detection of short-lived phenomena	Coverage every 18 days between N 82° and S 82°	No change
<u>Reception and Processing Time</u> Dist of selected data in cartographic form in 3 to 7 days	Time critical data must be in the hands of the user in a matter of days	Dist. of data (imagery) normally takes one to several months	Centralize reception and processing, provide for selective data processing in automated cartographic form
<u>Geometry of Image</u> Capable of 1:1,000,000-scale independent positioning. Capable of 1:250,000-scale positioning with control (all at NMAS)	1:1,000,000 is adequate for delineation of gross features and change thereto. 1:250,000 scale is needed to portray changes in developed areas and indicate where larger scale mapping is required	Capable of independent positioning at 1:6,000,000 NMAS. With control image can be fitted to 1:1,000,000 NMAS. Grid can be fitted to image of 1:250,000 scale. Scene corrected imagery meets 1:500,000 or 1:1,000,000 NMAS.	Improve positional and attitude determination to +300 m (rms). Convert bulk image to conformal projection. All processing to retain original image quality. Use one RBV band of increased spatial frequency and engineered reseau
<u>Image Repeatability</u> Hold successive images of the same scene to +13 km in the cross track direction and +5 km in the along track direction with respect to the nominal scene center.	The image format when repeated within stated limits becomes the basis for publication; it would involve perhaps 1/10 the time and effort of conventional quadrangle formats.	Orbit drift involves +15 km, attitude variations +11 km - both cross track, along track variations are within +5 km	Hold cross track imagery variations to +13 km, maintain along track image centers to +5. Keep same nominal scenes as for ERTS-1

Requirements	Rationale	Present Performance	Changes and Suggested Solution
<u>Sensor Alignment</u> Nominal square format for MSS	Same coverage as RBV is needed. Square format is more efficient and esthetic	MSS has 3° nominal skew at midlatitudes	Skew spacecraft or sensors 3° to the right of the space- craft velocity vector



United States Department of the Interior

GEOLOGICAL SURVEY

~~XXXXXXXXXXXXXXXXXXXX~~
1340 Old Chain Bridge Road
McLean, Virginia 22101

August 1, 1973

Memorandum for the Record (EC-18-ERTS)

By: Cartography Coordinator, EROS Program

Subject: Map Projection of the Bulk (System Corrected) ERTS MSS Image

Defining the Projection

Recently the USGS successfully fitted the Universal Transverse Mercator (UTM) grid to selected ERTS Multispectral Scanner (MSS) bulk images and mosaics of images at 1:250,000 scale. Maps so produced are in fact cast on the projection of the MSS image, which to date has not been fully defined as a specific map projection. The conventional mapping approach is to use a projection of the earth's figure, such as the UTM, and either transform the image to this projection (precision processing) or force the bulk image to the best analog fit on the projection. Because ERTS provides near orthographic imagery, the grid of a conventional projection, such as the UTM, can with only minor distortions be fitted to the MSS bulk imagery, except in isolated areas of extreme relief. The grid distortions are real and can be measured with precision instruments but they are less than 1 part in 1,000--which is the criterion, more or less, for maps of scaling accuracy. Moreover the fit appears consistent, which indicates that the bulk image of ERTS is itself a map projection of the earth's surface.

NASA/ERTS Users Data Handbook (1)* describes the orbit, MSS scanner, and geometric corrections made to the imagery; and Konecny (2), Kratky (3), Forrest (4), and the undersigned (5) have described the basic geometric and mathematical relationships of the ERTS image to the earth sphere and the UTM projection. Konecny further indicated that ERTS bulk imagery would be printed out in the UTM projection, whereas Kratky defined the corrected MSS image (bulk) as representing the equidistant cylindrical or Cassini projection. However an analysis of the geo-

*According to this reference, one of the corrections is a scale change in the along-track direction to approximate the perspective view of the RBV frame image. In practice this so-called correction--which is actually undesirable except for correlation to the RBV--has not been generally applied by NASA.

metric corrections made by NASA (1) indicates that neither the UTM nor the Cassini is the actual case. NASA has in fact retained the geometric conditions of perspective, which transform the individual panoramic sweep of the scanner (six lines) into a narrow horizontal strip on the plane normal to the vertical and at an equivalent focal distance* above the optical center of the primary mirror of the scanner. Attached are diagrams and notes which cover the basic geometry and mathematics of the MSS scanner. The resulting thin strips when properly composited and normalized to a scale of 1.00000 form a cylindrical surface around the earth normal to the orbital plane and tangent to the figure of the earth.

This cylinder or ring is fixed in space with respect to the polar axis, and forms a simple cylindrical surface of projection. The perspective centers of the strips that comprise this projection form a circle which is the loci of points occupied by the optical center of the scanner. Since a cylinder can be converted to a plane without distortion, we have the essential elements of a map projection. At any given instant of time the MSS scanner is pointed to a discrete (79 m) element of the earth, and this element is in turn recorded as a discrete picture element on the described projection. Map projections are normally defined and fixed with respect to the surface of the earth, but in this case the projection is independent, and an equation involving four motions as functions of time must be introduced to relate the projected image to the earth's surface. The four motions, all of which have a defined time relationship, are involved in the image formation as follows:

- The mirror sweep in the nominally cross-track direction
- The satellite orbit in the along-track direction
- The rotation of the earth, which provides the continuous shifting of the earth scene with respect to the orbit (and projection).
- The precession of the orbit.

These four motions result in the (potentially) complete mapping of the earth from 82° N to 82° S every 18 days on the same defined projection and in a sun synchronous mode.

For want of a better term, this projection is dubbed Space Cylindrical Strip Perspective: Space because it is defined and fixed in space, Cylindrical because of its shape, and Strip Perspective because it retains the geometric properties of perspective in the strip resulting from the scanner sweep. Such a projection could undoubtedly be applied

*This distance is irrelevant but is introduced to equate the MSS to an optical imager. For convenience a scale of 1.00000 is suggested. However the diameter and F number of the scanning mirror provide a focal length of about 0.76 m.

to other circular orbit systems which utilize a point or slit type imager (scanner, panoramic or strip camera). Insofar as is known, NASA or NOAA have not used this approach for meteorological satellite imagery, which they normally transform to one of the conventional projections, such as Miller cylindrical, azimuthal equidistant, or point perspective (for ATS).

Characteristics of the Present MSS Projection

The basic characteristics of the MSS projection are summarized as follows (see attached notes):

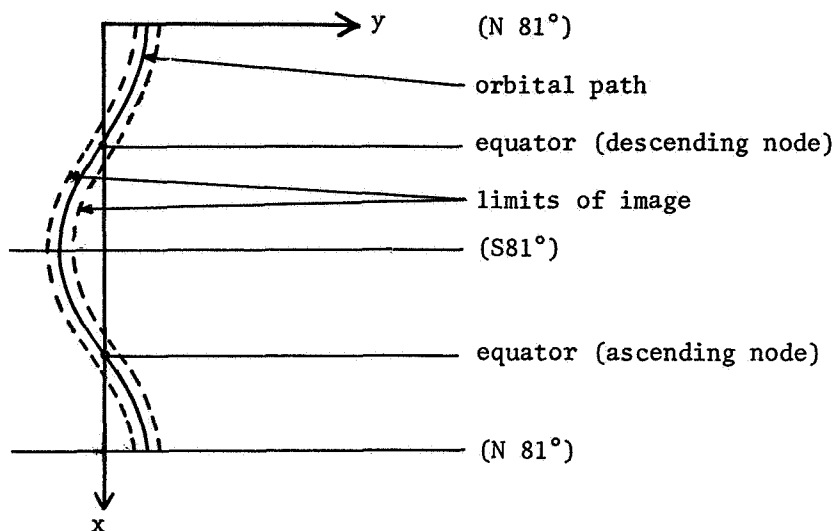
- Scale at nadir can be any desired scale, but we will normalize it with a scale factor of 1.00000.
- Cross track scale factor at image edge (end of scan lines) is 0.99916.
- Along track scale factor at image edge is 1.00011.

This results in a nonconformal projection in which an affine condition exists except along the nadir path. Thus the scale is different in different directions, and angular relationships will not truly hold as they do on a conformal projection. Nevertheless it is a true map projection insofar as NASA can correct for the various anomalies involved (1) and a system of plane cartesian coordinates can be applied to the projection. These coordinates become related to the earth's surface only when the four described motions are introduced as a function of time. This relates a specific element of the earth's surface to a specific element of the projection. Developing this transformation presents an interesting mathematical exercise which is by no means trivial if such refinements as the ellipticity of the earth's figures are considered. However if the projection is to be used as such, the rigorous transformations must be developed. Konecny (2) and Kratky (3) have indicated the general form of the mathematical relationships involved. Although the cylinder is fixed in space at a prescribed angle of about 9° to the polar axis, the earth or the cylinder must move back and forth along the cylindrical axis. This relative linear motion provides for the continuous imaging of the rotating earth on the cylinder without discontinuities.

If we start with an origin at the point of maximum inclination ($N 81^\circ$) the (x) along-track coordinate value will increase indefinitely.* The mapping equations of the earth surface must account for the various orbits, which after 18 days (251 orbits) would mathematically repeat themselves providing that the prescribed corrections are all properly made. The y or cross track coordinate value must accommodate the linear motion of the earth in the cylinder of projection. This motion results

*By treating the projection plane as a cylinder (which is mathematically acceptable) the x values repeat themselves each orbit.

in the orbital path (and the image strip) being record on the projection as a sinusoidal line (strip) which oscillates back and forth in the y direction as follows:



Map projection of MSS

Although the imagery is recorded on a single projection, there are always discontinuities between imagery of adjacent orbital passes when it is laid on the same plane (map). This is because the scale must change in the cross-track direction, and the orbital passes are convergent. Thus the cross-track distance from the nadir (center line) is constantly changing. The discontinuities are very small when the imagery is correctly processed, but they are real and are equivalent to the gores one sees in the zone boundaries of such transverse Mercator projections as the UTM.

Practical Application

The MSS projection (Space Cylindrical Strip Perspective) is in fact being used today for experimental mapping by the USGS and any others who map directly with MSS bulk imagery. In order to produce maps that are readily understandable, we are imposing a conventional plane coordinate grid to this heretofore unconventional projection. The grid selected is the UTM, and the resulting distortions of the UTM grid on this projection are so small (generally less than 1:1,000) that the average map user cannot detect the discrepancies. By relating image points to the local grid lines there is no measurable error due to the projection, and it is only when stable base manuscripts are measured on a precise measuring machine, such as a coordinatograph, that the discrepancies in scale and direction can be detected.

Recommended Changes

NASA's printing of the MSS bulk imagery is modulated by a computer (EBRIC).^{*} Thus there is no great problem in introducing a mathematical change in the printing procedure. Rather than print out on the presently used semiperspective affine projection, it is recommended that the projection if possible be made conformal. A cylindrical surface is still involved, and the only defined conformal cylindrical projection is the Mercator which may be normal, transverse, or oblique to the earth's polar axis. This is the oblique case with the plane of the orbit that defines the cylinder at 9.092° to the polar axis. The equations relating the oblique Mercator to the figure of the earth have been developed in detail for the various ellipsoids as well as the sphere, (6) but all are based on the static case. Here, as with the present MSS projection, we must develop the transformations as a function of time. A suitable name for this recommended projection is Space Oblique Mercator. As defined herein, this projection is not truly conformal since the two axes on which the equal-scale condition of conformality are established vary up to 4° from orthogonality. Thus a truly circular feature on the figure of the earth will have a very slightly elliptical form to it on the projection, depending on its position on the orbit. This elliptical distortion of a circle is known as Tissot's indicatrix and graphically illustrates the mathematical condition of nonconformality. Since the geometric conditions which create this slight deviation from conformality can be expressed mathematically, the relationships between the figure of the earth and the projection are still rigorous. Insofar as the actual image is concerned, the deviation from conformality will not be measurable and for analog applications can be disregarded. Perhaps Gerhard Kremer (Mercator) would object to having his name applied to a projection which is not truly conformal, but since conformality is the primary consideration applied, it is believed that this projection should be associated with Mercator.

The projection cylinder can be defined as either tangent or secant to the (sea level) figure of the earth. U.S. sponsored projections such as the UTM and those of the State plane coordinate systems are secant, whereas most Europeans use tangent projections, the most common being the Gauss-Kruger which is transverse Mercator. The projection of the Space Oblique Mercator creates scale distortions of only slightly over 1:10,000 and it is recommended that the European practice of tangency be followed. On a tangent cylinder, the scale factor of the projection, except along the orbital track, is too large with respect to the figure of the earth. However the land masses of the earth (where the MSS is principally employed) have mean elevations of 340 m or more (the mean elevation of North America is reported as 720 m). A mean elevation of 340 m, which is found in Europe and Australia, would compensate for the projection scale factor so that insofar as projection distances are concerned, as compared to actual ground distances, there is no valid

^{*}Electron Beam Recorder Image Corrections.

argument for making the projection secant. Insofar as fitting the MSS projection to the UTM, it makes no real difference since the scale factor of the UTM varies from 0.9996 (at the central meridians of the zones) to 1.0010 at the zone edges along the equator. Thus it is recommended that the MSS projection scale factor be 1.0000 along the orbital path and 1.0001 along the image edge.

Although they are probably not feasible to implement on ERTS-1, certain other alternatives should be considered relative to the projection of the MSS for future ERTS-type satellites. For instance, the EBRIC could include an along-track scale change based on the UTM zones. This would modulate the scale factor from a maximum of 1.001 to 0.9996. Such modulation would be an irregular approximation and require updating from ephemeris data. Moreover, scale modulating the imagery would be a disadvantage to anyone not using the UTM or the Soviet Unified Reference System, which is generally compatible with the UTM. Such UTM simulated modulation would not be implemented in the polar regions where another modulation might be introduced to approximate the scale factors of the two polar stereographic projections as now defined for the precision processing of ERTS imagery in the polar regions. Actually the precise UTM (and polar stereographic) projections could be used, but this involves discontinuities (breaks in the imagery) at the zone boundaries, the application of complex mapping equations, and calibration against ground control to fully implement. Perhaps such a system can be developed for near-real-time application in the future, but for the present, it is believed that NASA should concentrate on the relatively simple space Oblique Mercator for bulk processing. Insofar as possible, NASA should experiment with the alternate proposed projections (and perhaps others) to assist in the formulation of definitive plans for the processing of imagery from an operational ERTS-type satellite.

Significance

Defining the projection of the MSS in mathematical terms is essential to all who would relate the ERTS pixel* to the figure of the earth. The form of this projection is immaterial to those who deal strictly in analytics (computations) as long as it is rigorously defined. For those who use the MSS image for mapping in analog mode, the image projection should conform as close as possible to the mapping projection used for final display. ERTS imagery, except for that of polar regions, is customarily displayed on the UTM projection. The adoption of the Space Oblique Mercator by NASA would provide a continuous single projection which develops projection scale distortions of only about 1 part in 10,000 and which has geometric properties somewhat comparable to the UTM. Eventually, the automated casting of the image on the actual UTM projection is a distinct possibility.

From a practical standpoint, any attempts to fully automate an MSS mapping system will be limited by the precision of ephemeris and at-

*picture element

altitude data, which to date results in errors in the order of 2 km (rms). However the user can normally find at least one control point against which he can calibrate an MSS image or even several contiguous MSS images of the same orbital pass. With such calibration data and the mapping equations developed in rigorous form, he can then compute and superimpose on his image the figure of the earth in the form of lat/long or plane (UTM) coordinates. There are today indications that with control of perhaps 100 to 200 km spacing a printed map can be prepared that meets National Map Accuracy Standards at 1:250,000 scale (80 m rms). On the present MSS projection the resulting maximum distortion of the UTM grid is in the order of 0.25 mm (0.01 in.) on a 1:250,000-scale map, but on the recommended Space Oblique Mercator projection this distortion would be considerably less. The MSS, as system-corrected by NASA, is creating a continuous image of the earth on one single projection. Moreover it is doing it with a precision which opens the door to semiautomated image mapping today and perhaps fully automated image mapping within a decade. In this context the word mapping refers to digital as well as analog relationships.

It is important to note a basic advantage of the scanner as compared to the frame imager (camera). A frame imager creates its own discrete projection with each exposure. At aircraft altitudes, the effect of earth curvature is minimal, but from space it is significant. If a map is to be made by analytical procedures, there is no problem; but if the image is to be used in analog form as a map base, the problem is real because the discontinuities between images become measurable. With a scanner such as MSS the image produced is more or less continuous and (insofar as corrections are made) always on the same projection. For the first time the entire earth (between N 82° and S 82°) is being mapped on a single map projection on which the projection scale distortion is always less than 1:1,000 and, if made conformal, about 1:10,000. It is true that the imagery from two adjacent orbital passes cannot be fitted together without some discontinuity, but the imagery itself has the same geometric characteristics which continue without disruption along the orbital path.

The net effect of this new concept of mapping cannot be forecast at this time. Its basic importance to the mapmaker is obvious, but it is probably of equal or greater importance to those who use the digital approach to store and analyze data relative to the earth's surface. In theory, if not in actual practice, the mathematical relationship between the ERTS pixel and its location of the earth can, through the projection, be rigorously defined.

Acknowledgement

This memo represents a combined effort on the part of the EROS Cartography Program. In addition to those cited the branches of Photogrammetry and Field Surveys, Office of Research and Technical Standards, Topographic Division, U.S. Geological Survey performed the computations and measurements which led to the definition of this projection. In essence it is NASA who created the projection when they defined ERTS

and then so successfully applied corrections to the raw MSS data.

Alden P. Colvocoresses
Alden P. Colvocoresses

References

1. NASA, Earth Resources Technology Satellite Data Users Handbook. Prepared and maintained by General Electric Corporation, 1971 - to date.
2. Konecny G., Geometric Aspects of Remote Sensing. Invited paper Commission IV International Congress of Photogrammetry, Ottawa, 1972.
3. Kratky, V., Cartographic Accuracy of ERTS Images, Proceedings of the American Society of Photogrammetry 30th Annual Meeting, March 1973, Washington, D.C.
4. Forrest, R.B., Mapping from Space Images, Bendix Technical Journal Summer/Autumn 1970.
5. Colvocoresses, A.P., ERTS-A Satellite Imagery, Photogrammetric Engineering, June 1970.
6. Thomas, Paul D., Conformal Projections in Geodesy and Cartography, Sp. Pub. No. 251 of Coast and Geodetic Survey, G.P.O. Washington, D.C. 1964.

A.P.C. August 1, 1973

Notes on ERTS MSS Projection of Bulk Imagery*
(see attached diagrams)

H = altitude of satellite = 900-950 km

R = mean radius of earth = 6,367 km

β = viewing angle of scanner with respect to nadir (max = 5.76°)
The plane of the scanner motion is now defined as perpendicular to the plane of the orbit

γ = angle of earth curvature involved (max = 0.83°)

f = effective focal length of scanner. Based on mirror size and F number this is 730 mm, however, this dimension is immaterial with respect to the projection.

N = nadir point

P = point on earth imaged by MSS sensor

Present MSS projection (space cylindrical strip perspective)

C = line on which scanned image is recorded. Panoramic effect of scanner has been corrected to provide a true to scale image of a flat earth as depicted by tangent plane T. When scanner and satellite motions are introduced the line C generates a cylinder at height $H + f$ above the spherical earth.

Assume scale factor at nadir = 1.00000 (tangent cylinder)

$$\text{Perspective cross-track scale at P} = M = \frac{H}{H+D} \cos \gamma = \frac{H \cos \gamma}{H+R(1-\cos \gamma)}$$

(dist. effect) (primary obliquity effect)

At max scanning angle $M = 0.99916$

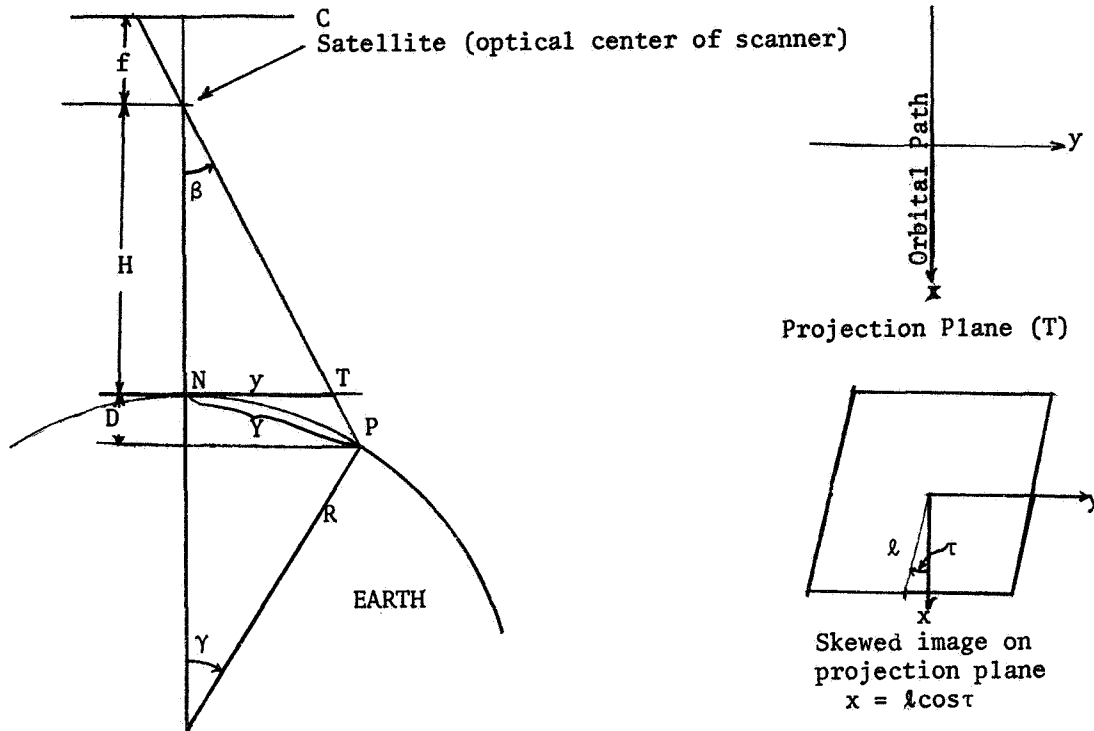
This cross-track scale varies from 1.00000 at nadir to 0.99916 at image edge.

In the along track direction the nadir point N and image point P at a fixed scanning angle (β) must describe lines on cylinder C (image) of equal length in order to provide the continuous image of the MSS. This condition requires that the along track scale at P must be larger than at N by an amount equal to the secant of γ . At maximum scan angle this along track scale equals the secant of 0.83° or 1.00011.

Projection is cylindrical and perspective in cross track direction only. One single projection (zone) maps the entire earth between the 82° parallels every 18 days.

*All figures given are approximations. NASA is expected to make available exact figures which might be required for rigorous computations.

Geometry of ERTS, MSS (orbital plane is perpendicular to this plan).



Let X = dist. along suborbital path on earth figure (stationary sphere)*
 Y = dist. normal to suborbital path on earth figure $Y = \gamma R$ *
 x = dist. on projection plane (cylinder) in orbital plane
 y = dist. on projection plane from orbital plane
 l = actual orbital path as imaged τ = skew angle (varies with latitude)

On present MSS projection:

$$x = X$$

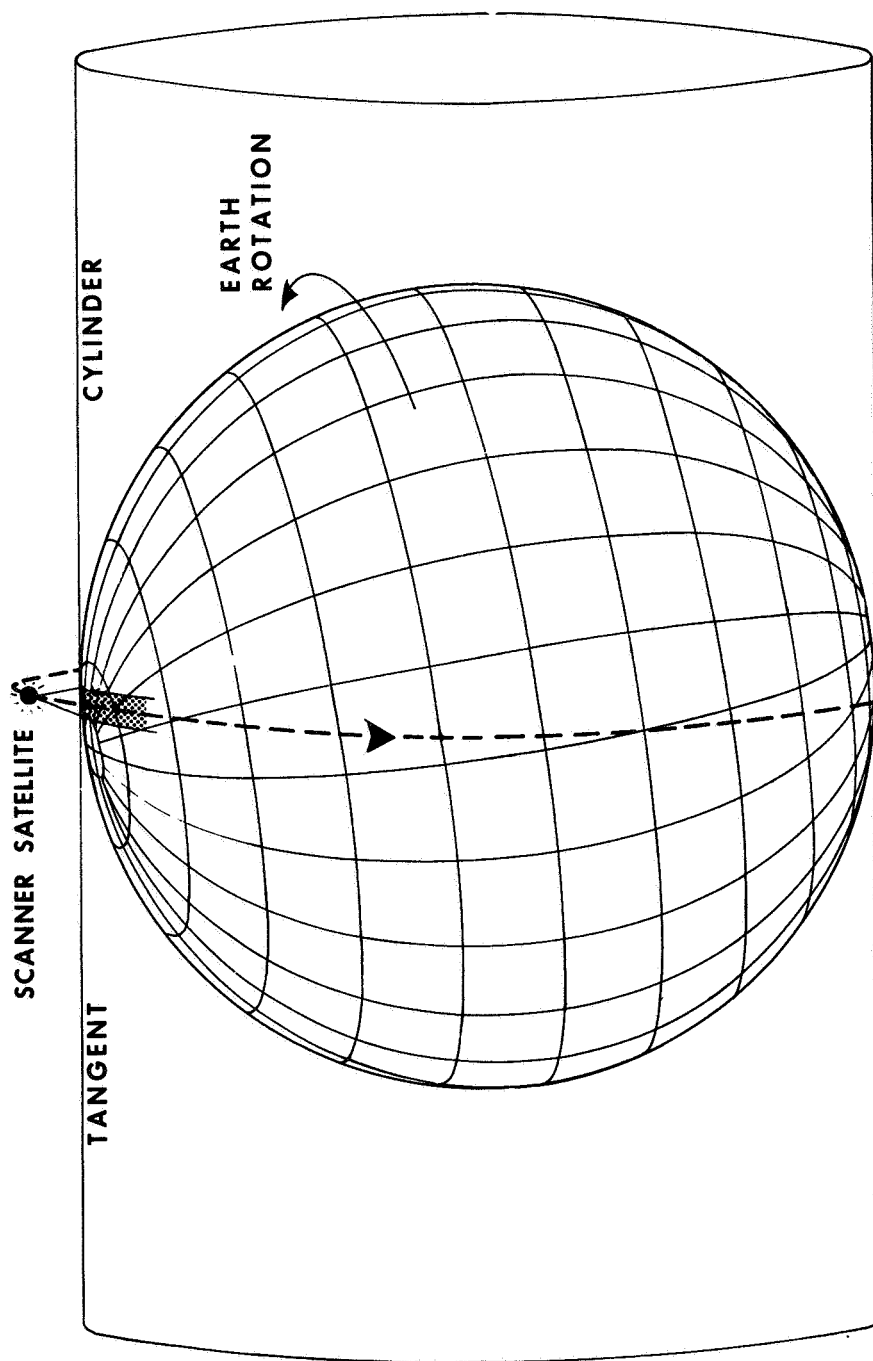
$$y = R \sin \gamma \left(\frac{H}{H + R(1 - \cos \gamma)} \right)$$

On recommended projection (Space Oblique Mercator)

$$x = X$$

$$y = R \int \sec \gamma \, d\gamma = R \log_e (\sec \gamma + \tan \gamma) = R \log_e \tan \left(\frac{\gamma}{2} + \frac{\pi}{4} \right)$$

*If one disregards the small error introduced by earth rotation during the scan sweep (The maximum displacement in the x direction is only about 200 m for the 185 km scan length), the y direction on the actual image is that of the scan lines (as now configured). However the x direction of the projection will be skewed on the image by as much as 4° with respect to the image orbital path, again due to earth rotation.



SPACE OBLIQUE MERCATOR PROJECTION

Images the Earth from N 82° to S 82° every 18 days

MOTIONS INVOLVED

- Scanner sweep
- Earth rotation
- Satellite orbit
- Orbit precession



7/73

**EARTH RESOURCES TECHNOLOGY SATELLITE DATA COLLECTION PROJECT,
ERTS - BOLIVIA**

Dr. Carlos Brockmann, *Geological Survey of Bolivia, La Paz, Bolivia*

ABSTRACT

The Earth Resources Technology Satellite program of Bolivia, under the direction of the Geological Survey, has developed a multidisciplinary project to carry out investigations in cartography and to prepare various thematic maps. In cartography, investigations are being carried out with the ERTS-1 images and with existing maps, to determine their application to the preparation of new cartographic products on one hand and on the other to map those regions where the cartography is still deficient. The application of the MSS images to the geological mapping has given more than satisfactory results. Working with conventional photointerpretation, we were able to prepare regional geological maps, tectonic maps, studies relative to mining, geomorphological maps, studies relative to petroleum exploration, volcanological maps and maps of hydrologic basins. In agriculture, the ERTS images are used to study land classification and forest and soils mapping. We use the ERTS images processed in black and white and in color, with Diazo film on a 23 x 23 cm format. We obtain 40% more information from the color composites than from the corresponding black and white images.

INTRODUCTION

The Bolivian ERTS Program began its studies in December 1972 with the arrival of the first images covering the Desaguadero River area, a portion of the primary test site area south of La Paz. Later, we received images from other zones of the country in an irregular and sporadic fashion and which has finally resulted in coverage of about 80% of the country (Fig. 1). Cloud cover problems, however, have reduced the useful coverage to about 50% of Bolivia (Fig. 2), mainly in the southwest. The eastern flanks of the Andes and certain orbits in which no data was taken must be obtained before coverage is complete.

*Text of report translated by W. D. Carter, EROS Program, USGS.

1 N74 30744

PRECEDING PAGE BLANK NOT FILMED

In consideration of the importance of the information that would be provided by ERTS images, a thematic multidisciplinary program was developed which includes cartography, geology, agriculture and hydrology.

Cartography

The objective of the cartography program is to evaluate the use of ERTS-1 bulk images and to study their applications in developing a photoimage map of Bolivia at a scale of 1:1,000,000. A study was undertaken to compare the ERTS images with World Air Navigation Charts (ONC 26-27), taking into consideration the following parameters:

- a. Displacement of coordinates of the ONC maps with reference to the ERTS images
- b. Drainage patterns
- c. Drainage density
- d. Width and variations in the courses of the rivers
- e. Drainage divides
- f. Representation, form and extension of lakes and lagoons
- g. Mountain ranges, volcanoes, shape and extent
- h. Direction of mountain ranges
- i. Snow fields
- j. Salars and other closed basins
- k. Zones of moist soil and flooded areas
- l. Plains, form and extent
- m. Cultural features, highways, railroads
- n. Zones covered by vegetation

The study was done using 11 bulk images (nos. 1010-14033, 14035, 14042; 1065-14091; 1100-14034; 1099-13591; 1008-13531 and 13524; 1045-13570; 1153-13583 and 1045-13563) and resulted in identifying 128 important discrepancies with existing maps. We determined that ERTS images provided cartographic information in sufficient detail to prepare small-scale photoimage maps. As a consequence of this work, we proceeded

to prepare an experimental space photomap of the Sucre area using a bulk processed image no. 1008-13522-1 from the Return Beam Vidicon (RBV) system (Fig.3). The experimental space photomap, published at a scale of 1:250,000, was prepared by the Instituto Geografico Militar (IGM), our national map making agency. They determined the cartographic control points, photo-identified cartographic details, prepared the U.T.M. grid system and printed the map using a color intensification system.

Considering the need that exists in our country for a new national map, this same organization recently published the "Preliminary Map of Bolivia" at a scale of 1:1,000,000 on a Lambert Conformal Conical Projection (Fig. 4). The publication was a result of these studies and field work which began in 1948.

It must be pointed out that north of parallel 16°S, there is very little and sporadic aerial photography. It was therefore necessary to rely heavily on several images from the ERTS/ Bolivia project to bring up to date existing information on the representation of rivers, lakes, lagoons, and other cartographic features that were not found on existing maps. The images used in this revision were nos. 1191-14055, 14082, 14084; 1045-13563 and 13570; 1007-13445; 1005-13341; 1111-13243; and 1006-13411 (Fig. 5).

These images were only partially used because we found coordinate displacements up to 10km, and this impeded their complete utilization.

Recently we received a precision processed image (no. 1010-14032) which covers an area where adequate cartography exists. This image is under study for the preparation of a new photoimage map which will help us determine how to use this type of product to prepare a new map of Bolivia.

Geology

Among the basic objectives of the geologic investigations project we are undertaking several different thematic studies, among which are regional geologic mapping, tectonics, mineral resources, geomorphology, petroleum exploration, volcanology and so forth.

a. Regional Geologic Mapping:

To determine the application of ERTS images to regional geologic mapping, we examined the four bands of the multispectral system to determine which of them is most useful for the extraction of geologic information. These

studies have indicated that, in general, band 7 provides the best information in the high plains (Altiplano), the western and eastern cordilleras, but that band 6 of the MSS is best for the chaco plains of the Beni River region.

We also attempted to determine the volume of information that could be extracted from color composite images in comparison with images processed in black and white by making transparent overlays of the respective scenes. We found that the color composites provided at least 50 percent more information.

In general, we have been able to indicate geomorphologic criteria, drainage, and tonal patterns and identify large lithologic units with great precision. We have also prepared geologic structure maps (Fig. 6) in which we have been able to extend known north-trending faults and structural lineaments. More significant, however, is the mapping of W-E and NW-SE lineaments identified for the first time on ERTS images and checked in the field. These correspond to fractured zones 50 to 100 meters in width, where normal and overthrust faults of small displacement occur.

In view of the excellent results obtained from ERTS images, we are now considering preparation of a new Geologic Map of Bolivia at a scale of 1:1,000,000. At the same time we also plan to use them to prepare geologic maps of the country at a scale of 1:250,000.

b. Tectonics:

Recently the Geological Survey of Bolivia in cooperation with the University of San Andrés, Department of Geosciences, published the first tectonic map of the country, based on existing information and without taking into consideration ERTS images. It is now obvious that this map will have to be corrected on the basis of preliminary interpretations that have revealed new tectonic elements that have never before been recognized. (Fig. 7).

Under this subproject we will include a map of the epicenters of the principal seismic movements and attempt to determine their relation with lineaments identified in the ERTS images.

- c. Studies of mineralized zones:
To evaluate the applications of ERTS images in the study of mineralization in Bolivia, we are making a compilation of all previous mineral resource studies. This work, being done on geologic maps published at a scale of 1:250,000, consists of plotting known mine locations and other information. Once this is compiled we plan to correlate it with existing aeromagnetic surveys and geologic interpretation of ERTS images with the objective of studying the relationships that may exist between them.
- d. Petroleum Exploration Subproject:
The petroleum exploration subproject is attempting to delineate those areas that appear to be appropriate for the accumulation of hydrocarbons in known petroliferous provinces and to define new areas for exploration. We will also attempt to evaluate new basins found as a result of this study.

In a morpho-structural interpretation of images covering the chaco-plain of the Beni River region, also known as the Lake Rogaquado region, lakes and lagoons not previously shown on any maps, show rectilinear shorelines with orientations of N43-68E and N21-45W which appear to be influenced in response to trends of the Brazilian Shield. From this, we deduced that the northeast sector is underlain by crystalline shield rocks and the limits of which are found in the Mamora River valley. This corresponds to a central zone covered by a thick sequence of Quaternary alluvial sedimentary deposits where there is persistent preferential orientation of the lakes, lagoons and rivers. This indicates a marked influence of the crystalline basement over the younger features (Fig. 8).

At exploration wells, La Esperanza and Peru drilled by the Shell-Bolivia Oil Company, it was determined that in this general area Quaternary sedimentary rocks 441 to 812 meters thick rest directly upon crystalline rocks of the Brazilian Shield. With the interpretation of ERTS images it is possible for one to determine that the most important area for petroleum exploration is restricted to the southwest sector, where there is a possibility of finding structural and stratigraphic traps.

In the interpretive work comparing conventional aerial photographs (scale 1:40,000) and ERTS images in the area of the Madre de Dios River, it was found that the rivers

are influenced by a marked structural control. We determined that there are probable anticlinal structures and lineaments oriented principally in NE-SW and NNE-SSW directions. There are also other less important linears oriented NW-SE and which are probably related to faults and fractures (Fig. 9). As a result of this comparative study we were able to determine that the ERTS image provided 40% less than that obtained from conventional methods, probably due to factors of scale (1:1,000,000).

e. Geomorphology:

The objective of this subproject is to prepare the first geomorphologic map of Bolivia, with the idea of applying this information to 1) determine the locations of possible secondary mineral resources (alluvial placer deposits), and 2) in civil engineering to assist the construction of highways and other civil works projects, and 3) in hydrology, to determine ground water basins.

In a general way, we are attempting to interpret land forms and land forming processes. For example, it is possible to distinguish features formed by diastrophism as homoclines, synclinal valleys and volcanism and where destructional forms such as volcanic collapse, borders of calderas, craters and parasitic cones are identified by their typical forms. Depositional forms are related to eruptions along fissures from which have come deposits of ignimbrites and basalts and andisites from central eruptions. Between these processes and distinctive forms we have distinguished intermediate features such as block lava fields (being a constructional colluvial shape) and mapped forms of fluvial and fluvio-glacial origin (Fig. 10).

f. Volcanism:

With the advent of space images providing large areal coverage the first map of the volcanology of Bolivia was planned with the objective of determining the points of origin of pyroclastic rocks and their regional distribution; to map volcanic structures and delimit the rocks of volcanic origin.

The example presented here (Fig. 11) corresponds to the area of the Salar de Coipasa, where we have differentiated basaltic lavas and ignimbrites (welded tuffs) from the rest of the volcanic rocks, the latter being light gray in tone and folded and, therefore, considered to be oldest

of the volcanic sequence (B). The ignimbrites were recognized by their grayish green tones and generally smooth surface while the basaltic lavas are dark in tone and rough textured. This rock group are considered to be of Miocene age on the basis of existing information.

Ignimbrites of Paleo-Pliocene age (c) are localized primarily on the southwest flank of the Andean Cordillera near the Chilean coast. Strato-volcanoes of Pleistocene-Holocene age are variable in development and extension but are recognized by their well preserved craters. Composite volcanoes are recognized by craters that are in various stages of collapse or destroyed by later activity. Calderas have a half-moon shape and notable changes in relief with scars left by collapse that were later filled by the emplacement of new cones and volcanic debris.

g. Structural Geologic Studies:

All of the above studies have clearly demonstrated that ERTS-1 images can best be applied to structural geologic mapping. With its broad areal coverage, it is possible to obtain regional information on the tectonic grain and other structural elements such as folds, faults, fractures and lineaments. In the Coipasa image, where the area is largely volcanic and the lithology is similar, it was impossible to obtain much detailed information on folding, but we did identify a large synclinal area in the northeast part of the image (Fig. 12).

Lineaments with trends dominantly NW-SE, E-W and NE-SW are most abundant and were identified on the basis of truncation or changes in strike of the sedimentary strata, sharp changes in geomorphology, lineation of morphologic features, and appreciable displacements. These criteria are believed to be associated with and indicative of large faults of significant offset. Other lineaments of less significance are probably related to fracture systems.

Agriculture

a. Soils:

Image interpretation of soils was conducted mainly in the western part of the country, principally in the western cordillera, the altiplano and the central sector of the eastern cordillera of the Andes. We have also done some work in the Beni River plain using black and white images at a scale of 1:1,000,000. In the Beni River area we

were able to determine the amount of information acquired from black and white images as compared to that acquired from color composites. We determined that we got 40 percent more information from color and for this reason we are now processing all ERTS data in color, using the Diazo process.

Because of the small scale (1:1,000,000) we are mapping only the major soil units and their principal subdivisions. They are distinguished by their color tones and physiography as expressed in the color composite images, processed in black and white as shades gray in bands 4, 5, and 7 from the MSS system.

To illustrate the types of information acquired by interpretation of image no. 1045-13563 processed in black and white and in color please refer to table 1. It was possible to identify the following list of features:

- 1) Natural dikes
- 2) High swamps
- 3) Dry areas
- 4) Low swamps with lake sediments
- 5) Alluvial plains alternating with high meadows
- 6) Dry alluvial plains
- 7) Alluvial plains, occasionally flooded
- 8) Abandoned meanders
- 9) Alluvial plains, frequently flooded

As a result of the excellent results we have obtained in these studies the ERTS/Bolivia Program is now planning to make a soils map of the entire country at a scale of 1:250,000, as soon as we have complete cloud-free coverage.

b. Forestry:

As in the soils mapping subproject, the fundamental objective is to make the first forest map of the country using ERTS-1 images. Unfortunately, most of the available coverage is in western Bolivia where there are few forests. Interpretive work is restricted to the sub-andean hills and chaco plains of the Beni River valley where a few images without cloud cover have been acquired.

Table 1: Table showing hydrologic analysis of ERTS-1 images compared to World Aeronautical Charts (ONC), 1:1,000,000 Scale

Type of Image: MSS		Number of Image: 1045-13563	Location: Lake Rogaguado	
<u>No. of Observation</u>	<u>ERTS Image</u>	<u>World Navigation Chart</u>	<u>Evaluation Image</u>	<u>Map</u>
A-102	Displacement of X and Y coordinates	Displacement of X and Y coordinates	X	X
B-103	Shows excellent drainage patterns.	Drainage pattern deficient. No information on river flood plains.	XXXX	X
C-104	Provides good data on drainage density.	Drainage densities incorrectly represented.	XXXX	XX
D-105	Representation of width and shape of river is realistic.	Widths of the Mamori, Yacuma and Endere Rivers exaggerated. Shapes not realistic.	XXXX	X
E-106	Drainage divides easily defined.	Drainage divides not indicated.	XXX	X
F-107	Large and small lakes clearly indicated faithfully, as are shape, extent, and geographic position; also humid areas related to phenological changes.	Principal lakes are partially shown. Generally not in the correct place. Density of lakes is poor. Small lakes and ox bow lakes are not shown. Forms of lakes are very generalized and dimensions almost always incorrect.	XXXX	XX

<u>No. of Observation</u>	<u>ERTS Image</u>	<u>World Navigation Chart</u>	<u>Evaluation Image</u>	<u>Map</u>
G-108	Wet (humid) and dry zones shown faithfully.	Wet zones not shown.	XXXX	X

Key:
~~XXXX~~ Excellent
 XXX Good
 XX Average
 X Deficient



1) Map showing total ERTS-1 coverage of Bolivia

The study thus far completed was done on images 1045-13563 and 1191-14084, corresponding to the Lake Rogaguado and Madre de Dios river areas respectively. Figure 13 represents a preliminary interpretation after evaluating the bands of the MSS system.

The key to this preliminary image interpretation is based on the relationship of physiography and forest formation according to characteristics of tone and texture presented in images from bands 4, 5, 6 and 7. In this manner the following preliminary legend was developed:

- 1) Tropical forests
 - 1.1) Low swamps forest
 - 1.2) Low terrace forest
- 2) Tropical forests of the high plains and hills
 - 2.1) Terrace forest
 - 2.2) Hill forest
 - 2.3) Forest in wet valleys
- 3) Subtropical forests of highland regions
 - 3.1) Forests on steep slopes
 - 3.2) Forests of the high plain zone

Special Formations

S - Savannah vegetation

SH Savannah - wetland herbs (pampas)

Sa Savannah - dry herbs (pajonales)

Sar Savannah - low crown trees

Sb Savannah - high crown trees (galeries)

P - Pantano (open areas with dammed water bodies)

PB Open forests

Y - Areas where human influence is visible; clearings, plantations, etc.

Because of the lack of information that exists in the country where this study was undertaken, it was not possible to make a comparative study to evaluate these results. Nevertheless, we plan to evaluate future work of this type where aerial photography exists in zones covered by ERTS images.

Hydrology

Because Bolivia has no relatively precise map of its hydrography, it was necessary to plan the development of this hydrographic subproject with the objective of establishing the hydrographic net of the country and delineating the principal basins and sub-basins. By interpretation of ERTS images it has been possible to determine the different types of drainage patterns; where the principal rivers are clearly

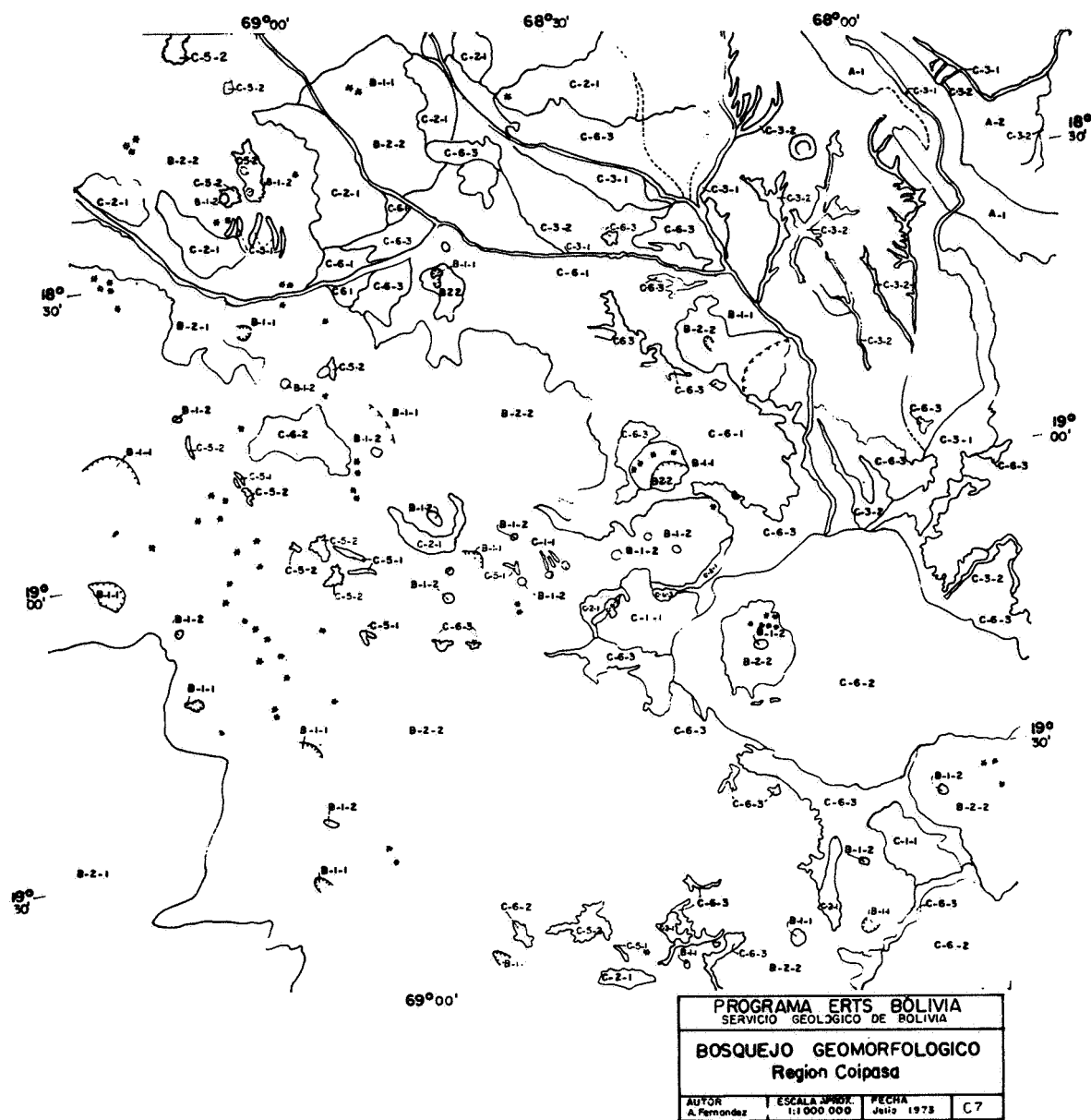
defined it has been possible to identify tributaries of fourth order (Fig. 14).

It is interesting to note that the specular reflectance of lakes and lagoons (not represented on any of the existing maps) are clearly defined and on the basis of tone, indirectly reflect their relative depth and degree of turbidity. It is clear that an appropriate hydrologic application of ERTS-1 images is the selection of adequate points for measuring water levels and stream flow, selecting dam sites, diversion structures and reservoirs and to determine areas where ground water resources are most likely to occur.

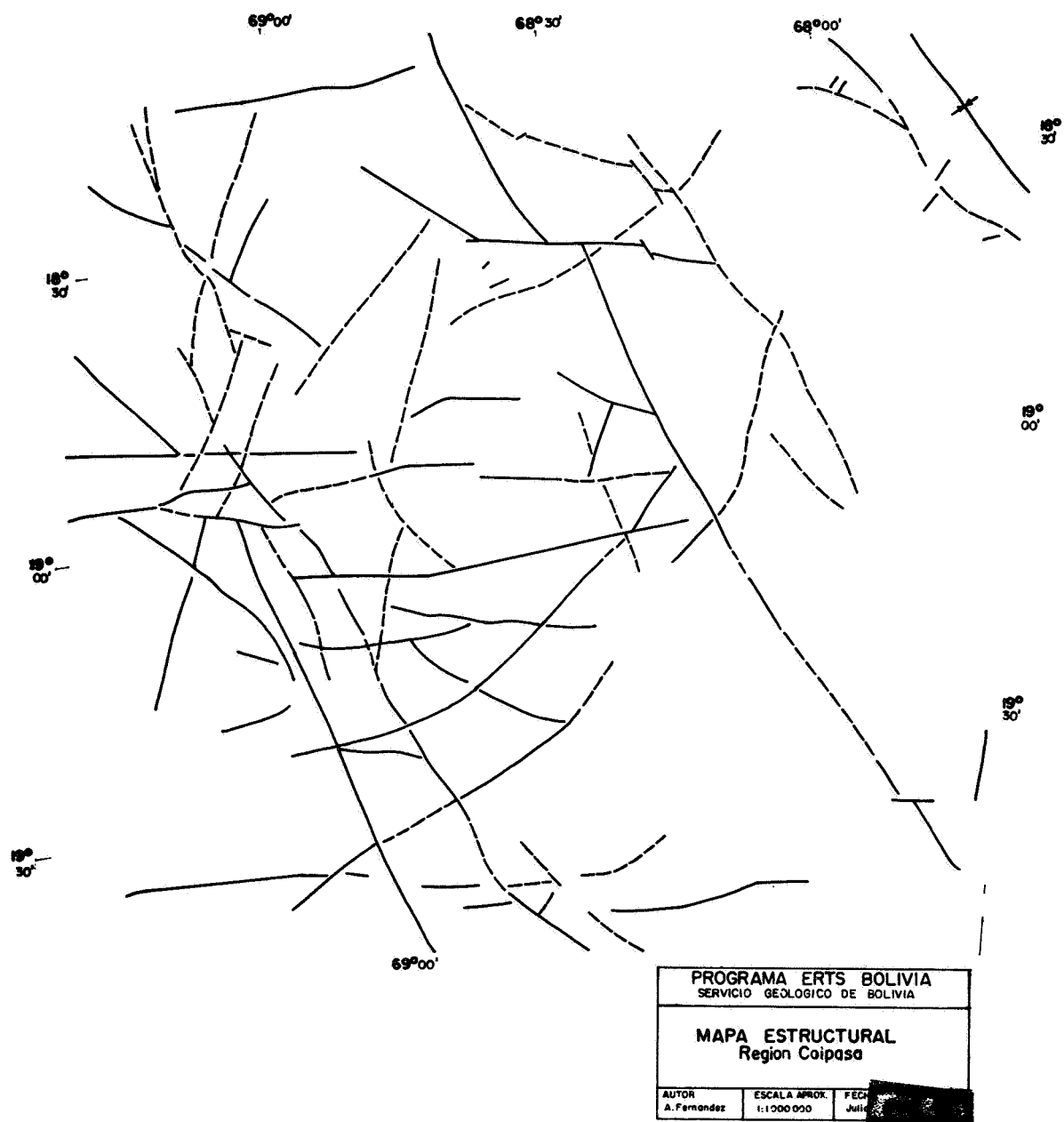
An immediate result of this investigative program, using image number 1010-14035, trellis drainage was observed and believed to be caused by zones of weakness related to fault zones. Centripetal drainage appears as an anomaly related to a collapse crater; irregular arcuate drainage appears to indicate areas of infiltration; anastomosing drainage patterns appear to indicate areas of little relief in the zone; radial drainage patterns indicate volcanic structures; and subparallel drainage patterns indicate the presence of ignimbrites. Many of the rivers have courses oriented in very definite directions which we postulate are controlled by fault traces.

References

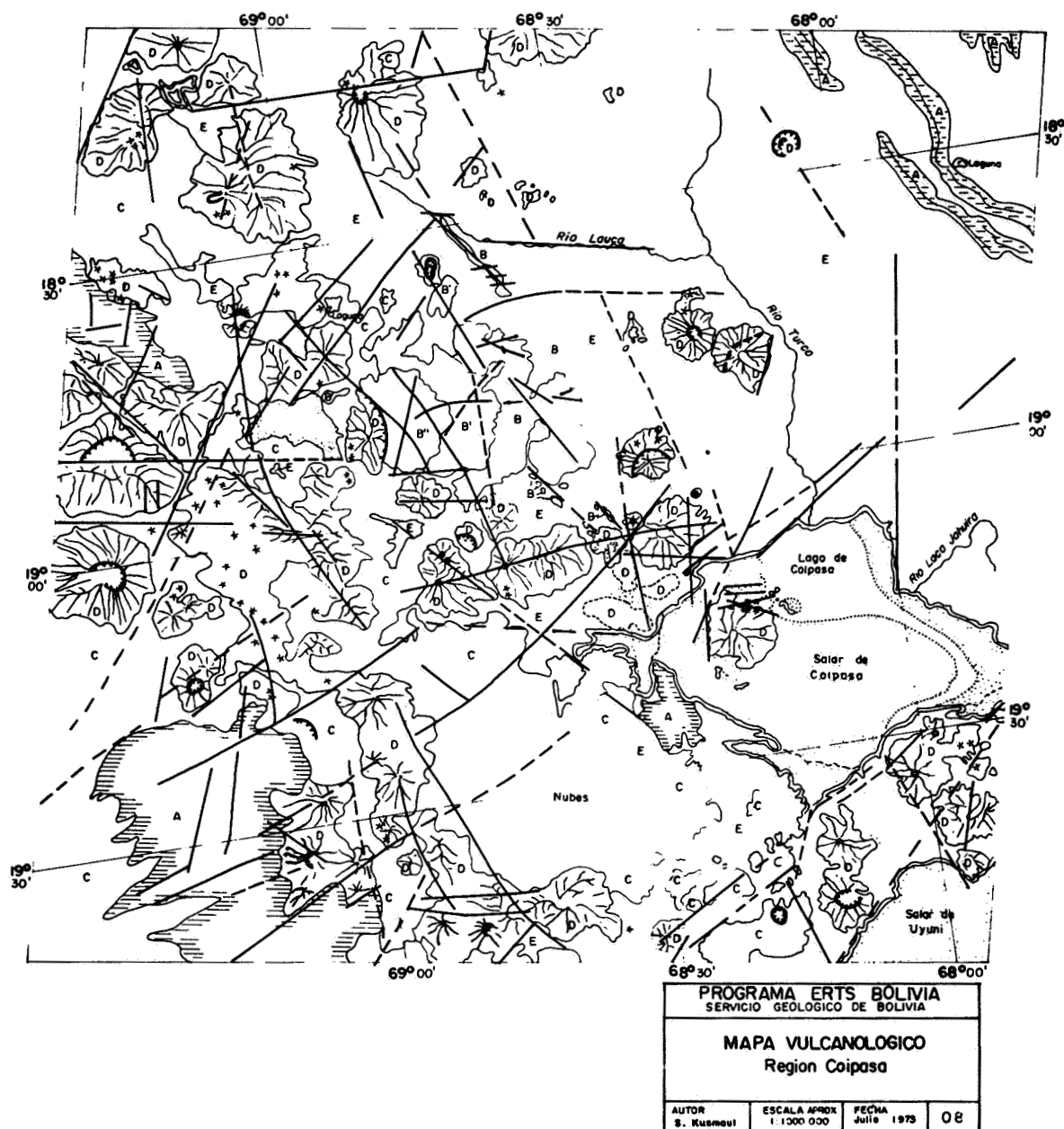
- Ballón Agllón, Raul, 1973, Regional Geologic interpretation of ERTS images, Western Region of Bolivia: Sub-Programa Geologia Regional, Programa ERTS/Bolivia; Servicio Geologico de Bolivia, La Paz, Bolivia, 8 p.
- Brockmann, Carlos E., Fernández C., Alvaro and Plaza Martinez, Basilio, 1973, Application of ERTS images to Cartography and Geology: Programa ERTS/Bolivia Servicio Geologico de Bolivia y Instituto Geografico Militar de Bolivia, La Paz, Bolivia, 12 p. 8 figs.
- Fernández, C., Alvaro, Aranibar R., Oscar and Ballón A., Raul, 1973, Application of ERTS images to Geologic Mapping: Programa ERTS/Bolivia; Servicio Geologico de Bolivia, La Paz, Bolivia, 5 p., 8 figs.
- Ilijic G., Mateo, 1973, Preliminary Study of the Salar de Uyuni and Coipasa Region: Sub-Programa Hidrologia; Programa ERTS/Bolivia; Servicio Geologico de Bolivia, La Paz, Bolivia, 4 p.
- Kussmaul, Dr. Sicfried, 1973, Volcanologic interpretation of the southern part of the Western Cordillera of Bolivia, using ERTS images; Sub-Programa Vulcanismo; Programa ERTS/Volivia; Servicio Geologico de Bolivia, La Paz, Bolivia, 8 p.
- Suarez, M., Milton, 1973, Geomorphologic Sketch Map of the Western Region of Bolivia, using ERTS Images: Sub-Programa Geomorfologia, Programa ERTS/Bolivia; Servicio Geologico de Bolivia, La Paz, Bolivia, 5 p.



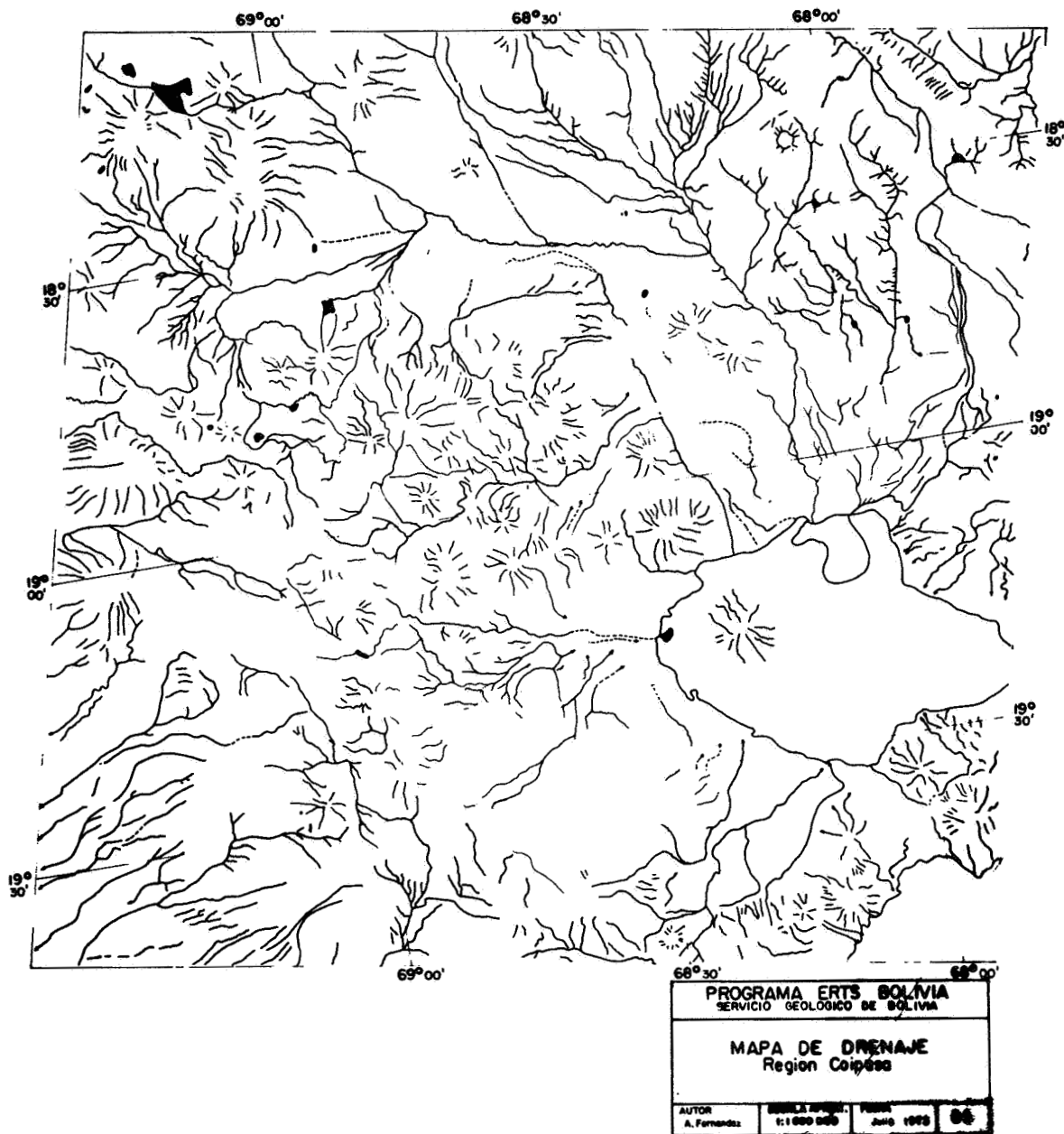
2) Map showing cloud-free ERTS coverage of Bolivia



- 3) Experimental photoimage map of the Sucre area, scale 1:250,000



- 4) 1973 map of Bolivia, scale 1:1,000,000 based on improvements provided by ERTS-1 images



- 5) Annotated ERTS image used in revising national map of Bolivia

AN OPERATIONAL APPLICATION OF ERTS-1 IMAGERY TO THE ENVIRONMENTAL INVENTORY PROCESS

James D. O'Neal and James R. Bwins

The organization which I represent, The Engineer Agency for Resources Inventories, is an element of the U. S. Army Engineer Topographic Laboratories. My agency is concerned primarily with the application of new technologies to current problems relating to environmental analyses in both civil and military functions of the army. We do this in the course of conducting studies aimed at specific user requirements. We have performed these kinds of services for \ numerous organizations within the Department of Defense, Department of State (Aid) and others, since our establishment in 1963, originally as an element of the office, Chief of Engineers. Experience gained during the past 10 years in supporting the USAID Foreign Assistance Program, in various developing nations overseas, with environmental resources assessments, has more recently been applied to domestic requirements of the Corps of Engineers. Over the past two years we have been conducting an environmental inventory program in support of civil works elements of the Corps. The earliest results of these efforts were reconnaissance inventories of Vermont, Washington, North Carolina, and the Charleston Engineer District. These were pilot studies to investigate the feasibility and desirability of a nationwide program. Their objectives were extremely narrow, involving primarily the earliest stages of project planning, and they dealt with only the most significant resources and amenities of the environment that should be approached with careful deliberation.

A more recent effort, which I plan to discuss today, is an in-depth inventory of substantially broader scope, aimed at providing basic input data for the preparation of environmental impact statements. This is a study of south Louisiana, with emphasis on the Atchafalaya basin, prepared on behalf of the New Orleans engineer district. The first Figure is a photograph of the cover of the study. The South Louisiana area includes a number of projects for which EIS's must be prepared. A single, overall inventory permitted a systematic approach and, we believe, substantial economy as compared with what the cost would be for separate inventory efforts for each project. The study area covered approximately 25,000 square miles and included all or part of 36 parishes in Louisiana and 8 counties in Mississippi.

Presented at the Third ERTS Symposium, Washington, D.C., 12 December 1973, by James D. O'Neal, Acting Chief, Engineer Agency for Resources Inventories, USAETL.

N 74 30745

The chief application of remote sensing in this study was in the mapping of land use and vegetative cover for publication at a scale of 1:250,000. This involved parts of 8 quarter-million-scale quadrangles of the national map series. The categorization used was based on the classification, to second level, developed by the inter-agency steering committee on land use information and classification, published in USGS circular 671. This classification scheme is shown in Figure 2.

Our application of remote sensing technology in this effort was necessarily very conservative. Quite literally, our results would have to be able to "stand up in court", and only techniques of proven reliability could be used. This argued strongly for conventional exploitation of aerial photography and full use of ground truth and other available collateral data. The aerial photography available for most of the study area was 1:62,500-scale and 1:120,000-scale color and color-infrared imagery provided by NASA. Figure 3 is an example of this coverage. Our experience, and that of other agencies, indicated that the compilation effort by conventional means would require about 36 man-weeks. This created a definite problem because the allocation of effort available for this phase of the study was only 20 man-weeks, in a total elapsed time of 2-1/2 months. It was therefore decided to search for means of employing ERTS-1 imagery, illustrated by this next figure, showing coverage of most of the study area, to achieve substantial savings of time in a hasty operational mode. Experiments were conducted subject to two ground rules: first, while degradation in locational precision was permissible, the amount had to be known and controllable; and second, category identifications had to be accurate and directly verifiable without lengthy testing and evaluation. These ground rules dictated that ERTS imagery be used as a supplement to airphotos and collateral data, rather than as a source.

The experimentation was in two phases: single-band operations using Band 5 imagery, and multiband operations using false-color composites of Bands 4, 5, 6 and 7. Both operations were limited to the use of film-chip imagery. Under limitations of time and resources we did not undertake any processing of computer-compatible tapes. However, during our next study we plan to extend our experiments into this area.

The single-band operations addressed the problem created by intricate "salt and pepper" patterns of woodlots and clearings, as shown by Figure 5, which were particularly common in the terrace uplands of the study area. In our judgement, the degree of detail observable on the airphotos was excessive, both from the viewpoint of information requirements, and from the standpoint of publication scale. We recognized that the analyst could readily become bogged down in this intricate detail. To keep compilation time and effort manageable, it was essential to find some objective means of controlling the level of detail. ERTS

Band 5 imagery such as that shown in Figure 6, was found to exhibit very nearly the exact level of detail desired. It further appeared that, in the "salt and pepper" areas, delineation from ERTS of the single boundary between forest and open areas would result in completion of the major part of the total line work required for a complete land use map.

We devised two separate experimental approaches for exploiting the ERTS imagery. Both approaches provided for the use of aerial photography to correct gross errors and to make final identifications of categories.

The first approach was a sequential process. One analyst drew all boundaries between forest and open areas on a 1:250,000 scale black and white print of the Band 5 image. His sole source of information was the print itself. The print was developed in high contrast to minimize decision time. The Figure you are looking at was made from such a print. The completed boundaries were enlarged to 1:120,000 scale for use as overlays to the airphotos by two separate teams in succession. The first team worked entirely within the forest areas, classifying to the second level (evergreen, deciduous, and mixed) by adding appropriate symbols and, in relatively few areas, internal boundaries. The second team worked entirely in the non-forest areas, classifying urban, agricultural, and nonforested wetland categories to second level. Both teams were charged with correcting registry errors in the original forest boundary that were beyond acceptable limits - approximately 1/4 mile ground distance. Both teams were also charged with correcting gross errors resulting from misidentification of forest on the ERTS print. This occurred chiefly in residential areas having numerous trees: areas which appeared as forest on the high-contrast ERTS print. This assembly-line process allowed a maximum application of specialized skills to the land-use mapping process. Interpreters trained in forestry, and equipped with the best collateral data on forest types, made the final forest classifications. Interpreters trained in cultural geography and equipped with the best collateral data on urban and farm land use, made the final urban and agricultural classifications. The greatest difficulty of this approach was in coordinating the correction of gross errors.

In our second experimental approach during the single-band phase of operations, one analyst was assigned responsibility for all aspects of land-use mapping within a defined portion of the study area. He used airphotos and collateral data as sources, and a print of ERTS Band 5 enlarged to 1:250,000-scale as his plotting base. The ERTS print was in normal gray tones, rather than high contrast, to permit maximum recognition of detail. Again, most of the land-use delineations were related to features visible on the ERTS print. As a result, most of the delineation could be done effectively by "eyeballing". A relatively few cases involved boundaries unrelated to features visible on the ERTS. In these cases, boundaries were first drawn to an overlay to the photograph and then projected

onto the ERTS base. After land-use mapping was completed to the second level of classification, the annotated ERTS print was turned over to the drafting staff for transfer to the 1:250,000-scale topographic map base. The fit was good. Horizontal control, and frequent checks on locational accuracy, were possible because of the many features, including roads, streams, shorelines, and small urban centers, that were visible on the ERTS image.

While this second approach avoided coordination problems and bottlenecks, because the work of multiple analysts was in parallel rather than in series, it lacked the capability of the first approach for a continuing quantitative check on locational accuracy. And it required broader expertise on the part of the interpreter. For these reasons, we consider it inferior to the first approach. It was in fact employed only in those parts of the study area where external considerations related to security classification of collateral source data warranted its use.

The second phase of experimentation involved multiband operations with ERTS imagery. Our initial investigations were broadly based, concerned with the potential not only for land-use mapping but also for identifying vegetation stands significant as wildlife habitats, water turbidity and shoreline configuration in areas of rapid sedimentation, and significant soil and soil-moisture variations. Using the I²s additive color viewer, illustrated in Figure 7, composite images were put through various configurations of filter and illumination. Each configuration was selected to enhance one or more particular elements, and was recorded photographically to give the analyst a hard copy for annotation and transfer to the base map. As an example, the Figure 8, covering parts of the Mississippi River Delta, shows a configuration used to enhance water turbidity patterns in an area of rapid sedimentation. It also provides good discrimination between cropland and forests. Next, Figure 9, located immediately north of the preceding one, is configured to enhance forest distributions and it permits good differentiation between bottomland hardwoods and upland hardwood-softwood associations. Agricultural land use is also readily visible, and distinction within these is made between terrace soils (in the north central area) and recent alluvial bottomland soils. The results of some 20 or 30 configurations were tabulated in this manner for future reference as shown in Figure 10. Prior to these experiments we had reviewed similar work and recommendations by other investigators. For the south Louisiana area with which we were concerned, we arrived at configurations which we preferred for our specific elements of interest.

As we focused more sharply on the specific data gaps and operational problems of the study, it was decided to emphasize one particular application of the multiband operations — that of distinguishing evergreen and deciduous forest in

areas where color and color infrared aerial photography were lacking. This composite, shown in Figure 11 using October 1972 ERTS imagery, renders a sharp color contrast between the two forest types, which was verified by detailed national forest maps covering part of the imaged area. The print was made at approximately 1:1,000,000-scale with the use of a film pack inserted in the holder of the I²s viewer.

Various means are readily available for transfer of this information to a base map. Our own preference for this operation is the B&L (Bausch & Lomb) zoom transfer scope, shown in Figure 12, an instrument based on concepts originally developed by the engineer topographic laboratories.

In our atchafalaya study, the overall land-use compilation was completed during a 10-week period with a total interpreter effort of slightly more than 19 man-weeks. Considering the area covered and its complexity in the light of previous experience by our agency and others, it appears that there may be as much as a 45 percent savings in effort as compared with conventional utilization of high-altitude aerial photography. With respect to identification of categories, no compromise has been made with the best available results of airphoto interpretation, supported by collateral sources. With respect to detail and locational accuracy, the product is undeniably an expedient effort. It can be considered only for applications tolerating accuracies of, say 80 to 90 percent of all lines within plus or minus 1/4 mile. But for such applications, the method deserves consideration because of the real economies achievable.

I will spend the last few minutes in putting this effort into perspective with the overall product to which it contributed. This is an environmental inventory document designed primarily to provide basic input data for the preparation of environmental impact statements of a sizable number of Corps projects in the south Louisiana area. We believe that a broad integrated study such as this permits a systematic approach and an economy of scale not possible with separate, project-by-project inventories. The first and most direct contribution of this effort to the inventory is a series of eight 1:250,000-scale quadrangles treating land use, one of which is shown on Figure 13. The following Figure 13a is an enlargement of the NE corner of the graphic for greater detail. These maps permit the identification of land use types within a specific project area, and the determination of approximate acreages of each. The next Figure, 14, a shot of the 1:500,000-scale vegetation map from the study, permits further analysis of the forest, marshland, and cropland areas.

With the aid of collateral data supplied in the supporting text of the map, it is possible to make some estimate of the associated rare species, the sensitivities and vulnerabilities of the plant communities, and their value in both economic and ecological terms. This is illustrated by the next 4 figures. The type

size of this Figure of a complete page of text on Flora is too small for you to read, but it shows the format: the following 3 Figures are enlargements on which we may be able to read the headings. The next Figure shows type, predominant species, and associated rare species; the next Figure, significance of the principal vegetation types including value to wildlife; and, the next Figure, sensitivity.

Further analysis and interpretation in the light of ecological data allows the recognition of major ecosystems and some quantitative estimates of their wildlife carrying capacities as illustrated in Figure 16. For example, the coastal marsh system of Louisiana (one of the ecosystems portrayed on the map) is known to support approximately 13 to 18 muskrat nests per 100 acres early in the year, and 6 to 14 late in the year. It also supports a significant alligator population, and is a breeding ground for numerous bird species, some of which are rare or very rare. Bottomland hardwood forests (another ecosystem treated) can be described in terms of numbers of deer, squirrel, swamp rabbit, turkey, wood duck, and migrant waterfowl that can be supported per unit area.

In summary, ERTS has taken a useful place as one of many tools we require to produce a comprehensive environmental inventory. In the overall study contents shown here on my last figure, we have so far made application of ERTS to those items which are outlined. In subsequent studies we plan to explore further applications in the areas of geomorphology and surface drainage. Because our applications are operational, and high-volume, we must continue to be conservative and to use readily verifiable procedures.

To conclude — as a supplementary source, used in conjunction with air-photos, ERTS has proven itself to us as a significant means of economy. As a primary source, we are not yet ready to accept ERTS for our own particular applications; but we believe that through digital tape processing experiments, some objective evaluations can be made, and this is the way we hope to move in the near future.

PHOTOINTERPRETATION OF ERTS-A MULTISPECTRAL IMAGES ANALYSIS OF VEGETATION AND LAND USE FOR THE VALENCIA LAKE BASIN REGION

F. Salas, M. Pineda, A. Arismendi

ABSTRACT

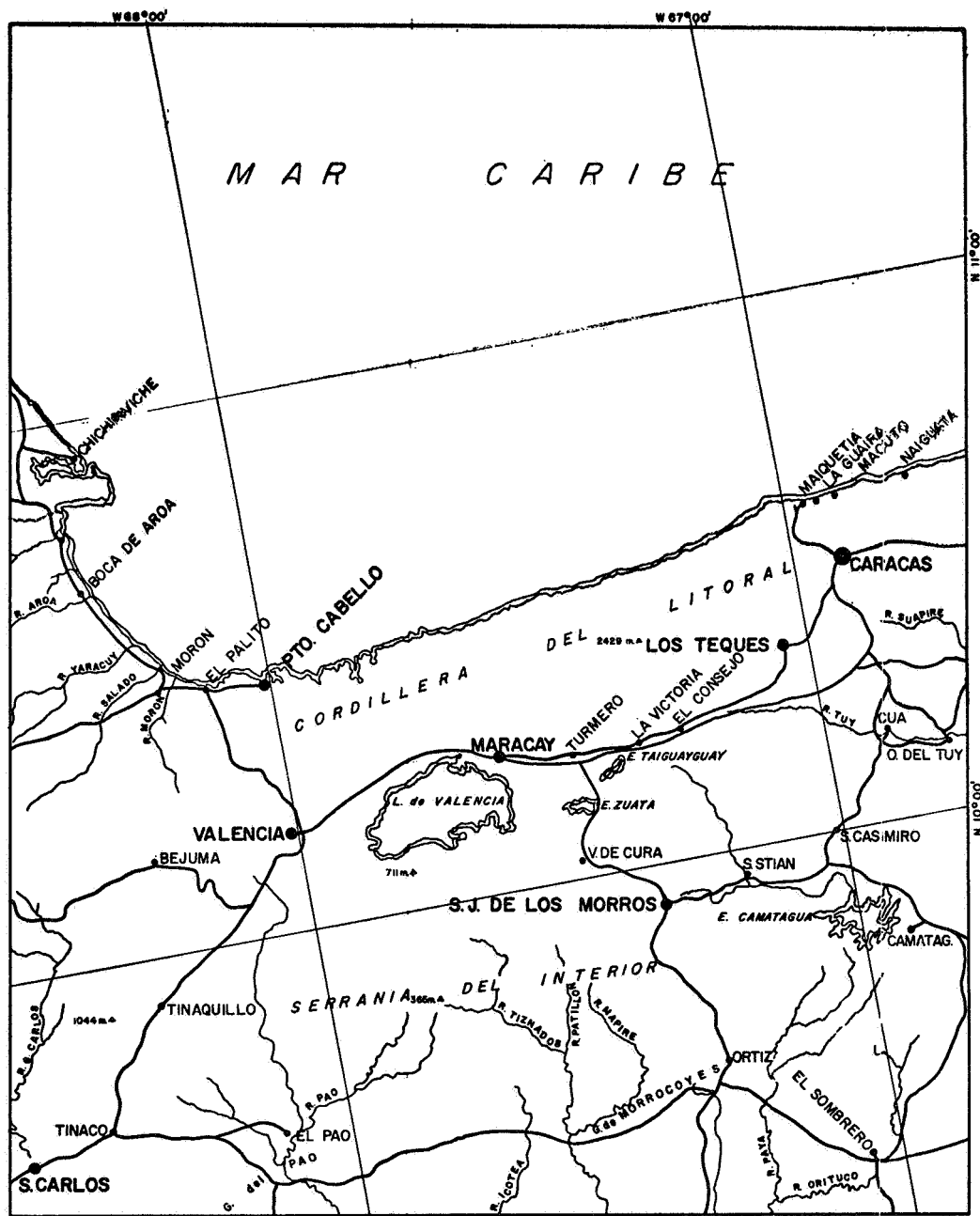
The area under study includes part of the Central and Capital Region of Venezuela (coord: $9^{\circ}30'$ - $11^{\circ}00'$ lat. N. and $67^{\circ}00'$ - $68^{\circ}00'$ long. W). Climatic conditions define the existence of different ecological associations with biological forms well defined in their physiognomic complexity as they reach complete development in environments related to gross geomorphic units: Coastal area, Northern mountain range, fluvio-lacustrines plains, Southern mountain range, southern ridges and parts of Venezuelan central plains. In this area, rainfall varies from 600 mm to 2000 mm and evapotranspiration indexes indicate the existence of vegetation for semiarid conditions (tropical very dry forest) as well as vegetation for very humid conditions (very humid premontane forest).

This project has been designed with the following objectives:

- Location of areas with representative ecosystems for the purpose of managing planning.
- Identification of structural and physiognomic characteristics of vegetation.
- Assessment of human activity effects on environmental debasement.
- Definition of the content and possibilities of orbital ERTS images for the study of urban and rural land use.
- Setting photointerpretation patterns applicable to areas of similar gross environmental conditions.

During the first stage of the project, orbital images were analyzed at scales of 1:100,000 and 1:500,000 tonal differences were correlated with categories derived from Holdridge's method. Techniques utilized were the identification of tonal contrasts in false color composites esc. 1:1.000,000 (February and March 1973) and in bands 5 & 7, with the use conventional photointerpretation methods (magnifying glass and microfilm viewer).

1 N 74 30746



LOCALIZACION DEL AREA
ESC. 1:1.000.000

Figure 1.

Tonal variations were compared with those observed through a random 25% sample in conventional panchromatic photographs at scales of 1:50,000 and 1:25,000.

We have not arrived yet to a finished map at the scale of 1:500,000 with completely proved categories. Nevertheless, results obtained allow us to think it possible as well as to further precision to the 1:250,000 scale as soon as statistical work advances and permit the correlation of climatic conditions, geoforms and solar radiation to the tonal responses of vegetation.

As for the tectonic part of the project, conventional photointerpretation techniques were applied to multispectral images at the scales of 1:1,000,000 to obtain maximum information. At regional scale, principal faults trending E. were identified as they divide the area in tectonic blocks. Sedimentary rocks have been identified as well as folds, faults and small linears.

1. Regional Structure. The evaluation of geoforms and regional faults trending E. allowed N. to S. separation of principal tectonic blocks. Structural units of the area were identified and further analyzed with the help of drainage photointerpretation.

Northern side of Coastal Range is separated of the La Guaira platform by Sebastian fault. The southern side of Coastal range is separated from "Serranía del Interior" by the La Victoria fault. A subsidence area is formed by the valleys of Valencia, Aragua, Santa Teresa and Santa Lucía. These intermontane valleys have a limit on the South at the normal E-W fault of Santa Rosa and at the piedmont of Serranía del Interior. Further on to the South, there can be observed a tectonic block formed by Paracotos Strip and the block of Villa de Cura. At the southernmost part of the study area, it is observed as a structural system of E-W lineaments almost parallel corresponding mostly to sandstone outcrops of Galeras del Pao.

The La Guaira platform, located at the N. is covered by the Caribbean Sea and is separated from the Coastal Range by the Sebastian zone of faults, evident in the straight shape of the shoreline.

In the tectonic block of the Coastal Range there were identified the fault of Tacagua and the fault zone of Macuto as well as some lineaments of the Valencia fault. In this block predominate incompetent rocks and the faulting pattern is oriented NW-SE, normal to the principal faulting system. A normal NE-SW lineament, of which there was no previous knowledge, was identified as the Petaquire fault.

2

The fluvio lacustrine area of lago de Valencia is a depressed block. Its principal structural characteristics are covered by Quaternary sediments over Miocene rocks.

At the tectonic block of the Serrania del Interior, faulting pattern is transversal. There were identified some features of the following faults: Santa Rosa, Agua Fría, La Puerta and Guárico. The strip of Paracotos is formed by a series of faulted blocks among volcanic competent rocks.

At the block of Villa de Cura there were observed the fault of Cantagallo (of difficult topographic expression) and the more recent fault of La Puerta. Both faults contact the V. C. block with Upper Cretaceous rocks of the mountain front.

The southern mountain front is folded and thrust to the south as they reach the limits of the Central Plains sedimentary basin.

2. Vegetation - photomorphic units. For the vegetation project, a first level was reached through the classification of tonal groups by aggregating tonal similarities to macrorelief units and sociological aspects of vegetation. There were identified the following units:
 - a. Litoral - Predominant dry and very dry tropical forest.
 - b. North and Central sector of Coastal Range - Predominant humid and very humid forest as well as premontane and lower premontane forest.
 - c. South Sector of Coastal Range - Predominant humid premontane and dry premontane forest.
 - d. Aluvial and Lacustrine Valleys of Aragua, Carabobo and Cojedes - Dry premontane forest and dry tropical forest.
 - e. Interior Rangeland - Dry premontane forest, dry tropical forest and humid premontane forest.
 - f. Plains - Dry tropical forest.
3. Classification of Vegetation and Land Use Categories. At a second level of the analysis, tonal characteristics reached in the first level were detailed and separated according to ecological conditions determined for photomorphic gross units. Classification was checked with

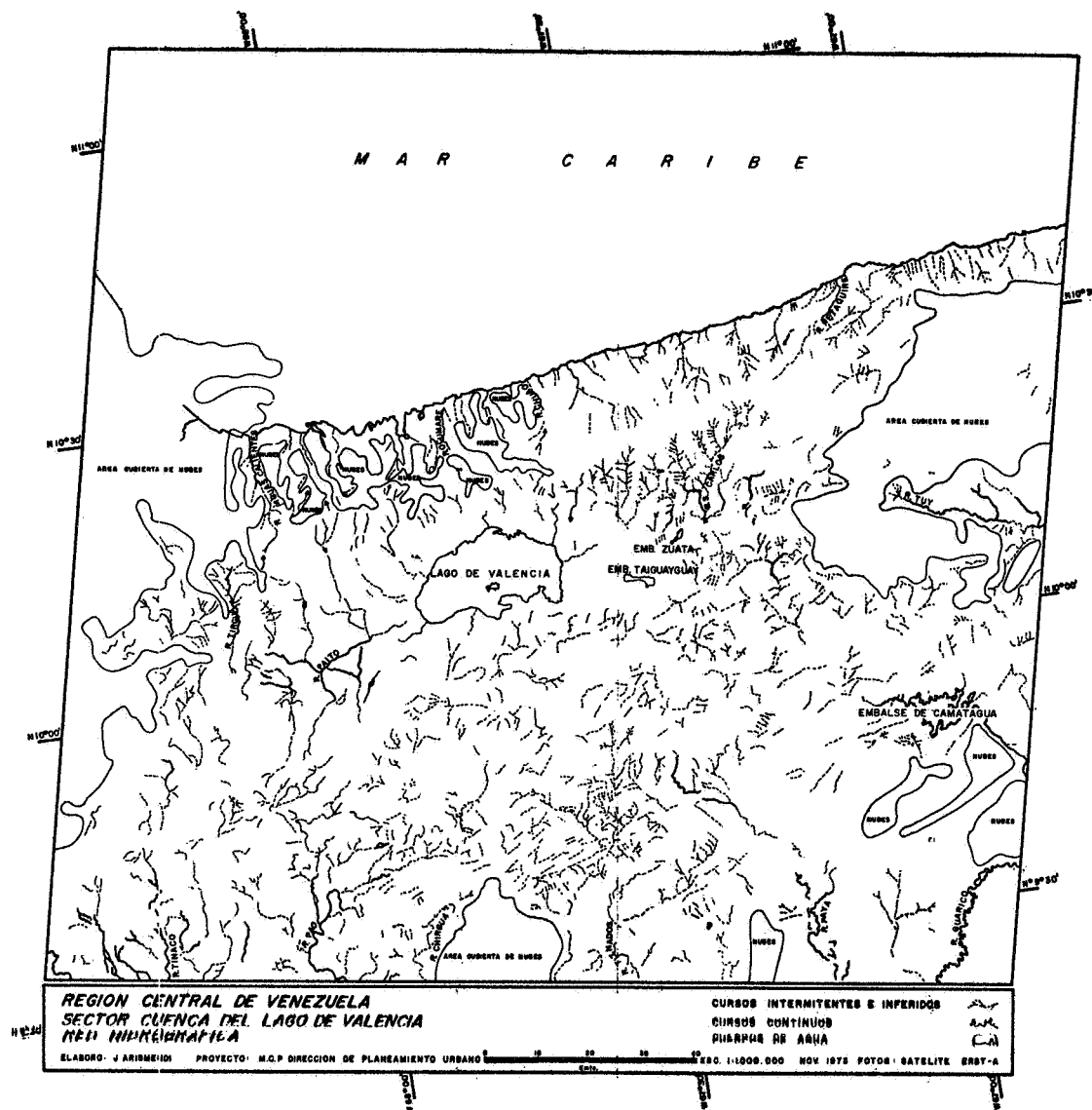


Figure 3.

samples ran in conventional 1:50,000 and 1:25,000 panchromatic photographs as well as with ground truth. Sampling allowed inference on the degree of human intervention, more exact definition of vegetal associational borders, agricultural types and some appreciation about density on the urban level.

Categories identified were the following:

- Vegetation
- Dry and very dry tropical forest
- Dry tropical forest
- Dry premontane forest
- Humid premontane forest
- Humid tropical forest
- Very humid premontane and lower premontane forest
 - a. Well developed gallery forest
 - b. Regularly developed gallery forest
 - c. Herbaceous vegetation scarcely developed with discontinuous arboreous and arbustive
 - d. Herbaceous vegetation scarcely developed
 - e. Burns

Each of the formerly mentioned vegetation categories has been qualified as follows: little intervention, medium intervention and very intervened.

Land use categories are the following:

- Urban area
- Industrial zones
- Vacant urban
- Airports
- Natural pastures
- Agricultural in big lots
- Sugar cane
- Agricultural in small lots

4. Evaluation. The geologic interpretation is comparable to the one we possess at scales of 1:200,000 drawn as photointerpreted from conventional 1:50,000 panchromatic images.

As for vegetation, the method used has permitted a diagnosis of actual conditions of vegetative coverage and the gross evaluation of the extension and quality of urban and rural land use. The repetitive character of images has been used (although not shown in this paper) to evaluate land use dynamics.

Tonal variations and its correlation with vegetational association is determined more exactly with false color composites due to plants chlorophyll absorption of visible light and reflection of I.R. In band 5, urban areas are easily identified and center part of cities (Maracay) can be delineated. Band 5 is also very sensitive to increase of biomass per unit area and tonal response is darker the more dense is the forest.

It is convenient to state the difficult task of approximating borders of vegetal formations due to ecotonal characteristics at transition levels.

**MINERAL RESOURCES, GEOLOGICAL STRUCTURE
AND LANDFORM SURVEYS**

APPLICATION OF THE ERTS SYSTEM TO THE STUDY OF WYOMING RESOURCES WITH EMPHASIS ON THE USE OF BASIC DATA PRODUCTS

Robert S. Houston, Ronald W. Marrs, Roy M. Breckenridge and D. L. Blackstone, Jr., *Department of
Geology, University of Wyoming, Laramie, Wyoming 82071*

ABSTRACT

Many potential users (for example, consultants, small companies and independent geologists) of ERTS data products and other aircraft and satellite imagery are limited to visual methods of analyses of these products. Illustrations are presented from Wyoming studies that have employed these standard data products for a variety of geologic and related studies. Possible economic applications of these studies are summarized. Studies include regional geologic mapping for updating and correcting existing maps and to supplement incomplete regional mapping; illustrations of the value of seasonal images in geologic mapping; specialized mapping of such features as sand dunes, playa lakes, lineaments, glacial features, regional facies changes, and their possible economic value; and multilevel sensing as an aid in mineral exploration. Examples of cooperative studies involving botanists, plant scientists, and geologists for the preparation of maps of surface resources that can be used by planners and for environmental impact studies are given. Emphasis is placed on the use of these maps in areas, such as the Powder River Basin of Wyoming, facing critical environmental problems that will result from the development of energy resources.

These various studies illustrate that certain user requirements can be satisfactorily met with ERTS alone, but that others require higher cost (to the user) aircraft and ground data or special data enhancement techniques. However, the ERTS system has given us both complete and sequential regional coverage at a crucial time in our effort to assess the effects of resource development.

INTRODUCTION

The basic goal of investigators of the ERTS-1 imagery in Wyoming is to discover applications of ERTS-1 data to earth resource studies. The ERTS standard data products can be used to produce many interrelations of economic value and there is nothing that competes with the ERTS synoptic view for regional geologic studies. The system does suffer, however, from resolution limitations and this has led some to question the utility of ERTS. For example, a recent editorial in *Nature* (1973, p. 345) states that the ERTS system,

NOV 24 3 07 42

. . . suffers from one major defect -- it is too generalized. It is not possible simultaneously to please a large constituency and provide each of them with what they need. Furthermore, it is by no means clear that many of the users of the ERTS data can make much of it beyond the 'gee-whizz' stage. When more detailed work is attempted the resolution is too poor (objects less than a few tens of meters across may be invisible), the time of the photograph is unsuitable for the problem or the effect is not suitably sampled in 18-d intervals . . .

. . . Much has been made of the geological uses of ERTS; indeed the publicity has tended to imply that geology is the study of lineations, and lineations can mean metal deposits. One cannot imagine why any geologist would be prepared to make a partial map of his area -- partial because of the finite resolution and because structures not visible at 9:30 a.m. would not be recorded.

This criticism exemplifies the feelings of some, even among the scientific community. At the very least, it seems that such statements are premature, considering that the system has been in operation for just longer than a year and there has been little time in which to realize most tangible benefits. If 'gee-whizz' refers to visual analysis of standard image products, certainly many users (private citizens, consultants, independent geologists and representatives of small companies) will be confined to that approach -- for the present. Even so, can they make profitable use of the standard ERTS-1 data products? The investigators at the University of Wyoming remote sensing laboratory have found that visual analysis of ERTS-1 data can produce real benefits. In fact, these studies indicate that visual analysis is the essential step in most earth resources applications.

From the outset, it was realized that any evaluation of ERTS-1 data applications would require thorough checking of the results. Some of the checking must, of course, be done in the field, but the very large areas studied from ERTS-1 cannot be effectively covered on the ground in a few months' time. It was therefore necessary to supplement field reconnaissance with data from the literature wherever possible and with interpretations of high-resolution aerial photography. Color, color infrared, and/or multiband photography is now available for much of Wyoming (Fig. 1) as a result of ERTS- and EREP-support flights flown by NASA aircraft. The aircraft data is, in itself, a valuable product and provides not only a means of checking interpretations of ERTS data, but also an opportunity to approach some problems by a multilevel remote sensing program. Starting with geologic mapping, we hope to illustrate a variety of applications of ERTS and supporting aircraft imagery, that can be made at low cost to the user.

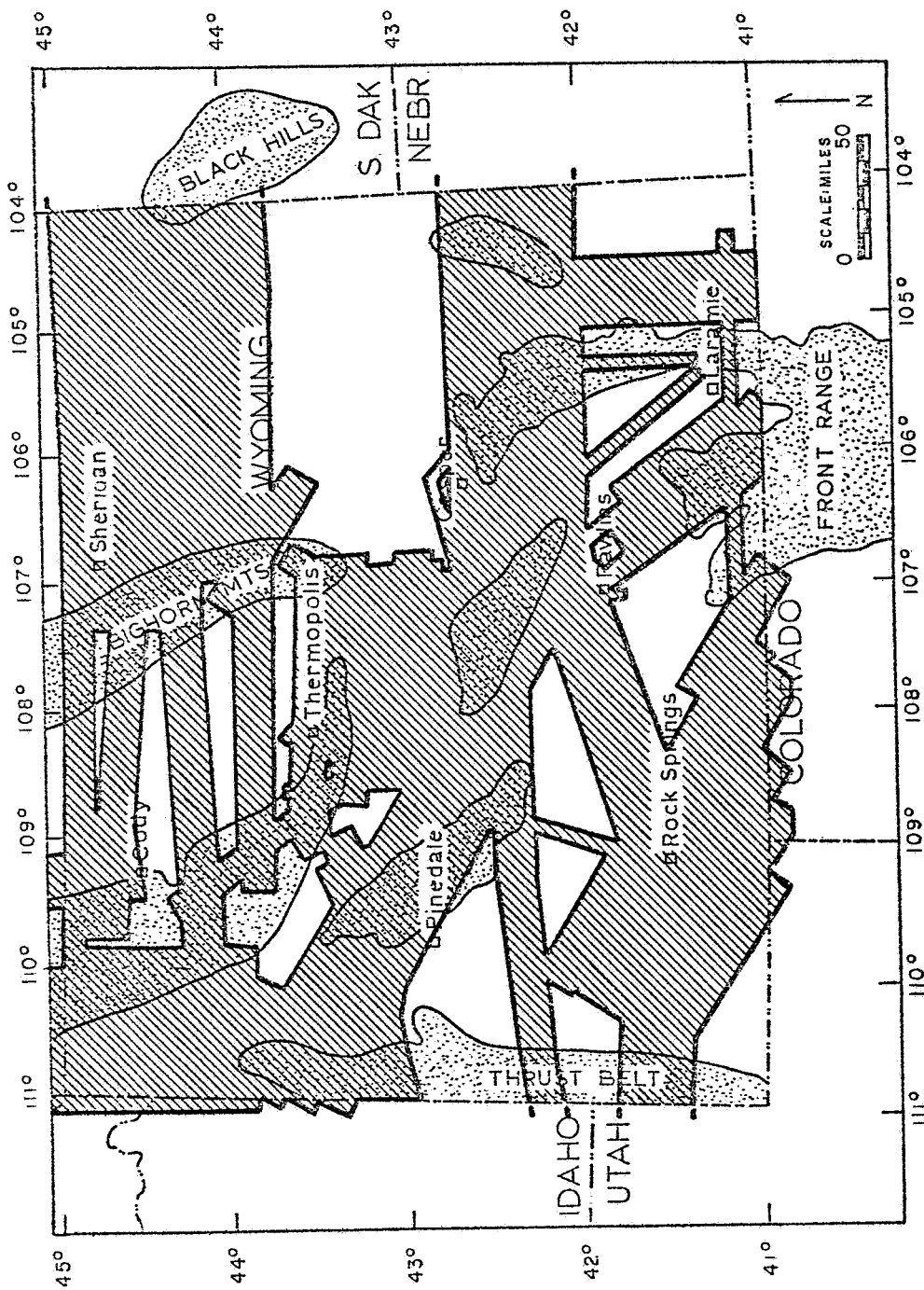


Figure 1. Index map showing current NASA air photo coverage of Wyoming.

GEOLOGIC MAPPING

Figure 2 shows a geologic map prepared from an ERTS color composite (image 1030-17235) of an area northwest of Casper, Wyoming and compares this ERTS map with the best surface mapping (Fig. 3). This area is one of complex geology at the south end of the Owl Creek and Bighorn Mountains where large blocks of Precambrian crystalline rocks have been uplifted and thrust over younger sedimentary successions. Major lithologic units include Precambrian gneisses (p6u), Cambrian sandstones (6f) and limestones and siltstones (6gl), Mississippian limestone (Mm), Pennsylvanian sandstone (Ppt), Permian dolomite, phosphatic siltstone and shale (Pf), Triassic siltstone with gypsum beds (Trcd), Triassic red siltstone and sandstone (Trc), Jurassic shale and siltstones (Js), Cretaceous sandstone (Kcr), Cretaceous black shale (Kt), Cretaceous sandstone (Kmd), Cretaceous black shale and siliceous shale (Kmr), Cretaceous shale overlain by massive sandstone beds (Kf), Cretaceous shale (Kc), Cretaceous sandstones, shale, and coal beds (Kmv), Cretaceous shales, carbonaceous shales and sandstones (Klml), Tertiary sandstones, siltstones and conglomerate (Tfu), Tertiary dolomitic siltstones (Tlb), Tertiary red beds (Trb), Tertiary units undivided (Tu), Quaternary gravels, Quaternary alluvium, and Quaternary sand dunes.

Twenty-three major lithologic subdivisions were differentiated for this area and many others could be made depending on the detail of mapping desired. Obviously the ERTS photogeologic map cannot compete with surface mapping in an area as complex as this, but note what was achieved. Eighteen subdivisions were made of the exposed units and these subdivisions correspond generally to units mapped by field geologists. Most major faults and many minor faults were mapped although there is a tendency (depending on the interpreter) to over-map lineaments. The distribution of sand dunes (Qs) was defined more accurately than on the geologic map, and some additional mapping was done in R. 88 W., Tps. 39 and 40 N., where no ground mapping had been done previously. Summarizing, then the ERTS image can be used to map the regional geology of complex areas (keeping in mind that limited field checks are necessary for lithologic identification), but the imagery is of little value, except for checking possible errors or filling in gaps, where careful surface mapping has been done previously.

Figure 4a shows a geologic map prepared from the same ERTS color composite (image 1030-17235) of an area north of Casper, Wyoming and compares this ERTS map with the 1955 geologic map of Wyoming (Fig. 4b). Much of this area has not been mapped in detail and no mapping is available in published or open-file form. The geologic map shows nine lithologic subdivisions where as the ERTS photogeologic map shows twenty-five lithologic(?) subdivisions. This area has not been fully field-checked so we cannot be certain that all subdivisions shown on the ERTS photogeologic map correspond to changes in lithology. The large area shown as Cody Shale (Kc) on the geologic map has been subdivided into

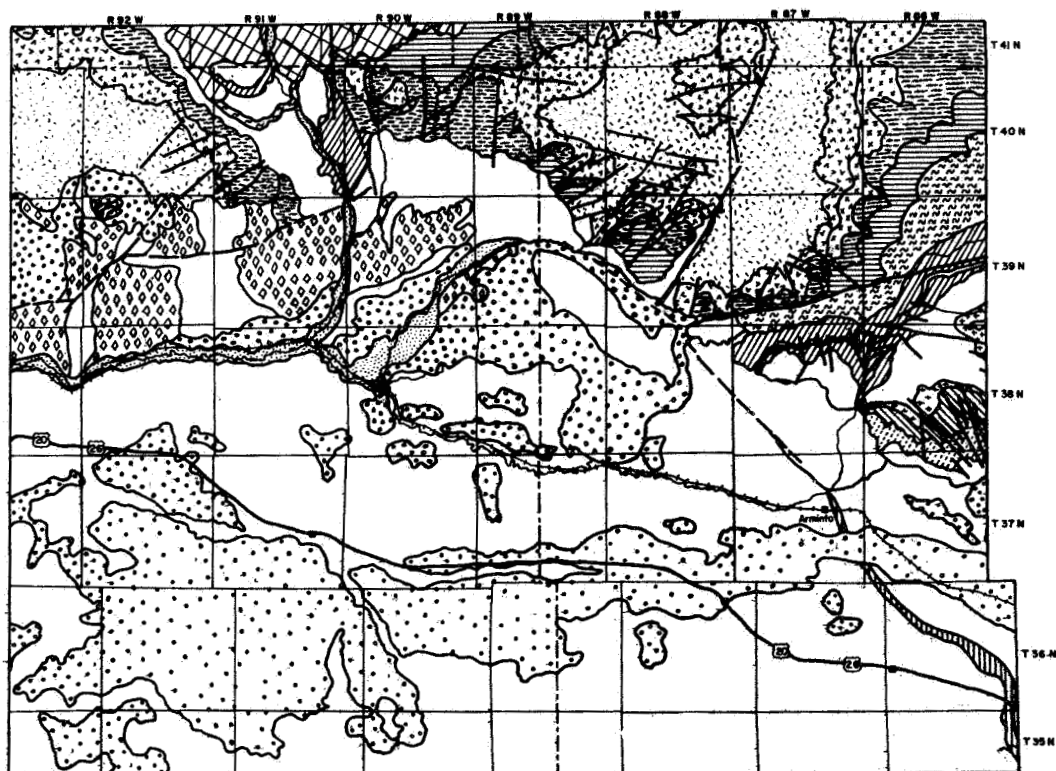


Figure 2. Photogeologic map prepared from ERTS color composite (image 1030-17235) of area northwest of Casper, Wyoming. Patterns of units are keyed to the nearest geologic field subdivision shown on figure 3.

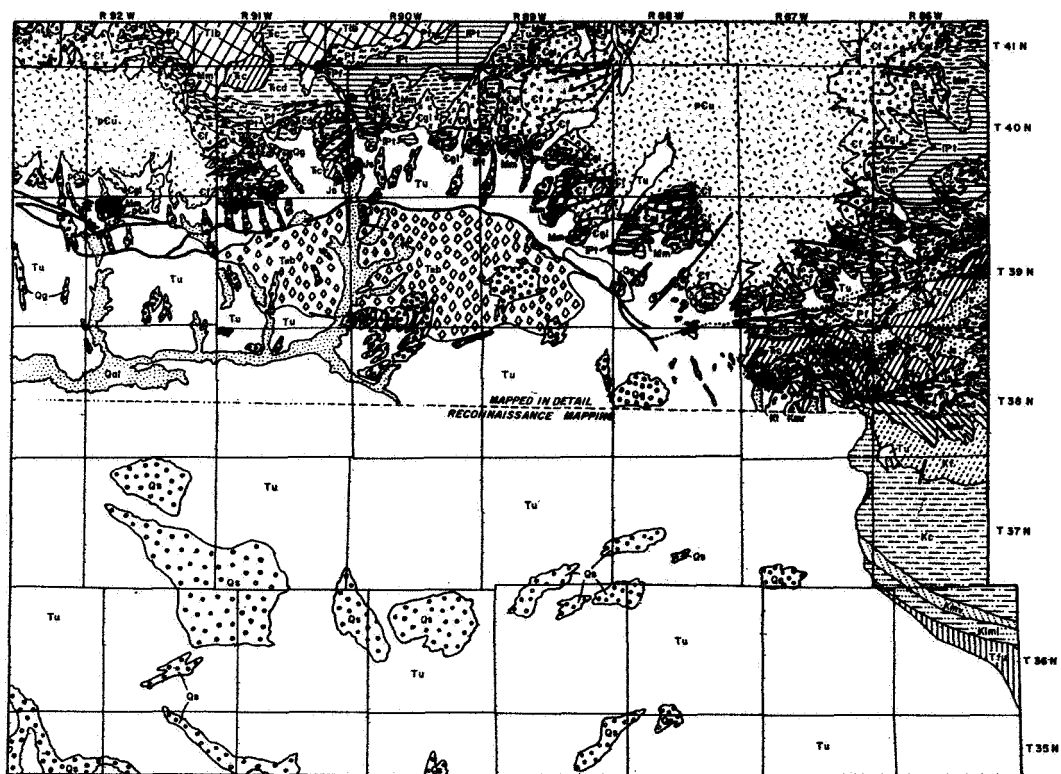


Figure 3. Geologic map of same area as in figure 2, modified from Tourtelot (1953), Woodward (1957), Rich (1962), and Keefer (1970). See text for explanation of units.

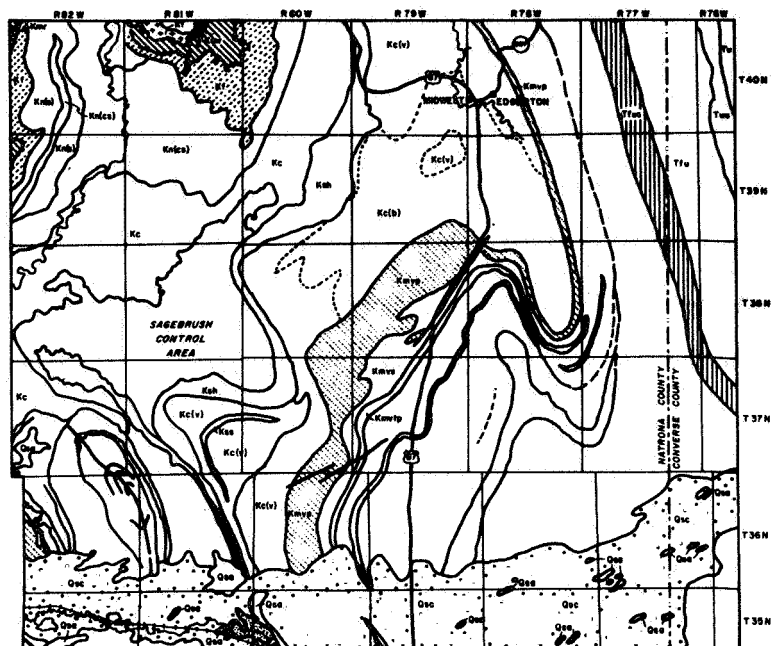


Figure 4a. Photogeologic map prepared from ERTS color composite (image 1030-17235) of area north of Casper, Wyoming.

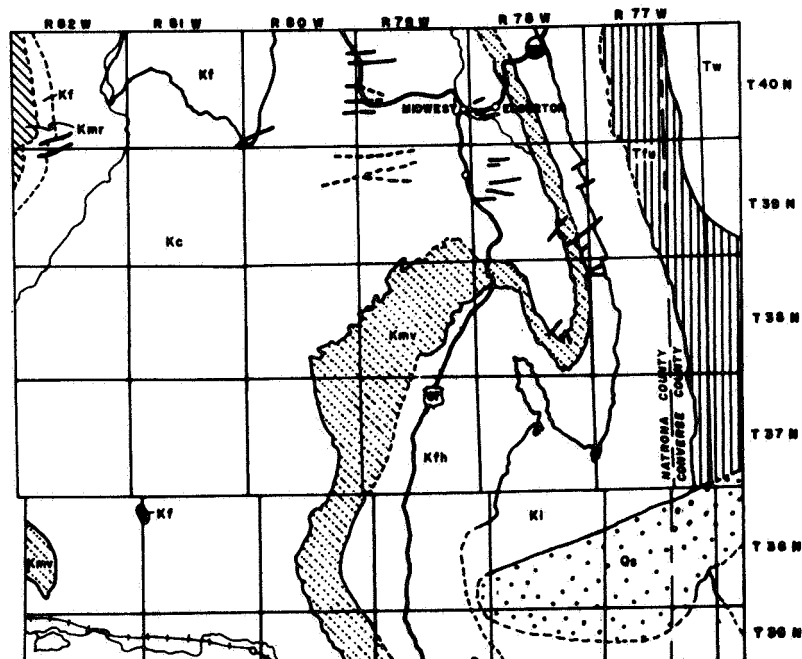


Figure 4b. Geologic map of above area modified from state geologic map of Wyoming (Love, Weitz, and Hose, 1955). See text for explanation of units.

several units; the areas shown as Kn(cs) and Kn(s) probably correspond to calcareous shales and shales of the Niobrara Formation. The area shown as Kc is typical Cody Shale. The area shown as Ksh is the Shannon Sandstone member of the Cody Shale. The area shown as Kc(b) is Cody Shale with very little vegetative cover and that shown as Kc(v) is Cody Shale with varying vegetative cover. Finally, the lens shown as Kss is probably the Sussex Sandstone member of the Cody Shale. The reason for the varying vegetative cover on the upper Cody Shale bed is not determined but it (Kob) does coincide with the location of a major oil field. The curious area in T. 38 N., Rs. 81 and 82 W. is an area where the natural vegetation has been disrupted by extensive spraying to kill sagebrush so its significance is probably not lithologic.

The Mesaverde Formation can also be subdivided into the Parkman Sandstone Member (Kmvp), a shale unit (Kmvs), and an upper unit called the Teapot Sandstone member (Kmvtp). Distinctions can also be made within the Fox Hills Sandstone (Kfh) and Lance Formation (Kl), but their significance is not known. The lower massive sandstone of the Fort Union (Tfus) and a similar sandstone in the Wasatch Formation (Tuss) can also be distinguished. Finally, stabilized sand dune areas (Qsc), active sand dunes (Qsa), and alluvium (Qal) are readily mapped to complete the more accurate ERTS map of this area.

This second mapping illustration clearly shows the advantage of an ERTS color composite in regional mapping (up to 1:250,000) in areas where detailed surface mapping has not been done. Many areas of this type still exist in the United States and a great many more exist outside of this country. Naturally, where good aerial mosaics are available, accurate mapping can be done by use of the mosaic but at higher cost to the user and without the major advantage of the color infrared mode and other multispectral enhancement procedures.

Color photographs or film positives are considered by most geologists (Wilson, 1970) the best tool for photogeologic mapping. Color is not a specific guide to rock type, but in a given region certain lithologies have characteristic colors that persist over broad areas so that color is extremely valuable in formation identification. Where characteristic colors of rocks or rock-vegetation units have been established for a geologic section, under these circumstances the geologist can map units with some assurance that he is identifying the rocks correctly. Color infrared offers the same possibilities once the interpreter is familiar with the color shift. We have attempted to define the "typical" color shift and have derived several false-color infrared rock guides (Fig. 5) which relate certain key beds to their typical color on a false-color image. With the color guide and/or experience, the interpreter can use the false-color imagery more efficiently.

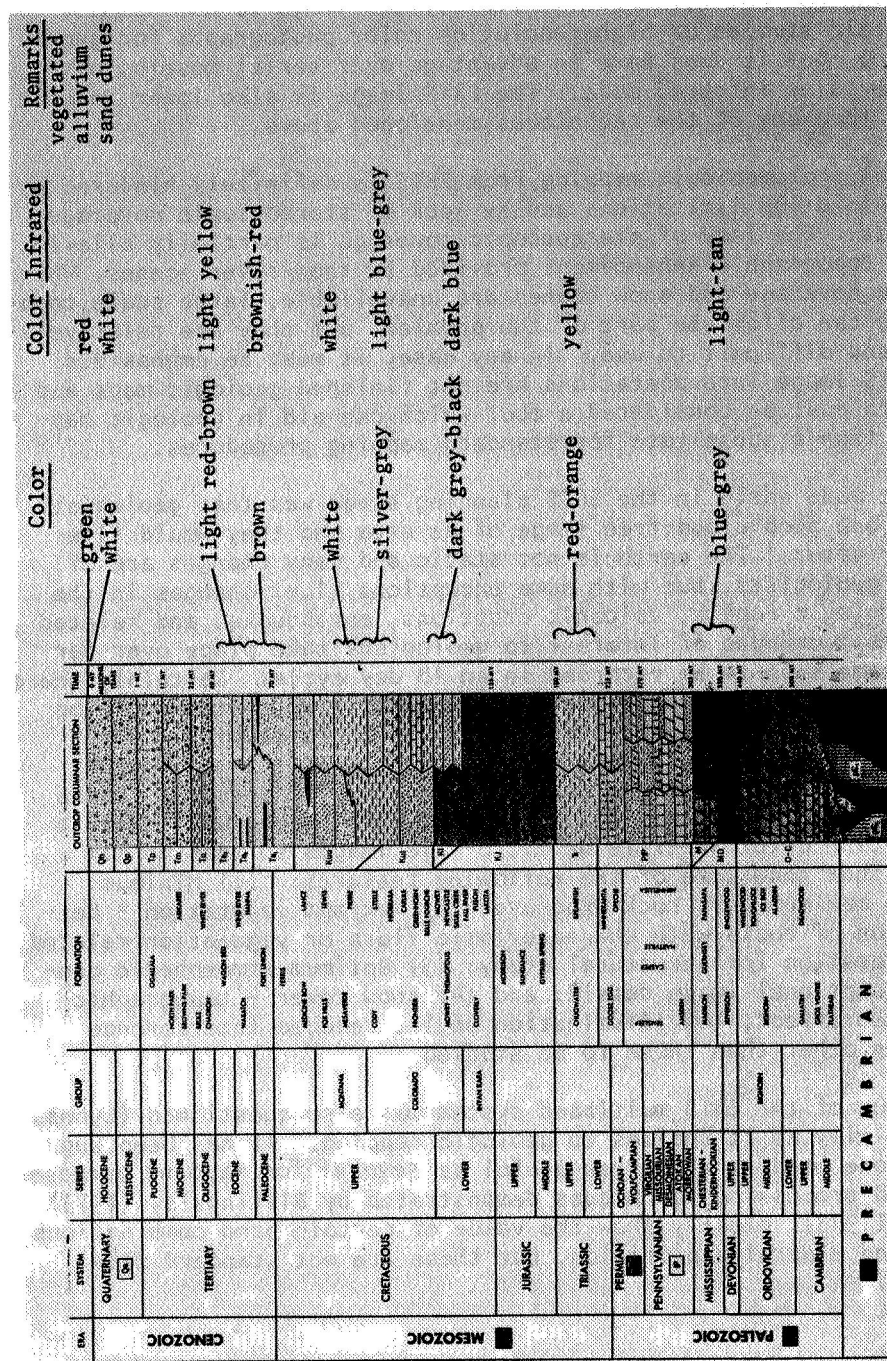


Figure 5 Color guide relating key units in the stratigraphic section of eastern Wyoming to their typical color representation on color and color infrared imagery.

The ERTS color composite is thus an extremely useful tool for geologic mapping in arid regions such as Wyoming, especially where detailed mapping has not been done. Obviously the image is not competitive with field studies or high-resolution color photographs for geologic mapping, but it does have an advantage over aerial mosaics because of the color infrared mode. The ERTS image is also lower in cost to the user than any of the techniques mentioned above.

Regional photogeologic mapping from ERTS is definitely hindered by the image-resolution limitations and by lack of stereoscopic coverage in many areas. The lack of stereoscopic coverage is partially alleviated by the topographic enhancement provided by snow-cover scenes. When stereoscopic coverage and snow scenes are unavailable, large scale topographic maps can alleviate part of the problem, but they are relatively cumbersome and difficult to use. In any case, it must be emphasized that the ERTS image interpretations are not finished geologic maps and the ERTS data must be considered a tool which can aid in geologic mapping rather than a substitute for standard mapping procedures.

A point made early in the ERTS planning stage was that geologists needed only one good cloud-free image of an area and they would live happily ever after. The earth is not static and many changes are of interest to geologists, but with some exceptions (i.e. changes in the surface hydrologic regime, volcanic eruptions, earthquakes and related phenomena) most changes of interest to geologists take place over far too long a time span to be recorded in an 18 day cycle. Certainly there was no compelling reason to suggest that a repetitive system would be useful to the individual interested only in geologic mapping.

An 18 day cycle may not be required but study of seasonal images does facilitate geologic mapping. A user of ERTS images will benefit from examination of browse-file or micro-file images so that he can pick images that show some of the following features: (1) Minimum vegetation - maximum bare rock exposure; (2) Maximum vegetation - better definition of rocks with characteristic flora or vegetation related to water saturation for structural study; (3) Optimum atmospheric conditions - exceptional image detail; and (4) snow cover - topographic effect, stereo-effect, low illumination angle, reduced interference from features other than those to be studied.

The value of the ERTS multiband system was also questioned (Lyons, 1970); especially as it applies to geologic mapping. It has been suggested that one band is almost as useful as several for mapping purposes. The multiband processing techniques demonstrated by Billingsley (1973) and Vincent (1973), clearly show the value of certain band combinations in mapping and mineral exploration, but these are not standard data

products from ERTS. The infrared color composite which is a standard data product requires three of the four bands for its construction and is demonstrably superior to a black and white product for geologic mapping. In addition, the individual ERTS bands tend to enhance contrasts between certain rock types. For example, bands four and five often show a strong contrast between rock types that are marked by characteristic vegetation, and band seven generally enhances contrast between iron rich and iron poor rocks such as granite-basalt contacts (Rowan, 1973; Houston and others, 1973).

TOPICAL MAPPING

The ERTS data is better suited to certain topical studies than to general mapping programs. Several such studies have been completed as a part of the Wyoming investigation. They include determination of extent of Pleistocene glaciation and related geomorphic features (Breckenridge, 1973), mapping of sand dunes (Kolm, 1973), playa lakes, pediments, regional facies changes, average slopes, major strip mines, large areas of surface instability, linear features, and large-scale tectonic elements.

The study of lineations has become a major facet of the ERTS-1 geologic applications and has attracted more than a fair share of attention and criticism. Lineations have always been somewhat of a special problem to the geologist because, as an aspect of megatectonics, the study of lineations and their implications is a field under constant criticism. The chief problem is the difficulty in compiling data on a group of lineations, faults, or shear zones without including a few, and sometimes many, features of questionable validity. This allows a critic to discredit an entire concept by disproving a small part of the supportive evidence.

The synoptic view of ERTS lends itself so well to mapping of lineations that even an experienced interpreter can become somewhat over-zealous, and map lineations that are unrelated to geology. Linear features that must be dealt with in compiling a "tectonic" interpretation include roads and highways, railways, fire lines, fence lines, tornado swaths, condensate trails, aeolian features, dikes, faults, shear zones, joints, topographic breaks, snow-lines, moisture and cloud patterns, and vegetation changes. The resolution limitations of ERTS and the extremely high-altitude overview often make distinction between these features difficult. Consequently, even the experienced photo-geologist can be embarrassed by finding that he has erred in his interpretation. Ordinarily one would resolve such problems by a simple field check. However, subtle linear features have been located on ERTS which appear on several image cycles and yet defy identification in the field (Blackstone, 1973c). These we hope to identify from very low-level aerial photography.

Despite the confusion with non-geologic linear features and the difficulty in field checking, we are convinced that most of the linear features identified on ERTS have geologic significance. As yet, no particular economic significance has been attached to the newly discovered linear elements, but we anticipate that some of these will prove economically important.

The ERTS imagery quite frequently suggests extensions of fault systems beyond their mapped limits, with some systems showing expression into younger rocks than were previously known to be involved. From these relationships we can establish better dates for some episodes of crustal movement.

Another aspect of tectonics being pursued with the aid of ERTS imagery is the interrelationship between structures in the Wyoming mountain ranges and those in the basins. The ERTS imagery allows rapid compilation of orientations for major faults and joints in the exposed cores of mountains and similarly rapid assessment of the axial trends of adjacent basin folds. These can then be compared to determine possible interrelationships. Figure 6 is a generalized map of the major faults, folds, and linear elements of the Bighorn-Pryor Mountains area. These features were mapped by photogeologic interpretation of ERTS images. Figures 7a and 7b are rose diagrams comparing the orientations of linear features in the mountains to fold axes. In this case, no strong correlation was seen (Blackstone, 1973b). A similar study for the Laramie Range and Laramie Basin showed a strong similarity in the orientations (Figs. 8 and 9), suggesting a common genesis (Blackstone, 1973a). The economic significance of such information, if any, will come with continued study of the tectonic systems and their local implications.

MINERAL EXPLORATION

The utility of standard ERTS data products in direct mineral exploration is still somewhat in doubt. Tests in which the standard imagery was used to locate exposed alteration zones give variable results.

In the Absaroka Mountains of Wyoming (Fig. 10d) attempts were made to map zones of reddish alteration that might be related to intrusive activity and mineralization. To eliminate some of the subjectivity, two separate maps were made. One (Fig. 10b) was compiled by a geologist who has extensive experience in the area and the other (Fig. 10a) by a geologist with no experience in the area. Both were asked to look for anomalously red (yellow on the false-color composite) areas. The obvious similarities between the two interpretations and their mutual correlation with a map of known mineralization (Fig. 10c) indicates that some areas of alteration, although subtly expressed, can be identified from ERTS. Areas identified on the image interpretations and not corresponding to known mineralization have yet to be checked.

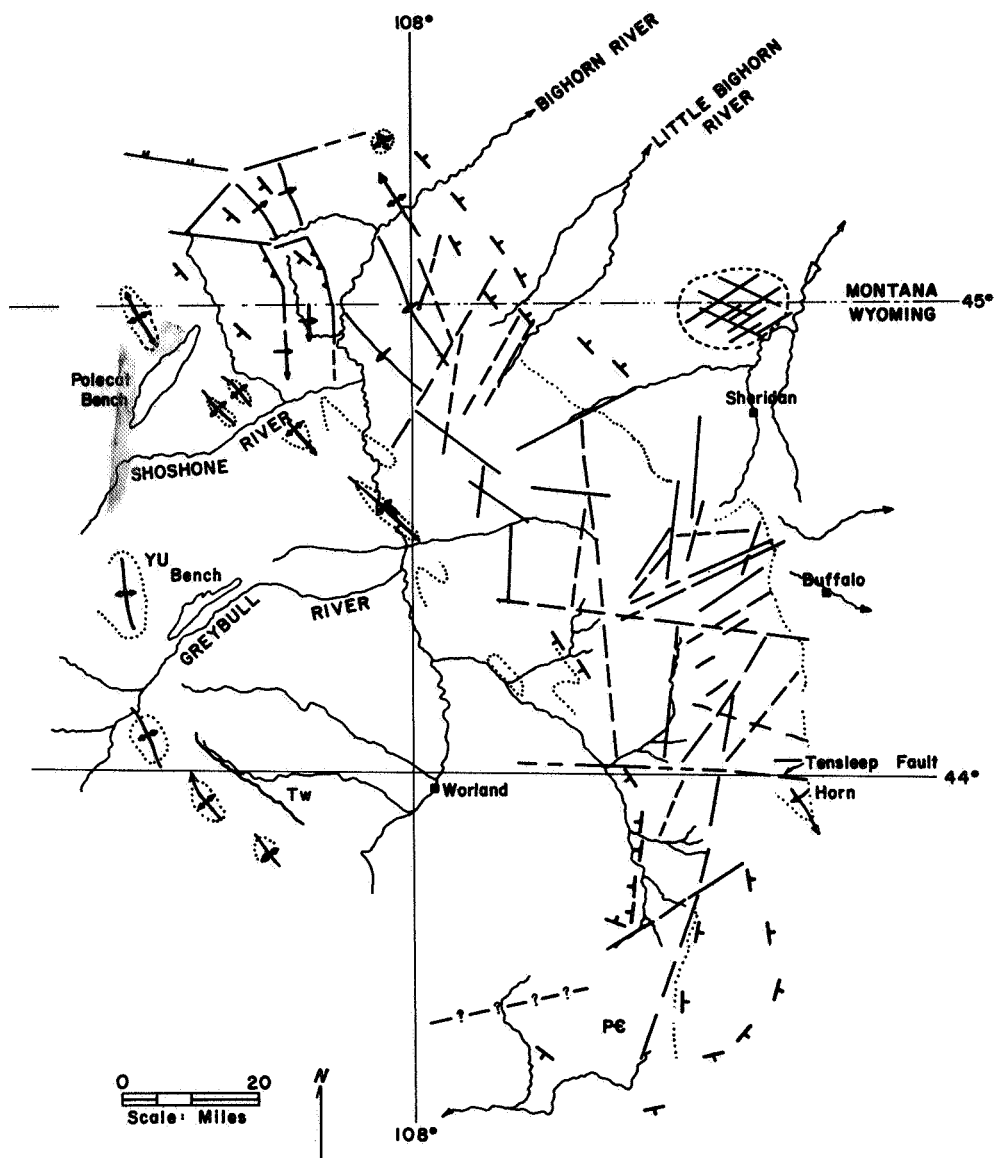


Figure 6. Major linear elements of the Pryor and Bighorn Mountains.
(after Blackstone, 1973c)

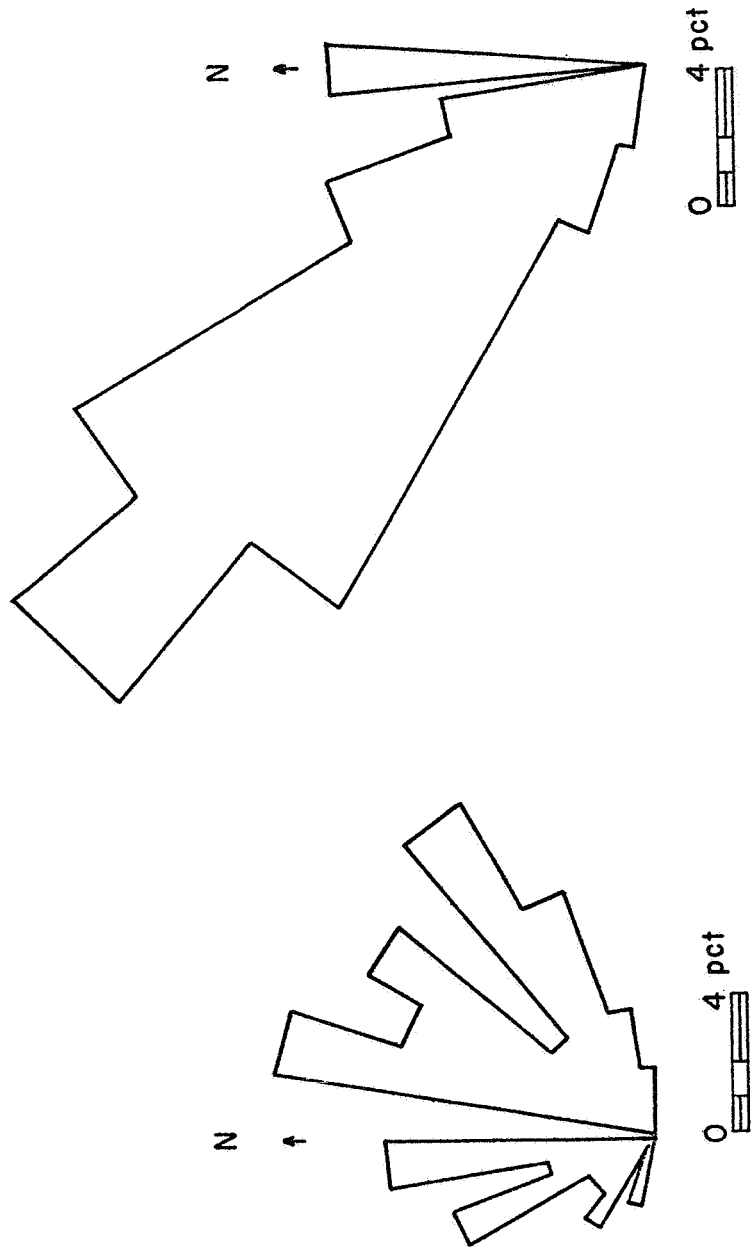
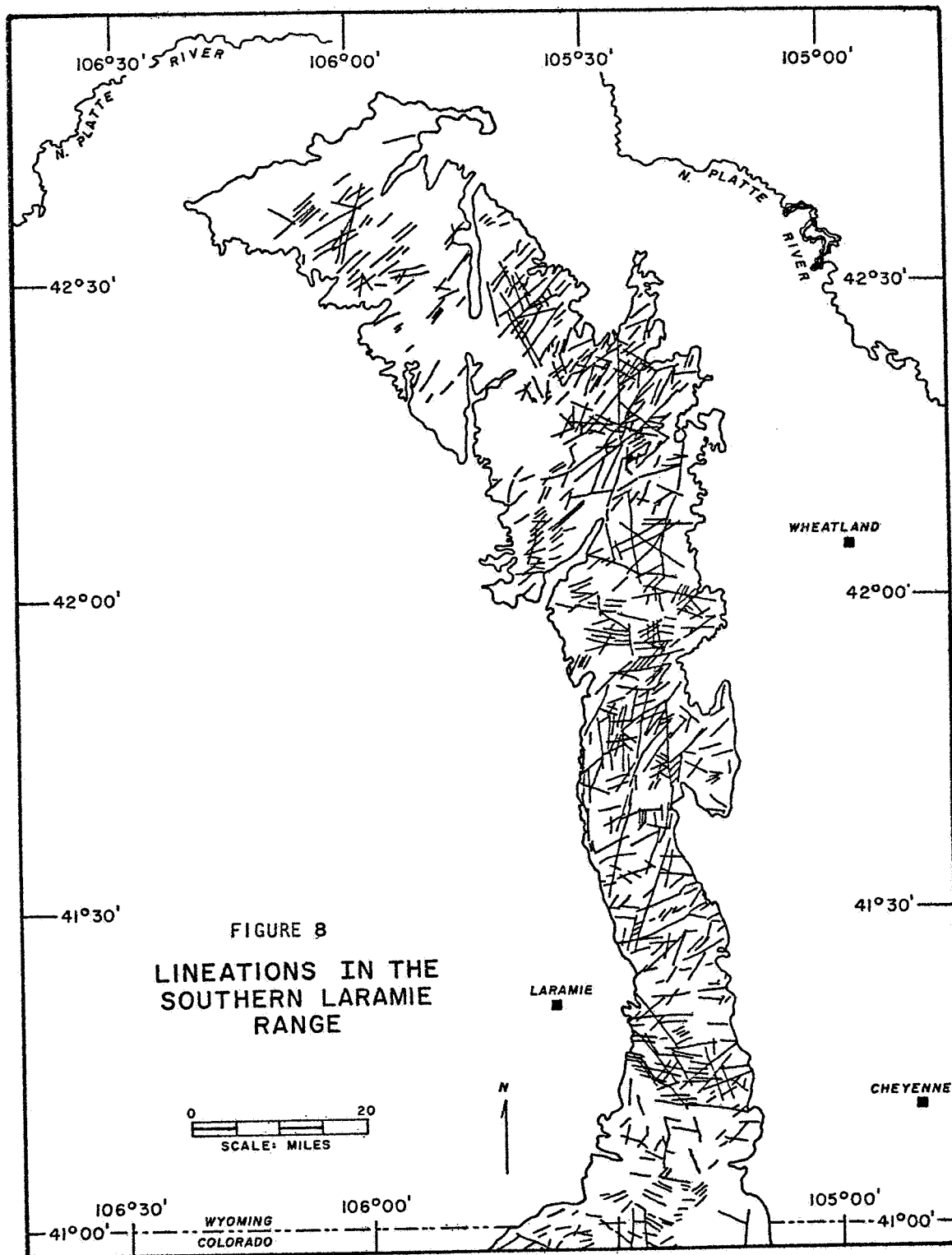


Figure 7b. Rose diagram showing the orientations of fold axis in the Bighorn Basin.

Figure 7a. Rose diagram showing trends and orientations of observed linear elements.



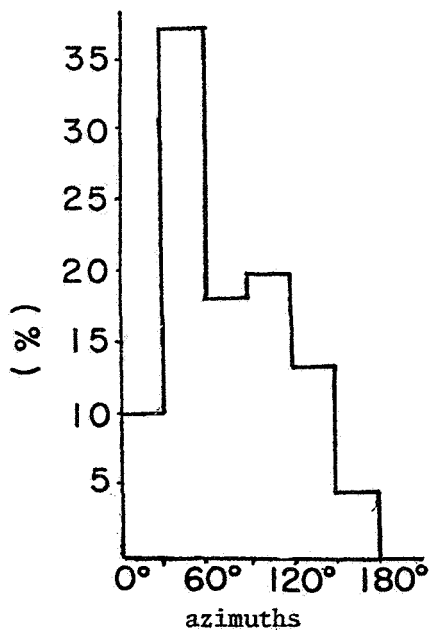


Figure 9a. Orientation of axial surfaces of the folds, surface and subsurface.

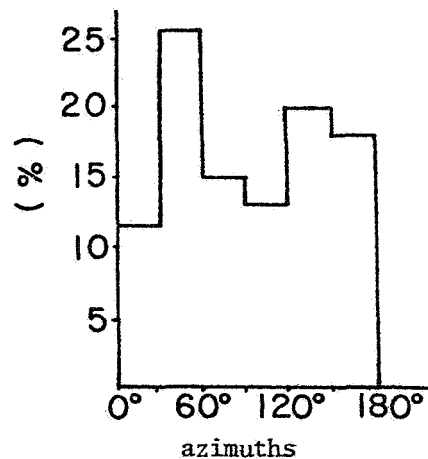
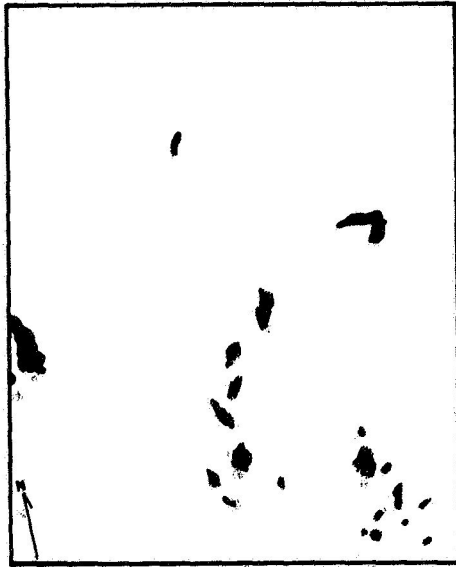


Figure 9b. Orientation of Precambrian linear features in the Laramie Mountains, such as faults, folds, fractures and foliations.

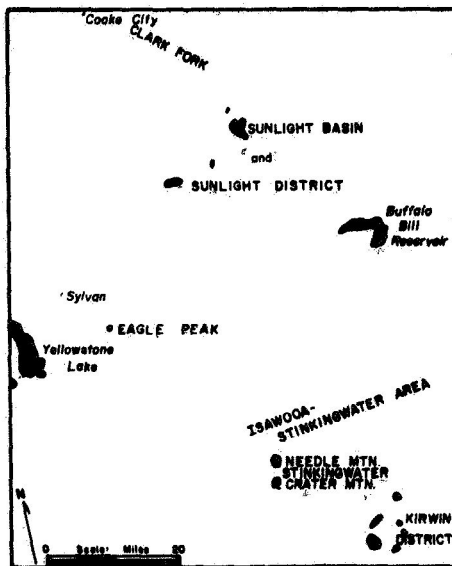
Figure 9. Comparison of orientation histograms for Laramie Basin folds and structures in the Laramie Mountains. Note the twin peaks of the Laramie Basin histogram relation fold axis that are both parallel and orthogonal to the dominant structural trend of the Laramie Mountains. (after Bekkar, 1973)



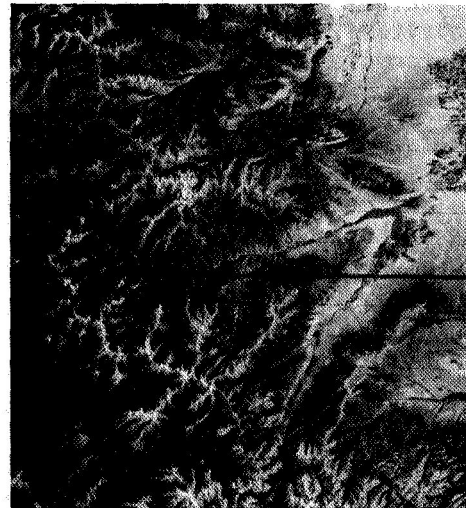
10-a. Alteration zones mapped by an interpreter unfamiliar with the study area.



10-b Alteration zones mapped by an interpreter with extensive experience in the study area.



10-c. Map of previously known areas of alteration.



10-d. Portion of ERTS-1 image 1014-17350 showing the Absaroka study area.

Figure 10 Maps of alteration zones in the Absaroka Mountains of northwest Wyoming. Interpreted from ERTS-1 color composite image 1014-17350.

A similar attempt was made to identify oxidized arkosic sandstone associated with uranium mineralization. In all major uranium producing areas of Wyoming the uranium occurs at the interface between oxidized and unoxidized sands (Fig. 11). The interface is generally marked by a distinct color change, with the oxidized sandstone being red or yellowish red and the unoxidized sandstone being tan or grey. We had hoped that the contrasting sandstones could be detected from ERTS, but our test study in a known uranium area of the Powder River Basin was unsuccessful (Fig. 12). A subtle contrast was noted in the test area, but when it was mapped and compared to the known color changes in the sands, the correspondence was slight. The lack of correspondence is greatest toward the southern end of the test area where the sandstone exposures are poorest. Coincidence of the mapped and known zones is considerably better in the northern part of the area, and there is some hope that such zones may yet be mapped in areas of good exposure. At the present time, however, we consider this an unsuccessful application of the ERTS data.

One of the earliest indications of the economic potential of ERTS resulted from a program in which the ERTS imagery was used to map greenstone belts in an area of granite-gneiss terrane of central Wyoming (Houston, 1973). Two greenstone belts were recognized on the ERTS image interpretation; a known greenstone belt in the southern Wind River Mountains and an unmapped belt in the northern Granite Mountains (Fig. 13). Detailed inspection of the Granite Mountains greenstone belt from high-altitude aerial photographs revealed several very distinct, dark colored outcrops. These proved to be outcrops of iron formation (Fig. 14).

The iron formation outcrops could not be detected on the ERTS-1 imagery, but they are confined to the greenstone areas that can be recognized on ERTS imagery. This, then, is a situation in which ERTS provides a means of "narrowing down" the area of interest so that the real exploration target (the iron formation) can be sought more efficiently by more detailed surveys.

ENVIRONMENTAL STUDIES

Wyoming, Montana, and North Dakota share enormous reserves of low-sulphur, sub-bituminous coal and lignite that will undoubtedly be developed by strip-mining techniques as soon as it becomes politically possible. Many of the necessary environmental surface resource studies to be done in conjunction with this development can be aided by remote sensing. The NASA programs in earth resources remote sensing come at a very opportune time in that the ERTS and aircraft data acquired in 1972-73 will not only serve as base line for detection of change, but also provide a great deal of the data necessary for planning and resource studies.

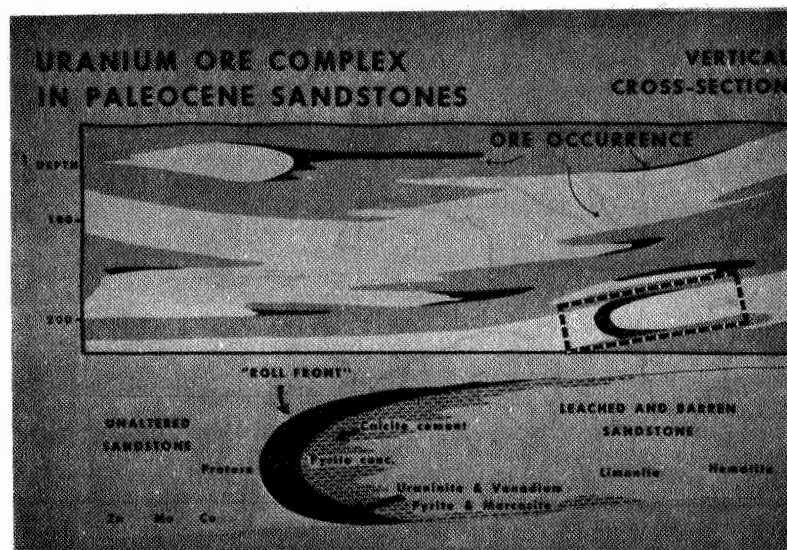


Figure 11. Diagram showing typical pattern of uranium deposition in Wyoming sandstones.

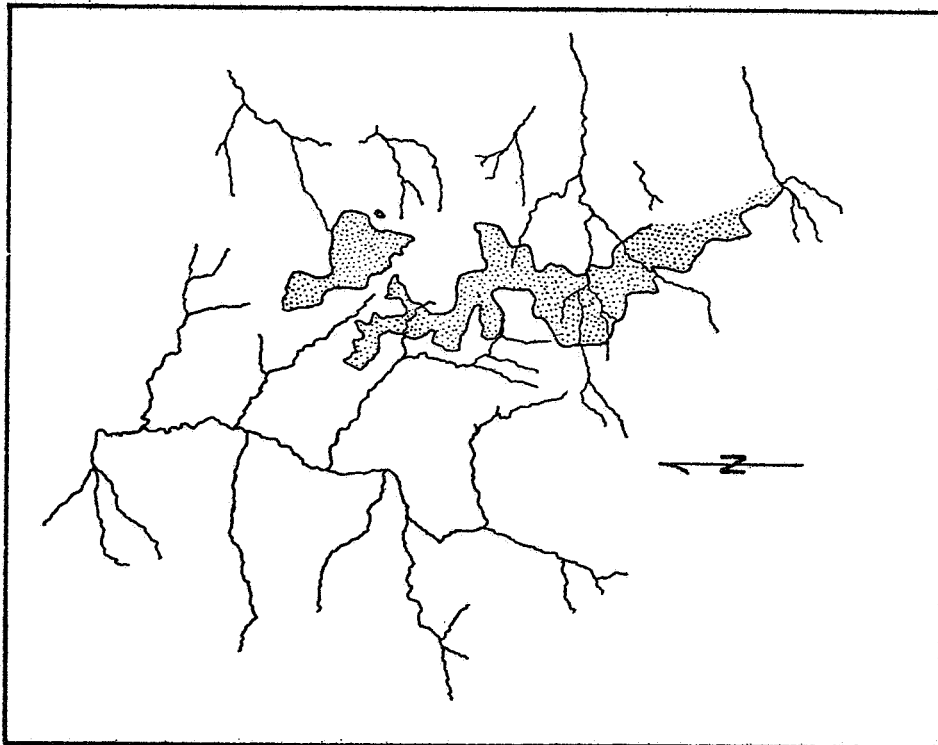


Figure 12a Surface color-change map of Pumpkin Buttes area, southern Powder River Basin, Wyoming. Anomalous zone interpreted from color composite ERTS image 1047-17182.

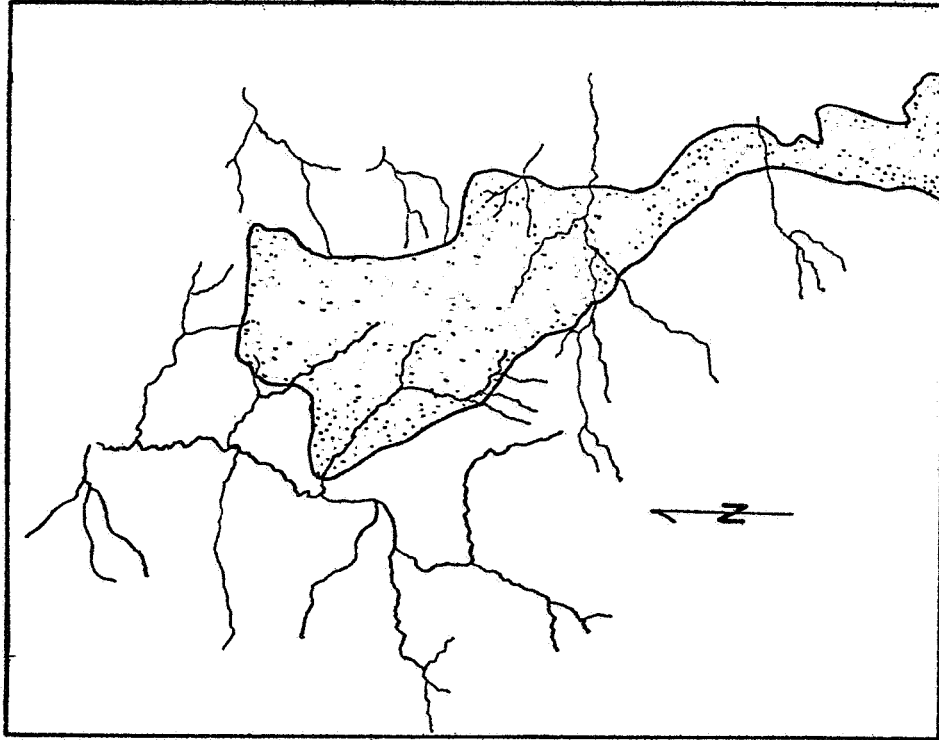


Figure 12b, Map of Southern Powder River Basin uranium area. Stippled area represents area of altered coarse-grained to conglomeratic sandstone. (after Sharp and Gibbons, 1964, plate III)

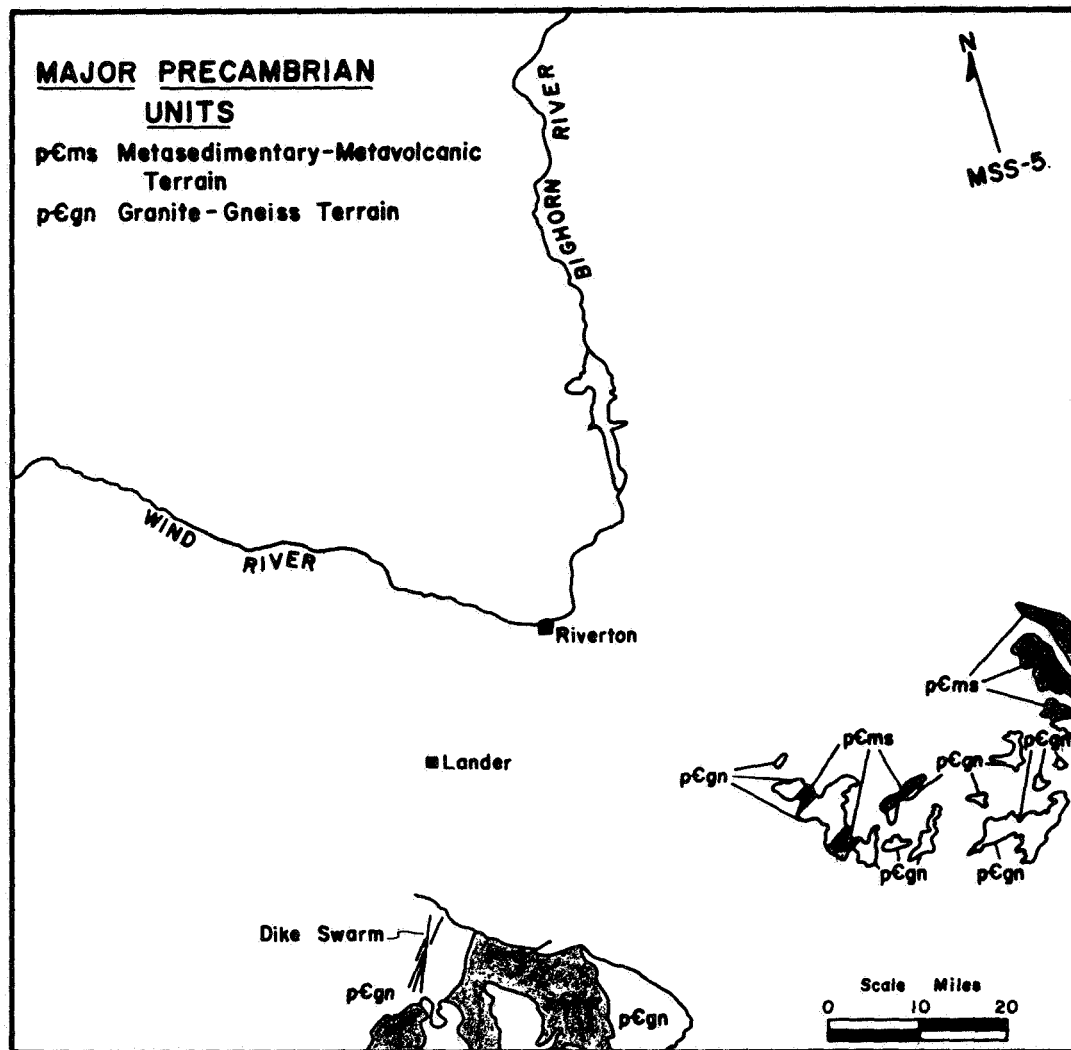


Figure 13 Map of Precambrian terrane of the southern Wind River Mountains and Granite Mountains showing greenstone belts pCms mappable from ERTS imagery.



Figure 14. Horseshoe-shaped bed of iron formation, Barlow Gap, Wyoming.

In January, 1973, a pilot program designed to test the applications of ERTS-1 data to land-use and resource management in Wyoming was completed for the Wyoming Department of Economic Planning and Development (Breckenridge and others, 1973). This pilot study demonstrated successful applications of ERTS image interpretation in ten land-use related studies. In the Powder River Basin test area, the study resulted in a 14-class land-use map, a regional soils map, a 6-class subdivision of range land, a water-impoundments map, a map of present open-cut mining operations, a map of coniferous and deciduous forests in the Bighorn Mountains, maps of several small urban areas, an average-slope map and several other topical maps related to geology. Density analysis and color-additive image enhancement proved of considerable value in several of these analyses.

SPECIALIZED INTERPRETIVE TECHNIQUES

Computer enhancement techniques employed in the various earth resources studies at the University of Wyoming include density analysis, clustering, and image ratioing. Such techniques are of demonstrated value in some applications, but, for the geologist, it appears that standard photointerpretation and image enhancement are still the chief means of using the ERTS and other remote sensor data. When special enhancement procedures appear to be necessary, the geologist (or other earth scientist) should have access to processed data. The processed data in such cases should be displayed in image form so that the interpreter can compare it to standard images and interpret it efficiently. Because the equipment necessary to process and re-display the data is prohibitively expensive, it seems that the processed data should be made available as an optional product along with the data original.

CONCLUSION

As the above studies illustrate, the present ERTS system has many applications in geology and related surface resource studies. Improved resolution and a narrower band selection will make future systems even more useful. There are probably very few geologists, regardless of their interests who cannot gain a new prospective and new information from ERTS. A major goal of the ERTS investigator should be to persuade these geologists to look at the images.

SELECTED REFERENCES

- Bekkar, Hamed, 1973, Laramide structural elements and relationship to Precambrian basement, southeastern Wyoming; unpublished M.S. Thesis, University of Wyoming, Laramie, 70p.
- Billingsley, F. C., 1973, Some digital techniques for enhancing ERTS imagery; in Symposium on Management and Utilization of Remote Sensing Data, Sioux Falls, South Dakota, Nov. 1, 1973, p. 285-293.
- Blackstone, D. L., 1972, Tectonic analysis of southwestern Wyoming from ERTS-1 imagery; NASA Technical Report CR-129651, 8p.
- _____, June 1, 1973a, Analysis of photo linear elements, Laramie Mountains, Wyoming; NASA Technical Report CR-132172, 16p.
- _____, June 10, 1973b, Analysis of photo linear elements, Bighorn-Pryor Mountains, Montana and Wyoming; NASA Technical Report CR-133017, 15p.
- _____, August 15, 1973c, Geology of photo linear elements, Great Divide Basin, Wyoming; NASA Technical Report NASA-CR-133634, 14p.
- Breckenridge, R. M., 1973, Glaciation in northwestern Wyoming; in Symposium on significant results obtained from the ERTS-1 Satellite, March 5-9, 1973, p. 363-370.
- Breckenridge, R. M., Marrs, R. W., and Murphy, D. J., 1973, Remote sensing applied to land-use studies in Wyoming; Symposium on significant results obtained from ERTS-1, March 5-9, 1973, p. 981-990.
- Houston, R. S., 1973, Distinguishing major lithologic types in rocks of Precambrian age in central Wyoming using multilevel sensing with a chapter on possible economic significance of iron formation discovered by use of aircraft images in the Granite Mountains of Wyoming; NASA Technical Report CR-130557, 34 p.
- Houston, R. S., Zochol, F. W., and Smithson, Scott B., 1973, Reconnaissance geologic mapping in the Dry Valleys of Antarctica using the Earth Resources Technology Satellite; NASA Technical Report CR-135665, 33p.
- Keefer, W. R., 1970, Structural geology of the Wind River Basin, Wyoming; U.S. Geol. Survey Prof. Paper 495-D, 35p.
- Kolm, K. E., 1973, ERTS multispectral scanner imagery applied to mapping of sand dunes in Wyoming; Univ. of Wyoming Department of Geology, Special Report under Contract NAS5-21799.

- Love, J. D., Weitz, J. L., and Hose, R. K., 1955, Geologic map of Wyoming; U.S. Geological Survey Map.
- Lyons, R. J. P., 1970, The multiband approach to geological mapping from orbiting satellites: Is it redundant or vital?; Remote Sensing of Env., Vol. 1, No. 4, p. 237-244.
- Nature, 1973, ERTS-technological success, scientific failure?; Nature, volume 245, no. 10, p. 345.
- Rich, E. I., 1962, Reconnaissance geology of Hiland-Clarksen Hill area, Natrona County, Wyoming; U.S. Geol. Surv. Bull. 1107-G, p. 540.
- Rowan, L. C., 1973, Iron-absorption band analysis for the discrimination of iron-rich zones; NASA Technical Report CR-129286, 4p.
- Sharp, W. N., and Gibbons, A. B., 1964, Geology and uranium deposits of the southern part of the Powder River Basin, Wyoming; U.S. Geol. Survey Bull. 1147-D, 60p.
- Tourtelot, H. A., 1967, Geology of the Badwater area, central Wyoming; U.S. Geol. Survey Oil and Gas Map OM-124.
- Vincent, R. K., 1973, Ratio maps of iron ore deposits of Atlantic City District, Wyoming; in Symposium on Significant Results Obtained from the ERTS-1 Satellite, March 5-9, 1973, p. 397-386.
- Wilson, J. E., 1970, Sensor detection capabilities study; U.S. Geol. Survey Circ. 616, 26p.
- Woodward, T. C., Geology of Deadman Butte Area, Natrona County, Wyoming; American Assoc. Petroleum Geologists Bull., v. 41, no. 2, p. 212-262.

SUMMARY OF AN INTEGRATED ERTS-1 PROJECT AND ITS RESULTS AT THE MISSOURI GEOLOGICAL SURVEY*

James A. Martin, William H. Allen, David L. Rath, and Ardel Rueff, *Missouri Geological Survey, Box 250, Rolla, Missouri 65401*

ABSTRACT

The aims of the Missouri Geological Survey ERTS-1 project have shifted significantly since its original inception. Initially, the non-funded study was to evaluate environmental and geologic engineering parameters along the St. Louis to Kansas City Corridor from ERTS imagery. However, normal work loads took precedence and problems developed in budgeting time. Though the corridor study suffered, utilization of both ERTS-1 imagery and NASA-supplied aerial photography provided a significant impetus to a number of other Survey projects.

Use of the imagery involved the recognition and interpretation of various ground patterns. Analysis and application are tied to ongoing programs. Specific studies utilizing the imagery and NASA aircraft photography are: a statewide lake and dam inventory; assessment of flooding and floodprone areas along the Missouri portion of the Mississippi and Missouri Rivers; land-use classification for several counties; structural features in selected areas, and Pleistocene features in northern Missouri.

Though it has been suggested that repetitive coverage is not necessary for geologic studies, it is this specific feature along with the synoptic view of large portions of the State that provided the potential for the utilization of the ERTS imagery in Missouri. Other State agencies, Departments of Conservation, Agriculture, and Community Affairs, have expressed interest in the potential application of ERTS data in their respective fields.

INTRODUCTION

Unlike funded projects which are tied directly to a specific subject, a diversified, nonfunded program has evolved within the Missouri Geological Survey. ERTS imagery and NASA photography are being used in 10 active Survey programs and 11 projects that are underway or have been completed by sister-state agencies, industry, or the federal government. A direct outgrowth of this interest in remote sensing has been the establishment by the Governor of a committee on Technical Data Sharing. The committee has the responsibility of making recommendations at the State government level on acquisition and use of remote sensing data.

*Publication authorized by the State Geologist, Missouri Geological Survey

PRECEDING PAGE BLANK NOT FILMED

N 74 30748

This report is a compilation of the significant geologic features defined on the ERTS-1 imagery. Many of the features shown have been previously described (Allen, Martin, and Rath, 1973, and Martin, Allen, and Rath, 1973).

Study of the imagery to date has been restricted to visual examination of the bulk product, both positives and negatives. False color infrared and color enhanced images are prepared from the bulk product on color diazochrome film. The method is simple, fast, and inexpensive -- exposed under a sun lamp and developed in a wide-mouth jar. The resulting product can be used directly or photographed for slides. Because of the varying densities found in the positive transparencies, it is necessary to experiment with exposure times in making the diazo enhancements.

DEVELOPMENT OF THE PRESENT ERTS-1 PROGRAM

The ERTS-1 investigation at the Missouri Geological Survey has changed completely both in aim and personnel from the original proposal. The initial study, to apply imagery data to urban and engineering geology problems along the St. Louis-Kansas City Corridor, did not develop. Two problems became apparent. One, most of the anticipated goals could not be realized from detail available on the imagery and two, the normal work load did not permit time for the project.

Examination of selected frames by the Mineral Resource and Areal Geology Sections of the Survey led to their use in several ongoing programs. This resulted in rather wide interest and utilization of the imagery both within the Survey as well as other State agencies. An outgrowth was the presentation at the NASA-sponsored second ERTS symposium, March 3-5, 1973 (First-Look Analysis of the Geologic Ground Patterns on ERTS-1 Imagery of Missouri, Allen, Martin, and Rath) and a paper presented at the American Society of Photogrammetry Remote Sensing Symposium October 29 - November 1, 1973 (Geologic Ground and Drainage Patterns from ERTS-1 Imagery of Northern Missouri, Martin, Allen, and Rath).

It was realized by mid-summer, 1973, that a revised program must be submitted to NASA if the Survey was to continue as an ERTS-1 investigator. This was done, accepted by NASA, and in September, 1973, the four authors listed replaced the original investigators. The principal aim of the modified study is a statewide inventory of geologic-related ground patterns, particularly in those areas of active programs, and as a prelude to our ERTS-B proposal.

NASA-supplied data have provided input into the following: structure, stratigraphy, mineral resources Pleistocene studies, Precambrian studies, geomorphology, physiography, pedology, land-use inventory, flood assessment, and dam inventory.

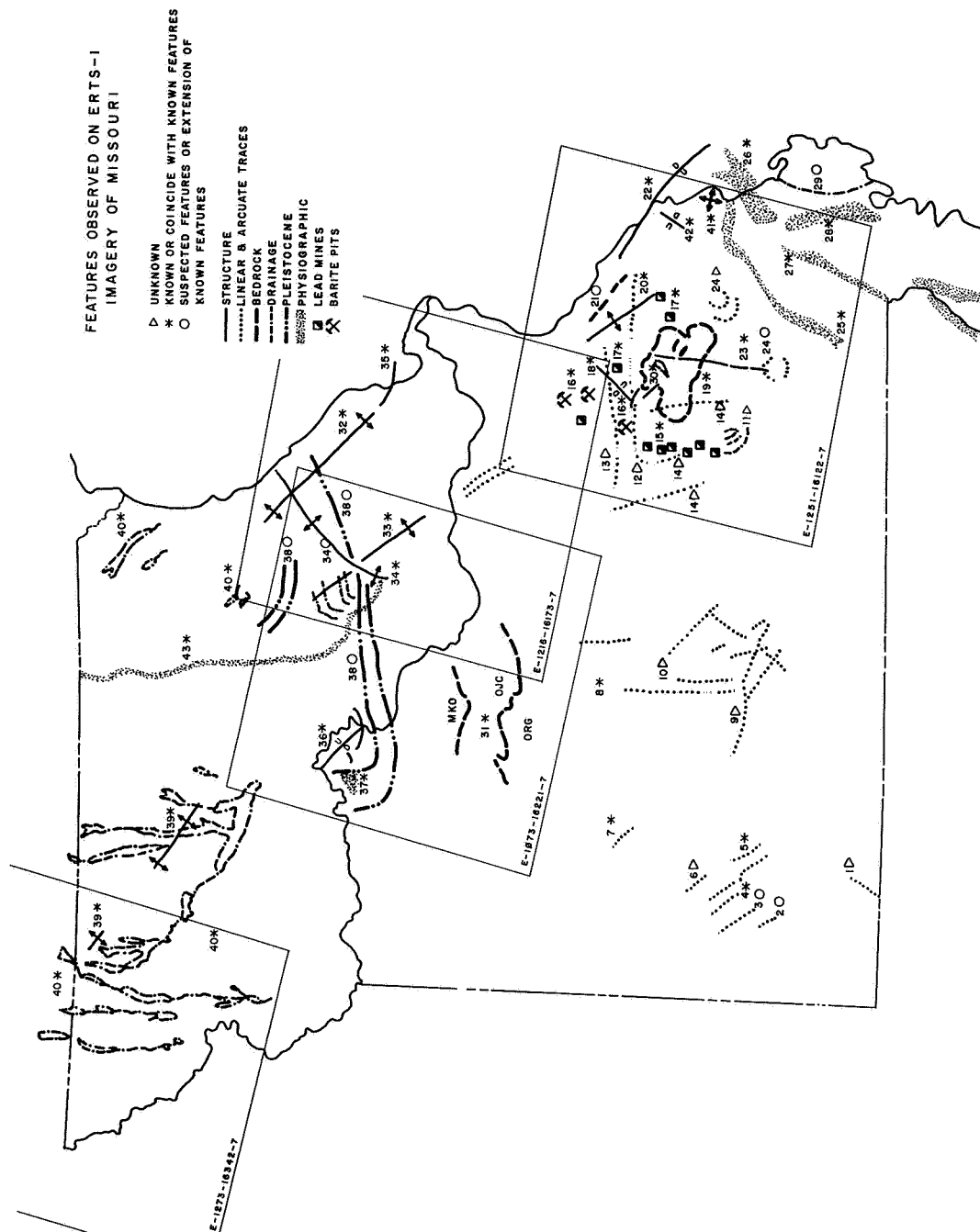
Three projects are summarized as examples of programs which utilize the ERTS and NASA aerial photography. These are followed by a listing and brief discussion of the ground patterns observed on the imagery of southwest, southeast, central and northwest Missouri.

PROJECTS UTILIZING ERTS AND OTHER NASA-SUPPLIED DATA

Dam Inventory: ERTS-1 imagery is being used in state-wide inventory of lakes and dams conducted by the Missouri Geological Survey for the Corps of Engineers in compliance with the 1972 National Dam Safety Act (PL 92-367). Lakes are transferred from the $9\frac{1}{2}$ " x $9\frac{1}{2}$ " Band 7 imagery to the 1:250,000 scale topographic maps and from this scale to the $7\frac{1}{2}$ ' quadrangle map series. Magnification capability does not permit direct transferring from 1:1,000,000 imagery to $7\frac{1}{2}$ ' quadrangle maps. Lakes of five to ten surface acres are plotted with certainty and those as small as two to five acres are identified with a fair degree of confidence. It is estimated that there are nearly 2,500 man-made lakes in Missouri. The ERTS imagery is playing a major role in determining lake locations, approximate surface acreages, greatly shortening the time required and keeping the inventory current.

Forest Inventory: Late in 1972, the Survey was contacted by the Forestry Division of the Missouri Department of Conservation on the feasibility of using ERTS imagery for forest mapping. We advised and assisted them on interpretation, provided imagery, and showed them the use of diazochrome transparency material. ERTS imagery was used in the determination of forest cover for 7 million acres in northwest Missouri and slides of the imagery were used by the Forestry Division at meetings with other state agencies to illustrate vegetation patterns as related to urban expansion. Coniferous forest cover can be distinguished from deciduous cover, but its recognition is dependent upon the time of year the image was recorded.

Flood Evaluation of the Missouri River, March-May 1973: Beginning March 10, 1973, flooding occurred on the Mississippi, Missouri and major tributary streams. For 9 weeks river level at St. Louis was above flood stage and four separate crests were recorded. Large areas of the Mississippi and Missouri River floodplains were inundated as the State experienced its longest flood of record. When it was realized flood period would be long ranging, a request was made to NASA/Goddard for U-2 or RB-57 coverage. On April 12, 1973, the Missouri River from Kansas City to St. Louis and the Mississippi River from St. Louis to the southern tip of the State was flown. The third and highest crest occurred on April 28th and 29th. Six days later on May 4, 1973, the Missouri Geological Survey underwrote a multispectral low altitude flight along the Missouri River from Boonville to St. Louis. The flight was made by the Kansas University Space Technology Center.



The Missouri River floodplain from Kansas City to St. Louis has been mapped to show areas flooded, areas of seep water, and major levee breaks. Comparison of the U-2 photos with the lower altitude photography shows the U-2 color infrared photography to be the more useful because of its greater areal coverage per frame and equal or better resolution. The larger areal coverage reduces evaluating time and allows for assessment of backwater along tributaries. The availability of this type data when needed emphasizes the importance of the NASA underflight program.

FEATURES OBSERVED ON ERTS IMAGERY

The main coverage studied is that of the southeast, east-central and the northwest. The geologic setting ranges from Precambrian through Tertiary with thick recent alluvium in the southeast; Ordovician through Mississippian with thin Pleistocene till cover in the east-central; and Pennsylvanian with thick glacial till and loess cover in the northwest.

The figure is a compilation of the significant linear, arcuate and other features observed on the imagery. In the following listing, structure names are used where the ERTS trace coincides with a known feature. Only the major features in each area are discussed. McCracken, 1971, is the principal reference to geologic structures in the State.

Southwest Missouri: Most of the coverage for this area has been cloud-covered and only a brief examination has been made. Bedrock in the area on which ERTS traces are plotted is lower Ordovician dolomite and sandstone in the east and Mississippian limestone in the west. Linears 4, 5, 7, and 8 coincide with the Golden City-Miller anticline, the Chesapeake fault, Humansville anticline and the Decaturville crypto-explosive structure, respectively. The other linears parallel or appear to be closely related to known structures.

Southeast Missouri: The majority of traces observed on the imagery of this area were described in Allen, Martin, and Rath, 1973. The principal mining areas, Barite District (16), Old Lead Belt (17), and the New Lead Belt or Viburnum Trend (16), are all quite apparent. Contrast in water reflectance aids in distinguishing tailings ponds from lakes. The major structural features that coincide with linears are the Ste. Genevieve fault system (22), the Big River fault (18), the Iron-ton fault (30), the Roselle lineament (23) and the Farmington Anticline (20). An almost E-W linear (12) appears on all coverage of the area. The trace roughly coincides with the postulated 38th Parallel Lineament of Heyl (1972) and others. Physiographic features prominent on all the coverage of the area are the Ozark Escarpment (25), Benton Hills (26), and the Sikeston Ridge (28). Crowley's Ridge (27) is prominent only on the "wet-weather" imagery. False color IR diazo-chrome of wintertime coverage highlights the outline of the igneous core (19) of the St. Francois Mountains. Three major soil classifications were distinguished on the

imagery of the southeast Missouri "Bootheel", an area of thick alluvium. Soil types delineated are sand, clay loam and silt loam. Separation was based mainly on drainage characteristics and the boundaries compare favorably with available soil maps.

Central Missouri: Three traces seen on most of the coverage of this area coincide in part with known structures -- Lincoln fold (32), Mineola structure (33) and the Mexico anticline (34). The Mexico and Mineola traces extend well beyond the known limits of these structures. Arcuate traces (38) are quite prominent on imagery of this area and are thought to represent or be related to early Pleistocene recessional moraines. These features are important to a better understanding of the Pleistocene history in Missouri. Bedrock boundaries (31) are enhanced on the imagery by changes in vegetation, soil, rock types and topography.

Northwest Missouri: The greater part of northern Missouri is blanketed by glacial drift ranging upwards to 400 feet. Bedrock exposures are quite limited. In addition to the present drainage system developed mostly on drift, there is a buried system developed entirely on bedrock and filled with sand, gravel and till. Stream patterns in this part of the State were rather indistinct on the early coverage. However, imagery made last spring and early summer, a period of heavy rainfall, was quite striking in that it gave the regional drainage an overall "chain-of-lakes" (40) appearance.

Wide floodplains are present where streams flow on drift; narrow segments are where flow is across bedrock highs resulting from thinning of drift, topographic highs on the bedrock surface, and regional structure. "Moisture-damming" takes place at these constrictions. Soil moisture accentuates the wide portions of the floodplain and appears to increase where the two drainage systems are superimposed.

Although glacial drift ranges upwards to several hundred feet in this area, a faint linear trace (39) on the imagery coincides with one of the known anticlinal structures.

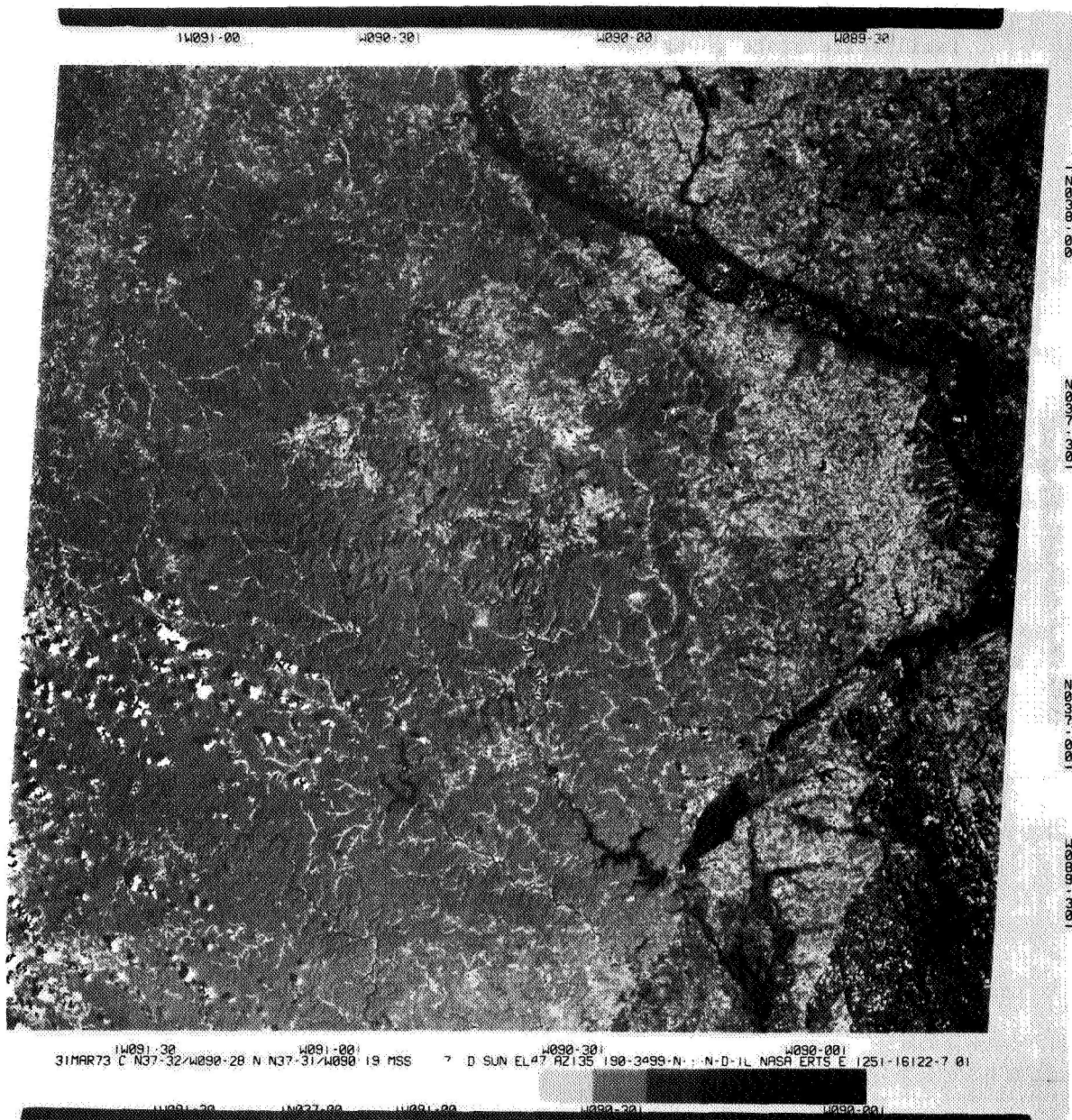
CONCLUSION

1. The variety of ERTS traces that coincide with known geologic features establishes the position of satellite imagery as a major reconnaissance tool.
2. Identification of ground patterns in a known setting is an important aid in the analysis of an unmapped area.
3. The repetitive coverage and wide synoptic view provided by the imagery are in themselves major enhancement features. Repetitive coverage was found to be a must for most geologic evaluations.

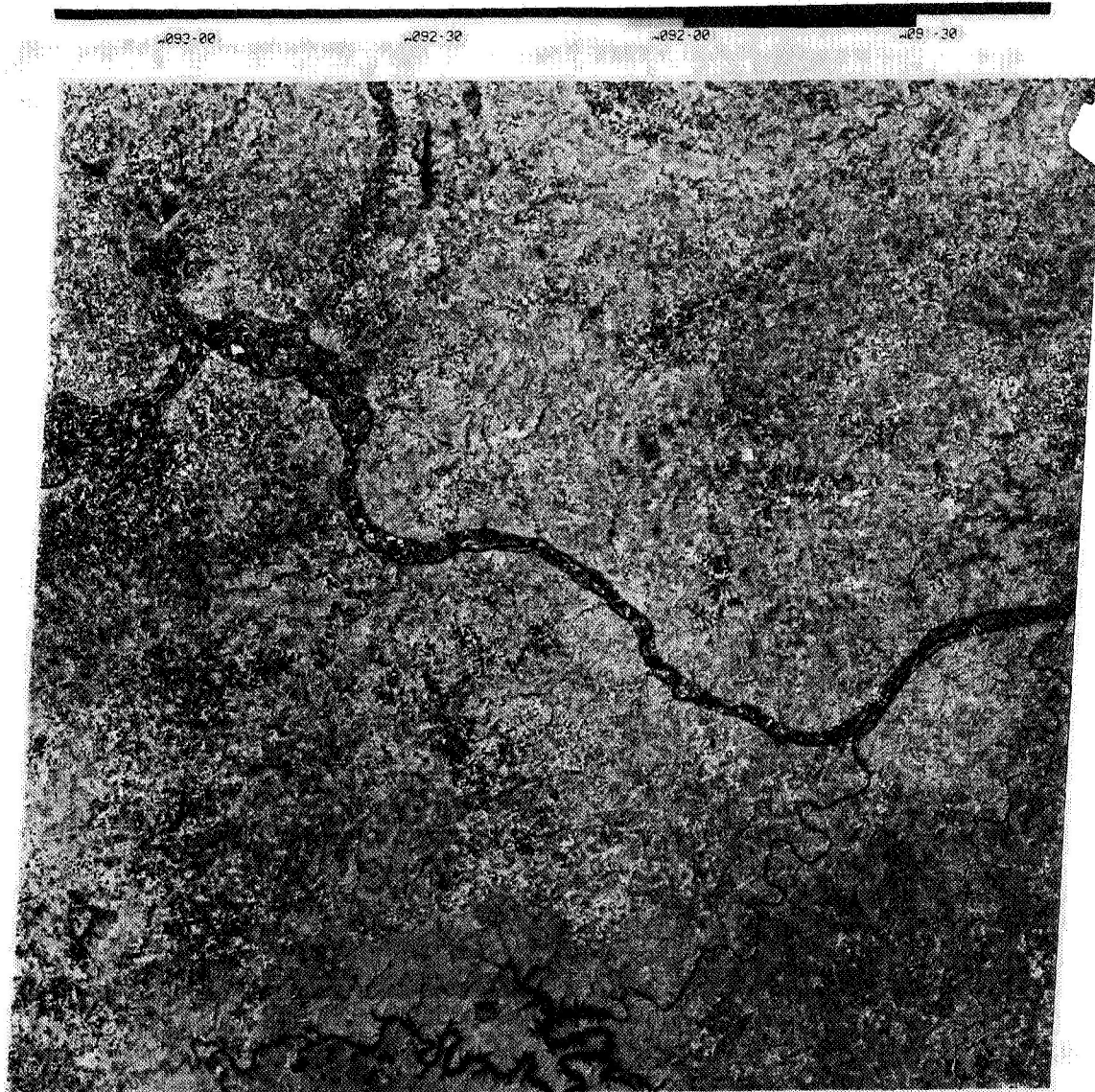
4. The number of geologic features identified on imagery of a mid-western setting shows its use in geologic studies is not limited to mountainous, arid, or barren shield terrain.
5. The use of satellite and high altitude imagery and photography provided by the NASA ERTS-1 program is being utilized by several state agencies and a Governor's committee is presently working to familiarize state government with the potential application of remote sensing data.

REFERENCES

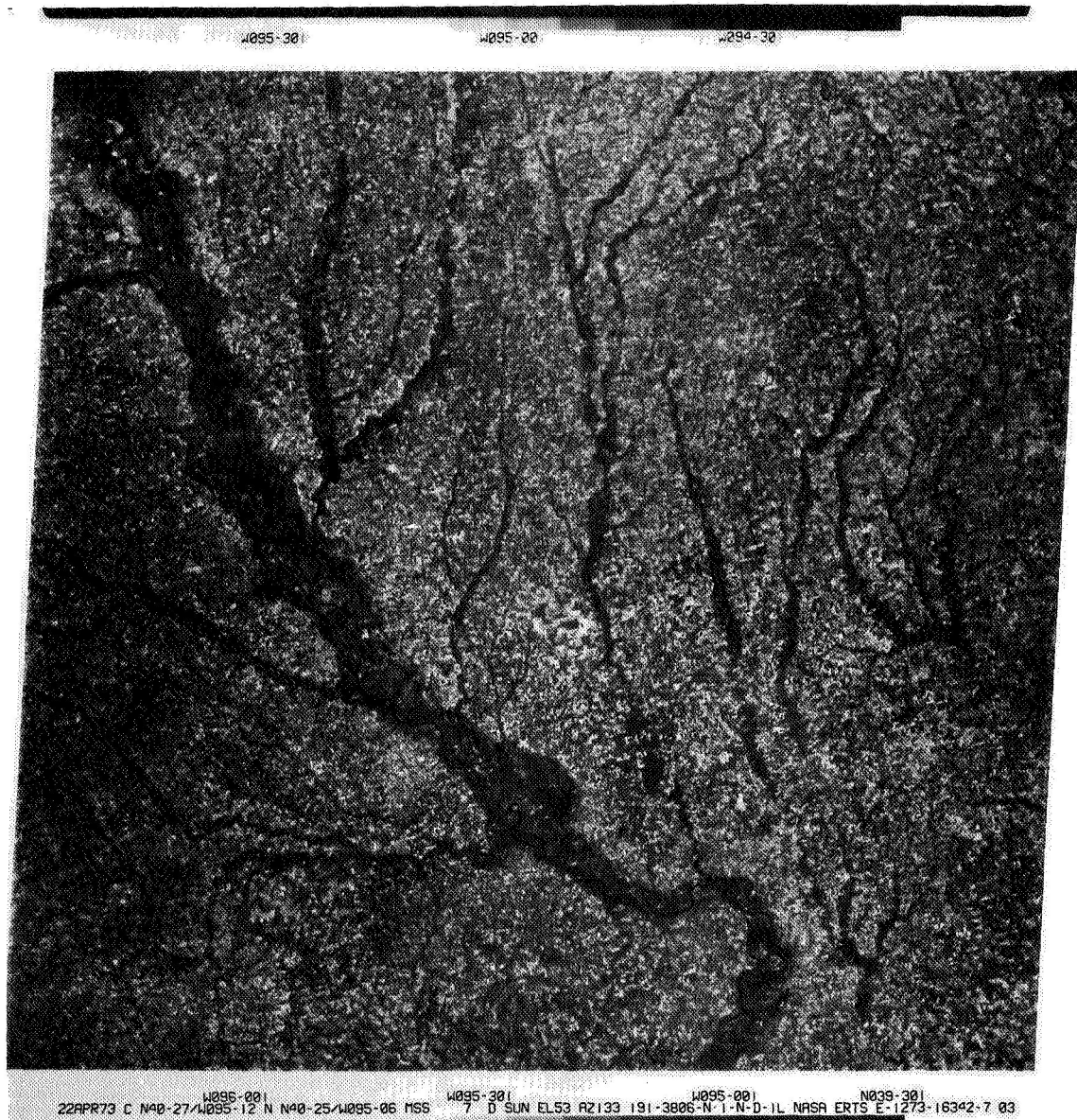
- Allen, William H., Martin, James A. and Rath, David L., 1973, First-look analysis of geologic ground patterns on ERTS-1 imagery of Missouri: in symposium on significant results obtained from the earth resources technology satellite-1, v. I: Technical Presentations Section A, NASA/Scientific and Technical Information Office, Washington, D. C.
- Heyl, Allen V., 1972, The 38th parallel lineament and its relationship to ore deposits: Econ. Geology, v. 67, p. 879-894.
- Martin, James A., Allen, William H. and Rath, David L., 1973, Geologic ground and drainage patterns from ERTS-1 imagery of northern Missouri: in Symposium proceedings on management and utilization of remote sensing data, American Society of Photogrammetry, Falls Church, Virginia.
- McCracken, Mary H., 1971, Structural features of Missouri: Mo. Geol. Survey Rept. Inv. 49.







04OCT72 C N38-58/W092-32 N N38-54/W092-27 MSS 7 D SUN EL41 AZ147 191-1017-G-1-N-D-IL NASA ERTS E-1073-16221-7 I



ANALYSIS OF STATE OF VEHICULAR SCARS ON ARCTIC TUNDRA, ALASKA

Ernest H. Lathram, *U. S. Geological Survey, Menlo Park, California*

ABSTRACT

Identification on ERTS images of severe vehicular scars in the northern Alaska tundra suggests that, if such scars are of an intensity or have spread to a dimension such that they can be resolved by ERTS sensors (> 20 meters), they can be identified and their state monitored by the use of ERTS images. Field review of the state of vehicular scars in the Umiat area indicates that all are revegetating at varying rates and are approaching a stable state.

INTRODUCTION

Umiat, Alaska was the hub of intense vehicular activity during the exploration of Naval Petroleum Reserve No. 4 in the period 1945 to 1952. It has since been used, though less intensively, by private industry as a staging area for petroleum exploration of sites outside the reserve.

Much concern has been expressed over the permanency of scars to the tundra resulting from damage to insulating vegetation and disturbance of the underlying permafrost brought on by such vehicular traffic. The more extreme conjectures purport that such scars will never heal and will spread unchecked.

Preliminary examination of ERTS-1 image 1004-21395 (taken in 1972), which covers the area around Umiat (fig. 1), revealed no trace of scars resulting from this activity (W. A. Fischer, *in* Lathram, Tailleux, Patton and Fischer, 1973, p. 38). Because ERTS sensors lack the resolving power (> 20 meters) required to recognize features as narrow as these tracks were originally, Fischer observed "This does not mean that the scars are gone, for I am confident they are not wholly healed and could be observed on the ground or from a low-flying plane, but it does mean that they are not spreading like cancer, as some purport, over the northern tundra." Subsequent study of this image under the microscope at enlargements up to 1:80,000 revealed that a scar on the ridge north of Umiat can be identified on Band 5 (reflected red light) images of the area.

During the summer of 1973, Robert L. Detterman, Geologist, U.S. Geological Survey, accompanied by John Koranda, Botanist, Lawrence Livermore Laboratory, made a one-day review of the status of the scars in this area. The area surrounding Umiat, in the eastern part of image 1004-21395, and to the east beyond its borders was examined from the air and on the ground. Weather prevented observations in the western part of the image area and was generally poor, with a ceiling of 100 feet and visibility of one-fourth mile, which also reduced the quality of illustrative photography. Comments herein that refer to the surface state of scars are based on the observations of Detterman and Koranda.

PRECEDING PAGE BLANK NOT FILMED

1 N 74 30749

During the planning, a report of a similar field study by the Bureau of Land Management in 1969 (Hok, 1969) was utilized, and it was possible to revisit areas previously studied for comparison and recognition of changes that had occurred over the intervening four years.

DISCUSSION

All scars observed in the Umiat area are being revegetated at varying rates depending on the nature, degree and age of the disturbance or are approaching a stable state. At all places where sites studied by Hok were re-examined, revegetation had proceeded further in the intervening four years.

The extent of scarring depends, as Hok found, on the season of occurrence, substrate (particularly with respect to water content, i.e., ice-wedge occurrence), degree of vegetation removal, and slope. Trails made by small tracked vehicles such as weasels and bombardiers have left little trace. LVT trails are most intensely scarred. Cat-tracks, with little or no blading, and used only in winter, do not cause extensive scars.

The scars presently visible from the air will remain visible from the air for a few years after the physical effects of the disturbance have been healed (fig. 2). The principal indicator of trails is the presence of grasses in the tracks that are not present in surrounding terranes, giving the tracks a greener appearance. Old trails are difficult to see on the ground at present and in 5 to 10 years will probably not be visible on the ground (fig. 3).

On lightly bladed trails in which only the tops of the tussocks were removed, while the rhizomes were left intact, growth is resuming in the original tussocks, and they will attain their original size in four to five years.

Trails crossing ice-rich lowlands that have been heavily bladed are assuming the appearance of the beaded stream prevalent in the tundra, a linear vegetated depression with irregularly spaced water-filled potholes up to 6 feet where an ice wedge was exposed (fig. 4). The beaded lakes will probably enlarge to the size of the ice wedges exposed, but interlake parts of the trails are not becoming wider, and the trails are approaching a stable state.

Although vegetal damage along trails in ice-poor soils is slightly wider than the original vehicle track, this damage is not propagating, i.e., the trails are not becoming wider.

Hok noted one site near the Colorado Oil and Gas Company Gubik test well, where a bladed trail made since 1960 crossed a 10° slope in ice-poor silt. Re-examination in 1973 shows increased revegetation of the main scar (fig. 5, compare with Hok, 1969, photographs 29 and 32), increased revegetation of part of the silted area at the foot of the slope (Hok, 1969, photograph 30), and little active siltation at present, indicating a reduction and early cessation of active erosion.

The most striking example of scarring, which Hok apparently did not visit, occurs on the ridge north of Umiat. Here a heavily used cat trail, bladed bare of vegetation, leads up a 10° slope to the site of several drill holes. Not only was the trail bladed, but it was also used summer and winter during the 1945 to 1952 period and crosses the exposed area of a bentonitic shale formation. The trail has spread to a depression on the slope about 150' wide and up to 15' deep (fig. 6). This is the scar noted on Band 5 ERTS images of the Umiat area. Here, revegetation is proceeding, with felt-leaf willow, equisetum, and a grass (stipa) not noted elsewhere, indicating the onset of healing, although much more slowly than elsewhere.

Study is continuing of images of this area and that to the south and east where exploration activity has occurred since 1960. Preliminary results indicate that younger scars may be more apparent on ERTS images than the older scars in the Umiat area. To date these studies have all been visual inspection of imagery. No attempt has been made yet to employ computer enhancement techniques to identify less severe scars or changes in scars.

CONCLUSIONS

The recognition of the scar north of Umiat on ERTS images indicates that if scars are large enough, or if they spread sufficiently to be resolved by ERTS sensors they can be recognized by use of ERTS data. Preliminary results of study of other images suggest that ERTS imagery can be used to identify young severe scars and monitor their healing.

REFERENCES

- Hok, J. R., 1969, A reconnaissance of tractor trails and related phenomena on the North Slope of Alaska: U.S. Dept. of Interior - Bur. Land Management, 65 p.
- Lathram, E. H., Tailleux, I. L., Patton, W. W., Jr., and Fischer, W. A., (in press), Preliminary geologic application of ERTS imagery in Alaska, in Symposium on significant results obtained from Earth Resources Technology Satellite-1: Nat. Aeronaut. Space Adm., Spec. Pub. SP-327, v. II, p. 31-38.

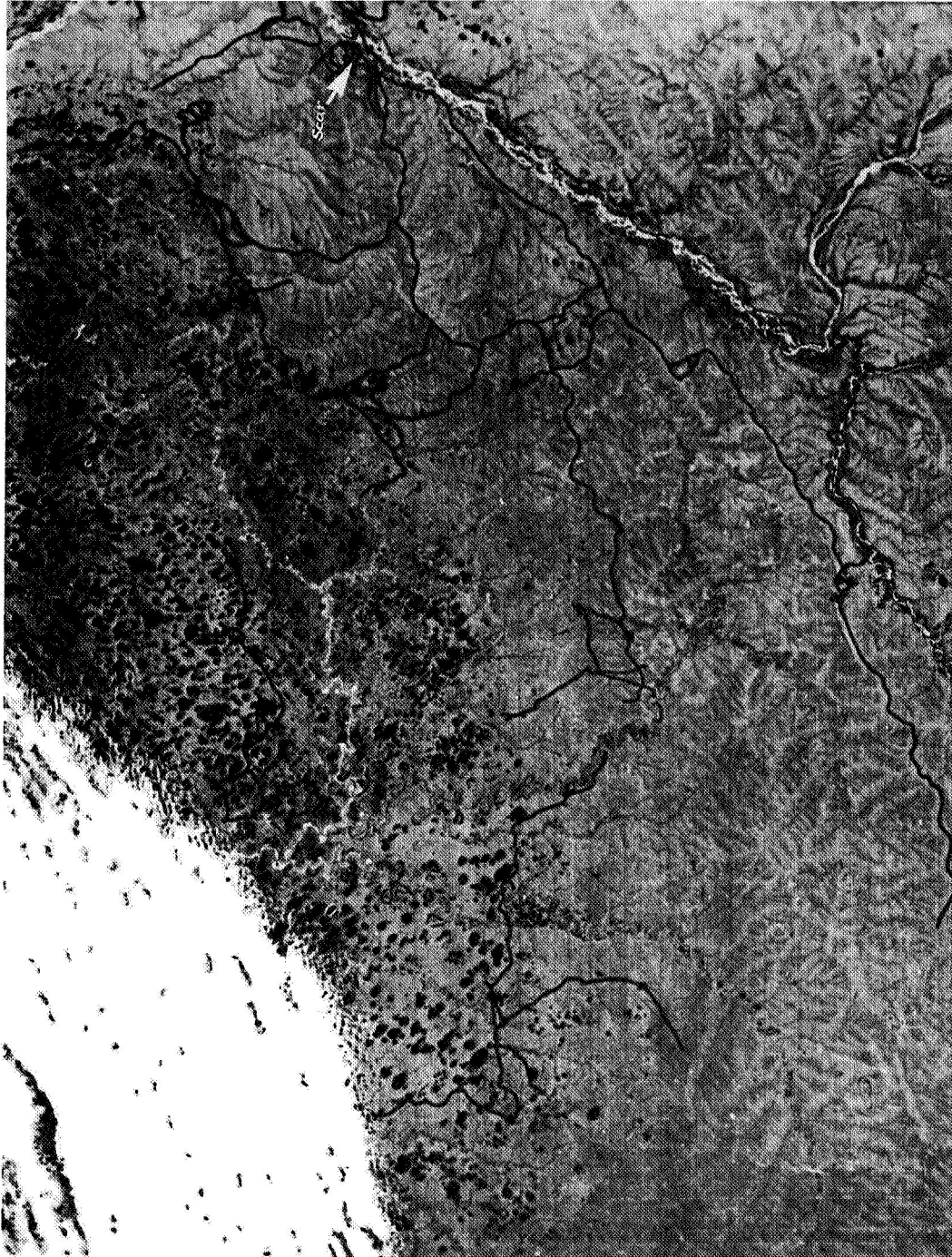


Figure 1 Known trails in the Umiat area.
Arrow shows location of scar visible on band 5 image of ERTS-1 scene 1004-21395.



Figure 2. Old trails on hills near Umiat.



Figure 3. Old trail in ice-poor soil near Umiat seen from ground.



Figure 4. Trail across ice-rich lowlands assuming appearance of beaded stream on right.



Figure 5. Scar formed by more recent activity than 1952



Figure 6. Severe scar on ridge north of Umiat.

THE INFLUENCE OF SEASONAL FACTORS ON THE RECOGNITION OF SURFACE LITHOLOGIES FROM ERTS-IMAGERY OF THE WESTERN TRANSVAAL

Jan Grootenboer, (*Spectral Africa (Pty) Limited, P.O. Box 2, Randfontein, Rep. of South Africa*)

ABSTRACT

The value to geological studies of repetitive ERTS-imagery was investigated by comparing two images gathered during different seasons over an area in the western Transvaal Province of the Republic of South Africa.

The first of the two images (1050-07355) was gathered on September 11th., 1972, co-inciding with the end of the dry winter season. The second image (1158-07363) was gathered in the middle of the summer rainfall season on December 28th., 1972.

A comparison of the two images reveals striking differences in the amount of recognizable geological detail. The most pronounced difference is the marked enhancement on the December image of tonal variations associated with individual surface lithologies. This contrast in tonal values is evident in all four spectral bands, though particular bands emphasize individual lithologies more clearly than others. Basic igneous rocks of the Bushveld Complex, for instance, are most clearly defined on bands 6 and 7, while certain areas underlain by granite are distinguishable only on band 4.

Tonal variations on the September image permit recognition of the major lithological units to a degree which is slightly inferior to that displayed by a 1:1 000 000 scale geological map. The very marked tonal differences displayed by the December image, however, permit recognition of detailed lithological units compatible with published geological maps at 1:250 000 scale. In addition, this image reveals the presence of distinct stratigraphic subdivisions within the previously undifferentiated Dolomite Series of the Transvaal System.

The differences exhibited by the two images clearly demonstrate the importance of repetitive ERTS coverage in geological investigations, particularly in areas of marked seasonal variations. In the present case variations in soil moisture content and atmospheric haze appear to constitute the most important factors exerting an influence on the tonal characteristic of different surface lithologies and consequently on the ease of recognition of such lithologies. Under different conditions, however, other seasonal factors may be of equal or greater importance.

N 74 30750

PRECEDING PAGE BLANK NOT FILMED

INTRODUCTION

This report summarizes the results of a comparison of two ERTS-images of the same area under different climatic conditions, allowing a preliminary assessment to be made of the importance of seasonal factors on the ease of recognition of geological features from ERTS imagery.

The images (1050-07355 and 1158-07363) cover a portion of the western Transvaal Province of the Republic of South Africa, centered on a latitude of approximately 26°S and a longitude of 27°E. The area covered by the images has a steppe climate with the annual precipitation averaging from 900 mm in the east to some 650 mm in the west. Precipitation is almost exclusively in the form of showers and violent thunderstorms, and falls mainly during the summer months from October to March.

Physiographically most of the area lies within the Transvaal Highveld region, a flatlying or gently undulating plateau at an altitude of between 1 800 and 2 200 m above sea level. The topography is strongly dependent on the underlying geology with the more resistant rock units frequently forming conspicuous elongated ridges. The Highveld area is covered largely by prairie grasslands, though the ridges frequently support some acacia thornbush and various indigenous and cultivated trees line the local streams. Large areas are devoted to the cultivation of corn.

- The northeastern portion of the image forms part of the Transvaal Plateau basin, consisting of an even flat terrain which is only occasionally broken by low inselbergs of rock outcrop. The vegetation consists almost exclusively of Thornbush savanna but a few small areas are under irrigation and devoted to citrus groves, tobacco and wheat farming.

The area is of considerable geological interest as it includes the gold and uranium mines of the central and west Rand, the platinum and chrome mines of the Bushveld Complex, the Lichtenburg diamond fields, the Marico lead/zinc deposits, as well as numerous other mineral occurrences. Intense geological investigation has been in progress over the last 90 odd years following the discovery of gold in 1886, and the area has been repeatedly mapped both by mining companies and the Geological Survey.

ERTS DATA AND ANALYSIS

The two images compared are 1158-07363 gathered on the 28th of December, 1972 and 1050-07355 gathered on September 11th., 1972. Both images are completely free of cloud cover. All four spectral bands on image 1050-07355 are rated "G" but definition in all four bands on 1058-07363 is poor and all were rated "P".

A detailed comparison of the geological information contained in the two images was based on "conventional" false colour composite prints of spectral bands 4, 5 and 7, enlarged to a scale of 1:500 000. In addition to the detailed comparison between the false colour composite prints, a more rapid comparison was made between black and white paper prints of all four spectral bands of the two images at 1:500 000 scale.

Interpretation of the geological information on the images centered mainly on the recognition and accurate delineation of surface lithologies. Structural features such as lineaments fracture patterns, and faults were given only scant attention.

REGIONAL GEOLOGY

Figure 1 illustrates the regional geology of the area covered by the images.

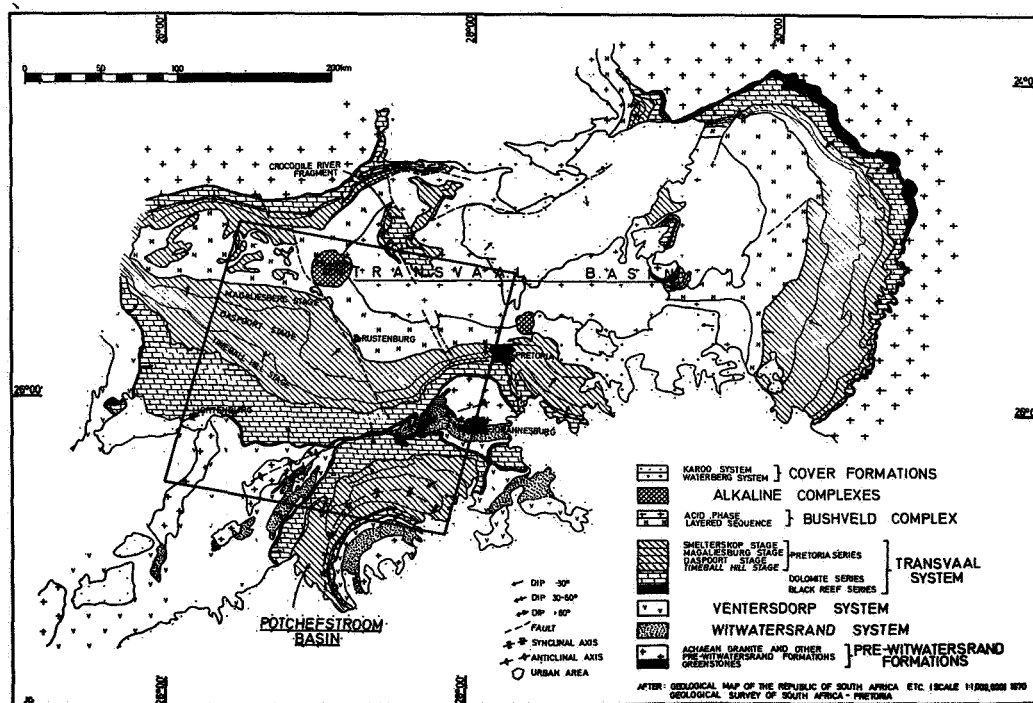


FIG. 1 : Regional geology of part of the Transvaal Province showing the approximate area covered by ERTS-images 1050-07355 and 1158-07363

Most of the area is underlain by rocks belonging to the Transvaal System of late Proterozoic age, consisting of a very thin basal clastic unit (Black Reef Series) overlain by a 1 700 m sequence of massive dolomitic limestone (Dolomite Series), which is in turn overlain by a thick sequence of alternating quartzites and shales with occasional volcanic horizons, (Pretoria Series). Intrusive diabase sills become abundant near the top of the Pretoria Series. The rocks of the Transvaal System have been folded into two synclinal basins, portions of both being represented on the imagery. The northern 2/3 of the images cover the south western portion of the Transvaal basin, characterized by regular structure and shallow dips. The south eastern corner of the images includes a portion of the curved Potchefstroom basin of more complex structure and steeper dips.

The two major basins of the Transvaal System are separated by a major N.E.-trending anticlinal axis along which older rocks of Archaean and Proterozoic age are exposed, the former consisting predominantly of granite with a few scattered occurrences of greenstones. Proterozoic rocks are represented by the Witwatersrand and Ventersdorp Systems, the former sequence consisting largely of quartzites with occasional interbedded shales while the latter comprises andesitic volcanics with interbedded sediments.

The centre of the Transvaal Basin is occupied by the Bushveld Igneous Complex comprising the Layered Sequence of basic igneous rocks and the Bushveld Granite consisting of granitic material. The structure of this area is very regular and dips are shallow. West of the Pilansberg, however, the structure is more complex and numerous outcrops of quartzitic floor rocks protrude the basic rocks. The Pilansberg Complex, a circular ring structure made up of a variety of alkaline rocks, intrudes the Bushveld Complex at the northern extremity of the images. Throughout the area small scattered patches of flat-lying and deeply weathered Karroo sediments (tillite, sandstone and shale) occur. Locally surficial deposits of alluvium, surface limestone, windblown sand and scree may obscure bedrock geology. Intrusive rock types include diabase sills in the Pretoria Series, alkaline dykes related to the Pilansberg Complex, and numerous post-Karroo dolerite dykes and sills.

Outcrop conditions are poor and most of the western Transvaal is covered by residual soil. The only units which form significant outcrops are the quartzites of the Witwatersrand and Transvaal Systems, the Pilansberg and occasional inselbergs within the Bushveld Complex.

ERTS-1 IMAGE 1050-07355

This image (fig. 2) was gathered on September 11, 1972 at the end of the dry winter season. At this time of the year the area was largely covered by "khaki-coloured" dry grass with all

indigenous vegetation being virtually leafless and the cornfields lying fallow. The false colour composite image of bands 4, 5 and 7 shows a relatively uniform predominantly light brown colour tone. The most distinctive tonal variations are related to areas of dense vegetation along stream channels and areas of wheat agriculture and orange groves. Areas of recent burning are marked by very dark colour tones. Slight tonal variations are associated with certain surface lithologies allowing recognition of the major geological units to a degree roughly comparable to that shown on published 1:1 000 000 scale maps. (Figs. 1 and 4).

The distribution of the Transvaal System is readily recognized and some individual lithological units can be distinguished, particularly in the central portion of the image where the structure is regular. The Magaliesberg quartzite is very evident, primarily due to a shadow effect. Shale bands are characterized by light colour tones though becoming more purple near the top of the sequence. The Dolomite shows a uniform darker tone with particularly the basal zone, immediately above the Black Reef being readily distinguishable. Towards the eastern extremity of the image outcrop areas of dolomite are clearly evident. The pre-Transvaal areas generally show very uniform tonal qualities but textural patterns permit recognition of Witwatersrand rocks. Basic rocks of the Bushveld Complex are readily distinguished by their dark colour tones but a detailed assessment of their distribution is hampered by the effects of numerous areas of burning over their outcrop area. The area underlain by Bushveld granite is characterized by a textureless light colour tone. The Pilansberg Complex can be recognized primarily on the basis of textural characteristics which very clearly accentuate the concentric ring structure. Throughout the image outcrop areas are characterized by uniform darker colour tones. Fracture patterns are clearly visible, as are some of the more prominent dykes.

ERTS-1 IMAGE 1158-07363

The image (fig. 3) was gathered on December 28th., 1972 at the height of the rainy summer season. At this time the area was covered by green grassland with the indigenous vegetation in full leaf. The majority of the cornfields, however, were still largely bare with plants in a very youthful stage. The false colour composite image of bands 4, 5 and 7 shows very strong tonal variations, the majority of which appear to be directly related to surface lithologies, particularly where shallow dipping rocks of the Transvaal System and the Bushveld Complex are concerned. The major geological units are immediately apparent and can be accurately delineated. (Fig. 4).

Areas underlain by Archean Granite in the eastern portion of the image are characterized by a mottled reddish colour tone, and show a uniform textural pattern. The slightly darker tone associated

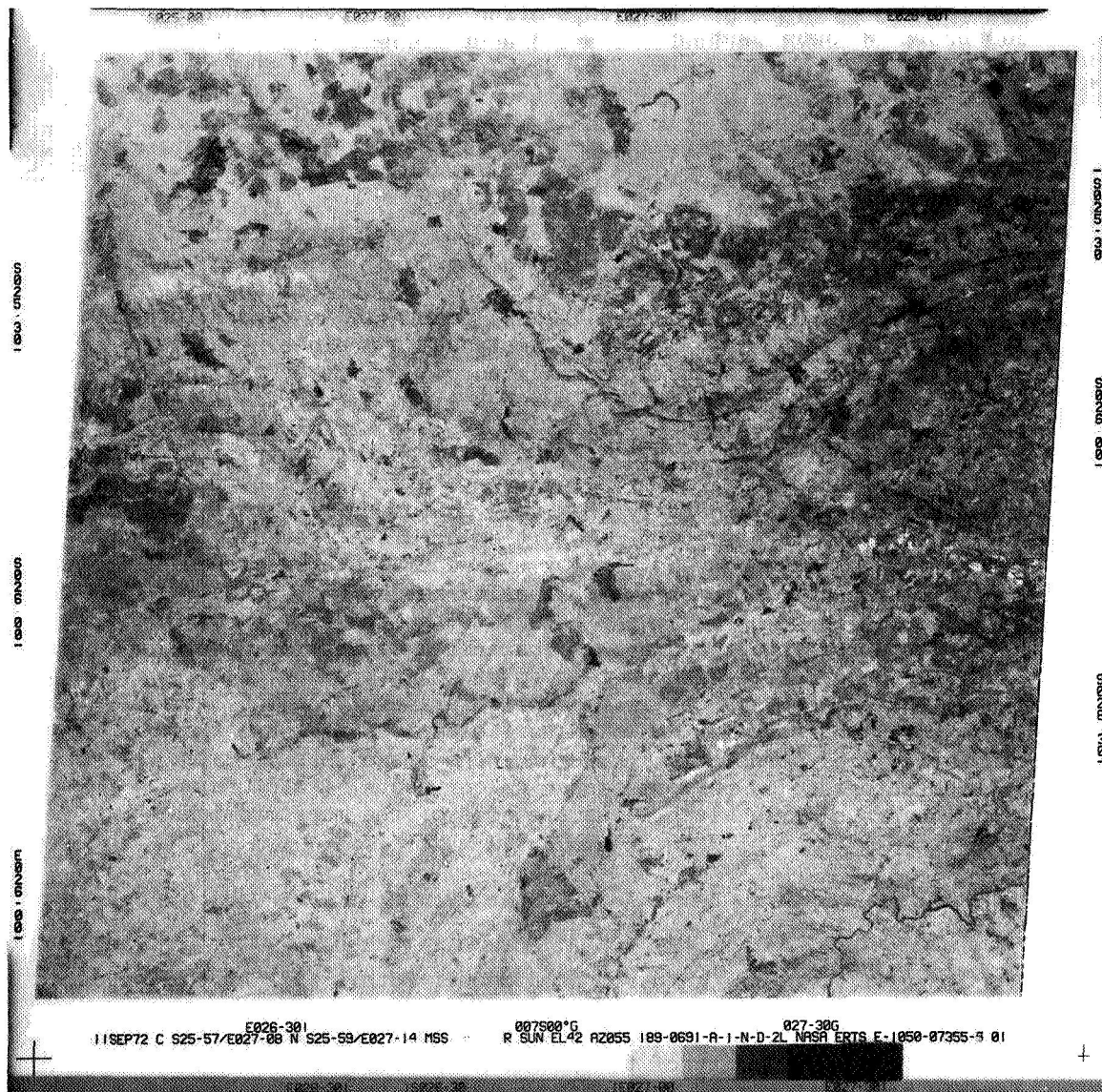


FIG. 2 : Composite colour print of bands 4, 5 and 7 of ERTS-image 1050-07355 gathered on September 11, 1972 at end of dry Winter season.

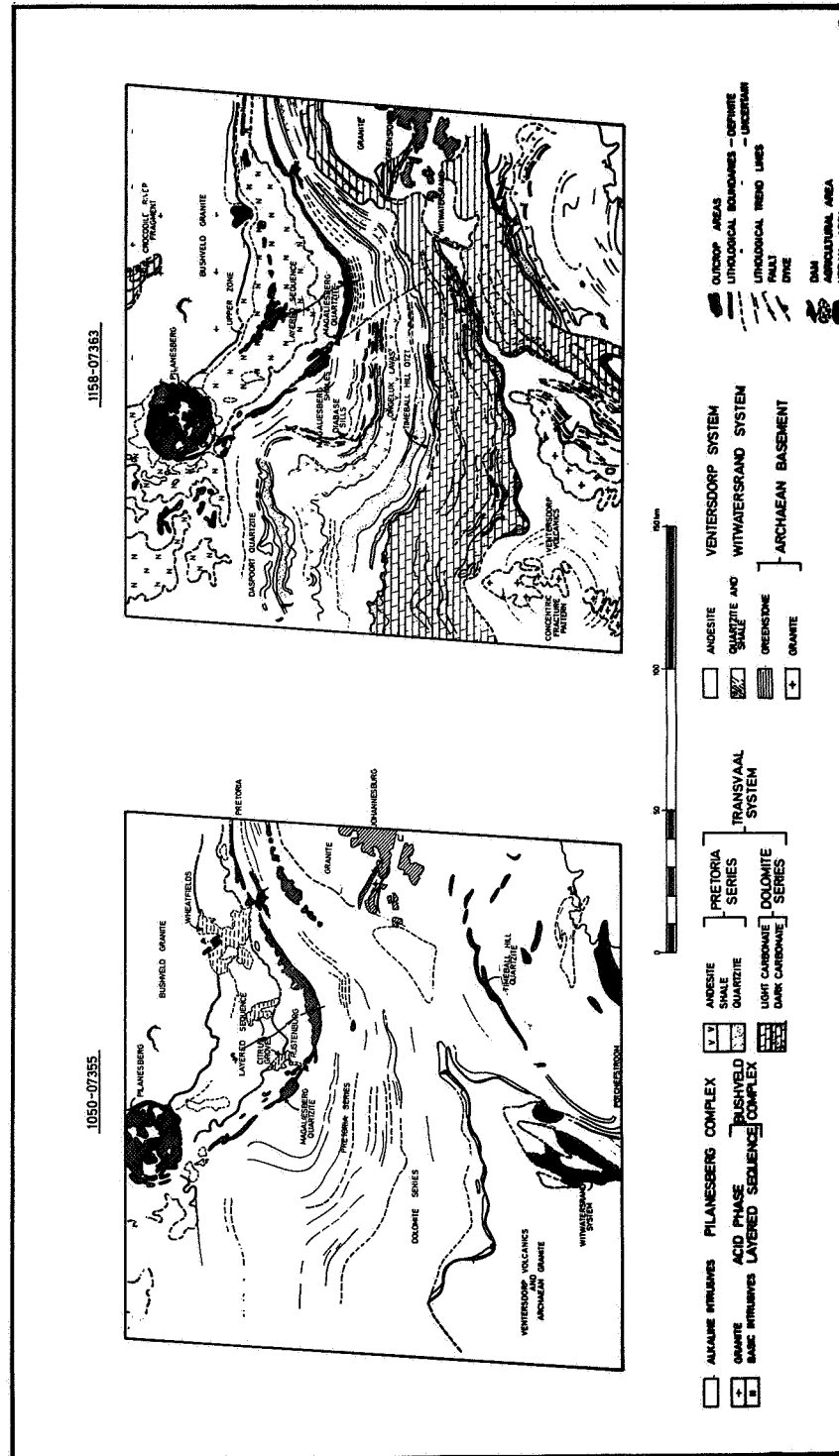


FIG. 4 : Geological interpretation of ERTS-Images 1050-07355 and 1158-07363 with emphasis on Lithological Features.

with greenstones can be distinguished only with difficulty. Darker colour tones are also associated with the Witwatersrand Quartzites, though generally these rocks are more readily distinguished on the basis of their distinct linear texture. The Ventersdorp rocks in the south western corner of the image are characterized by a uniform, textureless, green colour tone. The area is one of very poor outcrop but it is nevertheless possible to recognize areas underlain by granite, these exhibiting a yellow colour tone.

Strong tonal variations permit identification and accurate delineation of detailed lithological units in the Transvaal System. Within the Pretoria Series, all significant lithological units can be recognized, with detail in the central portion of the image being comparable with that shown on the official published 1:125 000 map of the area. Quartzite units have an intermediate grey colour tone, (fig. 4), the interbedded shales exhibit a very light colour tone, and the Ongeluk volcanics are locally clearly distinguishable by their green colour tone. The shales of the Magaliesberg Stage exhibit a variable colour tone ranging from light-, to dark-brown, and this may be due to the presence of diabase sills, some of which can be distinguished individually. A few lithological units not shown on the published geological maps can be identified including thin discontinuous shale units immediately above the upper Daspoort Quartzite and lithostratigraphic detail within the Magaliesberg shales. The Transvaal Dolomite is characterized by broad alternating zones of light green and dark grey colour tones. These clearly reflect broad stratigraphic units which to date had not been recognized from this area in spite of the long history of geological activity. Field investigations (Grootenboer, Eriksson and Truswell, 1973) identified the zones as corresponding to units of chert-rich light-coloured and chert-poor dark-coloured dolomitic limestone which could be correlated with the detailed stratigraphy established elsewhere. Certain areas within the Transvaal Dolomite show a distinct uniform green colour tone. Stratigraphic detail is absent in these areas and they almost certainly correspond to local thick soil cover, much of which may be of a transported nature.

Basic rocks of the Bushveld Complex show a distinctive dark-blue colour tone, resulting from their low reflectance in band 7. Areas of outcrop within the Layered Sequence are clearly identifiable. The basal contact of the Sequence is invariably obscured by surficial scree, but the upper contact with the Bushveld Granite is clearly defined and can be accurately traced. Of particular interest is the recognition of a distinct zone of darker tone at the top of the Layered Sequence coinciding with the so-called "Upper Zone", a unit of relatively more magnetite rich gabbroic rocks. To the west of the Pilansberg the numerous small occurrences of quartzite, with associated scree, penetrating the basic rocks of the Complex, are clearly visible. Whilst the granitic rocks of the B.I.C. as a whole are readily recognizable, a more detailed subdivision into granite, granophyre and felsite is not possible. Interpretation is rendered difficult by variable land use patterns, surficial deposits and the effects

of donga erosion. A small folded outlier of Transvaal rocks (Crocodile River Fragment) within the Bushveld granite is recognizable only on the basis of its textural characteristics.

Additional features of geological interest which are clearly recognizable on the image include dykes, lineaments, joints, faults, concentric ring structures (all characterized by distinctive textural patterns), areas of scree cover and surficial deposits. Outcrop areas are characterized by a relatively uniform dark-grey colour tone, and their lithologies are frequently indistinguishable on the basis of colour tone alone, in strong contrast with areas of poorer outcrop where strong tonal contrasts reflect the various lithologies. Non-geological features include natural vegetation patterns, agricultural land use patterns, urban areas, dams, streams, rivers, mine dumps, and roads.

DISCUSSION

A comparison of the colour composites of the two images (figs. 2 and 3) reveals striking differences in the tonal contrast between various surface lithologies differences. The depth of colour and tonal contrasts on the December image are enhanced, relative to the September image, permitting recognition of a great amount of geological detail in spite of its technically poor quality. The wealth of tonal variation on the former image does to some degree obscure other geological features such as fracture patterns and areas of outcrop. An examination of the individual spectral bands reveals that the tonal contrasts displayed by the colour composite is present in every individual spectral band. In virtually every instance a particular geological feature is more clearly displayed on a particular band of the December image compared to the same band on the September image. Table 1 provides a summary of the degree to which various geological features are characterized by tonal differences in individual spectral bands and on the colour composites.

A number of factors could be responsible for the differences in tonal contrast between the two images. The uniform tonal enhancement over the whole area of the image and in every individual band strongly suggest that a major large scale seasonal influence is at work. While factors like vegetation, and differential land use could all contribute to the effect, such contributions would generally be confined to individual bands only or to particular areas. It would seem that two factors, both indirectly related to rainfall, are largely responsible for the variation in tonal contrast; viz. soil moisture contrast and atmospheric haze. Fig. 5 illustrates the weekly rainfall for a number of stations in the western Transvaal as well as the dates on which the images were gathered. Over the 4 month period preceding the September image the total precipitation did not exceed 20 mm at any one of the stations. The December image on the other hand was gathered in the middle of the rainy season with weekly precipitation reaching up to 60 mm.

Table 1

TONAL CHARACTERIZATION AND RECOGNIZABILITY OF GEOLOGICAL FEATURES IN VARIOUS SPECTRAL BANDS

	Colour Composite		Band 4		Band 5		Band 6		Band 7	
	1050-07355	1158-07363	1050-07355	1158-07363	1050-07355	1158-07363	1050-07355	1158-07363	1050-07355	1158-07363
NASA rating of image quality			G	P	G	P	G	P	G	P
Topographical detail	Distinct	Distinct	v. Poor	Fair	Fair	v. Dist.	Distinct	Fair	Fair	Fair
<u>General Geological Features</u>										
Overall tone contrast of lithological units	Poor	v. Distinct	v. Poor	Fair	Poor	v. Distinct	Poor	v. Distinct	Poor	v. Distinct
Outcrop areas	Distinct	Poor	v. Poor	Fair	Fair	Distinct	Poor	Poor	Distinct	Poor
Fractures	Fair	Fair		Fair	Distinct	Distinct	Poor	Fair	Fair	Poor
Faults	v. Poor	Distinct		Fair	Distinct	Distinct		Fair	Fair	Fair
Dykes	Distinct	Distinct		Distinct	Poor	Fair		v. Poor	Poor	Poor
<u>Individual Lithologies</u>										
Bushveld: Granite	Fair	Distinct	v. Poor	Distinct	Fair	Fair	Poor	Distinct	Poor	Distinct
	Distinct	v. Distinct	Poor	Fair	Distinct	Poor	Distinct	v. Distinct	Distinct	v. Distinct
		v. Distinct		v. Distinct		Fair				Poor
	Distinct	Distinct	Poor	Distinct	Distinct	Distinct	Distinct	v. Distinct	Fair	v. Distinct
Pillanesberg Complex	v. Poor	Distinct		Distinct		Distinct	v. Poor	Poor	Poor	Poor
Pretoria Series: Quartzites	Distinct	v. Distinct	Poor(T)	Distinct	Poor(T)	v. Distinct	Poor(T)	Distinct	Poor(T)	Distinct
Shales	Poor	Distinct	Poor	Poor	Poor	Distinct	v. Poor	Fair	Poor	Fair
		v. Distinct		Distinct		v. Distinct	Fair	v. Distinct		v. Distinct
		Distinct		Poor				Distinct		Distinct
		Fair				Poor		Fair		Distinct
Diabase	Poor	Distinct	Poor	Poor	Poor	Distinct	Distinct	Distinct	Fair	v. Distinct
		Fair		Fair		Distinct	Distinct	Distinct	Distinct	Distinct
Screes	v. Distinct	Fair	Poor	Fair	Fair	Distinct	Distinct	Distinct	Distinct	Distinct
Outcrop Areas										
Dolomite Series:	Poor	v. Distinct	Poor	Fair	Poor	Fair	Fair	Poor	Poor	Fair
		Distinct		Fair		Fair	Fair	Poor	Poor	Fair
		Distinct		Distinct		Distinct	v. Poor	v. Distinct	Distinct	v. Distinct
		Poor		Fair	Fair	Fair	Distinct	Fair	Distinct	Distinct(T)
Chert-rich zones	v. Poor	v. Distinct				Distinct	v. Distinct			Poor
		Distinct								
		Poor								
		Distinct		Fair		Fair	v. Poor	Poor		
Chert-poor zones										
Outcrop Areas										
Thick Soil										
Dykes										
Pre-Transvaal: Granite in east	Poor	v. Distinct	Poor	Distinct	v. Poor	Fair		Poor	v. Poor	Distinct
		Distinct		Distinct						
		Distinct		Distinct						
		Distinct		Distinct						
Granite in southwest	Poor	Distinct	Poor	Distinct	v. Poor	Fair		Poor	v. Poor	Fair
		Distinct		Distinct						
		Distinct		Distinct						
		Distinct		Distinct						
Ventersdorp volcanics	Fair(T)	v. Dist. (T)	Poor(T)	Fair(T)	v. Poor(T)	Distinct	Poor	Poor	Poor	Distinct(T)
Wilwatersrand quartz.										
Greenstones										

Note: (T) indicates distinctive textural pattern influencing recognizability.

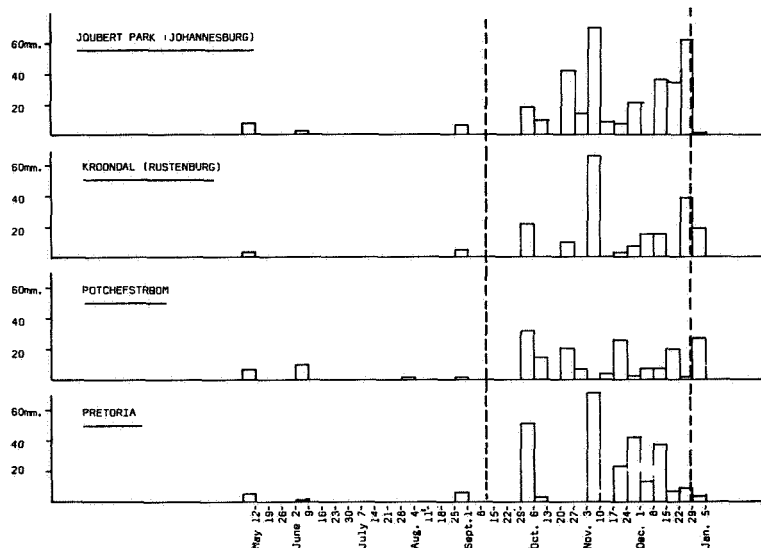


FIG. 5 : Weekly rainfall figures for several towns in the western Transvaal for the period May, 1972 to January, 1973.

During the dry winter months atmospheric haze occurs over most of South Africa, with windblown dust being the main constituent. Such material produces significant back reflection of sunlight and also scatters much of the radiation reflected from ground objects. Both effects result in reduced contrast in ground scenes. During the summer months most of the dust is removed by rainfall, thus producing a clear atmosphere and good contrast.

The effect of soil moisture content is important inter alia in so far as it affects the texture of the reflecting surface of a ground object. Dry soil will approximate a matt surface which may result in significant spectrally non-selective reflection from the top surface. A wet soil (or a soil which has been wet but not disturbed) will presumably exhibit greater spectrally selective absorption.

SUMMARY

1. Two sequential ERTS images of a portion of the western Transvaal Province gathered during the dry winter and rainy summer seasons were compared to investigate the value of repetitive ERTS imagery in geological studies.
2. A detailed comparison was based on colour composite prints of bands 4, 5 and 7, but this was followed by examination of all four individual bands for the two images.
3. The winter image proved to be of low tonal contrast and lithological detail, roughly comparable to that shown on a 1:1 000 000 scale map could be recognized. Fracture patterns and areas of outcrop are readily evident.
4. The summer image (in spite of a NASA rating of "P" for all four bands) shows very marked tonal contrast related to surface lithologies, locally permitting recognition of lithological detail comparable to that indicated on 1:250 000 maps of the area. The intensity of these tonal variations tends to obscure other geological features.
5. The summer image reveals new lithological information particularly in the Transvaal Dolomite where major stratigraphic units are clearly evident. In spite of 90 years of continuous geological activity in the western Transvaal, no such stratigraphic subdivisions had ever been recognized.

6. The enhancement of tonal contrast is evident in every single band of the December image. A comparison of all bands of both images indicates that virtually every single band of each image may display particular geological features to a greater degree than any other.
7. Atmospheric haze and soil moisture content appear to constitute the most important factors in enhancing the tonal contrast of the December image. Both these factors are directly related to rainfall.
8. The investigation clearly indicates the importance of repetitive coverage in the enhancement of particular geological features, in an area of strong seasonal changes.

REFERENCES

Grootenboer, J., Eriksson, K., and Truswell, J., 1973.
Stratigraphic Subdivision of the Transvaal Dolomite from
ERTS Imagery : ERTS Investigation Symposium, Dec. 10-14,
Goddard Space Flight Center.

STRATIGRAPHIC SUBDIVISION OF THE TRANSVAAL DOLOMITE FROM ERTS IMAGERY

Jan Grootenboer, (*Spectral Africa (Pty) Ltd., P.O. Box 2, Randfontein, Rep. of South Africa*);
Ken Eriksson, John Truswell, (*Department of Geology, University of the Witwatersrand, Jan Smuts Avenue, Johannesburg, Rep. of South Africa*)

ABSTRACT

ERTS imagery has revealed the presence of broad stratigraphic subdivisions in the previously undifferentiated Transvaal Dolomite of the western Transvaal, Republic of South Africa.

While detailed field mapping in areas of good outcrop, as well as borehole logging has recently led to the recognition of a stratigraphy in the Transvaal Dolomite of the central Transvaal, poor outcrop in the western Transvaal has to date prevented this. The ERTS-imagery, however, clearly reveals the presence of six, and in the far west seven, distinct stratigraphic zones extending along strike for a distance of at least 200 km. Ground truth selected on the basis of ERTS imagery, identified these zones as corresponding to alternating units of dark-grey, chert-poor and light-grey relatively chert-rich carbonates. With an appreciation of the defined stratigraphy of the central Transvaal, the detailed geology mapped along the traverses was readily related to the zones evident on the imagery, extending the established stratigraphic subdivision of the carbonate sequence over an area of some 4000 sq. km.

The investigation clearly demonstrates the potential applications of ERTS-imagery in geological studies, even in a country where the geology is supposedly well known.

INTRODUCTION

ERTS Image No. 1158-07363 covers much of the western part of the Transvaal Province of South Africa. The area is of considerable geological interest as it includes the gold and uranium mines of the central and west Rand, the platinum and chrome mines of the Bushveld Complex, the Lichtenburg diamond fields, the Marico lead/zinc deposits, as well as numerous other mineral occurrences. Intense geological investigation has been in progress over the

• N 74
30751

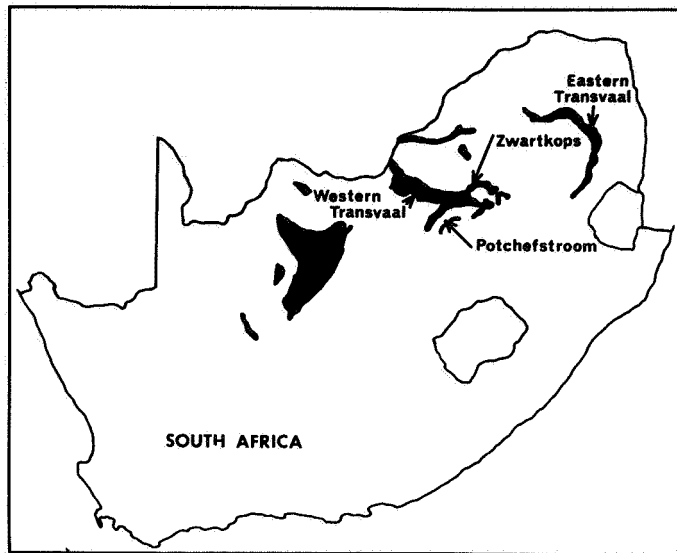


FIG. 1 : Distribution of the Transvaal Dolomite in South Africa.

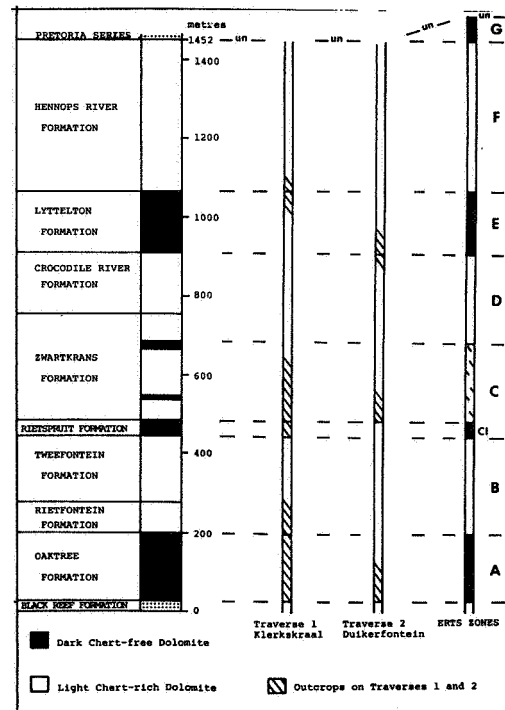


FIG. 2 : Stratigraphy of the Transvaal Dolomite from the Zwartkops area and relationship to outcrops along Ground Traverses and ERTS-zones.

last 90 odd years following the discovery of gold in 1886, and the area has been repeatedly mapped both by mining companies and the Geological Survey.

The image includes an area of some 4 000 sq. km. underlain by the Transvaal Dolomite. Over most of this region the northerly dipping Dolomite is characterised by extremely poor outcrop, generally being covered by residual soil. It is only near the eastern extremity of the image, south of the Hartbeespoort Dam that better outcrop occurs. Until recently it was considered that the Dolomite was relatively uniform in nature and as a result no subdivision of this unit was recognised, even on geological maps published as late as 1967. However, logging of borehole cores in the Potchefstroom area (Eriksson, 1972), and field mapping in the eastern Transvaal (Button, 1973) and at Zwartkops south of the Hartbeespoort Dam (Eriksson and Truswell, in press) (fig. 1) has now revealed the existence of a stratigraphy.

Broad zones of contrasting colour tone within the area underlain by the Transvaal Dolomite are clearly evident on the ERTS image. The conformable nature of these zones which extend over a strike length of some 200 km. strongly suggest that the colour tones reflect broad stratigraphic units. This was confirmed by ground traverses which identified these zones as reflecting alternating major zones of dark-grey chert-poor and light-grey chert-rich dolomite which could be directly related to the broad stratigraphic zones mapped at Zwartkops.

THE STRATIGRAPHY OF THE TRANSVAAL DOLOMITE

The Lower Proterozoic, essentially non-clastic Transvaal Dolomite was previously mapped as a single unit between the clastic Black Reef and Pretoria Series (fig. 2). Detailed examination of borehole cores from the Potchefstroom area resulted in a stratigraphic subdivision of the Transvaal Dolomite based largely on the presence or absence of chert and the colour of the dolomite (fig. 1), (Eriksson, 1972). In a general sense 3 dark chert-poor zones, the middle of which is the thinnest, and 3 light chert-rich zones were recognized. Button (in press) extended this stratigraphy in a regional study in the eastern Transvaal (fig. 1) an area of good outcrop where, however, the thin middle dark chert-poor zone of the Potchefstroom area was not traced. He noted the appearance of an additional dark chert-poor mixed dolomite-limestone zone stratigraphically above those developed in the Potchefstroom area. The succession developed in the eastern Transvaal can be shown to extend around the northern flank of the Transvaal basin into the extreme western Transvaal. Moving eastwards into the area under consideration this uppermost chert-poor zone is truncated by an erosional unconformity (un, fig. 2).

In the Zwartkops area north-west of Johannesburg, where exposures are good, a detailed stratigraphy has now been established in the Transvaal Dolomite (Eriksson and Truswell, in press) through detailed field mapping. In the broadest sense eight formations of alternating chert-rich and chert-poor dolomite can be recognized (fig. 4) but a considerable amount of detailed lithological information has also now become available. The chert-poor zones are the basal Oaktree Formation, the thin Rietspruit Formation and the Lyttelton Formation. In addition there are thin chert-poor zones in the Zwartkrans Formation above the Rietspruit Formation (fig. 2).

ERTS IMAGE 1158-07363

The distribution of the Transvaal Dolomite is evident on a colour composite of Bands 4, 5 and 7 of image 1158-07363 (fig. 3). The Dolomite is characterized by a greenish colour tone and occurs as a zone trending across the centre of the image, and again in a less distinct arc in the Potchefstroom area to the southeast.

Where good outcrop conditions prevail, as at the eastern extremity of the image, the Dolomite is characterized by a relatively dark uniform colour tone in which tonal variations are difficult to distinguish. Over the remainder of the western Transvaal, however, distinct zones of varying colour tone can be recognized within the Dolomite. Four zones of dark colour tone are recognizable, although the uppermost of these is developed only in the western extremity of the image. These dark zones are separated by three wider zones of light green colour tone. The various zones will be referred to in alphabetical order from the base upwards as indicated in figs. 2 and 4.

The conformable nature of the zones strongly suggests that they represent major stratigraphic subdivisions within the Dolomite which are continuous over a distance of at least 200 km. The termination of the uppermost dark unit is related to a major erosional unconformity at the top of the Dolomite.

GROUND TRUTH

Ground truth was gathered over a period of three days and involved traverses by car along roads over the area underlain by the Dolomite. The first two days were devoted exclusively to locating areas where sufficient outcrop was available for



FIG. 3 : Portion of ERTS Image 1158-07363 with limits of Transvaal Dolomite outlined.

further study. Over large areas outcrops are virtually absent rendering accurate identification and correlation with the established stratigraphy impossible. Traverses covered and the outcrops encountered along them are indicated in fig. 4. Only the Klerkskraal traverse contained any significant outcrop, and this was confined mainly to the lower half of the succession. This and scattered outcrops on the Duikerfontein traverse were investigated on the third day.

The Klerkskraal Traverse: Fair outcrop was encountered near the base of the Dolomite on this traverse, permitting recognition of the Oaktree Formation of dark chert-free dolomite, coinciding with Zone A (fig. 2) of dark colour tone on the image.

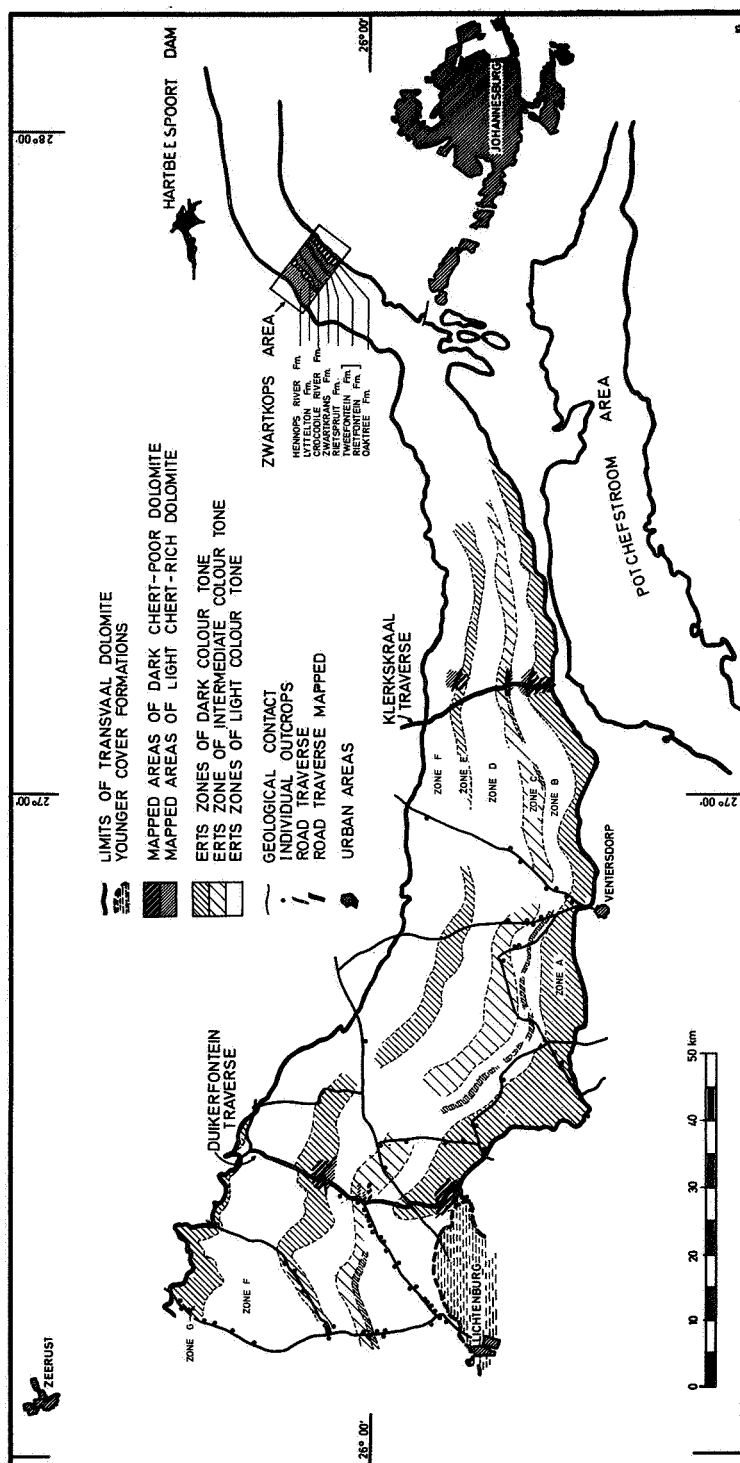


FIG. 4 : Extension of the stratigraphy of the Transvaal Dolomite from the Zwartkops area into the western Transvaal based on ERTS.

The contact between the Oaktree Formation and the overlying chert-rich, light-grey Rietfontein Formation was accurately located in the field and coincides with the change in tone on the ERTS image (Zones A-B). Outcrop conditions deteriorated from this point northwards, but the dark dolomite of the Riet-spruit Formation (Zone C-1, fig. 2) characterized by linked columnar stromatolites, was located in the field and could be correlated with the thin unit of very dark colour tone (fig. 4). At the base of Zone C this unit was overlain by alternating thin bands of dark chert-poor dolomite and lighter chert-rich dolomite which probably represents most of Zone C. Towards the north this material graded into uniform light-coloured chert-rich dolomite referred to as the upper Zwartkrans and Crocodile River Formations (Zone D, fig. 2). Farmlands obscured the remainder of the succession but in an area slightly to the east the contact between the chert-poor Lyttelton Formation and Hennops River Formation was located and found to coincide approximately with the contact between Zones E and F (fig. 2) on the image.

The Duikerfontein Traverse: In the south of this traverse isolated outcrops of dark chert-free dolomite were found near the base of the Dolomite. Some occurrences of chert-rich dolomite were noted in this area, still well within Zone A, but these probably represent thin units of local chert development. Further north along the traverse thick soil covers the remainder of Zone A and all of Zone B. A thin unit of dark dolomite, strongly resembling that overlying the Rietspruit Formation on the Klerkskraal traverse, was found within Zone C on the image. Outcrops are virtually absent along the remainder of the traverse, the area being covered by thick soil, but the contact between the Lyttelton and underlying Crocodile River Formations could be accurately located and coincided with that between Zones D and E on the image (fig. 4).

SUMMARY

1. ERTS imagery has revealed the presence of broad stratigraphic units in the Dolomites of the western Transvaal.
2. Despite a long history of geological activity, no stratigraphic subdivision of the Dolomite had previously been recognized in the western Transvaal. This was largely the result of poor exposure and the uniform nature of the Dolomite.

3. The stratigraphic units revealed on the imagery can be correlated with the generalized stratigraphy of a better exposed area.
4. Four zones of dark colour tone are distinguished on the image and correspond to dark chert-free dolomite. One of these units is very thin (50 m). The uppermost Zone (G) is truncated by an unconformity.
5. Three zones of lighter tone correspond to light-coloured chert-rich dolomite.
6. These seven zones are best seen in those areas of the western Transvaal that are characterised by poor outcrop and low dips. In contrast the zones become indistinct in areas of better exposure or steeper dip.
7. The investigation has demonstrated the usefulness of ERTS imagery as a rapid mapping technique in the extension of a known Transvaal Dolomite stratigraphy into an area of poor outcrop.

REFERENCES

- Button, A. (in press). The stratigraphic history of the malmani Dolomite in the Eastern and Northeastern Transvaal.
Trans.geol. Soc. S. Afr.
- Eriksson, K.A. and Truswell, J.F. (in press). Stratotypes from the Malmani Group, northwest of Johannesburg, South Africa.
Trans. geol. Soc. S. Afr.
- Eriksson, K.A. (1972). Cyclic sedimentation in the Malmani Dolomite.
Trans. geol. Soc. S. Afr., 75, 85-98.

AN INVESTIGATION OF MAJOR SAND SEAS IN DESERT AREAS THROUGHOUT THE WORLD

Edwin D. McKee, *U.S. Geological Survey, Denver, Colo.*, and Carol S. Breed, *U.S. Geological Survey, Flagstaff, Ariz.*

ABSTRACT

This study of sand seas on a global scale consists of identifying and measuring characteristic sand forms, examining structures, determining the processes involved, and ascertaining the world distribution of various types of sand bodies. ERTS imagery has the advantages of permitting (1) direct comparison of areas because the same scale prevails on all images, (2) ready observation of relationships to surrounding features, and (3) recognition of major trends or lineations where minor details are obscured.

Fifteen major areas or sites in the Eastern Hemisphere and three sites in the Western Hemisphere have been examined to date. For each area, mosaics of false-color prints showing sand patterns have been prepared and these mosaics form a base map for all subsequent types of study.

Many attempts have been made in the past to classify sand bodies and assign names, but the studies have been mostly local in scope, and classification has been based in part on supposed genesis. In this study an attempt is made to develop a strictly objective classification of worldwide application. The principal types recognized are (1) parallel straight or linear, (2) parallel wavy or crescentic, (3) star or radial, (4) parabolic or U-shaped, and (5) sheet or stringer types. Numerous variations of each group are also recognized.

Principal controlling factors in forming the various types of sand bodies are believed to be wind direction and strength, topography, vegetation, moisture, available sediment, and distance from source. Efforts to recognize and delineate these factors for specific areas are being made and methods of illustrating the relationships on transparent overlays are being developed. Ground truth investigations to determine internal structures of sand masses also are under way.

Ultimate objectives of this study are threefold. First, a better understanding of stratification in ancient rocks of dune origin; such structures are important in the migration of water and oil. Second, a further insight into the controls of sand migration that in some areas adversely affects various enterprises of man may be obtained. Finally, an appreciation of certain similar patterns on Mars, apparently wind-formed, may result.

N 74 30752

INTRODUCTION

This investigation is a study of desert sand seas on a global scale and illustrates the use and value of ERTS imagery for this purpose. The study consists of the identification, description, and measuring of characteristic forms and structures within the principal sand bodies. It facilitates the determination of world distribution of the various dune types and the classification of these. In addition, the basic forms of sand deposits, analyzed together with data derived from ground truth studies, make possible an interpretation of the processes responsible for each dune type.

The advantages of employing ERTS images in this study are readily apparent. Because the same scale is represented in all images, direct comparisons of widely separated areas are possible. Further, the relations of sand areas to surrounding features are easy to recognize and major lineations or other patterns in the sand fields are clearly defined. Finally, mosaics that are developed from combinations of images make excellent map bases on which to superimpose many kinds of data.

For purposes of this study, 15 desert or semidesert areas, all of them in the Eastern Hemisphere, were initially selected (fig. 1). Subsequently some of these test site areas were combined and others were reduced in size in order to eliminate non-sandy areas and to consolidate mosaics for greater efficiency in handling data. A few relatively small areas located in the Western Hemisphere (fig. 2) were later added to the coverage primarily because they were easy of access. These areas were chosen because they can readily be checked by air photography and, in most of them, ground truth is available for interpreting genetic features.

The methods used in this investigation have gradually evolved with experience in employing various types of ERTS imagery as they have become available. Initially only small black-and-white negatives were received and these were scarcely adequate for careful analysis. With the arrival of relatively large prints, and the enhancement of these by photo processing methods, both through printing techniques and differences in paper, considerable improvement was made. A comparison of available prints from the green, red, and near-infrared bands was another major advance, for it facilitated the recognition of water, vegetation and other associated features bordering sand bodies. Finally, when false-color images became available, the discernment of sand through its yellow color places the interpretation of sand bodies through ERTS images on a high level of accuracy.

CLASSIFICATION

A partial review of the literature on eolian sand dunes has disclosed that more than 20 attempts have been made to name and classify dune types, at least locally. Many proposed names are based on inferred genesis; some are defined differently by different workers, others are overlapping in scope. As a result, the present status of the classification of sand bodies is chaotic.

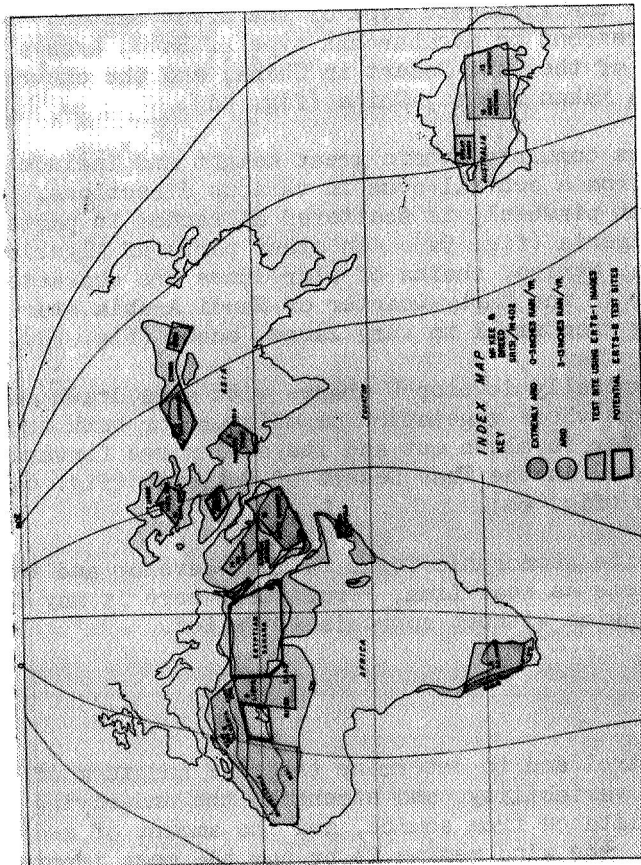


Figure 1.--Map of principal desert and semidesert regions and selected test sites (areas), Eastern Hemisphere.

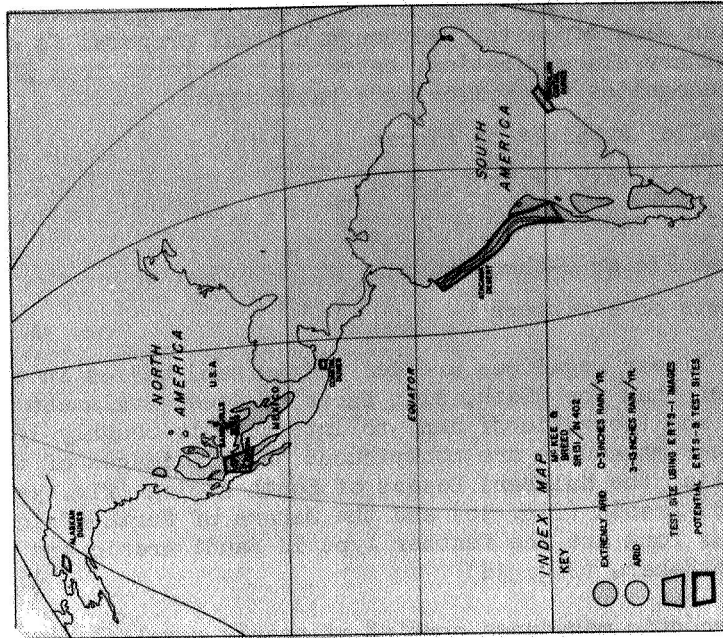


Figure 2.--Map of principal desert and semidesert regions and selected test sites (areas), Western Hemisphere.

A principal aim of this ERTS image study is to develop an objective classification of major eolian sand deposits. Although a final proposal is as yet far from ready, a preliminary classification, based on dune forms from ERTS imagery thus far examined, recognizes the following 5 basic types:

1. Parallel straight or linear
2. Parallel wavy or crescentic
3. Star or radial
4. Parabolic or U-shaped
5. Sheets or stringers

Parallel straight or linear megadunes are defined as sand bodies in which the length is much greater than the width, slip faces or steep avalanche surfaces occur on both sides, and the ratio of dune to interdune is roughly 1/1. Examples of such linear megadunes are conspicuous on ERTS images of the Simpson Desert of Australia, the Kalahari Desert of South Africa (fig. 3a), the Empty Quarter of Saudi Arabia (fig. 3b) and the Sahara of North Africa (fig. 3c). Variants of the linear form are the feather type in Saudi Arabia and the wide intradune type in the Sahara (fig. 3d).

Parallel wavy or crescentic megadunes consist of nearly parallel rows of cusped segments as represented in the Kara Kum Desert of the U.S.S.R. (fig. 4a), and in the Nebraska Sand Hills of western United States. Variants of the simple basic type are referred to as the fishscale type of the Great Eastern Erg of Algeria (fig. 4b), the giant crescent or megabarchan type of Saudi Arabia (fig. 4c), the bulbous warty type of the Gobi Desert in China, and the chevron or basket-weave type of the Takla Makan Desert, China (fig. 4d).

Star or radial megadunes commonly attain great height and include a few to many arms that project out from a central cone in various directions. The basic type, resembling a giant pinwheel, is scattered at random in parts of the Great Eastern Erg of Algeria (fig. 5a). In other parts of Algeria and in the Gran Desierto of Sonora, Mexico, chains of star dunes are characteristic (figs. 5b, 5c), whereas in the Empty Quarter of Saudi Arabia star dunes of graduated size, grading from small to very large, occur (fig. 5d).

Parabolic dunes that typically develop U shapes with arms drawn out on the sides are common in areas where vegetation or moisture or both tend to anchor the arms, while the center is blown out and its sand moves forward. These dunes are well illustrated in the Thar Desert of Pakistan (fig. 6a) and at White Sands, New Mexico (fig. 6b).

In some sand seas definite geomorphic forms fail to develop and the sand accumulates in flat sheets as near Lima, Peru. Elsewhere it may form stringers extending downwind without appreciable relief.

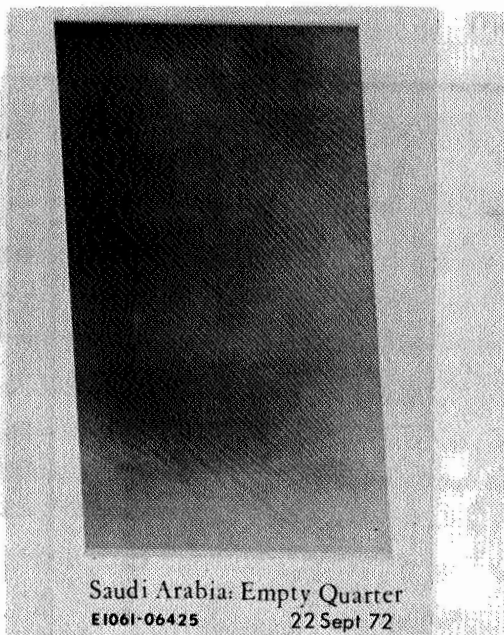
GENETIC IMPLICATIONS

Factors believed to control and to determine the size and form of dune bodies are the wind direction, variability, and strength, the underlying topography, vegetation, moisture, distance from source, and the amount of sediment available. Of these factors, the wind regime is by far the most important.



South Africa: Kalahari Desert
E1128-08105 28 Nov 72

(a)



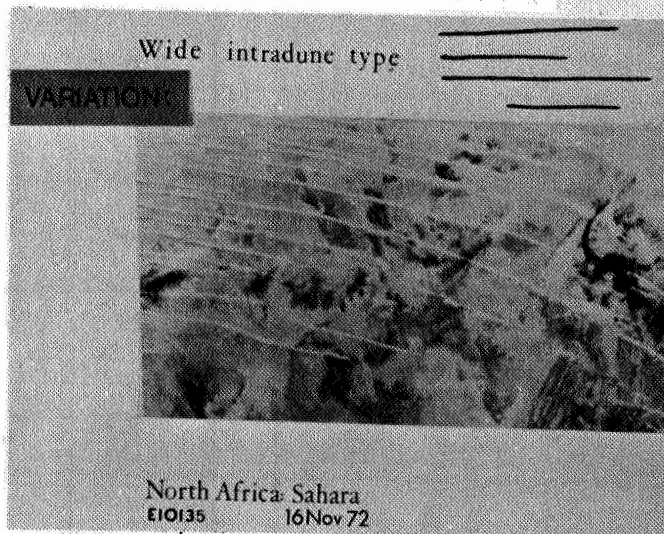
Saudi Arabia: Empty Quarter
E1061-06425 22 Sept 72

(b)



North Africa: Sahara
E1138-10374 8 Dec 72

(c)



North Africa: Sahara
E10135 16 Nov 72

(d)

Figure 3.--Parallel straight (linear) megadunes: (a) Kalahari Desert, South Africa; (b) Empty Quarter, Saudi Arabia; (c) Sahara Desert, North Africa; (d) Sahara, North Africa (wide intradune variety).

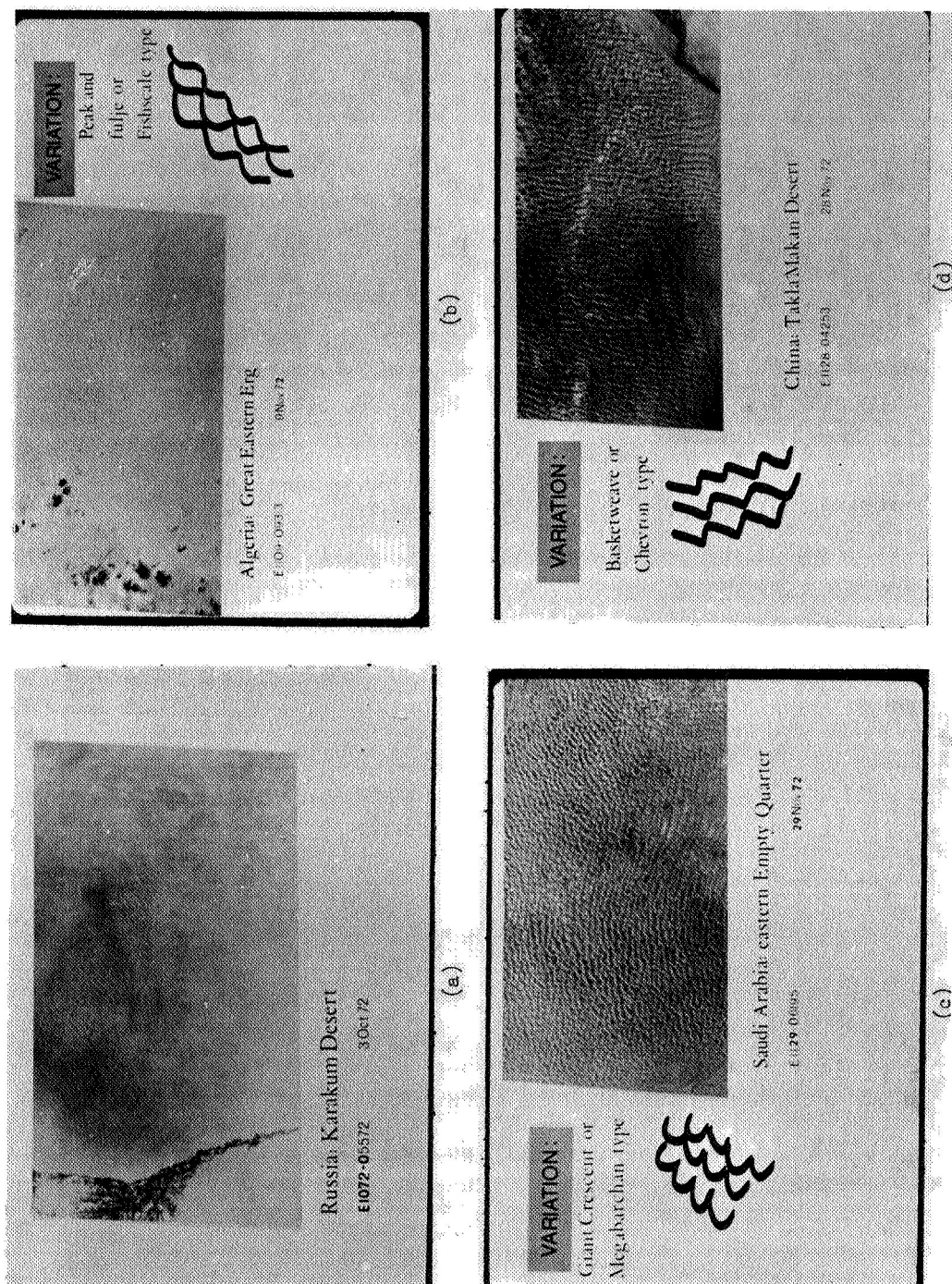


Figure 4. ---Parallel wavy (crescentic) megadunes: (a) Kara Kum Desert, U.S.S.R.; (b) Great Eastern Erg, Algeria (fishscale type); (c) Empty Quarter, Saudi Arabia (giant crescent type); (d) Takla Makan Desert, China (basketweave type).

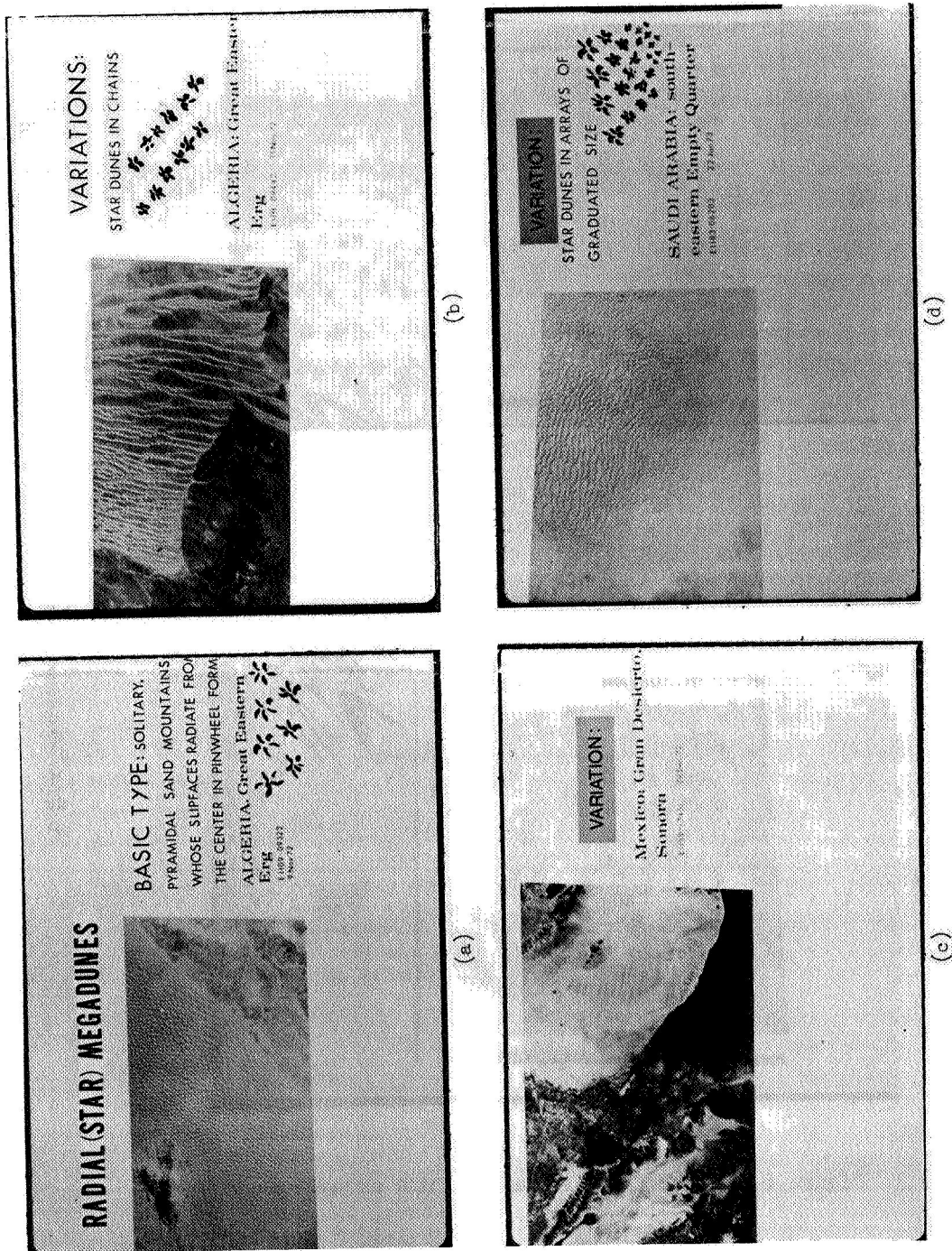
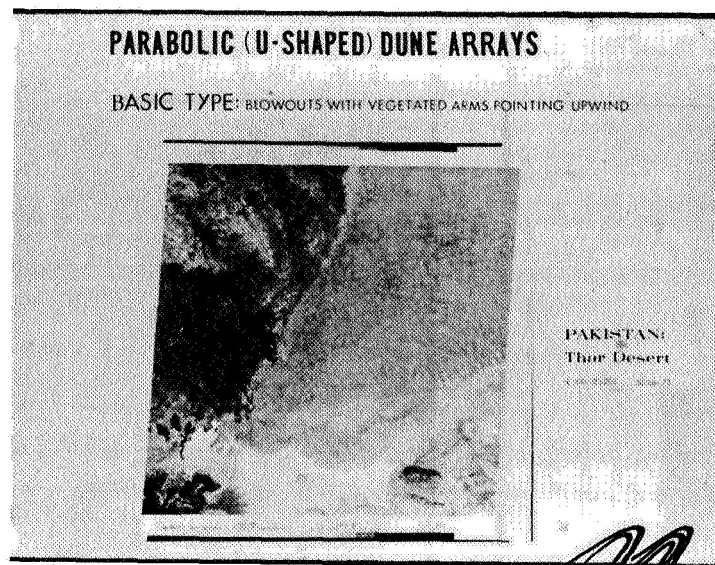
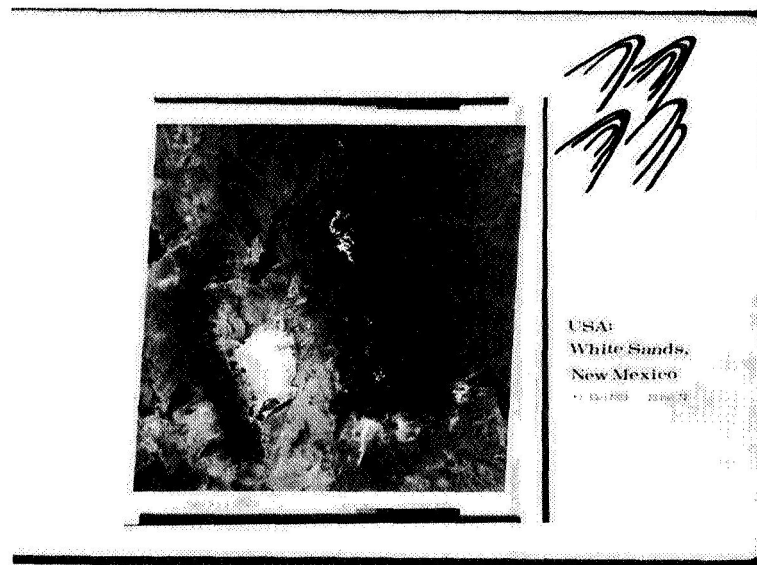


Figure 5.--Star or radial megadunes: (a) Great Eastern Erg, Algeria (random distribution); (b) Great Eastern Erg, Algeria (chain type); (c) Gran Desierto, Sonora (chain type); (d) Empty Quarter, Saudi Arabia (graduated size).



(a)



(b)

Figure 6.--Parabolic (u-shaped) dune arrays:
(a) Thar desert, Pakistan;
(b) White Sands, New Mexico.

Broad lineation and regional trends in sand seas are best recognized from ERTS images. Details of morphology which commonly reflect structure are shown best by Skylab photography and by airplane photos (fig. 7). Further details and ultimate confirmation of structural types must be established by ground truth, largely through the process of trenching.

The relations of wind strength and direction to dune form must necessarily be established by gathering data from meteorological sources where these are available. The data are then plotted on sheets as overlays to the ERTS imagery mosaics that display the dune patterns. Such overlays have been completed, in part, for South West Africa (fig. 8) and for White Sands, New Mexico (fig. 9), with air current information shown in the form of wind rose diagrams.

Considerable information on factors other than wind that affect dune form and size is furnished by ERTS imagery. The relation of vegetation and water bodies to dune sand in Mali (fig. 10a) and in Pakistan (fig. 10b) can be deduced from the color distribution in the false-color prints (vegetation appears red) from which the figure 10 pictures were made. Shifts in wind direction in Saudi Arabia (fig. 10c) are illustrated by the smoke of burning oil wells; the influence of topographic barriers on sand forms in Algeria is shown in figure 10d. A second example of wind-barrier effect is illustrated in figure 8 where a mountain system separates dunes of the Namib and Kalahari deserts.

In order to quantify data on the density of dune ridges as seen on ERTS images, visual counts are made, along a line, of the number of dunes per kilometer. From these counts isodensity maps are prepared showing possible relations of dune density to physical barriers or to wind roses. The isodensity map of Simpson Desert, Australia (fig. 11), has been compiled from 49 visual counts.

GROUND TRUTH

The acquisition of ground truth from field studies, especially data on the internal structure or stratification, represents the final and critical stage of sand sea investigation. This is best done by a direct approach consisting of wetting the sand, cutting trenches to expose stratification in three dimensions, and recording the patterns on rubber peels, scale drawings or photographs. Such field methods have been successfully tested in Libya, Saudi Arabia, U.S.A. and elsewhere. Although tedious and time-consuming, they furnish excellent records of the internal structures representative of each type of dune, thus enabling a reconstruction of subsurface patterns critical to various geological interpretations.

Ground truth should assist in establishing a new model for understanding eolian sand bodies. A general concept in the past has been that dunes are basically the result of sand migration by the processes of saltation and avalanching under the influence of a prevailing wind. This concept doubtless still applies in some regions, but a revised model incorporating the effects of multidirectional and variable winds that produce a complex of dune forms, with growth both vertically and laterally, is needed. Many aspects of this model are being tested in the present study.

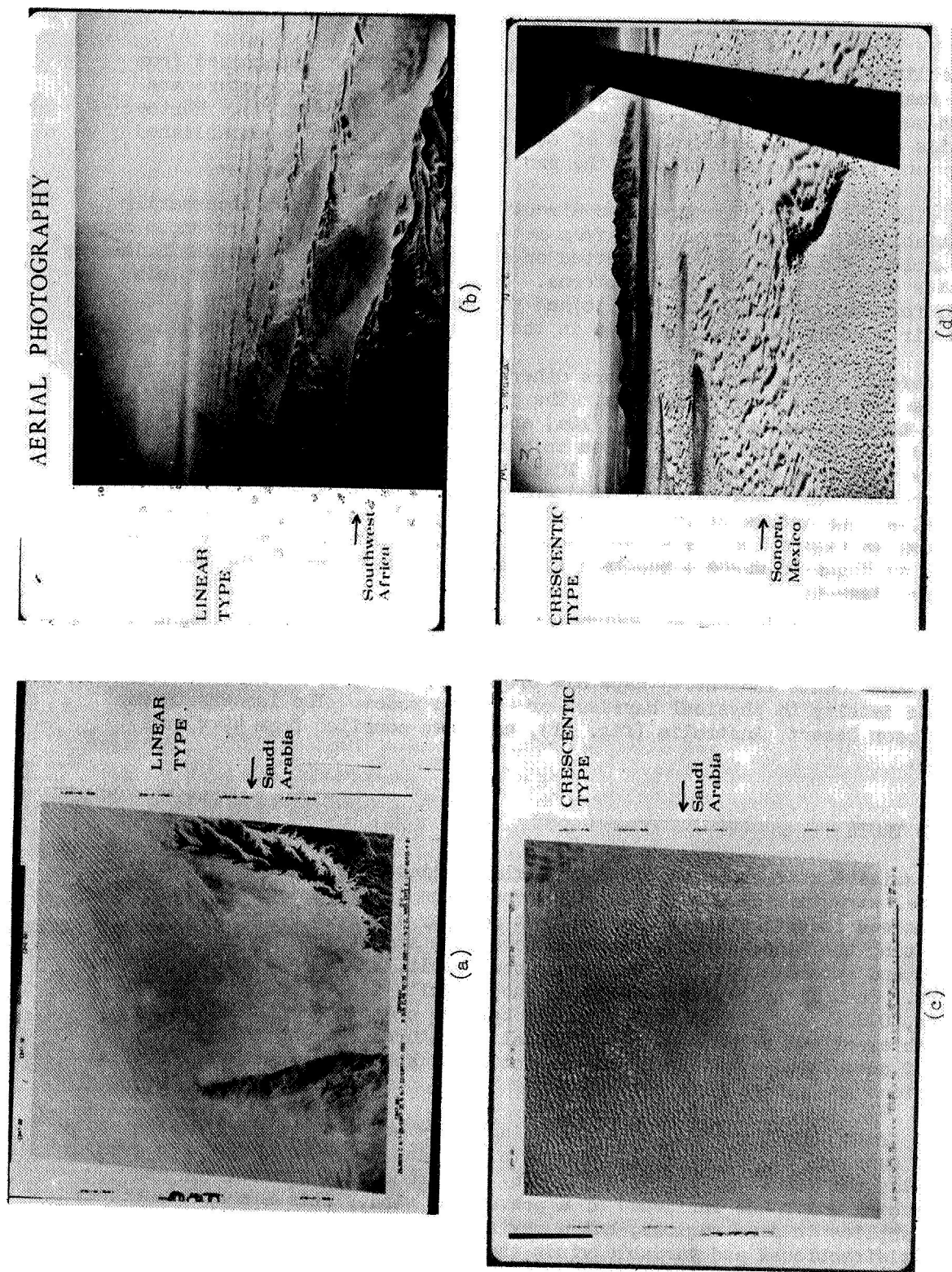


Figure 7.--Comparison of ERTS imagery and air photographs for two basic types of dunes: (a) Linear type, Saudi Arabia (ERTS imagery); (b) Linear type, South West Africa (Air photograph); (c) Crescentic type, Saudi Arabia (ERTS imagery); (d) Crescentic type, Sonora, Mexico (Air photograph).

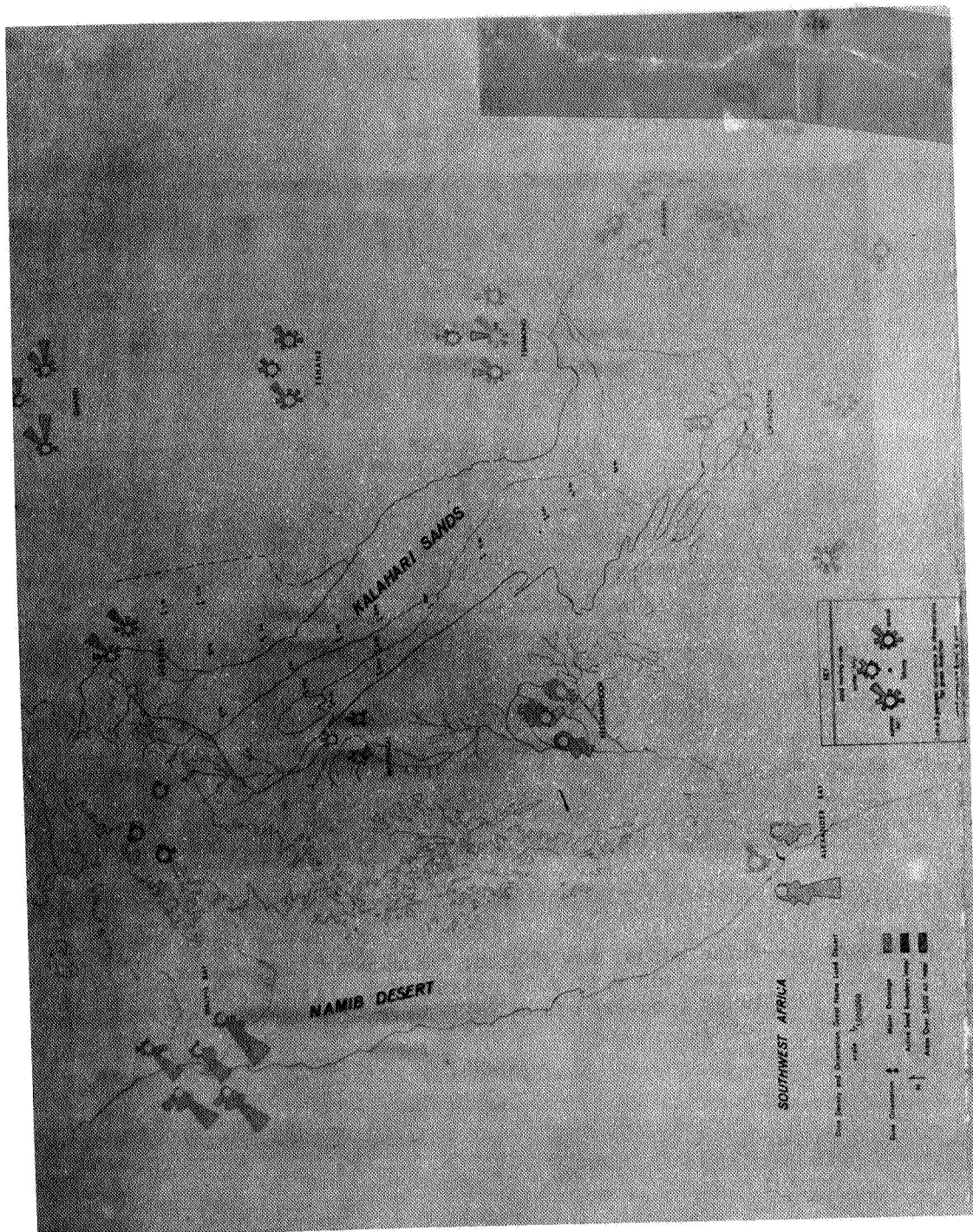


Figure 8.--Map of South West Africa showing dune density and orientation, Namib and Kalahari deserts.

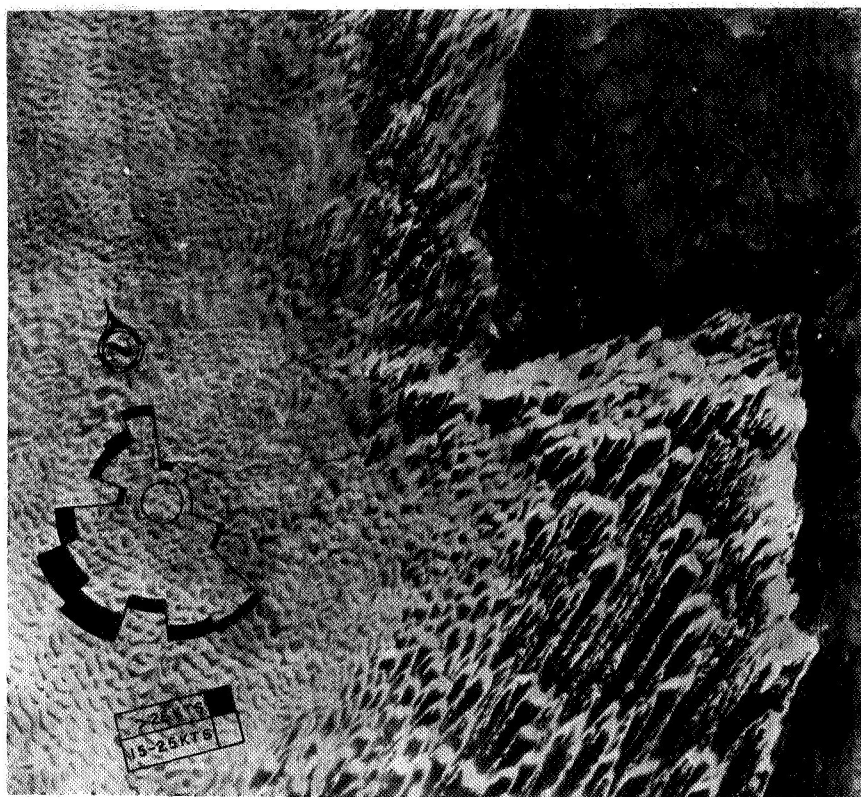


Figure 9.--White sands, New Mexico: wind rose diagram for comparison with dune orientation. (Enlarged image processed from ERTS-1 computer compatible tape).

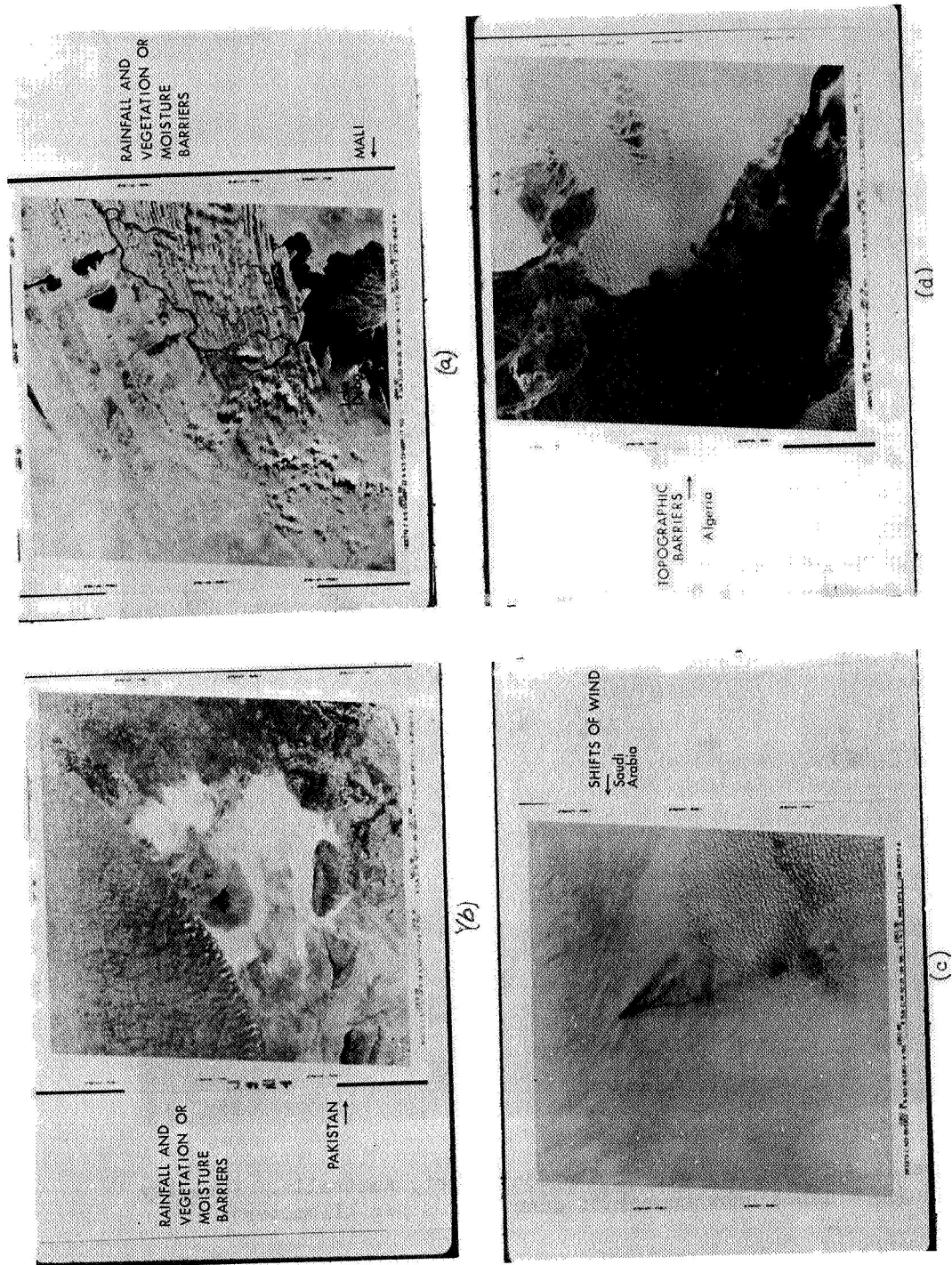


Figure 10.---Physical features affecting size and shape of dunes and megadunes in sand seas: (a) Mali (water and vegetation); (b) Pakistan (water and vegetation); (c) Saudi Arabia (shifts of wind); (d) Algeria (topographic barriers).

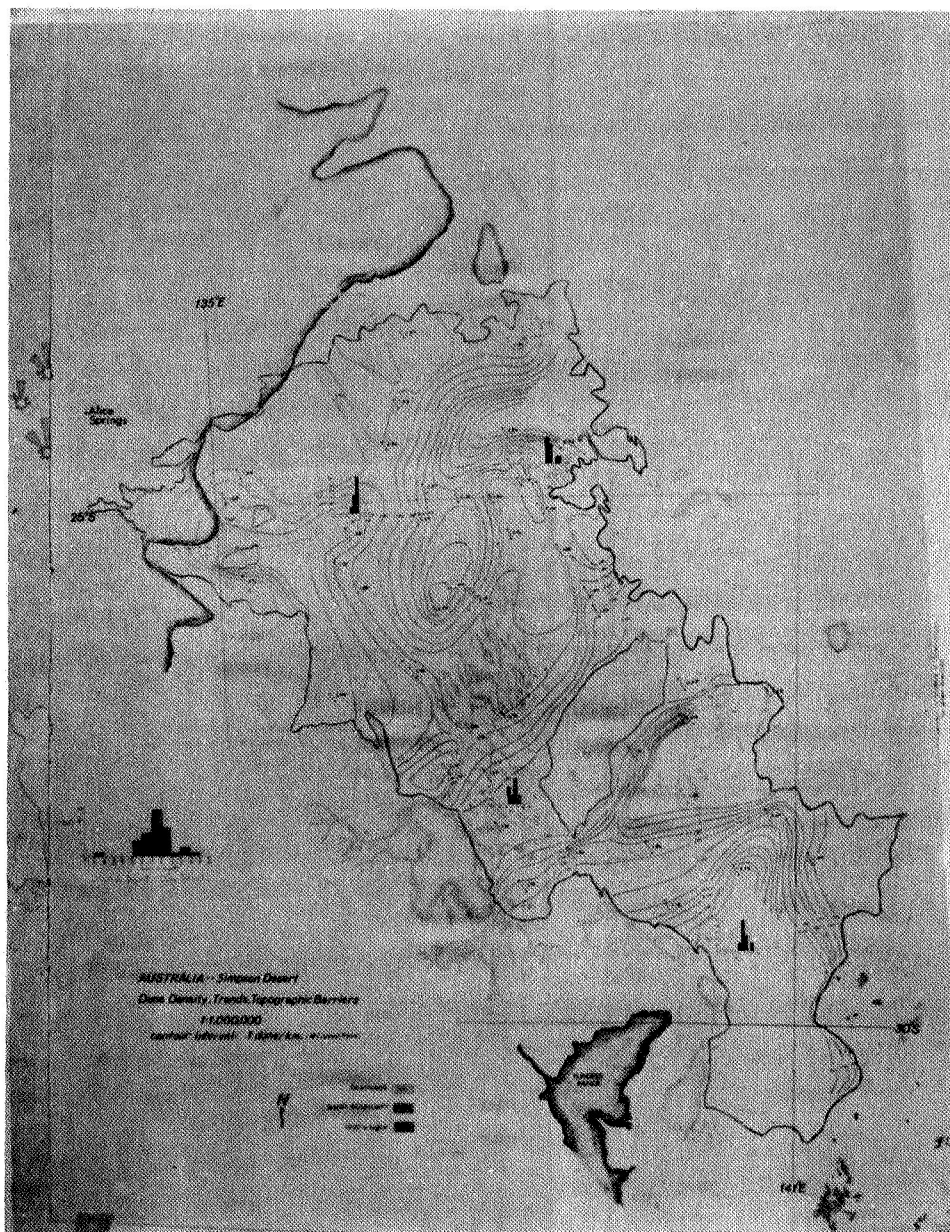


Figure 11.--Isodensity map of Simpson Desert, Australia. (Density lines show number of dune ridges per kilometer).

ULTIMATE GOAL OF INVESTIGATION

Long-term objectives of this study are to obtain an understanding of the overall structures in sand seas and by means of these structures to differentiate between various types of dunes. An understanding of major rock formations as the Navajo Sandstone and Coconino Sandstone of Western United States and many others considered to be of eolian origin, has economic application because such widespread sandstones control the underground movement of many fluids and locally serve as reservoirs. Ore-bearing fluids and also oil and gas migrate through such permeable rocks making a knowledge of their structural trends important in exploration programs.

Further benefits to be derived from a better understanding of windblown sands and their accumulations relate to the many problems of their encroachment on and burial of roads, agricultural areas and other developments of man. Adequate methods of controlling dune movements require a good knowledge of the factors that determine their growth and movement.

Finally, recent pictures of features on Mars that are considered the result of deposition from very strong wind action, seem to have analogies in ERTS images and probably can be understood and explained by correct interpretation of corresponding earth features.

A NEW METHOD FOR MONITORING GLOBAL VOLCANIC ACTIVITY

Peter L. Ward, Elliot T. Endo, David H. Harlow, Rex Allen and Jerry P. Eaton,
Seismology Program, U.S. Geological Survey, Menlo Park, California 94025

The ERTS Data Collection System makes it feasible for the first time to monitor the level of activity at widely separated volcanoes and to relay these data rapidly to one central office for analysis. This capability opens a new era in volcanology in which the hundreds of normally quiescent but potentially dangerous volcanoes near populated regions around the world can be economically and reliably monitored daily to warn when any one volcano is becoming active again. Before ERTS was launched, only a few volcanoes in the world were monitored continuously because of the high cost of building and staffing volcano observatories. Yet it is known from data collected in this century that while visible signs of pending eruptions may only occur minutes to days in advance, invisible but measureable signs may be detected days, weeks, months, and even years before a major eruption. While prediction of specific eruptions is still an evasive goal, early warning of a reawakening of quiescent volcanoes is now a distinct possibility.

A prototypical global volcano surveillance system was established under the ERTS program during the past year. Instruments were installed in cooperation with local scientists on 15 volcanoes in Alaska, Hawaii, Washington, California, Iceland, Guatemala, El Salvador and Nicaragua at the sites shown in Figure 1. Data from low-powered instruments in each of these many remote locations are being relayed six to ten times daily through the satellite to the ground tracking stations at Goldstone, California, and Goddard Spaceflight Center in Maryland. The data are processed at Goddard and then relayed within 90 minutes by teletype to the National Center for Earthquake Research in Menlo Park, California.

The sensors include 19 seismic event counters that count four different sizes of earthquakes and six biaxial borehole tiltmeters that measure ground tilt with a resolution of 1 microradian. Only seismic and tilt data are collected because these have been shown in the past to indicate most reliably the level of volcano activity at many different volcanoes. Furthermore, these parameters can be measured relatively easily with new instrumentation. The fourth-generation seismic event counter developed for this project is shown in Figure 2. This instrument compresses seismic data gathered at the rate of about 2 million digital bits per 12 hours to a small number of bits such as 64 that can be economically relayed through a satellite. This compression is not easy, and some data are lost. For the purposes of this project, however, the main data desired are simply the number of events of different sizes. These numbers typically change by orders of magnitude before eruptions. The criteria adopted for detecting events are that 10 peaks of the full-wave rectified seismic signal must be above a given threshold in 1.2 seconds and that

PRECEDING PAGE BLANK NOT FILMED

N 74 30753

there must have been no peak above this threshold in the previous 15 seconds. The second criterion effectively inhibits the counter during periods of high ground noise caused by wind, harmonic tremor, people, and so on. The time that a channel is inhibited is counted separately and indicates the relative level of ground noise. The number of earthquakes greater than four different amplitudes and the noise counts for each channel are relayed through the satellite. Each counter contains 120 COSMOS integrated circuits and has proven quite reliable. In fact the counters are significantly more reliable than the transmitters furnished by NASA, which use one-third as many integrated circuits but fail quite often.

The transmitter, event counter, seismic sensor, and batteries used for one year's operation are shown in Figure 3. The portability and low power consumption of these instruments makes them practical for operation in remote locations in all types of environments.

A typical installation on the Volcan San Cristobal in Nicaragua is shown in Figure 4. The equipment is locked in steel boxes cemented in place. The antenna is mounted about 12 feet off the ground with a plexiglass dome protecting the elements. A standard seismometer with VHF radio telemetry to some nearby recording site is also installed next to most event counters in this initial program to show whether the event counters are compressing the seismic data reliably. There has only been one minor case of vandalism so far. A few stations have been damaged by lightning.

The tiltmeter used in this project is shown in Figure 5. The bottom of the pipe, which is about 5 cm (2 in) in diameter, contains a precise electrically monitored level bubble that has been adapted for this use from a defense application. The pipe is placed in a 4-to-10-foot hole in rock or more typically sandy soil or ash. The output of the electronic equipment shown connects directly to the satellite transmitter. These instruments have worked very reliably except for some lightning damage that should be avoided in the future with some new design changes.

A sample of the tiltmeter data from Hawaii where three meters are set up several kilometers apart around the central caldera of Kilauea volcano is given in Figure 6. The graph in the upper left shows a comparison over several months of the output of one of these meters compared with the outputs of a mercury tube and a water tube tiltmeter that have operated in the same location for many years. This comparison is exceptionally good for tilt data. The scatter for the water tube meter is noise that represents the limit of resolution for the instrument.

The upper right-hand plot shows the tilt at one of these instruments for 5 months in early 1973 with a tilt event on May 5th. The lower plots show the same tilt event in detail as recorded by the three meters. The three tilt vectors show that the summit of the volcano subsided causing tilts on the order of 10 to 30 microradians or 10 to 30 mm of subsidence in 1 km. An eruption of lava from the flank of Kilauea closely followed this deflation. At present Pacaya volcano in Guatemala is inflating at

about 150 microradians per month, and a second tiltmeter was just installed to monitor this event more closely. Pacaya has had minor eruptions continuously for several years.

The number of earthquakes counted by an event counter on Mt. St. Helens in Washington is compared with those counted by a seismologist on standard instruments located next to the counter in Figure 7. Generally, we find that the counters accurately show the level of seismic activity. There is not a one to one correspondence between counts and earthquakes and this is not surprising since two seismologists might not agree on the exact number of earthquakes. The counts, however, do approximate the number of earthquakes except during periods of high noise that can be identified by the separate inhibit-time or noise counters.

The events of two different sizes counted on the volcano Fuego in Guatemala that erupted beginning on February 22, 1973 show an increase in activity during an eruption (Figure 8). The counter was installed in February. Note the significant increase in activity about 5 days before this small eruption began. The seismic activity was high during the eruption and returned to a low level after the eruption was over. A different counter 30 km from Fuego showed no change in seismic activity during the whole period. This implies the seismic activity was indeed at Fuego. The noise counts were high during periods of high harmonic ground tremor probably associated with the movement of lava underground.

Spurious event counts are usually flagged by the presence of significant noise counts. A second necessary criterion is also clearly shown here. The peak of events on March 18 on the high-gain channel is not observed on the low-gain channel. Since a large number of small earthquakes will always be accompanied by a few larger earthquakes, according to a well-established logarithmic relationship, we can infer that this peak is caused by spurious noise. In this case the spurious counts are caused by moderate harmonic tremor.

These event count data show the types of changes anticipated before destructive eruptions. More gradual changes should also be noted as the period of recording increases.

In conclusion a prototype global volcano surveillance system has been developed under the ERTS program with instruments on 15 volcanoes, in five countries. The instruments are working reliably and some data of the type anticipated have been collected. This work clearly demonstrates the technological feasibility of a global surveillance system although many details in the design of highly reliable instruments still need to be worked out. The primary effort in the future, however, needs to be the collection and analysis of data from these different volcanoes to establish clearly the scientific feasibility of this novel and potentially revolutionary approach to surveillance of hazardous volcanoes.

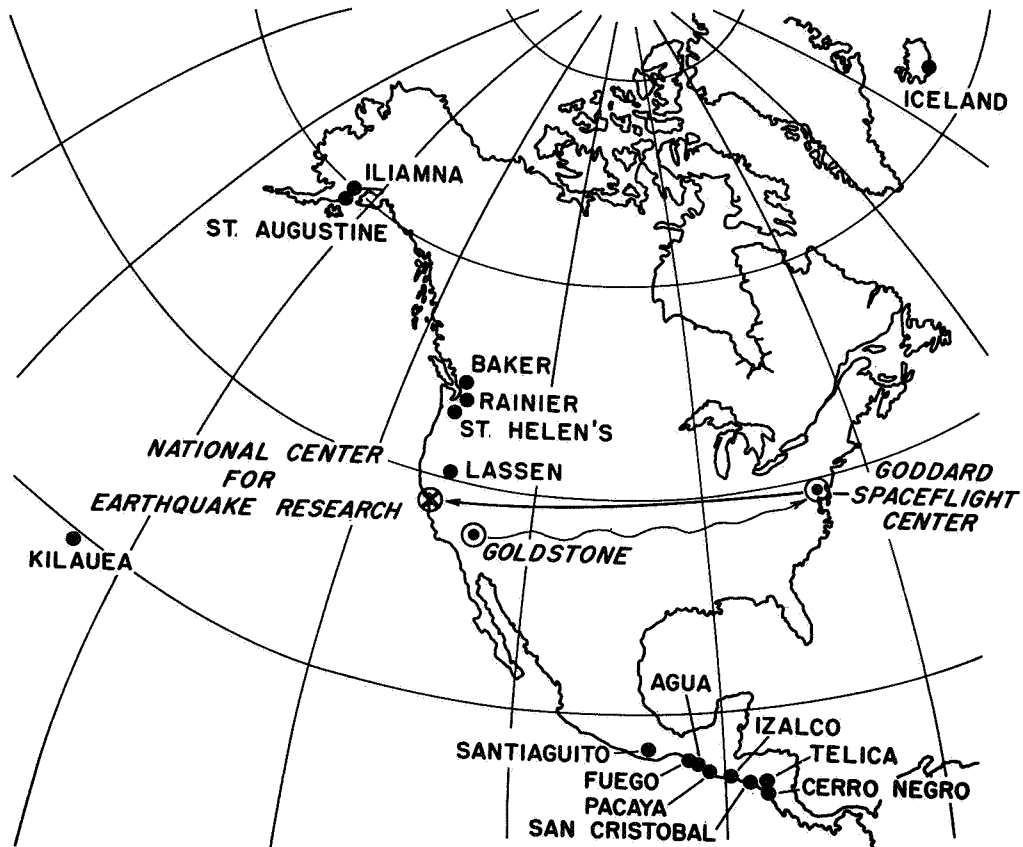


Figure 1: Map of volcanoes monitored in this study. Event counters are placed at all sites. Tiltmeters are placed on Mt. Lassen, Kilauea, Fuego, and Pacaya.

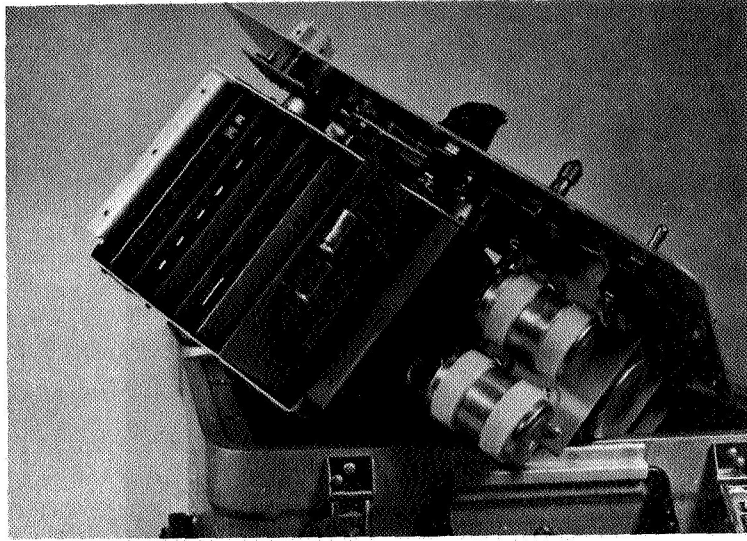


Figure 2: View of the inside of the seismic event counter showing some of the 8 circuit cards.



Figure 3: Satellite transmitter (left), seismic sensor (left foreground), seismic event counter (center), and batteries (right) used to monitor seismic activity and send the data to the satellite.

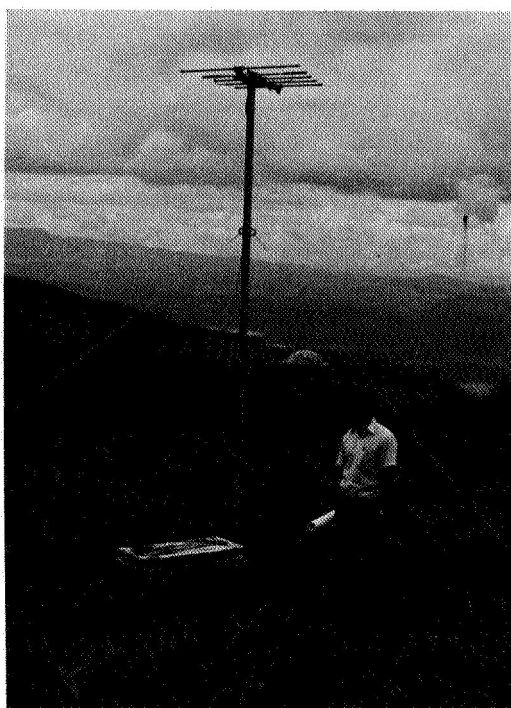


Figure 4: Installation of the standard seismometer (foreground) and seismic event counter system (background) on Volcan San Cristobal in Nicaragua.

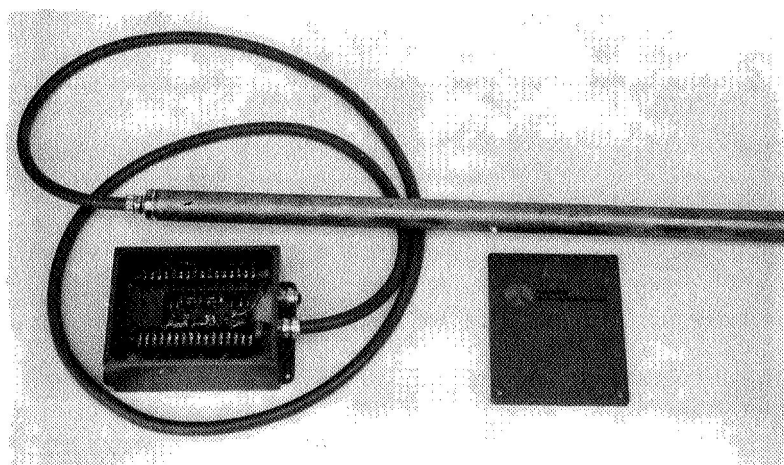


Figure 5: Biaxial tiltmeter and electronics used in this study. The tube is about 5 cm (2 in) in diameter and about 1.3 m (48 in) long.

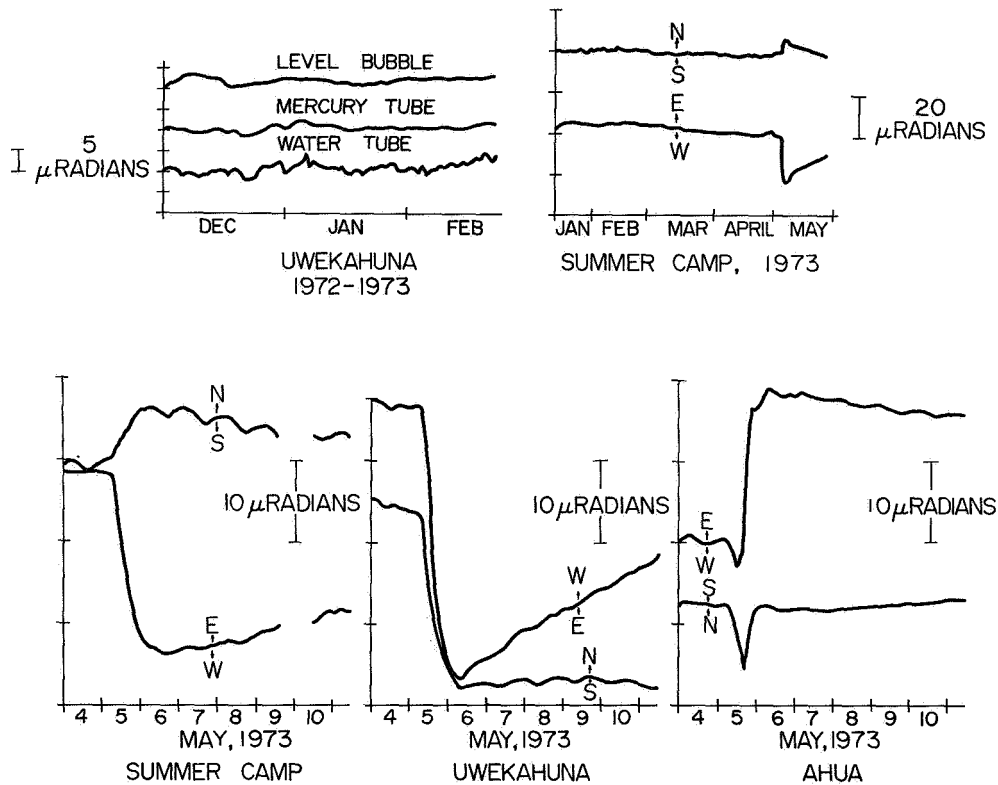


Figure 6: Typical data from three tiltmeters located around the central caldera of Kilauea Volcano during a collapse of the caldera area. The data in the upper left shows a comparison of the new level bubble tiltmeter with two other types of tiltmeters operated in Hawaii for several years.

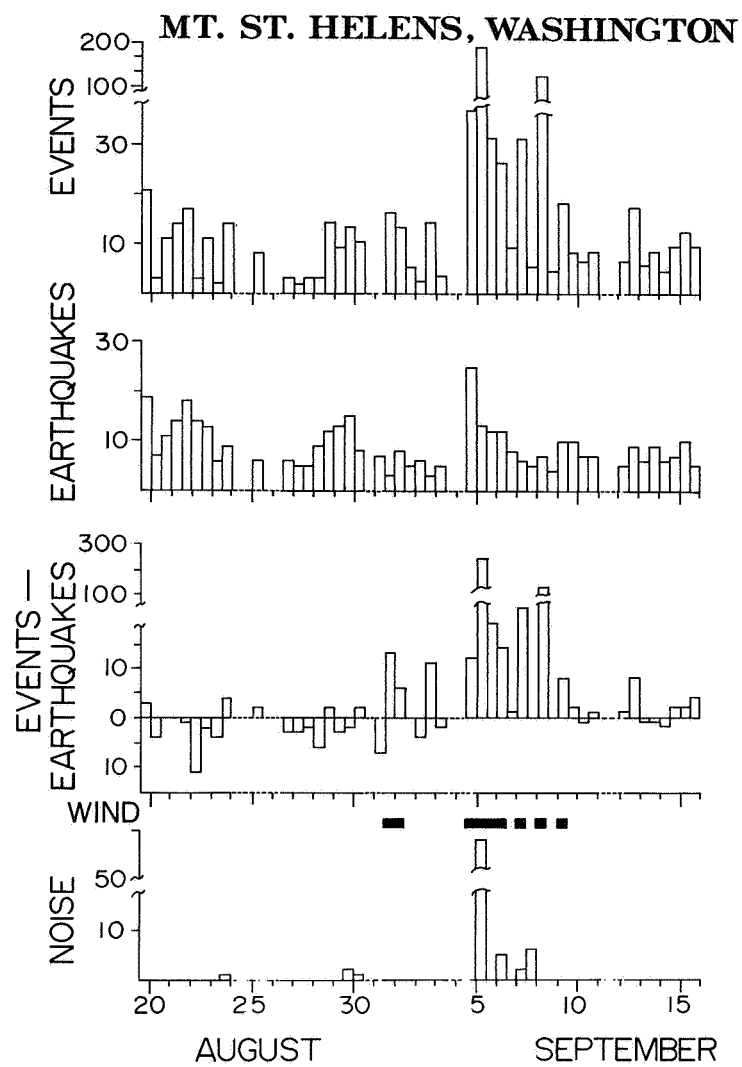


Figure 7: Seismic events counted by the event counter on Mt. St. Helens in Washington compared to earthquakes detected by a seismologist from a seismograph operated nearby.

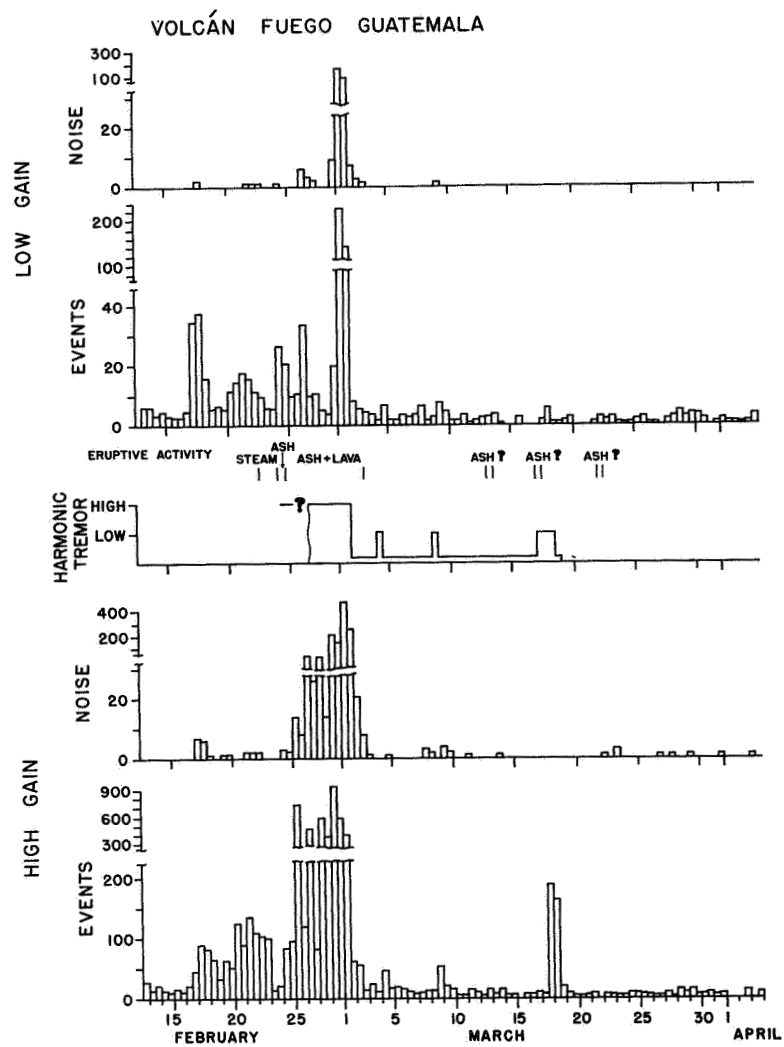


Figure 8: Seismic events and noise counted near Volcan Fuego in Guatemala in early 1973. Note the increase in seismic activity during during the eruption in February.

EVALUATION OF ERTS IMAGERY FOR SPECTRAL GEOLOGICAL MAPPING IN DIVERSE TERRANES OF NEW YORK STATE

Y. W. Isachsen, R. H. Fakundiny and S. W. Forster, *Geological Survey, New York State Museum & Science Service*

ABSTRACT

Linear anomalies dominate the new geological information derived from ERTS-I imagery, total lengths now exceeding 6000 km. Experimentation with a variety of viewing techniques suggests that conventional photogeologic analyses of band 7 results in the location of more than 97 percent of all linears found. Bedrock lithologic types are distinguishable only where they are topographically expressed or govern land-use signatures. The maxima on rose diagrams for ERTS-I anomalies correspond well with those for mapped faults and topographic lineaments, despite a difference in relative magnitudes of maxima thought due to solar illumination direction. A multi-scale analysis of linears showed that single topographic linears at 1:2,500,000 became segmented at 1:1,000,000, aligned zones of shorter parallel, en echelon, or conjugate linears at 1:500,000, and still shorter linears lacking obvious alignment at 1:250,000. Most circular features found were explained away by U-2 airphoto analysis but several remain as anomalies, the most notable being an elliptical "spoked wheel" anomaly which centers on Cranberry Lake. Neither shatter cones nor megabreccias have been found to date.

Visible glacial features include individual drumlins, best seen in winter imagery, drumlinoids, eskers, ice-marginal drainage channels, glacial lake shorelines and sand plains, and end moraines.

INTRODUCTION

This paper presents accomplishments to date on a continuing project to utilize ERTS-I multispectral scanner imagery in a tectonic synthesis of New York State, and is a supplement to an earlier publication by Isachsen and others, 1973a.

New York provides a highly varied test area for evaluating ERTS-I imagery as a source of new geological information not readily seen at conventional mapping scales. The State covers a number of well defined physiographic provinces, and contains lithologic units ranging in age from Proterozoic to Pleistocene (Broughton and others, 1966). It stretches east-west

*Published by permission of the Director, New York State Science Service, Journal Series No. 154.

1 N 74 30754

across five tectonic provinces as follows (Fisher and others, 1971): 1) a continental platform (Platform I) consisting of Lower and Middle Paleozoic strata resting on a Proterozoic basement which covers all except the eastern part of the State; 2) the Adirondack Dome Mountains which are located on the eastern edge of this platform and expose Proterozoic basement of the Grenville Province, 3) the Appalachian Foldbelt with its several subdivisions including the Hudson Highlands (reactivated Proterozoic basement) and the Taconic alloctheses, 4) the Triassic basin, and 5) Cretaceous coastal plain sediments on Paleozoic basement (Platform II).

For a general description of the geology and physiography of the State the reader is referred to Broughton and others (1966); the tectonic subdivisions are described in Fisher and others (1971).

INVESTIGATIVE PROCEDURE

The methods of handling and evaluating incoming ERTS-I multispectral imagery have been presented elsewhere (Isachsen, 1973), and are summarized by means of a flow diagram in Figure 1. Roman numerals signify the five stages of analysis which are as follows: I. photo-geologic identification of suspected geological signatures in ERTS-I imagery; II. laboratory screening of these signatures in terms of existing data in order to identify new ERTS-I anomalies; III. field investigation of representative anomalies, IV. preparation and analysis of ERTS-enhanced tectonic maps; V. publication of results.

EXPERIMENTATION WITH VIEWING METHODS

In a search for effective methods of treating ERTS-I imagery for photo-geologic analysis, experiments were conducted to compare the content of geological information in the following products (Isachsen and others, 1973b).

1. Positive transparencies and paper prints of each of the four spectral bands (4,5,6, and 7), as received from NASA.
2. Paper prints made from positive transparencies which were photo-geologically reprocessed to increase density contrast.
3. Log E dodged prints. This processing subdues density contrast to permit more detail to be seen in shadowed areas, if such detail is present.
4. Multispectral color-additive viewing of 70 mm positives of bands 4, 5,6, and 7, both as received from NASA and after photographic reprocessing to produce higher contrast positives.

The experiments described above were intended not as rigorous investigations, but rather as relatively rapid tests to help determine which methods, beyond the more conventional approaches, would yield a sufficiently greater amount of new geological information to justify the additional time involved. From the results obtained, we conclude that, for the region under study, the most advantageous method of photogeologically analyzing ERTS-I imagery is to study bands 7 and 5 separately. As for photogeologic linears, band 7 permitted detection of more than 97 percent of the total. A small additional increment of information may be derived by color additive viewing of photographically reprocessed imagery.

ERTS-I AND BEDROCK GEOLOGY

Introduction

ERTS-I imagery received through October 1973 totals 315 frames covering 34 scene areas over New York State and portions of adjacent states and Canada. An inventory of this imagery in terms of geological usefulness is as follows: useful (0-50 percent cloud cover), 55 percent; marginally useful (50-70 percent cloud cover), 12 percent; virtually useless (70-100 percent cloud cover), 33 percent.

The 1:1,000,000 film positives of the usable imagery were analyzed in transmitted white light (*i.e.* Stage I analysis) and the data were combined into a statewide "spectral geological map" at 1:1,000,000 (Isachsen and others, 1973a, Figure 2). For the late summer and fall imagery, it was found that bands 5 and 7 compliment each other and contain all the spectral signatures which appear to be geologically-linked; no additional data were found on bands 4 and 6. The data referred to above have subsequently received Stage II analysis, with a resultant ERTS-I anomaly map which will be discussed later.

Capability of ERTS-I Imagery to Delineate Major Geological Provinces

The synoptic value of ERTS imagery is readily appreciated from a single satellite image, but even more so from the mosaic of an entire State (Figure 2) where, despite the loss in resolution due to photo-reduction of the original mosaic, major physiographic, geologic and tectonic provinces can be seen. The tectonic provinces visible in the mosaic include Platform I which covers most of the State, the Adirondack Dome Mountains which comprise the northern part of the State, the narrow belt of upturned Silurian-Devonian rocks deformed during the Acadian Orogeny which define the westernmost part of the Appalachian Foldbelt and adjoin Platform I, the remainder of this Foldbelt, with the prominent Hudson Highlands, the Triassic basin between the Highlands and the Hudson River, and Platform II (Long Island). Two physiographic provinces within Platform I are clearly delineated in the imagery, namely the Tug Hill Plateau located between Lake Ontario and the Adirondacks, and the Catskill Mountains at the eastern end of the Allegheny Plateau of Platform I. (Both of these provinces are composed of erosionally-resistant deltaic rocks, one Ordovician, the other Devonian.)

Outlining the Adirondacks can be seen the major unconformity between the Grenville basement and the onlapping Paleozoic section which has at its base the Potsdam Sandstone of Upper Cambrian age. The contact is accentuated by a topographically-induced land use boundary, namely forest versus farmland, but it is also well delineated geologically, particularly along the southwestern, southern and eastern Adirondacks, by the abrupt termination of the east-west arcuate pattern in the basement at the Potsdam contact. This arcuate pattern results from differential erosion of the basement lithologies.

Along its northern, western, and southwestern borders, the crystalline Adirondack basement is expressed on ERTS-I imagery as a slightly dissected planar surface which dips gently away from the central part of the Adirondack Dome (Figures 2 and 3). This surface is exposed in a belt ranging in width from 10 km in the north to about 20 km along the western perimeter and corresponds closely to the physiographic section designated as the "Fall Zone Belt" by Buddington and Leonard (1968, p.8). It is doubtless a tilted erosion surface from which the Paleozoic units have been stripped by erosion. A striking feature of this paleoplane in the northern Adirondacks is its abrupt termination to the southeast, along a topographic lineament which had not previously been mapped, to produce a pseudo-cuesta. Along the northern border of the Adirondacks, the contact between this erosion surface and the Potsdam Sandstone is well displayed as a boundary between forest and cultivated farmlands. About 10 km to the north, is the contact between the Potsdam Sandstone and the Theresa sandy dolostone, again marked by a change in land use influenced by bedrock.

Along the southwestern border of the Adirondacks, the basement-Potsdam contact is accentuated by the Black River. In the intervening section, basement exposures are continuous from the Central Highlands, across the Frontenac Arch of the Northwest Lowlands, into the main Grenville Province of Canada. Potsdam occurrences are here limited to scattered, relict patches.

Within the Adirondacks, many geological structures can be identified. These include the major east-west arcuate folds extending across the southern Adirondacks (Figures 2 and 3) and a number of domical structures, plunging folds, refolds, and other structures which have topographic expression (Figure 3). More pronounced than these structural elements, however, is the strong expression of NNE-trending linear features. These will be discussed in a later section.

Within the Appalachian Foldbelt, major subdivisions can be seen in the ERTS-I imagery at the original 1:1,000,000 scale (albeit notably better at 1:500,000). In Figure 4, the Allegheny Plateau with the Catskill Mountains as its eastern projection, is readily identified by its dendritic drainage pattern. The straight eastern edge of the Catskill Mountains, which has long been referred to as the "Wall of Manitou", is prominently displayed. A major insight into its cause has been provided by ERTS-I imagery, as will be discussed later.

About 20 km south of the Catskills, the Shawangunk Mountains begin, and extend southwestward into New Jersey where they are known as the Kittatinny Mountains. They represent a belt of upturned Silurian and Devonian rocks, dominated by the Shawangunk conglomerate which marks the western boundary of the Appalachian Foldbelt.

An angular unconformity between the titled Shawangunk conglomerate and isoclinally-folded Ordovician shale and graywacke beds is seen on the imagery as the eastern edge of the Shawangunk Mountains. These beveled Ordovician rocks extend eastward to the resistant Proterozoic basement rocks of the Hudson Highlands, north of the wide portion of the Hudson River. Northwest of the Hudson Highlands a synclinal belt of down-faulted Silurian and Ordovician strata occurs. This belt is marked by the elongate Greenwood Lake at its southern end, and by the isolated Schunemunk Mountain mass at its northern end about 10 km southwest of the point at which the Hudson River enters the narrow gorge (fiord) through the Hudson Highlands. The Highlands extend northeastward, where they appear to merge, in the 1:1,000,000 imagery with the more highly-metamorphosed Paleozoic rocks of New England. (In the 1:500,000 imagery, the northern boundary of the Hudson Highlands is better delineated.) The elongate Housatonic Highlands, a separate Proterozoic mass, can be seen northeast of the Hudson Highlands. The belt of Taconic allocthonous north of the Hudson Highlands is not well defined in the 1:1,000,000 print, but can be seen at the 1:500,000 scale.

The Triassic Basin borders the Hudson-New Jersey Highlands along the Ramapo normal fault, and is bounded on the east by the Hudson River. The Palisades diabase sill forms a vertical escarpment along the west shore of the river. It can be seen in the imagery as a faint line parallel to and within 500 meters of the shoreline. The Hudson flows along the onlapping contact between the Triassic red beds and the high-grade Appalachian basement rocks to the east. This basement, in turn, forms the substrate for the Cretaceous and Pleistocene formations of Long Island.

ERTS-I Linears in New York State

In this report the word "linear" is used in the sense of Dennis (1967, p. 103) to designate lines of uncertain origin on aerial photographs or imagery. The term "lineament" on the other hand, is reserved for a naturally occurring linear feature (e.g. Hobbs, 1904, Latman, 1958), i.e. one that has been confirmed to exist on the ground.

Without question, the most significant geological contribution of ERTS-I imagery to date in New York State has been the location of more than 500 Stage II linears which had not previously been recognized. This linear detecting capability of ERTS-I imagery was the most frequently cited geological application at a recent Symposium of Significant Results from the Earth Satellite, ERTS-I (Short, 1973).

A work map of Stage II linears observed on ERTS-I imagery at 1:1,000,000 is shown in Figure 5. The linears represent those remaining from a Stage I work map (Isachsen and others, 1973a, Figure 2) after the removal of such "cultural linears" as transmission lines, railroads, abandoned railroad

beds, and highway segments. The Stage II linears range from strongly-developed topographic lineaments to very subtle linears which are defined by faint tonal, rather than topographic signatures. They range in length from 5 to 200 km, and the majority are straight. The combined lengths of these ERTS-I linear anomalies exceeds 6000 km, not including linear portions of the Hudson River and the Finger Lakes. It has been learned subsequent to the preparation of Figure 5 that topographic lineaments as short as 1.5 km are mappable on the 1:1,000,000 imagery. Hence additional linears can be extracted in the future.

ERTS-I Linears in the Adirondack Region

The most spectacular area of linear display in the State, if not in the entire northeast, is the Adirondack Mountain region (Figures 2 and 3). The linear features seen in the imagery include the majority of the major faults and topographic lineaments shown on the Geologic Map of New York at 1:250,000 (Fisher and others, 1971; Isachsen, 1973). Of those not visible in the imagery at 1:1,000,000 (Isachsen, 1973), most are short, and may turn out to be discernible at larger scales. The easternmost group occur in the Champlain Valley, an area of low relief, and are less likely to be expressed in the imagery.

A numerical summary of the Adirondack linear information obtained as of May 1973 is tabulated below:

<u>Category</u>	<u>Number</u>	<u>Combined length, km</u>
Previously mapped faults and topographic lineaments seen on ERTS-I imagery	232	1890
ERTS-I linear anomalies which have survived Stage II investigation	364	3131
Total linears seen on ERTS-I imagery	596	5021
Previously mapped faults and topographic lineaments not discernible on ERTS-I imagery	297	1750

The linear data shown in Figure 3 has had all obvious lithologically-controlled and "cultural" linears removed. Subsequent to this, each of the remaining linears in the Adirondacks were located by inspection on 1:62,500 airfoto index mosaics. They were thereupon classified as to photogeologic character (see Isachsen and others, 1973b for details). A summary of the photogeological classification follows:

Cultural linears	20
Linears parallel to lithological trends	51
Straight segments of stream courses	96

Straight stream valleys	27
Winding streams	7
Elongate lakes or straight shorelines	7
Ridge crests	3
Edge of topographic high or aligned segments of same	5
Alignments of vegetation:	
a. dark vegetation strips (may be valleys)	30
b. vegetation border	7
Combinations of one or more of the above	57
Unexplained	<u>125</u>
	TOTAL 435
Total, less cultural and lithological linears above	364

The ERTS-I linear anomaly data for the Adirondack region are summarized in the two rose diagrams of Figure 6. The upper diagram is an unweighted plot of the total number of linears, whereas the lower diagram takes the lengths of linears into account. The generally similar appearance of the two diagrams holds up well under closer scrutiny. The maxima appearing in the weighted diagram can also be seen in the unweighted one, namely: N75W, N45W, N20W, N-S, N25E, N40E, N50E, N60-70E, N85-90E. This close correspondence indicates that, in general, the lengths of the anomalous linears are proportional to their frequency for any give azimuth.

When the above diagrams are compared with analagous plots of previously mapped faults and topographic lineaments (Figure 7), both differences and similarities appear. The most notable difference is that the major concentration of ERTS-I linear anomalies occurs in the 30° sector N40E to N70E, whereas previously-mapped linear structures fall in the 35° span between N15E and N50E. This may reflect differences in the geological control and expression of these newly discovered linears. More likely, however, to the extent that they are topographic linears, they are so well expressed in this sector because it is essentially orthogonal to the azimuth of solar illumination in October (153°, 34° elevation). Consistent with this interpretation is the low incidence of linears parallel to the direction of illumination (N20-40W), despite the fact that linears in this direction are fairly abundant on the ground (Figure 7). Wise (1969) has demonstrated experimentally the critical effect of direction of illumination on the display of linears, although he used considerably lower elevations (5 to 20 degrees). The interpretation presented above is consistent with the conclusions reached by MacDonald and others (1969) from a look-direction study of side-looking radar images.

Despite the difference in relative magnitudes of the maxima, a very close correspondence exists for their directions, except for two. The maxima of Figure 7, which also appear as prominent directions (within 5 degrees) on the imagery, are as follows: N70W, N45W, N20W, N-S, N40E, N50E, N70E, and N80E. On the ERTS-I linear diagram, however, a N25E set is prominent rather than the N15E set mapped on the ground. The most prominent ERTS-I set (N60E) is very subordinate among the known ground linear features. However, its trend comes within 3° of being perpendicular to the direction of solar illumination, and this probably explains its prominence.

Stage III Investigation of ERTS-I Linear Anomalies in the Adirondack Mountains

A major problem associated with field checking of ERTS-I anomalies is

locating them on the ground. This is greatly facilitated by visually transferring data from the ERTS-I photographic product to another photographic product at a more useful field scale, namely airfoto index sheets at 1:62,500. It is then relatively easy to plot the feature in the approximately correct location on 1:62,500 topographic maps, particularly if it is topographic. The most economical and effective way to locate the feature on the ground is by viewing and photographing it from low level aircraft. Photographs taken on such a flight can be seen in Figures 8 and 9. They show an ERTS-I anomaly which is located entirely within a single geological unit, the Marcy Massif metanorthosite. The linear, a confirmed topographic lineament, turns out to be a 16 km-long southward extension of a previously mapped lineament. It extends both north and south of the portion shown in the photograph.

The contrast in relief between this new lineament and a previously mapped one (which has of course, a stronger expression in the imagery) can be seen by comparing Figures 8 and 10.

A far more subtle topographic lineament found in the ERTS-I imagery is shown in Figure 11. This broad, relatively short (6 km) linear valley extends WNW, transecting at nearly right angles the North River-Mt. Marcy range. The northern edge of the North River Mountains appears in the left middleground. The linear is terminated to the west by a major NNE linear which passes just east of Popple Hill, the dark mountain in the middle of the valley. It reappears to the west, as can be seen in Figure 3.

Geological Identification and Origin of ERTS-I Linears in the Adirondacks

Although data gathering and collation must continue to dominate our activity for some time before extensive synthesis and interpretation can be made, there is good reason to suspect that the NNE topographic lineaments will prove to be traces of high-angle faults and fracture zones. This is based on detailed geological mapping by Walton (unpublished) of four contiguous 15 minute quadrangles in the eastern Adirondacks where these linear fractures are so abundant. Walton (oral communication) found that fault breccias and/or stratigraphic displacement could generally be demonstrated for these structures.

Stage I Multi-scale Analysis of an ERTS-I Scene Covering Southeastern New York

A Stage I multi-scale photogeologic analysis was made of linears in southeastern New York (Figure 4) to determine their characteristics at various scales. ERTS-I data products at 1:1,000,000, 1:500,000, and 1:250,000, as well as a mosaic at approximately 1:2,500,000 (Figure 4) were used. Details of this study are given in Isachsen and others, 1973b. Selected results of the study are as follows:

- 1) Of the total number of linears visible on bands 5 and 7, and on a false color composite, more than 97 percent were visible on the band 7 image;
- 2) The features recorded as linears were simply lines having "sufficient length" to determine that they are straight. Following this criterion, the shortest lines classified as linears were 5 km at 1:2,500,000, 2 km at 1:1,000,000, 1 km at 1:500,000, and 0.5 km at 1:250,000. This

amounted to an unconscious selection of 2 mm as the shortest "reliable" straight line, whatever the scale.

- 3) Linears are abundantly expressed in the region, and, in general extend across physiographic, geologic, and tectonic boundaries.
- 4) What appear as continuous linears at the smaller scales, are zones of aligned segments at the larger scales. Furthermore, the segments may strike parallel to the zone of alignment, en echelon to it, or in conjugate relationship. As one example, the N65E trending set of linear segments near the northeast corner of Figure 4 produces at 1:2,500,000 what appears to be a single linear several hundred kilometers long, at 1:1,000,000 a dashed line (Figure 4), and at 1:500,000 a series of two sets of en echelon segment lying in a N65E zone. At 1:250,000 the individual linears are no longer recognizable as part of a major through-going structure. This study illustrates the value of multi-scale viewing in lineament analysis.

Stage III Investigations in the Catskill Mountains

General

Field work to date in the Catskill region indicates a direct relationship between the long axes of straight valley segments and the strike of major joint sets. If subsequent field investigations across the Allegheny Plateau confirm this relationship, ERTS-I imagery will prove to be the most economical method available for mapping major joint sets over large regions.

Field Study of the N20E Linear Set

The eastern edge of the Catskill Mountains is a notably straight steep escarpment (Figure 4) along which the Mountains rise abruptly for 800 m from the broad Hudson River Valley to adjacent summits which exceed 1000 m in height. This escarpment, long known as the "Wall of Manitou" extends south from the latitude of Catskill for a distance of 20 km.

West of the "Wall", the Catskill Mountains are eroded to produce prominent, northwest trending, ranges and valleys. Crossing these ranges at a high angle are numerous topographic lineaments which trend about N15E, and parallel the Wall of Manitou. The pervasive nature of this set, extending westward for at least 25 km, was never recognized before, and its geologic origin has only received brief mention. Chadwick (1944, p. 17) interpreted the two prominent valleys which occur 10 km west of the Wall of Manitou as being controlled by closely spaced joints along which "the internal settling known as 'keystone' faulting (Crosby, 1925)" might have occurred, although "as yet actual faulting has been demonstrated in only the easternmost of these lines, namely that which is tangent to the east end of North Lake." The fault referred to is located at the northern end of the "Wall" at the upper break in slope on Chadwick's geological map.

A vertical aerial photograph recently taken by NASA at 24,000 feet altitude of an area 12 km west of the Wall of Manitou (Figure 12) provides a useful

calibration device to determine how short a linear may be mapped on the ERTS-I imagery with confidence. As expected, the relatively long N20E linears are readily confirmed, a particularly good example being the Stony Clove linear. More impressive, however, is the fact that the two short N75E linears, spaced only 1 km apart, with the shorter one being less than 2 km long, can be discerned on the imagery.

Low level aerial reconnaissance of the Stony Clove linear confirms it as a well defined topographic lineament (Figure 13). A closer view of the Stony Clove drainage divide (Figure 14) suggests that vertical displacement may have taken place. Field altimetry, however, was inconclusive, inasmuch as an elevation difference of only 5 m across a valley width of 100 m in continental sediments can be explained without resort to faulting. Of interest, however, is the fact that the valley is developed along a steeply dipping conjugate joint sets. On the west side of the valley, east-dipping joints are dominant. On the east side, westward dips predominate (Figure 15). The orientation of the 32° acute angle is compatible with the interpretation that this set of conjugate joints, and the valley itself, are reflected basement structures such as might be produced by minor dip-slip reactivation along a basement fault such as those exposed along strike in the Adirondacks (Figure 5).

Circular Features on ERTS-I Imagery

A number of circular features appearing on the ERTS-I imagery covering New York State have been described and illustrated in some detail by Isachsen and others (1973b), and will be only briefly referred to here. Those which have survived Stage II analysis (*i.e.* are not fortuitous arrangements of urban signatures) are shown in Figure 5. A cluster of three occur southeast of Rochester, one north of Oneida Lake, and three in the Adirondacks. Of the three near Rochester, only the central one is well defined in a U-2 photograph covering the area. It results from a combination of a scalloped drainage pattern which forms the upper and lower parts of the circle, and elongate fields paralleling drumlins which define the sides. The drainage pattern is probably of glacial origin. The circular feature north of Oneida Lake is not visible on airfoto index sheets, and so remains unexplained. That located to the NNE across the Black River is formed in the main by a possibly fortuitous arrangement of two stream courses.

The most striking of the "circular" features is an elliptical "spoked wheel" centering on Cranberry Lake and here termed the Cranberry Lake anomaly (see Figures 3 and 5). Seven of the radial valleys are arms of Cranberry Lake, at least in part. The long axis of the feature measures about 30 km, the short axis about 22 km. In a very general way it has a central domal high surrounded by a ring depression, with a lake basin at the center of the feature. The maximum topographic relief measured from lake bottom to the higher mountains within the feature is about 830 m. In the eastern and southern parts of the feature, a suggestion of concentric rings can be seen in the imagery (Figures 2 and 3). A recently published gravity map of the Adirondacks (Simmons and others, 1973) shows a two milligal simple Bouguer negative gravity anomaly over the Lake basin. Taken together, the above observations suggest the possibility that the Cranberry Lake anomaly may be a cryptoexplosion structure.

The relationship between the topography of the anomaly and bedrock geology (Isachsen and others, 1973b) may be summarized by stating that the rim valley parallels bedrock foliation trends along part of its course, transects it along others, and fails to develop at all across an antiform of quartzofeldspathic units to the northeast.

Aeromagnetic trends in the Cranberry Lake anomaly area (unpublished map of Zietz) show no anomalous deviation from the mapped lithologic trends. Field work in the area to date has failed to disclose any criteria indicative of cryptoexplosion structures (e.g., Short and Bunch, 1968), particularly shatter cones, megabreccias, injection veins, or other anomalous fracturing. Thin section search for cryptoexplosion features remains to be made.

Beginning 15 km north of Childwold is a roughly circular feature 30 km in diameter which is bounded by a narrow valley (Figure 2, 3 and 5). This feature forms the major part of an irregularly-shaped area which has a northeasterly elongation. The topography and tone are clearly different in appearance from any other part of the Adirondacks. The area appears in the imagery as a broad depression with sparse, irregularly-scattered hills, suggestive of "broken ground" on a very large scale. The area is, in regional terms, a terrace (The Childwold Terrace of Buddington and Leonard, 1962, p. 8) with valley bottoms having elevations of 1200-1300 feet on the northwest and 1600 feet on the southeast. The scattered hills rise up to a maximum 400 feet above the valley floor. This physiographic belt has an anomalously high percentage of sand plains and swamps, and the lowest density of bedrock outcrops of any large area in the Adirondacks (see Fisher and others, 1971). The reason for this is not known. The area does not show any gravity anomaly (Simmons and others, 1972).

ERTS-I AND GLACIAL GEOLOGY

Numerous previously-mapped glacial features can be seen on ERTS-I imagery at 1:1,000,000. These include more than ten drumlin fields, drumlinoid glacial streamline forms, glacial lake sand plains and deltaic deposits, segments of glacial lake shorelines, ice-marginal drainage channels, and end moraines (Figure 16). No new glacial features have been identified to date. The search for mapped glacial features on ERTS imagery is greatly facilitated by using a scale-changing device such as the Bausch and Lomb Zoom Transferscope model ZT-4.

Several drumlin fields can be located on the summer and fall imagery due to the topographic effect of drumlin topography on land use pattern, but most are obscured. However, when snow cover obliterates land use patterns and the low sun angle of winter months highlights their relief, drumlin fields, and even individual drumlins, can readily be identified. Indeed, the stoss and lee sides of drumlins can be distinguished in some cases. Good examples can be seen south of the Mohawk River (1169-15123, 1170-15182) and in the Finger Lakes region (1243-15244). In the latter area, however, snow cover is less complete, and field patterns tend to camouflage the topography. For this reason only portions of the extensive drumlin fields of the Finger Lakes region can be identified, and of an estimated 10,000 drumlins in central New York State (Flint, 1957) only 228 could be recognized. South of the Mohawk River, 316 drumlins were counted. On the ground, the drumlins measure 2 km in length, 400 m in width and 25 m in height. It

appears likely that optimum winter imagery could be "calibrated" using topographic map information, and then used to make a rapid, relatively accurate, inexpensive inventory of the drumlins in any region of the State.

Numerous glacial features are visible east of Lake Ontario. On the Tug Hill Plateau, glacial streamline forms or drumlinoids with northwest axes are extensively developed. In contrast to the drumlin fields mentioned above, these are best shown on the fall imagery (1080-15180). This is understandable because the Plateau is evenly forested, rather than being camouflaged by agricultural patterns. On a topographic map, the drumlinoids average 2-4 km in length, about 80 m in width, and 15 m in height. No published data are available to indicate to what extent they are depositional landforms or erosional bedrock features.

A small drumlin field not apparent in earlier imagery can be seen in the winter imagery on the northwest slope of the Tug Hill Plateau (1170-15182, 1170-15175). Also visible in the winter image are several glacial lake drainage channels which roughly parallel the contours around the north slope of the Plateau. Although these could be seen to some extent in the fall imagery (1080-15180) they are enhanced in the winter imagery due to the contrast between shadowed channels (accentuated by low sun angle) and surrounding snow. On the ground they are 2-17 km long, 200-700 m wide, and 20-30 m deep.

Comparison of the imagery with existing glacial maps of the Tug Hill region (Stewart, 1958; Forster, 1971) revealed no correlation. Farther north, in the St. Lawrence Lowland, image 1080-15174 was compared with the maps of MacClintoch and Stewart, 1965, and a rough correlation was noted between the extensive areas of intermediate gray density located west of Malone, and areas mapped as peat and muck (swamp). An even better correlation was found when the imagery was compared with the woodland overprint on the 1:250,000 topographic map of the USGS (N118-11, 1961)--another example of a geological signature linked to land use.

In the Central Highlands of the Adirondacks, numerous segments of eskers show up in the imagery as narrow ridges bounded by bodies of water. On the ground these are 200-400 m wide and 15-25 m high.

At the northernmost part of the State, the Covey Hill drainage channels for glacial Lake Iroquois can be recognized on image 1079-15115. On the ground, these channels are 2-4 km long, approximately 300 m wide, and 20 m deep. On the same image can be seen an area south of Plattsburg which has a distinct, uniform, tonal density. This area was found to correspond quite closely with that of a sand plain mapped by Denny (1967) as a deposit formed in glacial Lake Vermont.

Farther south, two thirds of the distance to Albany, is a tonally distinct gray area whose borders were found to have a fair to excellent correspondence with the boundary of stratified drift and deltaic deposits associated with glacial Lake Albany, as shown on an unpublished 1:250,000 glacial map of the area prepared by R. Dineen.

In the southeastern part of the State, a series of moraines mapped by Connally and Sirkin (1967) in the Wallkill and Hudson Valleys were searched for on both fall (1079-15124) and winter (1205-15132) imagery. On neither image was any indication seen for these moraines.

Imagery of Long Island (1096-15074) was compared with a map of the Harbor Hill and Rankankama moraines using a direct overlay. A few short segments of these moraines were detected because of different land use on the moraine compared with surrounding areas.

Using a 1:1,000,000 enlargement of the Glacial Map of the United States east of the Rocky Mountains (Flint, et al, 1959) imagery for New Jersey and Pennsylvania (1205-15135, 1170-15184, 1243-15251) was searched for end moraines and other glacial features. As shown on Figure 16, only a few short segments of moraines are visible.

For the western part of New York State the imagery (1243-15244, 1243-15251, 1244-15303, 1046-15292, 1244-15305) was compared with a compilation of moraines and beach ridges (Muller, 1972). Perhaps because of land use camouflage and low relief of these ridges (10 m), only small sections of a limited number of each was seen. Moraines searched for include the Valley Heads, Olean, Almond, Arkport, Clymer, Findley Lake, Gowanda, Hamburg, Marilla, Alden, Buffalo, Niagara Falls, Batavia, Barre, Albion, Colton, Geneva, and Waterloo. Those sections seen are shown on Figure 16. Glacial lake shorelines of the following lakes were also searched for: Whittlesey, Warren, and Iroquois; only two sections of the Iroquois beach ridge were found (Figure 16).

CONCLUSIONS

The overwhelming majority of bedrock features which can be seen in ERTS-I imagery are identifiable either by their direct topographic expression or by differences in land use patterns governed by topography. Variations in bedrock lithology which lack topographic expression are only seen where they strongly influence land use.

By far, the greatest geological contribution of ERTS-I imagery is in the delineation of hundreds of hitherto unknown linear features, both topographic and tonal, long (up to 200 km) and short (less than 1.5 km). The new linear information will, in the short run, be incorporated into a regional tectonic synthesis now in progress. In the long run, because of its sheer magnitude it will doubtless occupy the attention of numerous field geologists for some time to come.

A comparison of ERTS-I linears with ground structures indicates that some linears parallel known major fault trends while others parallel regional joint sets. There are doubtless a number of other genetic categories represented.

It is anticipated that the ERTS-enhanced fracture map of the State now in preparation will prove to be invaluable in seismic studies now underway by Lamont-Doherty Geological Observatory and the New York State Geological

Survey. At present, virtually nothing is known about the relationship between seismicity and tectonics in New York. Both theoretical questions relating to seismicity within the North American Plate, and practical questions concerning seismic hazard are involved.

A number of potentially anomalous circular features seen in the imagery were explained through the use of U-2 aerial photography. An elliptical anomaly with a radial system of valleys, the Cranberry Lake anomaly, however, will require additional investigation.

REFERENCES

- Broughton, J.G., Fisher, D.W., Isachsen, Y.W., and Rickard, L.V. 1966. Geology of New York, a short account. N.Y.S. Mus. and Sci. Service Map Educ. Leaflet 20. 49 pp. and colored map.
- Buddington, A.F. and Leonard, B.F. 1962. Regional geology of the St. Lawrence County magnetite district northwest Adirondacks, New York. U.S. Geological Survey Prof. Paper 376, 145 pp.
- Chadwick, G.H. 1944. Geology of the Catskill and Kaaterskill Quadrangles. N.Y.S. Mus. Bull. 336, 251 pp.
- Connally, G.G. and Sirkin, L.A. 1967. The Pleistocene Geology of the Wallkill Valley. New York State Geological Association, 39th Annual Meeting Guidebook, pp. A1-A16.
- Dennis, J.G. ed. 1967. International Tectonic dictionary - English terminology. Am. Association Petroleum Geologists Mem. 7, 196 pp.
- Denny, C.S. 1967. Surficial geologic map of the Dannemora Quadrangle and part of the Plattsburg Quadrangle, New York. U.S. Geological Survey Map GQ-635.
- Fisher, D.W., Isachsen, Y.W., and Rickard, L.V. 1971. Geologic Map of New York, 1970, and Generalized Tectonic-Metamorphic Map of New York, 1971. N.Y.S. Mus. and Sci. Service Map and Chart Series no. 15.
- Flint, R.F., Colton, R.B., Goldthwait, R.P., and Willman, H.B. 1959. Glacial map of the United States East of the Rocky Mountains. Geol. Soc. Amer.
- Forster, S.W. 1971. Pleistocene Geology of the Carthage 15-minute Quadrangle. New York State: unpublished dissertation, Syracuse University, 129 pp.
- Hobbs, W.H. 1904. Lineaments of the Atlantic Border Region. Geol. Soc. Amer. Bull. 15:483-506.
- Isachsen, Y.W. 1973. Spectral geological content of ERTS-I imagery over a variety of geological terranes in New York State, in Anson, H., ed., Symposium Proceedings, Management and utilization of remote sensing data. Amer. Soc. Photogrammetry, pp. 342-363.

- Isachsen, Y.W., Fakundiny, R.H., and Forster, S.W. 1973a. Evaluation of ERTS-I imagery for geological sensing over the diverse geological terranes of New York State, in Symposium on significant results obtained from the Earth Resources Technology Satellite I, NASA/Goddard Space Flight Center, pp. 223-230.
- Isachsen, Y.W., Fakundiny, R.H., and Forster, S.W. 1973b. Evaluation of ERTS-I imagery for spectral geological mapping in diverse terranes of New York State. NASA Report, June 29, 1973, 77 pp.
- Lattman, L.H. 1958. Technique of mapping geologic fracture traces and lineaments on aerial photographs. Photogrammetric Engineering vol. 24, pp. 568-572.
- MacClintock, P. and Stewart, D. 1965. Pleistocene geology of the St. Lawrence Lowland, N.Y.S. Mus. and Sci. Service Bull. 394, 152 pp.
- MacDonald, H.C., Kirk, T.N., Dellwig, L.F. and Lewis, A.J. 1969. The influence of radar look-direction on the detection of selected geological features. Proceedings of the 6th International Symposium on Remote Sensing of the Environment. Univ. of Mich., pp. 603-615.
- Muller, E.H. 1972. Moraines of Western New York. unpublished map.
- Short, N. 1973. View from 570 miles. Geotimes, May 1973, pp. 16-20.
- Short, N., and Bunch, T.E. 1968. A Worldwide Inventory of Features Characteristic of Rocks Associated with Presumed Meteorite Impact Structures, in Shock Metamorphism of Natural Materials, B.M. French and N.M. Short, editors. Mono Book Corporation, Baltimore, pp. 267-285.
- Simmons, G. and Diment, W.H. 1972. Simple Bouguer anomaly map of northern New York. N.Y.S. Mus. and Sci. Service Map and Chart Series no. 17A.
- Stewart, D.P. 1958. Pleistocene Geology of the Watertown and Sackets Harbor Quadrangles, New York. N.Y.S. Mus. and Sci. Service Bull. 369, 79 pp.
- Wise, D.V. 1969. Pseudo-radar topographic shadowing for detection of sub-continental sized fracture systems. Proceedings of the 6th International Symposium on Remote Sensing of the Environment, Univ. of Mich., pp. 603-615.

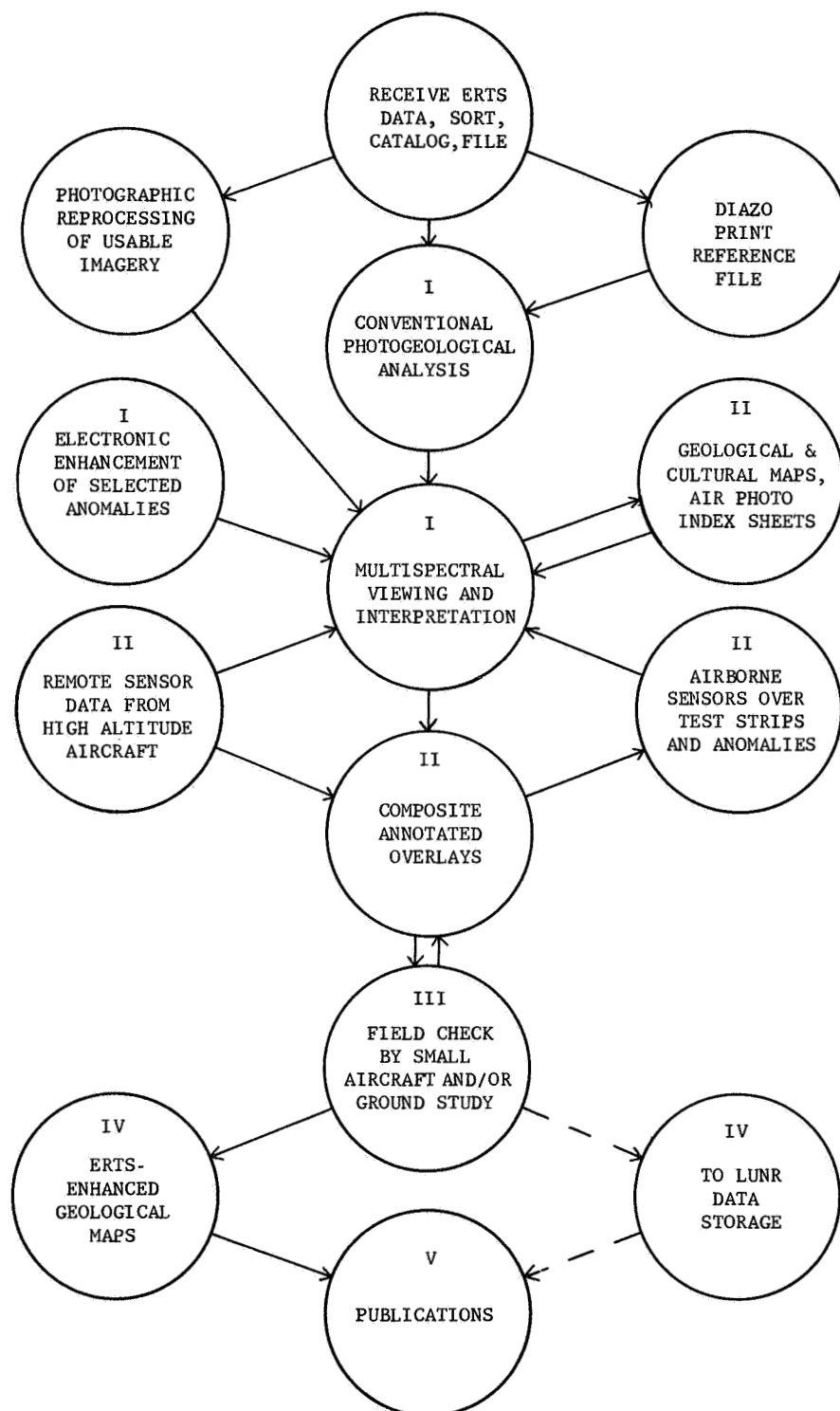


Figure 1. Flow chart of data handling and imagery analysis for ERTS-1 products. Roman numerals signify stage of study as discussed in text.

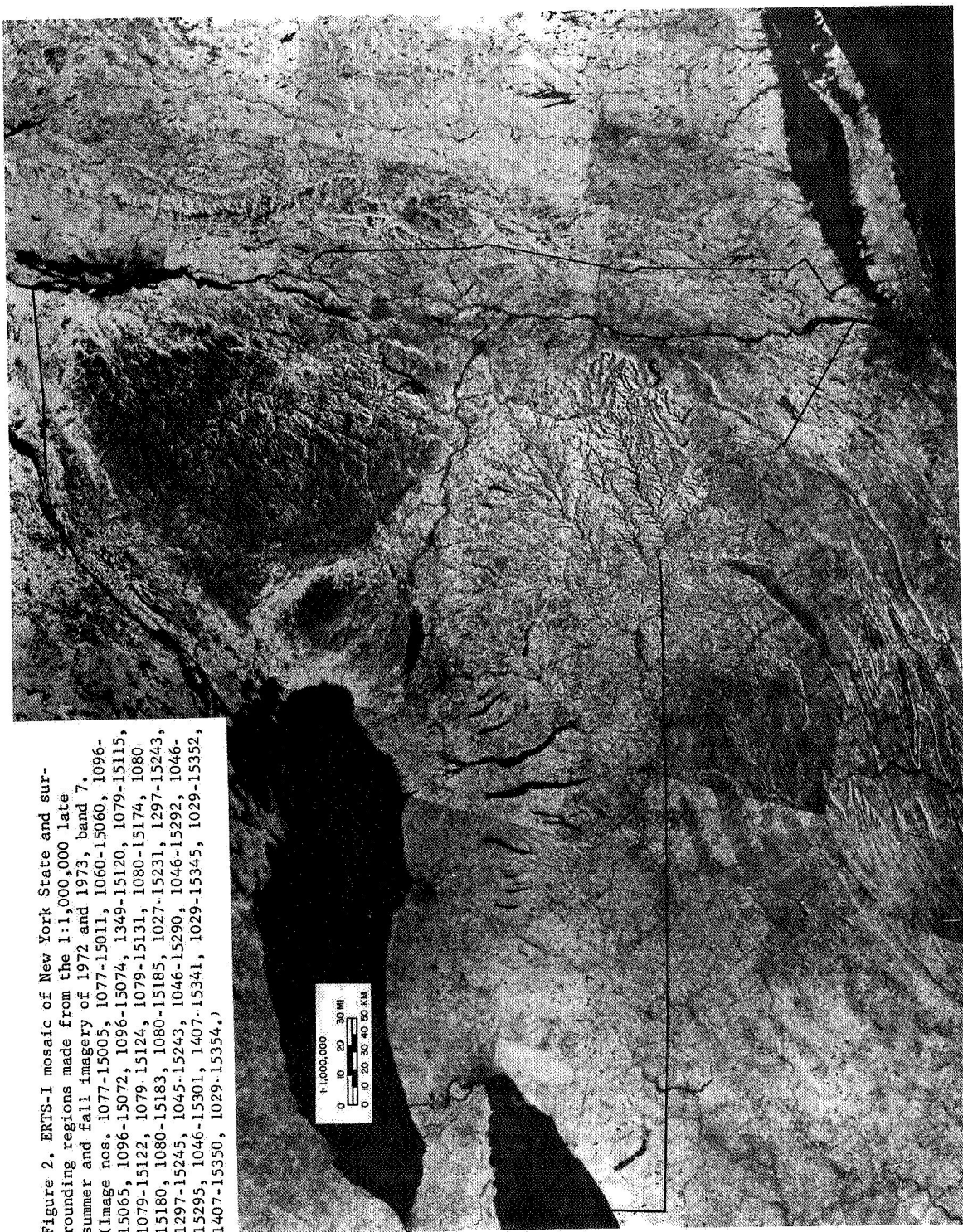


Figure 2. ERTS-I mosaic of New York State and surrounding regions made from the 1:1,000,000 late summer and fall imagery of 1972 and 1973, band 7. (Image nos. 1077-15005, 1077-15011, 1060-15060, 1096-15065, 1096-15072, 1096-15074, 1349-15120, 1079-15115, 1079-15122, 1079-15124, 1079-15131, 1080-15174, 1080-15180, 1080-15183, 1080-15185, 1027-15231, 1297-15243, 1297-15245, 1045-15243, 1046-15290, 1046-15292, 1046-15295, 1046-15301, 1407-15341, 1029-15345, 1029-15352, 1407-15350, 1029-15354.)

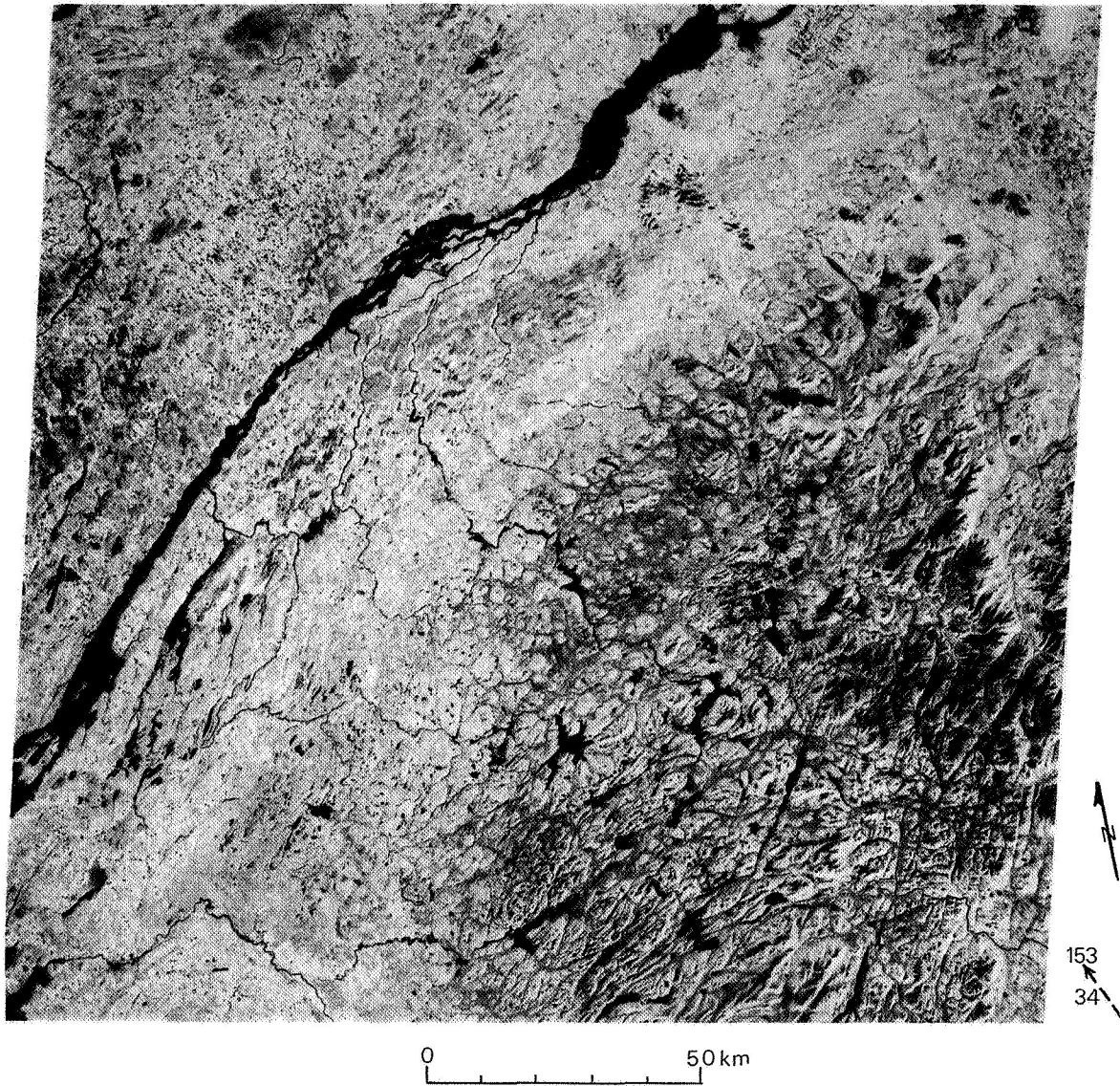


Figure 3. ERTS-I image of Adirondack area, band 7, taken 11 Oct 72 over the northern Adirondack region (image no. 1080-15174). Dashed arrow indicates sun azimuth and angle. From east to west, the dots in the high peaks region indicate sites from which were taken the photographs of Figures 8, 11, and 10 respectively.

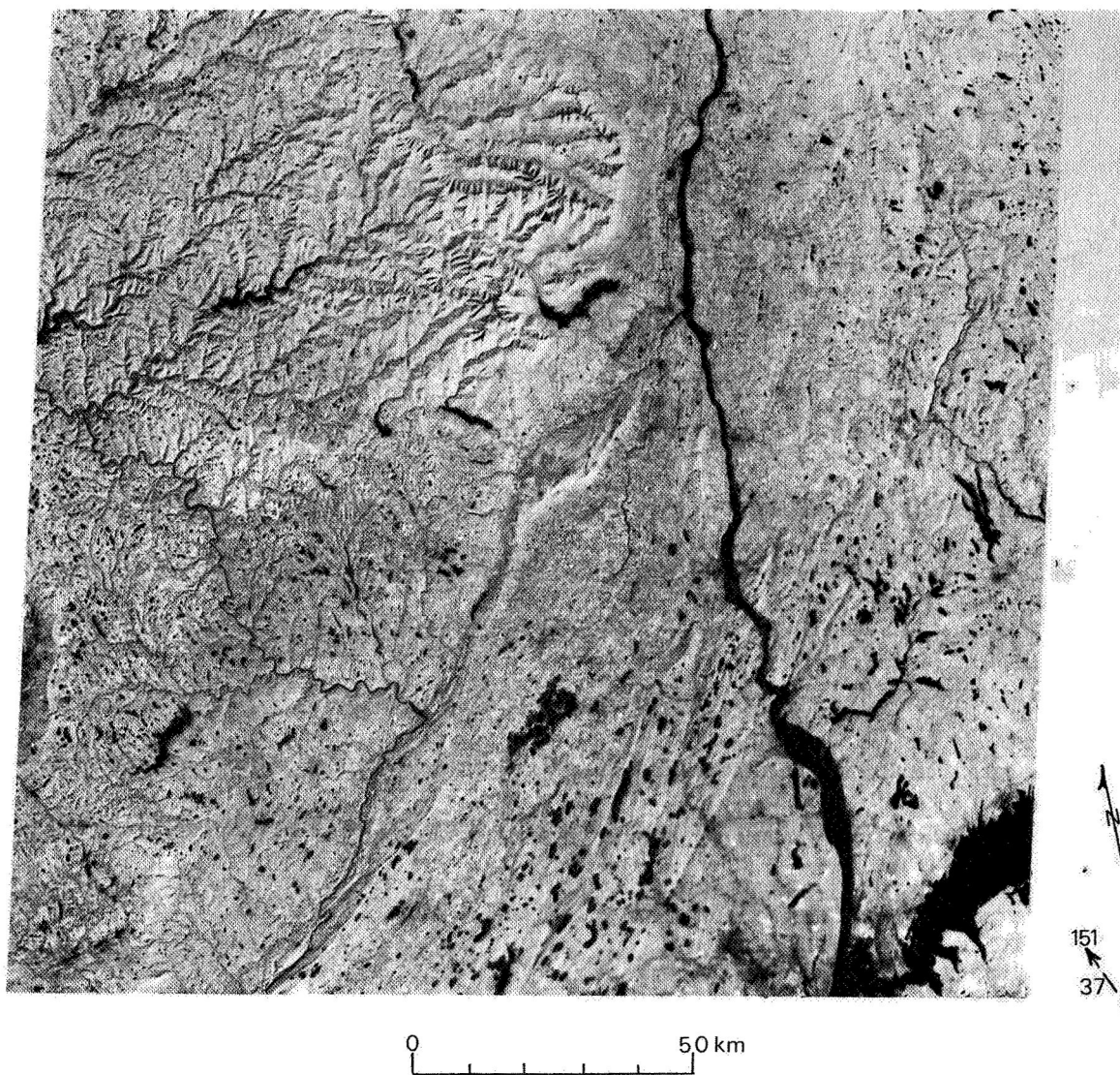


Figure 4. ERTS-I image over southeastern New York State, band 7 of 10 Oct 72 (image no. 1079-15124). Dashed arrow indicates sun azimuth and angle. Triangle in Catskill Mountains indicates site from which photograph of Stony Clove (Figure 13) was taken.

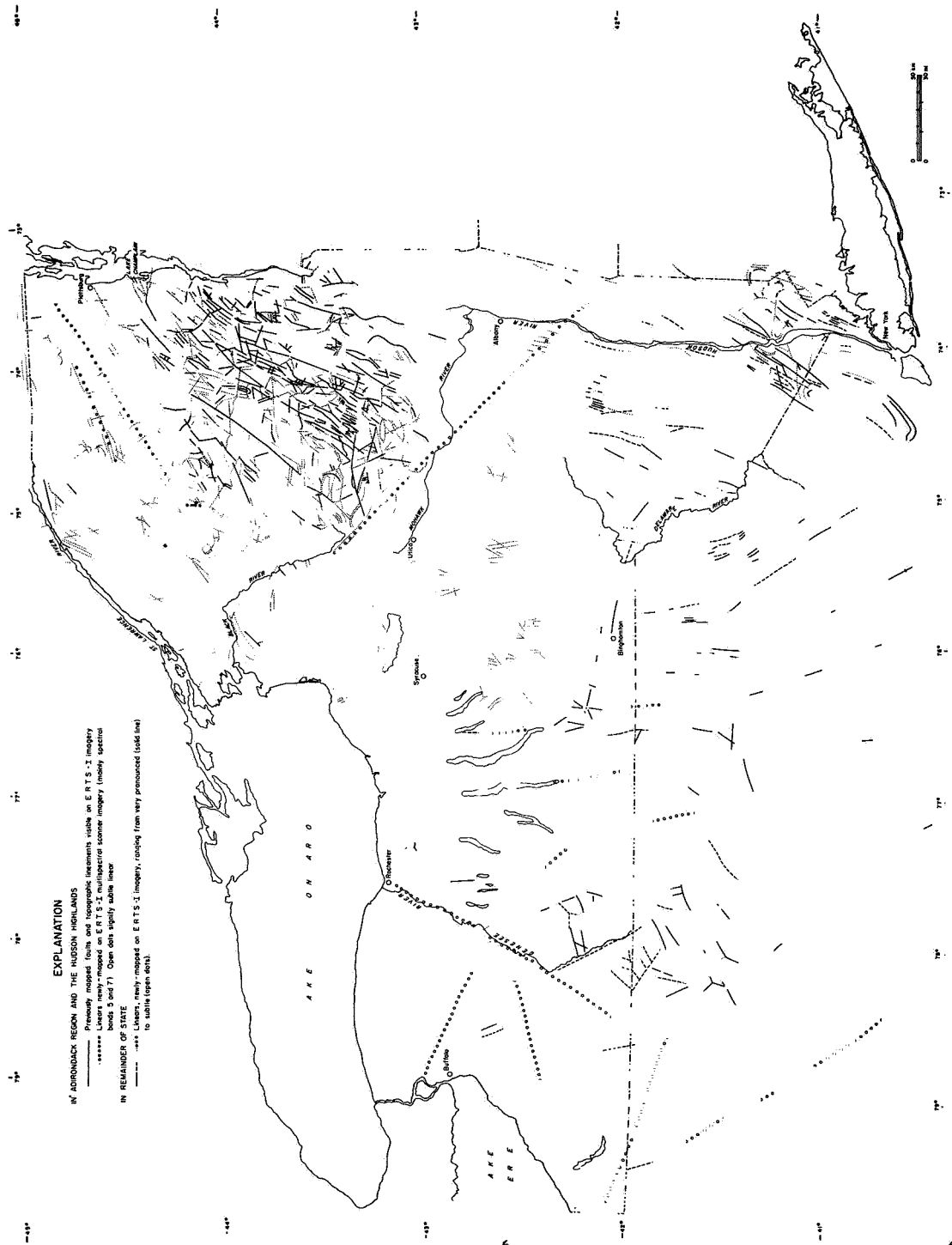


Figure 5. Stage II work map of ERTS-I anomalies mapped at 1:1,000,000.

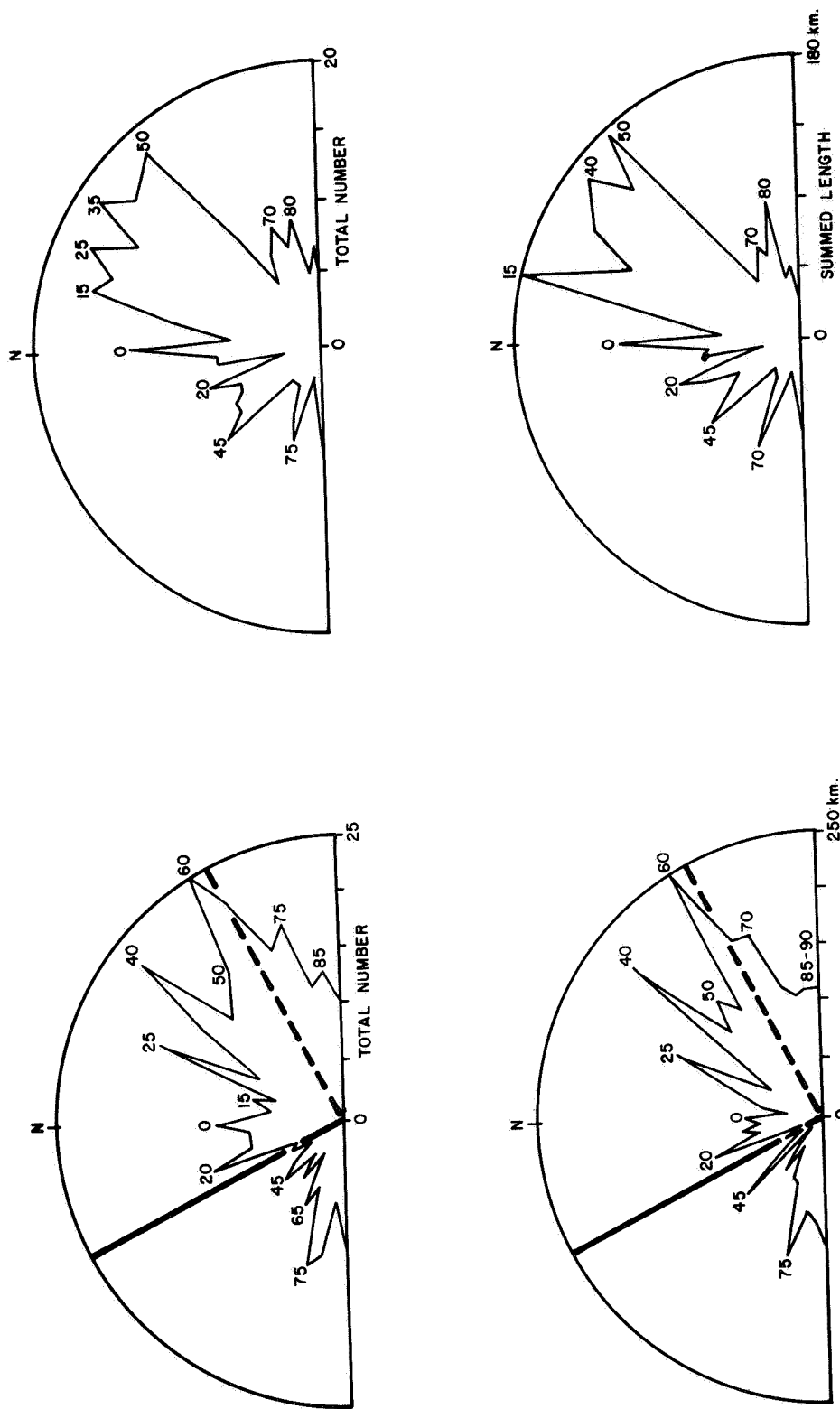


Figure 6. Rose diagram of ERTS-I anomalies, i.e. features which have survived Stage II analysis, in the Adirondack region, with data lumped into 5 degree intervals. Upper diagram is a plot of total number of linear features (364), whereas lower diagram sums total lengths. Curved lines were arbitrarily excluded.

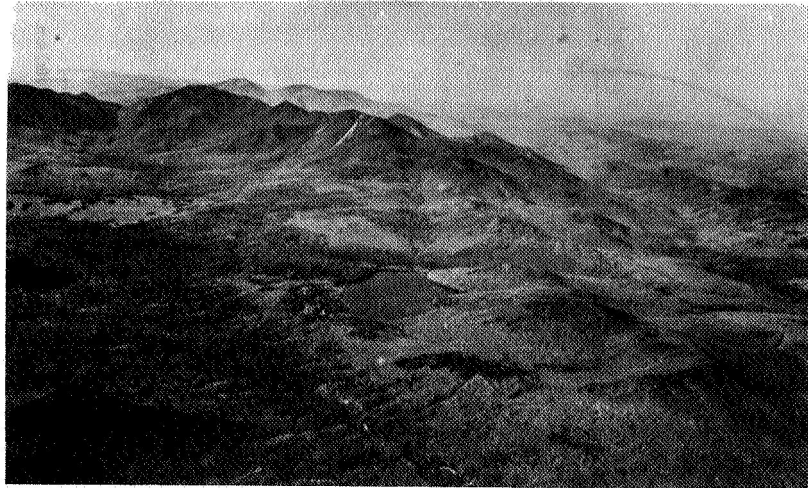


Figure 8. ERTS-I linear (no. 291), shown here to be a topographic lineament. It strikes N43E and extends in both directions across Clear Pond in the foreground. View is northerly. The mountain peaks west of the linear are McComb (with slide), Hough (sharp peak), Dix, and the valley of Hunters Pass. Hunters Pass is part of a previously-mapped topographic lineament 25 km in length which extends across Elk Lake in the middleground. All bedrock in clear view is metamorphosed anorthosite. Mt. Marcy 15' quadrangle. See Figure 3 for site of photograph on ERTS-I imagery.



Figure 9. Central and upper portion of linear shown in Figure 8. Topographic expression is slightly enhanced by the contrast between deciduous trees in the valley and conifers plus rock outcrop along the ridge.



Figure 10. View of Avalanche Lake topographic lineament, a previously-mapped feature, looking south. Avalanche Lake is in shadow at the base of Mt. Calden. Entire terrane except hazy background is located within Marcy Massif metanorthosite; Mt. Marcy 15' quadrangle. See Figure 3 for location on ERTS-I image.

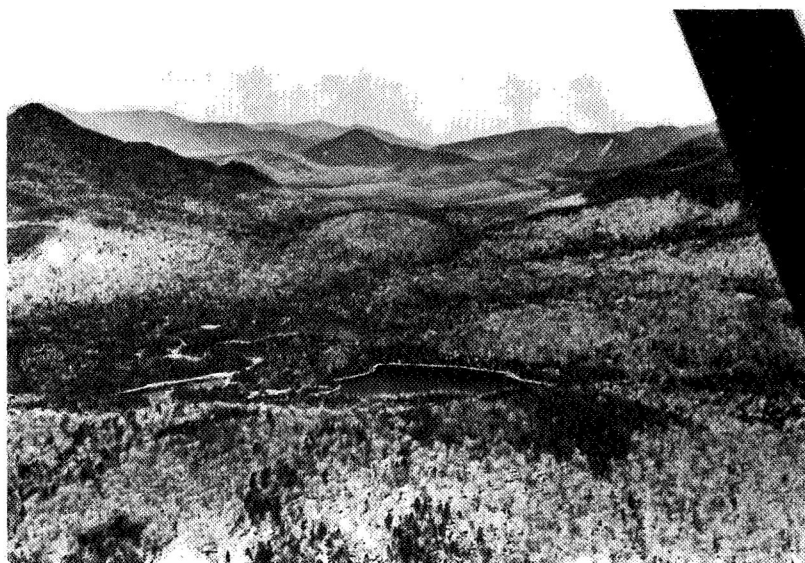


Figure 11. ERTS-I linear no. 287, extending N52W from White Lily Pond; entirely within Marcy Massif metanorthosite; Mt. Marcy and Santanoni 15' quadrangles.

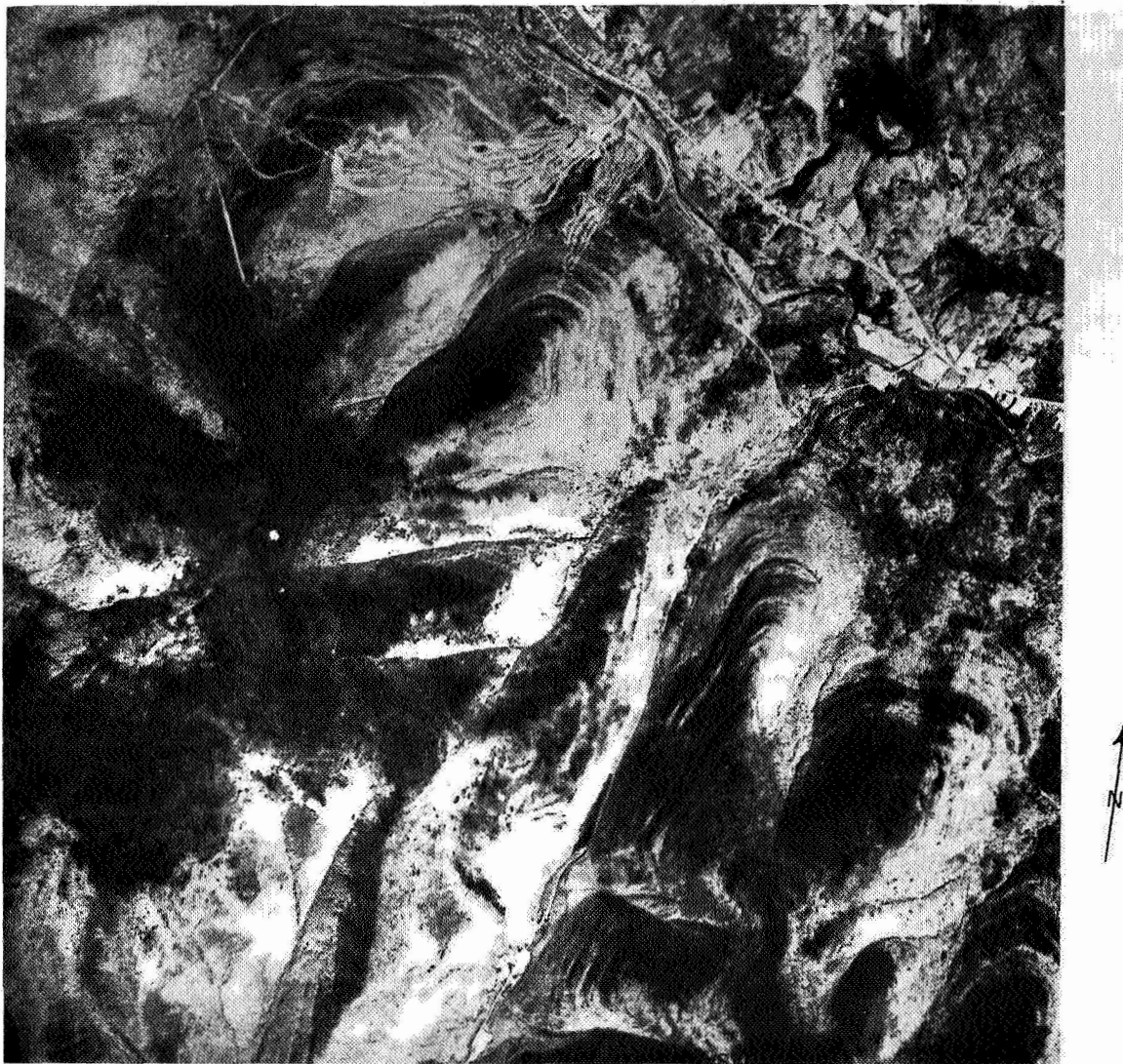


Figure 12. Print from color transparency aerial photograph over the eastern Catskill Mountains. Stony Clove topographic lineament extends about N15E from south center of photo; Hunter Mountain ski area is near north edge of photo. Note pair of N75E topographic linears. Photo by NASA, 30 Apr 73. For site of Stony Clove lineament on ERTS-I imagery, see Figure 4.

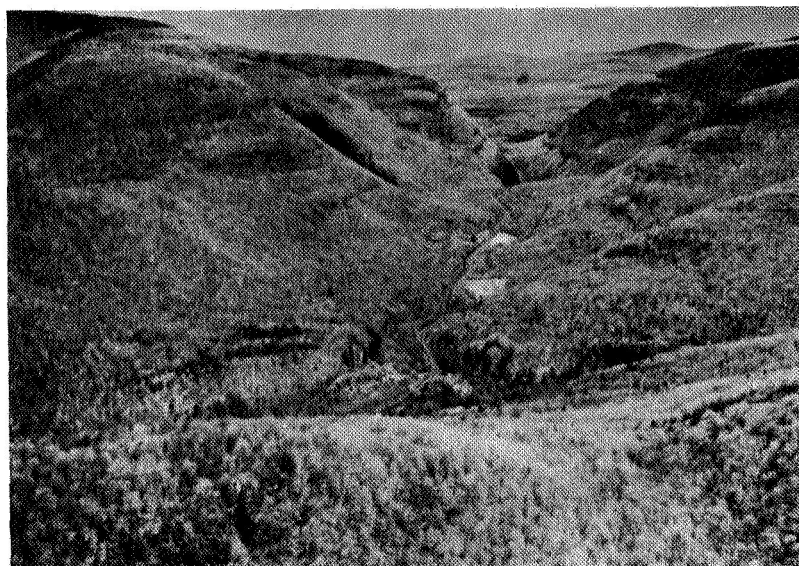


Figure 13. Stony Clove topographic lineament, looking N15E over Edgewood (hidden behind hill in foreground), with drainage divide at Clove in middleground; Hunter 7½' quadrangle. From color-infrared photo. See Figure 4 for location on ERTS-I image.



Figure 14. Stony Clove drainage divide of Figure 13, showing possible vertical offset of the resistant Stony Clove sandstones of the Upper Devonian Lower Walton Formation.

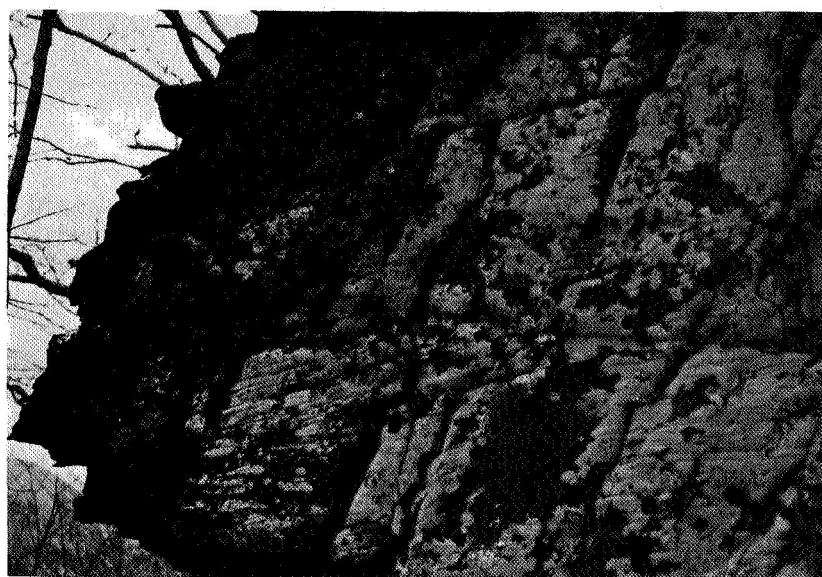


Figure 15. Cross-bedded sandstone unit along east wall of Stony Clove, looking north, showing dominance of westward-dipping joint set which parallels valley. Note conjugate joints at east side of outcrop; dips are 75° east and 73° west, making an acute angle of 32° .

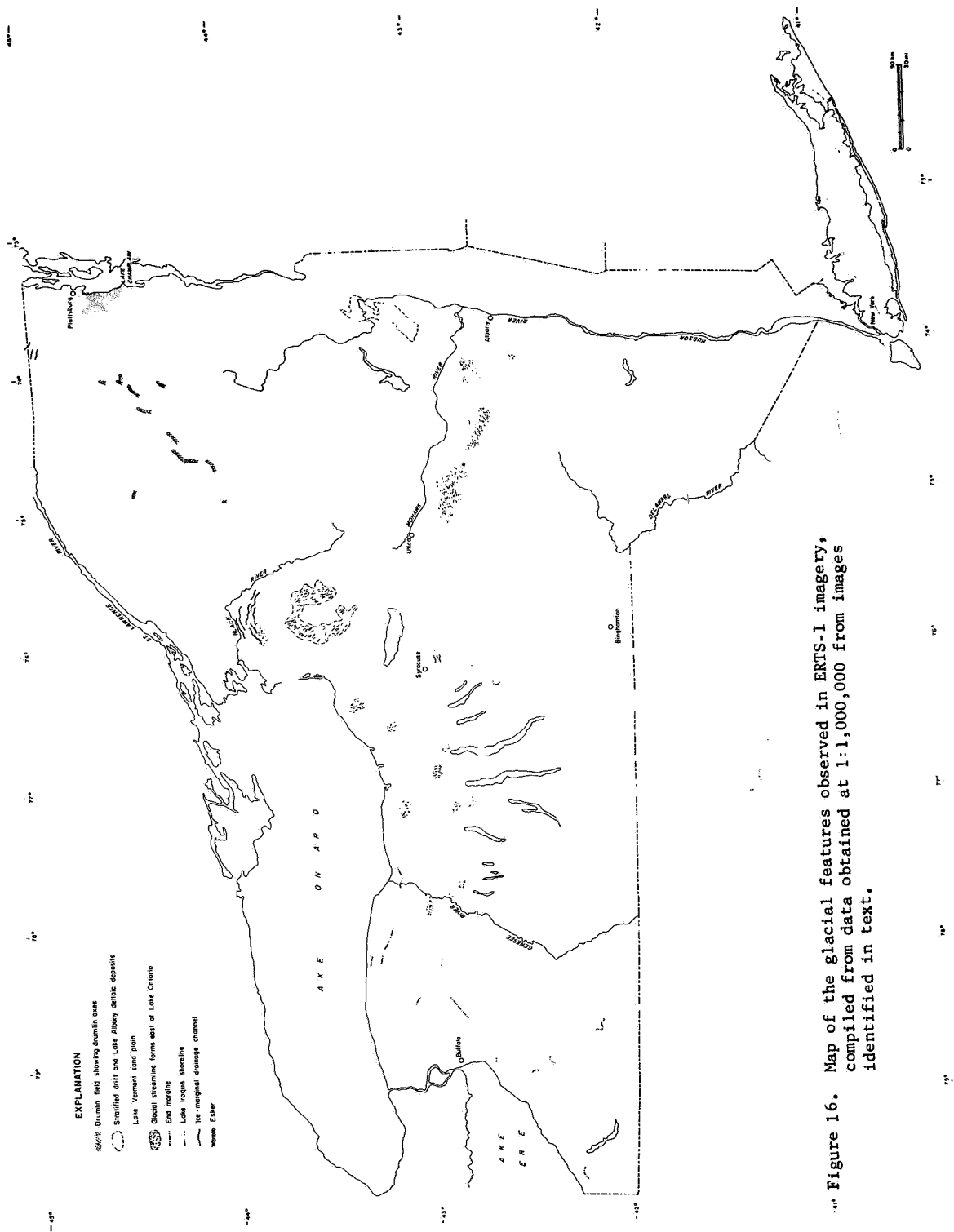


Figure 16. Map of the glacial features observed in ERTS-1 imagery, compiled from data obtained at 1:1,000,000 from images identified in text.

GEOLOGIC APPLICATIONS OF ERTS IMAGES ON THE COLORADO PLATEAU, ARIZONA

Alexander F. H. Goetz and Fred C. Billingsley, (*Jet Propulsion Laboratory, Pasadena, California*);
Donald P. Elston and Ivo Lucchitta, (*U.S. Geological Survey, Flagstaff, Arizona*); and Eugene M.
Shoemaker, (*California Institute of Technology, Pasadena, California*)

ABSTRACT

Three areas in central and northern Arizona centered on the 1) Verde Valley, 2) Coconino Plateau, and 3) Shivwits Plateau were studied using ERTS photography. Image enhancement techniques were developed to extract the most useful subsets from the digital tape images in each area. The value of color combined ratio images for geologic mapping was tested. Extensive new field mapping was completed on the Shivwits and Coconino Plateaus.

Useful applications results include: 1) Upgrading of the existing state geologic map of the Verde Valley region; 2) Detection of long NW trending lineaments in the basalt cap SE of Flagstaff which may be favorable locations for drilling for new water supplies; 3) Tracing of the Bright Angel and Butte faults to twice their previously known length and correlating the extensions with modern seismic events, showing these faults to be present-day earthquake hazards; 4) Discovering and successfully drilling perched sandstone aquifers in the Kaibab Limestone on the Coconino Plateau; 5) Determining the relationship between the Shivwits lavas and the formation of the lower Grand Canyon and showing that the lavas should be an excellent aquifer, as yet untapped.

This paper presents the results of one phase of research carried out at the Jet Propulsion Laboratory, California Institute of Technology, under Contract No. NAS 7-100, sponsored by the National Aeronautics and Space Administration.

74 30755

PRECEDING PAGE BLANK NOT FILMED

INTRODUCTION

Three regions having a combined area of approximately 30,000 sq. km have been mapped using ERTS photography. Work was carried out on the Shivwits Plateau, Coconino Plateau and in the Verde Valley area, marked as A, B and D respectively in Fig. 1.

Standard NDPF products, 1:200,000 and 1:125,000 scale enlargements, as well as computer enhanced digital tapes, were used. Several types of computer processing were applied to the images and each was evaluated for the type of application encountered. The applications discussed below were derived, in some cases serendipitously, through the process of regional geologic mapping at ERTS scales. The synoptic view provided the key to the results discussed below.

VERDE VALLEY

The north-central Arizona test site was chosen originally because of the good geologic map coverage and, therefore, as an area in which automatic mapping methods based on spectral reflectivity could be tested. This test site includes areas that have been mapped in detail at 1:48,000 and 1:62,500 scale. However, a large part of the area has only been mapped in reconnaissance at 1:375,000 scale for the Geologic Map of the State of Arizona (1969); published at 1:500,000 scale. A part of the state geologic map that includes the north-central Arizona test site is shown, without explanation, in Fig. 2.

Geologic Map

The ERTS-1 images allow details of the distribution of several of the geologic units to be improved with respect to the state geologic map. The images, employed with the detailed geologic maps, led to the identification of the units that are shown in Figs. 3a and 3b. The legend is given in Fig. 3c. The product is a regional geologic map referenced to a near-orthographic photo-base. Geologic detail is degraded with respect to standard geologic quadrangle maps, but is improved with respect to areas that only have been mapped in reconnaissance. A geologic map referenced to an orthogonal photo-base allows relations of geologic units to physiographic, vegetational and structural characteristics if the terrain to be evaluated from a single display. Transfer of the planimetric geology to a topographic base allows complementary analysis using standard techniques.

Basalt of late Tertiary age was easily discriminated on the ERTS images, but, not unexpectedly, appeared similar to gabbro of Precambrian age. A tuff-bearing area in a basaltic flow sequence was identified and mapped in the southeastern part of the map area. Such features are not represented on the state map. Quaternary and Tertiary sediments overlie and underlie the Tertiary basalts, and were mapped with fair ease. Details of their distribution were improved with respect to the state map. However, details of the stratigraphy in the paleozoic rocks could not be resolved, although the red Supai Formation of Pennsylvanian and Permian age was apparent on

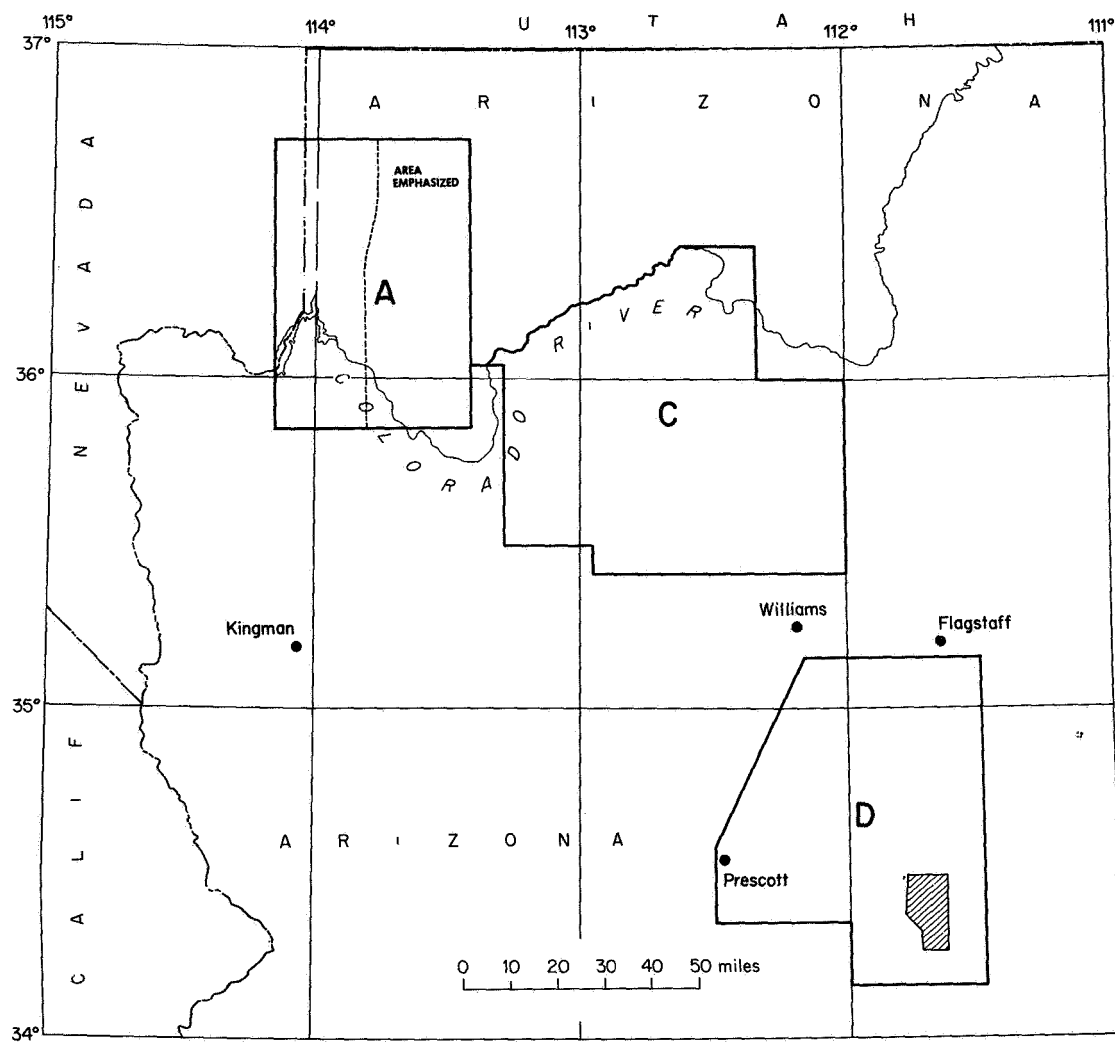


Figure I. Location map showing areas in which ERTS work was carried out, as discussed in this paper.

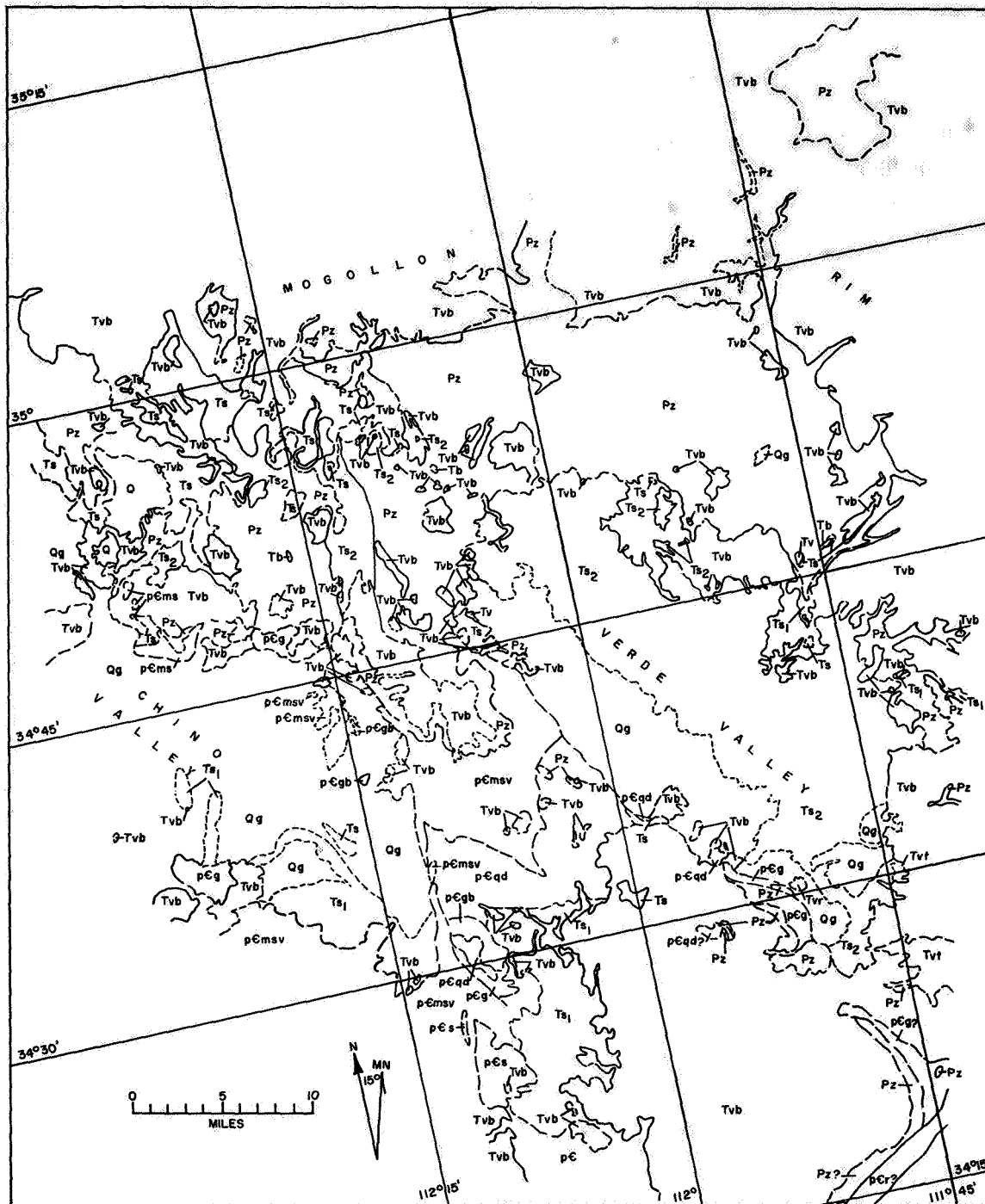


Figure 3a. Geologic map of north-central Arizona compiled from published and unpublished information on ERTS-I photobase. Legend is given in Figure 3c.

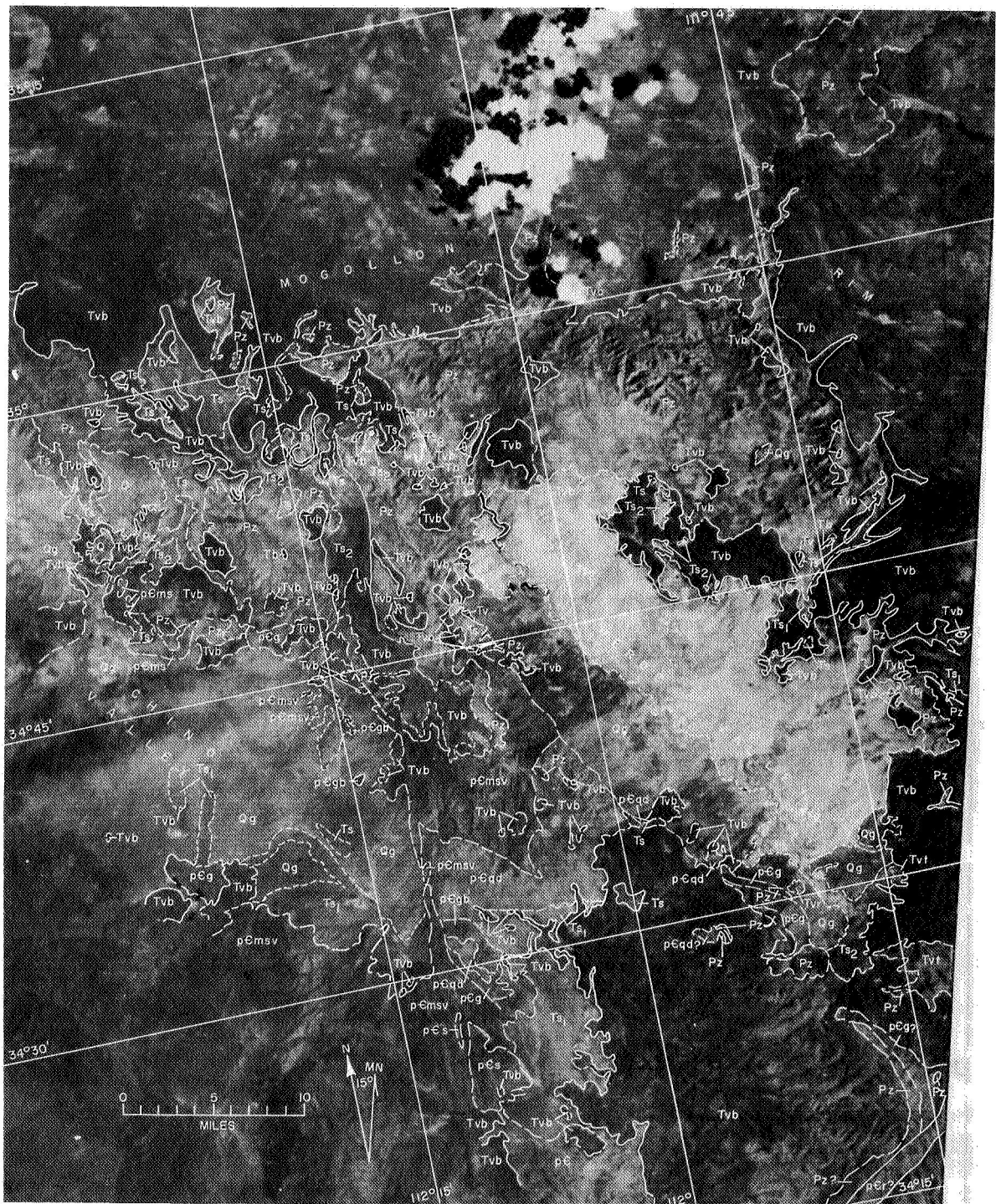


Figure 3b. Geologic map of north-central Arizona compiled on frame EI014-I7375 photobase from published and unpublished information. Legend in Figure 3c.

EXPLANATION

Sedimentary Rocks

Metamorphic Rocks

Igneous Rocks

Quaternary

Qg

Gravel and alluvium

Tertiary

Ts₂

Sandstone and lake beds

TS_1

Sandstone

Paleozoic

Pz

Sandstone and limestone,
undivided

Precambrian

p€ms

Quartzite

Volcanic Rocks

Tvb

Tvt

Basalt
Tuff

pEqd

 $p \in g$

Quartz diorite
and granite

per

Rhyolite

pEgb

Gabbro

pEmSV

Metasedimentary
and metavolcanic rocks

Contact. Dashed where approximately located; short dashed where indefinite

Fault and Lineament map:

Fault; from published geologic maps. Bar and Ball on downthrown side. Dashed where approximately located dotted where concealed.

Lineament Long traces reflect strongly developed trends, some of which are inferred to be faults. Intermediate and short dashed lines reflect degree of traceability of individual lineaments; dots reflect an alignment of one or more vague linear features.

Figure 3c. Legend for Figures 3 and 4.

false color composites of the multispectral images. As a consequence, all Paleozoic rocks were mapped as one unit. In this respect, the state geologic map is far superior. In contrast, more Precambrian units could be identified in the ERTS images than are shown on the state geologic map, and for the older rocks the ERTS "photogeologic" map is an improvement. We conclude that ERTS images at ~ 1:200,000 scale, employed with conventional photogeologic and field geologic techniques, can lead to improved geologic reconnaissance maps.

Fault and Lineament Map

The most striking geologic aspect of the ERTS images is the synoptic view they provide of fracture and lineament patterns that occur in basement rocks and in surficial deposits that mask the bedrock and basement. Faults and lineaments in north-central Arizona are shown on Figures 4a and 4b. The faults are from published maps. In a number of cases, the trace of a fault was less clear than the trace of nearby lineaments. Faults are shown as heavy lines on Figure 4 merely to allow them to be distinguished from the lineaments in this black-and-white illustration.

The north-central Arizona test site lies within the structural boundary of the Colorado Plateau Province, and only comparatively simple high angle normal or gravity faults displace the Paleozoic and Tertiary rocks. Thus, where Precambrian rocks are exposed, the structure that is seen principally reflects structure of Precambrian age. The dominant Precambrian lineament systems trend north, northeast and east. The north- and northeast-trending systems are strongly developed. In contrast, northwest-trending faults and lineaments mainly appear to reflect comparatively recent structural adjustments in the Tertiary, and they are subdued with respect to the Precambrian systems. However, the Precambrian structural grain has been imparted to the younger Phanerozoic rocks, and the major lineament systems have been sites of renewed structural adjustments. The Oak Creek fault in the northeast part of the map area, which is seen to displace only Paleozoic and Tertiary rocks, almost certainly overlies a north-trending fracture system in the basement, analogous to the Shylock fault one in the south-central part of the map area. Similarly, northeast-trending lineament systems occur near Williams, Arizona, in the northern part of the map area (35° 45'N, 112° 12'W). Eruptive centers of the late Tertiary San Francisco volcanic field in the Colorado Plateau are localized along these lineaments. Presumably, northeast-trending Precambrian fractures, analogous to the Chaparral and Spud faults in the southern part of the map area, underlie parts of the Plateau.

A myriad of fractures and lineaments occur in the Sedona area, west of the Oak Creek fault. ERTS images have revealed the existence of strongly developed east- and northeast-trending lineaments. Their existence apparently has led to the development of the erosional embayment in the margin of the Plateau here. Fracture systems in the Sedona area are currently being mapped in detail using NASA high altitude aircraft photographs in a first order photogrammetric plotter (Analytic Plotter Coordinograph). The photogrammetric analysis is being supplemented by geologic field mapping to produce ground truth data for comparative evaluations. Lineaments that have been plotted



Figure 4a. Fault and lineament map of north-central Arizona. Faults compiled from published information. Lineaments are from monoscopic and stereoscopic analysis of EIOT4-I7375.



Figure 4b. Fault and lineament map from Figure 4a combined with EIOI4-I7375-7.

from ERTS images, and lineaments that are to be plotted from Skylab images, will be referenced to the detailed map information. This geologic work in the Sedona area also has the practical objective of defining areas structurally favorable for the localization of ground water resources in an area of burgeoning population growth. This project is being carried out in close cooperation with the Water Resources Division of the USGS, Tucson as a part of their search for water in this area. Targets for future exploration of ground water are places where ancient and concealed karst (limestone cavern) ground in the Mississippian Redwall Limestone is intersected by through-going fracture systems at structurally favorable elevations, giving rise to potential underground 'rivers.'

On the plateau itself a set of northwest trending lineaments, seen on Fig. 4b near $35^{\circ}05'N$, $111^{\circ}40'W$, may also point to a favorable target for drilling for water in the Redwall Limestone approximately 700 m below the basalt cap. The lineaments have been provided to the City of Flagstaff and have been transferred to the city's working map. This map is being used for intermediate and long range planning for the development of Flagstaff's water resources.

Computer Enhancements

A number of types of enhancements were carried out using the digital data. The techniques are described in detail by Goetz and Billingsley (1973) elsewhere in these Proceedings. The most useful technique proved to be the simplest and least time consuming. Bands 4, 5 and 7 were contrast stretched by expanding the data to fill the dynamic range of the recording film. The color composites made from these stretched transparencies provided more information than any single band image. They also provided more than could be obtained from more sophisticated enhancements such as color ratio composites, and automatic classification routines. This result is due to the fact that most of the mapped units have strong absolute reflectivity differences in all bands, and a method such as ratioing which does not make use of the absolute brightness information fails.

COCONINO PLATEAU

Two specific problems and associated applications of the ERTS images evolved from the regional geologic mapping of the Coconino Plateau in the area shown in Figure 5. These applications are associated with faulting and the discovery of shallow, perched aquifers.

Faulting

Study of the low sun angle ERTS image of the Coconino Plateau (Fig. 6) revealed numerous faults in this previously, poorly mapped region (Fig. 7). In particular two parallel northeast-trending systems of normal faults, each of which can be traced at least 150 km, are seen. Many eruptive centers appear to be localized along these fault systems or along their extensions.

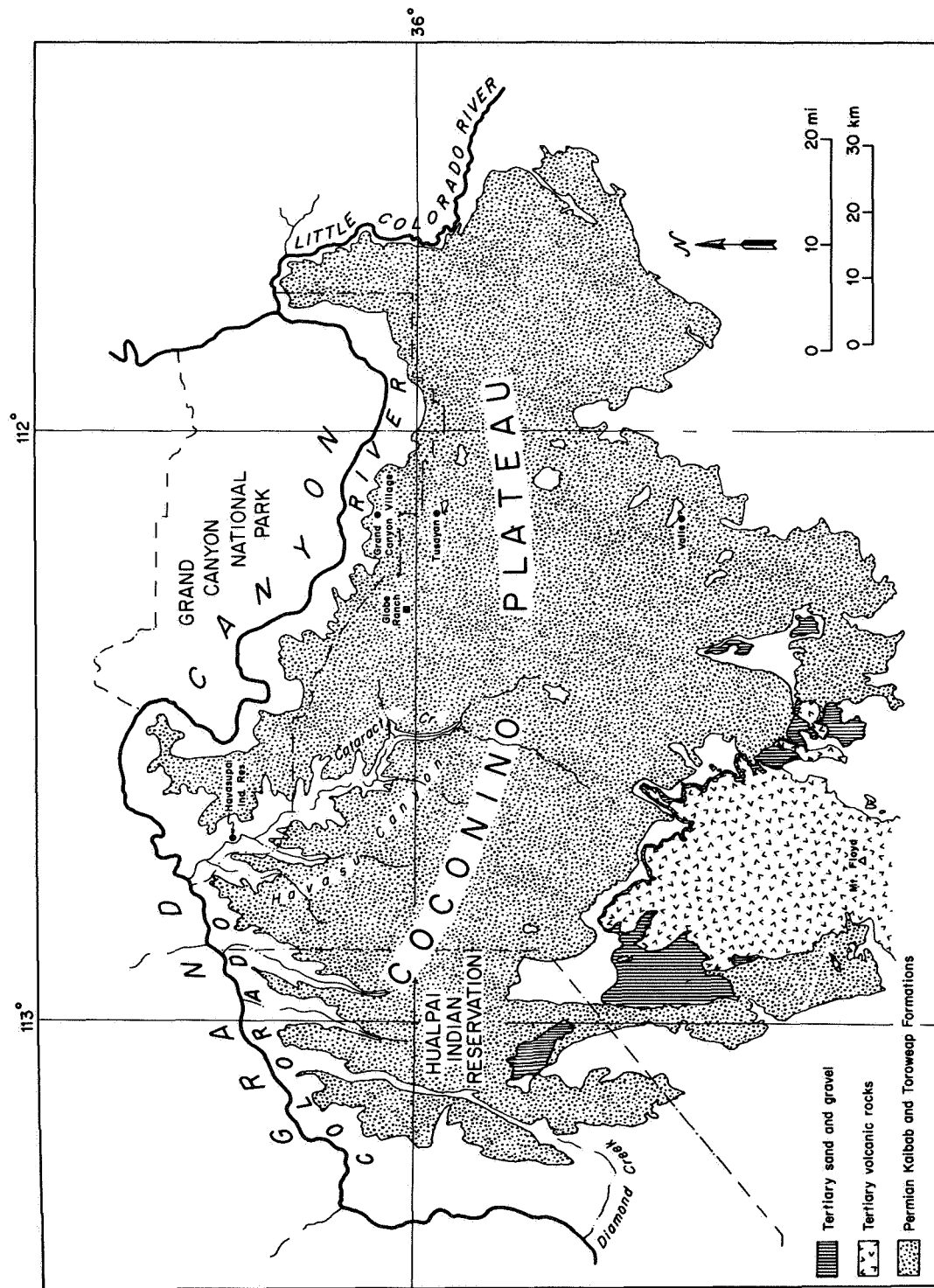


Figure 5. Simplified geologic map of the Coconino Plateau, Arizona.

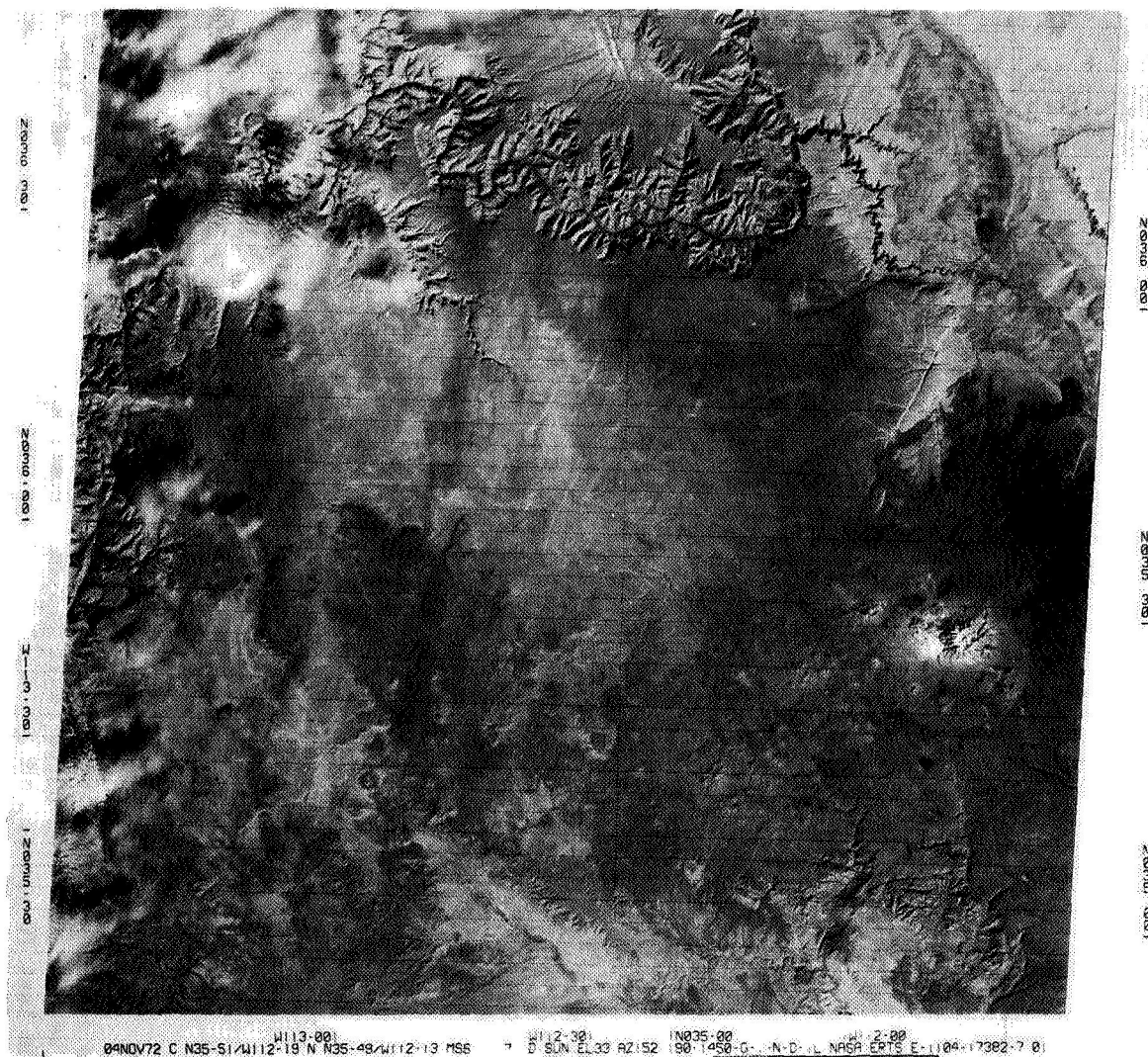


Figure 6. Frame II04-I7382-7 showing Coconino Plateau and Grand Canyon.

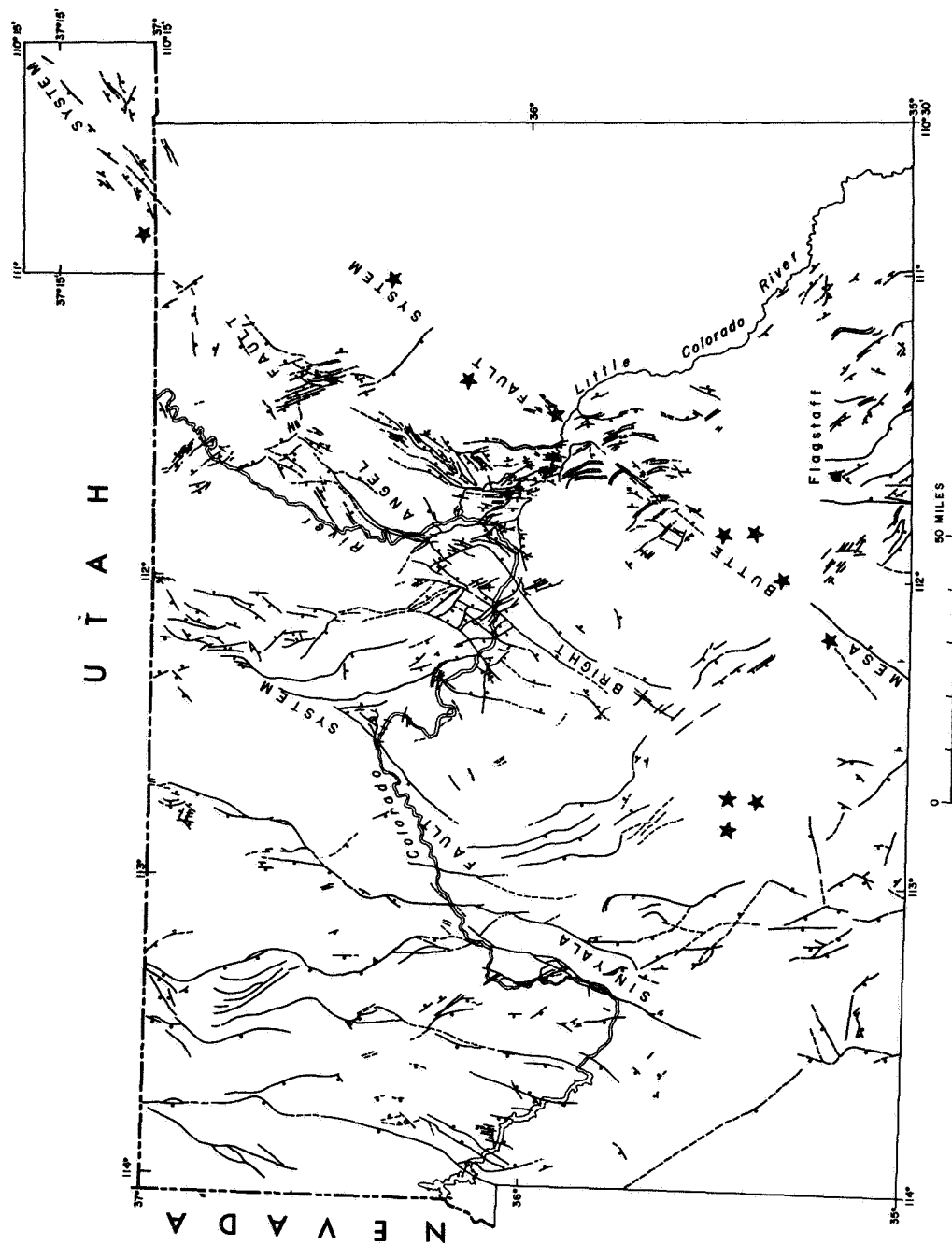


Figure 7. Faults compiled from existing publications and new faults seen on ERTS mainly south of the Grand Canyon and west of the Mesa Butte Fault System. Stars are epicenters of magnitude 4 or greater earthquakes in the last 10 years.

The faults are chiefly observed in Phanerozoic rocks and have minor displacement, but are interpreted by us to reflect fault zones of major displacement in the crystalline Precambrian basement.

The Bright Angel fault system extends as a continuous zone of normal faults from Cataract Creek on the southwest to the Echo Cliffs on the northeast. Beyond the Echo Cliffs, the system continues northeastward, to the vicinity of Monument Valley, as a more diffuse, discontinuous zone of normal faults. The Navajo Mountain intrusive center lies along the discontinuous part of the system. Three major intrusive centers of the Mount Floyd volcanic field lie on the southwestern projection of the Bright Angel fault system. The Bright Angel fault and the Eminence fault are among the larger previously mapped individual members of the total system. If the eruptive centers are included as part of the recognizable structural system, the Bright Angel system has a total known length of 175 miles.

The Mesa Butte fault system, as now recognized, extends from the Tonto Rim on the southwest to Shadow Mountain on the northeast. Bill Williams Mountain, Sitgreaves Peak, and Kendrick Peak are principal calc-alkaline eruptive centers of the San Franciscan volcanic field that appear to be localized along the fault system. Red Mountain, Mesa Butte, and Shadow Mountain are prominent basaltic eruptive centers along the system, and the monchiquite diatremes at Tube and Wildcat Peak lie on the northeast projection of the fault system. The total distance from the Tonto Rim to Wildcat Peak is about 180 km.

Comparison of the Bright Angel and Mesa Butte fault systems with the residual aeromagnetic map of Arizona (Sauk and Sumner, 1970) reveals a close correspondence between the positions of the observed relatively minor normal faults and the margins of a series of large northeast-trending magnetic anomalies. Perhaps the most noteworthy feature of the aeromagnetic map is a 400 km-long northeast-trending belt of large positive aeromagnetic anomalies that extends from the vicinity of Congress Junction to the northern border of Arizona. The Mesa Butte fault lies along the southeast margin of this anomaly belt. Another large positive anomaly, bounded on the southeast by the Bright Angel fault, corresponds to a sequence of metamorphosed basic volcanic rocks (Brahma Schist of Maxson 1961), where the crystalline Precambrian is exposed in the Grand Canyon. Precambrian displacement on the Bright Angel fault was described by Maxson (1961), where the Precambrian rocks are exposed. We believe that most of the large positive aeromagnetic anomalies along the Bright Angel and Mesa Butte fault systems probably correspond to bodies of basic metavolcanic rocks in the crystalline basement complex which have been offset along two major and perhaps several minor faults of Precambrian age. The normal faults that displace the overlying Phanerozoic rocks have been formed by renewed movement along these ancient fault zones, in response to dilation of the crust from late Tertiary time to the present.

The ancient fault zones are inferred to be present along these ancient fault zones, in response to dilation of the crust from late Tertiary time to the present.

The ancient fault zones inferred to be present along the Bright Angel and Mesa Butte fault systems may be related in origin to the Shylock fault zone and Chaparral fault described by Anderson (1967) in central Arizona. Both the Shylock fault zone and the Chaparral fault have right-lateral trans-current displacement. As shown by Anderson, the Shylock zone has a probable minimum horizontal displacement of five miles. A large contrast in the magnetic properties of the rocks on opposite sides of the fault zone, indicated by the aeromagnetic map, suggests the displacement may be several tens of miles or more. Comparably large right-lateral displacements may have occurred along the ancestral Bright Angel and Mesa Butte fault zones.

The location of epicenters of recent earthquakes, shown with stars in Fig. 7, and reports of earthquakes by residents in the region suggest that the Bright Angel and Mesa Butte fault systems are currently active. In 1912 an earthquake of intensity X (?) on the Rossi-Forel scale may have occurred on the Mesa Butte fault system.

Computer Enhancements

Figure 8 demonstrates a method for increasing the contrast greatly to enhance structural patterns. Figure 8a is an image of the relatively featureless Coconino plateau. Figure 8b is an image filtered to enhance the high spatial frequencies at the expense of radiometric accuracy. The origin of the fine NE and NW trending detail is not yet clear, although it may be a manifestation of the sub-resolution jointing pattern. Numerous faults, later mapped on the ground, can be seen in the otherwise featureless bright areas in the center of the image.

Figure 9a is a portion of Figure 6 near Cataract Creek and Havasu Canyon. Although the sun angle is only 33 degrees, the faulting in this region is barely visible. Figure 9b is a black and white rendition of a color combined ratio image, constructed specifically to locate perched sandstone aquifers discussed later. A side effect was to make visible the faulting in this area. The two white streaks in the lower left quadrant of the image are grabens filled with red colored alluvium. Without enhancement these faults are not visible or so faint that they could not be positively identified.

Water Studies

The Coconino Plateau is underlain chiefly by nearly flatlying to gently dipping sedimentary rocks of Paleozoic age. These rocks are locally offset along minor normal faults and along monoclines, structures which are typical of this part of the Colorado Plateau province. The Paleozoic rocks are locally overlain by the Moenkopi Formation of Triassic age and, in the southern part of the Plateau, by alluvial deposits and volcanic rocks of Tertiary and Quaternary age.

The Paleozoic rocks, about 1200 m thick, consist of an alternating sequence of sandstone, shale, and limestone (Fig. 10). These strata have been subdivided into ten mapped formations: The Tapeats Sandstone, Bright Angel Shale, and Muav Limestone, all of Cambrian age; the Temple Butte Limestone of

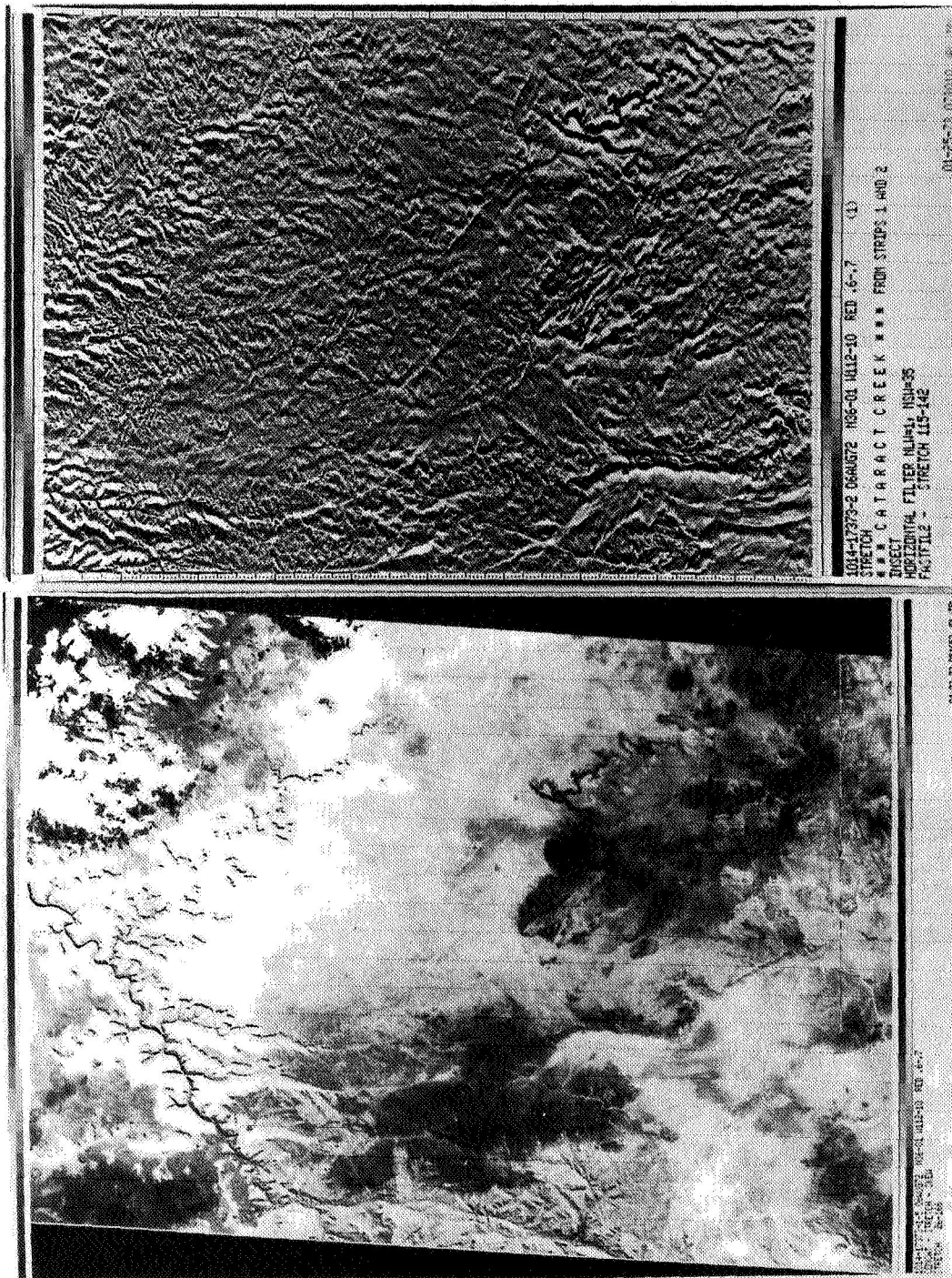


Figure 8a. Coconino Plateau EI014-I7373-5 from digital tape.
 Figure 8b. Spatially filtered version of Figure 8a to enhance linear elements.

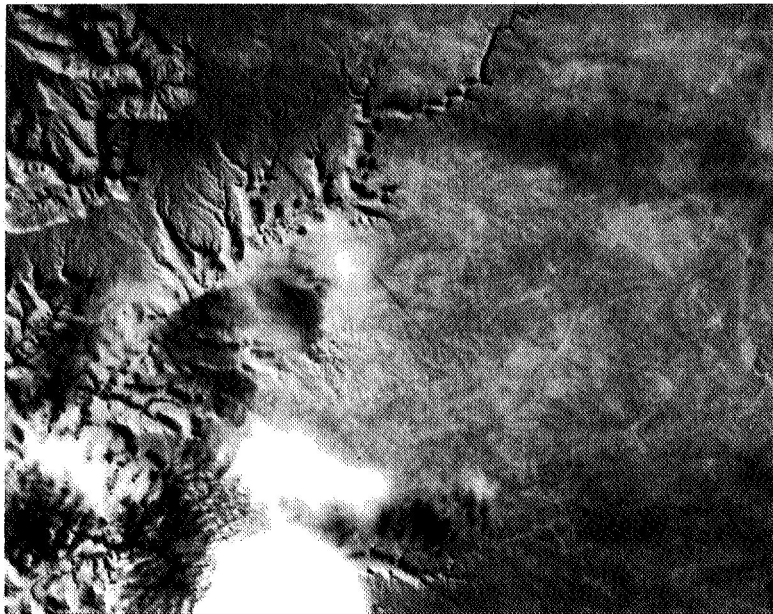


Figure 9a. Portion of frame EII04-I7382-7. Cataract Creek and Havasu Canyon bisects the image.

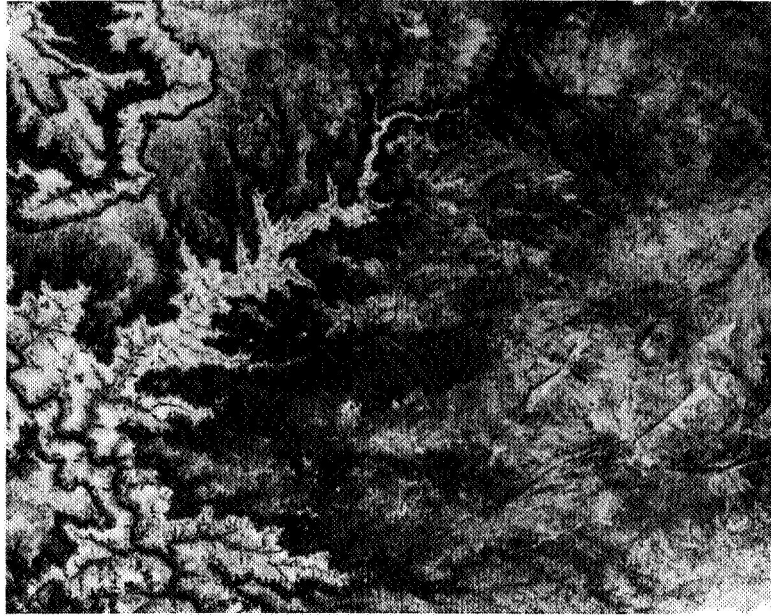


Figure 9b. Black and white print taken from a ratio color composite showing faults identified as white in the lower left quadrant.

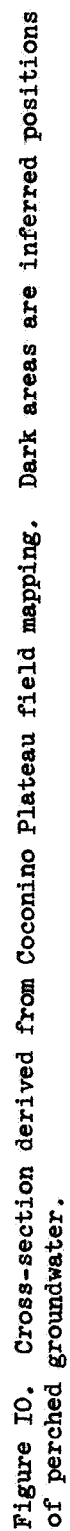
Devonian age; the Redwall Limestone of Mississippian age; the Supai formation of Pennsylvanian and Permian age; and the Hermit Shale, Coconino Sandstone, Toroweap Formation, and Kaibab Limestone, all of Permian age. About two-thirds of the Coconino Plateau is a stripped surface formed on the Kaibab Limestone, the highest Paleozoic unit; the total outcrop area of the Kaibab Limestone is about 8,000 square kilometers (Fig. 5). The older Paleozoic rocks are exposed chiefly in the Grand Canyon and in side canyons tributary to the Grand Canyon.

The Colorado River, at the bottom of Grand Canyon, flows at an elevation of about 1500 meters below the rim at the Coconino Plateau. Because the Canyon is so deep, and because most of the Paleozoic rocks underlying the Coconino Plateau are highly pervious, the water table beneath the Plateau lies at unusually great depth. In a general way, the water table slopes northward, toward the Grand Canyon. It descends from depths between 300 and 450 meters beneath the surface along the southern margin of the Coconino Plateau to depths as great as 900 to 1200 meters beneath the surface along the edge of the Canyon.

Only a small fraction of the annual precipitation on the Coconino Plateau is discharged directly by surface runoff. Most water not lost by evapotranspiration descends rapidly into the subsurface, along fractures and faults, and ultimately reaches the water table. This water is then discharged in two systems of very large springs, one deep in Havasu Canyon and the other deep in the Canyon of the Little Colorado River. The springs in Havasu Canyon are the source of a perennial stream that has sustained the simple agricultural economy of the Havasupai Indians for several centuries. The water issuing from both systems of springs is highly mineralized. A deep well that penetrates the water table south of Valle has shown that the water there is also highly mineralized.

Perched ground water occurs locally at depths much shallower than the water table (Fig. 10). This perched water is a major source of the water currently utilized on the ranches in the region and probably will continue to be a principal source of water produced locally for livestock, and for domestic consumption. The known supplies of perched ground water occur in five aquifers, the Coconino Sandstone, the Alpha Member of the Toroweap Formation, sandstone beds in the Alpha Member of the Kaibab Limestone, Tertiary deposits of alluvial sand and gravel beneath the Mount Floyd volcanic field, and Quaternary alluvium. The water is trapped, in a variety of structural settings above four different aquicludes. Water in the Coconino sandstone is trapped above the Hermit Shale. In the Alpha Member of the Kaibab Formation, water is trapped above claystone, siltstone and tightly cemented sandstone beds within the Kaibab. Important sources of water in Tertiary and Quaternary alluvial deposits are trapped above claystone and siltstone of the Moenkopi Formation.

In our investigation of the Cataract Creek Basin, the Alpha Member of the Kaibab Limestone has been divided into six stratigraphic units that have

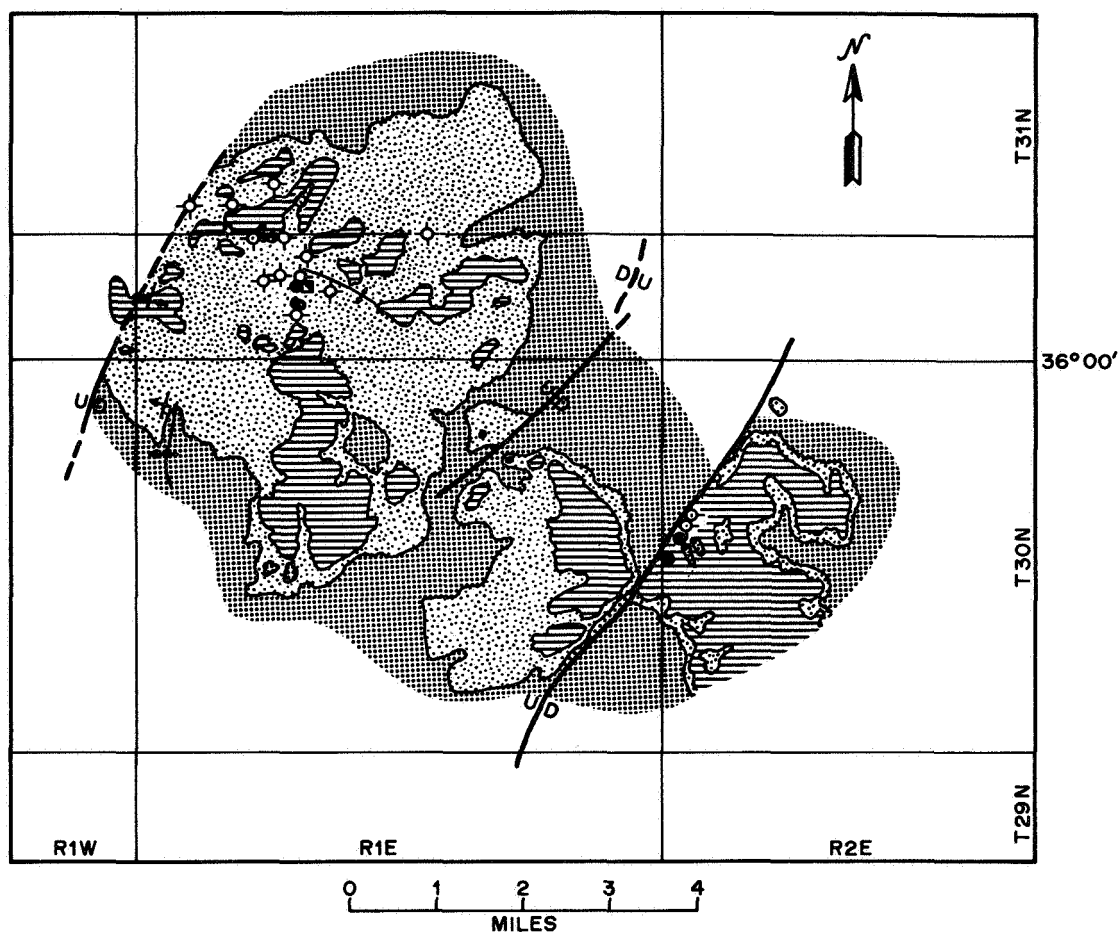


been successfully traced across a major part of the basin. Three of these units consist of limestone. The limestone units are separated by two units of clastic rocks, one of which also contains local deposits of gypsum. A third unit of clastic rocks occurs at the base of the Alpha Member. The limestone units are gray to buff in color and form benches and ledges, whereas the intervening clastic units are typically reddish-brown in color and are slope-forming. In the work to date, we have shown that color ratio ERTS images can be used to discriminate and map individual units within the Alpha Member of the Kaibab. Ratio images, color combined so that the ratios 4/5, 4/6 and 6/7 are produced as blue, green and red respectively, make possible identification of the red sandstone units within the Alpha Member of the Kaibab which can be local perched aquifers.

At the Globe Ranch, near the rim of the Grand Canyon, a small amount of water is produced from a shallow well in a sandstone lens within the Alpha Member of the Kaibab. The sandstone is interbedded with red claystone and siltstone which form an impervious layer beneath the sandstone. The perched water table is only 5 meters beneath the surface at the site of the well. Recharge occurs from local runoff and from direct precipitation on the outcrop belt of the sandstone. This well provided water for the original homestead at the ranch headquarters. Water is currently produced for stock at the rate of about 4,000 liters a week. Similar lenses of sandstone are scattered through the red clastic units of the Alpha Member. Many of these sandstone lenses may be local aquifers, which could constitute an accessible source of ground water for the ranches on the Coconino Plateau.

In order to explore this possibility, the distribution of sandstone in the uppermost unit of clastic rocks in the Kaibab Limestone was mapped over an area of about 130 square kilometers in the vicinity of the Globe Ranch (Fig. 11) as a part of our ERTS-I investigation. This area can be identified readily on the color combined ratio image discussed above. A series of very shallow test holes was then drilled in areas that appeared favorable for recharge of ground water in the sandstone. Two out of eighteen exploratory holes encountered water. The distribution of the water is controlled by variation in the permeability of the clastic rocks as well as by conditions of recharge. The two waterbearing holes are currently being monitored and tested to determine potential production of water from the local sandstone aquifer. The results at this study show that ground water supplies in the Alpha Member of the Kaibab Limestone can be found at depths as shallow as 6 to 15 meters by an inexpensive program of drilling guided by geologic mapping.

Water is so scarce on the Coconino Plateau that the development of even small additional supplies at sites convenient for watering of stock is a matter of importance to the ranching industry. At some ranches, the water obtained from a single existing well is distributed through an expensive system of pipe to strategically located storage tanks and watering tanks. Elsewhere, water is hauled by trucks. In some cases shallow wells that are capable of producing as little as 400 liters of water per day can be and are being utilized. One of the purposes of this investigation is to find additional widely distributed shallow sources of water.



- | | | |
|--|-------------------------------------|----------------------------------|
| | Limestones and shales above aquifer | } Moenkopi and Kaibab Formations |
| | Clastic unit with sandstone aquifer | |
| | Limestones and shales below aquifer | |
| | Fault | |
| | Anticline | |
| | Syncline | |
| | Monocline | |
| | Producing hand dug well | |
| | Test hole, wet | |
| | Test hole, dry | |



Figure II. Simplified geologic map of the Globe Ranch area, Coconino County, Arizona, with test hole locations.

SHIVWITS PLATEAU

The Shivwits Plateau is at the western boundary of the Colorado Plateau in northwesternmost Arizona and is seen in the upper center of Figure 12. The southern edge of the Plateau is marked by the Grand Canyon and the western margin by the Grand Wash Cliffs, which are a fault-line scarp along the Grand Wash fault. The eastern edge is at the Hurricane fault. The exceptional sharpness of the structural boundary between the plateau and the Basin and Range province makes the Shivwits critical for understanding the relations between the two provinces and the history of their common boundary. Because of its proximity to the mouth of the Grand Canyon and to the edge of the Colorado Plateau, the Shivwits Plateau also is very important for understanding the physiographic development of the region in general and the history of the Colorado River in particular. All these characteristics are being used in the present study, which is intended to combine conventional geologic techniques with the special advantages of ERTS photographs. During the course of this study an improved understanding of the geology of the Shivwits Plateau has resulted in practical applications that were not foreseen when the project was started. These applications are discussed below.

Structural Evolution

The Shivwits Plateau and adjacent parts of the Colorado Plateau differ from the Basin and Range terrane to the west in physiography, amount and kind of deformation, crustal properties, and geologic history. Many of these differences go back as far as Paleozoic time. Parallelism of the structural grain of the Plateau with that of the adjacent Basin and Range Province indicates that the two crustal blocks have been subject to the same stress field, but the more subdued deformation of the Plateau indicates that it has behaved as a competent, buttress-like block. Deformation of the Plateau has been controlled by the basement. Fractures in the basement -- some probably very old -- have repetitively localized and focused deformation occurring in response to varied stress fields. Thus, the Laramide compressive field resulted in deformation expressed at the surface by folding and warping; the subsequent extensional stress field related to basin-range deformation resulted in normal faulting along the same lines of weakness. The tectonic map of the western Plateau probably is a map of basement fractures. Shear stresses are reflected by transcurrent faults in the Basin and Range, and by sets of fractures with anomalous trends on the Plateau. These fractures have no transcurrent displacement, but were utilized by block faulting. Intersection of these anomalous fracture sets with the more common north-trending structures seems to have localized the only mineralization of commercial value in the area.

Physiographic Evolution

The physiography of the Shivwits Plateau has been controlled by these factors: (a) ancient uplift and erosion southwest of the present margin of the Plateau; (b) gentle structural dip to the northeast; (c) interlayering of hard and soft strata; (d) faulting; (e) effusion of lava; (f) incision by the Colorado River. These factors have resulted in the following physiographic elements: (a) cuesta scarps formed wherever hard layers lie over soft ones. These scarps originated from the ancient uplift southwest of the Plateau, and



12SEP72 C N36-01/4113-37 N N36-00/4113-31 HSS 7 D SUN EL48 RZ136 190-0711-G-1-N-D-IL NRSR ERTS E-1051-17432-7 81
 14114-30 14113-301 14113-001

Figure I2. Frame EI051-I7432-7 showing the Shivwits Plateau area in the upper center. The Shivwits lava is the dark material trending toward the upper left of the image.

have been retreating northeast down the structural slope; (b) cuesta troughs (strike valleys) at the foot of the cuesta scarps. They trend northwest to north-northwest and have been the major factor in controlling drainage directions; (c) stripped surfaces following particularly resistant strata; (d) erosion surfaces bevelling strata approximately equally resistant to erosion; (e) lava plateaus; (f) canyons. These are a relatively recent and minor, though impressive, element formed in response to incision by the Colorado River; (g) fault scarps produced by relatively recent movement on major faults.

Ancient drainages flowed mostly north-northwest along broad cuesta troughs. These drainages represent the pre-Grand Canyon drainages in northwest Arizona. In part, they may represent an ancient northerly trend of the Colorado River before the river established its westward course through the western Grand Canyon. One of these valleys was followed by the Shivwits lavas, which rest on a surface of low relief that is incompatible with a canyon landscape in the vicinity. If the 6 m.y. radiometric age for the lavas is correct, the western Grand Canyon must have been cut more recently than that date.

Ground Water

Water is extremely scarce on the Shivwits Plateau, and is the single most important factor in controlling the usability of the area. In the course of this study, it has become apparent that the few known shallow water resources on the Shivwits occur where the lavas rest on impermeable shales of the Triassic Moenkopi Formation. The lava is fractured, and serves as an aquifer. Where the lava rests on the Moenkopi Formation, the water percolating through the lava is trapped at the base of the lava, and flows down the axis of the ancient valley that had been partially filled by the lava. Where the lava and the Moenkopi are cut by faults transverse to the old valley, the down-valley flow is interrupted and ground water ponds up on the upstream side of the fault. These are the most favorable places for exploration and development of new shallow-water resources.

Value of ERTS

ERTS photographs have proven indispensable for providing the regional perspective in the Shivwits area, without which it would have been much slower and more difficult -- perhaps even impossible -- to reach an understanding of the structural and physiographic development of the Shivwits Plateau area. Thus, for example, the ERTS photographs have illustrated very clearly the structural grain of the Shivwits Plateau, its relation to the grain of the Basin and Range Province, and the location and alignment of anomalous structural features. In some instances, ERTS photographs have permitted extension of faults that were difficult to map on the ground because of poor exposure or difficult access. ERTS photographs have also pointed out the physiographic grain of the region, the importance of cuesta scarps in controlling drainage, and the relation between lava flows and ancient valleys. It is doubtful that any of these would have been understood without the perspective provided by the photographs. No large scale attempt has yet been made to use computer enhanced images.

SUMMARY

ERTS image data has been applied to three related geological provinces with diverse individual problems. The scale of ERTS has been shown to be valuable for reconnaissance geologic mapping and the synoptic view has proved to be invaluable.

Subtle reflectivity differences among rock units can be detected by computer enhancement techniques. These differences have been shown to be valuable for locating possible perched aquifers on the Coconino Plateau. However, intensive groundwork must be carried out to identify logical points for shallow test drilling in these areas.

Numerous faults and fractures have been identified for the first time. Their relative activity is important for seismic hazard evaluation. The fractures have an important bearing on where the drilling for water in the Flagstaff and Sedona areas should be attempted. The general orientation of this ERTS study toward applications results has been fruitful.

References

- Anderson, C. A. 1967, Precambrian Wrench Fault in Central Arizona; in Geological Survey Research 1967; U. S. Geol. Survey Prof. Paper 575-C, p. C60-C65.
- Goetz, A. F. H. and F. C. Billingsley 1973, Digital Image Enhancement Techniques Used in Some ERTS Application Problems, Proc. 3rd ERTS Symposium, Dec. 10-13, Washington, D. C.
- Maxson, J. S. 1961, Geologic Map of the Bright Angel Quadrangle, Grand Canyon National Park, Arizona: Grand Canyon Nat. History Assoc.
- Sauk, W. A. and J. S. Sumner 1970, Residual Aeromagnetic Map of Arizona: Univ. of Arizona.

ERTS-1, EARTHQUAKES, AND TECTONIC EVOLUTION IN ALASKA

Larry Gedney and James VanWormer, *Geophysical Institute, University of Alaska*

ABSTRACT

In comparing seismicity patterns in Alaska with ERTS-1 imagery, one is struck by the frequency with which earthquake epicenters fall on, or near, lineaments visible on the imagery. Often these lineaments prove to be tectonic faults which have been mapped in the field. But equally as often, existing geologic and tectonic maps show no evidence of these features. The remoteness and inaccessibility of most of Alaska is responsible, in large part, for the inadequacy of the mapping. ERTS-1 imagery is filling a vital need in providing much of the missing information, and is pointing out many areas of potential earthquake hazard. Earthquakes in central and south-central Alaska result when the north-eastern corner of the north Pacific lithospheric plate (roughly enclosed by the great bend in the Alaska Range near Mt. McKinley) underthrusts the continent. North of Mt. McKinley, the seismicity is continental in nature and of shallow origin, with earthquakes occurring on lineaments, and frequently at intersections of lineaments. South of Mt. McKinley, the seismicity is generally deeper and is associated with the subduction of the Pacific plate. The shallower events, however, still tend to align themselves with lineaments visible on the imagery.

* N 74 30756

INTRODUCTION

The recent emergence of plate tectonic theory as a unifying doctrine for the earth sciences is probably the most significant breakthrough of this century in explaining the recent evolution of our planet. The manifestations of sea-floor spreading -- magnetic and heat flow anomalies, oceanic ridges, arc and trench systems, volcanoes, earthquakes -- are explained with a simplicity which earlier workers would have envied. Yet, there are areas in the world which do not submit gracefully to various aspects of the theory. Central Alaska is one of those areas.

Ideally, the north Pacific plate "should" underthrust Alaska along the Aleutian trench east of Kodiak Island and the Kenai Peninsula. Indeed, this was one mechanism which was postulated for the great earthquake of 1964 (c.g., Plafker, 1972, p. 163). As a result of that earthquake, Alaska suddenly became a focal point of interest to seismologists, and the first seismographic nets in the state were established (the U.S.C.G.S. station COL near Fairbanks had been the only permanent installation in the state). With the enhanced seismographic coverage -- particularly from those stations operated by the University of Alaska -- it was possible to locate small earthquakes which had previously gone undetected, and the first clear picture of seismicity in Alaska began to emerge. It is this data which now lead us to claim that the subduction zone at the NE end of the trench-arc system does not lie offshore in the Aleutian trench, but instead

extends up Cook Inlet and along the base of the Alaska Range to a point north of Mt. McKinley. The dipping interface associated with the underthrusting is clearly delineated when one examines the seismic zone in profile (Fig. 1). However, all earthquakes within the state do not occur within the subduction zone. Transmittal of stresses from around the great bend in the Alaska Range (which appears to enclose a corner of the downgoing plate) is the agent most likely responsible for a broad area of shallow seismicity in the Alaskan interior. Thus, continental Alaska can be classified into two regions on the basis of seismicity. The first of these is the area enclosed by the bend of the Alaska Range, in which earthquakes of shallow and intermediate depth (to 250 km) occur. This is separated from the shallow seismic zone of central interior Alaska by the Alaska Range, and by the Denali fault (which trends generally along the mid-line of the range). The Denali fault is therefore a transform fault along which differential movement between continent and oceanic plate is occurring.*

With this knowledge as background, it is now natural to inquire into the question of where earthquakes are likely to occur. Little can be second-guessed on the basis of past experience, because such a short period of reliable data collection has elapsed. It has been our experience that large earthquakes (magnitude 6 or greater) can occur almost randomly in the interior, with no prior warning, and insufficient data have been accumulated to even indicate that such seismic zones might exist. Geologic mapping of the state is in such a preliminary stage that it is a certainty that many seismically active faults have gone unmapped.

Therefore, it was with a great deal of anticipation with which we awaited the first ERTS imagery of this area. We were gratified, indeed, when a first look at the data showed that the larger earthquakes in the state, more often than not, fell on or near lineaments which were clearly visible on the imagery. In most cases these lineaments were not mapped as faults. It therefore appears that ERTS imagery, in the next few years, will prove to be a most important tool in assessing earthquake hazards in areas where existing seismic and geologic data are minimal. This is an especially important matter in Alaska, which will be experiencing an unprecedented rate of growth and expansion now that resource development is so vital an issue to the nation.

South-central Alaska

Figure 2 is a mosaic constructed from 19 ERTS-1 images produced on four consecutive passes of the satellite on November 2,3,4 and 5, 1972. It shows south-central Alaska with Anchorage at the head of Cook Inlet near the right center, the Kenai Peninsula at lower right center, and the Alaska Range curving across the scene from the upper right to the lower left. Several well-known structural elements are readily apparent. Two of these

*The actual situation is not quite this simple. There are some problems with treating the Denali fault as a simple transform, but the matter will not be dealt with in this paper.

are large scale strike-slip faults which are among Alaska's most notable tectonic features. A portion of the Denali fault crosses the scene from upper right to upper left center, and it is roughly paralleled by the Lake Clark fault (which is somewhat less conspicuous) to the south. The solid circles on the key to Fig. 2 represent epicenters of earthquakes which occurred in this area during 1972. They are keyed by number to their respective parameters in Appendix I. Note that these are epicenters of earthquakes which were of magnitude 4 and larger. Many thousands of smaller events were recorded during this time. Most of the earthquakes are seen to occur in the vicinity of Cook Inlet, but it should be noted that this is largely deep-seated seismic activity related to the subduction zone, and it probably does not bear a direct relationship to lineaments which can be seen at the surface. A few earthquakes appear to be associated with the Denali fault, particularly in the vicinity of Mt. McKinley (which is casting the long shadow in the upper left quadrant), and there is an obvious clustering of earthquakes along the Lake Clark fault. Of particular interest, however, are those lineaments which are not geologically mapped as faults, but which could probably be so classified on the basis of ongoing seismicity. Particularly noteworthy are the set of sub-parallel lineaments trending off the Denali fault to the southwest, and the peculiar graben-like structure outlined by the mountains around Anchorage. The 1964 epicenter was very close to earthquakes 34 and 50 on the lineament near the right margin, although it is not clear whether or not this fault could have played a role in that earthquake. Note the extremely sharp escarpment of the Kenai Mountains which passes very close to Anchorage and the association of at least three earthquakes with this apparent fault. Even without the 1964 earthquake, this lineament should have provided Anchorage with the admonition: Build Well! Yet it is not even mapped as a fault.

Central Interior Alaska

Figure 3 is a mosaic of 6 ERTS-1 images collected on 4 and 5 November, 1972. Fairbanks is at right center, the Yukon River enters the scene at the top, the Tanana River crosses from right to left, and the Alaska Range is at bottom right. The scene is to the north of Fig. 2 and the mosaics partially overlap (although they are of different scales). First, faults which have been previously mapped on the ground are shown as solid lines on the key. In general, these are members of the same large scale strike-slip fault system to which the Lake Clark and Denali faults belong. Although not always topographically well-defined, large offsets have occurred along most of these since the Cretaceous. Second, the lineaments indicated by dashed lines appear to be large scale faults which supplement the known set. Included in this category is the northern escarpment of the Alaska Range which appears from the imagery to be a normal fault with considerable vertical displacement, although some workers believe that it is a fold feature. Finally, a very sharp set of conjugate lineaments is shown on the key as dotted lines. These intersect at an angle of about 55° and appear to be the result of compressive stress in an outward direction from around the bend of the Alaska Range. The angle of 55° is roughly the dihedral angle at which most brittle substances would be expected to fracture under compressive stress, with left-lateral offset on one set of fractures, and right-lateral offset on the other. The persistence of these features over large areas implies that they are continuous beneath the alluvium of the Tanana River valley.

The circles on the key relate to epicenters of the largest earthquakes to occur within the mapped area within recent years. The numbers correlate the earthquakes with their respective parameters which are given in Appendix II. It is significant that these have tended to occur at intersections of lineaments visible on the imagery. Focal mechanism studies have shown that the earthquake on the conjugate set of lineaments (number 2) was the result of left-lateral slippage on the prominent north-south trending fault, in agreement with the model proposed above. The Fairbanks earthquake of 1967 (number 1) appears to have been the result of left-lateral slippage on the NE-SW trending lineament -- a perplexing situation and one which indicates that the stress trajectories must curve across the region.

Much of the area of the mosaic will be under development in the years ahead. In particular, the trans-Alaska pipeline will cut across nearly every one of the major lineaments in the northeast quadrant. Since so little is presently known of the seismicity of these areas over long periods of time, we are compelled to regard each of these lineaments (and those in Fig. 2) as being potential sites for future earthquakes, particularly in view of the fact that some of them have produced sizeable events in only the brief period since 1967.

Reference

Plafker, George, Tectonics, The Great Alaska Earthquake of 1964, Seismology and Geodesy, pp. 113-174, Committee on the Alaska Earthquake of the Division of Earth Sciences, National Research Council, National Academy of Sciences, 1972.

APPENDIX I

The following table lists, by number, all the epicenters which are plotted on Fig. 2. All data in the table were produced by the University of Alaska seismology program, except those accompanied by an asterisk (*), for which the National Oceanographic and Atmospheric Administration (NOAA) was the source.

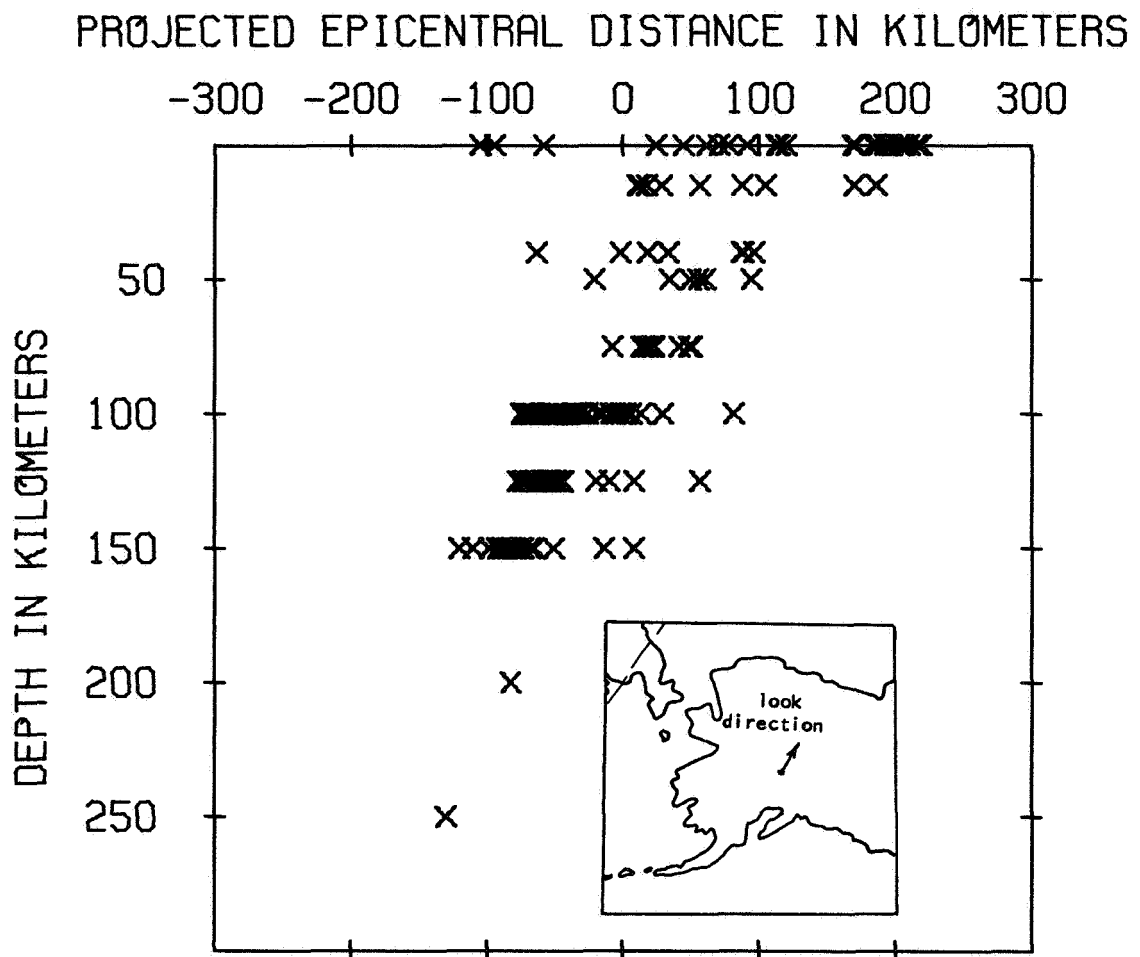
Date (1972)	Latitude (N)	Longitude (W)	Magnitude
1. Jan 2	59.3	153.6	4.4
2. Jan 9	59.5	156.6	4.0
3. Jan 19	59.4	156.9	4.3
4. Jan 24 *	59.6	151.4	4.0
5. Feb 5 *	60.3	153.8	4.6
6. Feb 13 *	59.9	154.2	4.9
7. Feb 16	59.5	152.9	4.3
8. Feb 25	61.3	149.4	4.0
9. Feb 27	59.2	151.6	4.4
10. Feb 29	63.2	150.5	4.0
11. Mar 1 *	59.6	152.8	4.6
12. Mar 7	60.0	155.3	4.0
13. Mar 12 *	64.1	148.4	4.2
14. Mar 12	61.6	147.7	4.0
15. Mar 14	60.8	152.3	4.0
16. Mar 21	60.1	150.3	4.0
17. Mar 23	59.7	153.2	4.3
18. Mar 25	59.8	155.6	4.0
19. Mar 25	59.3	155.3	4.1
20. Mar 28 *	59.8	153.4	4.3
21. Mar 29 *	59.9	153.1	5.1
22. Apr 2 *	59.9	153.6	4.9
23. Apr 5	61.4	151.9	4.0
24. Apr 7 *	60.1	152.8	5.1
25. Apr 9	64.0	150.9	4.5
26. Apr 9	61.6	151.0	4.1
27. Apr 11 *	62.0	150.4	4.2
28. Apr 15	60.8	153.6	4.1
29. Apr 16	63.4	147.6	4.6
30. Apr 16	63.5	147.6	4.1
31. Apr 19	58.7	155.6	4.1
32. Apr 20 *	60.2	152.1	4.7
33. Apr 20 *	59.9	153.6	4.5
34. Apr 25	61.1	147.1	4.0
35. Apr 25 *	62.0	147.8	4.6
36. Apr 28 *	63.6	149.9	4.7
37. May 7	61.1	152.1	4.1
38. May 8	59.6	155.7	4.1
39. May 8	58.8	153.0	4.1
40. May 14	62.4	151.1	4.0
41. May 14	61.8	150.3	4.1
42. May 19	59.6	152.9	4.1

Date (1972)	Latitude (N)	Longitude (W)	Magnitude
43. May 20	59.6	152.9	5.2
44. Jun 1	59.6	155.1	4.0
45. Jun 10	59.1	155.6	4.1
46. Jun 14	61.0	152.5	5.2
47. Jun 16	59.3	152.3	4.2
48. Jun 18	62.6	152.7	4.7
49. Jun 20	59.5	152.7	5.1
50. Jun 22	61.4	147.5	4.6
51. Aug 6	60.0	149.2	4.0
52. Aug 9	58.7	154.5	4.1
53. Aug 12	61.4	149.8	4.0
54. Aug 17	59.4	152.6	4.2
55. Aug 19	59.1	153.3	4.2
56. Aug 22	59.8	152.2	4.1
57. Aug 23	58.4	153.2	5.5
58. Sep 3 *	59.7	149.1	4.7
59. Sep 11 *	59.6	148.9	5.1
60. Oct 1	62.7	149.1	5.2
61. Oct 1	59.8	153.3	4.7
62. Oct 20	60.0	152.4	4.2
63. Oct 21	63.2	151.1	5.4
64. Nov 19	60.9	153.1	4.6
65. Nov 21	62.2	149.7	4.1
66. Nov 22	59.6	152.4	4.1
67. Nov 25	58.6	152.2	4.3
68. Nov 28	59.7	153.5	5.1
69. Dec 3	59.8	154.7	4.0
70. Dec 3	58.6	155.2	4.4
71. Dec 4	59.8	154.8	4.2
72. Dec 15	60.3	151.2	5.0
73. Dec 18	60.8	153.1	5.6
74. Dec 29	61.6	151.3	4.5

APPENDIX II

Listing of earthquakes plotted on Figure 3.

Date	Latitude (N)	Longitude (W)	Magnitude
1. 21 Jun 67	64.8°	147.4°	6.0
2. 29 Oct 68	65.4°	150.0°	6.5
3. 21 Jun 69	65.2°	147.6°	4.6
4. 9 Jun 70	64.9°	148.7°	4.2
5. 15 Aug 72	65.2°	148.7°	5.1



PROJECTION ORIGIN: 62.54N 150.08W
 LIMITING ORIGIN: 62.96N 149.74W
 AZIMUTH OF PROJ PLANE: 20 DEGREES
 NUMBER OF EVENTS PLOTTED: 162 OF 1847

Figure 1

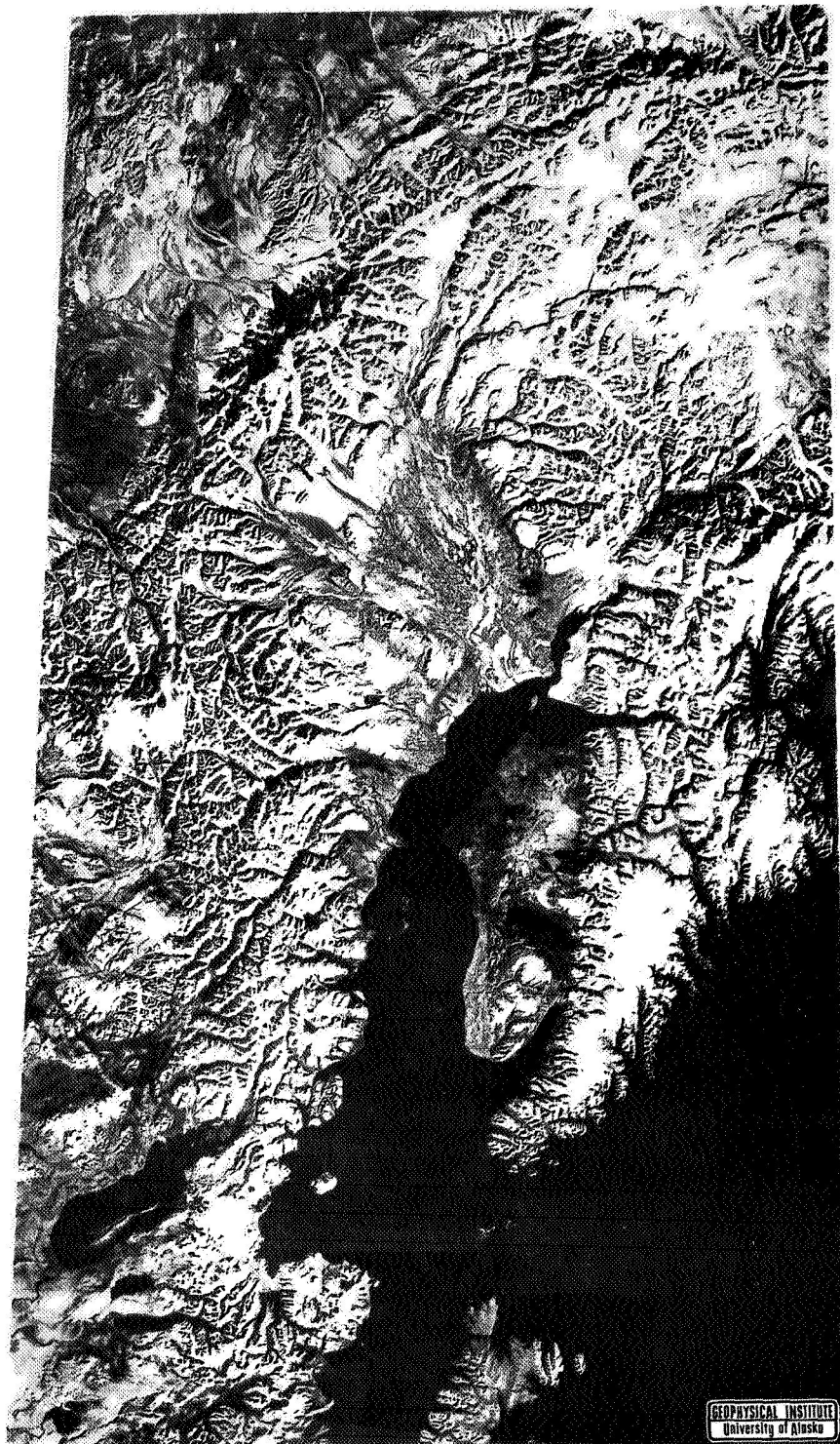


Figure 2

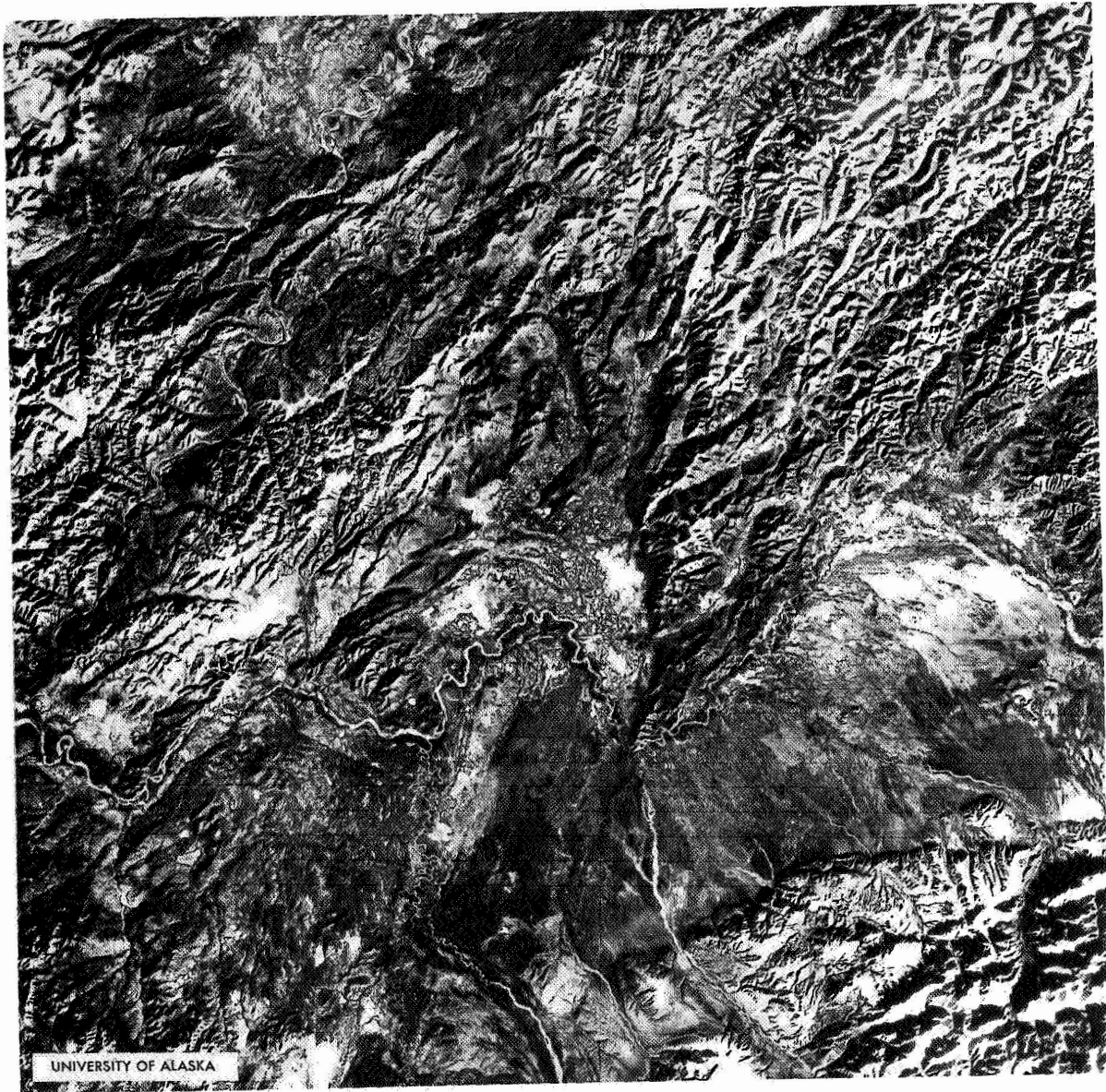
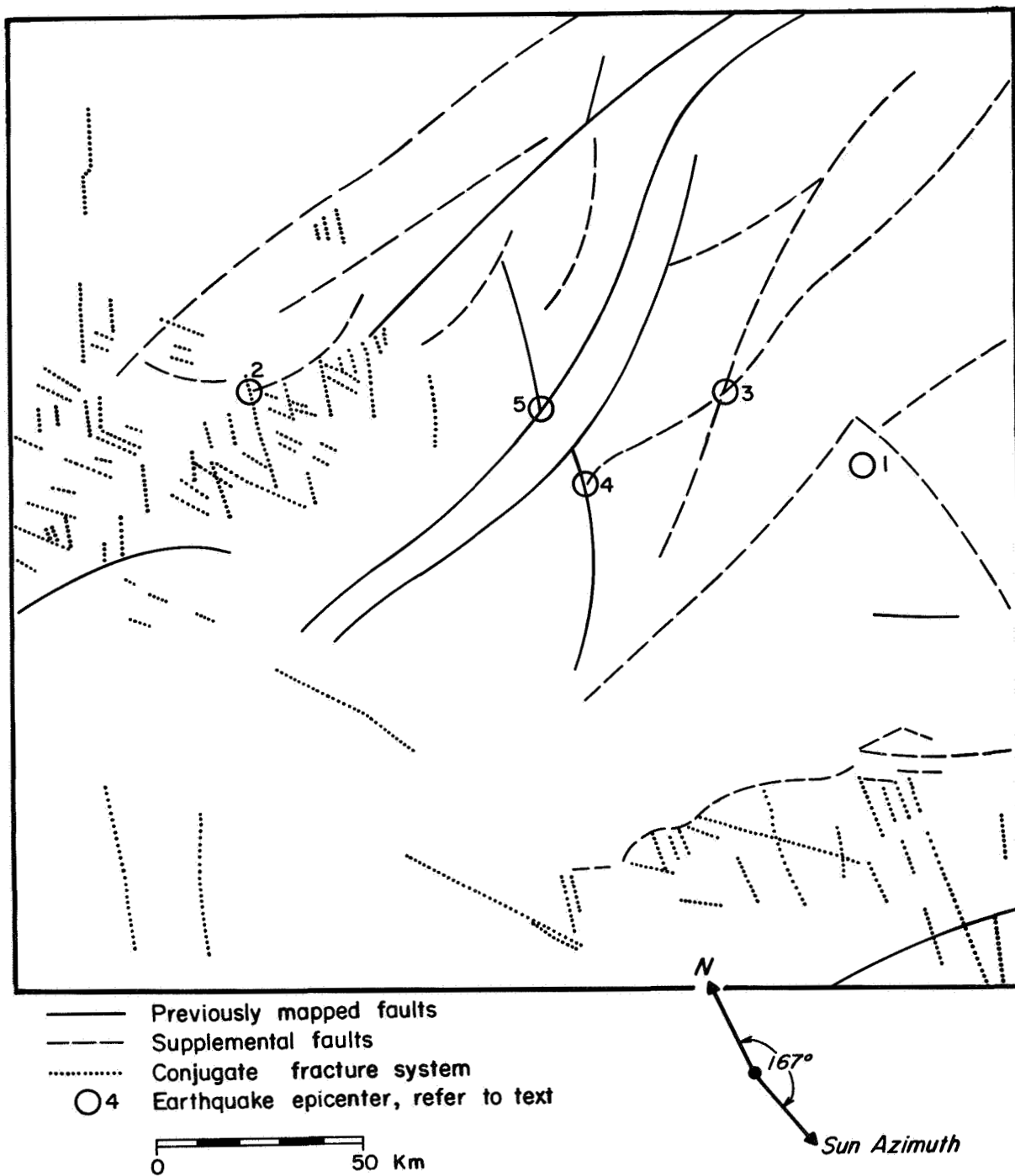


Figure 3



Key to Figure 3

STRUCTURAL INVESTIGATIONS IN THE MASSIF-CENTRAL - FRANCE -

J-Y Scanvic, *Bureau de Recherches Géologiques et Minières, Service Géologique National, B.P. 6009, 45018 - ORLEANS cedex - FRANCE -*

ABSTRACT

One survey we have achieved using ERTS imagery concerns the French "Massif-Central"—where cristallin and volcanic rocks outcrop—and its surrounding sedimentaries, "Bassin de Paris", Bassin d'Aquitaine" and Rhodanian valley.

The main purpose was the objective mapping of fracturing and the surveying of its relationship with known ore deposits. Then—eventually, to draw up a mineral research philosophy. During this survey we have shown the ability of ERTS imagery to outline lithology in some sedimentaries basins. On the other hand, in a basement area—under temperate climate conditions—lithology is rarely expressed. These observations can be related to the fact that band 5 gives excellent results above sedimentaries basins in France and generally band 7 is the most useful in a basement area.

Several examples show clearly the interest of ERTS imagery for mapping linear features and circular structures and confirm former ideas. All the main fractures are identified with the exception of a few—new ones are found both in sedimentaries and basement areas. Other interesting findings concern sun elevation which—stereoscopic effect not being possible—simulates relief in a better way under certain conditions. Then we have also found band 4, judged until now as not very useful by geologists can eliminate artificial details product by shadow of linear clouds (jet stream for instance, invisible on other bands).

At the least this paper aims to point out that ERTS images are a very useful tool but more time will be needed to prove its validity because details discovered have now to be carefully surveyed.

INTRODUCTION

The Massif-Central, located in the central part of France, is a fragment of the Hercynian chain peneplaned at the end of the Permian period.

N 74 30752

During the Westphalian it was divided by large fractures causing the formation of Stephanian coal basins (Saint-Etienne for example) over the whole area of the Massif.

The formation of graben during the Oligocene period (Limagnes, Aurillac, etc.) and of the high volcanic massifs (Mont Dore, Cantal, etc.) during the Neogene and Quaternary are the consequence of later evolution.

WHY THIS TEST SITE?

We have chosen this Massif to test the ability of ERTS images in the domain of tectonic geology because it is a very complex area where various geological phenomena are represented. Constituted by cristallin and volcanic rocks, showing exposures of Stephanian and Oligocene layers in more or less important graben, surrounded by sedimentaries basins (Parisian Basin, Aquitanian Basin, Rhodanian Valley), strongly affected by faulting, it is very interesting geological model.

Fracturing of different periods is very important all over the Massif-Central and metalliferous deposits, linked with it, have an economic interest: for instance the main lineament, called the "Sillon houiller" seems to be a boundary between two mineralized districts, the eastern one being the most important from a mining point of view. The study of the possible extent of this lineament toward the North (Sancerre fault), suggested by geophysical investigations is an interesting matter. Elsewhere we have seen that large fractures have permitted the formation of Stephanian coal basins but antimony, lead, gold, fluorite, baryte, zinc, silver and uranium appear in various districts. Some of them (fluorite) seem to be linked with coal basins and an accurate and objective mapping of fractures make it possible with ERTS images, could establish to research a good chronology and then become a useful guide for research of new deposits.

Let me point out, too, mineral springs, numerous in this country, are linked with fractures and here again the Sillon houiller seems to separate the Massif-Central into two districts, the eastern one only having the mineral springs: in France the economic value of thermal springs is certain.

Good maps exist for metalliferous deposits and mineral springs and a valid comparison is possible.

In another context, conscious of remote sensing ability in geology, the B.R.G.M. is involved, with other French geological societies, in experiments, mainly on the Massif-Central. Several investigations are being conducted in

cooperation with these companies—and with the national space agency—on four test sites (Villefranche, Meyrueis, Genolhac, Minervois) using colour and infra-red colour photographs, thermal infra-red imagery and multispectral scanning.

Finally for mineralized veins massive research is in progress over the Massif-Central and these surveys are very often conducted on the field with fractures maps interpreted by the B.R.G.M. photogeological team on 1/25 000 scale photographs. About twenty 1/50 000 scale fracture maps have been interpreted and checked in the field. Comparison between these photogeological fractures map and ERTS images interpretation demonstrates clearly the ability of orbital photographs and shows how many data they have registered.

Some of the surveys have been carried out at different scales (balloon photographs, 1/400 000, Mystere 20 photographs 1/100 000, classical photographs 1/25 000 and special cover 1/10 000) with different types of film while at the same time gravimetry and/or aero magnetism were used. Above the Villefranche test site these different scales aerial covers show, if some data exist on each one, some appear on ERTS image, for instance the circular structure we discuss in the "circular structure" part of this paper.

A fracture age map is scheduled and will be achieved in the next months.

Field mapping, drilling, geophysical surveys and remote sensing give us a very good control and make a valid interpretation of ERTS imagery possible on the Massif-Central. Several of these, in progress at the moment, will help us to obtain the necessary synthetic view of this complex area.

PROCESS OF SURVEYING

Each scene was carefully interpreted, using stereoscopic effect where possible, on the four bands at the beginning of the survey. However, it quickly appeared that only bands five and/or seven were useful and sometimes complementary for geological purposes. Band 6 generally is an image very similar to that obtained with band 7. Band 4 does not give any geological information; however, this band is necessary when the scene is apparently absolutely uncloudy. We have several examples where linear features, interpreted as possible fractures on bands 5, 6 and 7 are clearly related with the shadow of linear clouds with band 4.

One point is not clear. Why on some part of the test site band 5 is the best and on some others it is band 7? On the Massif-Central test site five scenes are interpreted on band five and nine scenes on band seven. For three of these

scenes the two bands present complementary features and for the others only one band can be exploited. Apparently, but this is not a rule, band 5 is better in sedimentaries formations, probably because vegetation is more contrasted there—and band 7 on basement areas. The Morvan scene illustrates this idea very well, but no conclusion can be drawn.

Another observation concerns sun elevation action. The Coiron volcanic massif is visible on two different scenes with two different sun elevations and only one shows the geological boundaries clearly; it is the one having a sun elevation of 35° (57° on the other).

Finally even if we have only one scene taken at two different seasons (March and September) we can assume the interest of multiseasonal images in geology by considering the results obtained on the eastern Parisian basin images. Comparison between the two images shows some differences which give a good idea of the geology of the "Bassin de Paris"; for instance, on band 7 taken in March, an important change appears towards North, in the Upper Cretaceous chalk, and also another one to the South. This change, not visible in September, corresponds to Quaternary argillaceous formations.

On the other hand, the extension of the Metz fault interpreted towards the West because the Seine river was seen without its alluvial terraces is not clearly observed in March these alluvium being not apparent.

All the interpretations we made on the test site were compared with existing documents:

- geological mapping at different scales,
- photogeological interpretation,
- geophysical exploration,
- drilling,
- various analysis,

and numerous results are confirmed by at least one of these methods. Such results in an area well known in the field are important and prove the validity of ERTS images.

RESULTS

We have not specially surveyed lithology but we can say that results are very irregular, and better in sediments than in the basement. Volcanic rocks were not generally observed. A fracture map at a 1 million scale is achieved and illustrates this paper. Some of the new results obtained from ERTS images are being checked at the moment or will be checked later. Features interpreted on ERTS images as possible fractures belong to four groups:

- fractures known in the field,
- extension of known fractures,
- fracture unknown in the field but corroborated by geophysical investigations, drilling and other methods,
- totally new fractures.

Notice that known fractures exist which are not visible on ERTS images but these represent only a small percentage.

Fractures we wish to discuss mainly correspond to group III and confirm that deep structural features under a thick cover are sometimes translated on the surface by indirect criteria.

The Aigueperse Fault

This fault was discovered by geophysical investigations and shows that the Limagne Basin is partitioned by North-East fractures. A field party is mapping this area at a 1/50 000 scale and if there is really a difference between the northern and the southern formations—sand and limestones to the North, marls to the South—there is no trace of fracturing on the ground except near Chatel-Guyon where thermo-mineral springs are known. However, on the ERTS image a linear feature we interpret as a fracture follows on the surface level the path of the fault found by gravimetry and confirmed by drillings, showing granite near the surface to the North and 1 800 meters deeper to the South.

The Toucy Fault

This fracture is known in the field at the jurassic level. An extension is found on ERTS images, towards the North, in the Cretaceous level and this ground trace corresponds quite exactly with a fault interpreted from drilling by petroleum geologists under 1 000 meters of Cretaceous chalk. We can assume this deep fault, probably not effecting Cretaceous levels is however visible on ERTS images through indirect criteria, difficult to interpret on the ground.

The Saint-Etienne Fault

The Saint-Etienne coal basin is strongly bounded on ERTS images on its southern limit. Another fracture, parallel to the North, is quite visible, but located in granites and migmatites, and shows the Westphalian graben is probably widest as indicated on the geological map even if there are no coal deposits in the northern part. These two faults extend across the Rhône Valley under thick fluvial sediments. We specially underline the southern extension because it follows quite exactly the basement high, known by drilling at 500 meters, which limits to the South the continuation, under the Rhône Valley of the Saint-Etienne coal deposit. This is a proof of the value of ERTS images in mineral research, a tool to explore ore deposit extensions.

ERTS images also show in this area a communication between the Roanne basin, filled with Oligocene sediments and the Saint-Etienne coal deposit and pose the problem of the ages of these two graben considered until now Oligocene for that of Roanne, Westphalian for the other.

The Bracieux - Gien and Cere - Romorantin Linear Features

These linear features are genuine ERTS discoveries. Geophysical and geological maps do not give a possible explanation of the phenomenon and unfortunately drillings are only a few there. It seems therefore that these two ERTS "fractures" each one hundred kilometers, or more, could reflect on the surface the Permian basin partly known by drilling and geophysics and named "the Cointre Fosse" by J. Lienhardt. These Permian sediments are at a thousand meters under the Jurassic and Cretaceous levels. Then on the "hypogeological" map of Weber the existence of a northern fault is confirmed near Villebourgeon, but very locally indeed.

Such a fault, trending north 80°, follows a direction that numerous authors have outlined in France (Guillemot, Duplan) and is parallel to the South with the extension of the Metz fault.

Then we can assert with Groslier and Letourneur, a displacement of nearly 70 kilometers along the main North-South trend (Sillon houiller - Sancerre Fault) because it is the distance between Gien and Montereau (see map). If we remember, we have shown on ERTS images the Metz fault follows westwards the Permian basin of Courgivaux - Trois Fontaines known under thousands of meters of sediments, we can assume that we begin to have a good knowledge of deep structures in the Parisian Basin, thanks to orbital imagery.

The Brive Fault

East of Rochechouart a 50 kilometers long fracture is visible on ERTS images, partly in Cristallin rocks, partly in Jurassic levels. This alignment is to be specially discussed because unknown until now on the geological map, it is partly described in a recent paper (J. Delfaud). This author shows that this fault, in its southern part, is the western margin of the "Occitan high", a paleo-relief he outlines with detailed sedimentology. Northwards we extend this fault across the Massif-Central in using the alignment interpreted on ERTS images.

Once again, with this example we demonstrate the interest of orbital imagery in tectonic research. On the other hand, and we specially want to underline this idea—we think it is absolutely necessary, checking in the field all the ERTS discoveries, to use not only the classical "hammer investigation" but also all other techniques available: geophysics, drilling, sedimentology . . . and others. Examples described in this paper, and in a recent one (ERTS-1 symposium) where we talk about the possible extension of the Metz fault, have been chosen to prove this idea and it is quite evident it will need some time to corroborate all the ERTS-1 discoveries in the geological tectonic domain.

Circular Structures

To end this paper we want to say a word about circular structures found on M.S.S. images and they are numerous.

The Rochechouart one is known from the time Raguin described it and demonstrated it was due to meteoritic impacts. B.R.G.M. and University of Paris Orsay are working on the topic (Lambert) and ERTS images are used, enlarged at a 1/200 000 scale. At the first glance a circular pattern is obviously visible, West of Rochechouart, and corresponds quite exactly to the breccia zone. Faults interpreted on ERTS images are partly known in the field and the North-South one, cutting the Vienne river West of Chabanais follows scattered microgranite veins and allows M. Lambert to draw up an interesting hypothesis we shall discuss in another paper. On the other hand a western extension of the meteoritic structure, found in the field but not evident is supported by M.S.S. images, even if not really obvious.

Other circular structures were found on ERTS images around Rochechouart. None is meteoritic structures; some are in relationship with oriented level in metamorphic rocks, some others are more interesting for this discovery, if confirmed by detailed surveying, could be important as it is in the vicinity of the already known circular structure of "Puy les Vignes" which is tungsten bearing.

BIBLIOGRAPHICAL REFERENCES AND MAPS

- Carte géologique de France - B.R.G.M. - 1/1 000 000
Carte de la végétation - Comité national de géographie - 1/1 000 000
Carte aéromagnétique B.R.G.M. - 1/1 000 000
Carte gravimétrique 1/1 000 000 publiée par le B.R.G.M.
Carte métallogénique B.R.G.M. - 1/2 500 000 - UNESCO - B.R.G.M.
Carte hydrogéologique du Bassin de Paris - B.R.G.M. - 1/500 000
- C. Cavelier, J-Y Scanvic, G. Weecksteen, A. Ziserman - Mars 1973
Capability of ERTS imagery to investigate geological and structural features
in a sedimentary basin - (Symposium ERTS)
- J. Delfau - 1973
Un élément majeur de la paléogéographie du Sud de la France au Jurassique
moyen et supérieur : le Haut-fond Occitan - (C.R. som. S.G.F.)
- L. Duplan - 1973
Les grands lineaments de la France (C.R. Acad. Sc. Paris)
- J. Grolhier et J. Letourneur - 1968
Evolution tectonique du grand sillon houiller du Massif-Central français -
XXIII - International geological congress - Vol. 1
- F. Heritier, J. Villemin - 1971
Mise en évidence de la tectonique profonde du Bassin de Paris d'après
l'exploration pétrolière - (La tectonique du Bassin de Paris) - (Bull. B.R.G.M.
Section 1 No. 2)
- J. Guillemot, Max Guy - 1973
Un système cohérent d'alignements structuraux communs aux Alpes et
aux Pyrénées mis en évidence par le satellite ERTS.1 (C.R. S.G.F.)
- M. J. Lienhardt - 1961
Etude stratigraphique, pétrographique et structurale du socle ante-Permien
du Bassin de Paris. (Annales Soc. géologique du Nord).
- E. Raguin - 1972
Les impactites de Rochechouart (Haute-Vienne) (Bull. B.R.G.M. No. 3)
- Sapin - 1967
Principaux résultats géologiques des travaux d'exploration réalisés par la
S.N.P.A. dans le Sud-Ouest du Bassin de Paris. (Bull. Soc. Géol. France -
7e série, No. 3)

Weber - 1972

Le socle antetriasique sous la partie sud du Bassin de Paris d'après les données géophysiques. (Thèse - Paris VI)

Division Geophysique - 1972

Carte magnétique B.R.G.M. : éléments interprétatifs de base obtenus à l'issue des levés aéromagnétiques, Massif-Central.

STRUCTURAL GEOLOGY OF THE AFRICAN RIFT SYSTEM: SUMMARY OF NEW DATA FROM ERTS-1 IMAGERY

P. A. Mohr, *Smithsonian Astrophysical Observatory, Cambridge, Massachusetts*

ABSTRACT

ERTS imagery reveals for the first time the structural pattern of the African rift system as a whole. The strong influence of Precambrian structures on this pattern is clearly evident, especially along zones of cataclastic deformation, but the rift pattern is seen to be ultimately independent in origin and nature from Precambrian tectonism. Continuity of rift structures from one swell to another is noted. The widening of the Gregory rift at its northern end reflects an underlying Precambrian structural divergence, and is not a consequence of reaching the swell margin. Although the Western Rift is now proven to terminate at the Aswa Mylonite Zone, in southern Sudan, lineaments extend northeastwards from Lake Albert to the Eastern Rift at Lake Stefanie. The importance of en-echelon structures in the African rifts is seen to have been exaggerated.

N 74 30758

INTRODUCTION

Unified mapping of regional structures of the African rift system (Figure 1) on a scale of 1:1 million has been completed except for a few persistently cloud-covered areas. The mapping has been done by direct tracing from 18-cm square black-and-white prints (spectral bands 5 and 7). Incorrect indication of coordinates on some images has been adjusted for using the USAF Operational Navigation Charts, and distortion from a precise 1:1 million scale has been allowed for by arithmetical scaling.

The results of the mapping have been charted on fifteen 100 x 50cm sheets, and they include Precambrian strike, Cainozoic faults, and lineaments of an uncertain nature. In some areas, young lava shields, calderas, cones and craters, and lithological boundaries have additionally been recorded. The area mapped covers nearly 5 million sq.km, and obviously it has been impossible to give full attention to fine detail, fascinating though this can be on the best ERTS images.

River courses and lake shorelines in eastern Africa are accurately seen for the first time, though due to uncertainties in satellite position the precise coordinates of mapped features can be subject to as much as 2-3 minutes of arc error in some areas.

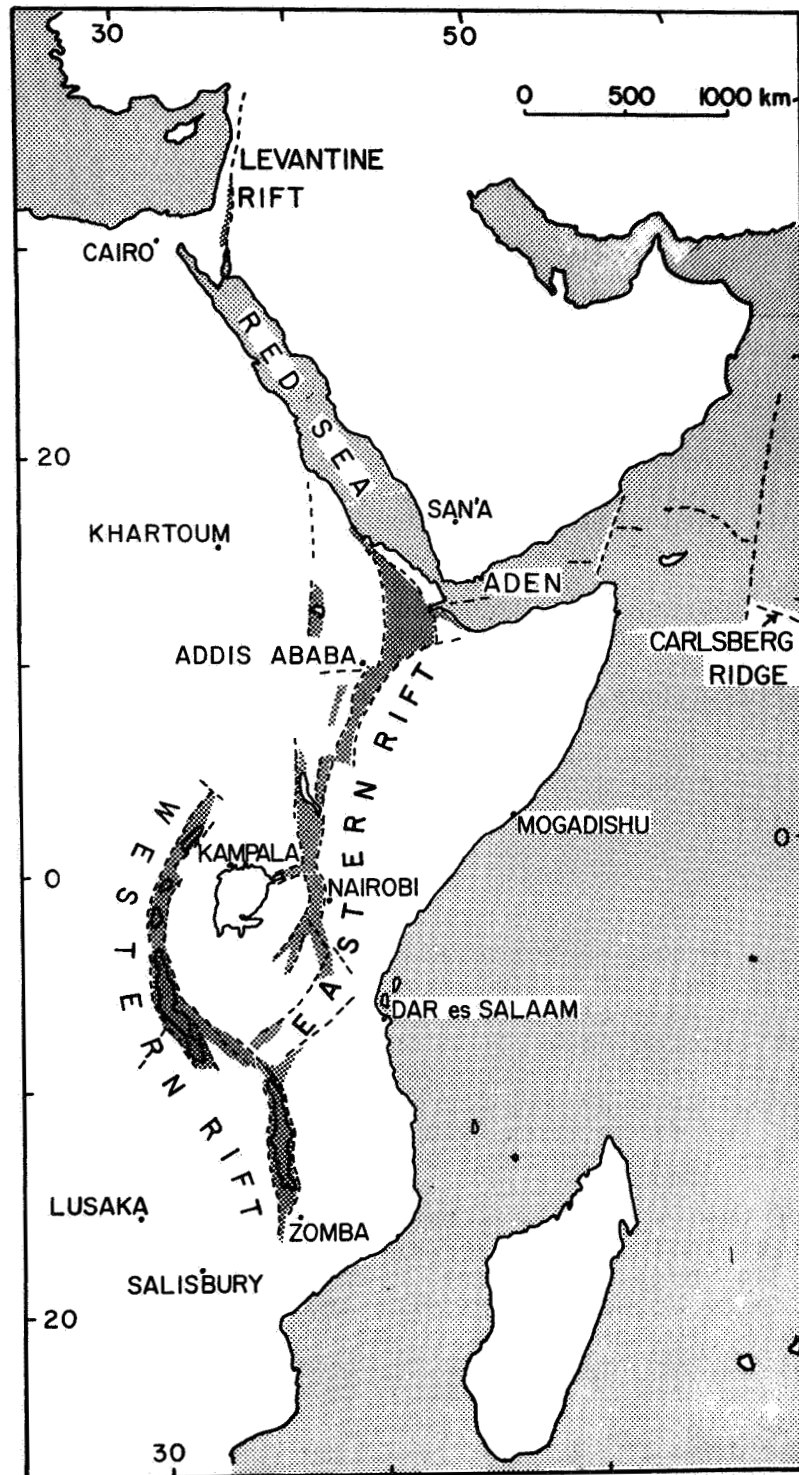


Figure 1. The East African rift system (rift valleys stippled).

This paper presents a summary of information interpreted from the mapped sheets. The sheets themselves will be published by Smithsonian Astrophysical Observatory in the final report on this work. In lieu of these sheets here, the reader should seek geographical assistance from the maps in Baker et al. (1972) and McConnell (1972).

METHOD OF MAPPING AND GROUND CONTROL

Although detailed mapping and study of the Precambrian fold-belts of eastern Africa falls outside the scope of the present work, an important question concerning the African rift valleys is the degree of parallelism of rift faults to pre-existing structures. Therefore, trends of strike-lines in exposed Precambrian terrain have been mapped from the ERTS imagery where these lines are clearly expressed. The problem is complicated by the fact that strike-lines are best observed in regions of appreciable topographic relief where the degree of lateritic palaeosoil cover is minimised. Instances of an apparent transition from strongly to weakly expressed Precambrian strike features, for example in Katanga and northern Ethiopia, can be related to the degree of soil cover and not to any change in structural style.

Precambrian strike-lines identified on ERTS imagery usually denote lithological strike of tilted or folded strata, particularly for younger Precambrian rocks such as comprise the Bukoban System of northwestern Tanzania, the Karagwe-Ankolean of Burundi, the Lufilian and Irumide belts of northern Zambia, or the Precambrian sequence of northern Ethiopia. This type of strike-line is characteristically curvilinear and frequently reveals broad synclinoria/anticlinoria. Where deformation and metamorphism have been intense, lithological strike is obliterated or at least obscured to the extent that the identified strike-lines can be said to represent a new, refoliated grain. This is notably the case in zones of deep-seated cataclasis, known from ground surveys, as for example in the Rukwa rift and the central sector of the Lake Tanganyika rift, and in the Aswa Mylonite Zone of southern Sudan against which the Western Rift terminates. This type of strike-line is characteristically precisely linear over distances of the order of 100km, and when followed by Cainozoic rift faulting the two types of structure can become virtually indistinguishable on the ERTS imagery.

Boundaries between different, regional lithological types in Precambrian terrain, though in some places clearly expressed on the ERTS imagery, have not been mapped in the present work. Some circular structures, including ring-intrusions, have however been included as possibly marking otherwise masked lines of ancient crustal weakness.

The faulting which gives form to the present-day rift valleys of eastern Africa is generally recognised to be of Pliocene-Quaternary age (Baker et al., 1972). The topographical expression of

the faults is therefore usually sharp, and because of this they are easily detected on the ERTS imagery. This is especially so for east-upthrown faults, which cast a sun-shadow at the time of imaging. Northwest-upthrown faults can sometimes be detected by illumination of their scarp, showing as a bright strip on the imagery, but where the scarp is somewhat denuded then the modest increase in brightness can be lost amongst background variations. It cannot be denied, therefore, that in regions where ground-truth is lacking there may be a bias favouring representation of the eastern boundary faults of graben (and western boundary faults of horst) on the author's maps.

The direction of throw on rift faults can be detected not only from sun-shadow or illumination, but frequently also from identification of the drainage pattern. The darker tones of afforestation are not a reliable guide: in some semi-desert areas, forest occurs along the foot of fault-scarps, presumably where there is near-surface groundwater. In some hilly terrain, forests are denser above the scarps because prevalent mountain mists foster a cold, rain forest. Complete afforestation makes the detection of faults very difficult, even where strong faults are seen to enter such an area.

Evidence for large-scale transcurrent faulting in the African rift system has not been found in this study, and it is probably best that this phenomenon be sought initially from ground and aerial photographic surveys. Likewise, no thrust-faulting has been identified in the rift system; the Precambrian Nandi fault of western Kenya (Sanders, 1965) is remarked on the ERTS imagery, but its nature, controverted even on the basis of ground studies, is not revealed thereon. ERTS imagery is a suitable tool for determining the nature of regional faults only insofar as the linearity of the fault trace can be related to topography and lithological strike. Even here some ambiguity can arise, as shown by the fact that regional rift faults with steep hade can show an almost perfectly linear trace whereas small, short faults of the graben floor, also with near-vertical hade, yet have a characteristically sinuous trace.

The third class of structural feature identified in this work is covered by the non-generic, descriptive term of lineament. Lineaments usually have the form of a linear arrangement of topographic features, either continuous or interrupted, without clear evidence of crustal displacement that defines a fault. Many of them trend at a large angle to the main rift faulting. Where Precambrian structures are largely masked by superficial cover, their vague and intermittent surface expression can form a type of lineament; but lineaments as mapped in this study can also cut across the strike of well-exposed Precambrian terrain, and could represent regional jointing or an overprinted or secondary structural trend. Lineaments are distinctly rare in the Mesozoic-Eocene sedimentary basins of the Horn of Africa, perhaps

because of the weakly consolidated nature and low rigidity of the rocks concerned, but in the Cainozoic volcanic fields can be common. Where a volcanic field is only a thin pile of lavas, the structural trend from adjacent Precambrian terrain can, as in central-north Ethiopia, be traced as lineaments into the volcanic field; but other lineaments in such fields can be discordant both to the nearest exposed Precambrian structures and rift faults. Indeed, the latter form the most characteristic type of lineament, whose trace can extend, though discontinuous or offset, for several hundred kilometres.

A not-yet-understood property of the ERTS imagery is its differential emphasis of structural features according to the overall tone of an image. Some darker images emphasise linear faults and lineaments, whereas lighter, more contrasted images bring out faults with large topographic displacements. Differential emphasis also comes, of course, from the different spectral bands employed by the ERTS-1 satellite, and in the present work it has been consistently noted that band 5 (6000-7000Å) best brings out geological structures, except where the overall tone is dark when band 7 (8000-11000Å) yields a lighter and more contrasted image. Band 7 images are also preferred for regions of extensive vegetation cover, and for regions subject to partial cloud-cover.

Ground survey data have been referred to throughout the author's mapping as a check against doubtful features expressed on the ERTS imagery. Whilst a few structural lines were recognised on this imagery only subsequent to a search originating from knowledge of ground data, it must be emphatically pointed out that in all cases the mapping has proceeded first from the images and then been checked against ground data. In this process, for example, the direction of fault-throw, or the manner of bifurcation or intersection of faults, has occasionally required correction from closer re-scrutiny of the images. In no case whatsoever has the author indicated on his maps structures that cannot be discerned on the ERTS imagery, even though there be an important feature (according to ground surveys) which is actually present. Therefore it will be discovered that the new ERTS-based maps lack some structural data shown on geological maps, and add new data previously unsuspected. The ERTS-based maps add to, and do not supersede existing structural maps.

Owing to the present lack of cloud-free imagery, no mapping has yet been possible of the Western Rift between latitudes 1°N and 3°S, nor the southern end of the main Ethiopian rift, nor of the Kilimanjaro area.

RESULTS

Relation of rift faulting to Precambrian structures

This knotty and persistently controversial topic basically concerns two alternative interpretations: 1. the pattern of the

rift faults is a faithful reflection of major Precambrian structures, owing (to an extent which is disputed) to continuity of a single tectonic style from the Precambrian up till the present. The principal proponent of this viewpoint has been McConnell (1972, and numerous other papers referred to therein).

2. the rift faults have taken advantage of the pre-existing Precambrian tectonic 'grain', but the overall pattern of the rift system has not been determined by this grain but by a fortuitously superimposed, completely different structural event. This viewpoint has been advanced by, amongst others, King (1970) and Baker et al. (1972).

The ERTS imagery provides, for the first time, an overview of the entire problem, and indeed this is the sort of task to which satellite imagery is well-suited. Precambrian rocks are extensively exposed in proximity to the African rift system, the centres of the Ethiopian and Kenyan swells excepted, and along much of the Western Rift the rift faults themselves occur in exposed Precambrian terrain.

It immediately has to be admitted that, on a regional scale, the frequent coincidence of Precambrian structures and rift faults is uncanny. The Eastern Rift, from Tanzania to Ethiopia, essentially follows the meridional Mozambique Belt, whose final activity is dated at 550 ± 100 m.y. (Clifford, 1970; Shackleton, 1967). The Western Rift commences in the south (L. Malawi rift) by following the Mozambique Belt, but then turns northwestwards along the Ubendian (1850 ± 250 m.y.) deformation zone before bending round to the north-northeast along the Kibaran (1100 ± 200 m.y.) deformation zone (Clifford, 1970). The Western Rift abruptly terminates in the north against a cross-cutting Precambrian structure, the NW-trending Aswa Mylonite Zone (Whiteman, 1971). The essentially upfaulted crustal blocks between the rift zones in eastern Africa are formed of cratonic nuclei, typically older than about 2500 m.y.

Some specific regions mapped from the ERTS imagery can now be discussed. In Yemen, major ENE-NE trending fracture zones in the Precambrian appear to have been reactivated by tectonism accompanying the opening of the Red Sea and Gulf of Aden, and some were sites for Cainozoic basaltic volcanism (Mohr, 1972b). However, typical Precambrian terrain in eastern and northern Yemen takes the form of a curving mesh of strike-lines with interspersed granitic intrusive bodies: young faults in this terrain are rarely identifiable, but where they are they usually run markedly oblique to the Precambrian strike. In fact, non-parallelism of Precambrian and rift structures in Yemen is hardly surprising in view of the proximity of an RRR-triple junction at Afar, unless this coincides with a Precambrian nexus. South of the Gulf of Aden, in northern Somali, non-parallelism is general (Mohr, 1962; Beydoun, 1970).

In Ethiopia, Precambrian zones of possible cataclastic deformation

(Mohr, 1972b) trend NNE from western Tigray province into Eritrea, where they turn to a meridional trend with several bifurcations and reunions. It is difficult to allow these structures as being parallel to the adjacent Red Sea basin. Central Tigray province exposes broad synclinoria and anticlinoria trending NNE-NE (Beyth, 1972): this regional Precambrian trend is slightly but definitely oblique to the Cainozoic margin structures of western Afar further east (Mohr, 1972a, 1973), and to the Tana graben further south. In northern Ethiopia and eastern Sudan, strongly expressed E-ESE Precambrian lineaments are not related to any known rift structures.

In central Ethiopia the Precambrian is masked by thick volcanic cover, but east of the main Ethiopian rift, along meridian 39°E, persistent and rather linear Precambrian structures (Chater and Gilboy, 1970) trend N-S, oblique to the NNE strike of Ethiopian rift faulting (But N-S faulting determines the Amaro horst and Galana graben at the southern end of the rift - see Levitte et al. 1974). Strongly discordant angles separate the meridional Precambrian strike of the Kenya-Ethiopia border region from superimposed NW-SE Cainozoic faulting, though numerous small basaltic centres appear to be aligned at intersections along the Precambrian trend.

East of the Gregory rift, in north-central Kenya between latitudes 2°N and 0°, the detailed ground-mapping of Baker (1963) is fully confirmed. The Precambrian strike here trends N-NNW, whereas the rift faulting immediately to the west trends NNE. This might seem to be a clear case of non-parallelism, yet the Precambrian structures project northwards into the precise alignment of the Mt Kulal volcanic range and related rift structures, east of Lake Rudolf. To the south, the same ancient structures pass via the Pleistocene volcanic centre of Mt Kenya (Baker, 1967) to the Cainozoic volcanics and faulting of the Yatta plateau. If the Gregory rift itself is following a 'discordant' NNE Precambrian trend, this is of course hidden by young volcanics and sediments. However, this possibility is rendered less likely by the fact that, west of Lake Rudolf, the western margin structures of the rift are precisely parallel to again NNW Precambrian strike-lines, though the rift structures are notably more linear than are the Precambrian ones (Mohr, 1972b).

The Western Rift is often regarded as the example par excellence of a rift valley determined by pre-existing structures, and a description of the polyphase Precambrian tectonism of the region and its influence on the Cainozoic rift faulting has been given by McConnell (1972). The Western Rift meets important NE-SW faulting at a structural node at latitude 9°S, longitude 33½°E; here the rift trends NW-SE and its unusually linear faulted margins are strongly developed in the southern L. Tanganyika-L. Rukwa-northern L. Malawi sector. This strong expression and linearity are matched in the precisely parallel Ubendide structures the

cataclastic character of which emphasises a zone of intense crustal deformation separating two cratonic nuclei (Sutton and Watson, 1959; Brown, 1962; McConnell, 1972). By contrast, the NE-trending Cainozoic faulting, expressed both northeast of the node (Usangu and Fufu faults) and to the southwest (Luangwa valley faults), are seen on the ERTS imagery to be superimposed on mild, NE-trending Irumide structures that are obliterated by the ostensibly older Ubendide structures at the node itself. At any rate, the predominant Precambrian trend is also the predominant Cainozoic fault trend here. Directly to the west, NE-SW faulting of the Upemba and Mweru half-graben is generally close to parallelism with structures of the relatively mildly deformed Kibaride belt (Cahen, 1970); however, no important Cainozoic faults are revealed along the imposing structural arc of the end-Precambrian Katangides (Cahen, 1970).

The L. Tanganyika rift, roughly 70km wide, is at first glance strongly controlled by the NW-SE Ubendide structures. In fact this only holds for the central sector of the rift; at latitude 6°S the rift trough is offset dextrally and thus, proceeding northwards, the rift escapes from the influence of the Ubendide structures continuing west of the lake, and follows the meridional trend of the related Rusizian structures though with some influence also from the Kibaride belt. Again, this younger Precambrian belt is largely obliterated where it crosses the older Rusizides (see McConnell, 1972, for a discussion on this problem). Similarly, proceeding southwards from the central sector of the L. Tanganyika rift, the Ubendide structures run straight, southeast across mountainous terrain to the L. Rukwa rift. But the L. Tanganyika rift itself, maintaining its normal width, extends SSE-wards until terminating in a region of Cainozoic cross-faulting.

ERTS imagery of the L. Tanganyika region therefore suggests two key points for an understanding of the Precambrian-Cainozoic structural relations problem. First, where Precambrian crustal deformation has been most intense, rift faulting is also more strongly developed. It is as though the Precambrian cataclastic zones provided trans-crustal sutures which became planes of weakness when tensional strain accumulated during the Cainozoic. Second, the L. Tanganyika trough persists in its curving arc, even where forced to make a lateral offset, in defiance of the linear Ubendide structures: the rift here is not a straight NW-trending valley superimposed on the length of the Ubendide belt.

In conclusion of this section, Precambrian structures have a powerful local influence on the Cainozoic rift structures. On the regional scale revealed by the ERTS imagery, however, the rift valleys are seen to persist in trends that transgress the Precambrian structures, suggesting that a new stress-field has been imposed with the generation of the rift valleys. Whether, on the sub-continental scale, the near parallelism of the African rift system and the Mozambique Belt is of fundamental structural significance cannot be answered here, but the question is of importance to possible relations of thermal plumes and plate motions.

The regional fault pattern

The fault pattern of the African rift system is known from ground and aerial surveys in varying degrees of detail for different sectors of the system. Ground surveys are fairly complete for the southern and central sectors of the Gregory rift, for the southern and western regions of the L. Malawi rift, and for Afar; they are only of reconnaissance type for much of the Western Rift and the Ethiopian rift, and are virtually non-existent for the graben occupied by lakes Tana, Stefanie and Mweru, and the Luangwa valley.

The great merit of the ERTS imagery is that, for the first time, it provides the means for a unified mapping of the major structures of the whole African rift system, formidable task though this is. As emphasised previously, this mapping is not a substitute for, but an adjunct to ground mapping. Nevertheless the satellite imagery enables a first interpretation to be made of unsurveyed regions in the light of what it reveals about well-surveyed regions. Furthermore, some significant additions and revisions are provided from ERTS imagery of even well-surveyed regions.

The fault pattern in Yemen is revealed by ERTS imagery to show a coastal zone of major warping and associated antithetic faults, both for the Red Sea and the Gulf of Aden (Gass et al., 1965). In the interior of the Yemen plateau, NE-ESE trending fracture zones have been identified. Other important faulting runs south-east across northern and eastern Yemen, parallel to the Red Sea structural trend north of it in Yemen, SSE-trend narrowing. These and other features have been discussed by Mohr (1972b).

The African rift system meets the Red Sea and Gulf of Aden at the Afar triple junction (Tazieff, 1970, 1972; Mohr, 1970, 1972a). Mapping of Afar margin structures from ERTS imagery has been described elsewhere (Mohr, 1973). Essentially, the western margin of Afar shows a gently sinuous plan which, in detail, reveals the powerful influence of NNW-trending 'Red Sea' structures. As the western margin runs close to meridian 40°E throughout its extent, this requires that the NNW-trending structures be offset dextrally. These offsets occur in sectors where the dominating structural trend is NNE; this trend parallels the Precambrian 'grain' west of northern Afar, and in the south occurs as a forceful extension of main Ethiopian rift faulting projecting right across southern Afar. Marginal warp-zones, and marginal graben associated with belts of antithetic faulting can be identified on the ERTS imagery.

The southern margin of Afar can be mapped accurately for the first time from the ERTS imagery. The western sector of the margin shows the influence of dextrally offset Ethiopian rift structures that turn off northwards into Afar (Mohr, 1973); this pattern changes abruptly near longitude 41°E where a Gulf of Aden trend is imposed, though this fades out south of the Aisha horst (Canuti

et al., 1972; Mohr, 1967, 1972a). Further east, along the northern margin of the Somalian plateau, the dominant fault trend is WNW and is especially strongly developed in the Asseh graben and on the Cape Guardafui peninsula - the latter is revealed for the first time on the ERTS imagery. Inland, WNW faulting again determines the Nogal and Darror graben (Azzaroli and Merla, 1957).

The SSW-trending faulting of southern Afar continues directly as the main Ethiopian rift to almost latitude 5°N (Baker et al., 1972; DiPaola, 1973). The aerial photographic mapping of DiPaola is largely confirmed and amplified by the ERTS imagery, which shows however that the importance of dextral en-echelon offsets in the rift has been exaggerated (eg. Mohr, 1967). Only the axial Wonji fault belt of the rift floor shows such offsets (Mohr, 1962), and as in places this belt can show two parallel developments, and elsewhere can be absent, the term en-echelon is a misnomer on the regional scale. Immediately west of the main Ethiopian rift, the parallel structures of the Omo valley can be traced northwards via the Guder valley to possibly as far as the Tana graben. The asymmetrically developed Tana graben occurs within the Ethiopian plateau block, and its fault pattern has been accurately mapped for the first time, using the ERTS imagery.

The regional link between the Ethiopian and Gregory (Kenyan) rifts was poorly known until the advent of the ERTS imagery. This reveals that the faulting at the southern end of the Ethiopian rift, and the Kino Sogo fault belt east of L. Rudolf, lie on a common NNE-oriented alignment. An unfaulted 'gap' of about 100km length separates the terminal faults of the two rifts (note: to the west of this region the Omovalley faulting passes through a broad zone of horst-graben structures into the Lake Rudolf basin). The transition of the rift system across this gap was thought by Mohr (1967) to be effected through the L. Stefanie graben via a dextral offset; but the imagery shows that this graben lies west of the alignment, and is formed of NNW-trending faults crossed by secondary but important ENE-faulting.

The transverse faulting of the L. Stefanie graben projects as lineaments across the structural gap between the Ethiopian and Gregory rifts. In the opposite direction it projects across Turkana, where lineaments line up with WSW-SW faulting on the eastern side of the L. Albert rift. Here is tentative evidence that the Western Rift, though indubitably terminating against the Aswa Mylonite Zone north of L. Albert, may persist through a minor tectonic offshoot across to the Eastern Rift, though not, it must be emphasised, as a graben. The structural gap between the Ethiopian and Gregory rifts is likewise a gap to some NW-SE tectonism, superimposed on a prominent, parallel Precambrian structure, extending from Moyali to the Omo valley.

The regional structures of the northern half of the Gregory rift (Baker et al., 1972) are shown in their unity on the ERTS imagery as a magnificent, regular fanning-out northwards. The rift widens from 60km at latitude 0° (at the junction with the transverse

Kavirondo rift) to 130km at latitude 2°N, and to about 300km for less clearly defined structural margins at latitude 4°N. Within this structural widening, the weakly faulted L. Rudolf basin shows a northward fanning-out into the southern Ethiopian plateau. Two major points require emphasising here: firstly, that although the northward widening of the Gregory rift structures coincides with the topographic decline from the centre to the margin of the Kenyan swell, it also coincides with a widening of the Precambrian structures. This raises a fundamental question: would swell uplift in the Cainozoic have formed a continuous, quasi-midoceanic ridge from Ethiopia to Tanzania if dissipation had not been enforced by a pre-existing structural pattern? Second point: strongly expressed rift structures do cross from the Kenyan to the Ethiopian swell without apparent diminution in strength (N.B. the gap noted above lies upon the fringe of the Ethiopian swell, and not between the two swells), though there does seem to be a greater complexity and less regularity to the structural pattern in the boundary region.

At the conjunction of the ENE-trending Kavirondo rift with the main Gregory rift, the latter undergoes an abrupt change from a N-NNE structural trend in the north, to a NNW-NW trend in the south. The southern half of the Gregory rift comprises a majestic curve, concave to the west, from the equator to latitude 4°S where the structural trend has finally turned to NE-SW. Characteristic platforms, not found in the Ethiopian or Western rifts, occur along the eastern side of the Gregory rift (Baker et al., 1972), and from the western margin several turn-off structures are revealed on the ERTS imagery. West of the rift, within the L. Victoria block, several important structures trend ENE-NE: these include the Kavirondo rift, the Uitimbara-Siria faults, the Speke Bay graben, and the L. Eyasi faults at the southern end of the Gregory rift. If these tensional features are contemporaneous with the Gregory rift, what homogeneous stress-field could have given rise to the overall fault pattern? Has there been a slight anti-clockwise rotation of the L. Victoria block?

Although the Gregory rift terminates southwards in a fanning-out zone, this phenomenon is shown on the ERTS imagery to be much more abrupt and less symmetrical than at the northern end of the rift (Baker et al., 1972). The main faulting, as mentioned above, turns to a SW direction, and lineaments of this trend continue across the Dodoman nucleus to the Western Rift. Faults of S and SE trend are relatively minor in the fanning zone, and the ERTS imagery shows that there is no significant connexion of the Gregory rift with the Usangu-Fufu faults farther south (see also Hepworth, 1972). Therefore it seems misleading to speak of the Eastern Rift as meeting the Western Rift at Mbeya: the Eastern Rift has already terminated further to the north.

East of the Gregory rift, a NNW-trending belt of strongly deformed Precambrian rocks extends from southern L. Rudolf, passes close to Mt. Kenya and along the Yatta plateau, and reaches northeastern

Tanzania at the Pare-Usambara graben-horst structures (McConnell, 1972). Once again, the control of Precambrian 'grain' on in this case extra-rift tectonism is emphasised: the corollary of course is that there must be important structural sub-divisions to be made within the Mozambique Belt.

We now turn to the Western Rift. Near the northern end of the Western Rift, the powerful NE-trending faulting of the Lake Albert sector curves, proceeding northwards, to a NNE-trend and a weak graben is juxtaposed west from the northern end of the lake. The faults of this weak graben impinge upon, and are abruptly terminated by the Aswa Mylonite Zone, on the Uganda-Sudan border (Whiteman, 1971). No NE-trending faults are revealed by ERTS imagery to continue northeast of the Aswa Mylonite Zone, where rather the tectonic trend is NW-SE, related to the northward widening of the Gregory rift.

The Aswa Mylonite Zone is a strongly, almost violently expressed structure for which there is as yet little ground-survey information. It forms a narrow, linear zone of cataclasites, about 150km long, whose ends are splayed with a slight clockwise bias; the southern splay is closed, indicating the presence of a broad folded structure. Cainozoic faulting is almost certainly imposed upon the Mozambiquian Aswa structures (Almond, 1969), with upthrows to the southwest if interpretation from the ERTS imagery is correct; Almond (1969) also regards the zone as being one of sinistral shear, and this is compatible with the clockwise splay. Faults continue northwestwards for at least a further 200km from the Aswa zone. Lineaments are also observed to project southeastwards from the zone, and pass via the southern fringe of Mt Elgon to the Precambrian Nandi thrust fault (Sanders, 1965). However, this southeastward continuation of the Aswa zone across northern Uganda cannot be matched with the narrow, continuous belt of cataclasites indicated by Almond (1969), perhaps owing to the effect of variably masking soil cover on the ERTS imagery. It is interesting to note that the Aswa Mylonite Zone and its continuations form a major Precambrian structure that has not been utilised in the development of the African rift system: this gives further support to the view that the rift system is a new and distinct structural unit rather than an ongoing re-activation of ancient transcrustal sutures.

ERTS imagery of the Western Rift southwards from Lake Albert is largely cloud-covered, and no useful structural maps can be constructed for as far as the northern end of the L. Tanganyika rift. The important relationships between the faulting of this rift and the Precambrian structures have been discussed briefly in the preceding section. The northern part of the L. Tanganyika rift is a graben superimposed on the Rusizian trend (N-S), but with some intersecting or adjusting faults of NNE-NE, Karagwe-Ankolean trend immediately east of the rift. The central sector of the L. Tanganyika rift is faulted parallel to the NW-NNW Ubendide structures, though the rift trough itself jumps across these structures at latitude 6 S: thus the Kiyimbi horst west of the lake lies on

the precise alignment of the Kungwe horst east of the lake, such that the rift is asymmetrically developed in one sense north of latitude 6° S, and in the opposite sense south of 6° S. At latitude 7½° S there is a further, 35km dextral offset of the graben faulting, which continues SSE as far as latitude 9° S. On the western side of the graben, however, at latitude 8½° S the marginal faulting is largely overruled by strong NE-SW faulting that extends southwest to the Mweru Wantipa graben-horst structures.

West of the L. Tanganyika rift, NE-ENE faulting, with predominant southeasterly upthrows, forms the Kabamba-Upemba and L. Mweru half-graben as well as more doubtful features north of the lower Lukuga river. It is of interest that the same NE-ENE trend is manifested in graben faulting west of the Eastern Rift (see above), as well as in numerous lineaments between the two Rifts. The termination of the L. Tanganyika rift in the south may be related to the presence of such cross-lineaments.

The L. Rukwa rift develops south of latitude 7° S, and runs about 130km east of the L. Tanganyika rift and with a SE trend that is significantly different from the SSE trend of the L. Tanganyika rift at the same latitudes. The intervening terrain is also strongly faulted, with a prominent high horst. The ERTS imagery reveals this faulting accurately for the first time. The faults of both margins of the L. Rukwa rift are exceptionally long and linear, and follow Precambrian cataclastic zones (Brown, 1962) of the Ubendides. The faulting of the L. Rukwa rift continues beyond the Mbeya node and into the L. Malawi (Nyasa) rift, and is particularly strongly developed on the northeastern side of the latter, in the Precambrian migmatites of the Livingston Mts. Mapping of the L. Malawi rift (Bloomfield, 1966) is not yet completed from ERTS imagery (Mohr, 1972b), and so discussion on the southern end and termination of the Western Rift is deferred.

In summary, the overall pattern of the African rift system as revealed from ERTS imagery suggests an incipient plate boundary struggling to express itself. The diffuse complexity of the pattern perhaps stems from both the slow rate of extensional movement in thick continental crust (McKenzie et al., 1970), and from the influence of the pre-existing Precambrian structures. It can be remarked that the Red Sea and Gulf of Aden cut straight enough and singly in their respective traverses across the Arabo-African continent, but their spreading rates are appreciably faster and there were no cratonic nuclei to deflect their initial paths. The Tanganyika block (Dodoman nucleus) has surely played an important role in the division of the Western from the Eastern Rift.

Other features

The ERTS imagery reveals numerous other features of interest to the structural geologist, the volcanologist, the glaciologist, the sedi-

mentologist and the economic geologist. Not all these features can be even briefly referred to here.

Noteworthy from the ERTS mapping is the persistent occurrence of ENE-trending lineaments. As mentioned in the previous section, there are important extra-rift normal faults of this trend, branching from or intersecting with the western margins of both the Western and Eastern Rifts. However, these faults tend to be curvilinear or even sinuous, whereas the lineaments, as their name implies, are linear. Well then, are these lineaments real structural elements, or are they 'hallucinosutures' (Shackleton, 1973; Tazieff, 1973)? Whilst the regular sun-angle obtaining during ERTS imaging might be expected to favour addition to ENE-NE trending hallucinations, in fact there is sufficient variation of this angle with latitude and season that hallucinosutures might be expected to vary more in their trend than they actually do. In this work, given lineaments have been identified regardless of season, though their intensity of expression may vary. Also, although the writer once grossly exaggerated the importance of ENE-trending lineaments in Ethiopia (Mohr, 1967), yet there is sufficient ground-knowledge to relate some lineaments of this trend to linear faults, lines of warping, dykes, and possible fracture lines without significant displacement, such that their existence must be faced and not pre-diagnosed. The lineaments, now precisely located from ERTS imagery, require to be examined carefully on the ground, though their structural significance will probably only be realised from a synthetic study of the fracture pattern of the African continent as a whole.

Calderas, volcanic craters and associated young lava fields are usually prominent on the ERTS imagery of eastern Africa. Mapping from the imagery is revealing that at least some of the major volcanic centres are situated at tectonic nodes. That this is the case for the Rungwe volcanoes at the Mbeya node of the Western Rift was evident enough from ground surveys. But it is now seen, for example, that Alid caldera in northern Afar lies on the intersection of the Precambrian Atsbi horst (Kazmin and Garland, 1973) lineament of the Ethiopian plateau with the Quaternary fault-belt of the floor of northernmost Afar.

Glaciated valleys can generally be recognised without difficulty on the highest mountains of eastern Africa. In the Sagatu Mts, east of the main Ethiopian rift, such valleys cut across the margin dyke-swarm of the rift valley and have been mapped by the author and E.C. Potter (in preparation). The largest glaciated valleys in the whole of eastern Africa have been recognised from the ERTS imagery of the Simien Mts, northern Ethiopia (Mohr, 1963). There, glaciers as long as 40km flowed south and east from the southeastward tilted crest of the Miocene Simien shield volcano.

No certain meteorite craters have been identified from the ERTS imagery of eastern Africa. Worthy of possible attention, however,

are the circular feature at 10°45'S, 27°45'E, and a better preserved but less symmetrical feature at 7°25'S, 28°15'E.

REFERENCES

- Almond, D.C., 1969, Structure and metamorphism of the Basement Complex of north-east Uganda. *Overseas Geol. Min. Resources*, 10, 146-163.
- Azzaroli, A., and Merla, G., 1957, Carta geologica della Somalia e dell'Ogaden (1:500,000). *Agip Mineraria-Consig. Naz. Ricerche*, Firenze.
- Baker, B.H., 1963, Geology of the Baragoi area. *Geol. Surv. Kenya*, Rep. 53, 74pp.
- Baker, B.H., 1967, Geology of the Mount Kenya area. *Geol. Surv. Kenya*, Rep. 79, 78pp.
- Baker, B.H., Mohr, P.A., and Williams, L.A.J., 1972, Geology of the Eastern rift system of Africa. *Geol. Soc. Amer.*, Spec. Paper 136, 67pp.
- Beydoun, Z.R., 1970, Southern Arabia and northern Somalia: comparative geology. *Phil. Trans. R. Soc. London, A*, 267, 267-292.
- Beyth, M., 1972, To the geology of central-western Tigre. *Rheinische Friedrich-Wilhelms Univ., Bonn*. 159pp.
- Bloomfield, K., 1966, Geological map of Malawi. *Geol. Surv. Malawi*.
- Brown, P.E., 1962, The tectonic and metamorphic history of the Pre-Cambrian rocks of the Mbeya region, southwest Tanganyika. *Quart. J. Geol. Soc. London*, 118, 295-317.
- Cahen, L., 1970, Igneous activity and mineralisation episodes in the evolution of the Kibaride and Katangide orogenic belts of central Africa. In: *African Magmatism and Tectonics* (eds, Clifford, T.N., and Gass, I.G.), Oliver & Boyd, Edinburgh, p. 97-117.
- Canuti, P., Gregnanin, A., Piccirillo, E.M., Sagri, M., and Tacconi, P., 1972, Volcanic intercalation in the Mesozoic sediments of the Kulubi area (Harrar, Ethiopia). *Boll. Geol. Soc. Ital.*, 91, 603-614.
- Chater, A.M., and Gilboy, C.F., 1970, Stratigraphic and structural relations in the Shakisso-Arero region of southern Ethiopia. 14th Ann. Rep. Res. Inst. Afr. Geology, Univ. Leeds, 8-11.
- Clifford, T.N., 1970, The structural framework of Africa. In: *African Magmatism and Tectonics* (eds. Clifford, T.N., and Gass, I.G.), Oliver & Boyd, Edinburgh, 1-26.
- Di Paola, G.M., 1973, The Ethiopian rift valley (between 7°00' and 8°40' lat. North). *Bull. Volc.*, 36, 517-560.
- Gass, I.G., Cox, K.G., and Mallick, D.I.J., 1965, Royal Society volcanological expedition to the South Arabian Federation and the Red Sea. *Nature*, 205, 952-955.
- Hepworth, J.V., 1972, The Mozambique orogenic belt and its foreland in northeast Tanzania: a photogeologically based study. *J. Geol. Soc. London*, 128, 461-500.
- Kazmin, V., and Garland, C.R., 1973, Evidence of Precambrian block-faulting in the western margin of the Afar depression, Ethiopia. *Geol. Mag.*, 110, 55-57.

- King, B.C., 1970, Volcanicity and rift tectonics in East Africa. In: African Magmatism and Tectonics (eds. Clifford, T.N. and Gass, I.G.), Oliver & Boyd, Edinburgh, p. 263-283.
- Levitte, D., Columba, J., and Mohr, P.A., 1974, Reconnaissance geology of the Amaro horst, southern Ethiopian rift. Bull. Geol. Soc. Amer., (in press).
- McConnell, R.B., 1972, Geological development of the rift system of eastern Africa. Bull. Geol. Soc. Amer., 83, 2549-2572.
- McKenzie, D.P., Davies, D., and Molnar, P., 1970, Plate tectonics of the Red Sea and East Africa. Nature, 226, 243-248.
- Mohr, P.A., 1962, The geology of Ethiopia. Univ. Coll. Addis Ababa Press, 268pp.
- Mohr, P.A., 1963, Geological report on an expedition to the Simien Mountains. Bull. Geophys. Obs. Addis Ababa, 6, 155-167.
- Mohr, P.A., 1967, The Ethiopian rift system. Bull. Geophys. Obs. Addis Ababa, 11, 1-65.
- Mohr, P.A., 1970, The Afar triple junction and sea-floor spreading. J. Geophys. Res., 75, 7340-7352.
- Mohr, P.A., 1972a, Surface structure and plate tectonics of Afar. Tectonophysics, 15, 3-18.
- Mohr, P.A., 1972b, ERTS-1 imagery of eastern Africa: a first look at the geological structure of selected areas. Smithsonian Astro. Obs., Spec. Rep. 347, 57pp.
- Mohr, P.A., 1973, Structural elements of the Afar margins: data from ERTS-1 imagery. Bull. Geophys. Obs. Addis Ababa, 15 (in Press)
- Sanders, L.D., 1965, Geology of the contact between the Nyanza Shield and the Mozambique Belt in western Kenya. Geol. Surv. Kenya, Bull. 7, 45pp.
- Shackleton, R.M., 1967, Complex history of the Mozambique Belt. 11th Ann. Rep. Res. Inst. Afr. Geology, Univ. Leeds, 12-13.
- Shackleton, R.M., 1973, In: Implications of continental drift to the earth sciences (eds. Tarling, D.H., and Runcorn, S.K.). Academic Press, London (in press).
- Sutton, J., and Watson, J., 1959, Metamorphism in deep-seated zones of transcurrent movement at Kungwe Bay, Tanganyika Territory. J. Geology, 67, 1-13.
- Tazieff, H., 1970, The Afar Triangle. Scientific Amer., 222, 32-40.
- Tazieff, H., 1973, About air and space photo interpretations of Afar. Trans. Amer. Geophys. Un., 54, 470 (abstract only).
- Tazieff, H., Varet, J., Barberi, F., and Giglia, G., 1972, Tectonic significance of the Afar (or Danakil) depression. Nature, 235, 144-147.
- Whiteman, A.J., 1971, The geology of the Sudan republic. Oxford Univ. Press, 290pp.

Paper G 13

TECTONIC ANALYSIS OF EAST AND SOUTH EAST IRAN USING ERTS-1 IMAGERY

Khosro Ebtehadj, Remote Sensing and Data Collection Division, Plan & Budget Organization, Tehran, Iran, and Ali Ghazi, Remote Sensing and Data Collection Division, Plan & Budget Organization, Tehran, Iran, and Farrokh Barzegar, Reza Boghrati and Bahman Jazayeri, Remote Sensing and Data Collection Division, Plan & Budget Organization, Tehran, Iran

ABSTRACT

Based on a tectonic study using 1:1,000,000 ERTS-1, MSS Band 7 photo-mosaic covering an area of approximately 500,000 sq. kms. of East and South East Iran, several tectonic units, and many new faults along previously recognized fault trends, were identified.

Futhermore, detailed tectonic interpretations were also carried out over selected areas, and different tectonic styles were recognized.

(Paper not available at time of printing)

MINERAL EXPLORATION WITH ERTS IMAGERY

Stephen M. Nicolais, *Colorado School of Mines*

ABSTRACT

74 N 74 30759

Ten potential target areas for metallic mineral exploration were selected on the basis of a photo-lineament interpretation of the ERTS image 1172-17141 in central Colorado. Of the ten target areas selected, five included the following mineral districts: the Breckenridge district, the Leadville-Climax-Alma area, and the Tomichi, Bonanza and Cripple Creek districts. An evaluation of bias indicated that prior geologic knowledge of the region had little, if any, effect on target selection. In addition, a contoured plot of the frequency of photo-lineament intersections was made to determine what relationships exist between the photo-lineaments and mineral districts. Comparison of this plot with a plot of the mineral districts indicates that areas with a high frequency of intersections commonly coincide with known mineral districts. The results of this experiment suggest that photo-lineaments are fractures or fracture-controlled features, and their distribution may be a guide to metallic mineral deposits in Colorado, and probably other areas as well.

INTRODUCTION

Mineral exploration is an often-cited potential application of orbital remote sensing data. However, before a new method, system or instrument is employed by industry, it must show potential use and economic feasibility. In this light, an experiment was designed to test the application of photo-lineament information obtained from ERTS imagery to the selection of potential target areas for mineral exploration. The objectives of the experiment were:

- 1) To select potential target areas based on the distribution of photo-lineaments and their intersections, as obtained from the ERTS image.
- 2) To evaluate the target areas.
- 3) To determine what relationships, if any, exist between the distribution of photo-lineament intersections and the location of mineral districts.

PRECEDING PAGE BLANK NOT FILMED

The test area was defined by a single ERTS image of central Colorado (Fig. 1), which includes a part of the Colorado Mineral Belt, and thus, several major mining districts. The northeast-trending mineral belt is characterized by intrusive porphyries of Late Cretaceous and early Tertiary age (1). Ore deposition, in most cases, was structurally controlled by faults and shear zones.

ANALYSIS AND RESULTS

Photointerpretation

Photointerpretation was performed on the 11 January 1973 image 1172-17141 (Fig. 2) using a Bausch & Lomb zoom stereoscope in both stereoscopic and monoscopic modes. The 9.5 x 9.5-inch positive transparencies of all four MSS bands were used; however, most of the data was obtained from band 7. This image was chosen over other images of the same scene because the topography is enhanced by the low-angle solar illumination (23° inclination) and snow cover in the mid-winter imagery. The first step of the experiment consisted of interpreting the ERTS image and plotting the photo-lineaments on an overlay (Fig. 3). Two types of elements were plotted: straight lineaments and curvilinear, or circular, features.

Target Area Selection

Potential reconnaissance target areas were selected on the basis of the lineament data obtained. Selections were made under the following assumptions:

- 1) We are looking for metallic mineral deposits
- 2) Mineralization is probably structurally related to faults and shear zones, which may, in turn, be spatially related to intrusive stocks, plugs and volcanic centers.

Target selection consisted of two steps. First, about 40 small, specific targets were chosen based on the numbers and kinds of photo-lineament intersections. Next, the 10 best target areas (Fig. 4) were selected from the first group. Each target area corresponds to a circular area on the ground about 14 km (9 mi) in diameter or approximately 165 sq km (64 sq mi). The 10 final target areas were broken down into three orders of priority (1, highest, etc.) based on the complexity, type and strength of the intersections and the presence or absence of curvilinear or circular features. Of these criteria, complex areas of intersections and intersections of photo-lineaments with curvilinear or circular features were felt to be the most important.

Target Area Evaluation

A map of Colorado mineral deposits (2) was used to evaluate the target areas. The location of the larger mineral districts and the selected target areas are shown in the overlay in Figure 5. Most of the annotated mineral districts have produced over \$100,000 in metals; however the combined production of Climax, Leadville and Cripple Creek has been over \$1,000,000,000 in precious and base metals. Other important mineral districts which have had production figures over \$1,000,000 include Breckenridge, Kokomo, Alma, and Bonanza. Five of the 10 target areas coincide with the following mineral districts: Breckenridge, the Leadville-Climax-Alma area (covered by one target area), Tomichi, Bonanza, and Cripple Creek. These results were better than expected, so the influence of prior geologic knowledge of the test area on target selection was tested.

Bias in Target Selection

Copies of just the lineament interpretation were distributed to a test group of 15 Colorado School of Mines professors and graduate students. After being instructed on the basic assumptions made during the selection of the Phase I target areas (those chosen in the first part of the experiment), each member of the group was asked to select 10 circular, 14 kilometer-diameter target areas. Analysis of the test group's selections (Phase II target areas) showed a remarkably strong agreement for 8 target areas, 5 of which coincide with mineral districts; 4 of these 5 were also picked during Phase I of the experiment. The test group's successful targets (i.e. coincidence with a mineral district) are tabulated and compared with the successful Phase I targets in Figure 6. There is a fairly strong agreement among members of the test group for the target areas that outline the following mineral districts: the Leadville-Climax-Alma area, Tomichi, Monarch, Bonanza and Cripple Creek districts.

Statistical analysis was used to evaluate both the test group's results and the method of target selection used in the experiment. The probability of selecting one successful target area in ten tries by random process is .32; this value decreases to .01 for selecting five successful target areas. In addition, the probability of 5 people choosing the same successful target area by random process is a mere 1.4×10^{-9} . The analysis was performed by placing a square grid with the approximate dimensions of a target area (9-x9-mile squares) on the lineament interpretation and the mineral district overlays. The probabilities were calculated assuming that there are 12 chances for a target area to coincide with a mineral district and there are 70 possible choices (target areas-squares) which coincide with photo-lineaments occurring on the overlay.

Analysis of the test group's results indicate that bias had very little, if any, effect on the selection of the Phase I target areas, and suggests that some of the mineral districts are defined by photo-lineament information.

Photo-Lineaments and Mineral Districts

To determine what relationships exist between mineral districts and photo-linears, the frequency of photo-lineament intersections was plotted using a computer program originally designed to plot stereonet data in a form suitable for contouring. The contoured plot shows the density, or concentration, of all types of intersections on the photo-lineament overlay (Fig. 7).

The Cripple Creek district is well defined by a high density of lineament intersections, and the Kokomo, Climax-Alma, Goldbrick-Pitkin and Tomichi districts are moderately-well defined. The Leadville and Bonanza districts were not discriminated by this method. It should be noted that the Kokomo and Goldbrick-Pitkin districts do not coincide with the previously-selected Phase I target areas, but they are discriminated by a high density of photo-lineament intersections. It is also interesting to note that the 8 target areas that show good agreement among members of the test group, also coincide with areas having a high concentration of lineament intersections.

SUMMARY

A promising approach to the selection of mineral exploration targets using ERTS imagery has been demonstrated. This study reduced an original search area of 33,500 sq km (13,000 sq miles) to ten 165 sq km (64 sq mi) reconnaissance target areas that appear to have the structural relationships commonly associated with mineralization in this region. Major mineral districts exist in 5 of the 10 target areas selected. In addition, this experiment shows a definite correlation between some of the major mineral districts in this part of Colorado and areas having a high density of photo-lineament intersections as interpreted from ERTS imagery.

CONCLUSIONS

The results of this experiment suggest that photo-lineaments on ERTS imagery are fractures or fracture-controlled features and that their distribution may be a guide to metallic mineral deposits in Colorado, and probably other areas as well. Analysis of photo-lineament information contained on ERTS imagery can be a very valuable and inexpensive first step in any mineral exploration program, especially if it is used in conjunction with other sources of geologic information. Imagery acquired from space will

probably prove most useful in areas of the world in which less is known about the geology. Moreover, the favorable results of this study suggest that those target areas that do not correspond with known areas of mineralization may, in fact, be new targets for mineral exploration in Colorado.

ACKNOWLEDGMENTS

Support for this study was provided by the Colorado School of Mines/ERTS project, funded by NASA Contract NAS5-21778. Appreciation is extended to Daniel H. Knepper, Gary Raines and Drs. Donald Sawatzky and Milton Wiltse for their help and suggestions during this investigation.

REFERENCES

1. Ogden Tweto and P.K. Sims. Precambrian ancestry of the Colorado Mineral Belt. Geol. Soc. America Bull., v. 74, p. 991-1014. 1963.
2. J.W. Vanderwilt. Mineral Resources of Colorado, Plate 4. State of Colorado Mineral Resources Board, Denver, 547 p. 1947.

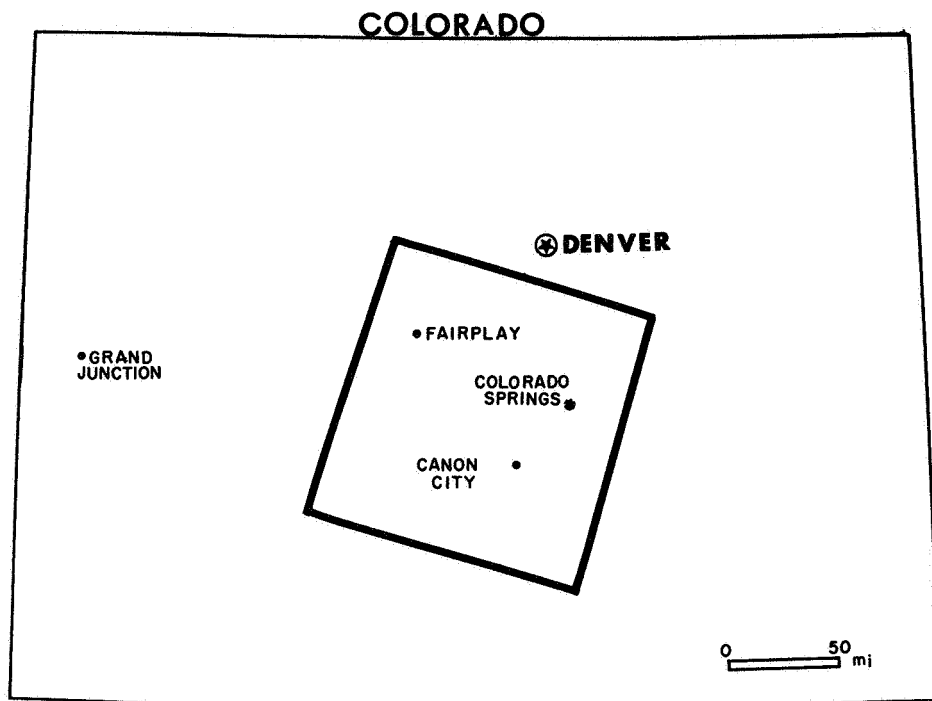


Figure 1. Colorado index map. Geographic location of the ERTS imagery used in this investigation.



Figure 2. 11 January 1973 ERTS image 1172-17141-7.

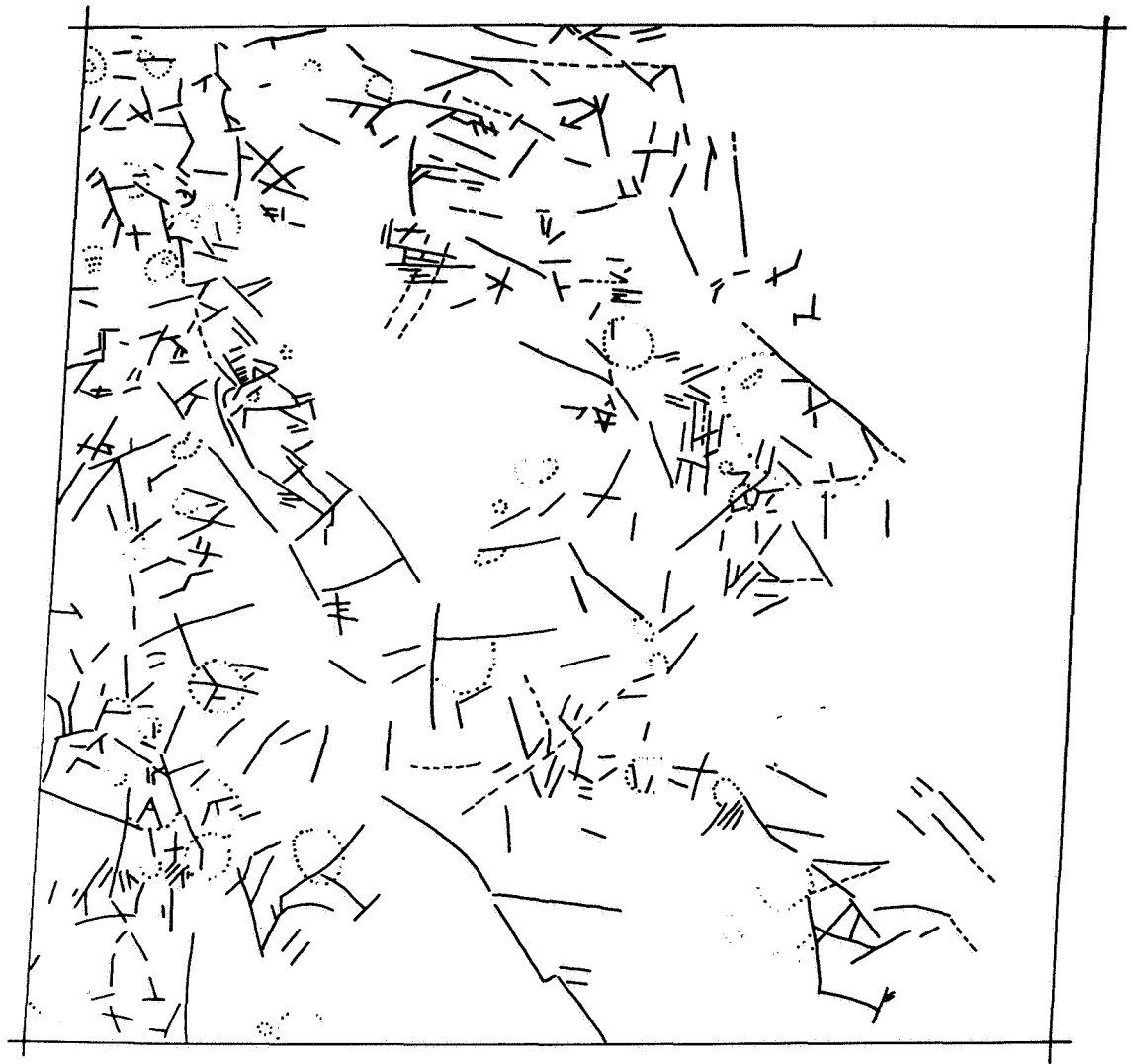


Figure 3. Photo-lineament overlay. Solid lines are well-defined linears; dashed lines are possible or moderately expressed linears; dotted lines are curvilinear or circular features.

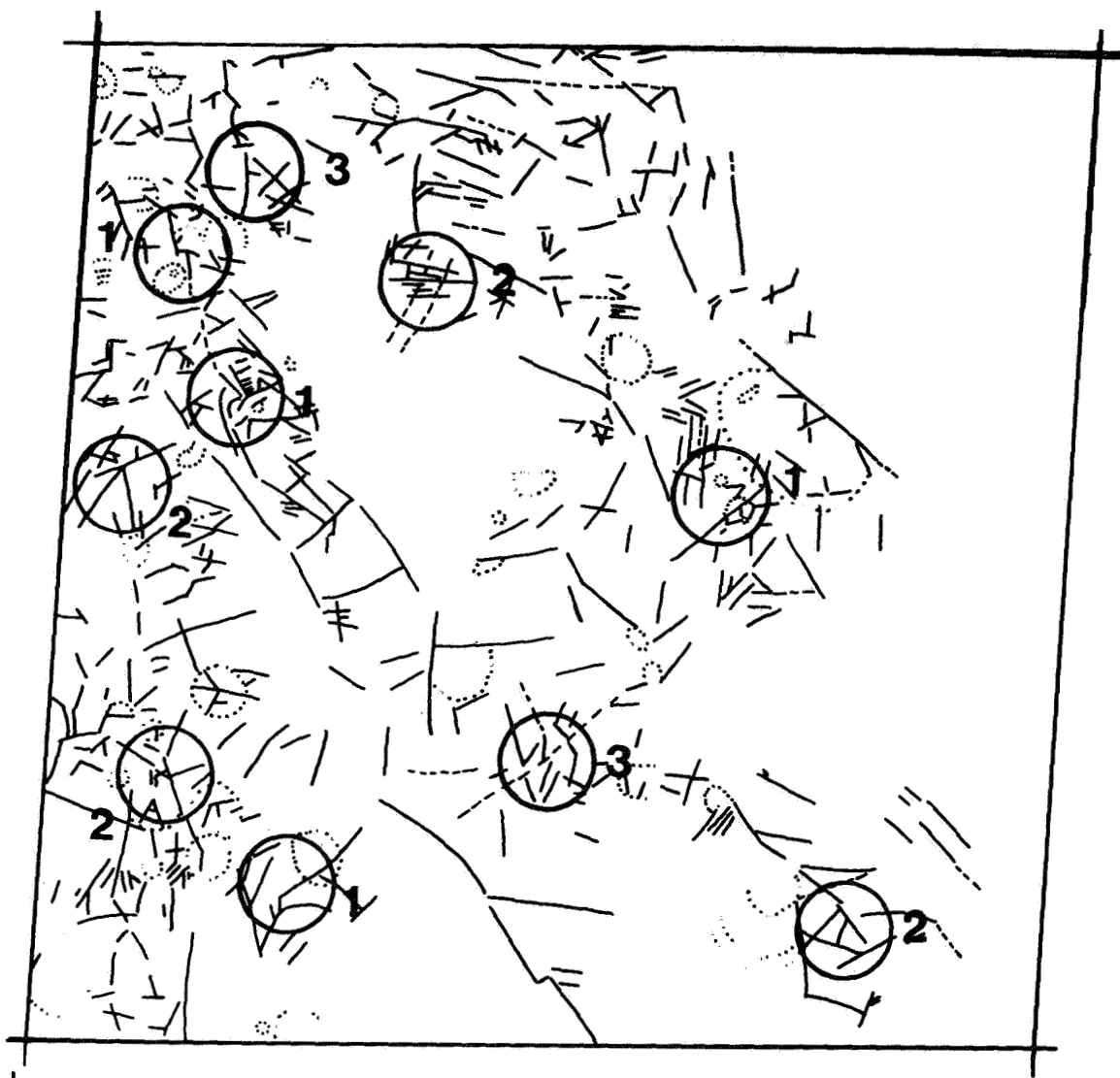


Figure 4. Location of target areas selected on the basis of photo-linears. The priorities (1, highest, etc.) are indicated by the number next to each target area.

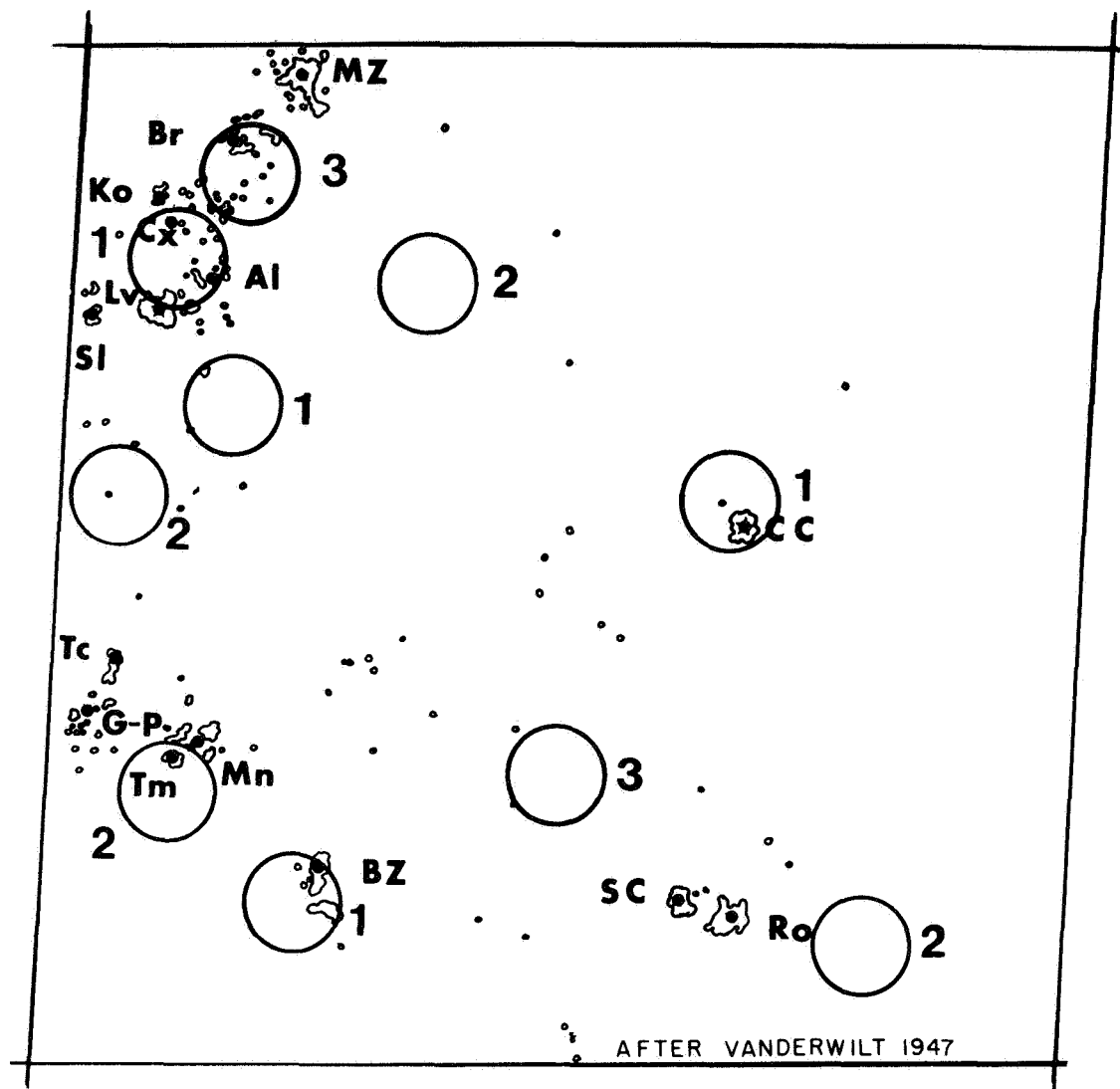


Figure 5. Location of major mineral districts and selected target areas. The small circles are isolated areas of mineral production, generally of low value. The larger mineral districts indicated by a black dot have irregular outlines and are annotated by an abbreviation: MZ-Montezuma, Br-Breckenridge, Ko-Kokomo, Cx-Climax, Al-Alma, Lv-Leadville, Sl-Sugarloaf, Tc-Tincup, G-P-Goldbrick-Pitkin, Tm-Tomichi, Mn-Monarch, BZ-Bonanza, CC-Cripple Creek, SC-Silver Cliff, Ro-Rosita.

TEST GROUP RESULTS

MINERAL DISTRICTS	A	B	C	D	E	F	G	H	I	J	K	L	M	N	O	P	%
MONTEZUMA																	
BRECKENRIDGE												X				0	13
KOKOMO				X	X	X							X		X		31
CLIMAX	X			X	X	X	X	X		X	X		X	X	X	0	75
LEADVILLE	X		X	X	X	X	X	X	X	X	X			X		0	75
ALMA	X		X	X	X	X	X	X		X	X		X	X	X	0	81
SUGARLOAF																	
TINCUP									X								6
GOLDBRICK-PITKIN					X												6
TOMICHI			X		X	X		X			X	X		X	X	0	56
MONARCH	X	X			X	X	X			X				X			44
BONANZA	X					X	X	X		X				X		0	44
SILVER CLIFF																	
ROSITA																	
CRIPPLE CREEK			X	X		X	X	X	X	X		X	X	X	X	0	75

Figure 6. Test group's successful target areas. Each letter across the top corresponds to a member of the test group. Coincidence of a mineral district with a target area is indicated by the letter X. The letter O in column P represents the successful target area selections of Phase I. The last column indicates the percent agreement for successful target areas selected during Phase I and Phase II of the experiment.

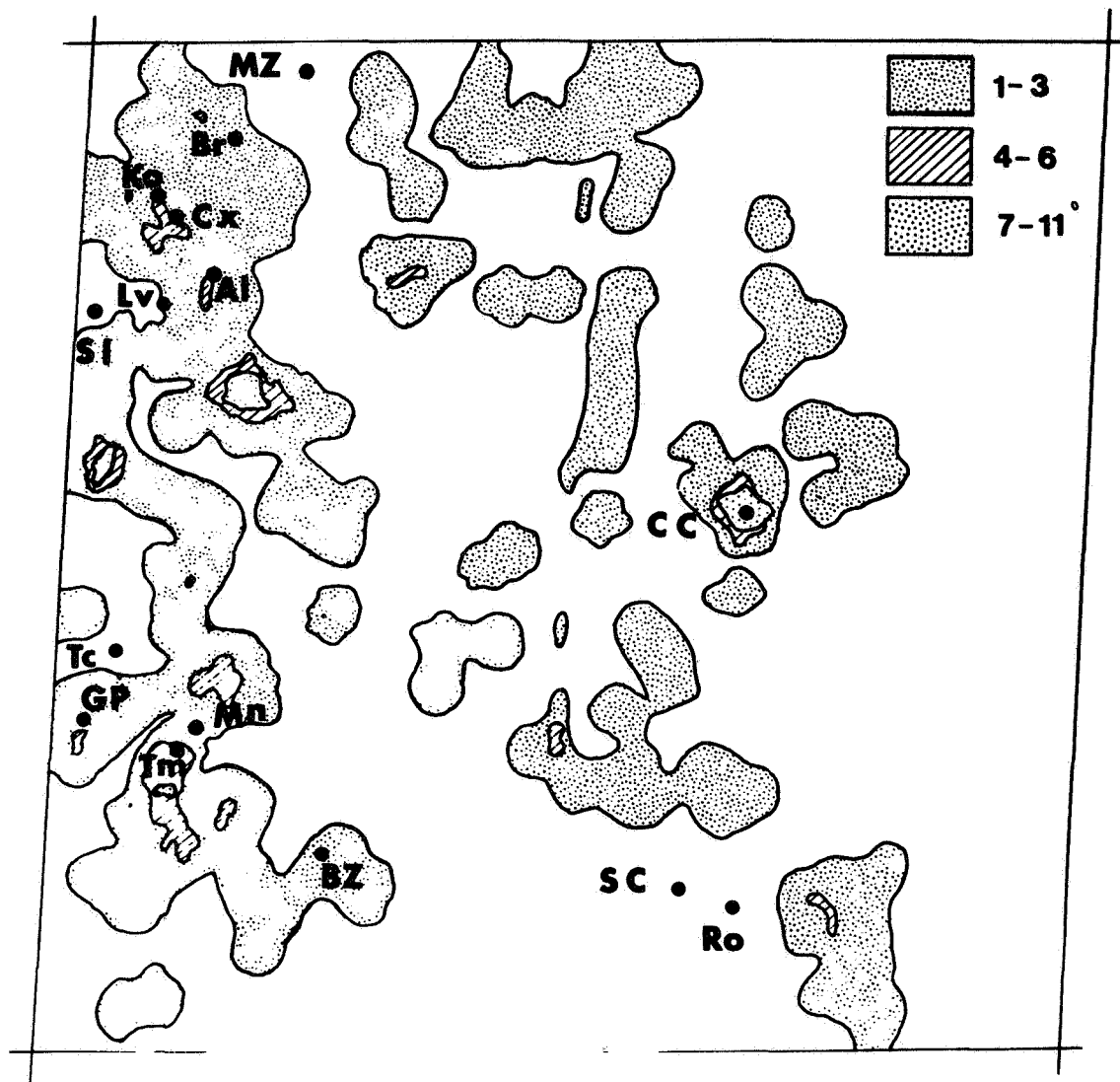


Figure 7. Density of photo-lineament intersections and the location of major mineral districts. The numbers in the legend represent the number of photo-lineament intersections per unit area.

**'ERTS-1 IMAGERY' AS AN AID TO THE UNDERSTANDING OF THE REGIONAL
SETTING OF BASE METAL DEPOSITS IN THE NORTH WEST CAPE PROVINCE,
SOUTH AFRICA**

Dr. Richard P. Viljoen, *Geological Research Department, P.O. Box 2, Randfontein. Rep. of South Africa*

ABSTRACT

A number of base metal finds have recently focussed attention on the North Western Cape Province of South Africa as an area of great potential mineral wealth. Extensive exploration programmes were initiated by many organizations but these programmes were hampered by the fact that the area is geologically unsurveyed. Available geological maps cover only a strip of country along the south bank of the Orange river, and areas to the west and south of the Springbok - O'Kiep copper mining region.

From the point of view of competitive mineral exploration it was essential that an insight into the regional geological controls of the base metal mineralization of the area be obtained as rapidly as possible. Conventional methods of producing a suitable regional geological map were considered to be too time-consuming and ERTS-1 imagery was consequently examined.

This imagery has made a significant contribution in the compilation of a suitable map on which to base further mineral exploration programmes. Major structural features, including folds, faults and lineaments, as well as the lateral extent of various important stratigraphic units, are clearly discernable on the available images. Important new data have come to light even in areas where published maps are available. In some instances, older stratigraphic trends can be deciphered through thin flat lying younger cover sequences.

Reconnaissance field work aimed at the identification of major rock units and other conspicuous features seen on the images was found to be important prior to interpretation. In addition a more detailed map was produced by identifying less obvious features on the images from a light aircraft flying at an altitude of approximately 2 000 m above ground level.

The time involved in the compilation of maps of this nature was found to be only a fraction of the time necessary for the production of similar maps using other methods. ERTS imagery is therefore considered to be valuable in producing accurate regional maps in areas where little or no geological data are available, or in areas of poor access. Furthermore, these images have great potential for rapidly defining the regional extent of metallogenic provinces

7
N74 30760

INTRODUCTION

The region discussed in this paper comprises a portion of the north western Cape Province of the Republic of South Africa and lies mainly to the south of the Orange river. It also includes a small portion of southern South West Africa on the northern side of the river and is bounded by latitudes 28°S - 31°S and longitudes 16°E - 24°E . (Figure 1).

The region is one of very low rainfall, so that in most places vegetation cover is sparse or non-existent. Erosion caused by the Orange river has resulted in the development of a broad strip of excellent rock exposures along both flanks of the river. To the north and south of this zone, outcrops become progressively poorer and eventually the older geological formations of the river valley are covered by flat lying younger strata at an elevation of some 500 meters above the river bed.

Despite the fact that copper deposits associated with small plugs of basic igneous rock have been known and mined in the western portion of the terrain (Springbok - O'Kiep area) for many years, the rest of the area was never considered to be particularly interesting as far as base metal mineralization was concerned. With the discovery of a major Cu - Zn deposit in the eastern part of the region (Prieska area) several years ago, followed by other significant base metal finds between this occurrence and the Springbok - O'Kiep copper occurrences, it became apparent that the entire region might represent a metallogenic province of considerable economic importance.

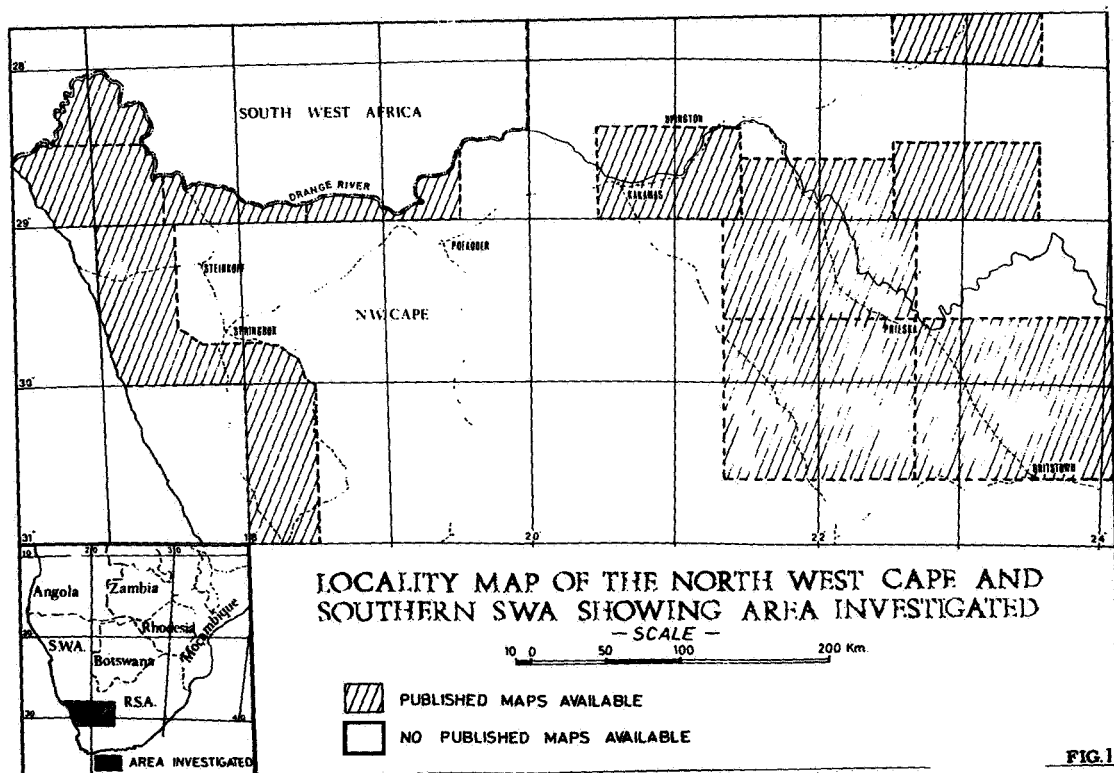
Numerous organisations commenced exploration in the area and from a competitive point of view it was imperative that the relationship between the various deposits and the regional geology of the area be established as rapidly as possible.

Previous geological work in the region included good mapping along the Orange river by the South African Geological Survey, as well as mapping in areas to the west and south of the Springbok - O'Kiep copper mining district where most of the work has been carried out by Dr. Joubert of the Precambrian Research Unit of the University of Cape Town. (See fig. 1). Nevertheless, large areas and particularly those where the new base metal finds were made, remained unmapped and the regional structure of the terrain was not understood. Conventional methods of producing suitable regional geological maps were considered to be too time consuming and ERTS-1 imagery was consequently examined.

METHODS OF STUDY

Eight ERTS-1 colour composite images enlarged to a scale of 1:500 000 were used for the compilation of a regional geological map of the area. A mosaic constructed from the images used in this compilation has been reduced in fig. 2 to a scale of approximately 1:2 000 000. A generalized map illustrating the interpretation is shown in fig. 3. A number of details have been omitted from this interpretation because of the competitive nature of mineral exploration in the area at the present time.

Before any interpretation was carried out, a detailed study of all the available published maps was made in order to correlate the expression of various formations with features seen on the ERTS images. Reconnaissance road traverses were undertaken in both the mapped areas and unmapped areas to establish ground truth. Final interpretation was carried out after a certain amount of mapping had been done directly on the images correlating geological features from a light aircraft flying at an altitude of about 3 000 meters above ground level. These data were then plotted onto 1:500 000 topographic sheets, somewhat simplified and finally reduced to a scale of approximately 1:2 000 000 (fig. 3).



GEOLOGICAL INTERPRETATION

Introduction

The area under consideration is divisible into four main geological entities, the most important of which is an extensive 1 000 million years old, metamorphic gneiss terrain, the Bushmanland Metamorphic Complex, which is well exposed in the valley of the Orange river. This metamorphic terrain is terminated to the east of Upington by a major NNW - SSE trending zone of dislocation (the Kibbos fault zone). This fault zone separates the Metamorphites from a very much older granite-greenstone terrain lying to the east and known as the

Kaapvaal craton. In the area under consideration the Kaapvaal craton is for the most part largely covered by relatively unmetamorphosed, predominantly sedimentary rocks belonging to a series of extensive ancient cratonic basins. Geochronological studies indicate that most of the basement granites of the Kaapvaal craton have ages in excess of 2.5 billion years.

In the western portion of the area, in a region known as the Richtersveld (fig. 3), the structural style and the grade of metamorphism changes and a series of vulcano-sedimentary formations striking roughly north-south are associated with granite (the Violsdrift granite) which has an age of about 1 800 million years. In the north and south central portions of the area the Bushmanland metamorphites are overlain by much younger flat-lying sedimentary formations belonging to the Nama and Karroo systems. Each of these major geological entities will be described in turn.

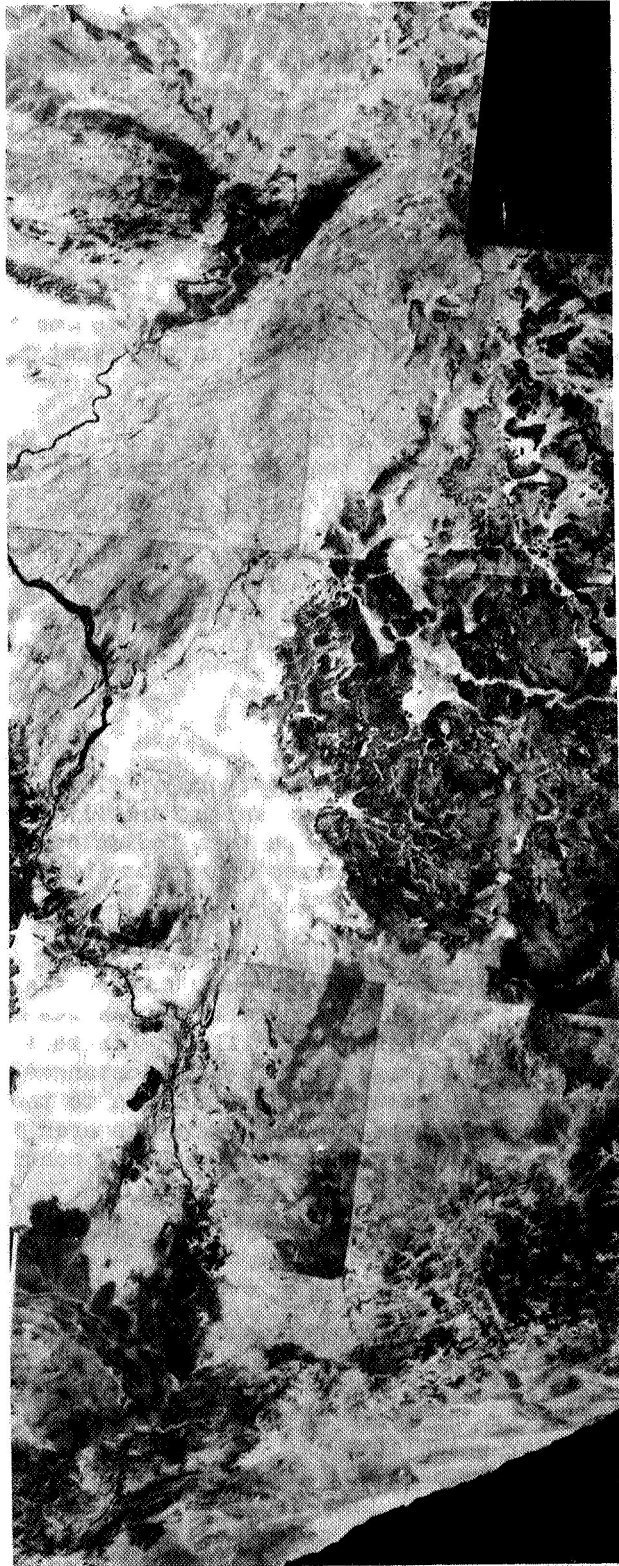


Figure 2.

Sedimentary formations of the Kaapvaal craton

One of the most striking features seen on the ERTS images is the spectacular discontinuity (the Brakbos fault zone) that separates the Kaapvaal craton in the east from the Bushmanland metamorphic complex in the west. Although this zone has been described briefly by a number of authors and detailed mapping aimed at establishing geological relationships is at present being undertaken, no definitive results have as yet been published. In this respect a number of features observed on ERTS imagery might well prove to be invaluable in the final assessment of the problem. These are:-

- a. The existence of a number of major faults parallel to and lying east of the Brakbos fault zone, clearly discernible in the country immediately west of the town of Prieska.
- b. Intense deformation mainly in the form of folding of the north-south striking sedimentary formations as they approach the Brakbos fault zone from the north east.
- c. All the sedimentary formations appear to have been abruptly truncated by the Brakbos fault zone and there is no evidence of them straddling this discontinuity and thus being represented within the Bushmanland metamorphic complex as has been suggested.

Flat-lying Sedimentary cover rocks

The imagery clearly reveals the distribution pattern of flat lying sedimentary beds belonging to the Karroo and Nama systems which formerly covered most of the Bushmanland metamorphic complex. This pattern indicates both the erosive action of the Orange river and its tributaries and yields information regarding the underlying basement structure (see later).

The Karroo sediments are clearly recognisable by their grey or dark grey colours whereas the Nama strata are characterized by brownish hues. Areas of thick and thin Karroo cover are also apparent, especially in the region to the south of Pofadder. In addition dolerite dykes and sills within this formation can be mapped in great detail from the images and in many instances appear to be partly controlled by major linear features as in the area to the south west of Kenhardt (fig. 3). Numerous salt pans especially in the area to the south of Kenhardt (not indicated on the map) are even more strongly controlled by these linear features.

Older volcano-sedimentary formations of the west coast

A number of generally north-south trending volcano-sedimentary formations have been mapped in the Richtersveld area adjacent to the west coast (fig. 3). These rocks have not been involved with the 1 000 million years old metamorphic overprinting which has affected the rocks of the Bushmanland sequence. They have been intruded by granites which have radiometric ages of approximately 1 800 million years and thus form part of a zone that is probably marginal to the Bushmanland Metamorphic Complex. The extent of the Stinkfontein formation, which comprises one of the most important components of the volcano sedimentary formation under consideration, is clearly discernible on the ERTS imagery (fig. 3).

The geology and structure of the Bushmanland Metamorphic Complex

The Bushmanland Metamorphic Complex forms part of a more extensive belt of 1 000 million years old metamorphic rocks which extend across the southern portion of

South Africa and includes both basement and supracrustal sequences. Rock types encountered in the latter group are of considerable importance from an economic point of view and comprises a large variety of quartz-felspathic gneisses with variable amounts of biotite and muscovite, banded amphibolitic and calc silicate assemblages and a variety of quartzitic rocks. The basement upon which they rest is ill defined but is probably represented by porphyroblastic augen gneisses.

The entire assemblage has undergone intense deformation and several periods of folding have been described by Joubert from the area to the west and south of the Springbok - O'Kiep mining district. Numerous fault zones and lineaments also feature prominently and have played an important part in the overall tectonic framework of the region.

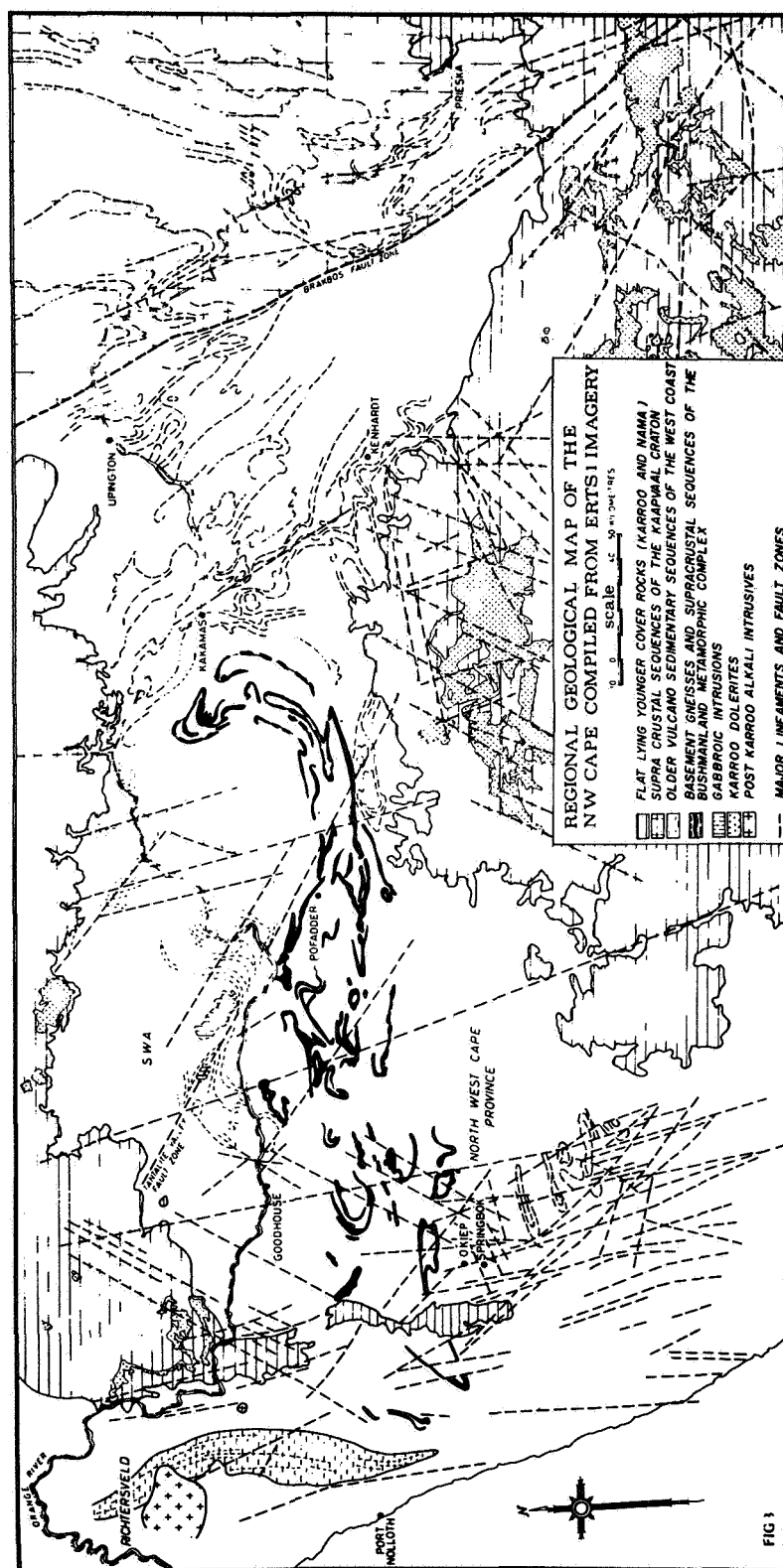
The supracrustal sequence has been recognised from a point some 30 kilometers from the west coast striking in an easterly direction towards a major zone of dislocation (the Tantalite valley fault zone) situated a short distance to the north east of the town of Pofadder and trending NW - SE (fig. 3).

As each major sequence of east-west striking rocks crosses this zone of dislocation it is deflected to form large refolded lobate structures on the north eastern side. The latter structures have a general north-south strike but are themselves deformed by younger folds with axes trending parallel to the Tantalite valley fault zone. This phenomenon is well illustrated in the area immediately north of the Orange river by the sequence of rocks which commences in the Goodhouse area. It is also shown by the sequence portrayed by the black ornament which commences in the region to the north west of the Springbok - O'Kiep mining district and strikes in an overall east east direction towards the town of Pofadder. Immediately east of the town the assemblage swings sharply northwards and then north west culminating in a position to the west of Kakamas on the Orange river (fig. 3).

The stratigraphic sequence lying to the south of the Springbok - O'Kiep mining district also strikes east - west but is covered as one proceeds east, firstly by sand and then by younger flat lying sediments of the Karroo system. When these rocks again make their appearance from under the Karroo cover in the vicinity of Kenhardt, they strike in a generally north west direction from this town to Kakamas on the Orange river (fig. 3). The relationship between mineral deposits and various stratigraphic components of the sequences described above is naturally of great importance and in this respect the regional geological map presented in this paper has acted as a most important and invaluable guide to the longer term planning of mineral exploration programmes. The results of the exploration carried out to date are encouraging and further work is continuing.

Faults and linear features

Numerous well defined linear features, some of them undoubtedly representing faults and in most cases not mapped previously, constitute conspicuous features



on the imagery. A number of prominent directions have influenced the geology to a large extent.

a. NNW - SSE Direction

A very strong set of fractures conforming to this direction, which parallels the west coast, occurs in a strip of country occupying the coastal region for a distance of some 120 kilometers inland. Features such as the termination of younger cover sequences at this point, the preservation of cover sequences in a NNW - SSE trending belt between the eastern Richtersveld and the Springbok - O'Kiep mining area, the north south trending zones of older vulcano-sedimentary rocks in the Richtersveld and the general attenuation of the Bushmanland supracrustal rocks in this area, suggest that the entire coastal strip has been an area of active uplift with attendant faulting which has preserved both younger and older sedimentary sequences in the area.

This direction of fracturing becomes less intense further east but is again manifested by the large fault zone to the east of Goodhouse which clearly controls the distribution pattern of the younger flat lying cover sequences. Features with the same direction are also clearly to be seen in the area to the north east of Pofadder and to the south west and north west of Kenhardt, and the Brakbos fault zone itself, further east, constitutes a spectacular expression of this direction.

The latter zone with its associated parallel faults also represents a zone of relative uplift as is manifested by the southward swing of the outcrop pattern of younger cover rocks between Kenhardt and Prieska and the northward swing of similar rocks to the north of Upington.

b. NW - SE Direction

The Tantalite Valley fault zone is the most important linear feature conforming to this direction and can clearly be traced through Karroo cover in the area to the south east of Kenhardt. This fault zone has acted as the basis for the intrusion of gabbro plugs in the area to the north west of Pofadder. (fig. 3). Parallel linear features are to be seen to the north and south west of Pofadder and in the area surrounding the Springbok - O'Kiep copper mining district.

c. NE - SW Direction

Linear features conforming to this direction are well developed along the west coast zone particularly between the Richtersveld and the Springbok - O'Kiep area. The intersection of these with the other fracture directions described probably acts as the locus for the emplacement of younger igneous rocks including the Post Karroo alkali intrusives of the Richtersveld. (fig. 3).

CONCLUSIONS

ERTS imagery has proved to be invaluable in compiling a regional geological map of the N.W. Cape Province of South Africa. The area represents one in which few published geological maps exist but in which important base metal deposits have been located. Interpretation of the imagery was carried out with a limited amount of ground truth. Mapping directly onto the images from a light aircraft has clearly defined the lateral extent of potential zones of mineralization and is considered to be an important technique. This has acted as the main basis for the implementation of regional mineral exploration programmes in the area. The structural framework of the area has been well established and significant geological features have been recorded even in areas where published maps exist. Major linear features not appreciated before are clearly seen on the imagery and have played a large part in contributing to the overall geological pattern. The use of ERTS images in defining accurately the extent of metallogenic provinces in a relatively short period of time, especially in unmapped or poorly mapped areas, is unrivalled. Techniques developed during this study could act as the framework for similar investigations in other regions.

Paper G 16

MAPPING OF HYDROTHERMAL ALTERNATION ZONES AND REGIONAL ROCK TYPES USING COMPUTER ENHANCED ERTS MSS IMAGES

Lawrence C. Rowan and Pamela H. Wetlaufer, *U.S. Geological Survey National Center, Reston, Virginia*, and F. C. Billingsley and Alexander F. H. Goetz, *Jet Propulsion Laboratory, California Institute of Technology, Pasadena, California*

ABSTRACT

A combination of digital computer processing and color compositing of ERTS MSS images has been used to map hydrothermal alternation zones and regional rock types in south-central Nevada. The technique is based on enhancement of subtle visible and near infrared reflectivity differences between mineralogically dissimilar rocks, especially unaltered and altered rocks. MSS spectral bands are ratioed, pixel by pixel, in the computer and subsequently stretched. These ratio values are used to produce a new black and white image which shows the subtle spectral reflectivity differences. Additional enhancement is achieved by preparing color composites of two or more stretched ratio images.

The choice of MSS bands for rationing depends on the spectral reflectance properties of the rocks to be discriminated. For south-central Nevada, the most effective composite for detecting the alternation zones and for discriminating the rock types was prepared using the following color and stretched ratio image combination; blue for 0.5-0.6/0.6-0.7 μm ; yellow for 0.6-0.7/0.7-0.8 μm ; and magenta for 0.7-0.8/0.8-1.1 μm . Altered areas appear green to brown and show a pronounced correlation with known mineralized areas. These altered areas are not apparent on the individual MSS images, color IR composites images, or SKYLAB S190A color photographs. Silicic volcanic and intrusive rocks are mapped as a single rock type on the color ratio composite; some of these rocks have large intrinsic albedo differences, which commonly prevents their discrimination from mafic rocks in the other types of images.

Although this technique is in the initial stage of development and is untested in other areas, it already appears to have considerable potential for targeting mineral prospects and for regional geologic mapping.

(Paper not available at time of printing)

N74 30761

AN EVALUATION OF THE SUITABILITY OF ERTS DATA FOR THE PURPOSES OF PETROLEUM EXPLORATION

Robert J. Collins, F. P. McCown, L. P. Stonis, Gerald Petzel and John R. Everett

I. INTRODUCTION

- The overall objective of this experiment is to determine the types and amounts of information valuable to petroleum exploration extractable from ERTS data and the cost of obtaining the information using traditional or conventional means.

In particular, we wanted to evaluate this new petroleum exploration tool in a geologically well known area in order to assess its usefulness in an unknown area. In light of the current energy situation, we feel that such an evaluation is important in an effort to:

- Best utilize technical effort with customary exploration tools by rapidly focusing attention on the most promising areas;
- Reduce the time required to go through the exploration cycle;
- Maximize the cost savings in both of these.

* Eason Oil Company, Oklahoma City, Oklahoma
** Earth Satellite Corporation, Washington, D.C.

N 74 30762

II. DESCRIPTION OF TEST SITE

- The Anadarko Basin lies in western Oklahoma and the panhandle of Texas. It was chosen as a test site because there is a great deal of published information available on the surface and subsurface geology of the area; there are many known structures that act as traps for hydrocarbons. The Anadarko Basin is similar to several other large epicontinental sedimentary basins. Eason's geologists know the area well, and it is convenient for our offices in Oklahoma City. ●

Climate, Vegetation and Terrain

- As a result of climatic variation across the site, native vegetation ranges from scrub oak in the east, seen in this slide, to short prairie grass and sage in the west.
- The entire area is extensively farmed and ranched, and divided along township and range survey lines. This imposes a north-south and east-west cultural and vegetation pattern over the area.
- The eastern part of the area is characterized by gently rolling hills with a local relief of 60 meters. ● In the west, the topography consists of mesas and undissected uplands with sharply incised canyons producing local relief of up to 400 meters.

Geology

- The basin is a large west-northwest trending asymmetrical syncline with the south flank much steeper than the north flank. The axis of the basin where the Kodachrome was taken lies about 40 kilometers north of the Wichita Mountains, seen in the distance, which exposes early Cambrian crystalline rocks. ● The basin is filled with approximately 7,000 meters of late Pre-Cambrian and early Cambrian sedimentary and layered igneous rocks. The Paleozoic rocks include approximately 5,000 meters of Pre-Pennsylvanian limestone, shale and sandstone, approximately 5,000 meters of Pennsylvanian clastic sedimentary rocks deposited during rapid subsidence and orogenic deformation, and approximately 1,000 meters of Permian rocks, mostly red beds and evaporites accumulated during late gentle subsidence marked by periods of restricted circulation.
- Rocks at the surface include gently dipping Permian red beds and evaporites in the eastern half of the area. Tertiary continental clastic rocks of the Ogallala formation cover the western part. Quaternary deposits occur along major rivers and in large areas of wind-borne sand on the uplands.
- Most of the structures that trap hydrocarbons (marked by colored dots) were created during the intermittent tectonism that began in earliest Pennsylvanian time and continued into earliest Permian time. Many of these traps are located in the

highly deformed frontal zone north of the Wichita-Amarillo Mountain trend.

Exploration for structurally trapped hydrocarbons in the basin is exceedingly difficult because the important structures are buried by 300 to 1,000 meters of essentially undeformed Permian and younger rocks. Surface features that reflect the deeply buried structures are extremely subtle and may be interrupted by much younger solution collapse structures.

Our hypothesis was that the synoptic view provided by ERTS imagery might allow integration of a sufficient number of these subtle features so as to, in effect, see the deeply buried structures through the overlying rocks.

- Intensive petroleum exploration in the basin began in 1917. However, it is only during the past 5 years that the deeper portions of the basin have received extensive exploration attention. The deepest well in the world, the Lone Star #1, Baden, with a total depth of 30,050 feet, completed drilling last year west of the Elk City field. It is a \$5 million dry hole.

III. TECHNICAL ANALYSIS

From a total of 49 ERTS scenes received, we interpreted 16 scenes in black and white and color composite form. The

remaining 33 scenes are of limited use because they are peripheral to our test site or they contain a high percentage of cloud cover. ● We interpreted paper prints, transparencies, mosaics, and digitally-enhanced imagery. This is an optical enhancement, color combining Bands 5, 6, and 7. It brings out closed anomalies such as these.... and linears like these. ● This frame combines and offsets a negative of Band 6 and a positive of Band 7, emphasizing linears like these... ● The MSS imagery was interpreted for a variety of features. These include linear features, ● lithology, ● tonal, textural and closed anomalies, and a variety of other features such as drainage and topography. We interpreted all four MSS bands and color composites. This has resulted in more than 120 individual interpretations.

From these frame-by-frame studies, we went in two directions. One approach was to focus our attention on small areas selected by ERTS interpretation and on the basis of known oil and gas exploration interest. The second approach was to compile the various interpretations into regional overlays.

The regional compilations, selected site studies, and interpretations of individual frames were analyzed and compared to existing information. The information included published maps and reports, auxiliary imagery, and interviews with geologists in Oklahoma.

IV. RESULTS AND CONCLUSIONS

Evaluation of Imagery

- Bands 5 and 7 together have the greatest versatility and widest range of easily extractable information. Bands 5 and 7 are generally of high overall contrast and, in fact, the contrasts are frequently reversed between the two.

However, all bands must be carefully interpreted in order to derive the maximum amount and kinds of geologic information. Each band contains different features which are more easily detectable than on the other bands. On this illustration you can see linears interpreted from Band 7 of this scene. ● Combining this successively with Bands 5 and 4, you can see Band 5 linears such as A and B which were added to the interpretation previously done from Band 7. Linears C and D were visible on Band 4, but not on Band 5 or Band 7.

- Seasonal differences increase the amount of information available from ERTS. We have found that imagery of extremes of vegetation growth, that is, maximum vigor and maximum die-back, to be most useful. However, so many subtle but important differences appear throughout the year that study of imagery from an entire year or even several years is necessary for optimum results. We will next look at interpretation of the area shown here ● and in this

view. This is the Cimmaron River, North and South Canadian, a badlands area, and a gently rolling upland. ● This illustration compares our interpretation of inferred lithologies made from spring and from fall imagery.

Area A demonstrates the great amount of detail frequently obtained from spring imagery which is near-absent in the fall. Points B and C locate boundaries interpreted from fall imagery, but not seen in the spring. At D you will note more detailed and precise location of a lithologic boundary on spring coverage. Boundary E, while noted on both images, is more confidently drawn from fall imagery.

Summary of ERTS-1 Interpretation

Using ERTS-1 imagery, we have defined the major features of the Anadarko Basin and refined our understanding of many smaller areas within our test site.

- Regional analysis of the inferred lithologic distribution defines the general features of the basin. This map was compiled from interpretation of ERTS Band 7 imagery without reference to existing maps. ● Here is a generalized geologic map for comparison.
 - Analysis indicates a gentle south dip on the north flank of the basin. The dip becomes southwesterly as one moves east, indicating a plunging basin.

- Outcrop width on two sides of the basin shows asymmetry.
 - Horizontal rocks cover the west end unconformably.
 - Basement rock outcrops and alignments define the Wichita Uplift on the south.
- Our study defined several regional sets of linears. Field checks indicate these linears represent fractures. The sets trending approximately N 40 W (yellow) and N 80 W (green), in particular, are associated with or control many of the structural hydrocarbon fields. ● A few fields are located by the dots. The N 30 E set (blue) coincides with the edges of solution collapse areas and with the edges of a large thin area shown in a thickness map of Middle-Pennsylvanian rocks on the north flank of the basin. The north to N 10 W set of linears (brown) is associated with the Amarillo-Wichita Uplift on the south side of the site. These associations suggest that the regional linears are either faults or fault-related features which have been active in the past and control the location of many structural hydrocarbon traps.
- This diagram locates known and hypothesized faults and linears within the basin. ● Here, we have overlaid our working interpretation of linears made on fall imagery and have

marked in red the places where our interpretations match or extend the diagrammed linears.

The regional map of anomalies also was compared to other pertinent information. We were able to locate most known structures of interest on ERTS imagery prior to referring to existing data. ● On one composite overlay of fall imagery we counted 76 anomalous features. We classified these as geomorphic, tonal, and "hazy" areas. These "hazy" areas appear on the imagery as if image detail had been smudged or partially erased. They are not artifacts. Of 76 anomalies, 59 correlate with producing oil and gas fields, 11 are on known but non-producing structures, and the remaining 6 could not be correlated with known features. Of 35 "hazy" anomalies, 33 correlate with producing fields or drilled structures. On a recent compilation, 42 of a total of 57 "hazy" areas occur where producing fields exist. Six additional areas correlate with known but non-productive structures. ● Several "hazy" anomalies are shown on this illustration along with a few tonal, textural and geomorphic anomalies. ● Here is the same scene without the overlay.

Next, we will look at an air photo of this area. ● This is a color infrared photo taken from 60,000 feet; it is 15 miles across. The ERTS "hazy" area is outlined. After study of all air photographs taken over the "hazy" areas,

we conclude they cannot be recognized except on ERTS imagery.

We have studied small areas selected from the anomaly maps, from published reports, and at the suggestion of our petroleum geologists. In every instance, we find that focusing our attention in this fashion increases the detail we perceive in an area. Our interpretations occasionally differ somewhat from suggested or published analyses. In a few instances, notably over the Cement-Chickasha fields, we can add details to the known structure but have not been able to confidently define these large features, which are fairly shallow, strongly folded and faulted structures.

- Some of our interpretations closely match conventional interpretations as at the Mobeetie field. Its closed structure and faulted nature can be seen here,
- as well as in our ERTS interpretation. In sum, interpretation of ERTS imagery enables us to locate areas for more detailed analysis on ERTS and for aerial photographic and geophysical studies.

Auxiliary Imagery

Auxiliary imagery, particularly high altitude aerial photography, is exceedingly valuable to studies of ERTS data. The side-looking, airborne radar and thermal infrared imagery we used, despite their generally poor

quality, proved of value in defining, locating and understanding linear and geomorphic features. High altitude, small-scale, multiband, aerial photography provides a means of understanding local image responses and patterns seen on ERTS imagery. It provides a means of verifying and refining interpretations and relating field observations to ERTS imagery. The photography provides details on features which are best interpreted in the regional context provided by ERTS.

V. APPLICATION TO PETROLEUM EXPLORATION AND COSTS

We have found that the ERTS imagery is an excellent tool for reconnaissance exploration of large sedimentary basins or new exploration provinces. The imagery allows rapid interpretation of large features and quickly focuses attention on anomalous areas. For the first time, small and medium size oil companies can rapidly and effectively analyze exploration provinces as a whole.

- Let me list specific types of information derived from ERTS that are useful for petroleum exploration:
 - There is a vast quantity of information on linear features -- much more than is generally available, even on large-scale maps.

- Many of the general lithologic relationships that are known to exist in the basin are visible on the imagery.
- A large number of closed anomalies of various types appear on the imagery. The majority of these correlated with known structural features or oil and gas fields.
- Many of the details of the structures controlling hydrocarbon accumulation are visible in the imagery, once one's attention is directed to a particular area.
- The overall structure of the basin and many of the major internal structures are visible on the imagery.
- The imagery provides overall geologic context of the exploration province.

Cost Analysis

So much for ERTS data and information itself. How does the cost of a petroleum exploration program employing ERTS compare to a standard program? Because of a variety of options available for obtaining reconnaissance geological and geophysical data, cost comparisons are difficult.

Moreover, the types of data obtained by the two approaches are not precisely comparable.

Savings produced by incorporating ERTS into an exploration program might be 20% to 50% of the cost of a standard survey. The savings would be made primarily by reducing the amount of seismic and other geophysical surveys needed.

The ERTS approach would also greatly reduce the time required for regional reconnaissance and analysis of the basin and would conserve technical manpower. It is difficult to assign a dollar figure to either of these types of savings.

- In conclusion, we should mention several questions which require more study. We need to determine the exact nature and source of several anomaly types, particularly "hazy" areas. Are the anomalies man-made or man-induced? Are they geochemically-induced soil or vegetation effects, or merely fortuitous? Are the "hazy" anomalies characteristic of hydrocarbon provinces, unique, or ubiquitous? What anomalies are related to stratigraphic oil and gas traps? Which to structural traps? What aspects of this study apply to other deformed sedimentary basins? And, finally, what savings will result from incorporation of Earth Resources Satellite data into an actual exploration program?

Thank you.

**PRELIMINARY ROAD ALINEMENT THROUGH THE GREAT KAVIR IN IRAN BY
REPETITIVE ERTS-1 COVERAGE**

Daniel B. Krinsley, *U.S. Geological Survey National Center Stop 908, Reston, Virginia 22092*

ABSTRACT

The Great Kavir in north central Iran is an extensive elevated peneplain composed of intricately folded Miocene and Pliocene sediments which are rich in evaporites. Interfingering within the peneplain surface are salt-encrusted depressions which occupy 37 percent of the area of the Great Kavir. The salt, derived from the evaporites, has no bearing strength through most of the year when it is saturated; it may form rough surfaces that are unstable.

Access to the Great Kavir is generally limited to the period August through October when some salt crusts will support limited vehicular movement. The condition of the salt crusts and their parent sediments during the long wet season have been unknown. This absence of information about the surface of the Great Kavir has prevented an intensive study of a possible road alignment which could shorten the present route between northern and central Iran by 760 km.

False color diazo composites of bands 4, 5, and 7 were prepared from positives of ERTS-1 MSS images taken of the Great Kavir on September 2 and 20, 1972; December 19, 1972; February 11, 1973; March 1, 1973; and May 12, 1973. These scenes presented a record of the seasonal hydrologic changes that occurred from the dry to the wet season. During the period of maximum inundation and lowest bearing strengths, as inferred from the image of May 12, 1973, it was possible to select a preliminary road alignment that would avoid the wettest or roughest areas and take advantage of the best terrain and shortest distance. The eventual road alignment should be based on a longer record of observation and on-site investigations.

(Paper not available at time of printing)

PRECEDING PAGE BLANK NOT FILMED

N74 30763

RELATIONSHIP OF ROOF FALLS IN UNDERGROUND COAL MINES TO FRACTURES MAPPED ON ERTS-1 IMAGERY

Charles E. Wier, *Indiana Geological Survey*; Frank J. Wobber, Orville R. Russell, Roger V. Amato and Thomas V. Leshendok, *Earth Satellite Corporation*

ABSTRACT

ERTS imagery is of unique value for mapping of certain fractures that are not identifiable on aircraft imagery. Because color infrared and ERTS imagery complement each other both sources of data were used to map fractures in western Indiana and eastern Illinois. In the Kings Station Mine, Gibson County, Indiana, most roof falls reported had occurred in areas where mapped fractures were closely spaced and intersecting. Using this information as a basis for extrapolation, roof fall hazard maps were prepared for other mine sites. Various coal resources programs related to energy and environment also were conducted.

N74 30764

INTRODUCTION

The purpose of this project is to relate lineaments on imagery to fractures in bedrock, which are related to frequency and location of roof falls in underground coal mines. Hazardous areas of potentially frequent roof falls can then be predicted. The importance of such an application is emphasized by the current energy crisis.

Coal production today represents a vital national resource, which, with the shortage of petroleum products, has taken on increased importance. The need for greatly expanded coal production can most readily be fulfilled by increased surface, or strip, mining. However, expanding strip mine production is complicated by limited strippable reserves, the drastic disturbance of the landscape, and the national concern for the environment. Regardless of the pros and cons of this environmental conflict, it is certain that there will be an increase in underground coal mining operations.

Underground mining is generally more complicated than surface mining and the hazards to the miners are greater. About 75 percent of all coal mining fatalities occurred in underground mines. The U.S. Bureau of Mines identifies roof falls as the number one killer in coal mining. More than 40 percent of the fatalities in underground mining are the direct result of roof falls and wall collapse. Any method or technique which will provide greater safety to the miners is desirable and this is the prime objective of this ERTS experiment.

The area studied is the Indiana coal field that lies on the east side of the Eastern Interior Coal Basin (also called the Illinois Basin), the center of which is in southeastern Illinois. This is both a structural and a sedimentary basin and the coal bearing rocks in Indiana dip to the west and

southwest toward the center of the basin at an average rate of 25 feet per mile. Coal deposits in Indiana occur in 25 counties in the southwestern part of the state and underlie an area of about 6,500 square miles (Figure 1).

There are eight major mineable coals interbedded with some 1500 feet of shale, sandstone, underclay, limestone, and at least 25 thin coals. The rocks are covered by a foot to more than 100 feet of glacial drift, loess, alluvium, and residual soil.

Coal reserves in Indiana are estimated to be slightly more than 33,000 million tons. Most of this will be mined by underground methods. About 2,000 million tons of this is considered recoverable by current strip mining methods, and 15,000 million tons by present underground mining methods.

OBJECTIVES

The primary objectives of this project are to:

1. evaluate the utility of ERTS and aircraft imagery for fracture mapping,
2. map fractures in the coal mining area in southwestern Indiana,
3. demonstrate the extent which fractures coincide with known roof falls, and
4. predict and delimit hazardous areas for underground mining.

Related objectives of the Indiana coal resources program include:

- o Surface mined lands inventory and monitoring: A prototype national mined lands map series is being prepared in response to state and national (S425 and HR 5988) legislation.
- o Subsidence in underground mined areas: Graphic products showing zones of subsidence that may be spatially related to fracture systems are being planned.
- o Refuse bank and slurry pond inventory: Maps and tabulations to assist in setting a fair tax on coal produced; data to be used by the Indiana State Legislature.
- o Energy related data acquisition: Various production statistics for surface mining will be made available to State offices in response to the energy crisis.

UTILITY OF ERTS DATA FOR FRACTURE MAPPING

Each spectral band of ERTS imagery was evaluated for use in fracture mapping. Bands 5 and 7 were of greatest value. Band 6 was largely redundant of band 7 (Table 1). Bands 6 and 7 also proved extremely useful for delineating strip mine land, evaluating the amount and kind of reclamation, and mapping the size and shape of water bodies.

TABLE 1. ERTS Imagery Evaluation

ERTS MSS spectral band	4	5	6	7	Color Composite
Fracture detection		XX	X	X	X
Mined land delineation			X	XX	X
Reclamation (vegetal cover)		X	X	XX	XX
Water bodies (size and shape)			X	XX	X
Water discoloration and turbidity	XX				XX
Physiographic features		X	X	X	XX

X = fair to good

XX = good to excellent

Independent analysis of imagery from repeated overpasses indicated that there is considerable seasonal effect on fracture information and that only with such in-depth analysis was it possible to extract full fracture (lineament) information. Prevailing atmospheric conditions (especially haze) at the time of overpass had a marked effect on information content and analysis capabilities.

Indiana is located in a temperate climatic zone that receives substantial rainfall and is exposed to a wide range of temperatures which cause the vegetative cover to undergo drastic seasonal changes. This is especially crucial in fracture detection in the Illinois Basin where many streams reflect structural control.

Although cloud cover and haze prevent a precise comparison of the time-lapse imagery, it is evident from consecutive ERTS band 5 imagery that tree-lined drainage systems which are relatively obscure in August, are most highly contrasted in October and diminish in contrast in November (Wier, et al., 1973). This is the result of a relatively uniform vegetal cover over the entire area consisting of cultivated crops in the flat uplands and natural vegetation along the stream courses. The die-back of the cultivated species occurs earlier than the natural growth along the streams; consequently, as the remaining green vegetation becomes dormant, the stream courses again become subdued. Imagery through 13 September is uniformly white indicating a high degree of infrared reflectance throughout the scene. By 1 October the farmlands appear darker, but the vegetation along the streams is still highly reflective. The situation becomes reversed by 6 November when tree-lined streams are darker in tone than the farmlands (Figure 2).

Table 2 summarizes the seasonal dependency of the various fracture manifestations observed in the investigation:

TABLE 2 Seasonal effects on lineament detection and mapping

Kind of lineament manifestation	Optimum season for detecting
Expressed by topography	Winter, when lowest sun angle has greatest shadowing effect.
Controlled by small streams and expressed by vegetational differences.	Fall and early spring, when a differential between natural and cultivated plant growth is at a maximum.
Expressed as linear changes in soil tones	Spring, after most fields are bare from plowing and before cultivated crops effectively cover the soil

TABLE 3. Suitability of ERTS data.

Characteristic	Fracture Mapping	Mapping Subsidence
Scale	Excellent	Fair
Resolution	Very Satisfactory	Unsatisfactory
Frequency	Good	-----
Timeliness	Good	Good
Optimum Bands	5 and 7	5 and 7
Optimum season	Fall	Fall

In summary, (Table 3) ERTS imagery is suitable for lineament studies in the Midwest. Scale and resolution are more than adequate and, with the normal amount of cloud cover, good imagery is available at least once each season of the year. In general, the imagery also is more than adequate for mapping surface subsidence except for resolution constraints. Most sinkholes or individual subsidence areas are too small to be detected because they cover less than an acre (about 4047 square meters).

RELATIONSHIP OF LINEAMENTS AND FRACTURES

It is hypothesized that fracture systems are reflected through the lithological column above coal seams and show up as lineaments on orbital and aerial imagery even in areas where thick unconsolidated overburden conceals the bedrock. Work done by Mollard (1957) and by Wobber (1967) have demonstrated that fractures can exert an influence at the surface and can be mapped as lineaments through as much as 250 feet of unconsolidated drift material. Mollard discussed the causes for fracture trace development in glaciated regions, and suggested that there are two basic mechanisms for fracture development:

1. An oscillatory or rhythmic mechanism caused by short-duration stresses in which the earth's crust behaves like an elastic material with a definite strength limit; and
2. A non-oscillatory deep-seated tectonic mechanism induced by long-duration stresses to which the earth's crust behaves like a plastic material with a yield point.

The first mechanism results mainly from earth tides and is most responsible for maintaining existing fracture traces through thick unconsolidated cover. The second mechanism is related to continental isostatic adjustment and is similar to the stress buildups associated with earthquakes, though of smaller magnitude. Once a break has been established within the glacial cover, the fracture trace is accentuated and deepened by long-continued leaching and settlement of the overburden which eventually causes slight surface depressions. These subtle depressions may in turn be accentuated by surface runoff. Differences in microrelief and soil permeability localize soil moisture and therefore accelerate vegetal growth. Both of these phenomenon may be expressed by variations in image tone.

Thus, the principal two kinds of phenomena to be observed includes (1) fracture lineaments at or near the surface, and (2) fracture traces, i.e., bedrock fracture lineaments identified through an unconsolidated overburden at the surface.

A lineament map was prepared for southwestern Indiana (Figure 3). The lineaments were mapped on both ERTS imagery and color infrared aerial photography (Scale of 1:120,000). In general, orientation of lineaments from the two sources agree but are not identical. The aircraft and ERTS imagery complement each other in that fractures were mapped on each that were not found on the other. The most common set of lineaments trend northeast-southwest and northwest-southeast. Some areas show a paucity

of fractures and others show close-spaced and intersecting fractures.

Ground truth, that is, measurement of fracture orientation on the ground, is not easily done. In the coal-bearing rocks bedrock is effectively concealed by glacial drift, loess and wind-blown sand, alluvial deposits, and thick residual soil. However, directional measurements were made in roof rock of coal beds in the highwall of strip mines, roofs of a few underground mines, and road cuts. In general, the directions matched closely with the lineaments mapped on the imagery.

ROOF FALLS AND MINE SUBSIDENCE

A roof fall results when the roof rock in an area of the mine falls into the opening left when the coal is removed. Massive roof falls fill the mine room or entry with a pile of rock rubble and leave a pyramid shaped opening extending upward as much as 30 feet. Anything that contributes to weakening the supporting strength of roof rock will increase the likelihood of roof falls. Some contributors are poor mining practices, swelling due to water, lithologic irregularities, and fractures.

A study by Wier (1970) showed that in the Thunderbird Mine, an underground coal mine in Sullivan County, Indiana, fractures in the roof rock did contribute to roof falls. Unfortunately additional costs of maintaining a safe roof and cleaning up roof falls caused the mine to close before the present study got underway. Thus mapping additional areas was not possible.

Surface evidence is available in some areas to show where roof falls have occurred in mines that have been abandoned and are no longer accessible. These are the sinkholes and subsidence areas. However, not all roof falls cause subsidence at the surface. Subsidence due to underground mining has long been recognized in the Indiana coal field, especially over many of the old, relatively shallow mines. In many areas, mine subsidence has created serious environmental and engineering problems as it has caused road beds to shift, utility lines to break, building foundations to collapse, and farmland to become swamps.

Subsidence in an area east of Sullivan, Sullivan County, Indiana, was noted on the 1:30,000 scale color infrared photography. Extensive underground mining has occurred in the Sullivan area during the first half of this century, but nearly all mining had ceased operation by 1950. Coal was extracted mainly from Coal V, (Figure 4) which in this area is about 200 feet beneath the surface. A lesser amount of mining was done in Coal VI which occurs about 70 feet higher in the stratigraphic section.

The black and white infrared photography (Figure 5) was taken in March 1973, (NASA C-130 underflight) after considerable rainfall and when most surface depressions were filled with water. These depressions, predominantly on the floodplain of Busseron Creek, reflect the room and pillar configuration conventionally used in underground coal mining. The area along Busseron Creek appears to be unusually susceptible to subsidence. It is a broad low-lying valley filled to a substantial depth with unconsolidated sand, silt, and clay which hold moisture longer than the surrounding uplands. In this area, the downward percolation of water through the overlying bedrock, possibly along zones of fracturing has caused the mine supports to weaken

and collapse with subsequent subsidence which extends to the surface. That the presence of the floodplain is a significant factor in the occurrence of subsidence is indicated by the minimal subsidence which occurs in the better drained undermined uplands.

FRACTURES IN TEST SITES

A primary objective of this investigation is to relate fractures to roof fall problems in underground mines. Thus four underground sites and one strip mine site (Figure 1) are being used for detailed investigations of the relationship between fracture patterns and mine safety. Fracture analyses have been completed for each mine site. The test mine sites are:

- o Kings Station Mine, Gibson County: Until its closure in late 1973 this mine was the largest underground coal mining operation in Indiana. Glacial cover is thin, being generally less than 50 feet thick. Roof falls occurred in scattered areas in the mine.
- o Thunderbird Mine, Sullivan County: This mine experienced extensive roof fall problems; many associated with roof rock fractures. As a result, the mine was closed in 1972.
- o Mecca Mine, Parke County: This site was selected because of the topographic relief and apparent fracture control on the drainage systems.
- o Keensburg Mine, Gibson County, Indiana and Wabash County, Illinois: This mine is being developed with mining to commence at the 800-foot level. Fracture data in this area can be of substantial value to this operation, and possibly serve to reduce roof fall hazards.
- o Lynnville Strip Mine, Warrick County: Four large strip mines are operating in this area (Lynnville East, Lynnville Main, Lynnville West, and Log Creek Mines). Fracture analysis in this test site will be applied to blowouts and wall failures associated with strip mining.

Detailed information on the Kings, Thunderbird and Mecca Mines are discussed herein.

Kings Station Mine

A preliminary fracture analysis of the Kings Station Mine was done in late 1972 and refined in early 1973. A serious roof fall in November 1972 claimed the life of a miner and injured three others. The investigators visited the mine in April 1973 and discussed the various types of roof fall problems with the mine operators. Three of the four main areas of concentrated and intersecting fractures were also areas of frequent roof falls. The pre-dominant fracture directions mapped from ERTS and high altitude color infrared photography are N 40° to 60° E and N 20° to 60° W (Figure 6). These correlate well with joints measured in the field which occur in two dominant directions of N 20 to 30° E, N 70 to 80° E, and N 40 to 60° W.

Thunderbird Mine

The Thunderbird Mine was plagued by roof fall problems throughout most of its operating period and the mine closed in September 1972 because of the increased expense associated with the high incidence of roof falls. Wier (1970) gathered considerable data on fractures, roof falls, and clay squeezes before the mine closed.

A summary of the directions of the fractures measured in the Thunderbird Mine are shown in Figure 6. Major fractures associated with clay squeezing in the eastern part of the mine were measured in Coal VI with trends averaging N 40° E. Several smaller fractures were measured with trends in a northwesterly direction. Dominant fracture directions of N 40° to 50° E and N 70° to 80° W later were measured in Coal VI in the western part of the mine.

Surface fracture traces have been compiled from ERTS and aircraft imagery and summarized (Figure 6). A total of 119 fracture traces were mapped and the rose diagrams indicate two predominant directions -- a major set of fractures oriented at N 40° to 50° E and a sub-ordinant set at N 30° to 50° W. This correlates very closely with the underground fracture data.

Mecca Mine

The Mecca Mine lies in an area of relatively rugged terrain in which the fracture-controlled drainage system is deeply incised and is easily recognized on both ERTS imagery and high altitude photography (Figure 7). The test site is actually a series of closely-spaced mine shafts which have been abandoned since the early 1900's; however, large reserves of coal remain in the area, and it is reasonable to assume that additional mining will take place in the future.

Coverage of the Mecca area includes ERTS images enlarged to 1:250,000 scale, and color infrared photography at 1:120,000 and 1:30,000 scale. A detailed fracture analysis of the area was conducted using these various scales of imagery. Ground truth data is unavailable in the Mecca area at this time, however, general agreement exists between the primary fracture directions mapped on the imagery and the available ground data outside the test site. However, analysis of the various scales and types of imagery within the Mecca area produced differing sets of fracture traces. Primary directions for the three types of imagery are:

COLOR IR 1:30,000	COLOR IR 1:120,000	ERTS
N 30-40° E	N 30-40° E	N 20-30° E
N 60-70° W	N 30-40° W	N 70-80° W
N 80-90° E	N 80-90° E	N 60-70° E

The primary directions of fracture traces were consistent for both the 1:30,000 and 1:120,000 scale color infrared photography (Figure 8). However, the fracture directions mapped from the ERTS imagery differ from those mapped on aircraft imagery by ten to twenty degrees. These differences are being investigated.

HAZARDS PREDICTION MAPS

Various criteria were examined and tested for the preparation of a hazards classification map. Many lineaments mapped, particularly on ERTS imagery are believed to be zones of fractures rather than a single joint. Although the fracture represents a zone of bedrock weakness, fracture junctions are particularly significant and these were rated as the highest hazard areas. The zone of influence around a junction is conjectural, and an arbitrary value of 200 foot radius was selected as realistic figure for the scale maps being produced.

Verification of the validity of the hazards maps by underground mine data is limited by the lack of mine records. At the Kings Station Mine there was good correlation with predicted hazards zones and known roof fall areas (Figure 9).

The Thunderbird Mine closed due to excessive roof fall problems just before work was initiated on this experiment. Thus underground data is limited. Mapped fractures (from ERTS and aircraft imagery) show good trend correlation with existing underground mine data, however, predicted hazard zones do not show the same degree of coincidence as that of the Kings Station Mine. This is in part due to the lower quantity of detected fractures. Disturbed surficial material over and near the mine site reduces the ease of fracture identification.

OTHER COAL RESOURCES PROGRAMS

A prototype of a National Mined Land Inventory Map series has been prepared in Indiana and distributed to interested members of Congress and various State offices. A coal refuse bank (gob pile) inventory is being completed to aid the Indiana State Legislature in drafting laws and to establish tax requirements on coal production. This will be completed in January 1974 in time for the Spring legislative session. Some work has been done in utilizing ERTS imagery for evaluating the amount of revegetation in a variety of reclamation practices.

Maintaining high levels of safe underground mine production and protecting the environment following surface mining operations are increasingly important elements with the impact of the energy crisis. The ERTS program has provided opportunities to demonstrate the application of satellite imagery and integrated high altitude aerial platforms to address coal resources problems in Indiana. ERTS can produce equally important benefits to other coal producing states, as well.

CONCLUSIONS

Most lineaments mapped on ERTS imagery and aircraft color infrared photography do represent bedrock fractures. After mapping fractures a conference with mine officials indicated that three areas of dense and intersecting fractures in the Kings Station Mine had roof fall problems while mining. Hazardous areas can be predicted from ERTS and aircraft photography, but further work must be done to evaluate the degree of accuracy.

REFERENCES CITED

Mollard, J. D., Aerial mosaics reveal fracture patterns on surface materials in southern Saskatchewan and Manitoba, Oil in Canada, August 5, 1957.

Wier, C. E., Factors affecting coal roof rock in Sullivan County, Indiana, Indiana Academy of Science, V. 79, 1970.

Wier, C. E., F. J. Wobber, O. R. Russell and R. V. Amato, Fracture mapping and strip mine inventory in the Midwest by using ERTS-1 imagery, in Symposium of significant results obtained from the Earth Resources Technology Satellite-1, NASA, V. 1, 1973.

Wobber, F. J., Fracture Traces in Illinois. Photogrammetric Engineering V.33, May, 1967, pp. 499-506.

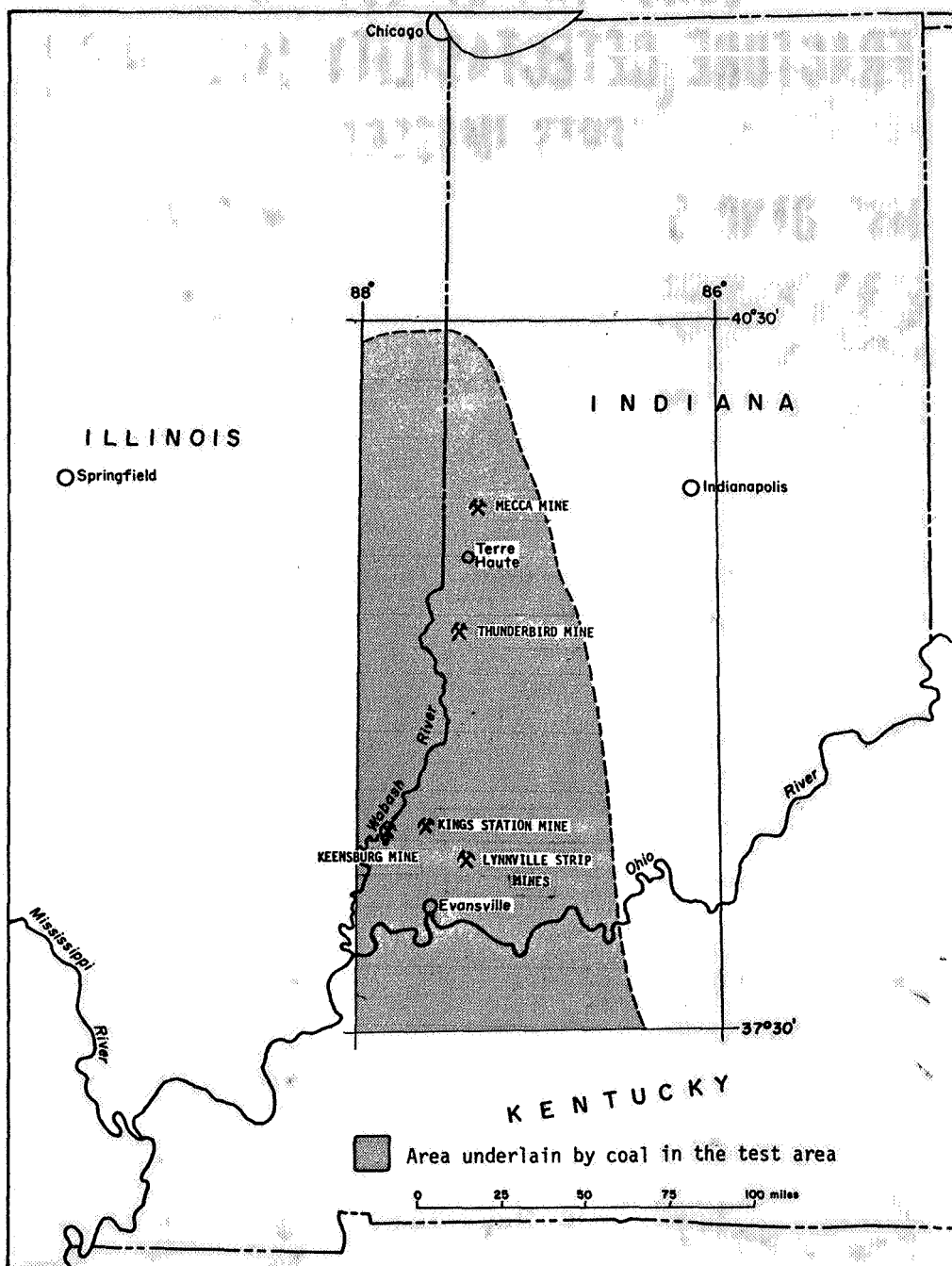
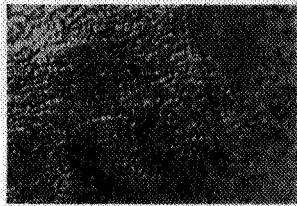


Figure 1. Map of Indiana and parts of Illinois and Kentucky showing the boundaries of the test area and the location of the individual test mine sites.

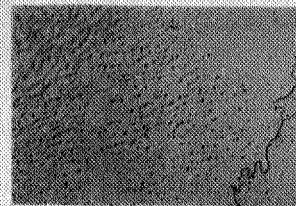
SEASONAL EFFECTS ON FRACTURE DETECTABILITY (ILL.-IND.) ERTS IMAGERY

MSS BAND 5

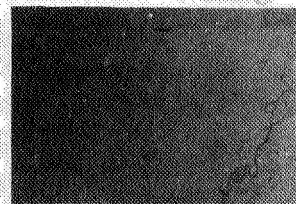
MSS BAND 7



26 Aug. 1972



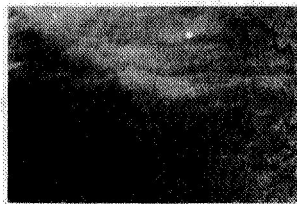
13 Sept. 1972



1 Oct. 1972



19 Oct. 1972



6 Nov. 1972



Figure 2. A series of ERTS-1 images of the same area (Illinois-Indiana) demonstrating the seasonal effects on fracture detectability in the temperate climate of the midwest.

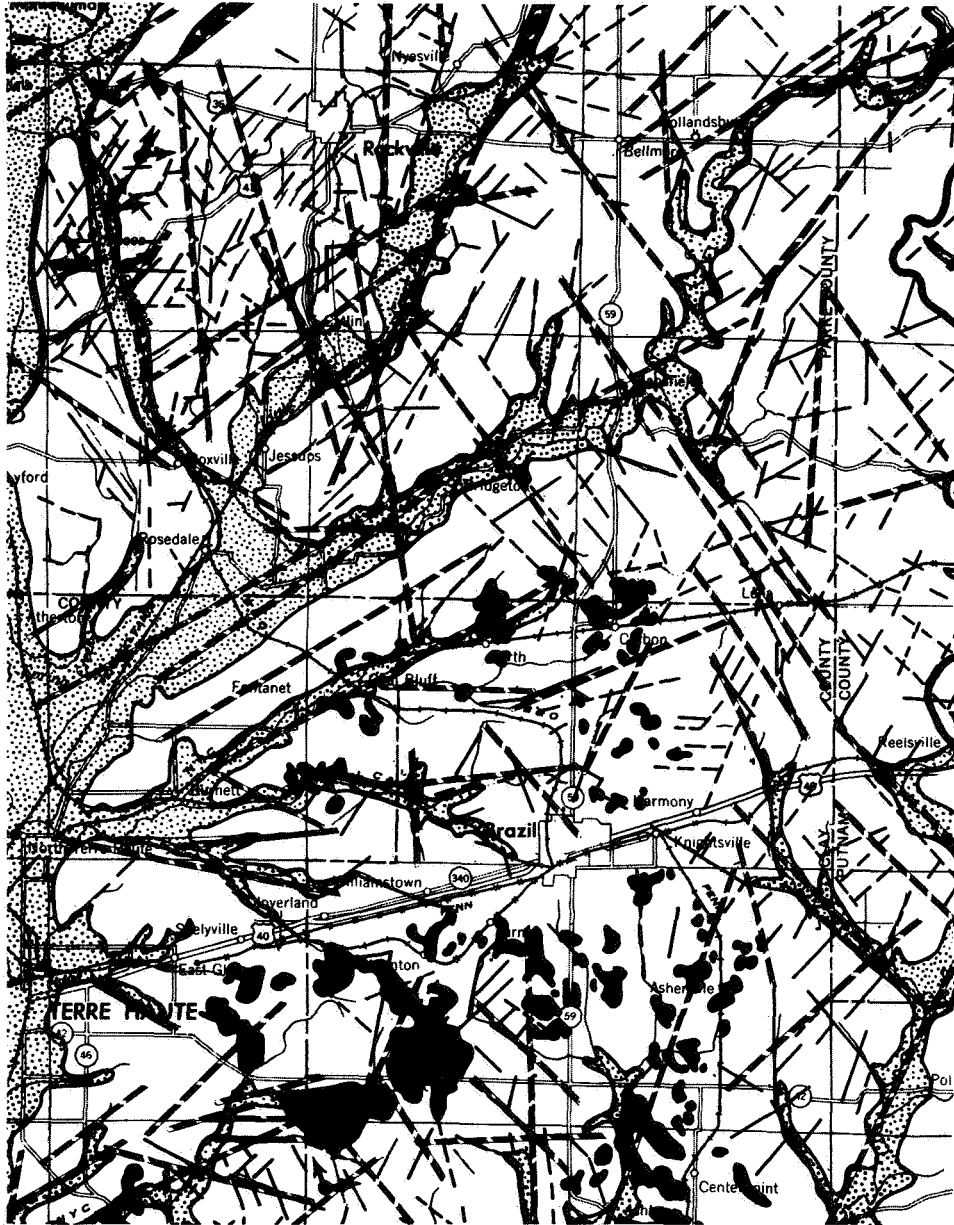
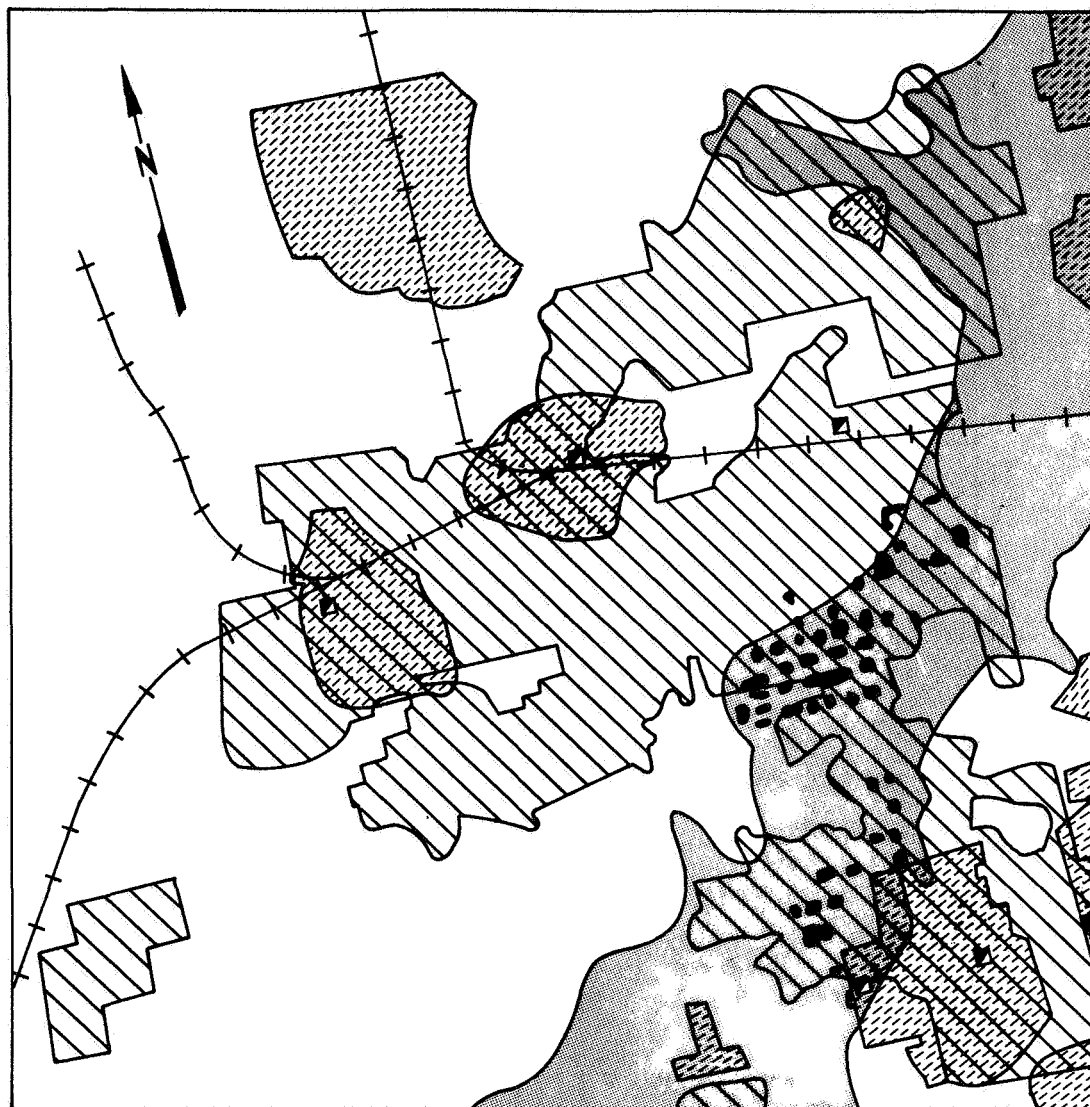


Figure 3. This portion of the Indianapolis 1x2° Quadrangle is representative of the fracture and lineament data derived from ERTS and aircraft imagery. The heavy diagonally dashed lines represent interpreted lineaments from ERTS imagery and the thin lines from small-scale aerial photography. Black areas are coal strip mines. Maps of this type have been prepared for the entire Indiana coal field.



Approximate Scale 1:40,000

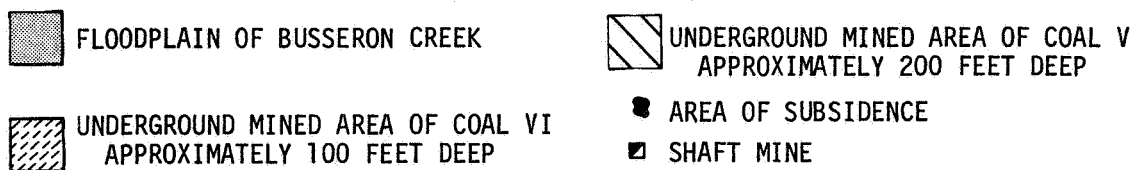


Figure 4. Map of a part of Sullivan County, Indiana, showing area from which coal has been mined by underground methods, and area of subsidence derived from analysis of image in Figure 5.



Figure 5. Black and white infrared image of part of Sullivan County, Indiana, showing extensive surface subsidence along Busseron Creek caused by underground coal mining.

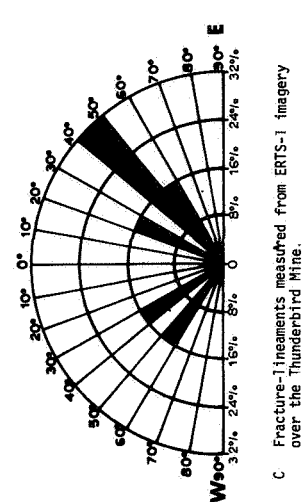
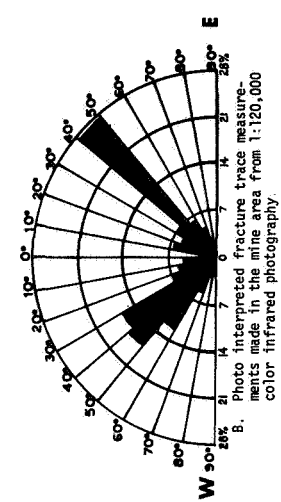
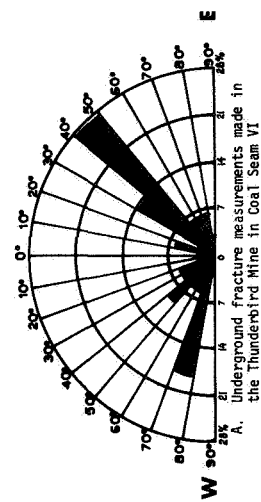
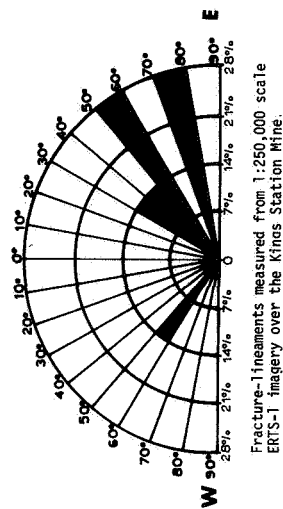
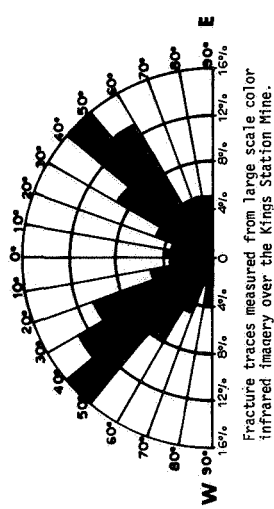
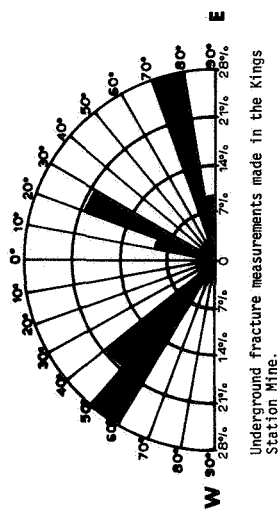


FIGURE 6. ROSE DIAGRAMS OF FRACTURE MEASUREMENTS FROM THE KINGS STATION MINE AREA, GIBSON COUNTY (LEFT COLUMN) AND THE THUNDERBIRD MINE AREA, SULLIVAN COUNTY, INDIANA (RIGHT COLUMN).



Figure 7. Black and white rendition of a color infrared image of the Mecca Mine area, Parke County, Indiana, showing area of underground mining and fractures mapped.

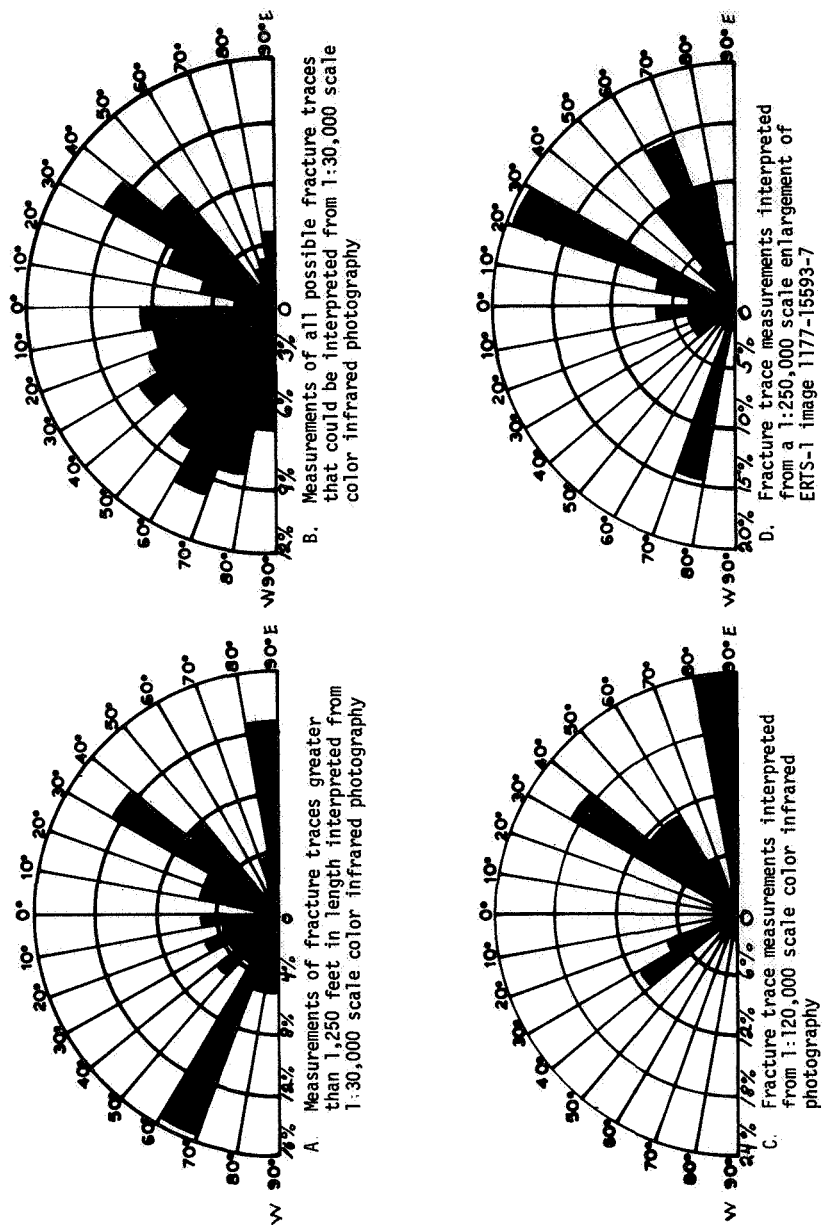


Figure 8. Rose diagrams of fracture measurements in the Mecca Mine area, Parke County, Indiana.

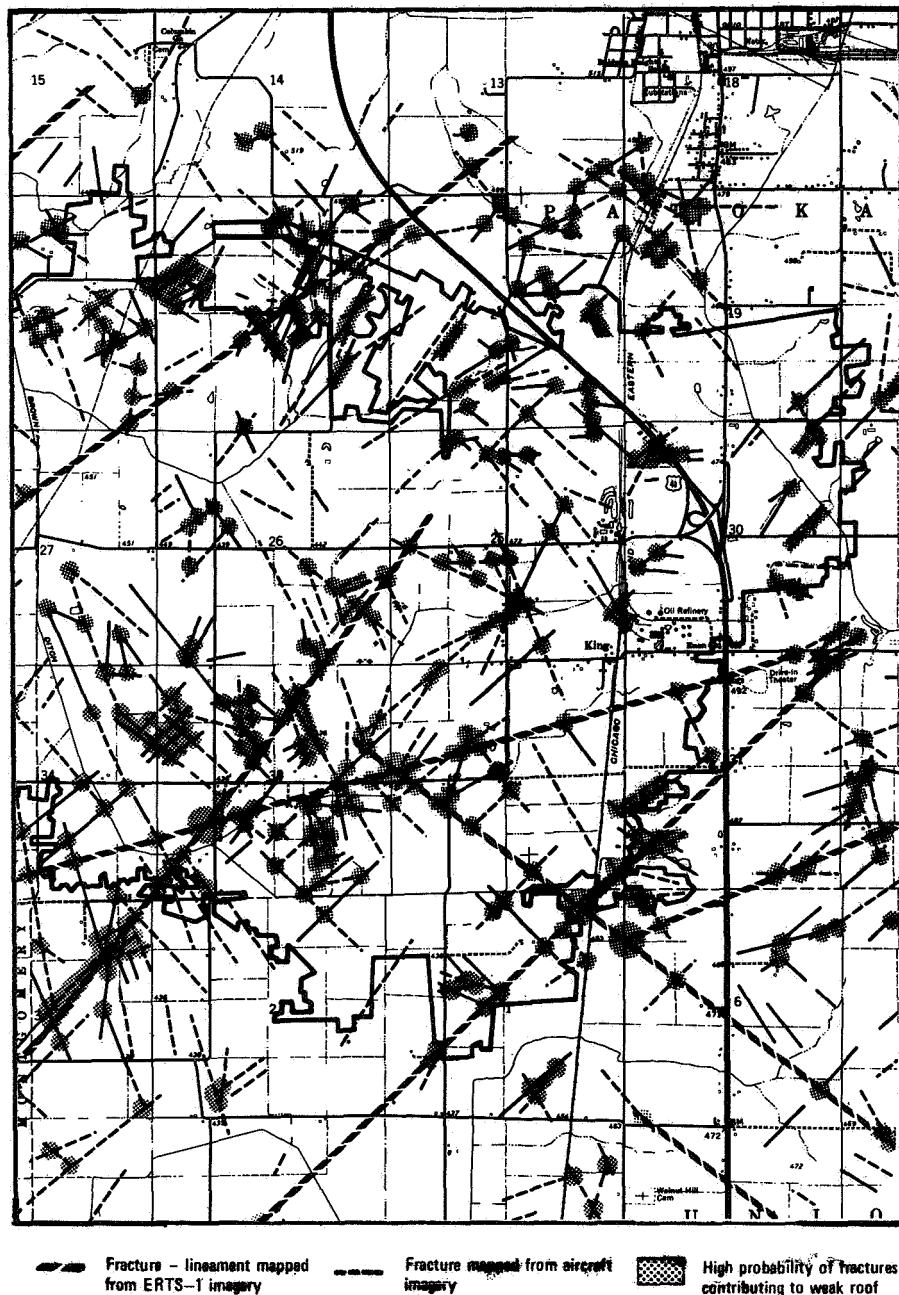


Figure 9. A portion of the King Station Mine Hazards Prediction map showing the distribution and concentration of fractures and lineaments mapped from ERTS and aircraft imagery. Stippled areas represent predicted zones of high probability of roof fall occurrence.

**A STUDY OF THE TEMPORAL CHANGES RECORDED BY ERTS AND THEIR
GEOLOGICAL SIGNIFICANCE**

Harold D. Moore and Alan F. Gregory, *Gregory Geoscience Ltd., 1750 Courtwood Cr., Ottawa*

ABSTRACT

The temporal changes that are recorded by ERTS were evaluated for an area around Bathurst Inlet in the North West Territories. The seasons represented by the images included: early winter, spring, early summer, summer, and fall.

Numerous surface characteristics (vegetation, drainage patterns, surface texture, lineament systems and topographic relief, etc.) were used to relate the change in observable features with the different seasons.

It was found that the time of year when an observation is made has a strong control over the amount and type of information that can be derived by an experienced interpreter.

An example of this type of seasonal control over observables, is the fact that on the winter images one can see an extensive hummocky morainal deposit and much bedrock structure which cannot be seen, or not as easily so, on the summer image. In a similar fashion, one can see on the summer image a vegetation pattern which may be related to the distribution of lacustrine and marine clay deposits. Such a vegetation pattern is of course covered during the arctic winter. Many other such examples of temporal changes were recorded in the study.

It is therefore concluded that a detailed study of temporal changes is an important part of any ERTS interpretation for geology.

PRECEDING PAGE BLANK NOT FILMED

N 74 30765

Introduction:

The data from ERTS-1 over the past year have recorded a full cycle of the seasons. In view of this, a company-supported project was started to study and evaluate, by means of visual analysis, the attendant spectral and temporal changes, and their significance to geological interpretation.

Terrestrial Canada, being located in the northern latitudes between 42°N and 83°N, has a wide variety of seasonal conditions which are faithfully recorded by ERTS. Canadian terrain is even more varied than the seasonal conditions, with geology ranging from Precambrian rocks over 2.5 billion years old to unconsolidated Pleistocene sediments deposited during the last ice age.

With such a great variety of seasonal and surficial conditions, it is obvious that the conclusions drawn from this study for one particular area in the Arctic tundra may have to be modified for use in a different area. However, this study should comprise a useful foundation for similar studies in other areas with different environments.

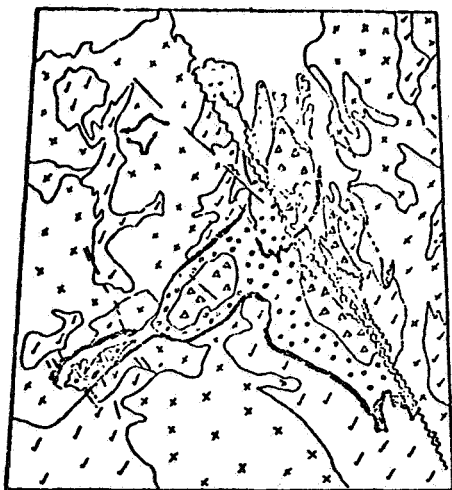
Area of Study:

The Bathurst Inlet area was chosen for this study because of its great variety of surficial and seasonal conditions. Other favourable factors were good continuous ERTS coverage and up to date mapping of the bedrock and surficial geology.

The Bathurst Inlet area is located on the Arctic coast of Canada and is cut by the Arctic Circle. As described by Fraser (1964) and Tremblay (1968), the topography is rugged, rising from sea level to over 650 m. with relief as great as 500 m. in some places.

The Pleistocene features in this area are quite varied in size and distribution ranging from eskers up to 120 km. long and 58 m. high to hummocky morainal deposits, which may cover thousands of square km. (Bird, 1961). Although the area is north of the tree line, one can still find a wide range of plant life. (Bird, *ibid*).

A generalized geological map of the area taken from work done by (Fraser, 1964, Tremblay, 1968) is present in (figure 1). All the rocks of the area are of Precambrian age, with a thick group of Proterozoic sedimentary rocks lying unconformably above Archean basement rocks. The unconformity between the Proterozoic and Archean has had a



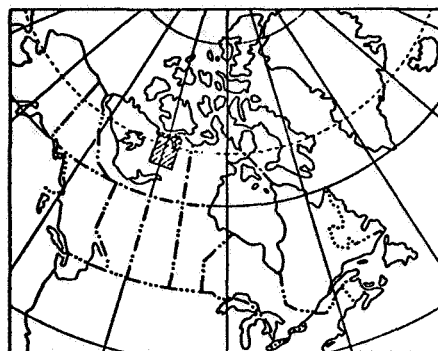
A	GREENSTONE	P	GABBRO, BASALT
R	SEDIMENTARY	T	QUARTZITE
C	GRANITE GNEISS	R	ARGILLITE, CARBONATE
H	GRANITES	O	SANDSTONE
A	DIABASE DYKES	G	FAULT
N		C	

GEOLOGY



M	MARINE DEPOSITS	D	GLACIAL DIRECTION
L	GLACIAL LAKE DEPOSITS	E	ESKER
D	DISINTEGRATION MORaine		
A	AREA OF LAST GLACIATION		

GLACIAL



INDEX MAP

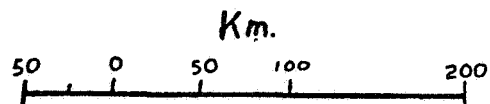
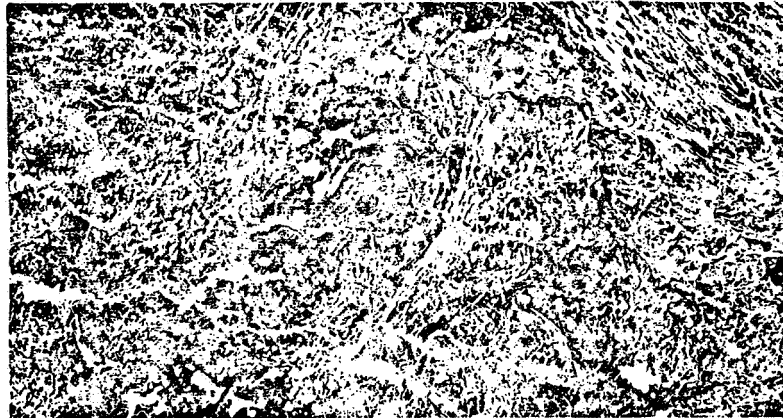


Figure 1. Bedrock and Surficial Geology Maps
Bathurst Inlet, NWT. (after Bird & Bird 1961,
Douglas 1968, Fraser 1964, Prest et al 1967,
Tremblay 1968)

October 9, 1972



May 30, 1973



June 18, 1973



Figure 2. ERTS 1 imagery for three different seasons.
Bathurst Inlet, NWT.

very strong control over the emplacement of an extensive group of gabbroic sills which almost completely rim the Proterozoic basin. Numerous diabase dykes, with a common strike of N 25° W, are found in the western part of the area. Several fault sets cut the area, the most prominent of which is the Bathurst fault zone with vertical relief of up to 330 m (Fraser 1964).

Method of Interpretation

Before starting the interpretation, data for all the seasons should be studied to find suitable imagery. Because ERTS images of any given area are obtained every eighteen days, there is a good possibility that high quality images can be found for each of the seasons.

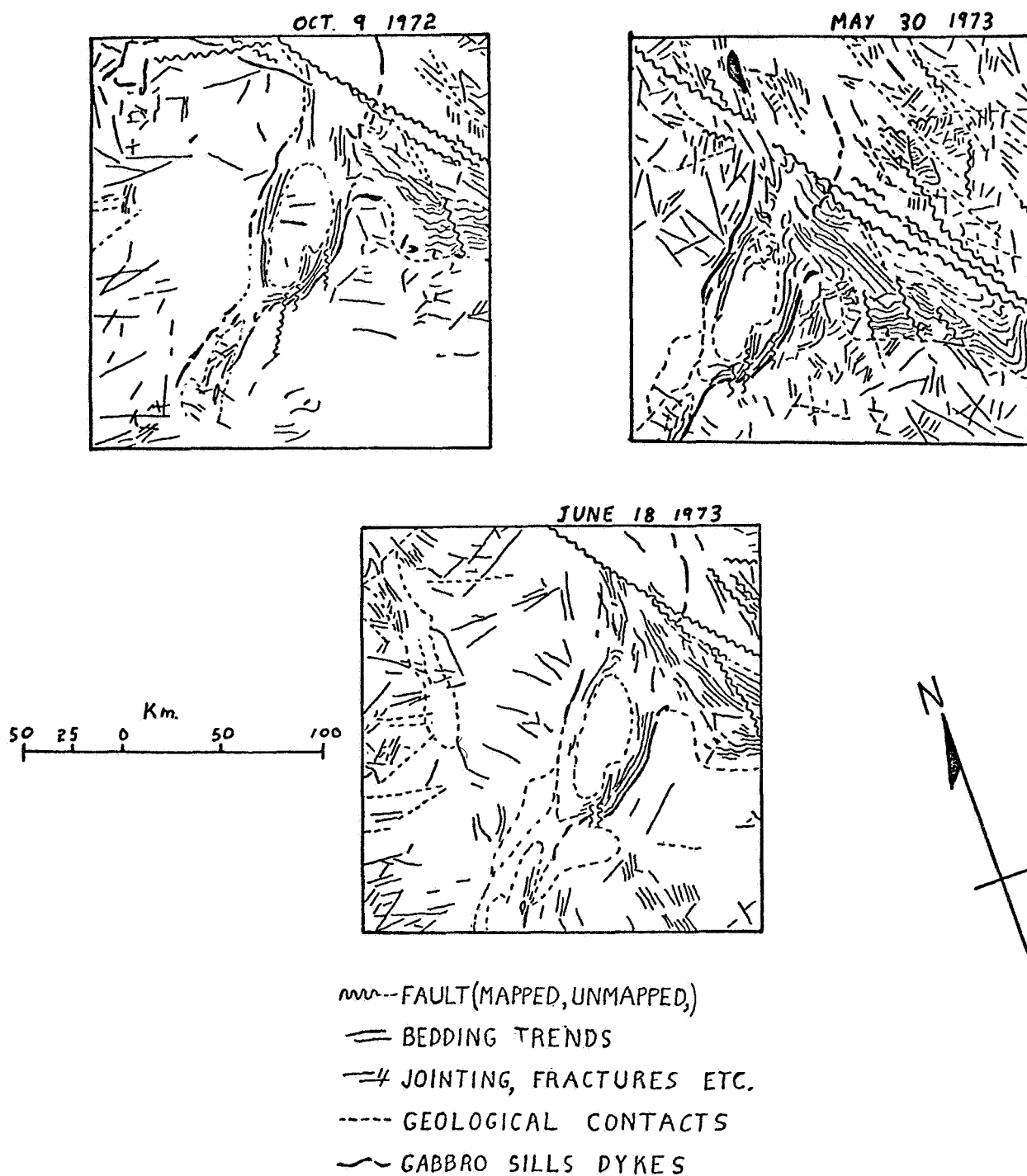
Three sets of images suitable for study were available for this area at the time this investigation was started (summer 1973). Since that time, however, two more sets of images have become available, thus completing the full annual cycle. The two latest sets of images have not yet been analyzed.

The great volume of data which is used in a geological interpretation was found to be a problem when one tried to do a temporal analysis for the three sets of images without an organized plan of attack. Therefore all the observables which can be used in a geological interpretation were divided into groups to be analyzed one at a time (structure, geomorphology, vegetation, lithology, drainage patterns, etc.)

The interpretative procedures were thus based on the sequential analysis of the different types of observables. This allowed the interpreter to concentrate on one type of observable at a time, and therefore pick out changes of a more subtle nature. The information which was gained from the interpretation was then validated by comparison with existing maps. Ultimately a composite interpretation will be prepared by integrating the individual interpretations.

In summary the establishment of a systematic procedure for interpretation provides two major benefits:

1. A step-by-step approach is repeatable, and therefore all the seasonal imagery can be analyzed in the same way.
2. Sequential focusing on selected sets of data in the image allows the interpreter to obtain a maximum amount of information from subtle details in the least amount of time.



GEOLOGY FROM ERTS

Figure 3. Structural geology from ERTS. Interpretations showing variation in interpretable structural details for three different seasons. Bathurst Inlet, N.W.T.

Observations:

Validation of the interpretations was based on published data (Fraser 1964, Tremblay 1968, Bird 1961, Douglas 1968, Prest et al 1967) which are compiled at small scale in (figure 1). The degree of correlation between the ERTS data and the existing maps was found to vary depending on the type of geological feature that was being studied. The ability of ERTS to record geological data through the seasons can be summarized, from this study as follows:

1. Structure:

As other investigators have reported, ERTS data record structural details, commonly revealing high correlation with existing maps, or, in many cases augmenting them. There is however a difference in what can be seen in images for each of the seasons (figure 3). These seasonal differences are in the amount and type of structural detail. As can be seen in the structural interpretations for the three seasons (figure 3), the larger structural features were recorded in all seasons. However, it is obvious that the May 30 image has the greatest amount of information. On the other hand, the May 30 image required a longer time for interpretation relative to the October image.

Seasonal feature-enhancement is the primary reason for the differences in structure which were interpreted for the three seasons. The three types of seasonal enhancement of structure which were found in this study are:

- 1.1 Shadow enhancement which occurs in October when the angle of sun elevation is quite low (Gregory 1973). The sun elevation for the image used in this study was 25° , however elevations as low as 3° have been used in other areas.
- 1.2 Residual snow enhancement is found in the May image with the last snows of winter remaining in shaded and low-lying areas.
- 1.3 Drainage pattern enhancement can be found in the June image with melt waters filling the drainage system, and outlining joints, faults, fractures, and topographic lineaments.

When the recorded data were compared with the ground truth, it was found that many structural features could be identified in addition to those on the maps.

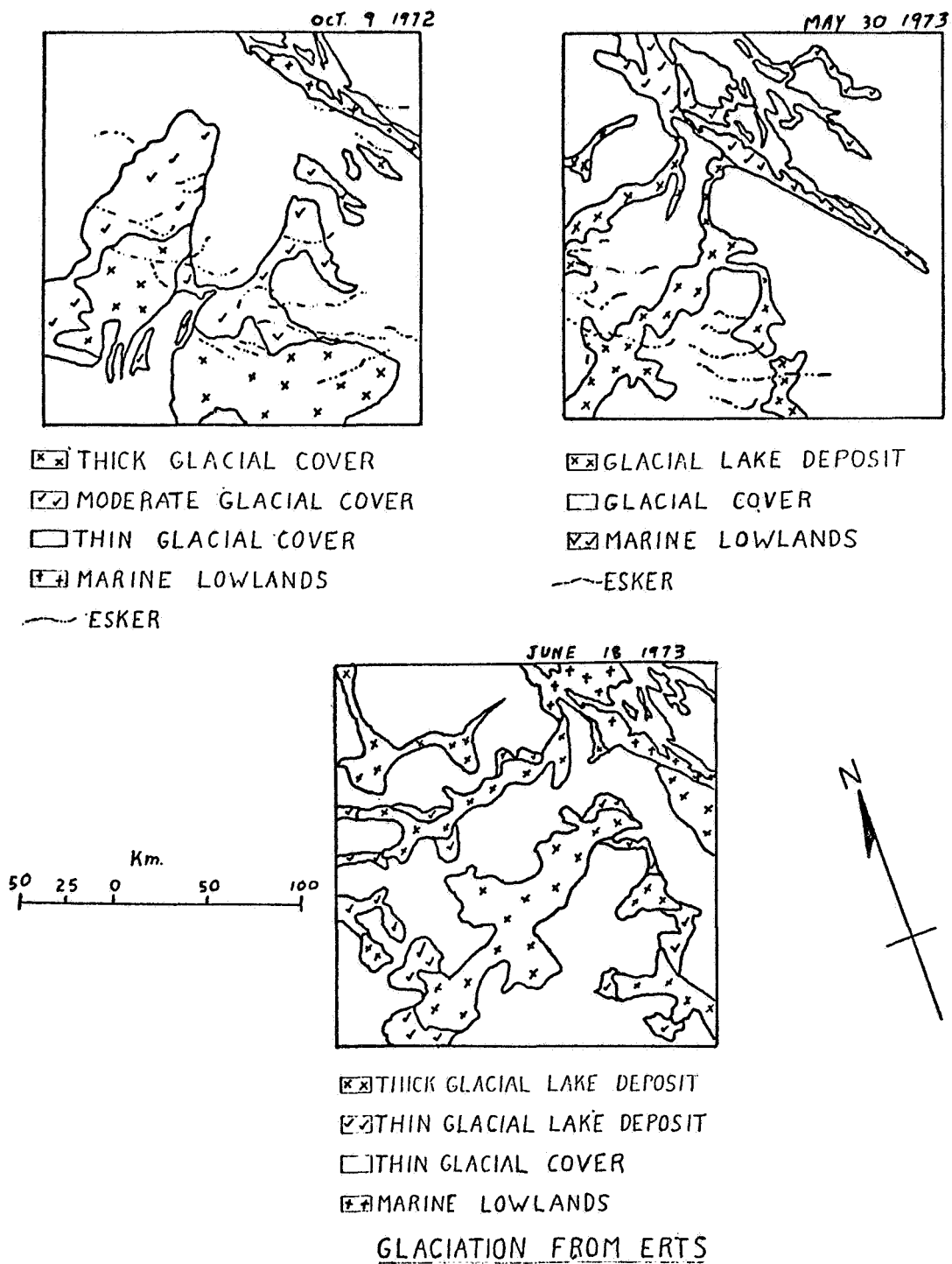


Figure 4. Glacial geology from ERTS. Interpretations showing variation in interpretable glacial observables for three different seasons. Bathurst Inlet, N.W.T.

Thus it would appear that selected ERTS images comprise an excellent basis for mapping structural feature, and that a temporal study of structure provides additional information at little extra cost.

2. Glacial Deposits:

The Glacial Map of Canada (Prest et al 1967) which is a compilation of airphoto interpretations for the whole country was the source of ground truth for this part of the interpretation. As can be seen in (figure 4), each of the seasonal images recorded a different distribution of surficial materials. The reasons for these differences are believed to represent different types of seasonal feature-enhancement. Some of these are the same as those for structure, but vegetation is tentatively considered to provide an additional type of enhancement.

- 2.1 In the October image, the low sun angle enhances the eskers and moraines. The blanket of snow also helped enhance the morainal material by cutting out other "Terrain noise".
- 2.2 Residual snow enhancement is prominent in the May image, especially for drumblin fields and esker swarms. Note also the first signs of new vegetative growth which seem to be related to the distribution of marine and lacustrine clay deposits. This apparent relationship between the lush vegetative growth and clay deposits possibly is caused by a higher content of nutrients in the clay, and abundance of water as a result of poor drainage in the clays.
- 2.3 In the June image the vegetative enhancement is a lot more prominent and along with drainage patterns gives a good outline of the marine and lacustrine clay deposits.

Without this temporal analysis a lot of information about the glacial deposits of the area would have been lost even though ERTS had recorded it.

3. Lithology:

As it has been observed by Chagarlanudi (1973) and many others, ERTS will, in most cases, give only a fair to poor picture of the true lithological distribution. Most lithological information is gained from ERTS data by the identification and extrapolation of geomorphological features. All the seasonal feature enhancements previously mentioned will help in identifying geomorphological feature and, therefore, lithological features. Thus depending on the abundance of outcrop it may be possible for a person without prior knowledge of the area to prepare from an ERTS image

a rapid though tentative analysis of the distribution of rock types. If some ground truth is available, it may be possible to prepare a preliminary, small scale geological map.

Conclusions:

1. Nearly all geological studies of ERTS images can benefit to some degree by a temporal analysis.
2. Temporal analysis will probably be very useful in other disciplines.
3. Four types of seasonal feature-enhancement were found in this study. They are: shadow enhancement, residual snow enhancement, drainage pattern enhancement, and vegetative enhancement.
4. Analysis of such seasonal changes in observables can increase the amount of information that can be derived from ERTS data, or help to enhance one type of data.
5. The amount of information which can be obtained from ERTS data can be maximized by doing a temporal analysis and afterwards compiling the individual interpretations into a composite interpretation.
6. Temporal analysis will increase the already proven ability of ERTS to record structural data. This new perspective and detail may help to solve the geological problem of the long-hypothesized link between ore deposits and lineaments.
7. The most significant temporal changes are those related to glacial deposits; therefore, the study of such deposits will benefit from temporal analysis.
8. Where formations are reasonably well exposed ERTS data can be used to prepare a preliminary map, especially if some ground truth is available to assist in identifying rock types.

References

1. J. B. Bird "Bathurst Inlet NWT." Department of Mines and Technical Surveys Geographical Branch Memoir #7.
2. P. Chagarlamudi "Correlation of Geology, Geophysics and Satellite Imagery Information in the Stoney Rapids Area N. Sask." Unpublished.
3. R. J. W. Douglas (1968) "Geological Map of Canada 1:5,000,000" Map # 1250 A.
4. J. A. Fraser (1964) "Geological Notes on Northeastern District of Mackenzie" Geological Survey of Canada paper 63-40.
5. A. F. Gregory (1973) "Preliminary Assessment of Geological Applications of ERTS-1 Imagery From Selected Areas of the Canadian Arctic". ERTS-1 Symposium on Significant Results. March 5 - 9 1973, Vol.#1 Sec. A.
6. V. K. Prest
D. R. Grant
V. N. Rampton (1967) "Glacial Map of Canada 1:5,000,000" Map #1253 A
7. L. P. Tremblay (1968) "Preliminary Account of The Goulburn Group NWT. Canada" Geological Survey of Canada paper 67-8

GEOLOGIC EVALUATION AND APPLICATIONS OF ERTS-1 IMAGERY OVER GEORGIA

S. M. Pickering and R. C. Jones, *Georgia Geological Survey, Department of Natural Resources*

ABSTRACT

ERTS-1 70mm and 9"x9" film negatives are being used by conventional and color enhancement methods as a tool for geologic investigation. Prints at 1:500,000 and 1:250,000 scale are made, gridded with latitude and longitude, and distributed to each of our field geologists for regional and local studies. These black-and-white working products are supplemented with color enhancements, made by addcol and density slicing. The Georgia Geological Survey has also prepared several state mosaics and regional interpretations from ERTS which have been widely used by state and local government.

Geologic mapping and mineral exploration by conventional methods is very difficult in Georgia. Thick soil cover and heavy vegetation cause outcrops of bed rock to be small, rare and obscure. ERTS imagery, and remote sensing in general have helped delineate: 1) major tectonic boundaries; 2) lithologic contacts; 3) foliation trends; 4) topographic lineaments; and 5) faults. The ERTS-1 MSS imagery yields the greatest amount of geologic information on the Piedmont, Blue Ridge, and Valley and Ridge Provinces of Georgia where topography is strongly controlled by the bedrock geology. Seven band imagery taken at low sun angle near the winter solstice (Dec. 21) is greatly superior for discriminating lineations and landforms.

Coastal Plain geology from MSS imagery may be inferred from land use and drainage patterns. Imagery taken during wet, winter condition seems best for southeastern Coastal Plain studies.

Color enhancement analysis using 5 and 7 band negatives gives more visual contrast and allows the greatest amount of geologic discrimination.

ERTS imagery, and general remote sensing techniques, have provided us with a powerful tool to assist geologic research; have significantly increased the mapping efficiency of our field geologists; have shown new lineaments associated with known shear and fault zones; have delineated new structural features; have provided a tool to re-evaluate our tectonic history; have helped to locate potential ground water sources and areas of aquifer recharge; have defined areas of geologic hazards; have shown areas of heavy siltation in major reservoirs; and by its close interval repetition, have aided in monitoring surface mine reclamation activities and the environmental protection of our intricate marshland system.

No NASA or other federal funds are involved in our remote sensing program. We would, however, like to gratefully acknowledge the assistance of the EROS Mississippi Test Facility in simplifying our standing order with the National Data Center, and in encouraging our use of their imagery enhancement equipment.

INTRODUCTION

Since shortly after launch in the summer of 1972, the Georgia Geological Survey has maintained a standing order for all clear weather MSS imagery of our state. Our standing order provides us with all 8-1 or better quality 70mm and 9x9 inch negatives, from which prints at 1:500,000 and

N74 30765

1:250,000 scale are made. Each print is gridded with latitude and longitude and copies are provided to each field geologist for regional and local studies.

These black and white working products are supplemented with color enhanced imagery derived by density slicing or a color additive viewer. Color products are useful in the recognition of particular features and for magazine articles or presentations of public interest. Our agency has also prepared state mosaics of bands 5, 6, and 7, and various regional interpretations which have been widely used by schools, universities, and state and local government for natural resource inventory and land use planning purposes. An ERTS interpretative atlas of the entire state for MSS bands 5 and 7 has been prepared and is currently in press.

Geologic Applications:

Geologic mapping and mineral exploration by conventional methods is very difficult in Georgia. Thick soil cover and vegetation cause outcrops of bedrock to be small, rare, and obscure.

Satellite imagery, and other remote sensing tools and techniques, have provided a powerful tool to assist geologic research and have significantly increased the efficiency of our efforts. For the past year the Georgia Geological Survey has been engaged in regional mapping for the new state geologic map. ERTS images enlarged to compatible mapping scales have increased our field efficiency by at least 25%. There are a number of areas where data from ERTS imagery has allowed a notably higher level of precision than has been available with any amount of field work on the ground. The following examples demonstrate how the imagery is being used as a tool for solving geologic problems in Georgia.

Major faulting is commonly apparent on MSS 5, 6, and 7 imagery in the form of topographic lineaments and zones of abrupt vegetation change. The Warwomen Shear (Fig. 1) has been noted



Figure 1

as a small structure in northeast Georgia, thought to be associated with the major Brevard Fault Zone. This 7 band frame shows that the shear is a part of a major fault zone connecting the Ashland and Brevard Faults. This relationship was not previously known.

The Cartersville Fault, shown in Fig. 2, is the prominent fault which separates the Paleozoic sediments from the crystalline rocks of the Piedmont. As such, it has been recognized and mapped since the 1840's. ERTS images indicate that what was regarded as a single fault is actually a series of overlapping thrust plates, and that there is at least one area where an abrupt fault does not exist.



Figure 2

Figure 2 also shows a tight elongate fold in high grade metamorphic rocks, the Murphy syncline. The pure marble deposits which allow our state to lead the nation in marble production are localized in the axial areas of cross-folds in this structure. This ERTS image is allowing a re-evaluation of the tectonic history of the area, and is of great interest to marble exploration.

In Figure 3, the Red Mountain Formation, a Silurian sandstone, in the Paleozoic area of northwest Georgia, is folded into a complex pattern of tight, plunging anticlines and synclines, which can for the first time be viewed as a structural unit, rather than as single folds.



Figure 3

Pennsylvanian sandstone capping Lookout Mountain is cut by a series of cross faults which have never been mapped (Fig. 4). This area of rapidly developing second homes has no extensive source of surface or ground-water, and these faults may localize zones of aquifer recharge.



Figure 4

Large areas of southwest and northwest Georgia are troubled by the collapse of limestone caverns, which cause limesinks as much as 700 feet in diameter and 100 feet deep. These limesinks are of great concern if they occur in developed areas or are used as areas of refuse disposal, allowing pollutants a direct entry to the aquifer. Late winter band 7 ERTS images (Fig. 5)



Figure 5

enable our Geological Survey to make a limesink inventory map of these areas. Similar interpretative techniques were used to construct a farm pond inventory of Georgia, mapping all open water bodies as small as 4.0 acres.

Aquifer recharge is evident in winter band 7 imagery (Fig. 6) along rivers at areas where they cross permeable cavernous limestone. This ERTS image shows the water saturated alluvial valleys of the major rivers clearly. Where the rivers cross aquifer recharge zones (at A), the alluvium is well drained by underground recharging, and therefore light in tone. This image makes it possible to map both floodplain and areas of aquifer recharge along our rivers.



Figure 6

ERTS images of the Georgia Coast (Fig 7) offer spectacular definition of our Sea Island Section and intervening marshland. These marshes have been recognized by biologists as among the most productive nutrient systems on earth. The 1971 session of Georgia's General Assembly passed a strict marshlands protection Act which limits filling, dredging, and development in this area. Without remote sensing techniques, it is very difficult to define a consistent boundary for our salt marshes which will be legally acceptable.

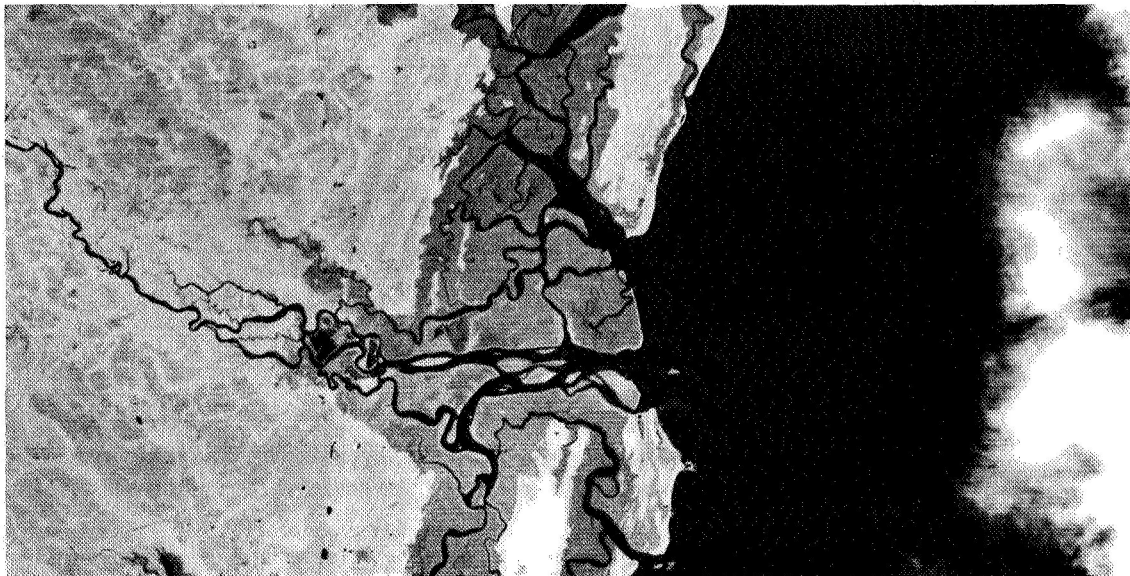


Figure 7

The immense organic productivity of the coastal marshlands is a direct product of the complex network of tidal circulation and drainage. Detail of a small portion of 5 band imagery allows classification and study of tidal flow (Fig. 8). The rich suspended nutrient washed from the marsh is carried to the fishing and shrimping grounds of the open ocean by a system of currents not previously well known.

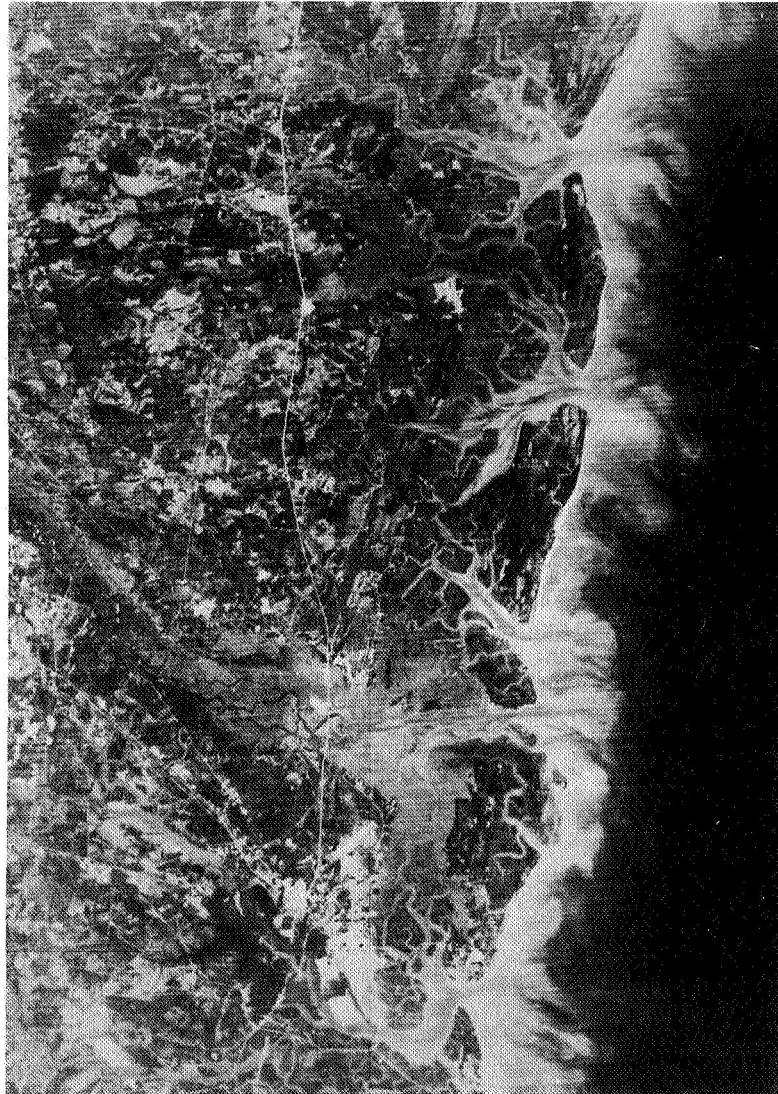


Figure 8

The Okefenokee Swamp is the largest elevated warm swamp on the North American continent and one of the most prolific of our nation's wildlife preserves. The origin of the swamp has never

been well understood. This detailed 7 band image (Fig. 9) gives a new perspective to our studies. It is evident that the swamp was a shallow Pleistocene marine bay during a time of higher sea level. A major longshore bar, Trail Ridge, developed along the east side of the bay and restricted drainage as sea level gradually lowered, thus impounding water behind the bar forming the present day swamp. ERTS imagery allows for the first time, a study of the gross morphology and drainage patterns of the swamp.



Figure 9

Wet weather 7 band imagery has allowed a new survey of the shallow elliptical depressions known as "Carolina bays" (Fig. 10). ERTS data have tended to support speculation on the extra-terrestrial origin of these features, which range in size from a few hundred feet to three miles. It may be only coincidence that the bays are elongated toward the Georgia tektite strewn area. Five Carolina bayfields have been identified from ERTS imagery over Georgia.

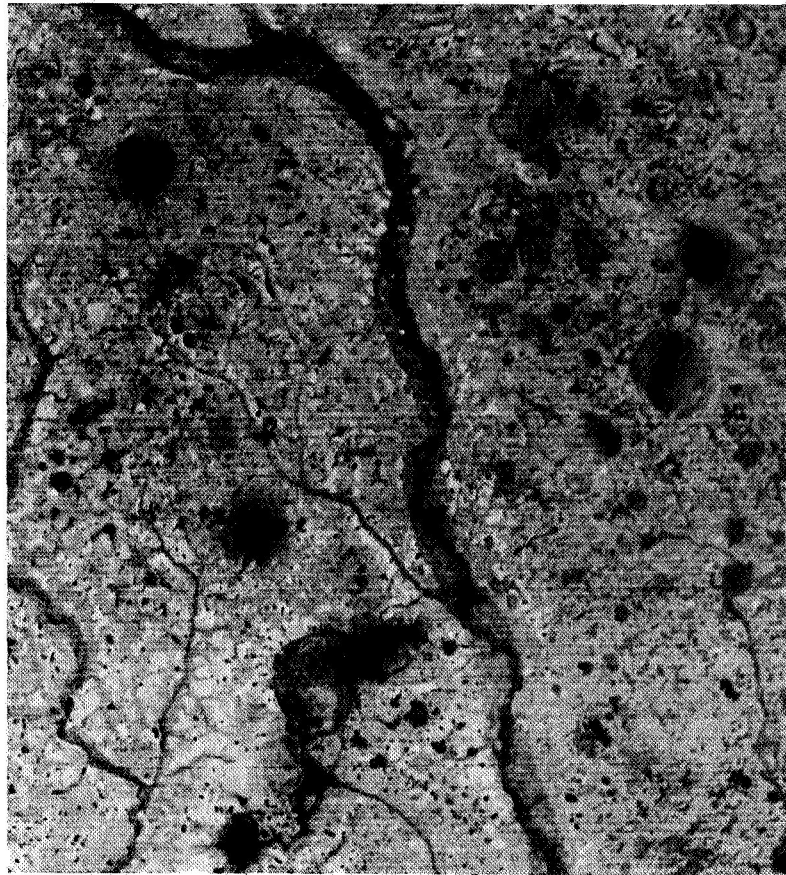


Figure 10

Long trains of striking parabolic dunes as much as four miles in size have been identified along several rivers in southeast Georgia. Such windblown sand features have not been previously described in the humid eastern United States (Fig. 11).

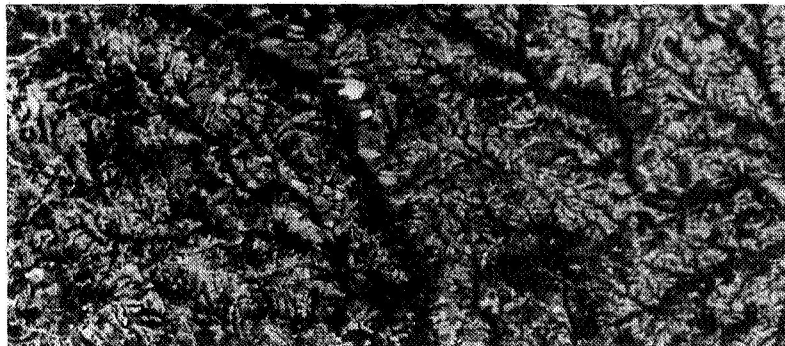


Figure 11

Commonly, unusual land use by man can result in a feature apparent on ERTS imagery which resembles a major geologic structure (Fig. 12). This large circular feature along the Georgia-South Carolina border resembles a major caldera or collapse structure. It is actually land under federal ownership at the Savannah River Nuclear Plant. Since the Atomic Energy Commission's only concern is plutonium production rather than farming, their land has grown up in forest, in contrast to the surrounding cultivated area.

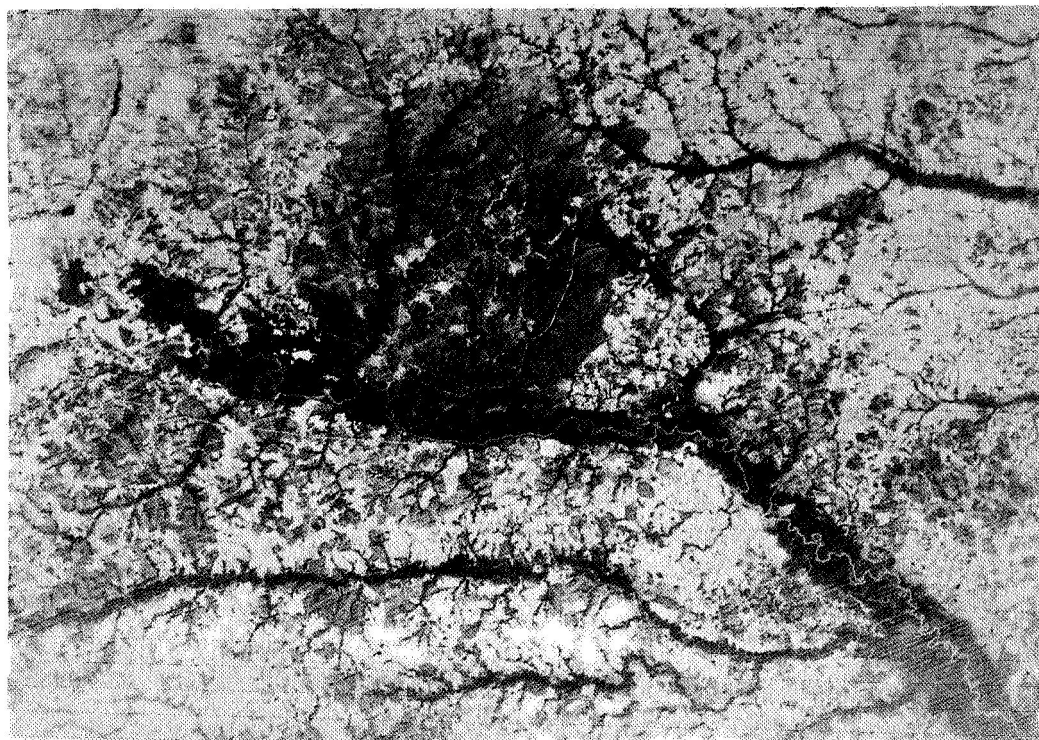


Figure 12

The Department of Natural Resources of the State of Georgia requires reclamation of all mined land in the state within one year of completion of mining. The monitoring of this industry, which produces over one-quarter billion dollars each year, is a major task. Figure 13 shows the extent of Georgia's kaolin mining district, which produces over \$150,000,000 in industrial clays yearly. Each pit is clearly discernable as a white spot, and reclamation efforts may be readily evaluated. This ability results in considerable savings in enforcement costs, and provides an inexpensive, impartial referee in disputes.

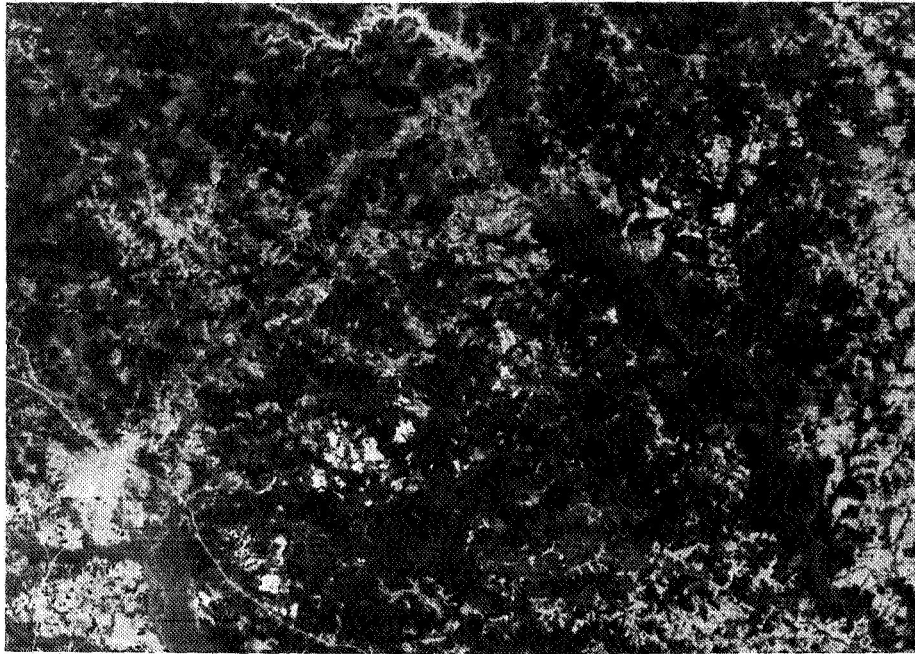


Figure 13

The ERTS system has provided a valuable tool and a new perspective for natural resources research in Georgia. It would be a considerable setback to Georgia's remote sensing program if continuous satellite coverage of our part of the United States were interrupted.

**ALTITUDE DETERMINATION AND DESCRIPTIVE ANALYSIS OF CLOUDS ON ERTS-1
MULTISPECTRAL PHOTOGRAPHY**

Carlos Albrizzio and Adelina Andressen, *Ministry of Public Works, Directorate of Urban Planning, Venezuela*

S U M M A R Y

A simple method to determine the approximate altitude of clouds is described in this work, with the objective of refining their classification using only marginal data from the photographs.

The method is based on the application of an approximate equation of the type $a = d \cdot \tan s$, that relates cloud altitude (a), angle of sun elevation (s), and cloud image to corresponding shadow distance (d) measured directly on the photograph.

A qualitative analysis of the following factors affecting the measurements is presented: Cloud shape and the sun elevation angle, atmospheric refraction, Earth ellipsoid, and topographic relief. The error involved in this method is small, and does not transgresses the range of cloud genetic levels, thus being accurate enough for cloud classification.

The classification of clouds is a part of the descriptive analysis of weather condition of a region. It includes analysis of the form, altitude, structure, density and cloud association characteristics which can be determined on the ERTS-1 multispectral photography.

Clouds and their corresponding shadows commonly found in the photographs, are undesirable for the interpretation of Natural Resources. A cloud analysis however, show features, such as wind direction, sea current direction, long-shore drift, sediments transport and other geomorphic and geologic processes that are useful on Geoenvironmental studies.

Results of the application of this method on photographs of the Goajira Península, Paraguaná Península and the Central Coast of Venezuela are presented. Here, the altitudes computed are used to classify clouds and to identify the genus of others without typical form. Instability of air masses through clouds vertical development, and wind direction as well as other local climatic characteristics such as moisture content, loci of condensation, etc. are determined using repetitive coverage for the time interval of the photography. Applications for the regional and urban planning (including airport location and flight schedule) and Natural Resources evaluation are suggested.

CA/AAR/Lcr.
21-11-73. -

N 74 30767

METHODOLOGY FOR THE ALTITUDE DETERMINATION OF CLOUDS.

Introduction. The space photographs of the earth are taken from satellite ERTS-1 on its orbit at 915 Km of altitude, by an optical-mechanical scanner of a 11.56° visual angle, converging a large area includes in a paralelogram 185 Km on the side (Fig.) Clouds and their corresponding shadows commonly found in the photographs, are undesirable for the interpretation of Natural Resources. The classification of clouds is a part of the descriptive analysis of weather condition of a region. It includes analysis of the form, altitude, structure, density and clouds association, characteristics which can be determined on the ERTS-1 multispectral photography.

Clouds are seen at a scale slightly larger than the terrain scale, and all the features useful for classification can be determined. A cloud analysis however, show features, such as wind direction, sea current direction, longshore drift, sediments transport and other geomorphic and geologic processes that are useful on Geoenvironmental studies.

A simple method to determine the approximate altitude of clouds is described in this work, with the objective of refining their classification, using only marginal data on the photograph. The error involved in this method is small and does not transgresses the range of cloud genetic levels, thus being accurate enough for cloud classification. Results of the application of this method on photographs of the Paraguana Peninsula are presented.

Cloud altitude ratio to the cloud-shadow image distance. Sun elevation and solar azimuth (SUN EL 54° AZ 126° of Fig.) are the marginal information provided by the ERTS-1 photograph. These terms are respectively the vertical angle of incidence of the sun rays above the horizon, and the bearing of their path on the horizontal plane, Fig.

. The direction of displacement of corresponding points of the clouds and shadows images occur along the solar azimuth.

Clouds located at similar atmospheric level show similar cloud-shadow image distance, but those located at different levels show different distances, being larger for the higher clouds.

Fig. show 3 levels of clouds illuminated by solar rays with a constant sun elevations angle (54° as in Fig.). For the demonstration, 3 clouds at different levels are used, with a border coinciding planimetrically in the photograph. The visual ray from the satellite records the images of the 3 boundaries on the same point of the photograph, but the boundaries of their respective shadows will be recorded at increasingly larger distances, the higher the clouds are located. Thus the cloud-shadow distance for the low level clouds is the short distance d_b ; for the intermediate level of clouds is the intermediate distance d_i , and for the high level of clouds is the long distance d_a .

Computation of clouds altitude. For the computation of the clouds altitude, trigonometric relations of the triangles built with the following parameters are used (Fig.).

- Sun elevation angle (s), given in the photograph.
- Clouds-shadow image distance (d), measured in the direction of the solar azimuth directly on the photograph with micrometer. This distance is converted into meters by multiplying it by the photographic scale.
- Cloud altitude (a) measured in meters vertically from the edge of the cloud (n).
- Line (a) drawn from the edge of the cloud (n) on the atmosphere, to its photographic image (i). This line is not vertical, but it approaches closely altitude (a), departing a maximum of 5.78° , that is, half of the optical scanner visual field.
- Angle (n) complementary of angle (s) whose value can varie from $90-s$ to $84.22-s$. The $90-s$ value is only a close approximation, valid when the cloud is at the center of the photograph, but its value can varie to a minimum of $84.22-s$ when the cloud is at the edge of the photograph.

From these triangles the following relations are obtained:

$$\frac{\sin s}{a'} = \frac{\sin n}{d}, \text{ then:}$$

$$a' = d \cdot \frac{\sin s}{\sin n} \quad (1)$$

Equation (1) provides slightly higher than the true altitude values, when the exact value of angle (n) is used. On the contrary, when approximate equation (2) is used, slightly lower values are obtained when angle (n) is used as complement of angle (s), on the following relationship:

$$\frac{\sin s}{a''} = \frac{\sin (90-s)}{d}, \text{ then}$$

$$a'' = d \cdot \frac{\sin s}{\sin (90-s)}, \text{ and}$$

$$a'' = d \cdot \operatorname{tg} s \quad (2)$$

The clouds altitude computation is not however exact,, because besides the approximate equations used also approximate measurements and data without correction is used. Among these factors are the following:

1. Cloud shape and solar elevation angle
2. Atmospheric refraction
3. Earth ellipsoid
4. Topographic relief.

Cloud shape and solar elevation angle. The cloud and shadow images are formed by the visual and sun rays tangent to the cloud edges (Fig.).

The cloud image tends to resemble the cloud map, as the visual rays from the camera, tangent to the clouds, depart little from the vertical (up to 5.78°), while the shadow image is the tilted section at the angle of the sun elevation, that varies according to latitude and hour. There is more resemblance on their images and therefore better accuracy on the measurement of their distance when the cloud is thin and the angle of sun elevation wider.

When the cloud is thin and the sun elevation angle high (over 45°), the tangents formed by the sun ray and the visual ray from the satellite tend to coincide on the same border of the cloud, and therefore the shadow image resembles much the cloud image.

When the cloud has a medium thickness, the shadow image is produced by a section, tilted steeper than the one producing the cloud image.

When the cloud has a high vertical development (even with a mushroom or anvil profile on its top), the cloud image may be formed at a lower level, while, the shadow image is formed by a steeper tilted section, including parts of a vertical profile at higher levels, with shapes not necessarily corresponding with the ones at lower levels. These dissimilar shapes of the images are easily detectable and indicate clouds with high vertical development. In both latter cases, the planimetric difference of location of the edges used for the cloud and shadow projections, is small and even more so considering the usual photographic scales of 1:1.000.000 to 1:500.000. This difference is reduced further with steeper sun elevations angles.

Atmospheric refraction. The refraction of the visual and solar rays on their crossing of the atmosphere to produce the cloud image and its shadow projected on the ground, causes the displacement of these images located at different altitude and on the ground (Fig.).

The refraction is a direct function of the atmosphere density (p), which depends on its temperature, pressure, etc., data which unfortunately is not easy to obtain. It can be generalized however that objects located in the high atmosphere will be less refracted than the ones close to the ground, where atmospheric density is greater; and during the dry season there will occur less refraction than on the wet season. The greater the thickness (E) of atmosphere crossed by the rays, the greater refractions they will undergo, thus the images on the ground will be displaced further than the images floating on the air, as the atmospheric distance crossed by the rays is larger. A cloud image undergoes little refraction due to the less dense (P_2) atmosphere separating it from the satellite. A shadow image on the ground surface undergoes larger refraction due to the greater thickness and denser (P_1) atmosphere separating it from the satellite. The resultant of this differential displacement is the cloud-shadow distance registered in the photograph and the basic data used without correction to compute the clouds altitude.

Earth ellipsoid. A small angularity is formed between the earth ellipsoid and the tangent plane of the photographic projection (Fig.). This angularity increases toward the edges of the photograph. The images displacement follows the solar azimuth direction, and it is always toward the sun. The magnitude of the displacement increases toward the photograph edges. This displacement is not noticeable toward the center of the photograph, especially at the scales commonly used, not appreciably influencing the computation of the clouds altitude.

Topographic relief. In areas of low relief, the clouds height is also approximately their altitude, however in mountainous areas, the clouds shadow is projected over the ground, located not at sea level but at an altitude that can be obtained from topographic maps (The Cartografía Nacional maps at a scale of 1:100,000 are enough). Adding the mountain altitude to the computed cloud height, the cloud altitude above sea level is obtained (Fig.).

Applications. Through the usage of equations (1) or (2) approximate altitude of different cloud levels seen on the Paraguaná Peninsula photographs (scale 1:500,000 taken from the ERTS-1 satellite at 10:30 a.m. October 19, 1972, (Fig.)) can be computed. From the photograph marginal information, a sun elevation angle of 54° and an azimuth of 126° is obtained.

Above the Paraguaná Peninsula a cloud level of cumulus type trend in a ENE-WSW to E-W direction. A sampling of the cloud-shadow distance (d) results in a variable range between 600 to 800 m. Table 1 (Fig.). Using equation (2) and multiplying those values of (d) by the tangent of angle s ($\tan 54^\circ = 1.376$), a cloud altitude range of 826 to 1,101 m. is obtained for this level, verifying in this way the preliminary classification of cumulus.

Other computations are made with Sierra de San Luis Cumulus, with the previously classified as Sierra de Baragua stratocumulus, and later on reclassified by their altitude as cumulus nimbus. Finally the Golfo de Venezuela (west of the Paraguaná Peninsula) cirrus filamentosus altitude could not be computed by their lack of shadow.

CA/aa.

Fig 5

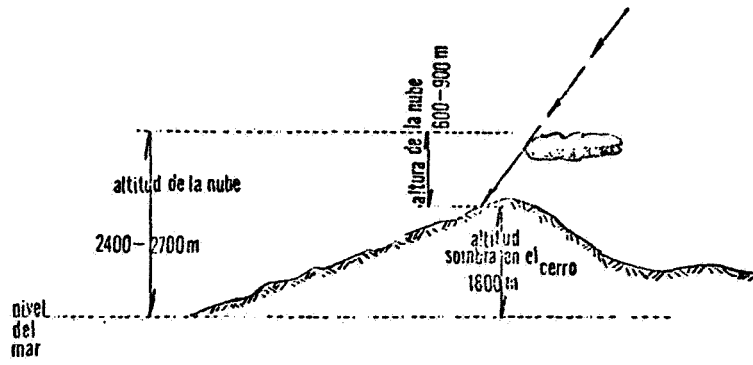
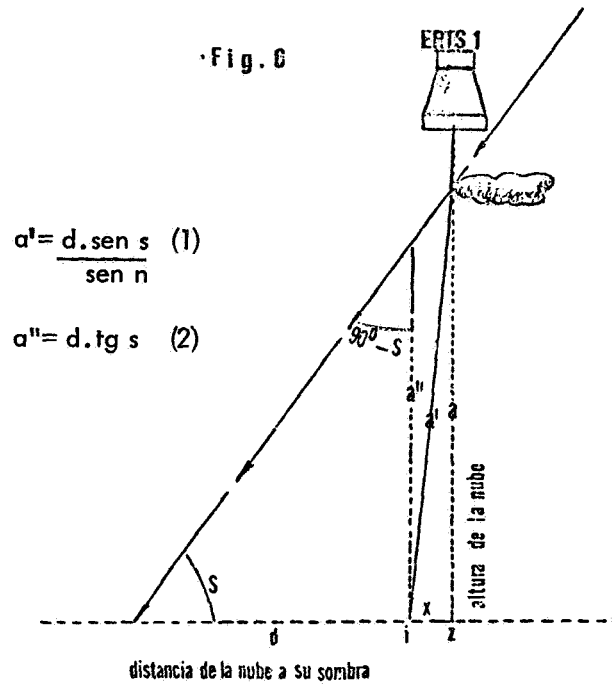
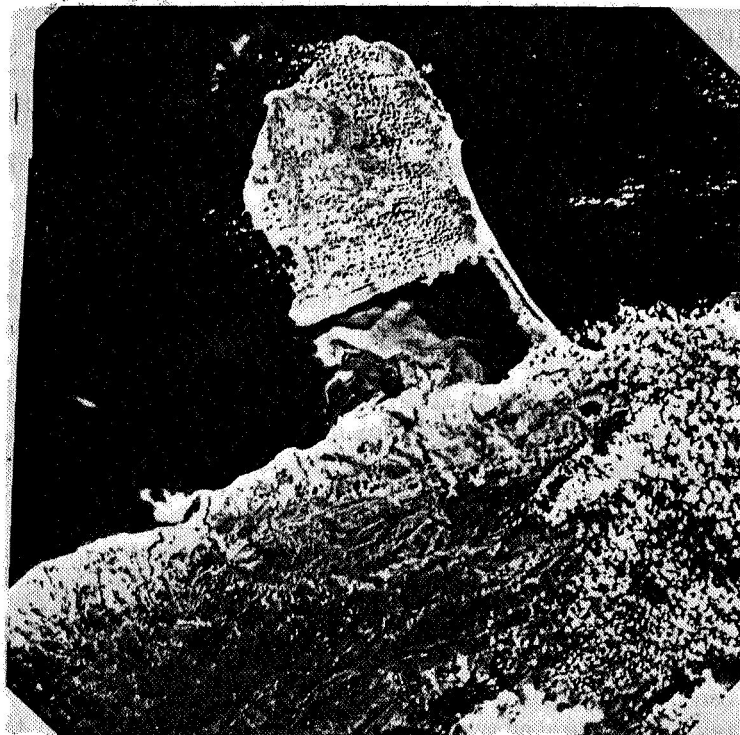


Fig. 6





DESCRIPTIVE ANALYSIS OF CLOUDS IN THE GOAJIRA PENINSULA, PARAGUANA PENINSULA AND THE VENEZUELAN CENTRAL REGION.

Introduction. The clouds study on the satellite photographs is aimed to different facets:

- a. Cloudiness determination, or finding the percentage of cloud coverage at the time the photograph was taken, and consequently its degree of usefulness.
- b. Cloud altitude determination, useful for their classification.
- c. Clouds classification, based mainly on their shape, which in turn depends on the altitude of their condensation process. Temperature, moisture and air movements varies at different level over the ground surface, and clouds formed at different altitude differ generally in shape.
- d. Determination of air mass instability, in the cloud, which is proportional to the cloud vertical development.
- e. Determination of the prevailing wind direction at the time of the take, as indicated by low altitude clouds with low vertical development, over regions of low relief.
- f. The areas of greater condensation can be located through a repetitive series of photographs covering a region over a period of time. This analysis is useful in the selection of airport locations and optimum flight time schedules.

Methodology. Black and white photographs scale 1:500,000 of bands 5 and 7 were used, complemented with photos scale 1:1,000,000 and band 4. False color photographs were used to differentiate water bodies from cloud shadows.

Shorter wavelengths (bands 4 and 5) allow better discrimination of shadows on water bodies. The greater water penetration renders a light tone for a shallow bottom as a background for the dark cloud shadows. These bands also show better the structure of the less dense clouds, a useful characteristic for their classification. Dense clouds (cumulus type) show better in band 7.

The cloud-shadow distance was carefully measured with parallax bar, thus avoiding additional inaccuracies in the method.

The cloud classification is based on the identification of cloud genus, except for some cases where cloud species were identified.

Analysis. From the cloud altitude computations, the following clouds types were identified:

- a. Clouds of low vertical development, less than 600 m thick, located from 700 to 1,600 m of altitude, dense, piled up, with sharp boundaries, identified as cumulus.
- b. Other clouds show similar features as the ones above but are located at 2,000 m and above, with this altitude indicating the measurement of the clouds upper level rather than their base; as well as their high vertical development. When these clouds show sharp boundaries and a cauliflower shape, they are named cumulus congestus.

Goajira Peninsula. Cumulus congestus can be seen in the W side of the photograph of October 2, 1972; (Fig.) besides their relatively low moisture content, they imply a strong vertical draft due to a large pressure gradient on the lower strata of the air mass. In fact, the trade winds from the NE, with some moisture content and less warmer than the ground surface, as they enter the the Goajira, get warmer in contact with the ground and begining their condensation as they rise. The greater their heating, the higher being their vertical development. An intense solar radiation is needed to generate the vertical displacement of the air.

Band 7 shows a high of penetration power through atmospheric water vapor, thus reducing the cloudiness. Band 5 shows entirely the large cirrus covering a great area of Golfo de Venezuela; as opposed to band 7 showing only the denser part of the main cloud with the shape of a fish skeleton, thus identifying it as a fibratus species.

Alto cumulus are seen in the SE part of the photograph of February 23, 1973 (Fig.), with a structure of very fine ripples resembling Cirrocumulus, but their computed altitude of 2,553 m. place them in the intermediate level common for Alto cumulus.

Clouds of low vertical development at altitudes from 350 to 1,550 m. are observed above the peninsula in the same photograph; their low altitude indicates air with low moisture content favorable for saturation at a minimum cooling. These cumulus are aligned parallel, forming the commonly named "Cloud alleys", indicating the prevailing wind direction for that hour, which was blowing from the NNE as confirmed by meteorological record. These cumulus are evidences of the regional good weather conditions prevailing for that date.

Band 5 show a sort of nebulus without obvious details above Golfo de Venezuela. NW of the Peninsula, filament shaped Cirrus fibratus are identified, resembling the cirrus of the previous photograph but with finer loose elements.

Paraguaná Península. A level of cumulus at an altitude of 800 to 1,100 m. are observed over the Peninsula in the photograph of October 19, 1972 (Fig.). Their low vertical development attained is due to the small extent and low relief land on their path. Larger Cumulus development by orographic winds are found in the Sierra de San Luis, with altitudes ranging from 1,600 to 2,200 m. for their upper boundaries. Toward Sierra de Baragua in the southern end of the photograph there is a cloud formation composed of rounded elements with rippen edges, revealing their cumulus origin. This cloud of high vertical development, with altitudes ranging from 9,630 to 11,000 m, is identified as a cumulonimbus, possibly originated by the exaggerated growth of a cumulus, a common fact occurring during the warmer months. The clouds albedo on the photograph indicates a day of strong radiation.

Toward the NE of the photograph and over the sea, low density cirrus are observed on band 5; they are absent in band 7.

Lake Valencia. A series of clouds of convective origin are observed in the photograph of October 17, 1972 (Fig.). According to their vertical development the following types are found:

a./ Clouds of medium to high vertical development located at 1,200 to 3,400 m. of altitude, are formed where the relief has forced a steep climb of the air masses. Some of these clouds are found along the crest of the Cordillera de la Costa. Normal to this range are N-S trending clouds, following the wind path through the valleys. Many of these clouds climb the range and continue their trend attaining greater altitude in the opposite flanks.

b./ Cumulus between 700 and 1,600 m of altitude are found in the Galeras del Pao area, on the southern part of the photograph. Some of them show a faint E-W trending alignment, thus pointing the wind direction at the time of the take.

This photograph shows a high percentage of cloudiness, a consequence of the convergence of local and tropical air masses, an event foreseen at 8 a.m. of the day of the take, by the Weather Bureau.

The photograph of February 2, 1973 (Fig.) shows a better alignment of cumulus trending NE-SW. The altitude of the smaller cumulus ranges from 1,300 to 1,500 m. or an average altitude higher than in the previous photograph. This higher altitude indicates a lower moisture content of the ascending air mass reaching a higher condensation level.

Clouds of medium size show their crests between 1,200 and 1,800 m. of altitude, thus indicating their approximate vertical extent and the air mass instability and moisture content.

A comparison of bands 4 and 7 is used for the classification of the large cloud formation over the Cordillera de la Costa. A cloud formation without typical features is seen in the former band, while large bodies of Cumulus-congestus of rounded edges, partially overlain by a faint layer of Altostratus is shown in band 7. This cloud formation is the result of the moisture condensation from the NE winds on their path through the Barlovento coastal plain. In this connection a repetitive series of photograph could provide useful data on the loci of recurrent moisture condensation from these winds, where the normal operation of airports would be critical from December to March, when the NE wind blows with its greatest intensity.

Over the sea a degeneration into patches of a layer of Altostratus, could be misidentified by patches of dense Cirrus, their considerable horizontal extent however, their gray tone and altitude of 3,500 m. allows their identification as Altostratus.

Barlovento Area. An homogeneous type of clouds are shown on the photograph of March 27, 1973 (Fig.). Cumulus with heights from 0 m. (Sticked to the crest of Serranía del Litoral) to 1370 m. are found over the land. Their low-altitude and the similarity of the cloud and shadow images indicate a low to moderate vertical development.

The low cloud base is another important fact to point out, this implies a high moisture content of the air masses on the area, a fact partly explained by the vicinity to the sea and of moisted surfaces such as the dense vegetative formations of the Guatopo jungle and Barlovento Coastal plain, made of deltaic deposits.

The display, somehow disordered of the clouds reveal a dominante wind direction, however the small cumulus show a SE-NW trending coastal plain of Barlovento.

The raising of air along the flanks of the Serranía del Litoral explains the existence of clouds along its crest. The absence of clouds in the coastal belt implies a dominant southern wind; the previously mentioned NW-SE aligned Cumulus confirms a prevailing wind direction from the SE.

Cirrus uncinus (of hook shape) are found over the sea, they are commonly formed on clear air with few component in suspension. Band 5 shows them move obviously. North of these an extensive Altocumulus generated by vertical displacement of air located on the atmospheric layers is observed.

In summary of the photographs studied, clouds with vertical development (cumulus type) are found generally along the coast and inland, thus confirming their thermal convection and differential gradient origin. On the contrary over

the sea surface the constant movement of water favors a continuous heat transfer toward greater depths, with the air above maintaining a greater density and moving toward the coast, the void being filled with air from the upper layers, thus causing subsidence and consequently fine weather. This fact is observed at the time of the lagoon, when wind blows from the sea.

In conclusion the coastal belt of northern Venezuela show a characteristic homogeneity of cloud types, which belonged mostly to the Cumulus genus; except for some examples of Cirrus, Altostratus y Altocumulus generally found over the sea.

The clouds altitude plus their shape and structure obtained through the comparative study of the different photographic bands, become the necessary tools for their identification. Their classification provides information on the physical processes developed in the atmosphere as well as certain regional climatic characteristic, such as moisture content, wind direction, etc.

Fig. 1 Tabla de alturas de nubes (Table of clouds altitude)

Nubes	Distancia (d)	tg	Altura m.	Orientación
<u>Península de la Goajira 2-10-72</u>		tg 56°		
Cumulus	600-1012 m.	1,4825	889-1500	NE-SO
" congestus	944-1281	"	1400-1900	
23-2-73				
Cumulus	300-1400 m.	1,1106	333-1554	NE-SO
Altos Cumulus	2300	"	2553	
<u>Península de Paraguaná 19-10-72</u>		tg 54°		
Cumulus de poco desarrollo vertical . Paraguaná	600- 800 m.	1,376	826-1101	ENE-OSO
Cumulus de mediano desarrollo vertical S. San Luis	1200-1600	"	1652-2202	SSE-NNO
Cumulunimbus .S. Baragua	7000-8000	"	9635-11011	
Cirrus filamentosso Golfo de Vla.	sin sombra		no determinada	
<u>Lago de Valencia 17-10-72</u>		tg 55°		
Cumulus de poco desarrollo vertical ,Galeras del Pao	500-1100 m.	1,428	714-1570	E-O
Cumulus en el Litoral	850-1200	"	1213-1713	N-S
Cumulus de mediano desarrollo vertical	1200-1400	"	1713-1999	
Cumulus congestus	1800-2380	"	2570-3398	
E. del Lago de Valencia				
2.2.73		tg 45°		
Cumulus. Galeras del Pao	1300-1500 m.	1	1300-1500	NE-SO
Cumulus de mediano desarrollo	1200-1800	1	1200-1800	
Nubes adosadas a la Cordillera de la Costa	600-1000	"	600-1000	
Altostratus sobre el mar	3500	"	3500	
<u>Cabo Codera 27-3-73</u>		tg 55°		
Cumulus.				
Cresta Serranía del Litoral	0-450	1,428	0-643	E-O
Cumulus.				
Llanura costera Barloventaña	400- 850	"	571-1214	SE-NO
Cumulus.				
Serranía Interior	800-960	"	1142-1371	
Cumulus.				
Altos llanos Centrales	690-950	"	985-1356	

BIBLIOGRAFIA (References)

1. Clausse y Facy. 1968 - Las Nubes. Martínez Roca S.A. 188 p.
2. Fontseré, Eduardo. 1943 - Elementos de Meteorología. C. Gili S.A. 358.
3. Gol A. M. 1963 - La Observación Meteorológica. Servicio de Meteorología de la Comandancia General de la Aviación. 251 p.
4. Guevara, José. 1970 - Meteorología para Geógrafos. U.C.V. 429 p.
5. NASA. 1972 - Manual para usuarios de datos ERTS
6. Organización Meteorológica Mundial. 1957 - Atlas Internacional de Nubes (Compendio). Servicio de Meteorología de la Comandancia General de la Aviación. 70 p.

GEOLOGICAL PHOTOINTERPRETATION OF THE PARAGUANA PENINSULA USING ERTS-A MULTIESPECTRAL PHOTOGRAPHY

Carlos Albrizzio

ABSTRACT. The objective of this study is the development of a methodology to evaluate multispectral analysis of orbital imagery on the interpretation of geology, coastal geomorphology and sedimentary processes, in manners useful for Urban Regional Planning and in the evaluation of Natural Resources.

The images analyzed were obtained during the pass of ERTS satellite through the Center Region of Venezuela in October 19-1972, at 69° 20' to 71° 00' long. W and 10° 45' to 12° 15' lat. N. (Paraguana Peninsula) ERTS-A multispectral images in black and white paper copies and transparencies of the 4 bands and false color composites at scales of 1:1,000,000 and 1:500,000 were interpreted with the aid of a magnifying glass and microfilm viewer.

Lithology and outcrop patterns of the following geological formations have been interpreted: igneous and metamorphic basement of Cocodite and Santa Ana, Jurassic-Cretaceous metamorphics of Pueblo Nuevo, Cantare Miocene-Pliocene sediments, and Quaternary alluvium, dunes, beach ridges, bars and reefs. A prominent and extensive "Paraguana tonal anomaly" shaped as an 8 has been discovered at the NW of the Peninsula. Its erosional origin has exposed light toned lower beds at the center, with additional evidence of topographic depression and development of underground drainage of karst origin.

The Peninsula structure is a plateau with near horizontal beds, with two gentle domes culminating in the basement cores of Cocodite and Santa Ana, with the E-W trending Buena Vista syncline in between; all the folding due to sedimentary dip and differential compaction. The Punta Salinas normal fault, down thrown to the north, trends ENE-WSW for over 35 Km from the coast to Mesa de Cocodite. Other smaller fault systems are the NW-SE trending Punta Macolla, and the NNE-SSW Bahía de Amuay systems.

Coastal geomorphology, its processes and energy has been interpreted with the help of wind direction analysis (ENE-WSW) at sea level through the orientation of transported materials (water vapor, water and sediments) by clouds, waves, sea current, plumes of suspended sediments associated to river outlets, dunes, sediment sources and shoreline orientation.

The Paraguana coastline has been sectorized (according to its linearity, orientation and typical geoforms) as follows: the Southern coast, straight with gentle dip slopes and 3 sand bodies, the Eastern coast straight with a few beach ridge systems and embayments with barrier reefs, sand bars, lagoons and salt flats; the Northern coast, straight with few beach sediments and some dunes; and the Western coast with embayments and 2 sand spits.

N 74 30768

Surface water bodies and drainage beds have been interpreted using soil pattern and vegetation of the gallery forest type.

For the current land usage, the following has been interpreted: cultivated plots and grazing lots on the rural areas around Adicora, Pueblo Nuevo, Buena Vista, Amuay, Cardón and Coro; the urban areas of Coro and Amuay-Cardón, and the industrial area refineries with details of oil tanks, their retaining walls and large sheds. Engineering works were also identified such as dams, airports, roads, oil pipes and a water pipe.

1. STRATIGRAPHY . Most important rock outcrops of pre-Tertiary age Igneous-Metamorphic basement are located in the Western sector of the Peninsula, at the Santa Ana Hill (covered in the image by a well developed cumulus) and at the Cocodite Mesa. Both areas are observed in the 4 bands with dark grey tones and in the color composite (4, 5, 6) appear with dark to very dark grey due to their composition of white granitic rocks (quartz, white feldspar and mica) which reflect I.R.

Marine shallow water sedimentation took place during the Tertiary. Clay, sand and coral reefs developed around the nuclei of the basement. Tertiary Formations are observed as Mesas Slightly tilted. They cover the entire Peninsula and originate a plain where light and dark grey tonal responses alternate according to the predominance of ground material (limestones, sandstone or clay and vegetation).

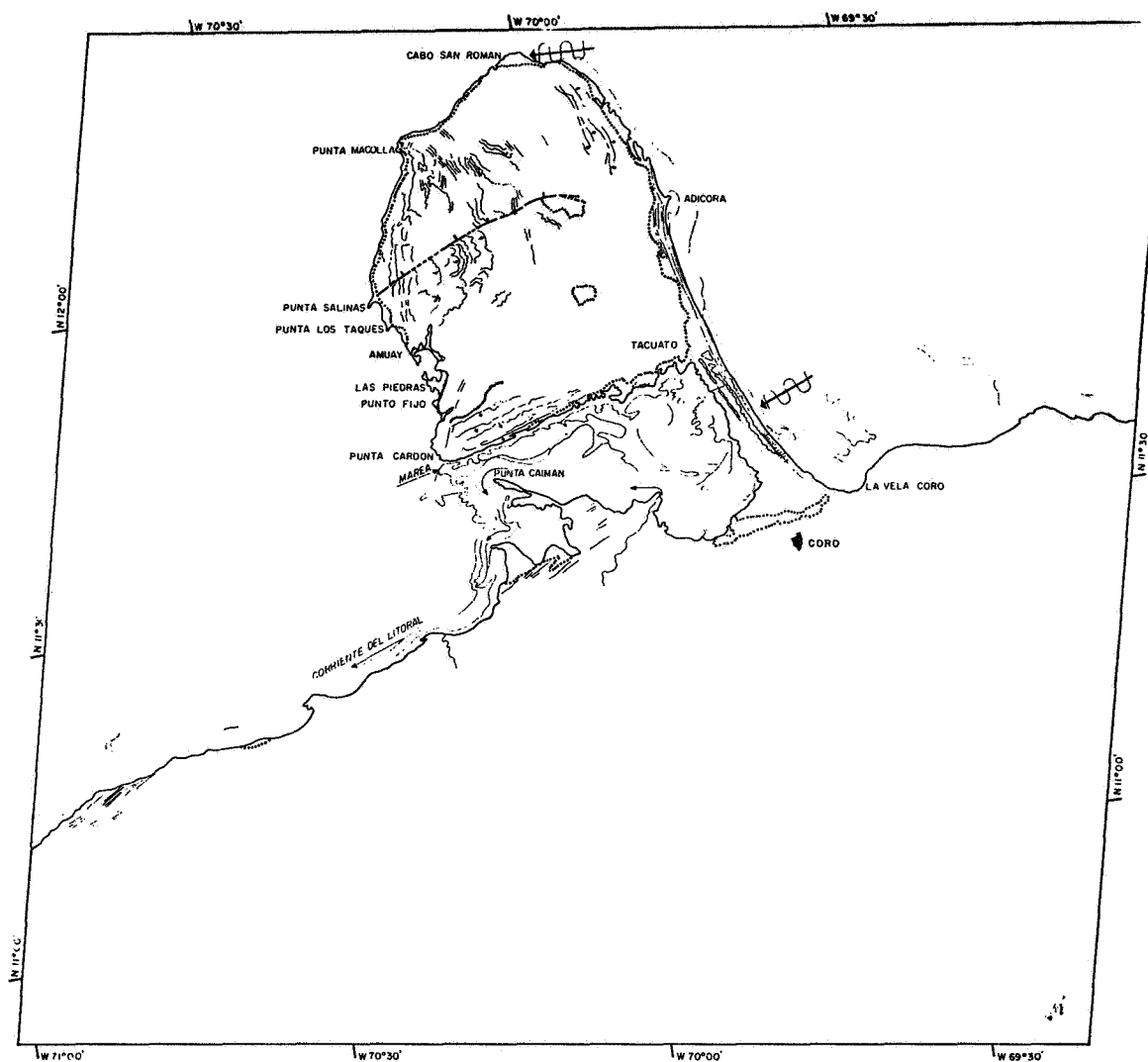
In the N.W. side of the Peninsula, two circular tonal anomalies are observed in all 4 bands, as well as in the color composite. Light gray to white linears shape an 8 form on a medium gray base. These tonal anomalies are present in areas of erosion and removal of overlying -possibly Pliocene- strata of almost horizontal position, identified by medium gray tones. Erosion has discovered older strata -possibly Miocene- formed by limestone and sandstone, identified by white to light gray tones.

The origin of these anomalies, as well as that of the depression of Amuay Bay, could be karstic. Both circles of the 8 shape are separated by the Punta Salinas Fault. Existing maps at scale 1:1.000.000 show some topographic evidence for the northernmost circle as well as some surface drainage which disappear and may continue underground within the circle, at the place called Orejitas, S.W. of Macolla. The Southern circle is surrounded by important topographic evidence; within it there is a depression, W. of Jadacaquiva.

Geologic contact of Quaternary and Tertiary has been drawn with great detail. Quaternary forms a narrow strip of light to white gray tones which surround the Peninsula. This strip has been formed by littoral sedimentation processes and in its composition predominate quartz sand. There exist dunes and some alluvial materials. Salt flats, barrier bars and coastal lagoons present an intermediate gray tone in all bands but in color composites (4, 5, 6) acquire a light blue color. Barrier reefs are distinguished in all 4 bands with medium gray tonal response with light gray tones at the border.

2. STRUCTURE. The Peninsula appears at the borders as a Mesa with strata dipping almost horizontal. At the center, regional structure resembles two soft domes which culminate at the nuclei of the basement and are seen as follows:

<u>SIDE</u>	<u>SLOPE</u>	<u>SLOPE DIR.</u>	<u>OTHER</u>
South	Gentle to Nil	South	---
East	Medium-Gentle	East	---
North	Gentle to Nil	North	Faulted
West	" to Nil	West	---



- | | | |
|----------------------------------|--|---|
| ----- CONTACTO GEOLOGICO | — LINEACIONES | Q ALUVION (A) DUNAS (D)
CUATERNARIO |
| — ESCARPADO | ↔ DIRECCION DEL VIENTO | MPc FORM. CANTAURE
PLIOCENO
MIOCENO |
| ↗ RUMBO Y BUZAMIENTO
DE CAPAS | ↗ DIRECCION DE LAS
CORRIENTES MARINAS | JKpn FORM. PUEBLO NUEVO
JURASICO
CRETACEO |
| — FALLA NORMAL | — PLUMA DE SEDIMENTOS
EN SUSPENSION | ROCAS IGNEAS PRE-JURASICAS |

**REGION DE LA PENINSULA DE PARAGUANA
GEOLOGIA Y GEOMORFOLOGIA**

ELABORO C ALBRIZZIO

Km. 0 10 20 30 40 50

OCT. 1972 FOTOG. SATELITE ERTS-1 IDENT 1088-14300

Between both nuclei there is a gentle syncline trending E.W. the dome of Cocodite, the dome of Santa Ana and the syncline of Buena Vista form a system of folds with origin due to depositional dip and differential compaction over a basement with topographic relief.


There are numerous evidences of faulting, with faults grouped in systems. The Midwestern part of the Peninsula is cut by the Punta Salinas fault extends ENE-WSW for 35 Km from Punta Salinas to the N of Cocodite Mesa. This fault is detected in all 4 bands by: a) the topographic expression of the lineament; b) the displacement of the strata on the west coast and central plateau; c) the light gray tonal response of outcrops along river beds. Northern side of the fault has been relatively lowered.

At the northern side of the Peninsula, East of Punta Macolla, it is observed a NW-SE faults system 16 Km long which controls numerous creeks. these faults are evident by their linearity, by the drainage or by the light gray tones of outcrops.

In the S.W., near the bay of Amuay, it is observed a system of faults extending NNW-SSE for 5 Km, faults are evident along the Jayana creek, at the cliffs and by their topographic expression.

3. LITORAL DYNAMICS. Accumulation of sediments is controlled by winds, wind direction, river discharge, long shore drift and by the energy balance of rivers and the sea.* The rivers of the region do not penetrate long within the sea, and this fact indicates that sea energy controls the distribution of sediments along the shoreline. The di-

* Wind is the most important energy element intervening in the formation of waves and ocean currents. Both waves and ocean current as well as fluvial currents are the most important components of litoral dynamics. Wind direction was determined at different places and altitudes by interpreting directional movement of the elements transported



rection of Eastern wind is constant along the coastal region. Sea current is the variable which controls the distribution of sediments.

Both at the Eastern coast of the Peninsula and of the Istmo, shorelines are oriented NW-SE, almost normal to wind direction and offers a barrier to the transport of sediments by the sea current. The wind diminishes its energy and local deposition takes place giving way to wide strips of sediments along the shoreline which is redistributed by longshore drift. Part of those sediments are transported by wind to form different types of dunes inland. **

The N and NE coast of the Peninsula are oriented from E-W. to NE-SW, almost parallel to wind direction. As they do not offer great resistance to sediment transportation, they only accumulate narrow strips of litoral and eolic sediments.

The West coast is oriented NW-SE and has little accumulations for it is protected from sea current by the Peninsula. At the West coast of the istmo, eolic and fine marine sediments are being accumulated, the latter being carried by the current of the Golfo de Coro.

* ... (water, water vapor and sediments). At sea level, waves, long shore drift and eolic sediment patterns were used as evidence. At other altitudes, patterns of clouds were used as evidence. The elongation of eolic geoforms indicate a persistent regional direction of wind ENE to WSW at sea level.

- ** Accumulation of dunes are encountered at the following places:
- Istmo de Médanos: extensive and frequent longitudinal dunes.
 - Cape San Román and Punta Macolla: longitudinal dunes.
 - Médanos de Coro: abundant and well developed transversal dunes.
 - Llano de Chenguító: interpreted as an accumulation of sand. Possibly transversal dunes not verified by field work.
 - Delta del Río Mitare: covered with longitudinal dunes.

The direction of waves and its refraction are not visible in the images at the scale of 1:500.000, but litoral dynamics is evident by plumes of densely suspended sediments that are observed associated with river outlets. Directional elongation of plumes indicate their transport direction as well as the direction of the long shore drift.

The general direction of the marine current is ENE-WSW as indicated by wind direction and by the pattern of the lower level of clouds. The direction of the long shore drift is indicated by the direction of plumes. Sediments plumes are observed in the following places:

- Punta Manzanillo (from Puerto Cumarebo to Ricoa river). Sediments from this river form 3 plumes extended towards the N.W. which disappear at the Bahía de la Vela where apparently sedimentation takes place. The longest plume is 4 Km long and the others are 1 Km long each one. Along side and continuing the largest plume, there can be observed a tonal anomaly that can be interpreted is a plume although it could be the shadow of a cirrus.
- Punta Taimataima to La Vela de Coro. There can be observed a narrow strip of 4 lobuli extended towards the NW. One of the plumes reaches the Istmo de Médanos where sedimentation occurs.
- Vela de Coro to East coast. a narrow strip of suspended sediments from river Coro is observed.
- Golfete de Coro. Its waters are rather shallow, with mean depth of 6 m. and with a narrow channel 8 m. depth. River Mitare's sediments are constantly filling the golfete. It is evident that the delta has been progressively displaced to the E. Ahead of the river Mitare Delta, it can be observed a dense plume of suspended sediments with numerous

lobuli displaced counter clockwise along the shoreline. Other minor plumes are displaced C.C.W. towards the E. of the golfete, creating thus a C.C.W circulation cell in the midpart of the golfete.

River Mitare's plume has irregularities of anomalous forms. They have been interpreted as the affect of friction among the sediments and clean seawater that is carried Eastwards.

At the west coast of the Golfete there is a narrow strip of suspended sediments from the rivers Codore, Mitare, Zazárida, Capatárida and Borojó. The plumes are displaced WSW following the litoral current and deposit their sediments along this coast.

4. LITORAL MORPHOLOGY. The coast line of the Península has been sectorized according to orientation of shoreline and predominant geomorphs:

a. SOUTHERN COAST. Extends from Punta Cardon to Tacuato, oriented NNE except at the eastern extreme where it is interrupted by 3 accumulations. Geologic contacts between Holocene sediments and interstratified Miocene-Pliocene rocks can be observed through tonal changes from white to light yellow to dark yellow in the false color composite. This coast is controlled NNE and by the dip angle SSE of the strata that crop out. There have been recognized 12 parallel bands where dark gray tones (clay) alternate with light gray tones (limestone and sand).

At the West part of this coast sedimentation and sea energy are at equilibria. At the East part, there can be observed 3 sand bars possibly old keys partly eroded.

b. EAST COAST. The east coast (Tacuato to cape San Román) is strigh trends SSE-NNW. The Istmo de Médanos with similar features is also included here. The coast line is divided in the following sections after their geomorphic characteristics :

La Vela de Coro-Adfcora coast line is 70 Km long and show a gentle curvature with a 200 Km. radius. The littoral zone is 3.5 to 5 Km wide and show predominantly beach ridges as alternate strips of white color (quartzose sands) with wider strips of pale gray tone (vegetation and higher moisture content on the low areas between ridges). Up to 15 of them have been identified at a scale of 1:500,000 on band 5.

Three systems of beach ridges are found in this area:

- The oldest system extends intermitently for 15 km from Tacuato to halfway the istmo, where it is totally destroyed and covered by longitudinal dunes.
- The intermediate system extends for 15 km from Adfcora to Tura (half way to Tacuato); it is 2 km wide and has a curvature radius of 10 km.
- The youngest system extend for 70 km from Adfcora to La Vela de Coro, it is 1.5 km wide and has a curvature radius of 200 km.

The coast line north of Adfcora has a general NNW-SSE trend, and show frequent reentrants, associated with reefs, embayments and coastal lagoons. It has been divided in 3 areas:

- Adfcora-San Pedro, of similar features to the area south of Adfcora.
- San Pedro-Puerto Escondido, with barrier reefs, coastal lagoons and sand bars.
- Puerto Escondido-Cape San Román, of narrow beach and a 2 km wide belt of longitudinal dunes.

c. NORTH COAST. The north coast (Cape San Román to Punta Macolla) is a straight NE-SW trending line with a gentle embayment NE of Punta Macolla. The rocks outcrop extend to the beach, except for the narrow belt of longitudinal dunes of Punta El Infierno.

d. WEST COAST. The west coast (Punta Macolla to Punta Cardón) characteristically lacks sediments, and has been divided in the following 4 parts according to their geomorphic features:

- Punta Macolla to Punta Salinas, a straight NNE-SSW trending coast controlled by the beds and fractures that outcrop along the beach.
- Punta Salinas to Amuay Bay, with 2 embayments and sand spits (Punta Salina and Punta Los Taques) with their source being Las Tres Marías creek.
- Amuay Bay to Punto Fijo, with a series of embayments and points along the cliffs controlled by fractures. Although this area resembles a sunken coast, it lacks the supporting evidence for this origins, and a control by fractures and karstic origins is more likely.
- Punto Fijo to Punta Cardón, with a SW trend that changes to SE on the south, shows no cliffs, and a small salt flat.

Drainage.

Water bodies. The free surface of water bodies are better identified as black areas on band 7 of black and white photographs, due to the shallow penetration of IR radiations. On false color composition (bands 4,5 and 6) they are identified by a blue color, of a dark to pale tone, depending on an increasing amount of suspended sediments.

River beds and depressions. River beds, coastal lagoons, salt flats and dam reservoirs are better identified on bands 5 and 7 of black and white photographs.

On band 5, areas above water appear with a pale gray to white tone (Bajarigua salt pond, coastal lagoons north of Adicora, and rivers of Falcón). Some of these river beds of white tone appear with a dark gray to black background from their gallery forests.

On band 7, the river beds show dark gray to black in a pale gray background of their gallery forests.

Land usage.

The interpretation of land usage has been done according to the following types:

Rural areas. Small land plots are identifiable in the Peninsula near Adfcora, Pueblo Nuevo, Buena Vista, Amuay-Cardón and large plots west of Coro. These features are identified by their rectangular shape, of pale gray tones on a darker background, and are interpreted as agricultural land, grass fields and plowed land.

Urban areas. Coro and other smaller urban areas such as Amuay and Punta Cardón, Jadaquiva, etc are identified. These areas show a geometric outline of pale to medium gray on a darker background, with radial roads and dark cultivated vegetation.

Industrial areas. Tank farms, safety dikes and large sheds have been identified in the oil refineries of Punta Cardón and Amuay. On black and white photographs the tanks appear as black spots, framed by pale gray dikes, with their tones changing to yellow on false color compositions.

Engineering works. Water dams, roads, airports, oilpipes and water pipe and associated features are identified.

The El Isiro water dam is identified on band 7 by its free surface of water. El Cayude small dam is under clouds in the southern part of the peninsula.

The roads are obvious in bands 4 and 5 as fine white to pale gray lines of geometric design in black and white photographs and pale yellow in false color compositions.

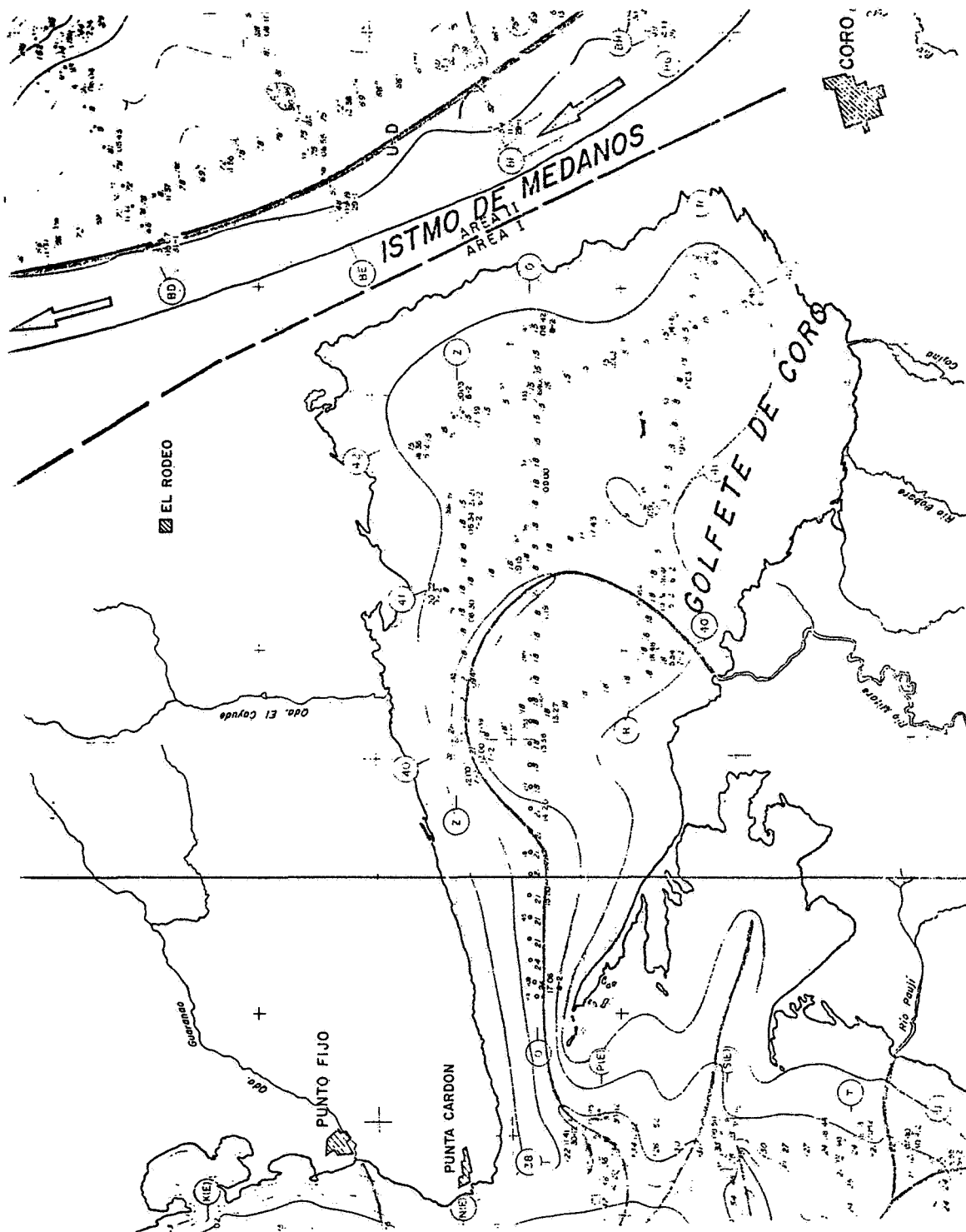
The two airports of the Peninsula are identified by the dark gray tone of the landing strip, inside a paler gray safety belt and on a darker background of the surrounding ground. Their trend is parallel to the directions of the prevailing wind.

The oil pipes from the state of Zulia to Paraguaná crosses the Golfete de Coro from Punta Caimán and are identifiable by their service roads.

The water pipe from the Siburúa water seeps to Paraguaná follows the Istmo de Médanos, and are identifiable by its paved road.

REFERENCE

Albrizzio Carlos, 1.969. Geomorphology of the Continental shelf of Venezuela: Goajira Peninsula -Gulf of Venezuela - Paraguaná Peninsula. 17 p. Texaco Report 11-173.



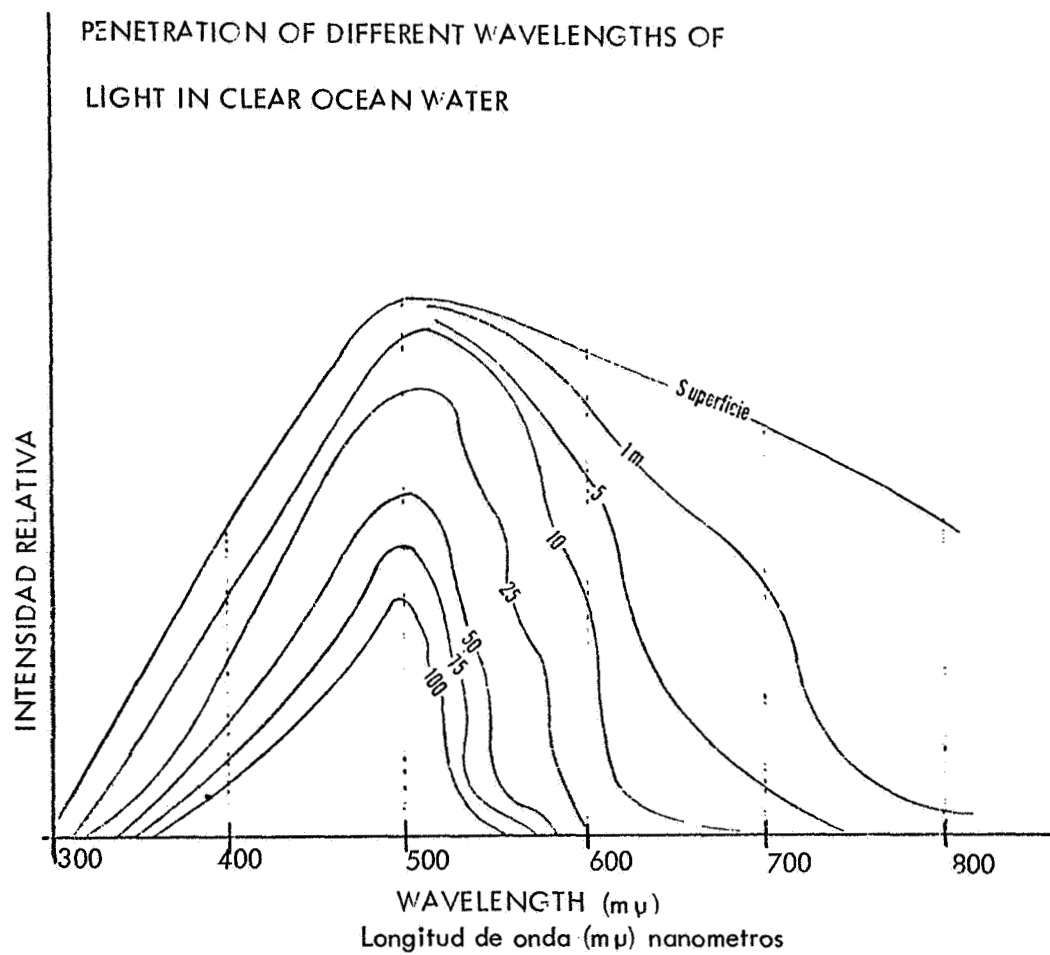


Fig. Penetración de la luz de diferentes longitudes de onda en agua clara del oceano.

SIGNIFICANCE OF SELECTED LINEAMENTS IN ALABAMA*

James A. Drahovzal, Thornton L. Neathery, Charles C. Wielchowsky, *Geological Survey of Alabama, P. O. Drawer O, University, Alabama 35486*

ABSTRACT

Four lineaments in the Alabama Appalachians that appear on ERTS-1 imagery have been geologically analysed. Two of the lineaments appear to have regional geologic significance, showing relationships to structural and stratigraphic frameworks, water and mineral resources, geophysical anomalies, and seismicity. The other two lineaments are of local geologic significance, but, nevertheless, have important environmental implications.

INTRODUCTION

With the advent of orbital photography, a few geologists have reported hitherto unknown alignments, variously termed, "linears," "lineations," "lineaments," or "linear features" (e.g., Lowman, 1969; Powell and others, 1970; Lathram, 1972). Following the launch of ERTS-1 and with the subsequent acquisition of virtual world-wide coverage, a greatly increased number of workers have reported these features (e.g., Gold and others, 1973; Isachsen and others, 1973). In spite of the many reports, few lineaments have been carefully field checked, consequently their nature and genetic relationship remain largely unknown. In this paper, four selected lineaments in the Alabama Appalachians for which field data have been collected will be discussed. Two of the lineaments are relatively long, extending across the entire state and appear to have regional geologic significance; the other two are shorter and have only local geologic significance. Based on the field data collected in each case, speculations as to the nature of the lineament-causing features will be discussed and the importance of such information to the operations of the Geological Survey of Alabama will be pointed out.

MAJOR LINEAMENT COMPLEXES

The Geological Survey of Alabama first became aware of lineaments through an analysis of Apollo 9 multispectral photographs of east-central Alabama (Powell and others, 1970; Drahovzal and Copeland, 1970; Drahovzal and Neathery, 1972). Two lineaments were exceptionally well displayed on the areally limited Apollo photography. Recent ERTS data have permitted extension of these lineaments into areas of the state where satellite imagery was previously unavailable. Careful study of ERTS imagery at a scale of 1:250,000 has shown that the two lineaments are actually lineament complexes. The complexes are linear zones composed of a series of shorter discontinuous, enechelon lineaments, with an overall trend approximately at right angles to Appalachian structural strike. The individual

*Approved for publication by the State Geologist.

segments occasionally cross one another or bifurcate, but generally are parallel to subparallel. Over the past several years, fairly extensive field data have been collected that show relationships and provide clues to the nature of the two lineaments.

Structural Relationship

Anniston Lineament

The northeastern lineament complex (A-A', fig. 1), herein designated the Anniston lineament (for the city of Anniston, Calhoun County, Alabama), is approximately 290 kilometers long in Alabama. The lineament extends from the vicinity of Riverview on the Chattahoochee River northwestward across the Piedmont province (not shown in fig. 1). It crosses the Brevard fault zone (BF, fig. 1) with no apparent disruption and continues northwest to the Little Tallapoosa River where it parallels a short stream segment (not shown in fig. 1). Extensive field studies in this area, however, have not revealed the presence of any major structural features correlative with the Anniston lineament complex. The lineament complex northwest of this area parallels the Tallapoosa River for several kilometers before crossing it at a major gap through a series of moderately high ridges (not shown in fig. 1). Before transecting the metamorphic front (MF), the lineament trace passes along the northeast limit of Talladega Mountain (TM) whose topographic expression is controlled by the underlying quartzites. North of the lineament, the quartzites change to fine-grained meta-arkose with interbedded slate. The lineament crosses the metamorphic front near the northeast side of a left-lateral 10-11 kilometer recess. Just beyond the metamorphic front, the lineament trace transects a prominent quartzite ridge at the point where the ridge abruptly changes strike from north-south to nearly east-west (not shown in fig. 1). The northwest flank of the ridge is bounded by the Jacksonville thrust fault (JF) where the main lineament and a short branch pass along either side of a narrow 5-6 kilometer southeasterly recess on the fault trace (fig. 2). The overridden block contains a small northwesterly elongate fenster (A, fig. 2) and several abruptly terminated, faulted synclines (B, fig. 2) near where the lineament complex passes. To the northwest, the lineament complex crosses just northeast of a 7-kilometer right-lateral displacement in the Pell City thrust fault (PCF, fig. 1) and crosses a narrow zone characterized by block klippen and thin imbricate thrust sheets on the lower plate (C, fig. 2). Much of the complexity of this zone appears to result from the abrupt change in strike near where the lineament complex crosses it. Southeast of the Lookout Mountain syncline (LMS, fig. 1), the main lineament trace is intersected by other traces having slightly different orientations. Near the intersection points, the lineament complex crosses an east-dipping homocline at a point where it is right-laterally offset 5-6 kilometers (D, fig. 2). Farther to the northwest, the Gadsden-Rome fault (GRF, fig. 1) abruptly cuts obliquely to regional structure for 10-11 kilometers, terminating the Lookout Mountain syncline. Just southwest of the lineament trace, the Helena thrust fault (HF) terminates. Northwestward, the lineament crosses Wills Valley anticline (WVA) near a point where its structural style changes from an asymmetrical thrust-faulted fold to the northeast to a more nearly symmetrical anticline to the southwest. The lineament continues northwestward

crossing the end of the Murphrees Valley anticline (MVA) and the terminus of the Straight Mountain fault (SMF). The lineament crosses the Sequatchie anticline (SA) with little apparent effect and bisects the sharp bend in the trace of the Cumberland escarpment (CE). The southwest-flowing Tennessee River abruptly veers out of the Sequatchie anticlinal structure and flows northwest paralleling the lineament for about 40 kilometers. The lineament extends beyond the state line into Giles County, Tennessee, where its trace coincides with the northwest-southeast structural grain on the southwest flank of the Nashville dome (Wilson, 1949, pl. 1). Charles Wilson (1949, p. 333) has speculated that the grain, expressed by closely spaced sharply asymmetrical minor parallel folds, was the result of vertical movement along a set of northwest-southeast fractures in the basement complex. More recent mapping in Tennessee has revealed low-magnitude normal faulting in the vicinity of and on trend with the lineament (Miller and others, 1966).

Harpersville Lineament

The Harpersville lineament complex (named for the town of Harpersville, Shelby County, Alabama; B-B', fig. 1) crosses the low-rank metamorphic rocks of the Piedmont, and passes near the point where the Brevard fault becomes covered by the Coastal Plain onlap (not shown in fig. 1). If the Towaliga fault to the southeast is part of the Brevard zone and they together make up an Inner Piedmont mega-nappe as suggested by some (e.g., Bentley and Neathery, 1970), then the lineament passes very near to the southern termination of this feature. The lineament crosses within approximately 6 kilometers of the southern terminus of Talladega Mountain (fig. 1). The lineament trace transects the metamorphic front along the southwestern edge of the major recess in the front. Northwestward along the lineament, the Pell City fault block is folded into a series of overturned structures that include rocks younger than those composing the block to the immediate northeast and southwest. These younger rocks suggest downwarping where the lineament crosses the block. The Pell City fault itself splays and becomes less distinct in the vicinity of the Harpersville lineament. The rocks within and just northwest of the Pell City block along the lineament complex exhibit a north-northwest strike orientation rather than the typical northeast strike. In addition, overturned thrust slices occur in this block in contrast with the right-side-up thrust slices to the immediate northeast. Northwestward, the lineament trace crosses the Coosa thrust fault at a point where it is left-laterally offset 3-4 kilometers. On the downthrown side of the Coosa fault in the Coosa synclinorium (COS), the lineament passes through a narrow structural high separating two oppositely plunging synclines (not shown in fig. 1). Farther northwestward, in the Coosa and Cahaba (CAS) synclinoria, the lineament transects several major ridges at points of saddle development. The northeast prong of the complex crosses a synclinal feature on the southeast flank of the Birmingham anticlinorium (BA) at a point of major gap development in the ridge and structural change. At this locality, the Middle Ordovician Chickamauga Limestone has been interpreted as being absent across a narrow zone, although 140-180 meters of the unit are present in the immediate vicinity (Butts, 1910). Detailed field studies have not located the limestone in the narrow zone, but have shown that the dip of overlying and underlying beds is markedly steeper where the lineament crosses the

syncline. These dips are more than 80°SE as opposed to 10-15°SE on either side of the zone along strike. It is quite probable that the limestone is completely masked in the area of steep dip by the thick mantle of colluvium. Both prongs of the lineament complex cross the southern terminus of the Blount Mountain syncline (BMS) and the Straight Mountain fault. The lineament cuts across the Birmingham-Murphrees Valley anticlinal complex where a change in structural style occurs. Southwest of the lineament, the Birmingham anticlinorium has a steep to overturned northwest limb that is cut by steep southeast-dipping faults including the Opossum Valley fault (OVF). Northeast of the lineament, however, the Murphrees Valley anticline exhibits a vertical to steeply overturned southeast limb cut by the nearly vertical northwest-dipping Straight Mountain fault. The northeast prong of the complex continues to the northwest where it intersects the Sequatchie anticline, the Warrior Basin (WB), and the Cumberland escarpment. At the present time, no known structural changes are apparent along its trace northwest of the Murphrees Valley anticline, but some gap development appears to correlate. The southwest prong crosses the Sequatchie anticline at the point where local upwarp along the anticlinal axis brings to the surface beds as old as Silurian. The prong crosses the eastern part of the Warrior Basin and becomes indistinct.

The offsets, terminations, and changes in structural style apparent along the two major lineaments may reflect the influence of geofractures that bound basement blocks. Because offsets along individual lineaments are not in the same direction, and because faults and folds terminate rather abruptly or change in style near the lineaments, vertical, rather than horizontal movement of the basement blocks may be the dominant form of displacement. Offsets in opposite directions along the same lineament may be explained by block rotation in the vertical plane. Similar situations have been described by Gwinn (1964, p. 891) in the Central Appalachians but have been attributed to upward shearing, inclined or vertical nonoutcropping faults that connect two glide levels along strike. The changes in the decollement-glide levels of local sole thrusts or higher branching stepped thrusts both across and along strike, may be the result of vertical movement in basement blocks. The foregoing structural studies have had an influence on the Geological Survey's concept of the tectonic framework of the southern Appalachians and are currently influencing geologic mapping programs in the province.

Stratigraphic Relationships

In addition to structural relationships, the two major lineaments appear to coincide with variations in Paleozoic stratigraphy in the southern Appalachians.

A succession that appears to show a strong relationship to the major lineaments is the Middle Ordovician. Over much of the southeastern United States, the Lower Ordovician is separated from the Middle Ordovician by a paleokarst unconformity, and the basal Middle Ordovician locally consists of conglomeratic beds having clasts that range from sand to boulder sizes. In Alabama, this unit is called the Attalla Chert Conglomerate Member of the Chickamauga Limestone. In general, the coarsest and thickest development of the Attalla in Alabama lies adjacent to the two major lineaments

(fig. 3). The conglomerate is unknown northeast of the Anniston lineament complex. Immediately southeast of the Anniston lineament complex on Wills Valley anticline and near the termination of the Helena thrust fault, clasts, ranging from 15 to 92 cm in diameter occur in pockets as much as 21 m thick (Drahovzal and Neathery, 1971, p. 11, 185). The conglomerate becomes finer and thinner southwestward ranging in thickness from 1-6 m. Immediately southwest of the Harpersville lineament, at the up-plunge end of Blount Mountain syncline, another locally coarse deposit approximately 13 m thick occurs with chert clasts ranging up to 50 cm (Thomas and Joiner, 1965, p. 13). The thickest and coarsest development of the Attalla immediately adjacent to the major lineaments suggests that the lineament-causing structures are in part responsible for the anomalous occurrences. Differential vertical movement of the individual basement blocks contemporaneous with or prior to deposition may have formed the restrictive pockets, or selective karst development along lineament-related fractures during the Early Ordovician may be responsible for the anomalous distribution.

Similar lineament-related changes in lithologies and thicknesses for Cambrian, upper Middle Ordovician and Mississippian rocks of the Alabama Appalachians are known. The apparent relationships between the two lineaments and Paleozoic depositional cycles suggest that differential movement prior to or contemporaneous with these cycles occurred along lineament-related crustal block boundaries.

Relationship to Water Resources

Results of Apollo 9 studies in Alabama have shown relationships between the occurrence of water resources and lineaments in the Valley and Ridge and Piedmont provinces. High-yield springs and wells show a number of excellent lineament correlations (Powell and others, 1970). In addition, it has been demonstrated that certain surface flow anomalies in eastern Alabama are directly related to the occurrence of lineaments. Detailed low-flow studies made in adjacent subdrainage areas along Talladega Creek in Talladega County, Alabama have shown that there is an abrupt pickup in flow at a point where two lineaments intersect the stream. Pickup at the intersection point increases more than 70 times from a flow of $6.6 \times 10^{-4} \text{ m}^3/\text{sec}/\text{km}^2$ to $4.7 \times 10^{-2} \text{ m}^3/\text{sec}/\text{km}^2$ (Powell and LaMoreaux, 1971; U. S. Geological Survey, 1972, p. 190-191).

The recent extension of the Anniston lineament into Madison County, Alabama through the use of ERTS-1 data has been significant to the intensive study of the hydrology of limestone terranes presently being carried out by the Geological Survey of Alabama. The region, therefore, provides an excellent test area for determining the nature of relationships between lineaments and the occurrence of ground-water resources in limestone terranes. Preliminary results indicate a striking correlation between high-yield springs and wells and areas of lineament concentration. In the southwestern part of Madison County, where the Anniston lineament complex crosses, data for nearly 80 wells and springs are available (fig. 4). The 4-kilometer-wide zone associated with the Anniston complex encompasses wells whose yields range as high as $0.318 \text{ m}^3/\text{sec}$ and average nearly $0.032 \text{ m}^3/\text{sec}$.

Wells located on either side of the zone exhibit markedly lower yields, averaging only about 0.010 m³/sec. For the area, yields greater than 0.016 m³/sec are considered to be anomalously high (George Moravec, oral communication, 1973). Structural data for the area indicate a series of low, undulating folds that trend generally northwest-southeast, sub-parallel to the lineaments (fig. 5). High well yields only generally correspond to structural lows and are probably influenced more by fracturing in the underlying limestone. Correlation of high-yield wells and springs to the lineaments suggests that the lineaments represent fractures and possibly low-magnitude faults that influence the movement and distribution of ground-water resources. Low variabilities in water-level fluctuation amplitudes for some of the lineament-related wells in Madison County appear to parallel the low-discharge variability noted by Powell and others (1970) for lineament-related limestone springs in the Valley and Ridge province. Low variabilities, uncommon for wells and springs in limestone terranes, suggest special recharge conditions. The plotting of lineaments derived from ERTS-1 and other available imagery is becoming an important part of exploration procedures for ground-water resources at the Geological Survey of Alabama.

Relationship to Mineral Resources

The lineaments show remarkable correlation with many of the hydrothermal mineral deposits of Alabama. The occurrence of barite and lead and zinc sulfides in the Valley and Ridge and barite, gold, manganese, tin, and copper, lead, zinc, arsenic, and iron sulfides in the Piedmont has been related to lineaments derived from Apollo 9 photography (Smith and Drahovzal, 1972). Barite appears to show the closest correlation with about 40 percent of the known prospects coinciding with the two major lineament complexes (fig. 1). The richest barite deposits known in Alabama occur along the Anniston lineament where the main branch changes trend slightly and is intersected by a number of shorter segments. Many of the other barite prospects correlate with shorter, less prominent lineaments.

To further evaluate the apparent mineral-lineament relationship, "B" horizon soil samples were collected at about 300-meter intervals along traverses crossing selected lineaments and analysed for eight metals. Preliminary results have been mixed, however, a number of traverses show anomalously high metal concentrations at the points of intersection with the lineaments. Two geochemical profiles across the Anniston lineament complex show excellent correlation (figs. 6 and 7). One traverse (A, fig. 6) crosses an area in the Piedmont province underlain by garnet schist. Despite a consistent lithology along the traverse, three metals - lead, zinc, and chromium - show anomalously high concentrations where the traverse intersects the Anniston lineament (A, fig. 7). Chromium concentration reaches 179 ppm, more than 4 times the estimated background of 40 ppm; whereas lead and zinc anomalies are about twice their estimated backgrounds. The other traverse (B, fig. 6), also in the Piedmont, crosses a variety of metamorphic lithologies and exhibits two anomalously high chromium concentrations (B, fig. 7). The higher chromium peak reaches a concentration of

374 ppm, more than 5 times the estimated background for the area, and is related to a branch off of the main trace of the Anniston lineament. The second peak is lower, being only about twice the estimated background, but is, nevertheless, sharp and distinct. It correlates extremely well with the main segment of the Anniston lineament.

On the basis of this work, it appears that the distribution of some potentially important mineral resources is related to the lineament-causing structures. The relationship suggests that these structures may be crustal penetrating fractures that serve as migration channels for mineralized fluids and sites of deposition for certain hydrothermal minerals. Additional studies are currently underway in other parts of the state and especially near lineament intersections where samples will be collected on a grid pattern rather than along single line traverses. The lineament-geochemical sampling approach to exploring for potential mineral resources is becoming an important procedure for the Mineral Resources Division of the Geological Survey of Alabama.

Geophysical Evidence

In addition to the geochemical surveys, several gravity surveys have been conducted in the vicinity of the Anniston lineament complex of northern Alabama. Although regional gravity shows no particular relationship to the lineaments, detailed surveys utilizing approximately 160-meter station spacing exhibit anomalies that are correlative with the linear features. A gravity survey conducted in a Mississippian limestone terrane just southwest of Huntsville in Madison County, Alabama (A, fig. 6) shows a sharp 0.4 milligal negative anomaly at the point where ERTS imagery indicates the presence of the main branch of the Anniston lineament complex (A, fig. 8). Figure 8 shows only a small part of the 13-kilometer profile, but to the southwest the anomaly slowly decreases in intensity for a distance of about 2 kilometers. Beyond that point, gravity readings vary only slightly from the regional gradient. To the northeast, several other smaller, but nevertheless sharp, anomalies are present. These appear to relate very closely to northeastern segments of the Anniston lineament complex. The sharpness of the 0.4 milligal anomaly suggests that it represents either a sharp flexure or a fault downthrown to the southwest. Applying the "half-maximum" rule, the anomaly could originate as much as 1,500 meters below the surface. Depth to basement in the area is unknown, but is estimated to be between 1,500 and 1,900 meters below the surface based on scattered well information. The anomaly, therefore, could reflect offset in the basement complex or possibly in the Cambrian Copper Ridge Dolomite. A structure map contoured on the top of the Devonian Chattanooga Shale in the vicinity of the profile and lineament shows a structural low trending in a subparallel fashion to the lineament trace (fig. 5). Some workers have preferred to interpret the data of figure 5 with a fault that parallels the lineament (Geological Survey of Alabama, open file maps). This flexure or fault may also be responsible for the gravity anomaly. A second gravity survey was run across the Anniston lineament complex in the Cumberland Plateau province (B, fig. 6). A negative anomaly of about 0.17 milligal correlates with the lineament complex (B, fig. 8). If the anomaly represents a fault, it is downthrown to the northeast rather than to the southwest as in previous case. It is possible that the thick Pennsylvanian

succession has the effect of masking and thereby reducing the magnitude of the anomaly, but final interpretation awaits detailed analysis and correlation with other recently conducted surveys in the area.

Gravity results to date look most encouraging and suggest that, at least in part, the Anniston lineament is the surface expression of a sharp flexure or fault in the subsurface. Future gravity surveys are being planned along both complexes and magnetic surveys will be conducted in association where possible. Some preliminary ground magnetic surveys seem most encouraging but await confirmation before being reported in detail. Detailed ground geophysical surveys appear to be extremely important in evaluating the nature of the lineament-causing structures.

Relationship to Seismicity

Between 1886 and 1971, 14 earthquake epicenters have been reported in Alabama (Eppley, 1965; Woollard, 1968; U. S. Department of Commerce, 1971; G. A. Bollinger, written communications, 1971-1973). Although the earthquakes are rather infrequent and of relatively low intensities (between I and VIII on the Modified Mercalli Intensity Scale of 1931), they may be highly significant to the understanding of the nature of the two major lineament complexes. Those epicenters occurring in the north-eastern quarter of the state are shown in figure 1. Four of the epicenters lie directly on the main branches of the Anniston lineament complex and two on the main segment of the Harpersville lineament complex. Coincidence of epicenters with the major lineament traces not only implies that the lineaments are related to basement structures, but also indicates that they may represent structures that are currently active. Microseismic studies are planned as part of proposed ERTS-B research.

TWO MINOR LINEAMENTS

In addition to the two major lineaments, there are a myriad of other lineaments for which very little or no field information is available. The latter are presently considered to be of lesser geologic significance and are classified herein as minor lineaments. There are, however, two minor lineaments for which fairly extensive field data are available.

Wesobulga Creek Lineament

As part of routine geologic investigations and ERTS-1 research, lineament analyses and a ground investigation were conducted in a 420 km² area of the northern Alabama Piedmont. Lineament locations and orientations were derived from ERTS-1 and side-looking airborne radar (SLAR) imagery supplemented with low-altitude conventional photographs. Two hundred-forty-two tonal and topographic lineaments were transferred from the various images and plotted on 7½-minute topographic maps for field checking. In the course of the field investigation, more than 2,500 stations were established for which structural data including the orientation of cleavages,

foliations, joints, faults, and folds were recorded. The relationships of most of the structural data to lineament traces is inconclusive, although a rough correlation appears to exist between joint orientations (273 stations) and the lineament orientations (fig. 9). Correlation is somewhat better than one might at first believe because compilation of the lineament data on a SLAR base has imparted as much as a 10-degree north-bias due to variable distortion of the SLAR imagery.

A detailed search was made over approximately 195 km² of the study area for surface manifestations of any of the image-derived lineaments. A small normal fault that is exposed in a road cut (fig. 10) was discovered and found to coincide with the trace of a lineament expressed both on ERTS-1 and SLAR imagery. The lineament, herein referred to as the Wesobulga Creek lineament, is approximately 4 kilometers in length on SLAR imagery and corresponds with an ERTS lineament about 15 kilometers in length. On both SLAR and ERTS data, orientation of the lineament averages N45°W. The Wesobulga lineament is no more prominent than many other such features for which no structural evidence exists.

The corresponding Wesobulga Creek fault zone is approximately 3 meters wide and has an approximate strike of N40-45°W with displacement of 3-15 meters in the roadcut. The principal zone of movement occurs on the east end of the fault zone where a mylonite-phylionite zone 10 cm wide marks the fault. The remaining 2.9 meters of the zone is composed of a series of closely spaced vertical shear joints that decrease in number to the west end. To fully investigate the orientation and extent of the fault, eight trenches were dug across its projected trace (fig. 11). Six of the eight trenches nearest to the road exposure cut the fault. One trench located approximately 700 meters north of the road failed to intersect the fault trace (not shown in fig. 11). The trenches show that the fault zone narrows in both directions from the 3-meter-wide zone at the road cut to a half-meter-wide kink band in trench TN-4 and to a disturbed zone less than 2 meters wide in trench TS-3. The trend of the fault, as exposed, coincides with the orientation of the lineament derived from both SLAR and ERTS data. The general shape of the fault zone and its topographic position along the flank of a steep-sided valley suggest that the feature may not be tectonic, but may represent a recent rotational shear related to slumping. Radiogenic age dates (K/Ar) are currently being determined on the mylonitic rock of the principal fault zone. Approximately 500 meters east of the fault, on the adjacent valley wall, another small fault and drag fold are exposed in a road cut, but the relationship of this feature to the Wesobulga Creek fault is unknown at this time.

This example of a positive relationship of one of the ERTS-derived lineaments to a small fault is noteworthy, but certainly not statistically significant. It is not to be regarded as indicating that all or even most lineaments are related to faulting. On the contrary, evidence based on this test area suggests that most of the minor lineaments are not related to obvious structural features. More detailed work is required to determine the significance, if any, of the many other lineaments to the structure of the area.

Kelly Creek Lineament

The other minor lineament for which considerable field data exists was originally discovered on Apollo 9 photography (Powell and others, 1970). Follow-up studies utilizing SLAR and ERTS-1 data have added to our understanding of the feature. The lineament also appears on U-2 photography and conventional panchromatic photo mosaics. Low-level aerial reconnaissance has revealed erosion-deepened hollows and gaps along the lineament, as well as linear regions characterized by trees whose foliage appeared to be slightly darker green than those of the surrounding area (Bailey, 1970). The lineament strikes about N49°W and has been traced for 8 kilometers on SLAR imagery, but appears on ERTS-1 imagery to be part of a somewhat longer linear feature.

The lineament has been the subject of extensive study because it strikes along the axis of Logan Martin dam on the Coosa River (fig. 12). Since impoundment in 1964, leakage from the reservoir has occurred beneath and to the sides of the dam through the highly weathered and fractured limestones and dolostones that underlie the area. Flows of up to 20 m³/sec have been measured below the dam and during one 2-year period total leakage increased, though it has now stabilized (Alverson, 1969). Structural, hydrologic, subsurface, and seismic data show that the lineament represents a deeply weathered fracture zone. Vertical joints coincident and parallel with the lineament were measured at several locations northeast of the dam (Spigner, 1969). The existence of hydraulic connection through solution-widened fractures developed along the lineament has been demonstrated by the following: 1) dye injected into well 262 was detected in well 222 within 24 hours (fig. 12); 2) well 238 has an anomalously high specific capacity of such a magnitude that it must be connected to the reservoir; 3) the lowering of water in a cofferdam on the west side of the river resulted in the lowering of water levels in two wells along the lineament on the east bank (not shown in fig. 12); and 4) sizable increases in surface flow have been noted during low-flow periods where the lineament crosses Kelly Creek just northwest of the dam (Alverson, 1970; Powell and LaMoreaux, 1971). Test drilling west of the dam on the lineament trace encountered nearly 200 meters of highly fractured rock before solid bedrock was encountered. Holes not on the lineament penetrated solid rock at much shallower depths. Several seismic and resistivity profiles confirm the presence of the fracture zone in the areas that correspond to the trace of the lineament (W. L. Scarbrough, oral communication, 1973).

The Kelly Creek lineament, in part at least, most certainly represents a fracture zone. At the present time, it is not known whether this fracture is a fault, but it is contributing to reservoir leakage.

CONCLUSIONS

The major lineaments such as the Anniston and Harpersville lineament complexes are probably related to basement structures. Because the structural offsets and changes do not necessarily parallel the lineament traces and because the lineaments may affect all parts of the Paleozoic succession, the lineaments appear to represent basement geofractures, which have been vertically active throughout much of geologic time. The geofractures may be partly responsible for the present geologic configurations of the Appalachians because of their direct tectonic effect at the time of deformation and their earlier tectonic control of sedimentation. Coincidence of high-yield wells and springs, hydrothermal mineral deposits, geochemical highs and geophysical anomalies with the major lineaments suggests that fracturing of the basement is also expressed in the Paleozoic cover. Seismic activity along the same lineaments indicates that they are related to basement geofractures that are still active.

The evidence relating to these lineaments leads us to speculate about their significance to the tectonic framework of the Appalachians. It is possible that much of the driving force for the thin-skinned tectonics of the Appalachians was derived from primary vertical movement in the basement. The vertical uplift and the attendant development of tectonically unstable conditions in the overlying Paleozoic cover may have resulted in horizontal forces that expressed themselves in the formation of decollement-glide planes in the incompetent units of the Valley and Ridge synclinorium. Such a concept combines parts of both "thin-skinned" and "thick-skinned" ideas which have been expressed before (e.g., Cloos, 1948; Boos and Boos, 1957; and Eardley, 1963), but generally not for the Appalachians.

The northwest orientation of the major lineaments in Alabama is closely similar to the trend of the postulated Bahama fracture zone off the southeast coast of North America (LePichon and Fox, 1971). This and other fracture zones along and seaward of the present coast of North America are thought to be genetically related to the open ocean fractures lying perpendicular to the Mid-Atlantic ridge and to complimentary marginal fracture zones along the African coast. Some of the marginal fracture zones are known to be related to basement ridges farther onto the continent, such as the Cape Fear fracture zone that is aligned with the axis of the Cape Fear arch. The similarity in orientation between the major lineaments in Alabama and the Bahama fracture zone may represent an analogous relationship. This concept is consistent with J. T. Wilson's (1965) suggestion that the pre-rift continental mass was broken by faults or ancient lines of weakness that after rifting and rotation, represent less tectonically active continental equivalents of active Mid-Atlantic transform faults.

The minor lineaments are believed at the present time to have limited geologic significance. The two discussed--the Wesobulga Creek and Kelly Creek lineaments--have demonstrated local geologic and environmental importance. Most of the minor lineaments, however, seem to have little or no obvious relationship to the local geology, but detailed information is lacking in most areas.

A great deal of field data and analysis will be required to determine the genetic nature and significance of the lineaments. It is hoped that this paper has presented a beginning in that direction. The ERTS-1 program in some respects has not saved the geologist field time and expense, as may be validly claimed for some problems, but it has sharpened his sensitivity to certain aspects of regional geology that may be highly significant to a fuller understanding of geologic relationships and environmental perspectives.

REFERENCES CITED

- Adams, G. I., Butts, Charles, Stephenson, L. W., and Cook, Wythe, 1926, Geology of Alabama: Alabama Geol. Survey Spec. Rept. 14, 312 p., geologic map.
- Alverson, R. M., 1969, Evaluation and interpretation of hydrologic and geologic data in the vicinity of Logan Martin dam, St. Clair and Talladega Counties, Alabama: Alabama Geol. Survey, open-file report, 31 p.
- 1970, Hydrologic implications of features observed on side-look radar photographs taken in the vicinity of Logan Martin dam: Alabama Geol. Survey, open-file report, 5 p.
- Bailey, B. L., 1970, A study of lineation on side-looking radar imagery of the Logan Martin dam area, Shelby, St. Clair, and Talladega Counties, Alabama: Alabama Geol. Survey, open-file report, 14 p.
- Bentley, R. D., and Neathery, T. L., 1970, Geology of the Brevard fault zone and related rocks of the Inner Piedmont of Alabama: Alabama Geol. Soc. Guidebook 8th Ann. Field Trip, 1970, p. 1-79.
- Boos, C. M., and Boos, M. F., 1957, Tectonics of eastern flank and foothills of Front Range, Colorado: Am. Assoc. Petroleum Geologists Bull., v. 41, no. 12, p. 2603-2676.
- Butts, Charles, 1910, Birmingham folio, Alabama: U. S. Geol. Survey Geol. Atlas, Folio 175, 24 p.
- Cloos, Hans, 1948, The ancient European basement blocks--preliminary note: Trans. Am. Geophys. Union, v. 29, p. 99-103.
- Drahovzal, J. A., and Copeland, C. W., 1970, Geologic and hydrologic interpretation of multispectral Apollo 9 space photographs in Alabama (abs.): Geol. Soc. America, Abstracts with Programs, v. 2, no. 3, p. 206.
- Drahovzal, J. A., and Neathery, T. L., 1971, Middle and Upper Ordovician stratigraphy of the Alabama Appalachians, in Drahovzal, J. A., and Neathery, T. L., (eds.), The Middle and Upper Ordovician of the Alabama Appalachians: Alabama Geol. Soc. Guidebook 9th Ann. Field Trip, 1971, p. 1-62.

- _____. 1972, The structural significance of multispectral Apollo 9 photographs to Appalachian geotectonics (abs.): Internat. Geol. Cong., Montreal, 1972, sec. 9, p. 3.
- Eardley, A. J., 1963, Relation of uplifts to thrusts in Rocky Mountains, in Childs, O. E., and Beebe, B. W. (eds.), The backbone of the Americas: Am. Assoc. Petroleum Geologists Mem. 2, p. 209-219.
- Eppley, R. A., 1965, Earthquake history of the United States, pt. 1, Stronger earthquakes of the United States (exclusive of California and western Nevada): U. S. Dept. Commerce, Environmental Sci. Services Admin., Coast and Geod. Survey, 120 p.
- Gold, D. P., Parizek, R. R., and Alexander, S. A., 1973, Analysis and application of ERTS-1 data for regional geologic mapping, in Symposium on Significant Results Obtained from Earth Resources Technology Satellite-1: Natl. Aeronautics Space Adm., SP327, v. 1, sec. A, p. 231-245.
- Gwinn, V. E., 1964, Thin-skinned tectonics in the Plateau and northwestern Valley and Ridge provinces of the Central Appalachians: Geol. Soc. America Bull., v. 75, p. 863-899.
- Isachsen, Y. W., Fakundiny, R. H., and Forster, S. W., 1973, Evaluation of ERTS-1 imagery for geological sensing over the diverse geological terranes of New York state, in Symposium on Significant Results Obtained from Earth Resources Technology Satellite-1: Natl. Aeronautics Space Adm., SP327, v. 1, sec. A, p. 223-230.
- Latham, E. H., 1972, Nimbus, IV view of the major structural features of Alaska: Science, v. 175, p. 1423-1427.
- LePichon, X., and Fox, P. J., 1971, Marginal offsets, fracture zones, and the early opening of the North Atlantic: Jour. Geophys. Res., v. 76, no. 26, p. 6294-6308.
- Lowman, P. D., Jr., 1969, Geologic orbital photography--experience from the Gemini Program: Photogrammetria, v. 24, p. 77-106.
- Miller, R. A., Hardeman, W. D., Fullerton, D. S., Sykes, C. D., and Garman, R. K. (compilers and eds.), 1966, Geologic map of Tennessee: Tennessee Dept. Conserv., Div. Geology, West Central Sheet.
- Powell, W. J., Copeland, C. W., and Drahovzal, J. A., 1970, Geologic and hydrologic research through space acquired data for Alabama--delineation of linear features and application to reservoir engineering using Apollo 9 multispectral photography: Alabama Geol. Survey Inf. Ser. 41, 37 p.
- Powell, W. J., and LaMoreaux, P. E., 1971, Apollo 9 photography reveals geologic structures controlling ground-water movement and reservoir leakage in Alabama: Alabama Geol. Survey, open-file report, 9 p.
- Smith, W. E., and Drahovzal, J. A., 1972, Possible geofracture control of ore deposition in Alabama: Soc. Mining Eng. of AIME, preprint no. 72-H-316, 8 p.

- Spigner, B. C., 1969, Notes on the geology and photographic lineaments of the Logan Martin dam area, St. Clair and Talladega Counties, Alabama: Alabama Geol. Survey, open-file report, 9 p.
- Thomas, W. A., and Joiner, T. J., 1965, Attalla Conglomerate Member of Chickamauga Limestone, in Thomas, W. A. (ed.), Structural development of the southernmost Appalachians: Alabama Geol. Soc. Guidebook 3rd Ann. Field Trip, 1965, p. 13-15.
- United States Department of Commerce, 1971, Preliminary determination of epicenters: Washington, U. S. Govt. Printing Office, monthly listing March 1971, 8 p.
- United States Geological Survey, 1972, Geological Survey research 1972, Chapter A: U. S. Geol. Survey Prof. Paper 800A, 320 p.
- Wilson, C. W., 1949, Pre-Chattanooga stratigraphy in central Tennessee: Tennessee Dept. Conserv., Div. Geology Bull. 56, 407 p.
- Wilson, J. T., 1965, A new class of faults and their bearing on continental drift: Nature, v. 207, p. 343-347.
- Woollard, G. P., 1968, A catalogue of earthquakes in the United States prior to 1925 based on unpublished data compiled by Harry Fielding Reid and published sources prior to 1930: Hawaii Instit. Geophys., Data Rept. 10, HIG-68-9, 170 p.

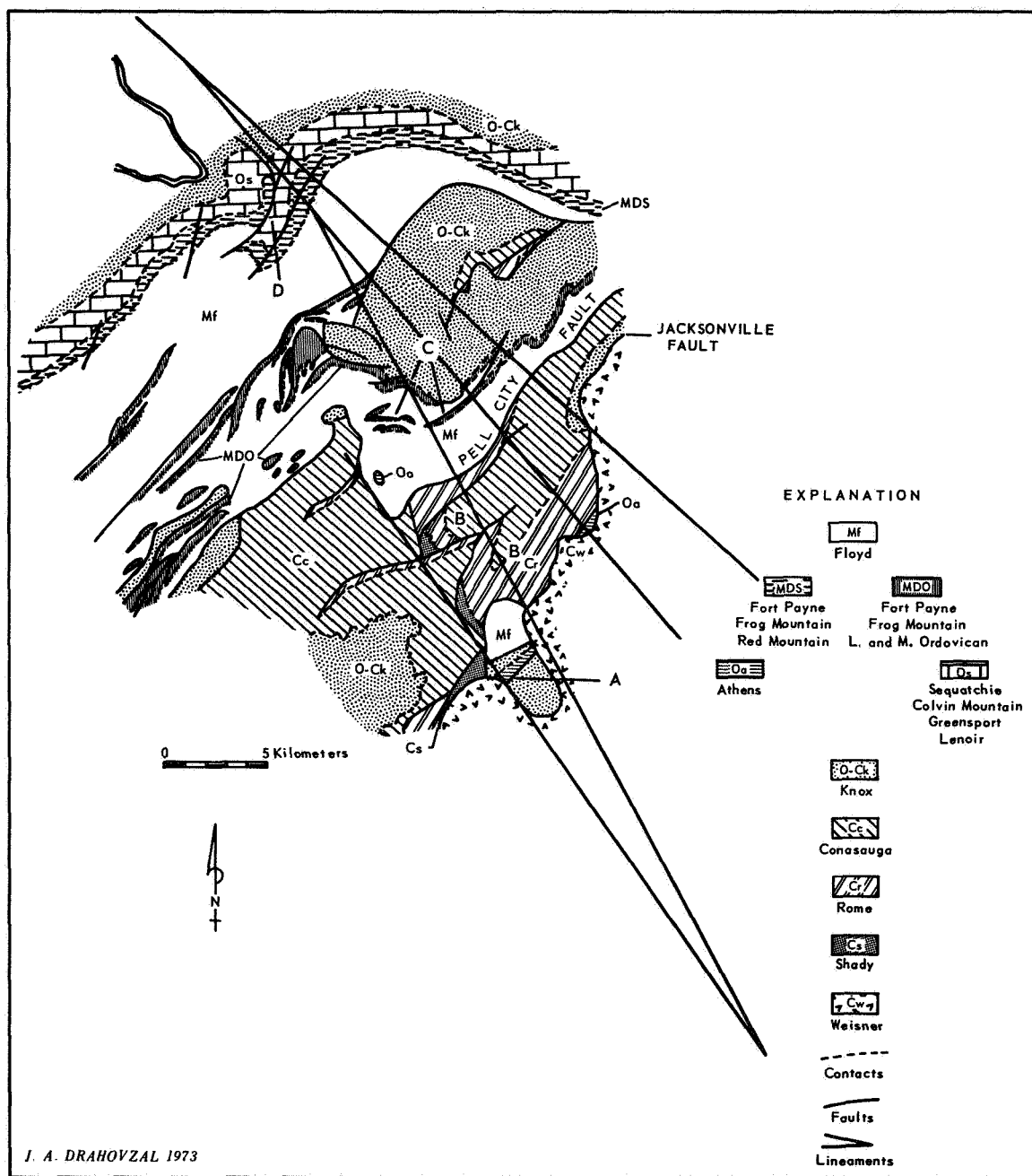


Figure 2.—Generalized geology of the Anniston-Gadsden area, Alabama showing its relationship to the Anniston lineament complex. Geology modified from unpublished field maps of T. L. Neathery (1968) W. A. Thomas and J. A. Drahovzal (1969-1970) and J. A. Drahovzal (1971-1973).

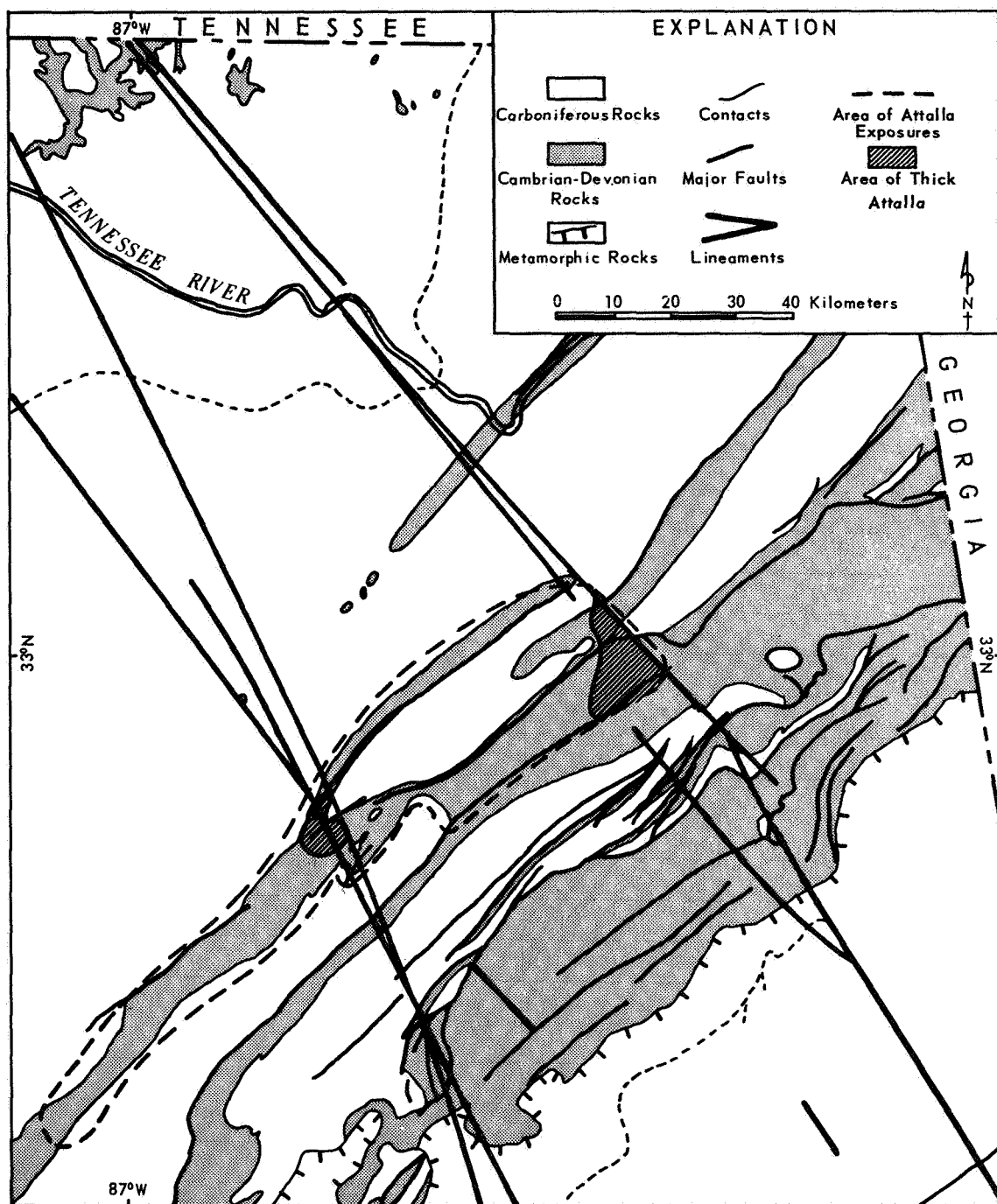


Figure 3.—Generalized geology of northeastern Alabama showing the approximate limits of the Attalla Chert Conglomerate Member of the Chickamauga Limestone and the areas of thick and coarse development. Data modified from Butts (1910), Thomas and Joiner (1965), and Drahovzal and Neathery, (1971).

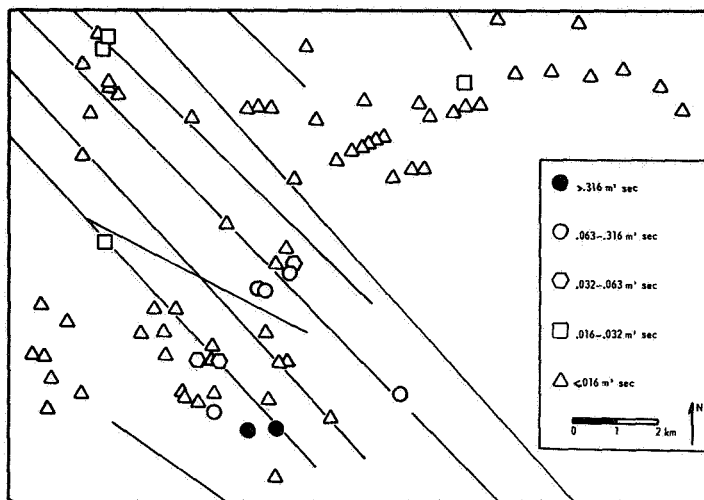


Figure 4.—Spatial relationships of water wells and springs to lineaments associated with the Anniston lineament complex in southwestern Madison County, Alabama. See figure 6 for location.

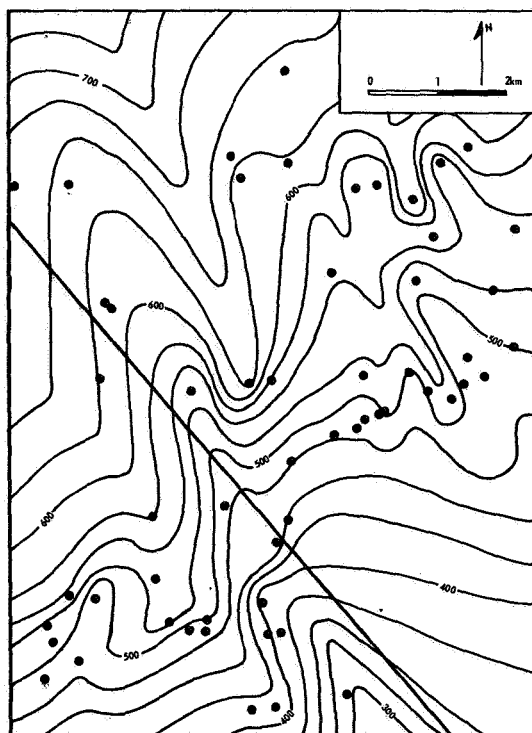


Figure 5.—Structure contour map of the southwestern part of Madison County, Alabama, showing the trace of the Anniston lineament. Contour interval is 25 feet and is drawn on the top of the Chattanooga Shale. Dots represent well locations.

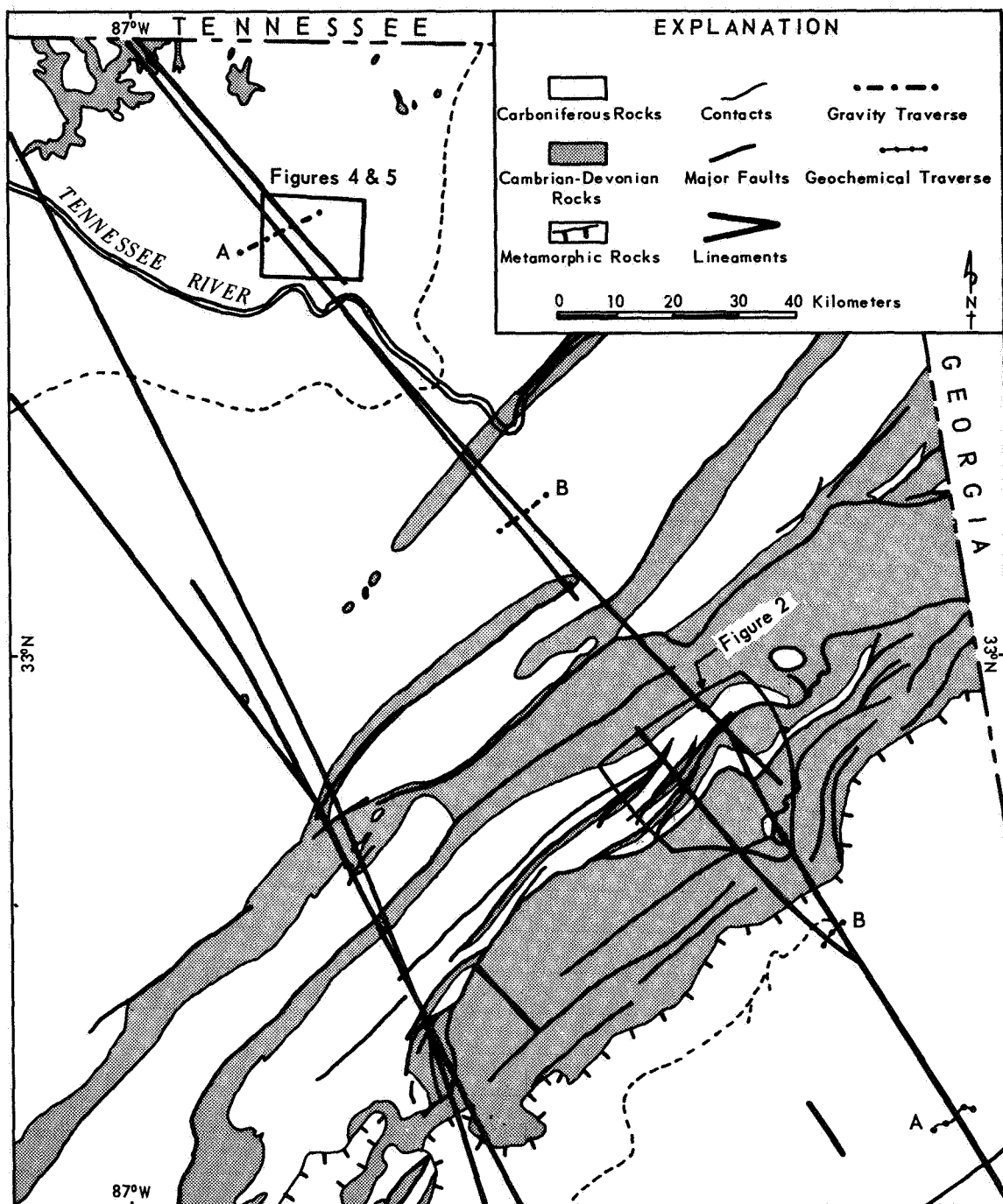


Figure 6.—Locations of geochemical and gravity profiles across the Anniston lineament complex and locations of figures 2, 4, and 5.

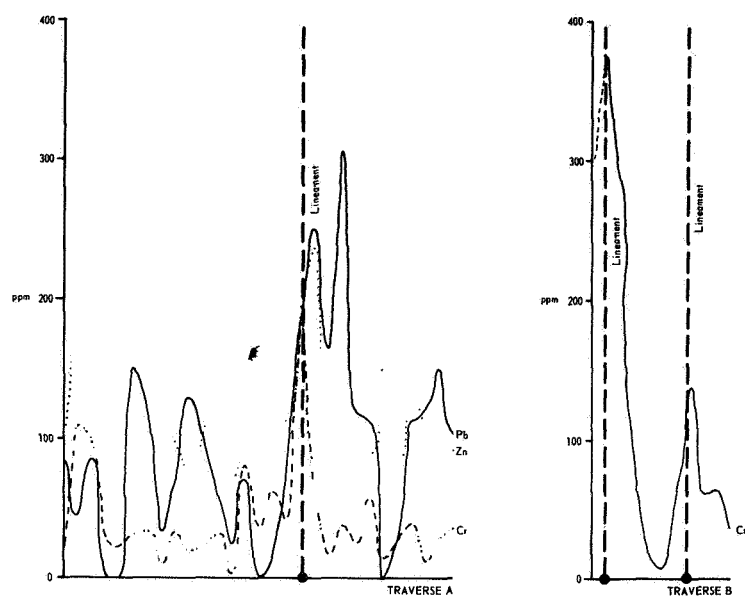


Figure 7.—Geochemical profiles across the Anniston lineament complex. See figure 6 for locations. From unpublished field and laboratory data (W. E. Smith, J. A. Drahovzal, and N. A. Lloyd, 1972).

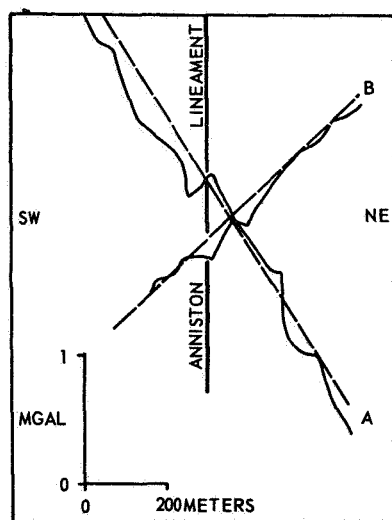


Figure 8.—Gravity profiles across the Anniston lineament complex. See figure 6 for locations. Dashed lines represent interpreted regional gravity; solid lines gravity anomalies. From unpublished field data collected by G. V. Wilson (1973).

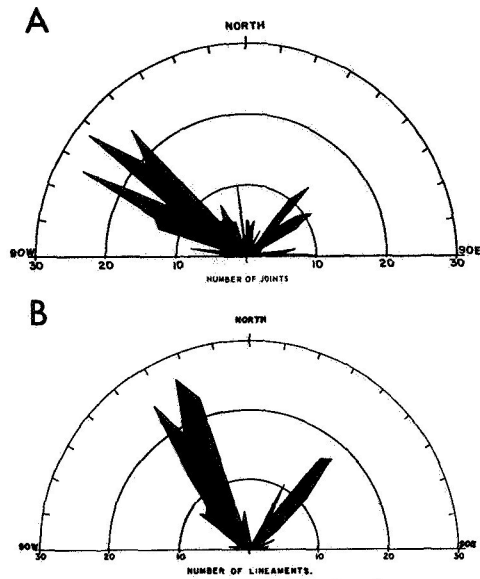


Figure 9.—Rose diagrams comparing the orientations of lineaments to joints in the vicinity of the Wesobulga Creek lineament.

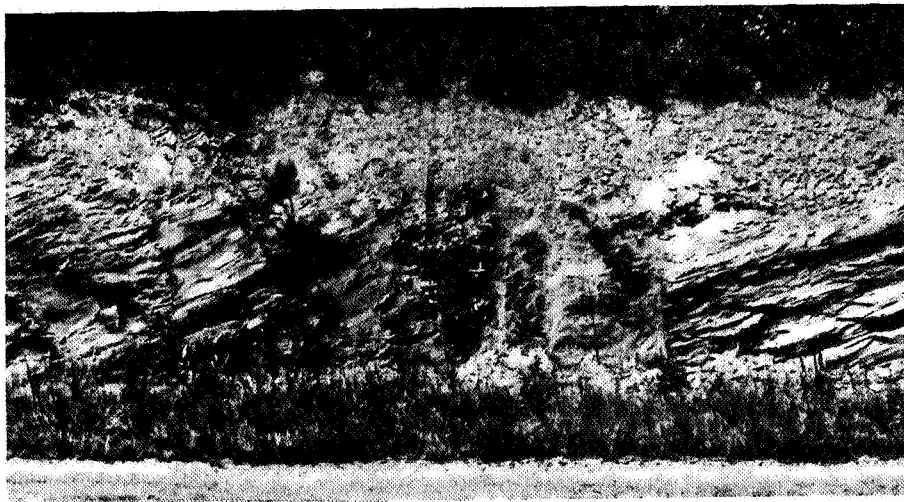


Figure 10.—Road cut exposing a normal fault that coincides with Wesobulga Creek lineament. Fault is 3 meters in width and downthrown to the right.

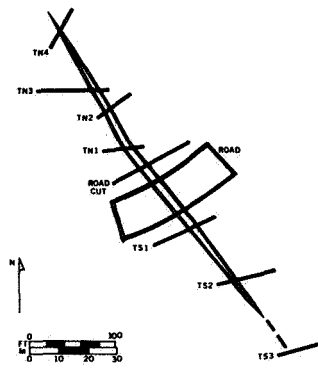


Figure 11.—Map showing the fault trace, road cut and trenches associated with the Wesobulga Creek lineament.

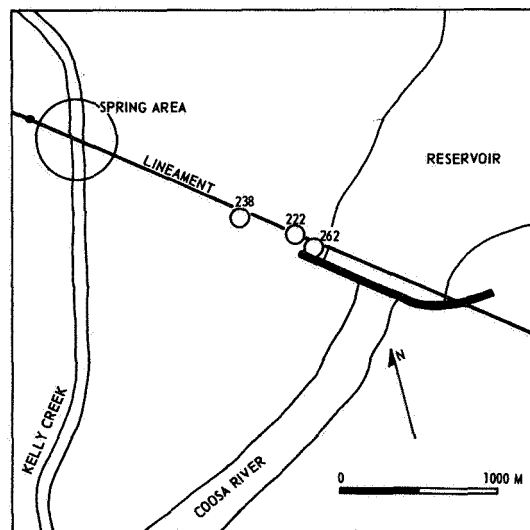


Figure 12.—Kelly Creek lineament in the vicinity of Logan-Martin Dam (modified from Alverson, 1970).

GEOLOGIC INTERPRETATION OF ERTS-1 SATELLITE IMAGES FOR WEST ASWAN AREA, EGYPT

E. M. El Shazly, M. A. Abdel-Hady, M. A. El Ghawaby and I. A. El Kassas

ERTS-1 images of West Aswan area are interpreted in terms of geology, drainage and structure, and this interpretation is compared with previous investigations on this area. The drainage pattern of the Nile is mainly controlled by structural elements of N-S, NNW-SSE, NNE-SSW trends and the slope towards the Mediterranean, while the wadis are usually taking the ENE-WSW, E-W fractures and directed by the slope towards the Nile in the eastern part of the area and by the slope towards the depressions in the Western Desert in the western part. The branches of Lake Nasser (Aswan Dam Reservoir) in its northern part are occupying the wadis and the fracture systems.

The structure of the area is dominated by the ENE-WSW folding of the open type occurring on a regional and minor scale, while the fractures and faults belong to several trends and are either extending for long distances or they may be short and grouped together in parallel arrangement echoing the major fractures.

-
- 1 Deputy Director of the Atomic Energy Establishment, and Director of the Geological Group of the Remote Sensing Project, Academy of Scientific Research and Technology, Cairo, Egypt.
 - 2 Professor of Civil Engineering, Oklahoma State University, USA, and Director of the Remote Sensing Project, Academy of Scientific Research and Technology, Cairo, Egypt.
 - 3&4 Geologists, Geology and Raw Materials Dept., Atomic Energy Establishment, Cairo, Egypt.

N 74 30770

Apart from cultivation and vegetation, twenty two geological units are distinguished on ERTS-1 images in West Aswan area covering geological formations and erosional levels within some formations ranging from the Precambrian to the Quaternary. Apart from the distinction of Aswan monumental granite, which is characteristic of Aswan, the investigated area shows very interesting exposures of sedimentary rocks ranging from the Cretaceous to the Quaternary. Of special interest from the economic geology point of view is the delineation on ERTS-1 images of the iron-ore member of the Nubian Sandstone and the phosphate-bearing formation. From the scientific point of view the tracing of the geological formations from south to north and the distinction of the varied geological units within the Pliocene and Quaternary, and the discussion on the origin of tufa are of particular significance.

Also, the tracing on these images of major fractures and faults intercepting Aswan Dam Reservoir and their significance on the seepage and possible future development of diversion channels from reservoir is emphasized.

GEOLOGIC INTERPRETATION OF ERTS-1 SATELLITE IMAGES
FOR WEST ASWAN AREA, EGYPT

BY

E.M. EL SHAZLY¹, M.A. ABDEL-HADY², M.A. EL GHAWABY³, I.A. EL KASSAS⁴

INTRODUCTION

This report complements a previous one published in July 1973 by the Academy of Scientific Research and Technology (Egypt) on the "Geologic Interpretation of ERTS-1 Satellite Images of East Aswan Area, Egypt". The report is considered a part of the continued effort initiated by the Remote Sensing Research Project, presently conducted by the Egyptian Academy of Scientific Research and Technology in cooperation with the U.S. National Science Foundation, Oklahoma State University, and the Remote Sensing Institute at South Dakota, to evaluate the significance of ERTS-1 satellite images in regional geologic and natural resources survey and mapping.

The clear weather all year around over Egypt permits excellent and clear satellite images which allows excellent exposure of geologic and other surface features. Undoubtedly a survey from such images can assist in revising and complementing present geologic maps compiled by limited ground survey techniques. Information

-
- 1 Deputy Director of the Atomic Energy Establishment, and Director of the Geological Group of the Remote Sensing Project, Academy of Scientific Research and Technology, Cairo, Egypt.
 - 2 Professor of Civil Engineering, Oklahoma State University, USA, and Director of the Remote Sensing Project, Academy of Scientific Research and Technology, Cairo, Egypt.
 - 3&4 Geologists, Geology and Raw Materials Dept., Atomic Energy Establishment, Cairo, Egypt.

provided by these images would yield significant information necessary for the regional development of agriculture, mineral exploitation, and transport in such arid areas as Egypt. It is also hoped that results obtained and experience gained from this investigation can assist in interpretation of satellite images over similar arid regions in the world.

The present report deals with the drainage, structure and geology of a large area in the southern part of Egypt namely West Aswan area, as interpreted from ERTS-1 satellite images. The area under study covers some 34000 km², and is limited by the following points of coordinate intersections : lat. 25°15'00" N, long. 31°25'40" E, and lat. 24°57'30" N, long. 33°15'10" E from the north, and lat. 23°22'30" N, long. 32°50'30" E, and lat. 23°37'30" N, long. 31°04'30" E from the south.

The River Nile passes from south to north in the eastern side of the area which overlaps with the western side of the previously investigated East Aswan area (El Shazly, Abdel-Hady, El Ghawaby and El Kassas, 1973). In contrast to the previously examined area the great part of the present area lies in the Western Desert of Egypt to the west of Aswan town (Fig. 1).

The area covered in these images is significant in the fact that it shows the pattern of filling of the Aswan Dam Reservoir and some of the significant geologic features in the surrounding region, e.g. some of the faults intercepting the reservoir did not appear in other available geologic maps for this area. Such features warrant very careful detailed investigation to study their effects on the seepage from the reservoir and their impact on the future development of the Aswan Dam region.

To demonstrate the value of information provided by ERTS-1 satellite images, geologic and structural maps compiled from these images for this area are shown in comparison to the geologic map for the same area compiled from various sources by the Geological Survey and Mineral Projects Authority published in 1971.

DRAINAGE ANALYSIS

West Aswan area is essentially covered by Foreland sediments ranging from Cretaceous to Quaternary with the exception of the igneous-metamorphic basement exposures of limited distribution in the vicinity of Aswan town and to its south.

The eastern part of the drainage map (Fig. 2) is dominated by the Nile drainage, including that of the present Nile and the plains surrounding it especially on the west side. The present Nile is controlled by the N-S, NNW-SSE, NNE-SSW fractures as already mentioned by the same authors in their interpretation of ERTS-1 images of East Aswan area. In this report more observations are available on the northern part of Lake Nasser (Aswan Dam Reservoir) extending from south of Aswan town to Kalabsha.

It is evident that branches of the Lake penetrating in the desert are formed by water back filling the wadis (valleys) draining the desert to the east and west of the River Nile. At Kalabsha the branches of the Lake are particularly well developed and they are controlled by the NNW-SSE, ENE-WSW, and E-W faults.

This phenomenon should be carefully evaluated in relationship to the possible future development of other significant branches

from the Lake along major faults traced on the satellite images. Detailed investigation should be carried out to show the nature of these faults (e.g. activity, openness, filling material, etc). This will help to predict whether in the future erosion along these faults would allow branches from the reservoir to grow rapidly causing significant seepage and water diversion problems.

On the west side of the present Nile the area is geomorphologically distinguished into two major units, namely the wide plain adjacent to the Nile and the plateau with its escarp towards the west. The plain - which normally ranges in the width from 20 to 30 km - has been the scene of activity of the older Nile in the Quaternary and Tertiary (Butzer and Hansen, 1968). It is sometimes called Kalabsha plain to the south where the bed rock is mainly Nubian Sandstone and Darb El Gallaba plain to the north where the most important bed rock is Darb El Gallaba gravel produced by the Nile drainage in the Pleistocene. The plateau - Sinn El Kaddab and its continuation - starts from the plain and extends westwards to the Kharga Oasis depression and southwards and northwards outside the boundary of the present map.

The wadis running from the plateau towards the Nile are mainly controlled by the ENE-WSW and E-W fractures, although their tributaries are controlled to a considerable extent by the other fractures and rock texture. In the north the wadis including W. Rimidin and W. El Magal are interrupted by the plain. In the south, however, the wadis run directly from the plateau to the Nile, these include W. El Kobbaniya, W. Kurkur and W. Kalabsha.

In the western part of the map the wadis are better developed southwards in comparison to the north where they drain westwards into the depression of Kharga Oasis being controlled largely by the ENE-WSW and E-W fractures. Southwards, the drainage is complicated, however, by the presence of various fracture systems and the gentler slope towards the west and south. Accordingly, W. Abu Silla, W. Mareef and other wadis draining the southwestern part of the plateau are essentially running in southwestern and southern directions.

STRUCTURE

The linear structural elements delineated by the examination of ERTS-1 satellite images are given in (Fig. 3) and they are represented essentially by folds and fractures.

Folds

The presence of sinuous trace extending NNW-SSE along Sinn El Kaddab escarp at the centre of the images and of more or less parallel crenulated lineations or traces in many parts of the investigated area reveals a major dominant folding system of ENE-WSW trend. These traces indicate that the folding which is of a regional nature is of the open type and slightly plunging WSW. Minor crenulations of the same type and trend are noted, thus proving the presence of smaller folds within the regional ones.

The folding influences the Cretaceous and early Tertiary sedimentary rocks in the area west of Aswan. Accordingly it is believed to have been caused essentially by the Upper Cretaceous-Tertiary diastrophism. It is noted that the trend of folding in

the presently investigated West Aswan area is ENE-WSW which is in agreement with the dominant younger fold trend in East Aswan area as given in Interim Report No. 4 of this series.

Fractures (Including Faults)

There are two major fault trends delineated in the images of West Aswan area, namely the NW-SE faults making notable horizontal separation and the NNW-SSE faults showing horizontal separation and indicated vertical separation along geological and relief boundaries. Furthermore, the NNE-SSW fault west Kurkur Oasis shows marked horizontal left-lateral separation of the Lower Esna Formation, Gebel Garra Formation and Upper Esna Formation.

Furthermore, two major fracture trends are widely distributed in the area namely the NE-SW and the ENE-WSW, E-W groups. The NE-SW fractures do not show separation, and they may be major tension fractures perpendicular to the principal force creating the previously mentioned two major fault trends. The ENE-WSW, E-W fractures seem to represent tension zones along the hinges of major folds which may have been faulted along the same zones.

Other shorter lineations are found in closely spaced patterns which are usually related to major fractures and faults. The NW-SE lineaments are observed to the west of Idfu and Kom Ombo towns, and near the northern part of the escarp. The NNW-SSE lineaments are noted to the west of Aswan town, and near the middle and southern parts of the escarp. Near Kalabsha on the western side of Lake Nasser lineaments are abundant in a N 35° W - S 35° E direction. Furthermore, crenulated lineaments of a N-S trend have been also recorded near the escarp. At the western side of the plateau notable widely separated lineaments are noted trending N-S to N 10°E-S 10° W.

As it was mentioned earlier in this report, some of the fractures and faults, particularly the NNW-SSE and ENE-WSW, E-W trends intercepting Lake Nasser (Aswan Dam Reservoir) should be given careful detailed investigation. This is essential to determine their significance on the seepage and possible future development of diversion channels from the Lake.

Comparing the present investigations with previous studies related to the structure of West Aswan area (Issawi, 1968; Barakat and Ashri, in press) it may be noted that major folds and faults reveal in general greater continuity in the present work, and the groupings of short lineaments echoing large fractures and faults are better delineated. However, the small structural basins and domes associated with faults which have been mapped by the previous authors have not been noted in the present work.

GEOLOGY

The geology of West Aswan area is dominated by a sedimentary succession ranging from Cretaceous to Quaternary. The igneous-metamorphic rocks are represented by the exposures of Aswan monumental granite and associated rocks in the vicinity of Aswan town on the east side of the Nile, as well as, by small outcrops on the west bank of the river, apart from small parts of outcrops of gneisses and pink granite. The igneous-metamorphic rocks are of Precambrian age passing into early Paleozoic and their characteristics in ERTS-1 images have been given already in Interim Report No. 4 of the present series (El Shazly, Abdel-Hady, El Ghawaby and El Kassas, 1973).

The most important point revealed by ERTS-1 images in this respect is the distinction of Aswan monumental granite by its medium grey tone and medium texture from the pink granite with its light tone and fine texture. This distinction is of particular importance in the geology of Egypt and the evolution of granites in relation to major tectonics (El Shazly, 1970).

The sedimentary column in West Aswan area starts by the Cretaceous Nubian Sandstone which covers the southern part of the plain on the west side of the Nile termed Kalabsha plain, as well as, large exposures north of Aswan town. In the studied area the Nubian Sandstone is distinguished on the ERTS-1 images into four units each possessing characteristic tone and texture. The basal unit is of coarse texture and of darker grey colour. The iron-ore member is the darkest in colour among the Nubian Sandstone exposures and has a medium texture. The undifferentiated unit is of grey tone and with a medium to fine texture, while the Nubian Sandstone with wind-blown sand is light grey to yellowish in tone with medium texture and lineated with sand of greyish tone.

The Fourth Calcareous Sediments cover the greatest part of West Aswan area especially on the Western side of the Nile. They range in age from Upper Cretaceous to Lower Eocene being represented by seven geological formations, the youngest one of them namely Gebel Serai Formation has been distinguished into two units of variable tone and texture. The Upper Cretaceous formations namely Wadi Abbad Formation, Gebel Duwi Phosphate Formation, and Lower Esna Formation have been described in Interim Report No. 4 of the present series. Of economic importance, however, is the distinction on the satellite images of G. Duwi Phosphate Formation - which incorporates the phosphorite beds - by its very coarse texture and medium grey tone.

The escarp on the western side of the Nile starts at the base with the Lower Esna Formation, followed upwards by the essentially Paleocene Gebel Garra Formation and the Lower Eocene Upper Esna Formation and Gebel Serai Formation. Gebel Garra Formation is made up of chalk and limestone with subsidiary marl and shale (Issawi, 1968), and it is well developed in the investigated area although it tapers off northwards. This formation possesses a fine to medium granular texture, a medium grey tone and is lineated parallel to the escarp.

The plateau covering the central and western parts of the images is capped by: the Upper Esna Formation - especially towards the south and exposed in the wadis, and Gebel Serai Formation - which is distinguished into a basal unit covering in particular the higher elevations in the southern part of the plateau and the proper well developed formation in the northern part of the plateau with its typical limestone lineated in the images with widely spaced fractures. The geology of the southern part of the plateau and plain are in general agreement with the investigations of Issawi (1968) on Kurkur-Dungul stretch. Kurkur Formation has been, however, distinguished in the images only in Gebel Marawa.

The Fifth Detrital-Calcareous-Evaporite Sediments are of particular interest in the investigated West Aswan area and they show great variation. Tufa and calcite are delineated towards the eastern and western side of the plateau. According to Butzer and Hansen (1968) tufa is of Pliocene age passing into Quaternary being related in origin to paleoclimatic conditions. The delineation of the tufa northwards of Kurkur Oasis has been established in the geological map of West Aswan area interpreted from ERTS-1 images, as well as, the possible relation between the tufa and the fracture systems observed in the area especially in their intersections. The authors of the present work are accordingly advancing the theory that the

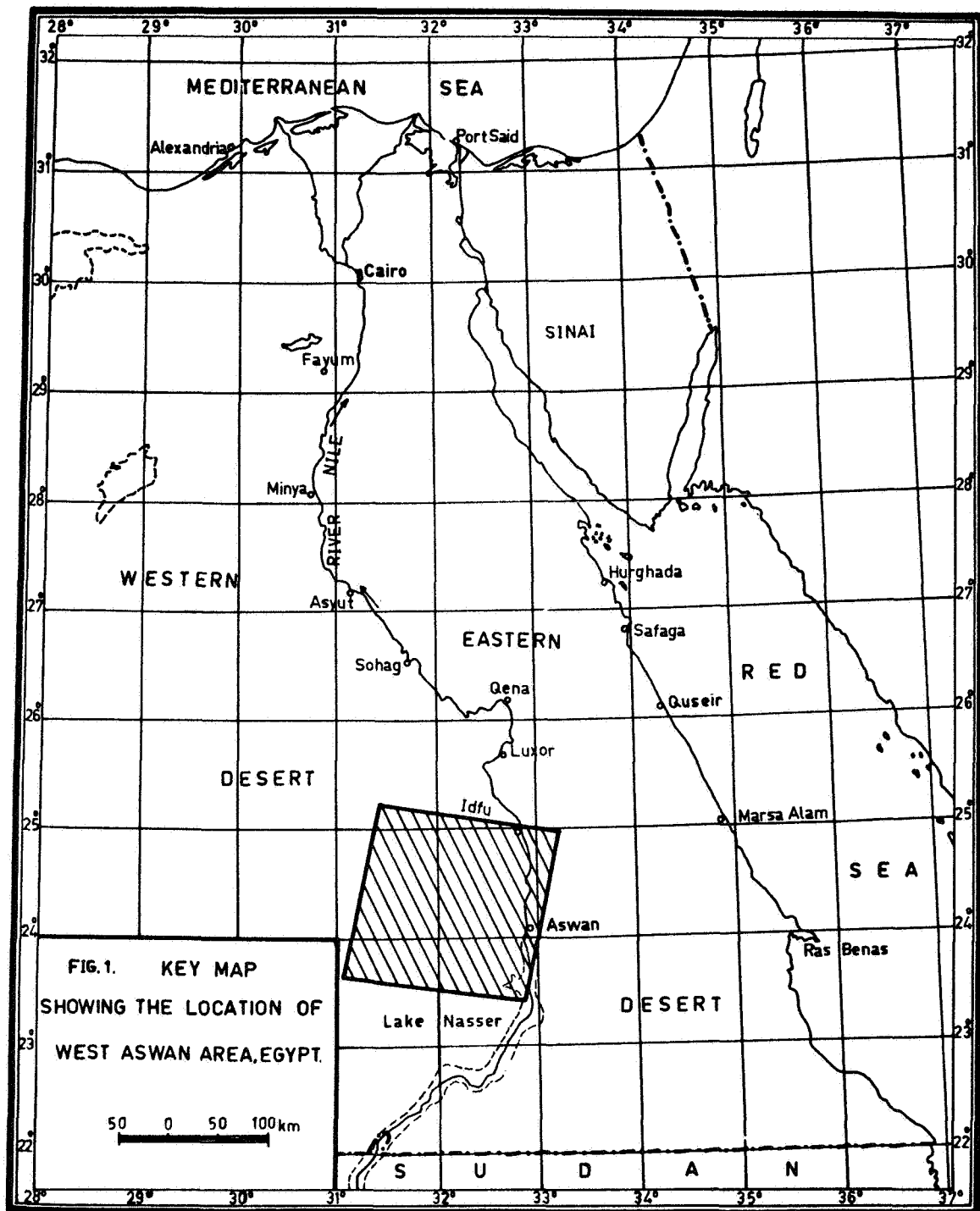
tufa and calcite are originally related to the hydrothermal activities of the tectonic movements of the late Pliocene-early Quaternary, which have been partly mobilized and redeposited by the climatic conditions prevailing in the later Quaternary.

The Quaternary deposits in West Aswan area have been distinguished into Darb El Gallaba gravel, conglomerate, playa, alluvium-eluvium and surficial deposits which are mainly alluvium, each of these is characterized by its particular texture and tone. Darb El Gallaba gravel covers the northern part of the plain west of the Nile, the gravel is accumulated by a Pleistocene Nile running at this locality to the west of the present Nile (Butzer and Hansen, 1968). Conglomerate accumulated on the southern part of the escarp slope, while playas are superimposed on the Nubian Sandstone plain not far from Kalabsha. One of the points of interest provided by studying ERTS-1 images is the distinction between the alluvial-eluvial deposits which have not been transported for long distance from their source rocks and the alluvial deposits which have been moved for longer distance from their source - in West Aswan area the former have been found to be relatively coarse in texture than the latter.

The compiled geological map of West Aswan area has been reproduced in (Fig. 6) (after the geological map of Egypt - published by the Geological Survey and Mineral Projects Authority in 1971) for the purpose of comparing it with the present geological map of West Aswan area interpreted from ERTS-1 satellite images (Fig. 4). The number of the geological units distinguished on our satellite images interpreted map are 22, while the number of geological units separated in the compiled map are only 7. Of particular importance is establishing the continuity of the geological units in the northern part of the area in (Fig. 4) as well as the continuity of the structural elements in the presently constructed structural lineament map in (Fig. 3) as compared to the compiled map in (Fig. 6).

REFERENCES

- BARAKAT, M.G., and A.H. ASHRI (in press), "Airphoto Interpretation of some structural features in the area southwest of Aswan". Egypt J. Geol., Cairo.
- BUTZER, K.W., and C.L. HANSEN (1968), "Desert and River in Nubia". The University of Wisconsin Press, Madison, Milwaukee and London.
- EL SHAZLY, E.M. (1970), "Evolution of Granitic Rocks in Relation to Major Tectonics". The West Commemoration Volume, University of Sagar, India.
- EL SHAZLY, E.M., M.A. ABDEL HADY, M.A. EL GHAWABY, and I.A. EL KASSAS (1973), "Geologic Interpretation of ERTS-1 Satellite Images for East Aswan Area, Egypt". Interim Report No.4, Remote Sensing Research Project, Academy of Scientific Research and Technology, Cairo, Egypt.
- GEOLOGICAL SURVEY AND MINERAL PROJECTS AUTHORITY, comp. (1971), Geological Map of Egypt, 1:2,000,000, Cairo.
- ISSAWI, B. (1968), "The Geology of Kurkur-Dungul Area". General Egyptian Organisation Geol. Research and Mining, Cairo, Paper No. 46.



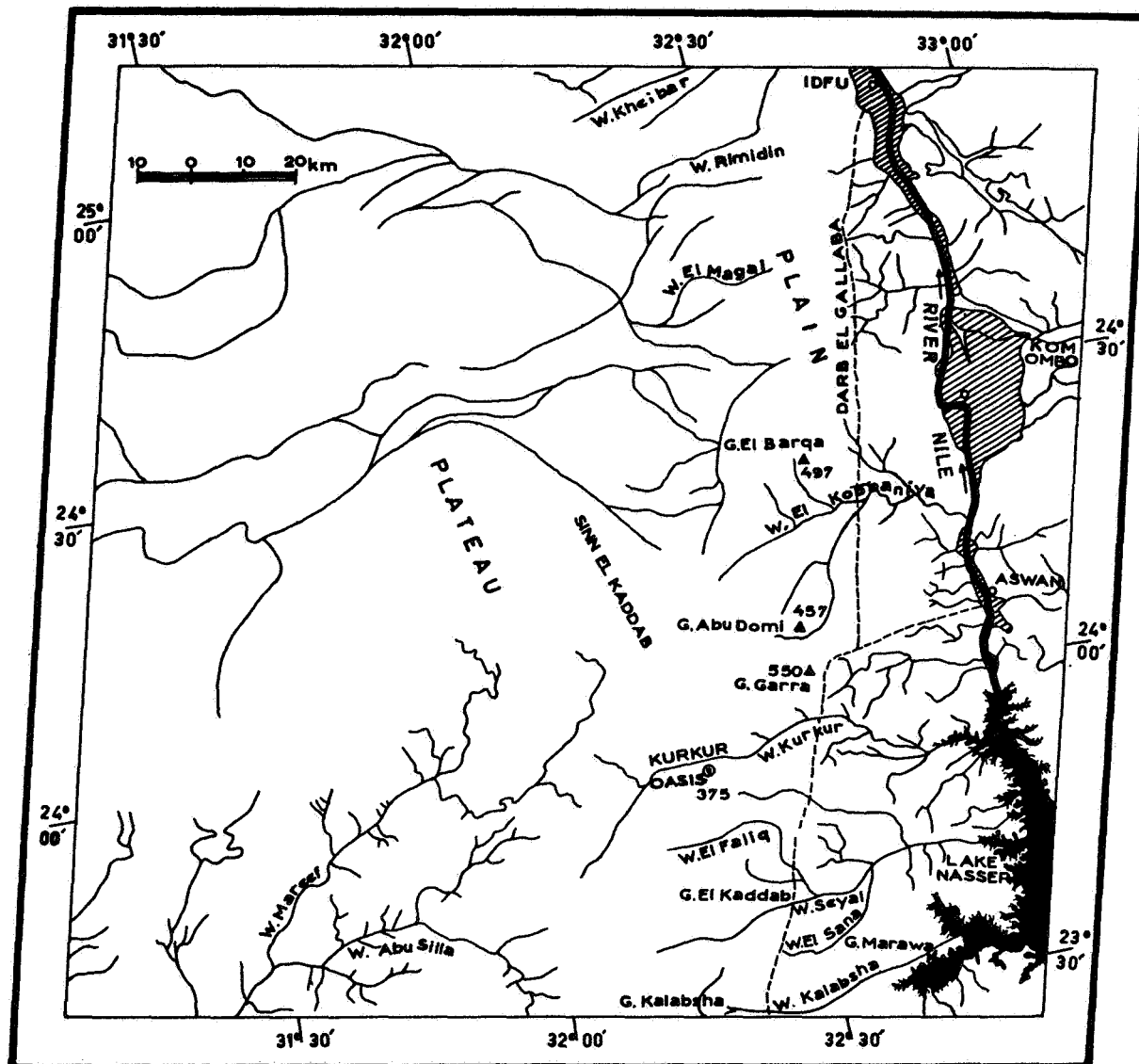


FIG.2. GENERAL DRAINAGE MAP OF WEST ASWAN AREA
(FROM ERTS -1 SATELLITE IMAGE)

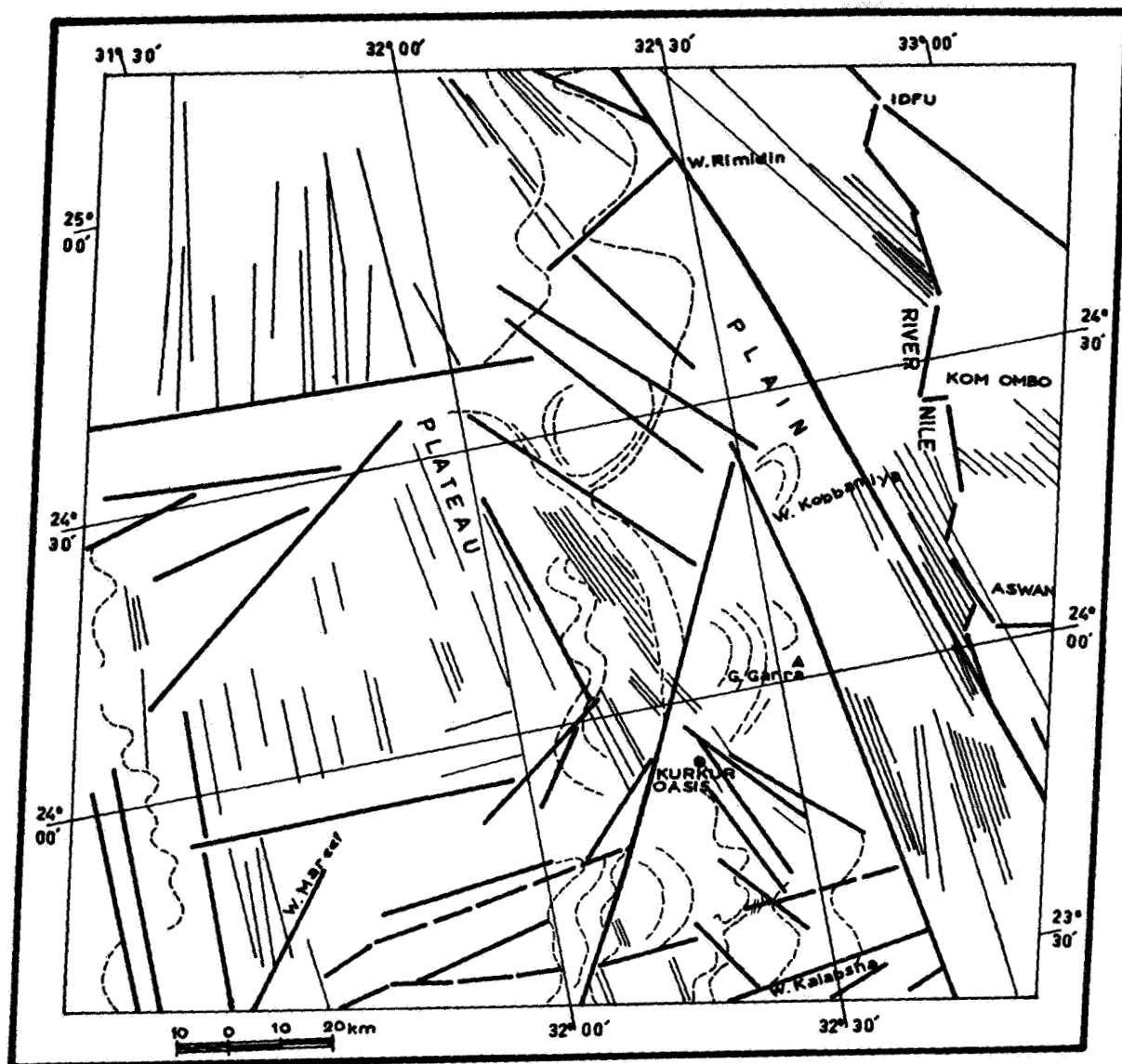





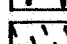
FIG.3. STRUCTURAL LINEATION MAP OF WEST ASWAN AREA
 (FROM ERTS-1 SATELLITE IMAGES)


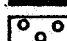
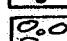
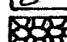
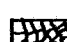
FOLDS FRACTURES INCLUDING FAULTS OTHER LINEAMENTS

LEGEND OF FIG. 4



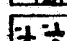
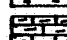
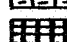
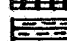


FORELAND SEDIMENTS

Fifth Detrital Calcareous-Evaporite Sediments




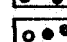
- | | |
|--|--|
|  Cultivation |  Vegetation |
|  Surfacial deposits,
mainly alluvium |  Alluvium-eluvium |

- | | |
|--|---|
|  Playa | |
|  Conglomerate | |
|  Darb El Gallaba gravel | |
|  Tufa |  Calcite |

Fourth Calcareous Sediments

- | | |
|---|--|
|  Gebel Serai Formation | |
|  Gebel Serai Formation, basal | |
|  Upper Esna Formation | |
|  Gebel Garra Formation ≈ Tarawan Formation | |
|  Kurkur Formation | |
|  Lower Esna Formation ≈ Dakhla Formation | |
|  Gebel Duwi Phosphate Formation | |
|  Wadi Abbad Formation | |

Third Detrital Sediments

- | | |
|---|--|
|  Nubian Sandstone, lineated with wind-blown sand | |
|  Nubian Sandstone, undifferentiated | |
|  Nubian Sandstone, iron-ore member | |
|  Nubian Sandstone, basal | |

POST OROGENIC PLUTONITES

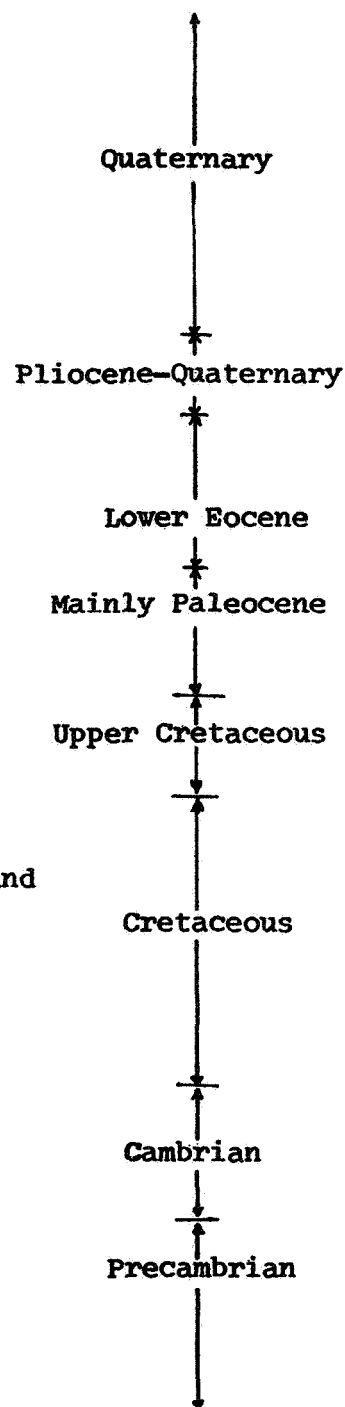
- | | |
|---|--|
|  Aswan monumental granite
and associated rocks. | |
|---|--|

LATE OROGENIC PLUTONITES

- | | |
|--|--|
|  Pink granite | |
|--|--|

GEOSYNCLINAL SEDIMENTS

- | | |
|---|--|
|  Metasediments | |
|---|--|



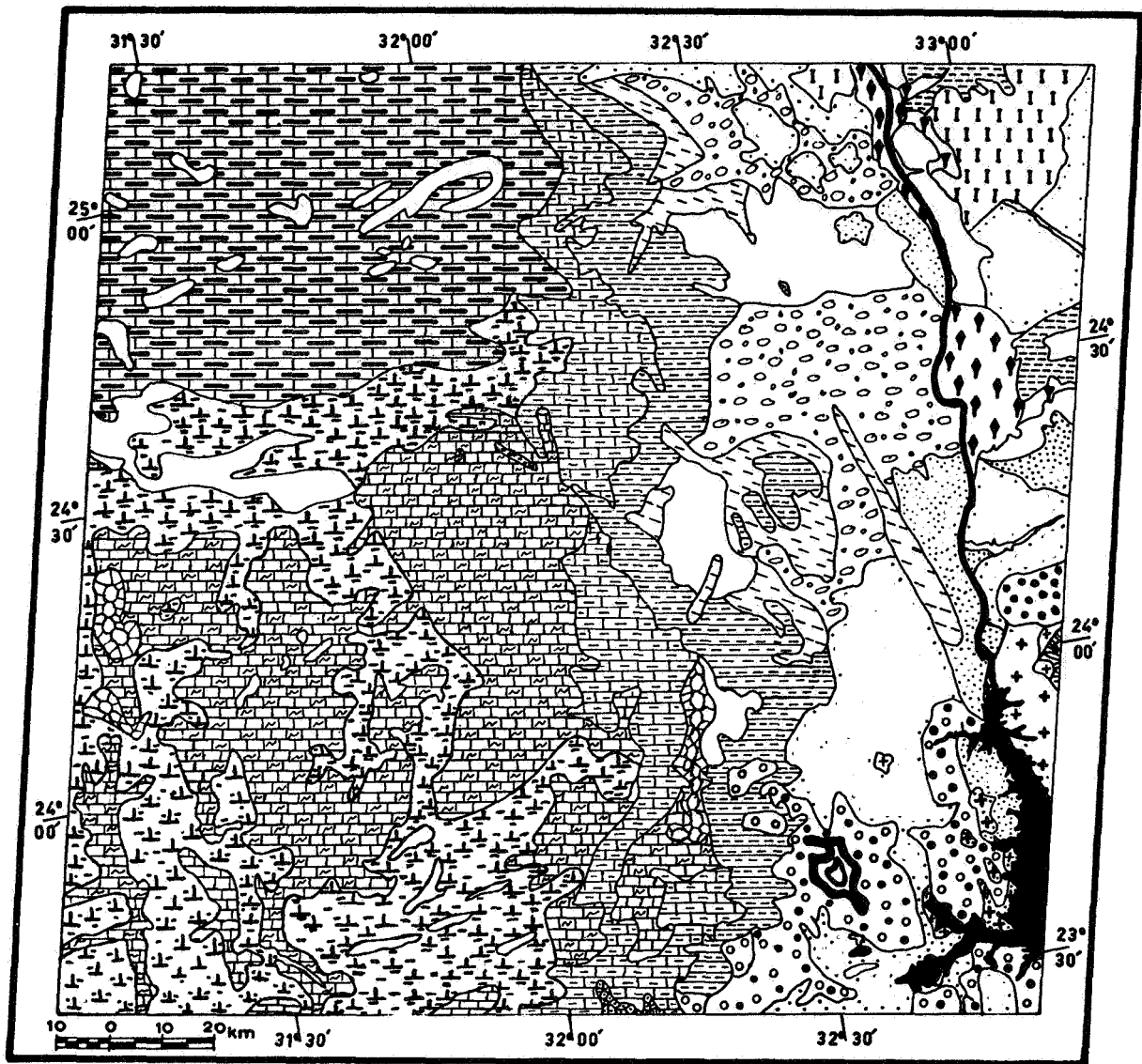


FIG 4. GEOLOGICAL MAP OF WEST ASWAN AREA

(FROM ERTS-1 SATELLITE IMAGES)



FIG.5. INFRARED IMAGE OF WEST ASWAN AREA
(ERTS-1 SATELLITE, NOV.1972)

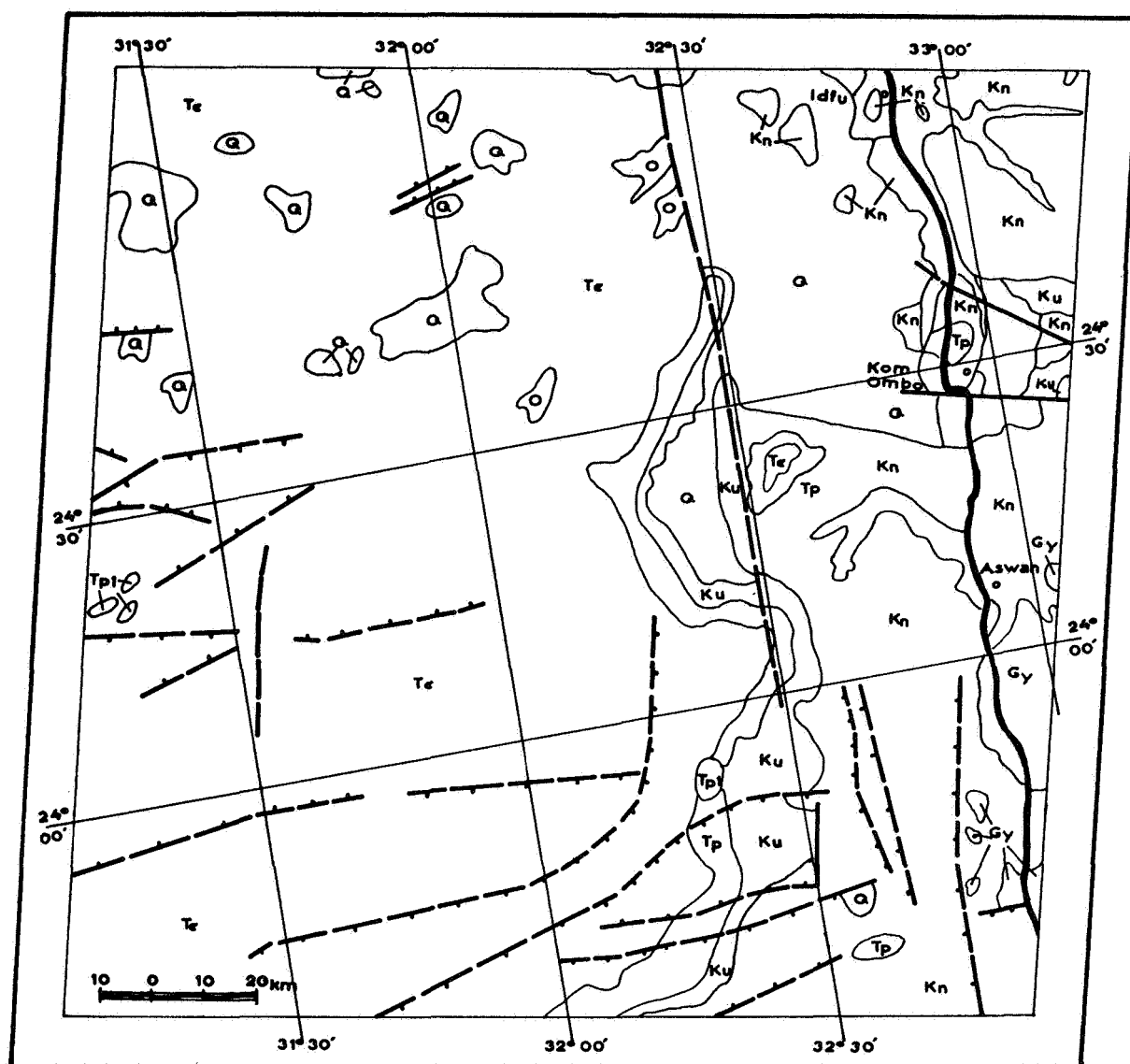


FIG.6. COMPILED GEOLOGICAL MAP OF WEST ASWAN AREA

(AFTER GEOLOGICAL MAP OF EGYPT, 1:2 000 000, 1972)

a	QUATERNARY	Ku	UPPER CRETACEOUS
Tp1	PLIOCENE	Kn	NUBIAN SANDSTONE COMPLEX
Te	EOCENE	Gy	YOUNGER GRANITES AND GRANODIORITES
Tp	PALEOCENE		FAULT

وبسيط على تركيب منطقة غرب اسوان الطيات المفتوحة والمتجهه شرق شمال شرق - غرب جنوب غرب ، ويظهر هذا النوع من الطي اقليميا وعلى المستوى الصغير كذلك . وتتبع الكسورات والفوالق عدة اتجاهات وقد تمتد لمسافات طويلة او قد تظهر كمجموعات قصيرة موازية للكسورات الكبرى .

وقد أمكن في هذه الدراسة من صور سفينة الفضاء سفتا - ١ (ERTS-1) حصر ٢٢ وحدة جيولوجية وضعت على الخريطة الجيولوجية لمنطقة غرب اسوان ، بينما اظهرت الخريطة الجيولوجية السابقة المجموعة من مصا در مختلفة والمنشورة في عام ١٩٧١ سبع وحدات جيولوجية فقط بنفس المنطقة . وتتراوح هذه الوحدات من حقب ما قبل الكمبري المتوغل في القديم الى الحقب الرباعي الذي يستمر حتى عصرنا هذا . وقد أمكن في هذه الدراسة تمييز جرانيت اسوان من الأنواع الاخرى من الجرانيت ، وكذلك الحجر الرملي النوبي الحامل لخامات الحديد ، والتكوين الجيولوجي الذي تتخله طبقات الفوسفات ، مما يدعم الاهمية الاقتصادية للدراسة الحالية . وقد تم التوصل من الناحية العلمية الى استنتاجات هامة تختص بامتدادات التكاوين الجيولوجية من الجنوب الى الشمال ، والتفريق بين الأنواع المختلفة من الرواسب الحديثة نسبيا ، ومناقشة نشأة التوفنا وطريقة تكوينها .

وقد تعرضت الدراسة الحالية لمسألة الكسورات والفوالق التي تعترض بحيرة ناصر وأوصت بالقيام بدراسات تفصيلية لمعرفة خصائصها من ناحية نشاطها وانفتاحها ومادتها المائلة حتى يتسنى تقييم احتمالات تأثيرها على المياه المخزونة في البحيرة ، وهي دراسات اساسية ولها اهميتها الكبيرة من الناحية الهندسية - الجيولوجية ولتلافى اى تأثيرات ضارة مستقبلا تنشأ عن تأثير بعض هذه العوامل الجيولوجية على الجوانب الهندسية لمشروع الحيوى الهام .

ويعطى هذا التقرير أمثلة واضحة للفوائد الكثيرة التي يمكن استنتاجها من دراسة الصخور المأخوذة عن طريق سفن الفضاء الخارجى لاغراض مسح واستكشاف الثروات والموارد الطبيعية للأرض ، والكشف عن بعض الظواهر والعوامل الجيولوجية التي تؤثر على المشروعات الهندسية والقومية الهامة .

الدارسة الجيولوجية للصور الالكترونية
المجموعة بواسطة سفينة الفضاء سفتا - ١
لمنطقة غرب اسوان ، جمهورية مصر العربية
اعتماد

الشاذلى محمد الشاذلى^١ محمد احمد عبد الهادى^٢ محمد عبد الرازق الخوايى^٣ ابراهيم القصاص^٤

الملخص

درست الصور الالكترونية المجموعة بواسطة سفينة الفضاء سفتا - ١ (ERTS-1) والمأخوذة في اربعة مجالات ضوئية مختلفة لمنطقة غرب اسوان ، من الناحية الجيولوجية والتركيبية وخطوط الصرف ، ثم قورنت هذه الدراسة بالابحاث السابقة عن نفس المنطقة في المجالات سالفه الذكر . ويعتمد صرف النيل في المنطقة المدروسة أساسا على العناصر التركيبية ذات الاتجاهات شمال - جنوب ، شمال شمال غرب - جنوب جنوب شرق ، شمال شمال شرق - جنوب جنوب غرب وكذلك على الانحدار ناحية البحر الابيض المتوسط . وتتخذ الوديان وهى مجارى السيول عامة اتجاه الكسورات شرق شمال شرق - غرب جنوب غرب ، شرق - غرب وتتجه مع الانحدار الى النيل في الجزء الشرقى من المنطقة ومع الانحدار ناحية المنخفضات بالصحراء الغربية في الجزء الغربى منها . وتشغل تفرعات بحيره ناصر من ناحيتها الشمالية (التى تظهر في الصورة) الوديان والكسورات الارضية . وهذه ظاهرة لها أهميتها القصوى من الناحية الهندسية - الجيولوجية لما قد يترتب عليها مستقبلا من فاقد بالتسرب مع خلق تفرعات رئيسية من البحيرة قد تساعد فى تكوينها عوامل النحر من تسرب المياه من البحيره خلال الشقوق والفوالق المفتوحة او المغطاه بمواد غير صلبة .

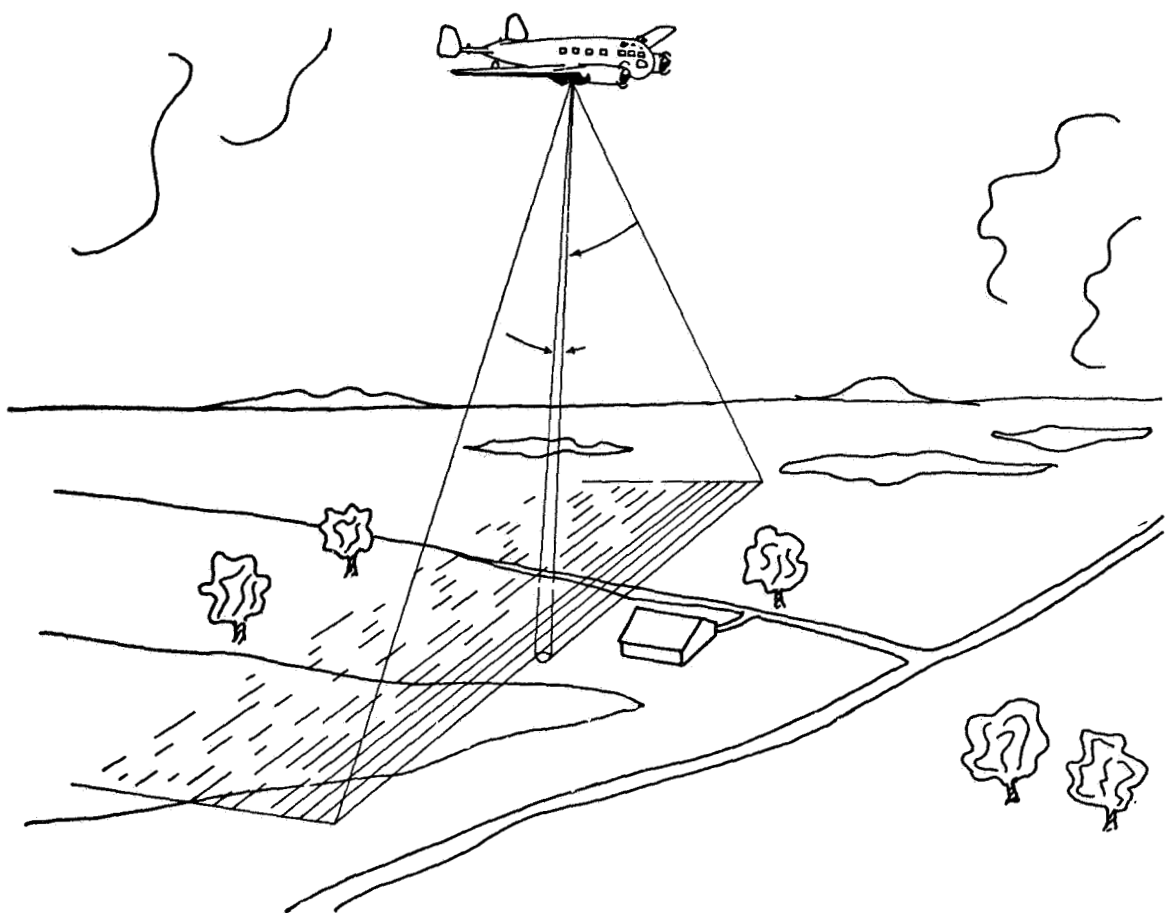
-
- (١) نائب مدير هيئة الطاقة الذرية ، ورئيس المجموعة الجيولوجية بمشروع الاستشعار من البعد
اكاديمية البحث العلمى والتكنولوجيا - القاهرة .
(٢) أستاذ الهندسة المدنية بجامعة ولاية اوكلاهوما بالولايات المتحدة الأمريكية ، ومدير مشروع
الاستشعار من البعد - باكاديمية البحث العلمى والتكنولوجيا ، القاهرة .
(٣ ، ٤) جيولوجيان بهيئة الطاقة الذرية بالقاهرة .

جمهورية مصر العربية
أكاديمية البحث العلمي والتكنولوجيا

الدراسة الجيولوجية للصور الالكترونية
المجموعة بواسطة سفينة الفضاء - ١ (ERTS-1)
لمنطقة غرب اسوان
جمهورية مصر العربية

تقرير بدئي رقم ٥
مشروع الاستشعار من البعد
بالتعاون مع
- مؤسسة العلوم القومية ، واشنطن ، الولايات المتحدة الأمريكية
- جامعة أوكلاهوما ، ستيلووتر ، أوكلاهوما ، الولايات المتحدة الأمريكية

الناشر
أكاديمية البحث العلمي والتكنولوجيا
القاهرة - ج ٠ م ٠ ع ٠
(أكتوبر ١٩٧٣)



ACADEMY OF SCIENTIFIC RESEARCH AND TECHNOLOGY

REMOTE SENSING RESEARCH PROJECT

ERTS-A MULTISPECTRAL IMAGE ANALYSIS CONTRIBUTION FOR THE GEOMORPHOLOGICAL EVALUATION OF SOUTHERN MARACAIBO LAKE BASIN

F. Salas, O. Cabello, F. Alarcón and C. Ferrer

Multispectral analysis of ERTS-A images at scales of 1:1,000,000 and 1:500,000 has been conducted with conventional photointerpretation methods (direct observation with the aid of magnifying glass). Specific methods have been developed for the geomorphological analysis of southern Maracaibo Lake Basin ($71^{\circ}30' - 72^{\circ}30'$ long. W, $8^{\circ}00' - 9^{\circ}00'$ lat. N) which comprises part of the Venezuelan Andean Range, Perijá Range, the Táchira gap and the Southern part of the Maracaibo Lake depression.

A steplike analysis was conducted to separate macroforms, landscapes and relief units as well as drainage patterns and tectonic features, which permitted the delineation of tectonic provinces, stratigraphic units, geomorphologic units and geomorphologic positions. The method of analysis allowed further knowledge on types of faults, lithologic characteristics as well as the identification of paleoprocesses and actual processes and the application of geochronological criteria on certain forms. The geomorphologic synthesis obtained compares favorably with conventional analysis made on this area for accuracy of 1:100,000 scale, and in some features with details obtained through conventional analysis for accuracy of 1:15,000 and field work.

Geomorphological units in the mountains were identified according to changes in tone, texture, forms orientation of interfluves and tectonic characteristics which control interfluvial disimetrics. Observation of tonal variation and contrast within interfluves allowed the identification of paleoforms. Geochronological inference was based on actual modeling and topographic position of forms.

Units were identified at Piedmont according to forms and topographic expression. Sedimentary deposits were identified (terraces, terraces-colluvial fans and other colluvial forms), and again, its modeling and topographic position gave way for geochronological induction.

At the plains, units were separated through a comparative analysis of tone and textural patterns as well through the evaluation of drainage characteristics. These units were redetailed according to fluvial dynamics.

N 74 30771

1. Introduction. The main objective of this project has been to develop a method for the analysis of natural resources, valid at different physiographic media. Physical environment is being analyzed and its results are comparable with those obtained through other conventional methods, in terms of time, precision and maximum details. With this paper, a first level of analysis has concluded pertaining to Hidrography, Geology and Geomorphology. Thematic maps were prepared to the scale of 1:500,000 and details obtained were compared with fieldwork. Multispectral image (ID 1071.14361) prints at scales of 1:1,000,000 and 1:500,000 were analyzed with the aid of a magnifying glass. Analysis was conducted stepwise with the separation of macroforms, lands capes and units of relief. Interpretation of drainage patterns and of structural characteristics permitted to establish tectonic provinces, stratigraphic units, sectors and geomorphologic positions.

The methodology utilized permitted definition of type of faults, the identification of paleoprocesses, actual processes and the application of geochronologic criteria to certain geomorphological units. A geomorphological synthesis of each one of the environments analyzed was prepared and its results are comparable in some instances to those obtained at scales of 1:25,000. Nevertheless, the method needs further revision and more sophisticated equipment in order to reach a final pattern definition stage.

At the mountains, units were defined according to tonal changes, texture, forms and orientation of interfluves as well as for those tectonic characteristics which control disimetrics of interfluves. Tonal variations, actual modeling and relative position of deposits permitted to identify paleoforms and to conduct geochronological inferences. At the piedmont, units were defined according to form and topographic expression. Accumulations such as terraces, and aluvial fans were detected and through their modeling and position, geochronological inferences were conducted.

At the planes, units were differentiated by tone, textural pattern and drainage pattern. Those units were redetailed according to predominant fluvial dynamics.

2. Relief. A thematic map was drawn based on analysis of linears, drainage and depth of image (especially band 5). Mountains, piedmont and plains were evaluated as separated units. Valleys were not identified in the map due to cartographic scale of 1:500,000.

In the mountains, the analysis of principal, secondary and elementary interfluves permitted a detailed appraisal of drainage as well as an approximation to the qualification of watershed modeling. Difficulties were encountered because of tonal changes due to the effects produced by the zenital angle. Shadows derived from contrasting altitude of mountains interfered form and structural characteristics differentiation.

At the Andean piedmont, modeling patterns, degree of dissection, disposition of accumulations and relative location have been taken into account. At the Perijá Region, according to its own morphographic characteristics, it was necessary to take into account tonal contrasts as well as dissection of materials to separate areas of different slope.

Towards the Macizo Avispa-Capaz area, mountain-piedmont-plains transitional areas are very short. Piedmont has been poorly developed as formed by detritic early quaternary materials.

At the planes, two subunits were defined, according to topographic characteristics: High planes and flooded planes. There were observed some semicircular tonal anomalies that could correspond to an old showline. North of this linear slope decreases and further on predominate areas of bad drainage. Flooded areas increase E to W and S-N.

Lake shore is contrasting. Eastwards, rivers Santa Ana, Catatumbo, Escalante and Chama have drawn sequences of bays and keys with combined processes of fluvial and lacustrine sedimentation. At the west coast, the sedimentation discharge is smaller; thus morphological characteristic, are more regular and gentle.

3. Hydrography. Differences in tone, relief and vegetation (bands 5 and 7) permit enough information on principal, secondary and tertiary drainage, permanente and temporal lagoons, wetlands and marshes.

The three gross landscape units condition drainage characteristics and thus, the method to analyze its patterns. A more complete morphometric analysis was left for next level of analysis.

At the mountain, with the help of preliminary morphometry, it has been possible to obtain information on sporadic (elemental) drainage aided by topographic expression. Bodies of water of glacial lagoons at the Serranías de la Culata, Tovar and Sierra Nevad are observed distantly in band 7.

At the Piedmont, the study of drainage patterns depends on topographic expression, although tone and texture are good indicators of drains. In the plains, contrasting tonal responses and textural patterns permit the recognition of permanently and temporally flooded areas. Some vestiges of paleochannels were identified, and its identification was of great help for the study of fluvial dynamics. Comparison of bands 5 and 7 was very useful in the evaluation of drainage density.

Band 7 permits a precise and detailed analysis of drainage patterns. Results obtained with orbital images better considerably 1:50,000 cartographic work at hand. In the mountains, structure exerts an important control on water channels, on their organization and on their hierarchy. At the piedmont there can be observed two combined patterns, one dendritic controlled and the other parallel.

At the plains, it was encountered that the river beds or some of their sectors, presented anomalous shapes due to structural influence. Badly drained areas are identified by the presence of wetlands, marshes, floods and are frequently marginal to the rivers and to the shoreline.

4. Geology. Two different thematic maps have been obtained: structural and stratigraphic. The criteria applied for the identification of structural characteristics was the observation of lineaments expressed mainly through significative variation of texture and tone. The presence of aligned surfaces was detected through conventional methods: Topographic expression, structural control over drainage, drastic changes in modeling, displacement of strata, etc. Faults detected (principal and secondary) were ground truthed and when there doubts they were drawn as simple lineaments. Synoptic characteristics of images permitted the detection of new regional faults as the one called falla frontal del piedemonte, which could be a quaternary fault.

The analysis of strata (dip and direction) allowed identification of folds, syncline and anticline.

In order to systematize the observation of structural characteristics, a synthetic map was drawn which shows tectonic blocks: Andes, depresión del Táchira, Perijá y Llanos.

For the identification of geological units, tone, texture and modeling were keyed. Further work is being concentrated on differentiation of rock units.

5. Geomorphology. Methodological approach varied with landscape gross units.

At the mountains sectors were identified according to tone, texture, form and disposition of interfluves and tectonic activity. At the Perijá Region, lithological differences were introduced as a criteria for sectorization. Same criteria were taken into account for details within sectors. Additional criteria were introduced (actual modeling and topographic position) for relative geochronology of accumulations. It was also possible to define the presence of altered materials (when thickness is important) through the analysis of watershed slope and softness, modeled by deep water channels. In some cases, disposition and regularity of interfluves permitted a comparative analysis of processes.

In the Macizo de Capas, it was possible to identify processes of solifluxion type. At the Piedmont the identification of sectors was mainly based on form, topographic expression and dissection of forms. There were distinguished Piedmont accumulations, terraces, cones-terraces and colluvial valleys. Their relative geochronology was inferred same as in the mountains.

For the Perijá region identification parameters were tone and texture predominant forms identified were glacis and colluvial glacis.

At the plains, three different sectors were identified according to morphogenetic differentials:

East of Chama Catatumbo-Zulia-Tarra System	Chama Escalante - System Central flooded System
---	--

East of Chama river corresponds to a transitional system formed by rivers Mucujepe, Capaz and Frío. According to tone and textural patterns there were identified the following units:

- An area of gradual and transitional sedimentation. Some paleochannels within.
- A coalescent drainage outing.

The system Escalante-Chama contains a deltaic outing. Through textural and tonal patterns there were recognized the following:

- Channels of periodical heapage.

- Granulometry inferred from drainage patterns and resulting topographic forms.
- Heavy material has been carried near the lake shore.

In the Catatumbo-Zulia and Terra system, river outing is common with heapage of channels. Small basins and heapage channels were identified. At the central flooding sector there were identified blocked basis, areas of permanent decantation and frontal basins near the lake shore.

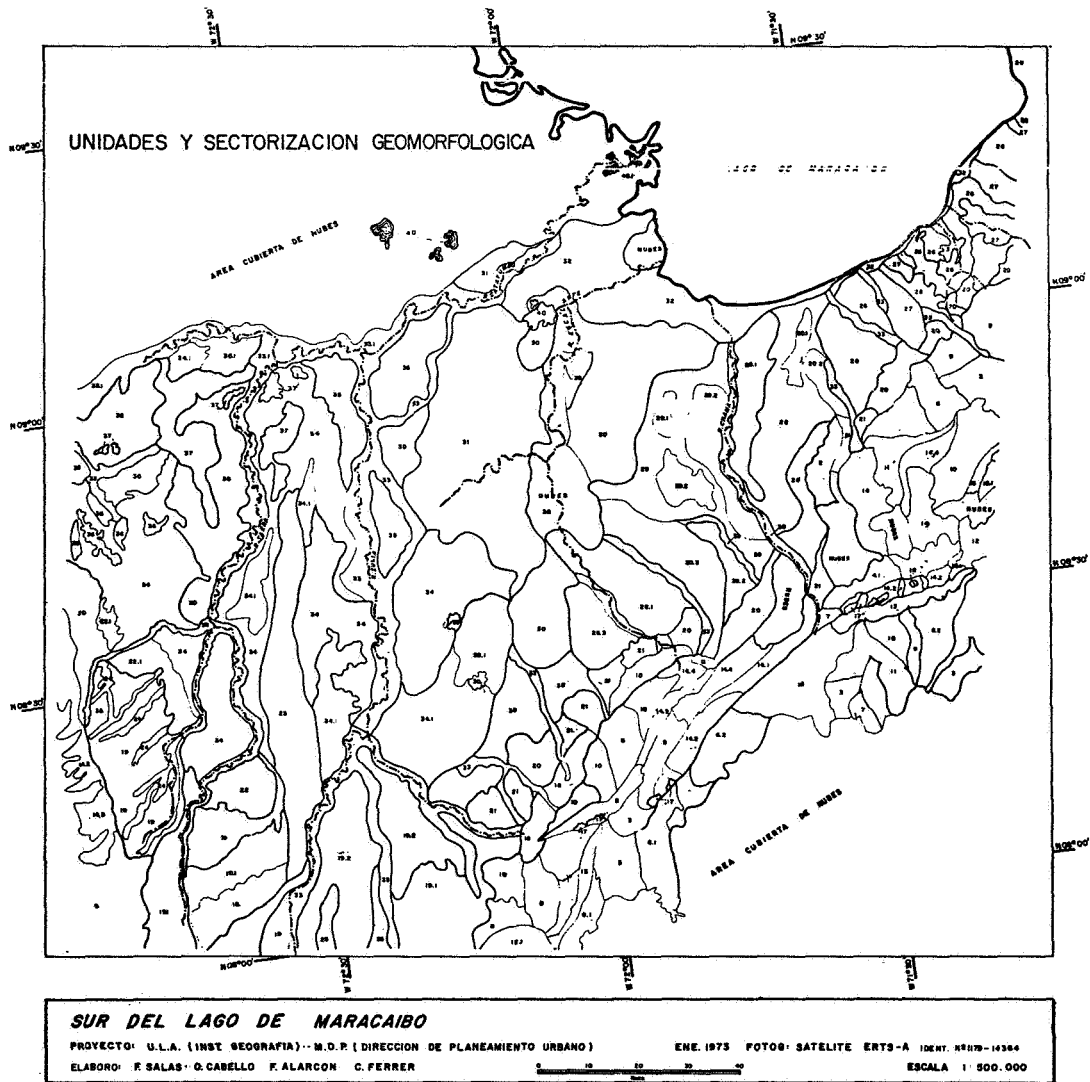


Figure 2.

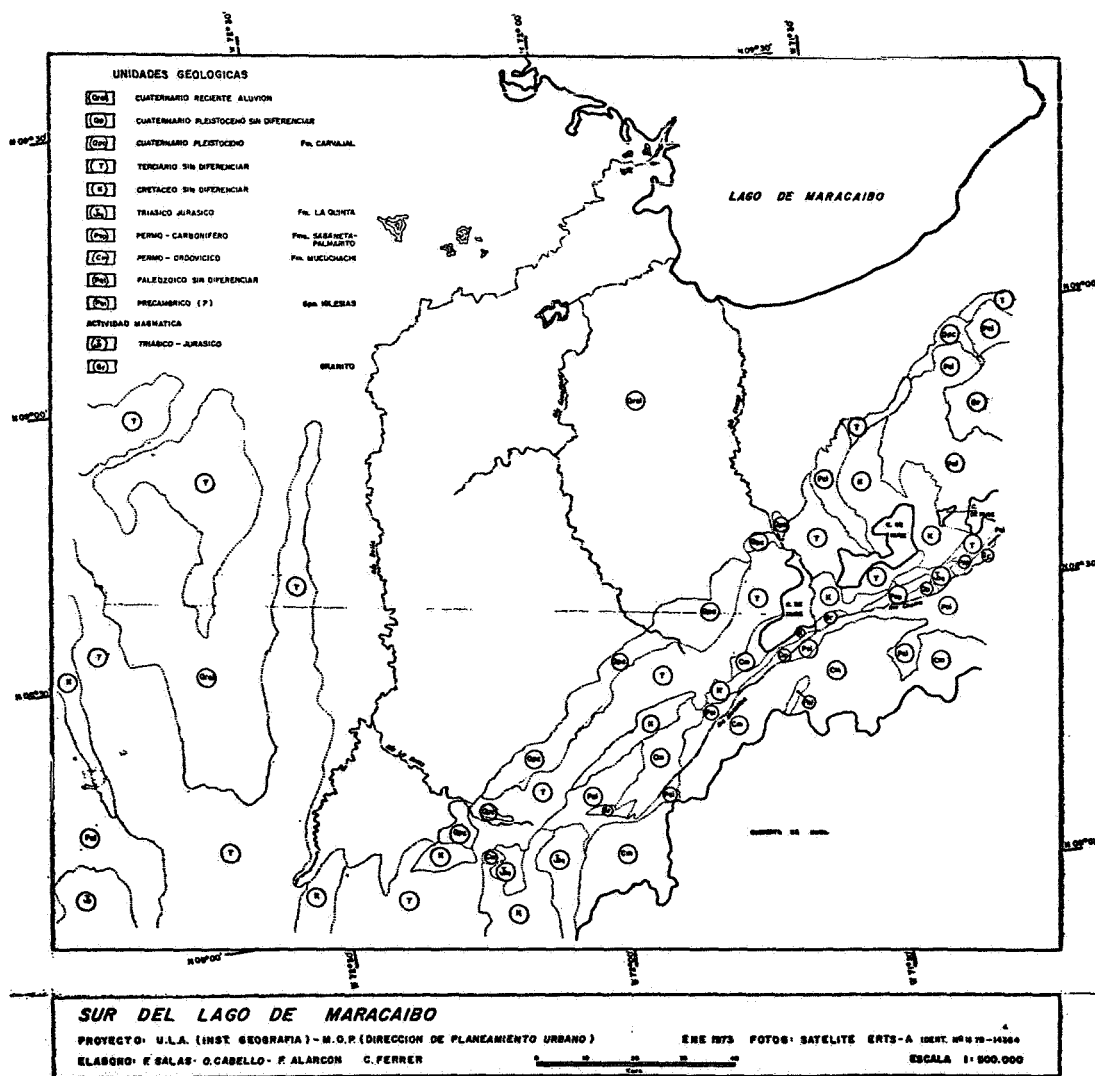


Figure 3.

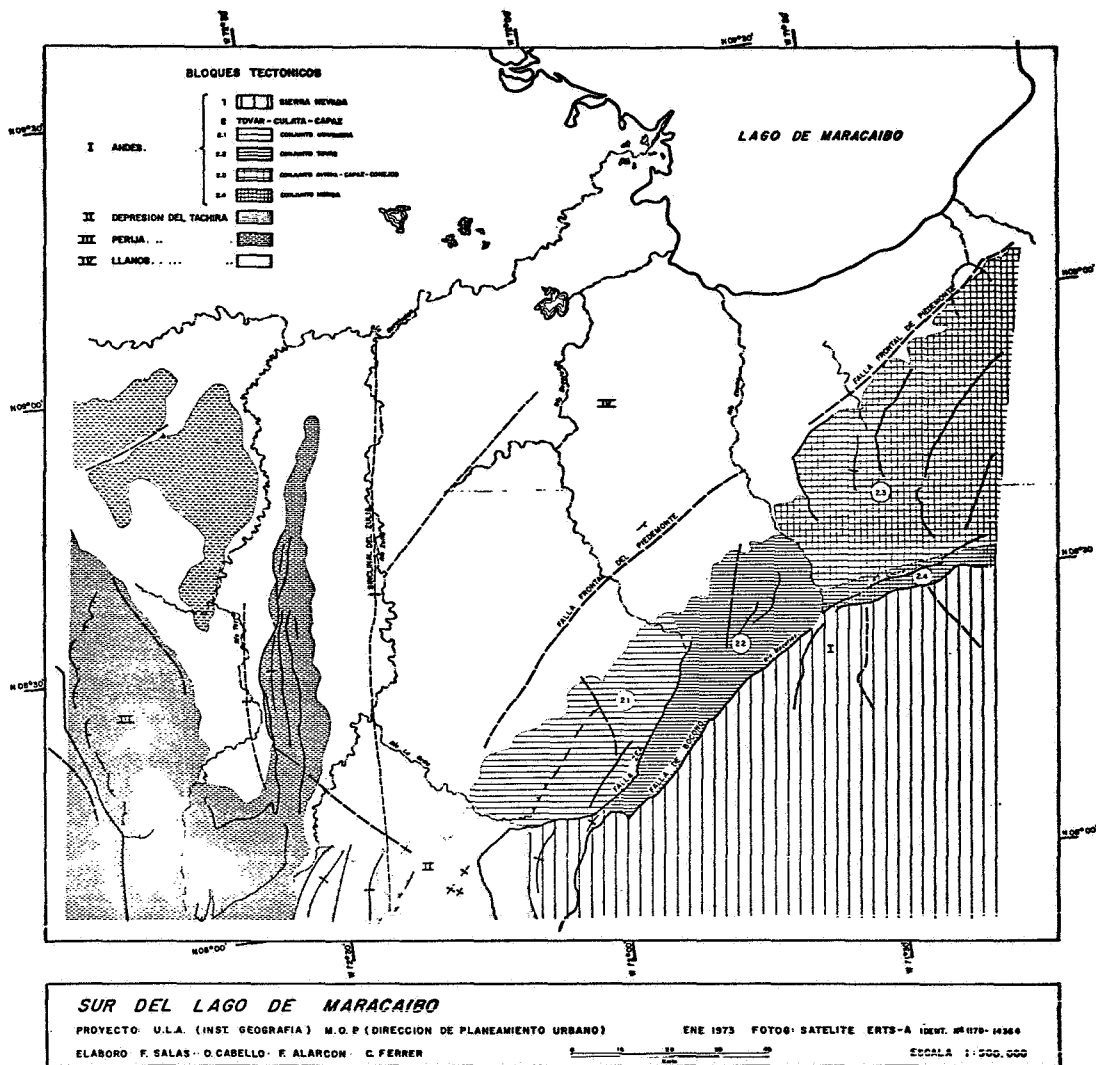


Figure 5.

GEOLOGIC HYPOTHESES ON LAKE TANGANYIKA REGION, ZAIRE, DRAWN FROM ERTS IMAGERY

Ulyera Wolyce and Sendwe Ilunga, *Bureau du President, Zaire*

INTRODUCTION

Based on initial work in the Lake Tanganyika area of eastern Zaire, we conclude that ERTS imagery is extremely useful for reconnaissance level geologic mapping and analysis in this region of the humid tropics. In particular, ERTS imagery has proven useful for recognizing and mapping regional structural units, for recognizing major structural features, and for arriving at some preliminary hypotheses about the mineral potential of the area. Results so far indicate that ERTS imagery can make a major contribution to the development of the mineral resources of our country. We hope to continue our research as principal investigators in the ERTS-B program.

The Government of Zaire is not a selected ERTS-1 principal investigator. We learned of the program too late to successfully propose an experiment. However, recognizing the wide range of potential applications that ERTS imagery could have in the field of resource inventory, management and development in our country, and anticipating the possibility of participating as Principal Investigators in the ERTS-B program, the Government of Zaire undertook an independent research program on the applications of ERTS imagery to several resource problems.

PRECEDING PAGE BLANK NOT FILMED

N 74 30772

Our research has concentrated on applications of ERTS imagery in the field of cartography, geology, forestry, hydrology and agriculture. For the work in geology reported here, we chose a test site in eastern Zaire on the shore of Lake Tanganyika in the vicinity of the Lukuga River. This area was selected because of its varied geology and the existence of two frames of cloud-free ERTS imagery.

The ERTS imagery used for the experiment includes 70mm transparencies, 1:1,000,000 scale black-and-white prints and selected enlargements, and a limited number of color composites. For the most part, we used standard photo interpretation techniques and checked our interpretations with field work and existing work.







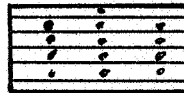
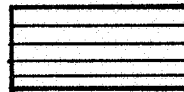
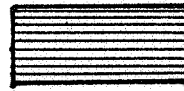

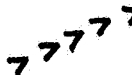
GEOLOGIC INTERPRETATION

The following observations are based on interpretation of ERTS frames 1052-07411 and 1052-07413 by geologists in the Bureau du President of Zaire (Figure 1).

Structural Units

The area covered by the two images can be divided into two zones separated by the Lukuga River. Within these two zones we were able to recognize and delineate nine major tectonic units. Several other large structural features are expressed clearly. The region studied covers the portion of Zaire lying south of 4°S and bounded by Lake Tanganyika on the east, meridian 28°30'E on the west, and the Lufira sector on the south.

LEGEND FOR FIGURE 1

9		Tertiary
8		Beach Sand
7		Red Grits
6		Kwango Series
5		Lukuga and Walikale or Niemba-Karoo Groups
4		Granitic Rocks
3		Katanga or Shaba Supergroup, including Kundelungu and Roan
2		Ruzizi Group
1		Kibasa Group
		Faults
		Axis of Anticline

* Unfortunately, the overlay for Figure 1 was mailed separately and has been lost or delayed in transit.



Southern Zone. In this zone, lying essentially south of 6°S and east of 28°E, one of the most prominent features is a large anticline or dome in the eastern part of the region known as the Grand Dome. In this part of the zone, the Kibasa Group crops out on the dome and are flanked on the north by a narrow band of Lukugian and Wasakalien rocks which lie along the south bank of the Lukuga River. The area underlain by Lukugian rocks is actually divided by the Lukuga River, with a strip of these rocks forming the north valley wall of this river.

The Grand Dome is covered by the Kibasa Formation and surrounded by the Rukugien through Niemba Formations and the Walikien Formation (Carboniferous through Upper Permian). The base of the Niemba is known elsewhere as the Karoo. The Karoo is equivalent to the Gres de Carnot which is well known as a diamond-bearing formation in the Central African Republic. This unit has yielded a few precious stones in the Equator Province of Zaire. In addition to scattered granitic intrusions, the southern part of the area is underlain by the Kundelunga Group, the upper part of the well known Katanga Supergroup which contains the rich copper deposits of Zaire in its lower unit called Roan.

Two large northeast trending faults cut the southeastern part of the Grand Dome. One of these lies essentially on the axis of this breached anticline. The second, essentially parallel to the first, passes through the Baudoinville area.

The rock unit exposed in the southern crestal portion of the anticline is clearly different from the surrounding units. This is the Kundelunga system.

The shores of Lake Tanganyika are composed of recent sediments derived from the upland described above. These sediments may contain detrital deposits of minerals present in the Dome.

Progressing to the west, the western flank of the Dome is bordered by Kibasien rocks which underlie the valley walls of the Niemba River. The region west of the river is essentially a granitoid terrain characterized by a large number of intrusions.

Immediately north and south of the Lukuga River, banks of the river expose a lithologic unit which Cahan has called Red Sandstone.

Northern Zone. This zone extends north of the Lukuga and is dominated by the Muhomba Plateau, an extension of the Mt. Mitumba upland in Maniema.

The units cropping out in the region are, in order of importance, the Ruzizi Group whose synclinal axes are occupied by the Kwango and Lualaba series and overlain by the red sandstones and the Tertiary rocks. It is in these Rheatic age plunging synclines that the coal beds were deposited. Three coal beds are the only mineral deposits currently exploited in this region.

The area is dominated by a large northwest trending fault system, which appears to be traceable in Tanzania across the lake. The

fracture system is composed of a large number of individual faults, all essentially parallel. Another important fault direction is suggested by a northeast trending fault oblique to the larger northeast trending fault.

One interesting feature should be pointed out here. There is a white polygonal area visible in the highlands of the Northern Zone. It has not yet been identified, but it may be a geometrically shaped, light colored granite cut by numerous joints.

As in the Southern Zone, the Northern Zone has a large number of granite intrusions.

Analysis of Mineral Potential

1. The Karoo is a continental deposit (Carboniferous, Permian, Triassic and Jurassic). Rocks of these ages are coal-bearing all over the world and are diamond-bearing in the Central African Republic (Gres de Carnot, for example) and in the Equator Province of Zaire. This unit also forms an extension of the "Golden Belt" of Kivu.
2. Alteration halos surrounding granitic intrusions in the area offer the possibility of supplemental mineralizations such as uranium, beryllium, tin, gold, zinc, lead, silver, etc. Systematic study

of these intrusions, particularly their alteration halos, may lead to economic discoveries depending on the degree of erosion.

3. The faulted areas north of former Baudoinville should be prospected, since they may have related copper and possibly cobalt mineralization. Indeed, these faults cut the underlying Roan copper belt formation. In general, the Katanga or Shaba Supergroup includes three units:

- Kundelungu;
- Dolomitic schist, called Minier;
- Roan (Faisceau des Mines).

Continental Basin

Because we are dealing with a continental depositional site, it might be well to consider the type of deposits we are likely to encounter. In general, a former continental basin is also a former river basin. Thus, there were waters running downhill and converging in the basin. The discovery of current direction indicators in these paleo-channels will indicate the direction to the deepest part of the basin.

There is a wide variety of minerals associated with continental basin deposition, including uranium, vanadium, copper, nickel, etc. For example, the uranium associated with vanadium of the Colorado

Plateau is found in a paleo-river basin, now a desert. Similarly, the uranium in Agades, Niger occurs in a desert paleo-river basin. In fact, these beds are saturated with non-replenished fossil water which defines the extent of the old basin. Copper as well as uranium can be concentrated in the paleo-river channels and basins.

In assessing the mineral potential of continental sedimentary terrains, one must consider both primary and secondary features, that is, depositional and post-depositional possibilities such as secondary enrichment, alteration, etc. These two types of mineralization offer the possibility of not only hydrocarbons and placer deposits such as gold, but also gold, uranium, beryllium, wolframite, copper and zinc.

In light of these possibilities, it is particularly important to consider structurally disturbed areas such as the Permian beds present in the Hercynien folds of the Kibasa region situated on the edge of the African Shield peripheral to the Zaire basin. These are deeply eroded folded chains that contain some volcanic rocks. These are known to contain some deposits of magnetite, ilmenite, nickeliferous minerals, gold in quartz, and tourmaline. Deposits of monazite, uranium and ilmenite result from erosion of the Karoo or Gres de Carnot.

For example, the grits of the thick Karoo in Africa are diamond carriers. As mentioned above, in Central Africa Republic there are diamonds in the Gres de Carnot, the lateral equivalent of the Karoo of Zaire. A few stones have already been found in the Equator Province of Zaire.

In the faulted zones in the region north of Lake Moero and from Kapula to Moba, Seremi has found indications of wolframite, tin, copper, some graphite schists, and indications of gold.

Mineralization Found in the Southern and Northern Zones

The following description of prospecting tends to verify some of the hypotheses based on the interpretation of ERTS data. Regional prospecting work was completed in 1973. In Kivu, block Zer No. 166 probably contains the following deposits:

1. Tin and wolframite on the Grand Dome are considered certain.
2. Tin minerals, ilmenite and tourmaline exist in the metamorphic series and in the black sands on the beaches of Lake Tanganyika.
3. Prospecting in the zone of altered Kibasien evaporites around granites has yielded indications of gold, tin, copper and other associated minerals.

In Shaba, block Zer No. 165 has even more promising possibilities with about fifteen anomalies of copper/cobalt active, gold, tin, wolfram discovered in Haute Luizi and Kongolo, and the discovery of an extension of the Katangian rocks in the southeast part of the block.

The Katanga Supergroup includes the Roan Formation which contains the copper beds. This is a fortunate discovery and prospecting is in progress. Copper and zinc anomalies also were found in Kikwanga, Ngaza in the Cretaceous rocks of Mwajhidi.

Other very recent discoveries include:

August 1973 - Shaba, No. 165

1. Alluvial samples of gold, tin and wolfram in Kongolo and Haute Luizi.
2. The discovery of a deformed Katanga granite outcropping over an area of approximately 1,000 km² in the south-eastern part of Zer.
3. Granite and muscovite exposures in the Kibasien.

- Kivu, No. 166

1. Cassiterite in the Kawa River.
2. Syenite and granite-bearing muscovite.
3. Quartz and tourmaline, cassiterite and wolframite bordering the Kivu Permian.

4. Various quartz veins containing wolframite in the northeast of Zer. These indications seem to be promising.

September 1973 - Shaba, No. 165

Several significant samples in terms of their analysis suggest there may be as many as fifteen copper/cobalt anomalies.

- Kivu, No. 166

Several alluvial samples analyzed in the course of a regional geologic study of Kinshasa show concentrations of cassiterite.

CONCLUSION

Our preliminary testing of ERTS imagery for the purpose of assessing mineral resource potential in Zaire involved preliminary delineation of tectonic units and structural features on the imagery, developing hypotheses about mineral potential of the area based on what we saw in the imagery and general knowledge of the geologic units in the area, and preliminary testing of these hypotheses using the most recent information available on results of mineral prospecting in the area. To date, we have used ERTS imagery covering only a small part of our country. From this work we conclude that ERTS imagery can probably make a material

contribution to assessing the mineral resource potential of our country and will be particularly valuable in the less known areas. We very much look forward to ERTS-B and an opportunity to test ERTS imagery for geologic exploration over larger areas.

ACKNOWLEDGEMENTS

We are deeply grateful to the Government of Zaire for its support of this work, and particularly to M. Bisengimana Rwema, Director of the Office of the President. We would like to thank the people of Earth Satellite Corporation for their advice and assistance during this study, particularly Mr. Jack Palgen and Dr. John Everett, for translating this report into English and editing it for publication.

Paper G 28

PRELIMINARY RESULTS OF ERTS-INVESTIGATIONS BY W-GERMAN INVESTIGATORS

Richard Mühlfeld, *Federal Geological Survey, Hannover, Germany*

INTRODUCTION

This report deals with the results of the following ERTS-proposals.

SR No. 328 "Multidisciplinary geoscientific experiments in Central Europe"

PI: D. Bannert

CIs: J. Bodechtel, F. Fezer, H.-G. Gierloff-Emden,
H. Knorr, P. Kronberg, R. Mühlfeld, S. Schneider

MMC No. 330 "Hydrogeological Investigations in the Pampa of Argentina"

PI: D. Bannert

CIs: H. Bender, W. Kruck

For several reasons this is only a preliminary report:

1. Delivery of existing ERTS-imagery was very incomplete until recently.
2. Repeated coverage showing different seasonal conditions is very poor.
3. NASA-processing of 1 : 1 million imagery results in the loss of an important part of the information existing on the tapes. Only recently has processing in Germany reached the point where it is possible to produce 1 : 200,000 scale prints directly from the tape without loss of information.

MULTIDISCIPLINARY GEOSCIENTIFIC EXPERIMENTS IN CENTRAL EUROPE

Original Aims of the Proposal

Geology: Structural and lithological interpretation;
Study of sediment transport in coastal areas.

Pedology: Mapping of soil units in glacially affected areas.

Geography: Study of field patterns and land use, pollution monitoring.

Cartography: Investigation of suitability of space imagery for small-scale map production.

Data processing: Automated map production, sensor calibration.

Results of the Studies

Central Europe is almost completely covered by vegetation. Since the type of vegetation is governed by morphology, soil, and bedrock, information on geological and soil units can only be derived from the type and distribution pattern of the vegetation.

Three main types of vegetation can be discriminated on imagery taken in September 1972 by comparison of MSS bands 4-7; pasture land (light toned in band 6 and 7), coniferous trees (dark toned in all 4 bands), and deciduous trees (light in band 6 and 7, dark in band 4 and 5).

From the distribution pattern of these vegetation types it is possible to identify a number of geological units, marshlands, sandy uplands, river terraces, peatbog, sandstone, and limestone (in part represented in Fig. 1 and 2). These units coincide with typical soil types.

In areas where the vegetation delineates the outcrop pattern of dipping sedimentary rocks, subsurface structure can be inferred.

Two findings resulted from the study of linear tectonic features.

The present knowledge of linear tectonics, especially in mountainous regions of Central Germany and the Alps, could and will be considerably improved. The significance of this improvement for the understanding of the tectonic history of the area will be object of future studies. In the Alps the obvious persistence of long, linear features even through faulted and overthrust zones has impact on the concepts of the mechanism of orogeny.

In the North German Lowlands a linear anomaly was found which corresponded to a major fault buried beneath unfaulted Tertiary and Quaternary sediments (A - B in Fig. 2). A seismic cross-section shows the lineation following the downthrown block (C - D in Fig. 2 and Fig. 3). At the surface the lineation is marked by vegetation anomalies caused by relatively high soil moisture content. Experience in other sedimentary basins would suggest that differential compaction of sediments in the upthrown and the downthrown blocks has caused a slightly greater subsidence in a narrow zone following the downthrown block.

Studies of the tidal flats off the German coast showed the suitability of ERTS-imagery taken during high tide for mapping the topography with better accuracy than existing maps. Sediment transportation could not be studied because neither imagery taken during low tide nor repeated coverage where available.

The study of land use and field patterns resulted in a very detailed subdivision into small geographical units which makes the imagery suitable for regional planning.

The smog of industrial areas could be monitored with additive color techniques. The influence of air pollution on land use was difficult to recognize because of small field size, limited resolution, and lack of repetitive coverage over an extended period of time.

Studies on the preparation of small scale photomaps show an incomplete registration of the traffic network. Possible improvement with recently received imagery taken in different seasons is being investigated.

Experiments with data processing developed ratio-methods which can identify 10 different surface signatures with 90% accuracy. In addition an electron beam recorder was designed which produces imagery without loss of resolution inherent in the system. In the future it will allow more accurate studies than was so far possible with NASA-furnished imagery.

HYDROGEOLOGICAL INVESTIGATIONS IN THE PAMPA OF ARGENTINA

It was proposed to map the distribution of fresh and salt contaminated groundwater mainly by type and pattern of vegetation.

A first investigation of the imagery proved their value for the proposed study (Fig. 4): Areas having patterns of agricultural fields have fresh groundwater. The dark areas indicated with an S are depressions where the water table is so close to the surface that high evaporation results in high groundwater salinity. Narrow elongated depressions without surface drainage called "bajos" collect surface rainfall runoff. The water percolates into the ground and forms fresh water bodies which are mainly used for cattle raising. On the river terraces areas covered by sand dunes are also favorable for the accumulation of fresh groundwater. Tectonic lineations most of them never before observed, also influence the groundwater conditions. They can be mapped readily from the imagery.

As has been checked with data gathered on the ground, the imagery shows all major elements necessary for a reconnaissance hydrogeologic study. The

work will be extended further South into a less known area, to prepare an experimental hydrogeological map based on the results from the ongoing studies.

CONCLUSIONS

The main goals of the investigation were achieved. The studies have given a good idea of the possibilities and limitations of ERTS-imagery depending on the objectives in question and on the geographical conditions of the areas under investigation. Even in the well known region of Central Europe, ERTS has proven its ability of improving our present knowledge. This ability is by no means fully explored. Therefore future coverage is highly desirable. In fields such as pollution monitoring and regional planning the satellite techniques should have distinct practical value. For any regional study of less known areas, the value of ERTS-imagery can hardly be overestimated.

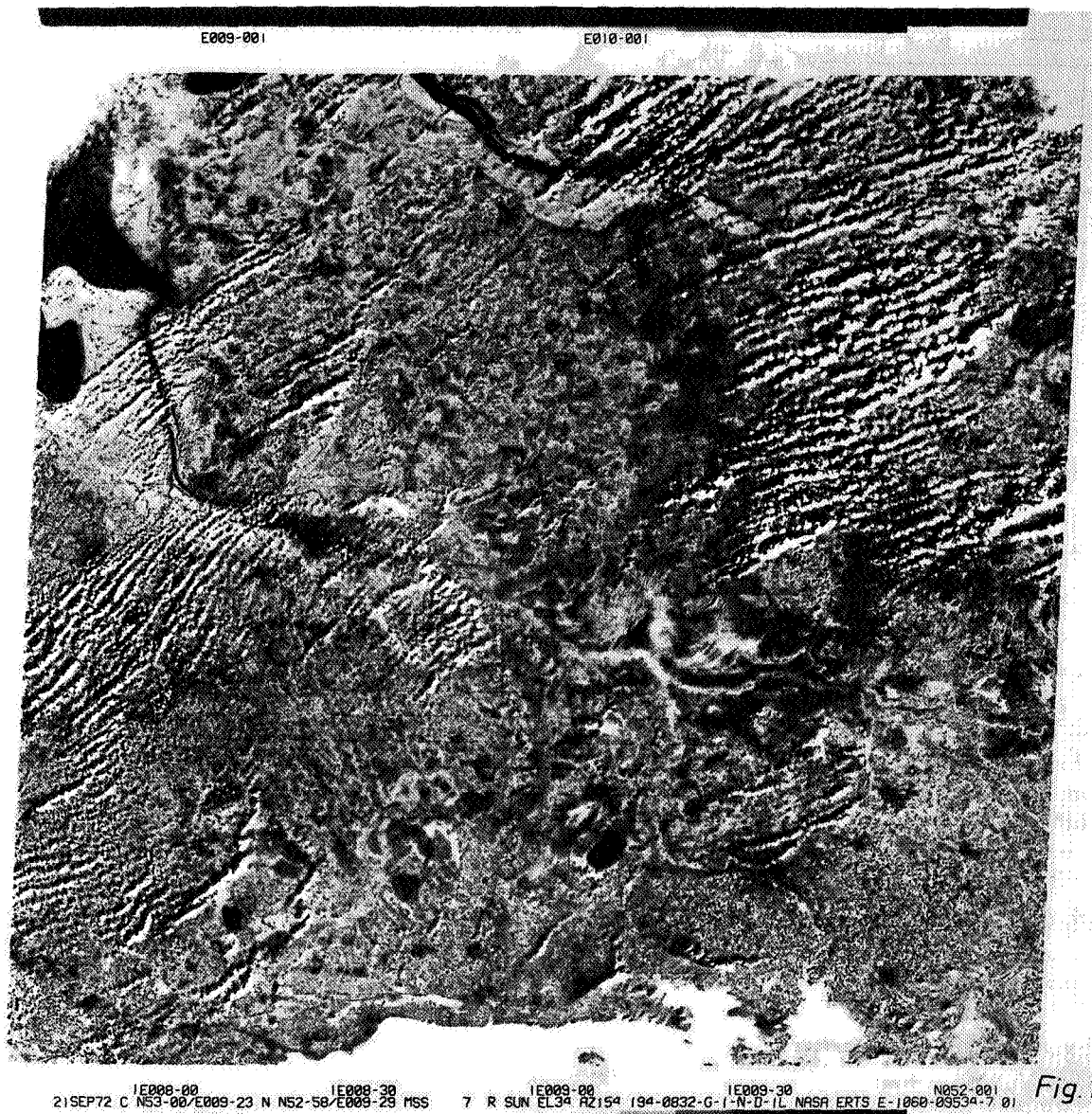
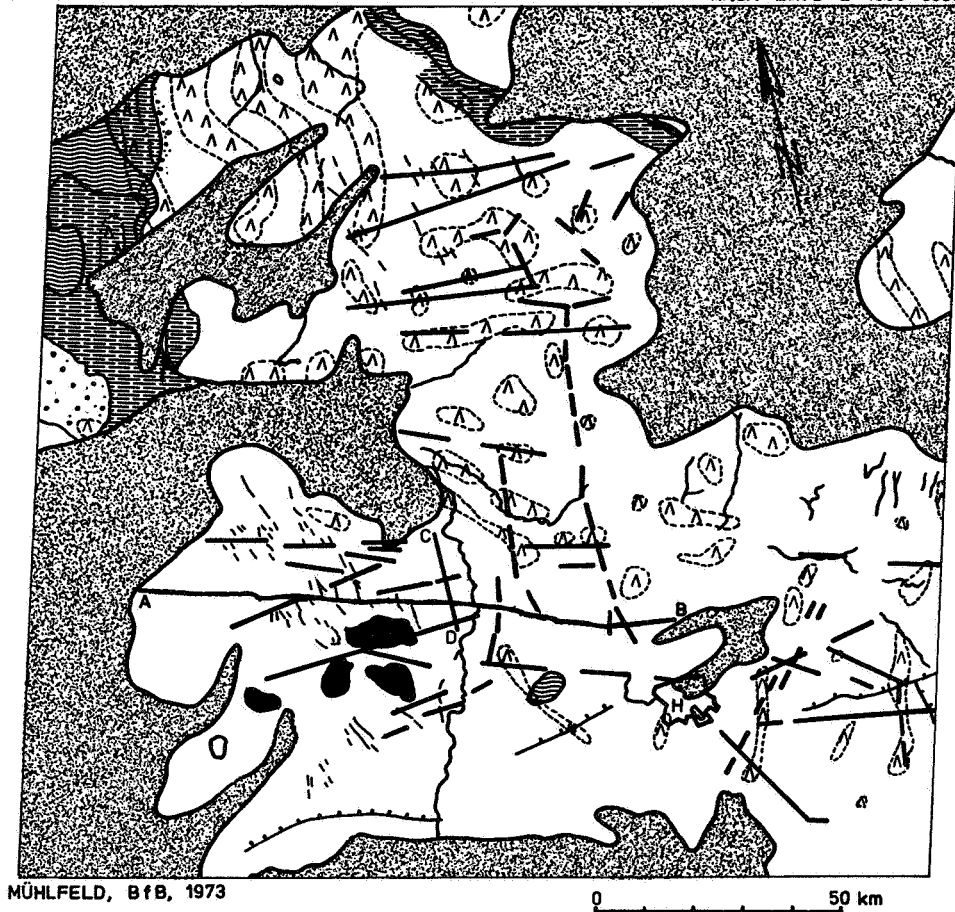


Figure 1. ERTS-1-Image of Parts of NW-German Lowlands

Parts of NW - German Lowland

21. SEP. 1972

NASA ERTS E-1060-09534



LEGEND

	Clouds		Peatbog
	Water surface		Glacial drainage network
	River		Photolineations and faults
	Canal		Salt diapirs (from geophysical investigation)
	Marshlands		HANNOVER
	Sandy uplands	A B	(Explanation compare with the text)
		C D	{ " " " " }

Figure 2. Interpretation of ERTS-1-Image of Fig. 1 Combined With Distribution of Salt Diapirs (After Geophysical Data)

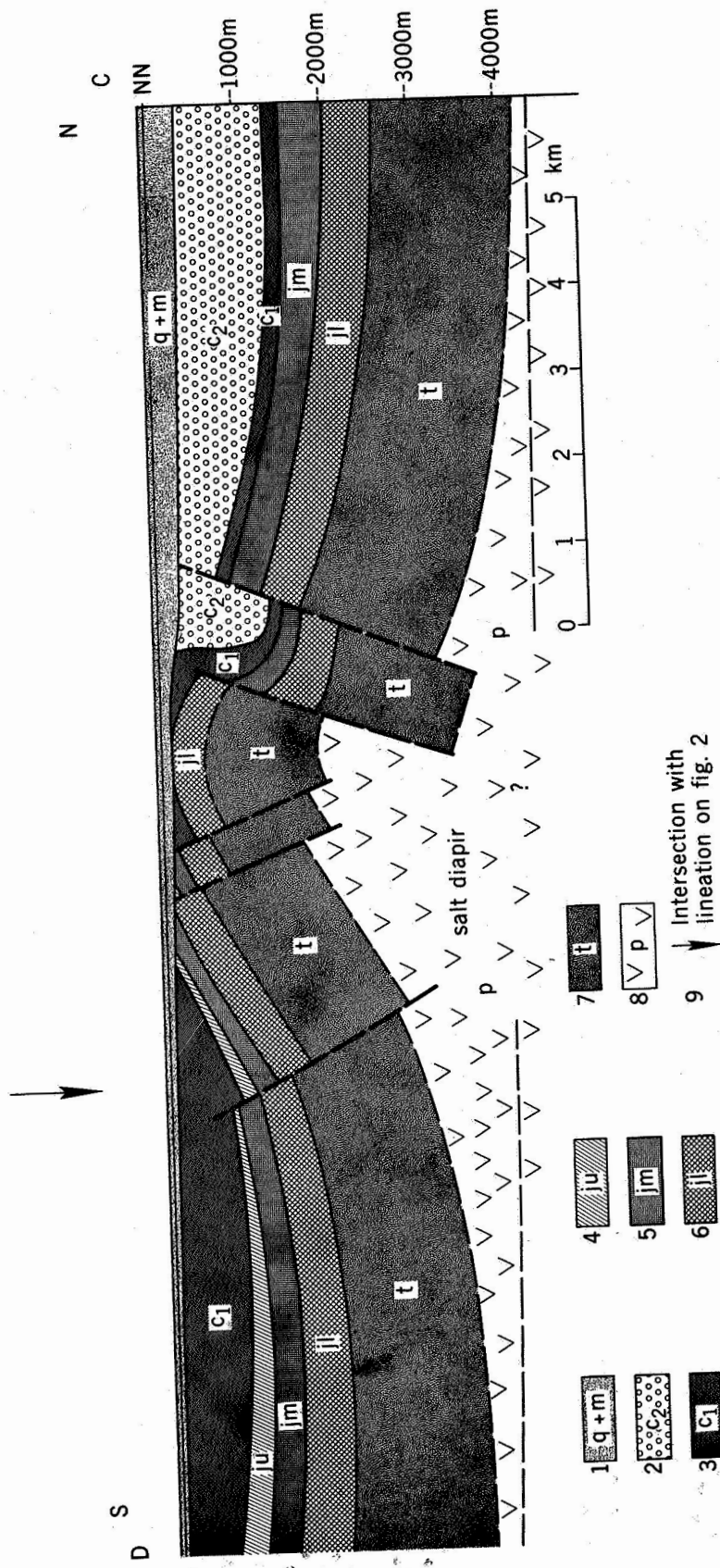
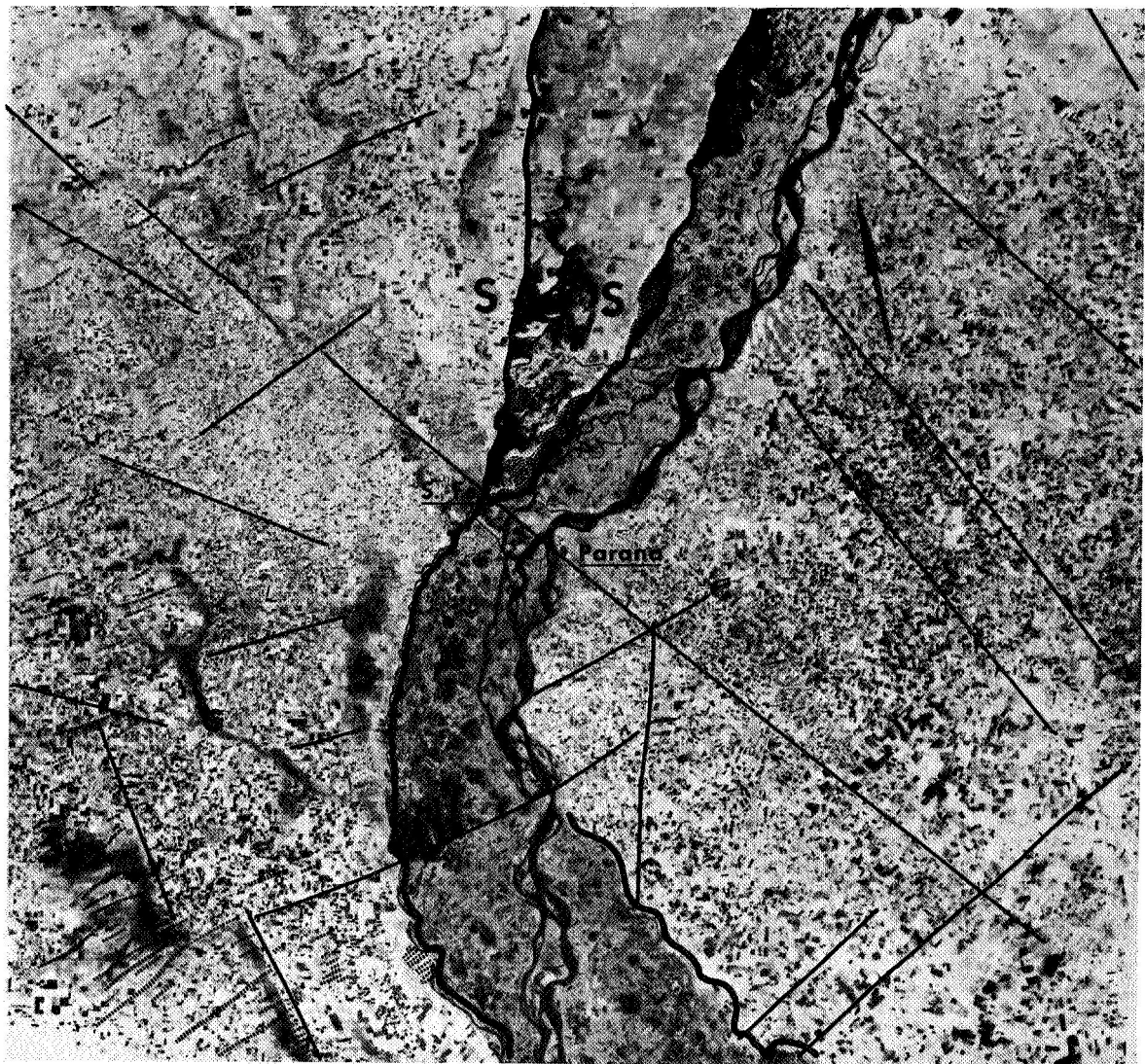


Figure 3. Seismic Section Across Lineation Observed on ERTS-Image Fig. 1



LEGEND

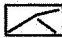


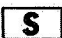

	LINEATIONS		BAJOS (ELONGATED DEPRESSIONS)
	TERRACE MARGINS		AREA WITH HIGH GROUND-WATER LEVEL, SALINE GROUND-WATER
	DUNES		

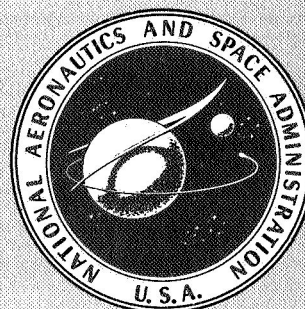
Figure 4. Hydrogeologic Evaluation of ERTS-1-Image of Parts of NE-Argentina

THIRD EARTH RESOURCES TECHNOLOGY SATELLITE-1 SYMPOSIUM

Volume I: Technical Presentations Section A

Addendum. Technical Presentation G 3.1
GEOLOGIC APPLICATION OF ERTS IMAGERY IN ALASKA
by Ernest H. Lathram

A symposium held by
GODDARD SPACE FLIGHT CENTER
Washington, D.C.
December 10-14, 1973



NATIONAL AERONAUTICS AND SPACE ADMINISTRATION

GEOLOGIC APPLICATION OF ERTS IMAGERY IN ALASKA

Ernest H. Lathram, *U. S. Geological Survey, Menlo Park, California*

ABSTRACT

ERTS imagery has been used to develop an hypothesis that provides an additional exploration rationale to mineral exploration, to suggest new areas of potential for petroleum exploration, and to improve small- and medium-scale geologic mapping in Alaska.

INTRODUCTION

Energy, minerals, and environment--the three primary concerns of the continuation of our way of life--come sharply into focus in Alaska. Estimated potential resources of 82 billion barrels of oil (Cram, 1973), 366 trillion cubic feet of gas (Rassinier, 1973), and 130 billion minable tons of coal (Barnes, 1967) constitute major elements in the nation's quest for energy sources. The discovery at Prudhoe Bay of the largest petroleum deposit in North America emphasizes the importance of this energy potential. Mineral resource production in 1972 was less than \$4 million (State of Alaska, 1972), whereas comparison with the geologically similar area of the 11 Western States suggests a potential annual production at least 50 times greater. The environment presents logistic problems that not only result in high cost but demand imaginative solutions in exploration and production to maintain the integrity of the sensitive physical, chemical, and biological balance in Alaska. The use of innovative methods such as ERTS is not only appropriate but essential in Alaska to develop and use its resources wisely and at the least cost to man and his environment.

It is the purpose of this investigation to employ ERTS data to update and develop new regional analyses and hypotheses of mineral and mineral fuel resource potential and to improve medium- and small-scale geologic maps that provide the information required to explore for and develop these resources. The preliminary results were reported in March (Lathram and others, 1973). This paper reports additional results, and presents some examples of practical application of ERTS imagery.

REGIONAL ANALYSES

Mineral Resources

Studies of Nimbus and ERTS imagery resulted in the formulation and strengthening of an hypothesis that mineralized areas in Alaska may be spatially related to a regional set of northeast- and northwest-trending linears--many previously unrecognized--that possibly reflect crustal fractures (Lathram and Gryc, 1973; Lathram and others, 1973; fig. 1). Linears representative of this set are clearly apparent on an ERTS mosaic of the Yukon-Tanana Upland east of Fairbanks (fig. 2). Both the Yukon and Tanana Rivers follow the northwest-trending linear direction, although both deviate from this trend near the western part of the figure. The northeast-trending linears of the set are clearly apparent in the highlands between the two rivers.

According to the conventional metallogenic hypothesis (fig. 1, top), areas deemed favorable for occurrence of various types of ore deposits are assumed to describe arcuate belts through southern and central Alaska, consonant with the arcuate pattern of distribution of stratigraphic, orogenic, and orographic features. The new hypothesis postulates that favorable areas would form belts parallel to major northwest- and northeast-trending fractures, and deposits would be more abundant where such fractures crossed. For example, using the conventional concept one would expect to find copper-molybdenum porphyry deposits in an arcuate belt south of the Denali fault, whereas according to the new hypothesis (fig. 1, bottom) such deposits could be found in two northeast-trending belts that could extend northeast of the Denali fault.

Following the ERTS-1 Symposium of March 1973, at which the new hypothesis was discussed, word was received that the hypothesis had been substantiated (E. R. Chipp, written commun., 1973). In 1970 and 1971, independent mineral exploration utilizing northeast and northwest fracture systems as a guide resulted in the discovery of a number of copper-molybdenum deposits in the area of the Tanacross quadrangle (fig. 2, southeast quarter), two of which are currently being explored by drilling. These deposits lie northeast of the Denali fault (fig. 2, north-convex arc at bottom left).

Although these deposits were not found directly by use of ERTS imagery, their discovery in an area and in a geologic setting predictable by the new hypothesis developed solely through use of space imagery, leads to two important conclusions:

1. The new hypothesis can be profitably used as an additional exploration rationale by the mineral resource industry.
2. ERTS imagery can be employed effectively to improve existing concepts of mineral resource potential and develop new ones.

Energy Resources

Examination of ERTS image 1004-21395 revealed hitherto unrecognized lineations in Coastal Plain lakes north of Umiat, Alaska. Comparison of the trend of these lineations with available geologic, magnetic, and gravity data suggests that concealed structures may exist in this area that may be favorable for concentrations of gas in shallow strata and of oil in deeper strata at or near basement (Fischer and Lathram, 1973; Lathram and others, 1973).

Study of ERTS images of northern Alaska acquired in 1973 not only substantiates observations made of the Umiat area but also shows that the east-trending lineation is prominent throughout the Coastal Plain to the east, extending as far as the Canning River (fig. 3). This area includes the sites of Prudhoe Bay and other recently discovered oil fields.

The newly observed lineation is prominent only in the area east of the Ikpiuk River. This restriction in the area characterized by the east-trending lineation lends support to the conclusion that it reflects buried geologic structure. In addition, the recognition of the lineation in the Coastal Plain between the Colville and Canning Rivers substantially increases the area in which the lineation may provide an additional guide to oil exploration.

Improvement in Geologic Maps

ERTS images are being used to complete a revised 1:1,000,000-scale regional map of northern Alaska. For example, in the earlier compilation (Lathram, 1965), the lowland area of the Ipewik and Kukpuk Rivers is largely devoid of structural data (fig. 4). Despite several seasons of exploration by private companies, and by the U.S. Geological Survey, the ubiquitous tundra cover and paucity of outcrops along the shallow streams and rivers prevented recognition of the distribution of structural elements in this area. Interpretation of conventional aerial photographs revealed little additional data. ERTS images 1009-22090, 1046-22143 and 1046-22145, however, displayed a startlingly clear and detailed representation of the area (Lathram, and others, 1973, fig. 2). The new map compilation of this area (fig. 5), although as yet unedited, shows clearly the complexity of structure revealed by the ERTS image, and the pronounced difference between the structural pattern in this area and that in the area of strata of comparable age to the north and east. This change in structural complexity may be due to oroclinal bending around an axis trending northeast through the lowlands (Tailleur and Brosge, 1970) or, more probably, to the superimposition of a western and younger belt of east-directed thrust faults upon an eastern and older belt of north-directed thrust faults (Grantz and others, 1970). Recognition of the structural complexity, and determination of its cause, are critically important in determining the potential for petroleum accumulations at depth in the area.

Enlargements of ERTS images to a scale of 1:250,000 are also being used in medium-scale geologic mapping. In the Kukpuk-Ipewik Rivers area of northern Alaska, compilation of known geology on the ERTS images has permitted extrapolation of data into unmapped areas, and has resulted in the recognition of structural and stratigraphic anomalies that suggest new interpretations of the geology (Tailleur, in Gryc and Lathram, 1973). In field mapping in 1973, W. P. Brosge, I. L. Tailleur, and others successfully used ERTS images to determine the location of lithologic contacts between successive field stations (Tailleur, oral commun. 1973). G. Plafker, R. L. Detterman, and others employed ERTS images in field studies of the location and continuity of major faults in southern Alaska, as a part of the U.S. Geological Survey's Earthquake Hazards Reduction Program. The images were particularly useful in mapping in the snow field areas bordering the Gulf of Alaska. Not only is the location of field observations more easy and accurate in the ERTS image (fig. 6) than on the most recent topographic map (fig. 7), but the distribution of perennial snow is more true on the near real-time image than on the more than ten year-old map (G. Plafker, oral commun., 1973).

CONCLUSIONS

Geologic study of ERTS images of Alaska during the first year of the satellite operations has resulted in:

1. Development of a new metallogenic hypothesis for Alaska that will provide an additional guide to those exploring for new sources of minerals.
2. Recognition of regional geologic features that may guide in the location of hitherto undiscovered oil and/or gas accumulations in northern Alaska.

3. Demonstration of the effectiveness of ERTS data in updating and developing new regional analyses and hypotheses concerning mineral and energy resource potential, and in improving medium- and small-scale geologic maps.

The results to date demonstrate the practical application of ERTS data to the study of the geology of Alaska. Future investigations will be focused on the most effective means of applying this new and powerful tool.

REFERENCES

- Barnes, F. F., 1967, Coal resources of Alaska: U.S. Geol. Survey Bull. 1242-B, p. B9.
- Cram, I. H., 1973, Future petroleum provinces of the United States: Their geology and potential: Summary, in Cram, I. H., ed., Future petroleum provinces of the United States--their geology and potential: Am. Assoc. Petroleum Geologists Mem. 15, v. 1, p. 24.
- Fischer, W. A., and Lathram, E. H., 1973, Concealed structures in Arctic Alaska identified on ERTS-1 imagery: Oil and Gas Journal, v. 71, p. 97-102.
- Grantz, Arthur, Hanna, W. F., Holmes, M. L., and Creager, J. S., 1970, Reconnaissance geology of Chukchi Sea as determined by acoustic and magnetic profiling (abs.): Am. Assoc. Petroleum Geologists Bull., v. 54, no. 12, p. 2483.
- Gryc, George, and Lathram, E. H., 1973, Identification of geostructures of continental crust, particularly as they relate to mineral resource evaluation: U.S. Dept. Commerce, Natl. Tech. Inf. Service, NASA-CR 131316, 5 p.
- Lathram, E. H., 1965, Preliminary geologic map of northern Alaska: U.S. Geol. Survey open file report, scale 1:1,000,000.
- Lathram, E. H., and Gryc, George, 1973, Metallogenic significance of Alaskan geostructures seen from space: Proceedings, Eighth Internat. Symposium on Remote Sensing of Environment, Ann Arbor, Mich., p. 1209-1211.
- Lathram, E. H., TAILLEUR, I. L., Patton, W. W., Jr., and Fischer, W. A., 1973, Preliminary geologic application of ERTS imagery in Alaska, in Symposium on Significant Results Obtained from Earth Resources Technology Satellite-1: Nat. Aeronaut. Space Adm., Spec. Pub. SP-327, v. I, Section A, p. 257-264.
- Rassinier, E. A., (chm.), 1973, Potential supply of natural gas in the United States (as of Dec. 31, 1972): Potential Gas Comm., Potential Gas Agency, Mineral Resources Institute, Colo. Sch. Mines Foundation Inc., Golden, Colo.
- State of Alaska, Annual Report 1972: Dept. of Natural Resources, Division of Mines and Geology, Juneau, Alaska, Table 1, p. 44.

Tailleur, I. L., and Brosge, W. P., 1970, Tectonic history of northern Alaska, in Adkison, W. L. and Brosge, M. M., eds., Proceedings of the geological seminar on the North Slope of Alaska: Los Angeles, Pacific Sec., Am. Assoc. Petroleum Geologists, p. E1-E19.

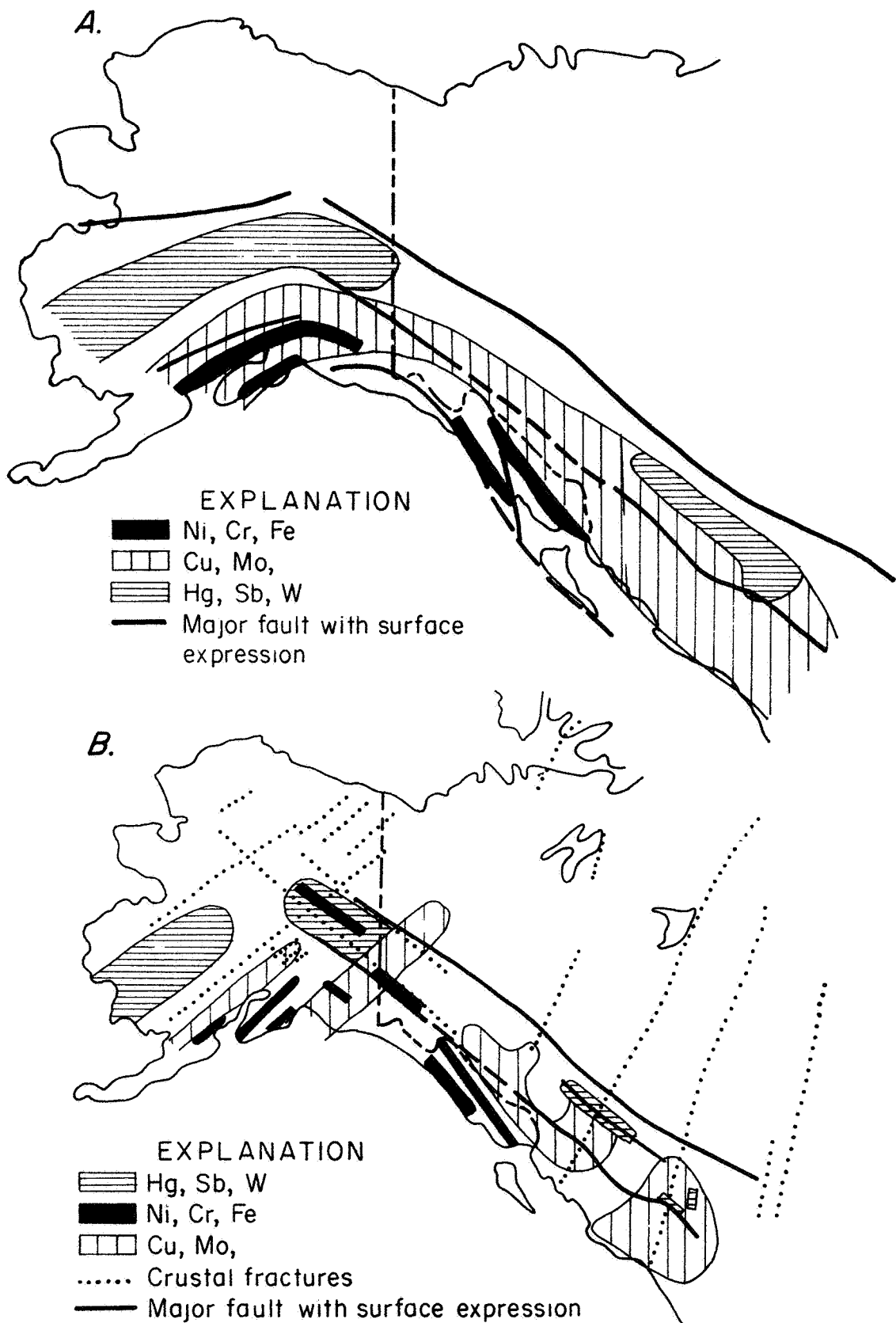


Figure 1. Areas of Alaska and western Canada considered favorable for location of deposits of selected metals based on extrapolation of geologic conditions at known occurrences. (A) Conventional concept guided by north-convex arcuate distribution of lithologic belts. (B) Postulated alternative assuming that linears seen on Nimbus IV and ERTS images are crustal fractures and have influenced mineralization.

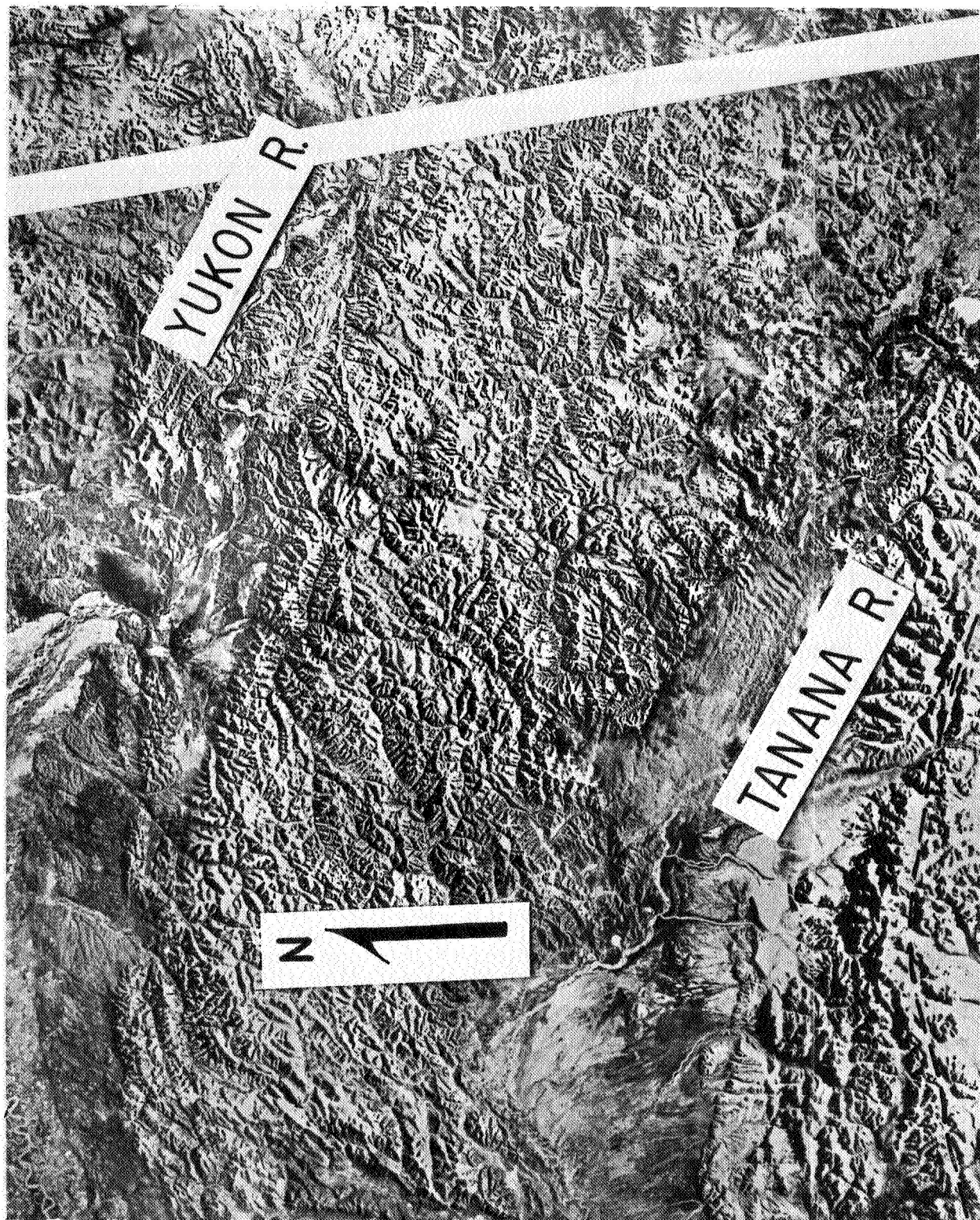


Figure 2. ERTS mosaic of Yukon-Tanana upland showing pronounced northeast- and northwest-trending linears and Denali fault (dashed line).

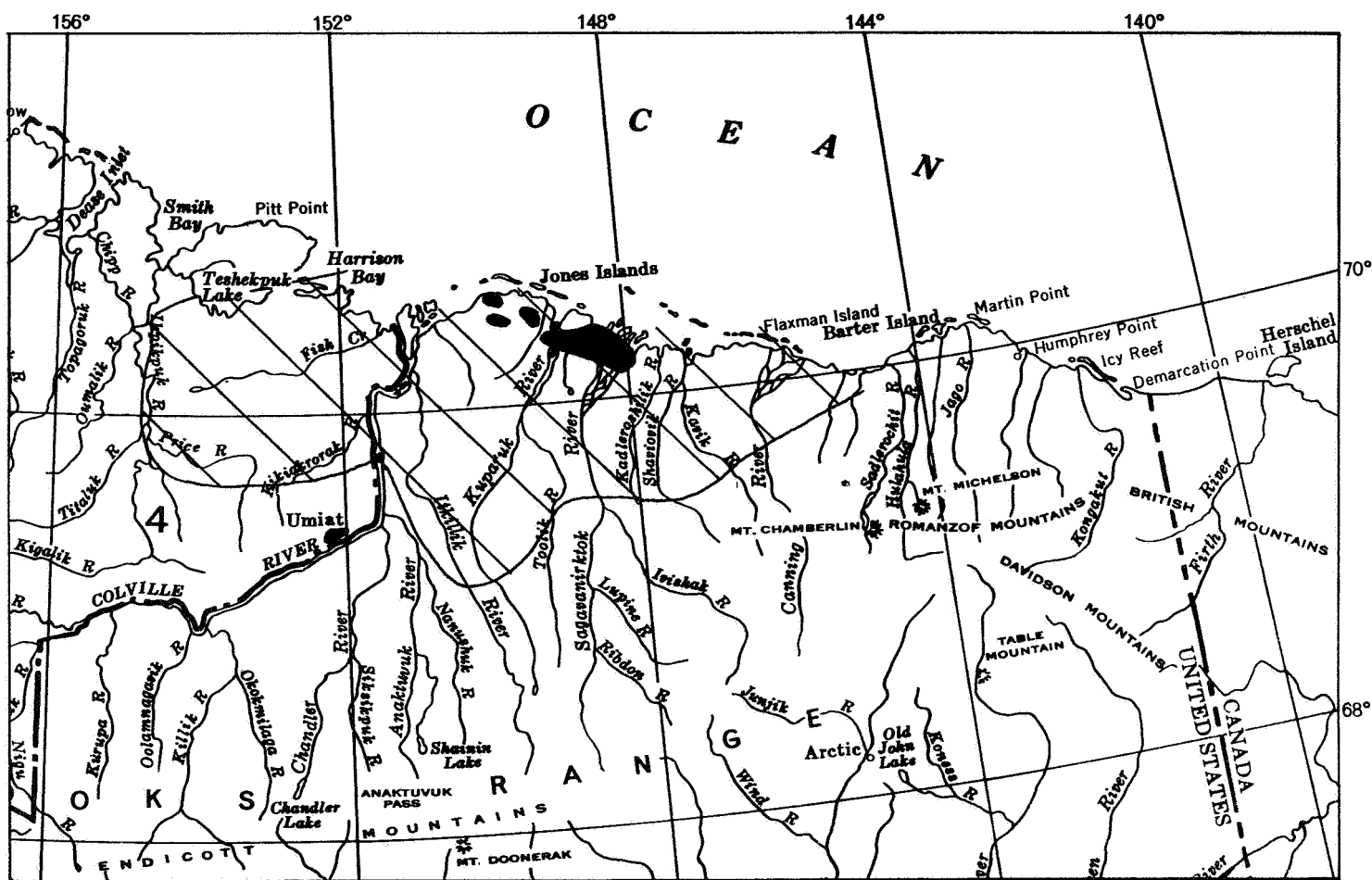


Figure 3. Excerpt from map of northern Alaska showing oilfields (in black) and area characterized by lineation in lakes (ruled).

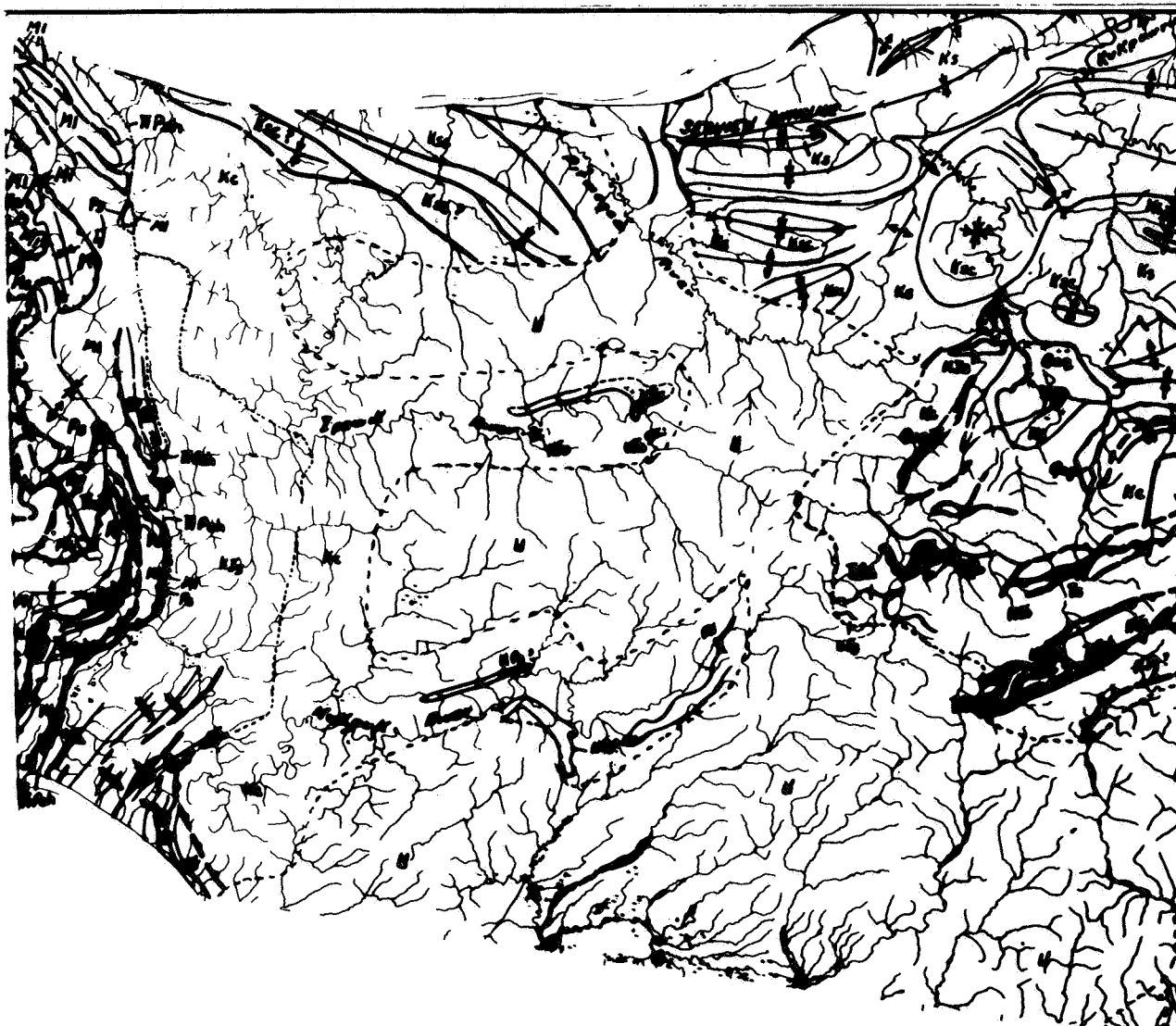


Figure 4. Part of regional geologic map compilation prepared in 1965 showing paucity of data in lowland of Ipewik and Kukpuk Rivers.



Figure 5. Part of revised regional geologic map compilation prepared in 1973 showing additional structure data obtained from ERTS images.

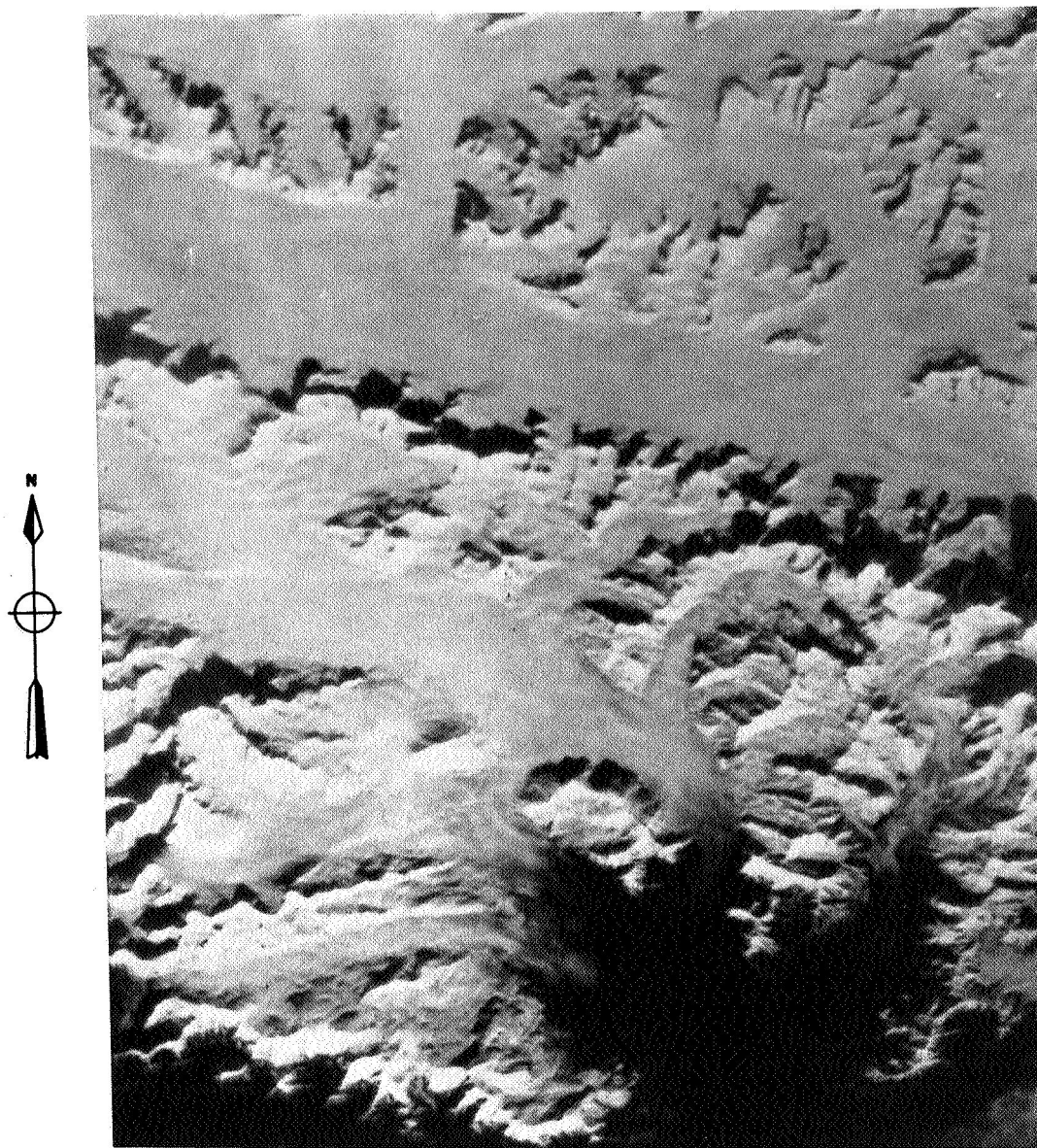


Figure 6. Part of ERTS image of Bering Glacier area, approximate scale 1:250,000.

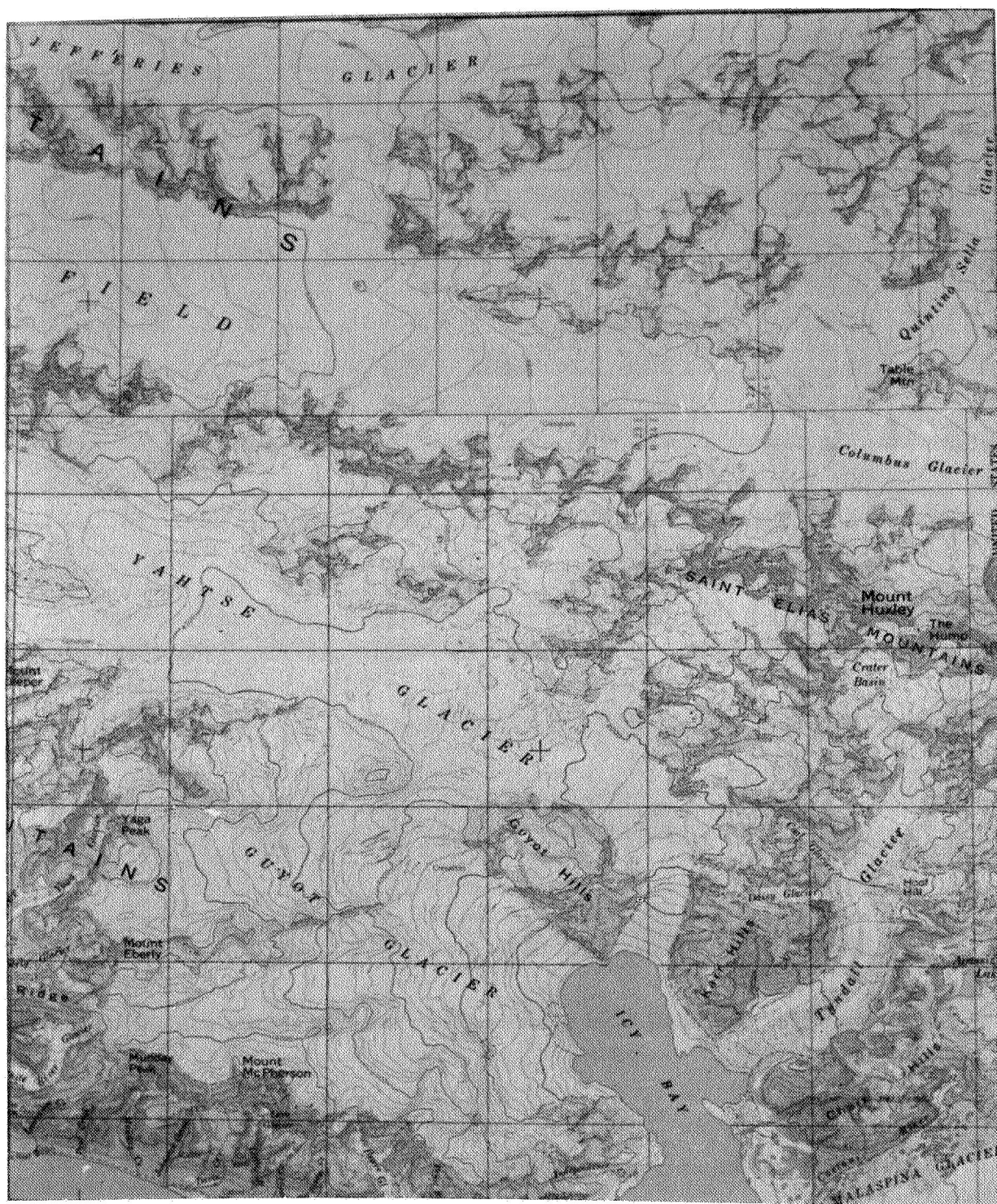


Figure 7. Part of standard topographic map of Bering Glacier area, scale 1:250,000, showing stylized representation of nunataks.

NATIONAL AERONAUTICS AND SPACE ADMINISTRATION
WASHINGTON, D.C. 20546

OFFICIAL BUSINESS
PENALTY FOR PRIVATE USE \$300

SPECIAL FOURTH-CLASS RATE
BOOK

POSTAGE AND FEES PAID
NATIONAL AERONAUTICS AND
SPACE ADMINISTRATION
451



POSTMASTER

If Undeliverable (Section 158
Postal Manual) Do Not Return

"The aeronautical and space activities of the United States shall be conducted so as to contribute to the expansion of human knowledge of phenomena in the atmosphere and space. The Administration shall provide for the widest practicable and appropriate dissemination of information concerning its activities and the results thereof."

—NATIONAL AERONAUTICS AND SPACE ACT OF 1958

NASA SCIENTIFIC AND TECHNICAL PUBLICATIONS

TECHNICAL REPORTS Scientific and technical information considered important, complete, and a lasting contribution to existing knowledge.

TECHNICAL NOTES Information less broad in scope but nevertheless of importance as a contribution to existing knowledge

TECHNICAL MEMORANDUMS Information receiving limited distribution because of preliminary data, security classification, or other reasons. Also includes conference proceedings with either limited or unlimited distribution.

CONTRACTOR REPORTS Scientific and technical information generated under a NASA contract or grant and considered an important contribution to existing knowledge.

TECHNICAL TRANSLATIONS Information published in a foreign language considered to merit NASA distribution in English.

SPECIAL PUBLICATIONS Information derived from or of value to NASA activities. Publications include final reports of major projects, monographs, data compilations, handbooks, sourcebooks, and special bibliographies.

TECHNOLOGY UTILIZATION PUBLICATIONS Information on technology used by NASA that may be of particular interest in commercial and other non-aerospace applications. Publications include Tech Briefs, Technology Utilization Reports and Technology Surveys.

Details on the availability of these publications may be obtained from:

SCIENTIFIC AND TECHNICAL INFORMATION OFFICE

NATIONAL AERONAUTICS AND SPACE ADMINISTRATION
Washington, D.C. 20546